

TN
1
AS
Vol. 186
NIC

TRANSACTIONS

of the

American Institute of Mining
and Metallurgical Engineers

(Incorporated)

*American Institute of Mining, Metallurgy
and Petroleum Engineers //*

VOLUME 186

PETROLEUM DEVELOPMENT

AND TECHNOLOGY

1949

PETROLEUM BRANCH

PAPERS AND DISCUSSIONS PRESENTED BEFORE THE BRANCH AT MEETINGS HELD AT DALLAS, OCT.
4-6, 1948; LOS ANGELES, OCT. 14-15, 1948; AUSTIN, DEC. 16-17, 1948; SAN FRANCISCO, FEB. 13-17, 1949,
AND SAN ANTONIO, OCT. 5-7, 1949.

PUBLISHED BY THE INSTITUTE
AT THE OFFICE OF THE PETROLEUM BRANCH
601 CONTINENTAL BUILDING
DALLAS, TEXAS

Headquarters of the Institute are at 29 West 39th Street, New York, N. Y.

COPYRIGHT, 1949, BY THE
AMERICAN INSTITUTE OF MINING AND METALLURGICAL ENGINEERS
(INCORPORATED)

PRINTED IN THE UNITED STATES OF AMERICA

STORM PRINTING COMPANY, DALLAS, TEXAS

FOREWORD

THIS volume of *Transactions* contains the technical papers that had their first publication in the *Journal of Petroleum Technology*. The officers and committees of the Branch take pride in the fact that the volume contains many more papers than any other *Petroleum Transactions* volume of recent years; and that in length, considering the new larger page size, it is the equivalent of any two such volumes since 1932. This evidence of the continuing increase in importance of the Branch as forum for petroleum engineers cannot be discounted, as the same high standards of selection prevailing in previous years were applied to this volume.

As would be expected, the sharp increase in the number of papers submitted was paralleled by the other indications of a progressing organization. Total membership in the Branch moved to new record levels, while the number of applicants also exceeded that of any year in history. Attendance at the principal meetings in San Antonio and Los Angeles was double that of very few years ago. The number of regional AIME petroleum organizations increased, as 1949 saw the formation of the Illinois Basin and Rocky Mountain Chapters of the Branch, and of the San Joaquin Valley Section of the Pacific Chapter; as well as creation of the South Plains (Lubbock) Sub-Section of the Permian Basin Local Section. These developments increased to 15 the number of AIME regional organizations to which the Branch is closely related. With the possible future organization of an Appalachian group, and expansion of Rocky Mountain activities, our national geographic foundation will be complete in outline.

The *Journal of Petroleum Technology*, new in 1949, found favor with the membership and can be considered the most fundamental influence toward the continued growth and capacity of the Branch. Other highlights of 1949 were achievement of a closer liaison with the Institute administrators, and a series of vital discussions with these administrators which has brought clearer understanding of principal problems and placed us, we believe, on the road to their solution.

The favorable developments of the past year, and of the past several years, are not happenstance, but reflect the conscientious attention, insight and leadership of the Chairman, the Executive Committee, and the specialized standing Committees of the Branch. Our thanks and many compliments are due Lloyd E. Elkins for his leadership in 1949. In becoming your chairman for 1950 I am confident of receiving the same fine cooperation of the Committees and the membership, and earnestly hope that I, too, can contribute full measure to the enlargement of the Branch and to increasing its value to each of its members.

JOHN E. SHERBORNE, *Chairman for 1950*
Petroleum Branch, AIME

WILMINGTON, CALIFORNIA
January 1, 1950

PETROLEUM BRANCH OFFICERS AND COMMITTEE CHAIRMEN

For the Year ending February, 1950

CHAIRMAN

LLOYD E. ELKINS
Stanolind Oil & Gas Co.
Tulsa, Oklahoma

VICE-CHAIRMEN

GAIL MOULTON
Chase National Bank
New York, N. Y.

JOHN E. SHERBORNE
Union Oil Company of California
Wilmington, California

EXECUTIVE COMMITTEE

JOHN E. SHERBORNE

LLOYD E. ELKINS

GAIL MOULTON

IRWIN W. ALCORN
The Pure Oil Company
Houston, Texas

HAROLD DECKER
Pan-American Companies
Houston, Texas

PAUL ANDREWS
Signal Oil & Gas Company
Los Angeles, California

JOHN H. MURRELL
DeGolyer & MacNaughton
Dallas, Texas

STUART E. BUCKLEY
Humble Oil & Refining Company
Houston, Texas

DEAN H. SHELDON
Consulting Engineer
Los Angeles, California

BENJAMIN C. CRAFT
Louisiana State University
University, Louisiana

CHARLES B. CARPENTER
U. S. Bureau of Mines
Dallas, Texas

TREASURER

MEMBERSHIP COMMITTEE

FRANK BRIGGS
Houston, Texas

Vice-Chairmen

JOHN K. WRIGHT, JR.
Mississippi Oil and Gas Board
Jackson, Mississippi

V. J. MERCIER
Mountain Iron & Supply Co.
Wichita, Kansas

BURTON ATKINSON
Humble Oil & Refining Company
Midland, Texas

N. A. D'ARCY, JR.
Manufacturers' Representative
Huntington Park, California

J. H. BARNETT
Stanolind Oil & Gas Company
Casper, Wyoming

PRODUCTION REVIEW COMMITTEE

(Serves until Oct. 15, 1950)

D. V. CARTER
Magnolia Petroleum Company
Dallas, Texas

Vice-Chairman

R. B. GILMORE
DeGolyer & MacNaughton
Dallas, Texas

GAS TECHNOLOGY COMMITTEE

Co-Chairmen

H. C. SPOOR, JR.
Commerce Building
Houston, Texas

FRANK DOTTERWEICH
Texas College of A&I
Kingsville, Texas

EDUCATION COMMITTEE

JOHN C. CALHOUN, JR.
University of Oklahoma
Norman, Oklahoma

Vice-Chairman

CHARLES R. DODSON
University of Southern California
Los Angeles, California

PRODUCTION TECHNOLOGY COMMITTEE

JOHN E. SHERBORNE
Union Oil Company of California
Wilmington, California

Vice-Chairmen

MORRIS MUSKAT
Gulf Research & Development Co.
Pittsburgh, Pa.

PAUL TURNBULL
La Gloria Corp.
Corpus Christi, Texas

LINCOLN ELKINS
Sohio Petroleum Company
Oklahoma City, Oklahoma

ECONOMICS COMMITTEE

R. J. BRADLEY
Dallas, Texas

Vice-Chairman

PAUL SCHULTZ
Stanolind Oil & Gas Co.
Tulsa, Oklahoma

PUBLICATIONS COMMITTEE

(Serves until Oct. 15, 1950)

OWEN E. THORNTON
The Texas Co.
Houston, Texas

Vice-Chairman

J. M. BUGBEE
Shell Oil Co., Inc.
Houston, Texas

CONTENTS

FOREWORD. BY JOHN E. SHERBORNE	iii
PETROLEUM BRANCH OFFICERS AND COMMITTEE CHAIRMEN	iv
THE ANTHONY F. LUCAS FUND AND MEDAL	vii
ERRATA	viii
TECHNICAL NOTES	325
INDEX	330

PAPERS

OFFSHORE OPERATION

Outline of Weather and Wave Forecasting Techniques. By A. H. GLENN and J. E. GRAHAM	49
Gulf of Mexico Floating Drilling Tender. By C. P. BESSE and G. W. OSBORNE	87
Wave Forces Computed for a Typical Drilling Site. By PAUL L. HORRER	299

DRILLING AND PRODUCTION EQUIPMENT, METHODS AND MATERIALS

(See also *Technical Note on Cementing by Roscoe C. Clark, Jr., p. 327.*)

A Hydraulic Process for Increasing the Productivity of Wells. By J. B. CLARK	1
Semi-Automatic Power Operated Drilling Equipment. By M. E. TRUE and B. L. STONE	27
The Core Recorder. By CLARK MILLISON	33
Method of Establishing a Stabilized Back Pressure Curve for Gas Wells Producing from Reservoirs of Extremely Low Permeability. By E. R. HAYMAKER, C. W. BINCKLEY and F. R. BURGESS	71
Pilot Gas Injection—Its Conduct and Criteria for Evaluation. By LINCOLN F. ELKINS and JOHN T. COOKE	180
Factors Involved in Removal of Sulphate from Drilling Muds by Barium Carbonate. By W. E. BERGMAN, H. B. FISHER and P. G. CARPENTER	197
Bottom Hole Flow Surveys for Determination of Fluid and Gas Movements in Wells. By C. R. DALE	205
Correction of Gas Volumes for Compressibility and Temperatures. By ALBERT D. BROKAW	248
Fundamental Forces Involved in the Use of Oil Well Packers. By JACK D. WEBBER	271

ELECTRICAL LOGGING

Relationship of Drilling Mud Resistivity to Mud Filtrate Resistivity. By W. H. PATNODE	14
A Quantitative Analysis of the Electrochemical Component of the S.P. Curve. By M. R. J. WYLLIE	17
Introduction to Induction Logging and Application to Logging of Wells Drilled with Oil Base Mud. By H. G. DOLL	148
The Relation Between Electrical Resistivity and Brine Saturation in Reservoir Rocks. By H. F. DUNLAP, H. L. BILHARTZ, ELLIS SHULER and C. R. BAILEY. (See Discussions by G. E. ARCHIE, p. 324, and by M. R. J. WYLLIE and WALTER D. ROSE, p. 325)	259

RESERVOIR PERFORMANCE—FIELD STUDIES

A Study of Oil and Gas Conservation in the Pickton Field By J. R. WALSH, R. E. SIMPSON, J. W. SMITH and C. S. YUST	55
Production of Oil Under Unitization in the Wertz Dome Field, Wyoming. By E. A. SWEDENBORG	163
Reservoir Performance of a High Relief Pool. By E. P. BURTCHAELL	171
The Performance of the Ten Section Oil Field. By W. TEMPELAAR LIETZ	251

RESERVOIR ENGINEERING

Use of Permeability Distribution in Water Flood Calculations. By W. E. STILES	9
Effects of Transient Conditions in Gas Reservoirs. By D. T. MACROBERTS	36
Estimation of Reserves and Water Drive from Pressure and Production History. By E. R. BROWNSCOMBE and FRANCIS COLLINS	92
Relation Between Pressure and Recovery in Long Core Water Floods. By J. N. BRESTON and R. V. HUGHES	100
The Effect of Well Spacing and Drawdown on Recovery from Internal Gas Drive Reservoirs. By RAYMOND G. LOPER and JOHN C. CALHOUN, JR.	211
A New Compressibility Correlation for Natural Gases and Application to Estimates of Gas-in-Place. By E. B. ELFRINK, C. R. SANDBERG and T. A. POLLARD	219
Some Examples of Fluid Flow Mechanism in Limestone Reservoirs. By W. O. KELLER and R. A. MORSE	224
A Calculation of the Effect of Production Rate upon Ultimate Recovery by Solution Gas Drive. By C. C. MILLER, E. R. BROWNSCOMBE and W. F. KIESCHNICK, JR.	235
Application of the LaPlace Transformation to Flow Problems in Reservoirs. By A. F. VAN EVERDINGEN and WILLIAM HURST	305

(Continued on following page)

CAPILLARITY — PERMEABILITY

(See also *Technical Notes* by Walter Rose on pp. 325 and 329, and by Owen Thornton on p. 328)

Capillary Pressures — Their Measurement Using Mercury and the Calculation of Permeability Therefrom. By W. R. PURCELL	39
Theoretical Generalizations Leading to the Evaluation of Relative Permeability. By WALTER ROSE	111
Evaluation of Capillary Character in Petroleum Reservoir Rock. By WALTER ROSE and W. A. BRUCE	127
Experiments on the Capillary Properties of Porous Solids. By JOHN C. CALHOUN, JR. and R. C. NEWMAN	189

RESEARCH ON PHASE RELATIONSHIPS

Methane Hydrate at High Pressure. By RIKI KOBAYASHI and D. L. KATZ	66
Gas Hydrates of Carbon Dioxide — Methane Mixture. By CARL H. UNRUH and D. L. KATZ	83
Behavior of Binary, Ternary and Multicomponent Systems at States Similar to Those Encountered in Condensate Fields. By B. H. SAGE and W. N. LACEY	143
Multiple Condensed Phases in the Methane-Decane-Tetralin-Bitumen System. By J. S. BILLHEIMER, C. G. YUNDT, B. H. SAGE and W. N. LACEY	265
Multiple Condensed Phases in the Decane-Tetralin-Bitumen System. By J. S. BILLHEIMER, H. H. REAMER and B. H. SAGE	279
Multiple Condensed Phases in the N-Pentane-Tetralin-Bitumen System. By J. S. BILLHEIMER, B. H. SAGE and W. N. LACEY	283

RESERVOIR ENGINEERING EQUIPMENT

An Electrical Computer for Solving Phase Equilibrium Problems. By MORRIS MUSKAT and J. M. McDOWELL	291
--	-----

TECHNICAL NOTES

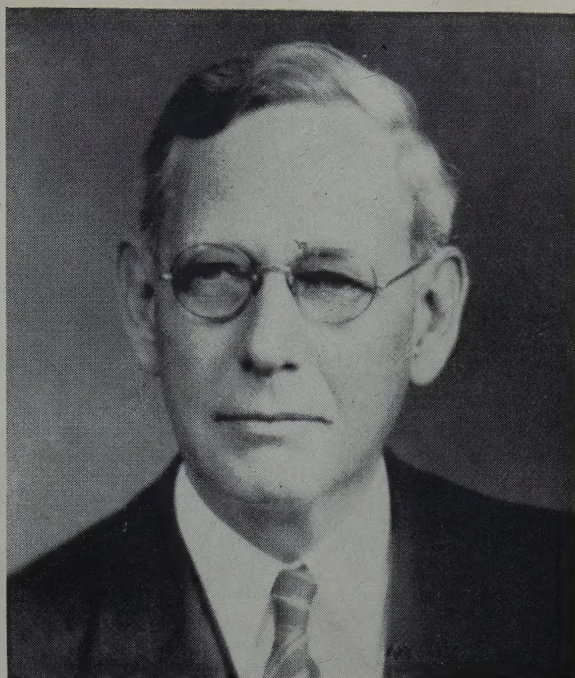
On the Application of the Capillary Pressure Method for the Determination of Oil Recovery. By WALTER ROSE	325
On Well Cementing at Low Temperatures. By ROSCOE C. CLARK, JR.	327
On the Valuation of Relative Permeability. By OWEN THORNTON	328
On the Theoretical Description of Wetting Liquid Relative Permeability Data. By WALTER ROSE	329

Papers published in the *Journal of Petroleum Technology* in 1949, but not in the Transactions Section of the *Journal*, are referred to in INDEX, page 330.

WILLIAM EMBRY WRATHER

Lucas Medalist, 1950

"For his untiring leadership in guiding and developing the science of petroleum geology, for reducing this science to effective application in practice, and for the inspiration he has given to others in the profession by his dedication to public service."



THE ANTHONY F. LUCAS FUND AND MEDAL

In 1936 the Institute established the Anthony F. Lucas Gold Medal, to be awarded from time to time "for distinguished achievement in improving the technique and practice of finding and producing petroleum." These awards are sponsored by the Petroleum Branch.

Captain Lucas was a pioneer in the oil industry, one of the early wildcatters and a leading mining and petroleum engineer. He was famous as the discoverer of Spindletop. He became a member of the Institute in 1895 and in 1913 was the first Chairman of the Petroleum and Gas Committee of the Institute, the forerunner of the present Petroleum Branch. He also headed the Committee in 1914, 1917 and 1918.

MEDALS AWARDED

J. EDGAR PEW, February 1937
HENRY L. DOHERTY, February 1938
E. DEGOLYER, February 1940
CONRAD (posthumously) and MARCEL SCHLUMBERGER, February 1941
JOHN ROBERT SUMAN, February 1943
CHARLES VAN ORMER MILLIKAN, February 1944
JAMES OGIER LEWIS, 1946
WILLIAM NOBLE LACEY, 1947
WALLACE EVERETTE PRATT, 1948
WILLIAM EMBRY WRATHER, 1950

COMMITTEE ON AWARD

HERBERT HOOVER, JR., *Chairman*

Until Feb. 1950

HERBERT HOOVER, JR.
JAMES O. LEWIS
H. H. POWER

Until Feb. 1951

HERBERT F. BEARDMORE
W. N. LACEY
THEODORE E. SWIGART

Until Feb. 1952

A. R. DENISON
M. GORDON GULLEY
HOWARD C. PYLE

Until Feb. 1953

J. E. BRANTLY
FRED M. NELSON
WALLACE E. PRATT

Members Ex-officiis

C. W. TOMLINSON
President AAPG

W. R. BOYD, JR.
President API

L. E. YOUNG
President AIME

JAMES BOYD
• Director, B. of M.

E R R A T A

Page 34 The entire caption opposite the middle chart, including chart number, applies to the bottom chart, and vice versa.

The following data applies to Chart 2 (Bottom Chart) :

<i>Depth</i>	<i>Recorded</i>	<i>Not Recorded</i>
3920-21'	1'	0
21-22'	0	1'
22-23'	1'	0
23-24'	1'	0
24-25'	2"	10"
25-26'	1'	0
26-27'	1'	0
27-28'	5"	7"
28-29'	6"	6"
29-30'	4"	6"
30-31'	0	1'
31-3931'-9"	0	9"
11'-9"	6'-5"	5'-4"

Page 94 Table II, footnotes c and d:

For δ substitute σ

For δ^2 substitute σ^2

Page 96 Table III:

For: "From standard deviation 13.1% 25.0%, substitute

"From average deviation 13.1% 25.0%"

Page 141 Table III, line 13 in column headed: K Permeability (md)

For 1.75×1^4 substitute 1.75×10^4

A HYDRAULIC PROCESS FOR INCREASING THE PRODUCTIVITY OF WELLS

J. B. CLARK, MEMBER AIME, STANOLIND OIL & GAS CO., TULSA, OKLA.

ABSTRACT

The oil industry has long recognized the need for increasing well productivity. To meet this need, a process is being developed whereby the producing formation permeability is increased by hydraulically fracturing the formation.

The "Hydrafrac" process, as it is now being used, consists of two steps: (1) injecting a viscous liquid containing a granular material, such as sand for a propping agent, under high hydraulic pressure to fracture the formation; (2) causing the viscous liquid to change from a high to a low viscosity so that it may be readily displaced from the formation.

To date the process has been used in 32 jobs on 23 wells in 7 fields, resulting in a sustained increase in production in 11 wells.

INTRODUCTION

Need For Process

Although explosives, acidizing, and other methods have long been used, there still exists a need for artificial means of improving the productive ability of oil and gas wells, particularly for wells which produce from formations which do not react readily with acids. This paper discusses the development of a hydraulic fracturing process, "Hydrafrac", which shows distinct promise of increasing production rates from wells producing from any type of formation. The method is also considered applicable to gas and water injection wells, wells used for solution mining of salts and, with some modification, to water wells and sulphur wells.

Requirements of Process

In considering such a possible process, it appeared that certain requirements must be met. Some of these are as follows:

A. The hydraulic fluid selected must be sufficiently viscous that it can be

injected into the well at pressure high enough to cause fracturing.

- B. The hydraulic fluid should carry in suspension a propping agent, such as sand, so that once a fracture is formed, it will be prevented from closing off and the fracture created will remain to serve as a flow channel for oil and gas.
- C. The fluid should be an oily one rather than a water-base fluid, because the latter would be harmful to many formations.
- D. After the fracture is made, it is essential that the fracturing fluid be thin enough to flow back out of the well and not stay in place and plug the crack which it has formed.
- E. Sufficient pump capacity must be available to inject the fluid faster than it will leak away into the porous rock formation.
- F. In many instances, formation packers must be used to confine the fracture to the desired level, and to obtain the advantages of multiple fracturing.

Development of Process

As a necessary step in the development of this process, it was deemed advisable to determine if the Hydrafrac fluids were actually fracturing the formation or whether these special fluids were merely leaking away into the surrounding formation. To determine this, a shallow well, 15 feet deep, was drilled into a hard sandstone. Casing was set, the plug drilled, and the well deepened in the conventional manner. A fracturing fluid dyed a bright red was used to break down the formation. Sand mixed with distinctively colored solids was injected into the well with the fracturing fluid to prop open any fracture made in the formation. A simulated gel breaker solution dyed a bright blue was then pumped into the well to determine if the gel breaker would follow the first solution.

The results are shown in Figure 1. It was noted that a fracture was formed about the well bore, that the propping

agent was transported back into the break, and that the breaker solution did actually follow the fracturing gel out into the fracture.

While it is realized that this shallow well test is probably not exactly equivalent to a deep test, the results were interpreted as being a definite indication of what happens down the hole during a Hydrafrac job.

Of interest in this connection is an investigation reported by S. T. Yuster and J. C. Calhoun, Jr.¹ This study, reported after the Hydrafrac work was under way, presents some excellent field data supporting the theory of fracturing a formation with hydraulic pressure.

METHOD

Steps of Hydrafrac Process

Figure 2 shows a simplified cross-sectional view of a well treated by one version of the process. The first step, formation breakdown, is done with a viscous fluid, usually consisting of an oil such as crude oil or gasoline, to which has been added a bodying agent. Due to availability and price, war-surplus Napalm has been used in the majority of experiments to date. Napalm is the soap which was used in the war to make "jellied gasoline". The next step consists of breaking down the viscosity of the gel by injecting a gel-breaker solution and then after several hours, putting the well back on production. Figure 3 shows diagrammatically, a typical field hookup. The oil or gasoline is unloaded into the 10 bbl. tank shown on the left rear of the truck. This base fluid is picked up by the mixing pump and pumped through the jet mixer, where the granular soap is added. Next it goes into a small mixing tub, from which the high-pressure pump takes suction. The solution is then pumped into the well. The breaker solution is then taken from an extra tank and is displaced into the well immediately following the gel. When required, additional trucks may

¹References are at the end of the paper.

Manuscript received at office of the Division August 17, 1948 (preliminary) and September 30, 1948 (final). Presented at Petroleum Division Fall Meeting, Dallas, Texas, October 4-6, 1948.

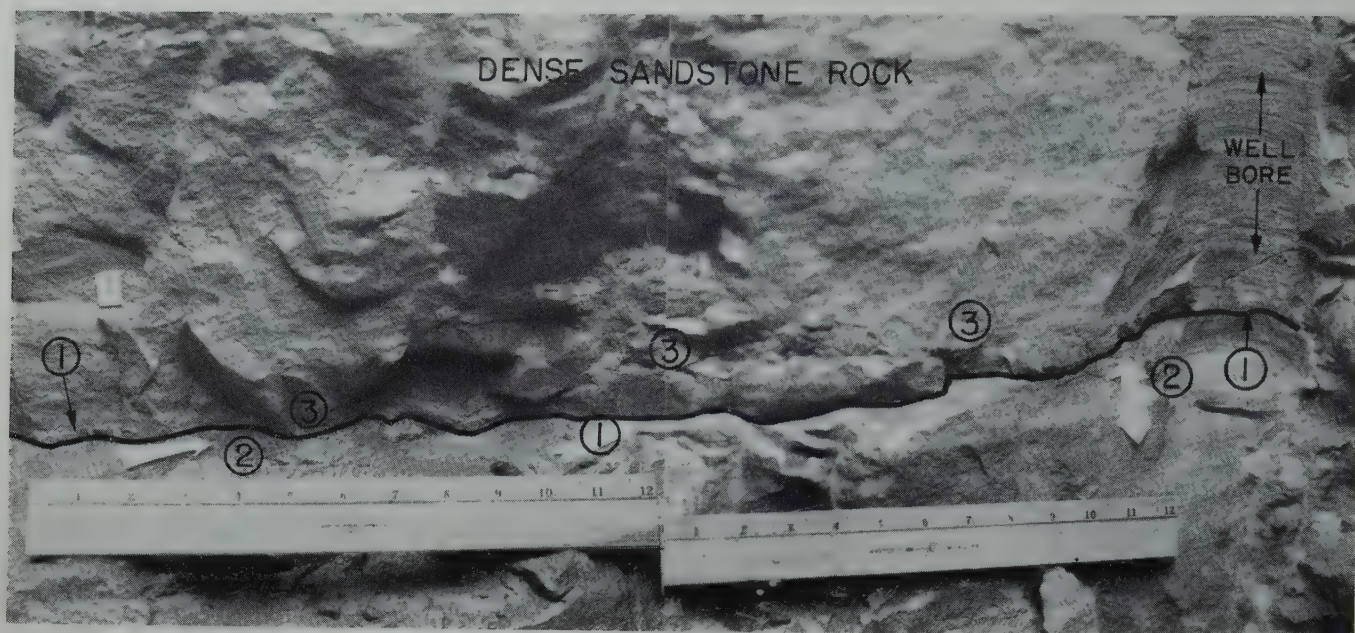


FIG. 1 — SHALLOW WELL HYDRAFRAC JOB, SHOWING (1) FORMATION FRACTURE CONTAINING FRACTURING LIQUID (2) EXPOSED FORMATION PROPPING AGENT AND (3) ROCK ADJACENT TO THE FRACTURE PARTIALLY SATURATED WITH SIMULATED GEL BREAKER SOLUTION.

be connected to the well so as to pump the fluids at a faster rate.

Planning the Field Job

The planning of a Hydrafrac job requires detailed consideration of the individual well conditions. Selection of the pumps and of the kind and amount of hydraulic fluid, for example, depends upon the thickness and permeability of exposed producing formation; the bottom hole formation pressure; the well depth; the pipe size and condition; and upon the weight, strength, and compressibility of the overburden.

Individual items that must be considered in the planning, and the method of meeting the detailed requirements for the fracturing fluid and equipment are discussed in detail below, under the corresponding headings of hydraulic fluid requirements, pump requirements, and packer requirements.

Hydraulic Fluid Requirements

The usual hydraulic fluid requirement is for an oil phase material with viscosity between 50 and 150 centipoises or higher, depending on the individual job. It has been found that Napalm soap and similar soaps provide the desired characteristics. Napalm can be added to gasoline, kerosene or other refined petroleum cuts to produce gels having any desired viscosity up to considerably over 300 centipoises.

Hydraulic Base Fluids: The ideal fluid should be an oily one rather than a water base fluid, to avoid decreasing the permeability of the formation to oil or gas. This requirement is met by the Napalm gel being used. Water base fluids, however, would be

advantageous in treating water wells, or water injection wells used in either the oil industry or industries where water is used in solution mining of salts, and in the Frasch process of mining sulphur. There is also some reason to believe that a water base fluid could be used successfully in oil or gas wells. In other words, it is entirely possible that the benefits derived from hydraulically fracturing the formation may be great enough to overcome the decrease in permeability caused by water wetting of the oil or gas sand. It is known, for example, that limestone reservoirs can be acidized with an acid solution that is as high as 80 or 90 per cent water, with a resulting increase

in well productivity. Future work with this process may indicate that it is more economical to use a water base for the hydraulic fracturing fluids than the more expensive gasoline and crude oil base fluids, particularly in formations not appreciably contaminated with argillaceous materials.

Sand Carrying Capacity of the Fluid: It is often desirable that the hydraulic fluid should carry in suspension a sufficient amount of strong granular material such as sand to be used as a propping agent to keep the fracture from closing off after release of pressure. The high viscosity of the Napalm gels makes them well suited to transport such material.

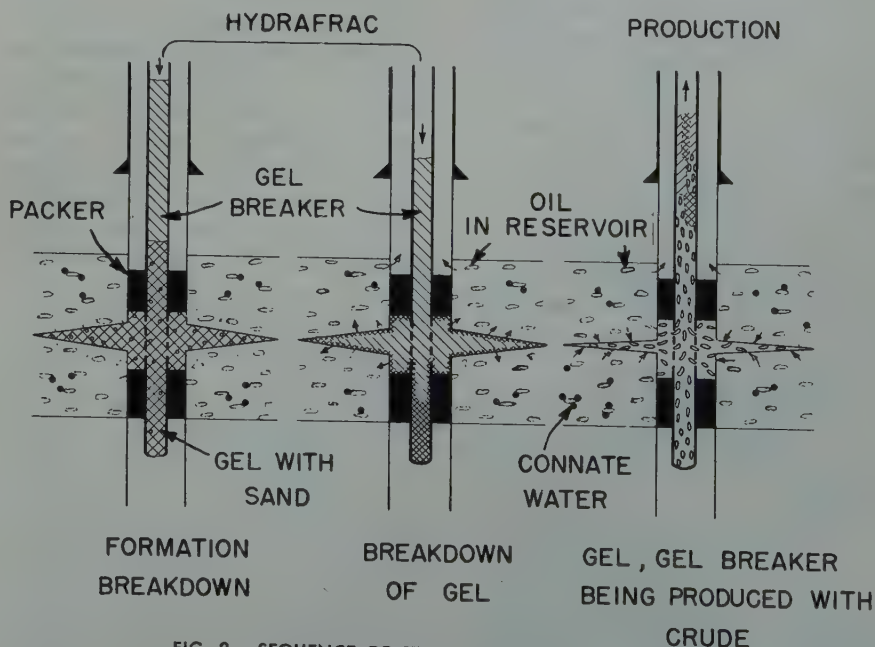


FIG. 2 — SEQUENCE OF STEPS IN HYDRAFRAC PROCESS.

Breaking of the Fracturing Fluid Viscosity: After the fracture is made, the fracturing fluid must be thin enough to flow back out of the well. The Napalm gels have the advantage of being relatively unstable, so that the viscosity of the solution will revert to approximately that of the base oil after the fracture is formed.

A further advantage of the Napalm gel is that its time of reversion to a sol is controllable within definite limits. For example, it has been found that ½% to 1% of water added to a Napalm-gasoline gel will cause reversion to a sol within 8 to 24 hours, which gives ample time for performing the Hydra-frac job. Napalm-gasoline gels will revert to sols within an hour or two if they are in quiescent contact with either salt water or many types of crudes. Furthermore, it is also possible to use solutions which will break these gels in a few minutes under quiescent contact conditions. One example is a 2% solution of petroleum sulphonates in gasoline or crude oil. This allows one to follow the Napalm gel with a second solution to insure its more rapid reversion to the sol condition.

Pump Requirements

Field experience has shown that the successful Hydrafrac treatment requires a definite fracturing of the formation, as indicated by a decrease in injection pressure; this decrease in pressure is clearly shown on several of the charts presented later.

Starting with well depth, fluid viscosity, formation thickness and permeability, and bottom hole pressure, it is possible to compute with fair accuracy, by an empirical method, the pump rate necessary to fracture a formation and to extend the fracture after it is made. It is also possible to determine the necessary fluid viscosity to fracture and to extend the fracture in the formation with a given pump rate.

Table 1 compares calculated breakdown pressures with those observed in the field. A comparison of the data presented in this table indicates a close agreement between the two figures.

Table 2 illustrates typical results of such computations. It is apparent from this table that, in formations of normal permeability, it is impossible to employ a fluid of high penetrating ability, such as the usual low-viscosity crude oil, for fracturing or extending the fracture. On sands such as in the East Texas Field, it would require a

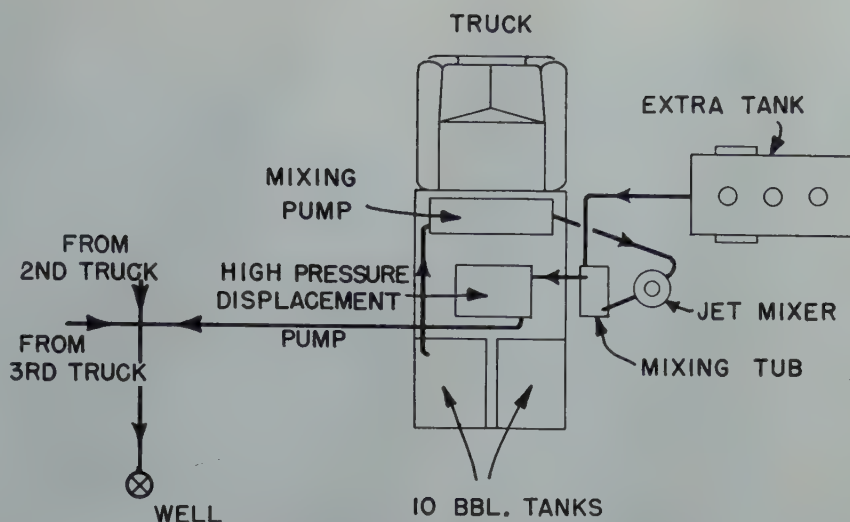


FIG. 3 — WELL HOOK-UP USING SERVICE COMPANY EQUIPMENT

TABLE 1

Calculated vs. Actual Formation Breakdown Pressures

Field	Well	Bottom hole Pressure (psi)	
		Calculated	Actual
East Texas.....	GA	3,000	3,350
Rangely, Colorado.....	EF	4,800	4,900
Hugoton, Kansas.....	AA	2,500	2,000
East Sasakwa, Oklahoma.....	FA	2,600	2,400
Frannie, Wyoming.....	BB	2,700	2,750

TABLE 2

Pump Rate to Fracture Hydraulically

	East Sasakwa Field Booth Sand	Hugoton Field Ft. Riley Lime	East Texas Field Woodbine Sand
Amount of open hole.....	35 ft.	35 ft.	20 ft.
Average formation permeability.....	150 md	13 md	2,000 md
Bbl/min to fracture.....			
Crude oil—5 centipoises.....	2	.13	21
Gel—100 centipoises.....	0.1	.007	1
Bbl/min to extend fracture to 50 ft. radius.....			
Crude oil—5 centipoises.....	11	1	213
Gel—100 centipoises.....	0.6	0.05	10.7
Pressure to fracture.....	2,100* 1,250**	1,700* 900**	2,900* 1,700**
Pressure to extend fracture.....	1,700* 850**	1,350* 550**	2,600* 1,400**

*Bottom hole pressure (psi)

**Surface pressure (psi)

crude oil injection rate of 21 bbl/min at approximately 2,000 psi in order to fracture the formation, which is beyond practical limits, since the largest portable oilfield pumps deliver only about 3 bbl/min at this pressure. However, it is obvious from Table 2 that by using a higher viscosity material such as a 100 centipoise gel, the pump requirements are dropped to within practical limits both for fracturing and for extending the fracture.

Packer Requirements

In wells where the exposed sand section is quite thick, special precautions must be taken so that the hydraulic fracturing operation can be performed at more than one depth. Ordinarily, the formation will fracture but once, and the relative increase in production due to this single fracture might be negli-

gible in a well having a large amount of productive sand thickness. To obtain the benefits of multiple fracturing, it is necessary to set special formation packers against the wall of the hole so as to isolate sections of a few feet in thickness before applying the Hydra-frac process. This technique is also important where it is necessary to prevent the fracturing fluids from entering non-productive formations which may alternate with the producing zones exposed to the well. Packers are also required in some instances to keep the high pressures of the process from injuring pipe. Inflatable packers have been found best for this work, but due to the fact that such packers are still in the development stage, considerable mechanical difficulty has been experienced with them.

Hazards

The Hydrafrac process is accompanied by a considerable hazard to personnel. The materials usually used are inflammable and explosive, and this, together with the use of internal combustion engines, makes this process rather hazardous. It is believed, however, by exercising due caution such as covering mixing tubs and piping off engine exhausts that this process need not be more hazardous than the handling of any other inflammable liquid. The treating solutions have not ignited on any of the jobs done to date.

FIELD RESULTS

Wells Showing Sustained Increases in Production

The experimental application of the Hydrafrac process to oil and gas wells has resulted in sustained and significant increases in productivity on 11 wells out of the 23 in which it has been tried. A compilation of some of the key data obtained on these wells is shown in Table 3.

Six of these 11 successes are gas wells in the Hugoton Field; in one instance, a combination Hydrafrac-acid job was done, resulting in increasing deliverability from 53 to 439 MCF per day; an increase from 53 to 322 MCF per day was the result of the Hydrafrac treatment, with a further increase to 439 MCF per day being the result of the subsequent acid job. On a Hydrafrac treated well, the deliverability was increased from 0 to 258 MCF per day, where the average of the offset wells completed by acidization indicated an increase in deliverability from 0 to 230 MCF per day. It is not possible at this time to make a complete evaluation of the advantages or disadvantages of a Hydrafrac-acid job or of a Hydrafrac job, over an acid job alone, but a program of comparison is in progress which will involve a sufficient number of wells to arrive at a definite answer.

A much stronger case for the economic possibilities of the process is found in the five oil wells in which Hydrafrac has resulted in sustained production increases. These are as follows:

Frannie Field, Wyoming: Well BB increased from 60 to approximately 160 bbl/day and the Well BC from 60 to 72 bbl/day as the result of Hydrafrac treatment; both these increases have been sustained for over a year.

East Sasakwa Field, Oklahoma: Well FA in this field, which was producing no oil and was to be abandoned, has

TABLE 3
Results of Hydrafrac Field Tests

Field, Well	Formation Breakdown	Sand Injection	Production			Percent Increase
			Before	After	Increase	
Hugoton (Gas) Field, Kansas (A)						
Well AA.....	Yes	No	769 MCF	1015 MCF	246 MCF	32*
Well AB†.....	Yes	Yes	53	322	269	508
Well AC†.....	Yes	Yes	0	258	258	Infinite
Well AD†.....	Yes	Yes	0	322	322	Infinite
Well AE†.....	Yes	Yes	0	**	—	—
Well AF†.....	Yes	Yes	0	**	—	—
Frannie, Wyoming (B)						
Well BA.....	Yes	Yes	27 BOPD	27 BOPD	0 BOPD	0
Well BB.....	Yes	Yes	60	160	100	167
Well BC.....	Yes	No	60	72	12	20
Well BD.....	Yes	No	65	65	0	0
Elk Basin, Wyoming (C)						
Well CA.....	No	Yes	0 BOPD	0 BOPD	0 BOPD	0
Winkelman Dome, Wyoming (D)						
Well DA.....	No	Yes	91 BOPD	91 BOPD	0 BOPD	0
Rangely, Colorado (E)						
Well EA.....	No	Yes	100 BOPD	65 BOPD	-35 BOPD	- 35
Well EB.....	No	Yes	100	100	0	0
Well EC.....	No	Yes	40	30	-10	- 25
Well ED.....	No	Yes	106	100	- 6	- 6
Well EE.....	No	Yes	25	25	0	0
Well EF.....	Yes	Yes	75	140	65	87
East Sasakwa, Oklahoma (F)						
Well FA.....	Yes	Yes	0 BPOD	6 BPOD	6 BOPD	Infinite
East Texas (G)						
Well GA.....	Yes	Yes	0 BPOD	50 BPOD	50 BOPD	Infinite
Well GB.....	No	Yes	4	4	0	0
Well GC.....	Yes	Yes	8.25	8.25	0	0
Well GD.....	Yes	Yes	3.5	3.5	0	0

*Combined effect of Hydrafrac and acid.

†One of four producing zones treated.

**No post-Hydrafrac production this date.

MCF—1000 cubic feet per day.

BOPD—Barrels of oil per day.

produced from five to six barrels per day for nine months since Hydrafrac treatment.

East Texas Field: Well GA which had produced no oil for two years produced more than 50 barrels of oil per day for several weeks while under special test after a Hydrafrac treatment, before being returned to its 20 barrels per day allowable rate. This well has been producing at the 20 barrels per day rate for five months since then, with periodic productivity

tests to determine the maximum potential of the well. The last special test of this type indicated a well potential of 61 barrels of oil per day.

Rangely Field, Colorado: Well EF which was producing approximately 75 barrels of oil per day before treatment, is now producing approximately 140 barrels of oil per day as the result of Hydrafrac treatments.

Figures 4, 5, 6, and 7 show for four of the above wells, the production curve before and after treatment, and the

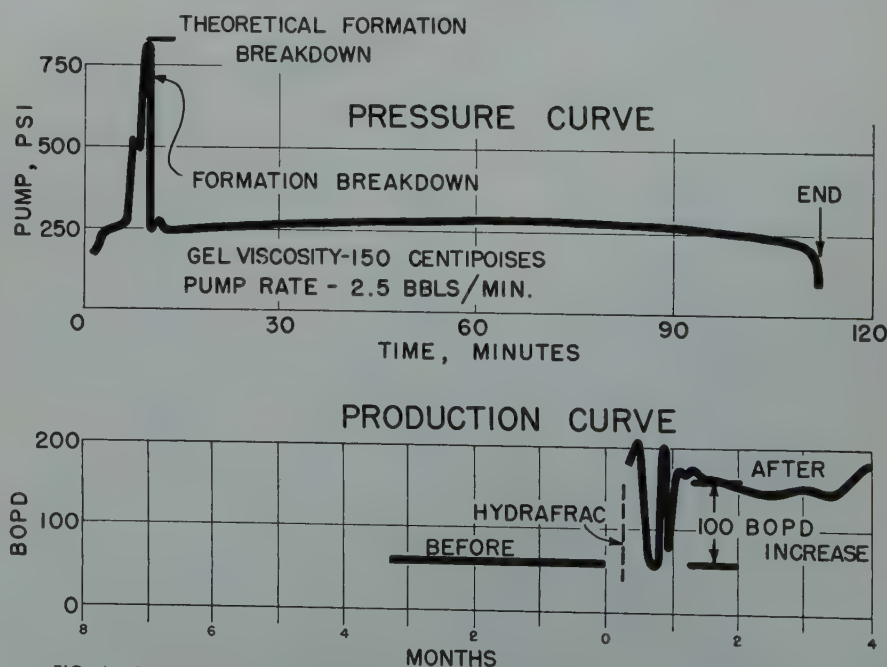


FIG. 4—PRESSURE AND PRODUCTION CURVES FOR WELL BB, FRANNIE FIELD, WYO.

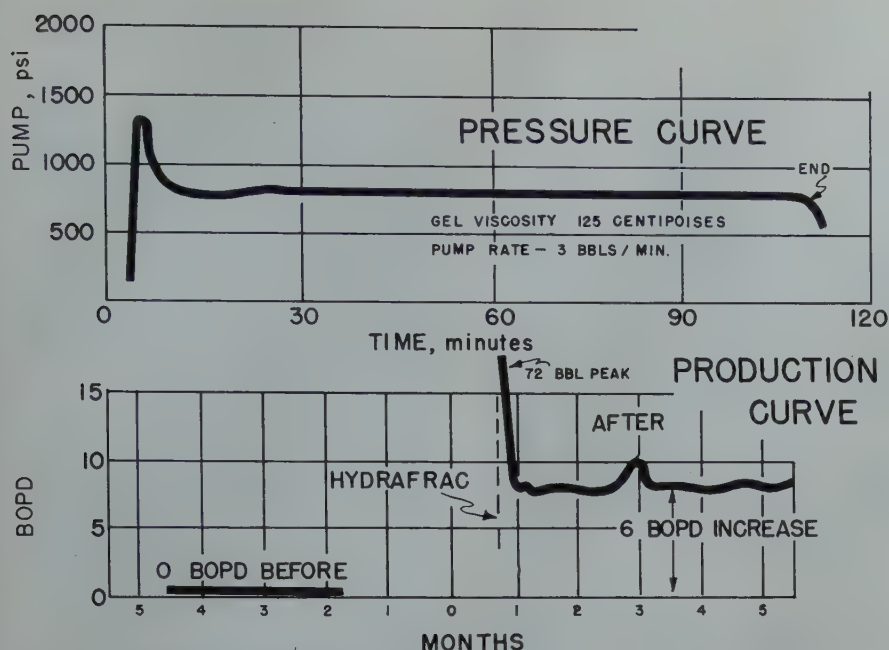


FIG. 5—PRESSURE AND PRODUCTION CURVES FOR WELL FA, EAST SASAKWA FIELD, OKLA.

pressure curve taken during the Hydrafrac job showing the formation breakdown.

The effect on the permeability of selectively fracturing the producing formation of Well EF, Rangely Field, Colorado, is shown in Figure 8 by a comparison of permeability profiles run before and after the Hydrafrac operation. The location of each Hydrafrac job is shown between the two permeability profiles. An effort was made to have the same injection pressure for both permeability profile tests, but pump capacity prevented obtaining as high an injection pressure after Hydrafrac as was obtained before. Some of the permeable zones indicated on the "Before Hydrafrac Permeability Profile" are not evident on the "After Hydrafrac Permeability Profile" due to the lower injection pressure. However, the increase in the permeability of those sections treated as the result of hydraulically fracturing the formation is clearly evident in this figure.

Figure 9 shows the production after Hydrafrac for these five oil wells: successfully treated by this process. It will be noted in all instances that a sustained increase in production was accomplished by Hydrafrac.

Well Showing No Sustained Increase in Production

No increase in production was obtained in 12 of the 23 wells treated in the preliminary experimental program. Considering the many variables involved, and the imperfections of present special packers, the proportion of failures at this stage of development is

not discouraging. Both theory and field experience show that it is necessary to obtain a definite formation breakdown in order for the process to function satisfactorily. Figure 10 shows the pressure curve and the production curve of Well EC, Rangely Field, Colorado, in which the formation did not breakdown and, as expected, no increase in production was obtained.

A comparison of Well EF and Well EC in the Rangely, Colorado Field illustrates the need for the proper isolation of the desired zones to be treated. It was possible on Well EF with suitable formation packers to confine the Hydrafrac fluids to the desired zones thus fracturing the pay formation in the most prolific sections. However, on

Well EC where the Hydrafrac operations were attempted without the benefit of packers, the hydraulic fracturing fluid was dispersed over the entire area of the open hole with a resulting failure to increase well production.

Production data on the 23 wells treated by Hydrafrac are shown in Table 3. It may be noted that the productivity of three of the wells treated in the Rangely Field seem to have been slightly decreased by the Hydrafrac treatment. This decrease in well production after treatment is believed to be a result of either well workovers before treatment, or normal production decline during the well testing period. For example, the pay zone in Well EA was charged with crude oil before Hydrafrac treatment during a cleanout of the hole while using crude oil as a drilling fluid, and sufficient time was not allowed for the well production to level off before the well test taken before Hydrafrac treatment. The decrease in production of Well ED after treatment represents the normal production decline for this well. Part of the production decrease of Well EC may be attributed to normal production decline; however, trouble occurred which it is believed accounted for most of this decrease.

Predictability of Results

If the engineering factors surrounding a proposed Hydrafrac job are known, experience has shown that correct prediction of success or failure of the job is usually possible. A careful review of the jobs done to date leads to the conclusion that, even with due regard to the fact that "hindsight is clearer than

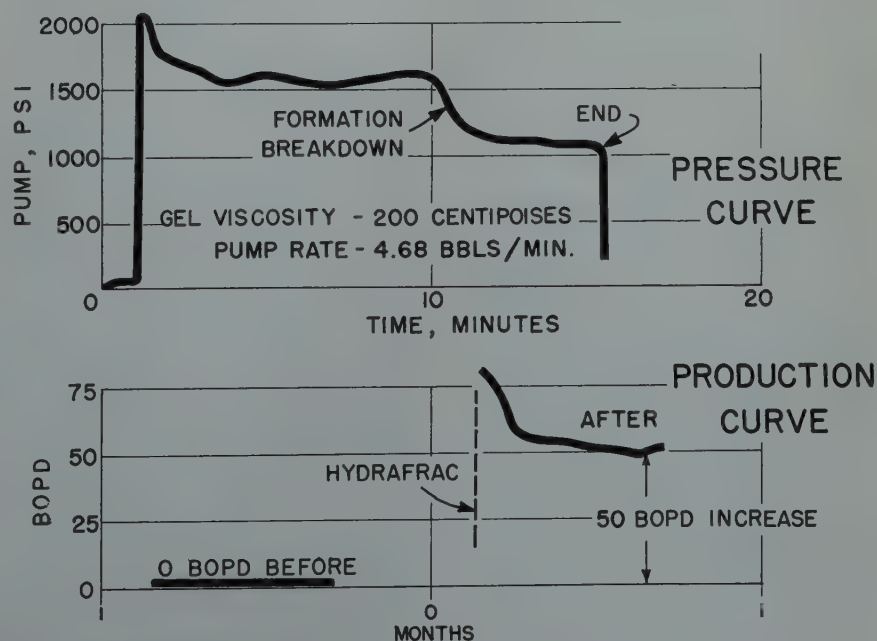


FIG. 6—PRESSURE AND PRODUCTION CURVES FOR WELL GA, EAST TEXAS FIELD

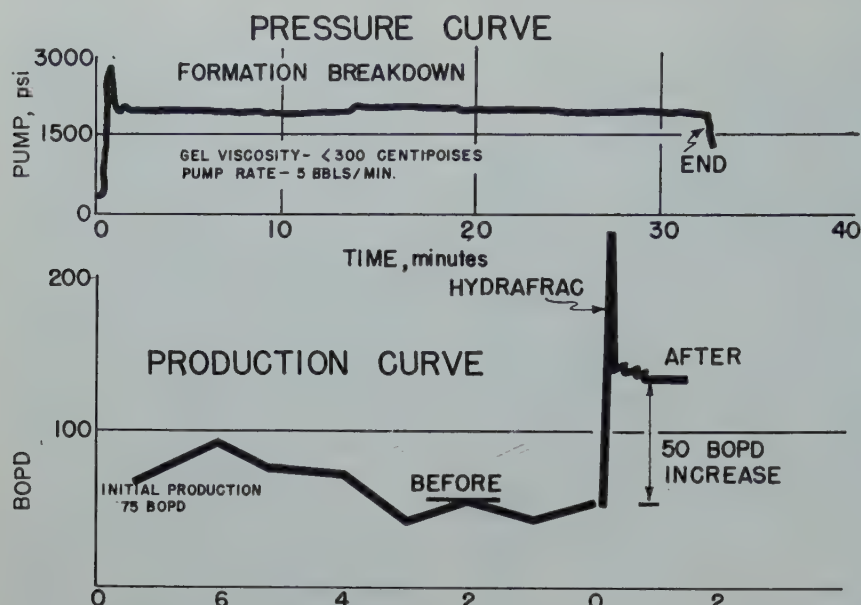


FIG. 7 — PRESSURE AND PRODUCTION CURVES FOR WELL EF, RANGELY FIELD, COLO

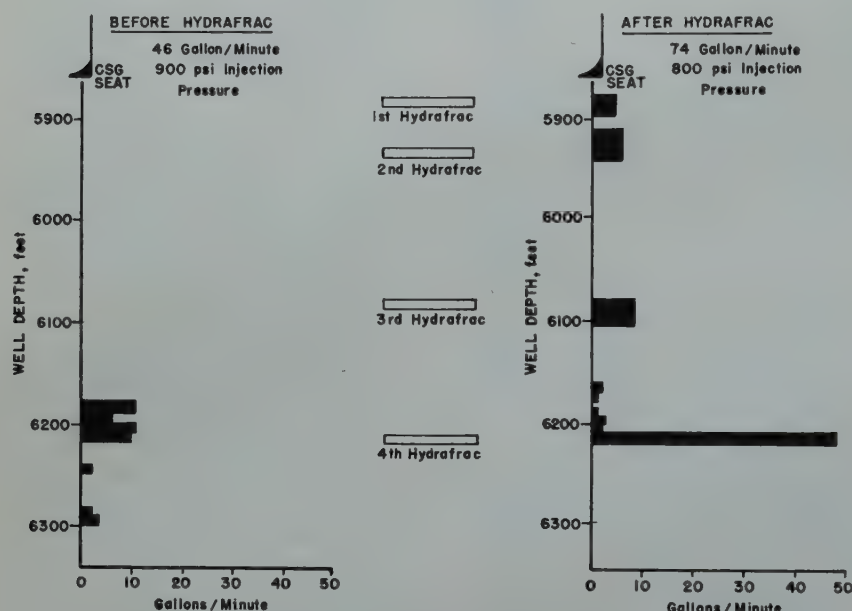


FIG. 8 — PERMEABILITY PROFILES INDICATING RESULTS OF HYDRAFRAC TREATMENT, WELL EF, RANGELY FIELD, COLO.

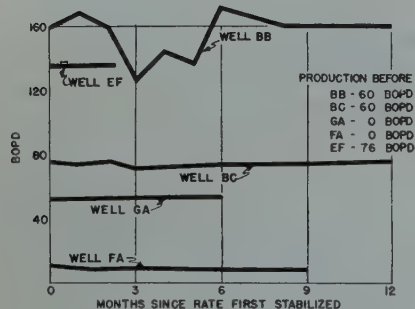


FIG. 9 — PRODUCTION AFTER SUCCESSFUL HYDRAFRAC TREATMENT.

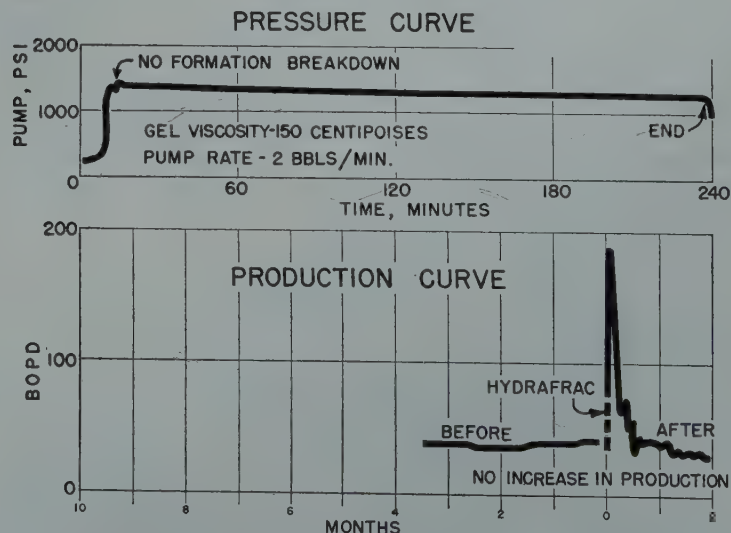


FIG. 10 — PRESSURE AND PRODUCTION CURVES, WELL EC, RANGELY FIELD, COLO.

foresight," it would have been possible to predict correctly at least 75% of the failures, and 95% of the successes, had all of the present field experience been available before each of the jobs done. As a matter of fact, many of the failures were predicted as such, and the jobs purposely done in the face of unfavorable well conditions in order to obtain research data. Incidentally, one of the treatments done under such circumstances (Well FA) was successful in spite of predicted failure.

Cost

When put into routine commercial use, the cost should be not much more than the cost of an acid job of corresponding gallonage. Where crude oil from the lease can be used as the base fluid in the Hydrafrac process, it is quite probable that the cost will be less than that for acidizing.

It is significant that the value of the additional oil and gas produced to date through the benefits of this process has already exceeded the combined cost of research, development, and all field tests.

ACKNOWLEDGMENTS

Acknowledgment is due Messrs. R. F. Farris, C. R. Fast, G. C. Howard, J. A. Stinson and other members of the staff of the Stanolind Oil and Gas Company's Research and Producing Departments for their part in the development of this process. Appreciation is expressed to the Management of Stanolind Oil and Gas Company for permission to publish this paper.

REFERENCES

1. Yuster, S. T., and Calhoun, J. C., Jr.: Pressure Parting of Formations in Water Flood Operations. *The Oil Weekly* (March 12 and March 19, 1945).

DISCUSSION

☆

By Wm. D. Owsley, Technical Adviser,
Halliburton Oil Well Cementing Co.,
Duncan, Okla.:

I wish to highly commend Mr. Clark and his associates for this important contribution to oil production. Even at this early date in the development of this process, it is apparent that Hydrafrac can be of great value to oil producers, especially in view of the present high price of crude oil, attended by scarcity of casing and heavy increases in drilling costs. In spite of this statement, this process should not be regarded as a cure-all for any and every well.

Considerable thought has been given to the hazards attendant to the use of the Hydrafrac process. These hazards to personnel and equipment must be recognized; however, they can be minimized by simple and easily applied safety precautions. The mixing equipment can easily be arranged to prevent splash over. Precautions must be taken against leakage on all lines during the course of the job. It is suggested that this process be performed during daylight hours to reduce hazards attendant to accumulation of vapors during the night. Diesel engine powered pumping equipment offers an advantage over gasoline engine equipment in the elimination of possible fire hazards. Precautions can be taken in piping away exhaust stack gases and cooling of manifolding to prevent possible explosion.

The pumping of crude oil, diesel fuel, or gasoline, under high pressures is not considered dangerous, provided leakage in the system is prevented. There will be no occurrence of diesel effect to give explosion within the pumps or pipes unless large volumes of air be trapped within the system. Even then an intimate mixture of the vapors with air and a rapid increase in pressure to produce heat would be necessary in order to produce an explosion.

The problem of packers for segregation of short sections of open hole does offer several difficulties, and it appears that a packer design different than anything now known to be in existence is necessary. It is assumed that Hydrafrac can be applied to wells which have been gun perforated for production, in which case, the packer problem is much less difficult, since packers are already in existence which will adequately

handle this condition.

There has been some thought given to difficulty with reciprocating pumps in the handling of a sand-laden fluid of the nature described. Experience in the past in handling sand of large granular size through reciprocating pumps has not been good; however, it appears that the use of thickened oil phase agents eliminates this problem.

In the use of this process, it is recommended that surface piping and manifolding to the well head be kept as simple and direct as is practical to offset line losses during rapid pumping. This will greatly assist in obtaining high injection rates into the well itself without excessive pump pressure.

While this paper presents Hydrafrac in its application to wells which have been partially depleted, it would appear that in many cases of new wells initial potential might be considerably improved by application of this process. It is believed that with proper study of all data on any well which is being considered for the use of this process, its correct application should result in a high percentage of success.

☆

By Paul E. Fitzgerald, Dowell Incorporated, Tulsa, Okla.:

Mr. Clark has presented a paper on a subject which has been discussed by petroleum engineers for years. Most engineers realize that pressure parting or formation lifting probably plays an important part in many wells where fluids are injected for various reasons. The author has furnished some valuable quantitative data bearing on this interesting phenomenon.

The pressure parting phenomenon has long been recognized in well acidizing operations. In numerous cases where the formation permeability is quite low it has been observed that the initial acidizing pressure will exceed the pressure required to lift the overburden. At pressures below this critical value the formation will take substantially no fluid but when a pressure sufficiently high to part the formation has been reached it will take fluid and the rate of fluid injection can be raised with little or no increase in the injection pressure.

After the acid enters the formation a chemical reaction takes place in which a portion of the formation is actually dissolved away thus further enlarging the previously established

fracture. As the characteristics of the rock are not uniform, more rock will be dissolved by the acid in some places than in others so when the treatment is concluded the pressure parted fractures will not close but will still be open and will serve as flow channels to the well.

Mr. Clark has extended the application of the pressure parting idea by using fluids of increased viscosity and inert solid particles. These materials make the process applicable to wells having high permeability and to wells in which the producing section is not acid soluble.

☆

By C. P. Parsons, Houston, Texas:

There is considerable need for such a process.

Step 1 in the process calls for "injecting a viscous liquid, containing a propping agent, under high pressure to fracture the formation". This step is amply supported by the established practice of fracturing formations and squeezing cement and other fluids into oil sands.

Step 2 calls for "causing the viscous liquid to change from a high to a low viscosity so that it may be readily displaced from the formation". For this step there is no precedent in oil well cementing, primarily because the fluids used are viscous because of suspended solids; also because the fluids are intended to remain in the formation. Cement slurry, for instance, after injection into the fracture under high pressure increases in viscosity and changes into a plastic and finally a solid.

The second step presents the main problem in the process. The paper indicates two ways to overcome it. One way is by the use of an oil base liquid that temporarily has been made highly viscous but which will automatically revert to low viscosity after it is in place in the formation. That, of course, is the ideal answer to the problem. The other way is to follow the injection of the viscous gel with an injection of a gel-breaker. The paper does not make it clear which of the two alternatives were used in the actual field tests.

With regard to the following up with a gel-breaker, it is difficult to understand how the breaker could effectively reach out through the tightly confined thin layer of viscous gel to cause the change from high to low viscosity. It is conceivable, however, that the gel-

breaker could physically push the viscous gel ahead of it, causing the gel to spread out to a distance where the gel can no longer hold itself into a continuous ring and must disperse further in streaks, leaving openings for the gel-breaker to physically break through. The low viscosity of the breaker would permit it to come back out of the channels followed by newly released oil out of the formation. In addition, the gel-breaker, by having increased contact with the gel, would cause some of the gel to become less viscous. This would allow some of the gel to come out of the formation and thereby assist in the return of the breaker and release of oil. As to the propping agent, due to drag, it might not completely follow the viscous gel through the fracture. This could be an advantage when the gel breaker and released oil come out of the formation.

The process is a distinct contribution to the industry's important aim of increasing the productivity of oil. It is

along sound, practical lines and should be encouraged and followed up with many more field tests.

☆

Author's reply to Mr. C. P. Parsons:

Mr. Parsons in his comments discussed the breaking of the fracturing fluid viscosity. He mentioned two of the methods used and asks which of these methods were used in the field experimental work.

Three methods are currently available for breaking the viscosity of the Napalm gel, any one of which we believe will do the job. These methods are:

- (1) The unstable nature of the Napalm gel at bottom hole temperatures and pressures, in the presence of crude oil, will cause this gel to revert to sol in 8 to 24 hours.
- (2) The addition of a small amount, $\frac{1}{2}\%$ to 1%, water to the Napalm gel, plus the quiescent con-

tact of this gel with salt water, will cause it to revert to sol within an hour or two.

- (3) Napalm gels, when in quiescent contact with gel breakers such as petroleum sulphonates, will revert to sol in a few minutes.

Actually in field practices all three of these methods have been used to insure complete reversion to sol of all the Napalm gel in the well, and thus to avoid the danger of plugging of the formation with the viscous oily medium.

The action of the gel breaker in the fracture filled with a viscous gel solution may be very much as Mr. Parsons describes. It is believed, however, that the quality of the Napalm gel that causes it to revert to sol on quiescent contact with petroleum sulphonates, salt water, and some type of crude oil, is the primary reason why these gels do not plug the formation.

USE OF PERMEABILITY DISTRIBUTION IN WATER FLOOD CALCULATIONS

WM. E. STILES, MEMBER AIME, CORE LABORATORIES, DALLAS, TEXAS

ABSTRACT

A method is presented for predicting the performance of water flooding operations in depleted, or nearly depleted, petroleum reservoirs. The method makes use of permeability variations and the vertical distribution of productive capacity. From these two parameters can be calculated the produced water cut versus the oil recovery. Derivations of the mathematical analogy is shown and sample calculations and curves of prediction are presented. Comparison is made of the predicted and actual performance of a typical 5-spot in an Illinois water flood.

INTRODUCTION

The use of water as a flooding medium in both depleted and "flush" oil reservoirs is gaining greater recognition and acceptance. Many of the shallower fields, depleted by primary production, have been and are being subjected to water injection in order to obtain some part of the large volume of oil remaining after primary production. Some of the earlier water flood installation proved highly discouraging and the value of water flooding was often questioned. Many of these earlier floods were haphazardly selected and developed as little was known of the physical characteristics and contents of the producing formations. The prior evaluation of the flood performance was impossible.

During the past decade the development of the required reservoir engineering tools—core analysis, reservoir fluid analysis, electric logs, fluid flow formulae, etc.—has allowed the engineer to construct and apply the methods which are presently being used to evaluate the economic and mechanical susceptibility of a reservoir to flooding.

This discussion will present a method for taking into account the effect of

permeability variations in predicting the performance of water floods in depleted reservoirs.

PERMEABILITY AND CAPACITY DISTRIBUTION

It is generally agreed by most investigators that in a single phase system fluid will flow in a porous and permeable medium in proportion to the permeability of the medium.

Producing formations are usually highly irregular in permeability, both vertically and horizontally. However, zones of higher or lower permeability are often found to exhibit lateral continuity. Thus, while structurally comparable stringers in adjacent wells may differ several fold in permeability values, they usually bear resemblance as being part of a general continuous higher or lower permeability section. It is generally agreed that where such stratification of permeability exists, injected water sweeps first the zones of higher permeability, and it is in these zones that "break-through" first occurs in the producing well. It is a basic assumption of the presently described method that penetration of a water front follows the individual permeability variations as if such variations were continuous from input to producing well. This is admittedly not rigorously true, but can be justified as making possible a simplifying mathematical approach to an otherwise extremely complicated three dimensional flow problem.

As a basis for study of the lateral flow of fluids in formations of irregular permeability, the irregularities may be conveniently represented by a permeability distribution curve and a capacity distribution curve. In obtaining these curves, the permeability values, regardless of their structural position in the formation, are rearranged in order of decreasing permeability.

If these permeability values so arranged are plotted against the cumulative thickness, a permeability distribu-

tion curve is obtained. This curve may then be likened to a "smoothed" permeability profile of the formation.

In making comparison between different distribution curves it is convenient to state the permeabilities in terms of the ratio of the actual permeability values to the average permeability of the formation. These ratios termed "dimensionless permeabilities", are used in this paper rather than the permeabilities in terms of millidarcys.

The capacity distribution curve is a plot of the cumulative capacity (starting with the highest permeabilities) versus the cumulative thickness. The capacity and thickness are given as fractions of the total capacity and thickness. Mathematically, the capacity distribution is the intergration of the permeability distribution curve.

In practice it is convenient to first obtain the capacity distribution curve and derive from it a smoothed dimensionless permeability curve.

The method of obtaining the capacity distribution curve is illustrated in the successive column of Table 1, in which capacity and thickness are derived as fractions of their respective totals. If only a small number of permeability values are available, it is generally desirable to smooth the resultant curve. This has been done to give the capacity distribution curve shown in Figure 1.

The differentiation of the capacity distribution curve to obtain the permeability distribution curve is shown in Table 2. Here, the capacity values are read from the smoothed curve at intervals of cumulative thickness, and the increments of capacity are divided by the increments of thickness to obtain the dimensionless permeability, K' . Due to this stepwise procedure of calculation these permeability values must be plotted at the midpoints of the successive increments of thickness. The curve so obtained from these data is shown in Figure 1. The total area under the K' curve is equal to unity.

TABLE 1
Calculation of Capacity Distribution

Cumulative Thickness; Feet	h=Fraction of Cumulative Thickness	K=Permeability; Millidarcys	ΔC=Increment of Total Capacity	C=Cumulative Capacity; Fraction
1	.0345	776	.153	.153
2	.0690	454	.089	.242
3	.1034	349	.069	.311
4	.1380	308	.061	.372
5	.1724	295	.058	.430
6	.2070	282	.056	.486
7	.2414	273	.054	.540
8	.2759	262	.052	.592
9	.3103	228	.045	.637
10	.3448	187	.037	.674
11	.3793	178	.035	.709
12	.4138	161	.032	.741
13	.4483	159	.031	.772
14	.4828	148	.029	.801
15	.5172	127	.025	.826
16	.5517	109	.021	.847
17	.5862	88	.017	.864
18	.6207	87	.017	.881
19	.6552	87	.017	.898
20	.6897	77	.015	.913
21	.7241	71	.014	.927
22	.7586	62	.012	.939
23	.7931	58	.011	.950
24	.8276	54	.011	.961
25	.8621	50	.010	.971
26	.8966	47	.009	.980
27	.9310	47	.009	.989
28	.9655	35	.007	.996
29	1.0000	16	.004	1.000
		Σ 5,075		

Derivation of Water Cut and Recovery Equations

The derivation of the water cut and the recovery equations is based on two principal assumptions: (1) fluid flow is linear and (2) the distance of penetration of the flood front is proportional to permeability.

With these assumptions, a cross section of the flood front would show penetration proportional to the permeability distribution. At the time when all permeabilities greater than a given value, K' , have "broken through" to water at the producing well, a schematic diagram of the water penetration would be as shown in Figure 2.

In the diagram of Figure 2, the intake well exposed to water injection is represented by the line ab and the producing well by line cd . The rectangle $abcd$ represents the floodable volume of the formation (total acre-feet of formation times the unit water flood recovery per acre-foot).

The curve gfb represents the water front and the enclosed area $agfba$ is the permeability distribution curve. Since dimensionless permeability is used, the area under this curve is equal to unity.

$$\text{Area } abcd = X + Y + Z = 1$$

$$= \text{floodable formation} =$$

$$ab \times fe = ab \times K'$$

$$\text{Area } agfba = W + X + Y = 1$$

Since the capacity distribution curve is the integration of the permeability curve, $W + X = C = \text{capacity corresponding to the formation thickness } h$ and

permeability K' , also:

$$Y = 1 - (W + X) = 1 - C, \text{ and}$$

$$X = fe \times ac = K'h$$

Areas X and Y represent the portion of the formation from which oil has been displaced by the encroaching water. The oil recovery expressed as a fraction of the total floodable formation is then:

$$\text{Recovery} = \frac{X + Y}{X + Y + Z} = \frac{K'h + (1 - C)}{K'}$$

In the producing well, it has been assumed that all permeabilities greater

than K' are flowing only water. The capacity flowing water is therefore C , and the capacity flowing oil is $(1 - C)$.

The water and oil production rates are calculated from these capacities by including relative permeability and viscosity terms, and in the case of oil, a formation volume factor, u .

$$\text{Rate of water production} = C \left(\frac{K_{rw}}{\mu_w} \right)$$

$$\text{Rate of stock tank oil production} = (1 - C) \left(\frac{K_{ro}}{\mu_o} \right) \left(\frac{1}{u} \right)$$

$$\text{Rate of total fluid production} =$$

$$C \left(\frac{K_{rw}}{\mu_w} \right) + (1 - C) \left(\frac{K_{ro}}{\mu_o} \right) \left(\frac{1}{u} \right)$$

Thus, water cut =

$$\frac{C \left(\frac{K_{rw}}{\mu_w} \right)}{C \left(\frac{K_{rw}}{\mu_w} \right) + (1 - C) \left(\frac{K_{ro}}{\mu_o} \right) \left(\frac{1}{u} \right)}$$

$$= \frac{C \left(\frac{K_{rw}}{\mu_w} \cdot \frac{\mu_o}{K_{ro}} \cdot u \right)}{C \left(\frac{K_{rw}}{\mu_w} \cdot \frac{\mu_o}{K_{ro}} \cdot u \right) + (1 - C)}$$

Assigning the term A to

$$\left(\frac{K_{rw}}{\mu_w} \cdot \frac{\mu_o}{K_{ro}} \cdot u \right)$$

$$\text{Water Cut} = \frac{CA}{CA + (1 - C)}$$

The water cut is expressed as a fraction, the ratio of the water production rate to the total fluid production rate.

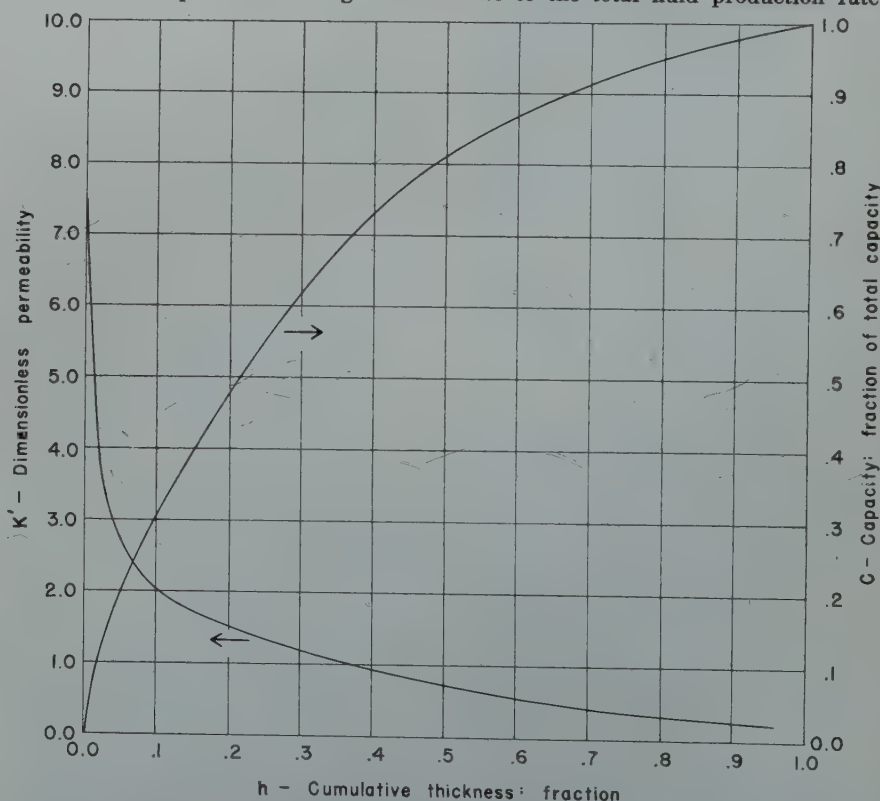


FIG. 1—PERMEABILITY AND CAPACITY DISTRIBUTION.

TABLE 2
Calculation of Permeability Distribution

h = Fraction of Cumulative Thickness	Δh = Increment of Cumulative Thickness	C = Cumulative Capacity; Fraction	ΔC = Increment of Cumulative Capacity	$K' = \frac{\Delta C}{\Delta h}$ Dimensionless Permeability	$h' =$ Average Cumulative Thickness Fraction
.01	.01	*.065	.065	6.50	.005
.02	.01	.110	.045	4.50	.015
.05	.03	.200	.090	3.00	.035
.10	.05	.308	.108	2.16	.075
.20	.10	.476	.168	1.68	.150
.30	.10	.620	.144	1.44	.250
.40	.10	.731	.111	1.11	.350
.50	.10	.812	.081	.81	.450
.60	.10	.870	.058	.58	.550
.70	.10	.917	.047	.47	.650
.80	.10	.952	.035	.35	.750
.90	.10	.980	.028	.28	.850
.95	.05	.991	.011	.22	.925
1.00	.05	1.000	.009	.18	.975

*From capacity distribution curve.

APPLICATION OF THE WATER CUT AND RECOVERY EQUATIONS

Sample calculations for recovery and water cut based on the previous permeability distribution data are shown stepwise in Tables No. 3 and 4.

In these tables water cut and recovery are calculated independently of each other, but as functions of the thickness h as a parameter.

A plot of the resultant water cut versus recovery data is shown in Figure 3.

The percentage recovery values can be converted to barrels of oil per acre foot by multiplying by the unit recovery at 100 per cent water cut and the appropriate flood coverage factor.

The unit recovery is calculated as shown in the following example:

Connate water saturation = 24 per cent of pore space.

Reservoir oil saturation (after primary depletion) = 59 per cent of pore space

Residual oil saturation after complete flushing = 21 per cent of pore space

Porosity = 19 per cent

Formation Volume Factor = 1.073 barrels/barrel

TABLE 3
Calculation of Recovery

h = Fraction of Cumulative Thickness	$K' =$ Dimensionless Permeability	$C =$ Cumulative Capacity; Fraction	$K' \cdot h$	$K' h + (1-C)$	$\frac{(K' h + (1-C))}{K'} =$ Recovery Fraction of Total Recovery
.00	*7.50	*.000	.000	1.000	.133
.01	5.32	.065	.053	.988	.186
.02	3.83	.110	.076	.966	.252
.05	2.69	.200	.135	.935	.348
.10	2.03	.308	.203	.895	.441
.20	1.55	.476	.310	.834	.538
.30	1.19	.620	.357	.737	.619
.40	.92	.731	.368	.637	.692
.50	.71	.812	.355	.543	.765
.60	.55	.870	.330	.460	.836
.70	.41	.917	.287	.370	.902
.80	.31	.952	.248	.296	.955
.90	.25	.980	.225	.245	.980
.95	.20	.991	.190	.199	.995
1.00	.00	1.000	0.000	0.000	1.000

*From permeability and capacity distribution curves.

Unit Recovery =

$$7758 (.19) \left(\frac{.59 - 1.073 (.21)}{1.073} \right) =$$

501 barrels of stock tank oil per acre foot

The total liquid saturation in this example is the sum of the 59 per cent oil saturation and the 24 per cent water saturation, or 83 per cent. The remaining 17 percent of pore space is occupied by the free gas remaining after primary depletion.

In order to increase reservoir pressure sufficiently to attain the desired production rate it is necessary to compress this gas space with injected water.

RECOVERY EQUATION

$$\text{Recovery} = \frac{X + Y}{X + Y + Z} = \frac{K' h + (1 - C)}{K'} \quad (1)$$

WATER CUT EQUATION

$$\text{Water Cut} = \frac{(W+X) \left(\frac{K_{rw}}{\mu_w} \cdot \frac{\mu_o}{K_{ro}} \cdot u \right)}{(W+X) \left(\frac{K_{rw}}{\mu_w} \cdot \frac{\mu_o}{K_{ro}} \cdot u \right) + (1 - (W+X))}$$

since $W+X = C$, and $\left(\frac{K_{rw}}{\mu_w} \cdot \frac{\mu_o}{K_{ro}} \cdot u \right) = \text{constant} = A$

$$\text{Water Cut} = \frac{C \cdot A}{C \cdot A + (1 - C)} \quad (2)$$

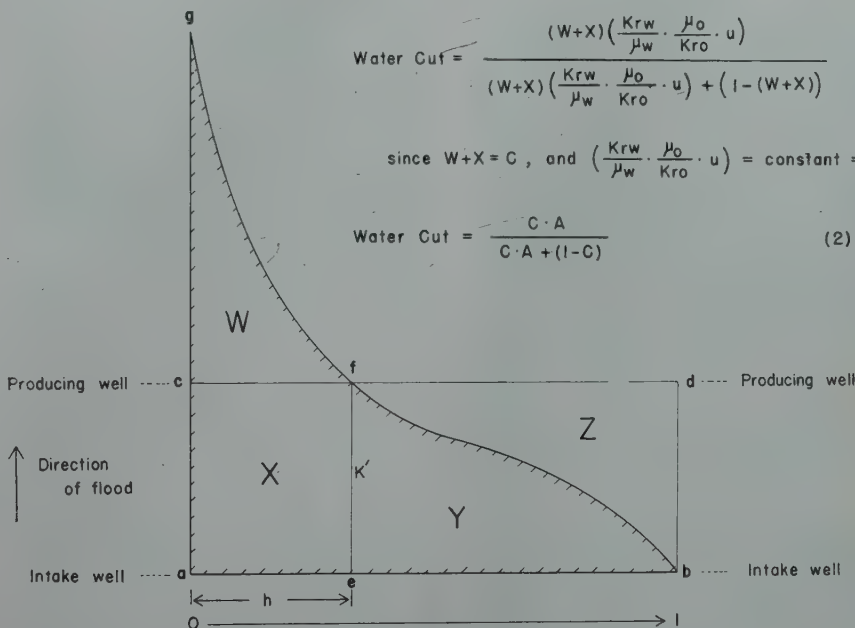


FIG. 2 — BASIC EQUATIONS AND SCHEMATIC ILLUSTRATION OF FLOOD FRONT.

Since reservoir pressure is built up as this gas is compressed, a "kick" in production rate is obtained somewhat before an amount of water equivalent to the gas space has been injected. However, for purposes of predictions the volume of water required to fill up is generally assumed equal to this gas space.

For example, using the above 17 per cent gas space, a 5-spot unit pattern containing 100 acre feet of formation and a porosity of 19 per cent or 1474 barrels per acre foot, the amount of water required for fill up is 100 (1474x.17), or 25,000 barrels. The time required at an injection rate of

100 barrels per day per 5-spot is, therefore, 250 days.

It should be noted that thus far the calculations have not included a flood coverage factor which even under the most favorable conditions may limit the actual recovery to some 70 to 90 per cent of the calculated maximum value at 100 per cent water cut. (The term "water cut", as used in the text, is intended to be synonymous with the phrase "water per cent by volume".) The flood coverage factor may be estimated from experience or electrical model studies.

After the flood coverage factor and the unit recovery to 100 per cent water cut have been determined they may be applied to the previously obtained water cut versus recovery data to convert to recovery in terms of barrels. These data and the assumed water injection rate furnish the necessary information for determining the time behavior of the flood unit. Illustrated in Table 5 are the stepwise calculations for determining the cumulative oil recovery, oil rate, and cumulative water injected versus time.

From these basic results and other derived information, such as total injection water requirements and time to reach economic limit, can be determined the economic feasibility of a water flood project.

TABLE 4

Calculation of Water Cut

h = Fraction of Cumulative Thickness	C = Cumulative Capacity; Fraction	$C \cdot A^1$	$C \cdot A + (1 - C)$	$\frac{C \cdot A}{C \cdot A + (1 - C)}$ = Water cut Fraction
.00	*.000	.000	1.000	—
.01	.065	.092	1.027	.090
.02	.110	.156	1.046	.149
.05	.200	.284	1.084	.262
.10	.308	.437	1.129	.387
.20	.476	.676	1.200	.563
.30	.620	.880	1.260	.698
.40	.731	1.038	1.307	.794
.50	.812	1.153	1.341	.860
.60	.870	1.235	1.365	.905
.70	.917	1.302	1.385	.941
.80	.952	1.352	1.400	.966
.90	.980	1.392	1.412	.986
.95	.991	1.408	1.417	.994
1.00	1.000	1.420	1.420	1.000

*From capacity distribution curve.

$$^1A = \frac{K_{rw}}{K_{ro}} \times \frac{\mu_o}{\mu_w} \times Q = \frac{.20}{.80} \times \frac{4.34}{.82} \times 1.073 = 1.42$$

COMPARISON OF ACTUAL AND PREDICTED BEHAVIOR

The presently described method of taking into account the variations in permeability has been used in a number of engineering studies of water flood projects. Figure 4 shows a comparison of the predicted and the actual recovery versus water cut relationship in one of these earlier projects which has now progressed sufficiently to make possible such comparison. The behavior of this project, a Benoist Sand flood in Illinois, was calculated by the above method prior to the start of injection.

LIMITATIONS

The limitations of the above method of calculating water flood behavior should be pointed out. In particular, this method should not be applied where there is present a gas zone or water zone immediately above or below the oil zone under consideration. In this event there would be by-passing of the oil zone by injected water, or there would be coning and the oil recovery to any given water cut would be less than the calculated recovery. However, in the case of gas or water zones of known permeability certain modifications can be made in the basic equations to adjust for those conditions.

The water cut recovery curve should not be interpreted as a prediction of the behavior of any individual well, since structural consideration may make individual recoveries greater or less than the calculated value. Instead, the water cut recovery curve must be considered an average relationship for an entire field assuming a uniformly spaced flood is established therein. The water cut-recovery relationships should be based on the permeability and capacity distribution of a large number of permeability measurements from many wells in the area to be flooded.

This method does not take into account all factors which may influence the production history, such as the presence of gas or water zones, distance from fluid contacts, rate of production, structural position of the individual wells, lateral versus upward encroachment, shape of field, spacing pattern effect, etc. As more data and experience is obtained the effect of these factors will be better understood. In

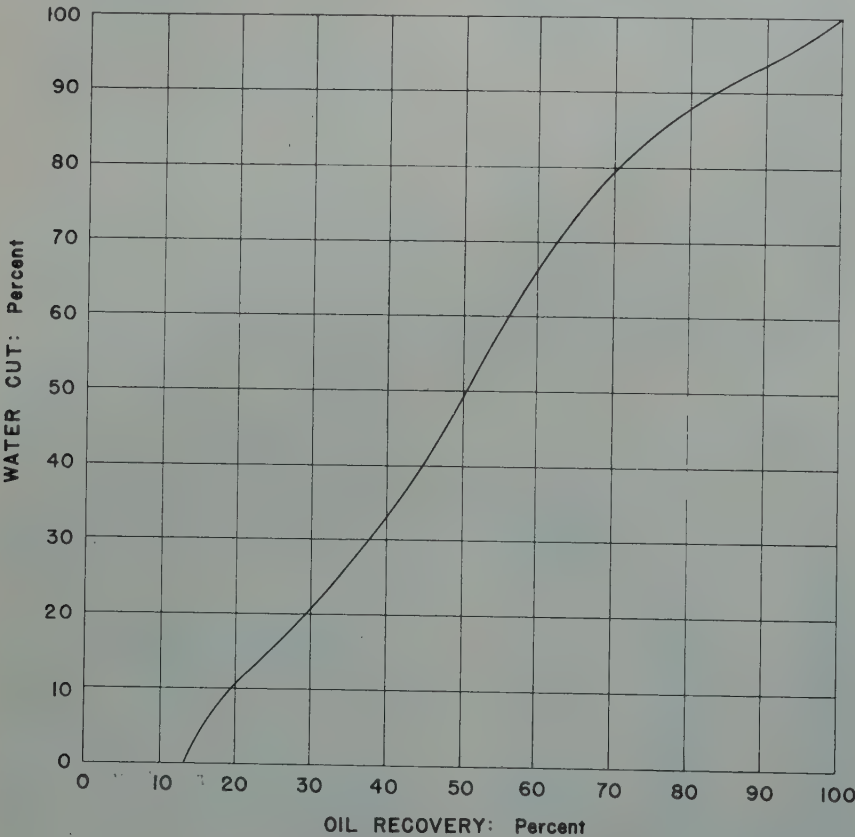


FIG. 3 — CALCULATED WATER CUT VS. RECOVERY

TABLE 5
Predicted Performance of 5-Spot at 100 Bbls/Day Injection Rate

Cumulative Recovery; Fraction of Total	Cumulative Recovery; Barrels	Δ Recovery; Barrels	Water cut; Fraction	Average Water cut; Fraction	Average Oil Rate; bbls/day = 100(1-W)	Days to Produce Δ Recovery at Average Oil Rate	Cumulative Days after Fill-up	Cumulative Water Injected; Barrels
.000	*0		.000	.000	100.0	—	0.0	25,100 (fill-up)
.133	5,664	5,664	.000	.000	100.0	56.6	56.6	30,760
.200	8,517	2,853	.102	.051	94.9	30.1	86.7	33,770
.250	10,646	2,129	.147	.125	87.5	24.3	111.0	36,200
.300	12,776	2,130	.204	.176	82.4	25.8	136.8	38,780
.350	14,905	2,129	.264	.234	76.6	27.8	164.6	41,560
.400	17,034	2,129	.328	.296	70.4	30.2	194.8	44,580
.450	19,163	2,129	.397	.363	63.7	33.4	228.2	47,920
.500	21,293	2,130	.485	.441	55.9	38.1	266.3	51,730
.600	25,551	4,258	.667	.576	42.4	100.4	366.7	61,770
.700	29,810	4,259	.799	.733	26.7	159.5	526.2	77,720
.800	34,068	4,258	.882	.841	15.9	267.8	794.0	104,500
.850	36,197	2,129	.911	.897	10.3	206.7	1,000.7	125,170
.900	38,327	2,130	.938	.925	7.5	284.0	1,284.7	153,570
.950	40,456	2,129	.964	.951	4.9	434.5	1,719.2	197,020
.970	41,307	851	.977	.970	3.0	283.7	2,002.9	225,390
.990	42,159	852	.991	.984	1.6	532.5	2,535.4	278,640

*Total recoverable oil in 5-spot=100 acre-feet \times 501 bbls/acre-ft. \times 85% coverage=42,585 bbls.

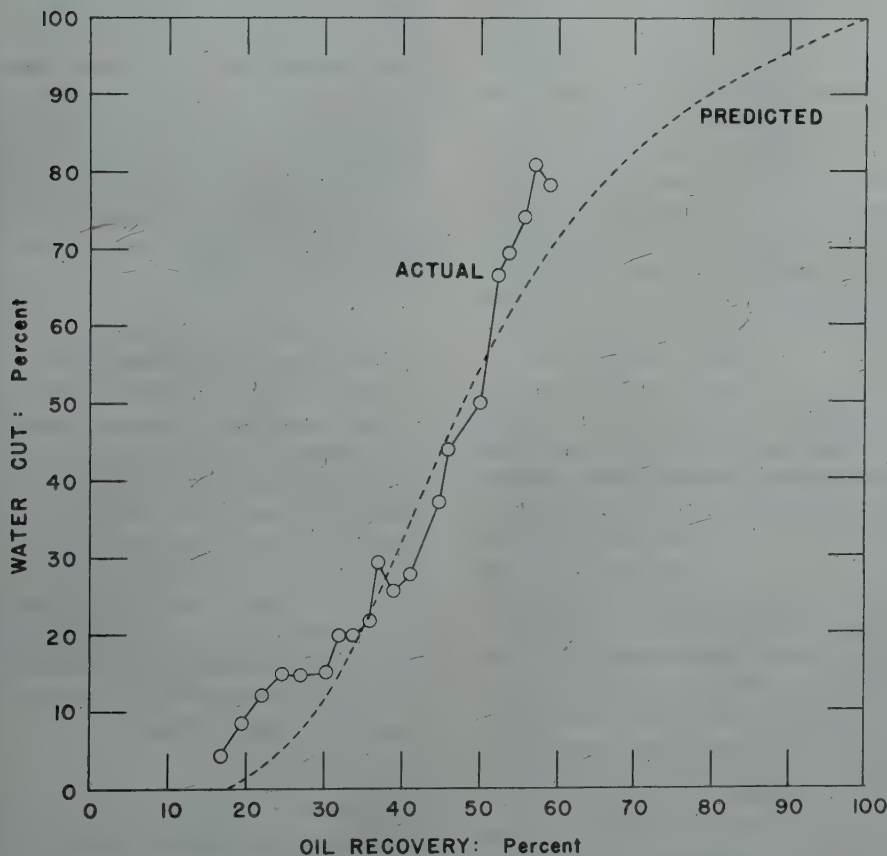


FIG. 4 — COMPARISON OF PREDICTED AND ACTUAL FLOOD PERFORMANCE.

the meanwhile the method herein presented must be considered an approach towards a mathematical treatment of the effect of permeability distribution in water flood performance.

SUMMARY

It has been shown that permeability variations in a reservoir may be represented by a permeability distribution curve and a capacity distribution curve.

Equations have been derived to incorporate mathematically the effect of the permeability distribution in the calculation of water flood recoveries.

Examples are presented to show the application of the equations to predictions of water flood performance in a depleted reservoir; however, the method may be applied to studies in "flush" fields.

A comparison of predicted and actual water cut-recovery relationship is shown.

Certain limitations of the method are presented and it is pointed out that the method is essentially an approximation intended to take into account principally the distribution of permeability in a reservoir.

ACKNOWLEDGMENT

The author wishes to acknowledge the assistance given in the preparation of this paper by Dr. Frank C. Kelton, Core Laboratories, Inc., whose original work serves as a basis for the methods outlined.

RELATIONSHIP OF DRILLING MUD RESISTIVITY TO MUD FILTRATE RESISTIVITY

H. W. PATNODE, GULF RESEARCH & DEVELOPMENT CO., PITTSBURGH, PA.

ABSTRACT

The effect of suspended solids on the resistivity of slurries is discussed and the relationship between drilling mud resistivity and mud filtrate investigated. It is concluded that it is erroneous to substitute mud resistivity for mud filtrate resistivity in electric log calculations. A recommendation is made that both the mud resistivity and the mud filtrate resistivity be determined when electric logs are run.

INTRODUCTION

The electric log is influenced not only by the resistivity of the drilling mud in the borehole at the time of logging but also by the resistivity of the drilling mud filtrate.

Sherborne and Newton¹ investigated the relationship of mud resistivity to mud filtrate resistivity and concluded that, "The resistivity of the mud in most cases closely approximates that of its filtrate," and "In fact, with the exception of Aquagel and its filtrate, the figures for any particular mud and filtrate are almost identical." Present practice is to determine only the drilling mud resistivity and apply this same value to calculations involving the mud filtrate.² The purpose of this study is to reexamine the factors governing the relationship between mud resistivity and mud filtrate resistivity.

EFFECT OF BOREHOLE FLUID ON THE ELECTRIC LOG

Resistivity Log

The resistivity log may be modified by the resistivity of the borehole fluid in two different ways:

- (1) The apparent resistivity of a formation may be different from the true resistivity of the formation because of the flow of some current through the drilling mud in the borehole. Therefore the resistivity of the mud is an important factor.
- (2) The apparent resistivity may differ from the true resistivity, if a formation is invaded by mud filtrate, because of displacement by

the mud filtrate of some of the interstitial fluid in the formation. In this case the resistivity of the mud filtrate rather than the resistivity of the mud is the important factor.

Self Potential Log

The self potential arises, in part, from electrochemical effects resulting from the interaction of connate waters in porous formations and the fluid in the borehole. Expressed in simple form,

$$E = K \log \frac{\rho_1}{\rho_2}$$

where E is the electrochemical self potential, K is a derived constant, ρ_1 is the resistivity of the borehole fluid, and ρ_2 the resistivity of the water in the formation. A theory of the electrochemical component of the self potential in boreholes has been recently set forth by Wyllie.³ In the above equation resistivities have been substituted for activities of the ions in the fluids.⁴ It is therefore apparent that the resistivity of the mud filtrate is more nearly representative of the activities of the ions than is the resistivity of the mud. However, it is possible that in some instances the ionic activities of cations from certain clays may contribute to the total cationic activity of the drilling fluid to such an extent that the mud resistivity is more nearly representative of the activities than the filtrate resistivity. This is particularly the case when the resistivity of the mud is less than the resistivity of the mud filtrate.

In addition the apparent self potential may be influenced by the resistivity of the drilling mud because of current flow through the borehole.

RESISTIVITY OF SLURRIES

Aqueous drilling muds are slurries containing fine-grained solid particles. The solid constituents consist mainly of added clays and weighting materials in addition to solids contributed by the drilled formations. The filtrate is primarily water in which quantities of salts or other chemicals are dissolved. The resistivity of the filtrate is a function of the type and quantity of dissolved material whereas the resistivity of the mud is a function of the combined resistivities of the filtrate and the

resistivities of the suspended solids.

Experiments have been carried out to determine the relationship between the resistivity of solutions and the quantity and type of solid matter in suspension. Solid materials of high resistivity, as well as solid materials of relatively low resistivity, have been used. The data obtained make possible the evaluation of the probable effect of suspended solids on the resistivity of drilling mud.

Procedure

Resistivities were determined by means of a conventional conductivity cell with platinized-platinum electrodes. Total resistance between the electrodes was measured by Kohlrausch's alternating current bridge method using a General Radio Company Type 650-A impedance bridge with telephone. The cell was standardized with potassium chloride solutions of known normalities in order to calibrate the cell so that measured resistances of slurries could be converted to resistivities.

Resistivities were determined for mixtures of potassium chloride solution and solid materials by placing a measured quantity of solution in the cell and adding weighed quantities of solid materials in small increments to the solution. The net change in resistance on addition of solid materials was measured. Even distribution of the solid particles was maintained within the cell by a motor-driven glass propeller before measurements were made.

Slurries Containing High-Resistivity Solids

Powdered silica sand having a maximum diameter of about 60 microns and precipitated chalk of commercial grade were used to make the slurries whose resistivities were measured. Both of these substances have high resistivities, are virtually insoluble, and effectively do not carry current in a slurry. The resistivities of slurries composed of potassium chloride solution and these two solid materials are given in Table 1.

The ratio of the resistivity of the solution to the resistivity of the slurries was computed and was found to follow the relationship established by Archie⁵

Manuscript received at office of the Division September 25, 1948. Paper presented at Division Fall Meeting, Dallas, Texas, Oct. 4-6, 1948.

¹ References are at the end of the paper.

for fluid-saturated rocks with intergranular porosity, i.e.:

$$\frac{\text{Resistivity of rock sat. with water}}{\text{Resistivity of water}} = \frac{1}{(\text{Porosity})^m}$$

Since, for slurries, percent fluid by volume is analogous to porosity, this same relationship can be expressed by inversion as:

$$\frac{\text{Resistivity of water}}{\text{Resistivity of slurry}} = (\text{Percent fluid})^m$$

The value of the factor m for slurries of powdered silica and precipitated chalk was found to be consistently close to 1.6, which is higher than the value of 1.3 computed for packed uniform spheres.⁹ This higher value may be attributed to the fact that the powdered materials are unsorted and non-spherical in shape.

Additional experiments were made using fine steel shot and rounded Ottawa sand of uniform size. The steel shot were covered with a resistant oxide film so that they were non-conductive. The factor m for these materials was calculated to be 1.22 which is slightly less than the theoretical value of 1.3 for packed uniform spheres.

A sample of well sorted, angular quartz sand was found to give a value of m equal to 1.39.

Slurries Containing Low-Resistivity Solids

The relationship derived for slurries containing solids of high resistivity does not hold for drilling muds. Certain solid materials contained in drilling muds, notably Aquagel, have a low effective resistance since some clays may partially dissociate in water and conduct current as true electrolytes. This property of clays has been extensively investigated by Marshall.⁷

The relationship of Aquagel mud to the resistivity of the mud filtrate for muds of different resistivities is given in Table 2. These figures have been calculated from data given by Sherborne and Newton¹ and are supplemented by determinations made by the writer. These data indicate that when the filtrate has a relatively high resistivity, the clay particles may be more conductive than the filtrate, thus giving a lower resistivity for the mud than for the mud filtrate. When the resistivity of the filtrate is relatively low, the resistivity of the mud may be appreciably greater than the resistivity of the filtrate because the particles are less conductive than the fluid in which they are

Volume of Fluid (percent) P	Resistivity of Slurry at 82.4° F. (ohm-meters)	Resistivity of Water Resistivity of Slurry	Factor m
Powdered Silica Sand			
100.0	0.184	1.00	1.00
98.2	0.195	0.94	3.12
94.1	0.195	0.94	0.96
93.7	0.231	0.89	1.81
92.3	0.208	0.85	2.01
89.3	0.223	0.83	1.68
89.0	0.209	0.85	1.35
84.7	0.246	0.75	1.72
81.5	0.256	0.72	1.59
80.0	0.262	0.71	1.58
74.0	0.296	0.63	1.57
70.8	0.318	0.58	1.59
65.4	0.348	0.53	1.50
64.3	0.365	0.51	1.55
61.2	0.432	0.43	1.74
57.8	0.424	0.43	1.52
57.5	0.457	0.40	1.64
56.0	0.454	0.41	1.56
53.7	0.501	0.37	1.61
50.0	0.596	0.31	1.70
46.6	0.668	0.27	1.69
45.6	0.680	0.27	1.68
44.8	0.674	0.27	1.61
44.4	0.710	0.26	1.66
Precipitated Chalk			
100.0	0.184	1.00	1.00
95.0	0.198	0.93	1.32
92.5	0.202	0.91	1.34
92.5	0.209	0.88	1.68
90.0	0.209	0.88	1.38
86.3	0.228	0.81	1.46
85.1	0.248	0.74	1.86
82.2	0.262	0.70	1.83
79.0	0.268	0.69	1.58
77.5	0.290	0.63	1.77
74.4	0.307	0.60	1.73
70.7	0.318	0.58	1.58
67.5	0.348	0.53	1.62
67.1	0.368	0.50	1.73
65.2	0.374	0.49	1.67
Ottawa Sand			
100.0	0.151	1.00	1.00
93.5	0.167	0.90	1.55
85.6	0.195	0.77	1.69
79.6	0.228	0.66	1.83
72.8	0.253	0.60	1.63
69.1	0.267	0.57	1.56

suspended. This is analogous to the relationship of the individual resistances of two resistors to their total resistance when in parallel.

Drilling Muds

The composition of drilling muds may be complex. Composition not only varies from well to well but may alter considerably during the drilling of a well. The suspended particles may consist of both resistant particles and conductive clays. The over-all effect of the suspended resistant solids is to increase the mud resistivity relative to the mud filtrate. The effect of the suspended clays may be conversely to decrease the mud resistivity. The combined effect of the two types of solids may be either to increase or decrease the resistivity of the mud, depending on the relative effective conductivities of the suspended clay and the filtrate. Because of these uncertainties, it is impractical to determine the resistivity of the mud filtrate from the mud resistivity.

The resistivity of a drilling mud is

usually greater than the resistivity of the mud filtrate. The ratio of mud filtrate resistivity to mud resistivity for several muds is given in Table 3. The first five examples are summarized from data on modified muds taken from the paper by Sherborne and Newton.¹ The others are measurements made on muds from four different wells of the Gulf companies. The ratio of mud filtrate resistivity to mud resistivity for all determinations varies from 1.5 to 0.66.

TABLE 2
Relationship of Filtrate Resistivity to Resistivity of Aquagel Mud

Resistivity at 80° F. (ohm-meters)		Filtrate Resistivity
Mud	Filtrate	Mud Resistivity
7.6	10.2	1.34
6.9*	10.5	1.52
4.9	6.0	1.22
3.3	3.9	1.18
2.4	2.4	1.00
1.4	1.3	0.93
0.80*	0.70	0.88
0.71	0.56	0.79

* These two determinations were made by the writer. Other data taken from Sherborne and Newton.¹

TABLE 3
Relationship of Filtrate Resistivity
to Resistivity of Some
Drilling Muds

Mud	Number of Determinations	Filtrate Resistivity	
		Mud Resistivity	
		Range	Average
Mojave*	20	1.00-0.70	0.84
Wilmington Slough*	24	1.00-0.81	0.90
Aquagel*	42	1.30-0.79	1.16
McKittrick*	40	1.00-0.73	0.83
Oxo*	44	1.56-0.80	0.95
Well A.	9	1.04-0.81	0.99
Well B.	14	1.24-0.69	0.80
Well C.	14	0.94-0.66	0.78
Well D.	3	0.85-0.82	0.84

* Calculated from data taken from paper by Sherborne and Newton.¹

CONCLUSIONS

1. The relationship between the resistivities of a series of slurries composed of fine-grained particles of high resistance and the resistivity of the suspending fluid has been found experimentally to satisfy the equation:

$$\frac{\text{Resistivity of water}}{\text{Resistivity of slurry}} = (\text{Percent fluid})^m$$

where m is a constant.

2. A slurry made with a clay such as Aquagel may have a higher or a lower resistivity than the mud filtrate, de-

pending on the effective relative resistances of the suspended clay and the fluid it displaces.

3. The resistivity of a drilling mud filtrate is usually appreciably less than the resistivity of the mud but may be the same or greater. The ratio of mud filtrate resistivity to mud resistivity has been found experimentally to range from 1.5 to 0.66.

4. In making quantitative calculations from electric log data it is erroneous to assume that the mud filtrate resistivity is the same as the mud resistivity. It is therefore essential that both mud resistivity and mud filtrate resistivity be determined at a specified temperature when electric logs are run.

ACKNOWLEDGMENTS

The writer wishes to thank Mr. A. C. Godbold for supplying data on the resistivities of muds and mud filtrates from drilled wells. The writer is indebted to Dr. Paul D. Foote, Executive Vice President of the Gulf Research & Development Co., for permission to publish this paper.

REFERENCES

1. J. E. Sherborne and W. M. Newton: Factors Influencing Electrical

Resistivity of Drilling Fluids. AIME Tech. Pub. 1466, *Petr. Tech.* (March 1942) 5 (2) 17 pp. Also *Trans. AIME* (1942) 146, 204-220.

2. H. Guyod: Electrical Logging Developments in the U.S.S.R., art 2. *World Oil* (January 1948) 127 (9) 67-70.

3. M. R. J. Wyllie: A Quantitative Analysis of the Electrochemical Component of the S. P. Curve. *AIME Jnl. of Petr. Tech.* (January 1948).

4. Samuel Glasstone: Introduction to Electrochemistry, Chapter V. New York, 1942. D. Van Nostrand Co. 557 pp.

5. G. E. Archie: The Electrical Resistivity Log as an Aid in Determining Some Reservoir Characteristics. AIME Tech. Pub. 1422, *Petr. Tech.* (January 1942) 5 (1) 8 pp. Also *Trans. AIME* (1942) 146, 54-62.

6. S. J. Pirson: Electric Well Logging, Factors Which Affect True Formation Resistivity. *Oil and Gas Jnl.* (November 1, 1947) 46 (26) 76-77.

7. C. E. Marshall and C. A. Krinbill: The Clays as Colloidal Electrolytes. *Jnl. of Phys. Chem.* (1942) 46, 1077-1090.

A QUANTITATIVE ANALYSIS OF THE ELECTROCHEMICAL COMPONENT OF THE S. P. CURVE

M. R. J. WYLLIE, GULF RESEARCH & DEVELOPMENT CO., PITTSBURGH, PA.

ABSTRACT

The relationship between the electromotive force (E.M.F.) across a shale barrier and the concentrations of sodium chloride solutions on either side has been investigated.

It is shown that the action of a shale barrier is analogous to a glass membrane separating two acid solutions of different hydrogen ion concentrations. The shale behaves as a sodium electrode and is responsive to the activities of the sodium ions in the two solutions in such a way that the potential can be calculated by means of the Nernst equation. This conclusion is confirmed by laboratory experiments.

In a borehole the total E.M.F. of a shale cell is the algebraic sum of the potential across the shale and a boundary potential. The relationship between total E.M.F. and the resistivity ratio of two sodium chloride solutions is indicated for a number of formation temperatures. The E.M.F. thus predicted is then compared with the self potential read from an electric log and good agreement is demonstrated.

Based on both the self potential and resistivity curves of the electrical log, a method is given for calculating connate water content in a bed having intergranular porosity and containing both connate water and hydrocarbons.

INTRODUCTION

The first paper on electrical well logging by C. and M. Schlumberger and E. G. Leonardon in 1934¹ attributed the self potential curve principally to streaming potentials, i.e. to electrokinetic effects. Almost immediately great difficulties were encountered in reconciling many of the curves they obtained with this interpretation, and a second paper² by the same authors soon appeared. In this second paper self potentials were attributed to the combined

effects of streaming potentials and electrochemical potentials, the electrochemical potential being considered the result mainly of the interaction of fluids of differing salt concentrations, i.e. a boundary potential, and partly of potentials set up at the faces of impermeable materials. Some experiments involving a gray clay for the impermeable material were quoted. The Schlumbergers and Leonardon deduced from the equation for a simple boundary potential that the electrochemical potential, as opposed to the electrokinetic potential, could be expressed in the form

$$E = K \log \frac{\rho_m}{\rho_c} \dots \dots \dots 1$$

where K is a constant, ρ_m the mud resistivity, ρ_c the resistivity of the connate water in a porous bed. However, no general expression for the constant K was obtained.

Although the literature between 1934 and 1943 contains a number of quotations of their results, the valuable work of the Schlumbergers and Leonardon was not extended so that the electrochemical potential has been generally attributed wholly to boundary potentials between the mud in the borehole and the connate waters in porous formations. Unfortunately, however, the fundamental premise of all these papers, that a boundary potential can give rise to current flow in a borehole, is thermodynamically untenable. As will be shown, the fact that the electrochemical potential can be fairly accurately expressed as $E = K \log \rho_m / \rho_c$, a form in which a boundary potential may also be written, is partly fortuitous. The boundary potential is indeed an integral part of the expression for the electrochemical potential in a borehole, but in magnitude it represents only about 20% of the total potential.

In 1943 an important step in the elucidation of electrochemical potentials was made by Mounce and Rust³ who showed that if a wall of shale separated two compartments which contained

saline solutions of different concentrations, and if the two solutions were themselves brought into contact in the pores of a porous inert membrane (such as unglazed porcelain) a current flowed through the shale and saline solutions. The direction of positive current was from the shale into the more dilute solution. The paper of Mounce and Rust, while repeating some of the observations of the Schlumbergers and Leonardon, seems to be the first to show that the shale was the seat of a genuine electrochemical effect capable of causing current flow. In the same paper Mounce and Rust pointed out the similarity between the fundamental conditions of their experiment and the conditions which existed when a bed of shale in the ground was simultaneously in contact with a porous sand containing saline connate water and mud fluid of salinity different from that of the water in the sand.

Since it is now generally recognized that the S.P. curve measures ohmic potential changes in the mud fluid in the well bore resulting from changes in current flow, it is apparent that currents having their origin in the electrochemical interaction of mud filtrate and connate waters with shale beds are a very important portion of the total S.P. The work of Mounce and Rust³ and others appears to indicate that, in general, the electrochemical portion of a particular kick on a S.P. curve far exceeds any electrokinetic potentials resulting either from streaming potentials or Dorn effects. The Dorn effect, or sedimentation potential, arises when small particles are allowed to fall through certain fluids under the influence of gravity, a difference of potential being observed between two electrodes placed at different levels in the stream of falling particles. The Dorn effect is unlikely to affect seriously the S.P. curve as now measured.

A successful analysis of the electrochemical aspects of the S.P. log should

Manuscript received at office of the Division September 15, 1948. Paper presented at Division Fall Meeting, Dallas, Texas, Oct. 4-6, 1948.
¹ References are given at the end of the paper.

thus give information of a very wide applicability to electrical log interpretation. Such an analysis, supported by a number of laboratory and field results, is attempted below.

Theoretical Analysis of the Shale Cell

The primary measurement which can be made from a conventional S.P. electrical log curve is the potential difference between points in the borehole opposite a porous formation and points opposite a shale formation, i.e. the amplitude of a S.P. peak above the shale base line. For the purpose of this analysis the porous and shale formations will both be considered thick and of fairly low resistivity, since decrease in bed thicknesses or high bed resistivities will markedly reduce the magnitude of the potential difference recorded on the log. This aspect of the S.P. curve problem has recently been admirably discussed by Doll¹ who also pointed out that if V is the recorded potential difference on the S.P. curve, and E the total theoretical E.M.F. giving rise to current flow, V will be sensibly equal to E under the conditions set forth above.

Although the nature of the metal is theoretically immaterial, lead electrodes are customarily used in the practical logging device. The cell whose true E.M.F., E , is being measured appears to be the following:

Lead/Mud//Interstitial water in the porous bed/Shale/Mud/Lead.

Here, following the normal electrochemical practice, the cell is written so that the direction of positive current flow within the cell is from left to right, i.e. the right-hand lead electrode is the positive pole of the cell. Single oblique lines represent boundaries between solid and liquid phases and double oblique lines a liquid junction between two solutions. Assuming that the potential difference at each lead/mud interface is the same (which implies that the electrodes have come to equilibrium with the mud fluid, that they are not being scratched, and that no significant differences in the composition of the mud surrounding the two electrodes exist), these potential differences are opposed in direction and hence cancel each other. Thus the net E.M.F. of the shale cell may be considered to be:

Mud//Interstitial water in the porous bed/Shale/Mud.

This net E.M.F. is composed of the algebraic sum of two potentials, namely a boundary potential at the mud//

interstitial water in the porous bed interface, and an E.M.F. between the interstitial water and the mud across the shale. The E.M.F. across the shale has been shown by Mounce and Rust to give rise to a sustained current flow. The quantitative aspects of the generation of this E.M.F. will be considered below. The boundary potential at the interface of the porous bed and mud fluid is, however, a better known phenomenon and will be considered first. For the purpose of this discussion the principal electrolyte in the waters comprising the borehole mud and the interstitial water in the porous bed is presumed to be sodium chloride.

A boundary potential results from the separation of electrical charge which occurs at the interface of two saline solutions of different concentrations when the speeds of migration of the positive and negative ions composing the salts are dissimilar. In sodium chloride solutions the negative chloride ion diffuses more rapidly than the positive sodium ion. Since at an interface of sodium chloride solutions of different concentration the sodium chloride will diffuse from the region of high to low concentration, as electrical double layer tends to be set up at the interface such that the low concentration side of the interface is negative and the high concentration side positive. The initial separation of electrical charges does not increase since the negative ions which diffuse across the boundary are attracted back by the positive ions left behind, and diffusion of one salt solution into the other can only occur by diffusion of both positive and negative ions together. Thus at the boundary there is no sharp change in concentration, but the potential difference between the bulk of one solution and the other tends to remain fairly constant. Technically the type of boundary formed by the mud//interstitial water interface in a porous material would be of the "constrained diffusion" type since mixing of the two solutions by diffusion would be slow.

The general expression for a boundary potential between salts of different types and valencies as given by Henderson² is, for dilute solutions:

$$E_b = \frac{RT}{F} \left(\frac{(U_1 - V_1) - (U_2 - V_2)}{(U_1 + V_1) - (U_2 + V_2)} \right) \ln \frac{U'_1 + V'_1}{U'_2 + V'_2} \quad \dots 2$$

where U_1 , V_1 , etc. are defined as:

$$\begin{aligned} U_1 &\equiv \sum (c_1 u_+)_1 & V_1 &\equiv \sum (c_1 v_-)_1 \\ U'_1 &\equiv \sum (c_1 u_+ z_+)_1 & V'_1 &\equiv \sum (c_1 v_- z_-)_1 \end{aligned}$$

and where c_+ and c_- are the concentrations of cations and anions respectively, u_+ and v_- are the corresponding ionic mobilities and z_+ and z_- are their valencies. The suffix 1 refers to the ions in solution 1 and similar expressions hold for U_2 , V_2 , etc. in which the ions in solution 2 are concerned. R is the gas constant, F the Faraday, T the absolute temperature.

For dilute solutions of monovalent salts of different concentration this reduces to:

$$E_b = \frac{RT}{zF} \left(\frac{v - u}{v + u} \right) \ln \frac{c_1}{c_2} \quad \dots 3$$

where c_1 and c_2 are the concentrations of the two solutions. For monovalent ions such as sodium and chloride z is 1.

More accurately the concentrations should be replaced by the mean activities³ of the electrolytes in the two solutions when,

$$E_b = \frac{RT}{zF} \left(\frac{v - u}{v + u} \right) \ln \frac{a_1}{a_2} \quad \dots 4$$

where a_1 and a_2 are the mean activities of the electrolytes in the two solutions.

For sodium chloride solutions at 25° C. the numerical expression of this relationship is:

$$E_b = 11.5 \log \frac{a_1}{a_2} \text{ millivolts} \quad \dots 5$$

The determination of the mean activities demanded by equations 4 and 5 is possible. It is, however, more convenient to replace the ratio of the activities of the electrolytes in the solutions by the ratio of the conductivities of the two solutions. Although the relationship between conductivity and activity ratios becomes less accurate at higher concentrations, this approximation is permissible for dilute solutions. From the standpoint of electrical logging techniques this may be more familiarly expressed as a resistivity ratio, and equation 5 becomes:

$$E_b = 11.5 \log \frac{\rho_{mt}}{\rho_c} \text{ millivolts} \quad \dots 6$$

where ρ_{mt} is the resistivity of the mud filtrate derived from a mud composed solely of an aqueous sodium chloride solution and inert solid materials in suspension, and ρ_c is the resistivity of the connate water in a porous formation, assuming that the principal electrolyte is sodium chloride.

It should be emphasized that the value of ρ_{mt} is frequently different from ρ_m (the mud resistivity) and it is not permissible to use ρ_m instead of ρ_{mt} . This statement is not in agreement with the conclusions of Sherborne and Newton,⁷ but has been substan-

tiated by the work of H. W. Patnode of these laboratories.

It has been stated above and it is reiterated here, that a boundary potential is wholly incapable of giving rise to current flow. However, the boundary potential is always measured when voltage determinations are made of any cell containing the boundary through which current is either flowing or is made to flow. Since flow of current through the system,

Mud//Interstitial water in porous bed/Shale/Mud,

is known to take place, it is reasonable to infer that the seat of the driving E.M.F. lies in the interaction of the shale faces with the aqueous solutions differing in salt concentration. It remains to examine the quantitative aspects of this inference.

A primary constituent of most shales is clay. Clays are known to be both complex and chemically reactive mineral substances. No quantitative work on the electrochemical properties of shales appears to have been published, but some work by Marshall⁹ on the electrochemical properties of a number of relatively pure hydrogen clays appears to be germane. Marshall showed that thin membranes prepared from colloidal dispersions of several different hydrogen clays developed a potential difference between their faces if they were interposed between salt solutions of different concentrations. It was found that the potentials so developed were very sensitive to concentrations of monovalent cations, but were in general less sensitive to solutions containing divalent and trivalent cations. In particular it was found that for monovalent cations, e.g. sodium and potassium ions, the membranes tended to give E.M.F.'s which followed the Nernst equation:

$$E = \frac{RT}{F} \ln \frac{a_1}{a_2} \quad \dots \quad 7$$

where E is the E.M.F. developed, a_1 is the activity of positive ions in the more concentrated solution, and a_2 is the activity of the positive ions in the less concentrated solution. For solutions of sodium chloride at 25° C. this reduces to:

$$E = 59.15 \log \frac{a_1}{a_2} \text{ millivolts} \quad \dots \quad 8$$

This relationship was found by Marshall to hold with great precision for monovalent salt concentrations less than 0.1 molal, a concentration which represents about 5800 parts per million

sodium chloride.

The mechanism whereby this E.M.F. is set up is by no means clear, but the explanation may lie in the sieving action on the ions of the salt solutions which would result if there were a high negative charge on the clay lattice. Thus negative ions, e.g. chloride ions in the case of sodium chloride solutions, would be repelled by the clay and would be unable to enter the clay lattice, whereas the sodium ions would not be similarly disbarred. Thus, effectively, two Donnan potentials would be set up at the faces of the clay membrane as postulated in the membrane theories of Meyer and Sievers⁹ and Teorell.¹⁰ The total effect of such a mechanism is clearer, inasmuch as the clay membrane would then behave as a sodium electrode in a manner very analogous to that in which the well-known glass electrode for pH determinations behaves as a hydrogen electrode. Marshall's results indicate that this action can only be expected in the case of clay membranes for solutions more dilute than 0.1 molal, since at concentrations in excess of this it was found that the potential developed across the clay membranes was always very much less than that anticipated from equation 7.

The E.M.F. set up across a clay membrane, unlike a boundary potential, derives its energy from the difference in the chemical potential of the ions in the concentrated and dilute salt solutions and is therefore capable of giving rise to a small but sustained flow of current. The direction of this current flow is such as to endeavor to equalize the sodium ion concentrations on each side of the membrane, i.e. a positive sodium ion current passes effectively through the membrane from the concentrated to the dilute sodium chloride solution.

The question then is whether or not it is justifiable to extrapolate the results, which Marshall obtained using artificially prepared clay membranes, to include shales. The chemically reactive mineral constituents of the clay membrane and the shale may be assumed to be reasonably similar, but the fact that the resistivity of a clay membrane was found to be of the order of 10⁵ ohm-meters compared with the order of 10 ohm-meters for a shale indicates that the heating process used by Marshall in preparing the clay membranes may have radically changed many of the properties of the clays. Nevertheless, as a first approximation

it would seem that shales might also give E.M.F.'s with sodium chloride solutions which tended to follow equation 7, in which case the circuit, Mud//Interstitial water in bed/Shale/Mud, would be electrochemically equivalent to a sodium concentration cell with transport, i.e.

Na electrode/NaCl of molality m_2 //NaCl of molality m_1 /Na electrode.

The total E.M.F. of such a cell is the algebraic sum of the electrode potentials and the boundary potential, and is thus the sum of the potentials given by equations 4 and 7. Replacing activities of sodium chloride once again by ρ_{mf} and ρ_c , it follows that, at 25° C.:

$$\begin{aligned} E_{\text{Total}} &= E + E_b \\ &= 59.15 \log \frac{\rho_{mf}}{\rho_c} + 11.50 \log \frac{\rho_{mf}}{\rho_c} \\ &= 70.65 \log \frac{\rho_{mf}}{\rho_c} \text{ millivolts} \quad \dots \quad 9 \end{aligned}$$

It should be pointed out that the potential across the shale and the boundary potential reinforce each other in the case of sodium chloride solutions.

Equation 9 shows that the total E.M.F. of the shale cell as it exists naturally should be capable of expression in the form (for any particular temperature):

$$E_{\text{Total}} = K \log \frac{\rho_{mf}}{\rho_c} \quad \dots \quad 10$$

This assumes that the shale behaves as a perfect sodium electrode and, consequently, obeys the Nernst equation. The form of this equation is thus the same as that of equation 1 derived by the Schlumbergers and Leonardon, but the magnitude of the constant K involved is very different.

Experimentally it is necessary to determine:

- (A) Whether or not shales behave electrochemically in a manner similar to artificially prepared clay membranes.
- (B) The range of solute concentration over which the Nernst equation is obeyed, assuming (A) to be generally true.

No experiments involving simple boundary potential measurements appear to be necessary since at low and moderate solute concentrations the boundary potential should be calculable from equation 4 with an accuracy well within that obtained in electrical logging.

Experiments carried out to these ends are described below and consist of both laboratory and field studies.

EXPERIMENTAL RESULTS

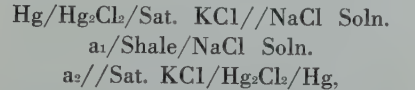
Laboratory Data

For this work two principal types of shale were arbitrarily chosen, both types being obtained by coring with a diamond bit.

The first type was a Conemaugh shale of Pennsylvanian age taken from depths of between 26 and 80 feet. This shale was taken from a zone where leaching by surface waters had probably taken place.

The second type was a Woodford carbonaceous shale of Devonian (?) age taken from the West Edmond field, Oklahoma, at depths between 6808 and 6810 feet. This shale overlies the productive Hunton limestone.

Both types of shale had been air-dried before use. For purposes of measurement the following cells were set up:



the concentration ratio of the sodium chloride solutions being varied as shown in Table 1. Several techniques were satisfactorily used to bring the sodium chloride solutions into contact with the cleavage surfaces of the shale, but a particularly successful method consists of cementing a flanged 24/40 male glass taper to the shale by means of a mixture comprising 100 grams of green optical pitch and 1 cc. of oil. L-shaped glass tubes are then fitted to the standard tapers to hold the sodium chloride solutions. Care was taken to make the boundary potentials between the saturated calomel electrodes and the salt solutions as reproducible as possible and to prevent contamination of the potassium chloride with sodium chloride. Most of the shale specimens used were for convenience about 3 cms. long. However, the length is not critical and has no apparent effect on the results obtained. Specimens so mounted had a total resistance of between 10,000 and 20,000 ohms and the potential could be satisfactorily measured to an accuracy of 0.1 M.V. using a Leeds & Northrup Type K potentiometer. For resistances in excess of 20,000 ohms the same potentiometer was used in conjunction with a Leeds & Northrup thermionic amplifier.

The resistivities of the sodium chloride solutions were measured using a conductivity cell with platinized-platinum electrodes and a General Radio Company Type 650-A impedance bridge. The activities of sodium ions in solu-

tions of concentration up to 1.0 molal were estimated by making the following non-thermodynamic assumptions:

- (A) That in dilute potassium chloride solutions the activities of potassium and chloride ions are equal.
- (B) That the activity of the chloride ion in sodium chloride solutions is the same as that of the chloride ion in potassium chloride solutions of the same ionic strength.

Owing to the unknown accuracy of the assumptions that would be necessary, activities of sodium ions in solutions of concentration in excess of 1.0 molal were not computed.

Table 1 contains the mean values for measurements made at 20° C. Reproducibility was in general extremely good, particularly at the lower concentrations. Cracked shale specimens were unsatisfactory and were rejected. One result obtained with a mud filtrate in which the anion was principally sulfate is included.

Several tentative conclusions appear to be justifiable from the data presented in Table 1:

- activity determinations do not appear to be feasible but, both in this range and at low concentrations, the Woodford shale gives fairly good agreement between measured potentials and those calculated from resistivities. The measured value appears to be higher than the calculated except in the most dilute solutions.
- (C) The range of concentration over which the Nernst equation is obeyed with reasonable accuracy appears to be wider for both the Conemaugh and Woodford shales than for any clay membranes so far prepared by Marshall.
- (D) The range of concentration over which the Nernst equation is obeyed with reasonable accuracy may depend upon the nature of the shale used.

In general, for sodium chloride solutions, the laboratory experiments confirm the conclusion that the total E.M.F. of the shale cell giving rise to current flow in boreholes may be compared with the E.M.F. of a sodium concentration cell with transport.

TABLE 1
Effect of Sodium Chloride Concentrations
in the E.M.F. Across Shales

Type of Shale	Activities		Molalities		m1 as p.p.m. NaCl (approx.)	m2 as p.p.m. NaCl (approx.)	Potential Calculated from:		Potential Measured (millivolts)
	a1	a2	m1	m2			Activities (millivolts)	Resistivities (millivolts)	
Conemaugh.....	0.0335	0.00919	0.0398	0.0101	2,320	585	32.7	33.2	32.7
Woodford.....									
Conemaugh.....	0.282	0.0787	0.395	0.0995	23,200	5,850	32.2	31.2	32.2
Woodford.....									
Conemaugh.....	0.719	0.2856	1.0	0.4	58,450	23,380	23.3	19.1	23.0
Woodford.....									
Conemaugh.....	—	—	2.0	0.5	116,900	29,225	—	30.1	14.3
Woodford.....	—	—	2.0	0.5	116,900	29,225	—	30.1	34.2
Conemaugh.....	—	—	4.0	1.0	233,800	58,450	—	23.7	9.9
Woodford.....	—	—	4.0	1.0	233,800	58,450	—	23.7	28.5
Woodford.....	—	—	Saturated Mud Filtrate*	0.01	363,000	585	—	133.5	137.2
Woodford.....	—	—		1.0	See analysis below	58,450	—	35.4	33.8

*This filtrate was from a mud used during logging in the Brunson-Argo field in New Mexico. The approximate analysis was: Na+ 5,172 mg. per liter; K+ trace; Ca++ 680 mg. per liter; Fe++ Mg++ trace; + 340 mg. per liter; SO4 8,608 mg. per liter; Cl- 952 mg. per liter; HCO3- 1,232 mg. per liter.

- (A) Shales tend to give potentials with sodium chloride solutions which may be calculated from the Nernst equation.
- (B) Results at low concentrations indicate that the agreement between measured and calculated values is best when ionic activities are substituted in the Nernst equation. At high concentrations

Field Data

If it is accepted that the E.M.F. of the shale cell with sodium chloride solutions is equivalent to a sodium concentration cell with transport, the total E.M.F. of the cell may be expressed, by again generalizing equation 9, as:

E_{Total} = 2.303 $\frac{RT}{zF}$ $\left(1 + \frac{u-v}{u+v} \right) \log \frac{\rho_{mf}}{\rho_c}$ 11
Assuming that the mobilities of ca-

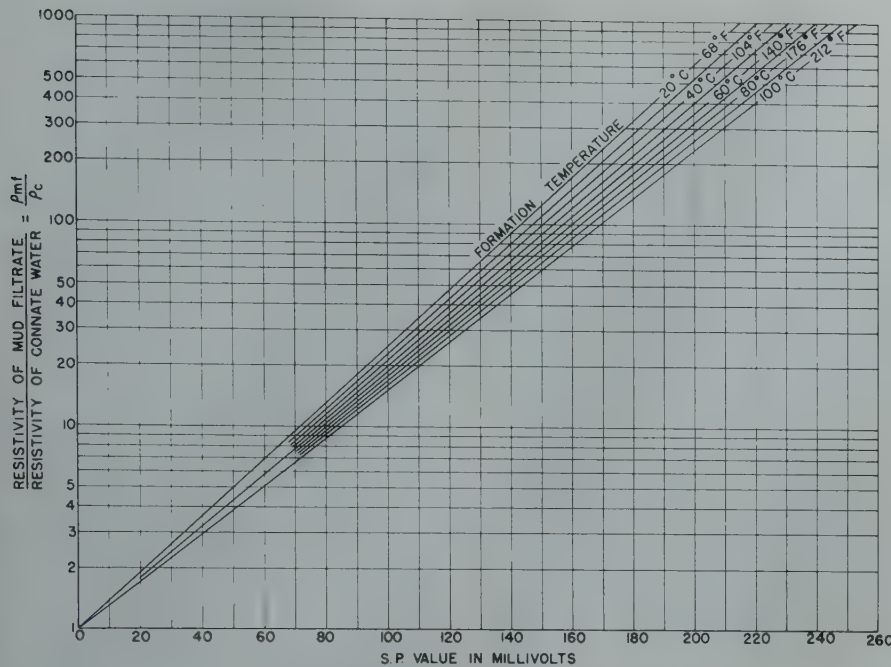


FIG. 1 — RELATIONSHIP BETWEEN SELF POTENTIAL

tion and anion used in this equation are independent of concentration, it is possible to plot a series of curves for different temperatures showing the effect of the resistivity ratio ρ_{mf}/ρ_c on the measured self potential of the shale cell. Such curves are shown in Figure 1 and refer to pure solutions of sodium chloride. In these curves an attempt has been made to consider the effect of temperature on the relative mobilities of the chloride and sodium ions.

The accuracy of these curves remains to be investigated from actual S.P. log measurements. Such an investigation

normally requires knowledge of the following variables:

- The resistivity of the filtrate of the mud used, sodium chloride being the principal soluble electrolyte in the filtrate.
- The resistivity of the connate water in the porous formation corresponding to the S.P. kick being examined and an analysis showing that sodium chloride is the chief electrolyte in solution.
- The temperature of the formation.

It is further assumed that the thicknesses and resistivities of the porous

formation and adjacent shales are such that the measured self potential is substantially equal to the true E.M.F. of the shale cell.

All these data are not easily acquired and, in fact, a reliable connate water resistivity is peculiarly difficult to obtain.

The problem is, however, greatly simplified if S.P. logs covering the same porous formation have been run with muds of two or more different resistivities. If ρ'_{mf} and ρ''_{mf} are the resistivities of two different mud filtrates, ρ_c is the unknown connate water resistivity and E' and E'' are the peak S.P. amplitudes corresponding to the same porous formation (using the two muds), then:

$$E' = K \log \frac{\rho'_{mf}}{\rho_c}$$

$$E'' = K \log \frac{\rho''_{mf}}{\rho_c}$$

$$\text{Therefore, } E' - E'' = K \log \frac{\rho'_{mf}}{\rho''_{mf}}$$

$$- - - - - 12$$

Thus, from equation 12, ρ_c is eliminated and the accuracy of the curves of Figure 1 can be tested using actual logs.

Such an examination was carried out on three logs of the Cypress sand section in Wayne County, Illinois. These logs were run in the same hole using muds of three different resistivities. The resistivities were altered by adding salt to the mud.

Analyses of the Cypress water from other wells showed it to be principally

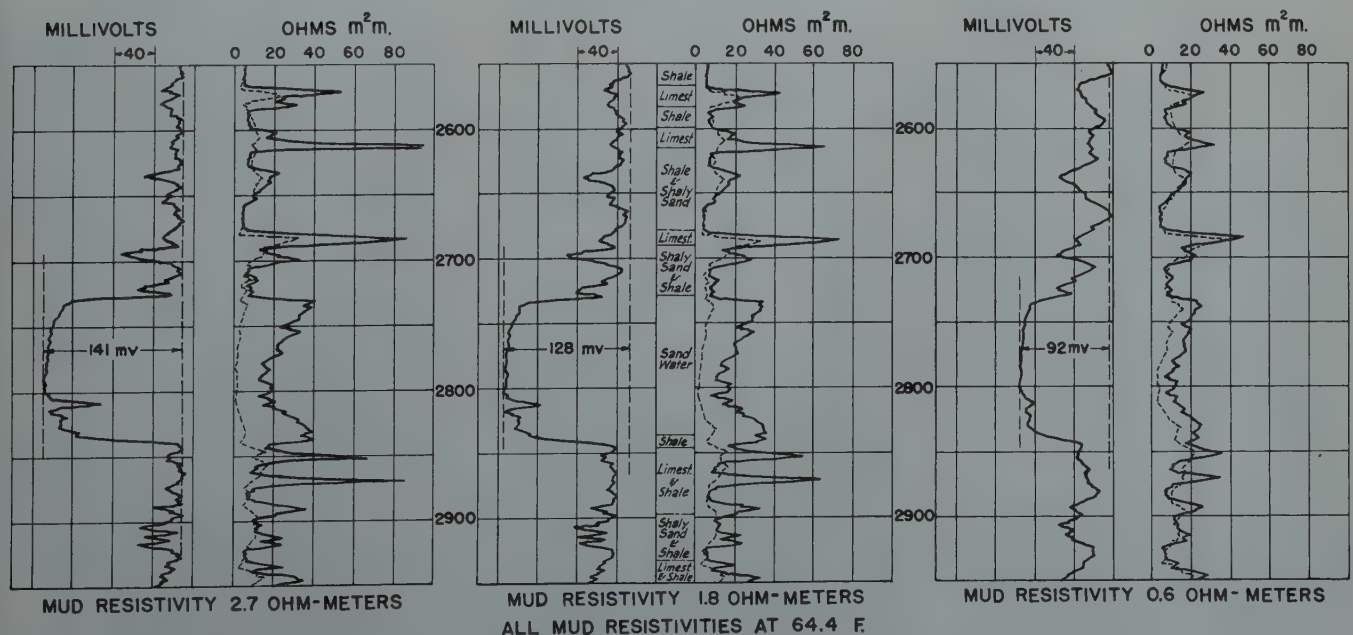


FIG. 2 — CYPRESS SAND LOGS

a sodium chloride solution, but no analysis of the Cypress water in the well logged was available.

Fig. 2 shows the three logs obtained of the Cypress sand. The shale base lines in each case have been taken, as shown, as the most positive kicks on the S.P. curve. The mud weights are given in Table 2 which summarizes all the essential data. Mud filtrate resistivities were not available and hence the mud resistivities have been used. This represents an error but, inasmuch as the mud weights were similar and the resistivities represented variations caused by salt additions to the same mud, it is believed that the comparative error will not be significant.* The borehole temperature opposite the formation was approximately 86° F. or 30° C.

tion of aqueous sodium chloride solutions were used.

** It should be noted that the mud resistivities could have been reduced to any convenient temperature, not necessarily 64.4° F., since the ratio of the resistivities, measured at a particular temperature, of any two sodium chloride solutions is almost independent of the temperature of measurement. The resistivity of the connate water will, of course, be determined for the temperature corresponding to that at which the mud resistivity was determined.

The connate water resistivities are shown in Table 4 to be in good agreement, which indicates that the calculated Nernst equation constant holds good. It should be noted that the resistivity values obtained are relative and not absolute in this case, since

nate water resistivities would be the existence of any constant error in the S.P. values read from the three logs.

The Cypress sand example quoted represents in every way a very nearly ideal case for application of the quantitative shale cell theory outlined above. It is instructive, however, to examine the relationship between calculated and observed potentials for a number of porous beds under conditions where the nature of the salinity of the mud given in Table 2 which summarizes filtrate and connate waters are less well-known. Such an example would have more in common with ordinary log interpretation.

Available for this purpose were two logs run with muds of different resistivity in an 11,000 ft. well in Kern County, California. As before the muds used were of the same weight (10.5 lbs. per gal.) and hence the mud resistivity to mud filtrate resistivity correction could be neglected for comparative purposes. The bottom hole temperature measured in this well was 220° F. or 105° C. Making the assumption that the geothermal gradient in the well is uniform, it is possible to estimate the temperature of porous beds at any depth. This method was used for the temperatures listed in Table 5. The mud resistivities in the two runs, reduced to a common temperature of 64.4° F., were 2.1 ohm-meters and 0.62 ohm-meters. The resistivity ratio was thus $2.1/0.62=3.4$. In Table 5 are plotted potentials calculated from this ratio for the estimated temperatures of the corresponding porous beds. Only those beds were considered where the measured potentials were believed to be substantially equal to the total potentials of the appropriate shale cells. The calculated potentials are compared with the difference in the measured potentials as for the Cypress example. Finally the connate water resistivities for

TABLE 2
Data From Log of Cypress Sand

Mud Weight (lbs. per gal.)	Mud Resistivity (ohm-meters)	at Temp (°F.)	Mud Resistivity (ohm-meters)	at Temp (°F.)	S. P. (millivolts)
10.2	3.2	54	2.7	64.4	14
10.2	1.9	61	1.8	64.4	128
10.0	0.63	61	0.6	64.4	92

From the data in Table 2 three resistivity ratios may be calculated from the mud resistivities at 64.4° F. and thus three expressions of the kind given in equation 12 may be derived.** Table 3 contains the numerical evaluations.

It will be seen that in this example the agreement between the S.P. values obtained from the log and those obtained from the calculated values plotted on Figure 1 for a formation temperature of 86° F. are in excellent agreement. It appears that for the relatively dilute salt solutions comprising the mud filtrates used, the shale adjacent to the Cypress sand gives potentials which follow the Nernst equation. Whether the Nernst equation holds for the cells involving the mud filtrates and the much more concentrated saline solution which constitutes the connate water, can be determined by calculating the connate water resistivity from the three S.P. values obtained.

* The mud resistivities recorded on the headings of the three logs were converted to a common temperature of 64.4° F. for comparative purposes. For this conversion the well-known curves relating the resistivity and concentra-

mud resistivities and not the more accurate mud filtrate resistivities were used in the calculations. It can be seen also from Table 1 that if the measured value of S.P. is approximately the theoretical E.M.F. of the shale cell (the case in the thick Cypress sands considered), the value of the connate water resistivity calculated may be too low.

TABLE 3
Comparison of Observed and Calculated S.P. Differences

Resistivity Ratio	S. P. Difference (millivolts)	S. P. from Fig. 1 (millivolts)
$\frac{2.7}{1.8}=1.5$	141-128=13	14
$\frac{2.7}{0.6}=4.5$	141-92=49	48
$\frac{1.8}{0.6}=3.0$	128-92=36	35

This would be the case with a shale of similar properties to the Woodford shale since the substitution of resistivities for ionic activities represents an error. This error varies with the concentrations of the two sodium chloride solutions, being greatest for solutions of high concentration. Another factor affecting the absolute value of the calculated con-

TABLE 4
Calculation of Connate Water Resistivity for Cypress Sand

S. P. (millivolts)	Resistivity Ratio from Fig. 1	Mud Resistivity Ratio	Connate Water Resistivity (ohm-meters at 64.4° F.)
141	82	$\frac{2.7}{82}$	0.0329
128	55	$\frac{1.8}{55}$	0.0327
92	18	$\frac{0.6}{18}$	0.0334

each porous bed computed from the two logs are listed for purposes of comparison.

In Figure 3 the observed S.P. differences from the two logs are plotted against the temperatures of the corresponding porous beds. The straight line represents calculated potentials over the same temperature range for the resistivity ratio 3.4. It will be seen that, although there is a considerable scatter, the straight line represents a fair curve through the plotted points.

On the whole the results given in Table 5 and Figure 3 indicate that the shale cells tend to yield potentials following the Nernst equation. The agreement between calculated and measured potentials, considering the assumptions made regarding the nature of the geothermal gradient and the type of fluids in the porous beds is, in fact, very encouraging. The last result in Table 5 (10,685 to 10,790 feet) is particularly interesting inasmuch as it shows a reversal of the S.P. kick when using the low resistivity mud, but no reversal with the high resistivity mud. This, of course, results from the fact that the connate water resistivity lies between

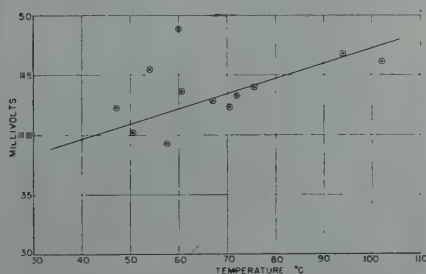


FIG. 3—COMPARISON OF OBSERVED AND CALCULATED SELF POTENTIALS, KERN COUNTY WELL.

the two mud resistivities. The negative sign ascribed to the reversed potential in Table 5 is only relative to the remaining values which are listed as positive for convenience.

The connate water resistivities calculated from the two logs for the twelve porous beds considered are in reasonable harmony. The absolute connate water resistivities will be different from these values for the same reasons as given above for the Cypress sand example, but it is apparent that the saline content of these beds is considerably smaller than in the Cypress example. The Nernst equation appears to be applicable in every case.

APPLICATIONS TO CONNATE WATER DETERMINATION

The quantitative evaluation of the shale cell potential offered here has

obvious applications to the determination of connate water content of oil sands from electrical log data. Assuming that the Nernst equation holds for the S.P. kick corresponding to a porous sand with intergranular porosity containing both connate water and hydrocarbons, the connate water resistivity, ρ_c , may be determined from the mud filtrate resistivity and measured S.P. using the curves in Figure 1. For an accurate connate water calculation it is necessary to know:

- The geothermal gradient in the hole.
- The mud and mud filtrate resistivities at specified temperatures. It is recommended that all electrical logs show the latter quantity on the log heading as a matter of routine.
- The true bed resistivity.
- The true resistivity of the invaded formation surrounding the borehole or the formation factor of the bed experimentally determined from cores. See Archie's paper.²¹

From the geothermal gradient the approximate temperature corresponding to the bed of interest is obtained. This figure permits the appropriate curve on Figure 1 to be selected for the determination of ρ_c .

The formation factor, F , if not known from cores can be calculated from a true value of the invaded resistivity, ρ_i , as follows:

$$F = \frac{\rho_i}{\rho_{mf}}$$

The resistivity of the sand 100% filled with connate water, is ρ_w , is then

the well-known relationship published by Wyckoff and Botset²² and others,

$$\frac{\rho_t}{\rho_w} = \frac{1}{w^2}$$

At present most electrical logs do not record all the data required for this method. It is hoped that this situation will be corrected in the future.

CONCLUSIONS

The analysis of the shale cell potential given above has been shown by both laboratory and field tests to be essentially correct. It seems possible that all shales have electrochemical properties of the same nature as those shales arbitrarily selected for examination in these studies but, until the method has been applied to the analysis of logs from as many wells as possible throughout the world, it is impossible to deny that serious anomalies may exist. Comparison of computed potentials or resistivities with reliable experimental data will ultimately determine this point. It should be pointed out that concentrations of dissolved salts frequently observed in connate waters represent molalities far outside the range of dilute solutions for which most electrochemical formulae have been derived. Thus any relationships based on classical thermodynamics must represent approximations when applied to many electrical log data. Results so far obtained indicate, however, that these errors may not be very serious from the practical standpoint.

The effects of salts other than sodium chloride in solutions in the mud filtrate or connate waters represent a problem which requires further study.

TABLE 5

Comparison of Observed and Calculated Data, Kern County Well

Depth Ft.	Temp. °C.	Self Potential (millivolts)		S P Difference		Calculated Connate Water Resistivity (ohm-meters at 64.4° F.)	
		Mud A (2.1 ohm-meters)	Mud B (0.62 ohm-meters)	Measured (millivolts)	Calculated (millivolts)	Mud A (2.1 ohm-meters)	Mud B (0.62 ohm-meters)
2,955-3,040	47.0	51.3	9.0	42.3	40.6	0.45	0.48
3,530-3,540	50.5	52.5	12.3	40.2	41.0	0.43	0.43
4,035-4,100	54.0	65.5	20.0	45.5	41.4	0.30	0.34
4,477-4,497	57.5	60.7	21.4	39.3	41.8	0.35	0.34
4,777-4,794	60.0	73.3	24.4	48.9	42.2	0.24	0.30
4,896-4,907	60.5	69.3	25.6	43.7	42.2	0.28	0.30
5,888-5,897	67.0	77.5	34.6	43.1	43.1	0.22	0.23
6,335-6,350	70.5	59.4	17.1	42.3	43.5	0.38	0.38
6,552-6,571	72.0	69.3	26.0	43.3	43.7	0.29	0.30
7,005-7,030	75.5	73.4	29.4	44.0	44.2	0.26	0.27
9,495-9,580	94.0	82.5	35.7	46.8	46.6	0.22	0.23
10,685-10,790	102.0	40.4	— 5.7	46.1	47.5	0.71	0.73

$$\rho_w = F\rho_c$$

The resistivity index is derived by dividing the true bed resistivity, ρ_t , by ρ_w , and the connate water content W , is obtained from this index using

For connate waters which are predominantly sodium chloride and for mud filtrates in which the cations are principally sodium, the relationships expressed by Figure 1 may still be satis-

factory. In the case of connate waters in which the sodium ion is not the predominant cation the relationships must break down. Laboratory and field studies alone will elucidate these complications. These studies are continuing.

ACKNOWLEDGMENTS

The writer is indebted to Mr. H. W. Patnode for his assistance in carrying out many of the laboratory experiments described and to Mr. A. C. Godbold and Mr. G. W. Ledingham for drawing his attention to suitable logs for use as examples. The writer's thanks for permission to publish this paper are due to Dr. Paul D. Foote, Executive Vice President, Gulf Research & Development Company.

REFERENCES

1. C. and M. Schlumberger and E. G. Leonardon: Electrical Coring; a Method of Determining Bottom-hole Data by Electrical Measurements. *Trans. AIME* (1934) **110**, 237-272.
2. C. and M. Schlumberger and E. G. Leonardon: A New Contribution to Subsurface Studies by Means of Electrical Measurements in Drill Holes. *Trans. AIME* (1934) **110**, 273-289.
3. W. D. Mounce and W. M. Rust: Natural Potentials in Well Logging. AIME Tech. Pub. 1626, *Petr. Tech.* (September 1943) **6** (5) 6 pp. Also *Trans. AIME* (1945) **164**, 288-294.
4. H. G. Doll: The S.P. Log, Theoretical Analysis and Principles of Interpretation. AIME, *Petr. Tech.* (September 1948).
5. P. Henderson: The Thermodynamics of Liquid Cells. *Z. Physik. Chem.* (1907) **59**, 118-127.
———: On the Thermodynamics of Liquid Cells. *Z. Physik. Chem.* (1908) **63**, 325-345.
6. Samuel Glasstone: Introduction to Electrochemistry, Chapter V. New York, 1942. D. Van Nostrand Co. 557 pp.
7. J. E. Sherborne and W. M. Newton: Factors Influencing Electrical Resistivity of Drilling Fluids. AIME Tech. Pub. 1466, *Petr. Tech.* (March 1942) **5** (2) 17 pp. Also *Trans. AIME* (1942) **146**, 204-220.
8. C. E. Marshall and C. A. Krinbill: The Electrochemical Properties of Mineral Membranes, V. Beidellite Membranes and the Determination of Sodium. *Jnl. Amer. Chem. Soc.* (1942) **64**, 1814-1819.
9. K. H. Meyer and J. F. Sievers: Permeability of Membranes. *Helv. Chim. Acta* (1936) **19**:—I. Theory of Ionic Permeability, 649-664; II. Studies with Artificial Selective Membranes, 665-677; III. (and H. Hauptmann) The Ionic Permeability of Layers of Nonaqueous Liquids, 948-962; IV. Analysis of the Structure of Vegetable and Animal Membranes, 987-995.
10. Torsten Teorell: An attempt to Formulate a Quantitative Theory of Membrane Permeability. *Proc. Soc. Exptl. Biol. Med.* (1935) **33**, 282-285. Also Farad. Soc. discussion to papers on Skin Potentials, *Trans. Farad. Soc.* (1937) **33**, 1054.
11. G. E. Archie: The Electrical Resistivity Log as an Aid in Determining Some Reservoir Characteristics. AIME Tech. Pub. 1422, *Petr. Tech.* (January 1942) **5** (1) 8 pp. Also *Trans. AIME* (1942) **146**, 54-62.
12. R. D. Wyckoff and H. G. Botset: The Flow of Gas-liquid Mixtures through Unconsolidated Sands. *Physics* (September 1936) **7** (9) 325-345.

DISCUSSION

☆

By Milton Williams, Humble Oil & Refining Co., Houston, Texas

Dr. Wylie has made an interesting approach to the solution of an intriguing and difficult problem. I wish to take issue however, with his implication that the shale, or Mounce, potential results from a mechanism which is electrochemically equivalent to a sodium concentration cell with transport.

Such a mechanism takes no cognizance of the fact that shale or other colloidal matter is a requisite to the development of the Mounce potential. It may be shown experimentally that only the expected liquid junction potential, usually of the order of 10 millivolts, is found when the two solutions of different salinities are separated by a barrier of low permeability non-colloidal material, such as cellophane, or fritted glass. On the other hand, naturally occurring shales or sandy shales of comparable permeability usually give relatively high Mounce potentials.

Following the same thought further, Dr. Wylie's concept gives only parenthetical consideration to the variation of the Mounce potential with variation of the character of the shale. I have had occasion to determine the values

of the Mounce potential for many shale samples, and have observed that the magnitude of the potential depends in a large measure upon the nature of the shale. Generally, the more hydrophilic the clay, the greater is the Mounce potential. Dr. Wylie's Figure 1, which gives no recognition to this dependence on the character of the shale, may therefore be misleading.

Another objection to Dr. Wylie's concept is that it may be shown experimentally that the Mounce potential is developed even when there is no ion common to the salts dissolved in the fluids separated by a shale barrier. For example, a shale barrier interposed between a relatively concentrated solution of sodium chloride and a dilute solution of, say, thorium nitrate, yields a Mounce potential of normal polarity and only slightly less magnitude than would be obtained if the thorium nitrate solution were replaced by a sodium chloride solution of the same molarity. If the molarity of the thorium nitrate solution be increased, and made greater than that of the strong salt solution on the other side of the shale, the polarity of the cell is reversed.

It is difficult to reconcile this behavior, as well as the dependence of the potential on the colloidal properties of the shale with the concentration cell concept. It appears likewise improbable that the explanation of the Mounce potential lies in the mechanistic concept of a shale barrier permeable only to particular ions.

An explanation of the Mounce potential which seems logical to me, and which is in keeping with experimental observations is briefly, as follows:

In its normal state, shale is in equilibrium, with respect to adsorption, with the saline water contained in its interstices. Chloride ion is more strongly adsorbed than sodium, so that the former is constrained by adsorptive forces, while the latter constitutes the contra-ion. When the shale is placed in contact with water, or with a dilute salt solution, a new adsorption equilibrium is approached. In attaining this new equilibrium, the sodium contra-ions may be supposed to diffuse away from the clay particles before the corresponding chloride ions are desorbed. This "leading" of the contra-ions should give rise to a potential effect, which may well be the Mounce potential.

As a corollary, the pH of the dilute solution should rise initially, then de-

crease as the initial migration of sodium ions is followed by desorption and migration of the chloride ions. Experimental work has indicated that such a change in PH does take place.

It might also be expected that colloidal materials other than clays would, under proper conditions, exhibit a Mounce potential. To test this, the compressed coagulum from a positive hydrous ferric oxide sol, which contained a high concentration of sodium chloride, was placed between strong and weak salt solutions. A Mounce potential of about 30 millivolts was observed, with the more dilute solution negative. A repetition of this test, using a coagulum of very coarse hydrous-ferric oxide, gave only a negligible potential.

The concept of the Mounce potential arising from the delayed migration of the more strongly adsorbed ions implies that the phenomenon is, in a relative sense, transient. That this is so is confirmed by experience both in the laboratory and, by numerous observations of gradually diminishing self-potentials, in logging practice in the field.

☆

*By Hubert Guyod, Well Logging
Consultant, Houston, Texas*

The paper's title conveys the impression that bore hole potentials comprise one or more significant components in addition to the electrochemical effect. This, however, does not seem to be substantiated by the experimental results discussed by the author in his paper, nor by some of the recent literature. A short statement expressing the author's view on this point would be of interest.

In view of the rather complete and interesting discussion offered by the author on the potential graphs from the Cypress sand section in Wayne County, Illinois, it would be of great value to other workers that the interstitial water analysis of this sand be included in the paper.

☆

*Author's Reply to Milton Williams
and Hubert Guyod*

Mr. Williams does not seem to be in accord with my concept of the mechanism of the electrochemical E.M.F. He does not, apparently, suggest any quantitative alternative explanation for the experimental observations made. However, it may be of interest to consider some of the experimental observations and theoretical comments made

by Mr. Williams in the light of the theory proposed in my paper.

The concept of a sodium concentration cell with transport as a quantitative explanation for the observed potentials recorded when the soluble electrolytes in the borehole and the connate water are sodium chloride is believed to be fundamentally correct. This case is probably the most important one in practice and was thus taken as a good example for use in a preliminary paper. It should be noted that if the anion of mud filtrate is not the chloride ion the effect on the total E.M.F. observed is twofold. Firstly the activity/resistivity relationship of the mud filtrate in terms of sodium ion activity and the resistivity of a sodium chloride solution is altered, and secondly, the value of the boundary potential between the mud filtrate and the sodium chloride in the connate water is no longer the simple relationship given in equation 6 above. For common mud filtrate anions such as sulfate, carbonate and bicarbonate, no serious activity error ensues as the appropriate calculations will show. The Henderson equation given as equation 2 above indicates that the predominant boundary potential influence, when the salinity of the connate water greatly exceeds that of the mud filtrate, is the principal salt in the connate water. Thus for the case of Na^+ as the principal cation in the mud filtrate and sodium chloride as the principal electrolyte in the connate water, the curves given in Figure 1 are essentially accurate.

As regards the existence of colloidal material in the shale to act as a source of the observed potential this is not disputed, except that the material need not necessarily be colloidal to produce analogous electrical effects. See, for example, the work of Marshall¹ using natural zeolites. Many materials which have a charged lattice will give rise to electrochemical potentials of the type under consideration. In this connection the papers by Sollner^{2, 3, 4} concerning membrane potentials in general and those across oxidized collodion membranes, in particular, provide an excellent introduction to the subject. In the case of shales, the fixed anionic charges which give rise to the observed potentials, according to the theory of Meyer and Sievers and of Teorell, are almost certainly those resulting from dissociation of the cations of the clay minerals.

These references are listed at end of author's reply.

Any membrane made from a charged sol will similarly give rise to a potential which will tend to the Nernst potential. The magnitude of the potential will, however, depend upon the charge on the sol forming the membrane and the degree of anionic conductivity within the membrane. Negatively charged membranes will be similar to shales, while positively charged membranes will respond to the activities of the anions present in the solutions in contact with them.

It is fully recognized that shale barriers will give rise to potentials when they separate solutions containing no common ions. These cases are covered by the theory of Meyer and Sievers and of Teorell quoted above. The potential is essentially dependent for sign and magnitude on the ratio of the activities of the cations on either side of the shale barrier and their relative mobilities within the shale barrier. On this basis Mr. Williams' results with thorium nitrate and sodium chloride could probably be explained both qualitatively and quantitatively.

The pH effects noted by Mr. Williams would follow from the fact that the current through the shale is mainly carried by cations, frequently sodium ions. Thus migration of these cations into the dilute solution will raise the pH. Correspondingly the pH in the concentrated side goes down, and in relatively small volumes of solution, if they are not changed periodically, some of the current is eventually carried to the low concentration side by hydrogen ions, resulting in a subsequent pH decrease on that side.

The fact that the Nernst potential may not be attained at high concentrations of electrolytes if the thermodynamic charge on the active materials in the shale is insufficient, was pointed out in my paper. The Conemaugh shale examined was a laboratory example of this effect and doubtless there are many others. A similar effect arises if there are physical imperfections, such as cracks, in the small shale samples examined. This makes laboratory work on the problem difficult although fractures can generally be detected. Calculations made from electrical logs tend to show that shales in situ frequently give closer approximations to the Nernst potential than do small laboratory samples of the same shale. This aspect of the problem needs further elucidation by the study of appropriate field data.

The falling off of potential with time which is frequently observed in boreholes may be due to equalization of the concentrations of the mud filtrate and connate water electrolyte concentrations caused by current flow in the borehole. The effect of mud filtrate invasion of the formation with time, which also leads to diminution of the S.P., has been ably demonstrated by Doll in the paper listed above, and it may be this effect which is predominant, since the solution volumes are relatively enormous, and concentration changes will thus be small.

It seems unfortunate that the excellent work of Mounce and Rust has led to the original work of C. and M. Schlumberger and E. G. Leonardon being largely forgotten. On re-reading the contributions of the latter workers, I would like to pay tribute to the fact that their original paper⁵ these workers showed that impervious materials such as shales and clays gave rise to an electromotive force which caused a current to flow from a porous bed through the impervious material to the mud in the borehole. They were thus responsible for the original shale cell concept, or electrochemical potential

effect, in well logging, which Mounce and Rust subsequently re-emphasized so effectively. I must apologize for not making this clear in my introduction.

Mr. Guyod's remarks are singularly germane. In writing my paper I have deferred to the rather widely held belief that in certain cases streaming potential or electrokinetic effects are of importance. It is hoped to deal with some aspects of this problem in a later paper, but I may say here that in rotary drilled wells it is my present belief that streaming potentials do not appear to be of very significant moment and to a first approximation, the S.P. may be treated as a simple electrochemical effect.

The Cypress sand example quoted is of considerable interest. It was pointed out in the paper that the absolute value of the connate water resistivity computed was not accurate, although the agreement in the three values obtained in Table IV showed that the Nernst equation was being obeyed. The mean resistivity of 0.033 ohm-meters at 64.4° F. represents a completely saturated sodium chloride solution, whereas the best information we possess regarding the salinity of the connate water in

this sand indicates a value of about 150,000 p.p.m. This error results from the employment of resistivities instead of activities in the calculations, since the ratio on the ordinate scale on Figure 1 is properly one of activities. Recalculating on the basis of computed activities gives a connate water salinity of 200,000 p.p.m. This value is obtained using the mud resistivity to compute the mud activity and hence, from the ratios obtainable from Figure 1, the connate water activities. A better value would probably have been obtained had the mud filtrate resistivity been available. The inaccuracies resulting from the use of resistivities instead of activities become progressively more serious as connate water salinities exceed about 60,000 p.p.m.

¹C. E. Marshall: The Use of Zeolitic Membrane Electrodes. *J. Phys. Chem.* (1939), 43, 265.

²Karl Sollner: The Nature of Physicochemical Membranes as Physicochemical Machines; Preparation and Properties of Membranes of Highly Pronounced Electrical Properties. *J. Phys. Chem.* (1945), 49, 47.

³Karl Sollner: The Physical Chemistry of Membranes with Particular Reference to the Electrical Behavior of Membranes of Porous Character II. *J. Phys. Chem.* (1945), 49, 171.

⁴Karl Sollner: The Physical Chemistry of Membranes with Particular Reference to the Electrical Behavior of Membranes of Porous Character III. *J. Phys. Chem.* (1945), 49, 265.

⁵Reference 2 of the paper under discussion, page 278.

SEMI-AUTOMATIC POWER-OPERATED DRILLING MACHINERY

MARTIN E. TRUE, MEMBER AIME, HUMBLE OIL & REFINING CO., HOUSTON

BERT L. STONE, CONSULTING ENGINEER, PALOS VERDES ESTATES, CALIFORNIA

ABSTRACT

To cope with the problems encountered when drilling at greater depths and to reduce the amount of physical effort required on the part of drilling crews in making round trips, a new type of semiautomatic power-operated drilling machinery has been developed which permits round trips to be made without the drill pipe being touched by hand. This equipment consists of hydraulically operated tongs which perform the stabbing, spinning, and tonging operations, and two power-operated racking units mounted in the derrick for carrying the pipe to and from the center of the hole and positioning it on the mat and in the rack. With this equipment all of the operations of the various units are controlled remotely by manipulation of hydraulic valve levers and electric switches.

INTRODUCTION

As horsepower rises to meet the demand for deeper drilling, it is necessary to increase the weight of surface drilling equipment. Also, the duration of repetitive operations in making round trips to change bits is greatly increased with depth. Harder formations encountered at greater depths reduce bit life rapidly, resulting in more frequent round trips and in some instances more time is consumed in changing bits than in drilling.

Since the introduction of the first rotary employed to drill for oil in 1895¹, there has been relatively little change in the general procedure for making up, breaking out, stabbing, and racking drill pipe in making round trips to

change bits. The conventional method of making round trips with the drill pipe requires that drilling crews lend strenuous physical assistance to manually operated tools.

Although many new devices have been developed to improve efficiency, increase speed of making round trips, improve safety, and reduce the amount of physical effort required in handling drill pipe, it is considered a vital necessity to substitute automatic or semiautomatic power-operated machinery for many of our more or less manual operations if extremely deep drilling is to be carried out successfully on a production basis in the same manner as our shallower drilling of today.

Field tests have been made of remotely controlled power-operated tongs, spinner, stabber, and racking equipment. The tongs, which include a built-in pipe spinner, are mounted on a column, are capable of gripping and supporting the weight of a 90-foot stand of drill pipe, and are provided with means for moving the pipe vertically as well as to and from the center of the hole. The racking equipment consists of two units, one at the level of the conventional monkey board and the other at the first girth on the ladder side of the derrick.

Most of the physical effort of making round trips with drill pipe has been eliminated in that all of the operations of tonging, spinning, stabbing, and racking of pipe on the floor are controlled by an operator in a seated position by manipulation of hydraulic and electric valve levers and buttons. The driller is relieved of operating the cathead, leaving only the hoisting and slips to be controlled. Complete round trips are made without the drill pipe being touched by the drilling crews.

Although the speed of pulling or running a single stand with the power-operated equipment is approximately the same as that with conventional equipment, it is possible to maintain this rate for long periods, whereas fatigue slows crews working conventionally during round trips, especially under adverse weather. After completing round trips with this equipment, drilling crews are not exhausted, consequently, are able to perform effectively their duties while drilling, which is essential for maximum over-all efficiency. Safety is substantially improved as the derrickman performs his duties from a platform enclosed by rails and the tong lines and spinning chain are eliminated from the derrick floor. The hazards encountered in racking drill pipe on the floor and in stabbing are also eliminated. Figure 1 shows a drawing of a derrick equipped with the power-operated drill pipe handling equipment.

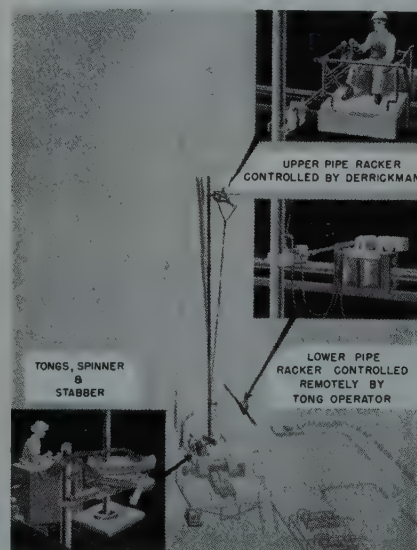


FIGURE 1—POWER OPERATED TONGS, SPINNER, STABBER AND PIPE RACKER.

Manuscript received at office of the Branch August 30, 1948. Paper presented at Division Fall Meeting, Dallas, Texas, Oct. 4-6, 1948.
¹ References are given at the end of paper.

METHOD

Remotely Controlled Pipe Racker

The remotely controlled pipe racker consists of two electrically powered arms, one between the eleventh and twelfth girths and one just above the first girth on the ladder side of the derrick. Each arm, which consists of a three-inch diameter, twelve-foot long screw having two threads per inch and three equally spaced keyways through the threads parallel to the axis of the screw, is caused to move in and out perpendicular to the side of the derrick in a horizontal plane. Each arm or screw is mounted on a carriage which in turn is supported on tracks attached to the ladder side of the derrick in openings which permit eight feet of travel for the upper unit and ten feet for the lower unit across the side of the derrick.

Upper Racking Unit

The upper racking unit, consisting of the carriage and arm, is equipped with a working platform having dimensions approximately the same as those of the conventional monkey board. This platform is enclosed with a rail 30 inches in height and is provided with a swivel seat adjustable in height. The end of the racking arm, which moves to and from the center of the derrick, is provided with a claw which automatically encircles the pipe on contact and is used for positioning the upper end.

Figure 2 (Page 29) shows a view looking down from the top of the derrick of the traveling monkey board and racking arm just before the claw engages a stand of drill pipe and Figure 3 shows a lower view of the same equipment after the pipe has been engaged by the claw.

Figure 4 shows a view of the racker removing pipe from the rack and Figure 5 shows a lower view of the racker moving pipe into the elevators. Figure 6 shows the position of the racker at the time the elevators are latched.

Referring to Figures 2 and 5, the claw consists of a "U" shaped fork that encloses 180 degrees of the circumference of the pipe and a hydraulically operated latch which is automatically closed around the pipe on engagement.

The claw latch is actuated by an arm which controls a solenoid valve admitting hydraulic fluid to a cylinder and piston. The claw assembly is provided with a knuckle joint and a pressure release as a safety measure in case the elevators are accidentally lowered onto it.

Transverse movement of the carriage and monkey board is produced by a stationary 3-inch diameter lead screw mounted parallel to the carriage track shown in Figure 3. A nut on the screw is powered by a 2-horsepower, 220-volt, 3-phase electric motor drive. The racking arm screw is likewise powered by a 3-horsepower electric motor driving a nut supported by bearings on the carriage assembly frame.

Control of the upper racker is accomplished by a single lever, shown in Figure 2, which has eight positions for actuating microswitches that determine the movement of the racking arm and carriage. Separate movement of the arm and carriage can be obtained or a combination movement of both will occur by proper positioning of the controller. The claw is released from the pipe by pushing the button shown on the control lever in Figure 2. Microswitches are provided with adjustable stops which provide means for limiting the travel of the carriage and racking arm screws to prevent jamming and to provide means for bringing the units automatically to a predetermined position.

Lower Racking Unit

The lower racking unit is essentially the same as that of the upper without the working platform. It consists of a carriage which moves back and forth across the side of the derrick and is provided with a power-operated screw or arm which travels out and in for positioning the lower end of the drill pipe. The end of the racking arm moves to and from the center of the derrick and is connected by a linkage to an auxiliary elevator which is provided to support the weight of the pipe and transfer it from the tongs to an elevated pipe mat. Figure 7 shows the lower racker transferring a stand of pipe from an elevated mat into the jaw of the make-up tong and Figure 8 shows a rear view of the lower racking unit mounted in the derrick just above the

first girth.

The auxiliary elevator, shown in Figure 9, consists of a "U" shaped member which is built to fit around the drill pipe being racked. A hydraulically operated spring returned cam with teeth located in one leg of the "U" shaped member is rotated into engagement with the pipe for hoisting. The elevator unit is provided with means for swiveling to accommodate any lean of the pipe that may be encountered. A hydraulic cylinder, mounted at the eleventh girth, is connected by a cable to the auxiliary elevator and is energized from the control panel on the derrick floor. The control for the lower racker is similar to that described for the upper unit and is mounted on the tong panel. Figure 10 shows the auxiliary elevator supporting a stand of pipe as it is being transferred from the tongs.

To facilitate moving, both the upper and lower power-operated pipe rackers, shown in Figure 11, are mounted on a single skid. The racking arm screws are pivoted on their frames and anchored in a position parallel to the carriage tracks.

Power-Operated Tongs

The power-operated tongs, shown in Figure 12, consist of two pipe-gripping units mounted on a side bracket attached to a hydraulically operated column with its base anchored rigidly to the derrick substructure. The upper portion of the column to which the tongs are attached is capable of a vertical travel of three feet, permitting operation at any height in that range and allowing the driller a liberal tolerance in setting the slips. The back-up tong unit is provided with a hydraulically operated gate and latch, actuated by a valve on the control panel, and a gripping cylinder which is energized by sequence valves causing the lower unit to grip the tool joint automatically after the gate has been closed. The make-up tong, mounted just above and on the back-up tong, is provided with an identical mechanism for opening and closing the gate and latch but requires the manipulation of a special control lever to produce a gripping force on the pipe. This tong is also provided with a pair of power driven rollers, shown in Figure

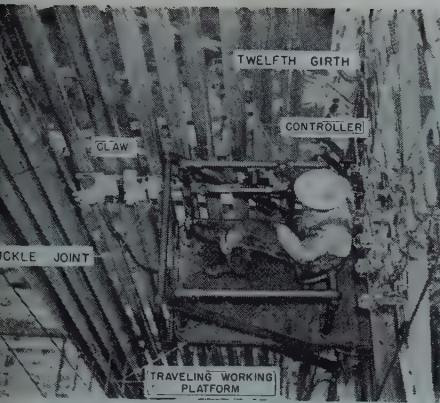


FIGURE 2
UPPER RACKING UNIT WITH CLAW APPROACHING STAND OF PIPE

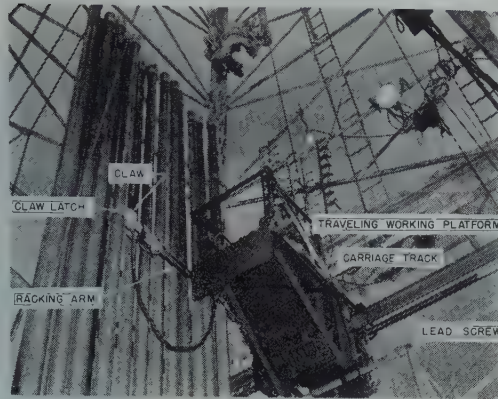


FIGURE 3
DRILL PIPE BEING REMOVED FROM RACKING FINGERS BY UPPER RACKER

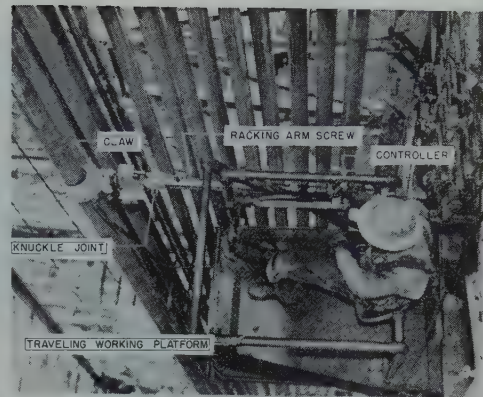


FIGURE 4
DRILL PIPE BEING REMOVED FROM RACKING FINGERS BY UPPER RACKER

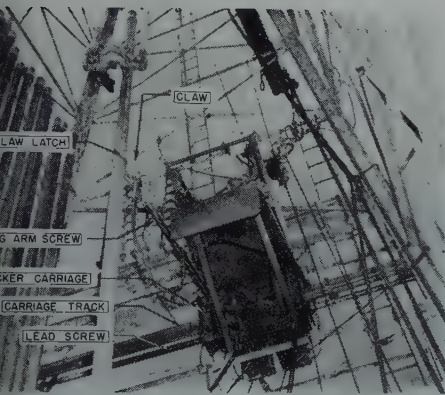


FIGURE 5
UPPER RACKER MOVING DRILL PIPE INTO ELEVATORS

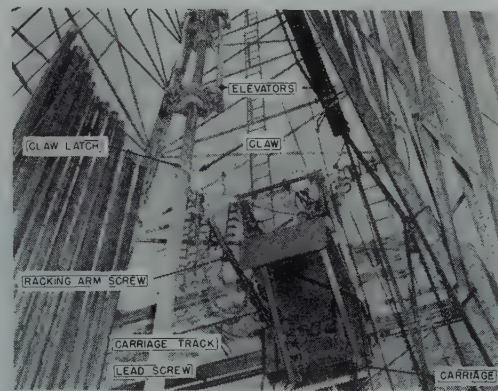


FIGURE 6
ELEVATORS LATCHED AROUND DRILL PIPE BY UPPER RACKER

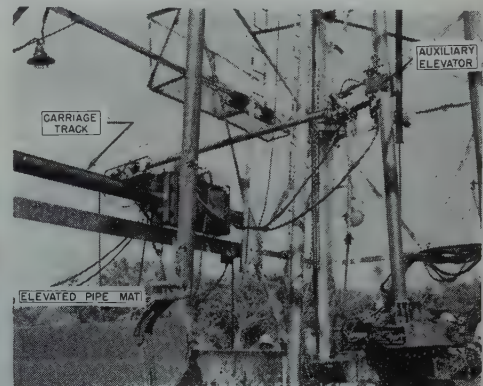


FIGURE 7
PIPE RACKER TRANSFERRING A STAND OF DRILL PIPE FROM MAT TO TONGS AT EXCHANGE POSITION



FIGURE 8
REAR VIEW OF LOWER PIPE RACKER

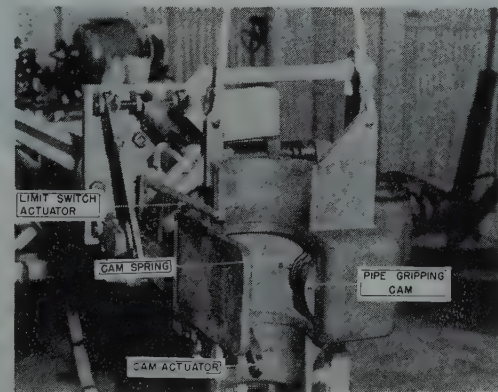


FIGURE 9
SINGLE STAND AUXILIARY ELEVATOR

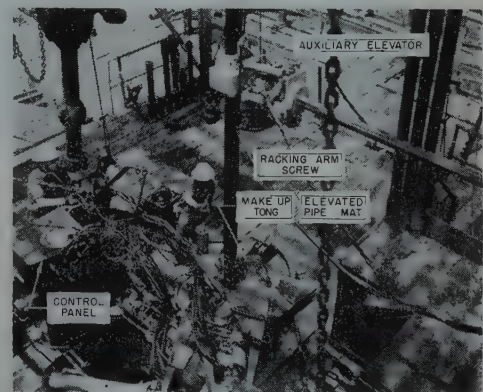


FIGURE 10
AUXILIARY ELEVATOR SUPPORTING A STAND OF DRILL PIPE AS IT IS REMOVED FROM THE TONGS

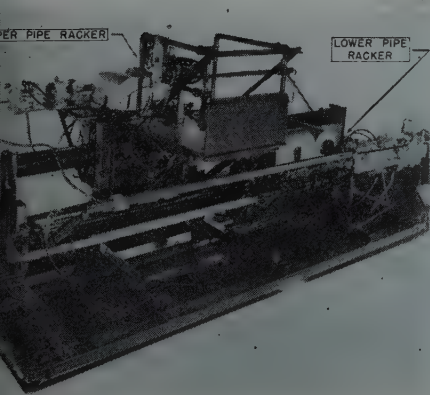


FIGURE 11
UPPER AND LOWER PIPE RACKERS MOUNTED ON SKID
February, 1949



FIGURE 12
POWER-OPERATED TONGS
PETROLEUM TRANSACTIONS, AIME

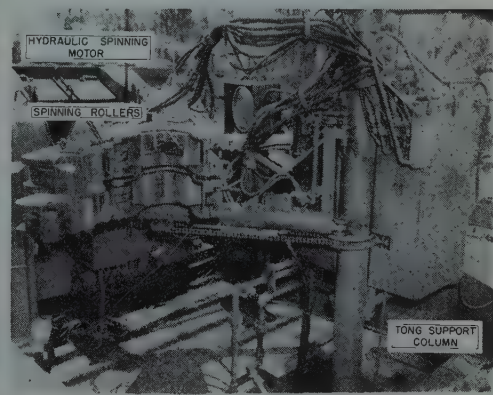


FIGURE 13
POWER TONG SPINNING ROLLERS

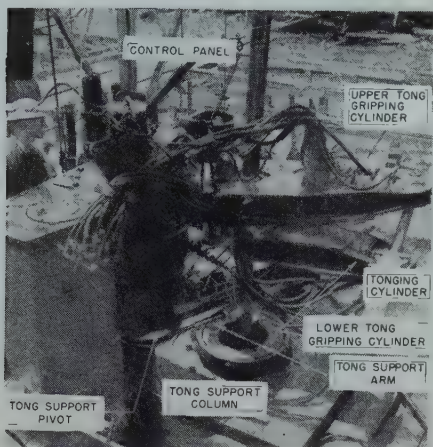


FIGURE 14
MAKING UP DRILL PIPE WITH POWER TONGS

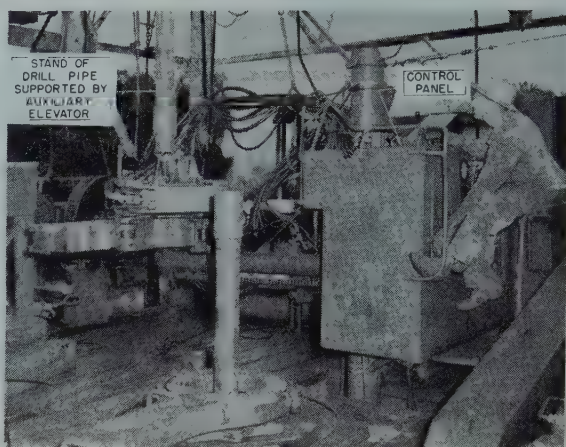


FIGURE 15
POWER TONGS JUST BEFORE MOVING UP TO GRIP AND SUPPORT
STAND OF DRILL PIPE

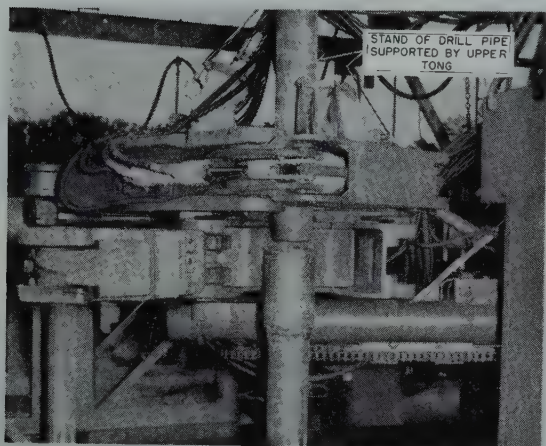


FIGURE 16
POWER TONGS STABBING DRILL PIPE

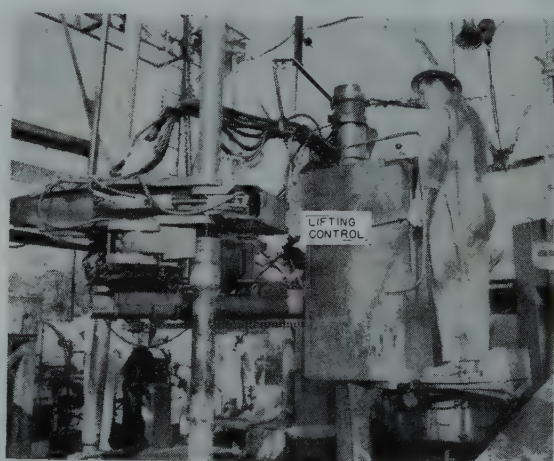


FIGURE 17
POWER TONGS LIFTING STAND OF DRILL PIPE AFTER SPINNING OUT

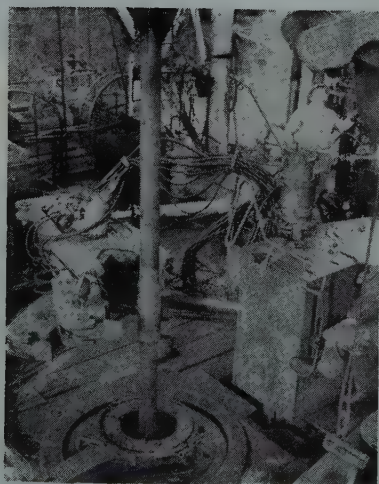


FIGURE 18
POWER TONGS MOVING INTO POSITION
TO BREAK TOOL JOINT

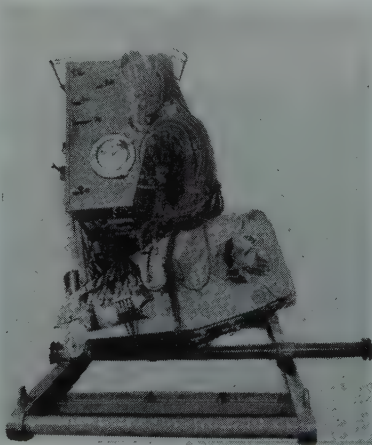


FIGURE 19
END VIEW OF POWER TONGS MOUNTED
ON SKID



FIGURE 20
SIDE VIEW OF POWER TONGS MOUNTED ON SKID

13, which are moved through the tong jaws by hydraulic pressure for engaging the pipe to produce the spinning operation.

The spinning rollers are capable of developing 1,950-foot pounds of torque when operating at 2,500 pounds per square inch hydraulic fluid pressure. A maximum force of 28,000 pounds can be exerted against the rollers for spinning. The spinning rollers which are six inches in diameter and capable of a speed of 147 rpm are powered by a hydraulic motor driving through sprockets and chains.

Make-up or break-out with the tongs is accomplished by a scissor action produced by a hydraulic cylinder, shown in Figure 14, connecting the two outer ends of the tongs. The tongs are capable of gripping from $2\frac{7}{8}$ -inch tool joints up to and including 8-inch OD drill collars. Each of the tongs can exert a gripping force of 400,000 pounds at an operating pressure of 2,500 pounds per square inch. The maximum tong make-up pressure is 591,000-pound inches and the maximum break-out pressure is 1,440,000-pound inches when operating at 2,500 pounds per square inch. Normal operating pressure is 1,500 pounds per square inch although 2,500 pounds per square inch is used for maximum torque and gripping force.

The hydraulically operated column, tong support, and tongs are capable of supporting the weight of a stand of 5-inch OD drill pipe. During normal operations, the lower racker is used for moving the stands of drill pipe to or from an exchange position which is approximately 4 feet from the center of the rotary in the direction of the draw-works on an arc scribed by rotation of the tongs on the column.

With the stand of drill pipe in the exchange position supported by the rackers and auxiliary elevator, Figure 15 shows the position of the tongs just before being raised to grip the tool joint in the case of going in the hole or the position after releasing the long grip in coming out of the hole. Figure 7 shows the tool joint in the jaw of the make-up tong. The tongs are shown in the stabbing position in Figure 16. Figure 17 shows the position of the unit prior to closing the gate on the back-up tong and spinning going in the hole or

immediately after spinning when coming out. Figure 18 shows the power tong unit moving onto the drill pipe after the slips have been set for breaking the tool joint.

The current procedure, used in coming out of the hole is to break the tool joints with the tongs, release the grip, and open the gate of the back-up or lower tong, and spin out with the rotary table. An alternate method to accomplish this is to rotate the stand of pipe out with the spinner.

Power for the spinner, tongs, and controls is supplied by a 35-horsepower pump and precharged piston and cylinder-type hydraulic accumulator.

Figures 19 and 20 show the power tongs mounted on a skid for moving. The entire unit, including controls, are unitized, requiring the connection of two hydraulic lines and one electrical plug.

Operation of the Remotely Controlled Power Tongs and Pipe Racker

All of the movements of the upper end of the drill pipe are by the racking arm, the derrickman's only manual operation being to unlatch the elevators when coming out of the hole. All tonging operations and pipe handling on the derrick floor are controlled remotely by the tong operator from either a standing or seated position on the control panel platform attached to the moving portion of the tong support column. One man is required on the floor for latching and unlatching the elevators.

Coming Out of the Hole

By the time the slips have been set, the jaws of the power tongs have been moved around the tool joint at the proper height following which the gates are latched, pressure is applied to the gripping jaws, and a 30-degree scissor action is produced to break the tool joint. The upper tong grips the lower end of the stand being broken out and produces a slight upward force as the spinning operation is accomplished with the rotary table. After the break-out operations are completed on the floor, the derrickman pulls the upper end of the stand in the direction of the monkey board by means of the power-operated

arm and in turn unlatches the elevators with the assistance of the catline. As soon as the threads clear the tool joint box, the lower end of the stand is carried to the transfer position by the break-out tong accomplished by rotating the tongs about the column through an arc of approximately 50 degrees. The transfer position, approximately four feet from the center of the rotary, allows clearance for the traveling block to return to the floor. The lower racking arm supporting the auxiliary elevator engages the pipe, lifts it from the tong, and moves it to and positions it on the elevated mat. The lower racker then returns automatically to the approximate vicinity of the exchange positions. The derrickman racks the upper end simultaneously with the lower.

Going Into The Hole

Both the upper and lower racking arms engage and pick up a stand of pipe from the mat and racking fingers and move it to the transfer position. The derrickman centers the racking arm and holds it in an approximately vertical position. With the lower end of the pipe supported by the auxiliary elevator moved to the transfer position by the lower racker, the make-up tong jaws move up around the tool joint which, in turn, is energized for gripping and supporting the entire stand. The operator then rotates the tong unit through a 50-degree arc in the direction of the center of the hole and lowers the column to allow the tool joint pin to enter the box. The make-up tong grip is released and the spinning rollers are energized, rotating the stand of pipe in a clockwise direction until shouldered. The make-up is completed by a clockwise rotation of the make-up tong to produce the final tightening. While the tonging operation is in progress, the derrickman moves the upper end of the stand into the open elevators, Figures 5 and 6, which automatically latch around the pipe. A conventional side door type elevator with a special toggle latching linkage is used with this equipment. While the stand of pipe is being lowered into the hole and the empty elevators returned to the top of the pipe, the tong operator and the derrickman have moved the next stand into the transfer position.

CONCLUSION

Although the power-operated tongs, spinner, stabber, and racking equipment have been used for drilling two wells to depths below 10,000 feet, the equipment is yet in the experimental stage and final development will be reached as drillers and their crews use it and suggest modifications and improvements.

REFERENCE

1. I. F. Bingham: Present Trend in Rotary Well Drilling and Completion. *The Science of Petroleum*, Volume 1, Pages 406-429.

DISCUSSION

☆

By J. M. Clark, *The Chicago Corp., Corpus Christi, Texas*

The semi-automatic drilling equipment described in this paper is certainly a big stride toward eventual full automatic operation. There are, however, certain considerations which must be taken into account as the new devices are developed. The chief advantage is in relieving the driller of sev-

eral routine operations which he must perform on a conventional drilling rig while making a "round trip". Most new conventional rigs have placed too many operations in the driller's hands.

A question of prime importance is, can all of the equipment described in this paper be instantly and surely disengaged in the event of power or mechanical failure? If this is not true, the drill stem might "freeze" in open hole in an emergency.

Conventional drilling equipment provides a dependable means of lifting drill pipe stands from the floor mat to the height required for tool joint make-up and vice-versa. Equipment to mechanically swing the stands to the desired positions could be very advantageous, but it would seem that a mechanism which also lifts the stands duplicates a function of the hoisting elevators and results in too many complicated devices. In addition, the weight of a stand while being lowered to the floor mat of a conventional set-up, helps accelerate the traveling blocks on the empty trip down. When a large number of lines are strung, traveling blocks accelerate slowly, thus lengthening trip time.

Drilling rigs have increased in size

to meet the demand for deeper drilling, but it should be noted that in spite of heavier equipment, the new rigs and the derrick floor tools are easier on the crew than the older lighter rigs. Tools are easier to handle, quite often, not because they are automatic, but because they are better designed and balanced.

Much of the fatigue resulting from repetitive operations of round trips is mental rather than physical, and semi-automatic tools will not necessarily be of great help. In fact, a reasonable amount of physical effort helps to relieve the monotony of a long round trip. Efficient automatic equipment which lessens the skill required to operate, promotes safety and frees personnel for other duties, should compensate for the extra investment and complexity, but semi-automatic equipment may retain the main disadvantages of both automatic and manually operated tools; that is, the intricate devices necessary for semi-automatic operation are, of course, more subject to breakdown than conventional tools, but they may not lessen the mental fatigue or required operational skill. Judging solely from a brief study of this paper, the tools described would seem to come under the latter category. ★ ★ ★

THE CORE RECORDER

CLARK MILLISON, CONSULTING GEOLOGIST, TULSA, OKLAHOMA

ABSTRACT

The core recorder, a mechanical instrument for determining the exact depth at which core is recovered, drilled up or lost, is described. Examples of charts from the recorder are explained and interpreted. The uses of the core recorder are discussed.

INTRODUCTION

In the experience of geologists and engineers during coring operations on drilling wells, many will recall the times when a full core was not recovered and particularly when the requirement was urgent that they know exactly what part of the core was lost. To make this determination, the core recorder was designed. Its uses are many, and only the most obvious will be presented here. Although this discussion will be limited to drilling wells for petroleum, the core recorder can be used in any type of coring operation.

The principle of the core recorder is the proportional reduction of the motion of core entering or dropping out of the core barrel to a stylus moving in such a manner as to record the reduced motion on a chart. The time element is registered on the same chart by the revolution of a clock which turns the chart drum. Thus the exact amount of core entering or dropping out of the core barrel is charted and the time of such entry or exit from the core barrel is precisely correlated to the depth at which the core is recovered or lost. Lack of movement of the stylus which is revealed by the continued revolution of the chart drum indicates that no core is entering the barrel.

The principles are accomplished by an instrument placed inside of the core barrel. A cylinder which contains the clock and mechanical apparatus has a

diameter smaller than that of the core barrel. Near the top of the cylinder is an eighteen hour clock which turns the drum that contains the chart. Near the

bottom of the instrument is a serrated wheel which by friction against the inside of the core barrel is turned as core enters or drops out of the barrel.

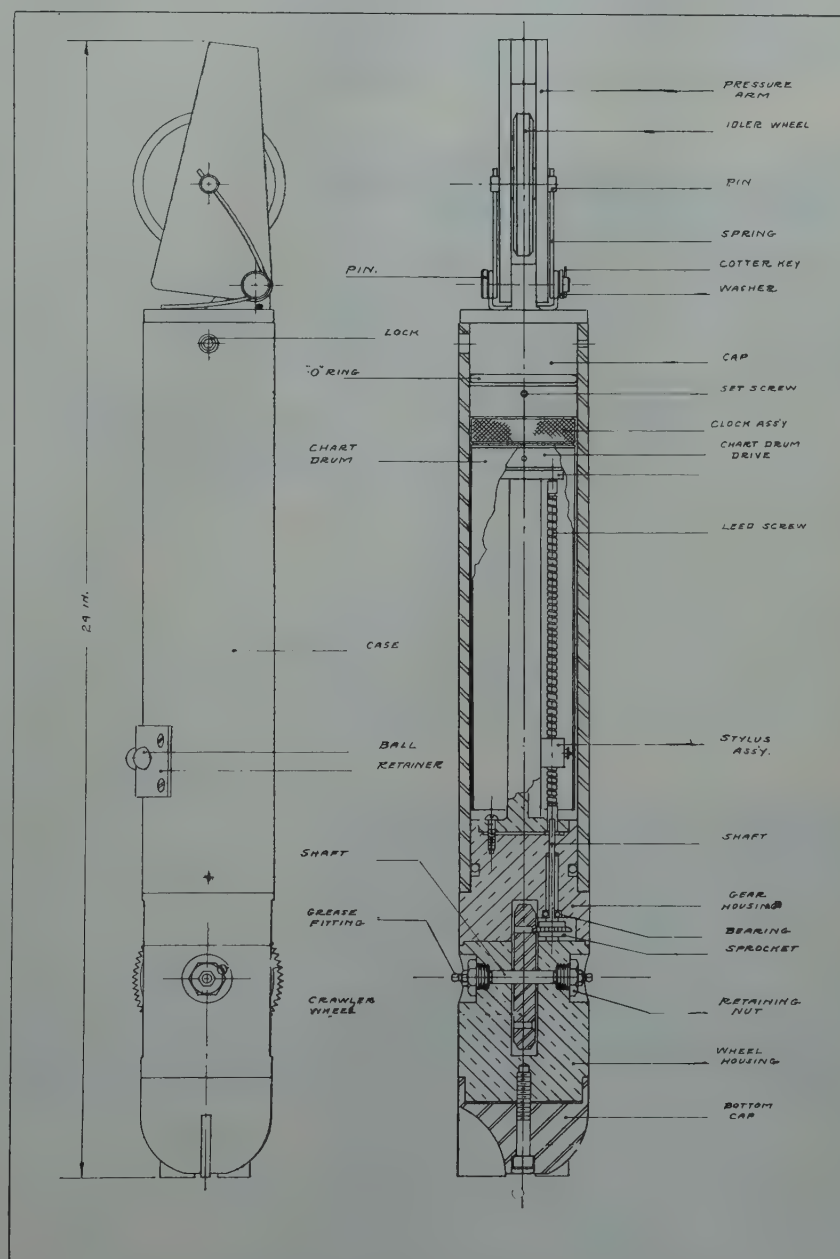


FIG. 1 — DETAILED VIEW OF THE CORE RECORDING INSTRUMENT.

Manuscript received at office of the Branch August 2, 1948. Paper presented at Branch Fall Meeting, Dallas, Texas, Oct. 4-6, 1948.

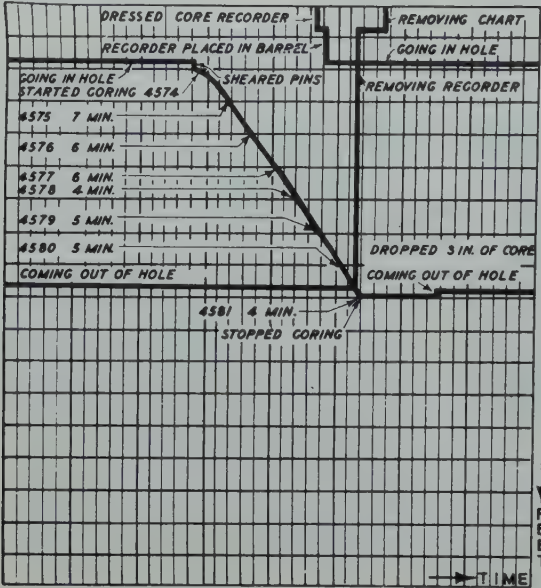


CHART 1—CORE RECORDING CHART WHERE FULL RECOVERY WAS OBTAINED.

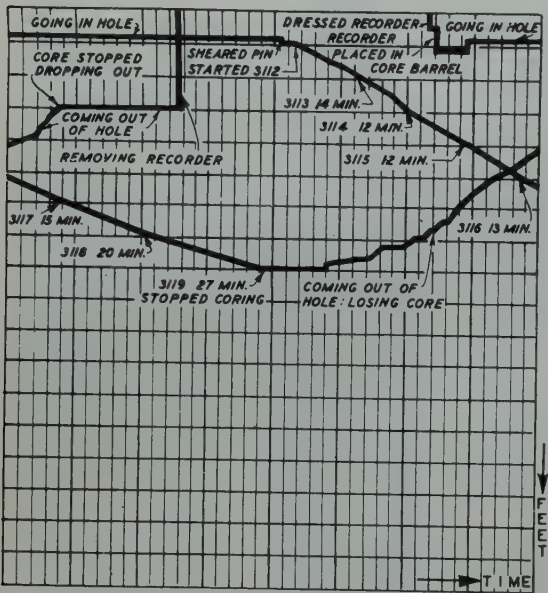


CHART 2—SHOWING THAT CORE IS NOT RECOVERED UNDER SOME CIRCUMSTANCES.

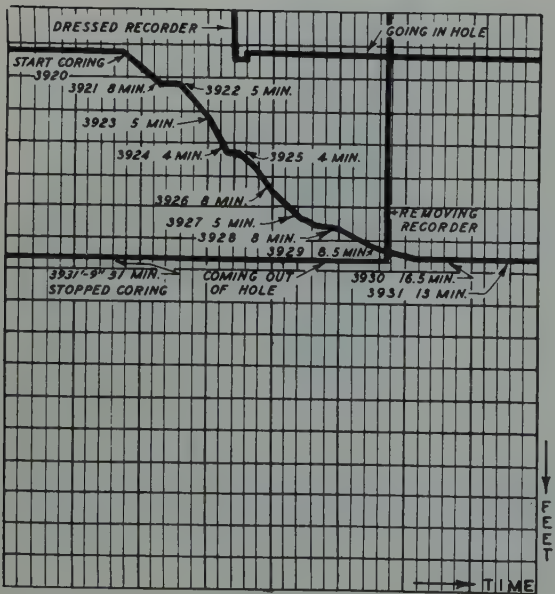


CHART 3—SHOWING THE RESULTS OF A DEFECTIVE CORE CATCHER.

To insure a positive friction against the barrel, a spring loaded idling wheel at the top of the instrument causes a stress against a ball bearing fulcrum below the center of the instrument which forces the serrated wheel against the inside of the barrel. The movement of the serrated wheel is transmitted through a sprocket to a lead screw on which a spring loaded stylus travels. The distance the stylus travels is in direct ratio to the length of the core barrel.

The vertical movement of the instrument is recorded on the chart by the stylus, and at the same time the clock is turning the chart horizontally. Consequently if core is entering the barrel, the stylus moves upward. If the core is being drilled up and none is entering the barrel, the stylus does not move but the clock continues to turn the chart. If core drops out of the barrel, the stylus moves downward.

Time of the coring operation is kept at the surface in the usual manner except that the time the recorder is placed in the barrel and the time it is removed are also recorded. Thus, the time it takes to go into the hole, the time required for each foot drilled and the time that is necessary to come out of the hole is known. A sort of closed traverse is recorded. Correlation of the time kept at the surface against the time recorded by the clock will reveal all of the events that occurred during the entire operation.

As examples of the charts made by the core recorder, the following cases offer many of the various types of occurrences. The first shows a case in which full recovery was obtained. The horizontal line near the top is that made by the stylus while resting on the plug during the operation of going in the hole. The first vertical line indicates when the pins in the plug were sheared. As core entered the barrel and the clock turned the chart, the individual feet cored were recorded. When the coring operation ceased, the stylus discontinued its movement and a horizontal line was made. As the core bit was lifted off of bottom, three inches of core dropped out as recorded by the small downward movement of the stylus. The next downward line shows when the core was removed from the barrel.

The second chart shows that core is not recovered under several different

circumstances. The second foot cored, from 3921 to 3922 feet, was not recovered although it took only five minutes to drill the foot. Conversely the last foot and nine inches took 44 minutes to drill and none was recovered. This record is from a well that cored from the Simpson dolomite into "Wilcox" sandstone. One and one half feet of sandstone was recovered. By analyzing the chart, the top of the sandstone could be determined at 3926½ feet and this information could not be determined from the core, samples, or drilling time. To show an example of the detail which can be expected from the core recorder, an analysis of this chart is presented.

The third chart shows the results of a defective core catcher. The sandstone which was cored is about 13 feet thick in this area. Eight feet of sandstone were drilled when it was decided to core. The coring time indicated that a slower drilling formation was encountered after coring five feet. Two more feet were cored, and the barrel was removed from the hole. Only two feet

of core was recovered, and it was shale. The presumption was made that five feet of sandstone had been drilled up, and only the two slower drilling feet, which were presumed to be shale, were recovered. But the core recorder showed that full recovery had been obtained and that five feet had dropped out of the barrel on the way out of the hole. Only the top two feet were left in the barrel, and the entire core was shale below the sandstone which had thinned at this particular location to eight feet.

If it is attempted by coring to find the top of a producing formation, the core recorder can be used with great benefit. Loss of core would make it difficult to establish the exact top of the producing zone and consequently the geological information, the drill stem test seat, and the casing seat would be questionable.

If a loss of core occurs while coring a producing formation the core analysis is inexact. A side wall core at the exact depth where core is lost can be taken

and it will supply the lacking data. A comparison of the core recording chart with the electric log will supply oftentimes the type of rock that was lost from the core.

Perhaps one of the most beneficial result of the use of the core recorder is the possibility of improving coring technique. While using the recorder, the data such as pump pressure, rotary table speed and weight, should be kept and correlated with recovery percentages. The experience with the recorder has been too limited to offer any concrete suggestions, but it is believed an accumulation of such data will offer improvements in technique and in the amounts of core recovery.

Only coring operations in holes drilled for petroleum have been considered in this paper. The core recorder might be useful in mining operations, holes cored for dam and bridge sites, and water wells. The instrument is simple enough to be adaptable to any coring operation.

★ ★ ★

EFFECTS OF TRANSIENT CONDITIONS IN GAS RESERVOIRS

D. T. MacROBERTS, MEMBER AIME, UNITED GAS PIPE LINE COMPANY, SHREVEPORT, LOUISIANA

ABSTRACT

A simple disturbance in a gas reservoir travels with a finite velocity which is nearly independent of the amplitude of the disturbance. As a result very complex transients may be set up which seriously affect observation at a well. The time of transient is much longer than commonly supposed.

INTRODUCTION

A change in pressure at a gas well is not propagated through the reservoir instantaneously but with a definite finite velocity. Knowledge of the period of this transient is of value because:

- 1. Observations of pressure and flow-rate during the transient may affect interpretation of back-pressure tests.
- 2. Interference effects between wells may be used to determine continuity of formation.
- 3. Additional information concerning the physical characteristics may possibly be deduced from the behavior of a well during the transient.

MATHEMATICAL DEVELOPMENT

It will be assumed that the well is initially closed in and that the pressure is constant throughout the reservoir. As the initial disturbance passes outward from the well it is further assumed that a logarithmic pressure distribution is established between the most distant point reached and the well, so that:

phi = (phi_r - phi_w) (log(r_r / r_w) / log(r / r_w)) + phi_w . (1)

r_r = distance to any point between r and r_w
r = radius of drainge
r_w = radius of well
phi = potential (P for incompressible fluids, P^2 for perfect gases)

Up to the time the effect reaches the point r the production from the well will be:

W = (pi * t * r^2 * f / P_b) * (P_r - P_m) . (2)

W = volume produced
t = sand thickness
f = fractional porosity
P_r = reservoir pressure

P_m = average pressure between r and r_w

P_b = atmospheric Pressure

All pressures will subsequently be stated in atmospheres and the constant P_b will be omitted.

This will be produced at a rate:

(dw/dtheta) = (pi * t * k / mu) * ((P_r^2 - P_w^2) / log(r / r_w)) . (3)

P_w = pressure at the well
k = permeability
theta = time
mu = viscosity

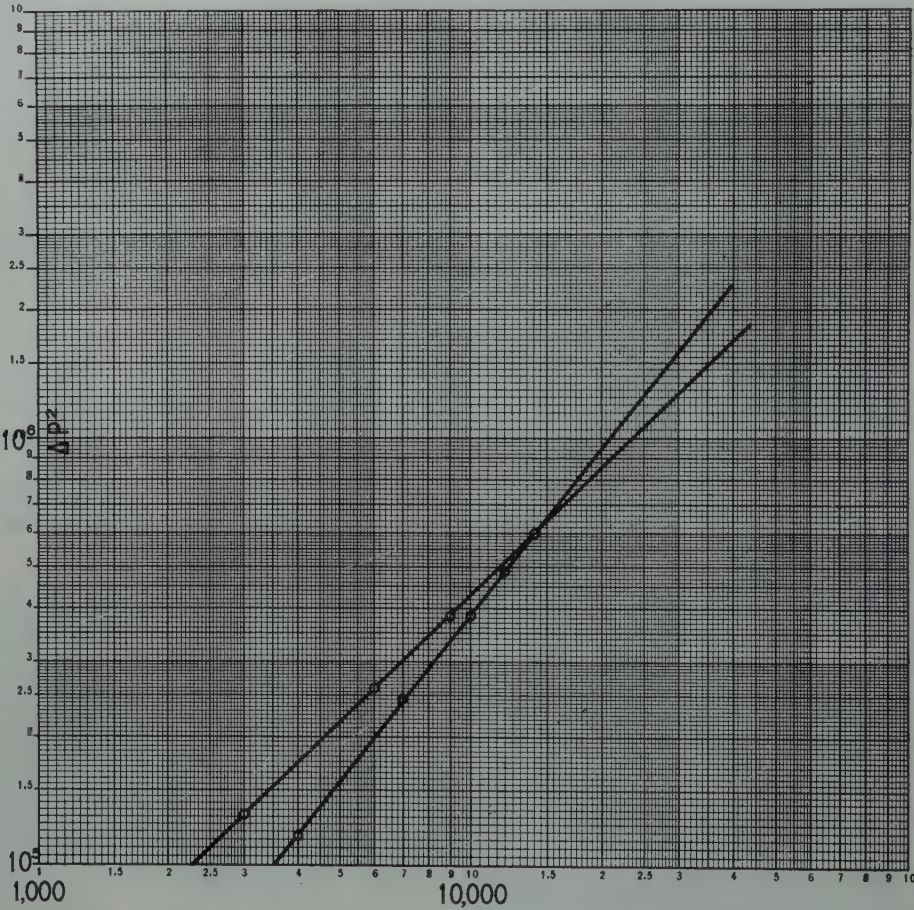


FIG. 1 — EFFECT OF TRANSIENT CONDITIONS ON BACK PRESSURE TEST.

Manuscript received at office of the Branch September 15, 1948. Paper presented at Branch Fall Meeting, Dallas, Texas, Oct. 4-6, 1948.

The average value of ϕ between r and r_w is:

$$\phi_m = (\phi_r - \phi_w) \left(1 - \frac{1}{2 \log \frac{r}{r_w}} \right) + \phi_w \quad (4)$$

The average pressure for a perfect gas will lie between the following limits:

$$P_m < \left[(P_r^2 - P_w^2) \left(1 - \frac{1}{2 \log \frac{r}{r_w}} \right) + P_w^2 \right]^{1/2} \quad (5)$$

$$P_m > (P_r - P_w) \left(1 - \frac{1}{2 \log \frac{r}{r_w}} \right) + P_w \quad (6)$$

For conditions of interest in actual gas reservoirs the limiting values of (5) and (6) are practically identical. The simpler incompressible fluid average (6) may be used.

Setting $x = r/r_w$ and substituting (6) in (2):

$$W = \frac{\pi t r_w^2 f (P_r - P_w)}{2} \left(\frac{x^2}{\log x} \right) \quad (7)$$

$$\frac{dw}{dx} = \frac{\pi t r_w^2 f (P_r - P_w)}{2} \left(\frac{x}{\log x} \right) \left(2 - \frac{1}{\log x} \right) \quad (8)$$

If the well pressure is dropped to and maintained at P_w , from (3):

$$d\theta = \frac{\mu \log x}{\pi t k (P_r^2 - P_w^2)} dw \quad (9)$$

$$\theta = \frac{\mu r_w^2 f}{2k(P_r + P_w)} \left[2 \int_x^\infty x dx + \int_x^\infty \frac{x dx}{\log x} \right] \quad (10)$$

Taking the lower limit of integration such that time is zero when $r = r_w$:

$$\theta = \frac{\mu r_w^2 f}{2k(P_r + P_w)} \left(x^2 - E_1(2 \log x) \right) \quad (11)$$

Residual terms of Euler constant and $\log 2$ have been dropped as negligible. The expression $E_1(2 \log x)$ is the exponential integral.

By another, possibly more direct, approach this expression becomes:

$$\theta = \frac{\mu f r^2}{2k(P_r + P_w)} \left(1 - \frac{1}{2 \log \frac{r}{r_w}} \right) \quad (12)$$

Disregarding the correction term for the moment, the variations of time with the other variables is seen to be:

1. Inversely proportional to the permeability
2. Independent of the sand thickness
3. Directly proportional to the porosity
4. Practically independent of the rate of production

As an illustration of the time involved Table 1 has been calculated for a sand having the following characteristics:

porosity	20%
viscosity	.015 centipoise
permeability	.050 darcy
Reservoir pressure	300 atmos.
Flowing pressure	295 atmos.
Radius of Well	10 cm.

TABLE 1

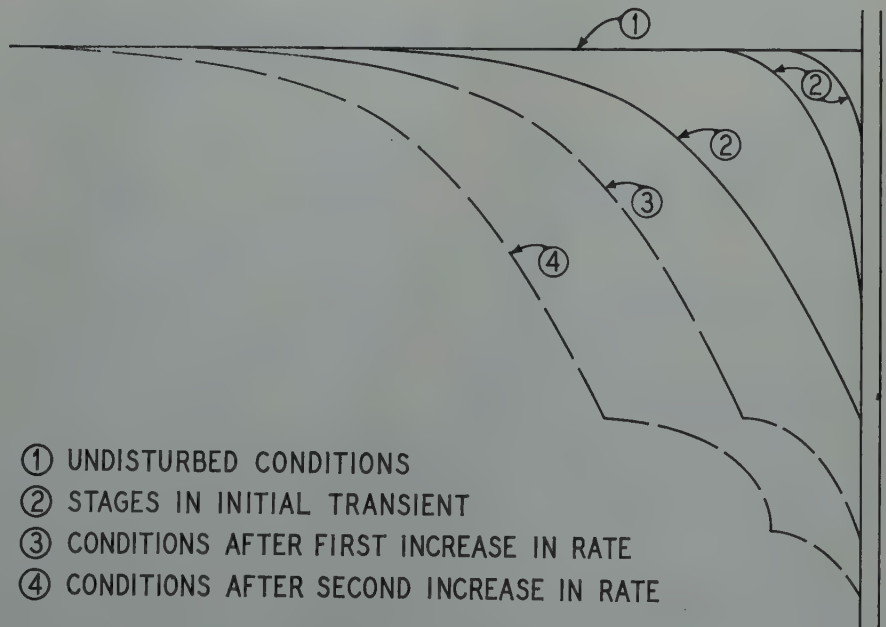
r (feet)	Time
10	4.0 seconds
50	1.75 minutes
100	7.0 minutes
500	3.0 hours
1000	12.2 hours
5000	13.0 days
10,000	51.5 days

CONCLUSIONS

The great length of time which may be involved in transients may be calculated from the appropriate constants. Thus the Monroe gas field contains areas having transient time of the order of years. This produced the anomaly of a field effectively depleted in one portion but with virgin pressure in another even though both were connected.

Some attempts have been made to establish or disprove continuity of formation by the observance of interference effects between wells. Although this is theoretically possible and such interference effects have been observed the observational difficulties are formidable and the probable existence of complex transients further decreases the likelihood of an extensive application of this method.

The same conclusions, even more forcibly, apply to attempts to measure reservoir constants by transient observation. Although equations (2) and (11) contain both porosity and permeability in such fashion that, at least theoretically, they may be determined from field observation, it is unlikely that the permeability is ever sufficiently uniform to permit an evaluation of the



- ① UNDISTURBED CONDITIONS
- ② STAGES IN INITIAL TRANSIENT
- ③ CONDITIONS AFTER FIRST INCREASE IN RATE
- ④ CONDITIONS AFTER SECOND INCREASE IN RATE

FIG. 2 — PRESSURE DISTRIBUTION IN RESERVOIR.

porosity to any usable degree of accuracy. However, a basic method very similar to this has been proposed for water reservoirs by Theis¹ and applied by Wenzel² and others.

Whether the transient phenomenon can be used or not its effects must be recognized: in particular its effects on the observations constituting back-pressure tests on gas wells. The basic difficulty arises from the fact that the velocity of propagation of each disturbance is practically independent of the intensity. The vicinity of a well soon becomes an area of complex disturbances. Although movement of gas is always toward the well the rate of movement is neither uniform nor uniformly distributed. Although the pressure decreases toward the well the time derivatives of pressure may have values differing in magnitude and sign. When

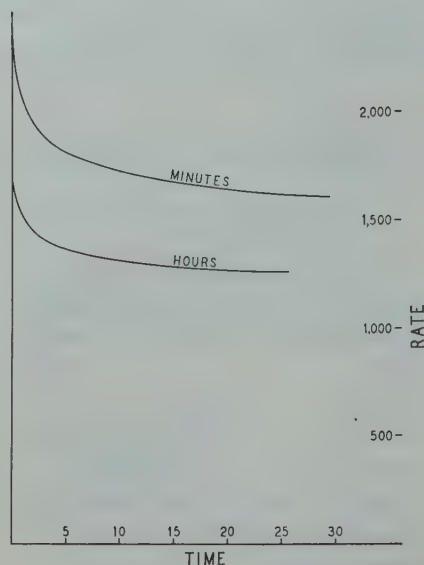


FIG. 3 — DECLINE IN RATE OF FLOW DURING INITIAL TRANSIENT.

more than one well is considered the complexity is compounded and even the direction of flow and of pressure gradients is not uniform. A field of moderate permeability and dimensions should, if closed in after producing for some time, show strange pressure behavior at many wells.

As a result of these complex transients, pseudo-stabilization readily occurs and test values may easily be recorded which have no validity. In back-pressure testing it has long been noted that in many instances the test was affected by the "direction" of the test, i.e., whether conducted from low to high rates of flow or vice versa. The differences are readily explained by transient theory. ★ ★ ★

¹ American Geophysical Union, 1935, p.519

² American Geophysical Union, 1944, p.940

CAPILLARY PRESSURES – THEIR MEASUREMENT USING MERCURY AND THE CALCULATION OF PERMEABILITY THEREFROM

W. R. PURCELL, JUNIOR MEMBER AIME, SHELL OIL COMPANY, HOUSTON, TEXAS

ABSTRACT

An apparatus is described whereby capillary pressure curves for porous media may be determined by a technique that involves forcing mercury under pressure into the evacuated pores of solids. The data so obtained are compared with capillary pressure curves determined by the porous diaphragm method, and the advantages of the mercury injection method are stated.

Based upon a simplified working hypothesis, an equation is derived to show the relationship of the permeability of a porous medium to its porosity and capillary pressure curve, and experimental data are presented to support its validity.

A procedure is outlined whereby an estimate of the permeability of drill cuttings may be made with sufficient accuracy to meet most engineering requirements.

INTRODUCTION

The nature of capillary pressures and the role they play in reservoir behavior have been lucidly discussed by Leverett¹, Hassler, Brunner, and Deahl², and others. As a result of these publications the value of determining capillary pressure curves for cores has come to be generally recognized within the oil industry. While considerable attention has been directed toward the subject in an effort to provide a reliable method of estimating percentages of connate water,^{3,4,5} it has been recognized that capillary pressure data may prove of value in other equally important applications.

This paper describes a method and procedure for determining capillary pressure curves for porous media where-in mercury is forced under pressure into the evacuated pores of the solids. The pressure-volume relationships ob-

tained are reasonably similar to capillary pressure curves determined by the generally accepted porous diaphragm method. The advantages of the method lie in the rapidity with which the experimental data can be obtained and in the fact that small, irregularly shaped samples, e.g., drill cuttings, can be handled in the same manner as larger pieces of regular shape such as cores or permeability plugs.

Based upon a simplified working hypothesis, a theoretical equation will be derived which relates the capillary pressure curve to the porosity and permeability of a porous solid, and experimental data will be presented to support its validity. This relationship applied to capillary pressure data obtained for drill cuttings by the procedure described provides a means for predicting the permeability of drill cuttings.

METHODS FOR DETERMINING CAPILLARY PRESSURES

Several techniques have so far been employed in determining capillary pressure curves and these fall into two principal categories:

- (1) Liquid is removed from, or imbibed by, the core through the medium of a high displacement pressure porous diaphragm^{3,4,5,6}.
- (2) Liquid is removed from the core which is subjected to high centrifugal forces in a centrifuge^{4,6}.

There are, however, certain limitations inherent in both methods.

The greatest capillary pressure which can be observed by method (1), above, is determined by the maximum displacement pressure procurable in a permeable diaphragm which at the present time appears to be less than 100 psi. An even more serious limitation of the diaphragm method is imposed by the fact that several days may be required to reach saturation equilibrium at a given pressure; hence, the time re-

quired to obtain a well-defined curve may be measured in terms of weeks. Furthermore, to date, no suitable technique for handling relatively small, irregularly shaped pieces of rock, such as drill cuttings, has been reported and, therefore, measurements must be made, in general, on cores, or portions thereof.

The centrifuge method offers the distinct advantage over the porous diaphragm method of arriving at saturation equilibrium in a relatively short time by virtue of the elimination of the transfer medium for the liquid. The calculation of capillary pressures from centrifuge speeds is somewhat tedious⁶, however, and the equipment required is fairly elaborate. While there exists the possibility that this method might be adaptable to the determination of the capillary pressures of cuttings, this particular ramification has not been investigated, as far as is known.

In view of the limitations of the two principal methods for determining capillary pressures, the apparatus described in the following sections has been devised in order that difficulties previously encountered might be circumvented.

MERCURY INJECTION METHOD FOR DETERMINING CAPILLARY PRESSURES

Theory

The methods described above for determining capillary pressures are characterized by the fact that one of the fluids present within the pore spaces of the solid is a liquid which "wets" the solid, i.e., the contact angle which the liquid forms against the solid is less than 90° as measured through that phase.

For these "wetting" liquids the action of surface forces is such that the fluid spontaneously fills the voids within the solid. These forces likewise oppose the withdrawal of the fluid from the pores of the solid.

Manuscript received at office of the Branch September 1, 1948. Paper presented at Branch Fall Meeting, Dallas, Texas, Oct. 4-6, 1948.
¹References are given at the end of the paper.

There is, however, a second type of system which may be considered in the study of capillary pressures. This system involves the porous solid and a single "non-wetting" fluid (mercury) which forms a contact angle of greater than 90° against the solid. In this case the action of the surface forces involved opposes the entrance of the liquid into the solid and pressure must be applied to the liquid to cause penetration of the pores of the solid.

This type of system has been employed by Drake and Ritter⁷ in studying the pore size distribution of catalysts, and the apparatus to be described below has been developed in order that similar techniques might be applied to materials exhibiting pore sizes of the order of that found in naturally occurring rock formations.

Apparatus and Procedure

An apparatus suitable for determining capillary pressures of porous media is shown in Fig. 1. The essential components of the apparatus are a mercury displacement pump A, a sample holder B, both shown in detail, and a manifold system C, shown schematically, wherein the gas pressure may be varied from small absolute values (high vacuum) to about 2000 psi, gauge.

The mercury pump consists of a pis-

such that one turn of the driving mechanism moves the piston through a distance sufficient to displace one cubic centimeter. The volume of liquid displaced from the pump is determined by successive readings of the scale D, and vernier E which is attached to the hub of the hand wheel.

The sample holder consists of two parts, both of which carry a lucite window, G, of frusto-conical shape which is cemented into the body of the holder and held rigidly in place by bushings. The displacement pump is connected to the sample holder and manifold by means of diametral conduits through the two lucite plugs. Reference marks, H, are incorporated in these conduits at about the midway point of the lucite windows and may be viewed through the openings in the supporting bushings.

The manifold is connected, as shown, to both a vacuum system and a high pressure (2000 psi) nitrogen bottle. To this manifold are also connected a manometer and pressure gauges suitable for measuring gas pressures ranging from a few millimeters of mercury, absolute, to 2000 psi, gauge.

In operation, one or more plugs drilled from a core, or a number of drill cuttings, which have been extracted and dried, are placed in the cavity, F, of the sample holder. The top

gasket makes the seal pressure tight.

With the mercury level somewhat below the reference line of the lower lucite window, a vacuum is drawn on the system until an absolute pressure of 0.005 mm. of mercury, or less, is registered by the McLeod gauge. The mercury level is then accurately positioned at the lower reference mark by advancing the piston of the displacement pump. The scales attached to the volumetric pump are set at zero following which the piston is further advanced until the mercury meniscus reaches the reference mark in the top lucite window. At this point a scale reading is made which indicates the amount of mercury required to fill the cell with the sample in place. This quantity is subtracted from the known volume of the sample holder (between the reference marks) to provide a measure of the bulk volume of the sample under test.

The vacuum pump is isolated from the manifold and gas admitted to the system in increments, thereby increasing the pressure on the mercury surrounding the sample. The entrance of mercury into the pores of the core or cuttings is indicated by a recession of the mercury-gas interface from the upper reference line, and the degree of penetration is determined by advancing the displacement pump piston until the mercury meniscus returns to this reference mark.

The procedure of alternately building up the pressure to cause recession of the mercury meniscus and advancing the pump piston to return the meniscus to the reference mark, thereby determining the amount of mercury injected into the porous solid under various pressures, is repeated until the pressure of the nitrogen cylinder is reached.

A pressure-volume correction curve is established for the apparatus by carrying out a run as described above without a sample in the holder. The volume readings obtained when testing cores or cuttings are corrected by subtracting amounts as determined by this blank run at corresponding pressures.

The pressure on the mercury entering the sample is taken as the pressure in the gas phase plus a hydrostatic head due to the weight of the column of

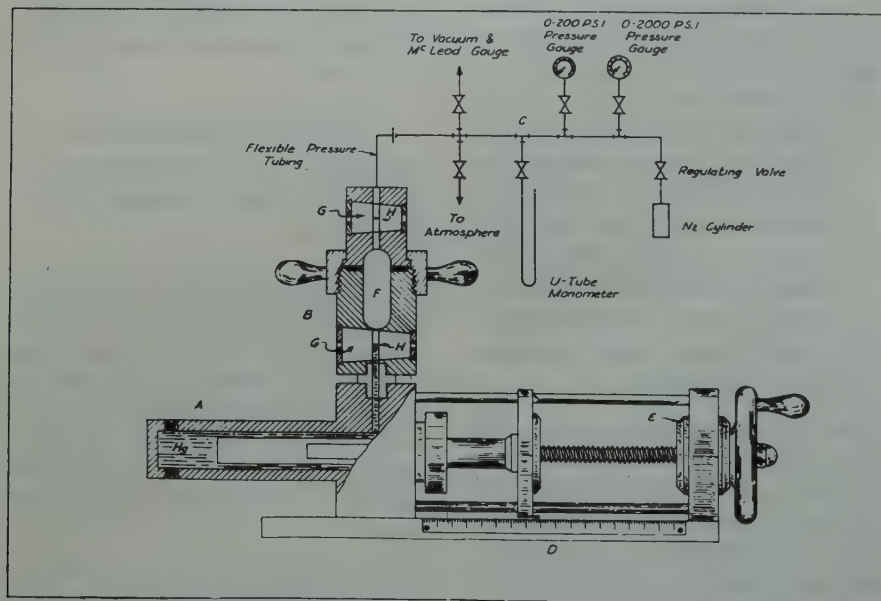


FIG. 1 — APPARATUS FOR DETERMINING MERCURY CAPILLARY PRESSURES

ton-cylinder arrangement, the former being moved by means of an accurately machined screw, the pitch of which is

portion of the sample holder is positioned and the two parts brought together by a make-up nut. A suitable

mercury between the upper reference line and the midway point of the sample. This hydrostatic head may be determined by direct measurement.

Inasmuch as saturation equilibrium is reached very rapidly at any particular pressure, an entire curve may be determined in from 30 to 60 minutes. Temperature fluctuations of the system are ordinarily not sufficiently great during this time to require corrections for thermal expansion or contraction.

Experimental Results

In Figs. 2 to 8, inclusive, (Pages 44 and 45), mercury capillary pressure curves determined in the manner just described are compared with curves determined with water* and air using the porous diaphragm method. The air permeabilities and total porosities of the samples are shown on the graphs.

In comparing these curves it must be recalled that the magnitudes of the capillary pressures are proportional to the product of the surface tension of the liquid being used and the cosine of its angle of contact against the solid. While the surface tensions of the liquids involved can be measured with fair accuracy, the uncertainty in values of the contact angles makes it difficult to predict in advance the exact ratio which should exist between mercury and water/air capillary pressures at corresponding saturations. As a first approximation, however, the following values can be assumed:

Surface tension of water: 70 dynes per cm.

Surface tension of mercury: 480 dynes per cm.⁷

Contact angle of water against the solid: 0°

Contact angle of mercury against the solid: 140°⁷

The required ratio is then,

$$\frac{(\text{Mercury Capillary Pres.})}{(\text{Water/Air Capillary Pres.})} = \frac{\text{corresponding saturations}}{\text{corresponding saturations}} = \frac{(480) (\cos 140^\circ)}{(70) (\cos 0^\circ)} \approx 5.$$

It will be seen that the curves of Figs. 2 to 8 have been plotted on scales such that this approximate ratio of 5 to 1

* The water used in all tests referred to in this paper contained 5 per cent by weight of sodium chloride.

is taken into account and hence they may be easily compared qualitatively by visual observation.

As evidenced by these curves, which are typical of those so far obtained, relatively close agreement has been found between mercury and water/air capillary pressure curves for the various types of formations studied and over the range of permeabilities and porosities encountered.

Fig. 9 (P.45) is included to show a capillary pressure curve over the entire saturation range (from 0% to 100%). With the apparatus just described it is possible to measure mercury capillary pressures of the order of 2000 psi. which corresponds approximately to a water/air capillary pressure of 400 psi. The apparatus could be adapted for measurements at higher pressure if this were deemed advisable.

The advantages of the mercury injection method over those previously used are that an entire curve of as many as twenty to thirty points may be determined in about an hour's time and small irregularly shaped pieces can be handled in the same manner as larger portions of regular shape. In addition, the range of capillary pressures that can be observed is considerably greater than for the porous diaphragm method.

CALCULATION OF PERMEABILITY FROM CAPILLARY PRESSURE CURVES

In reservoir analysis and production practice, the importance of that property of rock formations which is referred to as permeability has long been recognized by the exploitation engineer. The determination of air permeability has, for some time, been a routine core analysis test, but in order to obtain the required measurements for this determination, it is first necessary to procure a sample of regular shape and of appreciable dimensions. To accomplish this end, the expensive operation of coring is generally resorted to.

In the course of drilling, cuttings are usually available which, although too small to be suitable for permeability measurements, provide satisfactory samples with which to determine other important characteristics of the rock

formation from which they were cut. An apparatus has been described in the preceding sections which enables the measurement of capillary pressure curves for cuttings. An equation will now be developed which provides a means for calculating the permeability of a porous medium from capillary pressure data. This, in turn, of course, makes possible the estimation of the permeability of drill cuttings.

Theory

The rate of flow Q/t , of a fluid of viscosity, μ , through a single cylindrical tube or capillary of length, L , and internal radius, R , is given by Poiseuille's equation:

$$\frac{Q}{t} = \frac{\pi R^4 P}{8 \mu L}, \quad \dots \dots \dots (1)$$

wherein P is the pressure drop across the tube. Since the volume, V , of this capillary is $\pi R^2 L$, equation (1) may be written as,

$$\frac{Q}{t} = \frac{V R^2 P}{8 \mu L^2}, \quad \dots \dots \dots (2)$$

The capillary pressure for this single tube, is given by the Pressure of Displacement Equation,

$$P_c = \frac{2 \sigma \cos \theta}{R}, \quad \dots \dots \dots (3)$$

where P_c , the capillary pressure, is the minimum pressure required to displace a wetting liquid ($\theta < 90^\circ$) from or inject a non-wetting liquid ($\theta > 90^\circ$) into a capillary of radius R when the surface or interfacial tension at the interface is σ and the angle of contact which this interface forms with the solid of the capillary is θ .

Equation (3) indicates that capillary pressure is inversely proportional to pore radius and hence may be used as a measure of capillary size. Substituting equation (3) in (2) we have,

$$\frac{Q}{t} = \frac{(\sigma \cos \theta)^2 V P}{2 \mu L^2 (P_c)^2} \quad \dots \dots \dots (4)$$

Consider now a system composed of a large number, N , of parallel, cylindrical capillaries of equal length but random radii, each tube being identical in all respects except internal area to the capillary under discussion above. The total rate of flow (Q/t) , through this system must be equivalent to the sum of the contributions made by each of the N single tubes or capillaries.

The flow through each individual tube is given by equation (4); the total flow, therefore, may be represented as follows:

$$(Q/t)_s = \frac{(\sigma \cos \theta)^2 P}{2\mu L^2} \sum_{i=1}^N \frac{V_i}{(P_c)_i^2} \quad (5)$$

On the other hand, the rate of flow $(Q/t)_s$ through this same system of capillaries is also given by Darcy's Law:

$$(Q/t)_s = \frac{K A P}{\mu L} \quad (6)$$

where K is the permeability of the system, L is the length of the tubes, A is the total cross-sectional area of the system, and P is the pressure differential causing flow.

By equating the right-hand members of the equations (5) and (6) the following is obtained:

$$K = \frac{(\sigma \cos \theta)^2}{2AL} \sum_{i=1}^N \frac{V_i}{(P_c)_i^2} \quad (7)$$

To simplify equation (7) the volume, V_i , of each capillary may be expressed as a percentage, S_i , of the total void volume, V_T , of the system, i.e.,

$$\frac{V_i}{V_T} \times 100 = S_i$$

Furthermore, since AL is the bulk volume of the system we may introduce the per cent porosity, f , where

$$f = \frac{V_T}{AL} \times 100$$

and equation (7) becomes

$$K = \frac{(\sigma \cos \theta)^2 f}{2 \times 10^4} \sum_{i=1}^N \frac{S_i}{(P_c)_i^2} \quad (8)$$

Equation (8) relates the permeability of a system of parallel cylindrical capillaries of equal lengths, but various radii, to the porosity of the system and to the capillary pressures and volumes of its component parts.

Equation (8) is derived for a porous medium composed of non-interconnected capillaries of circular cross-section and equal length. Certainly no such system obtains in naturally occurring rock formations. The path by which a fluid may travel through a rock

is circuitous, for the pore spaces within these materials are usually interconnected to a greater or lesser degree. Furthermore, this path is neither uniform nor circular in cross-section. It is necessary, therefore, to modify equation (8) by introducing a so-called lithology factor, F , to account for differences between the flow in the hypothetical porous medium for which equation (8) was derived and that in naturally occurring rocks. Equation (8) becomes

$$K = \frac{F(\sigma \cos \theta)^2 f}{2 \times 10^4} \sum_{i=1}^N \frac{S_i}{(P_c)_i^2} \quad (9)$$

The amount of variation in the factor F (to be discussed below) for samples of equivalent and of different lithology will determine the practical utility of equation (9).

The evaluation of the quantity

$$\sum_{i=1}^N \frac{S_i}{(P_c)_i^2}$$

can best be presented by reference to Fig. 10, which shows a typical capillary pressure curve for a naturally occurring porous media such as a reservoir sandstone.

Consider the change in saturation, $\Delta\rho$, that occurs when the pressure is increased from $(P_c)_1$ to $(P_c)_2$. This change in saturation is a result of liquid either entering (non-wetting liquid) or receding from (wetting liquid) all pores having capillary pressures lying between $(P_c)_1$ and $(P_c)_2$. All pores in this interval may be treated as if they exhibited some intermediate average capillary pressure, $(P_c)_{av.}$, where,

$$(P_c)_1 (P_c)_{av.} \sqrt{f} (P_c)_2$$

If a number, r , of such intervals are chosen, and if n_j is the number of pores in the j th interval, then

$$\sum_{i=1}^{n_j} \frac{S_i}{(P_c)_i^2} \cong \left[\frac{\Delta\rho}{(P_c)_{av.}^2} \right]_j$$

Likewise,

$$\sum_{i=1}^N \frac{S_i}{(P_c)_i^2} = \sum_{j=1}^r \sum_{i=1}^{n_j} \frac{S_i}{(P_c)_i^2} \cong$$

$$\sum_{j=1}^r \left[\frac{\Delta\rho}{(P_c)_{av.}^2} \right]_j$$

and

$$\lim_{\substack{\Delta\rho \rightarrow 0 \\ r \rightarrow \infty}} \sum_{j=1}^r \left[\frac{\Delta\rho}{(P_c)_{av.}^2} \right]_j = \int_{\rho=0}^{\rho=100} \frac{d\rho}{(P_c)^2} = \sum_{i=1}^N \frac{S_i}{(P_c)_i^2}$$

It is seen, therefore, that the quantity

$$\sum_{i=1}^N \frac{S_i}{(P_c)_i^2} \quad \text{is equal to}$$

the integral of the reciprocal of the square of the capillary pressure expressed as a function of per cent liquid saturation. Such a function is shown in Fig. 10 (P.45). This integral may be determined by planimetry or, more readily, by applying Simpson's Rule.

In the calculation of permeability by equation (9) from mercury capillary pressure data a surface tension of 480 dynes per cm. and a contact angle of 140° are assumed. Equation (9) then reduces to

$$K = 0.66 F f \int_{\rho=0}^{\rho=100} \frac{d\rho}{(P_c)^2} \quad (9a)$$

where K is the permeability in millidarcies, f is per cent porosity, ρ is per cent of total pore space occupied by the liquid, and P_c the capillary pressure expressed in atmospheres.

Experimental Results

In an attempt to determine experimentally the utility of equation (9a), mercury capillary pressure curves have been obtained for numerous rock samples of two types of formations, the Upper Wilcox of Eocene age and the Paluxy of Cretaceous age. Samples of such size were used that their air permeabilities could be measured directly and these observed permeabilities were employed in determining the magnitude of, and the variation in, the factor F of equation (9a). The data obtained

TABLE 1
Observed Values of F

Sample No.	Factor F , Eq. (9a) Required to Make Calculated and Observed Permeabilities Identical	Permeability Calculated from Eq. (9a) Using an Average F of 0.216	Observed Air Permeability (md)
Upper Wilcox			
1	0.085	3.04	1.2
2(1)	0.122	21.2	12.0
3	0.168	17.3	13.4
4	0.149	53.5	36.9
5	0.200	61.9	57.4
6	0.165	91.6	70.3
7	0.257	92.3	110
8	0.256	97.5	116
9	0.191	163	144
10	0.107	680	336
11 (Fig. 6)	0.216	430	430
12	0.273	348	439
13	0.276	388	496
14(1)	0.185	902	772
15	0.282	816	1070
16	0.363	865	1459
Paluxy			
17	—	0.003	<0.1
18	—	0.10	<0.1
19	0.182	42.2	35.7
20	0.153	54.9	40.2
21	0.231	172	184
22	0.276	183	235
23	0.215	308	307
24	0.163	422	320
25	0.284	383	506
26	0.272	502	634
27 (Fig. 5)	0.338	734	1150
	Av. 0.216		

(1) "Cuttings"

with typical samples are recorded in Table I.

It will be seen in Table I that the factors F for the Upper Wilcox and Paluxy sands are of the same general order of magnitude. However, there is some indication that this factor may vary with permeability from a minimum of about 0.1 for samples of low permeability to about 0.4 for samples of high permeability.*

It may be possible, with the further accumulation of data, to establish values of the factor F for various perme-

ability ranges. Likewise, it may be found that the factor F will be different for samples of widely divergent lithology** since the two formations studied in detail and reported here do not vary greatly in lithology. The Upper Wilcox is in general a poorly sorted sandstone while the Paluxy is a well sorted sandstone. The establishment of more precise values of F , however, will serve merely to increase the precision of the method for estimating permeabilities from capillary pressure data. For the moment, with the information at hand, quite satisfactory accuracy may be obtained by merely taking an arithmetical average of the factors F over the entire permeability range.

** While F values have been determined extensively for only the Upper Wilcox and Paluxy sandstones, it is interesting to note that the following values are obtained from the data presented in Figs. 2, 3, 4, 7, and 8.

Fig. No.	Formation	Factor, F	Air Permeability (Md.)
2	Frio Sand	0.073	23
3	Frio Sand	0.271	170
4	Frio Sand	0.276	950
7	San Andres Lime	0.133	35
8	San Andres Lime	0.150	43

Although these values are in line with those reported in Table I for samples of comparable permeability, additional data must be obtained before it can be concluded that all four types of formations exhibit similar F factors.

Table I gives observed air permeabilities together with permeabilities as calculated from equation (9a) using an average value of the factor F of 0.216. These values have been plotted in Fig. 11.

In Table I, samples 2 and 14 are designated as "cuttings". These samples were prepared by crushing cores of known air permeability to obtain a number of small pieces in approximately the size and shape of drill cuttings. Mercury capillary pressure curves were determined for these sets of "cuttings" in exactly the same manner as employed for the larger single pieces. It will be noted in Fig. 11 that the data for these "cuttings" fit the average line as well as the data for the cores.

The procedure for estimating the permeability of drill cuttings (or any porous medium, regardless of size or shape) consists of determining the capillary pressure curve by the method described above, calculating a permeability from the curve by means of equation (9) using a predetermined value of F , and then reading the corresponding air permeability from a plot such as that shown in Fig. 11. The spread of points of Fig. 11 is such as to indicate that the permeability so determined will be sufficiently accurate for most engineering requirements.

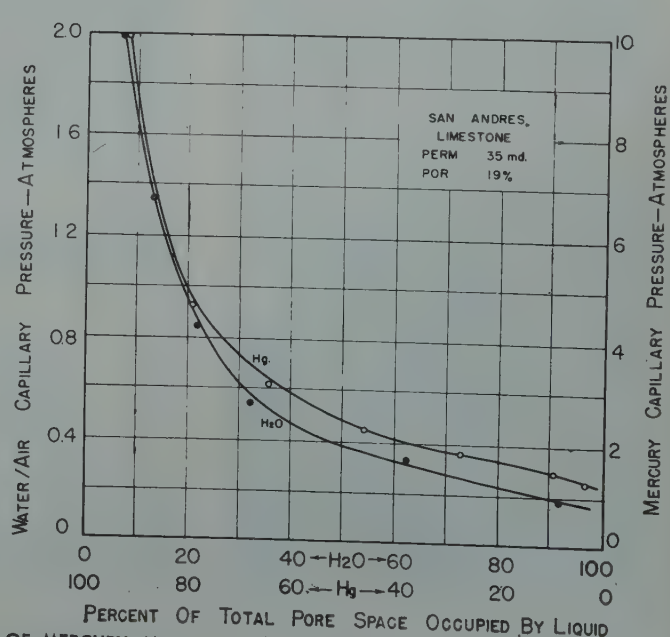
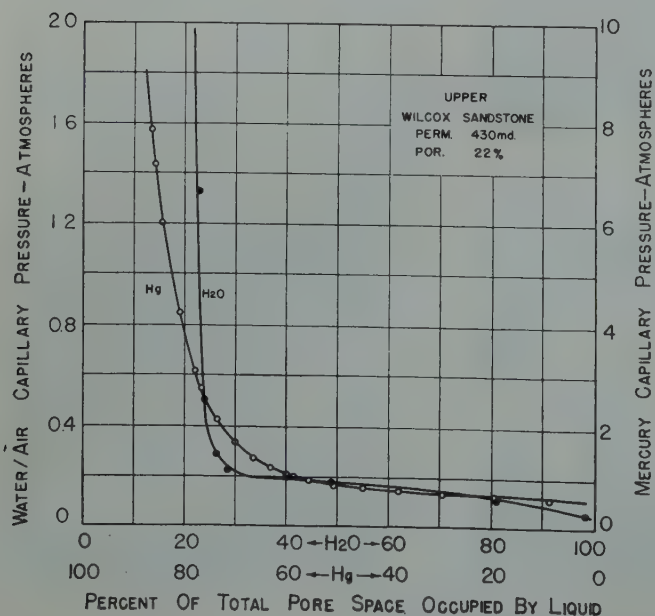
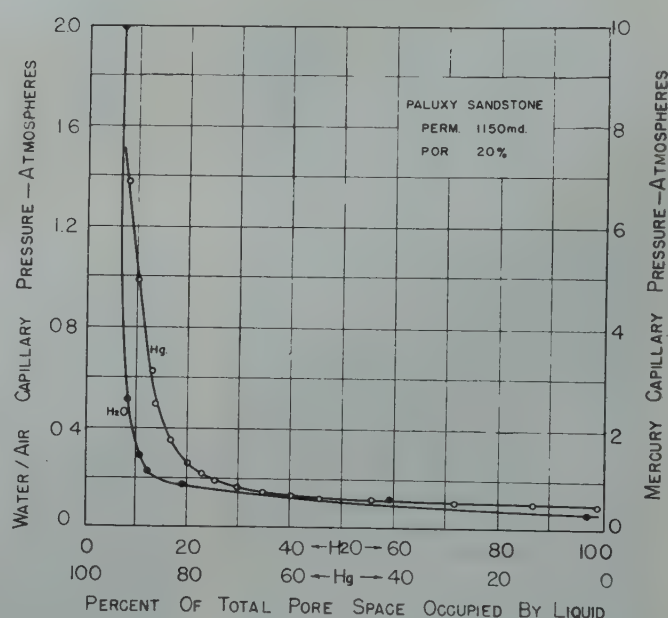
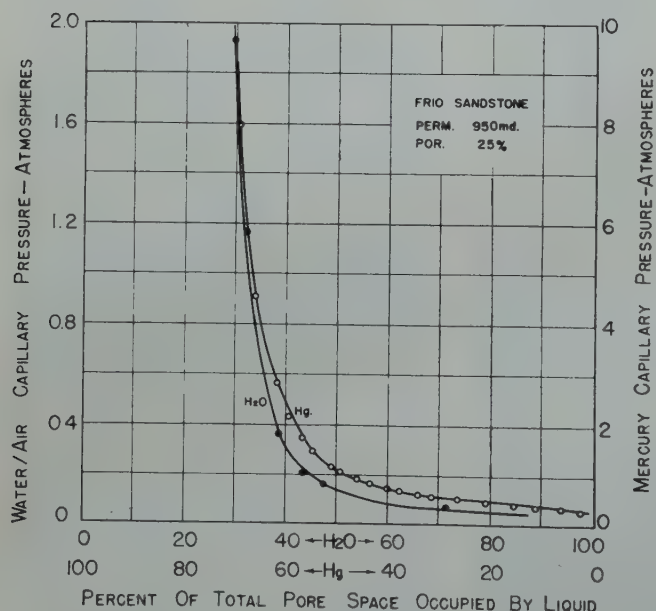
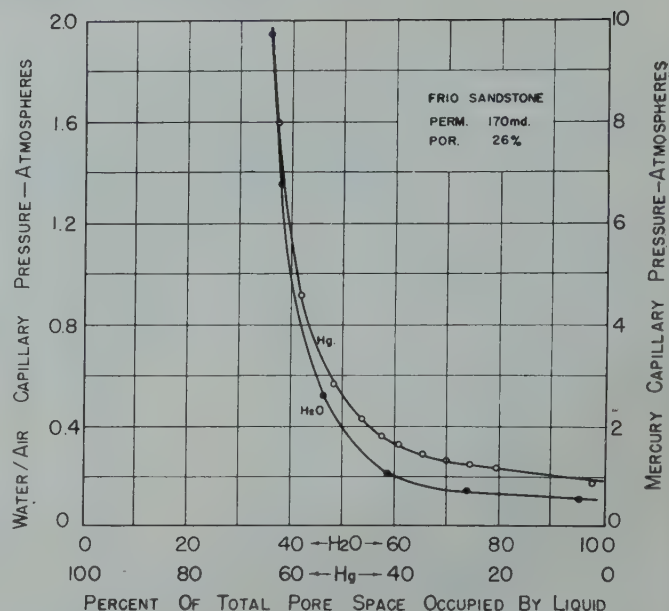
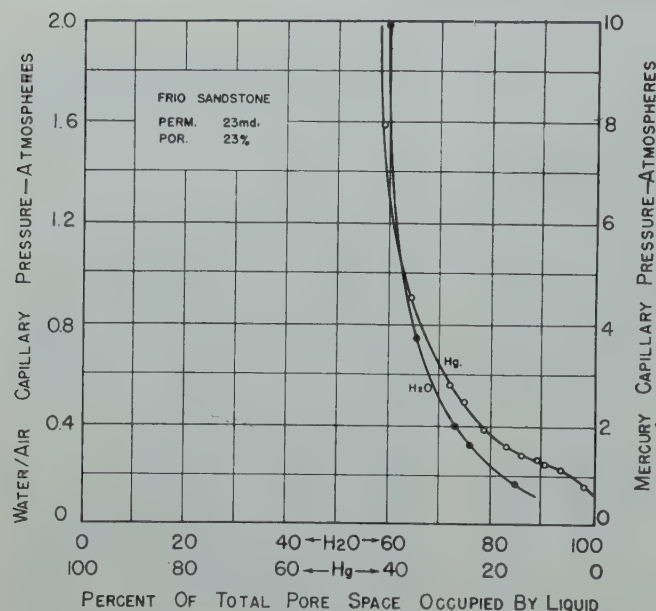
SUMMARY AND CONCLUSIONS

A method of determining capillary pressures for porous media wherein mercury is forced under pressure into the pores of the evacuated solid has been found to yield results which are reasonably similar to those obtained using the porous diaphragm technique. This method offers the following advantages over previously described procedures:

1. An entire capillary pressure curve consisting of as many as 20 to 30 points can be determined in a matter of hours rather than weeks.
2. Small, irregularly shaped pieces, such as drill cuttings, can be handled in exactly the same manner as larger, regularly shaped samples such as cores or permeability plugs.
3. The range of capillary pressures which can be observed is 5 to 10 times that of conventional methods.

* It may be shown both theoretically and experimentally⁸ that for close-packed spheres of uniform size the length of the path by which a fluid may pass through such a system is $\pi/2$ times as great as the length of the pack. Since the length of the path enters into the denominator of equation (6) as a squared term, it can be shown that the factor F for this pack is $(2/\pi)^2$ or about 0.4. The difference between this value and those actually observed (0.1 to 0.4) may be due in part to inaccuracies in the assumptions of values for σ and θ , but is probably chiefly the result of the difference in pore structure between that of the ideal pack of uniform spheres and that of naturally occurring rock structures. It is interesting to note, however, that the observed values for F of natural rocks are of the same order of magnitude as, but somewhat less than, that which can be calculated for an ideal "sand" pack.

CAPILLARY PRESSURES — THEIR MEASUREMENT USING MERCURY AND THE CALCULATION OF PERMEABILITY THEREFROM



FIGURES 2 THROUGH 7, L TO R, TOP, CENTER, BOTTOM — COMPARISON OF MERCURY AND WATER/AIR CAPILLARY PRESSURE CURVES.

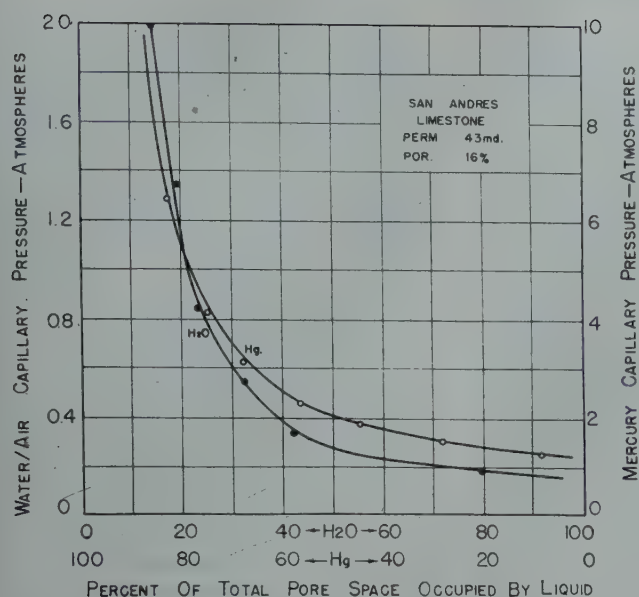


FIG. 8 — COMPARISON OF MERCURY AND WATER/AIR CAPILLARY PRESSURE CURVES

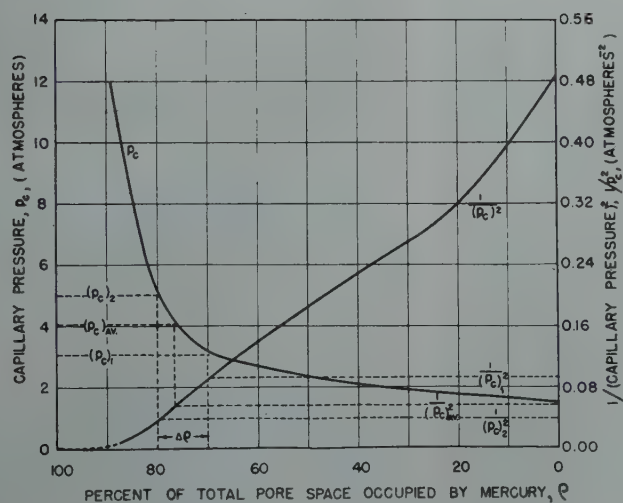


FIG. 10 — PERCENT SATURATION AS A FUNCTION OF CAPILLARY PRESSURE AND RECIPROCAL OF SQUARE CAPILLARY PRESSURE

An equation has been derived which indicates theoretically the relationship which should exist between the permeability of a porous medium and its capillary pressure curve. Experimental data have been presented to show that this equation provides a fairly reliable method of calculating permeability from capillary pressure data.

A combination of the method for measuring the capillary pressure curve of drill cuttings and the equation relating permeability to the capillary pressure curve so determined makes possible the estimation of the permeability of those cuttings.

ACKNOWLEDGMENT

The author wishes to express his appreciation for the aid and cooperation of Mr. G. E. Archie in the formulation of the problem, for the assistance rendered by Messrs. M. A. Westbrook and C. F. Blankenhorn in designing and assembling the apparatus, and for the many valuable suggestions offered by Mr. J. P. Murphy during the preparation of the manuscript.

REFERENCES

1. M. C. Leverett: Capillary Behavior

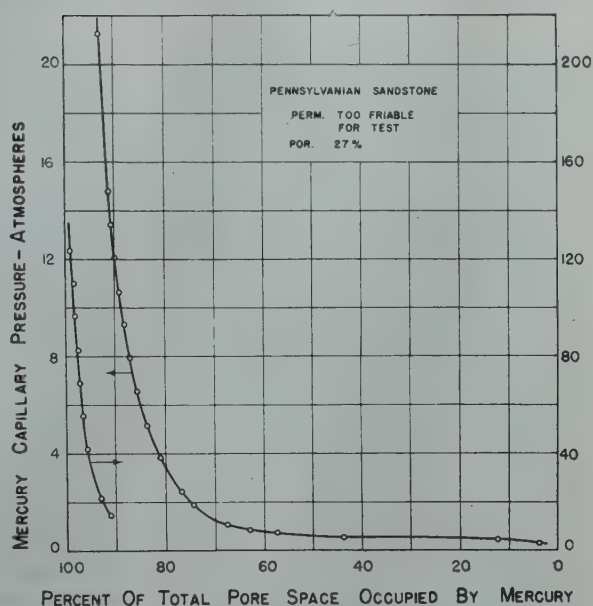


FIG. 9 — MERCURY CAPILLARY PRESSURE CURVE OVER THE ENTIRE SATURATION RANGE

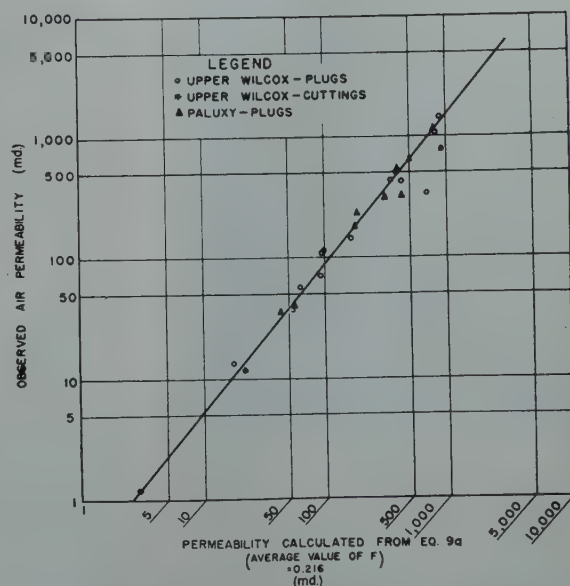


FIG. 11 — OBSERVED AIR PERMEABILITY AS A FUNCTION OF PERMEABILITY CALCULATED FROM EQUATION 9A

in Porous Solids. *Trans. AIME* 142, 152, (1941).

2. G. L. Hassler, E. Brunner, and T. J. Deahl: The Role of Capillarity in Oil Production. *Trans. AIME* 155, 155, (1944).
3. O. F. Thornton and D. L. Marshall: Estimating Interstitial Water by the Capillary Pressure Method. *Trans. AIME* 170, 69, (1947).
4. J. J. McCullough, F. W. Albaugh, and P. H. Jones: Determination of Interstitial-Water Content of Oil and Gas Sand by Laboratory Tests of Core Samples: *Drilling and Production Practice* (A.P.I.) 180 (1944).

5. W. A. Bruce and H. J. Welge: Restored-State Method for Determination of Oil in Place and Connate Water. *Oil and Gas Journal*, 46, 223, (1947).
6. G. L. Hassler and E. Brunner: Measurement of Capillary Pressures in Small Core Samples. *Trans. AIME* 160, 114, (1945).
7. R. L. Drake and L. C. Ritter: Pore-Size Distribution in Porous Materials. *Ind. Eng. Chem., An. Ed.* 17, 782, (1945), and Macropore-Size Distributions in Some Typical Porous Substances. *Ibid* 17, 787, (1945).
8. F. E. Bartell and H. J. Osterhof: Pore Size of Carbon and Silica Membranes. *J. Phys. Chem.* 32, 1553, (1928).

DISCUSSION

☆

By Walter Rose, Gulf Research and Development Company, Pittsburgh, Pa.

It is appropriate certainly to compliment Mr. Purcell on the interesting manner in which he has called attention to another laboratory method for measuring capillary pressure phenomena, and to another useful application for capillary pressure data. It appears that conventional methods for measurement have not been utilized fully to serve the purposes of routine laboratory core analysis because of the instrumentation and associated difficulties which have been encountered; and also it appears that the heretofore emphasized application for capillary pressure data to evaluate initial fluid phase distributions in virgin petroleum reservoirs can be discredited to some extent due to theoretical uncertainties. However, it is not to be expected that the results of Mr. Purcell's work immediately provide solutions for all the problems related to the evaluation and application of capillary pressure phenomena. This is because the data obtained by the mercury penetration method is not equivalent entirely to that obtained by conventional procedures, as perhaps implied by Purcell, in ways now to be discussed. Elsewhere it will be shown, however, that the data obtained by the mercury penetration method indeed lead to the other useful results suggested by Purcell.

It is to be assumed that when a difference in pressure is established at the interfaces of contact between immiscible fluids saturating the interstices of porous media, this capillary pressure (as an explicit function of fluid saturation and an implicit function of fluid distribution) is in effect a measure of the interstitial pore widths containing these interfaces of contact, assuming conditions of static equilibrium obtain. From this standpoint then it is apparent that Purcell's method and conventional methods of capillary pressure measurement all yield potentially the same kinds of data. To obtain the exact equivalence of these data by the various methods, however, requires that consideration be given to the well-known hysteretic possibilities, that the configurational character of the interstitial spaces not be variably affected by the method of measurement employed, and that the dynamic mechanism of wetting and non-wetting fluid flow (as static equilibrium is approached) be unrelated to the method of measurement employed. Presumably, the first requirement has been satisfied by Purcell's experimentation for he attempts comparison of data obtained only by the capillary drainage mechanism (i.e. where the invading non-wetting phase permits only drainage and no intermediate imbibition of the wetting phase) so that hysteretic uncertainties need not be considered. Regarding the second requirement, it is felt that only in the case of "inert" porous media will the character of the interstitial spaces be unrelated to the physico-chemical properties of the saturating fluids. As an example, the presence of interstitial surface clay coating in certain types of naturally occurring porous media will certainly result in a different pore structure when mercury and rarified gas are substituted for oil and brine as the saturating fluids, due to the dependence of the clay swelling effects on the nature of the fluids contacting the clays. Thus, even in conventional capillary pressure experimentation it has been recognized that use of reservoir-like fluids is to be preferred so that the data will truly reflect on the pore character representative of the natural reservoir condition. This refinement evidently cannot be employed in the use of Purcell's method. However, it is the inevitable disre-

gard for the third requirement as above stated which most seriously limits the possibility of attaining equivalence between the results of Purcell's method and conventional methods, but which nonetheless leads to the potential usefulness for Purcell type experimentation as described in his paper. For it can be anticipated on theoretical grounds, and indeed it can be established from an examination of Purcell's data (c.f. Purcell's Figures 2 through 8), that "irreducible" minimum wetting phase saturations (reflecting on zero wetting phase relative permeability due to the attainment of pendular configurations) will not be a result of the mercury penetration method, since this procedure involves a compression rather than a flow of the wetting phase as desaturation occurs. It is evident then that the data reported by Purcell reflect principally on a complete distribution of pore radii, as originally advanced by Ritter and Drake (c.f. Reference 7 of Purcell's paper), providing information not directly derivable from conventional capillary pressure curves and leading to a method for approximating permeabilities and lithology characteristics of porous media. However, it must be emphasized that exact equivalence between conventional capillary pressure data and that obtained by the mercury penetration method is not to be expected as a common result.

The interesting feature about Purcell's equation for permeability is that it can be arrived at by several processes, leading to a more complete interpretation of the lithology factor, F . For instance, in a recent paper (not yet generally available)* an expression for permeability is given as:

$$k = \frac{\left[\lim_{\rho_w \rightarrow 1} j(\rho_w) \right]^2 \left[\sigma \cos \theta \right]^2 f}{P_d^2 \times 10^2} \quad \text{Eq. (1)}$$

where ρ_w is the fractional wetting phase saturation, $j(\rho_w)$ is Leverett's capillary pressure function, P_d is the displacement pressure as commonly defined, and where the other notation follows that as employed by Purcell. In this cited reference it is shown that the limiting (minimum) value for the capil-

*Walter Rose and W. A. Bruce, "Evaluation of Capillary Character in Petroleum Reservoir Rock", *Jnl. of Petr. Tech.*, in press, (1949).

lary pressure function can be identified with the "rock" textural constant, t , appearing in the Kozeny equation for streamline fluid flow through porous media, as:

$$\lim_{\rho_w \rightarrow 1} j(\rho_w) = \left(\frac{1}{t}\right)^{1/2} \quad \text{Eq. (2)}$$

Now, it is observed that the constant, t , as used in Eq. (2) refers to its maximum value, which has been established as being greater than 5 (and sometimes, for instance, as great as 500) as related to the various types of unconsolidated and consolidated porous media encountered in natural reservoir rock. This implies that Purcell's lithology factor generally will be less than 0.4, as indeed predicted and observed, for it is seen on combination of Eq. (1) above and Purcell's Eq. (9) or (9a) that:

$$\frac{F}{2} > \left(\lim_{\rho_w \rightarrow 1} j(\rho_w)\right)^2, \quad \text{Eq. (3)}$$

since:

$$\int_0^1 \frac{d\rho}{P_c^2} < \frac{1}{P_d^2}, \quad \text{Eq. (4)}$$

Moreover, it can be shown from these equations that the lithology factor, F , is defined fundamentally as:

$$F = \frac{2}{1 \int_0^1 \frac{d\rho}{j(\rho_w)^2}} = \frac{2}{t_{\min}}. \quad \text{Eq. (5)}$$

The above considerations imply that in texturally similar porous media the lithology factor, F , and the limiting value of the j function will be related

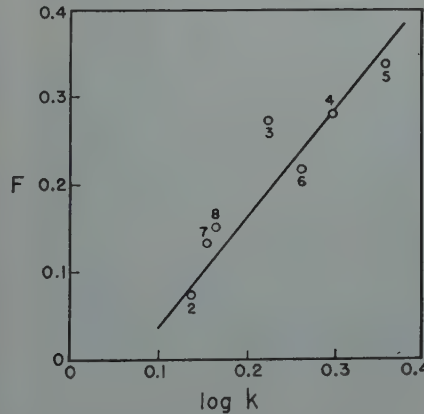
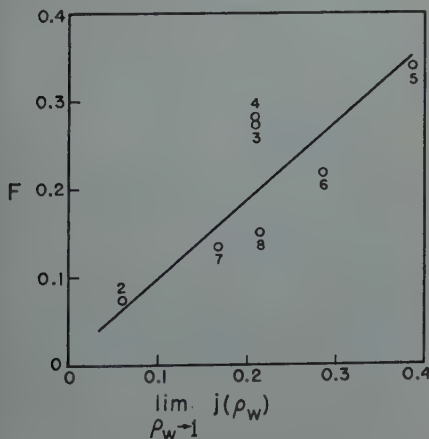


FIGURE 1

CORRELATION BETWEEN LITHOLOGY FACTOR, F , AND THE LIMITING VALUE FOR THE CAPILLARY PRESSURE FUNCTION, $j(\rho_w)$, (C.F. LEFT DIAGRAM), OR THE LOGARITHM OF PERMEABILITY, $\log k$, (C.F. RIGHT DIAGRAM). NUMBERS ASSOCIATE DATA POINTS WITH PURCELL'S FIGURE NUMBERS.

to each other by some constant factor characteristic of the media, and that in texturally dissimilar media a rough proportionality will still obtain between these parameters. This is clearly shown by Figure 1, constructed from Purcell's data where F has been plotted versus $\lim j(\rho_w)$. It would appear,

$$\rho_w \rightarrow 1$$

therefore, that Eq. (1) above has the same sort of validity and usefulness as Purcell's Eq. (9a), and its use is to be preferred since from the experimentation standpoint it is easier to evaluate. For only the initial segment of the capillary pressure curve need be measured (actually, only the displacement pressure need be measured) to solve Eq. (1) and to provide values reflecting on lithology or permeability characters of porous media equivalent to those obtained by Purcell. In this connection, a plot of F versus the logarithm of the corresponding permeability value is also given in Figure 1 and the linearity obtained by this plot suggests that in the classification of texturally dissimilar porous media a knowledge of permeability alone suffices sometimes to predict qualitatively lithological differences.

Figure 2 shows the results of some experimentation conducted recently to verify that the mercury penetration method of capillary pressure measurement would yield data equivalent to that obtained by conventional methods for inert porous media. Thus, Curve A of Figure 2 shows the capillary retention replot of the original Ritter and

Drake data characterizing pyrex fritted glass media. Curve B is a similar plot of data obtained on other fritted glass media by the conventional capillary pressure technique, and the close conformance between these two curves can be taken as evidence that both methods have provided a measurement of the same phenomena, at least at the saturation levels where the wetting phase is continuous throughout the interstitial spaces (i.e. at saturations greater than those obtaining when the wetting phase configuration is pendular). These results are offered to support further the validity of the experimentation described by Purcell, for it is regarded that Purcell's technique for laboratory

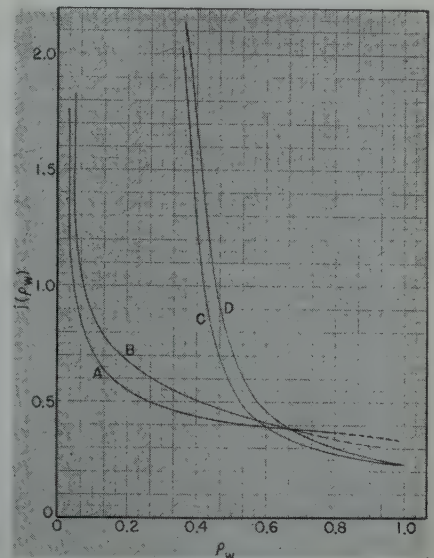


FIGURE 2

CAPILLARY RETENTION CURVES

CURVE A IS A PLOT OF THE RITTER AND DRAKE DATA.

CURVE B IS A PLOT OF DATA CONVENTIONALLY OBTAINED ON POROUS MEDIA TEXTURALLY SIMILAR TO THAT USED BY RITTER AND DRAKE.

CURVE C IS A RELOT OF PURCELL'S FIG. 3.

CURVE D IS A RELOT OF PURCELL'S FIG. 4.

measurement must have high order accuracy and precision. This is shown also by the replot of the Frio core data as Curves C and D in Figure 2 from Purcell's Figures 3 and 4, since essentially the same capillary retention curve has been obtained for these two cores of widely different permeability. For when capillary pressure data yield the same capillary retention plot for different porous media, a condition of textural similarity between these media

is implied, as already was established in the case of the Frio cores by the observed approximate equivalence of the measured lithology factor.*

To conclude, it is apparent that Mr. Purcell, in applying his method for capillary pressure evaluation, has accomplished probably as much as will be forthcoming from experimentation of this sort. That is, he has developed suitably a rapid and precise method to make valid measurements of capillary pressure on small rock fragments reflecting on the permeability and the lithological character of porous media. Such data undoubtedly will be found to be useful for correlation purposes in the interpretation of the results of other core analysis experimentation. However, it is noted that for some purposes at least conventional experimentation still will be required, and this should not be neglected because of the features of simplicity associated with the mercury penetration type experimentation, especially because it appears that Mr. Purcell's objections to use of conventional methods can be obviated somewhat through suitable instrumentation improvements. For instance, use of cellophane type capillary barriers permits measurements of capillary pressure in excess of 300 p.s.i., which is well above the values required to produce "irreducible" minimum saturations of the wetting phase in petroleum reservoir rock of practical interest. Also, it is noted that the equilibrium values of saturation can be obtained by extrapolation of rate of displacement data, thereby decreasing the time required for conventional laboratory experimentation. Finally, it is noted that the recently proposed "multi-core" procedure for capillary pressure evaluation (c.f. Rose and Bruce paper, loc. cit.) has a potential use for the study of small core fragments similar to that characterizing Purcell's method of evaluation. In this connection, however, it must be realized that no method presently described in the literature will provide satisfactory capillary pressure data in those

instances where the core fragments are so small that their total bulk surface area approaches the total interstitial surface area, thereby imposing a lower limit on these possibilities.

The consideration presented in this discussion have been directed to bear on the significance of the results of Mr. Purcell's excellent paper. It is to be recognized, however, that Mr. Purcell's paper, independent of these considerations, is a most valuable contribution to the literature, and the author is to be congratulated for his developments which contribute so significantly to our knowledge of capillary pressure phenomena.

Author's reply to Mr. Walter Rose:

It is indeed gratifying that Mr. Rose, through his discussion, has provided a link between the theoretical approach to the problem which is exemplified by his recent paper entitled "Theoretical Generalizations Leading to the Evaluation of Relative Permeability"† and the experimental approach of the author. It is believed that through a close intermeshing of these two general types of investigation our knowledge of capillary phenomena should increase substantially in the future.

Mr. Rose has very aptly pointed out certain conditions which must be satisfied if exact equivalence between mercury capillary pressures and those obtained by other means is to be obtained; likewise he has indicated that all of these conditions are not necessarily fulfilled. It would seem appropriate, therefore, to state that the author does not intend to imply, as indicated by Mr. Rose, that the mercury penetration method is exactly equivalent to conventional procedures but instead has chosen to show experimentally (as evidenced by Figures 2 to 8, inc.) that for the various types of formations studied and over the range of permeabilities and porosities encountered a reasonable similarity exists between mercury and water/air capillary pres-

ures. In the paper no conclusions are drawn from the comparison tests other than the one of similarity between the two types of curves and this same conclusion has been obtained by Mr. Rose for his fritted glass plates. Furthermore, it should be pointed out that only one application of capillary pressure data, namely that of estimating permeability, is discussed.

Mr. Rose's confirmation of equation 9 by the derivation outlined in his discussion adds materially to the subject. The calculation of permeability from but a single point of the capillary pressure curve, namely the displacement pressure, should perhaps be used with caution, although it must be admitted indications are that the results so obtained would compare favorably with those obtained by an integration of the entire curve. In this connection, it might be pointed out that an accurate determination of the displacement pressure is exceedingly difficult by means other than mercury penetration.

It is stated in the discussion that difficulties usually encountered in conventional methods of determining capillary pressures, can be alleviated by suitable instrumentation. While it is apparent that the range of pressures can be extended through the use of cellophane membranes, this may be accomplished, perhaps, only through the aggravation of a second difficulty, namely that of the length of the time involved. Yuster** has recently stated that the extrapolation method of estimating equilibrium saturations from rates of displacement data gave accurate results in only about 25 per cent of the tests for which it was employed; hence, it may be concluded that this method of reducing the time involved in conventional tests should be used with reservation. It is to be hoped that the paper of Rose and Bruce referred to in the discussion will soon be made generally available for it is believed that any method of determining capillary pressure curves for cuttings will find immediate application. ★ ★ ★

* Note, from Curves C and D of Figure 2 the validity of the definition presented as Eq. (5) above is readily verified.

† *Jnl. of Petr. Tech.*, in press (1949).

** *Producer's Monthly*, December 1948, p. 24.

OUTLINE OF WEATHER AND WAVE FORECASTING TECHNIQUES

ALFRED H. GLENN, METEOROLOGICAL CONSULTANT, NEW ORLEANS, LOUISIANA

JOE E. GRAHAM, HUMBLE OIL & REFINING COMPANY, GRAND ISLE, LOUISIANA

INTRODUCTION

Oil operators engaged in drilling on the Continental Shelf of Louisiana and Texas are in agreement that adverse weather and wave action are two of the greatest hazards to the safety and efficiency of their work. It was anticipated when the offshore operations commenced that such would be the case, and experience to date has verified this assumption. Because atmospheric conditions and wave action involve tremendous amounts of energy it is highly unlikely that it will be possible to control any but the most localized weather and wave phenomena within the foreseeable future. Thus, as long as the offshore operations involve the movement of small craft and barges over exposed waters, and the transfer of personnel and heavy equipment from these craft to either fixed structures or larger craft at close quarters, the weather and wave problem will remain.

Taking into consideration the persistence of the wave and weather problem and the improbability of achieving a direct solution, the Humble Oil & Refining Company, in planning its offshore campaign investigated the possibility of forecasting wave and weather conditions in order to provide warnings of dangerous conditions and increase efficiency in day-to-day planning of work. It was recognized that predictions of wave and weather conditions based on meteorology and oceanography, both geophysical sciences, are not 100 per cent accurate and application of forecasts in the offshore work was dependent on whether they provided information which was sufficiently greater in accuracy than the layman's guess to be worth the expenditure involved.

During World War II, meteorology and oceanography were used with success in reducing danger resulting from environmental conditions and increasing efficiency of operations exposed to the elements. This success was partially the result of improvement in the scientific techniques involved and the procurement and distribution of observational data, and partially due to the large scope of the military operations which meant that a reduction of losses of a relatively small percentage of the total cost amounted to a large figure expressed in terms of dollars. Since the offshore drilling involves an extremely large financial investment, it was considered that the experience of the Armed Services in successfully employing meteorology and oceanography might be duplicated in the oil industry. In addition, the oil industry's successful experience in utilizing seismology, geology, and terrestrial magnetism; all geophysical sciences, indicated that meteorology and oceanography, also of the family of geophysical sciences and sharing their scientific assets and liabilities, might be profitably put to use.

Since the immediate problem involving the sciences of meteorology and oceanography in the offshore campaign is wave action, a program was inaugurated within the Humble Oil & Refining Company during June 1947, the purpose of which was to ascertain the applicability and limitations of wave forecasting in the offshore campaign. A summary of the effective wave forecasting techniques developed during the war was prepared in the form of a forecasting manual for the Continental Shelf off Grand Isle, Louisiana, by Bates and Glenn. After completion of this manual, experimental forecasts were prepared daily over a two-month period by Graham and Thompson to determine the accuracy of the forecasts.

It was considered that the accuracy of the experimental forecasts justified a more extensive test under actual operating conditions in the offshore work and the firm of A. H. Glenn and Associates was set up under the sponsorship of the Humble Oil & Refining Company to work with the Humble Grand Isle District in providing forecasts of wave and weather conditions over a one-year period. This paper discusses the service now provided to the Grand Isle District, its applicability and limitations.

TYPE OF FORECASTS REQUIRED

It was apparent before the commencement of the forecasting service that a specialized type of forecast was required. Many of the weather elements of interest to the general public, such as rain and temperature, are of minor concern to offshore operators. On the other hand, such elements as wave height and wind speed and direction are of great concern in the offshore operations since variations in wave height of a few feet in the critical range divide safe from hazardous working conditions. To be of utility, a forecasting service for the offshore work must provide detailed forecasts of the elements which affect the operation. With this in mind, it was decided that forecasts would include the following information: average wave heights to the nearest foot, wind speeds within a range of approximately 5 miles per hour, and wind directions within $22\frac{1}{2}$ degrees. Since the procedure for forecasting these elements involves thorough analysis of weather data, it was decided to include a generalized forecast of weather conditions such as rain and cloud cover, although these are of secondary importance.

Manuscript received at office of the Branch September 30, 1948. Paper presented at Branch Fall Meeting, Dallas, Texas, Oct. 4-5, 1948.

These forecasts have been prepared twice daily for periods of 24 and 48 hours in advance since the inauguration of the forecasting service. The 48-hour forecast is prepared with the understanding that the accuracy of this forecast during rapid changes of weather conditions is expected to be low. It was decided that revised forecasts would be issued on the basis of more recent data whenever an appreciable change in conditions was expected that had not been predicted in the routine forecasts.

FACILITIES NECESSARY TO PROVIDE WAVE AND WEATHER FORECASTS

Before discussing specific forecast procedure, the facilities which must be available to the meteorologist before a weather service can be provided will be outlined. This is necessary in order to explain the problems of providing a weather service in the coastal areas of Louisiana and Texas and also to indicate what in general are the meteorologist's tools in preparing a forecast. There is considerable misinformation circulated concerning the science of meteorology. This is partially the result of the publicity given a number of "quacks" and partially because the two theoretical sciences on which meteorology is based, thermodynamics and hydrodynamics, are somewhat abstract in comparison to other physical sciences which have obvious applications in machines in everyday use.

The first requirement of the meteorologist is a source of up-to-the-minute weather data which permits the construction of a quantitative three-dimensional representation of the atmosphere within a radius of one to two thousand miles from the point for which short range forecasts are to be made. These data are provided by the U. S. Weather Bureau. The Weather Bureau makes observations of weather conditions at a large number of meteorological stations throughout the United States and in certain locations outside the continental limits. Such observations are also made by the meteorological services of other nations and these are communicated rapidly throughout the world. There are three types of standard meteorological observations: sur-

face, winds aloft, and radiosonde observations. Surface observations are made throughout the world at land stations and on certain ships simultaneously four times daily. They are standardized by international agreement and include data on cloud cover, winds, pressure, temperature, humidity, visibility, precipitation and a number of other elements. Winds aloft observations in the United States and the Gulf-Caribbean area are also made four times daily by tracking the rise of a free balloon into the upper atmosphere either visually by use of a theodolite or by tracking a radar target suspended from the balloon. Radiosonde observations provide a determination of temperature, humidity, and pressure in the upper atmosphere. The radiosonde unit consists of a small radio transmitter the signal of which is modulated by pressure, temperature, and humidity sensitive elements. The unit rises through the atmosphere suspended from a free balloon, and a continuous recording of the three meteorological elements is received at the ground station. Radiosonde observations are made simultaneously at about 60 stations in the United States and Gulf-Caribbean regions. The surface, winds aloft, and radiosonde observational data are encoded and placed shortly after their procurement on U. S. Weather Bureau teletype circuits which make them immediately available to those with receiving services on this teletype circuit.

By the use of these data it is possible to construct charts for various levels from the surface to 50,000 feet in altitude which give the distribution of temperature, pressure, and moisture at each level. These charts provide the meteorologist with a three-dimensional reconstruction of the atmosphere around his locality within a few hours after the time the observations were made. The problem in forecasting is to extrapolate from the past sequence of weather conditions the future movements of and the energy transformations in the atmosphere which account for variations in weather conditions.

The second requirement of the meteorologist is accurate, routine, quantitative observations of the weather conditions at the locations for which forecasts are made. In any particular locality the effect upon atmospheric condi-

tions of irregularities in topography, the configuration of land and water areas, the differential cooling and heating of land areas and water areas by night and day, and the variation of normal surface temperatures must be considered before accurate forecasting is possible. In many areas of the country, forecasts for specific locations such as cities and airports have been made for many years and the so-called local effects are distinguished from the large scale changes in weather conditions have been determined. Such is not the case for the preponderance of the coastal areas of Louisiana and Texas. Thus, at the present time it is necessary to determine the local effects on the large scale atmospheric conditions in the coastal areas.

Accurate instrumental observations are also necessary to obtain an objective evaluation of the accuracy of the forecasts. An analogy may be drawn between the meteorologist's need for local observations at his forecast location and the geologist's need for samples of well cuttings in order to verify his predictions concerning location of oil deposits and improve future predictions. The geologist can state in broad terms the characteristics of the subsurface strata and whether there is likelihood of oil bearing strata in a given geographical zone. The accuracy of predictions of the existence of recoverable oil deposits at a specific location would be extremely low, however, if he had to depend entirely upon such generalized information. If the petroleum geologist did not have available accurate data concerning conditions within a restricted locality he would not be able to discover small scale features of the local geology which are all important in locating commercial production areas. The meteorologist's problem is identical. A forecast may be excellent from the standpoint of large scale features but if the local effects are not properly evaluated, the forecast may be utterly useless in practical application. Thus, the second requirement of the meteorologist is accurate observations made at the locality for which he is forecasting.

The third requirement in maintaining a forecasting service is rapid and reliable communications. In most parts of the country this is no problem, but

unfortunately in the coastal areas where offshore operations are now progressing, communications are a major problem. For example, in providing forecasts for the Humble Grand Isle District it would be preferable to set up the forecasting office in the district office. However, there are no teletype line facilities to the south of New Orleans which would permit the installation of receiving drops on the Weather Bureau teletype circuits in the Grand Isle District office. This is typical of communications facilities over most of the Louisiana and Texas coasts. It is necessary, therefore, to establish the main forecasting office in New Orleans, which is serviced by Weather Bureau facilities, and depend upon radio or telephone communication of the forecasts and observations between the forecasting office and the center of offshore operations. At the present time public communications in most of the coastal areas of Louisiana and Texas are unreliable, crowded, or non-existent. This places a severe handicap on the success of a forecasting service because there is nothing more useless than a forecast received after the predicted weather has already occurred.

FORECASTING PROCEDURES

The ocean waves which are observed visually day after day are generated by the stress of the wind on the ocean surface. These waves may be subdivided into two types, wind waves and swell. Wind waves are those generated by the local wind. These waves are short and choppy; they increase rapidly in height when the wind increases and decrease rapidly when it decreases. Swell, sometimes called ground swell, consists of long, even, "rolling" waves. Swell is the end product after wind waves have moved away from the area in which they were generated. The movement of the wave energy through the water is such that the period and the wave length of the swell increases as it moves away from the generating area, accounting for the smooth regular characteristics of these waves. Swell may be observed at a location when calm wind conditions obtain locally. The appearance of the sea surface is the result of the local wind waves superimposed on the one or more swell wave trains which may be present.

In order to forecast wind wave conditions, it is first necessary to forecast the winds which will generate the waves, and second determine the characteristics of the waves produced by this wind. The wind conditions are predicted using meteorological charts and these predictions are subject to the errors of meteorological forecasting. The relationship between wind and wave conditions was developed for forecasting purposes during the war by a number of oceanographic research groups of which the work of Sverdrup and Munk at the Scripps Institution of Oceanography was outstanding. The height of ocean wind waves are now known to be determined by the speed of the surface wind; the distance over which it blows, known as the fetch; and the elapsed time during which the wind blows over the fetch, known as the duration. When the wind speed, fetch, and duration are determined, the wave height, period, direction of movement, and speed of movement can be ascertained. This process has been simplified by the use of graphs developed by Sverdrup and Munk.

To prepare forecasts of swell conditions, all the wind wave generating areas in the Gulf are considered as to the possibility of wind waves emerging from the leeward end of the fetch moving as swell to the offshore locations. The procedure employed in determining the decrease in height of the swell waves and the travel time of the swell wave train from its generating area to the offshore location has also been simplified to a rapid graphical technique.

Either wind waves or swell moving from deep into shallow water, or into areas where pronounced currents are present, undergo transformations as to direction of movement, height, and wave length and these factors must be considered in preparing the forecast. Forecasts of wave heights are prepared for specific locations, not for areas. Sometimes a group of off-shore rigs will have nearly similar characteristics as far as wave conditions are concerned, but this is not usually the case. In general, there will be differences in depth of water, bottom topography, exposure to open sea, length of fetch for offshore winds, and currents which result in variations in wave height from one rig location to another.

While strong winds and resulting high waves occur in a variety of meteorological situations, there are a number of weather phenomena of typical characteristics which occur repeatedly in the coastal areas of Louisiana and Texas causing high winds and waves for which a more or less standardized forecasting procedure has been developed. Discussion of the forecast procedure for such typical weather phenomena which affect the offshore work; northers, line squalls, hurricanes, may provide a more detailed explanation of the service being provided the Grand Isle District than can be ascertained from the preceding generalized discussion.

NORTHERS

During the period extending roughly from November to March the Gulf Coast area is subject to northers. Northers, known as polar outbreaks by the meteorologist, consist of a rapid southward flow of cold air in the low levels of the atmosphere. Where offshore locations are within 10 to 15 miles of the shore, the northwesterly winds immediately following the onset of the norther will rarely produce high waves even though wind speeds of 50 to 60 miles per hour obtain. However, the northers are frequently preceded by 20 to 25 mile per hour, southerly winds which over their long fetch across the Gulf have produced waves of the order of 10 to 15 feet in height moving from the south. The danger of the norther consists partially in the possibility of boats, ships, and barges moored adjacent to drilling platforms in such a position as to be braced against the southerly winds and waves to be suddenly subjected to action of strong northerly winds and choppy wind waves with little advance warning. The wind shift from south to north is likely to occur during a period of a few minutes with accompanying gusty winds and heavy rain showers. Ramping of the drilling platforms by the floating vessels is a possibility under these conditions. In addition to the dangers accompanying the onset of the norther, there is usually a gradual wind shift from northwesterly to northeasterly after the onset of the norther. The northeasterly winds are capable of raising considerably higher waves than the

northwest winds since they blow more nearly parallel to the coast and provide longer fetches for the generation of waves.

The forecasting for northers consists of a warning of 24 hours or more that a norther is moving towards the Gulf over the Great Plains, and a short range warning approximately 6 hours in advance of the movement of the norther to the rig locations. The latter short range warning can be supplemented by a 1- to 2-hour warning accurate within 30 minutes by use of radar. Radar is a very effective aid in forecasting weather conditions accompanied by rain cloud formations extending to high altitudes. Its use is described later under techniques utilized in forecasting line squalls. The long range warning of the norther is provided by analysis of the surface weather map based on weather observations made every 6 hours. The short range warning is provided by weather observations made every hour or at times of significant weather changes. For example, up-to-the-minute weather observations made at Biloxi, New Orleans, Baton Rouge, Lafayette, Lake Charles and Beaumont will permit the short range warnings for northers arriving along the Louisiana coast.

LINE SQUALLS

Line squalls are a common weather feature of the Louisiana coastal area, occurring four to five times per month with considerable severity in the spring months. Isolated squalls occur with much greater frequency but with less severity during the summer months. The line squall consists of a bank or cumulonimbus (thunderheads) clouds oriented along a northeast-southwest line. The line squall moves in a southerly direction approximately normal to its axis and is accompanied by strong, gusty winds, from a northerly or westerly direction; heavy rain; and lightning. During the spring months line squalls may be extremely hazardous. A severe line squall which occurred in the Grand Isle area on June 9 caused an increase of winds to 55 miles per hour with gusts to 75 miles per hour within a period of one-half hour. The moisture distribution and the wind conditions aloft which favor a development of line squalls are recognizable from

standard meteorological charts so that an initial warning of the likelihood of a line squall can frequently be made 6 to 8 hours in advance.

The short range warning of the movement of a line squall into the offshore area is made by utilizing hourly weather reports from stations to the north which have already been passed by the squall and by use of radar. The clouds associated with the squall ascend vertically to an altitude between 15,000 and 40,000 feet and contain large water drops which reflect a radar signal. Thus, a clearly defined image delineating the rain areas of the line squall may be observed moving across a PPI radar scope. By plotting successive positions of the squall on the scope and extrapolating the movement, the arrival time of the squall can be determined within 15 to 20 minutes and the strength of the gusty winds can be estimated from reports from U. S. Weather Bureau stations previously affected by the squall. If no such reports are available, the gusty surface winds can be estimated from wind conditions aloft.

In general, the short duration of the line squall precludes the formation of high waves; however, wave heights of 5 to 6 feet have been measured during a squall passage. Such waves are accompanied by winds sufficiently strong to break a barge from its mooring and cause damage to the floating equipment and drilling platforms unless proper precautions have been taken in advance. The high, gusty winds accompanying squalls can also inflict damage to the drilling and production equipment on the drilling platforms. Such items as drill pipe or tubing standing in the derrick can dangerously reduce its safe wind-loading characteristics. The pipe and the derrick can also be damaged by the pipe being blown around in the derrick if not properly tied down. The one-to-two-hour advance knowledge of the imminence of these severe squalls, which can be provided by the technique outlined above, is usually sufficient to take the precautions required for these severe blows of short duration.

HURRICANES

By far the most spectacular and dangerous phenomenon affecting offshore drilling and production operations is

the hurricane. Extremely high waves are possible during hurricane conditions depending mainly on the depth of water where the operations are under way. On the basis of past hurricanes that have occurred along the Gulf Coast, the maximum wave height to be expected would be about 32 feet in water from 40 to 100 feet in depth; 24 feet in water 30 feet in depth; 15 feet in 20 feet of water; and 8 feet in water 10 feet deep. In anticipation of hurricane conditions it is usually necessary to secure drilling and production operations and evacuate personnel to safe points ashore. Considerable time can be consumed in preparing for evacuation and transporting personnel to safety. Obviously, it is important to receive hurricane warnings as far in advance of the storm as possible. Even before the storm itself moves into an area, swell which extends well out in front of the storm center can produce sea conditions which make any type of hurricane mooring arrangement difficult to accomplish unless begun in ample time.

Hurricanes consist of a counterclockwise revolving vortex of warm, moisture-laden tropical air 20,000 to 40,000 feet deep. There are no successful techniques yet devised for predicting the movement of hurricanes for long periods in advance although the movement can usually be anticipated correctly 6 to 12 hours in advance. At present, hurricane warnings are based on tracking of the hurricane movement and short range extrapolation of past movement. Improvement in hurricane warnings in recent years has been primarily the result of improvement in methods of tracking, and in extension of observing facilities to include a dense network of land stations and a large number of ship reports. Improvement of tracking methods has included use of radar for short range tracking and hurricane reconnaissance aircraft for tracking hurricanes outside of radar range, rapid and reliable communications, use of automatic weather stations on certain locations in the Bahama area, use of LORAN for navigational fixes on aircraft flying in the vicinity of the storm, and the use of aircraft radar for fixes on the storm center, and other facilities which are of general use in routine forecasting or are still in the research stage. The hurricane warning

service now in operation in the southeastern United States is a joint project of the U. S. Weather Bureau, the Air Force, and the Navy. All hurricane advisories, whether issued by the Weather Bureau or private meteorological consultants, are based on data procured by this joint governmental service, and the accuracy of such advisories is initially dependent on the effectiveness of the facilities provided for obtaining data.

The forecasting procedure for hurricanes consists of fixing the center by analysis of all available data and the prediction of movement by use of extrapolation of past movement, knowledge of wind, pressure, and moisture conditions in the upper atmosphere, and application of knowledge gained in the past of the characteristics of hurricane movement. Because of the extreme danger of the hurricane and the desirability of securing offshore work in anticipation of hurricane conditions one of the most important functions of a weather service for the offshore operations is in assisting in arriving at a decision as to when offshore rigs should be evacuated.

THE FORECASTING ORGANIZATION

To apply the foregoing forecasting techniques efficiently, assure accurate observations at the forecast location, and make use of radar in providing short range warnings the forecasting service is organized to include a forecasting unit in New Orleans serviced with Weather Bureau teletype facilities, and a meteorologist on full-time duty at the Grand Isle District office, who is equipped with meteorological instruments, a wave gauge, and radar. He is furnished twice daily, from the New Orleans office, weather information which permits an evaluation of local weather conditions in terms of large scale conditions over the United States and Gulf-Caribbean area. The meteorologist in the district office handles the distribution of forecasts, maintains complete weather observations, provides routine maintenance of meteorological instruments, and assists the district personnel when decisions must be made which call for interpretation of the forecasts or require information not included in the forecast. This latter func-

tion is quite important because the ultimate goal of the weather service is to anticipate working conditions, not weather conditions. The weather conditions must be interpreted in terms of how they will influence the operations and this interpretation can be carried out most effectively by discussion between the meteorologist and the district personnel.

UTILIZATION OF FORECAST IN OFFSHORE WORK

After the preparation of the forecast and the briefing of field personnel who will make use of the information, the next problem is to determine whether a particular transportation, drilling or production operation is feasible under forecast conditions. It is not possible to define operating limits without actual experience under various sea and wind conditions because the type of operation that can be successfully and safely carried out under forecast conditions depends on the type of equipment involved, the experience of the personnel engaged in the operation, and the length of time required to complete the work.

The transportation phase of offshore drilling and producing operations is obviously the most critical from the standpoint of sea conditions. The importance of forecasts in scheduling open sea transportation depends to a varying degree on the following factors: (1) distance to be traversed in the open sea, (2) length of time required for round trip, (3) seaworthiness of equipment involved, (4) nature of cargo, (5) facilities for mooring in open sea or at destination, (6) number of drilling and production operations under way simultaneously, and (7) proximity of operations relative to each other. When sending deep-draft tugs over shallow outside bars or in shallow channels, wave height forecasts are important in determining the possibility of the vessel pounding bottom or running aground in heavy seas. Sea conditions also greatly affect the speed at which a barge can be towed as well as the number of tows which can be successfully handled by a single tug. After the tow has reached its destination, wave and wind conditions determine whether or not it can be moored at the drilling

or production site. A knowledge of expected wave conditions may dictate the necessity of having a tug stand by the tow at the drilling or production site in case of unfavorable weather.

Producing operations, where barging is the primary source of transportation, depend almost entirely on favorable sea conditions. To obtain as nearly as possible an uninterrupted flowing schedule, a forecast of sea conditions is important in order to make the most efficient and safe use of barges and tugs. A hazardous condition exists if a loaded barge of oil is caught in rough seas. There is danger that the barge will break loose from its mooring or its towing line and be set adrift. If loading or unloading operations are under way when wave heights increase, damage to the loading facilities, pollution of the water, or fire may be the result.

Forecasts of weather and wave conditions are important when long strings of casing are to be run. This operation to be successful must not be interrupted for any great length of time. Knowledge of expected sea conditions becomes even more critical when small platforms are used which do not contain sufficient pipe racks to hold the entire casing string. The job may be unsuccessful if it is necessary to remove the drilling tender due to rough seas when the string is being run. To minimize this hazard the amount of time required to lay down the drill pipe and run the casing string can be estimated and if unfavorable weather conditions which might interrupt the casing job were forecasted, the operation can be postponed to good advantage until more favorable conditions are expected.

During hurricane periods coordination between the meteorologist and the field personnel permits the continuance of drilling for a maximum period compatible with safety and resumption of work immediately after the danger is over. As a rule, evacuation of the offshore structures will require removal of drill pipe from the hole, movement of unpropelled vessels to hurricane anchorage, evacuation of personnel from rigs and anchored vessels by crew boats, and possibly evacuation from shore bases if storm tides are expected. This hurricane procedure is time con-

suming and may only be feasible under daylight conditions. After determination of the time required and conditions under which the evacuation must be carried out the meteorologist can assist in determining when the evacuation must be commenced to be completed under safe wind and wave conditions. Occasionally the initial movement of a hurricane may demand

immediate preparations for evacuation while a later change in course may permit resumption of work although the hurricane is still active. Under these conditions the meteorologist's advice may be instrumental in avoiding costly downtime.

The foregoing examples indicate the types of situations in which the meteorologist can be of assistance in reducing

the hazards and increasing the efficiency of the offshore work. The long-term utility of the present wave and weather forecasting service provided to the Grand Isle District can only be defined after a further period of test. Experience to date has justified extension of the period of test beyond the one-year period originally planned.

★ ★ ★

A STUDY OF OIL AND GAS CONSERVATION IN THE PICKTON FIELD

J. R. WELSH, R. E. SIMPSON, J. W. SMITH, AND C. S. YUST, MEMBERS AIME
HUMBLE OIL & REFINING COMPANY, HOUSTON, TEXAS

ABSTRACT

This paper presents the results of a complete reservoir study designed to determine a sound economic program for the conservation of oil and gas in the Pickton field, Hopkins County, Texas. The Pickton field produces from the Bacon Lime with all indications of the study being that production is predominately by dissolved-gas drive. Calculations of the total ultimate recovery to be expected under primary operations indicated only 16.7 per cent of the oil originally in place would be recovered. This unusually low recovery is due to the type of drive operating and the extremely high dissolved gas-oil ratio and shrinkage.

Results are presented for six plans of returning gas to the reservoir, evaluated to determine (1) comparative recoveries and economics of (a) returning gas at a constant rate by supplementing Pickton gas with extraneous gas during the early portion of the operation, and (b) conventional gas-return operations without using extraneous gas, and (2) the optimum size of compressor plant for each type of pressure maintenance.

The over-all economic program considers, for either type pressure maintenance operation, a gasoline plant to process the unusually rich casinghead gas. Since pressure maintenance will disturb equities, pooling of royalties is in the case of Pickton a prerequisite to conservation of oil by this type of operation, both from an economic and legal standpoint. In the event pooling of royalties cannot be achieved, the study considers a gasoline plant to operate under a modified primary production operation which will make the conservation of gas possible.

INTRODUCTION

The Pickton field, located in Hopkins County, Texas, was discovered in November, 1944, by the completion of Humble's C. D. Nichols 1, in the Bacon lime of the Lower Glen Rose formation, through perforations from 7,888 to 7,896 feet. The well initially produced 50.2 API gravity oil with a gas-oil ratio of 1,350 cubic feet per barrel. Subsurface samples of the reservoir fluid obtained soon after completion of the discovery well showed that the Pickton crude is unique in that it has an extremely high dissolved gas-oil ratio and is subject to very severe shrinkage.

Calculations of the future behavior of the Pickton reservoir indicated that ultimate oil recovery by primary operations would be 3,269,000 barrels, representing only 16.7 per cent of the oil in place (19,577,000 stock-tank barrels), and that recovery could be substantially increased by returning the

produced gas. The cumulative production of 1,382,694 barrels on November 1, 1947, amounted to 42.3 per cent of the estimated ultimate oil recovery from primary operations.

The purpose of this study is to determine and evaluate the optimum program for conservation of oil and gas in the Pickton field, including the desirability of conducting gas-return operations and of installing a gasoline plant.

LOCATION AND DESCRIPTION

Pickton Field

The Pickton field, as shown in Fig. 1, is located in southwest Hopkins County, Texas, 12.5 miles southwest of the New Hope field, 2.7 miles northeast of the Coke field, 16 miles southwest of Sulphur Springs, and 8 miles northwest of Winnsboro, Texas.



FIG. 1—INDEX MAP.

The low-relief, domal-type structure has about 100 feet of closure on the base of the Ferry Lake, or massive anhydrite section, that occurs immediately above the producing formation. Production is from the Bacon lime which occurs at the top of the Lower Glen Rose formation of the Commanche Series, Lower Cretaceous System, Mesozoic Era. Although the first few feet of the Bacon lime are usually dense and impermeable, the base of the massive anhydrite is used as the top of the producing formation. Fig. 2 is a contour map of the base of the massive anhydrite. New Hope and Winnsboro are the only other fields in the immediate area that produce from the Bacon lime.

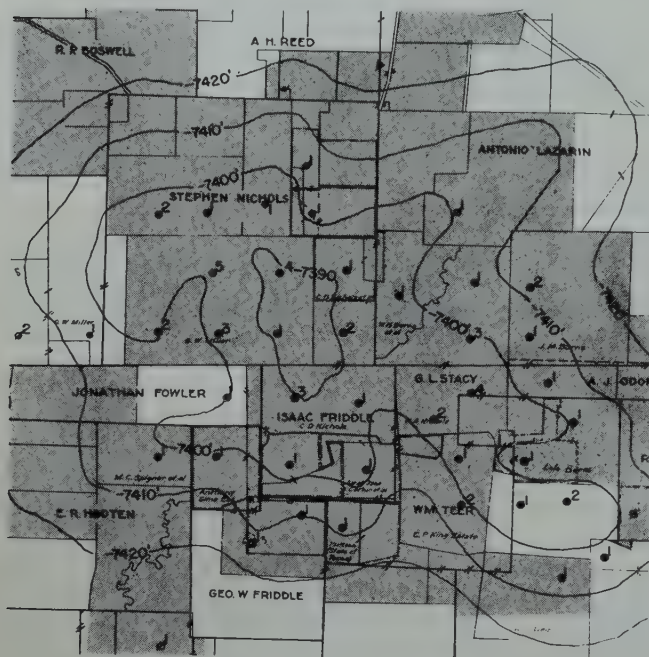


FIG. 2—CONTOUR MAP OF BASE OF MASSIVE ANHYDRITE (TOP OF BACON LIME)—PICKTON FIELD.

Bacon Lime

The Bacon lime at Pickton is oolitic and dolomitic, averaging 25 feet in thickness and having an average effective net producing section of 14 feet. Maximum porosity development is noted in structurally high wells and porosity decreases towards the edge of the field where low-permeability dense lime occurs. A decrease in the porosity is also observed throughout the reservoir at depths approaching the oil-water contact but does not correspond with the oil-water level because of the erratic nature of the porosity development. Examination of about 380 core samples from the productive portions of the formation in 19 wells indicates an average porosity of 19 per cent and average permeabilities parallel and perpendicular to the bedding plane of 379 and 183 millidarcys, respectively. A summary of reservoir data is presented in Table 1.

The producing formation has been encountered as high as 7,388 feet subsea, and the water table has been established at 7,425 feet subsea, indicating a maximum oil column of 37 feet. An associated gas cap could not be detected from information obtained on wells drilled high on the structure during the early development of the field.

TABLE 1
RESERVOIR DATA
Pickton Field

Original Oil-Water Contact, Ft. SS.	7,425
Average Porosity, Percent	19
Permeability, Millidarcys*	
Parallel to Bedding Plane	379
Perpendicular to Bedding Plane	183
Connate Water, Percent of Pore Space	25
Average Net Pay Section, Ft.	14
Estimated Oil in Place, MM Reservoir BBL	40.8
Original Reservoir Pressure, Lb. Per Sq. In. Ga. at 7,424 Ft. SS.	3,578
Reservoir Temperature, F.	209
Characteristics of Produced Oil**	
Dissolved Gas-Oil Ratio	2,220
Shrinkage Factor, BBL Stock-Tank Oil Per Reservoir BBL	0.413
Oil Gravity, API	46.0
Sodium Chloride Content of Connate Water, PPM	260,000
Viscosity of Original Reservoir Oil Centipoises	0.21

*Average of approximately 380 determinations on cores from 19 wells.

**Original reservoir oil produced under separator conditions of 0 lb. per sq. in. and 80° F.

A correlation of electric logs and core analyses indicates that a streak of dense low-permeability limestone (with an average thickness of about 2 feet) occurs generally throughout the producing formation approximately 15 feet below the massive anhydrite, as shown by representative north-south and east-west cross sections in Fig. 3. Pressure performance of wells completed in the upper and lower portions of the reservoir has indicated restricted communication across the dense streak with migration of oil from the upper to the lower portion from which the majority of the production has been obtained to date.

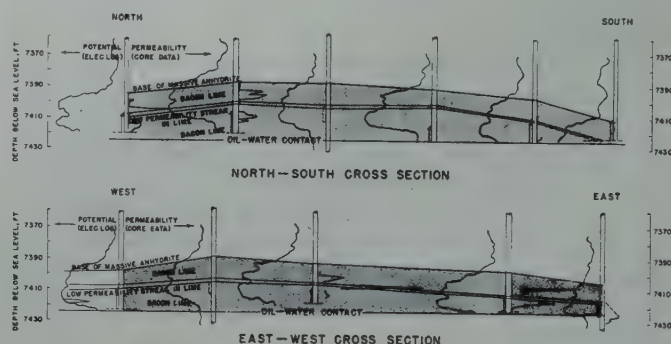


FIG. 3—TYPICAL CROSS SECTIONS—PICKTON FIELD.

Geologic data from wells drilled to the Bacon lime in the East Texas area indicate that the formation is permeable only in small areas and is, therefore, unlikely to have sufficient areal extent of adequate permeability to support an appreciable water drive for the Pickton reservoir, even though a water table is present. This has been further substantiated by the pressure-production performance of the reservoir.

HISTORY

Discovery

The presence of the Pickton structure was first indicated by geologic correlation of subsurface data and was later confirmed and isolated by geophysical data. The discovery well, Humble's C. D. Nichols 1, was drilled to a total depth of 8,850 feet in the Travis Peak and was plugged back for completion in the Bacon lime through casing perforations from

7,888 to 7,896 feet on November 6, 1944. On the initial potential test, the well produced 611 barrels of 50.2 API gravity oil through a 1/4-inch choke with a gas-oil ratio of 1,350 cubic feet per barrel.

Development

Drilling of the Pickton field has continued steadily since discovery, and as of November 1, 1947, the three operators in the field had completed a total of 36 producing wells, with 31 (86.1 per cent) operated by Humble, 3 operated by Magnolia, and 2 operated by Hunt. In addition, 4 wells (3 Humble) have been abandoned as dry holes, and of these, 1 abandonment has been converted and equipped for salt-water disposal into the Dexter section of the Woodbine formation. A drilling development program for the field is continuing.

Present estimates are that the field has 2,600 productive acres and 40.8 million barrels of reservoir space originally occupied by oil as summarized in Table 2. Railroad Commis-

TABLE 2
PRODUCTION AND RESERVE DATA
Pickton Field

	Total Field
Estimated Productive Area, Acres.....	2,600
Producing Oil Wells as of 11-1-47.....	36
Estimated Oil in Place, Reservoir Barrels.....	40,785,586
Estimated Recoverable Oil, Stock-Tank Barrels*	3,269,000
Cumulative Oil Production as of 11-1-47.....	1,382,694
Allowable, Barrels per Producing Day on 11-1-47.....	1,414
October 1947 Monthly Oil Production, Barrels.....	42,481
Cumulative Gas Production as of 11-1-47, Mcf.....	2,578,631
Cumulative Water Production as of 11-1-47, Barrels.....	81,743

*Estimated ultimate production to 100-pound-per-square-inch abandonment pressure under primary recovery.

sion field rules call for 40-acre spacing, with a tolerance of 20 acres granted the last well on a lease. The allowable is allocated on a 75 per cent acreage and a 25 per cent well basis with a penalty gas-oil ratio of 2,500 cubic feet per barrel.

Completion Practices

The early completions were of the gun-perforated type, but due to difficulty in obtaining satisfactory completions for wells located in the less permeable areas, the open-hole method of completion was tried and adopted for general use. The present completion method consists of drilling and coring to 7,423 feet subsea, obtaining an electrical log, and setting casing with 4 to 5 feet of the bottom porosity open to the well bore.

ANALYSIS OF PAST RESERVOIR BEHAVIOR

Reservoir Pressure-Production Data

The original reservoir pressure as measured in the discovery well, C. D. Nichols 1, was 3,578 pounds at 7,424 feet subsea and reservoir temperature was determined to be 209° F. At the time of the pressure measurement, the well had produced approximately 2,000 barrels of stock-tank oil and had been shut in for 134 hours. A total of 15 shut-in subsurface pressure surveys have been made in key wells with a maximum interval of 5 months between any 2 surveys. The reservoir pressure has been determined by arithmetically averaging the

individual well pressures. Fig. 4 illustrates the variation in individual well pressures for the survey effective October 23, 1947. A total of 18 flow tests were run to determine individual well producing characteristics.

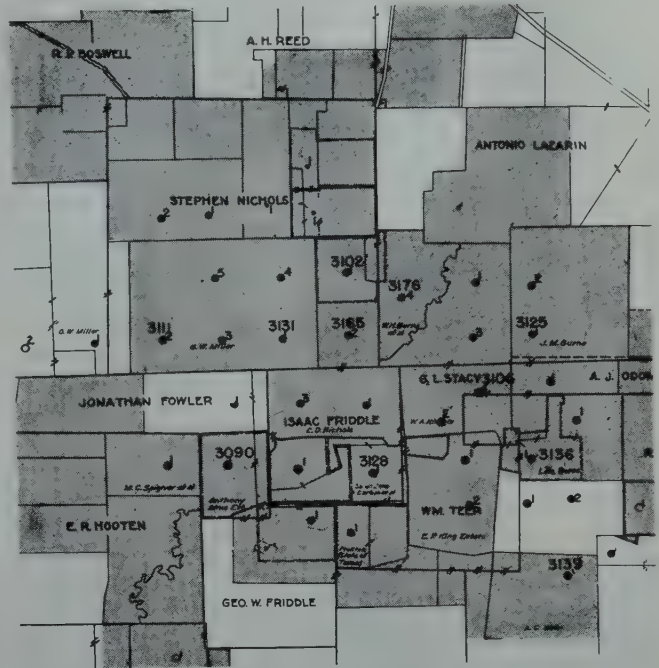


FIG. 4—SUBSURFACE PRESSURE MAP—PICKTON FIELD.

Effective November 1, 1947, the reservoir pressure was 3,123 pounds with a corresponding cumulative production of 1,382,694 barrels of stock-tank oil, which represents 42.3 per cent of the total oil that is estimated to be recoverable under primary operations. The reservoir pressure decline of 455 pounds as of November 1, 1947, (12.7 per cent of the original pressure) amounts to 329 pounds per million barrels of oil produced. Fig. 5 is a summary of the pressure-production performance of the Pickton reservoir.

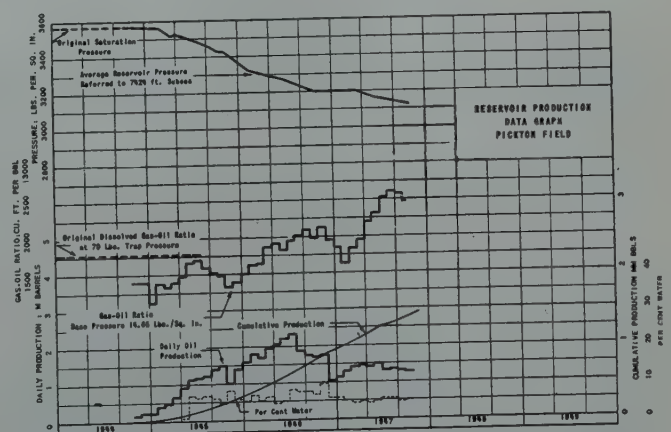


FIG. 5—RESERVOIR PRODUCTION—DATA GRAPH—PICKTON FIELD.

Reservoir Fluid Analyses

Two identical subsurface oil samples were obtained in the discovery well immediately following the initial pressure and temperature measurements. Gas liberation data, pressure-volume-temperature relationships, hydrocarbon analysis, A.S.T.M.

distillation of residual oil, and viscosity-pressure-temperature relationships determined from the two identical samples are shown in Fig. 15, and Table 5. The saturation pressure of the

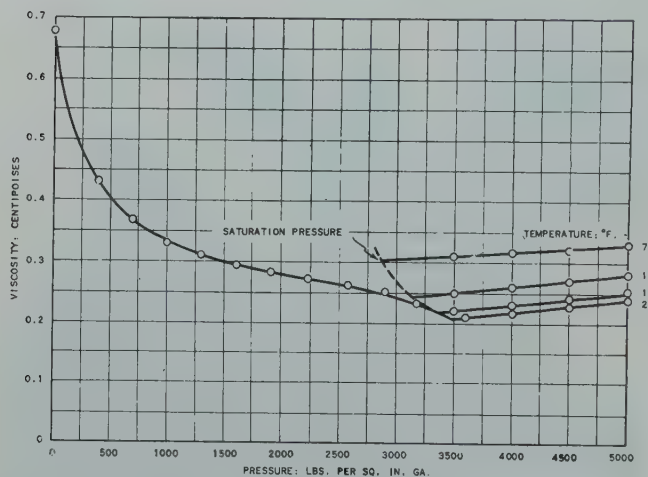


FIG. 15—VISCOSITY OF RESERVOIR OIL.—PICKTON FIELD.
(RESERVOIR TEMP. = 209° F.)

samples was 3,500 pounds at the reservoir temperature of 209° F, which was in close agreement with the pressure conditions existing when the subsurface samples were obtained and indicated the reservoir oil to be saturated with gas under original reservoir conditions even though no associated gas cap was detected in the reservoir. The dissolved gas-oil ratios of the sample oil were found to be 2,220 and 1,497 cubic feet per barrel of stock-tank oil when flashed at 80° F. for 0- and 150-pound separation, respectively. The corresponding shrinkage factors for the 0- and 150-pound flashes were 0.413 and 0.478 barrels of stock-tank oil per barrel of original reservoir oil, with the resulting residual oil gravities for these separation pressures being 46.0 and 50.5 API, respectively. The reservoir material is unique in that the dissolved gas-oil ratio and shrinkage are unusually high which accounts for the attendant pronounced effect that separator pressure has on oil shrinkage, produced gas-oil ratio, and residual oil gravity. The viscosity of the samples at 3,500 pounds and 209° F. was 0.21 centipoises. The effect of separator pressure on the properties of oil and gas was calculated, the results of which are shown in Figs. 12, 13, and 14.

Carefully controlled field tests for single- and two-stage separation were made which provided results that were in close agreement with the calculations.

Water Production

The original oil-water contact has been established at 7,425 feet subsea, based on completion experience, core data, and electrical logs. By November 1, 1947, there were only 7 down-structure wells producing more than 2 per cent water. The bottom of the completion interval in these flank wells varies from 7,416 feet subsea (9 feet above the oil-water contact) to 7,432 feet subsea (7 feet below the oil-water contact); pertinent data are included in Table 3. The water-production histories of 6 of these wells are interesting since the water percentage has remained constant in 1 well, decreased in 2 others, and in the remaining 3 has increased slowly. The reservoir apparently is experiencing very little water influx as demon-

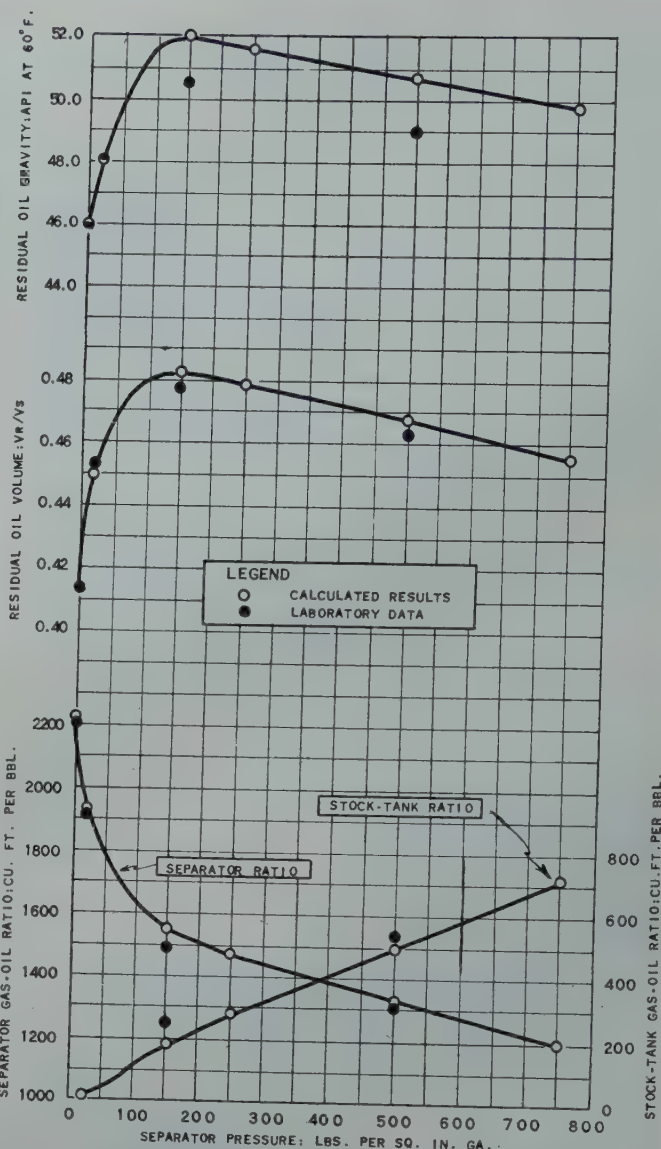


FIG. 12—EFFECT OF SEPARATOR PRESSURE ON PROPERTIES OF OIL AND GAS TEMP. 80° F. SINGLE-STAGE SEPARATION.—PICKTON FIELD.

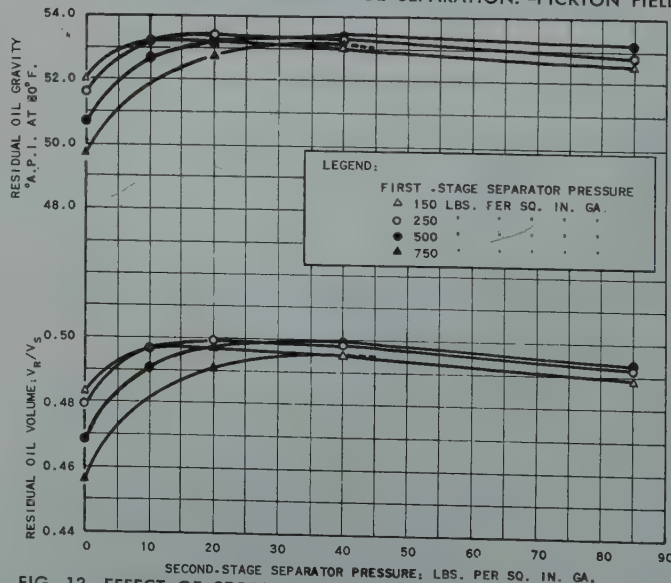


FIG. 13—EFFECT OF SECOND-STAGE SEPARATOR PRESSURE ON PROPERTIES OF RESIDUAL OIL FOR VARIOUS FIRST-STAGE SEPARATOR PRESSURES. TEMP. 80° F.—PICKTON FIELD.

TABLE 5

PROPERTIES OF SUBSURFACE OIL SAMPLE

Source: Pickton Field, C. D. Nichols 1

Date Taken: November 16, 1944

Sampling Conditions: Depth, 7,700 ft. Well was shut in.

Properties of Saturated Oil:

Temperature, F.....	76	150	179	209
Saturation Pressure, lb/sq in. ga.....	2872	3295	3412	3500

Gas Liberation and Shrinkage of Oil:

Flash:		Gas-Oil Ratio: cu ft per bbl. residual oil		Residual Oil Gravity API at 60° F	Sp Gr Gas at 60° F.	Vr/Vs*
Pres. (pl) lb/sq in. ga	Temp. F.	Flashed at pl	Flashed from pl to 0			
0	80	2,220	0	46.0	1.018	.413
20	80	1,924	—	48.1		.453
150	80	1,497	241	50.5		.478
500	80	1,316	527	49.0		.464

Differential at 209° F.:

Pres. lb/sq in. ga	Gas-Oil Ratio: cu ft at 60° F. per bbl reservoir oil at 3,500 lb/sq in. ga, 209° F.	Residual Oil Gravity API at 60° F.	V/Vs**
3,500	0		1.0000
3,200	154		.9064
2,900	264		.8398
2,600	350		.7907
2,300	423		.7519
2,000	486		.7167
1,700	542		.6875
1,400	593		.6614
1,100	643		.6370
800	691		.6123
500	739		.5878
270	783		.5600
148	806		.5418
0	882	47.6	.4820

*Vr, volume residual oil at 0 lb/sq in. ga, 60° F.

Vs, volume saturated oil at 3,500 lb/sq in. ga, 209° F.

**V, volume saturated oil at indicated pressure, 209° F.

Pressure-Volume-Temperature Relations of Subsurface Saturated Oil Sample:

Temperature: 76° F.			Temperature: 150° F.		
Pressure lb/sq in. ga	Relative Volume	Specific Volume cu ft/lb	Pressure lb/sq in. ga	Relative Volume	Specific Volume cu ft/lb
4,500	.9681		4,500	.9679	
4,000	.9766		4,000	.9799	
3,800	.9804		3,800	.9850	
3,600	.9842		3,600	.9905	
3,428	.9875		3,408	.9962	
3,220	.9918		3,295	1.0000	0.02768
3,022	.9960		3,273	1.0022	
2,872	1.0000	0.02582	3,240	1.0057	
2,816	1.0050		3,200	1.0102	
2,769	1.0097		3,160	1.0146	
2,723	1.0143		3,050	1.0279	
2,643	1.0238		2,790	1.0680	
2,540	1.0380		2,510	1.1262	
2,230	1.0953		2,202	1.2161	
1,938	1.1814		1,908	1.3423	
1,630	1.3254		1,615	1.5282	
1,290	1.6045		1,315	1.8268	
1,050	1.9339		1,110	2.1474	
890	2.2618		963	2.4555	
780	2.5927		850	2.7755	
692	2.9208		770	3.0838	
568	3.5905		645	3.7143	
480	4.2601		550	4.3473	

Temperature: 179° F.			Temperature: 209° F.		
Pressure lb/sq in. ga	Relative Volume	Specific Volume cu ft/lb	Pressure lb/sq in. ga	Relative Volume	Specific Volume cu ft/lb
4,500	.9668		4,500	.9635	
4,000	.9804		4,000	.9791	
3,800	.9866		3,800	.9863	
3,600	.9933		3,610	.9938	
3,412	1.0000	0.02843	3,500	1.0000	0.02925
3,385	1.0027		3,478	1.0021	
3,345	1.0071		3,440	1.0063	
3,310	1.0114		3,407	1.0105	
3,272	1.0158		3,375	1.0148	
3,170	1.0288		3,200	1.0378	
2,895	1.0723		2,900	1.0858	
2,600	1.1335		2,600	1.1566	
2,300	1.2214		2,317	1.2467	
2,000	1.3447		2,008	1.3894	
1,622	1.5829		1,723	1.5717	
1,322	1.8942		1,535	1.7327	
1,130	2.1950		1,310	2.0020	
985	2.5066		1,122	2.3125	
878	2.8077		1,000	2.5918	
720	3.4190		758	2.8507	
615	4.0359		600	3.4428	
			648	4.0349	

Production Research Division Progress Report: December 1944.

Hydrocarbon Analyses of Subsurface Oil and Gas Sample:

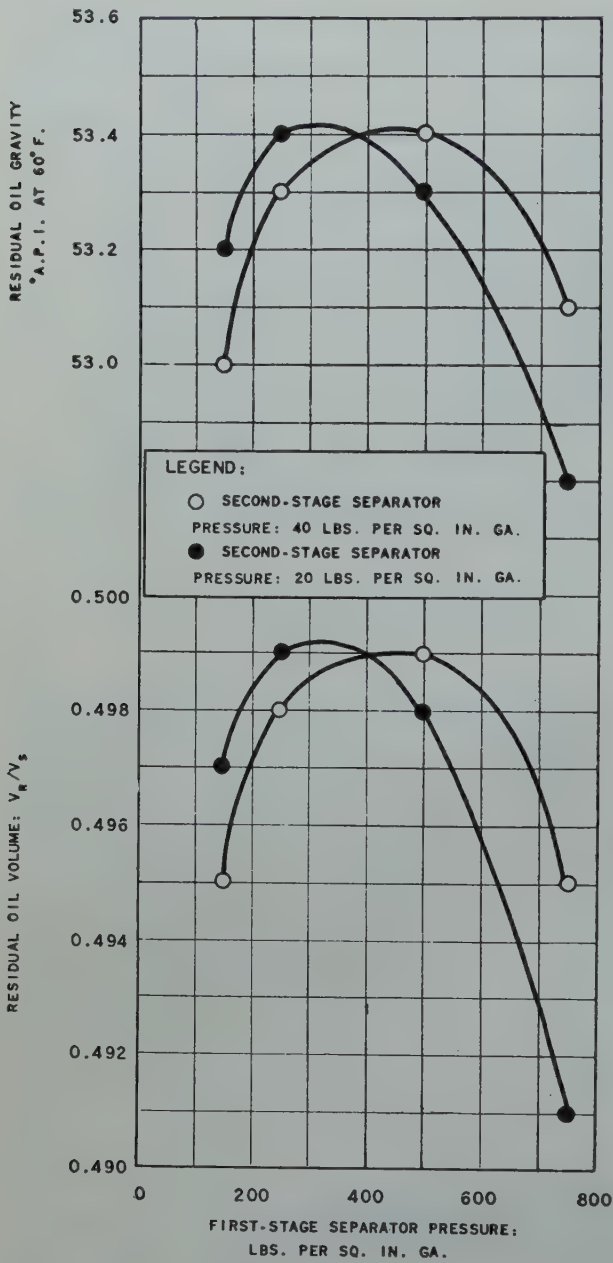
Analysis of: Component	Original Saturated Material			Solution Gas Flashed at 0 lb/sq in. ga. & 140° F.		
	Wt. %	Density gm./cc. at 60° F.	Molecular Weight	Vol. %	Density gm./cc. at 60° F.	Molecular Weight
Methane.....	13.80			59.97		
Ethane.....	3.52			7.88		
Propane.....	5.88			9.97		
Iso-butane.....	2.54			2.89		
N-butane.....	5.75			6.77		
Iso-pentane.....	1.26			1.26		
N-pentane.....	4.32			4.38		
Hexane.....	6.23			3.71		
Heptane.....	2.80	.7168	98			
Octane.....	5.42	.7346	105			
Nonane.....	6.61	.7611	111			
Heavier fraction.....	41.87	.8420	200	3.17	.7265	100
Total.....	100.00			100.00		
Hexane-free fraction.....		.8133	163			

A.S.T.M. Distillation of Residual Oil Sample*:

% Over	Temp.: ° F.
I.B.P.	110
5	160
10	186
15	220
20	251
25	276
30	297
35	333
40	362
45	398
50	432
55	468
60	508
65	550
70	595
75	645
80	685

Maximum temp.: °F.....	686
Recovery: % by vol.....	83
Residue: % by vol.....	15
Loss: % by vol.....	2
Gravity: API at 60° F.	
Distillation charge.....	48.0
Overhead product.....	51.2

*Sample obtained by flash gas liberation, from subsurface oil sample having saturation pressure of 3,500 pounds per square inch gauge at 209° F., to atmospheric pressure and 20 pounds per square inch at 80° F.



strated by (1) the failure of structurally low wells to produce large volumes of water and (2) the relatively small estimated cumulative water production of 81,743 barrels on November 1, 1947.

Gas-Oil Ratio Behavior

The original gas-oil ratio measured on November 9, 1944, during the Railroad Commission potential test of the discovery well, was 1,350 cubic feet per barrel. As shown in Fig. 5, there has been a general upward trend in the field average gas-oil ratio since discovery, and the average ratio over the 4-month period ending October 23, 1947, was 2,526 cubic feet per barrel. Although the optimum single-stage separator pressure is 130 pounds (as obtained from Fig. 12), the field separators are being operated at pressures between 90 and 106 pounds because of the separator specifications.

Individual well gas-oil ratios vary generally from 1,500 to 3,200 cubic feet per barrel, depending upon structural positions of the wells and the location of the completion intervals within the productive section. By comparison of the contour map on the base of the massive anhydrite (Fig. 2) and the gas-oil ratio map (Fig. 6), it may be seen that the high gas-



FIG. 6—GAS-OIL RATIO MAP—PICKTON FIELD.

TABLE 3
WELLS PRODUCING MORE THAN TWO PER CENT SALT WATER
Pickton Field

Lease and Well No.	Elev. (D. F.)	Date Completed	Total Depth Ft.—SS	Completion Interval Ft.—SS	Est. Orig Oil-Water Contact Ft.—SS	Distance Bottom Prod. Interval Above Oil-Water Contact—Ft.	Percent Water Produced		Approximate Date Started Producing Salt Water
							At Comp.	Effective 11-1-47	
J. M. Burns 2.....	502	3-25-46	7,424	7,418—7,424	7,425	1	15.0	3.0	3-46
S. J. Carbin 1.....	481	11-22 45	7,425	7,420—7,425	7,425	0	2.0	2.0	11-45
E. P. King 1.....	489	5-2-46	7,426	7,420—7,426	7,425	—1	3.4	4.0	5-46
G. W. Miller 2.....	498	11-19-45	7,432	7,420—7,432	7,425	—7	7.4	4.0	11-46
O. W. Miller 1.....	500	5-28-45	7,493	7,404—7,416	7,425	9	Not Known	45.0	Not Known
Pickton Statae 1...	495	1-23-46	7,426	7,409—7,426	7,425	—1	33.0	45.0	1-46
M. C. Spigner 1....	477	7-20-45	7,450	7,403—7,420	7,425	5	18.0	25.0	7-45

oil ratios generally occur in the upper part of the structure which indicates that gas segregation may be taking place. Also it appears that localized areas of high gas saturation exist below the streak of reduced permeability in the middle of the producing formation, as well as in the producing section immediately below the massive anhydrite as shown by Fig. 7 which represents a correlation of gas-oil ratios with completion depths for wells completed above and below the streak of reduced permeability. Evidence of possible gas segregation is more pronounced beneath the streak of reduced permeability since the majority of the wells (especially structurally high

wells) have been completed below the low-permeability streak; however, it cannot yet be determined whether gas segregation will become a factor in recovery efficiency.

Calculation of Past Reservoir Behavior

Volumetric balance calculations (Table 4 made for the Pickton reservoir indicated no appreciable water influx which led to the conclusion that the Pickton field was producing predominately by dissolved-gas drive. This confirmed previous opinions that were based on the increasing gas-oil ratio trend, the rapid decline of reservoir pressure, the lack of appreciable water production, the lack of off-structure porosity in the Bacon lime, and the absence of a gas cap. Conventional dissolved-gas-drive calculations were then made by using relative permeability curves of gas to oil as determined by Leverett for unconsolidated sand and by Botset for consolidated sand. It appeared from the past pressure-production history that the relative permeability curve for the Pickton field was between the limits set by the Leverett and the Botset data, and a new curve was constructed to permit duplicating the past reservoir pressure and gas-oil ratio trends of the Pickton reservoir. The agreement between the calculated field data and actual field data is shown by Fig. 8 (Next Page).

Predicted Reservoir Behavior Under Primary Operations

Predictions of reservoir behavior based on the relative permeability curve of gas to oil determined for the Pickton reservoir were made by using conventional dissolved-gas-drive calculations and by assuming water influx to be negligible. Results of these calculations are shown graphically in Fig. 8 and indicate that the total ultimate recovery at the assumed reservoir abandonment pressure of 100 pounds will be 16.7 per

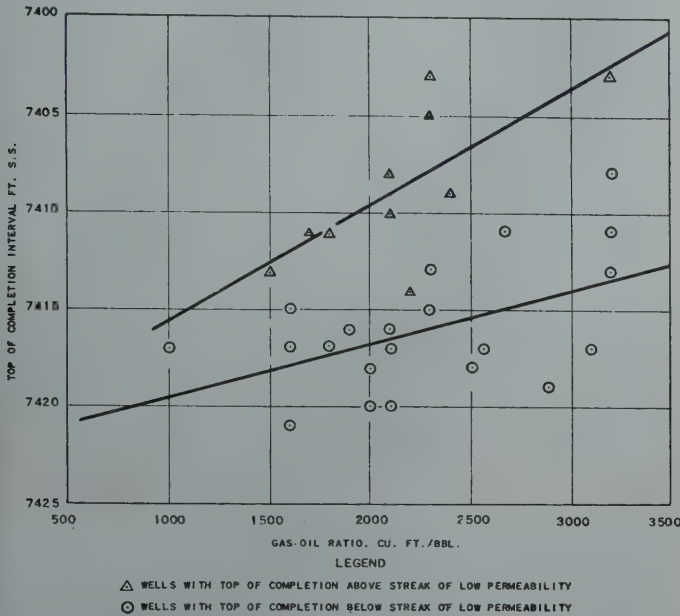


FIG. 7—VARIATION OF GAS-OIL RATIOS WITH COMPLETION DATA. PICKTON FIELD.

TABLE 4
SUMMARY OF VOLUMETRIC BALANCE CALCULATIONS
Pickton Field

Date	Reservoir Pressure lb/in ² @-7,424'	Cum. Oil in S.T. Bbl.	Cum. Oil Orig. Res. Bbl.	Recovery Percent of Orig. Oil in place	Cum. Water Prod. Bbl.	Cum. Gas Prod. Mcf	Avg. GOR Between Surveys Ft ³ /Bbl. S.T. Oil	Cum. Total Fluid With- drawals-Bbl.	Total Water Influx Bbl.	Net Water Influx Bbl.	Bbl. Net Water Influx Per Bbl. Orig. Res. Oil Prod.
1944 November 6	3,578	0	0	0	0	0	—	0	0	0	0.05
1945 January 15	3,565	10,547	22,600	0.055	0	—	—	22,550	— 31,150	— 31,150	—1.38
February 18	3,562	20,256	43,400	0.105	0	—	—	43,400	— 18,600	— 18,600	—0.43
April 11	3,527	46,135	98,800	0.239	0	56,830	—	99,100	—115,900	—115,900	—1.17
May 1	3,520	59,299	126,900	0.307	0	76,063	1.366	127,600	—120,400	—120,400	—0.95
June 6	3,505	92,488	198,000	0.478	666	127,643	1.472	199,800	—118,200	—118,900	—0.60
August 6	3,478	162,447	348,000	0.842	5,299	243,766	1.658	356,300	— 90,700	— 96,000	—0.28
September 16	3,448	214,395	459,000	1.110	8,609	330,410	1.548	473,600	—121,400	—130,000	—0.28
October 26	3,436	278,927	597,000	1.440	11,772	412,693	1.523	617,800	— 36,200	— 48,000	—0.08
November 24	3,432	304,879	653,000	1.580	14,214	457,063	1.398	678,200	4,200	— 21,700	—0.03
1946 March 15	3,359	477,860	1,022,000	2.489	25,925	716,925	1.514	1,076,000	21,000	— 16,700	—0.02
July 1	3,260	691,492	1,480,000	3.580	37,695	1,111,183	1.805	1,575,000	— 50,000	—115,600	—0.08
November 1	3,207	912,162	1,952,000	4.720	55,632	1,551,858	1.970	2,100,000	165,000	109,400	+0.06
1947 February 15	3,215	1,015,000	2,172,000	5.483	64,283	1,760,653	1.887	2,344,000	454,000	389,700	+0.18
April 1	3,202	1,083,707	2,320,000	5.600	67,063	1,873,591	1.887	2,504,500	537,500	470,400	+0.20
June 23	3,155	1,190,415	2,550,000	6.170	72,021	2,107,579	2,190	2,813,400	551,400	479,400	+0.19

General Data:
Original Reservoir Pressure=3,578 lb/sq in. ga.
Reservoir Temperature =209° F.
Original Oil in Place =41,368,000 bbl. reservoir oil.
Vr/Vs (@ 70 lb/sq in. ga. sep. pres.)=0.468 bbl. stock-tank oil per bbl. original reservoir oil.
Production Research Division
Pickton Reservoir Study Calculations

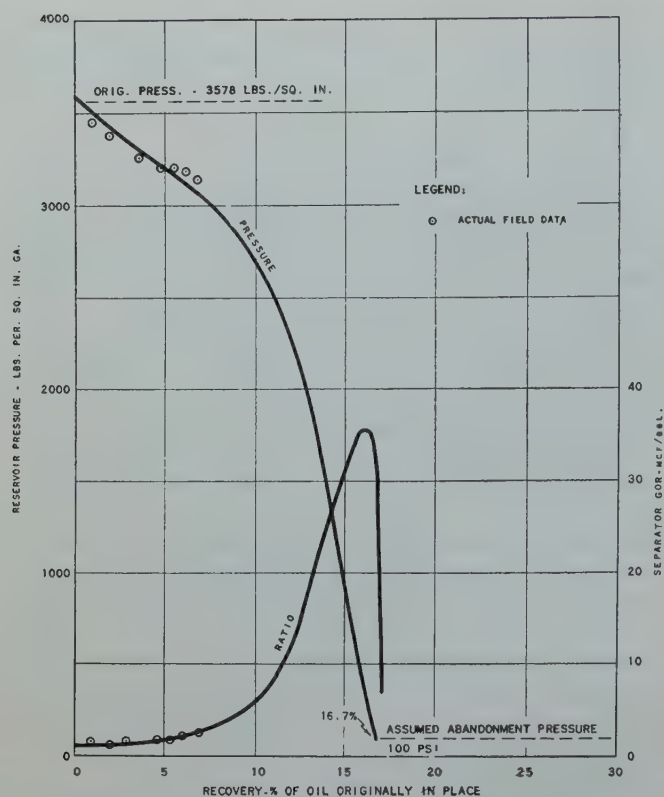


FIG. 8—EFFECT OF OIL RECOVERY ON PAST AND PREDICTED RESERVOIR PRESSURE AND SEPARATOR GAS-OIL RATIO FOR PRIMARY RECOVERY. PICKTON FIELD.

cent of the oil originally in place, or 3,269,000 barrels of stock-tank oil. The present cumulative production of 1,382,694 barrels as of November 1, 1947, represents 42.3 per cent of the expected ultimate oil recovery from primary operations. It will also be noted from Fig. 8 that, after approximately 10 per cent of the oil originally in place has been recovered, the reservoir pressure declines at an accelerated rate, and the gas-oil ratio increases very rapidly. As a result, a withdrawal rate of 1,400 barrels per day (the present withdrawal rate for the field) would deplete the field by the latter part of 1951.

In order to indicate the effect that the choice of a relative permeability curve of gas to oil has on the calculated recovery, it is pointed out that the calculated recovery would be 2,604,000 barrels of stock-tank oil when using Botset's curve and 5,286,000 barrels of stock-tank oil when using Leverett's curve. However, the calculated volume of additional oil to be gained by pressure maintenance is approximately the same when using any of the three relative permeability curves.

EVALUATION OF PRESSURE-MAINTENANCE OPERATIONS

Possible Programs

A preliminary study of pressure-maintenance indicated that the productive life of the Pickton field would be very short even if pressure-maintenance operations were undertaken immediately, and that the rapid increase in produced gas-oil ratio would require the handling of continually increasing

volumes of gas by the compressor plant. Further analysis of the data indicated that any gas-return operation should be undertaken at the highest possible reservoir pressure because of the very high shrinkage characteristics of the reservoir oil. The combination of high injection pressures, rapidly increasing volumes of gas to be returned and the short operating life indicated that the maximum profit from a pressure-maintenance project likely could be realized by a type of operation that would permit constantly operating compressors at capacity, thus insuring a maximum injection volume per installed horsepower. Also, it was apparent from an economic standpoint that it would be desirable to operate the compressors at the highest possible intake pressure, and that some kind of outlet other than returning gas to the reservoir would be required eventually under any type of pressure-maintenance operation. For these reasons, it was decided to evaluate the possibilities of (1) conventional pressure-maintenance operations wherein all available produced gas would be returned to the reservoir, with compressors added as needed until the gas production exceeded the maximum planned plant capacity and then the excess gas would be marketed or vented; and (2) a constant rate of gas-return program wherein the maximum planned compressor facilities would be installed immediately and operated continuously at capacity by obtaining extraneous gas for make-up until the produced gas equaled the plant capacity after which the excess produced gas would be marketed or vented.

Equity Considerations

Because of the preponderance of small leases, pooling of Pickton royalty interests will be necessary for a pressure-maintenance program from both the legal and the economic standpoints in order to (1) prevent changes in equity as a result of oil migration between leases, (2) permit using structurally favorable wells for injection without requiring new wells, (3) permit selective production from favorably located wells to take advantage of possible gas segregation and thereby minimize free gas production, and (4) permit an injection pattern conducive to the formation of an associated gas cap.

BASIS FOR PREDICTIONS

Conventional Pressure-Maintenance Operations

Predictions for conventional pressure-maintenance operations are based on returning to the reservoir 85 per cent of the produced gas after January 1, 1949, until such time as the installed plant capacity is reached and then injection at plant capacity for the remaining life of the field. Surplus produced gas will require a market to effect complete gas utilization after 1952, when the produced gas volume is expected to exceed the plant capacity. Conventional pressure-maintenance calculations for internal gas drive as employed in this analysis assume a uniform distribution of all reservoir oil and gas and all gas returned to the reservoir so as to provide similar oil and gas saturations throughout the entire reservoir at any given time. Oil production was assumed to be 1,400 barrels per day (the present withdrawal rate for the field), and the net water influx was assumed to be negligible (as indicated by the volumetric balance calculations).

Constant-Rate-of-Injection Pressure-Maintenance Operations

Predictions for constant-rate-of-injection operations were based on the assumption that an extraneous source of gas will be available for the Pickton project and adequate to supply make-up gas for injection rates of 10, 15, and 20 MMcf per day. The method of calculating the constant-rate-of-injection type of pressure maintenance as employed in this analysis is similar to that for the conventional pressure-maintenance calculations for internal gas drive and also assumes a uniform distribution of all reservoir oil and gas and all gas returned to the reservoir so as to provide similar oil and gas saturations throughout the entire reservoir at any given time. When the produced gas at Pickton exceeds injection requirements (during 1952), a market for the gas will be required if complete conservation of gas is to be achieved. The future oil production rate was assumed to be 1,400 barrels per day (the present withdrawal rate for the field), and the net water influx was assumed to be negligible (as indicated by the volumetric balance calculations).

RESERVOIR PERFORMANCE WITH PRESSURE MAINTENANCE

Conventional Pressure Maintenance (Injection to start January 1, 1949)

Calculations for conventional pressure-maintenance operations were made considering compressor plants of three different capacities (19, 30, and 37 MMcf per day) in an effort to determine the optimum size of plant. All pressure-maintenance oil recoveries were calculated on a common basis, using 750-pound single-stage separation. The predicted effect of oil production on reservoir pressure and separator gas-oil ratio for each of the three compressor plants is shown in Fig. 9. Pertinent oil recovery data for each of the three plants are summarized as follows:

Ultimate plant capacity, MMcf/Day	19	30	37
Calculated ultimate recovery, per cent of oil in place	21.9	23.7	24.5
Increase in recovery over primary operations:			
Per cent of oil in place	5.2	7.0	7.8
Stock-tank barrels	1,066,000	1,426,000	1,586,000

Constant-Rate-of-Injection Pressure-Maintenance Operations

Calculations for the constant-rate-of-return gas-injection project were made for compressor plants of three different capacities (10, 15, and 20 MMcf per day) in an effort to determine (1) the comparative economic advantages of a conventional gas-return program and a constant-rate-of-return program, and (2) the optimum plant size for gas injection at a constant rate. Pressure-maintenance oil recoveries were calculated in each case for 750-pound single-stage separation as well as for 750- to 40-pound two-stage separation. The predicted effect of oil production recovery on reservoir pressure and separator gas-oil ratio for each of the three compressor plants is shown in Fig. 10. A summary of pertinent oil recovery data for each of the three plants follows:

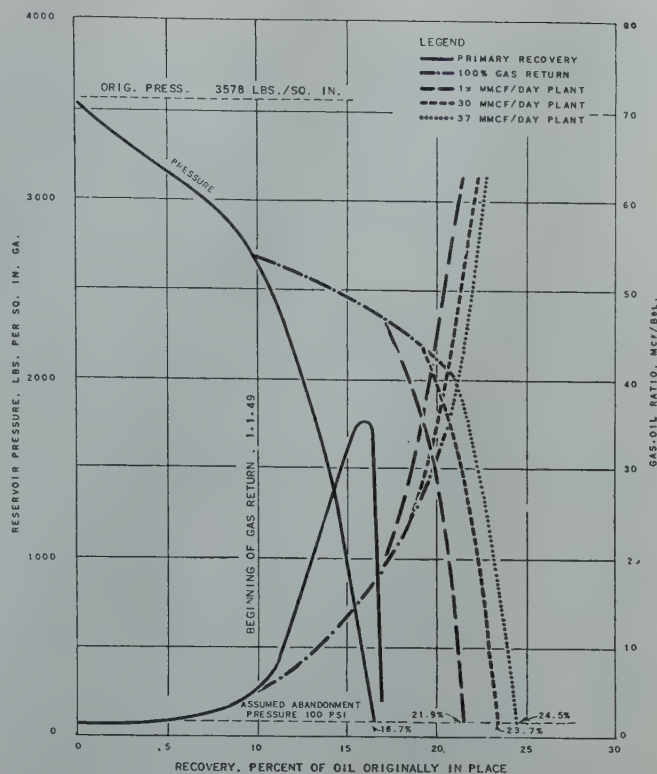


FIG. 9—EFFECT OF OIL RECOVERY ON PAST AND PREDICTED RESERVOIR PRESSURE AND SEPARATOR GAS-OIL RATIO (WITH AND WITHOUT CONVENTIONAL PRESSURE-MAINTENANCE OPERATIONS). PICKTON FIELD.

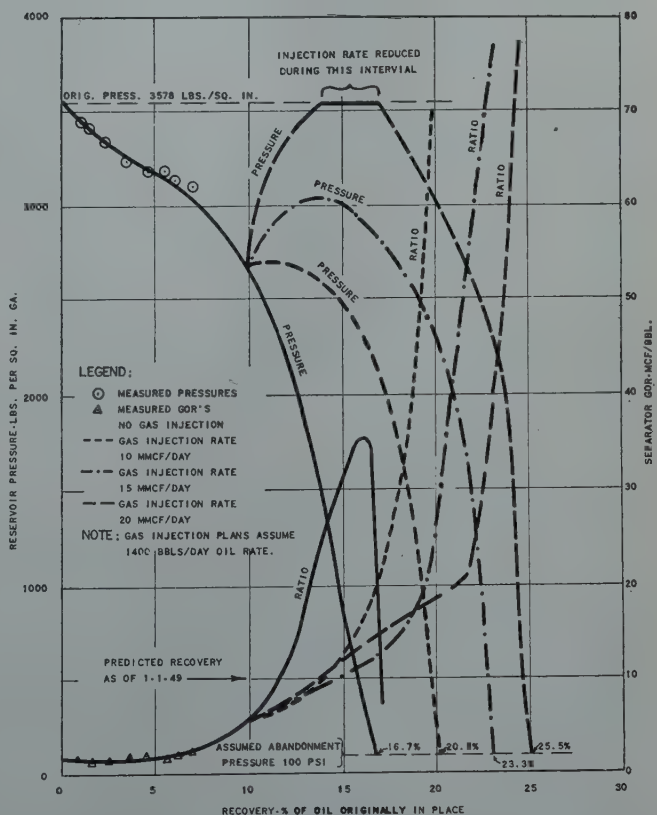


FIG. 10—EFFECT OF OIL RECOVERY ON PAST AND PREDICTED RESERVOIR PRESSURE AND SEPARATOR GAS-OIL RATIO (WITH AND WITHOUT CONSTANT-INJECTION PRESSURE-MAINTENANCE OPERATIONS). PICKTON FIELD.

Plant capacity, MMcf/Day.....	10	15	20
Calculated ultimate recovery, per cent of oil in place.....	20.3	23.3	25.5
Increase in recovery over primary operation			
Per cent of oil in place.....	3.6	6.6	8.8
Stock-tank barrels (single- stage separation).....	746,000	1,346,000	1,786,000
Stock-tank barrels (two- stage separation).....	927,000	1,579,000	2,058,000

OPTIMUM PRESSURE-MAINTENANCE PROGRAM

Optimum Program 15 MMcf/Day Constant Injection

From the two preceding summary tables it is apparent that returning 20 MMcf of gas per day would yield a larger oil recovery than either of the other two constant-rate-of-return programs; however, the cost is prohibitive. In addition, the extraneous source of gas which is apparently available does not appear adequate to supply the requirement for the 20-MMcf-per-day program. Because of the high cost and the accelerated decrease in oil recovery that would occur with the larger compressor plant in the event the injected gas channels to the producing wells, it appears that the 15 MMcf-per-day plant (with constant injection at plant capacity) would be the optimum pressure-maintenance program for Pickton. In order to determine the optimum over-all plan when considering a gasoline plant at Pickton, the optimum pressure-maintenance program was evaluated (based on the difference between primary operations and pressure maintenance) for single-stage separation (Plan 1: 750 to 0 pounds) and two-stage separation (Plan 2: 750 to 40 to 0 pounds). The 750-pound pressure was used in each case to permit a large saving in compressor horsepower.

Plan 1: Under Plan 1 (single-stage separation), the pressure-maintenance program would yield an estimated 1,346,000 barrels of oil with a value of \$2,611,000.

Plan 2: Under Plan 2 (two-stage separation), the pressure-maintenance program would yield an estimated 1,579,000 barrels of oil with a value of \$3,063,000.

Although Plan 2 (two-stage separation) is more attractive when only pressure maintenance is considered, Plan 1 (single-stage separation) is more advantageous to the over-all program when a gasoline plant is operated in conjunction with pressure maintenance.

Alternate Pressure-Maintenance Plan If Extraneous Gas Is Not Available

Since there is a possibility that the contemplated extraneous gas may not be available, the oil recovery was evaluated for the project without this outside source of gas. The evaluation assumed that all facilities required for Plan 1 would be installed as though outside gas were available, that gas return would be initiated by January 1, 1949, and that oil production would be maintained at the current withdrawal rate of 1,400 barrels per day.

From the summary it is evident that the optimum program for conventional pressure maintenance would require a 30-MMcf-per-day plant. The return of 85 per cent of the produced gas to the reservoir from January 1, 1949, until the gas production utilizes all of the plant capacity and the return of

gas at plant capacity thereafter (with excess gas marketed) would increase the oil recovery by 1,426,000 barrels when using single-stage separation. The final 15 MMcf per day compressor facilities would not be required until the early part of 1951, and the project should be reviewed in light of the then accumulated operating information before installation of the additional facilities to insure that they are justified.

EVALUATION OF GASOLINE PLANT OPERATIONS

A preliminary analysis of the feasibility of processing Pickton casinghead gas indicated that a gasoline plant would not be attractive in connection with conventional oil-field operations because of the anticipated constantly increasing casinghead-gas volumes and the very short operating life (ending in 1951), but suggested that a gasoline plant would likely be attractive under any type of operation which would permit processing practically all of the gas with a plant of reasonable capacity. For this reason, the feasibility of operating a gasoline plant was evaluated in connection with (1) the optimum constant-rate-of-gas-injection pressure-maintenance program, (2) the alternate conventional pressure-maintenance program with a plant of limited capacity and without an outside gas supply, and (3) primary operations with the daily rate of oil production reduced as necessary to limit gas production to 18 MMcf per day for supply of an assumed constant gas market.

BASIS OF EVALUATION

Gas Volumes and Compositions

Fields such as Pickton that produce by internal gas drive are subject to sharply increasing gas-oil ratios and to changes in the liquid content of the produced gas. In order to evaluate the recovery and economics of a gasoline plant in conjunction with primary and pressure-maintenance operations, it was necessary to develop reasonable estimates of the effect of depletion on both the volumes and the liquid contents of the produced gas. As previously mentioned, detailed flash vaporization calculations were made for the original reservoir fluid to determine the effect of separator conditions on the separator gas-oil ratio and the composition of the produced gas. The results of these calculations were later verified by laboratory analyses of Pickton separator gas samples; however, the calculated compositions are applicable only as long as the field is producing approximately at its dissolved gas-oil ratio.

The conventional internal gas-drive calculations, which were used to evaluate future reservoir behavior in this analysis, yield fairly reliable values for the gas-oil ratio as measured under reservoir conditions of pressure and temperature but provide no correction for either condensate dropping out of the gas phase in the separators or for gas stripping the lighter hydrocarbons out of the oil phase in the separators. In view of the unusually rich gas, which is liberated from the Pickton oil with decreases in reservoir pressure, it appeared that the effect of condensate dropping out of the gas phase in the separator would have to be evaluated to obtain a reasonable estimate of the potential liquid recovery of a gasoline plant. For this reason, detailed flash vaporization calculations were made for conditions during the optimum pressure-maintenance

program to provide a basis for adjusting the reservoir gas-oil ratio to standard surface conditions and a basis for estimating the liquid content of the produced gas. Results of these calculations are shown graphically in Fig. 11. The produced gas

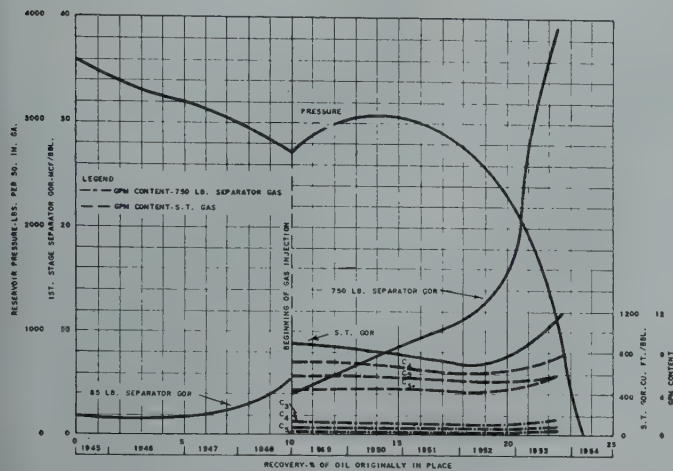


FIG. 11—VARIATION OF RESERVOIR PRESSURE, RATIO AND GPM CONTENT WITH RECOVERY AND TIME—750 TO 0 LBS. PER SQ. IN. @ 80° F. SEPARATOR CONDITIONS.—PICKTON FIELD.

volume and composition for the conventional pressure-maintenance program (without using extraneous gas) and for primary operations were estimated as a function of depletion from data accumulated during the detailed flash vaporization calculations for the optimum program.

Gasoline-Plant Evaluation

Due to the very rich composition of the Pickton casinghead gas and consideration of a gasoline plant in connection with types of field operation which would permit processing practically all of the gas with a plant of reasonable capacity, the

economics of a gasoline plant are favorable for (1) the optimum constant-rate-of-gas-injection pressure-maintenance program, (2) the alternate conventional pressure-maintenance program with a plant of limited capacity and without an outside gas supply, and (3) primary operations with a daily rate of oil production reduced as necessary to limit gas production to 18 MMcf per day for supply of an assumed constant gas market.

The optimum gasoline plant for use with the 15-MMcf-per-day constant-rate-of-gas-injection pressure maintenance project would be designed to recover 80 per cent of the propane when processing 18 MMcf of gas per day. At higher gas-producing rates, all the gas up to 30 MMcf per day could still be processed, but at a correspondingly reduced propane recovery (approximately 50 per cent propane recovery at 30 MMcf per day). Such a gasoline plant should recover approximately 1,597,000 barrels of products, which would have a value of \$4,686,000.

The evaluation of gasoline-plant operations in connection with limited capacity conventional pressure-maintenance operation (no outside gas available and compressor plant capacity of 30 MMcf of gas per day) was based on the use of a plant identical to the one selected for the optimum pressure-maintenance program. In this case, plant recovery would be 1,500,000 barrels of products, having a value of \$4,334,000.

If it is decided not to conduct pressure-maintenance operations because of difficulty in pooling royalty or some other consideration, it will be necessary to develop an immediate market for Pickton gas and probably to regulate production on the basis of gas demand. Gasoline-plant (identical to the one selected for the optimum pressure-maintenance program) operations were evaluated for a 15-MMcf gas market or 18-MMcf-per-day production before plant extraction and fuel losses. A gasoline plant on this basis (3-year operating life) should recover 1,500,000 barrels of products, which would have a value of \$4,334,000. ★ ★ ★

METHANE HYDRATE AT HIGH PRESSURE

RIKI KOBAYASHI, STANOLIND OIL AND GAS COMPANY

DONALD L. KATZ, MEMBER AIME, THE UNIVERSITY OF MICHIGAN

ABSTRACT

The conditions at which methane and water form solid hydrates have been extended from 4,000 to 11,200 pounds per sq. in. The curve at high pressure had been in doubt because of Villard's report of a critical decomposition temperature. The paper explains the nature of the hydrate curve at high pressure and its dependence on fluid phase behavior. Extrapolation of the methane hydrate curve indicates a pressure of 40,000 pounds per sq. in. will cause hydrates to form at a temperature of 100° F.

INTRODUCTION

The conditions under which natural gases form hydrates when liquid water is present have been studied by several investigators^{2, 3, 4, 8, 9, 15} up to pressures of about 4,000 pounds per sq. in. The early work by Villard on hydrates of methane and ethylene¹³, ethane¹², and propane¹⁴ included references to critical decomposition temperatures of the hydrates. Villard's work raised the question as to whether the pressure-temperature curve for methane-water hydrate continued above a temperature of 70.7°F. or whether this was the maximum temperature at which hydrates would form.

This paper extends the experimental data on methane hydrate to 11,200 pounds per sq. in. A discussion of phase relations in the hydrate region for the hydrocarbons and of the methane-water system at high pressures is included.

PREVIOUS WORK

Villard suspected that methane hydrates could not be formed at temperatures above 21.5°C. (70.7°F.)¹³ irrespective of the pressure of the liquid-vapor system. However, he was limited in his studies by his apparatus in 1888 to pressures not greater than 300 atmospheres (4,410 pounds per sq. in.)

Manuscript received at office of the Petroleum Branch July 1, 1948. Paper presented at the Branch Fall Meeting, Dallas, Texas, Oct. 4-6, 1948.

¹References are given at end of the paper.

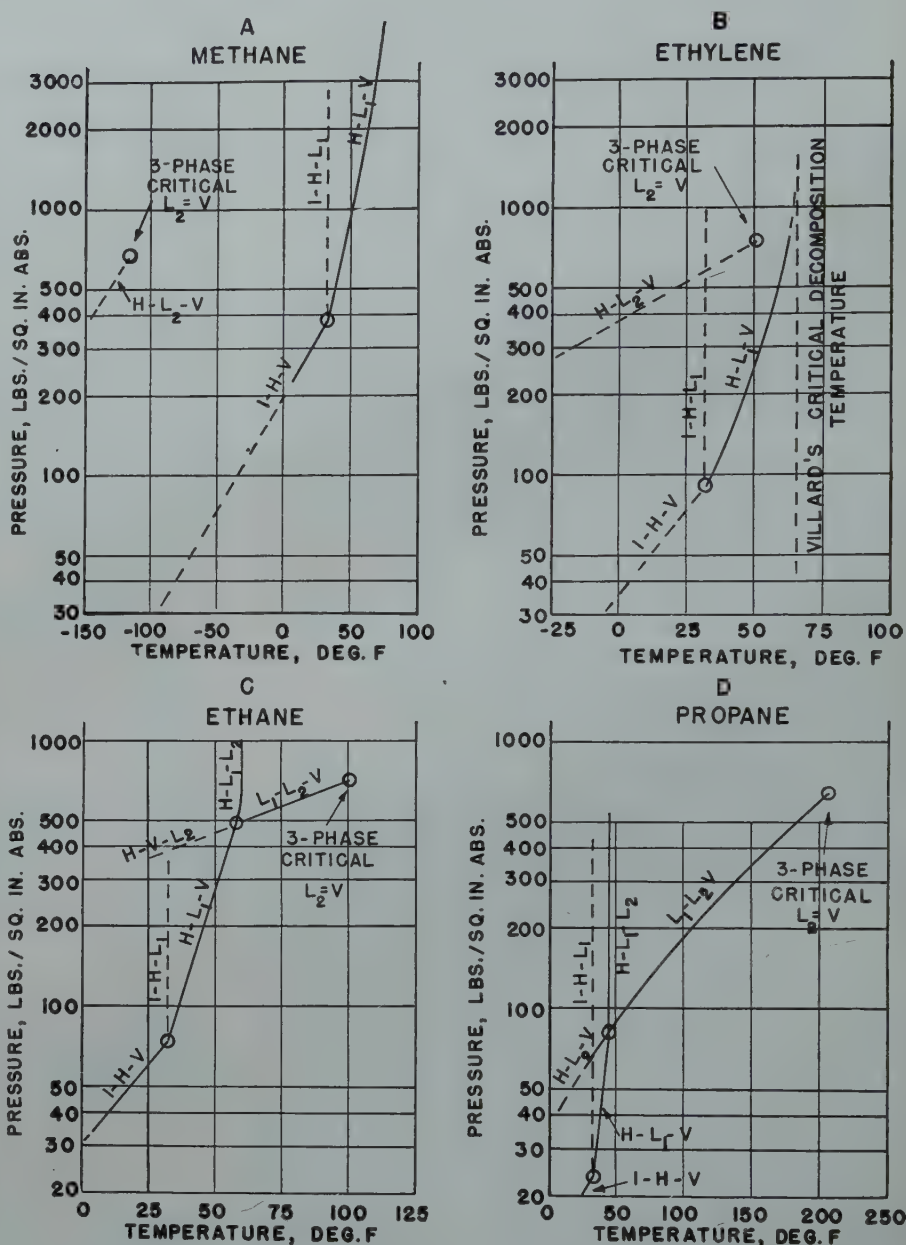


FIG. 1—PRESSURE-TEMPERATURE PROJECTION SHOWING RELATION OF HYDRATE FORMATION CURVES TO LOCATION OF HYDROCARBON CRITICALS.

so that there has remained some doubt as to the existence of such a maximum temperature in this region.

For the case of ethylene hydrates, however, Villard does specifically state the occurrence of what he terms a "critical temperature for the decomposition of the hydrates"¹³. Fig. 1B shows a

pressure-temperature projection of the three-phase locus, hydrate-ethylene rich liquid-vapor (H-L₂-V) terminating at the critical locus in which L₂ and V assume similar properties. Throughout this paper the following phase designations will be used: H for hydrate, L₁ for the water rich liquid, L₂ for the

hydrocarbon rich liquid, I for ice, and V for vapor. By extrapolating Villard's ethylene hydrate data it is found that the slope of the H-L₁-V locus approaches a large positive value as the temperature approaches 65.6°F. which he terms as the "critical decomposition temperature of the ethylene hydrate". Thus the pressure required to form hydrates at 68°F. would probably exceed 10,000 pounds per sq. in., a pressure unattainable in his apparatus.

For ethane-water and propane-water systems, critical decomposition temperatures were reported^{12, 14}, but the reason that such temperatures were observed is evident from Fig. 1C and Fig. 1D. The intersection of the vapor-hydrate-water rich liquid curve with the vapor-hydrocarbon rich liquid-water rich liquid (L₁-L₂-V) curve causes

a change in slope of the hydrate curve which now becomes a H-L₁-L₂ equilibrium locus. For propane, the effect of pressure on the liquid volume is small and the effect of pressure on the hydrate formation temperature is also very small. For ethane, the transition onto the H-L₁-L₂ curve is more gradual since the effect of pressure on the ethane rich liquid is more pronounced due to the proximity of the ethane vapor-liquid critical.

Ethylene does not show a quadruple point since the H-L₂-V line reaches its three phase critical (in which the phases L₂ and V become identical) before intersecting the three phase locus H-L₁-V. Nevertheless, the behavior of the H-L₁-V curve for the ethylene is similar to the combined H-L₁-V curve and the H-L₁-L₂ line for ethane. This

behavior may be attributed to the fact that the ethylene fluid assumes properties identical to that of ethane liquid (or fluid) as the critical pressure of ethylene is approached and exceeded. For the ethylene-water system there is no L₁-L₂-V curve since hydrate formation would deplete either the L₁ or the L₂ phase.

This analysis of the data gives little help on the prediction of the methane-hydrate curve at pressures above 4,000 pounds per sq. in. No sudden change in the curve would be expected due to effects of pressure on the methane density.

EXPERIMENTAL RESULTS

Experimental data for the three phase hydrate-water rich liquid-vapor (H-L₁-V) locus for the methane-water system has been obtained over the range from 4,900 pounds per sq. in. and 72.5°F. to 11,200 pounds per sq. in. and 83.9°F.

The formation and decomposition of the hydrate was detected by conducting the experiment in a glass-windowed pressure cell. The apparatus has glass windows capable of withstanding 25,000 pounds per sq. in. pressure and has been fully described by Rzasa¹⁰. Methane of 99+% purity was first passed through a purification train comprised of activated carbon, sodium hydroxide, and ascarite. Then the methane was compressed and injected into the cell. Water was pumped into the cell in amounts considerably less than the theoretical amount required for the complete utilization of the methane upon hydrate formation.

The cell temperature was lowered with agitation until hydrates were formed. It was necessary to supercool the liquid-vapor mixture by as much as 12°F. at the higher pressures in order to cause the formation of hydrates. This is probably the reason why Villard suspected that hydrates of methane could not be formed above 70.7°F. Once the hydrates had formed, the temperature was increased slowly until three phases, hydrate-water rich liquid-vapor, appeared. The thermocouple and pressure gage readings were taken at the first instant that the hydrates began to decompose. The results are presented in Table 1 and plotted on Fig. 2 along with previous hydrate data on methane

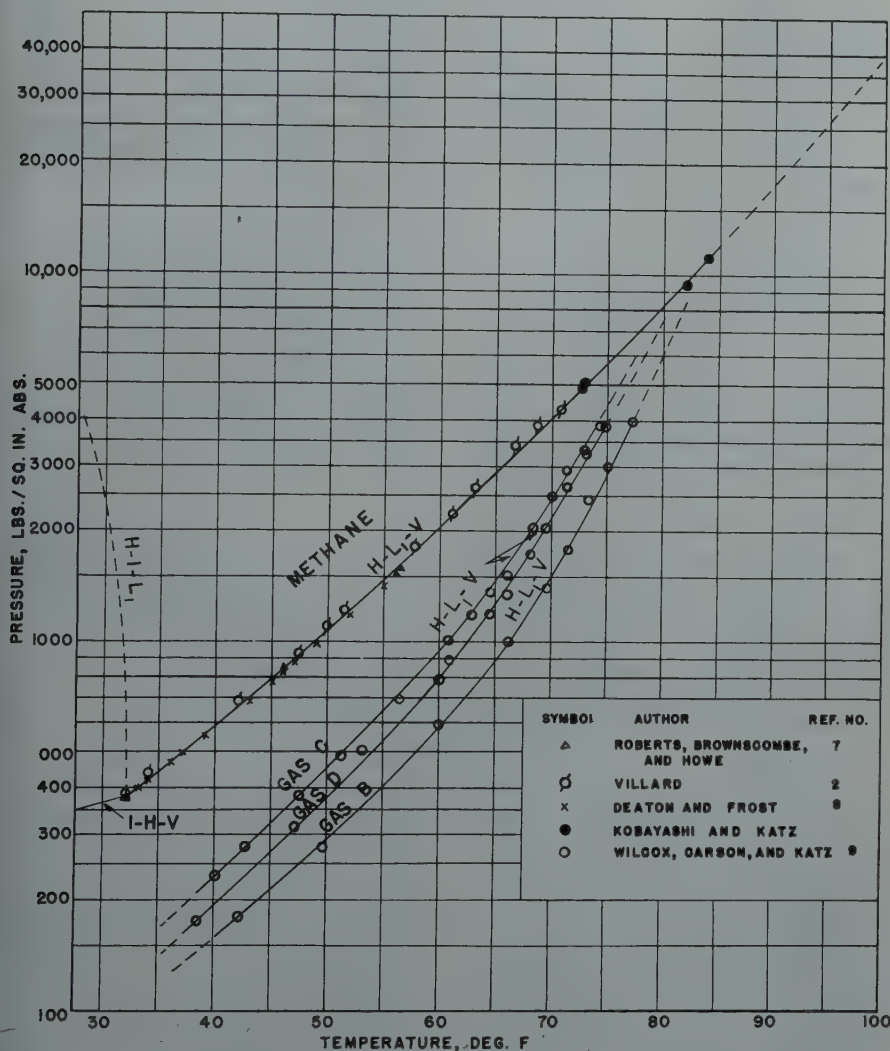


FIG. 2—PRESSURE-TEMPERATURE PROJECTION FOR METHANE-WATER AND NATURAL GAS-WATER SYSTEMS SHOWING HYDRATE FORMING CONDITIONS.

and natural gases. It is apparent that the methane hydrate curve continues to some high pressure. For example, the extrapolated curve indicates that methane and water would form solid hydrate at 100° F. under a pressure of about 40,000 pounds per sq. in.

TABLE 1

Experimental Data for Three Phase Equilibria, Hydrate-Water Rich Liquid-Vapor in the Methane-Water System

Pressure lbs./sq.in. abs.	Temperature deg. F.
4,930	72.6
5,120	72.9
9,400	82.1
11,240	83.9

PREDICTION OF METHANE-WATER PHASE RELATIONS

Existing data on the methane-water system seem to indicate that the critical phenomenon between the vapor (V) and the liquid phase (L_1) does not occur for low temperatures (150-250° F.) until pressures in excess of 100,000 pounds per sq. in. are reached. The relationship between such criticals and the hydrate equilibrium curves may be explored qualitatively by the application of the phase rule¹ to the data now available.

The Phase Rule may be simply stated as

$$F = C - P + 2$$

in which F is the degree of variance or freedom, C is the number of components, and P is the number of phases in equilibrium.

For two component systems, the phase rule reduces to

$$F = 4 - P$$

For the simplest case of heterogeneous equilibrium two phases are involved so that the degrees of variance or the number of independent variables that must be fixed in order to define the system is equal to 2. Since two independent variables imply a function of 3 variables, 2 independent and one dependent, such equilibria may be represented by a Pressure-Temperature-Composition (P-T-X) diagram. Two-phase equilibria are represented by a pair of surfaces, one for each phase. Three-phase equilibria are represented by three space curves, each formed by the intersec-

tion of two surfaces. The requirement of the uniformity of pressure and temperature for an equilibrium system requires that the space curves for all three-phases must furnish the same projection on the pressure-temperature plane. Four-phase equilibria are represented as four unique points in space, falling on a straight line perpendicular to the pressure-temperature plane at their respective phase compositions. From each of such points there must radiate three space curves which when projected on the pressure-temperature plane appear as four three-phase curves emanating from a four-phase (quadruple point).

Two-phase pressure-temperature relationship for two components appear as lines in the pure component planes of the P-T-X figure, while three coexisting phases are represented as an invariant point (triple point).

Constant pressure planes passed through the three dimensional P-T-X diagrams show possible phase relations occurring over the temperature range as a function of the phase compositions. Similarly, isothermal sections yield pressure-composition diagrams. For this particular study only the former will be considered.

Projections of the space curves on

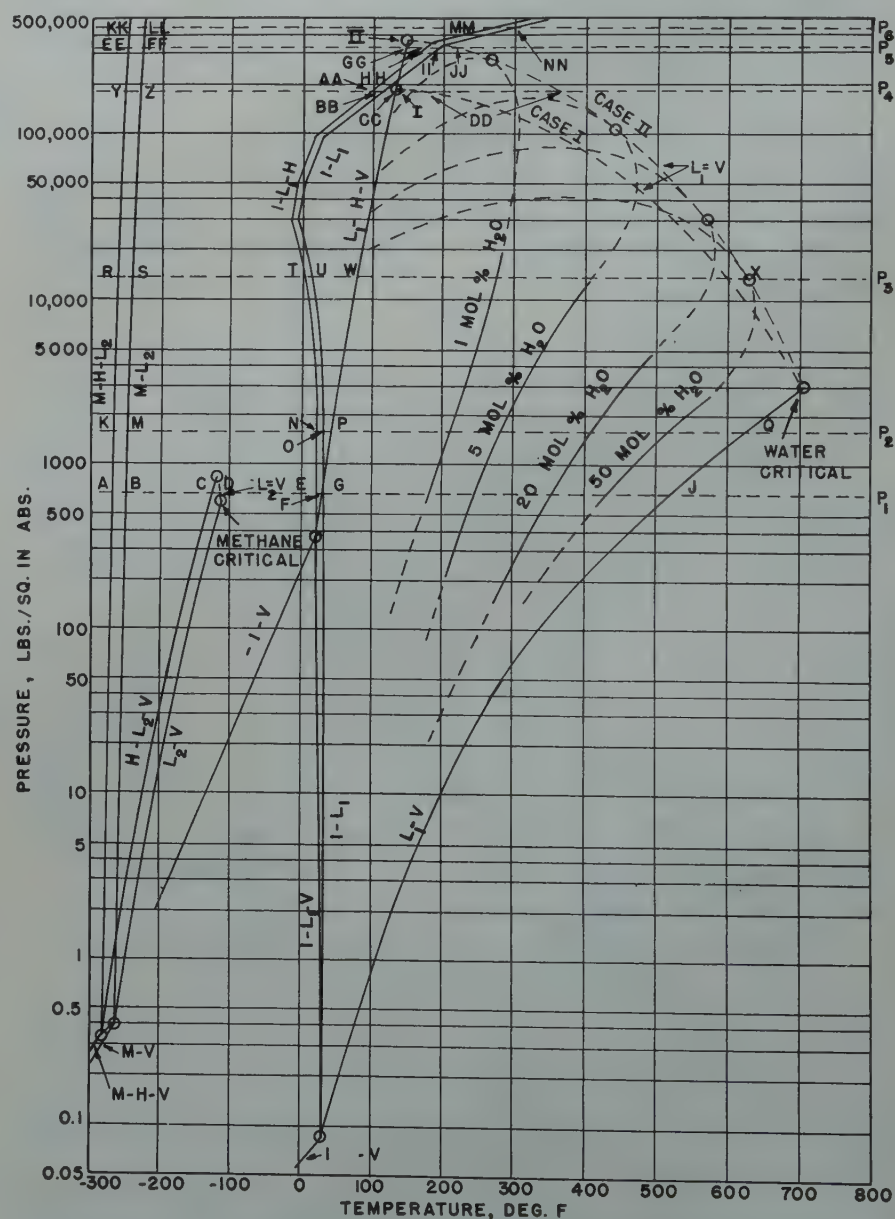


FIG. 3—COMPLETE PRESSURE-TEMPERATURE PROJECTION FOR THE METHANE-WATER SYSTEM.

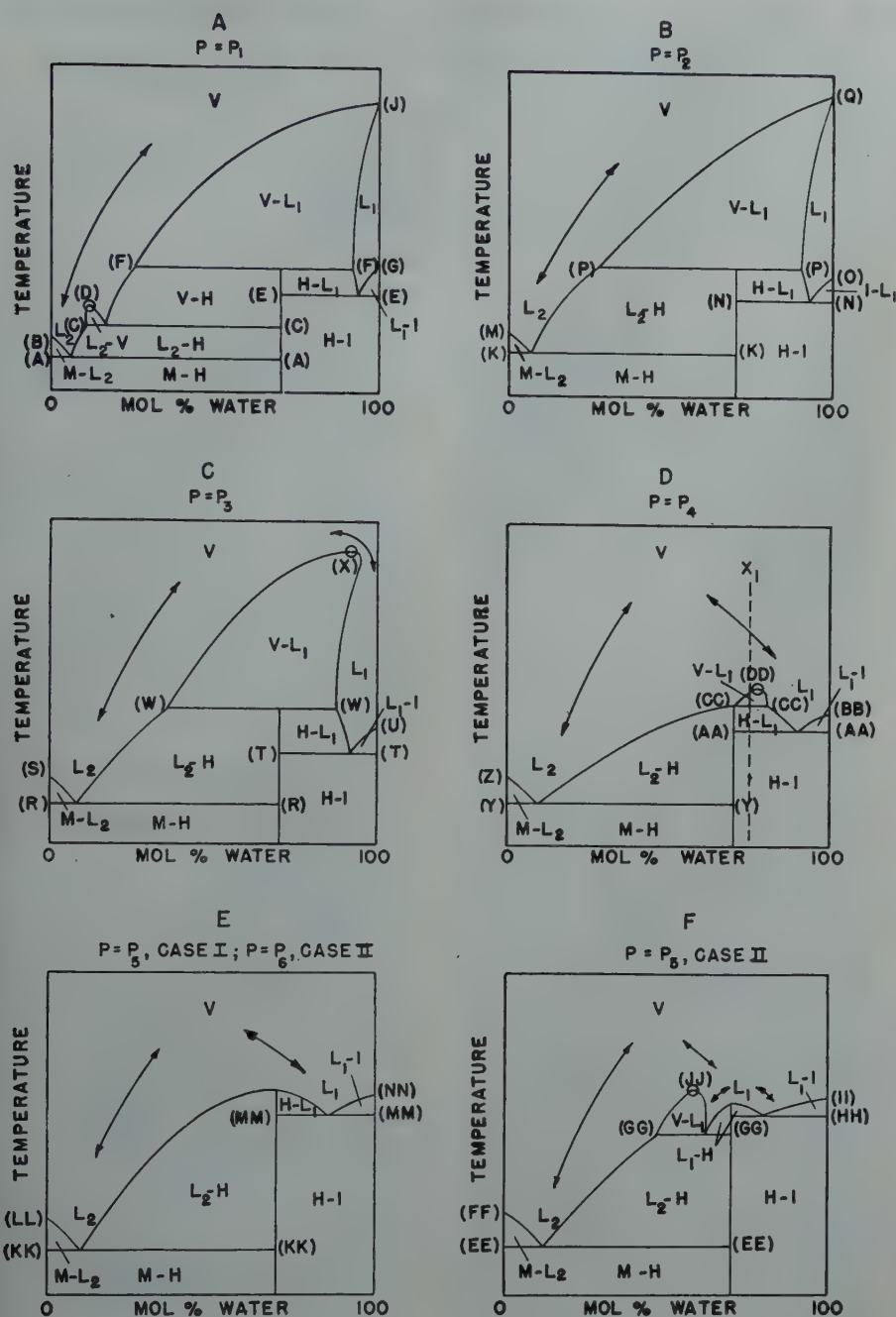


FIG. 4—SCHEMATIC TEMPERATURE-COMPOSITION DIAGRAMS FOR THE METHANE-WATER SYSTEM.

the pressure-temperature plane, Fig. 3, prove to be of considerable aid in determining the schematic temperature-composition diagrams shown in Fig. 4. The appearance of only one hydrate of methane and the absence of solid-solid solubilities is assumed in the foregoing treatment. No attempt has been made to keep an exact scale because of the wide range of pressures and temperatures covered and the practical coincidence of some of the important fea-

tures of the diagram. For instance, the line M-H-L₂ using the present graphical scale would coincide with M-L₂. In order to preserve such features, the distinctions have been exaggerated, but the correct relative positions maintained. The critical temperatures and pressures of the pure substances are known, and the points on the three phase locus, H-L₁-V, have been reported in this paper to 11,200 pounds per sq. in. The I-H-V locus has been deter-

mined by Deaton and Frost down to 12.6°F.⁵ The equilibrium line L₁-I has been determined by Bridgeman and others⁷. The line I-L₁-H has been estimated from it.

The termination of a three-phase locus for a two-component system could occur in the three following ways if the appearance of solid-solid solubilities is rejected:

- (1) by the addition of another phase to give an invariant quadruple point.
- (2) by the loss of a component in which the end point is identified as an invariant triple point of one of the components.
- (3) by critical behavior in which any two of the co-existing phases become identical.

Any predictions as to trends of the lines relating pressures and temperatures beyond the available data must remain consistent with the above implications of the phase rule. Thus, for the lines H-L₂-V and H-L₁-V a study of the pressure-temperature projection indicates their terminations are only likely through the appearance of critical behavior between the liquid and vapor phases. In the case of H-L₂-V since both the L₂ and V are rich in methane, the critical can be expected to occur very near the critical for pure methane. For the locus H-L₁-V, however, the extremely low solubility of natural gases in water¹¹ and the low concentration of water in the vapor phase for the lowest temperature at which the critical might be expected to occur (110-140°F.) indicate that the critical between L₁ and V probably does not occur until extremely high pressures are reached, perhaps as high as 250,000 pounds per sq. in.

A point of interest to note is that unlike totally miscible systems, for example methane-butane, a system such as methane-water involving components of limited miscibility and undergoing compound formation exhibit two distinct critical loci between the so-called liquid and vapor phases. One critical locus occurs for mixtures of very low water concentrations when the vapor phase, V, rich in methane in this case, becomes identical in properties with methane-rich liquid, L₂. The second critical locus occurs for higher concentrations of water when the vapor phase, V, becomes identical in properties with the water-

rich liquid phase, L_1 . For the critical involving L_1 and V, two possibilities, Case I and Case II are studied. Case I and Case II are distinguished by the appearance of the liquid water-ice line at pressures above and pressures below the Pressures I and II, of Fig. 3 respectively. The bubble point-dew point envelope have been drawn consistent with Case II only and have been omitted for Case I. In the neighborhood of the $L_1 = V$ critical the two cases yield slightly different temperature-composition sections as are shown on Fig. 4D and Fig. 4F.

With the aid of the dew-point data of Sage and Lacey for the methane-water system¹¹, typical bubble-point and dew-point curves have been sketched on Fig. 3. With the exception of mixtures of extremely low total concentrations in either water or methane the bubble point curves would be expected to terminate on the H- L_1 -V locus and the dew point on the I- L_1 -V locus.

The order of magnitude of the critical between L_1 and V was determined by a plot of the logarithm of the vaporization equilibrium constant versus the logarithm of the pressure using the dew-point data of Sage and Lacey for the methane-water system¹¹. The complete pressure-temperature projection for the system is shown in Fig. 3.

Six T-X diagrams corresponding to pressures P_1 through P_6 on Fig. 3 have been prepared. Points of intersection of the constant pressure plane with the three-phase-two component lines and the two-phase-one component lines are lettered on Fig. 3. Since each intersection corresponds to a definite temperature, three-phase-two component equilibria are represented on horizontal lines on the T-X diagrams and two-phase-one component equilibria as definite points on the edges of the T-X diagrams. The letters corresponding to points of intersection on the pressure-temperature projection appear at various temperature levels on the T-X diagrams.

The T-X diagram corresponding to the pressure P_2 will be discussed in detail. The diagram is shown in Fig. 4B. In review, H denotes the hydrate, I denotes Ice, V denotes vapor, M denotes solid methane, L_2 denotes methane rich liquid, and L_1 denotes water rich liquid. The composition scale is distorted to provide clearness to the

illustration and the temperature scale is purely relative. The arrows drawn between the phases labelled as liquid and vapor phases indicates the existence of a continuum between the phases. Under these conditions there is no complete boundary separating the two phases, but the designations L_1 , L_2 , and V have been maintained in order to avoid confusion. The first intersection, K, occurring at the lowest temperature represents three-phase equilibrium involving M, H, and L_2 and is located at the temperature K on the T-X diagram. Point M is located on the 100% methane axis at a slightly higher temperature. The equilibrium I- L_1 -H occurs at the temperature N, and I- L_1 occurs at the temperature O on the 100% water axis. P represents the L_1 -H-V equilibrium. Finally at point Q, L_1 and V are in equilibrium on the 100% water axis of the T-X diagram. The T-X diagram is completed by the joining of the points involving a common phase.

The T-X diagram may be used to illustrate what will occur if heat is slowly removed from a mixture of definite composition at a constant pressure. If such a mixture X, Fig. 4D, is cooled a second fluid layer appears as soon as the area L_1 -V is pierced. As the temperature decreases the compositions and the amounts of the phases change until the temperature CC is reached. At that temperature a third phase, the hydrate, forms. Further removal of heat from the mixture V- L_1 -H results in the complete disappearance of phase V at the same temperature CC leaving the equilibrium H- L_1 for temperatures below CC until another three-phase line is reached at the temperature AA. With additional removal of heat the appearance of the ice phase and the disappearance of the L_1 phase occur leaving equilibrium between hydrate and ice for all lower temperatures. In like manner any section may be studied in order to trace changes in a mixture which take place upon cooling.

This treatment of possible phase relations indicates that the methane hydrate curve continues until it intersects the $L_1 = V$ critical locus at a pressure roughly estimated to be in excess of 150,000 pounds per sq. in. It must be emphasized that a phase relation treatment such as this can be used to present the possible phase relations, but cannot predict which of the possibilities

is actually followed in nature.

CONCLUSION

Experimental data have extended the methane hydrate equilibrium curve to 11,200 pounds per sq. in. Theoretical considerations indicate that the curve may be extrapolated so that at 40,000 pounds per sq. in. methane hydrate would form at 100°F. The curve probably terminates on the vapor-liquid critical locus at pressures of the order of 250,000 pounds per sq. in.

ACKNOWLEDGMENT

This Research was made possible by a Fellowship supported by the Stanolind Oil and Gas Co.

The authors acknowledge the assistance of the Phillips Petroleum Co. in furnishing the pure methane. Prof. L. O. Case and Mr. D. B. Robinson aided in the development of the phase theory.

REFERENCES

1. Case, L. O., *Elements of Phase Rule*, Edwards Bros., (1939) Ann Arbor, Michigan.
2. Deaton and Frost, *AGA Monthly*, 19, 219 (1937).
3. Deaton and Frost, *Proc. Nat. Gas Dept.*, AGA, pp 112-119, (1938).
4. Deaton and Frost, *Proc. Nat. Gas Dept.*, AGA, pp 122-128, (1940).
5. Deaton and Frost, *Oil and Gas Journal*, 45, pp 170 (1946).
6. Dodson and Standing, *API Drilling and Production Practice*, pp 173, (1944).
7. Dorsey, N. E., *Properties of Ordinary Water Substances*, pp 603, Reinhold Pub. Corp. (1940).
8. Hammerschmidt, E. G., *Ind. Eng. Chem.*, 26, pp 851, (1934).
9. Roberts, Brownscombe, and Howe, *Oil and Gas Journal*, (Dec. 5, 1940).
10. Rzasas, M. J., Ph.D. Theses, Univ. of Mich. (1947).
11. Sage, Olds, Lacy, *Ind. Eng. Chem.*, 34, 1223, (1942).
12. Villard, M., *Compt. rend.*, 106, 1602, (1888).
13. Villard, M., *Compt. rend.*, 107, 395, (1888).
14. Villard, M., *Compt. rend.*, 111, 302-305, (1890).
15. Wilcox, Carson, Katz, *Ind. Eng. Chem.*, 33, 662, (1941). ★ ★ ★

METHOD OF ESTABLISHING A STABILIZED BACK-PRESSURE CURVE FOR GAS WELLS PRODUCING FROM RESERVOIRS OF EXTREMELY LOW PERMEABILITY

E. R. HAYMAKER, C. W. BINCKLEY, MEMBER AIME, AND F. R. BURGESS,
PHILLIPS PETROLEUM CO., BARTLESVILLE, OKLAHOMA

ABSTRACT

A method of establishing stabilized back-pressure curves for gas wells producing from formations of extremely low permeability is presented. Actual well performance under many different operating conditions is shown by the stabilized back-pressure curve. By use of the method, it is possible to conduct back-pressure tests with a critical-flow prover on wells that stabilize slowly, and save approximately 88% of the gas ordinarily vented to obtain satisfactory test data, with a great reduction in time required for testing.

INTRODUCTION

The reasons for establishing dependable back-pressure curves on gas wells have been pointed out by previous publications. The publication most referred to, of course, is the United States Bureau of Mines Monograph 7, titled "Back-Pressure Data on Natural Gas Wells and Their Application to Production Practices". The technique generally established therein has been accepted and used by many engineers; and, when proper tests are conducted, the results can be used for the analysis and solution of several practical problems concerning field operation and development.

Even where formations of low specific permeability are encountered, the determination of a well's actual performance by the back-pressure test method permits the engineer to analyze many problems in individual well operation and also to predict necessary future field development. Such problems as the determination of the ability of a well to produce into a pipe line at a predetermined line pressure, the design of gas gathering systems and meter settings, and the determination of the time and the number of wells required to be drilled to meet future market obligations, can be solved, in part, by the use

of a reliable back-pressure curve. In addition, the computed well delivery rates determined by data from back-pressure tests ordered by state regulatory bodies, when compared with the true back-pressure curve, permit the operator to ascertain whether such data represent unstable or relatively stabilized delivery rates for given pressure conditions of the well.

The technique of back-pressure testing, as described in this report, was developed by Phillips Petroleum Company engineers from data obtained during a testing program that started in 1944 and has been continued to date. Three hundred and eleven back-pressure tests were conducted on 299 wells located in the southern part of the Hugoton Field. The gas-bearing zone is composed of several dolomitic formations of the Permian Age; the important ones are the Herington, Upper Krider, Lower Krider, and Winfield. The average bottom-hole temperature is approximately 91°F., and the initial wellhead shut-in pressures range from 400 to 440 psig. The spacing pattern is 640 acres per well with each well located near the center of the section. The range of back-pressure potentials on wells tested was from 500 to 23,000 Mcfd.

All gas wells were acidized, and the quantity of acid used, expressed in 15% hydrochloric acid, varied from 12,000 to 22,000 gallons per well. The quantity and concentration of each treatment depended on the stage, the formation being treated, and experience gained from previously completed wells.

The gas in the Hugoton Field is a "dry" gas. It has a gasoline content of approximately 0.25 gallons per thousand cubic feet, as determined by charcoal test, and its specific gravity averages about 0.71 as compared to air (air = 1.00 at 60°F.).

Of the wells tested, 71 were completed with 7" casing, 3 with 9⁵/₈" casing, and

1 with 6⁵/₈" casing set on top of the upper producing formation with the well bore through the gas bearing formations being open hole. Two hundred and twenty-four were completed with 5¹/₂" O.D. casing set through the gas bearing formations and perforated.

For the purpose of establishing reliable back-pressure curves in the area, Phillips Petroleum Company personnel has computed data on the basis of 24-hour flows per point. Early in the program, many tests were actually permitted to flow 24 hours to obtain data for each plotting point, at great expense in man power and time. Presently, however, such tests have been replaced by tests of short duration flows which can be made to effect results that correspond to the tests obtained by flows of much longer duration.

METHOD

When a gas well producing from a reservoir of low permeability is opened for production through a constant size orifice, both the rate of flow and working pressure decline, first at a high rate and later at a lower rate until after several hours the decline becomes difficult to ascertain. In this paper the rate of flow and working pressure are considered to be stabilized when it becomes difficult to observe changes in working pressure during a period of three hours by the use of a deadweight pressure gage.

Stabilization of pressure in the literal sense is never obtained in a producing gas well. In formations of low permeability, such as those in the Hugoton Field, most wellhead working pressures approach stabilization closely enough to be used satisfactorily in the determination of a back-pressure potential curve after flow periods of 24 hours. We shall therefore describe the back-pressure curve calculated from observed rates of flow and working pressure at the end of 24-hour flow periods,

or an equivalent curve computed from 3-hour per flow test data, as a "Twenty-Four Hour Back-Pressure Potential Curve".

Rates of flow and working pressures at the end of 24-hour flow periods, often satisfactory for establishing the back-pressure potential curves, may be unsatisfactory for establishing a back-pressure curve for determining every day performance of a well producing into a pipe line. The back-pressure curve from which everyday working pressures and rates of flow can be determined is described as a "Stabilized Back-Pressure Curve".

To obtain reliable pressure decline data during a back-pressure test, the well must be producing under critical-flow conditions at the wellhead. This condition is obtained by the use of a critical-flow prover, a choke nipple with the gas vented to the atmosphere, or by controlling the flow from the well by a valve while producing into a pipe line. When a well is back-pressure tested by producing into a pipe line, the tester must carefully observe the pipe line operating pressure downstream from the control orifice or choke. If the downstream pressure is greater than 56 per cent of the wellhead working pressure, critical-flow conditions do not exist. During non-critical flow, changes in the pipe line pressure will affect the wellhead working pressure, and the well flow data will not be representative of the producing characteristics of the well.

It has been the practice throughout the testing program to use either a 2-inch or a 4-inch critical-flow prover on all wells back-pressure tested. The data thus collected have been very consistent and are used to study true reservoir performance where liquids do not accumulate in the well bores and where there are no severe temperature changes in the well bores during testing. These favorable conditions are found in the Hugoton Field.

Observed Data Taken During Short Flow Back-Pressure Tests On Hugoton Field Gas Wells

The first observation made for the determination of a back-pressure potential curve is the shut-in wellhead pressure which is gaged after the wellhead is closed in for a minimum period of

3 days; after 3 days shut-in the rate of pressure build-up of wells in this area has been found to be less than 0.1 psi per hour.

The back-pressure potential test as determined by the short flow method requires that four flows, each of three hours duration, be taken using a normal sequence of orifice plates. That is to say, after a sufficient shut-in period, the test is started with the smallest rate of flow and continued with increasingly greater rates of flow until four rates are taken.

The practice of reading wellhead working pressures with a dead-weight gage at regular time intervals has been maintained for the testing of all wells in the Hugoton Field. The starting time for taking data is when the well is first opened and a working pressure corresponding to the shut-in pressure is recorded. Subsequent working pressures are read and recorded at the end of the 0.5 hour, 0.7 hour, and 1.0 hour respectively. Thereafter, the working pressures are taken at 1.5, 2.0, 2.5, and 3.0 hours. At the end of the first flow, the well is shut-in and the orifice size is increased for the next flow. Of course,

there is a small amount of pressure increase while the well is closed-in for plate changing. However, this pressure build-up is soon dissipated after the well is opened, and the first reading of the second flow is taken one-half hour after the working pressure equals the last gage reading of the previous flow. Each flow thereafter is recorded as outlined above. At the end of each flow period, the prover pressure and temperature of the flowing gas stream are read and recorded for the purpose of calculating the rate of flow. Fig. 1 shows a typical data sheet used to record working pressure data during a back-pressure test.

The wellhead pressures observed throughout all the flows are used to calculate bottom-hole pressures; therefore, it is necessary to know other physical data such as the internal diameter of the casing, the specific gravity of the gas, and the average length and average temperature of the gas column. The computations necessary to make these conversions are the same as outlined in Monograph 7² and other publications such as "Calculations of Back-Pressure Tests on Natural Gas Wells" by J.

GAS WELL B.P. TEST PRESSURE DATA

Company Phillips Petroleum		Lease Gas Well "A"					
Data By:		Date					
Hrs.	Working Pressure Data			Crit. Flow Prov.			Remarks
	W.P. psig	(ΔP)	$\Delta P/Hr.$	psig	$^{\circ}F.$	Disc.	
0.0	383.9						First Flow
0.5	379.7	4.2	8.4				
0.7	379.1	0.6	3.0				
1.0	378.5	0.6	2.0				
1.5	377.9	0.6	1.2				
2.0	377.4	0.5	1.0				
2.5	376.9	0.5	1.0				
3.0	376.5	0.4	0.8	376.4	61	1/4"	Gas Dry Second Flow
0.0	376.5						
0.5	370.1	6.4	12.8				
0.7	369.3	0.8	4.0				
1.0	368.2	1.1	3.7				
1.5	366.9	1.3	2.6				
2.0	365.9	1.0	2.0				
2.5	365.2	0.7	1.4				
3.0	364.5	0.7	1.4	364.3	61	3/8"	Gas Dry Third Flow
0.0	364.5						
0.5	354.2	10.3	20.6				
0.7	352.7	1.5	7.5				
1.0	351.2	1.5	5.0				
1.5	349.0	2.2	4.4				
2.0	347.5	1.5	3.0				
2.5	346.1	1.4	2.8				
3.0	344.9	1.2	2.4	344.5	61	1/2"	Gas Dry Fourth Flow
0.0	344.9						
0.5	331.2	13.7	27.4				
0.7	329.4	1.8	9.0				
1.0	327.4	2.0	6.7				
1.5	324.8	2.6	5.2				
2.0	322.6	2.2	4.4				
2.5	320.8	1.8	3.6				
3.0	319.2	1.6	3.2	318.3	61	5/8"	Gas Dry

FIG. 1 — TYPICAL DATA SHEET USED TO RECORD WORKING PRESSURE DATA DURING A BACK-PRESSURE TEST.

William Ferguson³, and "Methods of Determining Gas Well Capacities in the Panhandle Field from Back-Pressure Data" by the Engineering Department—Oil & Gas Division, Texas Railroad Commission⁴. This paper makes reference to the above reports and does not present a detailed discussion of back-pressure test calculations.

Computed Data Required to Plot a 24-Hour Back-Pressure Potential Curve

In order to show a correlation and explain the method of calculating data for plotting a "24-Hour Back-Pressure Potential Curve", the data observed on a typical Hugoton Field gas well "A" will be used for illustration. In 1944, this well was tested by four 24-hour flow periods, in 1945 by three 24-hour flow periods, and again in 1946 by four 3-hour flow periods.

Reference to Fig. 2 shows the natural pressure decline curves of the well's working pressure plotted vs. time. From these curves it can be clearly seen that the rate of pressure decline is great at the beginning of each flow and gradually decreases until, at the end of each flow, the rate of change is very small. Also, it may be observed that each curve is different from the others with respect to rates of pressure decline. These differences are a function of the pressure at the beginning of the flow and the rate at which the well produces.

It is apparent from the above observations that extrapolated values of working pressures based on the curves of Fig. 2 would be very unreliable. For this reason, it is necessary to graphically represent the pressure data in a manner involving pressure differentials so the curve can be rectified to a

straight line. Such is conveniently done with the use of semi-logarithmic paper by plotting the time as the ordinate (log scale) vs. the logarithm of the difference between the bottom-hole shut-in pressure and the bottom-hole working pressure for the corresponding time as abscissa (equally divided scale). This is the same as plotting the pressure differential data on a logarithmic scale abscissa with a much larger modulus than that of the ordinate. It should be explained here that the rectification of the data to a straight line by the method suggested in no way changes the data. The method is merely a mathematical device permitting accurate extrapolation of the pressure decline with time. The data plotted are in the log vs. log form, and the type power equation is:

$$Y = a(X + K)^m$$

where Y = Time (hours)

X = Difference between bottom-hole shut-in pressure and bottom-hole working pressure (psi).

a , and m = Experimentally determined constants.

K = Rectification constant, calculated by "cut and try method" or computed directly by mathematical method⁵.

It is apparent from the above equation that the addition of a rectification constant " K " to the pressure differential data of the curve shifts the curve horizontally to the position where it becomes a straight line. Sometimes it is more convenient to shift the pressure differential curve vertically to obtain a straight line relationship of pressure differential and time. When such procedure is used, the following equation is the type power equation for the rectified curve:

$$Y + K = aX^m$$

In 1946, gas well "A" was tested by the short flow method using three-hour flow periods. The method of determining the sandface working pressure and subsequently the back-pressure curve that would be obtained had each flow been of 24 hours duration is described in the following step-by-step procedure: (See also Table No. 1 and Figs. 3 and 4.)

(1) In column one of Table No. 1,

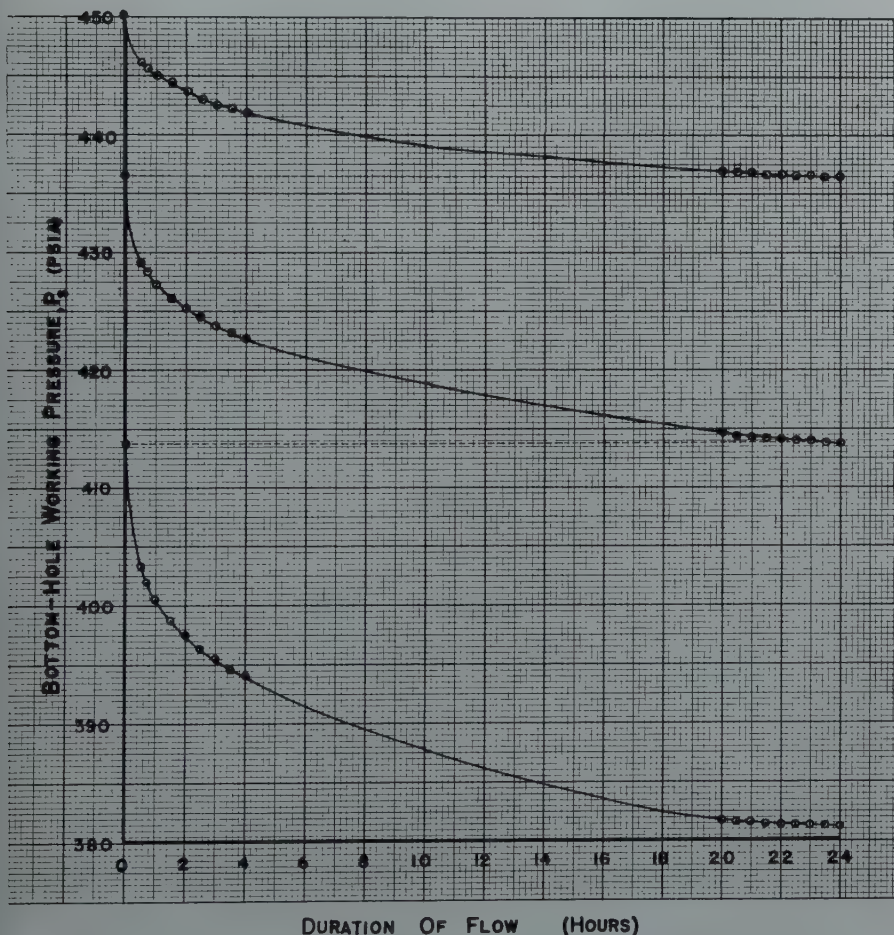


FIG. 2 — GAS WELL "A"

CURVES SHOWING THE NATURAL DECLINE OF PRESSURE DURING THREE SUCCESSIVELY INCREASED RATES OF FLOW.

enter the time intervals at which pressure readings are recorded. (T)

- (2) In column 2 (WP - psig), enter the working pressures observed opposite their respective time.
- (3) Use wellhead working pressures in column 2 to calculate the sandface working pressures which are entered in column 3 (P_s - psia).
- (4) Subtract each value in column 3 from the sandface shut-in pressure, P_r , and enter these values in column 4. These values are referred to as ΔP_b .
- (5) Take the common logarithms of the ΔP_b values and enter each of them in column 5.
- (6) Plot the log ΔP_b on the equally divided abscissa vs. T on the logarithmic divided ordinate of the semi-log graph paper. The alignment of the plotted points will indicate the type of rectification that may be conveniently used to develop a straight line from the data. For example, in Fig. 3 the curves for the first and second flows are concave and the addition of a rectification constant to the difference in pressure (or, $\Delta P_b + K$) will make each set of data plot on a straight line. For both the third and fourth flows the plotted data of Fig. 4 indicate convex curvature and are rectified by adding a constant to the time values (or $T + K$). These values are entered in column 6 or Table No. 1.
- (7) Determine the time to which the curves of Fig. 3 must be extrapolated to arrive at a pressure differential from which the sandface working pressure can be computed. In the development of a 24-hour back pressure potential curve, the three-hour data of the first rate of flow are extrapolated to the end of 24 hours and the logarithmic value of the pressure differential plus the rectification constant ($\Delta P_b + K$) is read from the curve. Subsequently, the value of the working pressure and rate of flow at the end of 24 hours is determined in a manner shown by Table No. 1.

The rate of pressure decline at the end of 24 hours is much lower than at the end of three hours flow. This difference in rate pressure drop results from the production of a quantity of gas from the end of the third through the twenty-fourth hour.

After rectification of the 3-hour rectification of the three-hour flow data of the second rate of flow on a short flow back-pressure test, and after extrapolation of the curve to the 24-hour point, the rate of working pressure drop will be greater than would

TABLE NO. 1
Extrapolation of 3-Hour Test — Gas Well "A"

(1)	(2)	(3)	(4)	(5)	(6)	(7)
FIRST FLOW						
T	W. P. (Psig)	P_s (Psia)	ΔP_b ($P_r - P_s$)	Log ΔP_b	$\Delta P_b + K$	Log ($\Delta P_b + K$)
0.5	379.7	420.8	4.5	.653	(K=1.7)	.792
0.7	379.1	420.2	5.1	.708	6.2	.832
1.0	378.5	419.5	5.8	.764	7.5	.875
1.5	377.9	418.9	6.4	.806	8.1	.908
2.0	377.4	418.3	7.0	.846	8.7	.940
2.5	376.9	417.8	7.5	.874	9.2	.964
3.0	376.5	417.4	7.9	.897	9.6	.982
24.0	370.6	411.0	14.3		16.0	1.204

Formation Pressure (P_r) = 425.3 psia

Rate of flow at 3 hours (Q_3) = 514 Mcfd

Extrapolate rectified curve to 24 hours and obtain Log ($\Delta P_b + K$) = 1.204

$\Delta P_b + K$ = antilog (1.204) = 16.0 psi

ΔP_b = 16.0 - 1.7 = 14.3 psi

P_s = 325.3 - 14.3 = 411.0 psia

$$Q_{24} = 514 \left[\frac{411.0}{417.4} \right] = 507 \text{ Mcfd}$$

(1)	(2)	(3)	(4)	(5)	(6)	(7)
SECOND FLOW						
T	W. P. (Psig)	P_s (Psia)	ΔP_b ($P_r - P_s$)	Log ΔP_b	$\Delta P_b + K$	Log ($\Delta P_b + K$)
0.5	370.4	410.8	14.5	1.162	(K=30)	1.648
0.7	369.3	409.7	15.6	1.194	44.5	1.660
1.0	368.2	408.5	16.8	1.226	45.6	1.670
1.5	366.9	407.1	18.2	1.260	46.8	1.683
2.0	365.9	406.0	19.3	1.286	48.2	1.693
2.5	365.2	405.3	20.0	1.301	49.3	1.699
3.0	364.5	404.5	20.8	1.318	50.0	1.706
34.0	354.0	393.3	32.0		50.8	1.706
					62.0	1.792

Rate of flow at 3 hours (Q_3) = 1087 Mcfd

$V = \frac{21}{24} \times 514 = 450 \text{ Mef}$; Approximate volume of gas that would have been produced if first flow had continued from the end of the three hours for twenty-one hours more.

$R_h = \frac{1}{24} \times 1087 = 45 \text{ Mcf/hr.}$; Hourly rate of gas production at end of 3 hours flow.

$T = \frac{V}{R_h} = \frac{450}{45} = 10 \text{ hrs.}$; Time beyond 24 hours to which second flow pressure differential curve must be extrapolated.

Extrapolate rectified curve to 34 hours and obtain Log ($\Delta P_b + K$) = 1.792

$\Delta P_b + K$ = antilog (1.792) = 62.0 psi

ΔP_b = 62.0 - 30.0 = 32.0 psi

P_s = 425.3 - 32.0 = 393.3 psia

$$Q_{24} = 1087 \left[\frac{393.3}{404.5} \right] = 1057 \text{ Mcfd}$$

(1)	(2)	(3)	(4)	(5)	(6)
THIRD FLOW					
T	W. P. (Psig)	P _s (Psig)	ΔP _b (P _f - P _s)	Log ΔP _b	T+K
0.5	354.2	393.5	31.8	1.502	(K=0.3) 0.8
0.7	352.7	391.9	33.4	1.524	1.0
1.0	351.2	390.3	35.0	1.544	1.3
1.5	349.0	387.9	37.4	1.573	1.8
2.0	347.5	386.3	39.0	1.592	2.3
2.5	346.1	384.8	40.5	1.608	2.8
3.0	344.9	383.6	41.7	1.620	3.3
42.0	320.9	357.7	67.6	1.830	

Rate of flow at 3 hours (Q_3) = 1854 Mcfd

$V = \frac{31}{24} \times 1087 = 1404$ Mcf.; Approximate volume of gas that would have been produced had the second flow continued for 31 hours longer.

$R_h = \frac{1}{24} \times 1854 = 77$ Mcf./hr.; Hourly rate of gas production at the end of 3 hours flow.

$T = \frac{V}{R_h} = \frac{1404}{77} = 18$ hours; Time beyond 24 hours to which third flow rectified curve must be extrapolated.

Extrapolate rectified curve to 42 hours and obtain Log $\Delta P_b = 1.830$

$\Delta P_b = \text{antilog } (1.830) = 67.6$ psi

$P_s = 425.3 - 67.6 = 357.7$ psia

$$Q_{24} = 1854 \left[\frac{357.7}{383.6} \right] = 1729 \text{ Mcfd}$$

(1)	(2)	(3)	(4)	(5)	(6)
FOURTH FLOW					
T	W. P. (Psig)	P _s (Psig)	ΔP _b (P _f - P _s)	Log ΔP _b	T+K
0.5	331.2	368.9	56.4	1.751	(K=0.3) 0.8
0.7	329.4	366.9	58.4	1.766	1.0
1.0	327.4	364.8	60.5	1.782	1.3
1.5	324.8	362.0	63.3	1.801	1.8
2.0	322.6	359.6	65.7	1.818	2.3
2.5	320.8	357.7	67.6	1.830	2.8
3.0	319.2	356.0	69.3	1.840	3.3
52.0	287.0	321.5	103.8	2.016	

Rate of flow at 3 hours (Q_3) = 2599 Mcfd

$V = \frac{39}{24} \times 1854 = 3013$ Mcf.; Approximate volume of gas that would have been produced had the third flow continued for 39 hours longer.

$R_h = \frac{1}{24} \times 2599 = 108$ Mcf./hr.; Hourly rate of gas production at the end of 3 hours flow.

$T = \frac{V}{R_h} = \frac{3013}{108} = 28$ hours; Time beyond 24 hours to which fourth flow rectified curve must be extrapolated

Extrapolate rectified curve to 52 hours and obtain Log $\Delta P_b = 2.016$

$\Delta P_b = \text{antilog } (2.016) = 103.8$ psi

$P_s = 425.3 - 103.8 = 321.5$ psia

$$Q_{24} = 2599 \left[\frac{321.5}{356.0} \right] = 2347 \text{ Mcfd}$$

be experienced if the second three-hour flow followed a first flow of 24 hours duration. To arrive at extrapolation data from which a 24-hour working pressure for the second rate of flow can be determined, it is necessary to extrapolate the second rate of flow curve of Fig. 3 beyond 24 hours to a point where the rate of working pressure decline is comparable to that which would have been experienced at the end of a second consecutive 24-hour flow. The time beyond 24 hours required for extrapolation of the curve for the second rate of flow is found by determining the approximate quantity of gas that would have been produced from the end of the third hour through the twenty-fourth hour of the first rate of flow had the first 3-hour flow continued for 24 hours and dividing such volume by the rate of flow at the end of the second 3-hour flow period.

The calculation for the 24-hour working pressure and rate of flow to be used for the second point of a 24-hour back-pressure potential curve based on 3-hour flow data is shown in Table No. 1. Also included in the table are the calculated 24-hour working pressures and rates of flow for the third and fourth flows of the short flow back-pressure test of gas well "A".

- (8) Having the calculated 24-hour sand-face working pressures and shut-in pressures, it is necessary to determine the rates of flow corresponding to the 24-hour pressures. This is done by multiplying the rate of flow at the end of three hours by the ratio of the 24-hour to the 3-hour sandface working pressures.

$$(Q_{24} = Q_3 \times P_{s24}/P_{s3})$$

Such procedure is convenient and satisfactory unless the flowing friction loss in the flow string is very large in which instance it is advisable to compute wellhead pressures and use the ratio of the twenty-four to the three-hour wellhead pressure rather than use the sandface

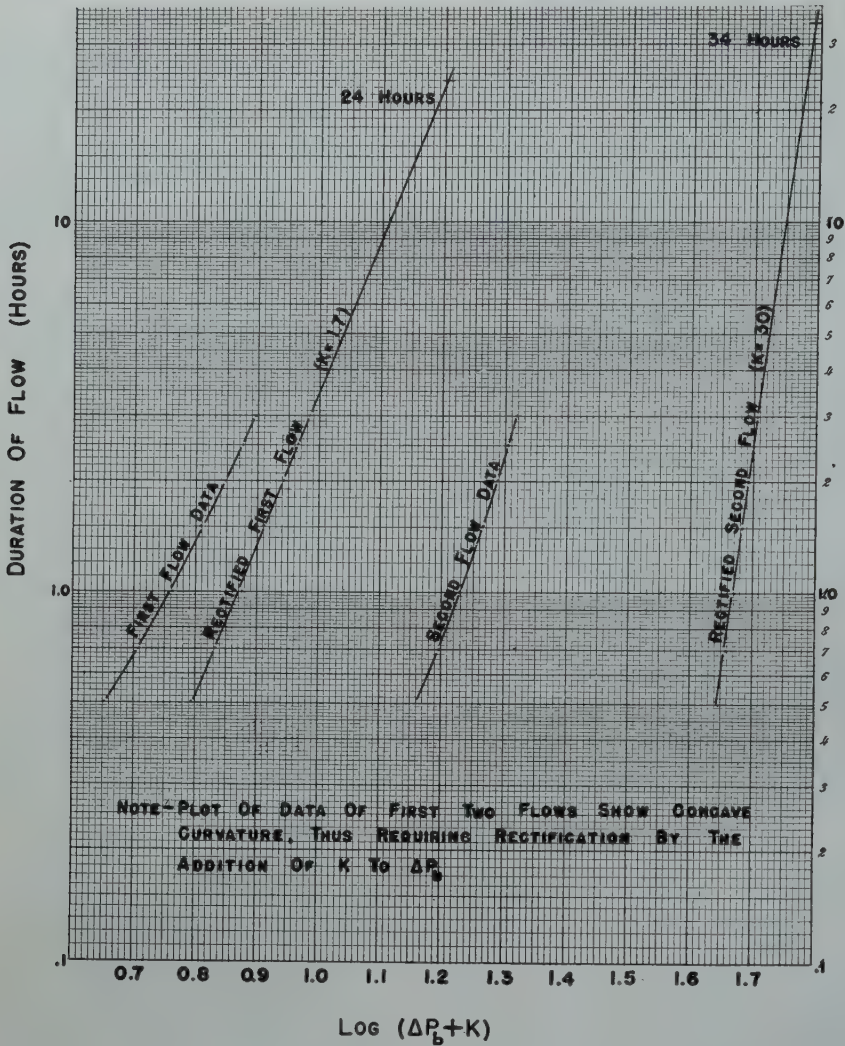


FIG. 3 — GAS WELL "A"
EXTRAPOLATION OF 3-HOUR TEST DATA TO OBTAIN THE BOTTOM-HOLE WORKING PRESSURES
EQUIVALENT TO THE PRESSURES THAT WOULD HAVE BEEN OBTAINED DURING
AN ACTUAL 24 HOURS PER FLOW BACK-PRESSURE TEST.

pressure ratio in the above equation.

(9) Having the calculated 24-hour rates of flow and working pressures at the sandface, the necessary computations for squared pressures are made, and the 24-hour back-pressure potential curve is plotted in the conventional manner. Fig. 5 is a copy of the work sheet used in the calculation of the short flow back-pressure test. The potential shown is that determined by a 3-hour per flow test. Figure 6 shows the 3-hour per flow back-pressure curve and the 24-hour back-pressure potential curve determined by the short flow meth-

od, and the plotted points for two 24-hour back-pressure potential curves determined from one set of data taken in 1944 and from another taken in 1945.

*Validity of the Method of
Determining a Back-Pressure
Curve by Extrapolation of
Pressure Differential and
Time Curves*

To further determine the validity of the above described procedures, several "Special Tests" were conducted on wells that had previously been tested using 24-hour flow periods. These tests listed below are titled:

- 1. The Short Flow Back-Pressure Test (12 tests)
- 2. The Maximum Flow Check Test (4 tests)
- 3. The Second Flow Check Test (4 tests)

The short flow back-pressure test is one conducted in the same manner as the 24 hours per flow test except that flow periods of 3 or 4 hours duration are used. The duration of flow for each flow period on nine tests was 3 hours and on three tests the flows continued for 4 hours each. Each of the twelve tests was conducted with four different rates of flow beginning with the lowest and ending with the highest. The back-pressure curves obtained by testing in this manner naturally gave highly unstabilized potentials which were much greater than the more stabilized potentials of the 24-hour potential curves.

TABLE NO. 2

*Comparison of Slopes of Curves Established by Short Flow Back-Pressure
Tests and 24-Hour Back-Pressure Potential Tests*

(1) Gas Well	(2) Duration of Each Flow	(3) Slope of Short Flow Test Curve	(4) Slope 24 Hr. Curve	(5) Difference in Slope
"C"	4 Hrs.	.848	.720	— .128
"D"	3 Hrs.	.725	.725	— .000
"E"	3 Hrs.	.744	.741	— .003
"G"	3 Hrs.	.733	.734	+ .001
"H"	3 Hrs.	.778	.811	+ .033
"I"	4 Hrs.	.771	.820	+ .049
"A"	4 Hrs.	.888	.799	— .089
"B"	3 Hrs.	.834	.803	— .031
"J"	3 Hrs.	.772	.763	— .009
"K"	3 Hrs.	.743	.791	+ .048
"L"	3 Hrs.	.803	.810	+ .007
	3 Hrs.	.743	.776	+ .048
Average 12 Tests		.779	.774	— .005

However, two interesting features were clearly observed during the short and long duration tests. One was the fact that if equal time intervals were used for each flow, the calculated back-pressure plotting points would lie on a straight line when plotted on logarithmic paper. The other was the similarity in the slopes of the short flow and 24-hour back-pressure curves. In all the tests, the back-pressure curves are nearly parallel (Table No. 2). Therefore, it is apparent that the duration of flows does not materially affect the slopes of the back-pressure curves when each flow during a test continues for the same time as the others. By referring to Figure 7, it can be seen that the slope of the curve is established by the computed data for each test, but the amount of displacement of the 24-hour curve to the left of the 3-hour curve is a variable that must be determined by the extrapolation method outlined heretofore or by the 24-hour per flow test.

In order to know what affect the starting pressure and duration of flow had on the final working pressure of a well, a maximum flow check test was initiated to check the working pressure on the last and largest flow of a back-pressure test without including the two flow periods prior to the last flow. It was expected that 24 hours would be sufficient flowing time to allow the well to stabilize and thus reproduce a similar working pressure to that on the last flow of a 24-hour back-pressure test. Instead, it was found that when the

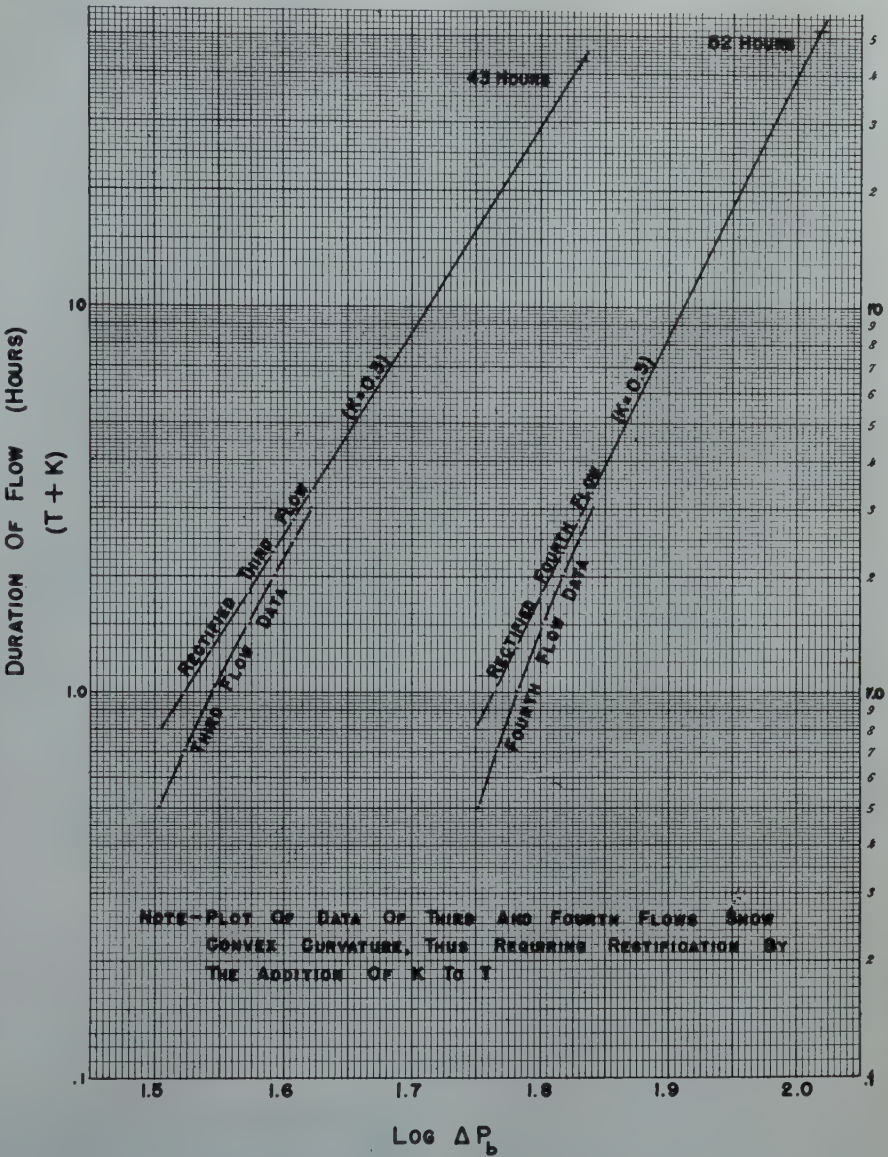


FIG. 4 — EXTRAPOLATION OF 3-HOUR TEST DATA — CONTINUED.

TABLE NO. 3
Gas Well "B"

Comparison of Rates of Pressure Decline During 3rd Flow of Back-Pressure Test and During Maximum Flow Check Test

Time (Hours)	3rd. Flow Back-Pressure Test			Maximum Flow Check Test		
	W. P. (Psig)	P ₃ (Psia)	ΔP ₃ (Psi/Hr.)	W. P. (Psig)	P ₃ (Psia)	ΔP ₃ (Psi/Hr.)
0.5	339.5	376.8	8.0	389.2	429.8	22.0
0.7	338.3	375.5	6.5	386.0	426.4	17.0
1.0	337.0	374.1	4.7	381.4	421.5	16.3
1.5	335.4	372.4	3.4	377.7	417.6	7.8
2.0	334.1	371.0	2.8	374.6	414.2	6.8
2.5	333.0	369.8	2.4	372.0	411.5	5.4
3.0	332.2	369.0	1.6	369.7	409.0	5.0
3.5	331.5	368.2	1.6	367.9	407.1	3.8
4.0	330.8	367.5	1.4	366.4	405.5	3.2
20.0	319.0	354.9	—	341.1	378.7	—
21.0	318.6	354.4	0.5	339.7	377.3	1.4
22.0	318.2	354.0	0.4	338.6	376.1	1.2
23.0	317.8	353.6	0.4	337.5	374.9	1.2
24.0	317.4	353.2	0.4	336.5	373.8	1.1
52.0	—	—	—	319.3	354.0	0.4

well started flowing from shut-in conditions at the maximum rate of the previous back-pressure test, the working pressure after 24 hours was much higher and the rate of pressure decline was much greater than that found on the last flow of the previous test. Reference to Table No. 3 and Fig. 8 illustrates one such test taken on gas well "B". The third flow of the original 24-hour back-pressure was started with a working pressure of 353.2 psig using a 5/8" orifice plate in the prover. At the end of 24 hours, the working pressure had dropped to 317.4 psig and the rate of pressure decline was 0.4 psi per hour. On the maximum flow check test, a 5/8" orifice plate was again used, but

PHILLIPS PETROLEUM COMPANY NATURAL GAS DIVISION
BACK-PRESSURE TEST SHEET

LEASE Gas Well "A"
DATE 11-29 1946

FIELD Hugoton COUNTY _____ STATE _____
SEC. _____ TWP. _____ RGE. _____ BLK. _____ SURVEY _____
CASING SIZE 7" O.D. WT. 22 lbs. SET AT 2727' PERF. TO _____
GAS PAY FROM 2771 TO 2846 L 2809 G 0.710 GL TO 1994
TUBING SIZE None WT. _____ SET AT _____ PERF. TO _____
SIZE PROVER 4" METER RUN TYPE CONN. BAROMETER 13.2
e^s 1.149 F_q 6.695 REMARKS Old Well Retest—Short Flow Back-Pressure Test
☐ Initial Test ☐ P.P.Co. only
☐ Retest ☐ Official

OBSERVATIONS

No.	Orifice Size	Meter Pressures			Flow Temp. °F.	Wellhead		Duration of Flow (hrs.)
		Static Psig	P _m Psia	Diff. hw		(W _P) Psig	(P _w) Psia	
1.					61	376.5	389.7	3
2.					61	364.5	377.7	3
3.					61	344.9	358.1	3
4.					61	319.2	332.4	3
5.								

FLOW CALCULATIONS

No.	Orifice Size	Coeff. C (24 hr.)	√hwP _m or	Working Pressure on Prover		Flow Temp. Factor F _{tb}	Gravity Factor F _g	Delivery Rate Mcf Per 24 hrs. Q @ 14.65 Psia
				Psig	Psia			
1.	1/4"	1.384		376.4	389.6	.9990	.9193	514
2.	3/8"	3.110		364.3	377.5	.9990	.9193	1,087
3.	1/2"	5.564		344.5	357.7	.9990	.9193	1,854
4.	3/4"	8.668		318.3	331.5	.9990	.9193	2,599
5.								

SIP 383.9 psig PRESSURE CALCULATIONS
(All squared pressures in thousands)

BAR. 13.2 psia
P₁ 397.1 psia P_c² 157.69 × e^s 1.149 = P₂² 181.19
WELL SHUT-IN _____ HOURS BEFORE OR AFTER TEST.

No.	Q (Millions) × F _q = R	P _w ² × e ^s = e ^s P _w ² + R ² = P _s ²				P _f ² - P _s ²	P _f ² - e ^s P _w ²		
1.	.514	6.695	3.4412	151.87	1.149	174.50	0.0	174.50	6.69
2.	1.087	6.695	7.2775	142.66	1.149	163.92	0.1	164.02	7.17
3.	1.854	6.695	12.413	128.24	1.149	147.35	0.2	147.55	33.64
4.	2.599	6.695	17.400	110.49	1.149	126.95	0.3	127.25	53.94
5.									

ABSOLUTE POTENTIAL 7,100 Mcf PER DAY @ 14.65 psia
ABSOLUTE POTENTIAL _____ Mcf PER DAY @ _____ psia
SHUT-IN WELLHEAD PRESSURE 383.9 psig
Commission _____ Company _____ Pipeline _____

FIG. 5 — TYPICAL WORK SHEET USED IN THE CALCULATION OF THE SHORT FLOW BACK-PRESSURE TEST.

the flow was started from a shut-in pressure of 428.5 psig. It is interesting to note that after 24 hours of flow on the check test the working pressure was approximately 20 psi above that of the third flow of the back-pressure test and the working pressure was decreasing at the rate of 1.1 psi per hour and that the flow would have had to continue for several hours before the degree of pressure stabilization obtained during the back-pressure test could have been reached on the check test.

By using the extrapolation method described earlier, it was found that the check test would require approximately 52 hours to reach the flow conditions of the maximum 24-hour flow of the back-pressure test. The working pressure at that time was calculated to be 319.3 psig, and the rate of pressure decline was approximately 0.4 psi per hour.

Further proof the extrapolation technique can be shown by the "Second Flow Check Test". The test consists of a 3-hour flow followed by a second flow permitted to continue for the calculated number of hours needed to lower the working pressure to a value equal to the working pressure at the end of the second flow of a 24-hour back-pressure test. The same orifice sizes used in the first and second flows of the 24-hour test were used in the check test.

Fig. 9 shows the bottom-hole working pressure for well "J" plotted vs. time. The upper scale of the abscissa is for the original 24-hour back-pressure test. The lower scale of the abscissa indicates the duration of flow of the second flow check test. The points A, B, C, D, and E, denote the following:

- A. Shut-in pressure. (Because of production from this well in the interim between tests, the shut-in pressure of the check test was corrected to that of the back-pressure test, and this common difference of 2.2 psi was also added to each working pressure of the check test.)
- B. Working pressure after 3 hours flow on the back-pressure and the check test.
- C. Working pressure at the end of first flow and beginning of second flow of the 24-hour back-pressure test.

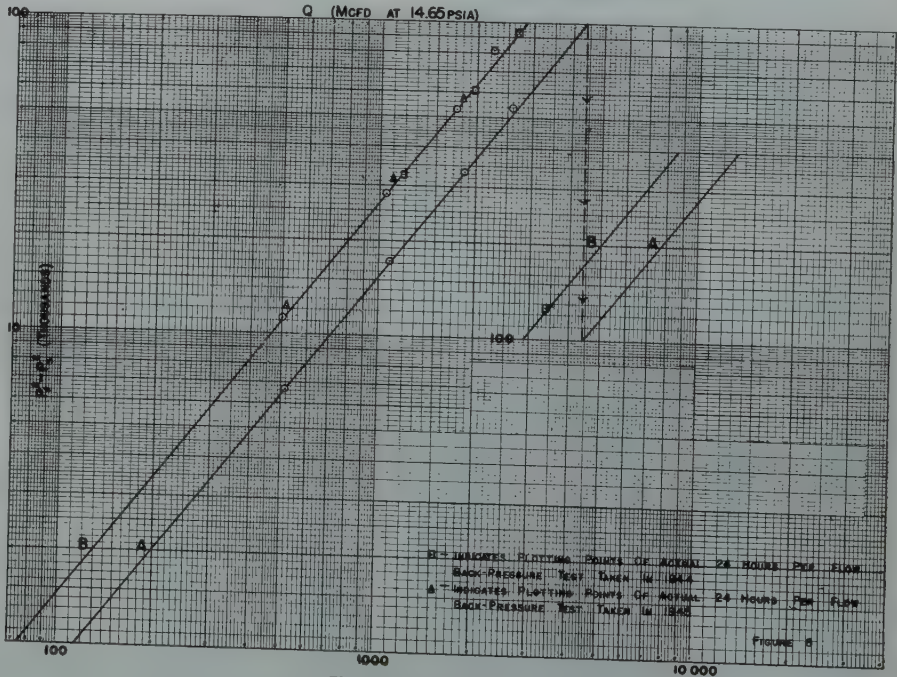


FIG. 6 — GAS WELL "A"
CURVE A — ACTUAL 3 HOURS PER FLOW BACK-PRESSURE TEST.
CURVE B — EXTRAPOLATED "24 HOURS PER FLOW" TEST.

D. Working pressure of the end of second flow of the 24-hour back-pressure test.

E. Working pressure of the end of check test flow.

It is interesting to note that the rate of pressure decline on the second flow of the check tests approximated the rate of decline of the back-pressure test second flows for the four wells tested. The arithmetic average of the working pressures for the four wells at the end of the check tests was .98 psi less than the average for the second flows of the back-pressure tests.

It has been found that 24-hour back-pressure potential curves on wells producing from formations of extremely low permeability are satisfactory for the determination of a back-pressure potential but cannot be used for determining the stabilized performance of gas wells producing gas into a pipe line. It is often necessary to establish a stabilized back-pressure curve from which actual operating conditions can be ascertained. Such a curve has been constructed and shown in Fig. 10 for gas well "J". The technique of extrapolating the pressure differential data is the same as that used in determining working pressures and rates of flow for the 24-hour back-pressure potential curves except that the pressure differ-

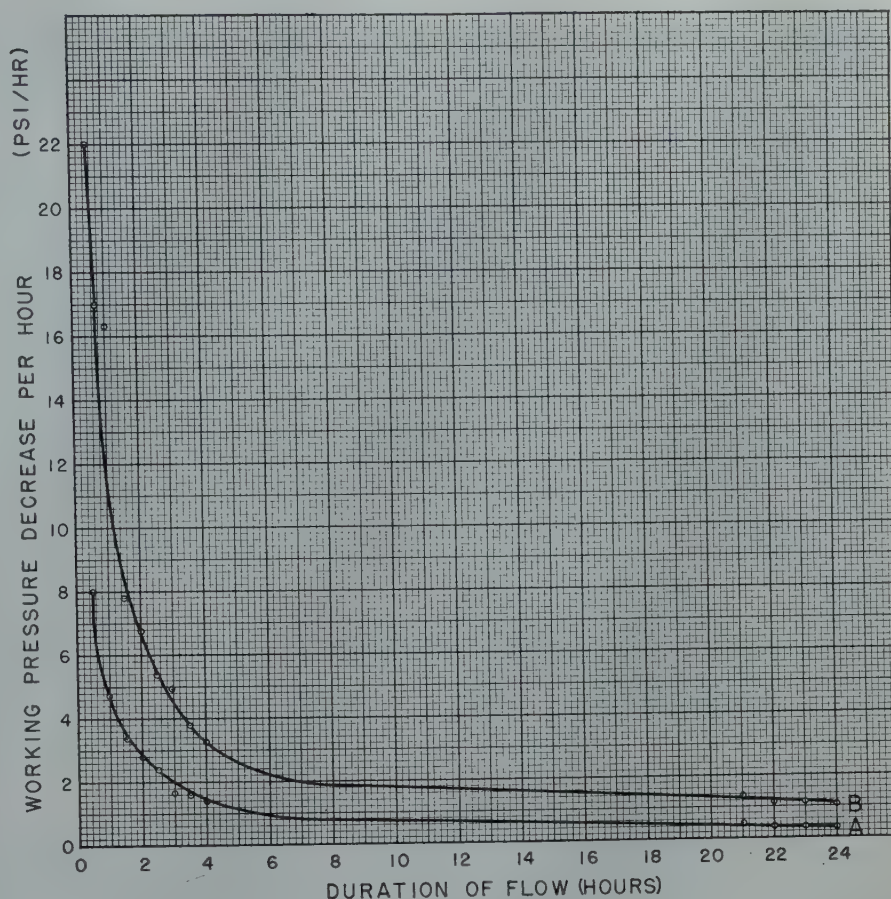


FIG. 8 — GAS WELL "B"

WORKING PRESSURE DECREASE PER HOUR VS. DURATION OF FLOW.
CURVE A — LAST FLOW OF ORIGINAL BACK-PRESSURE TEST.
CURVE B — MAXIMUM FLOW CHECK TEST.

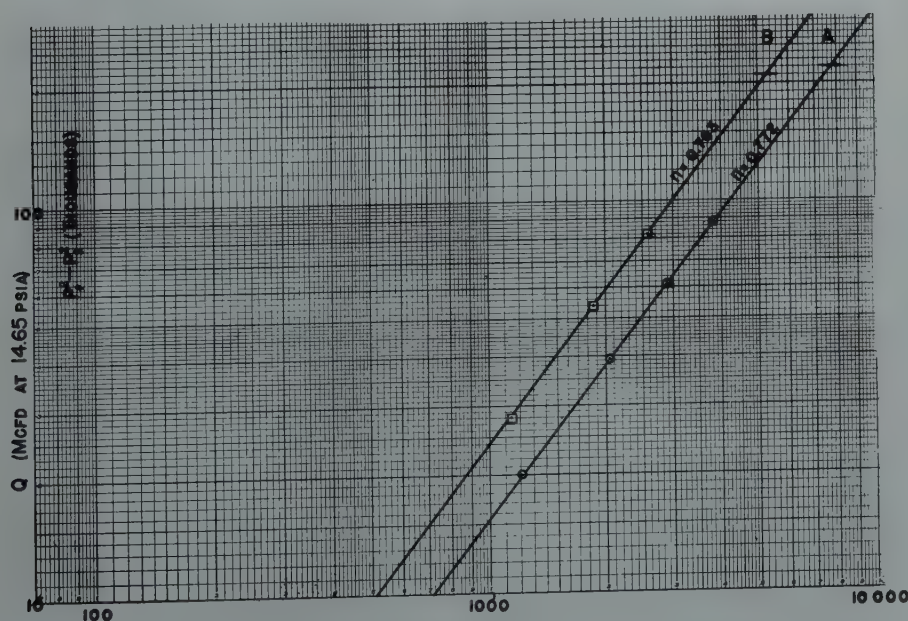


FIG. 7 — GAS WELL "B"

CURVE A — CURVE OF 3 HOURS PER FLOW BACK-PRESSURE TEST.
CURVE B — ACTUAL 24 HOURS PER FLOW BACK-PRESSURE POTENTIAL CURVE.
NOTE—SIMILAR SLOPES INDICATE CURVES ARE NEARLY PARALLEL.

ential curves are extrapolated to obtain data by which a curve equivalent to one that would be established by a back-pressure test taken with flows of 240 hours duration. Curves "A" and "B" are the three-hour back-pressure curve and the 24-hour back-pressure potential curve, respectively. Curve "B" was determined by the method described earlier in this paper. Curve "C" is the stabilized back-pressure curve determined by the extrapolation method using a flow duration such that a test obtained is equivalent to a 240-hour back-pressure test.

The numbered points between curves "B" and "C" were determined from data of actual shut-in pressures, working pressures, and rates of flow recorded at various times while the well produced gas into the pipe line. Point No. 1 was determined three days after the well started to produce into the pipe line. The well continued to deliver gas

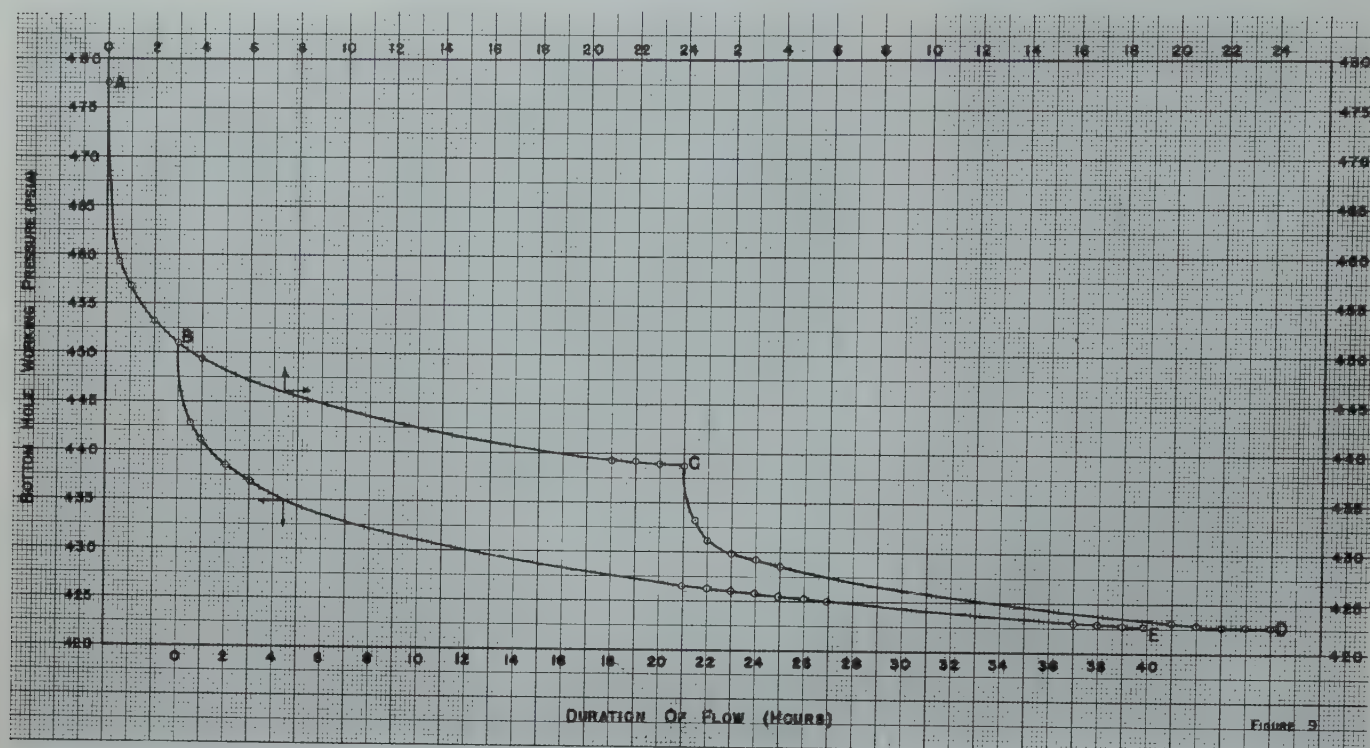


FIG. 9 — GAS WELL "J"

WORKING PRESSURE DATA OF "SECOND FLOW CHECK TEST".

CURVE AC — FIRST 24 HOUR FLOW (WITH $\frac{3}{4}$ " ORIFICE) RATE OF FLOW AT C = 4587 MCFD.CURVE CD — SECOND 24 HOUR FLOW (WITH $\frac{7}{8}$ " ORIFICE) RATE OF FLOW AT D = 6004 MCFD.CURVE AB — 3 HOUR FLOW OF SECOND TEST (WITH $\frac{3}{4}$ " ORIFICE) RATE OF FLOW AT B = 4732 MCFD.CURVE BE — 39.9 HOUR FLOW OF SECOND TEST (WITH $\frac{7}{8}$ " ORIFICE) RATE OF FLOW AT E = 6041 MCFD.

into the pipe line, and points No. 2 and No. 3 indicate the well performance at the end of seven and fourteen days, respectively. Since the stabilized back-pressure curve passes very closely to points No. 2 and No. 3, it is apparent that the curve represents actual operating conditions at rates of flow of approximately 4300 Mcfd. Approximately six weeks after the data for point No. 3 were obtained, well "J" was shut-in for a period of fourteen days and a new shut-in pressure was obtained. The well was then opened into the pipe line, and data for determination of points No. 4, No. 5, and No. 6 on Fig. 10 were obtained. Data for point No. 4 were obtained at the end of three days flow, point No. 5 at the end of ten days flow, and point No. 6 at the end of fourteen days flow. Again point No. 4 lies on the unstabilized 24-hour back-pressure potential curve "B", and points No. 5 and No. 6 are very close to the stabilized back-pressure curve "C", thus, indicating the dependability of curve "C" at rates of

flow of approximately 5,000 and 5,500 Mcfd.

The data on Fig. 10 are representative of many wells in the Hugoton Gas Field, and many stabilized back-pressure curves have been developed, and later verified, by observation of pressures and rates of flow from time to time during actual production of gas into the pipe line.

SIMILARITY OF THE DECLINING GAS WELL PRODUCTIVITY INDEX OF OIL WELLS

A paper was presented at the Houston 1944 meeting of the AIME by C. V. Millikan and Herbert F. Beardmore titled "*Significance of Declining Productivity Index*" in which the authors showed several logarithmic plots of oil well productivity indices (barrels of oil produced per day per pound per square inch of differential pressure between the reservoir and the bottom of the well) vs. time in hours.

In most cases a straight line relationship is shown for the decline of the productivity indices. Also, it was demonstrated that the productivity indices on the wells studied declined with time, but upon shutting in the wells and allowing the reservoir pressure to build up, the productivity indices were restored to their original values.

By defining the productivity index for a gas well as the thousands of cubic feet of gas produced per day per unit of difference between the square of the reservoir pressure and the square of the bottom-hole working pressure, it is possible to analyze the performance of gas wells in somewhat the same light as was done by Messrs. Millikan and Beardmore on oil wells. Due to the turbulent nature of the flow of gas through porous media into a well bore, we believe it advisable to use the flow exponent "n" (slope of back-pressure curve) in the gas well productivity index. Thus, the productivity index of a gas well becomes the coefficient of the

gas flow equation, and the index in terms of symbols is as follows:

$$C = \frac{Q}{(P_r^2 - P_s^2)^n} \text{ (Productivity Index)}$$

and

$$Q = C(P_r^2 - P_s^2)^n \text{ (Gas Flow Equation)}$$

WHERE:

Q = rate of flow Mcfd

P_r = shut-in reservoir pressure psia

P_s = working sandface pressure psia

n = slope of the back-pressure curve or gas flow exponent

C = productivity index

Fig. 11 shows the productivity indices of two gas wells, "F" and "G", plotted vs. time on logarithmic paper. The nature of the curves is very similar to that of the oil well curves discussed in the above mentioned paper. We have learned that declining gas well productivity indexes can be restored to original values by shutting in wells and permitting the reservoir pressure to build up.

SUMMARY AND CONCLUSIONS

From the foregoing discussion of the gas well test work performed during the last four years in the Hugoton Gas Field, it is possible to draw the following conclusions with regard to back-pressure testing of gas wells which produce from formations of extremely low

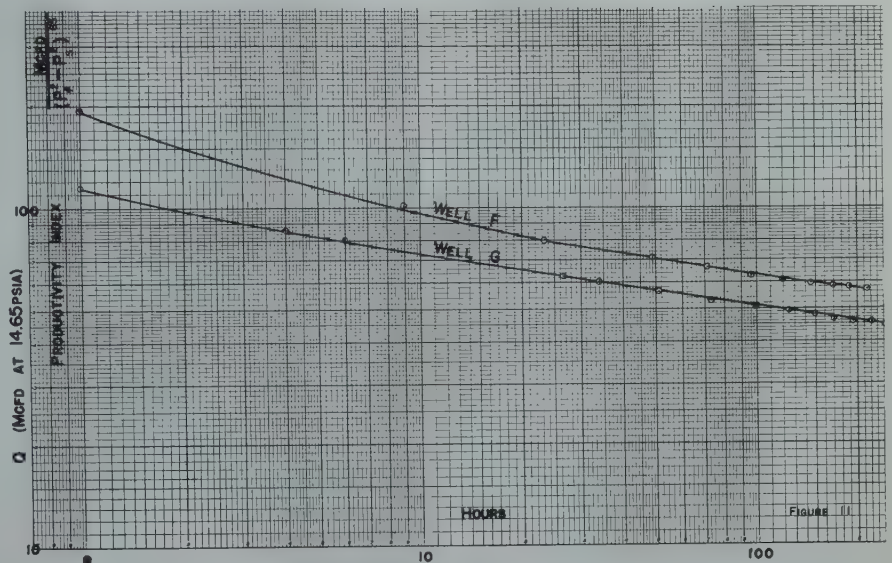


FIG. 11 — GAS WELLS "F" AND "G"
CURVES SHOWING DECLINING PRODUCTIVITY INDICES FOR TWO HUGOTON FIELD GAS WELLS.

permeability:

1. A method has been developed by which it is possible to determine reliable back-pressure potential curves and stabilized back-pressure curves for wells in the Hugoton Gas Field.
2. The stabilized back-pressure curve determined by use of the method reported herein can be used to determine actual rates of gas production into a pipe line for pre-

determined wellhead working pressures.

3. The stabilized back-pressure curve is satisfactory for use in the design of gas gathering systems and for the sizing of orifice meter settings.
4. By use of the method described, it is possible to save approximately 88% of the gas ordinarily vented by long duration back-pressure tests where pipe line pressures are such that it is necessary to use a critical-flow prover or choke nipple to measure the rates of gas production during well testing.
5. The productivity indices for gas wells producing from a low permeability reservoir plotted against time on logarithmic paper show a declining straight line or slightly curved trend similar to the oil well declining productivity indices described by Messrs. Beardmore and Millikan in the AIME Technical Publication No. 1872⁶.
6. Although the method described in this paper has been developed in the Hugoton Gas Field, it is the authors' conclusion that such procedure need not be confined to that area. By the proper evaluation of the physical data observed during back-pressure testing, it should be possible to apply the method to wells in many fields.

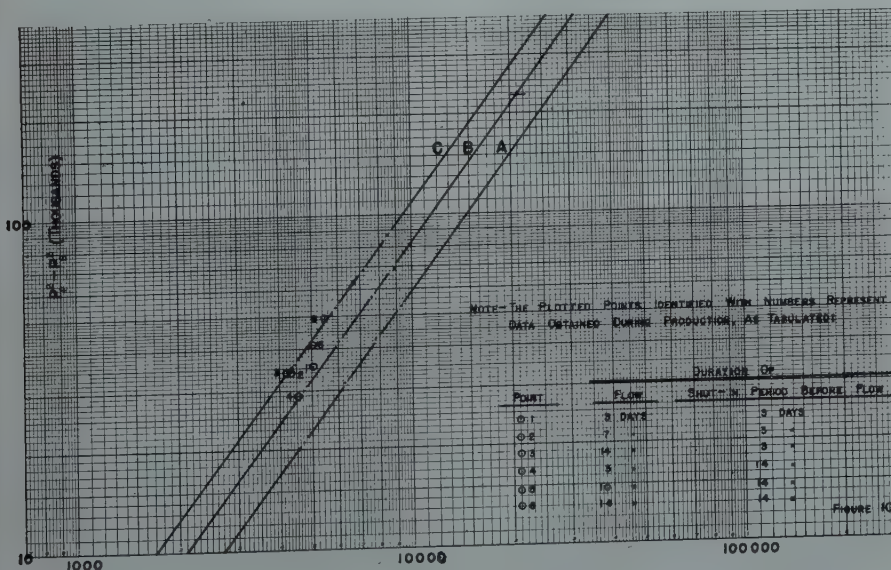


FIG. 10 — GAS WELL "J"

CURVE A — 3 HOUR PER FLOW BACK-PRESSURE TEST.

CURVE B — 24 HOUR BACK-PRESSURE POTENTIAL CURVE EXTRAPOLATED FROM DATA OF 3 HOUR PER FLOW BACK-PRESSURE TEST.

CURVE C — STABILIZED BACK-PRESSURE CURVE.

ACKNOWLEDGMENT

This description of a method for determining stabilized gas well performance for gas wells producing from reservoirs of extremely low permeability is published by permission of the management of Phillips Petroleum Company.

NOMENCLATURE

- W.P. — Wellhead working pressure (psig)
- ΔP — Difference between two successive wellhead working pressures (psi)
- P_r — Shut-in formation pressure (psia)
- P_s — Formation working pressure (psia)
- P_{s_3} — Formation working pressure after 3 hours flow (psia)
- $P_{s_{24}}$ — Formation working pressure after 24 hours flow (psia)
- ΔP_b — Difference between formation shut-in pressure and formation working pressure (psi)
- K — Rectification constant
- a & m — Experimental constants determined from rectified curve
- n — Experimental constant or slope of the back-pressure curve
- C — Productivity index or coefficient of gas flow equation
- Q — Rate of flow (Mcf/d at 14.65 psia)
- Q_3 — Rate of flow at end of 3 hours continuous flow
- Q_{24} — Rate of flow at end of 24 hours continuous flow
- R_h — Rate of flow (Mcf/hr. at 14.65 psia)
- V — Volume (Mcf at 14.65 psia)
- T — Time (hours)

REFERENCES

1. Binckley, C. W.: Open Flow and Back-Pressure Data and Their Application to the Production of Natural Gas — With Particular Reference to Hugoton Field — June, 1946,

Page 9 — FPC Docket G-669, Ex. 443.

2. Rawlins, E. L. and Schellhardt, M. A.: Back-Pressure Data on Natural Gas Wells and Their Application to Production Practice. U. S. Bureau of Mines Monograph 7.
3. Ferguson, J. William: Calculation of Back-Pressure Tests on Natural Gas Wells. *Oil and Gas Journal* (January 19, 1939).
4. Methods of Determining Gas Well Capacities in the Panhandle Field from Back-Pressure Data: Engineering Department—Oil & Gas Division, Texas Railroad Commission (June 1, 1939).
5. Davis, Dale S.: *Empirical Equations and Nomography*, McCraw Hill Book Company, 1943, Page 18.
6. Millikan, C. V. and Beardmore, Herbert F.: Significance of Declining Productivity Index, *Technical Publication* 1872 (1944).

★

DISCUSSION

By H. R. Sells, *Sohio Petroleum Co., Oklahoma City, Oklahoma*

The material presented outlines in detail a procedure for the construction of a "24 hour" back-pressure curve, or a "stabilized" back-pressure curve, when the actual data used are from flow tests of relatively short duration and during which the well has not reached stable conditions. This method, while involving considerable additional calculation, is an important addition to back-pressure testing procedure and should prove of much value to all operators of gas fields in which reservoir permeabilities are low. The reduction made in the time required for testing is always important, and in areas in which tests must be made using a critical flow prover, considerable gas may be saved using this procedure.

The paper is an excellent example of presenting a mathematical solution to a testing problem, and then proceeding to verify the results by actual field tests. Little criticism can be made of a paper which uses this procedure. The tests were made in one field only, but

the outlined method should apply equally well in other areas. It might be well to point out that these tests must be made with the well bore free of liquids or cavings. It would appear that a considerable error could be introduced if the method were used on gas wells in which the liquid conditions in the well bore had been improperly interpreted.

The method used to prove the calculated "stabilized" back-pressure curves which is graphically presented in Fig. 10, brings to mind the suggestion that this particular procedure can be used to check back-pressure curves which have already been made, if the well is presently producing under critical flow conditions into a pipe line.

Authors' Reply to H. R. Sells

I would like to point out first that the additional calculations involved to establish a 24-hour back-pressure curve from data of short flows can be accomplished in approximately two hours by an experienced clerk. The expense of the additional man-hours for such calculations is far more than offset by the saving in gas vented by ordinary testing procedures.

The importance of having a well clean prior to testing must be stressed. I agree with Mr. Sells that water or cavings in the wellbore will obstruct the flow of gas and the tester will obtain data that are not related to the true producing characteristics of the well. It is also unlikely that such data can be verified by production records of rates of flow and wellhead working pressures. It is our policy to investigate well-bore conditions prior to any test by 20 minute open flows, and by wire line surveys if it is suspected that foreign material remains in the wellbore after blowing.

I also wish to clarify a third point in the discussion of this paper in regard to the calculated stabilized performance curve and its verification by pipe line production records. Critical-flow conditions between the well and the pipe line are desirable but not necessary for, if pipe line pressures are held reasonably constant during a check flow period wellhead working pressures will not be materially affected and the plotting point will fall upon or very close to the stabilized performance curve. ★

DISCUSSION OF THIS AND ALL FOLLOWING TECHNICAL PAPERS IS INVITED

Discussion in writing (3 copies) may be sent to the Editor, *Journal of Petroleum Technology*, 601 Continental Building, Dallas 1, Texas, and will be considered for publication in the Transactions volume *Petroleum Development and Technology*. Discussion will close December 15, 1949. Any discussion offered thereafter should be in the form of a new paper.

T.P. 2578

GAS HYDRATES OF CARBON DIOXIDE-METHANE MIXTURES

CARL H. UNRUH, C. F. BRAUN AND COMPANY, ALHAMBRA, CALIFORNIA

DONALD L. KATZ, MEMBER AIME, UNIVERSITY OF MICHIGAN

ABSTRACT

Experimental data are presented for hydrate formation conditions for gas mixtures of carbon dioxide and methane. Equilibrium constants for carbon dioxide, defined as the mole fraction of carbon dioxide in the gas phase (dry basis) divided by the mole fraction of carbon dioxide in the hydrate (dry basis), were calculated using the equilibrium constants for methane developed in an earlier paper.

INTRODUCTION

A series of papers have been written on gas hydrates, giving temperatures and pressures at which hydrates would form.^{2, 3, 4, 5, 6, 9, 12, 13, 15} Vapor-solid equilibrium constants have been developed for methane, ethane, propane and iso-butane¹ by which it is possible to compute for a specific gas mixture the temperature and pressure at which hydrates will form.

Carbon dioxide is present in many natural gases in concentrations usually from 0.1 to 2.0 per cent. It also forms a gas hydrate with water and presumably enters the solid solution when present with a natural gas which is forming a hydrate. The equilibrium constant giving the ratio of the concentration of carbon dioxide in the gas phase to the concentration in the solid phase is required for including the effect of the carbon dioxide when computing the conditions for hydrate formation.

Direct determination of the concentration of carbon dioxide in solid hydrate requires a difficult separation to be made. Therefore, this research resorted to the measurement of the temperature and pressure at which specific mixtures of methane and carbon dioxide

would form hydrates. From the equilibrium constants previously mentioned for methane, it is possible to compute the equilibrium constant for carbon dioxide, without measurement of the composition of the solid phase.

Fig. 1 shows the conditions at which methane and carbon dioxide form hydrates. The methane curve FG extends to some high pressure while the carbon dioxide curve AB intersects the vapor-liquid water-liquid carbon dioxide

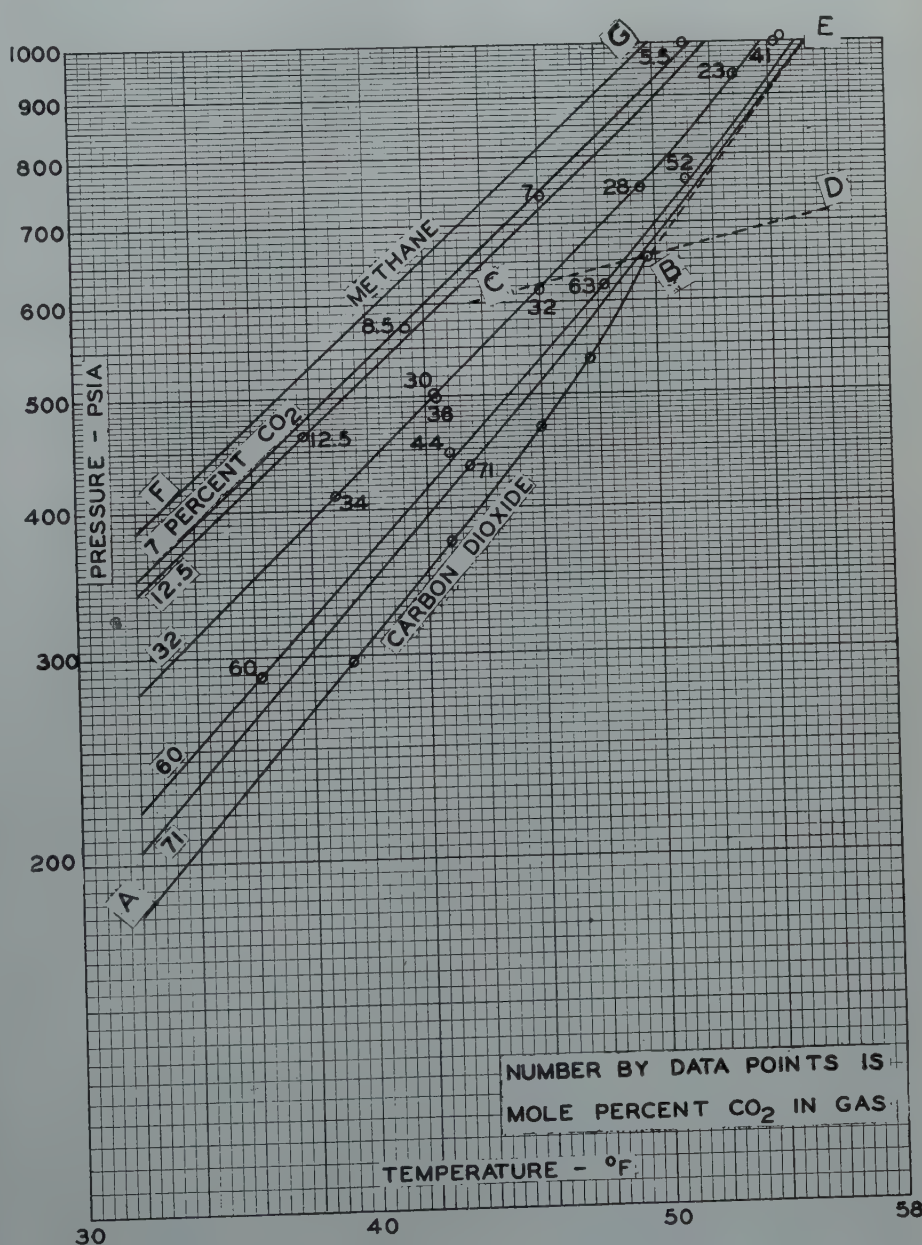


FIG. 1—HYDRATE FORMATION CONDITIONS.

Manuscript received at office of the Petroleum Branch July 22, 1948. Paper presented at the Branch Fall Meeting, Dallas, Texas, Oct. 4-6, 1948.

¹References are given at end of the paper.

(V-L₁-L₂) curve CD at B, the quadruple point. Curve BE is the locus of conditions at which four phases exist.

EXPERIMENTAL PROCEDURE

The apparatus used was similar to that described by previous investigators^{3, 15} with the addition of two gas mixing cells.

These two cells were used to meter carbon dioxide and methane separately by mercury displacement. The amount of each gas added was calculated from the quantity of mercury displaced, the pressure and temperature, and available compressibility factors for methane¹¹ and carbon dioxide^{7, 11}.

The gases were then pumped back and forth from one cell to the other several times. The gas was allowed to remain in one of the cells each time for twenty or thirty minutes to permit mixing. This gas mixture was introduced into the hydrate cell.

The hydrate cell had glass windows and was immersed in a constant temperature water bath. The cell could be rotated through an angle of 30° from the horizontal to agitate its contents. The cell was illuminated by means of an electric light bulb placed inside a large glass tube which was immersed in the constant temperature bath.

The hydrate cell was filled with distilled water by means of a pump. The gas mixture was then introduced into the cell, allowing about half the water in the cell to be displaced by the gas. The bath was then cooled by addition of ice to 32° to 33°F. or to 5° or 6°F. below the temperature for hydrate formation. The cell was then agitated until hydrate began to form. As the hydrate formed the pressure observed by a Bourdon gage decreased slowly. The bath temperature was then increased until the hydrate began to melt and the pressure began to rise. The bath was then heated slowly until almost all of the hydrate had disappeared. At this point the hydrate was present as small flakes distributed throughout the liquid phase. The bath temperature was then reduced several tenths of a degree so that hydrate would just begin to form again. The cell, with continuous rocking, was kept at a constant bath temperature and pressure readings were taken every five minutes until no no-

ticeable change in pressure occurred. The pressure and temperature readings were then recorded as the hydrate formation conditions for the composition of the gas in the gas phase. The pressure in the cell was then increased by addition of water by means of a pump, and the procedure was repeated. In this manner three or four points could be obtained for each gas sample.

This procedure made it necessary to calculate the composition of the gas phase. Solubility data for pure carbon dioxide in water¹⁴ and for natural gas in water⁸ are available in the literature. These data were extrapolated to the temperature range involved and calculations were made by a trial and error method. A gas composition was assumed and the quantities of each component in the liquid and in the gas

phases were calculated. The total gas composition was thus found. If it did not agree with the composition of gas charged to the cell, another assumption of gas composition was made and the calculation was repeated.

HYDRATE BEHAVIOR

Hydrates of pure carbon dioxide exhibited some characteristics different from those of the gas mixtures. Much more difficulty was experienced in getting the pure carbon dioxide to form hydrates than for the mixture. An effective method of getting hydrates to form in a sub-cooled mixture was to lower the pressure suddenly about fifty pounds. The carbon dioxide hydrate formed exceedingly fast and uniformly throughout the water phase. In a few seconds what had been the liquid phase

TABLE I
PHASE EQUILIBRIUM DATA
FOR CARBON DIOXIDE-METHANE-WATER SYSTEM
A. Conditions for Hydrate Formation with Carbon Dioxide-Methane-Water Mixtures.

Run	Point	Temp., °F.	Press., psia	Mole % CO ₂ in Charge	Calc. Mole % CO ₂ in Gas Phase	Vol. Gas Phase cc.	Vol. Liq. Phase cc.
1.....	1	38.9	412	53.9	34	47	47
	2	42.3	502		30	38	56
2.....	1	42.4	498	54.5	36	47	47
	2	46.0	615		32	38	56
	3	49.5	750		28	28	66
	4	52.8	938		23	20	74
3.....	1	36.2	289	77.7	60	42	52
	2	42.8	447		44	20	74
4.....	1	37.8	464	27.4	12.5	42	52
	2	41.4	573		8.5	28	66
	3	46.1	740		7	21	73
	4	51.1	1,000		5.5	15	79
5.....	1	43.5	435	82.4	71	47	47
	2	48.2	620		63	28	66
	3	51.1	765		52	15	79
	4	54.2	1,000		41	8.5	85.5
	5	54.5	1,015		41	8.5	85.5

B. Conditions for Hydrate Formation with Carbon Dioxide-Water Mixtures.

Temp., °F.	Press., psia
39.3	296
42.8	375
45.9	468
47.7	535
49.8	653 (Quadruple Point)

C. Vapor Pressure Data for Water-Rich Liquid, Carbon Dioxide-Rich Liquid, and Vapor

Temp., °F.	Press., psia	Temp., °F.	Press., psia
60.0	750	53.9	693
58.2	735	48.1	639
53.8	692	43.9	604

appeared to be completely solid even though a large excess of water was present. Apparently, the water was trapped in the honeycomb of crystalline hydrate. The pressure did not drop immediately, indicating that the hydrate had formed from the carbon dioxide in solution; but if the bath were not heated immediately, the pressure would drop fifty to seventy-five pounds in twenty or thirty minutes. As the bath was heated and the hydrate began to melt, the pressure would increase again.

The hydrate obtained from the mixture of carbon dioxide and methane formed much more slowly and appeared to be more of a surface phenomena. It would take, perhaps, twenty minutes for the pressure to drop fifty pounds. The hydrate formed in small flakes which resulted in a "slushy" liquid in the cell. As the bath temperature was increased, the pressure rose again. When almost all of the hydrate was melted, the flakes of hydrate would adhere to the glass and glisten so that there was no doubt about hydrate being present.

The hydrate of carbon dioxide is apparently less dense than water because it tended to accumulate at the surface of the water as it was melting from the original solid mass. At the quadruple point much of it would remain at the interface between the water-rich phase and the even less dense carbon dioxide-rich phase. The mixed gas hydrate was generally in the form of flakes and remained distributed throughout the liquid phase.

The methane used in the experiments (minimum purity of 99.0%) was supplied by the Phillips Petroleum Company. The carbon dioxide (estimated purity of 99.5%) was obtained from Pure Carbonic, Inc.

EXPERIMENTAL RESULTS

Data were first taken for hydrates of pure carbon dioxide in order to perfect the experimental technique. Results are given in Table 1(B). They agree very well with the data of Deaton and Frost⁵. The quadruple point, i.e., four phases present, was observed to occur at 49.8°F. and 653 psia. Vapor pressure data were also taken for the system, L_1 - L_2 -V, and are given in Table 1(C). A comparison of these values

with the vapor pressure of pure carbon dioxide as reported in the literature¹⁰ indicates that the pressure of the three phase water-carbon dioxide system is about three pounds higher than that of pure carbon dioxide. However, this may not be significant considering the accuracy of calibrating and reading the pressure gauge.

Hydrate formation conditions for mixtures of carbon dioxide and methane are given in Table 1(A) and on Fig. 1. From these data lines for various compositions were estimated and drawn in. These lines are cross plotted in Fig. 2.

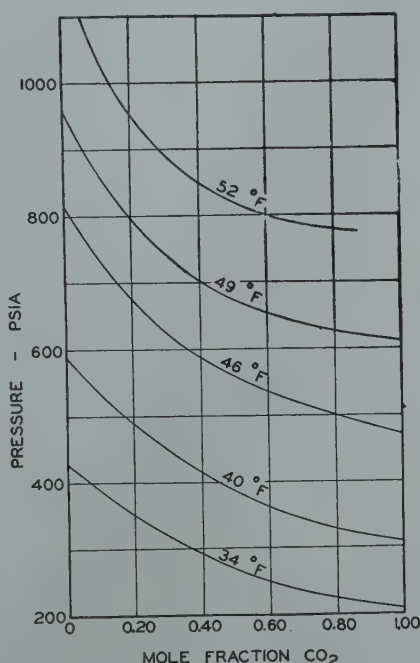


FIG. 2—HYDRATE FORMATION CONDITIONS FOR CO_2 - CH_4 MIXTURES.

EQUILIBRIUM CONSTANTS

Equilibrium constants, defined as the mole fraction of carbon dioxide in the vapor (dry basis) divided by the mole fraction of carbon dioxide in the hydrate (dry basis), were calculated and are plotted in Fig. 3. They were calculated using equilibrium constants for methane proposed by Carson and Katz¹. The hydrate formation conditions which were observed correspond to the dew point in vapor-liquid equilibrium so that $\sum x = \sum \frac{y}{K} = 1.0$, where x and y are the mole fractions of a component in the solid phase and vapor phase re-

spectively (both on a dry basis). Since the composition of the vapor phase and the equilibrium constants for methane were known, the equilibrium constants for carbon dioxide could be calculated.

To obtain equilibrium constants for carbon dioxide at values above 1.0, it is necessary to have data for a system in which carbon dioxide was the more volatile component. The curve for pure ethane lies at pressures below that for carbon dioxide. It was assumed that a plot of pressure versus mole fraction between CO_2 and ethane was similar to that for CO_2 and methane. This plot and the ethane equilibrium constants were used as a guide in the extrapolation of the CO_2 constants above unity.

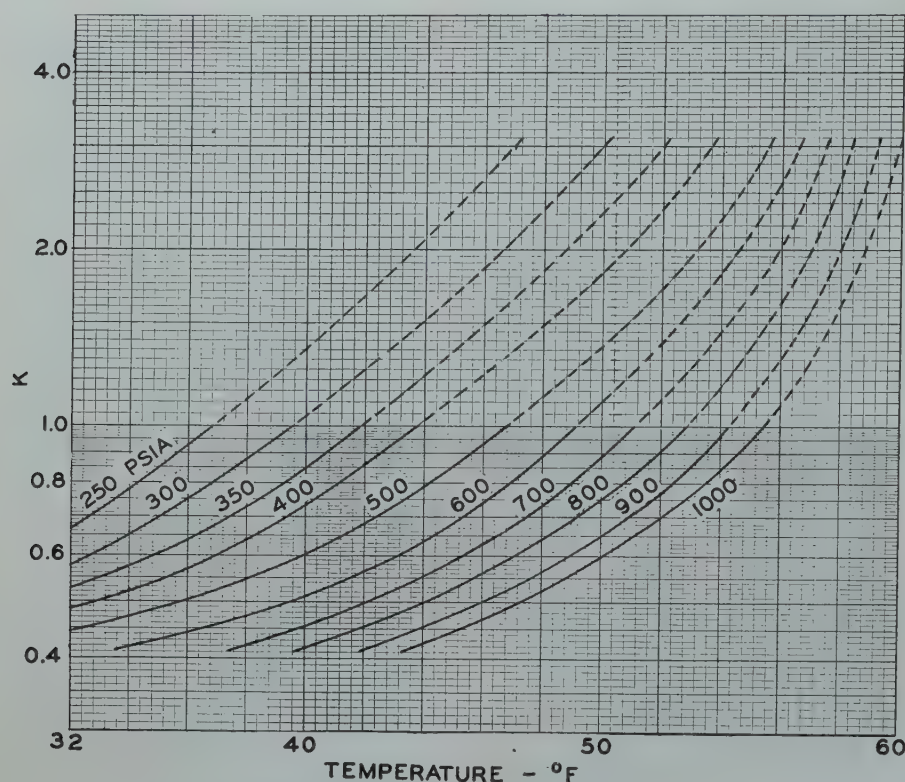
The hydrate equilibrium constants for carbon dioxide on Fig. 3 may be used along with the charts for the hydrocarbons¹ when computing the hydrate formation conditions of a natural gas containing carbon dioxide.

ACKNOWLEDGMENT

The previous work and observations on this subject by Mr. Eric R. Kent were of considerable help. The supply of pure methane by the Phillips Petroleum Company was appreciated.

REFERENCES

1. Carson, D. B., and Katz, D. L., *AIME Trans.*, **146**, 150-8 (1942).
2. Chinworth, H. E., and Katz, D. L., *Refr. Eng.*, **54**, 359-62 (1947).
3. Deaton, W. M., and Frost, E. M., *Am. Gas Assoc., Nat. Gas Dept., Proc.*, 23-31 (1937).
4. Deaton, W. M., and Frost, E. M., *Ibid.*, 112-9 (1938).
5. Deaton, W. M., and Frost, E. M., *Ibid.*, 122-8 (1940).
6. Deaton, W. M., and Frost, E. M., *Oil & Gas Jnl.*, **45**, No. 12, 170-8 (1946).
7. Demming, W. E., and Demming, L. S., *Phy. Rev.*, **56**, 108-12 (1939).
8. Dodson, C. R., and Standing, M. B., *Drilling and Production Practice (A.P.I.)*, pp. 173-79 (1944).
9. Hammerschmidt, E. G., *Ind. Eng. Chem.*, **26**, 851-5 (1934).
10. Meyers, C. H., and Van Dusen,

FIG. 3—HYDRATE EQUILIBRIUM CONSTANTS FOR CO₂

- M. S., *Bur. Standards, J. Research*, **10**, 381-412 (1933).
11. Reamer, H. H., Olds, R. H., Sage, B. H., and Lacy, W. N., *Ind. Eng. Chem.*, **36**, 88-90 (1944).
 12. Roberts, O. L., Brownscombe, E. R., and Howe, L. S., *Oil & Gas Jnl.*, **39**, No. 30, 37 (1940).
 13. Schroeder, F., in Ahrens' *Sammlung chemischer und chemischer-technischer Vorträge*, **29**, 1-98 (1927).
 14. Wiebe, R., and Gaddy, V. L., *J. Am. Chem. Soc.*, **62**, 815-7 (1940).
 15. Wilcox, W. I., Carson, D. B., and Katz, D. L., *Ind. Eng. Chem.*, **33**, 662-5 (1941).

☆

DISCUSSION

By Michael J. Rzasa, Stanolind Oil & Gas Co., Tulsa, Oklahoma

Unruh and Katz have extended our

knowledge of hydrates and hydrate-forming conditions by investigating the effects of a non-hydrocarbon component in a binary system. The presence of carbon dioxide in variable concentrations in many natural gases should be taken into account in prediction of hydrate forming conditions in the same way that its presence should be considered when dealing with vapor-liquid equilibria.

Many natural gases contain nitrogen, sometimes in concentrations up to 30 per cent. There does not seem to be complete agreement on whether or not nitrogen forms hydrates with water. I am familiar with a patent granted for the purpose of storing natural gas in hydrate form, in which it is stated that such so-called "permanent" gases as H₂S, CO₂, H₂, O₂, and N₂ do not form

hydrates. Actually, the hydrates of CO₂ and H₂S had been investigated as early as 1882 by de Forcrand and Villard². In 1902, de Forcrand summarized known information on gas hydrates in which nitrogen was included as a hydrate with the composition of N₂:4 or 5 H₂O. The above anomaly would seem to point to the need of investigating the possibilities of the existence of nitrogen hydrates and the conditions under which these hydrates may form. The effect of nitrogen on natural gas hydrate- may form. The effect of nitrogen on natural gas hydrate-formation could then be included.

The authors have obtained the gas phase by trial and error computations using extrapolated data for the solubility of carbon dioxide and natural gas in water. The possible errors inherent in the extrapolation process, together with the effect of mutual solubility of the two substances, might result in calculated compositions quite different from experimental. It is realized that analysis of the hydrate is a difficult process, but I would like to ask Katz about his estimate of the possible error involved in the above procedure.

A third point for discussion involves equilibrium constants for the carbon dioxide hydrate which were obtained by using the methane equilibrium constants proposed by Carson and Katz in a previous paper. The methane constants were computed from natural gas hydrates and as a result, might be quite different from the constants for methane in a hydrate system composed of one hydrocarbon and one non-hydrocarbon. For lack of experimental data on the actual composition of the carbon dioxide-methane hydrate, the procedure outlined by the authors is the best available, but it must be recognized that the results may have to be modified with further investigations. ★ ★ ★

GULF OF MEXICO FLOATING DRILLING TENDER

C. P. BESSE AND G. W. OSBORNE, THE CALIFORNIA COMPANY, NEW ORLEANS, LOUISIANA

Drilling operations on the Gulf of Mexico continental shelf are following two general plans. The first plan placed all buildings, equipment, and materials on a large platform while the second copies Lake Maracaibo drilling methods by placing a minimum of equipment on the platform and using a floating drilling tender or drill barge anchored adjacent to the platform in an attempt to take maximum advantage of flotation in an effort to reduce costs.

A complete power rig, mud pits, pipe racks, and small auxiliaries have been placed on the platform as shown in Figure 1, to assure proper handling of drilling operations under the most adverse weather. This has the economic advantages of eliminating the fabrication of a large structure, a material reduction of rigging up time on each structure, and elimination of delay time on equipment while quarters and equipment placed on the tender are being rigged up. These factors have certainly proved their economic value in drill barge operations in the Louisiana and Texas coastal area.

Naturally the heart of such an operation is the anchorage. This anchorage, to permit taking advantage of maximum economies, must hold the ship in a relatively fixed position under the following weather conditions:

- (1) Winter northwesters
- (2) Southeasterly gales
- (3) Severe rain squalls

In hurricane weather all operations must be suspended regardless of method of operation and the floating tender will, if possible, be moved to a protected location. However, in case of an emergency the floating tender should be prepared to swing with the wind and

seas on a single anchor as there is considerable doubt that either ship or anchorage could withstand the severe strains imposed by fixed anchorage in hurricane weather.

Northwesters are reported to have developed wind gust velocities as high as sixty miles per hour and steady winds of approximately forty-five miles per hour. Fortunately these winds do not travel a great distance over water before arriving at our location, and, while they can possibly develop seas approximately eight feet high, the waves are short, and if taken on the bow or stern of a ship 250 feet or more in length they should not present a difficult problem.

On the other hand southeast gales having a long fetch and maximum steady wind velocities of approximately

thirty miles per hour can possibly develop long swells approximately twelve feet in height. These should develop the most severe anchorage problem. To combat these waves any workable anchorage plan should permit maneuvering the ship in such a manner as to head the bow or the stern into the seas and still maintain contact with the structure.

Rain squalls develop wind gust velocities as great as sixty miles per hour. However, they are local and the seas have not been a source of great trouble. To permit continuous operation the anchorage must be able to withstand these winds broadside to the ship as the wind direction often changes radically in a very short time.

All of these weather conditions are dangerous to small craft, deck cargoes,

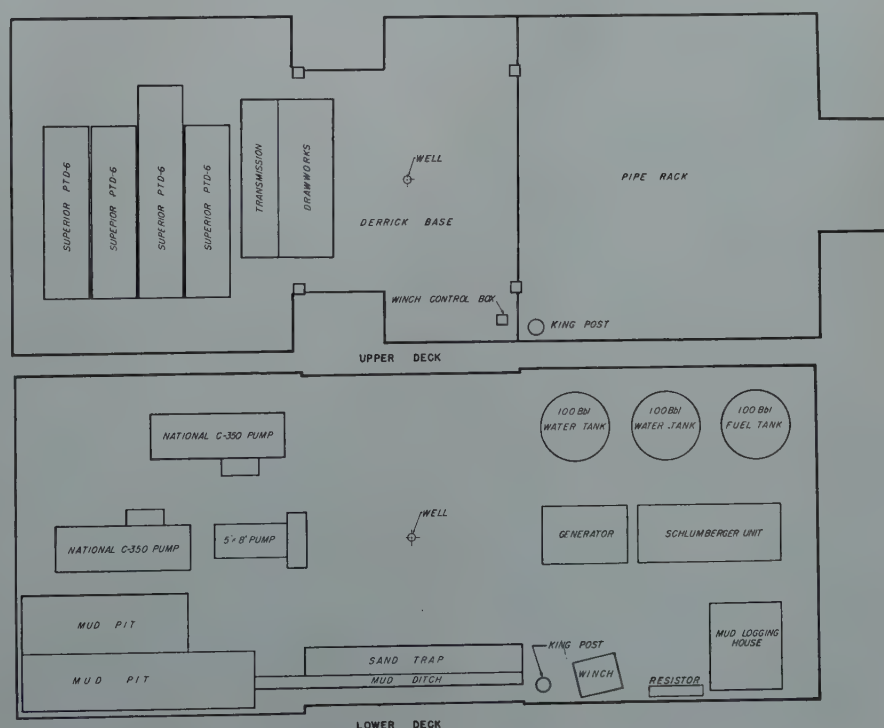


FIG. 1 — LAYOUT OF UPPER DECK AND LOWER DECKS OF DRILLING PLATFORM.

Manuscript received at the Petroleum Branch office September 1, 1948. Paper presented at Branch Fall Meeting, Dallas, Texas, October 4-6, 1948.

and improperly anchored barges. However, the objective of the drilling tender method is to develop an anchorage which will permit continuous operation under these weather conditions with the minimum amount of equipment placed on the platform.

As stated earlier it is our opinion that a ship less than 250 feet in length will have considerable difficulty in maintaining anchorage in the heavier northwester and southeast gales. This fact, coupled with cargo requirements of 2000 to 2500 tons for wildcat wells, limited selection to two war surplus items, Navy YF barges and L.S.T.'s. The latter was selected because of its structural strength, ability to ride heavy seas, greater cargo capacity, availability, and the possibility of self-propulsion. However, the YF barge, among others, has the advantage of shallow draft which will help on locations close to shore.

To accomplish the above objective of continuous operation under all except hurricane weather the mooring must be designed to permit the ship to rise and fall with the waves and to prevent impact loading of the moorings as a result of surging of the ship. No conceivable mooring can hope to withstand the forces imposed by a relatively fixed anchorage if these two requirements are not accomplished. The conditions can be obtained by the use of constant tension mooring winches or by the use of heavy anchor chains. The constant tension mooring winch can be set to maintain a predetermined tension and to pay out line to overcome impact loads in excess of the set tension. Paid out cable is recovered after the severe strain is relieved and the ship is thereby returned to its original position. Heavy anchor chain accomplishes an increasing load and flexibility by lengthening the catenary of the anchor chains suspended in the water. This permits movement and imposes a heavy load which moves the ship back to its original position. If an initial force of reasonable magnitude is applied to either method, impact loading due to surge should be prevented. The magnitude of this force will have to be determined for individual ships and anchorage locations.

After a careful study by a firm of consulting naval architects, 2 1/16" stud link anchor chain was selected as

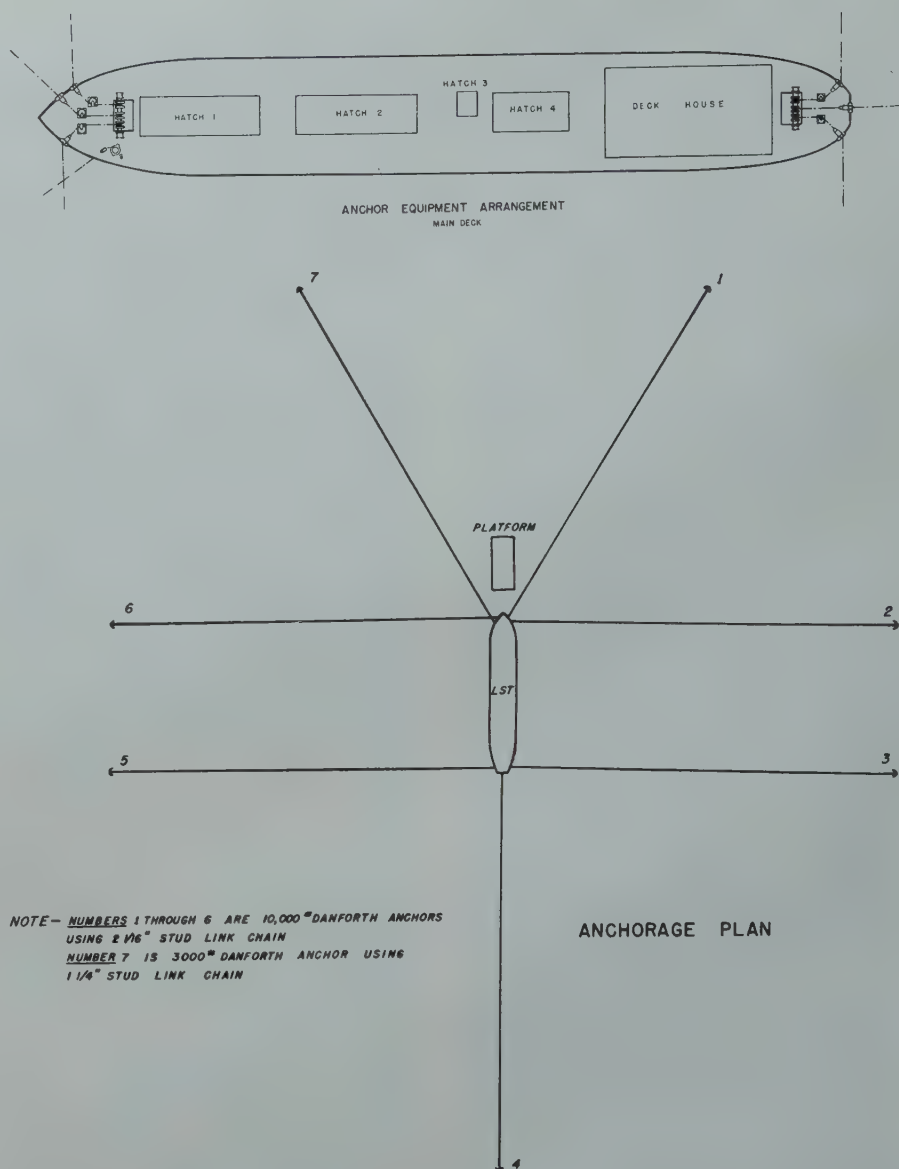


FIG. 2— LOCATION OF ANCHOR WINDLASSES AND POSITION OF ANCHORS.

being the more positive and less subject to mechanical breakdown. These chains, having an ultimate strength of 341,000 pounds, are stowed in chain lockers and handled by two anchor chain windlasses capable of developing a pull of 120,000 pounds. Each of these windlasses is equipped to handle three chains as shown in Figure 2. The windlass power can be applied to any or all of the chains at one time and each wildcat sheave is equipped with a brake capable of holding 200,000 pounds. In addition to the brake a chain stopped capable of developing the braking strength of the chain is installed on the deck for use after the ship is positioned. The bow chains are ten shots or 900 feet long and the stern chains are twelve

shots or 1,080 feet long. The longer stern lines were installed to permit maneuvering the ship to take heavy seas on bow or stern. In addition to these six anchor lines the ship's twelve shot or 1,080 feet long 1 1/4" anchor chain is used. This line is employed to help balance the bow mooring as the ship is directed toward the structure as shown in Figure 2. To facilitate breaking away from the moorings when a hurricane is approaching, the bitter ends of the chain may be disconnected from the ship.

In conducting these studies wind gust velocities were disregarded as they are of too short duration to overcome the inertia of the ship's mass and transmit forces to the chains and anchors. A

wind load coefficient of .0038 was selected as being a relatively conservative one for the calculation of wind loads on the side of the ship. With an average light draft of ten feet, the total exposed area of deck house and main hull above the water line is approximately 6,510 sq. ft. As this area will not be distributed equally between fore and aft anchor lines with a broadside wind, calculations are based on the assumption that the maximum area attributable to one anchor will be four thousand sq. ft. In addition to direct wind load an allowance of 25% of the total wind load has been made to account for current and surge effect on the anchorage. This was added in accordance with the practice employed by the Navy in the mooring of floating dry-docks in relatively open harbors. Under these circumstances the force imposed on one broadside anchor is as follows:

For a wind velocity of 50 mph the forces are:

Wind load on one broadside anchor:

.0038x4000x50 ²	38,000 lbs.
25% allowance for current and surge	9,500 lbs.
Total	47,500 lbs.

For a wind velocity of 70 mph the forces are:

Wind load on one broadside anchor:

.0038x4000x70 ²	74,480 lbs.
25% allowance for current and surge	13,620 lbs.
Total	88,100 lbs.

Another force of unknown magnitude is imposed by the waves. There is no accepted theory or empirical formula for the calculation of wave forces on a moored object. This fact occasioned a decision to keep the ship oriented to receive heavy seas on either bow or stern, thereby exposing a minimum area. To facilitate handling the ship under very difficult circumstances anchor windlass specifications require a maximum line pull of not less than 120,000 pounds.

In selecting an anchor to use in this mooring plan concrete blocks, pile anchors, Navy stockless anchors, mushroom anchors, and patented anchors were considered. For holding power and ease of use 10,000 pound patented an-

chors were selected. However, to insure against the doubtful and unknown factors involved, pile anchors were installed to back up the patented anchors in the three stern positions in Figure 2. These pile anchors consisted of sixty foot long 14" H-beams driven ten feet below the ocean bed with a length of 2 1/16" stud link anchor chain attached to the patented anchors with approximately ninety feet of slack to permit complete failure of the patented anchors before the pile anchor starts to function. Of course, the holding capacity of anchors varies with the soil characteristics and these vary over wide ranges as indicated by piling penetrations requires at the three locations on Figure 3. To carry identical loads, these penetrations were:

Location No. 1 — 243 feet

Location No. 2 — 196 feet

Location No. 3 — 137 feet.

meager; however, the following general information may be of value. At Location No. 2, Figure 3, one anchor was pulled to the ship in the process of mooring. When this anchor was placed a second time it held; and when the ship was moved after completion of the well, the full power of the anchor windlass applied to individual 10,000-pound patented anchors could not move them. This fact proves a holding capacity of over 120,000 pounds. In an effort to retrieve the 3,000-pound patented anchor, used on the ship's anchor windlass, the three wildcat windlass was secured to it and a sufficient load applied to part a link in the 1 1/4" chain which has a breaking strength of 129,000 pounds. This indicates a holding power of approximately forty pounds per pound of anchor.

Unfortunately, this condition does not exist at Location No. 1, Figure 3. Soil



FIG. 3 — AREA LOCATION MAP

Equipment is being assembled to conduct anchor holding and chain loading tests and to accumulate data on anchorage forces under various weather conditions. This equipment consists of a calibrated test link equipped with an SR-4 strain gauge, and necessary devil's claws to conveniently install the test link.

As the tests mentioned above have not been conducted, anchorage data is very

samples taken for foundation purposes show a very soft clay to a depth of forty feet below the Gulf bottom. In view of this poor soil quality an attempt was made to determine anchor holding capacities by laboratory tests of soil samples and field tests with a twelve-pound patented anchor. The anchor manufacturer conducted Jurgeson squeeze shear tests on undisturbed soil samples and correlated these with the results of load

tests on 10,000-pound patented anchors in soils of known Jurgeson shear values. The results of these tests were as follows:

Penetration into Gulf bottom	Jurgeson Squeeze Shearing Strength	Probable holding power 10,000-lb. anchor
10 ft.	52 lbs.	55,000 lbs.
30 ft.	116 lbs.	120,000 lbs.
50 ft.	232 lbs.	200,000 lbs.
80 ft.	522 lbs.	300,000 lbs.

These values for probable holding power are not based on reliable data as clay and organic matter content enter into holding power and data available are not sufficient to give more than a rough comparison of soil characteristics. Accurate correlation of soil data is very difficult, if not impossible; therefore, data of the type given above should be considered only as an indication of general conditions. Changes in soil characteristics over a short distance further complicate the problem.

Tests with the twelve-pound anchor were correlated with other available data by the manufacturer to give an estimated holding power of 40,000 pounds for a 10,000-pound anchor. This estimate is also very rough and is therefore considered a good correlation with the 55,000 pounds estimated for a penetration of ten feet by the Jurgeson shear test.

Experience while mooring at this location tended to verify this data as we had no difficulty moving the anchors with the windlasses. Later tests indicate that the anchors have settled to a greater depth and this combined with a consolidation or settling up of the soil around the anchor has increased the holding capacity. We have experienced difficulty in maneuvering the ship or holding it against severe rain squalls. No heavy seas were encountered at this location while the ship was moored.

The capacities indicated at Location No. 1 are not considered satisfactory. However, soil characteristics at this location are very exceptional, even for the Gulf of Mexico Continental shelf. For a comparison with other locations soil analyses indicate no soil shear value which can be interpreted by standard foundation laboratory analyses in the first thirty feet of depth and an average soil shear value for the section from thirty to sixty feet of fifty-nine pounds per square foot. This compares to an average shear value of 112 pounds

of soil penetrated at Location No. 2 and an average shear value of 274 pounds per square foot for the first thirty feet of soil penetrated at Location No. 3. The shear values established for foundation purposes were determined by standard compression cohesion tests and the writer has made no attempt to correlate them with the Jurgeson squeeze shear tests.

This data, though sketchy and incomplete, does indicate that anchor holding capacities of reasonable proportions can be developed at Locations Nos. 2 and 3.

The choice of a method for handling dry cargo was another problem that this operation presented. Casing, tubing, drill pipe, well head equipment, dry mud, and cement were the main items of dry cargo which required handling. The dry cargo had to be handled as follows:

1. From the dock to the drilling tender.
2. From the drilling tender to the drilling platform.
3. From barges or boats to the drilling tender.

The gear had to be capable of delivering casing from the drill tender to the platform as fast as the casing can be run into the well.

After carefully checking possible methods, the ordinary ship method of burtoning was selected for the handling of dry cargo. Burtoning is a term used to describe the handling of cargo with two or three booms rigged so that the top of one boom is fixed over the pick-up point and the top of another boom is fixed over the discharge point. The end of the load lines from each of the booms are attached to a common hook. With this arrangement, it is possible to pick up a load vertically under the point of one boom and by hauling in and paying out load lines to set the load down under the point of a second boom. The hook is returned to the loading point by reversing this procedure.

The booms were located as shown on Figure 4. The chief consideration in locating the booms was to arrange them so that all hatches could be reached with a minimum number of standard size booms. You will note that the booms are set off the centerline of the vessel to permit fore and aft burtoning as

well as thwartship burtoning. In addition to the ship's booms a single boom was placed on the platform.

The booms were designed for a five-ton load and are fifty-five feet long. The masts or king posts are approximately forty-eight feet high. The cargo winches are rated at a 14,400 lb. line pull at 110 feet per minute, and driven by a 50 h.p. D.C. electric motor.

Burtoning has proved satisfactory in all respects.

The space on the third deck level, aft of the pipe stowage was selected for locating a 7 $\frac{3}{4}$ "x18" mud pump, a 5"x8" mud pump, and skid mounted cementing unit. The mud pumps and cementing unit are powered by separate Diesel engines. Four of the third deck wing compartments, which are 10'x24'x6'-6" in dimension were utilized for mud pits. A sand trap was mounted in a second deck wing compartment directly over one of the mud pits. Mud was mixed and conditioned on the ship and either pumped to the pits on the platform or directly to the well.

A forty foot long personnel bridge connects the ship and platform. It is hinged on the bow of the vessel so that it is free to move both horizontally and vertically. The other end of the bridge is supported by a trolley attached to an I-beam located under the top deck of the platform. A 15' wide by 12' long hinged ramp extends out from the lower deck of the platform and under the bridge. Hence the bridge is free to move a maximum of twelve feet without destroying the connection between ship and platform.

Liquids are transferred from the ship to platform by means of hose connections. Each hose is approximately 120 feet long. The hose is attached at the bow of the ship to the ship's pipe lines with quick release couplings. The hose extends down into the water, to the ocean floor, and up to the platform where it is coupled into the pipe lines. Hoses are provided for liquid mud, fresh water, salt water, fuel oil, and cement. The hose connections allow a generous movement of the ship without interference to the transferring of liquids.

Power, telephone, and radio cables also extend from the ship to the platform and are rigged similar to the hoses, so that they do not interfere with

a reasonable ship's movement, and so that they can be quickly released.

Quarters are provided on the main deck and second deck for personnel. These quarters consist of eighteen rooms and a dormitory. Each room is equipped to quarter two men and the dormitory has twelve berths. The regular crew is housed in the rooms. Extra labor and service personnel are housed in the dormitory.

Galley and messing facilities are located on the Main Deck. The mess room is equipped with six four-person tables. The method of serving the food is decided upon by the tool pusher in charge. Cafeteria style is the method in use at present.

The communication system is a very important factor in successful operation of the unit. It is possible to talk from the platform to men in the following locations on the tender: mud pumps, cementing unit, generator room, boiler room, forward and stern anchor windlasses, and the office. In addition to this communication system within the drilling unit, two radio communication systems were provided. The principal

radio communication system is frequency modulated and provides communication between boats, land base, and the District Office. The second system consists of an amplitude modulated marine radio telephone equipped with channels for Coast Guard, ship to ship, and marine telephone communication. This dual system has been found to be of considerable value due to the lack of complete reliability of radio equipment in the most difficult emergencies.

With the above decisions made, the problem resolved into one of placing equipment, supplies, and personnel on the ship. Figure 4 gives a detailed layout of the arrangement selected. The following materials were loaded on the floating tender for the drilling of the first well:

MUD AND CHEMICALS

4,000 sacks weight materials
136 sacks quebracho
225 100-lb. drums caustic soda
800 50-lb. sacks of lime
600 sacks of drilling clay
600 50-lb. sacks of starch
300 sacks of Kembreak

800 sacks bentonite drilling clay
100 sacks soda ash
100 sacks cellophane flake

DRILL PIPE

415 joints 4½" drill pipe

CEMENT

1,200 sacks slow set cement
1,500 sacks portland cement
1,500 sacks high early strength cement

WELL PIPE

10 joints 16" casing
75 joints 10¾" casing
230 joints 7" 26-lb. N-80 casing
94 joints 7" 29-lb. N-80 casing
69 joints 7" 32-lb. N-80 casing
490 joints 2½" EUE tubing

LIQUID CARGO

225,000 gallons fresh water
170,000 gallons Diesel fuel
40 drums lube oil
and also miscellaneous supplies required for drilling operation.

During the drilling of our first well the crew requirements averaged thirty-five men. The thirty-five men were composed of the following:

- 1 Tool pusher
- 2 Drillers
- 12 Roughnecks
- 2 Electricians
- 2 Engineers
- 3 Able Bodied Seamen
- 2 Ship's roughnecks
- 7 Steward's Department
- Roustabouts as needed

The crew worked twelve-hour tours, two weeks on and one week off, with the exception of the able bodied seamen who worked eight-hour tours, two weeks on and one week off.

In the drilling of our first two wells we did not lose a single day due to bad weather. However, we did find several periods of twenty-four hours or less when seas were too rough to permit handling drill pipe and dry cargo from ship to platform. Even this most severe weather did not interfere with safe use of the personnel bridge or other communications. While we probably have not operated in the most severe weather, present experience has proved the operation successful. ★ ★ ★

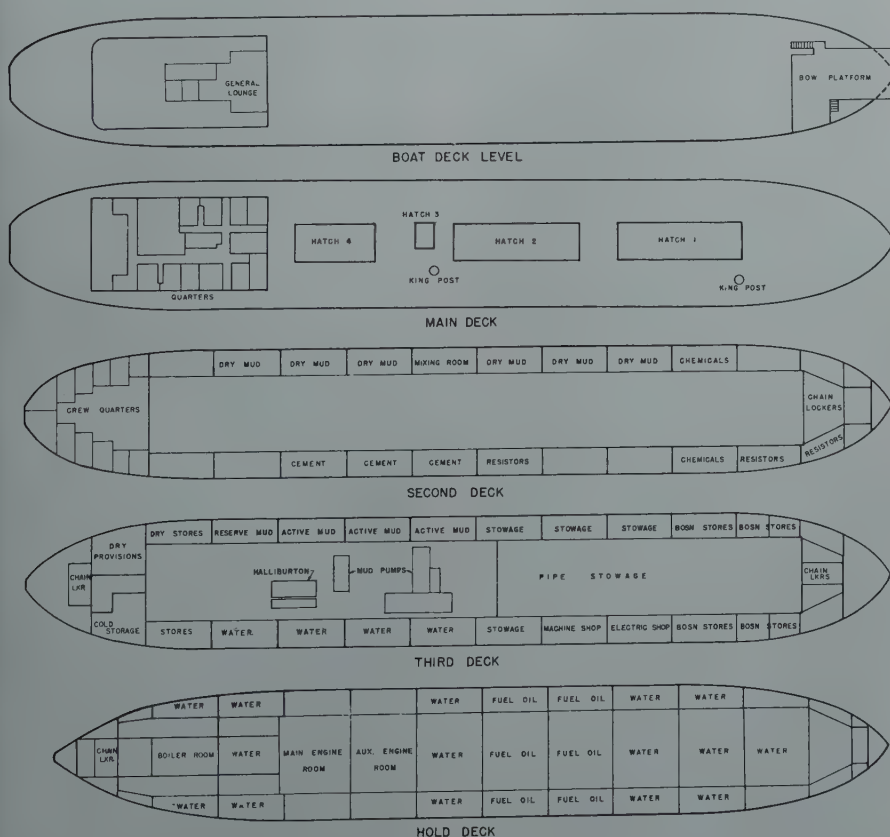


FIG. 4 — LST ARRANGEMENT PLANS FROM BOAT DECK TO HOLD.

ESTIMATION OF RESERVES AND WATER DRIVE FROM PRESSURE AND PRODUCTION HISTORY

E. R. BROWNSCOMBE, MEMBER AIME, AND FRANCIS COLLINS, JUNIOR MEMBER AIME
THE ATLANTIC REFINING COMPANY, DALLAS, TEXAS

ABSTRACT

A study has been made of the material balance-fluid flow method of estimating reserves and degree of water drive from pressure and production history data. By considering the effect of random pressure errors it is shown that in a particular example a standard deviation of three and one-half pounds in each of ten pressure surveys permits the determination of the reserves with a standard deviation of 8 per cent and the water drive with a standard deviation of 15 per cent, assuming that certain basic geologic data are correct. It is believed that this method of estimating reserves and water drive is useful and reliable in a number of cases. The method is particularly valuable when reservoir pressure data are accurate within a very few pounds, but may also be applied with less accurate pressure data if a relatively large reservoir pressure decline occurs early in the life of the field, as for example in an undersaturated oil field.

INTRODUCTION

A knowledge of the magnitude of reserves and degree of water drive present in any newly discovered petroleum reservoir is necessary to early application of proper production practices. A number of investigators have contributed to methods of relating reserves, degree of water drive, and production and pressure history.¹⁻⁸ Three types of problems of increasing complexity may be mentioned. If a reservoir is known to have no water drive, and if the ratio of the volume of the reservoir occupied by gas to the volume of the reservoir occupied by oil (which ratio permits

fixing the overall compressibility of the reservoir) is known, then only one further extensive reservoir property remains to be determined, namely the magnitude of the reserves. A straightforward application of material balance considerations will permit this determination.^{1,6,7} The problem becomes very much more difficult if we wish to determine not only the magnitude of the reserves but also the magnitude of water drive, if any, which is present. In principle, a combination of material balance and fluid flow considerations will permit this evaluation. Finally, if neither the magnitude of reserves, the degree of water drive, nor the ratio of oil to gas present in the reservoir is known and it is desired to determine all three of these variables, the problem could in principle be solved by a fluid flow-material balance analysis which determines the overall compressibility of the reservoir at various points in its history. The change in compressibility with pressure would provide a means of determining the ratio of gas to liquid present, since the compressibilities of gas and liquid vary differently with pressure variation. However, in practice this problem is probably so difficult as to defy solution in terms of basic data precision apt to be available.⁴

It is the purpose of this discussion to illustrate the second case, which involves the determination of two unknown variables, single phase reserves and degree of water drive, from pressure and production history and fluid property data, and to study the precision with which these unknowns can be determined in this manner in a particular case.

Although an electric analyzer developed by Bruce⁸ was used in making the calculations to be described, numerical methods necessary in carrying out the process have been devised and have been applied for this purpose.

Schilthuis,¹ for example, developed a comprehensive equation for the material balance in a reservoir. He combined this with a simplified water drive equation, assuming that the ratio of free gas to oil was fixed by geological data and that a period of constant pressure operation at constant rate of production was available to determine the constant for his water drive equation. On this basis he was able to compute the reserves and predict the future pressure history of the reservoir.

Hurst² developed a generalized equation permitting the calculation of the water drive by unsteady state expansion from a finite aquifer. He showed in a specific case how the water influx calculated by his equation, using basic geologic and reservoir data to fix the constants, matched the water influx required by material balance considerations.

Old³ illustrated the simultaneous use of Schilthuis' material balance equation and Hurst's fluid flow equation for the determination of the magnitude of reserves and a water drive parameter from pressure and production history. He used this method to calculate the future pressure history of the reservoir under assumed operating conditions. As a basis for determining reserves, Old assumed a value for his water drive parameter and calculated a set of values for the reserves, using the initial reservoir pressure and each successive measured pressure. The sum of the absolute values of the deviations of the resulting reserve numbers from their mean value was taken as a criterion of the closeness of fit to the experimental data possible with the water drive parameter assumed. New values of the water drive parameter were then assumed and new sets of the reserves calculated until a set of reserves numbers having a minimum deviation from the average was established. The average value of the re-

Manuscript received at office of the Branch September 1, 1948. Paper presented at Branch Fall Meeting, Dallas, Texas, Oct. 4-6, 1948.

¹References are given at the end of the paper.

serves for this set was taken as the correct value of the reserves and the value of the water drive parameter corresponding to this set was taken as a measure of the water drive.

Woods and Muskat⁴ considered four unknowns: the magnitude of the reserves, the ratio of free gas to oil, and two independent parameters to fix water drive. It was indicated that any accuracy reasonably expected of the basic data would not permit the evaluation of the four unknowns. It was also pointed out that the percentage root mean square deviation for the two sets of reserves corresponding to the optimum water drive and to the no water drive case, using Old's data, differed by less than one per cent of the reserves (being 1.51 and 2.16 per cent respectively). However, in the Shuler Field example used by Old and by Woods and Muskat the estimated water drive resulted in a reserves figure which was only 16 per cent less than that which would be calculated assuming no water drive. This relatively small effect of the water drive on the reserve estimate made it difficult to unequivocally evaluate the degree of water drive. It would also tend to minimize differences to be expected in the water drive by calculating the water drive by means of various water drive equations.

The following discussion will assume that two unknowns are to be evaluated, namely, the magnitude of reserves and the degree of water drive. In principle two independent parameters are required to fix the water drive calculation. However, as Old has pointed out, the calculation is relatively insensitive to one of these so that it is felt that it may be determined with sufficient precision in terms of geologic data likely to be available. The remaining unknown water drive parameter has been taken to be the permeability of the aquifer. We feel that it is advantageous to evaluate as well as possible the other field constants and to determine this parameter directly as a permeability in order to keep in mind better the implications of the quantities involved. It is proposed to use as the criterion of the best fit to the experimental data not the deviation of successively calculated values of reserves from the mean value³ but the best fit of the calculated pressure values to the measured pressure values. This

fit was obtained by varying permeability to obtain a minimum standard deviation from the measured pressure values for each assumed reserve value. Again we feel that this will enable us better to keep in mind the implications of the results and in particular to evaluate the deviations of the calculated pressure decline curves from the measured decline curves in terms of precisions likely to be attainable in the pressure measurements.

It may be noted that in the case here selected the water drive is reflected more significantly in the reserve estimate than in Old's case since here there is a difference of about a factor of 1.6 between reserves calculated with the estimated water drive and with no water drive, in spite of the fact that in Old's case the reservoir was 26 per cent depleted and in this case only 5 per cent depleted in terms of reservoir barrels at initial conditions produced per initial reservoir barrel of reserves. The criteria that govern the suitability of any particular reservoir example for determination of reserves and water drive from pressure decline curves are of considerable importance but have not been determined.

BASIC DATA

The example selected to illustrate the procedure and the accuracy of the results which were obtained is a gas distillate field which geological data indicate may be surrounded by a water zone of large extent. In determining the water influx with the electric analyzer the aquifer is in fact assumed to be infinite, and of uniform thickness and

TABLE 1
BASIC DATA USED IN
CALCULATIONS

h = thickness of aquifer = 38.3 feet
f = porosity of aquifer = 0.3
c = compressibility of water = 6.81×10^{-6} per lb. per sq. in.
μ = viscosity of water = 0.365 centipoise
a = radius of reservoir = 8470 feet
β = compressibility of reservoir gas ^a
$= \frac{1}{\rho} \frac{d\rho}{dp} = 1.87 \times 10^{-4}$ per lb. per sq. in.
$(\rho = \text{std. cu. ft. per reservoir barrel of gas})$

^aSubstantially constant over small pressure decline considered.

permeability. Flow from the aquifer into the reservoir is considered to be radial.

The basic data required for the calculations are given in Table 1. This information may be used with any suitable numerical procedure such as a combination of Hurst's water drive equation and Schilthuis' material balance, or the pressure decline curves may be obtained on the electric analyzer.

DECLINE CURVES

In setting up the problem on the electric analyzer, the aquifer was divided into concentric zones and an equivalent electrical network was set up, capacitances proportional to the volumes of the zones being connected through resistances inversely proportional to the permeabilities of the zones. An infinite aquifer was simulated by arranging the system so that no appreciable voltage drop occurred on the outer capacitor during the time required to make the analyzer runs. A single capacitor (referred to as the pool capacitor) was used to represent the reservoir expansibility.

For each assumed pair of values of reserves Q and permeability k a complete pressure decline curve was obtained by choosing aquifer resistors corresponding to the assumed permeability and a pool capacitance proportional to the assumed reserves. The system was then charged to uniform initial voltage and current withdrawn according to the production schedule in Table 2, column 2. The reservoir pressure decline is proportional to the voltage decline on the pool capacitor.

In this connection it should again be noted that in principle two parameters are required to define the aquifer performance. In Hurst's equation, for example, one parameter is the argument of the transcendental water drive function and the other parameter is included in the coefficient of the series. In the electrical analyzer one water drive parameter is represented by the electrical resistances in the aquifer (determined from the product thickness times permeability divided by water viscosity) and the other parameter by the capacitances in the aquifer (determined by the product thickness times porosity times water compressibility).

In principle only these products must

be specified rather than the component factors (Table 1). In practice the analyzer runs are found to be relatively insensitive to the value taken for the second product so that geologic data have been used to determine this product. Having determined the second product in this manner, it is possible to use the entire first product or any subgroup as the undetermined water drive parameter. The permeability k has been selected, using the best available values of thickness and water viscosity, because it is subject to large uncertainties, and as previously indicated, dealing with an individual factor rather than an overall parameter affords a check on the reasonableness of the values being selected.

EFFECT OF VARIATIONS IN RESERVES AND PERMEABILITY ON DECLINE CURVES

Taking the value of $Q_r = 83.9$ million reservoir barrels of gas for the reserves and a value of $k_r = 24.3$ millidarcies for the aquifer permeability together with the basic data in the preceding section, a run was made to give a reference pressure decline curve. The pressure changes for this run appear in column 3 of Table 2. Additional runs were then made, varying reserves Q and perme-

ability k . As an example the results of Run No. 1 for $Q/Q_r = 1$ and $k/k_r = 0.75$ are given in column 4 or Table 2. In each case the variance* σ^2 and standard deviation σ of the variation in calculated pressure from reference pressures at each of ten points on the reference curve were computed. This calculation for Run No. 1 is shown in columns 5 and 6 of Table 2.

For each value of Q assumed, a series of such runs was made using various values of k . To determine the value of k which gave the minimum variance from the standard curve the variance was plotted against k/k_r for each value of Q/Q_r as shown in Figure 1. Each of these curves has a minimum point giving the best value of k/k_r for the value of Q/Q_r for which the curve was obtained. A curve drawn through these minima has a minimum which gives the value of k corresponding to the closest possible fit to the reference curve. In this case, since the reference curve was obtained on the analyzer and contains none of the errors to which field measurements are subject, the minimum variance is zero and the best value of k/k_r is unity. The best value of Q/Q_r corresponding to this value of k/k_r may be found by replottting the minimum points in Figure 1 with the variance σ^2

as a function of Q/Q_r , each point on the curve corresponding to a different value of k/k_r . Such a curve has been drawn in Figure 3, giving of course for the reference curve the value $Q/Q_r = 1$.

The curves of Figure 1 were also used as a basis for drawing a series of contours corresponding to given standard deviations on a graph with Q/Q_r plotted against k/k_r as shown in Figure 2. The best values of Q/Q_r and k/k_r are represented by a point at the center of this contour system. It will be noted that the smallest standard deviation which can correspond to a condition representing no water drive, namely $k/k_r = 0$, $Q/Q_r = 1.64$, is only 3 lbs. per square inch. This would seem to confirm Woods and Muskat's contention that it is impossible by means of an analysis of this type to determine with any accuracy whether or not a water drive is present and what the reserves are. However, the low fluid viscosity and high permeability of this reservoir cause shut-in well pressures to reach reservoir pressure very rapidly, and as has been pointed out⁹ by the use of a field calibration technique it is possible to obtain a standard deviation of only 2 or 3 lbs. per square inch for an individual pressure measurement. The random error in an average of a number of check pres-

TABLE 2
CALCULATION OF DEVIATION FROM REFERENCE PRESSURE DECLINE CURVE WITH AND WITHOUT RANDOM ERRORS

(1)	(2)	(3)	(4)	(5)	(6)	(7)	(8)	(9)	(10)	(11)	(12)	(13)	(14)
Time	Cumulative Production	Reference Pressure Decline ^a	Run No. 1 Pressure Decline ^b	Deviation from Reference	Square of Deviation	Random Errors Added to Reference Curve					Case 1 Reference Pressure	Run No. 1 Deviation in Case 1	Square of Deviation
				(4)-(3)	(5) ²	Case 1	Case 2	Case 3	Case 4	Case 5			
Months	Reservoir Barrels	psi	psi	psi	(psi) ²	psi	psi	psi	psi	psi	psi	psi	(psi) ²
0	0	0	— 3.9e	-3.9	15.2	+2.5	-3.9	+3.9	+0.5	-0.5	2.5	-6.4	41.0
3	187,000	9.5	5.8	-3.7	13.7	-6.2	-2.5	-6.2	-1.4	-6.2	3.3	+2.5	6.3
6	374,000	17.5	14.3	-3.2	10.2	-2.5	-6.2	+0.5	-3.9	+1.4	15.0	-0.7	0.5
9	561,000	25.0	21.8	-3.2	10.2	+6.2	+0.5	+1.4	-6.2	+6.2	31.2	-9.4	88.4
12	1,084,000	48.6	46.7	-1.9	3.6	-1.4	+2.5	-3.9	-6.2	-2.5	47.2	-0.5	0.3
15	1,607,000	69.6	68.8	-0.8	0.6	+0.5	+6.2	-0.5	-2.5	-3.9	70.1	-1.3	1.7
18	2,130,000	88.0	89.1	+1.1	1.2	-0.5	+3.9	-1.4	+2.5	+2.5	87.5	+1.6	2.6
21	2,877,000	116.8	119.7	+2.9	8.4	+1.4	-1.4	+2.5	+3.9	+0.5	118.2	+1.5	2.3
24	3,624,000	142.0	147.1	+5.1	26.0	+3.9	-0.5	+6.2	+1.4	+3.9	145.9	+1.2	1.4
27	4,370,000	165.5	172.6	+7.1	50.4	-3.9	+1.4	-2.5	-0.5	-1.4	161.6	+11.0	121.0
					139.5 ^c								265.5 ^d

^a Reference run made at $Q_r = 83,900,000$ reservoir barrels, $k_r = 24.3$ millidarcies.

^b Run No. 1 made at $Q = Q_r$, $k = 0.75 k_r$.

^c Reference case: Variance of Run No. 1 = $\sigma^2 = \frac{139.5}{10} = 13.95$

Standard deviation = $\sigma = 3.74$ lb. per sq. in.

^d Case 1: Variance of Run No. 1 = $\sigma^2 = \frac{265.5}{10} = 26.55$

Standard deviation = $\sigma = 5.16$ lb. per sq. in.

^e See appendix for explanation of starting point of curve.

* The variance is the sum of the squares of the pressure differences between the two curves at the ten points divided by the number of points (ten). The standard deviation is the square root of the variance.

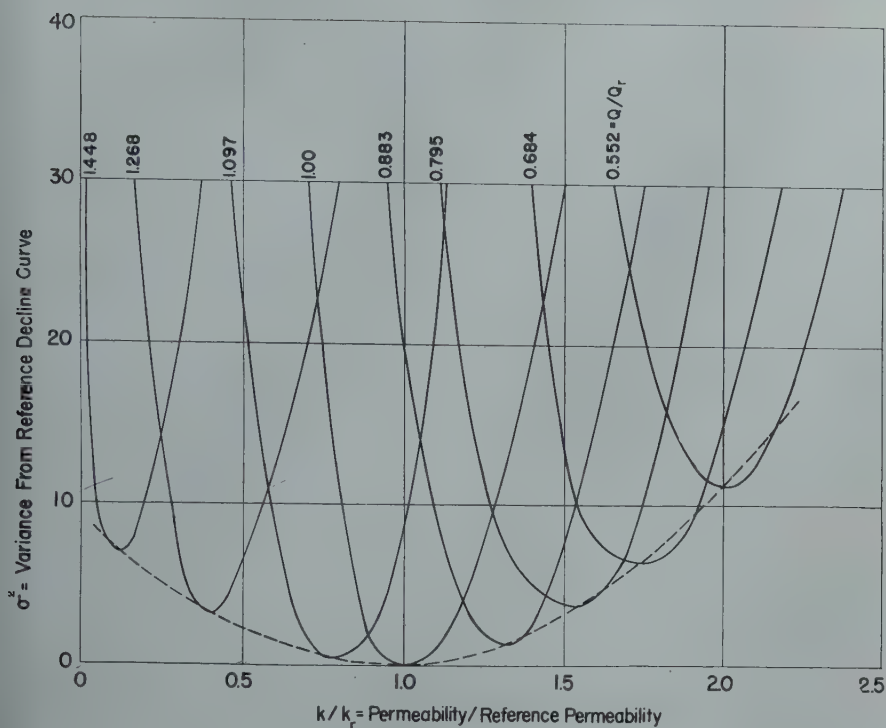


FIG. 1 — EFFECT OF RESERVES AND AQUIFER PERMEABILITY ON VARIANCE IN PRESSURE DECLINE CURVES

Individual solid curves are plotted for values of Q/Q_r (reserves/reference reserves) and give variance (square of standard deviation) of pressure decline curve from reference curve versus ratio of aquifer permeability to reference permeability. Minimum point on each curve gives best value of k/k_r for that value of Q/Q_r . Minimum of dashed curve through minima of solid curves gives best value of k/k_r (which is unity when comparing decline curves to reference curve).

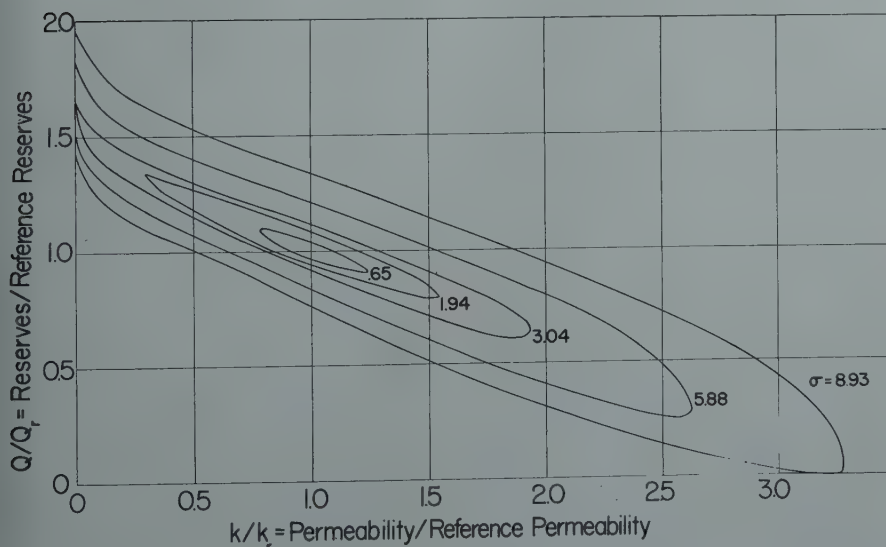


FIG. 2 — CONTOURS OF CONSTANT DEVIATION FROM REFERENCE DECLINE CURVE

The standard deviation σ is the square root of the variance, which is the average of the squares of the difference between a pressure decline curve (for arbitrary Q/Q_r and k/k_r) and the reference curve. The "valley" or point at the center of the system shows the Q/Q_r and k/k_r for which σ is a minimum. Curves on this graph may be obtained by reploting Fig. 1.

sure measurements would of course be less since its standard deviation is that of the individual measurement divided by the square root of the number of measurements.

Further, it should be kept in mind that for the deviations of the random errors in the pressure measurements to give a no water drive ($k=0$) condition it would be necessary to have a very specialized distribution of these errors. One would not anticipate that a random distribution of errors in pressure measurements would give nearly as wide a dispersion in Q and k as is indicated by the contours in Figure 2, since these represent the maximum variation in Q and k possible with the standard deviations shown.

EFFECT OF ERRORS IN PRESSURE MEASUREMENTS

In order to estimate what the effect of random errors in the pressure measurements might be on the precision obtainable in Q and k the same sets of data were recomputed from new reference curves containing random errors. It was assumed that the true pressure decline was represented by the reference pressure decline curve but that the pressure measurements available had a standard deviation of 3.5 pounds per square inch (which is substantially larger than the deviation corresponding to no water drive, and also substantially larger than the random error of a pressure survey average obtainable for this type of field). Since ten pressure surveys were assumed to be available, a probability distribution was calculated showing what errors would be present in the ten measurements if they were to have the given standard deviation and a random distribution. One of these errors was then assigned by chance selection to each of the ten measurements in the reference pressure decline curves (Cases 1 to 5 in columns 7 to 11 of Table 2 are five different chance arrangements of these same errors).

By adding these errors to the pressures on the reference curve a new reference curve was obtained for each of the five cases, the curve for Case 1 being given in column 12 of Table 2. The same analyzer runs were then used with each new reference curve to determine the variance and standard deviation of each run from the new reference

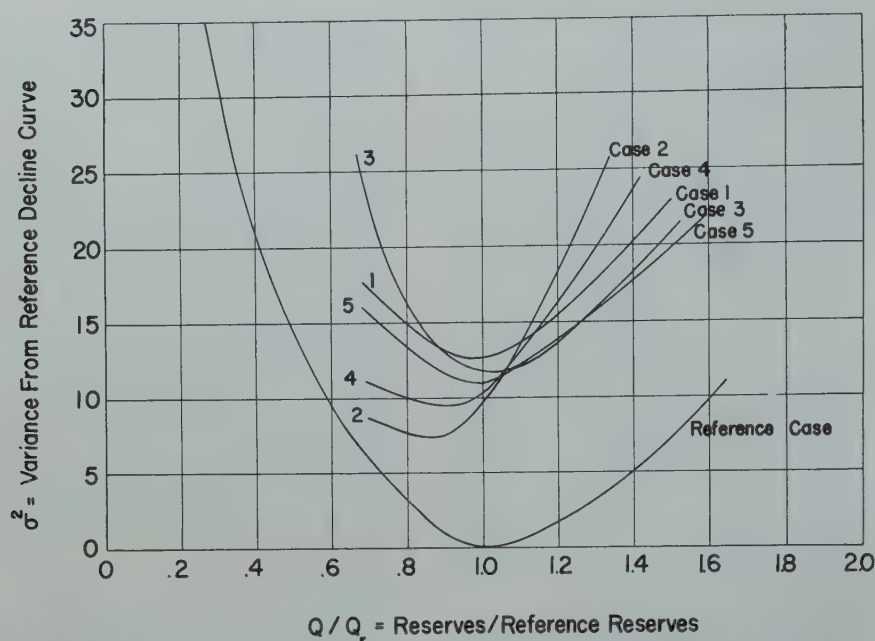


FIG. 3—EFFECT OF RANDOM ERRORS IN PRESSURE MEASUREMENTS ON ESTIMATION OF RESERVES AND AQUIFER PERMEABILITY

Curve for Reference Case is a replot of data in Figs. 1 and 2 showing the determination of Q/Q_r when comparing decline curves to reference curve. Curves for Cases 1 to 5 are similar plots for chance distributions of random errors in the reference curve (see Table 2 for distributions). Best value of k/k_r for these cases was obtained from a plot similar to Fig. 1 (see Table 3 for results).

TABLE 3
EFFECT OF PRESSURE
ERRORS ON ESTIMATES OF
RESERVES AND
PERMEABILITY

Per Cent Variation from Reference Values		
Case	Reserves	Permeability
1	— 2	6
2	—12	21
3	3	— 3
4	— 8	20
5	— 4	4
Standard Deviation of Individual Values*		
	Reserves	Permeability
	7.8%	15.0%
90% Error in Individual Value		
	Reserves	Permeability
From standard deviation	12.8%	24.9%
From standard deviation	13.1%	25.0%
Probable (50%) Error in Individual Value		
	Reserves	Permeability
From standard deviation	5.2%	10.2%
From average deviation	5.3%	10.2%

* Since a small number of values is available, the standard deviation was calculated from the formula

$$\sigma = \sqrt{\frac{1}{n-1} \sum X^2}$$

in which X is one of n deviations.

curve. The calculation for Run No. 1 in Case 1 is given in columns 13 and 14 of Table 2. An entire series of such calculations for the full set of analyzer runs gave data for drawing curves equivalent to Figures 1, 2, and 3 for each case and consequently for determining the values of Q/Q_r and k/k_r for minimum variance. As pointed out for the original reference case, the best value of k/k_r is obtained from a plot like Figure 1 while the best value of Q/Q_r is obtained from a plot like Figure 3. The curves for all five cases are shown with the original curve in Figure 3.

The results for the five cases with random errors introduced are shown in Table 3. The two columns give the per cent errors in estimated reserves and permeability which occurred because of the random errors introduced into the reference curve. These errors, which have a standard deviation of 7.8% in Q and 15.0% in k , correspond to a standard deviation of 3.5 lbs. per square inch in pressure measurement. Restating this in another manner, if the figures for thickness, porosity, field radius, water viscosity and water compressibility are taken as correct, then in this example, pressure survey averages

which have a 90% error* of 5.8 lbs. per square inch suffice to determine the reserves with a 90% error of 13% and the permeability with a 90% error of 25%.

While these numbers apply only to the example used, it is felt that they indicate a general usefulness of this method of determining reserves and water drive from pressure and production history. The example here used is generally similar to an actual Frio gas field in Louisiana. The 170 lb. per square inch pressure drop and 5% depletion of the reservoir represent an early period in the history; in general, a longer history would permit more ready determination of reserves and water drive. Relative to the effect of errors in basic geologic data, it should be noted that to a certain extent these will be compensated by changes in k necessary to give the best fit to the pressure decline curve. Although time has not permitted making an exact analysis of the many factors involved in a comprehensive study of the limits of usefulness of this method, it is felt that the material balance—fluid flow approach does offer useful possibilities of estimating reserves and water drive from pressure and production histories in a number of cases.

In this particular case the usefulness of the method depends upon the fact that accurate reservoir pressures are available. This example emphasizes the importance of taking steps to assure the attainment of reservoir pressures accurate within a very few pounds and of developing methods such as build-up curve analysis for correcting for differences between bottom hole pressures and actual reservoir pressures. However, the method is not necessarily inapplicable to all fields where such precision in pressure measurement is not available. In an undersaturated reservoir, for example, a pressure decline of several hundred pounds may accompany the production of a small percentage of the reserves, and larger uncertainties in reservoir pressures may be tolerated without leading to failure of the method.

ACKNOWLEDGMENTS

The authors are indebted to Mr. Phil-

* Defined so that there is a 90% chance that the true value will be within these error limits. The 90% error equals 1.66 times the standard deviation.

lip H. Braun who organized and supervised the project of securing the example given and to Mrs. Mary Hall who obtained the pressure decline curves with the electric analyzer.

REFERENCES

1. R. J. Schilthuis: Active Oil and Reservoir Energy, *Trans. AIME* (1936) 118, 33.
2. W. Hurst: Water Influx into a Reservoir and Its Application to the Equation of Volumetric Balance, *Trans. AIME* (1943) 151, 57.
3. R. E. Old, Jr.: Analysis of Reservoir Performance, *Trans. AIME* (1943) 151, 86.
4. R. W. Woods and M. Muskat: An Analysis of Material Balance Calculations, *Trans. AIME* (1945) 160, 124.
5. W. A. Bruce: Pressure Prediction for Oil Reservoirs, *Trans. AIME* (1943) 151, 73.
6. D. L. Katz: A Method of Estimating Oil and Gas Reserves, *Trans. AIME* (AIME) 1936 118, 18.
7. B. H. Sage and W. N. Lacey: Application of Phase-Equilibrium Data to the Estimation of Oil and Gas Reserves, *Amer. Petr. Inst. Drill. and Prod. Practice* (1937) 81.
8. W. A. Bruce: An Electrical Device for Analyzing Oil-reservoir Behavior, *Trans. AIME* (1943) 151, 112.
9. E. R. Brownscombe and D. R. Conlon: Precision in Bottom-hole Pressure Measurement, *Trans. AIME* (1946) 165, 159.

APPENDIX

VERTICAL ADJUSTMENT OF DECLINE CURVE

The drawing of all curves through the initial pressure implies that this measurement is absolutely correct and gives it too much weight. To give all points equal weight, the analyzer runs were first made through the initial pressure and then adjusted vertically to give a minimum value for σ^2 . To do this note that any vertical adjustment Δp to all the pressures $p_1, p_2 \dots p_n$ on the analyzer curve gives a variance from the

reference pressure values $p_1', p_2' \dots p_n'$ equal to

$$\sigma^2 = \frac{1}{n} \sum_{j=1}^n (p_j + \Delta p - p_j')^2.$$

To minimize this set the derivative with respect to Δp equal to zero,

$$\frac{d\sigma^2}{d\Delta p} = \frac{2}{n} \sum_{j=1}^n (p_j + \Delta p - p_j') = 0,$$

from which

$$\Delta p = -\frac{1}{n} \sum_{j=1}^n (p_j' - p_j).$$

The terms are taken with regard to sign, and Δp may be either positive or negative.

☆

DISCUSSION

By E. C. Babson, *Union Oil Co., Whittier, Calif.*

For those cases where it is necessary to estimate simultaneously the quantity of hydrocarbons originally in place and the strength of the water drive in a pool, the method of analysis developed by the authors seems to offer more promise than previously published methods. It must be recognized, however, that while the authors have somewhat minimized the uncertainties involved in this type of calculation the inherent difficulties still remain. It is, for instance, stated by the authors that the pressure decline for the case of no water drive would show a standard deviation of only three pounds per square inch from their reference curve.

While it may be possible to make pressure measurements in wells with sufficient accuracy to render this small standard deviation significant, it is not at all certain that the field pressure data can be interpreted with anything like this degree of precision except under ideal circumstances. Under most conditions it should be possible to estimate the quantity of hydrocarbons originally in place more accurately by the volumetric method than by the method outlined in this paper. Since there are conditions, however, in which it is not feasible to estimate the size of the reservoir by volumetric methods, it may be

pertinent to examine briefly the factors involved in some of these cases.

Probably the most common case of uncertainty regarding the volume of the reservoir is that of a pool which has been only partially developed. In this case, however, it is doubtful whether a more reliable result could be computed by the method developed in this paper unless it can be assumed that the pressure in the undeveloped portion of the reservoir is the same as the pressures actually measured in the wells. It is apparent that the uncertainty introduced by this, or any other reasonable assumption regarding pressure in the undeveloped area, can be many times three pounds per square inch and is likely to be in the same direction at all points of the pressure decline rather than having a random distribution. If it is desired to draw conclusions regarding the strength of a water drive during the early stages of development, it would seem advisable to utilize regional geological information regarding the continuity and the permeability of the reservoir rock rather than relying upon materials balance calculation.

Another source of uncertainty regarding the quantity of hydrocarbons originally in place results from the fact that portions of some producing formations may either be barren of hydrocarbons or may have such low permeabilities that they are not effective from the standpoint of production. Unfortunately, lithologic changes which result in these conditions are often gradational and there may be intermediate portions of the formation in which the permeability is high enough for appreciable production of oil or gas but is still too low to permit rapid equalization of pressure when the wells are shut in. Estimates of the reservoir pressure can, of course, be made from built-up curves, but there is always some uncertainty involved in these estimates, and even if the pressure is allowed to build up for a period of weeks, the significance of this pressure is still uncertain if there is reason to believe that there are pressure differences between various portions of the producing interval. It would seem much more desirable to estimate the effective hydrocarbons in place by the utilization of core analysis, electric logging, and flow meter surveys in producing wells rather than

by the use of materials balance methods unless it can be assumed that water encroachment is negligible.

Further uncertainties can be introduced into the reservoir pressure calculation by differences in pressure and in the sub-sea position of gas-oil or water-oil interfaces in the individual wells. If the pressures vary materially from well to well it immediately becomes necessary to devise some method of weighting the pressure from the individual wells to give a representative average pressure. While there are several reasonable methods of so weighting pressures, there is always some uncertainty regarding the pressure distribution in the areas between the wells when the pressures in the wells themselves vary materially. If the producing formation has appreciable closure it becomes necessary to project pressures to some datum plane and varying gas-oil and water-oil interfaces in the individual wells cause uncertainty regarding the well pressure which should be used as the basis for projection and the gradient on which the projection should be made to the datum plane. There are several different theories on this problem, none of which seem to give entirely satisfactory results in all cases. In most cases the uncertainties resulting from these factors will not be large but could well be of the order of several pounds per square inch.

There are undoubtedly cases where the method of analysis developed in this paper will furnish information useful in the control and operation of an oil pool. When this method is used, however, the possible uncertainties should be kept constantly in mind and an effort should be made to check the conclusions, at least approximately by some independent method.

☆

DISCUSSION

By Morris Muskat, Gulf Research & Development Co., Pittsburgh, Pa.

The paper by Brownscombe and Collins presents an interesting study of the possibilities of determining simultaneously the oil reservoir hydrocarbon content and effective permeability of the supporting aquifer, in partial water drive systems, by comparing observed and predicted pressure histories. While the authors refer incidentally to their

use of the electrical analyzer as a convenient tool in making the required flow calculations, it is felt that their results are especially pertinent to a general evaluation of electrical analyzer studies or equivalent reservoir treatments. For it has been common practice also to use in such studies the degree of agreement between the calculated pressure histories and those observed as the criterion of validity of the assumed aquifer characteristics. The use in the latter of the fluid expansion capacity and permeability of the aquifer as the two adjustable parameters and the variation of the oil reserves and aquifer permeability, as applied in the present paper, are essentially equivalent from an analytical standpoint. In fact, one could go still further, and in some cases more appropriately, and vary the oil reserves and fluid expansion capacity of the aquifer, keeping the average permeability fixed, and very likely obtain equivalent results regarding the poor sensitivity of the pressure predictions to the exact values of the reservoir parameters.

As to the quantitative aspects of the treatment, the significance of the magnitude of the deviations between the calculated and measured pressures will depend largely on the accuracy of the recorded pressure data and the physical significance of the individual values. The authors properly point out that to apply their method very high precision in the pressure determinations will be required. But the problem is more than one of gage accuracy and depth correction. It involves the perennial plague of pressure averaging. This may be especially serious during the early producing history where the effective reservoir volume is being continually enlarged until the field is fully developed, with corresponding changes in the significance of the various pressure averages. On the other hand, later in the producing life the development of pressure differences over the field—often by several hundred psi—will again lead to uncertainty as the true precision of pressure averaged with or without weighting. While these complications will be smaller in distillate or gas cap reservoirs, it would seem that to base the determination of the magnitude of water intrusion and reserves in most oil reservoirs on differences in mean pressure deviations of 1-3 psi would severely

tax one's faith in conventionally reported reservoir pressures.

Referring specifically to Fig. 1 of the paper, it will be seen that by choosing the permeability to be twice the reference or correct value the root mean square pressure deviation between the theoretically accurate reference pressure history and that calculated will be only about 3.5 psi, even though the assumed reserves be only 55.2% of the correct value. Conversely, one may take the reserves to be 44.8% greater than the correct value and still get agreement between the true and calculated pressure histories such that the root mean square deviation does not exceed 2.7 psi, by adjustment of the permeability parameter. Thus throughout a range of total variation of 88.6% in the reserves, and a factor of about 10 in the corresponding rates of water intrusion, it is always possible, for the system treated in the paper, to reach agreement between the supposedly true pressure history and those computed to within 3.5 of psi, on the average, for the production interval used in the analysis. It would appear, therefore, that the resolution or discriminating power of this method of treatment is subject to essentially the same limitations as are inherent in those previously developed from material balance principles. While this might have been anticipated qualitatively from earlier studies of the general problem of reserves estimation, the quantitative treatment of the authors does provide more specific estimates of the effects involved.

Author's reply to Morris Muskat and E. C. Babson:

The importance of securing accurate average reservoir pressures has been emphasized both in the preceding comments and in the original article. Both Muskat and Babson have outlined some of the difficulties and uncertainties attending the securing of such pressure data. While there are cases in which average reservoir pressures will be so unreliable as to rule out the material balance method of estimating reserves and water drive, it is believed that the accuracy will be sufficient to give useful results in a number of instances.

Muskat has suggested that the

method is less applicable to oil reservoirs than to gas reservoirs because of the greater uncertainty in average reservoir pressure. On the other hand, a greater uncertainty can be tolerated with an undersaturated oil reservoir since a larger pressure decline will accompany the initial period of production by liquid expansion, and hence a smaller fractional error in reservoir pressure decline will result from equally accurate absolute pressure measurements.

An important consideration is the fact that calculated decline curves are compared with reservoir pressure decline rather than with absolute reservoir pressures. Viewed in this light some of the problems of pressure estimation become less intractable. For example, as Babson has pointed out, in a relatively undeveloped field it is necessary to make assumptions about the pressure in the undeveloped area, and these assumptions may lead to errors which are likely to be in the same direction at all points of the pressure decline rather than having a random distribution. Pressure errors which are all in the same direction, however, would have less effect on reserve and water drive estimates than randomly distributed errors, since the calculated decline curves are vertically adjusted to secure the best possible fit. In fact, if the errors were all equal and in the same direc-

tion they would have no effect on the reserve and water drive estimates.

Further, with regard to the ever-present problem of averaging the well pressures to secure an accurate reservoir pressure, while it is very difficult, as both Babson and Muskat have pointed out, to devise a system of weighting the individual pressures which will produce a good absolute pressure in all cases, it is much simpler to find a system of weighting which will give a good approximation of the pressure difference existing between surveys made at different times. For example, a good approximation to such a system may be simply to use the same wells and the same system of weighting for all pressure surveys. This procedure might begin to break down as the field is depleted but the longer pressure history thus made available would be a compensating factor.

On the other hand, the question of non-uniform permeability raised by Babson is not readily answered by material balance methods. If a portion of the formation is extremely tight and contributes little production during the early history, it will be missed by a material balance reserve estimate. If the developed portion of the field is entirely surrounded by a very tight section which has experienced negligible pressure decline then no water influx will have occurred and both the reserves and

the water drive will be underestimated. Other work by the authors, however, indicates that even in a tight formation of a few millidarcies the pressure will soon decline at substantial distances from the producing area.*

It should be pointed out that the abbreviated statistical analysis given in the article does not cover all cases and that too much significance should not be attached to the quoted standard deviation of 3.5 lbs. per sq. in. The primary point of the analysis is to indicate that while an error of say 3.5 lbs. per sq. in., if properly chosen, could make a large difference in the results, the chances are that the natural distribution of such pressure errors will affect the results to a much smaller extent than that indicated by Muskat. For the example given it is believed that a 3.5 lbs. per sq. in. precision in pressure measurement would lead to worthwhile results. Other cases would of course require greater or less precision depending upon pressure decline, degree of water invasion and other factors. A quantitative answer to this more general question would require a much more comprehensive statistical analysis than has been attempted by the authors.

★ ★ ★

* Miller, Kieschnick, and Brownscombe; "The Effect of Production Rate Upon Ultimate Recovery from a Solution Gas Driven Reservoir," presented at the AIME Meeting in Dallas October 6, 1948.

and

Brownscombe and Collins; "Steady States in Single Phase Reservoirs," presented at the AIME Meeting in San Francisco, February 16, 1949.

RELATION BETWEEN PRESSURE AND RECOVERY IN LONG CORE WATER FLOODS

JOSEPH N. BRESTON AND RICHARD V. HUGHES, MEMBER AIME
PENNSYLVANIA GRADE CRUDE OIL ASSOCIATION, BRADFORD, PA.

ABSTRACT

Conclusions drawn by previous research workers with respect to the relation between pressure gradients and/or velocity and oil recovery obtained by laboratory water flood tests have been in disagreement probably due to variable procedures and unnatural conditions and materials. The Bradford Laboratory of the Pennsylvania Grade Crude Oil Association as part of its secondary recovery research program has conducted nineteen water floods on two long cores of widely differing characteristics in an attempt to clarify this relationship and make it an aid in predicting flooding pressures in the field. Unlike previous research procedures the present experiments were conducted with the aim of duplicating field conditions as closely as possible by using long unextracted consolidated cores, a live crude, and natural brines for both flooding and connate water content. Also, the pressure gradients and flooding velocities were representative of field conditions where similar sands were being flooded. Eleven floods on one core and eight floods on the other core showed increased recoveries and lower residual oil saturation with increased flood pressure gradients and flood velocities. A marked decrease in recovery was obtained from both cores at very low flood velocities. This pressure versus recovery relationship is shown to hold up to the point of water breakthrough and also up to the 100 and 1 produced water to oil ratio point.

INTRODUCTION

The possibility of water flooding oil sands was suggested by Carll of the Pennsylvania Geological Survey in 1880. It is not known when the practice was tried intentionally for the first time, but its beneficial effects were noted in the annual production rate of the Bradford field as early as 1907. The practice was illegal in Pennsylvania until 1921. Early water floods in the Bradford field usually consisted of shooting or splitting the casing secretly to permit subsurface waters to enter the producing sands under hydrostatic head. As it was

noted that the benefits of water flooding seemed to be proportional to the quantity of water dumped into the well many also began to utilize surface sources after the practice became legal. It was probably during the middle 20's before many producers realized that the pressurehead of the water upon the producing sand determined the rate and quantity of water that would enter the sand. Hence, rate and quantity of production appeared to be a direct function of input pressures.

By 1927 a few producers had ventured the installation of pressure pumps in order to increase water-input rates and production through the combination of hydrostatic and hydraulic pressures. The adoption of pressure flooding and the "five-spot" drilling pattern in the Bradford field were essentially simultaneous. Water-input pressures in 1930 seldom exceeded 300 p.s.i. at the well head or 1100 p.s.i. at the sand face. Since that time, water-flood producers in the Bradford-Allegany fields have gone to higher and higher pressure until today 600 p.s.i. at the well heads is called a low pressure flood. Many high pressure floods now operate at 1300-1400 p.s.i. at the well head. The limiting and advisable pressure at the sand face has been pronounced as that pressure just under what is required to lift the overburden or to cause formation parting.⁸ According to this rule any water flood operation utilizing well-head pressures nearly equal in pounds per sq. in. to 1.1 times the average depth in feet to the top of the producing sand would be considered as a high-pressure flood.

Despite the higher pressure trends in the Bradford-Allegany field operations and the results of early laboratory water flooding research, the desirability and benefits of high input pressures are still questioned by many operators, particularly in midwestern water flood operations.

The present paper recounts a series of 19 laboratory water floods using two long, consolidated cores of widely differing characteristics saturated with live crude and flooded with oil field brines in an effort to simulate field conditions under various pressure gradients and flooding velocities. For both cores, higher recoveries and lower residual oil saturations were obtained at higher pressure gradients and flood velocities. This relationship is shown to hold up to the water breakthrough point and also up to the 100 to 1 produced water to oil ratio point.

Manuscript received at Petroleum Branch Office February 2, 1948. Paper presented at AIME Annual Meeting, New York City, February 16-19, 1948.

¹References are given at end of paper.

REVIEW OF LITERATURE

Umpleby,¹ upon noting a marked increase in oil production rates caused by "dumping" wells nearer the producer, called attention to the beneficial effects of higher pressure gradients in 1925. Two years later Torrey² credits H. M. Ryder with having demonstrated in the field that the amount of water an input well would take was dependent upon the hydrostatic pressure of the water in the well bore. Producers in the Bradford-Allegany field at that time believed decreased development costs by wider spacing of wells to be the chief advantage of using higher input pressures. Russell,³ in 1932, as a result of laboratory tests, found it difficult to predict whether or not more oil would be recovered by higher pressures while maintaining constant well spacing.

Ryder⁴ as a result of field experiments and related observations and interpretations of laboratory floods conducted by Yuster at The Pennsylvania State College was probably the first to proclaim the benefits of higher flooding pressures upon recoveries. For more than a decade he has been the chief advocate of high flooding velocities,^{5,6} which for any given sand are a direct function of pressure gradient. His latest contribution,⁷ based upon field experiments, showed that on four Bradford oil properties, each of eight increases in the water pressure resulted in a substantial increase in the quantity of oil ultimately to be produced.

Parsons¹⁰ obtained greater recoveries at lower pressure gradients when flooding verticle unconsolidated sand columns where gravity separation became a factor. However, Miller¹¹ showed increases in recovery with higher flooding pressures and velocities in laboratory experiments using horizontal packed unconsolidated sand columns. Yuster,^{8,9} and Calhoun, McCormick, and Yuster,¹³ have reported increased flooding efficiency with respect to higher pressures in laboratory floods of low permeability consolidated sand cores from the Bradford-Allegany field. Later, Morse and Yuster¹⁴ in reporting upon 42 laboratory water flooding tests on three different long Venango sand cores from the Franklin, Pa., mine of widely varying permeabilities found that with the materials used there was no measurable effect of flooding gradient or velocity upon residual oil saturation. Holmgren¹⁵ recently reported on ten laboratory water drives at various pressure gradients using a long, high-permeability, consolidated core cut from sands outcropping near Sand Springs, Oklahoma. The core contained connate water and free gas throughout all tests. Holmgren concluded that for the range investigated, the water input rate and the resulting pressure gradient, during a water drive at low gas saturation, has no discernible effect on the final oil saturation of the core.

A paper by Earlougher,¹² based upon many laboratory floods of cored sands and related field observations has been widely accepted by water flood producers and research workers as indicative of what is to be expected under field operating conditions. He has concluded that:

1. For any given oil saturation there is a critical maximum velocity above which the recovery efficiency falls off rapidly.
2. When this critical velocity is exceeded, the water-oil ratio

rises extremely fast and thus shortens the economic life of the flood and in turn reduces the ultimate recovery.

3. The critical velocity of a sand varies with the percentage of oil saturation, with sands of higher saturation having higher critical velocities.
4. Recovery efficiency by flooding is largely dependent upon two factors; namely, percentage of oil saturation at the beginning of the flood and the velocity of the flooding water.

APPARATUS AND MATERIALS

Cores

One of the cores used in these flooding experiments was obtained from horizontal drilling in the Franklin, Pa., oil mine into what is locally called the First Venango sand. It was a cylindrical core approximately $4\frac{1}{4}$ inches in diameter and 51 inches long. The sandstone was well consolidated and had a nitrogen gas permeability of 135 millidarcies without extraction. Before the first crude saturation the brine permeability was measured as 49 millidarcies. After repeated saturations and measurement of the total fluid content, its porosity was estimated at 18 per cent. The core was not extracted or treated in any way before mounting nor during any of the tests.

The second core was very similar to the Third Bradford sand. It was taken from a sandstone outcrop corresponding strati-

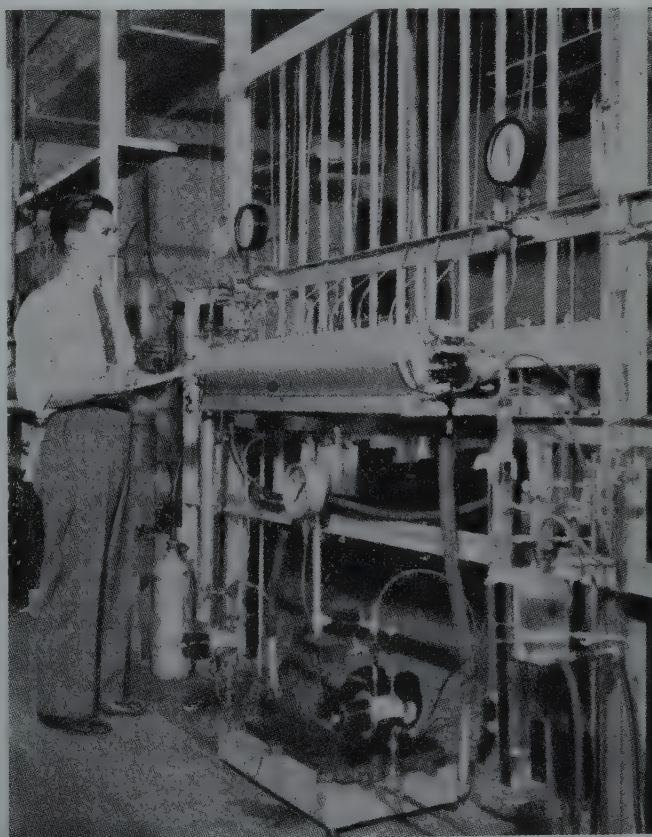


FIG. 1 — CORE FLOODING APPARATUS.

graphically to the Third Bradford sands at Rushford, New York, approximately 45 miles northeast of the Bradford field. It was cut to cylindrical shape approximately $4\frac{1}{4}$ inches in diameter and 12 inches long. The core had a measured air permeability of 15.3 md. and a brine permeability of 2.55 md. The porosity was determined as 16.9% by the sand grain density method. This core also was not extracted or treated in any way before mounting or during the experiments.

Core Mountings

Very shallow circumferential grooves were cut at eight locations along the Venango sand core and taped with cellophane tape. These were to simulate piezometer pressure rings. The core was coated with a polystyrene lacquer and mounted in hard sealing wax in $4\frac{1}{2}$ -inch steel pipe. Using the proper gaskets to completely isolate the core from the wax, end plates with two openings each were bolted to the ends of the pipe. The pipe and wax were tapped down to the piezometer rings and special fittings and valves inserted to complete the pressure taps into the mounted core.

The core mount was fitted with a jacket through which could be circulated water at a constant temperature.

The mounted core was placed on a steel rack, as illustrated in Fig. 1, and fitted with the auxiliary equipment. Saran plastic tubing and brass fittings were used wherever possible. Plastic tubing was also used for the U-tube pressure manometers. The manometers were connected to give the pressure gradients over nine sections of the core and the overall pressure drop.

Sufficient auxiliary equipment was installed (see Figs. 1 and 2) to allow for oil saturations and brine floods and for continuous measurement of all fluids going into and out of the core. This provided the necessary data for a continuous and absolute material balance on the core.

The Rushford sandstone core was mounted in $4\frac{1}{2}$ -inch steel pipe with hard sealing wax the same as the Venango core except that there were no pressure taps installed. The core was mounted on a rack and fitted with auxiliary equipment necessary for saturating and flooding. Equipment on a smaller scale than for the Venango core was provided for obtaining the necessary data for a material balance on the core. For this core provisions were made for disconnecting and weighing the core before and after each saturation and flood.

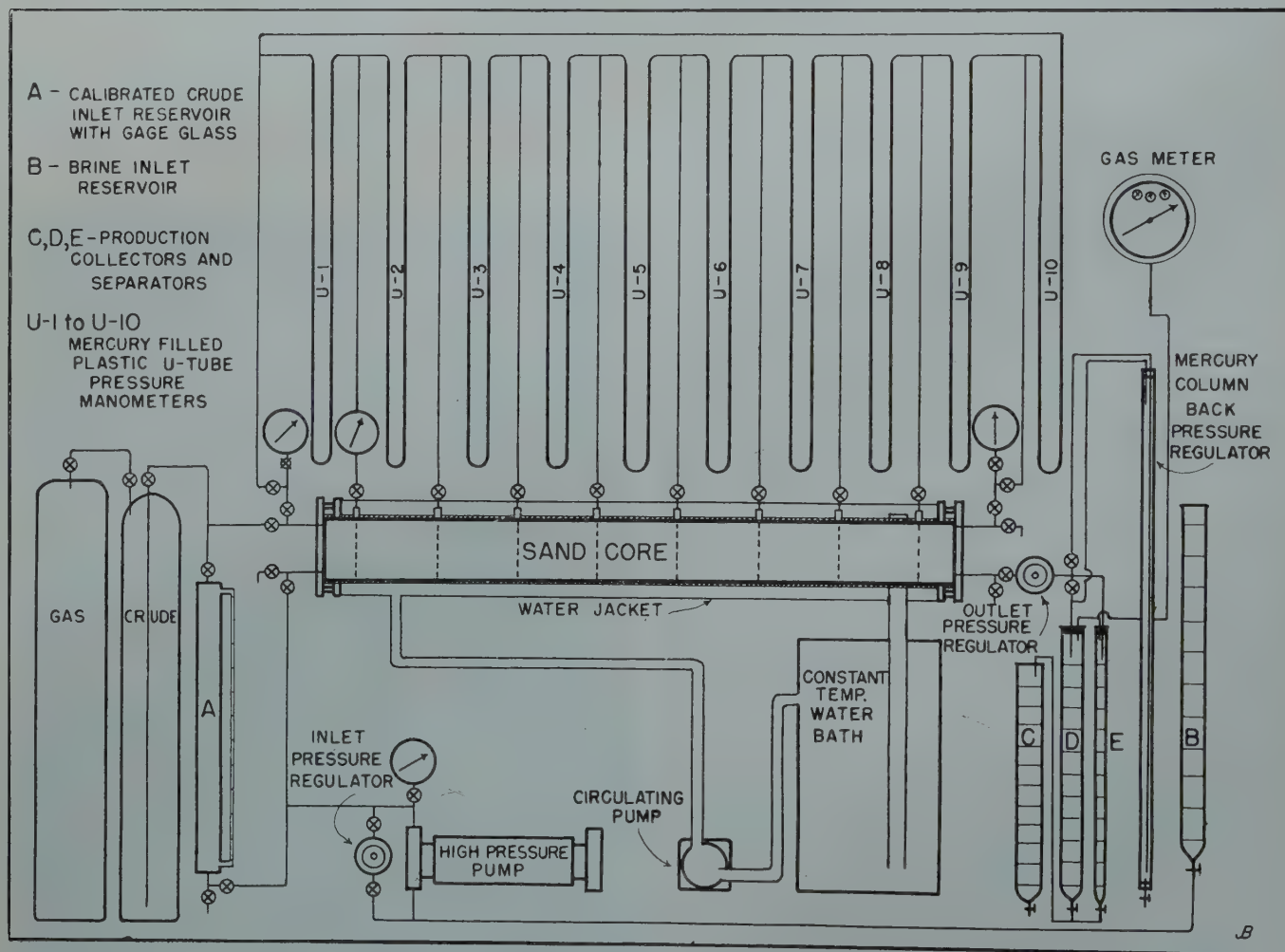


FIG. 2 — DIAGRAM OF CORE FLOODING APPARATUS.

Saturating and Flooding Materials

The crude oil used in the experiments on both cores was a live Bradford crude with a specific gravity of approximately 0.80. The crude used in the Venango core was gassed-up with natural gas to a bubble point of approximately 20 p.s.i. The crude used in the Rushford core was gassed-up to a bubble point of approximately 10 p.s.i.

Pressure pycnometer measurements showed that in depressing the live crude from 20 p.s.i. gauge to atmospheric pressure one liter of evolved gas (standard conditions) would account for a shrinkage in oil volume of 1 milliliter. This factor was used in correcting the produced oil volumes for shrinkage due to release of dissolved gas from the produced crude.

The brine used to saturate and flood the Venango core was a produced water from the Franklin mine from which the core material was obtained. It was natural brine diluted with fresh water to a specific gravity of 1.016. The chloride content measured 12,000 ppm. Except for clarification by filtering and settling the brine was untreated.

The brine used to saturate and flood the Rushford core was a strong natural brine produced by a Bradford oil well. It had a specific gravity of 1.126 and a measured chloride content of 127,000 ppm. It was clarified by settling, and kept from contact with air as much as possible.

The gas used to pressure-up the crude was a dry natural gas from the Bradford oil field.

OPERATING PROCEDURE

Saturating Cores

Except for determining the gas permeability, the cores were not subjected to any artificial preparation (such as extracting) before saturating. The first saturation was made with brine on the evacuated core. Brine was pumped in under pressure while a vacuum was pulled on the outlet end and pressure taps. After the brine came through the core was flooded with brine at a high pressure gradient until the increase in brine content of the core became negligibly small. The core was then ready for saturating with crude.

Saturating the Venango core with a live crude was performed as follows: The calibrated crude oil reservoir "A" in Fig. 2, was first loaded with brine. Then the brine was displaced by crude from the crude storage cylinder which in turn was displaced by gas from the gas cylinder. For obvious reasons, these operations were carried out under a pressure always in excess of the bubble point of the crude. Next, the crude was driven into the core by displacing it from the calibrated reservoir with brine from a high pressure pump. A back pressure slightly in excess of the bubble point of the crude was kept at the outlet end of the core by means of a diaphragm and spring action back pressure regulator or by a mercury column through which the produced fluids had to flow. The produced fluids were collected, separated, and measured in the apparatus illustrated. The crude saturation was continued until several pore volumes were flowed through at which point the brine saturation was reduced to a minimum, and only a negligibly small amount of brine was produced for each volume of crude. A complete material balance permitted the calculation of the oil and brine content of the core.

The Rushford core was saturated with crude in the same manner as the Venango core. The oil and brine contents were calculated by material and weight balance, provisions having been made to weigh the core before and after saturations.

Flooding Cores

The cores were flooded by pumping brine from an inlet reservoir into the core and collecting and measuring the produced fluids in the appropriate receivers (see Fig. 2). The flooding was performed at predetermined pressure gradients which were obtained by regulating the inlet pressure with a constant pressure regulator.

The Venango core was saturated with crude and then flooded with brine eleven different times, the core being resaturated before each flood. The flooding was done at pressure gradients from 0.10 to 11.15 p.s.i. per foot. The flooding pressures were not in ascending or descending order but were varied so the direction changed six times. The rate of advance of the flood front varied from 0.16 to 23.8 feet per day. Some rates were considerably slower and others much faster than the average of those considered prevalent in the field in sands of comparable properties. Frequent readings were made so that the point at which the flood water broke through could be determined accurately. Flooding was continued at least until an instantaneous produced water to oil ratio of 100 to 1 was obtained.

The Rushford core was saturated and flooded eight different times at pressure gradients varying from 1.02 to 49.5 p.s.i. per foot. The rate of advance of the flood front for this core varied from 0.04 to 2.32 feet per day, values which cover the average range of the flood rates in the Bradford field through sands of similar properties. As in the case of the Venango core sufficient readings were taken during the progress of the floods to determine the water break-through point and the point representing a produced water to oil ratio of 100 to 1. Due to the small amount of oil produced, the 100 to 1 produced water to oil ratio point for this core was more difficult to determine with accuracy.

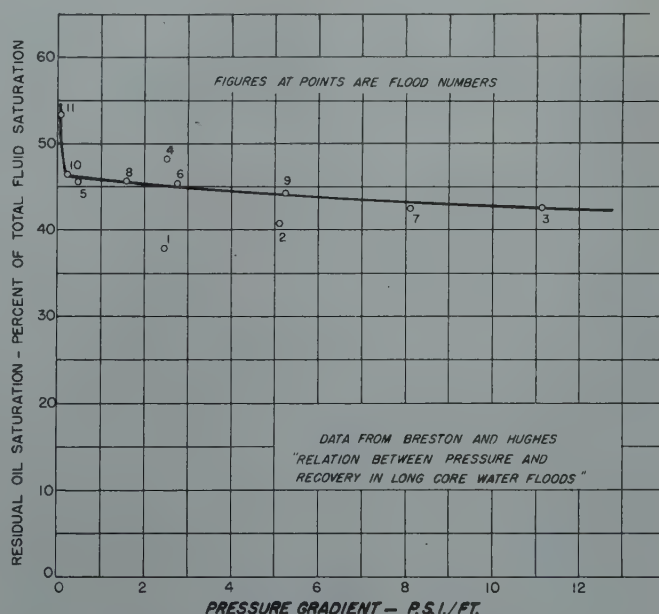


FIG. 3—VENANGO SAND CORE. EFFECT OF PRESSURE GRADIENT ON RECOVERY TO WATER BREAKTHROUGH.

RESULTS

Venango Core Floods

Data summarizing the results obtained from the eleven floods on the Venango core are found in Table I and illustrated graphically in Figs. 3 to 9. Inasmuch as the core increased in total liquid content with each successive saturation, as illustrated in Fig. 8, the recoveries at the various pressure gradients were based on an effective pore volume equal to the total liquid content at the time. This unintentional change in total fluid saturation and perhaps pore pattern introduces a certain variable which the authors feel can be minimized by calculating recoveries on the effective pore volume basis. Figs. 3 and 4 illustrate the recoveries at the point of water breakthrough and at the 100 to 1 produced water to oil ratio point in terms of residual oil saturation at the various pressure gradients. Discounting the values for floods 1 and 2 because of low total liquid content and correspondingly high unnatural recovery, the curves show a definite decreased in residual oil saturation at the higher flood pressure gradients. The poor recovery for the very low pressure gradient flood is reflected in the high residual oil saturation.

Since the ratio of oil to water content of the core at the end of each saturation was very nearly the same (except for sat-

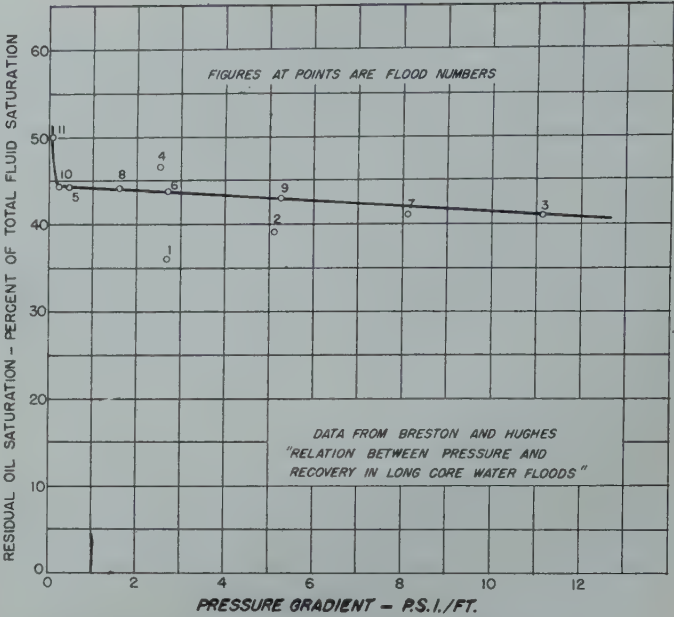


FIG. 4 — VENANGO SAND CORE. EFFECT OF PRESSURE GRADIENT ON RECOVERY UP TO 100 TO 1 PRODUCED WATER TO OIL RATIO.

TABLE 1

Summary — Water Flood First Venango Sand Core

Size: 51" x 4 1/8" Permeability: N₂ = 135 md.
Brine = 49 md.

Bulk Vol. = 11,171 cc.
Pore Vol. = 2,011 cc. (From an estimated porosity of 18%)

Operation	Pressure Gradient PSI/ft.	Flood Velocity ft/day	Oil Plus Water at End cc.	Total Oil Content in cc.			Percent Oil Saturation (18 Percent Por., 2011 cc.)			Percent of Initial Oil Content Recovered		Percent of Total Oil Recovered up to Water Breakthru	Oil Satn., Percent of Total Liquid Saturation	
				at Saturation	at Water Breakthru	at w/o ratio of 100:1	at Saturation	at Water Breakthru	at w/o ratio of 100:1	up to Water Breakthru	up to w/o Ratio of 100:1		at Water Breakthru	at w/o Ratio of 100:1
Brine Saturation...			1096.0											
1st Oil Saturation...			1136.5	761.5			37.9							
1st Brine Flood...	2.50	4.9	1129.0		425.5	406.5		21.2	20.2	44.1	46.6	94.6	37.7	36.0
2nd Oil Saturation...			1167.0	827.0			41.1							
2nd Brine Flood...	5.13	11.5	1163.5		471.0	455.0		23.4	22.6	43.1	45.0	95.7	40.5	39.1
3rd Oil Saturation...			1182.5	861.0			42.8							
3rd Brine Flood...	11.15	23.8	1203.0		510.0	493.0		25.4	24.5	40.7	42.7	95.4	42.4	41.0
4th Oil Saturation...			1260.0	930.5			46.3							
4th Brine Flood...	2.54	4.9	1210.5		581.5	565.0		28.9	28.1	37.5	39.3	95.5	48.0	46.7
5th Oil Saturation...			1186.0	914.5			45.5							
5th Brine Flood...	0.48	0.9	1295.0		588.5	577.0		29.3	28.6	35.6	37.1	96.0	45.4	44.4
6th Oil Saturation...			1330.5	982.5			48.9							
6th Brine Flood...	2.70	5.0	1360.0		613.0	597.0		30.5	29.7	37.6	39.2	95.8	45.1	43.9
7th Oil Saturation...			1360.0	991.0			49.3							
7th Brine Flood...	8.13	15.3	1401.0		594.5	576.5		29.6	28.7	40.0	41.8	95.7	42.4	41.1
8th Oil Saturation...			1462.5	1056.5			52.5							
8th Brine Flood...	1.60	2.5	1465.5		667.0	647.5		33.2	32.2	36.9	38.7	95.2	45.5	44.2
9th Oil Saturation...			1449.5	1055.5			52.5							
9th Brine Flood...	5.25	9.2	1477.0		651.5	634.5		32.4	31.6	38.3	39.9	96.0	44.1	43.0
10th Oil Saturation...			1507.0	1078.0			53.6							
10th Brine Flood...	0.22	0.35	1518.0		701.5	677.0		34.9	33.7	34.9	37.2	93.9	46.2	44.6
11th Oil Saturation...			1561.0	1144.0			56.9							
11th Brine Flood...	0.10	0.16	1584.5		842.5	795.5		41.9	39.6	26.3	30.4	86.5	53.2	50.2

urations 1 and 2) another way of interpreting the results whereby the variable of increasing fluid content is greatly eliminated is to plot the recoveries in terms of the per cent of initial oil content. This is shown in Figs. 5 and 6. Fig. 5 illustrates the greater recoveries obtained with increasing pressure gradient and Fig. 6 illustrates the greater recoveries obtained with increasing flood velocity. Inasmuch as there is a direct relationship between pressure gradient and flood velocity a close and expected similarity is shown between the curves of Figs. 5 and 6.

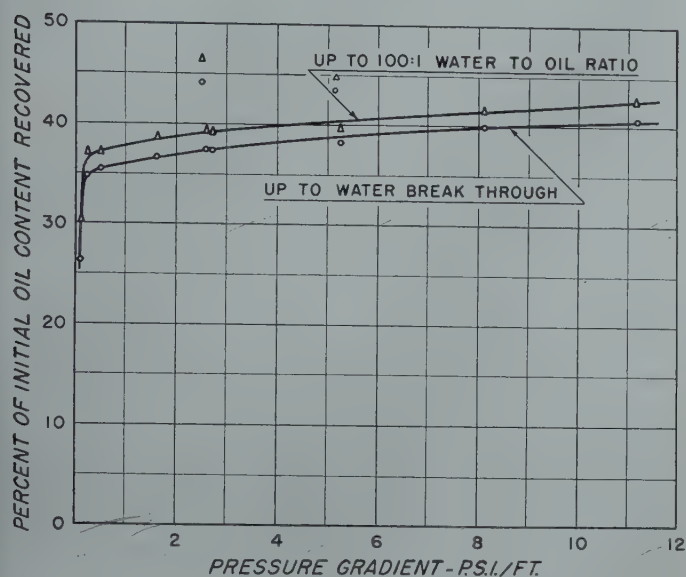


FIG. 5—GREATER RECOVERIES OBTAINED WITH INCREASING PRESSURE GRADIENT.

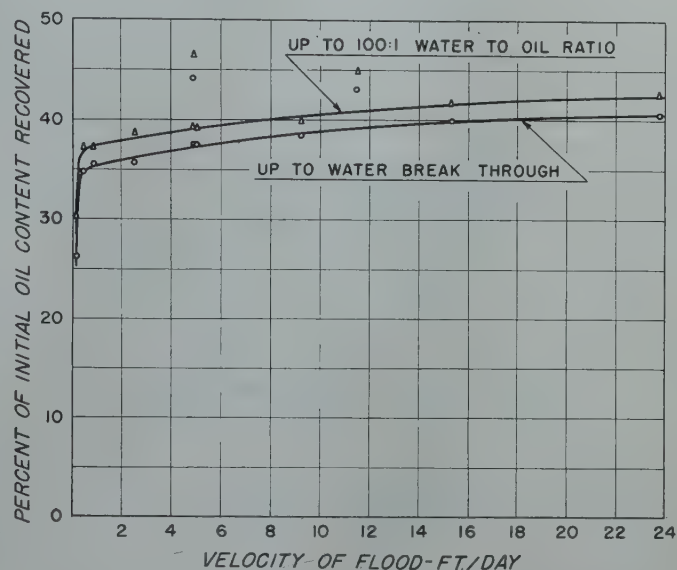


FIG. 6—GREATER RECOVERIES OBTAINED WITH INCREASING FLOOD VELOCITY.

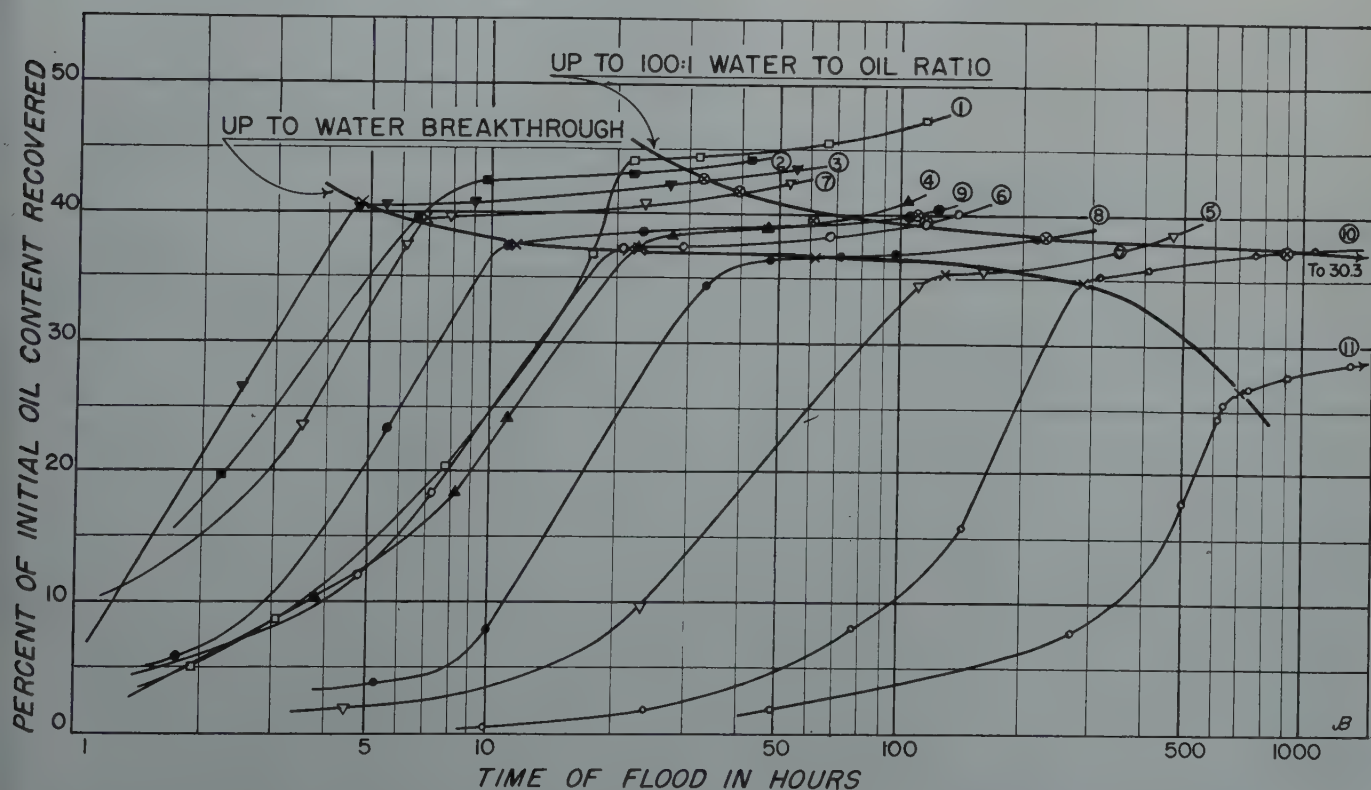


FIG. 7—ACCUMULATIVE OIL RECOVERIES FOR ELEVEN VENANGO CORE FLOODS WHEN PLOTTED AGAINST TIME

Fig. 7 is introduced to show the accumulative oil recoveries for the eleven Venango core floods when plotted against time. The semi-log scale was used to avoid an extended graph. Curves drawn through the water breakthrough points and the points representing a produced water to oil ratio of 100 to 1 also clearly show the higher recoveries obtained at the higher flooding pressure gradients.

Inferring that one must analyze the results on a basis of total pore volume and not effective pore volume, Fig. 9 was plotted to show that it would not change the interpretation of

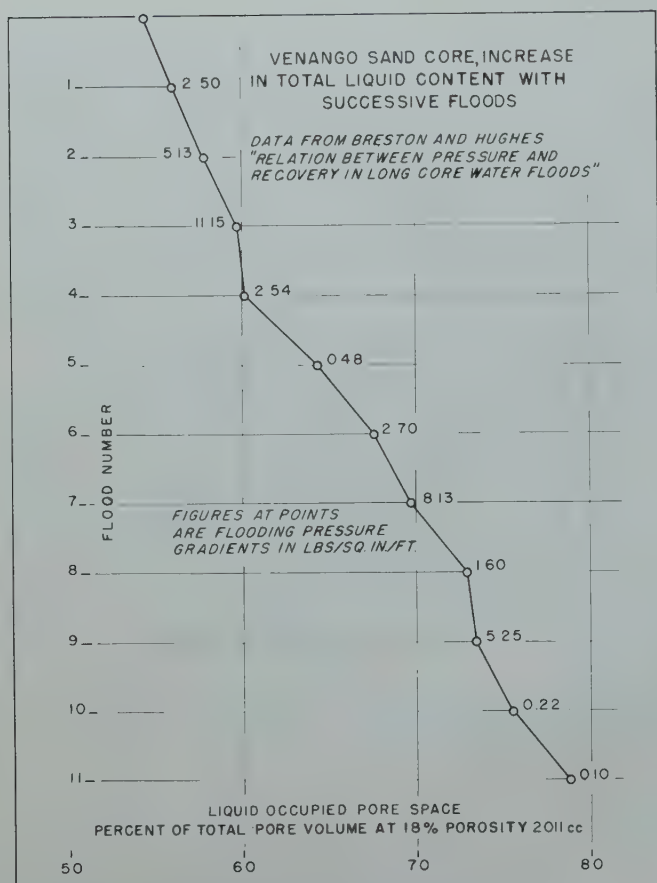


FIG. 8 — INCREASE IN TOTAL LIQUID CONTENT WITH SUCCESSIVE FLOODS

the data. The initial and final oil saturations for the eleven floods are plotted against each other as per cent of total pore volume. The dashed line was drawn through the points representing floods of approximately the same pressure gradient. An examination of the position of the points shows that those representing the high pressure gradient floods fall to the left of the curve and the low pressure gradient flood points fall to the right of the curve. The point for the extremely low pressure gradient flood (0.10 p.s.i./ft.) falls far to the right of the curve. Thus, it is shown that although the trend was to continuously higher residual oil saturation after each flood the effect of the pressure gradient of the flood on recovery and its attendant effect on residual saturation causes a deviation from this trend which is unmistakable.

Rushford Core Floods

The Rushford sand core was selected for similar flooding pressure gradient versus recovery experiments to see if a sand of markedly different characteristics would show the same relationships as indicated by the Venango core floods. The data summarizing the results of eight floods are found in Table II and illustrated graphically in Figs. 10 and 11. Unlike the case of the Venango sand core the total fluid content of this core did not change very much from flood to flood. As a result a direct relationship between pressure gradient and residual oil saturation was obtained as shown in the Figs. As in the case of the Venango core, lower residual saturations are obtained at the higher pressure gradients. The curves plotting per cent of initial oil content recovered versus pressure gradient show the same relationship. Inasmuch as the 100 to 1 produced water to oil ratio point was difficult to determine accurately for the floods on the Rushford core, the curves in Fig. 11 could not be located with certainty.

TABLE II

Summary — Flooding Rushford Sand Core

Size — 12" x 4 $\frac{1}{8}$ ", Air Permeability 15.3 md., Brine Permeability 2.55 md.

Operation	Pres. Grad. psi/ft.	Flood Veloc. ft./D	Oil Water at end cc.	Total Oil Content at end cc.	Percent of Initial Oil Content Recovered		Residual Oil Saturation Percent of Total Liquid Saturation		Percent of Total Oil Recovered up to Water Breakthrough
					to Water Breakthrough	to 100/1 Water Oil Ratio	to Water Breakthrough	to 100/1 Water Oil Ratio	
Brine Saturation			363.0	0					
1st Oil Saturation			450.5	306.0					
1st Brine Flood	49.5	1.7	425.0	129.5	54.5	57.6	32.7	30.5	94.6
2nd Oil Saturation			460.5	300.5					
2nd Brine Flood	7.0	0.21	449.0	152.0	41.2	48.4	39.3	34.5	85.2
3rd Oil Saturation			490.0	319.0					
3rd Brine Flood	29.0	2.0	488.0	164.0	44.0	47.6	36.6	34.2	92.5
4th Oil Saturation			495.5	314.5					
4th Brine Flood	5.5	0.23	497.5	173.5	37.8	44.8	39.3	34.9	84.4
5th Oil Saturation			490.5	309.5					
5th Brine Flood	19.5	1.00	492.5	154.0	43.0	48.8	36.8	32.2	88.1
6th Oil Saturation			503.0	318.5					
6th Brine Flood	40.2	2.32	495.5	144.0	44.4	53.1	35.5	30.0	83.6
7th Oil Saturation			508.5	320.5					
7th Brine Flood	10.25	0.45	516.5	161.5	42.7	48.6	35.5	31.8	87.9
8th Oil Saturation			542.5	332.5					
8th Brine Flood	1.02	0.04	(542.5)		33.1	39.1	(41.0)	(37.3)	(84.6)

Figures in parentheses are estimated from incomplete flood.

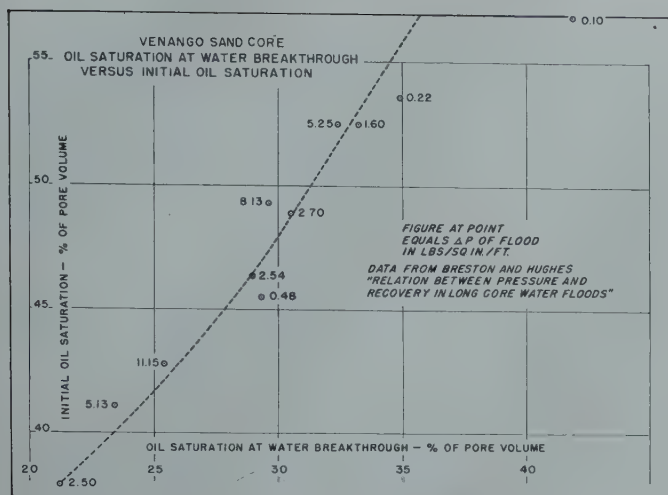


FIG. 9 — OIL SATURATION AT WATER BREAKTHROUGH VS. INITIAL OIL SATURATION

GENERAL DISCUSSION

Results of long core water flood research reported upon by Morse and Yuster and by Holmgren are of particular interest with respect to the work described above.

Morse and Yuster¹⁴ also used long cores from the Venango sand of the Franklin, Pa., mine. Some of their floods were started with 100 per cent oil saturations and others with representative percentages of connate water present. Pressure gradients covered those used in the present study. During 42 water floods there was no relationship indicated between flooding pressure gradient and residual saturation. Examination of the data presented by them also fails to show any relationship between flooding pressure gradient and percentage of original saturation recovered.

Fig. 7 shows the accumulative oil recoveries for the eleven Venango core floods plotted against time. The semi-log scale was used to avoid an extended graph. Curves drawn through the water breakthrough points and the points representing a produced water-oil ratio of 100 to 1 clearly show that higher percentages of recovery were obtained at the higher flooding pressure gradients. Holmgren¹⁵ has presented similar accumulative production-time curves for five of his long core water floods at varying pressure gradients. Fig. 12 is a reproduction of his figure with an added curve drawn through what may be assumed to be the water breakthrough points. If Holmgren's first flood is disregarded, the trend of the added curve also indicates higher percentages of recovery with higher flood pressure gradients which is contrary to the preliminary conclusions stated in his paper. The recovery obtained from his first flood may have been abnormally high and analogous to those obtained during the first two floods with the Venango core and the first flood with the Rushford core.

Past practices of plotting residual saturation against flooding pressure gradient may have caused conflicting interpretations of recovery versus pressure gradient because the cores were

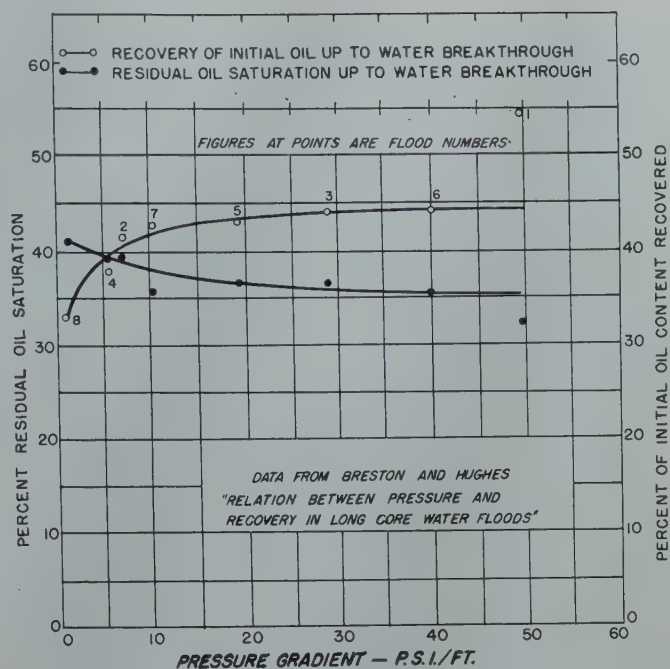


FIG. 10 — RUSHFORD SAND CORE. EFFECT OF PRESSURE GRADIENT ON RECOVERY TO WATER BREAKTHROUGH

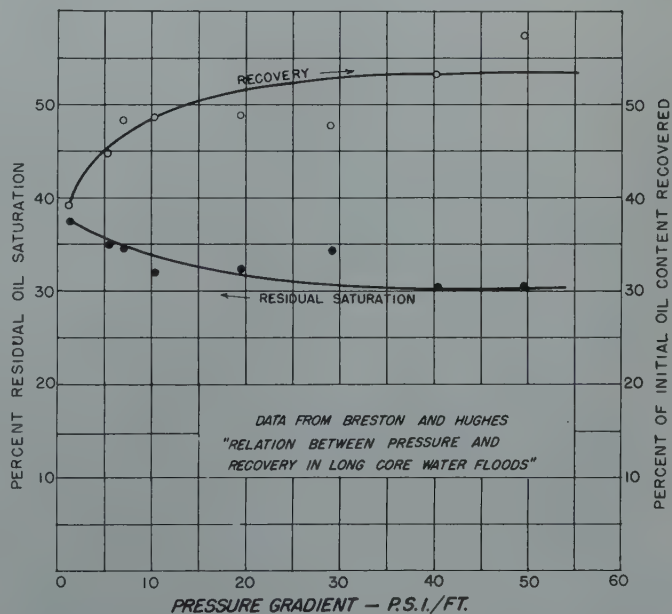


FIG. 11 — RUSHFORD SAND CORE. EFFECT OF PRESSURE GRADIENT ON RECOVERY UP TO 100 TO 1 PRODUCED WATER TO OIL RATIO

flooded only once before extraction and resaturation. It has been noted in the case of the Venango core that abnormally high recoveries were obtained on the first and second floods. Recovery from the first flood was greater than for the second even though the initial oil saturation of the core was less the first time. This indicates that the oil injected into the core during the first and second saturations penetrated only into the larger and more accessible pores from which it could be most easily flooded by the subsequent brine floods. Further saturation or additional saturations under pressure would be expected to force more of the oil and/or water into the smaller pores where it is logical to expect the effect of pressure gradients upon recoveries to be more pronounced.

As concluded by Earlougher¹² there apparently is a relationship between the relative amount of oil and water and its distribution within the sand and the amount that can be recovered by water flooding at a given pressure gradient. The distribution of the oil content of the sand both prior to and after water flooding is chiefly a function of the relative size and distribution of the pore restrictions. The smaller the restrictions the greater the pressure gradient necessary both to saturate all such pores and to flood contained oil from them.

simulate flood conditions as closely as possible, the same pressure gradients and flood velocities covering the ranges considered normally occurring in field operations were used. Also, a live natural crude was used for saturating the cores, as well as a natural brine for connate water content and for flooding. With the exception of the first three floods conducted a definite relationship between flooding pressure gradient and recovery has been shown in that higher flooding pressure gradients have given higher recoveries and lower residual oil saturations. As velocity is a direct function of pressure gradient, it has been shown also that higher rates of flooding resulted in higher percentages of recovered oil. Very low pressure gradients and flooding velocities resulted in markedly low recoveries.

The observations made during and as a result of these flooding experiments are not to be interpreted that every type of sand which can be water flooded will produce the maximum yield of oil at high pressure gradients. There may very well be an optimum pressure for many sands depending upon their physical and chemical characteristics and upon the ratio and mode of distribution of their water and hydrocarbon content. Proper pressure gradients for field use are still difficult to predict.

SUMMARY AND CONCLUSIONS

Nineteen laboratory floods on two long, consolidated sand cores were conducted to determine the effect of pressure gradient and/or flood velocity on oil recovery. In an attempt to

ACKNOWLEDGMENTS

These water flooding experiments were carried out as part of the overall secondary recovery research program of the Pennsylvania Grade Crude Oil Association in its laboratory at

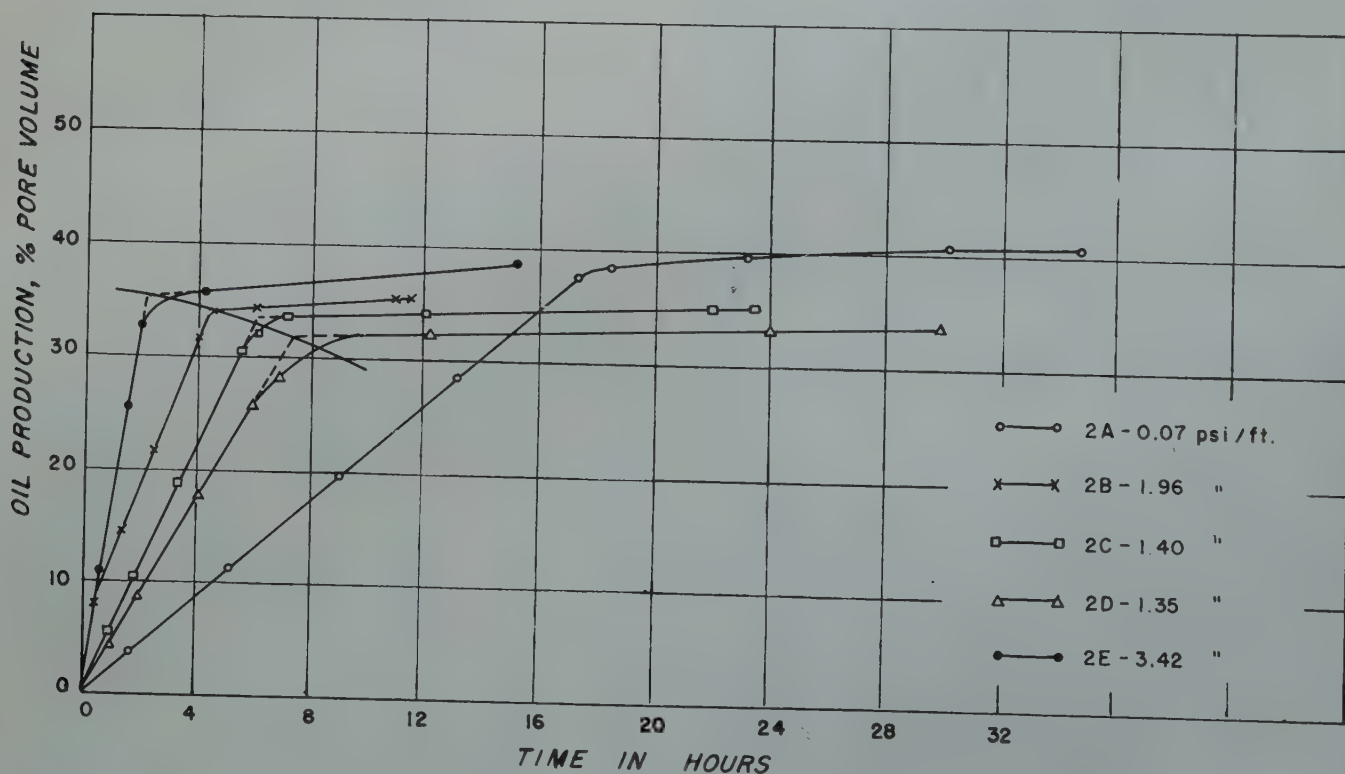


FIG. 12 — WATER DRIVE EXPERIMENTS, GROUP II (FROM HOLMGREN)

Bradford, Pa. The authors wish to express their appreciation and thanks to the many individuals and staff members who have aided in or otherwise made possible the conducting of these experiments. Particular thanks are due to Dr. R. J. Pfister, who formerly directed the Association's laboratory research, and to Willard Johnson, who ably assisted at all times during the experiments.

REFERENCES

1. Umpleby, Joseph B., "Increasing the Extraction of Oil by Water Flooding," *Petrol. Dev. and Tech. AIME*, (1925) pp. 112-129.
2. Torrey, Paul D., "Some Factors Influencing Production of Oil by Flooding in the Bradford and Allegany Fields," *AIME Tech. Pub. No. 39*, (1927).
3. Russell, William L., "Some Preliminary Experiments on Oil Recovery Processes," Circular No. 8, New York State Museum, Nov. 1932.
4. Ryder, H. M., "Effects of Higher Flooding Pressures," *Prod. Monthly*, Vol. II, No. 2, pp. 21-22, Dec. 1937.
5. "Economic Technology of the Water Drive—Its Application to Encroachment Water and Water Flooding," *Prod. Monthly*, Vol. VI, No. 8, pp. 12-26, June 1942.
6. "\$100,000,000 Increase Available in Bradford's Future Income," *Prod. Monthly*, Vol. VII, No. 2 pp. 12-18, Dec. 1942.
7. "Effect of Increase in Water Pressure on Water Flood Production," *Prod. Monthly*, Vol. XI, No. 7, pp. 18-26, May 1947.
8. Yuster, S. T., "Pressures in Water Flooding," *Prod. Monthly*, Vol. III, No. 11, pp. 25-27, Sept. 1939.
9. "Some Laboratory Studies and Their Field Application in Secondary Recovery," *Prod. Monthly*, Vol. VI, No. 10, pp. 8-11, Aug. 1942.
10. Parsons, R. L., "The Recovery Efficiency of a Water Drive as a Function of the Rate of Advance of the Oil-Water Interface," Grad. Thesis, Mech. Eng. Dept., Univ. Calif., 1940.
11. Miller, Frank G., "A Laboratory Study of Water Encroachment in Oil-Filled Sand Columns," R. I. 3595, U.S.B.M., October 1941.
12. Earlougher, R. C., "Relationship Between Velocity, Oil Saturation, and Flooding Efficiency," *AIME Trans.*, Vol. 151, pp. 125-137, 1943.
13. Calhoun, J. C., McCormick, R. L., and Yuster, S. T., "The Effects of Pressure Gradients and Saturations on Recovery in Water Flooding," *Prod. Monthly*, Vol. IX, No. 1, pp. 12-17, Nov. 1944.
14. Morse, R. A., and Yuster, S. T., "Water Flood Tests on Long Cores," *Prod. Monthly*, Vol. XI, No. 2, pp. 19-24, Dec. 1946.
15. Holmgren, C. R., "Some Results of Gas and Water Drive on a Long Core," *AIME Petr. Tech.*, July 1948.



DISCUSSION

By Harry M. Ryder, Consulting Engineer, Washington, D. C.

The problem attacked by the authors is of greatest fundamental importance to petroleum reservoir engineers. In work of this type, the simulation of field conditions is very important. The effort on the part of the authors is commendable but the extent to which simulation was in fact achieved is not evaluated. The old oil in both cores had been exposed to oxidation for extended periods prior to their use for the experimental work. The presence of oxidized organic material can affect interfacial conditions and may or may not have appreciably influenced the water-flood characteristics. The mean pressures used were very much lower than those usual in the field.

The percentage of the initial oil content recovered is not necessarily a measure of the effectiveness of a water drive. Extensive field observations at Bradford have provided no indication that the residual oil saturation is a function of the initial oil saturation. A flood which will leave 25 per cent of the pore space occupied with oil is equally effective whether the initial oil content is 90 per cent or 40 per cent of the pore space, but the per cent of the oil removed in the former case is far greater than in the latter. The residual oil saturation as per cent of pore space is the fairest criterion of flood effectiveness.

After the first two runs, the pore-filling behavior in the Rushford-sand core was much better than in the case of the Venango sand. In Fig. 1 the residual oil saturation is plotted

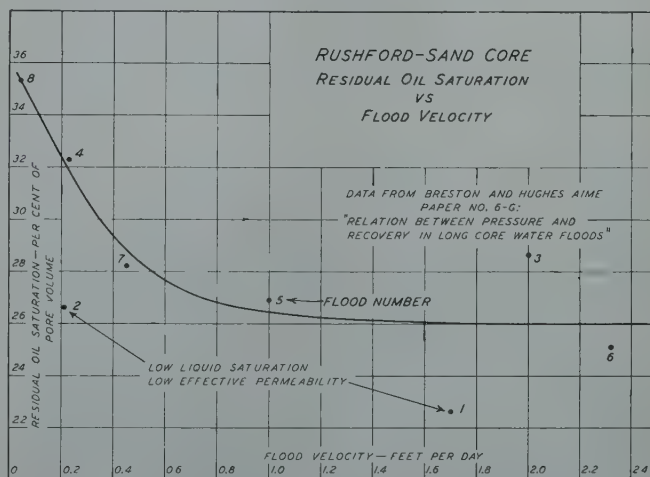


FIG. 1 — RUSHFORD SAND CORE, RESIDUAL OIL SATURATION VS. FLOOD VELOCITY.

directly against flood velocity. Disregarding the first two floods because of low total liquid content and corresponding low effective permeability, this curve strongly suggests an economically important increase in flood effectiveness with increasing velocity up to about one foot per day and under the circumstances of the investigation. A theory as to why this should be so has been reported.¹ The potential economic importance of this relation may the better be understood when it is realized that a large part of the Bradford field oil is produced as a result of flooding at a velocity of less than three inches per day, only a small part being produced at a velocity in excess of one foot per day.

Whether pressure or velocity in fact exercises a dominant control over residual oil saturation, and hence over flood effec-

tiveness, other factors being constant, can be determined only by comparative flood tests. For such tests, several long cores should be used, identical in every respect except for different permeabilities. The authors could contribute to this knowledge by flooding additional Rushford-sand cores of different permeabilities.

REFERENCE

1. Harry M. Ryder: Effect on Production of Fluid Distribution and Relative Permeability in Sand. *World Oil*, vol. 128, No. 2, June 1948, p. 142.

Author's reply to Harry M. Ryder

The authors greatly appreciate Ryder's remarks and his added analysis of the data reported.

We were aware of the fact that the presence of oxidized organic material may affect interfacial conditions and perhaps appreciably influence the water-flood characteristics. In order to eliminate or minimize such a possibility the cores were well

"flushed" by flowing through under pressure a goodly number of pore volumes of fresh, live crude before completing the first saturation. The first portion of the effluent crude was dark and viscous showing that much of the oxidized organic material was being removed.

Due to the pressure limitations of the apparatus the mean absolute pressures used were lower than those usual in the field. However, since the experiments were conducted on a basis of 100 per cent fluid saturation; i.e., no free gas, it was only necessary to maintain a pressure slightly in excess of the bubble point of the saturating crude. The pressure gradients used did cover the range common in the field.

Since the cores were saturated each time to the same water-oil ratio content, calculating the recoveries as percentage of the initial oil content automatically corrected for the changing total fluid content. It is the same as calculating the effectiveness of the water floods on a basis of residual oil saturation as per cent of effective pore volume if the effective pore volume is considered to be equal to the total fluid saturation at the time.

★ ★ ★

DISCUSSION OF THIS AND ALL FOLLOWING TECHNICAL PAPERS IS INVITED

Discussion in writing (3 copies) may be sent to the Editor, *Journal of Petroleum Technology*, 601 Continental Building, Dallas 1, Texas, and will be considered for publication in the Transactions volume *Petroleum Development and Technology*. Discussion will close December 15, 1949. Any discussion offered thereafter should be in the form of a new paper.

THEORETICAL GENERALIZATIONS LEADING TO THE EVALUATION OF RELATIVE PERMEABILITY

WALTER ROSE, JUNIOR MEMBER AIME

GULF RESEARCH & DEVELOPMENT CO., PITTSBURGH, PENNSYLVANIA

ABSTRACT

Theoretical expressions are presented to describe wetting and non-wetting phase relative permeability relations. These expressions have then been compared with existing published data, the conformance noted being sufficiently good to satisfy the requirements of some engineering use. As a consequence, it may be supposed that relative permeability characteristics of porous media now can be inferred from basic core analysis data, in a manner more convenient (although less direct) than presently available methods of experimental evaluation.

INTRODUCTION

This paper presents a new approach to the problem of relative permeability evaluation. A classification of published discussions of relative permeability concepts which have appeared in the petroleum literature will show that previously emphasis has been placed on methods of experimental measurement, on the interpretation of the data so obtained with respect to the variable properties of the system, and on theoretical and practical considerations which relate relative permeability to gross fluid behavior in petroleum reservoirs. Essentially, no detailed examination has appeared which treats the fundamental factors controlling the quantitative features of the relative permeability relation*, although cer-

tain references can be cited^{1,2,3,4,5,6,7} where a qualitative awareness of their existence and nature is indicated. This condition is explainable in terms of the recognized complexity of the problem, and in order to provide some basis for theoretical development, the general emphasis has been placed in the past on experimental procedures of evaluation, the validity of which, in principle, could be confirmed by the analysis of well and reservoir performance. However, because of the experimental difficulties which have been encountered (notably, difficulties due to the so-called "end effects"), and because of the general unreliability of field performance tests required to study the applicability of the data, relative permeability phenomena continue to be incompletely understood and described.†

In this paper is examined the possibility of predicting relative permeabilities entirely from fundamental considerations. In addition, attention is called to certain important factors, previously unemphasized in the published literature, which now can serve as a basis for the eventual experimental confirmation of this and similar theoretical approaches, as well as the experimental solution of the problem in general. Therefore, the analysis presented herein has the dual purpose both of orienting future experimental activity and also of providing an immediate solution for the relative permeability problem, sufficiently adequate for some engineering use. It will be seen that the conclusions reached are supported by theoretical and intuitive considerations, and they are not contradicted insofar as gross features are concerned by existing concepts and interpretations of published experimental data, except as specifically noted.

Darcy's law, expressed simply as:

$$q = \frac{k}{\mu} \frac{dp}{dx} \quad \dots \dots \dots (1)$$

where q is linear rate of flow (assumed horizontal), k is the

* Intuitively, at least, we may suspect that the factors controlling the quantitative features of relative permeability relations (where relative permeability of porous media to given fluid phases is plotted as function of the saturation of these phases) will be describable in terms of basic rock texture and in terms of the character of the distribution of the immiscible fluids within the interstitial spaces. The term basic rock texture is used here to refer to the pore configurational characters dependent on factors such as grain sizes and packing as modified by cementation and other secondary processes. It will be realized that there are other factors of importance which in practical instances also will control the quantitative features of the relative permeability relation, such as those related to the various possibilities for variable interaction between the saturating fluids and the surfaces of the interstitial spaces. Thus, interstitial clays can be responsible for variable conditions of pore configuration obtaining in a given instance depending upon the nature of the saturating fluids. Variable conditions of preferential wettability also can obtain expressive of analogous possibilities in ways which will control heterogeneous fluid flow behavior. For the purposes of this paper, however, fixed pore configurational and wettability characters will be assumed. Moreover, no attempt will be made to establish explicitly a dependence of relative permeability on strictly fluid properties.

Manuscript received at Petroleum Branch office April 28, 1948. Presented at Petrol. Fall Meeting, October 4-6, 1948.

References are given at end of paper.

† The poor comparison usually obtained between laboratory and field gas-oil ratios (c.f., Fig. 4 of paper by L. E. Elkins⁸) is illustrative of conditions which discourage unqualified acceptance of the results of previous studies except as presently useful approximations. In this connection, Evinger and Muskat⁹ have discussed in detail the discrepancy observed between field well productivity values and values obtained from the analysis of laboratory flow data.

permeability constant, μ is fluid viscosity, and dp/dx is the pressure gradient, defines completely the viscous flow of homogeneous fluids through porous media of uniform cross section. The permeability constant, k , then is an expression of the properties of a particular porous body which collectively require fluid flow to be controlled by fluid viscosity and pressure gradient in the manner indicated by Eq. (1). Now, in media variously saturated with two or more immiscible continuous fluid phases Darcy's law will still define the dynamic character of flow for each phase separately, if effective permeability constants are properly defined as functions of the distributions of the various saturating fluids. This point of view follows that accepted by Richards¹⁰, who considered the presence of one fluid saturating a porous body merely as a factor which controlled (in the same manner as the structure of the porous body itself) the geometry of the paths available for flow to another immiscible fluid simultaneously saturating the porous body. The analysis to follow requires assuming, as a simplification, steady state flow with the fluid phase saturation distribution uniformly constant during the time interval of measurement; and in the study of reservoir behavior this usually can be done rigorously, at least in principle, by selecting sufficiently small elements for consideration wherein the macroscopic flow character is nonetheless retained. Under such conditions, the observed effective permeabilities become significant constants functionally related to the saturation distribution in addition to the other porous body properties which, as noted above, themselves control completely the dynamic aspects of single-phase (homogeneous fluid) flow.

In developing the basis for the analysis to follow where relative permeability will be explicitly related to saturation distribution characters attention is called to certain previous attempts which have been made to relate specific and effective permeability to various rock properties. Traxler and Baum¹¹ defined specific permeability in terms of average pore radius, and Leverett² attempted to apply this concept to relative permeability. Hassler¹⁴ and Botset³ also discussed this supposed relationship, although none of these authors presented an exact definition of pore distribution, and Leverett¹² finally discarded the notion altogether because of the complicating factors related to saturation hysteresis effects. In this connection, Haines¹³, and more recently, Leamer and Lutz¹⁴ and Ritter and Drake¹⁵ showed the usefulness of relating pore distribution to the differential plot of the capillary pressure type relation,[‡] implying the possibility of deriving relative permeability relations therefrom, although this has not yet been entirely accomplished. Carman¹⁶ and others used the Kozeny equation in defining permeability in terms of surface area, porosity, and rock texture, and Krumbein¹⁷ and others have discussed the relationship between permeability and grain size parameters. The recent work of Brownell and Katz⁵ considers the connection between relative and specific permeability as based on correlations developed from existing data. Their approach

[‡] That is, the plot of some function of the fluid phase distributions versus some measure of the capillary pressure obtaining at the interfaces between phases (e.g. the interfacial curvature, or the height of the interface above some reference level of zero curvature, etc.).

[§] c.f. discussion following Eq. (9).

holds great promise, at least for engineering use, particularly if examination of newer data as they become available substantiates the general applicability of their correlations.

These attempts to explicitly relate permeability functions to rock properties can be expressed by the following analytical reasoning. Permeability can be defined functionally as:

$$k = F(T) \quad (2)$$

That is, there are a series of rock properties collectively represented by the symbol T which control permeability according to the prevailing physical requirements of the system. In general, the function, $F(T)$, will be known in simple systems (e.g., capillary tube), whereas it will be only partially or imperfectly known in more complex systems (e.g., petroleum reservoir rock). In practice this is a serious limitation to the extent that the approximations which are discovered to apply under one set of conditions become invalid under slightly different conditions such that empirical generalization is impossible. By analogy the effective permeability, k_e , can also be considered as formally defined in terms of other functions of rock properties, where at least one function of particular importance involves the fluid phase saturation distribution, or:

$$k_e = F_e(T_e, \rho), \quad (3)$$

where ρ is employed here to denote the saturation distribution of the fluid phases. The relative permeability, k_r , then can be expressed as:

$$k_r = \frac{k_e}{k} = \frac{F_e(T_e, \rho)}{F(T)} \sim F_r(\rho) \quad (4)$$

Eq. (4) calls attention to the simplification employed in the present treatment of relative permeability, which involves describing all of the properties of the system (responsible for the specific permeability in single phase flow) as implicit functions of saturation in polyphase flow. Therefore, the saturation (or more properly, the saturation distribution) explicitly becomes the only variable controlling relative permeability in polyphase flow, and this concept is developed in the paragraphs to follow. For example, the "effective" porosities* which contribute to the separate elements of polyphase flow can be related to the total porosity responsible for single phase flow according to the character of the prevailing saturation distributions in the polyphase system. Assuming for the moment, for illustrative purposes, that effective porosities and total porosity are the only factors which determine effective permeability and specific permeability respectively, a ratio of these factors as defined in terms of a saturation function will then serve uniquely as an expression for relative permeability.

Having now indicated a need for detailed examination of relative permeability concepts and having suggested a basis for the necessary analysis, extensions will be made below to provide a definition of relative permeability in terms of known saturation parameters. The development as presented in the next section applies principally to a consideration of the *wetting phase* relative permeability relation, although elsewhere in this paper it is shown that non-wetting phase relations and three phase relations also can be inferred, at least approximately, in a similar and related manner.

* Effective porosity is herein defined as the saturation of a phase under consideration per unit of bulk volume.

DEVELOPMENT OF THE GENERALIZED EXPRESSION FOR WETTING PHASE RELATIVE PERMEABILITY

In a recent paper³¹ the author investigated some of the possible applications of capillary pressure data, and arrived at the following equation for wetting phase relative permeability, as:

$$k_{rw} = \rho_w \left(\frac{P_D}{P_C} \right)^2 \quad \dots \quad (10)$$

Now, in order to contribute to a fuller interpretation of the theoretical considerations; to compensate for notational differences occurring in this paper and the above mentioned Rose and Bruce paper (loc. cit.); and to allow the desired emphasis of dynamical rather than static considerations of fluid behavior, the development of Eq. (10) will be reviewed as follows:

According to common usage the Kozeny equation for a single phase flow can be expressed as:

$$k = \frac{f}{A^2 t} \quad \dots \quad (5)$$

where f is the fractional porosity, A is the specific internal surface area of the pores (per unit of pore volume, and t is a dimensionless rock textural constant related to the shape and orientation (tortuosity) of the pores. Carman¹⁸ later, in studying the properties of unconsolidated sands, established empirically that:

$$A = \frac{P_D}{\sigma} \quad \dots \quad (6)$$

where P_D is the displacement pressure, and σ is the interfacial tension. Eqs. (5) and (6) can be combined to yield:

$$k = \frac{f \sigma^2}{P_D^2 t} \quad \dots \quad (7)^\dagger$$

Now, considering the wetting phase effective permeability (k_{ew}) in a polyphase flow system it can be argued by analogy to Eq. (7) that:

$$k_{ew} = \frac{f_{ew} \sigma^2}{P_C^2 t_{ew}} \quad \dots \quad (8)$$

where the effective porosity, f_{ew} , is defined as noted above; and where P_C , the capillary pressure, is accepted as being the effective displacement pressure characterizing the partially saturated system. The effective rock textural constant, t_{ew} , has not been evaluated as yet, and therefore, for the purposes of this analysis it will be assumed that $t_{ew} = t$ throughout the

saturation range of interest.[‡] These assumptions made for expediency, however, can be supported by the fact that a plausible conclusion is eventually obtained, as will be seen below. In any event, simply dividing Eq. (8) by Eq. (7) yields an expression for wetting phase relative permeability, k_{rw} , namely:

$$k_{rw} = \frac{k_{ew}}{k} = \left(\frac{f_{ew}}{f} \right) \left(\frac{P_D}{P_C} \right)^2 \left(\frac{t}{t_{ew}} \right) \quad \dots \quad (9)$$

which leads to Eq. (10) since $t = t_{ew}$ has been assumed, and since $\frac{f_{ew}}{f} = \rho_w$.

Eq. (10) can be differentiated to yield:

$$\frac{dk_{rw}}{d\rho_w} = k_{rw} \left(\frac{1}{\rho_w} + \frac{2}{r D_r} \right) \quad \dots \quad (11)$$

where:

$$D_r = \frac{d\rho_w}{dr} = - \frac{P_C}{r} \frac{d\rho_w}{dP_C}$$

is the pore radii distribution coefficient according to Ritter and Drake (loc. cit.), and r is the pore radius (i.e. a pore width) which under a given condition of saturation (ρ_w) contains the interfaces between the non-wetting and wetting phases.[§] Eq. (11) supports the view mentioned above that the relative permeability-saturation relation depends on the distribution of pores in the system being considered.

Actually, Eq. (10) can be derived more fundamentally by combining the Darcy and the Poiseuille equations for fluid flow in the manner suggested by Traxler and Baum (loc. cit.) to yield:

$$k = \frac{f r^2}{\text{const.}}$$

where r is presumed to be an average pore radius of the hypothetical system of capillary tubes equivalent to the porous media actually being considered. By analogy, then, an expression for effective permeability in terms of an effective porosity and a similar effective average pore radius can be derived, which on combination with the above expression for specific permeability yields an expression for relative permeability as:

$$k_r = \rho \left(\frac{r_e}{r} \right)^2 \quad \dots \quad (10a)$$

where r_e refers to the average pore radius of that portion of the system containing the phase under consideration having a saturation, ρ . To the extent that the ratio $(r_e/r)^2$ is related to the distribution of fluids within the interstitial spaces, Eq. (10a) shows how relative permeability depends both on phase saturation and distribution. In order to illustrate the significance of Eq. (10a) Curves E and F (as applied to non-wetting

[†] Although according to the derivations of Eq. (5), (6), (7), . . . these relations apply strictly to unconsolidated systems [c.f. Sullivan and Herte¹⁹ point out, for instance, that "where the media are consolidated, or where the media contain bridging, agglomeration or considerable channeling" there is some question as to the applicability of Eq. (5)], it is assumed that suitable adjustment of the rock textural constant, t , will make these relations applicable to a consideration of consolidated systems. Carman has recently discussed the applicability of Eq. (5) to consolidated porous media.³³

[‡] The constant, t , is defined fundamentally¹⁹ as a product of dimensionless pore shape and orientation factors. This could suggest that t_{ew} characterizing a polyphase system is approximately equal to the t characterizing the equivalent single-phase system in the sense that the incidental presence of a non-wetting phase does not appreciably alter the configurational properties of the pores containing the wetting phase, although its presence does reduce the porosity available for wetting phase saturation.

[§] Note, a plot of r versus ρ_w will exhibit the same hysteresis effects observed in the capillary pressure-saturation relation.

and wetting phase relative permeability respectively) are presented in Fig. 6, as calculated for a hypothetical case where it is assumed that a normal probability distribution of pores obtains and that at any given phase saturation condition the wetting phase is always contained in the smallest pores and the non-wetting phase is always contained in the largest pores. The shapes of these Curves E and F in Fig. 6 will be referred to later. In any event, it is noted that when considering wetting phase relative permeability Eq. (10a) reduces to Eq. (10) if use is made of the following well-known relations:

$$P_D = F(\sigma/r) \quad \text{and} \quad P_C = F(\sigma/r_s).$$

In order to solve Eq. (10) it is necessary to have available pressure versus saturation data such as are obtained in capillary pressure (static) experiments or displacement (dynamic) experiments.* It will be shown now, however, that a more general solution of the wetting phase relative permeability versus saturation relation can be derived, where the relative permeability is entirely described in terms of explicitly known saturation parameters. This has been accomplished conveniently by observing the properties of the family of curves produced by plotting the dimensionless group:

$$\phi(\rho_w) = \rho_w \left[\frac{P_D}{P_D + \int_{\rho_w}^1 P_C d\rho_w} \right]^2 \quad (12)$$

versus the wetting phase saturation, ρ_w .† The dimensionless group, $\Phi(\rho_w)$, itself was evolved by treating the Kozeny equation (Eq. (5)) in a manner similar to the derivation of Eq. (10) from Eq. (7); that is, by assuming $t = t_{ew}$ through the saturation range of interest, and by recognizing that: $f_{ew}/f = \rho_w$. Thus, by analogy to Eq. (5):

$$k_{ew} = \frac{f_{ew}}{A_{ew}^2} \frac{1}{t_{ew}} \quad (13)$$

or:

$$k_{rw} = \rho_w \left(\frac{A}{A_{ew}} \right)^2,$$

where A_{ew} may be regarded as the effective surface separating the wetting phase from all other elements of the system. Comparison of Eq. (13) with Eq. (10) shows that:

$$A_{ew} = \frac{P_C}{\sigma} \quad (14)$$

* It is developed later in this paper that terms which are the dynamic equivalents of capillary and displacement pressure can be substituted in Eq. (10) to define dynamically the relative permeability relation. The necessity of this extension is suggested by examining, for instance, Leverett's capillary pressure and relative permeability data obtained on unconsolidated sands.^{2,12} It will be seen that these data are not interrelated through Eq. (10), since the capillary pressure data describe fluid distribution in Leverett's systems under static conditions and the relative permeability data pertain specifically to dynamic conditions. In order, then, to employ Eq. (10) it is necessary to know the capillary pressures obtaining at the interfaces under the dynamic conditions of fluid phase distribution in the flowing system. The fact that these conditions of fluid distribution exhibit hysteretic behavior suggest that the relative permeability relation itself will be characterized by a related hysteresis, one limit of which it may be supposed will be that described by Eq. (10) when static capillary pressure data are substituted therein.

† It may be noted that Eq. (12) and the general considerations given here leading to its development but with special emphasis on its implications with respect to capillary pressure phenomena have also been presented by Rose and Bruce.²¹

is a reasonable definition for this effective surface area, § analogous to Carman's definition of specific surface area, (cf. Eq. (6)).

Eq. (13) also suggests the importance of the function $\Phi(\rho_w)$ on identifying A_{ew} with:

$$A + \frac{1}{\sigma} \int_{\rho_w}^1 P_C d\rho_w = \frac{P_D}{\sigma} + \frac{1}{\sigma} \int_{\rho_w}^1 P_C d\rho_w,$$

where:

$$\frac{1}{\sigma} \int_{\rho_w}^1 P_C d\rho_w$$

is the interfacial surface area previously defined by Leverett.¹²

It will be noted from Eq. (12) that $\Phi(\rho_w)$ has the following properties:

$$\lim_{\rho_w \rightarrow 1} \frac{d}{d\rho_w} \Phi(\rho_w) = 3,$$

since:

$$\lim_{\rho_w \rightarrow 1} \Phi(\rho_w) = 1, \text{ and } \lim_{\rho_w \rightarrow 1} P_C = P_D \quad (15)$$

Also:

$$\lim_{\rho_w \rightarrow \rho_{w1}} \Phi(\rho_w) = 0,$$

if it is assumed that:

$$\lim_{\rho_w \rightarrow \rho_{w1}} P_C = \lim_{\rho_w \rightarrow \rho_{w1}} \int_{\rho_w}^1 P_C d\rho_w = 0,$$

where the irreducible minimum wetting phase saturation, ρ_{w1} is defined as:

$$\lim_{k_{rw} \rightarrow 0} \rho_w = \rho_{w1}$$

Fig. 1 shows a plot of $\Phi(\rho_w)$ versus ρ_w obtained from capillary pressure data, as previously presented in the cited literature references^{4,12,20,21,22}. The general conformance of these experimental curves to the above outlined limiting conditions suggests the possibility of explicitly relating $\Phi(\rho_w)$ to the saturation parameters ρ_w and ρ_{w1} . This has been accomplished in the following manner.

First, the analogy between an assemblage of capillary tubes and porous systems of the type which constitute petroleum reservoir rock is accepted as applicable to the purposes of this analysis (cf. Brownell and Katz⁵ have recently stated a similar

§ Comparison of Eq. (13) with Eq. (10) implies that the effective surface area, A_{ew} , increases indefinitely as the wetting phase saturation is decreased to its minimum value. This simply means that in the process of desaturation the wetting phase is confined to smaller and smaller pores where the surface to volume ratio becomes larger and larger.

view, as have numerous others previously). It is further supposed that all porous systems of the type being considered can be classed, according to their fluid behavior properties, as intermediate between the limiting systems described as uniform sized, uniformly oriented capillary tubes on the one hand, and random sized, randomly oriented capillary tubes on the other. These two limiting systems, abbreviated U.S.O. and R.S.O. respectively, can be analyzed in detail as follows:

The uniform sized, uniformly oriented system of capillary tubes (which is actually equivalent to a single capillary tube oriented in the direction of flow) has this character as defined in terms of capillary pressure concepts. The capillary pressure equals the displacement pressure for all values of saturation,[†] and the irreducible wetting phase saturation in zero. It follows then that:

$$\int_{\rho_w}^1 P_0 d\rho_w = P_D (1 - \rho_w),$$

Or, by Eq. (12):

$$\Phi(\rho_w)_{\text{U.S.O.}} = \frac{\rho_w}{(2 - \rho_w)^2} \quad \dots \quad (16)$$

Eq. (16) satisfies the limiting requirements of Eq. (15).

The random sized and oriented system of capillary tubes (R.S.O.) simply is characterized by the fact that $\rho_{wi} = \frac{2}{3}$,

since it is supposed that the random orientation reduces two-thirds of the pore volume effectively to *cul-de-sac* porosity (i.e., porosity which cannot be invaded by the non-wetting phase since the zero permeability conditions prevent the escape of the wetting phase therefrom).^{*} Now, it is observed from Eq. (15) that the intercept on the ρ_w axis of the tangent to

$$\lim_{\rho_w \rightarrow 1} \frac{d}{d\rho_w} \Phi(\rho_w) \text{ is also } \frac{2}{3} \text{ such that the curve}$$

$$\Phi(\rho_w)_{\text{R.S.O.}} = (3\rho_w - 2) \quad \dots \quad (17)$$

is taken as the most convenient definition for $\Phi(\rho_w)_{\text{R.S.O.}}$. It is readily verified that Eq. (17) also satisfies the requirements of Eq. (15).

The limiting functions $\Phi(\rho_w)_{\text{U.S.O.}}$ and $\Phi(\rho_w)_{\text{R.S.O.}}$ are shown in Fig. 1, and, as assumed above, data obtained on any porous system should yield $\Phi(\rho_w)$ versus ρ_w plots belonging to the family of curves intermediate to these limits and having the properties indicated by Eqs. (15). A suitable generalized expression for $\Phi(\rho_w)$ which fits the required conditions stated

[†] Starting with a completely saturated capillary tube a displacing pressure which is infinitesimally greater than P_D is required before the non-wetting phase can enter the capillary and produce a desaturation of the wetting phase. However, at any saturation condition between 1 and 0, the pressure difference between the phases arbitrarily can be set exactly equal to P_D , thereby establishing condition of static equilibrium, so that $\frac{dP_0}{d\rho_w} = 0$.

^{*} Klippenberg²³ in his analysis of homogeneous flow through an R.S.O. system makes a similar sort of an assumption.

above, and which serves as a basis for deriving the desired expression for relative permeability, is:

$$\Phi(\rho_w) = \frac{4(\rho_w - \rho_{wi})(1 - \rho_{wi})}{[(3\rho_{wi} - 2)\rho_w + (4 - 5\rho_{wi})]^2} \quad \dots \quad (18)$$

Eqs. (12) and (18) can now be combined to yield:

$$\frac{P_0}{P_D} = \frac{2\rho_w^2(2 - 3\rho_{wi}) + 3\rho_w\rho_{wi}(3\rho_{wi} - 2) + \rho_{wi}(4 - 5\rho_{wi})}{4\sqrt{\rho_w(1 - \rho_{wi})(\rho_w - \rho_{wi})^3}} \quad (19)$$

It will be observed that the conditions:

$$\lim_{\rho_w \rightarrow 1} P_0 = P_D \quad \text{and} \quad \lim_{\rho_w \rightarrow \rho_{wi}} P_0 = 00$$

are satisfied by Eq. (19). Combining Eq. (19) with Eq. (10), we obtain finally:

$$k_{rw} = \frac{16\rho_w^2(\rho_w - \rho_{wi})^3(1 - \rho_{wi})}{[2\rho_w^2(2 - 3\rho_{wi}) + 3\rho_w\rho_{wi}(3\rho_{wi} - 2) + \rho_{wi}(4 - 5\rho_{wi})]^2} \quad \dots \quad (20)$$

where Eq. (20) evidently reduces to the limiting values 1 and 0, as ρ_w approaches 1 and ρ_{wi} respectively.

While Eq. (19) has been developed primarily as an intermediate relationship for the purpose of deriving Eq. (20), it has the same type of validity as the empirical representation of capillary pressure data by the function $\Phi(\rho_w)$ plotted in Fig. 1. It is not suggested that Eq. (19) gives a universal description of capillary pressure curves, although, in contrast to other proposed empirical equations,[†] it satisfies all the basic

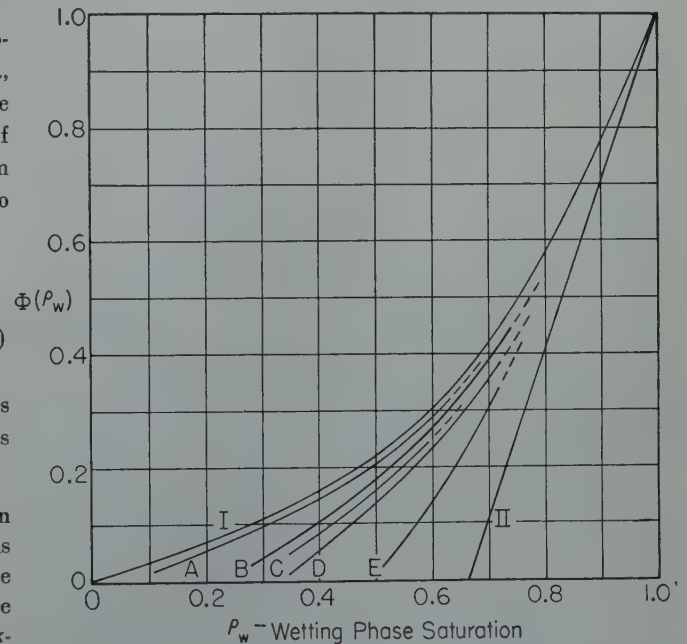


FIG. 1 — VARIATION OF THE RHO FUNCTION WITH WETTING PHASE SATURATION.

Curve I — Theoretical Curve applying to a U.S.O. system.

Curve II — Theoretical Curve applying to a R.S.O. system.

Curve A — Experimental Curve for Leverett's Sand III¹².

Curve B — Experimental Curve for an Ohio Sandstone.²⁰

Curve C — Experimental Curve for a Magnolia Limestone.²¹

Curve D — Experimental Curve for Thornton and Marshall "Well A".²²

Curve E — Experimental Curve for a California Sand.⁴

[†] c.f. for example, the equation of Hassler et al (loc. cit.).

physical requirements as expressed by Eq. (15). It is Eq. (20) which represents the immediate goal of the above outlined theoretical considerations. Its validity and usefulness will be discussed below.

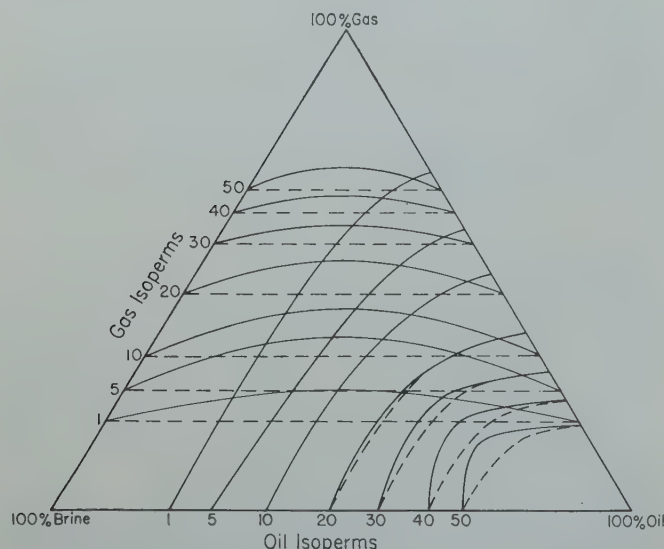


FIG. 2 — THREE-PHASE RELATIVE PERMEABILITY DIAGRAMS.
Solid Lines, Data of Leverett and Lewis.²⁴
Dashed Lines, Theoretical Gas and Oil Isoperms.
(Water Isoperms not shown.)

DISCUSSION OF RELATIVE PERMEABILITY CONCEPTS SUGGESTED BY AVAILABLE EXPERIMENTAL DATA

First, however, in order to develop the range of usefulness in which relationships of the type indicated by Eq. (20) can be applied to evaluate relative permeability, some consideration will be given to the published empirical results of previous workers. This is required, since the validity of Eq. (20) is not to be considered as rigorously proved by the above argument, so that conformance between theory and experiment is the only direct proof presently available. One danger in this approach to be noted and avoided stems from the uncertainty regarding the detail which justifiably can be employed in the examination of the data, since it is desired only to generalize on significant features independent of the experimental procedures followed and the experimental materials employed.[‡]

The data of Leverett and Lewis²⁴ which have been replotted in Fig. 2 for convenience provide an indication of the type of relative permeability relations which prevail in two and three phase systems. Although this work pertains specifically to the properties of unconsolidated media, the conclusions applying to two-fluid-phase systems are confirmed more or less by later studies of consolidated sand bodies. The conclusions applying to three-fluid-phase systems, however, have not yet been shown valid when applied to consolidated sands, and in the discussion to follow this fact is recognized to the extent that certain of the Leverett and Lewis statements about three-fluid-phase

systems will not be accepted simply because available data or intuitive argument does not require unqualified acceptance.

The data of Leverett and Lewis suggest that the following qualitative generalizations, expressed symbolically,[§] apply insofar as gross features are concerned to a consideration of the properties of a given porous body:

$$\frac{k_{rb}(\rho_b)}{b-g \text{ system}} = \frac{k_{rb}(\rho_b)}{b-o \text{ system}} = \frac{k_{rb}(\rho_b)}{b-o-g \text{ system}} \quad (21-1)$$

That is, the relative permeability to brine in a given porous body is independent of the fluid properties of the other saturating fluid(s) in those cases where brine is considered to be the wetting phase.

Also:

$$\frac{k_{rg}(\rho_g)}{g-b \text{ system}} = \frac{k_{rg}(\rho_g)}{g-o \text{ system}} > \frac{k_{rg}(\rho_g)}{g-o-b \text{ system}} \quad (21-2)$$

That is, the relative permeability to gas in two phase systems is independent of the nature of the wetting phase, and in three phase systems it is always less at a given saturation than in a two phase system.

Finally:

$$\frac{k_{ro}(\rho_o)}{o-g \text{ system}} < \frac{k_{ro}(\rho_o)}{o-b \text{ system}} < \frac{k_{ro}(\rho_o)}{o-g-b \text{ system}} > \frac{k_{ro}(\rho_o)}{o-g \text{ system}} \quad (21-3)$$

That is, at a given oil saturation, the relative permeability to oil is less in an oil-gas system than in an oil-brine system; the latter itself being greater than, equal to, or less than the oil relative permeability in a three-phase system; the oil relative permeability in the three-phase system in turn being always greater than that in a two-phase oil-gas system.

Now, to the extent that gas and oil can both be regarded as non-wetting phases in brine-oil or brine-gas two-phase systems, and to the extent that appropriate compensation is made for gas slippage (Klinkenberg) effects,* it is regarded that:

$$\frac{k_{rg}(\rho_g)}{g-b \text{ system}} = \frac{k_{rg}(\rho_g)}{g-o \text{ system}} = \frac{k_{ro}(\rho_o)}{o-b \text{ system}} \quad (21-4)$$

§ The following symbols are employed as subscripts:

- b refers to a brine (aqueous) phase
- g refers to a gas phase
- o refers to an oil phase
- n refers to a non-wetting phase (unspecified)
- w refers to a wetting phase (unspecified)

Thus, the notation:

$$\frac{k_{rb}(\rho_b)}{b-g \text{ system}}$$

implies we are concerned with the relative permeability of brine plotted as a function of brine saturation, in a brine-gas (two-phase) system.

* Detailed consideration has been given to the problem of slippage effects in gas relative permeability phenomena, and it has been concluded that these effects are often negligible as an approximation even in instances where appreciable slippage corrections must be applied to the values of effective and specific permeability used to calculate the relative permeability relation. The theory and data supporting this result have been reported elsewhere,³² together with a statement of the slippage term which must be employed when it is desired to derive *exactly* gas relative permeability as a function of gas mean free path.

‡ It is significant to note that all the cited references on permeability measurement emphasize the exploratory nature of the work as a precaution against the tendency to over-generalize on the experimental results.

this being more or less supported by experimental data.[†] Also, since oil can be regarded as a wetting phase in a two-phase oil gas system Eq. (21-1) can be expanded as:

$$\frac{k_{ro}(\rho_o)}{\text{o-g system}} = \frac{k_{rb}(\rho_b)}{\text{b-g system}} = \frac{k_{rb}(\rho_b)}{\text{b-o system}} = \frac{k_{rb}(\rho_b)}{\text{b-o-g system}} \quad (21-5)$$

On combining the equalities (21-4) and (21-5) with the inequalities (21-2) (and 21-3) we obtain:

$$\frac{k_{rn}(\rho_n)}{\text{2-phase system}} > \frac{k_{rw}(\rho_w)}{\text{2 or 3-phase system}} < \frac{k_{ro}(\rho_o)}{\text{o-g-b system}} \quad (21-6) \dagger$$

$$\frac{k_{rn}(\rho_n)}{\text{2-phase system}} > \frac{k_{rg}(\rho_g)}{\text{g-o-b system}} \quad (21-6) \ddagger$$

Eq. (21-6) shows how in a given porous body the relative permeability to the three phases, brine, oil and gas, compare with each other under conditions of two and three-phase saturation. Specifically, it is shown that of the nine possible systems of interest those pertaining to wetting phase relative permeability in 2 or 3-phase systems can be classed together, as can those pertaining to non-wetting phase relative permeability in 2-phase systems.[§] The relative permeabilities to gas and to oil in 3-phase systems according to presently available data provide an anomalous situation insofar as their description by the inequality (21-6) is not supported by theory nor entirely confirmed by experiment,^{*} and this will receive discussion below. However, first it will be shown how the various elements of Eq. (21-6) can be evaluated, at least approximately, from a consideration of various modified forms of Eq. (20).

APPLICATION OF THE GENERALIZED EXPRESSIONS FOR RELATIVE PERMEABILITY

Fig. 3 shows a plot of Eq. (20) where various values for the term, ρ_{w1} , are assumed arbitrarily in the interval 0 to 2/3. Also shown for comparison are the representative wetting phase

[†] Actually, this question is not entirely settled since the recent data^{25,26} in some instances suggest a dependence of the relative permeability on fluid properties. This paper does not consider systems where there is interaction between solid and liquid phases (e.g. clay hydration), it being assumed that in the absence of such interaction the flow of fluids will be controlled entirely by preferential wettability characteristics rather than by incidental fluid properties such as viscosity, etc.

[‡] That is, k_{rn} at a given saturation, ρ_n , in 2-phase systems will be greater than k_{rw} at an equivalent saturation, ρ_w , in 2 or 3-phase systems; which in turn is less than k_{ro} at an equivalent saturation, ρ_o , in 3-phase systems; which in turn is greater than, less than or equal to above mentioned k_{rn} in two-phase systems; which in turn is greater than k_{rg} at ρ_g in a g-o-b system.

[§] These are:

- (1) k_{rb} in b-o system
- (2) k_{rb} in b-g system
- (3) k_{rb} in b-g-o system
- (4) k_{ro} in o-b system
- (5) k_{ro} in o-g system
- (6) k_{ro} in o-g-b system
- (7) k_{rg} in g-b system
- (8) k_{rg} in g-o system
- (9) k_{rg} in g-o-b system

(1), (2), (3) and (5) may be expressed as k_{rw} in 2 or 3-phase systems. (4), (7) and (8) may be expressed as k_{rn} in 2-phase systems.

* In this connection, it is observed that the Leverett and Lewis data (representing all that is presently known about relative permeability in 3 fluid phase systems) merely support but in no way confirm or establish Eq. (21-6) above, even for the unconsolidated systems they specifically studied, as can be seen simply by reploting the ternary diagrams they reported. This observation, of course, does not detract from the pioneering accomplishment of their experimental work, or from the qualitative importance of their conclusions except where a theoretical contradiction can be established.

relative permeability data of Botset (loc. cit.), Martinelli *et al.*²⁷, Morse *et al.* (loc. cit.), and Bulnes and Fitting²⁸. A certain conformance is noted immediately between the shape and character of the experimental and theoretical curves, this conformance being of particular interest because the cited data were obtained variously in studies of several dissimilar porous systems (i.e. capillary tube, unconsolidated sands, consolidated sands and dolomites).

Now it has been mentioned that Eq. (20) was developed specifically as an expression for wetting phase relative permeability. In this connection it should be observed that Eq. (20) conforms to the experimental conclusion first reached by Wyckoff and Botset and later by Leverett and Lewis, that wetting phase relative permeability in a given porous body is a function of saturation alone (independent of fluid properties) as expressed by the relation (21-5). Therefore, by insertion of suitable saturation terms in Eq. (20) it may be assumed that the brine relative permeability in 2 and 3-phase systems and the oil relative permeability in oil-gas systems will thereby be established.[†]

At this point it becomes necessary to consider an apparent

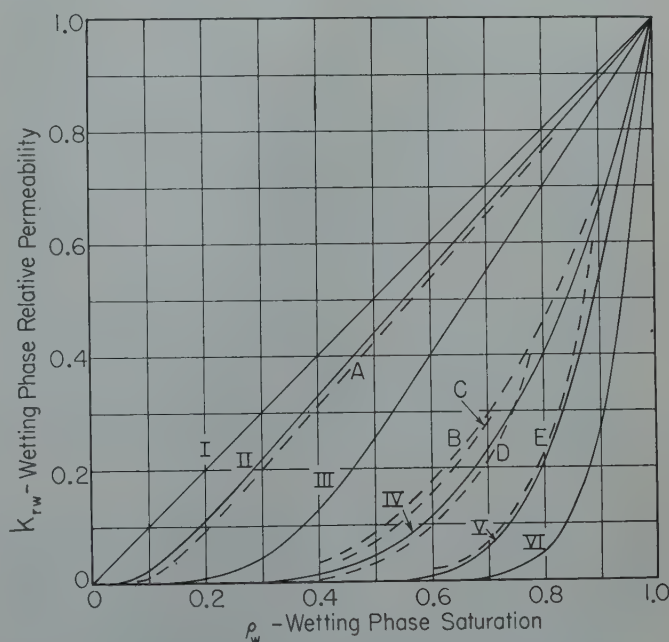


FIG. 3 — EXAMPLES OF WETTING PHASE RELATIVE PERMEABILITY.

Theoretical Curves (Eq. 20).

- I. ρ_{w1} assumed to be zero.
- II. ρ_{w1} assumed to be 0.01.
- III. ρ_{w1} assumed to be 0.1.
- IV. ρ_{w1} assumed to be 0.3.
- V. ρ_{w1} assumed to be 0.5.
- VI. ρ_{w1} assumed to be 0.67 ($\frac{2}{3}$)

Experimental Curves:

- A. Data obtained on single capillary tube²⁷.
- B. Data obtained on unconsolidated sand⁹.
- C. Data obtained on a synthetic core²⁵.
- D. Data obtained on a dolomite²⁸.
- E. Data obtained on a consolidated sand³.

[†] Here and elsewhere in this paper hydrophilic interstitial surfaces have been assumed merely to simplify the presentation.

discrepancy between existing data and the generally accepted theoretical concept symbolically stated as:

$$\lim_{\rho_w \rightarrow \rho_{w1}} k_{rw} = 0 \quad \text{where} \quad \lim_{P_0 \rightarrow 0} \rho_w = \rho_{w1}$$

In the development of Eq. (20) the validity of this concept was assumed and the difficulty arises from the fact that *apparently* in the general case:

$$\lim_{\rho_w \rightarrow \rho_{wm}} k_{rw} = 0 \quad \text{where} \quad \rho_{wm} > \rho_{w1} \quad (\text{usually})$$

For example, an examination of Leverett's capillary drainage experimental data¹² gives values of ρ_{w1} between 5 and 10 per cent, and these are to be compared with ρ_{wm} values of 20-30 per cent elsewhere reported on similar sands^{2,6,24†}. This apparent discrepancy is normally explained by assuming that the relative permeability at saturation ρ_{wm} is so small that it is mistaken for zero, and that actually conditions of pendular configuration must be attained (i.e. $\rho_w = \rho_{w1}$) before flow will cease and relative permeability will become zero.

Although this explanation is plausible, it is of interest to consider another point of view. Fig. 3 in the recent paper by Holmgren²⁹ calls attention to the fact frequently observed in the laboratory, that the production of a wetting phase from a porous system, effected by the displacing action of an invading non-wetting phase under pressure, depends upon various factors associated with the conditions of flow, and that maximum production will be attained generally in the static type capillary pressure experiment rather than in a dynamic flow type experiment. It seems reasonable that ρ_{wm} can be accepted as the dynamic equivalent of ρ_{w1} , which itself is an "irreducible" saturation attained only under conditions of static equilibrium. In this sense ρ_{wm} is not a fixed and unique saturation, but rather it is determined by the prevailing conditions of flow, and it becomes equal to ρ_{w1} only in the limiting case. Therefore, it will be assumed that ρ_{wm} is an appropriate value to substitute in Eq. (20) when the conditions of polyphase flow are such that $\rho_{wm} \gg \rho_{w1}$, and indeed this is required if Eq. (20) is to be accepted as a suitable generalized expression for wetting phase relative permeability. Thus, Eq. (20) is rewritten as:

$$k_{rw} = \frac{16\rho_w^2 (\rho_w - \rho_{wm})^3 (1 - \rho_{wm})}{[2\rho_w^2 (2 - 3\rho_{wm}) + 3\rho_w \rho_{wm} (3\rho_{wm} - 2) + \rho_{wm} (4 - 5\rho_{wm})]^2} \quad (22) \S$$

† Similar experimental discrepancies have been elsewhere noted. Recent capillary pressure experiments on Nichols Buff sandstone indicate ρ_{w1} values considerably lower than ρ_{wm} values obtained by the extrapolation of Botset's³ relative permeability data. Fig. 16 of the paper by Bulnes and Fitting (loc. cit.) illustrates this discrepancy as applied to limestones.

§ According to these views, Eq. (10) must also be rewritten as:

$$k_{rw} = \rho_w \left(\frac{\pi_D}{\pi_C} \right)^2 \quad \text{where} \quad \pi_D \text{ and } \pi_C \text{ are the dynamic equivalents of the}$$

static quantities, P_D and P_C respectively. In general, it will be found that for a given saturation $\pi_C > P_C$ and that $\pi_D > P_D$, which simply means that an interface in motion in a pore of a given size will have a larger specific surface area than the same interface in the same pore under conditions of static equilibrium. (In this connection, note that Eq. (10) was developed to apply to a *draining* system, i.e. one where ρ_w is always constant or decreasing in magnitude. Similar argument, however, can be applied also to an *imbibing* system, suggesting the possibility of extremely complex hysteresis effects). Eq. (19) then can be rewritten as:

$$\frac{\pi_C}{\pi_D} = \frac{2\rho_w^2 (2 - 3\rho_{wm}) + 3\rho_w \rho_{wm} (3\rho_{wm} - 2) + \rho_{wm} (4 - 5\rho_{wm})}{4\sqrt{\rho_w (1 - \rho_{wm}) (\rho_w - \rho_{wm})^3}}$$

in accordance with these views.

Fig. 4 is presented to illustrate the significance of the various saturation parameters employed in this paper. It is evident that whether ρ_{wm} is used in Eq. (22) or whether ρ_{w1} is used in Eq. (20) to derive relative permeability, this will depend upon the nature of the flow process being considered. Further, it is believed that these limiting saturation parameters can be approximated from existing data correlations* or experimentally obtained in a manner less involved than present methods of relative permeability measurement.† This is illustrated with the aid of Fig. 5 where an assumption is made (based on Botset's³ plot of gas-oil ratios) that 0.5 is a suitable value to use for ρ_{wm} when it is desired to fit Eq. (22) to Botset's data as obtained under his stated flow conditions. This gives curve "A" in Fig. 5, and for comparison Botset's original Nichols Buff data points are included. Also shown in Fig. 5 is a plot of Eq. (20) where ρ_{w1} is chosen to be 0.35 (curve "B"). Since this value ($\rho_{w1} = 0.35$) is a reasonable "irreducible" saturation for the Nichols Buff sand, it is concluded that curve "B" shows a limiting position of the relative permeability relation, which would characterize this sand under conditions quite different from those experimentally imposed by Botset.‡

In concluding this discussion on the applicability of Eqs. (20) and (22) to the evaluation of k_{rw} , it is of interest to note that these equations reduce to:

$$k_{rw} = \rho_w \text{ or } \frac{dk_{rw}}{d\rho_w} = 1 \quad \dots \dots (22a)$$

when the condition: $\rho_{wm} = \rho_{w1} = 0$ is satisfied, as identified with a system of uniformly sized capillary tubes oriented in the direction of flow. Eq. (22a) is of particular interest in connection with Leverett's argument² where he concludes that relative permeability curves characterizing "a system of non-interconnected, parallel capillary tubes" will be simply 45° lines when plotted conventionally (i.e. as in Fig. 3) according

* In this connection, Brownell and Katz⁵ develop the relation:

$$\rho_{wm} = \frac{1}{86.3} \left(\frac{k}{G \cos \theta} \frac{dp}{dx} \right)^{-0.264}$$

where G is the acceleration due to gravity and θ is the angle of contact. Now, this implies that the term ρ_{wm} is determined by the pressure gradients in the flowing phases, requiring (according to a strict interpretation of the equations appearing in this paper) that in some instances at least the entire relative permeability curve will be shifted upon variation in the pressure gradients. Experimental evidence of such possibilities as applied to non-wetting phase relative permeability can be found by examining Fig. 4 of the recent paper by Henderson and Yuster (loc. cit.). Actually, more recently at the 1948 Annual Conference on Secondary Recovery at the Pennsylvania State College these authors presented additional indications of such hysteretic shifts as applied to either wetting or non-wetting phases relative permeability, these shifts being entirely in accord with the theoretical interpretation presented in the legend for Fig. 4 of this paper (Private Communication, October 16, 1948). The recent paper of Childs and George gives further evidence of these hysteretic shifts.³⁴

† For instance, ρ_{w1} is simply the irreducible saturation observed in a drainage type capillary pressure experiment; that is, the maximum saturation where the wetting phase configuration is still entirely pendular.

‡ Curve "D" illustrates what might be expected if Nichols Buff capillary pressure data were used in Eq. (10) to describe wetting phase relative permeability. The deviation between curves B and D supports the view that *dynamic* flow data are not directly derivable from static capillary pressure data.

to the assumed requirement that in such a system the sum of the effective permeabilities for the separate phases should total the specific permeability. Although as Henderson and Yuster²⁸ have recently pointed out the experimental data of Martinelli *et al*²⁷ do not confirm Leverett's prediction,[§] at least the equations developed in this paper are in accord with the concept that in the absence of capillary interaction between immiscible fluid phases (as would prevail, for instance, in a hypothetical U.S.O. system of the type above mentioned) phase relative permeability is linearly related to phase saturation (c.f. Eq. (22a)).

Having indicated the usefulness of Eq. (20) and (22) to evaluate wetting phase relative permeability under the conditions described by Eq. (21-5) when reasonable values for ρ_{wi} (or ρ_{wm}) can be assumed or otherwise obtained, it is of interest now to see what further extensions can be made in the manner of evaluating specific non-wetting phase relations under the 2-phase saturation conditions described by Eq. (21-4).

It has been observed that if we define Ψ_w as the limiting wetting phase saturation associated with $k_{rn}(1)$; and then if we arbitrarily define the "effective" non-wetting phase saturation range of interest to be within the interval, $\rho_w(1)$ and $\rho_w(\Psi_w)$; and then if we substitute in Eq. (22) the effective non-wetting saturation terms so defined for the comparable wetting phase saturation terms; an expression is evolved which apparently can serve as an equation for non-wetting phase relative permeability according to the conformance with experimental data indicated in Fig. 5 (Curve "C") and Fig. 6.* Thus,

$$\lim_{k_{rn} \rightarrow 1} \rho_w = \Psi_w \quad (\text{Definition})$$

Also,

$$\rho_{en} = \frac{\rho_n}{1 - \Psi_w} = \frac{1 - \rho_w}{1 - \Psi_w} \quad (\text{Definition})$$

$$\rho_{enm} = \frac{\rho_{nm}}{1 - \Psi_w}$$

where ρ_{nm} will be identified with equilibrium non-wetting phase saturation as commonly defined. Then by analogy to Eq. (22):

$$k_{rn} = \frac{16\rho_n^2 (\rho_n - \rho_{nm})^3 (1 - \Psi_w - \rho_{nm})}{[2\rho_n^2 (2 - 2\Psi_w - 3\rho_{nm}) + 3\rho_n \rho_{nm} (3\rho_{nm} - 2 + 2\Psi_w) + \rho_{nm} (1 - \Psi_w)]^3} \quad (23)$$

where,

$$\lim_{\rho_w \rightarrow \Psi_w} k_{rn} = \lim_{\rho_n \rightarrow (1 - \Psi_w)} k_{rn} = 1$$

and

$$\lim_{\rho_n \rightarrow \rho_{nm}} k_{rn} = 0.$$

[§] Nor do these data deny Leverett's prediction since it may be supposed that the conditions of the Martinelli *et al* experiment are not entirely applicable to a consideration of phenomena occurring in Leverett's idealized system.

* Attention is called to the recent gas relative permeability data reported by the author²² where conformance between the results of experimentation and the theoretical analysis as presented above also has been obtained.

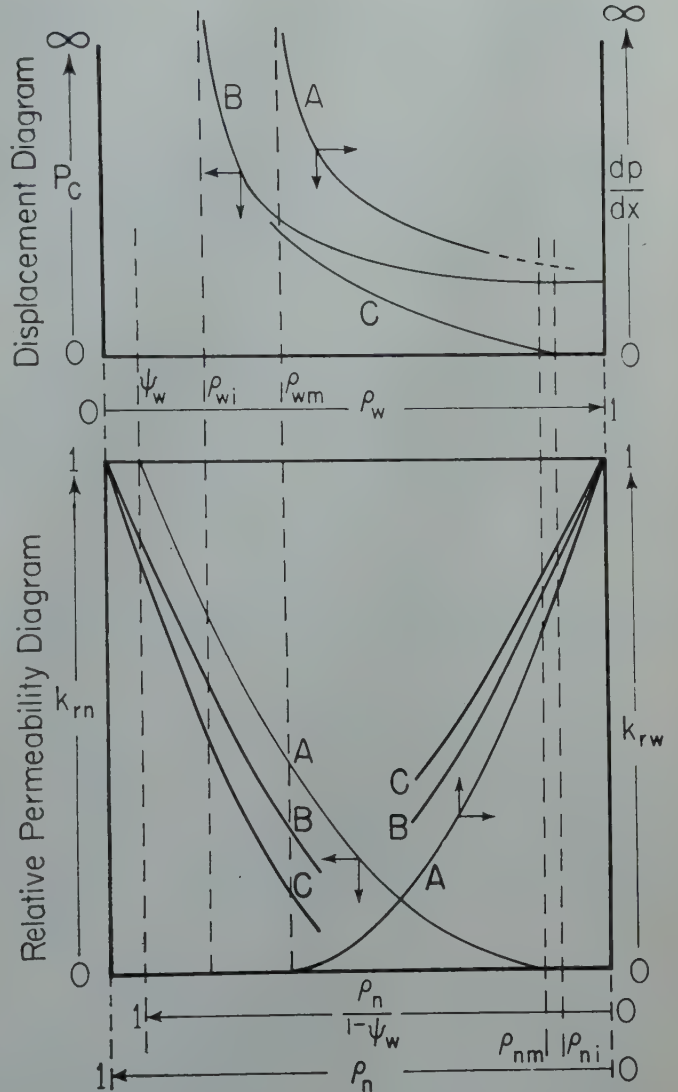


FIG. 4 — DEFINITIONS OF SATURATION PARAMETERS.

Curves A, B, and C refer to the plots of a dependent variable versus some function of fluid saturation as the independent variable. In the top diagram the dependent variable is either the capillary pressure difference measured across the interfaces of contact between the immiscible fluids saturating the interstitial spaces, or some function of the pressure gradients existing in these phases when they are flowing. In the bottom diagram the dependent variable is either the wetting phase or the non-wetting phase relative permeability. In particular, Curves A refer to fluid distributions obtaining under conditions of dynamic equilibrium (that is, under conditions of steady-state heterogeneous flow of immiscible fluids). Curves B and C refer to fluid distributions obtaining under conditions of static equilibrium which have been approached respectively by drainage or by imbibition capillary pressure processes. Thus, any given group of Curves A, B, and C show possible limits of hysteresis in the relation associated with these curves. Note, for instance, that the fluid distribution which yields the largest value for non-wetting phase relative permeability (at a given non-wetting phase saturation) invariably yields the lowest value for wetting phase relative permeability, and vice versa.

Thus, in the derivation of Eq. (23) the existence of limiting non-wetting phase saturation terms, ρ_{n1} and ρ_{nm} , analogous to the wetting phase terms, ρ_{w1} and ρ_{wm} , has been implied, as shown graphically by Fig. 4 and as discussed in greater detail below.

The manner in which existing experimental data are described by Eq. (23), of course, can be fortuitous, to the extent that insufficient data are available for examination. However, the applicability of Eq. (23) itself can be developed in a reasonable manner from more or less plausible concepts as follows:

In the first place, Brownell in his discussion of the Martinelli *et al* paper (loc. cit.), and later Brownell and Katz (loc. cit.) develop the view that the pore space saturated with capillary bound (immobile) wetting phase should be eliminated from definitions of saturation functions employed in flow equations. It is evident that if we identify the term Ψ_w defined above with the immobile wetting phase saturation, then the terms,

$$\frac{\rho_n}{1-\Psi_w} \quad \text{and} \quad \frac{\rho_{nm}}{1-\Psi_w}$$

which were substituted in Eq. (22) to yield Eq. (23) actually express non-wetting phase saturation parameters per unit of

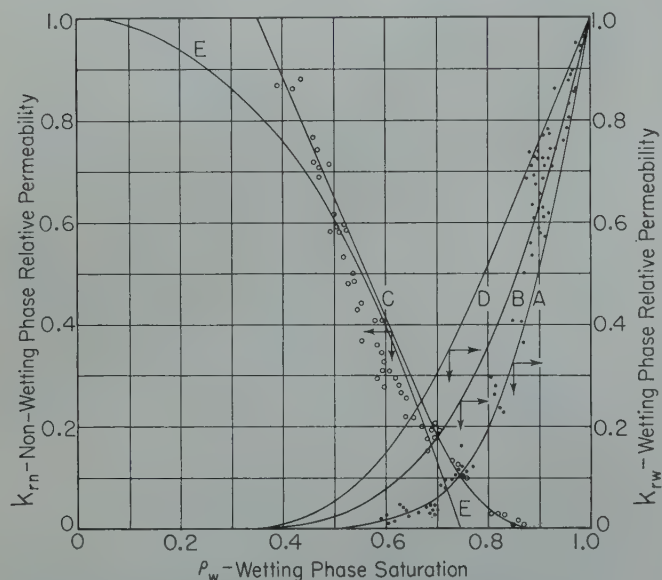


FIG. 5—CONFORMANCE OF EXPERIMENTAL DATA TO THEORETICAL PREDICTIONS.

Curve A—Theoretical Curve obtained by assuming $\rho_{wm} = 0.5$ in Eq. (22) in order to fit Botset's brine relative permeability data² on Nichols Buff (solid points).

Curve B—Theoretical Curve obtained by assuming $\rho_{w1} = 0.35$ in Eq. (20) to show the limiting position of the brine relative permeability relation.

Curve C—Theoretical Curve obtained by assuming $\psi_w = 0.35$, $\rho_{nm} = 0.1$ in Eq. (23) in order to fit Botset's gas relative permeability data² on Nichols Buff (circled points).

Curve D—Description of Nichols Buff "brine" relative permeability as suggested by Eq. (10).

Curve E—Description of Nichols Buff "gas" relative permeability data as suggested by Eq. (10a), where a normal probability distribution of pores is assumed and where Eq. (10a) is normalized to show a zero relative permeability at an assumed value for the equilibrium gas saturation.

pore volume from which the portion occupied by the immobile wetting phase has been eliminated.[†]

This discussion suggests that a character of symmetry is a common feature associating wetting and non-wetting phase relative permeability to each other, for it is evident that a comparison of Eqs. (22) and (23) will yield:

$$k_{rw}(\rho_w) = k_{rn}(\rho_n)$$

when:

$$\rho_w = \rho_n$$

in a 2-phase system where: $\Psi_w = 0$ and where: $\rho_{wm} = \rho_{w1}$. Physically, a condition of symmetry probably requires assuming that relative permeability is a function of saturation alone, and that "effectively" the pore configuration may be represented as an assemblage of equivalent capillary tubes. Thus, when a little non-wetting phase is introduced into an initially non-wetting phase saturated system it occupies several of the smaller pores, so that it is not unreasonable that a decrease in the non-wetting phase relative permeability should result approximately equivalent to the above referred to decrease in wetting phase relative permeability. (Note, how-

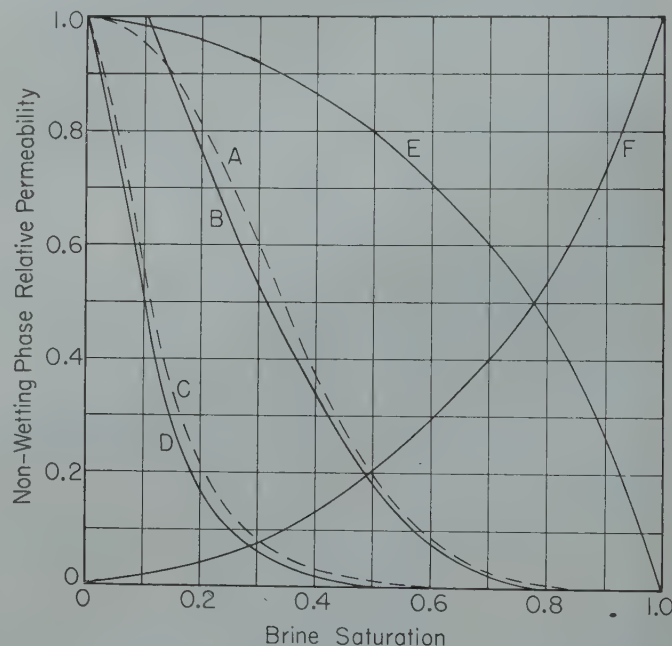


FIG. 6—EXAMPLES OF NON-WETTING PHASE RELATIVE PERMEABILITY.

Curve A—Described empirically by Hassler¹ as

$$k_{rn} = e^{-7.75\rho_w^{2.25}}$$

Curve B—Eq. (23) with limiting saturation parameters chosen to fit Curve A.

Curve C—Martinelli *et al* data²⁷.

Curve D—Eq. (23) with limiting saturation parameters chosen to fit Curve C.

Curve E—A generalized solution of Eq. (10a) as applied to a non-wetting phase.

Curve F—A generalized solution of Eq. (10a) as applied to a wetting phase.

[†] Brownell and Katz (loc. cit.) suggest that the wetting phase removed from flow is proportional to the non-wetting phase saturation, which evidently is not in accord with the data of Russell *et al*³⁰ where characteristics of high mobility are attributed to interstitial brines even under conditions of low saturation. In accepting herein the concept of an immobile wetting phase its magnitude will not be related to the incidental presence of the non-wetting phase, but rather to the physio-chemical rock properties responsible, for instance, for interstitial clay hydration effects, etc. In general, then:

$$0 \leq \Psi_w \leq \rho_{w1} \leq \rho_{wm} < 1$$

ever, this concept of symmetry has not been derived directly through analysis of the properties of any particular system). Presumably, this assumed character of symmetry has not been emphasized in the past simply because the end-points of the wetting and non-wetting phase relative permeability curves do not in general originate from comparable positions on the conventional data plot (cf. Fig. 4). Thus, whereas $k_{rw}(1)$ occurs at $\rho_w(1)$, $k_{rn}(1)$ does not occur at $\rho_n(1) = \rho_w(0)$; but rather it occurs at $\rho_n(1 - \Psi_w = \rho_w(\Psi_w))$ where $\rho_w(\Psi_w)$ only occasionally equals $\rho_w(0)$. In a like manner, $k_{rw}(0)$ occurs at $\rho_w(\rho_{wm})$ although $k_{rn}(0)$ occurs at $\rho_n(\rho_{nm})$, where ρ_{wm} usually is considerably larger than ρ_{nm} .†

In this connection it is observed that ρ_{wm} and ρ_{nm} are both limiting saturation parameters associated with saturation distribution conditions of the respective phases such that an infinitesimal decrease in either ρ_w or ρ_n beyond ρ_{wm} or ρ_{nm} would result in a phase discontinuity. ρ_{wm} then represents the end point of a displacement experiment where the non-wetting phase reduces the wetting phase to a minimum. (In a capillary pressure experiment $\rho_{wm} = \rho_{wi}$). Likewise, ρ_{nm} represents the end point when the non-wetting phase is reduced to a minimum. Referring to the generalized pressure-saturation diagrams in Fig. 4 it is noted ρ_{nm} is approached in a more abrupt manner than is ρ_{wm} . That is to say a funicular chord of non-wetting phase in the central pore portion of an assemblage of sand grains and surrounded by wetting phase will be abruptly pinched-off as globules by the wetting phase and thereby rendered immobile as ρ_n is decreased to ρ_{nm} . On the other hand, as ρ_w is decreased to ρ_{wm} (or ρ_{wi}) the wetting phase adhering to the pore wells is more gradually forced into a strictly pendular configuration, and, assuming 0° contact angle, actually never does become entirely discontinuous although it may so behave from a flow standpoint. In any event, there is reason to expect in the region of low phase saturation a departure from wetting and non-wetting phase symmetry in the respective relative permeability curves (that is, assuming as has been done above that a general character of symmetry does exist at other levels of saturation) which manifests itself in the form of a sharp non-wetting phase relative permeability cut-off in contrast to a more gradual wetting phase relative permeability cut-off. This then introduces a minor limitation into the unqualified use of Eq. (23) for non-wetting phase relative permeability, the quantitative magnitude which is suggested by observing the conformance between theory and experiment as presented in Fig. 5c and Fig. 6. Presumably, the theoretical relationship for wetting phase relative permeability (Eq. 22) does not invoke this limitation since it was developed from basic concepts to apply exactly to wetting phase flow in contrast to the intuitive development of the non-wetting phase relation (Eq. 23).

† It will be noted that Eq. (10a) appears to contradict the intuitively developed concept of inherent symmetry, as suggested by Curves E and F of Fig. 6. Indeed, all attempts at theoretical analysis of non-wetting phase relative permeability have led to monotonic curves concave downward (as opposed to the concave upward wetting phase relative permeability curves) when plotted as in the conventional diagram (cf. Fig. 6). In view of the conformance obtained between non-wetting phase relative permeability curves of this type and the experimental data of Botset, as illustrated by Curve E of Fig. 5, the concept of inherent symmetry should be accepted for the present only to the extent that it is useful for approximation purposes. For it is believed that in some respects at least more exacting experimentation and more rigorous theoretical development are yet to be accomplished before non-wetting phase relative permeability phenomena are completely understood.

In connection with the application of the developments presented in this paper to the three-phase flow problem some quantitative statements now can be made, again based on the concept of inherent symmetry. In the first place the evaluation of the relative permeability of a wetting phase in the presence of one or more non-wetting phases has already been accomplished to the extent that the equivalence of wetting phase relations for a given porous body is established by existing data to be independent of fluid properties (c.f. Eq. 21-5). The relative permeability to oil in a o-b-g 3-phase system has been described by Eqs. (21-3) and (21-6). In order to explain these experimental observations, one is inclined to observe with Leverett and Lewis²⁴ that starting with a gas-oil system and holding ρ_o constant, the oil changes its distribution by migrating from smaller to larger pores as some of the non-wetting gas is replaced by water. However, to say that this in itself tends to increase the oil relative permeability (as apparently observed) invalidates the argument presented above which lead to the concept of symmetry. That is to say, granted the average pore radius of the oil saturated portion of the system is increased as some of the gas is replaced by water, still the number of pores containing the oil is decreased simultaneously, such that it is assumed for the present that the resultant of these effects does not entirely (if at all) account for the observed facts expressed by the inequalities (21-3) and (21-6). Instead, the problem is simply solved by applying Eq. (22) when the oil acts as a wetting phase, to give the relative permeability of oil in an o-g system; and applying Eq. (23) when the oil acts as a non-wetting phase to give the relative permeability of oil in an oil-brine system. This has been done for a typical case as illustrated by the dotted lines in Fig. 2, and it is seen that the form of the inequality (21-3) should be changed by this argument to:

$$\frac{k_{ro}(\rho_o)}{\text{o-b system}} > \frac{k_{ro}(\rho_o)}{\text{o-b-g system}} > \frac{k_{ro}(\rho_o)}{\text{o-g system}}$$

since ρ_{wm} was chosen greater than ρ_{nm} according to the general case. Although indicating the relative permeability to oil in the three-phase system as immediate between that obtaining in oil-brine and oil-gas two-phase systems represents a departure from the Leverett and Lewis data (loc. cit.) intuitively it is a necessity since there has not appeared an argument which requires

$$\frac{k_{ro}(\rho_o)}{\text{o-b-g system}} \text{ to sometimes be greater than } \frac{k_{ro}(\rho_o)}{\text{o-b system}}$$

Thus, combining Eq. (22) and (23) in a manner suggested by the above discussion we obtain as an expression for oil

§ In a like manner Fig. 2 has been prepared to indicate that Eq. (21-2) should be modified as:

$$\frac{k_{rg}(\rho_g)}{\text{g-o system}} = \frac{k_{rg}(\rho_g)}{\text{g-b system}} = \frac{k_{rg}(\rho_g)}{\text{g-o-b system}}$$

Again, although this departs from the usual interpretation of the Leverett and Lewis data no argument is apparent which supports the observation that the gas non-wetting phase relative permeability relation should be different in three-phase systems than in two-phase systems. This latter would imply the gas *knows* the nature of the wetting phase(s) simultaneously saturating the porous system, which according to the concepts assumed or established in this paper would be true only in unsteady state flow. These arguments suggest that Eq. (21-6) should be modified as:

$$\frac{k_{rn}(\rho_n)}{\text{2-3 phase systems}} > \frac{k_{ro}(\rho_o)}{\text{o-g-b system}} > \frac{k_{rw}(\rho_w)}{\text{2-3 phase systems}}$$

which is herein accepted as a qualitative description of the manner in which wetting and non-wetting phase relative permeabilities compare with each other in a given porous medium under the indicated conditions of equivalent phase saturation. It is apparent that this modified form of Eq. (21-6) will hold only when $\rho_{wm} > \rho_{nm}$ and/or when $\Psi_w > 0$.

relative permeability in the presence of both brine and gas:

$$\frac{k_{ro}(\rho_o)}{\text{o-g-b system}} = \frac{x}{y^2 z^2} \quad (24)^*$$

$$x = 256\rho_o^2 (\rho_o - \rho_{om})^3 (1 - \rho_{b1} - \rho_{om}) (1 - \rho_{b1})^2 (1 - \rho_{b1} - \rho_{gm})^3 (1 - \psi_w - \rho_{gm})$$

$$y = 2\rho_o^2 (2 - 2\rho_{b1} - 3\rho_{om}) + 3\rho_o\rho_{om} (3\rho_{om} + 2\rho_{b1} - 2) + \rho_{om}(1 - \rho_{b1}) (4 - 4\rho_{b1} - 5\rho_{om})$$

$$z = 2(1 - \rho_{b1})^2 (2 - 2\psi_w - 3\rho_{gm}) + 3\rho_{gm}(1 - \rho_{b1}) (3\rho_{gm} + 2\psi_w - 2) + \rho_{gm}(1 - \psi_w) (4 - 4\psi_w - 5\rho_{gm})$$

and where we may specifically identify ρ_{b1} as the irreducible connate water, ρ_{gm} as the equilibrium gas saturation, and ρ_{om} as the minimum oil saturation resulting from a gas drive. Fig. 7 shows how oil relative permeability varies with connate water saturation as predicted by Eq. (24), this plot being somewhat of the form suggested by the cited data of Leverett and Lewis (c.f. Fig. 9 of their paper, loc. cit.) It is concluded then that Eq. (24) can be useful to calculate oil relative permeability in three phase systems, for instance, when only two-phase laboratory data are available for study or when assumptions can be made regarding the magnitude of the various limiting saturation parameters contained in Eq. (24).

To conclude, and in order to show the usefulness of the concepts developed in this paper for the solution of problems of practical importance, the following example is given. Gas-oil ratios, which in the past have been obtained either directly from the field data or indirectly from laboratory flow tests through a knowledge of the gas-oil relative permeability ratio are required in the study of certain problems of petroleum production. From a combination of Eq. (23) (applying to gas as a non-wetting phase) and Eq. (22) or Eq. (24) (applying to oil as a wetting phase with respect to gas) one obtains a k_{rg}/k_{ro} ratio which can be generalized and approximately described by:

$$\frac{k_{rg}}{k_{ro}} = \left[\frac{(1 - \rho_o - \rho_{b1} - \rho_{gm}) (1 - \rho_{b1} - \rho_{om}) (1 - \psi_w - \rho_{gm})}{(1 - \rho_{b1} - \rho_{gm}) (\rho_o - \rho_{om}) (1 - \rho_{gm})} \right]^2 \quad (25)^+$$

where:

$$\rho_o + \rho_g + \rho_{b1} = 1$$

Here again, ρ_{b1} represents the connate water, ρ_{gm} represents the equilibrium gas saturation, and ρ_{om} is the non-productible oil saturation by gas drive as was obtained for instance in the experiments of Holmgren (loc. cit.).

* Thus, Eq. (24) reduces to Eq. (22) when $\rho_{b1} = 0$ and the oil acts as a wetting phase; and Eq. (24) reduces to Eq. (23) when $\rho_{gm} = 0$ and the oil acts as a non-wetting phase. When all three phases (oil, gas and connate water) are present Eq. (24) implies that the oil is acting as a wetting phase with respect to gas in the pore spaces left when the connate water is considered as a part of the confining matrix along with the solid phase. This would seem to indicate that Eq. (24) should not be employed to predict the oil relative permeability when unreasonably high values are assumed for the connate water term, ρ_{b1} .

† More exact evaluation of this ratio entails appropriately solving Eqs. (20), (22), (23), and/or (24) as required by the conditions under consideration.

Fig. 8 shows a plot Eq. (25) as it compares with cited data,† and again fair conformance is noted, suggesting the applic-

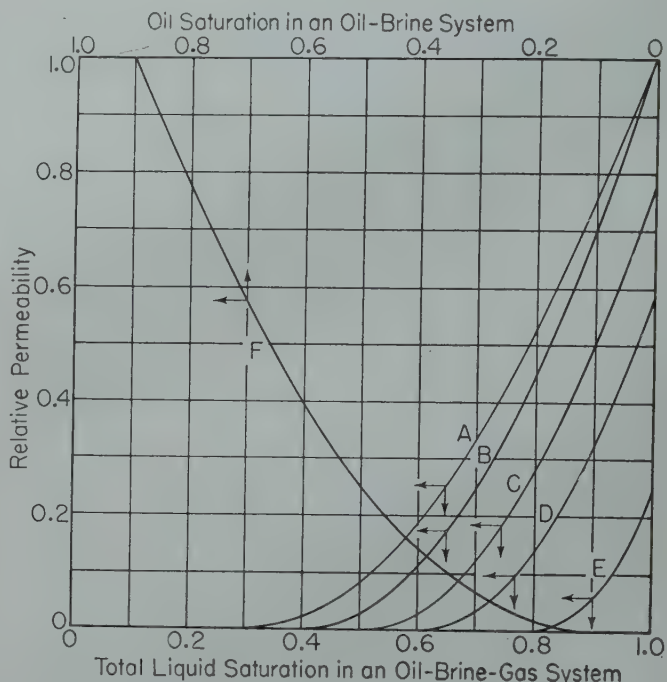


FIG. 7 — EFFECT OF CONNATE WATER ON THE OIL RELATIVE PERMEABILITY RELATION.

Curve A — Oil relative permeability in an oil-gas system containing no connate water (viz. Eq. (22)).

Curves B, C, D and E — Oil relative permeability in oil-gas-brine systems where ρ_{b1} is assumed to be 0.1, 0.2, 0.3 and 0.5 respectively and where ψ_w is assumed to be 0.1 in each case. (viz. Eq. (24)).

Curve F — Oil relative permeability in an oil-brine system. (viz. Eq. (23)).

‡ For example, in setting up Eq. (25) to describe a typical three-phase case the following assumptions were made:

$$\psi_w = 0.1; \rho_{gm} = 0.1; \rho_{om} = 0.3, \text{ and, } \rho_{b1} = 0, 0.1, 0.2 \text{ and } 0.4$$

for the four examples given, yielding curves which can be compared directly to the relations illustrated in Fig. 7. Eq. (25) is rewritten as:

$$\frac{k_{rg}}{k_{rw}} = \left[\frac{(1 - \rho_w - \rho_{gm}) (1 - \rho_{wm})}{(1 - \psi_w - \rho_{gm}) (\rho_w - \rho_{wm})} \right]^2 \quad (25a)$$

when it is desired to describe approximately two-phase experimental data. Therefore, in setting up Eq. (25a) to fit Botset's³ data

$$\psi_w = 0.35, \rho_{gm} = 0.1 \text{ and } \rho_{wm} = 0.5$$

were assumed as suggested by Fig. 5.

ability of the concepts presented in this paper at least for engineering use. Thus, it is seen that by Eq. (25):

$$\lim_{\rho_g \rightarrow \rho_{gm}} \frac{k_{rg}}{k_{ro}} = 0$$

and,

$$\lim_{\rho_o \rightarrow \rho_{om}} \frac{k_{rg}}{k_{ro}} = \infty$$

in accord with accepted concepts. Further, it is noted increasing ρ_{b1} , or increasing ρ_{om} , or decreasing ρ_{gm} , in each case holding the other limiting saturation parameters constant, will tend to increase the k_{rg}/k_{ro} ratio at a given total liquid saturation.

SUMMARY AND CONCLUSIONS

To summarize, this paper has treated the subject of calculated relative permeability according to the point of view that the configuration of the saturating fluid phases alone determines the relationships which will prevail in steady state flow. Specifically an expression for wetting phase relative permeability has been derived from fundamental considerations based on modified forms of the Kozeny equation for flow and Leverett's expression for capillary retention. Although the derivation presented is neither rigorous nor unique it is supported through the indicated conformance of predicted results with existing experimental data. Then, postulating the concept of inherent symmetry as a character interrelating wetting and non-wetting phase relative permeability relationships the limiting saturation parameters

$$\lim_{k_r \rightarrow 1} \rho \quad \text{and} \quad \lim_{k_r \rightarrow 0} \rho$$

have been defined. This in turn has led to an expression for non-wetting phase relative permeability which again is supported by conformance to existing data. Finally, general consideration has been given to the problems of three-phase relative permeability phenomena and gas-oil ratios.

In view of the considerations which have been examined in this paper it is concluded that the pore widths of the interstitial spaces in contact with the immiscible fluid phase interfaces saturating these spaces is the factor of importance in controlling the effective permeability of the porous body to these phases. Essentially, capillary pressure data identifies the distribution of pore widths with a range of fluid phase saturation configurations under conditions of static equilibrium, and it is shown herein how this fact can be employed to derive a generalized expression for the relative permeability relation explicitly defined in terms of saturation parameters. In suggesting that the effective permeability characteristics in poly-phase systems are controlled by the magnitude of the pore spaces available for flow under the prevailing conditions of saturation distribution, it is recognized that the limiting saturations where phase discontinuities occur also have an importance in defining the detailed features of the observed relations. Moreover, it has been suggested that in a given porous body the conditions of flow determine the effective distribution of pore widths associated with the prevailing

saturation configurations as well as determine the exact occurrence of the phase discontinuities. Therefore, hysteresis effects analogous to those observed in static capillarity studies are to be anticipated as observable phenomena in relative permeability work. In this connection, the generalized expressions for relative permeability presented in this paper presumably can be used to calculate the various limits of hysteresis through suitable selection of the saturation parameters, although experimental proof is nonetheless desired to further establish the validity of the assumptions which have lead to these expressions. Finally, it is concluded that insofar as confirmation is offered by available data a character of symmetry seems to interrelate wetting and non-wetting phase relative permeability relations in a manner requiring only the knowledge of the above mentioned limiting saturation param-

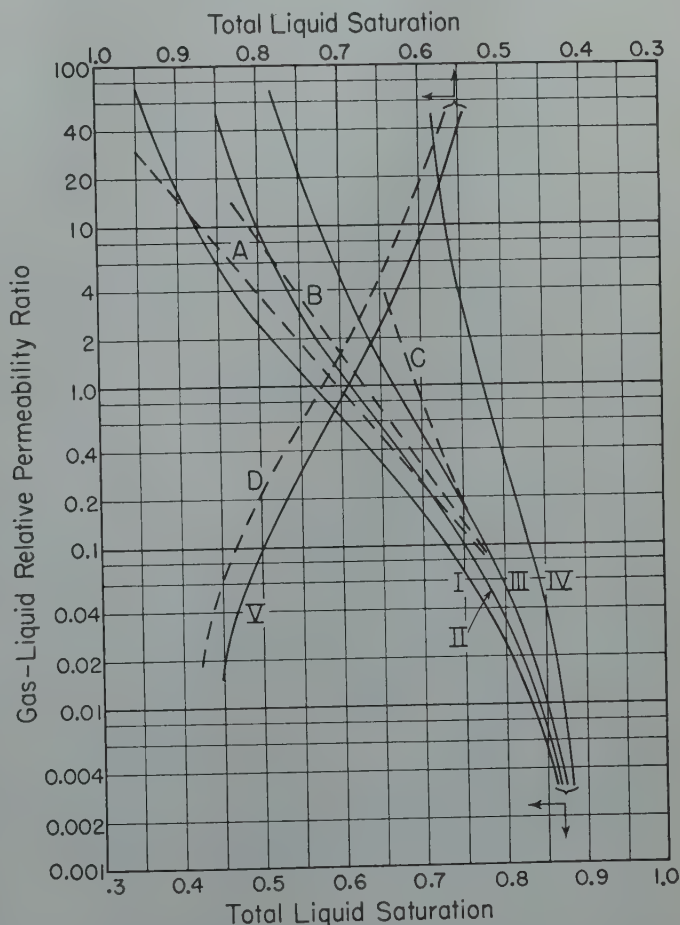


FIG. 8 — RELATION OF GAS-LIQUID RELATIVE PERMEABILITY RATIO TO TOTAL LIQUID SATURATION.

Curves A, B and C gas-oil ratio data of Leverett and Lewis²⁴ where $\rho_{b1} = 0, 0.2$ and 0.4 respectively.

Curves I, II, III and IV — Eq. (25) with limiting saturation parameters chosen to approximately describe the Leverett and Lewis data, and where $\rho_{b1} = 0, 0.1, 0.2$ and 0.4 respectively.

Curve D — Data of Botset⁷.

Curve V — Eq. (25a) with limiting saturation parameters chosen to approximately describe Curve D.

eters in order to treat the various problems of steady state polyphase flow.

ACKNOWLEDGMENT

The author has appreciated the opportunity to discuss this paper with Morris Muskat and to benefit from his critical comments. Acknowledgment is given to Paul D. Foote, executive vice-president of the Gulf Research and Development Co., for permission to publish this paper.

NOMENCLATURE

(1) Permeability Terms

- k — specific permeability
- k_e — effective permeability
- k_r — relative permeability (fractional)

(2) Saturation Terms (all per unit of pore volume expressed as fractions)

- ρ — fluid saturation
- ρ_1 — limiting minimum saturation attained in static capillary pressure experiment
- ρ_m — limiting minimum saturation attained in dynamic flow experiment
- ψ_w — immobile wetting phase saturation

(3) Rock and Fluid Property Terms

- A — specific surface area of pores per unit of pore volume
- f — porosity (fractional)
- t — Kozeny Rock textural constant
- T — collective term for Rock Textural Properties
- μ — fluid phase viscosity
- σ — interfacial tension
- P_c — capillary pressure
- P_D — displacement pressure
- π_c — dynamic equivalent of P_c
- π_D — dynamic equivalent of P_D
- $j(\rho_w)$ — capillary pressure function (wetting phase)
- dp/dx — pressure gradient in the x -direction
- q — linear rate of fluid flow
- D_r — distribution coefficient of pore radii
- r — pore radius
- θ — contact angle

(4) Miscellaneous Symbols

- F — denotes functional relationship
- G — acceleration due to gravity
- $\Phi(\rho_w)$ — Rho Function

(5) Subscripts

- w — refers to a wetting phase (unspecified)
- n — refers to a non-wetting phase (unspecified)
- b — refers to a brine (aqueous) phase
- o — refers to an oil phase
- g — refers to a gas phase
- e — denotes effective
- r — denotes relative
- m — refers to minimum saturation value attained under dynamic flow conditions
- i — refers to minimum saturation value attained in a static capillary pressure experiment.

REFERENCES

1. Gerald L. Hassler: The Measurement of the Permeability of Reservoir Rock and Its Application. *Science of Petroleum*, 1, 198-208 (1938).
2. M. C. Leverett: Flow of Oil-Water Mixtures Through Unconsolidated Sands. *Trans. AIME*, 132, 149 (1939).
3. Holbrook G. Botset: Flow of Gas-Liquid Mixtures Through Consolidated Sand. *Trans. AIME*, 136, 91 (1940).
4. G. L. Hassler, E. Brunner, and T. J. Deahl: The Role of Capillarity in Oil Production, *Trans. AIME*, 160, 155-174 (1945).
5. Lloyd E. Brownell and Donald L. Katz: Flow of Fluids Through Porous Media. *Chem. Engr. Progress*, 43, 601-612 (1947).
6. R. D. Wyckoff and H. G. Botset: The Flow of Gas-Liquid Mixtures Through Unconsolidated Sands. *Physics*, 7, 325 (1936).
7. Morris Muskat and Milan W. Meres: The Flow of Heterogeneous Fluids Through Porous Media. *Physics*, 7, 346 (1936); cf. Morris Muskat, The Flow of Fluids Through Porous Media, *J. App. Phys.*, 8, 274-282 (1937); Morris Muskat, Fluid Flow Through Porous Media, Proc. Sec. Hydraulic Conference, Bull. 27, University of Iowa Studies in Engineering, (1943).
8. L. E. Elkins: The Importance of Injected Gas as a Driving Medium in Limestone Reservoirs. *API Drill. and Prod. Practice*, 164, (1946).
9. H. H. Evinger and M. Muskat: Productivity Factor Calculations for Oil-Gas Water Systems in the Steady State. *Trans. AIME*, 146, 194 (1942).
10. L. A. Richards: Capillary Conduction of Liquids Through Porous Mediums. *Physics* 1, 318-333 (1931).
11. R. N. Traxler and L. A. H. Baum: Permeability of Compacted Powders-Determination of Average Pore Size. *Physics*, 7, 9-14 (1936).
12. M. C. Leverett: Capillary Behavior in Porous Solids. *Trans. AIME*, 142, 152-169 (1941).
13. William B. Haines: Studies in the Physical Properties of Soils. *J. Agr. Sci.*, 17, 264-290 (1927); *ibid*, 20, 97-116 (1930).
14. Ross W. Leamer and J. F. Lutz: Determination of Pore-Size Distribution in Soils. *Soil Sci.*, 49, 347-360 (1940).
15. H. L. Ritter and L. C. Drake: Pore-Size Distribution in Porous Materials. *Ind. Eng. Chem. Anal. Ed.* 17, 782 (1945).
16. P. C. Carman: Fluid Flow Through Granular Beds. *Trans. Inst. Chem. Eng.*, 15, 150-166 (1937).
17. W. C. Krumbein and G. D. Monk: Permeability as a Function of the Size Parameters of Unconsolidated Sands. *Trans. AIME*, 151, 153-163 (1943).
18. P. C. Carman: Capillary Rise and Capillary Movement of Moisture in Fine Sands. *Soil Sci.*, 52, 1-14 (1941).

19. R. R. Sullivan and K. L. Hertel: The Permeability Method For Determining Specific Surface. *Adv. Coll. Sci.*, 1, 36-80 (1942).
20. J. J. McCullough, F. W. Albaugh and P. H. Jones: Determination of the Interstitial Water Content of Oil and Gas Sands. *Am. Pet. Inst. Drill. and Prod. Practice*, 1944 (1945).
21. W. A. Bruce and H. J. Welge: The Restored State Method for Determination of Oil in Place and Connate Water. Presented Amarillo Meeting of the Division of Production, A.P.I. (May, 1947).
22. O. F. Thornton and P. L. Marshall: Estimating Interstitial Water by the Capillary Pressure Method. *AIME Petroleum Technology*, T.P. 2126 (Jan. 1947).
23. L. J. Klinkenberg: The Permeability of Porous Media to Liquids and Gases. *A.P.I. Drill. and Prod. Pract.* (1941), 200-213.
24. M. C. Leverett and W. B. Lewis: Steady Flow of Gas-Oil-Water Mixtures Through Unconsolidated Sands. *Trans. AIME* 142, 107-116 (1941).
25. R. A. Morse, P. L. Terwilliger and S. T. Yuster: Relative Permeability Measurements on Small Core Samples. *Oil & Gas J.*, 46, 109-125 (August 23, 1947).
26. J. H. Henderson and S. T. Yuster: Relative Permeability Studies. *Prod. Monthly*, 12, 13-20 (January, 1948).
27. R. C. Martinelli, J. A. Putnam and R. W. Lockhart: Two-Phase, Two-Component Flow in the Viscous Region. *Trans. Am. Inst. Chem. Engrs.*, 42, 681, 705 (1946).
28. A. C. Bulnes and R. V. Fitting: An Introductory Discussion of the Reservoir Performance of Limestone Formations. *Trans. AIME*, 160, 179 (1945).
29. C. R. Holmgren: Some Results of Gas and Water Drives on a Long Core. Paper presented AIME *Pet. Tech.*, July, 1948, T.P. 2403.
30. R. G. Russell, F. Morgan, and M. Muskat: Some Experiments on the Mobility of Interstitial Waters. *Trans. AIME* 170, 51 (1947).
31. Walter Rose and W. A. Bruce, Evaluation of Capillary Character in Petroleum Reservoir Rock", *J. Pet. Tech.*, (May, 1949).
32. Walter Rose: Permeability and Gas Slippage Phenomena. Presented before the Steering Committee of the Topical Committee on Petroleum Technology of the Division of Production, A.P.I., at Chicago during the 28th Annual Meeting, November, 1948. cf. *A.P.I. Drill. and Prod. Prac.*, in Press, (1948).
33. P. C. Carman: Some Physical Aspects of Water Flow in Porous Media, *Discussions of the Faraday Society*, 3, 72-77 (1948).
34. E. C. Childs and N. C. George: Interaction of Water and Porous Materials, *Discussions of the Faraday Society*, 3, 78-85 (1948).

DISCUSSION

By A. C. Bulnes, Shell Oil Co., Midland, Texas

Walter Rose is to be congratulated on an excellent paper and one which constitutes, in my opinion, a most important contribution to the subject of polyphase flow in porous media.

Particularly gratifying is the fact that it has been found possible to develop a comparatively simple expression for relative permeability from the fundamentals of capillary phenomena and the quantitative measures of rock properties, together with the aid of certain rather generous assumptions, instead of being forced to fall back upon some unobvious and complicated empirical result. Moreover, in the process of this derivation, the relationship existing between the measured data of relative permeability, capillarity, and the void structure of the medium is also brought out in a clear and simple fashion and should be of interest to many readers.

The relative permeability of the wetting phase is shown to be a function of p_w and of an irreducible saturation ρ_{wm} or ρ_{w1} . The determination of ρ_{w1} is relatively simple, or at any rate, it is easy to describe an experiment whereby it can be measured. This does not appear to be the case for ρ_{wm} ; in fact, it is not clear to me just how this quantity can be determined except in terms of the relative permeability; that is, by solving it in Eq. (22), a procedure that would defeat the purpose for which this equation was developed. Moreover, although it appears reasonable to conclude that ρ_{w1} is a lithologic property independent of the fluid properties, it is not evident that the same statement can be made as regards ρ_{wm} . I would appreciate the comments of the author on the foregoing observations.

The assumption that $t_{ew} = t$ is of considerable importance in the mathematical developments and may be accepted as a reasonable first approximation. Rose indicates that if not equal to t , t_{ew} is some function of the saturation. I would like to ask Rose if he considers that t_{ew} may be also a function of the interfacial tension, in which case we would expect the relative permeability to display a dependence upon this quantity. Granting the inequality of t_{ew} and t , I wonder whether Rose would care to express an opinion as to the range of variation to be anticipated in t/t_{ew} for normal variation in ρ_w and/or σ , and also whether abandonment of the assumption of unity as the value of the textural constant ratio would lead to fundamental changes in the shapes of the theoretical curves in Fig. 3.

☆

Author's reply to A. C. Bulnes

Upon reflection I find that my paper is an admixture of theoretical probabilities and theoretical possibilities. The latter are not to be too seriously considered, although perhaps it might be said they stimulate interesting argument. On the other hand the probabilities are believed to be of some importance, and Bulnes has cleverly focused attention on this importance by questioning a major assumption upon which the theoretical developments are based. In view of the fact that no one heretofore has dealt with the textural characterization of polyphase saturated porous media it is appropriate

therefore to set forth the rationale of the concept that the ratio, t/t_{ew} , is reasonably constant throughout the saturation interval of interest. This is best done by recalling that the textural factor is defined as the product of a pore shape factor and a pore tortuosity factor. There appears to be no reason to attempt to describe the variation of shape factors with fluid saturation since it is well established in the literature that these generally fall within the narrow range of 2.0 to 2.5, as applied to homogeneous fluid saturated media, and by implication at least as also applied to polyphase saturated porous media. § On the other hand, the tortuosity factor cannot be so easily disposed of as an universal constant, for values are found to range between 2 and over 200 for consolidated porous media. (A tortuosity value close to 2 is usually quoted for unconsolidated porous media of various particle size, shape and surface characters). Therefore, perhaps we should expect that as the "equilibrium" saturation of the non-wetting fluid is developed, the tortuosity factor will increase since a given element of flowing wetting liquid will have to pass around additional barriers of non-wetting fluid in the central pore spaces. However, it is suspected that once the equilibrium saturation of the non-wetting fluid is established, the tortuosity factor thereafter will remain sensibly constant at all other wetting liquid saturation levels above the minimum where the wetting liquid itself becomes discontinuous. This is because the tortuosity factor is a dimensionless ratio of actual length of fluid streamline to apparent length (i.e. actual bed length). By representing the non-wetting fluid saturation as interconnected spheres located in the central pore spaces it is seen that the ratio will be independent of the distribution of spheres (i.e. the non-wetting fluid saturation) as an approximation.

Thus, whereas t/t_{ew} has been assumed equal to unity in the paper, it would appear that the ratio actually tends to decrease initially as continuity in the non-wetting fluid is being established, thereafter remaining nearly constant and less than unity throughout the wetting liquid saturation interval of interest. Although this conclusion is based on highly speculative argument it is noted that better conformance between

Curve D of Fig. 5 in the paper and the associated experimental data follows if the above described variation of the t/t_{ew} ratio is employed in the solution of Equation 10. Actually, however, it appears that the development followed in the paper (based on the Rho function concepts) obviates the necessity of giving explicit treatment to the rock textural factors, for the analytical expressions finally developed to describe relative permeability phenomena give good conformance between theory and experiment. In any event, it will be clear from the definition of the texture factor that the term, t_{ew} , does not depend directly on fluid properties such as interfacial tension. In this respect, perhaps Bulnes implies that the dynamics of a given system might result in a dependence of the fluid distribution on such fluid properties, which conceivably could result in a dependence of tortuosity (and therefore texture) factors on fluid properties since tortuosity certainly must depend on fluid distribution character. Such dependence, however, will not be easily evaluated. Indeed, it may be regarded that an object of the writer's paper has been to present the view that the characters of polyphase flow through porous media are (a) inadequately understood, and (b) difficult to evaluate either experimentally or theoretically. This condition, sadly enough, permits theorists to say almost anything and empiricists to report almost any data without immediate fear of serious contradiction.

To reply to the comments of Bulnes about the difficulty of evaluating the term, ρ_{wm} , appearing in Eq. (22) of the paper, further reference is made to the correlation of Brownell and Katz as cited in the paper footnote following Eq. (22).* The qualitative correctness of the form of this correlation has been supported recently by the examination of certain unpublished data obtained at this laboratory. It is believed therefore that controlled flooding experimentation should serve adequately for the determination of the limiting saturation parameters such as ρ_{wm} and ρ_{nm} . In any event, the feeling expressed by Bulnes that these limiting parameters will be dependent on fluid properties is born out by the cited result due to Brownell and Katz.

★ ★ ★

§ See for example the recent Carman paper (*Discussions of the Faraday Society*, No. 3, 72-77, 1948), discussing these considerations.

* In the preprint version of the paper the Brownell-Katz equation for ρ_{wm} was incorrectly given.

EVALUATION OF CAPILLARY CHARACTER IN PETROLEUM RESERVOIR ROCK

WALTER ROSE, JUNIOR MEMBER AIME, GULF RESEARCH & DEVELOPMENT CO., PITTSBURGH, PA.
W. A. BRUCE, MEMBER AIME, THE CARTER OIL CO. RESEARCH LABORATORY, TULSA, OKLAHOMA

ABSTRACT

Improved apparatus, methods, and experimental techniques for determining the capillary pressure-saturation relation are described in detail. In this connection a new multi-core procedure has been developed which simplifies the experimental work in the study of relatively homogeneous reservoirs. The basic theory concerning the Leverett capillary pressure function has been extended and has been given some practical application. Some discussion is presented to indicate the relationship of relative permeability to capillary pressure, and to provide a new description of capillary pressure phenomena by introducing the concept of the psi function.

INTRODUCTION

For the purposes of this paper the capillary character of a porous medium will be defined to express the basic properties of the system, which produce observed results of fluid behavior. These basic properties may be classified in the following manner, according to their relationship to:

- (a) *The geometrical configuration of the interstitial spaces.*

This involves consideration of the packing of the particles, producing points of grain contact, and variations in pore size distribution. The packing itself is often modified by the secondary processes of mineralization which introduces factors of cementation, and of solution action which causes alteration of pore structure.

- (b) *The physical and chemical nature of the interstitial surfaces.*

This involves consideration of the presence of interstitial clay coatings, the existence of non-uniform wetting surfaces; or, more generally, a consideration of the tendency towards variable

interaction between the interstitial surfaces and the fluid phases saturating the interstitial spaces.

- (c) *The physical and chemical properties of the fluid phases in contact with the interstitial surfaces.*

This involves consideration of the factors of surface, interfacial and adhesion tensions; contact angles; viscosity; density difference between immiscible fluid phases; and other fluid properties.

Fine grained, granular, porous materials such as found in petroleum reservoir rock possess characteristics which are expressible by (1) permeability, (2) porosity, and (3) the capillary pressure-saturation behavior of immiscible fluids in this medium. These three measurable macroscopic properties depend upon the microscopic properties enumerated above in a manner which defines the capillary character.

Systems of capillary tubes or regularly packed spheres may be thought of as ideal and numerous references can be cited in which exact mathematical formulations are developed to show the relationships governing the static distribution and dynamic motion of fluids in their interstitial spaces. The capillary character of non-ideal porous systems such as reservoir rock also is basic in determining the behavior of fluids contained therein; although, in general, the connection is not mathematically derivable but must be approached through indirect experimental measurement. This paper gives consideration to the evaluation of petroleum reservoir rock capillary character. The methods employed may be applied to the solution of problems in other fields, and the conclusions reached should contribute to the basic capillary theory of any porous system containing fluid phases.

In this paper, a modification of the core analysis method of capillary pressure is employed and it is intended to show that the capillary character of

reservoir rock can be expressed in terms of experimental quantities. A very general method of interpretation correlating the capillary pressure tests with fundamental characteristics such as rock texture, surface areas, permeability, occasionally clay content and cementation is introduced. Eventually an attempt is made for establishing a method of deriving relative permeability to the wetting phase from capillary pressure data.

The experimental evaluation of capillary character must be approached in a statistical manner if reservoir properties are to be inferred from data on small cores. This is implied by the heterogeneous character of most petroleum reservoirs, and suggests that considerable intelligence should be applied in core sampling. Finally, this paper supports the view that once the capillary character of a given type of reservoir rock has been established by core analysis, fluid behavior can then be inferred in other similar rock. Although no great progress has been made in establishing what variation can be tolerated without altering the basic fluid behavior properties, evidence will be presented to indicate that certain reservoir formations are sufficiently homogeneous with respect to capillary character that the data obtained on one core will be useful in predicting the properties of other cores of similar origin. Tests have shown that cores under consideration can vary widely with respect to porosity and permeability and still be considered similar in capillary character.

EXPERIMENTAL METHODS AND TECHNIQUES

Various types of displacement cell apparatus for capillary pressure experiments have been described in the literature. Bruce and Welge¹; Thornton and Marshall²; McCullough, Albaugh and Jones³; Hassler and Brunner⁴; Lever-

Manuscript received at Petroleum Branch Office August 31, 1949.
¹References are given at end of paper.

ett⁶; and others have used various types of apparatus to measure the interstitial water in petroleum reservoir cores. Richards⁶ developed a similar apparatus to study soil sorption, and he gives references to the work and apparatus of ten previous experimenters in this field of soil physics. Of particular interest is the early work of Haines^{7,8} in which he describes methods of studying capillary pressure hysteresis effects, and the work of Leamer and Lutz⁹ in which they propose and use displacement cells to evaluate pore size distribution in porous systems. More recently Welge¹⁰ has described displacement apparatus to measure oil displacement, and Amyx and Yuster¹¹ have described apparatus which they are using in their secondary recovery study.

None of the conventional techniques referred to above are entirely suited to the purposes of the experimental program reviewed in this paper. This was due in part to the desire to develop multiple-core techniques; and also to the fact that conventional apparatus was characterized by (a) the limited range of temperature and pressure conditions which could be employed in experiments using the apparatus, (b) the complicated assembly and cleaning features which made experimental work tedious, and (c) by the semi-permeable barrier failure trouble which introduced apparatus errors into the experimental results. The modified apparatus described below was designed to overcome these limitations, and also to make the rapid accumulation of the experimental data discussed in this paper. It is of interest to mention here that Richards^{8,12,13,14,15} working in a different field (soil science) anticipated many of the requirements which should be incorporated into displacement cell design to satisfy the purposes of petroleum reservoir behavior study, and his pioneering work has contributed to some of the developments reported here.

A displacement cell should be regarded as a reservoir model system wherein the conditions which produce effects in the reservoir can be simulated adequately in a laboratory experiment. Fig. 1 shows how basic parts of the apparatus illustrated in Figs. 2 and 3 can be assembled in a variety of ways when various types of experiments are con-

templated. It can be supposed that the core element represents some volume portion of the reservoir under consideration. This core may be saturated with fluid phases according to the saturation condition of the represented portion of the reservoir at some initial state. Surrounding the core in a high pressure chamber is an environment of the displacing fluid phase. The core itself is placed in capillary contact with a semi-permeable barrier which is preferentially wetted by, permeable to, and saturated with the immiscible fluid phase to be displaced from the core. Thus, this membrane barrier separates the high pressure chamber containing the core and filled with the displacing phase from a low pressure chamber filled with the phase to be displaced. The establishment of a suitable pressure difference across the membrane barrier, in general, causes the displacing phase to

enter some interstitial portions of the core producing a displacement of the wetting fluid from the system.

This reservoir model system permits a quantitative measurement of the character of the displacement which is caused by the pressured advance of the displacing phase into the interstitial spaces, and which results in the displacement of the fluid originally occupying these spaces. The experimental data which can be obtained yield relationships involving capillary pressure, fluid saturation and rates of displacement.

The means for interchange of the semipermeable barrier is a special feature of the displacement cells illustrated in Figs. 2 and 3. This is desired particularly when changing from aqueous phase displacement to oil phase displacement since no single barrier can serve both of these purposes. Inter-

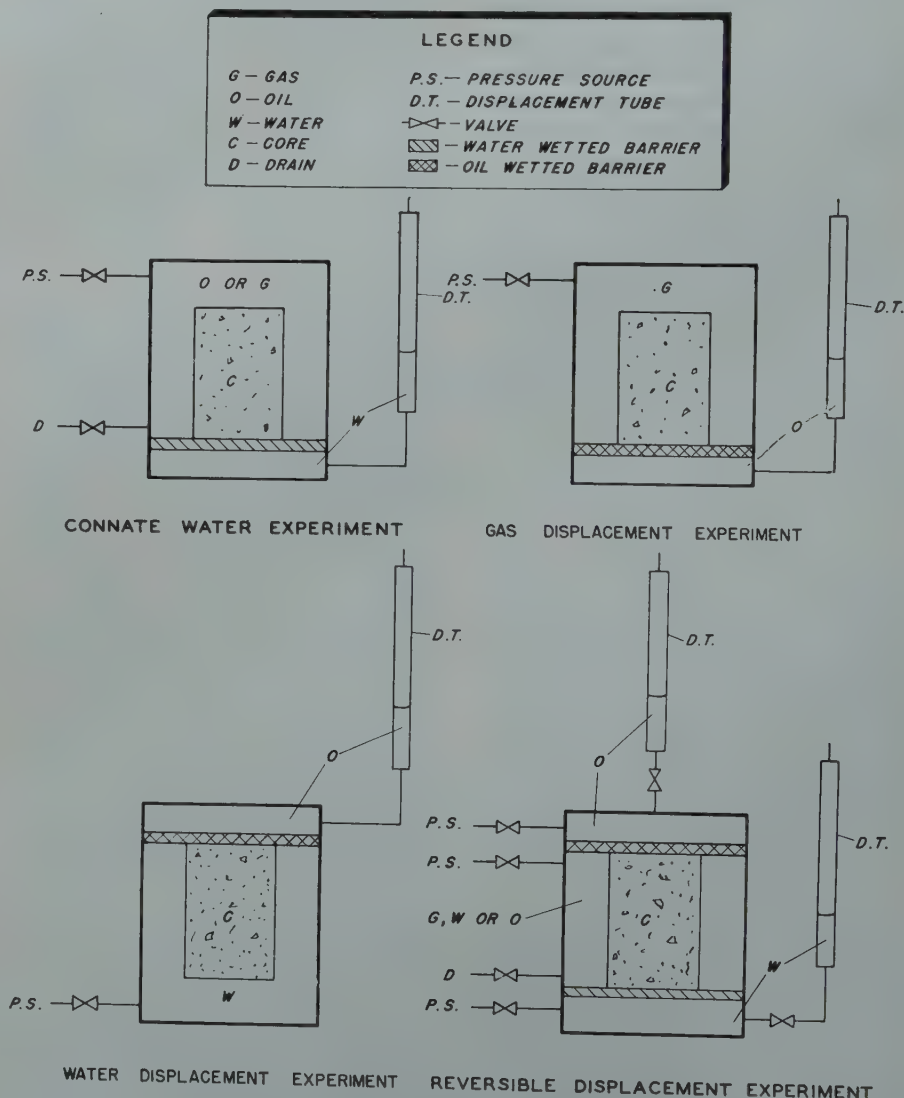


FIG. 1 — DISPLACEMENT CELL ASSEMBLIES.

changeability is also desired when changing from low to high capillary pressure operations, and when changing from one operation to another of the same type, additional barriers being required because of prior failure or similar reason. These considerations can be clarified by describing the necessary properties which characterize semipermeable barrier material. In the first place the barrier must have surface characteristics such that it is preferentially wetted by the phase to be displaced from the cores when it is saturated with this phase. This means that the non-wetting (immiscible) displacing phase

cannot permeate the barrier until some critical threshold pressure is exceeded, at which time the forces of capillarity are no longer sufficient to keep the pores of the barrier saturated with the wetting phase. On the other hand, the wetting phase can permeate the barrier under any condition of pressure difference across the barrier. It is evident then, that the semi-permeable behavior of a given membrane material can be realized only when the operating conditions are confined within a definite displacement pressure range. Many materials have been considered suitable to use as semipermeable barriers in dis-

placement cells. Among these might be listed porous ceramic and porcelain materials, cellophane and collodion type materials, sintered glass and metal, unconsolidated beds of barium sulfate and carbon, porous rubber, carbon discs, animal membranes, etc. Some of these materials are irreversibly water or oil wetted, while others can be rendered either water or oil wetted by suitable chemical treatment of the internal pore surface. The treatment of membranes to change their wetting character has been described by Welge¹⁰ and Amyx and Yuster¹¹.

Fig. 2 shows that the lid and base member are joined together by a threaded coupling to form a pressure chamber. A self-sealing type gasket provides the desired pressure seal. This diagram shows how a spring mechanism holds the core element in capillary contact with a cellophane type semipermeable barrier. The membrane barrier is in turn gasketed in a holder which has a central flow channel extending downward from the surface supporting the membrane and core, and thence outward through a series of tubes, adaptors and other parts to a volumetric fluid measuring (glass) tube located on the outside of the pressure chamber. Indicated also in the diagram is a porcelain semipermeable barrier cemented in another type holder which is interchangeable with the cellophane membrane holder, and which has a similar flow channel arrangement. The cell itself has several threaded ports through which the displacing fluid can be admitted and through which fluids can be drained out, according to the requirements of the experimental procedure followed.

Referring to Fig. 3 it is seen that the multi-core cell differs from the single core cell (Fig. 2) principally in capacity and size. The illustrated apparatus will accommodate eight one-inch core plugs, although other multicore cells have been built to accommodate more than twenty cores. It is often regarded as being more desirable to analyze rapidly a number of cores for approximate values than to devote excessive time to the accurate analysis of a single core. Therefore, the multi-core displacement apparatus is particularly useful for routine work. Another object of the multi-core approach is the possibility of filling the

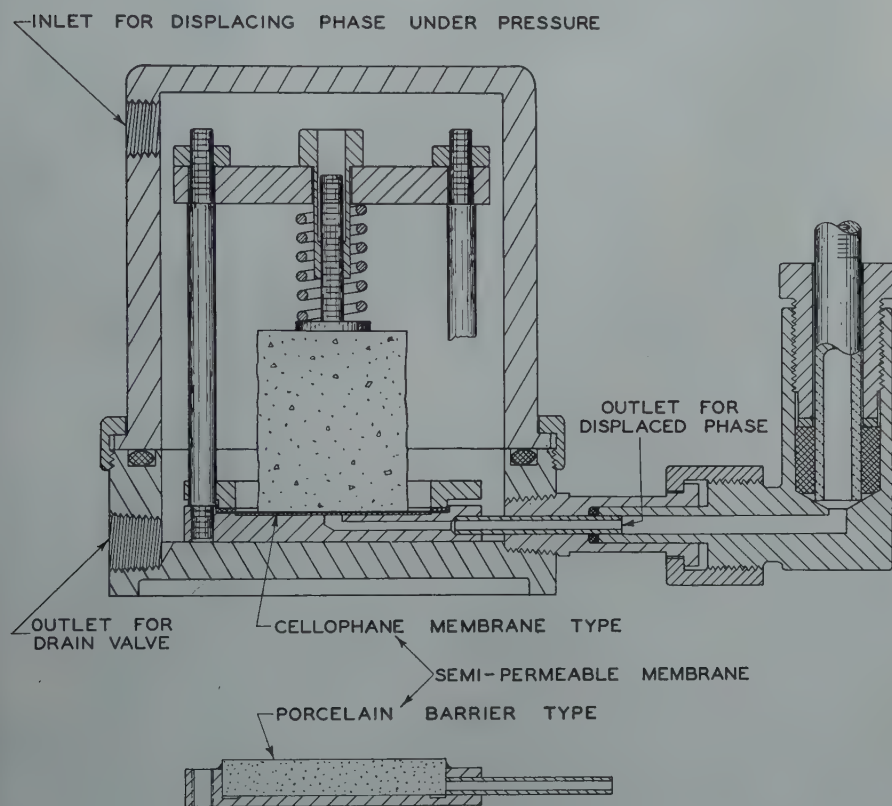


FIG. 2 — SINGLE CORE DISPLACEMENT CELL.

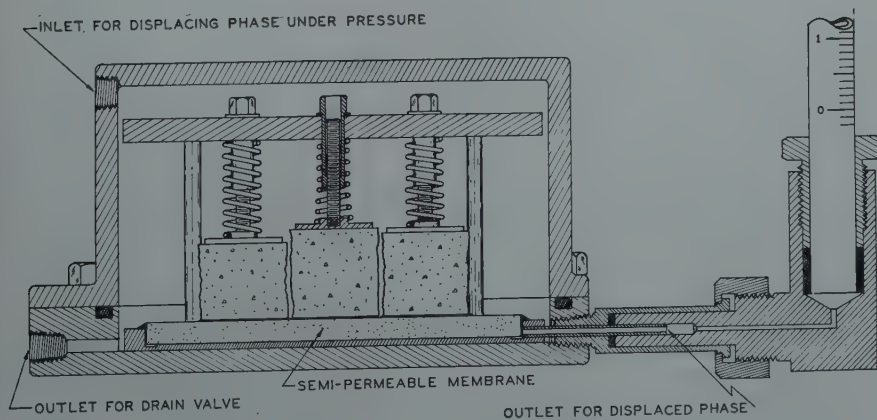


FIG. 3 — MULTI-CORE DISPLACEMENT CELL.

cell with a number of small core fragments and then, in the interpretation of the displacement data, collectively regarding these fragments as contributing to the behavior of some hypothetical core (or reservoir). This technique provides a rapid means of obtaining displacement data and a means of studying a collection of small rock fragments (e.g. cuttings) where individual analysis of any single fragment would be impractical because of the large relative error involved in accurately measuring small volumes of displaced fluid.

Several schemes have been devised to measure the degree of displacement in capillary pressure experiments. Volumetric measurement (visually or electrically) of the displacing phase entering, or the displaced phase leaving the displacement cell is a method commonly employed. Core conductivity measurements also have been employed to indicate core brine saturation. This scheme is satisfactory if sufficient care is taken to control electrode contact potentials, and if a calibration curve is available relating conductivity to saturation for the particular system being studied.

The most reliable and certain way of determining fluid saturation is by distillation and extraction. Fig. 4 shows a modified Dean-Stark apparatus which has been designed to be used according to the method of Rall and Taliaferro¹⁶ for water and oil measurement in core samples. This apparatus differs from the Bureau of Mines apparatus¹⁶ in ways which permit more accurate measurement of small quantities (0.1 ml. or less) of water. The vapor entry from the sample flask into the condenser tube is through the water jacket at the side so that the condensed solvent vapors are cooled as they pass the trapped water distillate in refluxing back to the sample flask. This eliminates loss of trapped water by secondary distillation out of the top of the condenser tube, and also allows ultimate recovery to be attained more rapidly. A second feature involves rendering water-repellent the entire inner glass surface of the apparatus as well as all ground glass tapered joints. This is accomplished by treatment with alkyl-chloro-silane (G. E. Dri-film).¹⁰ After such treatment it is observed that the condensed water droplets fall freely by gravity into the water trap rather than adhere to the glass

condenser surfaces. In designing the water trap a stopcock has been placed at the bottom of the calibrated tube. By filling this volume-calibrated water trap tube with mercury at the beginning of the analysis the trapped water collects in the large diameter upper portion of the trap. Withdrawal of the mercury at the end of the analysis through the stopcock draws this recovered water into the small volume-calibrated portion of the trap, and in this way smaller water values can be measured more accurately than with conventional apparatus.

THE CAPILLARY PRESSURE-SATURATION RELATION

It is a special purpose of this paper to describe apparatus, develop theory, and present data which will indicate a rapid and reliable way to measure the capillary pressure relationship and to indicate briefly the practical and theoretical importance of the data which are obtained. Experimental methods and techniques of the type described above have a wide range of usefulness in core analysis as is evidenced by the general acceptance of capillary pressure techniques to study connate water and oil production characteristics of petroleum reservoirs^{1,2,3,4,5,10,11}. Although Leverett¹⁷ and Hassler, Brunner and Deahl¹⁸ originally emphasized the importance of evaluating the entire capillary pressure curve including the zone of hysteresis, recent authors^{1,2,3} have concentrated more on the engineering applications of capillary pressure data. In this paper, the theoretical and practical importance of the entire capillary pressure curve is stressed along with the importance of certain critical portions of this curve.

The references cited attempt to show that certain types of capillary pressure study will reveal information about the saturation distribution of fluid phases which existed under some given reservoir condition. This represents a possibility only insofar as core properties are a true measure of over-all reservoir properties, which presumes a condition of homogeneity seldom encountered in petroleum reservoirs. Generally, this limitation is recognized and efforts are made to average the data statistically in a manner which permits inference of approximate fluid distribution. How-

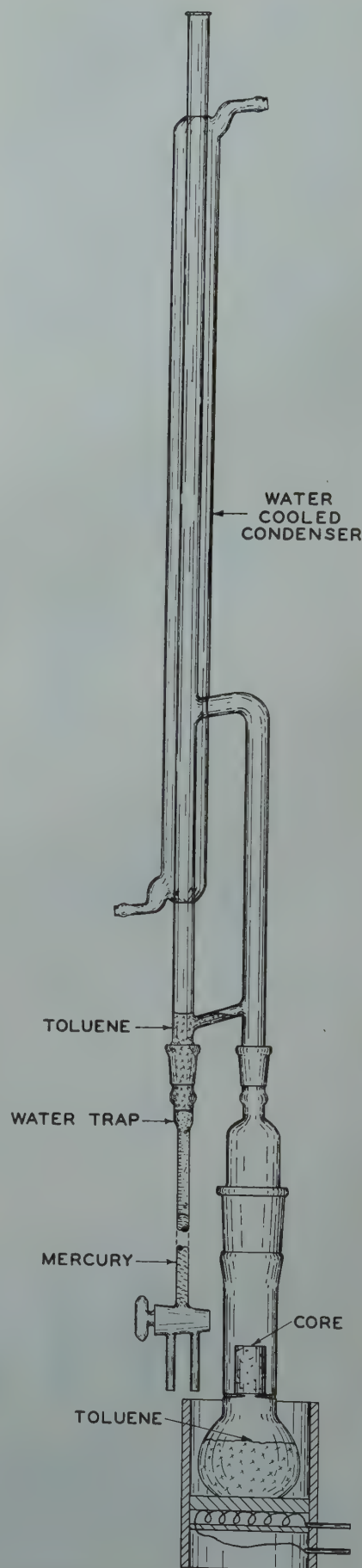


FIG. 4 — TOLUENE EXTRACTOR.

ever, another limitation must be recognized before these engineering applications of capillary pressure data will be acceptable on theoretical grounds. It has been stated that in the capillary pressure experiments an attempt is made to simulate reservoir conditions, in order to produce measurable reservoir-like effects on a core reservoir model. This requires a perfect knowledge of the reservoir processes to be simulated, and an ability to accomplish physically the desired processes. The fact that there is a marked hysteresis effect in the capillary pressure relation emphasizes this requirement. In certain instances, therefore, it may be questioned whether or not an adequate

knowledge can be had regarding what occurred in the reservoir over geologic time. For instance, it is desired in capillary pressure work to attain conditions of static equilibrium only to the extent that this state prevails in the reservoir, a factor which may or may not be known. These recognized limitations present problems which will be solved eventually. Although the data and methods presented contribute to the solution of these problems, the special object of this paper is to demonstrate that capillary pressure work has another value, unlimited by the considerations which limit the engineering applications of capillary pressure data. That is, the capillary pressure curve associated with

a porous system provides a characterization of the capillary properties of the system, and this is desired in the proper interpretation of observed fluid behavior in porous media.

A capillary pressure experiment is defined as a process in which a fluid phase saturating the interstices of a porous rock system is displaced by the advance of other immiscible displacing phases. This displacement is observed to continue until the displacing forces become balanced by the opposing forces of capillarity, approaching a condition of static equilibrium. Figs. 5, 6, and 7 shows a series of capillary pressure curves of the type commonly encountered. There is a finite threshold pres-

CALCULATED CAPILLARY PRESSURE CURVES, $P_c = \left(\frac{f}{K} \right)^{1/2} j(S_w) (\gamma \cos \theta)$

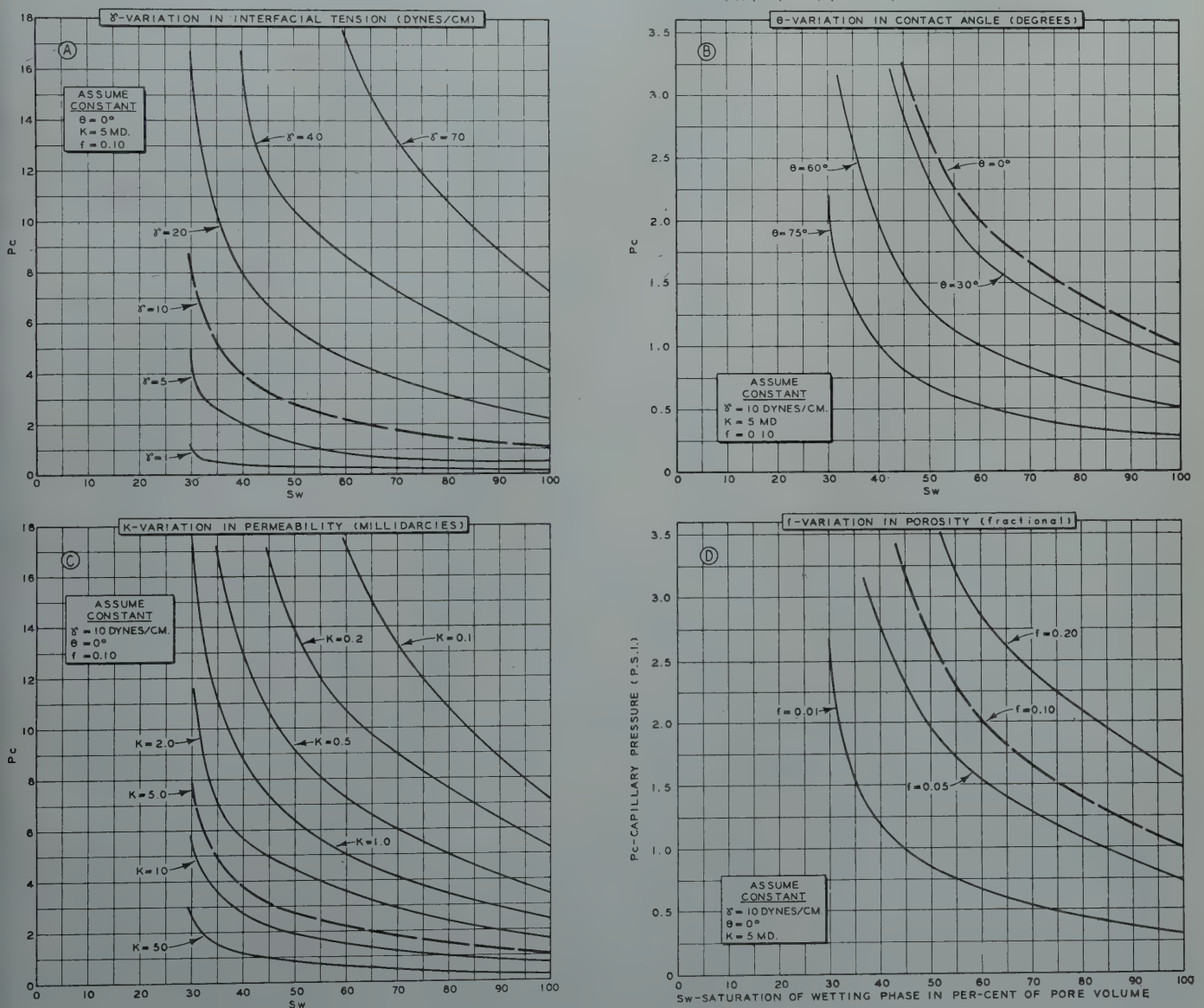


FIG. 5 — CALCULATED CAPILLARY PRESSURE CURVES, $P_c = \left(\frac{f}{K} \right)^{1/2} j(S_w) (\gamma \cos \theta)$

sure which must be exceeded before displacement occurs. This is followed by a near horizontal portion of the curve and then a near vertical portion which seems to indicate an asymptotic approach to some "irreducible minimum" value of the wetting phase saturation at high capillary pressures.

The concept of irreducible minimum water saturation has resulted from the nearly vertical character of the P_c vs. S_w curves. If these curves are going to approach zero wetting phase saturation at infinite capillary pressure, it is possible but not likely that a true irreducible minimum exists. For purposes of engineering work, it has been in the past assumed that a working irreducible minimum exists and can be determined experimentally. This minimum has been defined as that portion of the curve for which the saturation does not change appreciably for a fairly large change in capillary pressure. Experiments not reported here have indicated that oil as a displacing medium tends to produce a curve which becomes more definitely vertical than in the case when air is used to displace the wetting phase. Two phenomena may have a bearing on the wetting phase saturation in the region of low saturation. In the first place, conditions of wettability may be such that in the funicular saturation region water is distributed in the pores in a different manner when oil is the displacing fluid than it is when air is used. In the second place as the displacing fluid moves the water successively into smaller pores it is to be expected that some water will be trapped in the pockets from which there is no exit for fluid to move by viscous flow. If gas is the displacing fluid it is possible for the trapped water to escape by diffusion process and qualitative calculations indicate that the time for diffusion is of the order of days for 99% equilibrium. If oil is the displacing medium a pocket of water which has been trapped will require a time of the order of tens of years to move out by diffusion. While this time is long enough for equilibrium in a reservoir, it is not long enough for equilibrium in a laboratory experiment. Another way of stating this is that an irreducible minimum exists when oil displaces water and that this irreducible minimum is that saturation at which water ceases to move as a viscous fluid.

These considerations are important in the application of capillary pressure data to the study of interstitial water distribution of a virgin reservoir. It may be concluded that the use of reservoir fluids constitutes the preferred procedure in experimental work where the reservoir conditions of low capillary pressure are to be simulated. Under these conditions fluid properties such as interfacial tension are of importance.

On the other hand, it may be concluded that substitution of an inert gas

for oil as the displacing phase may be the preferred procedure when reservoir conditions of high capillary pressure are to be simulated. Under these conditions, fluid properties such as interfacial tension seem to have little or no effect on the resulting wetting phase saturations as is evidenced by the near, vertical shape of the capillary pressure curve in this region.

To conclude the section on the capillary pressure-saturation relation, reference is again made to Fig. 5 to show the

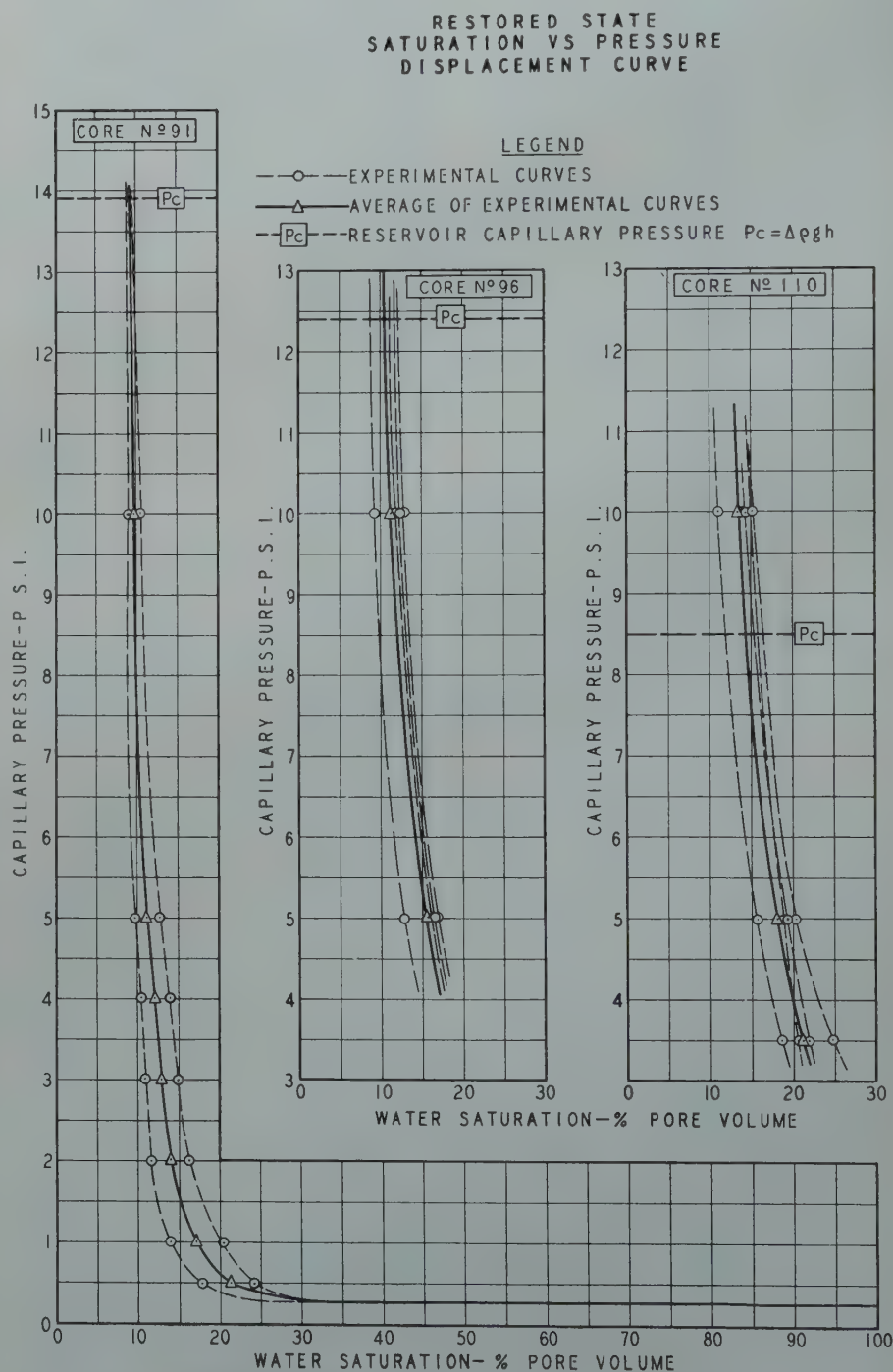


FIG. 6—RESTORED STATE SATURATION VS. PRESSURE DISPLACEMENT CURVE.

dependence of this relation on permeability, porosity, interfacial tension, and contact angle. The theoretical basis for this dependence and the technique of calculating capillary pressure curves are discussed in the next section. In each of the family of capillary pressure curves shown in Fig. 5 three of the above listed parameters are held constant and the fourth is varied over a reasonable range to show the relative effect of this fourth variable. It is observed that small deviations of the contact angle from zero only slightly displace the curve; that considerable variation in porosity can be tolerated without seriously displacing the curve; and that independent variation of interfacial tension or core permeability produces considerable distortion of the capillary pressure curves.

THE CAPILLARY RETENTION RELATION

Employment of apparatus such as that illustrated in Fig. 2 has been the common method of experimentally evaluating capillary pressure behavior. The following theoretical development based on the concept of capillary retention suggests the possibility of another approach using the multi-core apparatus illustrated in Fig. 3. Leverett in two of his theoretical papers^{17,21} developed the semi-empirical relation

$$j(S_w) = \frac{P_c}{T} \left(\frac{K}{f} \right)^{1/2} \quad (1)$$

which he accepted because it was indicated by dimensional analysis and was supported by experimental data. Here $j(S_w)$ is a dimensionless function of

the wetting phase saturation, termed the "capillary pressure function". P_c is the capillary pressure which Eq. (1) shows as being proportional to $j(S_w)$ and to the interfacial tension, T , and inversely proportional to the square root of the permeability-porosity ratio, $(K/f)^{1/2}$. This term, $(K/f)^{1/2}$, according to derivation from the Poiseuille and Darcy equations, can be shown to be equal to the "average pore radius" of the porous system being studied. Hence, there is theoretical justification for Eq. (1) since it conforms to basic concepts of capillarity as defined by Eq. (2). Leverett's data showed that a plot of the capillary function, $j(S_w)$, versus saturation of the wetting phase, S_w , yielded a unique curve which described in an adequate manner the capillary retention of wetting liquid existing in the clean, unconsolidated sands studied, when capil-

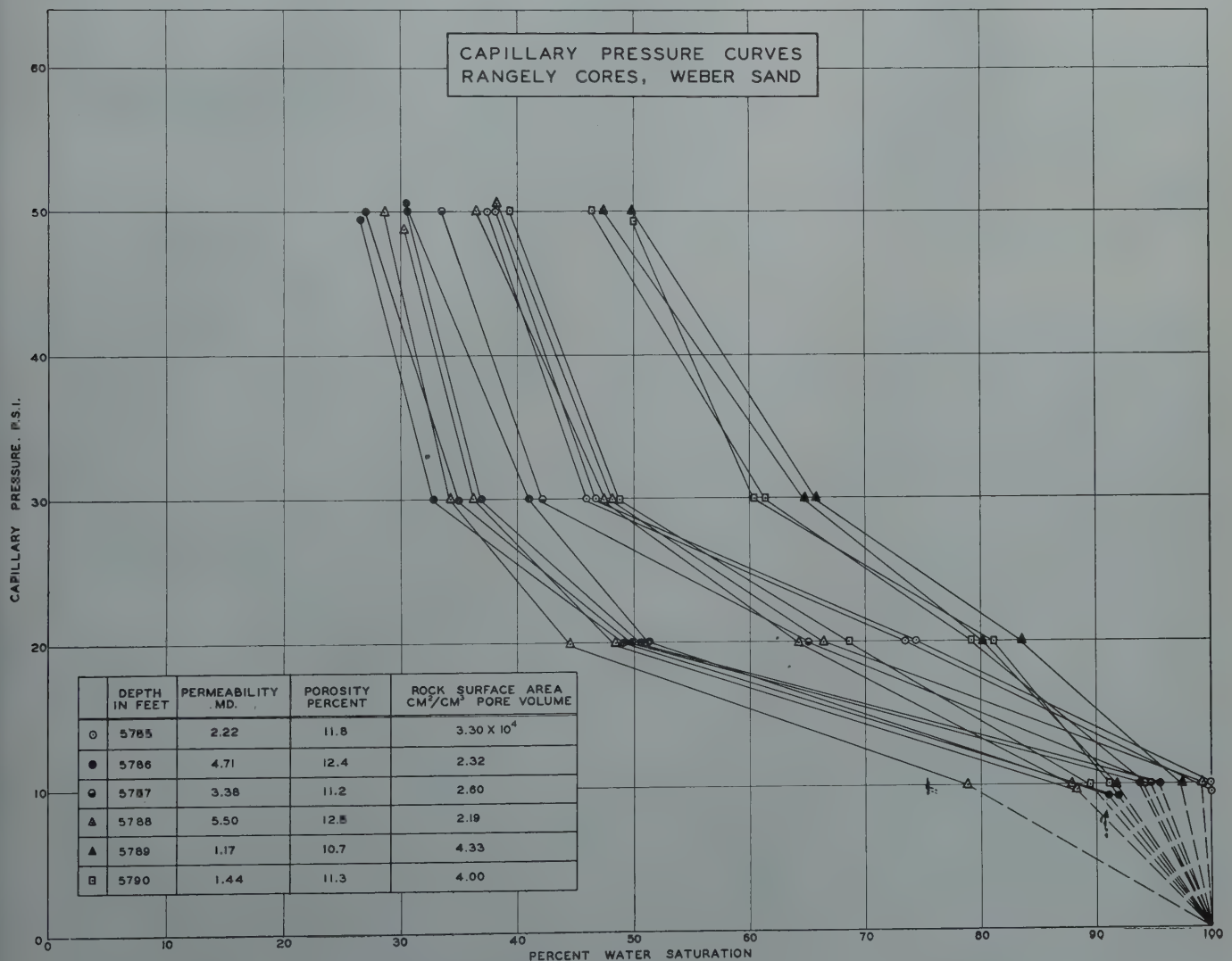


FIG. 7 — CAPILLARY PRESSURE CURVES RANGELY CORES, WEBER SAND

lary forces were balanced by gravitational forces (static equilibrium condition). A re-plot of Leverett's average data is shown in Fig. 8, along with data obtained on a number of consolidated systems according to the method presented in this paper. The theoretical aspects of this data plot are discussed below.

Starting from the basic concept of capillary rise in circular tubes, where

$$P_c = Dgh = \frac{2\tau}{r} \quad (2)$$

(complete wetting is assumed for the purpose of simplicity, that is, the contact angle, θ , is zero), Carman²² has shown how an evaluation of capillary rise in other more complex systems, such as random-packed, non-spherical sand systems, can be made by assuming that twice the "hydraulic radius" is suitable value to use for the radius, r , in Eq. (2). Since this "hydraulic radius" is defined as the ratio of porosity, f , to surface area in units of bulk volume, A , Eq. (3) can be derived where h indicates the height of capillary rise, D is the density difference between fluid phases, and g is the gravitational constant.

$$\frac{P_c}{\tau} = \frac{Dgh}{\tau} = \frac{A}{f} \quad (3)$$

Carman studied clean unconsolidated sand systems similar to those used by Leverett (loc. cit.) and seemed to obtain experimental confirmation to support his theoretical argument. The close connection between the work of Carman and Leverett is evident by considering the Kozeny equation^{23,24} which expresses specific surface area in terms of permeability and porosity and other constants (and which is rearranged here to conform with the units and dimensions of the other equations in this paper).

$$A = f \left(\frac{f}{K} \right)^{1/2} \left(\frac{1}{k} \right)^{1/2} \quad (4)$$

Here, k is the numerical (rock textural) constant which makes the Kozeny equation describe streamline motion through granular beds. This equation can be combined with Eq. (3) to yield an expression similar to Eq. (1). Thus, when S_w equals unity

$$\frac{P_T}{\tau} \left(\frac{K}{f} \right)^{1/2} = \left(\frac{1}{k} \right)^{1/2} \quad (5)$$

where P_T is the threshold pressure, defined as

$$\lim_{S_w \rightarrow 1} P_c = P_T$$

By replacing P_c by P_T in Eq. (3), a possible minimum value for A/f is obtained. Accordingly,

$$\lim_{S_w \rightarrow 1} j(S_w) = \left(\frac{1}{k} \right)^{1/2} \quad (6)$$

In this manner a numerical interpretation is given to the limiting value of the capillary pressure function. Eq. (6) shows the limiting value of the $j(S_w)$ function to indicate a minimum value of the square root of the reciprocal Kozeny constant, k . Carman^{25,26}, Fowler

and Hertel²⁷, and others have evaluated this constant, k , as it applies to a variety of unconsolidated systems by an independent method, and find experimentally that it is approximately 5. From basic capillarity as it applies to the geometry of the system it can be shown that for ideal systems (viz. regular packed, uniform spheres) k is equal to 5.

The replot of Leverett's data in Fig. 8 shows 0.42 to be the limiting $j(S_w)$ value, or according to Eq. (6), k equals 5.7. This value compared with the Fowler and Hertel (loc. cit.) have obtained a value of 5.5 for similar systems. Table

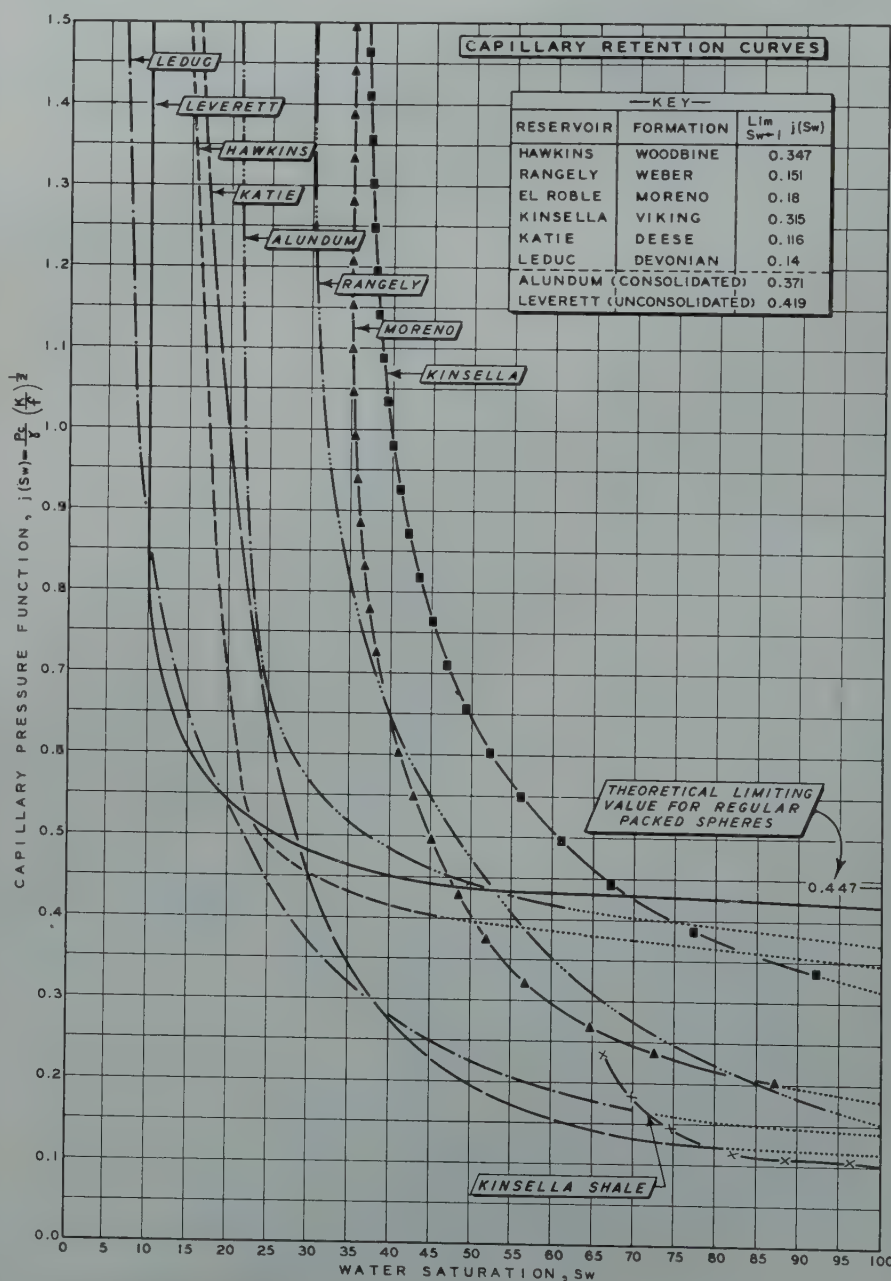


FIG. 8 — CAPILLARY RETENTION CURVES.

I (Page 137) correlates the limiting $j(S_w)$ values observed in Fig. 8 with the character of the porous system to indicate qualitatively a relationship between rock properties and deviations from ideal behavior.

Table II obtained from the analysis of data on several cores from the same reservoir presents evidence that the deviation of limiting values for $j(S_w)$ from 0.447 (ideal case) is related to the presence of fine interstitial material (in this case clays).

It is assumed in Table II that weight

Weight Pct. fine fraction (Sieve anal.)	Pct. Clay	Lim $j(S_w) \rightarrow 1$	k Values
5.1	—	0.17	35.0
5.7	5.9	0.18	31.2
5.9	5.7	0.21	23.0
8.9	8.5	0.08	155.0
11.6	—	0.05	400.0

per cent fines as determined in grain sieve analysis is a rough measure of interstitial clays. However, these data should not be interpreted to mean that the presence of interstitial clays is responsible entirely for deviations of lim-

iting j values from the ideal value. It is probable that cementation, secondary alteration of pore character, as well as other factors will likewise cause deviations. All other factors being equal, it can be inferred that an increase in interstitial clay content will cause a corresponding decrease in the experimentally determined limiting j values.

Aside from the fact the threshold pressure P_T can be derived, and limiting values of the Kozeny constant, k , evaluated from the $j(S_w)$ versus S_w data plot, there are several other interesting applications possible. Fig. 9 is a capillary retention plot of the capillary pressure data shown in Fig. 7. It is observed that the similar capillary retention behavior of these argillaceous cores is not at once apparent in Fig. 7, nor was it anticipated by the statements of Leverett (loc. cit.) who suggested that interstitial clays would present an anomalous situation. Fig. 9, on the other hand, shows how the porosity-permeability compensation of the j -function treatment suitably corrects capillary pressure data to show the basic behavior character of the porous rock. Fig. 10 shows how the J-Curve reveals the character of a type of limestone, even though these cores had a scattered permeability-residual water saturation plot.

USE OF NOMOGRAPH

Fig. 11 is a nomograph relating values for $j(S_w)$, P_c , or P_T , K , k , f , τ , to each other, such that any of these variables can be calculated by nomographic construction providing the others are known or assumed. The values for $j(S_w)$ plotted in Figs. 8, 9, and 10 were calculated in this manner and then associated with the proper wetting phase saturation values to yield these capillary retention curves. A more interesting application is to use this nomograph in the reverse process of calculating capillary pressure curves from capillary retention data. Thus, it is observed that once the capillary retention trend characterizing a given type of rock is obtained, values for capillary pressure can be related nomographically to $j(S_w)$ values, which are in turn related by the capillary retention curve to definite saturation, S_w , values. All that need be known (or assumed) are values for

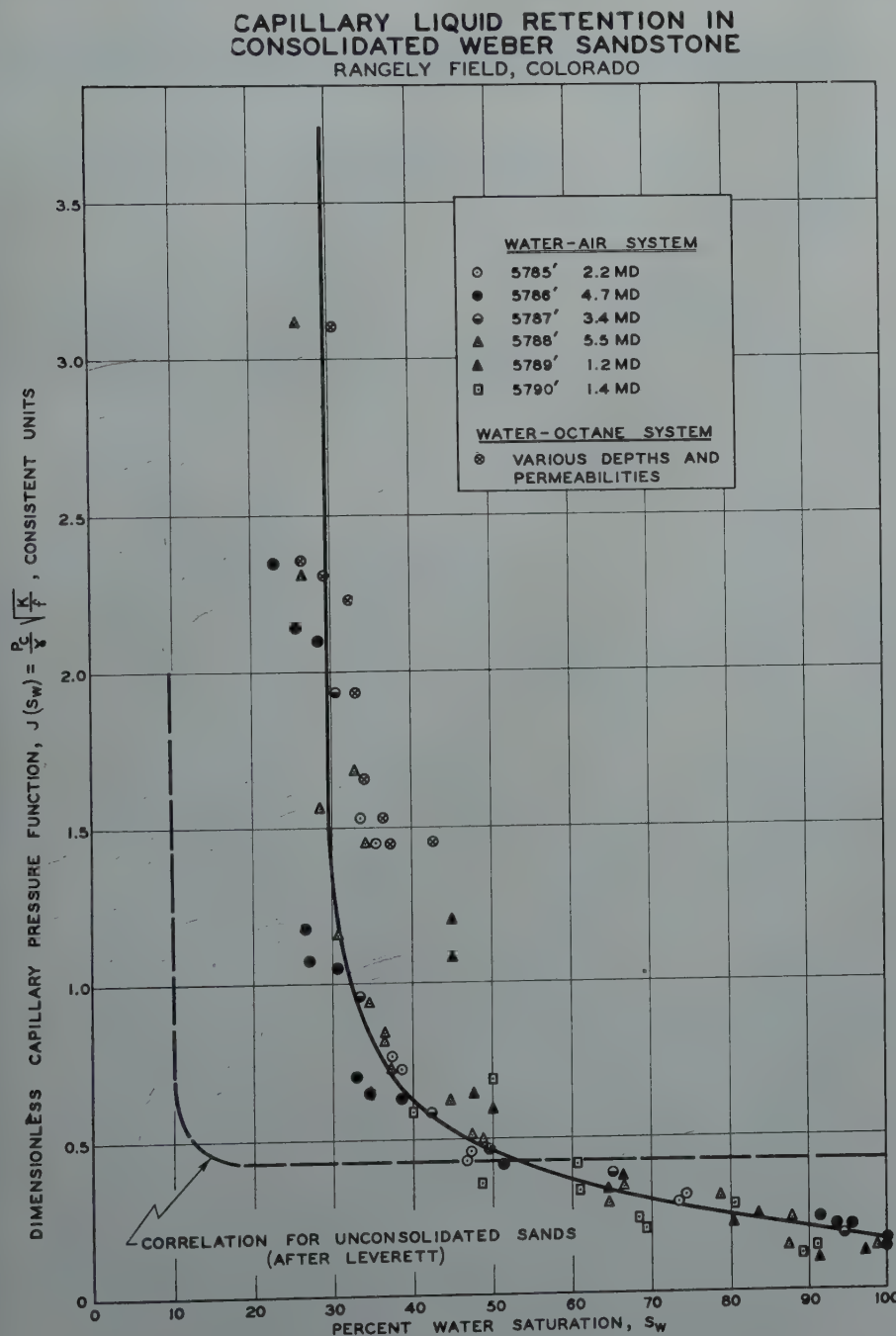


FIG. 9 — CAPILLARY LIQUID RETENTION IN CONSOLIDATED WEBER SANDSTONE.

permeability, porosity and interfacial tension. Fig. 5 has been presented above as a complete example of this calculation.

It is apparent that the multi-core apparatus described in the first part of this paper (Fig. 3) has special application in the derivation of calculated capillary pressure curves from capillary retention data plots. For example, if several cores from the same formation but differing in permeability, porosity, and other characteristics are assembled in the multi-core apparatus, in many instances sufficient data will be obtained to establish the capillary retention curve by merely applying a single displacing pressure to the apparatus and then measuring residual wetting phase saturations in the individual cores after static equilibrium has been attained. This is illustrated in Fig. 7 where saturations ranging between 45 and 85 per cent are observed to characterize this group of fifteen cores under conditions of 20 psi capillary pressure. There are enough data to establish part of the capillary retention curve presented in Fig. 8. Furthermore, the whole capillary pressure curve can be established for any of these cores if porosity, permeability, and interfacial tension are known.

The use of the nomograph entails first joining the porosity and interfacial tension values with a straight edge, producing a point of intersection on the multiplier scale. This point is then joined to the proper permeability value, producing another point of intersection on the

$$\gamma \left(\frac{f}{K} \right)^{1/2}$$

scale. Finally, a series of straight lines through this latter point intersecting the other two scales of the nomograph will give values of capillary pressure, (P_c) which are related to corresponding values of $j(S_w)$. Employing the capillary retention curve, values for P_c then can be associated with values of S_w to produce calculated capillary pressure curves of the type illustrated in Figs. 5. Since considerable time is required to measure experimentally a capillary pressure curve, this multi-core method of calculating the capillary pressure relation permits considerable saving of

experimental time. It is noted that these calculated curves deviate from experimental curves to the same degree that experimental data points deviate from the average trend when plotted on the capillary retention curve. In this connection, some deviation of individual values can be tolerated since the multiple core approach has been organized to reveal more about the capillary properties of the reservoir from which the core material was recovered, rather than to tell about the detailed anomalies in the properties of any particular core.

INTERPRETATION OF THE KOZENY RELATION, TORTUOSITY, AND SURFACE AREA

The Kozeny relation as stated in Eq. (4) can be given in a more explicit form. The actual streamline flow velocity through channels in a porous system is greater than the apparent velocity by virtue of the tortuous path which must be followed. Thus, the permeability may be expressed as

$$K = \frac{fm^2}{k_o} \left(\frac{L}{L_a} \right)^2 (\text{c.g.s. units}) . \quad (7)$$

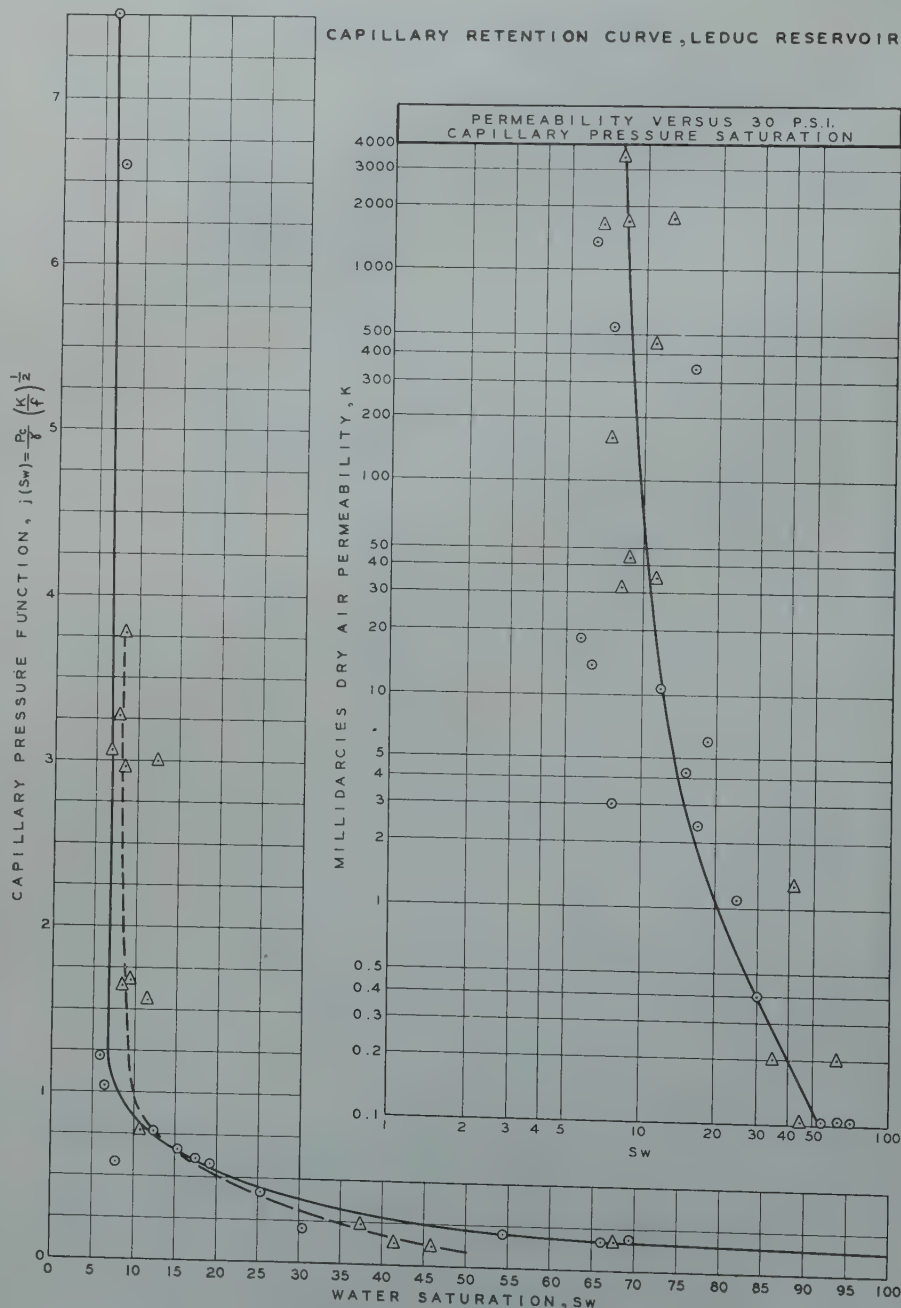


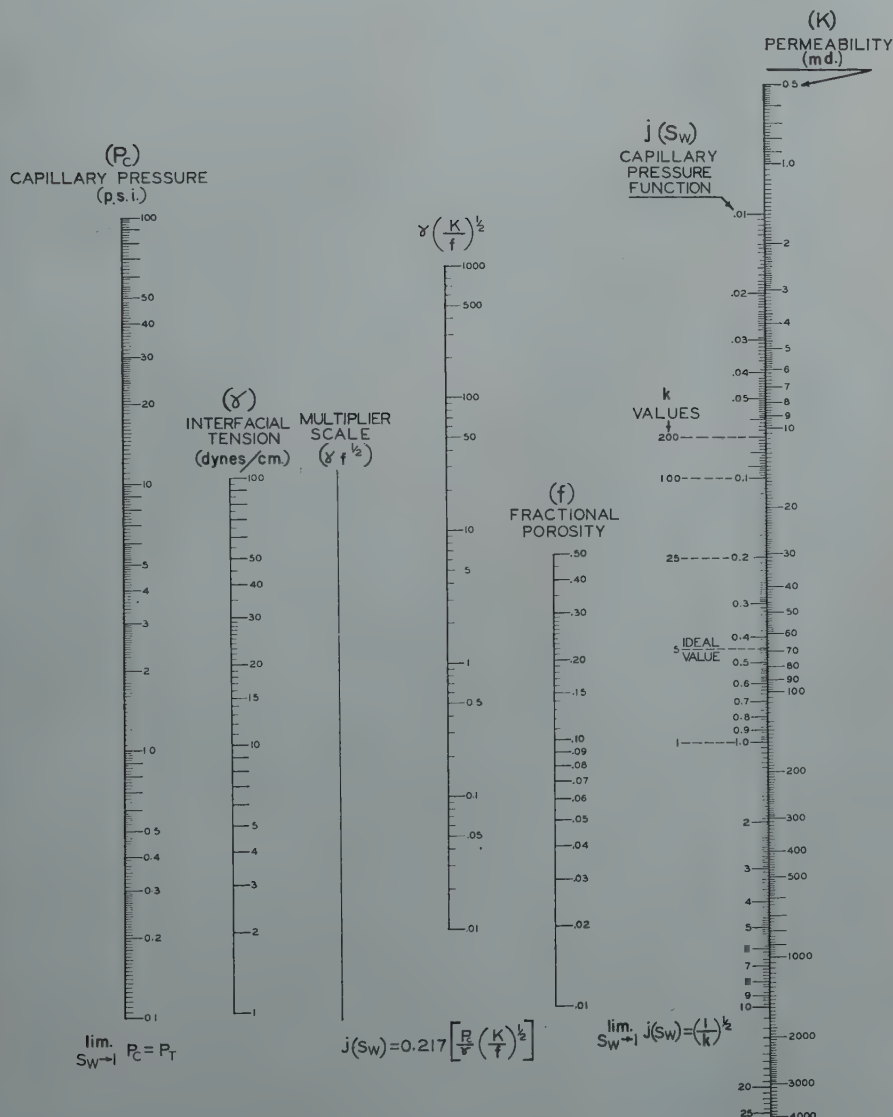
FIG. 10 — CAPILLARY RETENTION CURVE, LEDUC RESERVOIR.

TABLE I*

Type Rock	Rock Character	$\lim_{S_w \rightarrow 1} j(S_w)$	k	Permeability range, md.
Uniform pack spheres	Ideal system	0.447	5.	
Unconsolidated sand (Leverett)	Clean, random packed	0.42	5.7	50-2,000,000
Alundum synthetic cores	Sintered Alumina	0.37	7.2	50-1,500
Hawkins (Woodbine)	Clean Sandstone	0.35	8.2	2,000-6,000
Kinsella (Viking)	Fairly clean sand	0.31	10.5	500
El Roble (Moreno)	Argillaceous sand	0.18	31.2	5-500
Rangely (Weber)	Argillaceous bedded Sand	0.175	33.0	1-10
Leduc (Devonian)	Dolomitic Limestone	0.14	52.0	1-2,000
Katie (Deese)	Argillaceous Sand	0.12	70.5	50-250
Kinsella (Viking)	Shale with interbedded Sand	0.10	100.0	1-20

$\lim_{S_w \rightarrow 1} j(S_w)$

* Values for $S_w \rightarrow 1$ and k are indicated also in Fig. 8, 14, and 15 which occasionally differ from those reported in Table I. In general, the values reported in Table I are those which have been used in the calculations reported in this paper. They correspond to maxima in k .



NOMOGRAPH RELATING THE CAPILLARY PRESSURE CURVE TO THE CAPILLARY RETENTION CURVE

FIG. 11 — NOMOGRAPH RELATING THE CAPILLARY PRESSURE CURVE TO THE CAPILLARY RETENTION CURVE.

where m = mean hydraulic radius as previously defined

L = length of porous sample
 L_a = actual length of path taken by fluid in traversing depth, L , of the porous bed

k_o = a constant in the general law of streamline motion through channels of uniform, but non-circular, cross-section

Carman (loc. cit.) shows that $k_o = 2$ as a very general average for many uniform systems, and Bartell and Osterhof³³ accept the value $\pi/2$ for the minimum L_a/L ratio so that a value for $k = 5$ is obtained. Actually, the tortuosity, T_1 , of a porous system can be defined in terms of the $(L_a/L)^2$ function so that tortuosity,

$$T_1 = \left(\frac{L_a}{L} \right)^2 = \frac{k}{k_o} = \frac{k}{2} \quad (8)$$

(assuming $k_o = 2$). These relationships are of interest in defining the significance of the Kozeny constant, k .

Tables II and III suggest maximum values of tortuosity characterizing natural reservoir rock systems as high as $T_1 = 200$. This concept of tortuosity is useful, both from the standpoint of numerically evaluating the Kozeny constant, k , and from the standpoint of establishing another core analysis parameter related to the capillary character of porous systems.

The Kozeny equation (4) has been found useful to estimate interstitial surface area values for correlation purposes. Fig. 12 shows the trend which is observed when surface area values are plotted against connate water as determined by the capillary pressure method. The linearity of this curve suggests the possibility of inferring reservoir connate water character from porosity-permeability information (i.e. the variables appearing in the Kozeny equation) once the trend is established for a given type of formation. Leverett¹⁷ originally called attention to the dependence of the capillary pressure curve on surface area considerations and the present paper relates both threshold pressures (Eq. 3) and irreducible interstitial water values (Fig. 12) that is, both ends of the drainage loop of the capillary pressure curve to Kozeny calculated surface areas. Sullivan and Hertel³⁴ have stated in their review of this subject that the Kozeny equation has doubtful

significance when applied to consolidated systems, or to media characterized by bridging, agglomeration or channeling, since it is not certain how much of the surface is actually exposed to flow. From the standpoint of measuring true surface area this criticism may be justified although the usefulness of Kozeny surface areas for correlation purposes should not be overlooked. On the other hand, it has been shown in this paper that the Kozeny constant of proportionality (k) can be estimated by an independent method (Eq. (6) as it applies to consolidated systems; therefore it is probable that some compensation for the effects of consolidation, etc., are possible.

Table III is presented to illustrate the order of magnitude of the interstitial surface area for different types of porous media.

APPLICATION OF STATIC CAPILLARITY TO THE DYNAMIC PROBLEMS OF FLOW

For some time interest has been expressed in the possibility of obtaining relative permeability from capillary pressure data. The following development shows how the relative permeability to the wetting phase can be approximated at different saturations from capillary pressure data if certain assumptions are made.

Eq. (5) can be rearranged

$$K = f \left(\frac{1}{k} \right) \left(\frac{\gamma}{P_T} \right)^2 \quad \dots (5a)$$

to show that the specific permeability, (K), may in a first approximation be proportional to the reciprocal Kozeny constant, ($1/k$), to the porosity, (f), and to the square of the interfacial tension-threshold pressure ratio, (γ/P_T)². In this expression complete wetting is assumed, and the cosine of theta is therefore one. Eq. (5a), as it has been deduced, applies to a porous system completely saturated with a wetting phase. Now, if it may be assumed that as the porous system is desaturated during a capillary pressure experiment, Eq. (5a) may be rewritten so that it continues to apply, then

$$K_E = f_E \left(\frac{1}{k} \right) \left(\frac{\gamma}{P_c} \right)^2 \quad \dots (5b)$$

where (P_c) is the capillary pressure associated (on the capillary pressure diagram) with given values for the wetting phase saturation, S_w . K_E is the effective permeability to the wetting phase at saturation, S_w , f_E is the effective porosity defined as the volume of the wetting phase per unit of bulk volume.

That is, $f_E = f S_w$ therefore,

$$K_E = f S_w \left(\frac{1}{k} \right) \left(\frac{\gamma}{P_c} \right)^2 \quad \dots (5c)$$

The justification for these equations (5b and 5c) depends on the argument that values for P_c obtained in a capillary pressure experiment may be regarded as equivalent to the threshold pressures of pores of a definite size. In other words, the capillary pressure at satura-

tion, S_w , is actually a threshold pressure of the maximum sized pore which is completely filled under this condition of saturation, S_w . A further assumption is that the constant, k , appearing in Eqs. (5a), (5b), and (5c) is a unique constant which has the same value regardless of which pores in the system (or portions thereof) are being considered. This latter assumption is reasonable since, according to Eq. (8), the constant k may be defined as the product of a dimensionless pore shape factor and a pore orientation factor. That is, k is a function of pore configuration and not pore size.

Combining Eqs. (5a) and (5c) gives an expression for relative permeability of the wetting phase, (K_w).

$$K_w = S_w \left(\frac{P_T}{P_c} \right)^2 \quad \dots (9)$$

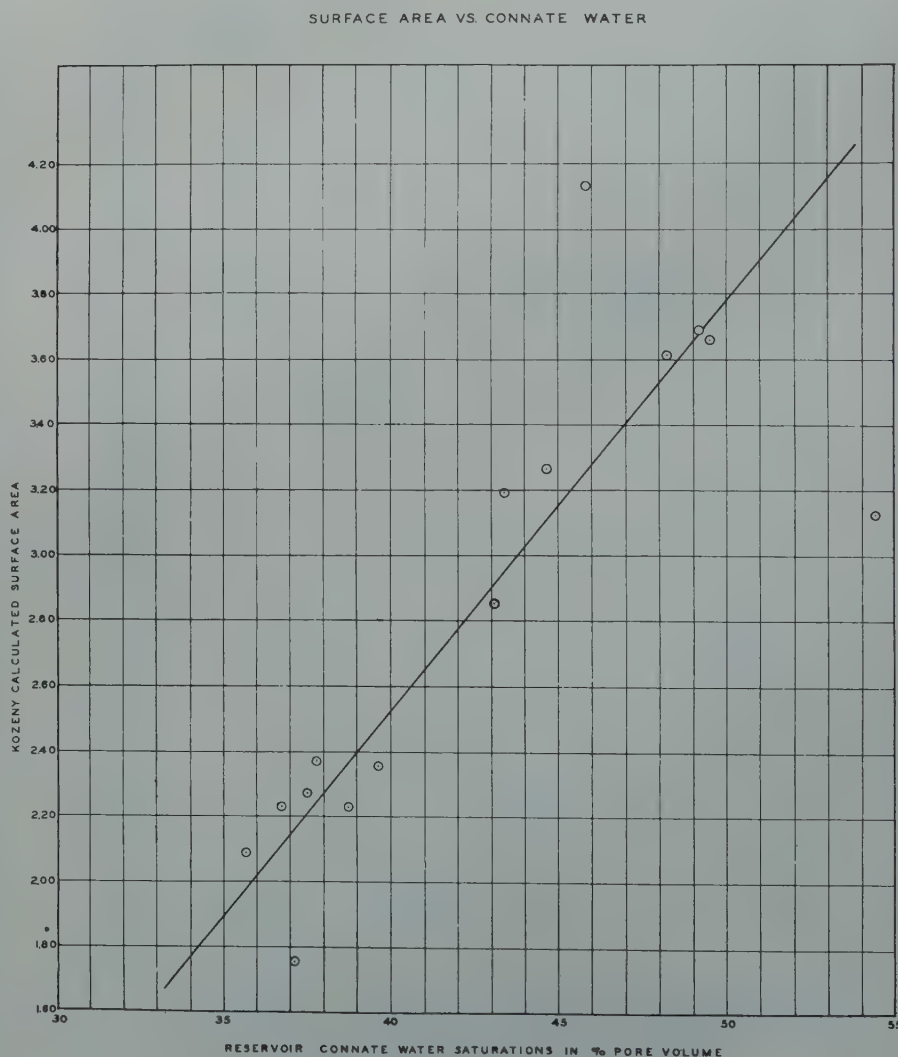


FIG. 12—SURFACE AREA VS. CONNATE WATER.

Martinelli *et al.*³⁰ recently have made an experimental study of the relative permeability characteristics of a capillary tube, and Fig. 13 illustrates the result they obtained. It is evident that their K_w - S_w curve is predicted entirely by Eq. (9) since in the case of a capillary tube $P_c = P_r$ for all values of S_w so that $K_w = S_w$ (approximately) as shown in Fig. 13

Fig. 13 not only shows relative permeability curves obtained by previous workers^{30,36} on capillary tube and unconsolidated sand systems, but it also illustrates a comparison of the K_w vs. S_w curves obtained by experiment and by theory (Eq. 9) as they apply to a consolidated sand core. Until more such direct comparisons can be made no speculation will be attempted to explain the discrepancy between theory and experiment. It is recognized that irreducible minimums are associated with the maximum saturation where the wetting phase has zero permeability, and that previous experimental work does not indicate consistently this condition. In this sense the calculated curve in Fig.

13 is more reasonable than the experimental curve, at least in the regions of low saturation.

In conclusion, it is pointed out that Eq. (9) predicts that the wetting phase relative permeability relation should be independent of rock and fluid properties (e.g. permeability, porosity, interfacial tension) as long as the group of cores being considered are characterized by the same capillary retention curve.

Thus, according to Eq. (9)

$$K_w = S_w \left(\frac{P_r}{P_c} \right)^2 = S_w \left(\frac{\lim_{S_w \rightarrow 1} j(S_w)}{j(S_w)} \right)^2 = \left(\frac{S_w}{k} \right) \left(\frac{1}{j(S_w)} \right)^2 \quad (9a)$$

Eq. (9a) offers theoretical explanation to an experimental fact (previously observed in the cited reference) that ideal systems (e.g. capillary tube, regular packed sand, etc.) are characterized by higher K_w values associated with given S_w values than non-ideal systems (e.g. consolidated sands). Eq. (9a) shows

that the system characterized by a low value of k will have a higher value of K_w than a system characterized by a high value of k . This condition is predicted by Eq. (9a) under conditions where the two systems being considered are further characterized by approximately the same capillary retention relation. It is shown in this paper that high values of k reflect non-ideal systems, and this supports the above conclusion made about the significance of Eq. (9a). Fig. 14 (offered to support this argument) has been obtained by plotting the capillary retention data shown in Fig. 8 in the way indicated by Eq. (9a). The various relative permeability curves obtained (with the exception of the curve for the Leduc limestone) are all oriented with respect to each other in the manner suggested by the above discussion, such that it may be concluded that this method of calculation qualitatively checks the cited experimentally observed trends.

UNIVERSAL CAPILLARY PHIS- PSI RELATIONSHIPS

The following development was attempted to provide a universal relationship which would define the capillarity of any porous system.

The fundamental Kozeny relation (Eq. 4) can be written as

$$K = \frac{f}{k(A')^2} \quad (4a)$$

where A' is now the interstitial surface area in cm^2 per cm^3 pore volume. If it is assumed as previously that Eq. (4a) can be extended over the whole saturation range, and by using Leverett's expression for interfacial surface area as given by

$$1/r \int_{S_w}^1 P_c dS_w,$$

the following dimensionless function can be derived:

$$\phi = S_w \left[1 + k^{1/2} \int_{S_w}^1 j(S_w) dS_w \right]^{-2} \quad (10)$$

Consideration of equation (10) shows that the slope of ϕ versus S_w as S_w approaches unity is equal to 3. For the

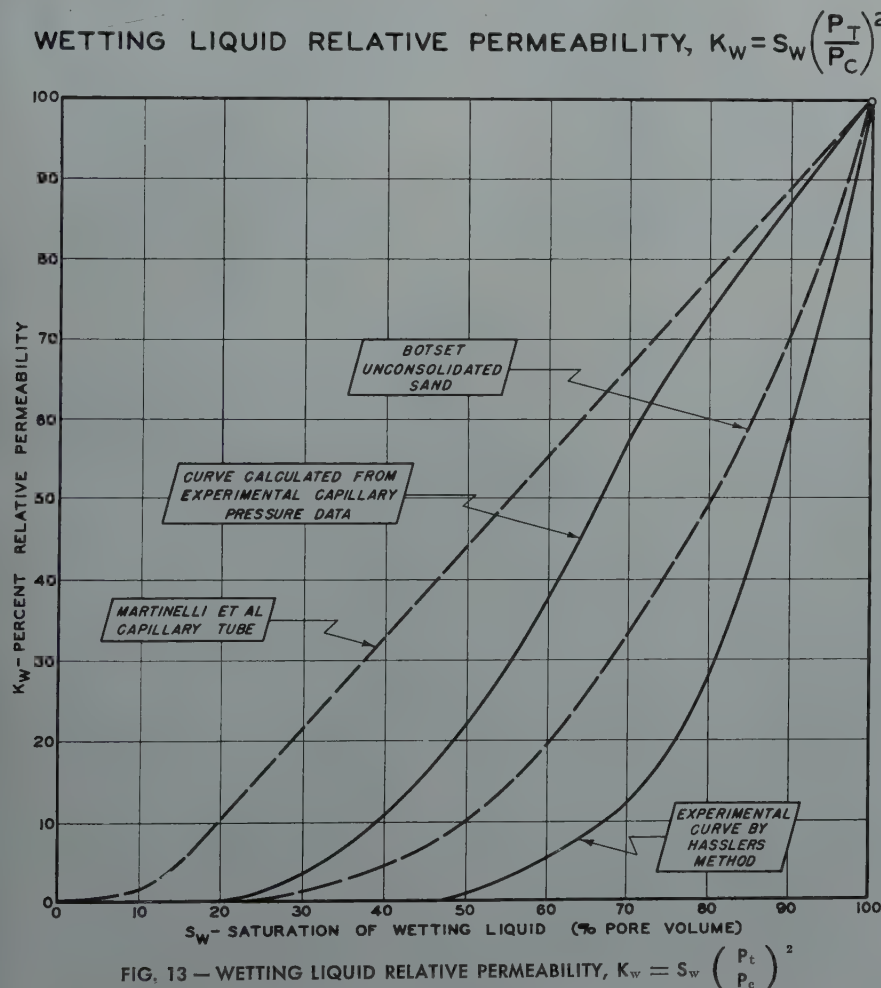


FIG. 13 — WETTING LIQUID RELATIVE PERMEABILITY, $K_w = S_w \left(\frac{P_r}{P_c} \right)^2$

special case of a capillary tube it can be shown that

$$\phi = \frac{S_w}{(2 - S_w)^2} \dots (11)$$

where the slope of ϕ is equal to 3 as S_w approaches unity and equal to 0.25 as S_w becomes zero.

Fig. 15 (Phi relation) shows a plot of ϕ versus S_w as it applies to a capillary tube according to Eq. (11). Also shown for comparison are similar plots and they apply to other porous systems according to Eq. (10). It is observed that all systems show limiting slopes of 3 as predicted.

It has been observed experimentally that $j(S_w)$ vs. S_w tends to become vertical as S_w approaches an "irreducible minimum" value. This minimum might be labeled, S_o , and defined as that value of S_w for which ϕ becomes vanishingly small. If the water is being displaced by oil, there is evidence that an S_o exists for which ϕ actually becomes zero.

This behavior suggests that a modified relation can be developed by defining a new variable, S , the saturation function

$$S = \frac{(S_w - S_o)}{(1 - S_o)} \dots (12)$$

After the manner of equation (10), it is now possible to write

$$\Psi = S \left[1 + k^{1/2} \int_S^1 j(S) dS \right]^{-2}$$

or in terms of more easily evaluated experimental quantities

$$\Psi = S \left[1 + \frac{k^{1/2}}{(1 - S_o)} \int_{S_w}^1 j(S_w) dS_w \right]^{-2} (13)$$

Fig. 15 also shows a plot of Ψ versus S as it applied to the porous systems discussed above.

CONCLUSIONS

The object of the work reported in this paper is to call attention to the theoretical aspects of capillary behavior which yield a characterization of the capillary properties of a porous system, such as petroleum reservoir rock. This permits a more exact description of fluid behavior in porous media. Considerations of pore configuration, rock sur-

face properties, and fluid properties contribute to this characterization. Although, certain of these factors can be independently measured, this paper attempts to show that the capillary pressure test provides a measurement of the combined effect of all of these factors. For instance, the data obtained from the capillary pressure test can be interpreted to reflect the distribution, orientation, shape, and tortuosity of pores; the interfacial and interstitial surface area; and finally relative permeability to the wetting phase. The new experimental techniques and computation aids described in this paper have been shown to be useful for this work.

ACKNOWLEDGMENT

The authors wish to thank the Carter Oil Company for permission to publish this paper. Not only are they indebted to R. C. West who assisted in obtaining most of the data used in this paper, but also they wish to thank Leo Rapoport,

E. F. Johnson and Charles Russell for their participation in helpful discussions bearing on the preparation of this manuscript.

NOMENCLATURE AND DIMENSIONS OF VARIABLES

Symbol	Meaning	Dimensions
a	Effective Interstitial Surface Area (Area per unit of pore volume)	1/L
A'	Interstitial Specific Surface Area (Area per unit of pore volume)	1/L
A	Interstitial Specific Surface Area (Area per unit of bulk volume)	1/L
A_I	Interfacial Specific Surface Area (Area per unit of pore volume)	1/L
D	Density difference between fluids	M/L ³
f_E	Effective fractional porosity	None
K_E	Effective permeability	L ²
f	Fractional porosity	None
g	Gravitational constant	L/T ²
γ	Interfacial tension	M/T ²
h	Height of fluid interface above level of zero curvature	L
$j(S_w)$	Capillary pressure function	None

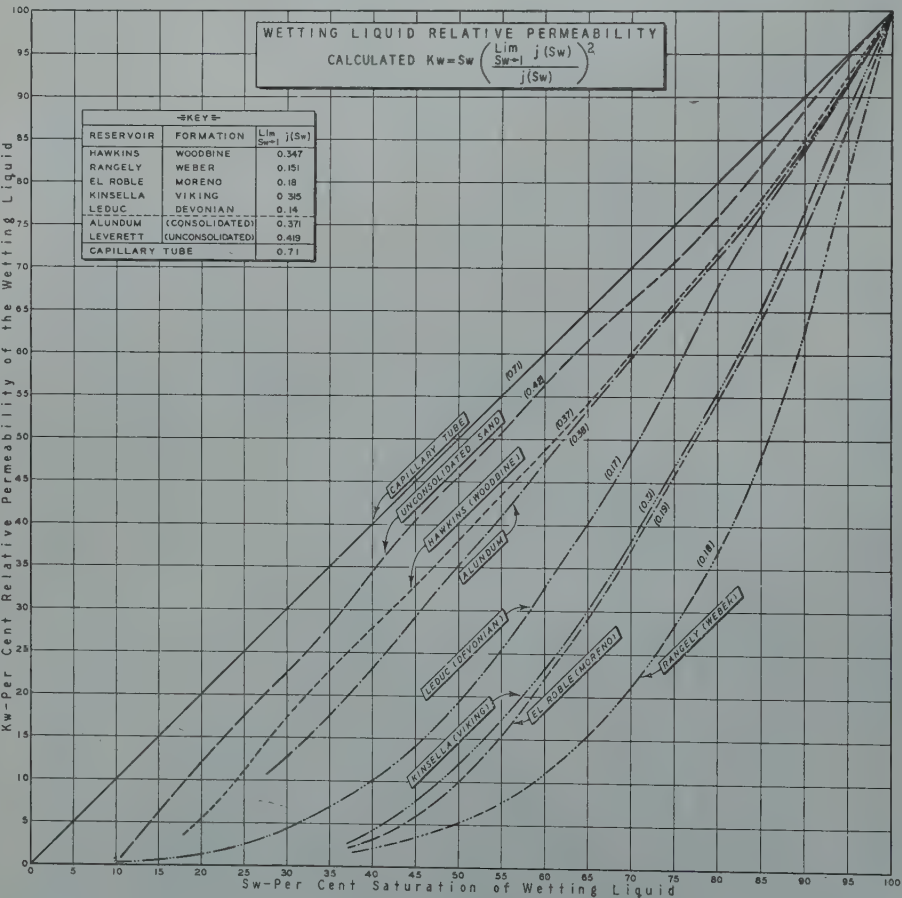


FIG. 14 — WETTING LIQUID RELATIVE PERMEABILITY CALCULATED $K_w = S_w \left(\frac{\lim_{S_w \rightarrow 1} j(S_w)}{j(S_w)} \right)^2$

TABLE III

Core Description	PT Threshold Pressure (psi)	Interfacial Tension (dynes/cm.)	A ⁽¹⁾ Surface Area (cm ² per cm ³ of pore volume)	f Porosity (fractional)	K Permeability (md)	$\lim_{S_w \rightarrow 1} j(S_w) = \left(\frac{1}{k}\right)^{1/2}$ (dimensionless)
Weber Sandstone.....	16.7	70	1.65 x 10 ⁴	0.118	2.1	0.20
" ".....	12.3	70	1.21	0.119	2.4	0.22
" ".....	8.1	70	0.80	0.124	4.4	0.17
" ".....	8.5	70	0.84	0.125	5.9	0.18
" ".....	6.5	70	0.64	0.112	3.4	0.17
" ".....	11.3	70	1.11	0.122	2.9	0.15
" ".....	7.4	70	0.73	0.132	5.9	0.17
" ".....	10.5	70	1.03	0.135	11.1	0.27
" ".....	7.0	70	0.69	0.121	2.2	0.07
" ".....	8.5	70	0.84	0.111	1.3	0.10
Viking Sandstone.....	3.7	70	0.36	0.17	10.0	0.10
" ".....	1.5	70	0.15	0.22	650.	0.31
Unconsolidated Sand (After Leverett).....	0.6	70	0.059	0.39	1.75 x 10 ⁴	0.42
Alundum.....	2.0	70	0.20	0.24	208.	0.38
" ".....	0.8	20	0.23	0.24	208.	0.38
Deese Sandstone.....	1.0	70	0.99	0.15	253.	0.16

k	Constant in general law of streamline motion through granular beds	None
k ₀	Constant in general law of streamline motion through channels of uniform cross section	None
K	Specific permeability	L ²
K _w	Relative permeability of wetting fluid	None
L	Apparent length of pore (actual length of core)	L
L _a	Actual length of pore	L
m	Mean hydraulic radius	L
P _c	Capillary Pressure	M/LT ²
P _T	Threshold pressure	M/LT ²
r	Interstitial pore radius	L
\bar{r}	Average interstitial pore radius	L
S	Saturation Function	None
S _w	Fractional wetting phase saturation (per units of pore volume)	None
S ₀	"Irreducible" wetting phase saturation	None

T ₁	Tortuosity	None
θ	Contact angle	Degrees
φ	Phi Function	None
ψ	Psi Function	None

REFERENCES

- W. A. Bruce and H. J. Welge, "The Restored State Method for Determination of Oil-in-Place and Connate Water", presented, Amarillo meeting of the Division of Production, A.P.I. (May, 1947).
- O. F. Thornton and P. L. Marshall, "Estimating Interstitial Water by the Capillary Pressure Method," AIME *Petroleum Technology*, T.P. 2126 (January 1947).
- J. J. McCullough, F. W. Albaugh and P. H. Jones, "Determination of

the Interstitial Water Content of Oil and Gas Sand by Laboratory Tests of Core Samples," Amer. Petr. Inst. *Drill. and Prod. Prac.*, 1944 (1945), 180.

- G. L. Hassler and E. Brunner, "Measurement of Capillary Pressure in Small Core Samples," *Trans.*, AIME, 160, 114-123 (1945).
- M. C. Leverett, "Method of Determining Connate Water Content of Cores," U. S. Patent 2,330,721 (Sept. 28, 1943).
- L. A. Richards, "A Pressure-Membrane Extraction Apparatus for Soil Solution," *Soil Sci.*, 51, 377-86 (1941).
- W. B. Haines, "Studies in the Physical Properties of Soils, IV," *J. Agr. Sci.*, 17, 264-290 (1927).
- W. B. Haines, "Studies in the Physical Properties of Soils, V," *J. Agr. Sci.*, 20, 97-116 (1930).
- R. W. Leamer and J. F. Lutz, "Determination of Pore Size Distribution in Soils," *Soil Sci.*, 49, 347-360 (1940).
- H. J. Welge, "The Displacement of Oil from Porous Media by Water or Gas," presented, Tulsa meeting, Petroleum Division, AIME (October 1947).
- J. W. Amyx and S. T. Yuster, "Capillary Pressure in Secondary Recovery," *Producers Monthly*, pp. 10-13, (December 1946).
- L. A. Richards and W. Gardner, "Tensiometers for Measuring the Capillary Tension of Soil Water," *J. Am. Soc. Agron.*, 28, 352 (1936).

CAPILLARY RELATIONSHIPS

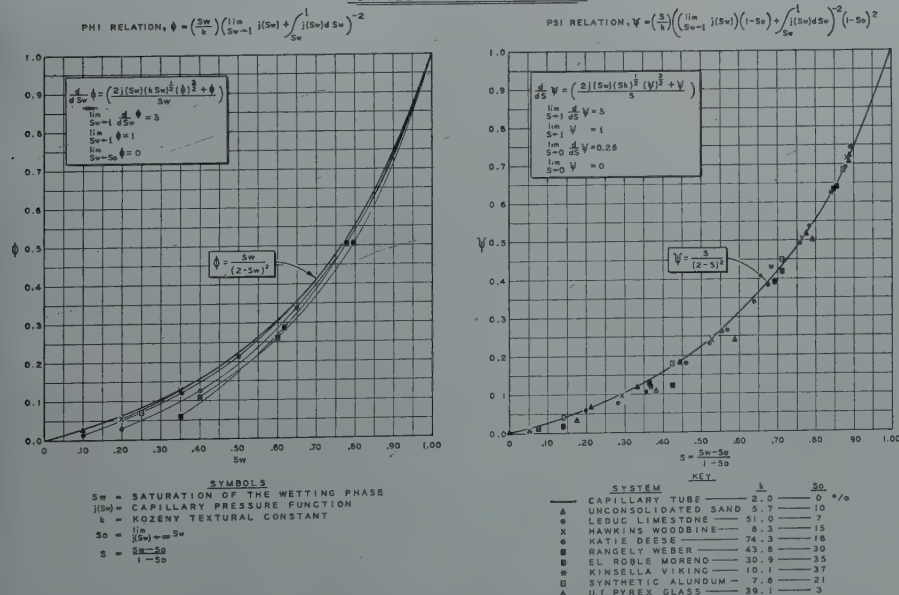


FIG. 15 — CAPILLARY RELATIONSHIPS.

13. L. A. Richards, "Soil Moisture Tensiometer Materials and Construction," *Soil Sci.*, 53, 241 (1942).
14. L. A. Richards and Milton Fireman, "Pressure-Plate Apparatus for Measuring Moisture Sorption," *Soil Sci.*, 56, 395 (1943).
15. L. A. Richards and L. R. Weaver, "Moisture Retention by Some Irrigated Soils as Related to Soil-Moisture Tension," *J. Agr. Res.*, 69, 215 (1944).
16. L. G. Rall and D. B. Taliaferro, "Determining Oil and Water Saturations of Oil Sands," U. S. Bureau of Mines, R. I. 4004 (December 1946).
17. M. C. Leverett, "Capillary Behavior in Porous Solids," *Trans. AIME*, 142, 151-169 (1941).
18. G. L. Hassler, E. Brunner and T. J. Deahl, "The Role of Capillarity in Oil Production," *Trans. AIME*, 155, 154-74 (1944).
19. W. D. Smith, "The Final Distribution of Retained Liquid in an Ideal Uniform Soil," *Physics*, 4, 425-438 (1933).
20. A. D. Garrison, "Selective Wetting of Reservoir Rock and its Relations to Oil Production," *A.P.I. Drill. and Prod. Pract.*, 130-140 (1935).
21. M. C. Leverett, W. B. Lewis and M. E. True, "Dimensional-model Studies of Oil-field Behavior," *Trans. AIME*, 146, 175-193 (1942).
22. P. C. Carman, "Capillary Rise and Capillary Movement of Moisture in Fine Sands," *Soil Sci.*, 52, 1-14 (1941).
23. J. Kozeny, "Über-Kapillare Leitung des Wassers in Boden," *Sitzb. Akad. Wiss. Wien., Math.-nature. Kl.*, 136, 27-306 (1927).
24. J. Kozeny, "Ground Water Movement," *Wasserkraft v. Wasserwirtschaft*, 22, 67, 86 (1927).
25. P. C. Carman, "Determination of the Specific Surface of Powders, I," *J. Soc. Chem. Indus.*, 57, 225-234 (1938).
26. P. C. Carman, "Determination of the Specific Surface of Powders, II," *J. Soc. Chem. Indus.*, 58, 1-7 (1939).
27. J. L. Fowler and K. L. Hertel, "Flow of Gas Through Porous Media," *J. Applied Phys.*, 11, 496-502 (1940).
28. M. C. Leverett, "Flow of Oil-Water Mixtures Through Unconsolidated Sands," *Trans. AIME*, 132, 149 (1939).
29. G. L. Hassler, "The Measurement of Permeability of Reservoir Rock," *The Science of Petroleum*, 1, 198-208 (1938).
30. H. G. Botset, "Flow of Gas-Liquid Mixtures Through Consolidated Sand," *Trans. AIME*, 136, 91 (1940).
31. Bernard A. Koon, "The Physical Properties of the Soil," London: Longmans Green (1931).
32. P. C. Carman, "Fluid Flow Through Granular Beds," *Trans. Am. Inst. Chem. Engr.*, 15, 150-166 (1937).
33. F. E. Bartell and H. J. Osterhof, "The Pore Size of Compressed Carbon and Silica Membranes," *J. Phys. Chem.*, 32, 1553-71 (1938).
34. R. R. Sullivan and K. L. Hertel, "The Permeability Method for Determining Specific Surface," *Advances in Colloid Science*, 1, 3280 (1942).
35. R. N. Traxler and L. A. H. Baum, "Permeability of Compacted Powders," *Determination of Average Pore Size*, *Physics*, 7, 9-14 (1936).
36. R. C. Martinelli, J. A. Putnam and R. W. Lockhart, "Two-phase, Two-Component Flow in the Viscous Region," *Trans. Am. Inst. Chem. Engr.*, 681-705 (1946).
37. R. A. Morse, P. L. Terwilliger and S. T. Yuster, "Relative Permeability Measurements on Small Core Samples," *Oil and Gas Jnl.*, 46, 109-125 (Aug. 23, 1947).
38. R. W. Leamer and J. F. Lutz, "Determination of Pore Size Distribution in Soils," 49, 347-360 (1940).
39. H. L. Ritter and L. C. Drake, "Pore Size Distribution in Porous Materials," *Ind. Eng. Chem. Anal. Ed.*, 17, 782-791 (1945). ★ ★ ★

DISCUSSION OF THIS AND ALL FOLLOWING TECHNICAL PAPERS IS INVITED

Discussion in writing (3 copies) may be sent to the Editor, *Journal of Petroleum Technology*, 601 Continental Building, Dallas 1, Texas, and will be considered for publication in the Transactions volume *Petroleum Development and Technology*. Discussion will close December 15, 1949. Any discussion offered thereafter should be in the form of a new paper.

BEHAVIOR OF BINARY, TERNARY, AND MULTICOMPONENT SYSTEMS AT STATES SIMILAR TO THOSE ENCOUNTERED IN CONDENSATE FIELDS

B. H. SAGE, MEMBER AIME, AND W. N. LACEY

CALIFORNIA INSTITUTE OF TECHNOLOGY, PASADENA, CALIFORNIA

ABSTRACT

The growing background of experimental information concerning the volumetric and phase behavior of binary and ternary hydrocarbon systems is used as the basis for a comparison of these systems with naturally occurring hydrocarbon mixtures under conditions representative of underground petroleum reservoirs. The qualitative and semiquantitative similarities and differences between the two types of systems are considered in reference to the possibilities and limitations of using experimental data on binary and ternary systems for predicting the volumetric and phase behavior of naturally occurring hydrocarbon mixtures of low molecular weight. The possible influence on such phase behavior of water, hydrogen sulphide, nitrogen, and components of relatively high molecular weight is discussed.

INTRODUCTION

During the past two decades much effort has been devoted to the study of the volumetric and phase behavior of pure paraffin hydrocarbons and of binary and ternary mixtures of these compounds. Many of these studies were carried out with the direct objective of utilizing a knowledge of the detailed characteristics of binary and ternary mixtures of the lighter paraffin hydrocarbons for predicting the behavior of more complex mixtures. The ability to make such predictions with accuracy would be of great value in petroleum production and refining. Although the behavior of the methane-propane system¹ served at one time as a qualitative illustration of the probable characteristics of the more complex hydrocarbon mixtures found in nature, it fell far short of requirements for quantitative predictions. The present paper endeavors to indicate the relation of the more recently accumulated information concerning the behavior of binary and ternary hydrocarbons to this problem. In discussing binary and ternary systems as examples pointing toward the behavior of multicomponent systems no effort is made to present new methods of predicting the characteristics of natural hydrocarbon mixtures. Preliminary proposals have been made elsewhere for the prediction of volumetric^{2,3,4}, phase equilibrium^{4,5,6,7}, and thermodynamic^{8,9,10,11} data for multicomponent mixtures, utilizing as a basis the behavior of binary and ternary systems.

Numerous other proposals have been made. That based upon the concept of a pseudo-critical state¹² has proved to be of value to the petroleum industry.

Concurrently with this study of binary and ternary systems investigations have been made of natural hydrocarbon systems. Of the many publications reporting such experimental information only a few examples will be mentioned. A number of studies of black oil and natural gas have been made^{13,14,15} and much attention has been directed to extended and detailed investigations of the behavior of fluids in condensate fields^{16,17,18,19,20}. This work has been supplemented by some studies of the separation of bitumen from natural hydrocarbon liquids^{21,22}. The over-all behavior of such systems has been used in predicting the volumetric and phase behavior of naturally occurring mixtures^{23,24,25,26}. This background of experimental and correlated information concerning the behavior of multicomponent hydrocarbon systems also permits a direct comparison of the characteristics of binary and ternary aliphatic systems with those materials produced from underground reservoirs.

PRESENTATION OF DATA

The primary limitation encountered in using binary and ternary aliphatic hydrocarbon mixtures as examples of the characteristics of the fluids encountered in underground reservoirs lies in the existing lack of knowledge of the quantitative effect upon behavior of the presence of several important constituents, notably hydrocarbons of high molecular weight, water, carbon dioxide, hydrogen sulphide, and nitrogen. The presence of substantial quantities of hydrocarbons of fairly high molecular weight serves to increase the complexity of the phase behavior of natural systems. No simple systems yet studied give adequate guidance in this regard. The influence of such materials of high molecular weight was indicated earlier^{21,22} to an extent which serves to show that definite limitations now exist in the correlation of simple and complex systems. However, significant progress is being made in filling gaps in the information. For example, similarities in the behavior of fluids in condensate fields with that of binary and ternary systems are becoming more systematically evident.

A few studies of the behavior of water in paraffin hydrocarbon systems have been made^{27,28,29}. Results of investigations of mixtures of carbon dioxide and the lighter hydrocarbons also are available^{30,31,32}. Limited work has been reported con-

Manuscript received at the Petroleum Branch Office February 22, 1949. Paper presented at the AIME annual meeting in San Francisco, February 13-17, 1949.

¹References are given at end of paper.

cerning the solubility of hydrogen sulphide in liquids^{33,34}. However, it appears that additional knowledge of the influence of hydrogen sulphide on the phase behavior of hydrocarbons must be obtained before its effect can be estimated with any surety.

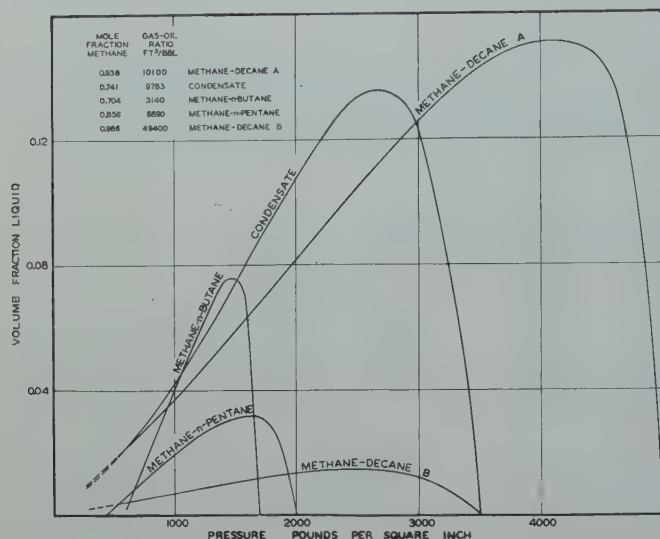


FIG. 1—FRACTIONAL VOLUME OF LIQUID PHASE IN SEVERAL SYSTEMS AT 160°F.

It is often important to know the influence of changes in pressure upon the separation of liquid from the gas phase of a reservoir during production operations. Fig. 1 shows for several systems the fraction of the volume of the system that is occupied by liquid as a function of pressure for a temperature of 160°F. The data for the natural mixture are taken from direct laboratory measurements of the behavior of high-gravity oil and related gas from a San Joaquin Valley Field⁴⁰. For comparison, curves showing the behavior of the methane-decane^{35,36,37}, the methane-pentane^{38,39}, and the methane-n-butane⁴⁰ systems are included. The gas-oil ratios⁴¹ of the binary mixtures are indicated and they are computed throughout this discussion on the basis that all the methane and ethane are considered to be "gas." A marked similarity of behavior appears between the multicomponent system and the binary systems. Suitable volumetric data for ternary systems have not yet been published and so no example could be included in Fig. 1. However, Fig. 2 shows the relative number of moles of liquid compared to the total moles constituting the system as found in several different ternary mixtures. These data relate to the methane-ethane-n-pentane system⁴¹ and the methane-propane-n-pentane system^{42,43}, the compositions of the mixtures being expressed in terms of the mole fractions of the components and of the gas-oil ratio. The arbitrary method of designation of gas and oil described above was followed here. The behavior of mixtures of methane and n-pentane containing the same and a higher mole fraction methane shows distinct similarity to that of the ternary mixtures.

The component of intermediate molecular weight in a ternary mixture is one of interest because it is analogous to com-

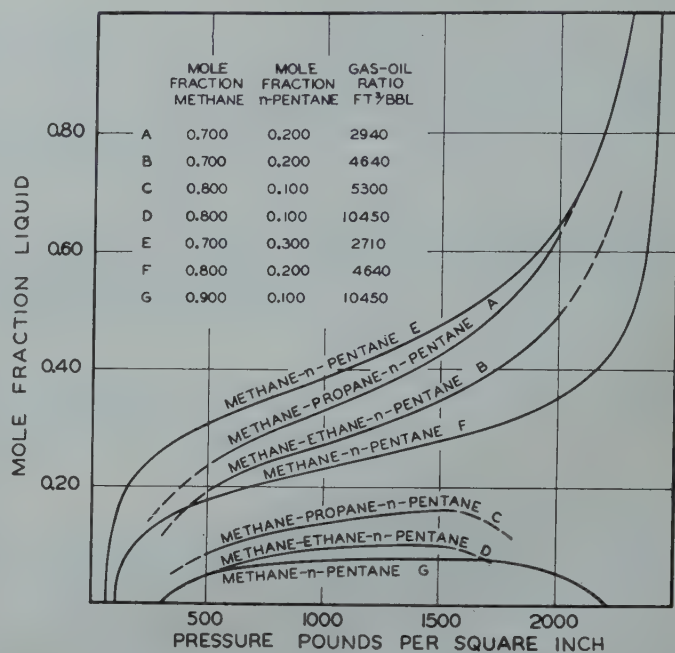


FIG. 2—RELATIVE MOLAL QUANTITIES OF LIQUID PHASE FOR BINARY AND TERNARY MIXTURES CONTAINING METHANE AND N-PENTANE AT 100°F.

ponents of intermediate volatility in a natural system. Fig. 3 indicates the mole fraction of the intermediate component which is present in the gas phase with varying pressure for the several mixtures covered in Fig. 2. The ordinate in Fig. 3 is the fraction of the intermediate component in the system which is found in the liquid phase under the conditions indicated by the figure. The curves serve to illustrate the marked changes in this quantity as the pressure is progressively decreased. This information serves to illustrate the similarity in the behavior of ternary systems to the more complex naturally occurring hydrocarbon mixtures.

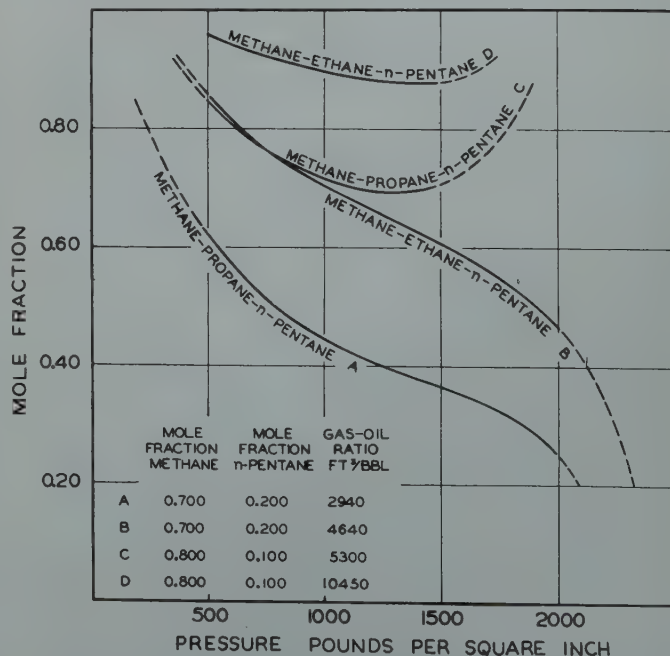


FIG. 3—DISTRIBUTION OF COMPONENTS OF INTERMEDIATE VOLATILITY IN TERNARY SYSTEMS AT 100°F.

*For present purposes the gas-oil ratio is taken as the volume of "gas," measured in cubic feet at 60°F. and 30-in. of mercury pressure, associated with one barrel of oil measured under the same conditions.

The generalized equilibrium constants^{5,44,45} which have been thus far published do not appear to be applicable at states approaching the retrograde dew point of the system. For this reason it is not possible to predict from them the distribution of components of intermediate volatility in naturally occurring mixtures corresponding to that shown for the ternary system in Fig. 3. However, as additional information, particularly that obtained from ternary and more complex systems, is employed, it will become feasible to make such calculations with reasonable accuracy for multicomponent systems. The data already available concerning the phase behavior of ternary systems^{41,42,43} reflect the marked influence of the composition of the phases, as well as pressure and temperature, upon the equilibrium constants. This fact makes it evident that utilization of experimentally established equilibrium constants for a ternary system in making predictions will be much less convenient than if it were possible to consider the equilibrium constant to be a function of pressure and temperature only.

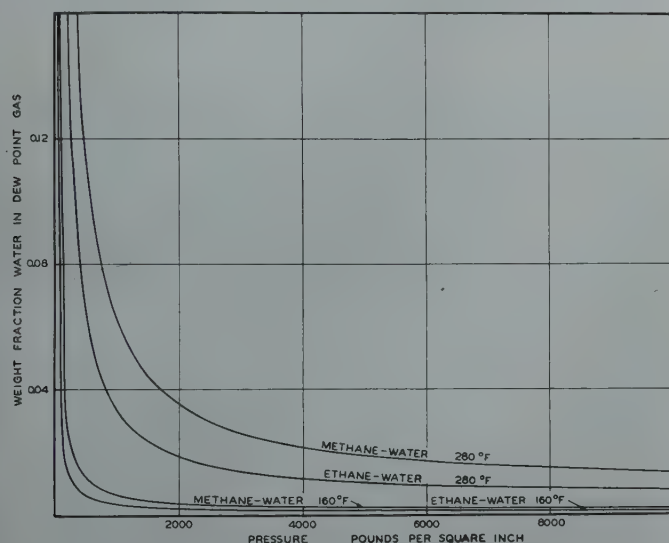


FIG. 4 — WEIGHT FRACTION WATER IN THE GAS PHASE IN THE METHANE-WATER AND ETHANE-WATER SYSTEMS.

In order to illustrate the extent to which water may occur in gas phases, Fig. 4 presents information concerning the compositions of the gas phase of the methane-water²⁷ and of the ethane-water²⁸ systems. In this diagram the weight fraction of water is shown as a function of pressure for the two binary systems at two temperatures. The weight of water in a cubic foot of gas space is shown in Fig. 5 as a function of pressure for 160° and 280°F.

Comparison of Figs. 4 and 5 shows that although the weight fraction of water in the gas phase decreases markedly with increase in pressure, nevertheless the amount of water in each cubic foot of gas space increases at higher pressures, the effect being large at the temperatures found in deep reservoirs. The condensation of water which would occur upon lowering of pressure and temperature during production of fluids from condensate fields would account for the fresh water frequently found in production traps. Because of the relatively small difference in behavior shown with methane and with ethane it is believed that for many practical purposes the curves shown in Fig. 5 may be used as a rough estimate of the behavior of natural hydrocarbon gas phases. In the

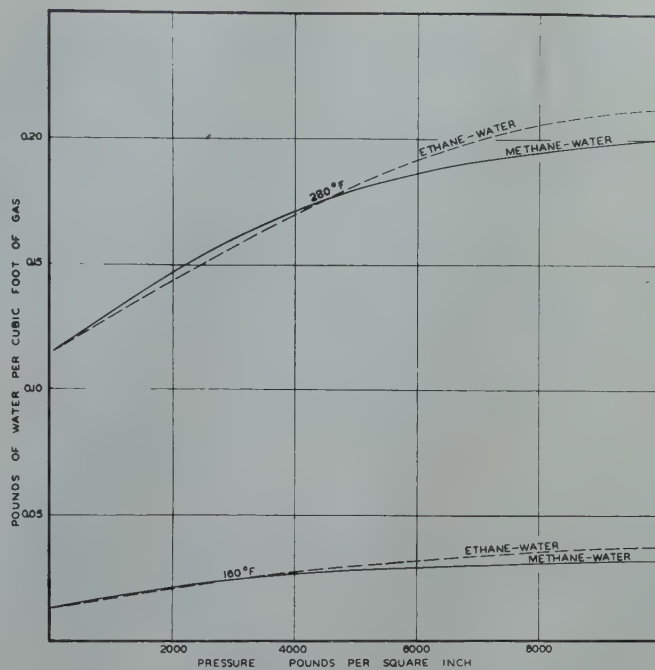


FIG. 5 — WATER IN A UNIT VOLUME OF GAS PHASE IN THE METHANE-WATER AND ETHANE-WATER SYSTEMS.

case of systems at equilibrium with salt water, the quantity of water in the gas phase will be slightly less than that shown in Figs. 4 and 5 because the fugacity of water in a saline solution at a given pressure and temperature is lower than that for pure water at the same conditions.

At low temperatures water-hydrocarbon systems form hydrates^{40,47,48}. The temperatures found in most underground petroleum reservoirs are above those at which hydrates are stable. However, these solid phases are of importance in surface production operations and in the transmission of natural gas. It appears that reasonable agreement can be found between the characteristics of hydrates of the lighter paraffin hydrocarbons⁴⁶ and the behavior of hydrates prepared from multicomponent hydrocarbon mixtures^{47,48}. In the latter case it

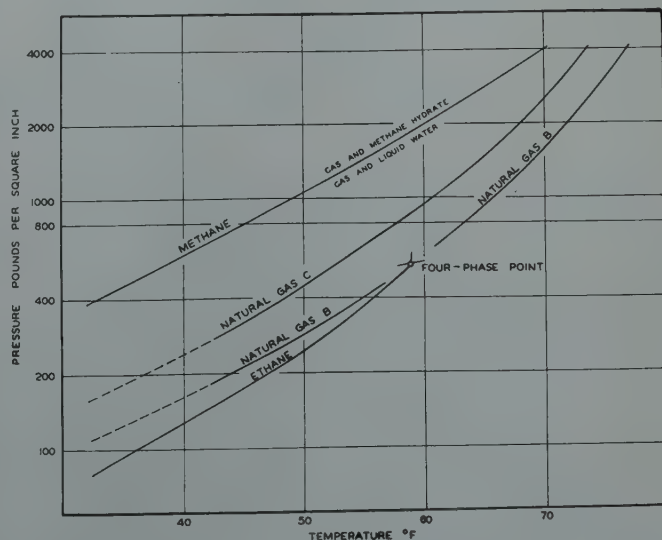


FIG. 6 — COMPARATIVE BEHAVIOR OF HYDRATES INVOLVING METHANE, ETHANE, AND A NATURAL GAS.

is probable that the hydrates are solid solutions and that decomposition or formation may occur over a range of temperature for a given pressure. Fig. 6 is a temperature-pressure diagram showing the behavior of the methane-water system, the ethane-water system, and a natural gas-water system under conditions where hydrates, hydrocarbon gas, and an aqueous phase coexist. Table 1 records the compositions of the natural gases represented in the figure. The similarity of the curves offers promise that a reasonable amount of additional data will suffice for predictions relating to multicomponent systems. Some steps in this direction have already been taken by Katz and his co-workers^{47,48}.

TABLE 1
*Composition of Natural Gases**

Component	Mole Fractions	
	Gas B	Gas C
Nitrogen	0.0064	0.0043
Carbon Dioxide	—	0.0051
Methane	0.8641	0.9320
Ethane	0.0647	0.0425
Propane	0.0357	0.0161
Isobutane	0.0099	—
n-Butane	0.0114	—
Pentane and all others	0.0078	—

Some of the similarities and differences of simple and complex hydrocarbon systems have been pointed out. An entirely satisfactory way to utilize the similarities for prediction purposes has yet to be found. If a simple characterization factor such as average molecular weight is used as a basis of comparison results such as are shown in Fig. 7 are obtained. In this figure the compressibility factors of four systems^{19,39,40,49} of approximately the same average molecular weight are compared at 160°F. The compositions of these systems are given in Table 3. Although the curves bear a similarity they differ markedly from each other.

Consideration of different systems at the same reduced state has been proposed on the basis of pseudo-critical states for binary and multi-component systems¹². Comparisons based upon the concept of a convergence pressure⁵⁰ have been made,

but the evaluation of this quantity in advance of experimental measurements may prove difficult. Predictions from partial properties (such as the partial volume) of the various components and their proportions in the system depend upon a knowledge of the effect of composition environment as well as those of temperature and pressure upon the partial property values. Table 2 gives a comparison between the experimentally determined behavior¹⁴ of a complex mixture and that predicted by a correlating method proposed by Brown⁵¹. Although the method requires extensive information it takes into account factors which have been shown to be pertinent. In any of these methods, prediction of behavior near the critical state of the system will be likely to have uncertainties.

One or more of the more elaborate equations of state^{52,53,54} may be of particular utility in predicting the thermodynamic behavior of multicomponent mixtures from data relating to binary, ternary, and possibly more complex hydrocarbon systems. There appears to be a limit to the efficacy of graphical methods when applied to such problems. The advent of commercial digital computing equipment with some memory

TABLE 2
Comparison of Observed and Calculated Compressibility Factors for Gas Samples from Santa Maria Valley Field†
100°F.

Component	Composition Mole Fractions	Compressibility Factor	
		Pressure PSI Absolute	Observed Calculated‡
Methane	0.7511	1250	0.7231 0.742
Ethane	0.0959	1500	0.6874 0.710
Propane	0.0813	1750	0.6651 0.681
Isobutane	0.0124	2000	0.6544 0.674
n-Butane	0.0266		
Isopentane	0.0065		
n-Pentane	0.0060		
Carbon Dioxide	0.0140		
Hexanes and heavier	0.0062		

† Data obtained from published information¹⁴.
‡ Calculated from published correlations⁵¹.

TABLE 3
Compositions of Mixtures for Fig. 7

System	Component	Mole Fraction
Methane-n-Butane-Decane	Methane	0.817
	n-Butane	0.121
	Decane	0.062
Condensate	Methane	0.7406
	Ethane	0.0772
	Propane	0.0485
	Isobutane	0.0101
	n-Butane	0.0209
	Isopentane	0.0084
	n-Pentane	0.0091
	Hexanes	0.0151
	Heptanes and heavier	0.0606
Methane-n-Pentane	Carbon Dioxide	0.0095
Methane-n-Butane	Methane	0.770
	n-Pentane	0.230
	Methane	0.704
	n-Butane	0.296

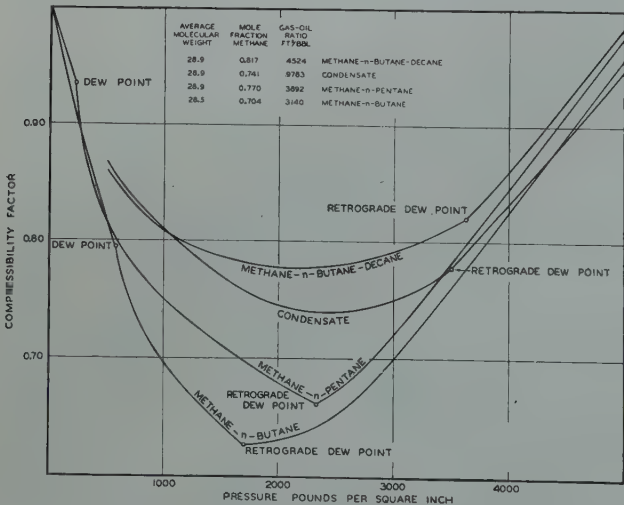


FIG. 7 — COMPARISON OF VOLUMETRIC BEHAVIOR OF NATURAL MIXTURE WITH SEVERAL SIMPLE MIXTURES AT 160° F.

* Data obtained from published information⁴⁷. Volumetric behavior of these gases shown in Fig. 6.

features appears to afford an avenue of approach to the prediction of the characteristics of multicomponent hydrocarbon mixtures at individual states of interest at a particular time. After nearly two decades of fairly intense experimental effort by a number of laboratories, the background of experimental information is nearly sufficient for the establishment of the characterization coefficients of equations of state which can be effectively utilized in predicting the behavior of naturally occurring mixtures. At present such methods cannot be extended accurately to mixtures involving large quantities of the heavier hydrocarbons nor can they deal with cases involving formation of solid or plastic bitumen phases or solid hydrates.

ACKNOWLEDGMENT

The assistance of Hugh Johnson and Elizabeth Kendall in connection with calculations and of Ann Jarvis in the preparation of the figures is acknowledged.

REFERENCES

1. Sage, Lacey, and Schaafsma: *Oil and Gas Jnl.* (1933) **32**, 12.
2. Sage, Hicks, and Lacey: Amer. Petr. Inst. *Drill. and Prod. Prac.*, 1938 (1939) 402.
3. Sage and Lacey: *Refiner and Nat'l. Gasoline Mfr.* (1939) **18** (11) 88. *Oil and Gas Jnl.* (1939) **38** (27) 189. Amer. Petr. Inst. *Drill. and Prod. Prac.*, 1939 (1940) 641.
4. Sage and Lacey: Amer. Petr. Inst. *Drill. and Prod. Prac.*, 1941 (1942) 308.
5. Sage, Hicks, and Lacey: Amer. Petr. Inst. *Drill. and Prod. Prac.*, 1938 (1939) 386. *Refiner and Nat'l. Gasoline Mfr.* (1938) **17**, 350.
6. Sage and Lacey: *Calif. Oil World* (1941) **16**, 31.
7. Sage and Lacey: *Ind. Eng. Chem.* (1938) **30**, 1296.
8. Sage, Olds, and Lacey: Amer. Petr. Inst. *Drill. and Prod. Prac.*, 1942 (1943) 162.
9. Holcomb and Brown: *Ind. Eng. Chem.* (1942) **34**, 590.
10. Maron and Turnbull: *Ind. Eng. Chem.* (1942) **34**, 544.
11. Edmister: *Petroleum Refiner* (1947, 1948) **46** and **47** (series).
12. Kay: *Ind. Eng. Chem.* (1936) **28**, 1014.
13. Sage and Reamer: AIME Tech. Pub. No. 1251; *Petroleum Technology*, November 1940. *Trans. AIME* (1941) **142**, 179.
14. Olds, Sage, and Lacey: AIME Tech. Pub. No. 1588; *Petroleum Technology*, March 1943.
15. Sage, Lacey, and Schaafsma: *Ind. Eng. Chem.* (1935) **27**, 162.
16. Eilerts: *Oil and Gas Jnl.*, February 1, February 8, and February 15, 1947.
17. Eilerts, Barr, Mullens, and Hanna: *Petroleum Engineer*, February 1948.
18. Olds, Sage, and Lacey: AIME Tech. Pub. No. 1861; *Petroleum Technology*, May 1945.
19. Olds, Sage, and Lacey: AIME Tech. Pub. No. 2412; *Petroleum Technology*, September 1948.
20. Sage and Olds: AIME Tech. Pub. No. 2153; *Petroleum Technology*, March 1947.
21. Botkin, Reamer, Sage, and Lacey: Amer. Petr. Inst. *Fundamental Research on Occurrence and Recovery of Petroleum*, 1944-45 (1946) 42.
22. Botkin, Reamer, Sage, and Lacey: Amer. Petr. Inst. *Fundamental Research on Occurrence and Recovery of Petroleum*, 1943 (1944) 62.
23. Standing: *Oil and Gas Jnl.* (1947) **46** (2) 95, 100.
24. Technical Committee, Natural Gasoline Association of America: *Ind. Eng. Chem.* (1932) **34**, 1240.
25. Standing and Katz: AIME Tech. Pub. No. 1323; *Petroleum Technology*, July 1941.
26. Katz and Hachmuth: *Ind. Eng. Chem.* (1937) **29**, 1072.
27. Olds, Sage, and Lacey: *Ind. Eng. Chem.* (1942) **34**, 1223.
28. Reamer, Olds, Sage, and Lacey: *Ind. Eng. Chem.* (1943) **35**, 790.
29. Reamer, Olds, Sage, and Lacey: *Ind. Eng. Chem.* (1944) **36**, 381.
30. Katz and Poettman: *Ind. Eng. Chem.* (1946) **38**, 330.
31. Reamer, Olds, Sage, and Lacey: *Ind. Eng. Chem.* (1944) **36**, 88.
32. Reamer, Olds, Sage, and Lacey: *Ind. Eng. Chem.* (1945) **37**, 688.
33. Frolich, Touch, Hogan, and Peer: *Ind. Eng. Chem.* (1931) **23**, 548.
34. Wright and Maass: *Canadian J. Research* (1932) **6**, 94.
35. Lavender, Sage, and Lacey: *Oil and Gas Jnl.* (1940) **39** (9) 48.
36. Sage, Lavender, and Lacey: *Ind. Eng. Chem.* (1940) **32**, 743.
37. Reamer, Olds, Sage, and Lacey: *Ind. Eng. Chem.* (1942) **34**, 1526.
38. Taylor, Wald, Sage, and Lacey: *Oil and Gas Jnl.* (1939) **38** (10) 46.
39. Sage, Reamer, Olds, and Lacey: *Ind. Eng. Chem.* (1942) **34**, 1108.
40. Sage, Hicks, and Lacey: *Ind. Eng. Chem.* (1940) **32**, 1085.
41. Billman, Sage, and Lacey: AIME Tech. Pub. No. 2232; *Petroleum Technology*, July 1947.
42. Carter, Sage, and Lacey: *Trans. AIME* (1941) **142**, 170.
43. Dourson, Sage, and Lacey: *Trans. AIME* (1943) **151**, 206.
44. Smith and Wilson: *Trans. Am. Inst. Chem. Engrs.* (1946) **42**, 5 and 927.
45. Hadden: *Chem. Eng. Prog.* (1948) **44** (1) 37 and (2) 135.
46. Roberts, Brownscombe, and Howe: *Oil and Gas Jnl.*, Dec. 5, 1940.
47. Wilcox, Carson, and Katz: *Ind. Eng. Chem.* (1941) **33**, 662.
48. Carson and Katz: AIME Tech. Pub. No. 1371; *Petroleum Technology* 1941.
49. Reamer, Sage, and Lacey: *Ind. Eng. Chem.* (1947) **39**, 77.
50. Hanson and Brown: *Ind. Eng. Chem.* (1945) **37**, 821.
51. Brown: *Deviation of Natural Gas from Ideal Gas Laws*. Clark Bros., Inc., Olean, New York (1940).
52. Beattie and Bridgeman: *Proc. Amer. Acad. Arts and Sciences* (1928) **63**, 229.
53. Benedict, Webb, and Rubin: *Jour. of Chem. Physics* (1940) **8** (4) 334.
54. Gouq-Jen Su and Chien-Hou Chang: *Ind. Eng. Chem.* (1946) **38**, 802.

★ ★ ★

INTRODUCTION TO INDUCTION LOGGING AND APPLICATION TO LOGGING OF WELLS DRILLED WITH OIL BASE MUD

H. G. DOLL, MEMBER AIME, SCHLUMBERGER WELL SURVEYING CORP., HOUSTON, TEXAS

ABSTRACT

A new logging method, called induction logging, is described; it measures the conductivity, or resistivity, of the strata traversed by a bore hole. The apparatus, which is briefly described, comprises a coil system coupled with the ground by induction, so that there is no need for direct contact with the mud, or with the formations. For that reason, the method is particularly useful in oil base mud, and it was first applied to that case.

A discussion concerning the respective contribution of each region of ground in the vicinity of the coil system is given. Through the concept of a geometrical factor, it is demonstrated that the total signal, which measures the apparent conductivity, is the summation of the partial products—geometrical factor by conductivity—for the different regions of the ground under consideration. It is thus possible to establish, for each type of coil arrangement, investigation characteristic as well as departure curves and correction charts for beds of various thicknesses. This should greatly facilitate the quantitative interpretation of the field logs, even in cases where such interpretation would have been difficult on electric logs taken with electrodes.

It is also shown that focussing combinations of coils can be used, which give, directly on the recorded log, a value close to the true conductivity, even for fairly thin beds, thus eliminating in most cases the need for corrections. These focussing systems also give a sharper definition of the boundaries between successive strata.

Manuscript received at Petroleum Branch Office February 7, 1949. Paper presented at AIME Annual Meeting in San Francisco February 13-17, 1949.

¹Reference given at end of paper.

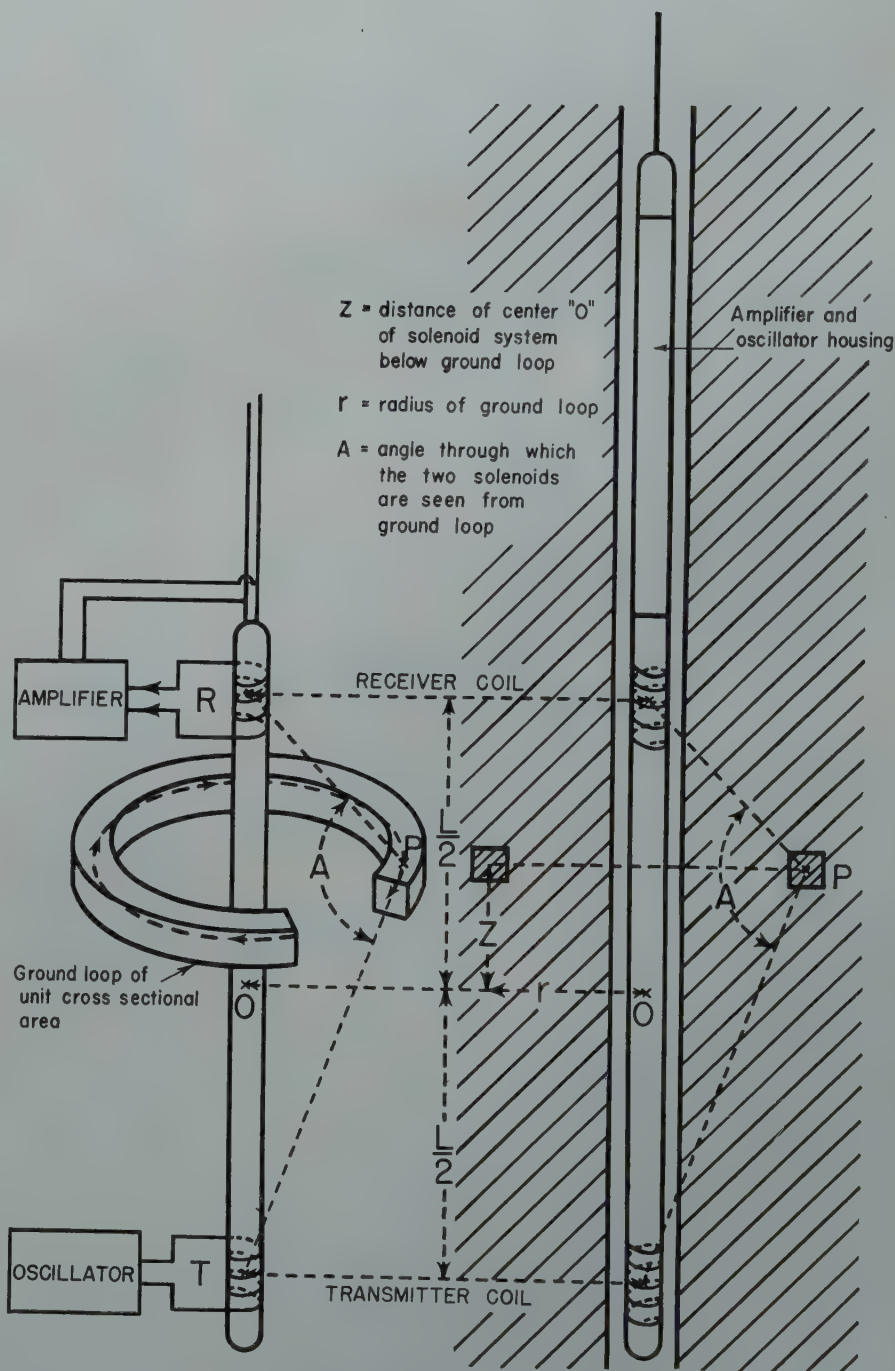


FIG. 1—A (LEFT) B (RIGHT) SCHEMATIC DRAWINGS OF APPARATUS USED FOR INDUCTION LOGGING.

INTRODUCTION

The measurement of the resistivity of the different formations traversed by drill holes has become standard practice in oil well drilling during the last 20 years. The technique used requires that direct contact be made with the mud filling the bore hole by means of electrodes which are connected to the insulated conductors of the supporting cable. A current of constant intensity is generally made to flow in the surrounding medium, by ohmic effect, potential differences which are proportional to its average resistivity. These potential differences, as picked up by one or more measuring electrodes in the bore hole, are recorded continuously at the surface of the ground, giving the resistivity log.

There are cases, however, where a direct contact between the electrodes and the drilling mud is not possible, for instance, in holes drilled with cable tools, which are generally dry, or in holes where non-conductive oil base mud is used in rotary drilling. The conventional electrical logging method then requires scratcher electrodes, which are forced by springs on the walls of the hole, to make direct contact with the formations. In some cases, the results are fairly satisfactory, but sometimes, particularly in wells drilled through hard formations, the measurements are not reliable because of poor contacts with the formations. It is, in particular, to surmount these problems that a new method of electrical logging, known as induction logging, has been introduced for resistivity measurements in oil base mud.

The induction logging system does not require any direct contact with the mud, or with the ground. As indicated by the name of the method, the formations surrounding the logging apparatus are energized by induction. To that effect, alternating current of appropriate frequency is made to flow through a coil, referred to as a "transmitter", which is supported by an insulating mandrel. The alternating magnetic field thus created generates eddy currents, which currents follow circular paths, coaxial with the coil system and the hole, in the formations surrounding said hole. These eddy currents create a secondary magnetic field which induces an electromotive force in a second coil, referred to as a "receiver", mounted on the same non-conductive mandrel at a certain distance, called "spacing", from the transmitter.

If the transmitter current is maintained at a constant value, the intensity of the eddy currents is proportional to the conductivity of the ground. Thereby, the conductivity of the ground determines the secondary field created by the eddy currents, and the signal generated in the receiver.

As in regular logging with electrodes, the signal is recorded continuously at the surface of the ground while the apparatus is moved along the hole. The record thus produced, which is frequently called an "induction log", because of the way in which it is obtained, shows the variations of the ground conductivity — and, consequently, of its inverse, the ground resistivity — with respect to depth. It is, therefore, equivalent to the resistivity log obtained by the conventional method of electrical logging with electrodes in water base mud.

The present paper is limited to the theory of the induction logging method, and to considerations concerning its application in holes drilled with oil base mud. In so doing, the paper simply follows the industrial development of this new technique to meet the challenge introduced by the use of oil base mud. In that case, the advantages of the method are more immediate, especially in view of the difficulties encountered by the conventional method of electrical logging. This does not mean that the induction logging method will not work in water base mud; on the contrary, it is believed that, in that case also, the

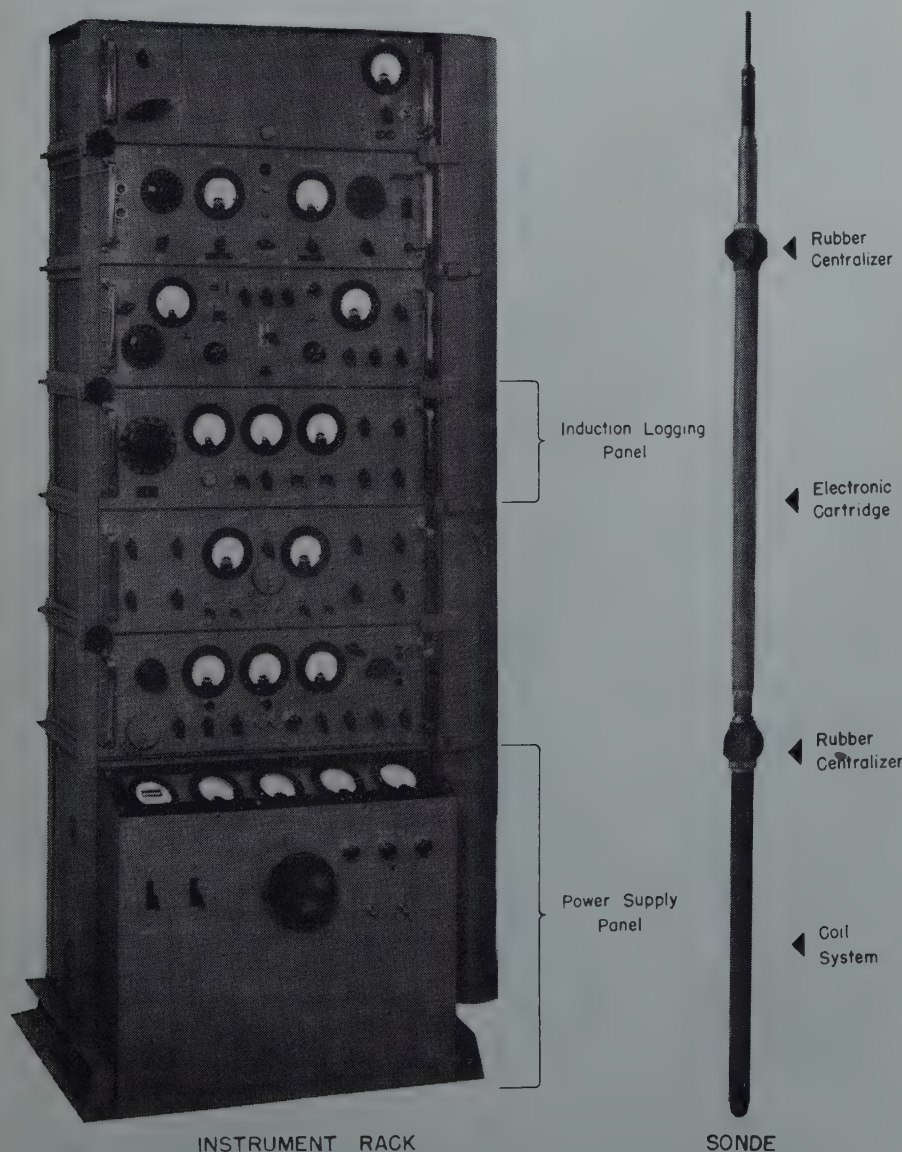


FIG. 2 — INDUCTION LOGGING EQUIPMENT.

method will have important advantages. Experience in water base mud is, however, still very limited, not only because the available instruments were all applied to oil base mud operations, where they were urgently needed, but also because certain improvements, which are still being studied, are to be introduced for best operation in water base mud. This is why it was felt advisable not to discuss the use of induction logging in water base mud at this time, and to wait for the results of field tests that will be made for that case.

Notation:

In the present paper, the following notation is used, in which "C" represents conductivity and "R" represents resistivity.

$$C_t = \frac{1}{R_t} = \text{true conductivity of a bed.}$$
$$C_i = \frac{1}{R_i} = \text{conductivity of the zone invaded by mud filtrate in a permeable bed.}$$
$$C_m = \frac{1}{R_m} = \text{conductivity of the drilling mud, which is considered as negligible in the case of oil base mud.}$$
$$C_{sa} = \frac{1}{R_{sa}} = \text{apparent conductivity of the formations surrounding, or adjacent to, a bed.}$$

In logging practice, the resistivity unit is the ohm-meter. Conductivities are expressed in mhos per meter. It is preferred, however, to use units of millimhos per meter for induction logging in order to get a range of values that does not require extensive use of decimal figures. Accordingly,

$$C \text{ mmhos/m} = \frac{1000}{R \text{ ohm-m}}$$

Thereby, a bed with a resistivity of 100 ohm-m has a conductivity of 10 mmhos/m.

PRINCIPLE OF RESISTIVITY MEASUREMENTS BY INDUCTION LOGGING

The apparatus used for induction logging is shown schematically on Figs. 1A and 1B; it is, in fact, a mutual impedance bridge. It comprises essentially a transmitter coil T, fed with alternat-

ing current by an oscillator, and a receiver coil R connected through an im-
plifier to the recording galvanometer. In the absence of any conductive medium around the apparatus, as, for example, when it is suspended in the air from a wood frame high enough above ground, the coupling between the transmitter and receiver coils is fully balanced, so that the measuring apparatus reads zero. When the apparatus is in a drill hole,

the alternating field set up by the trans-
mitter coil produces in the surrounding medium — i.e., in the ground — induced currents, generally known as "eddy currents", which are proportional to the conductivity of the ground. The electro-
motive force induced in the receiver coil by the eddy currents, referred to here-
after as "the signal", and designated by the letter E, is proportional to the con-
ductivity of the ground. If, therefore.

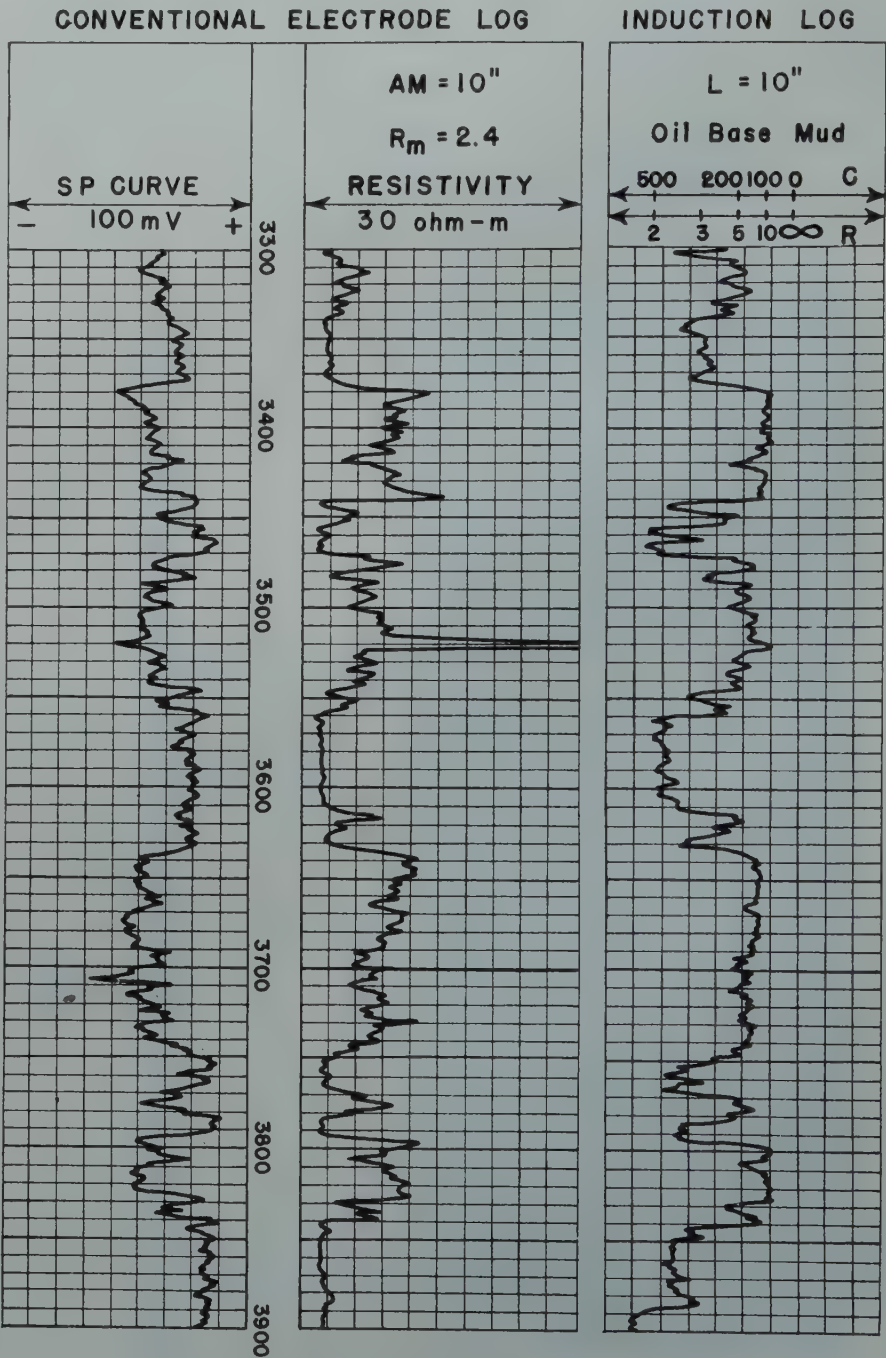


FIG. 3 — COMPARISON OF CONVENTIONAL ELECTRIC LOG IN WATER BASE MUD AND INDUCTION LOG IN OIL BASE MUD.

the apparatus is properly calibrated, a measure of the signal constitutes a quantitative determination of the conductivity* of the ground.

The signal is amplified and rectified into direct current for transmission in the cable to the surface where it is automatically recorded. A remote controlled test signal is provided in the apparatus to check the calibration.

The oscillator and the amplifier are contained in a pressure-proof housing, called the electronic cartridge, on top of the coil assembly. The subsurface instrument is represented schematically in Fig. 1B. A photograph of the equipment used for induction logging is shown in Fig. 2, where the sonde corresponds to Fig. 1B. An induction log recorded in oil base mud by this equipment is given on Fig. 3, alongside the

conventional electric log of the same well recorded later in water base mud for comparison.

When the ground surrounding the coil system is homogenous, as is practically the case for a thick bed which is not appreciably invaded by the mud fluid, the conductivity C_a , as measured by the apparatus, is substantially equal to the true conductivity C_t of the ground. When, however, the ground around the coil system is not homogenous, as for example, in the case of a thin bed surrounded by formations of appreciably different conductivity, the conductivity C_a , as measured by the apparatus, represents a combination of the conductivities of the different media surrounding the coil system, and is referred to as the "apparent conductivity." This is similar to what happens for electrical logging with electrodes where the apparatus also measures an apparent resistivity, R_a . In both cases, a

better approximation of the true conductivity can be obtained by applying corrections deduced from the departure curves* or correction charts.

As will be explained in more detail later in this paper, an important advantage of the induction logging system is that the measured values, even without corrections, are already nearer to the true values; furthermore, the corrections themselves are much easier to compute than in the case of logging with electrodes, particularly when influence of bed thickness is to be taken into consideration.

* Departure curves for electrical logging with electrodes have been published earlier in a booklet entitled "Resistivity Departure Curves," 1947, by Schlumberger Well Surveying Corporation, Houston, Texas. The application of the curves was discussed in a paper on "True Resistivity Determination from the Electric Log—Its Application to Log Analysis," by H. G. Doll, J. C. Legrand and E. F. Stratton, presented at the Spring Meeting, 1947, of the Pacific Coast District at Los Angeles, California, Division of Production, American Petroleum Institute.

* The words "conductivity" and "resistivity" are used indifferently in this paper both in the text and in the charts, inasmuch as one quantity is the inverse of the other.

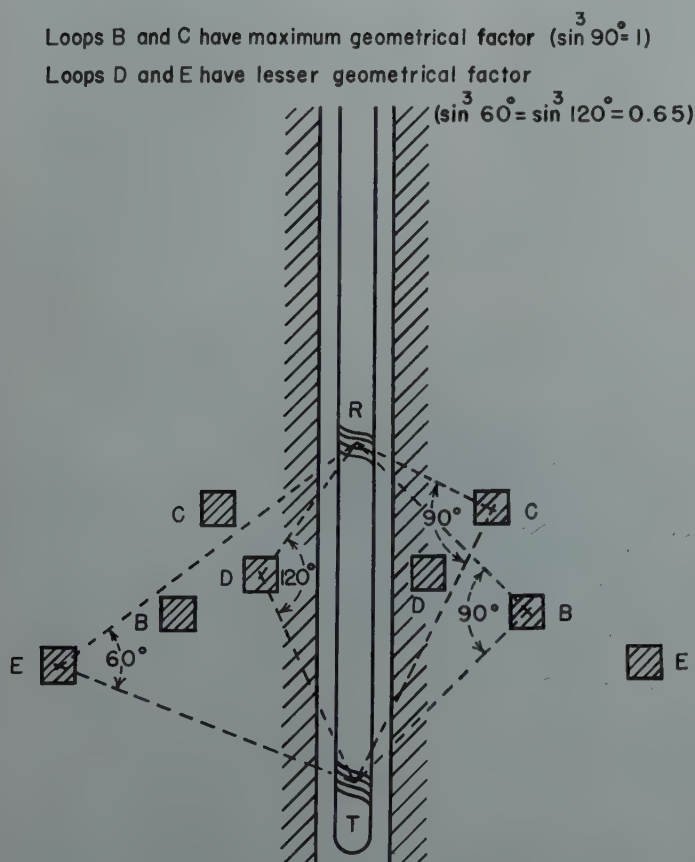


FIG. 4A — THE UNIT GROUND LOOP AND ITS GEOMETRICAL FACTOR.

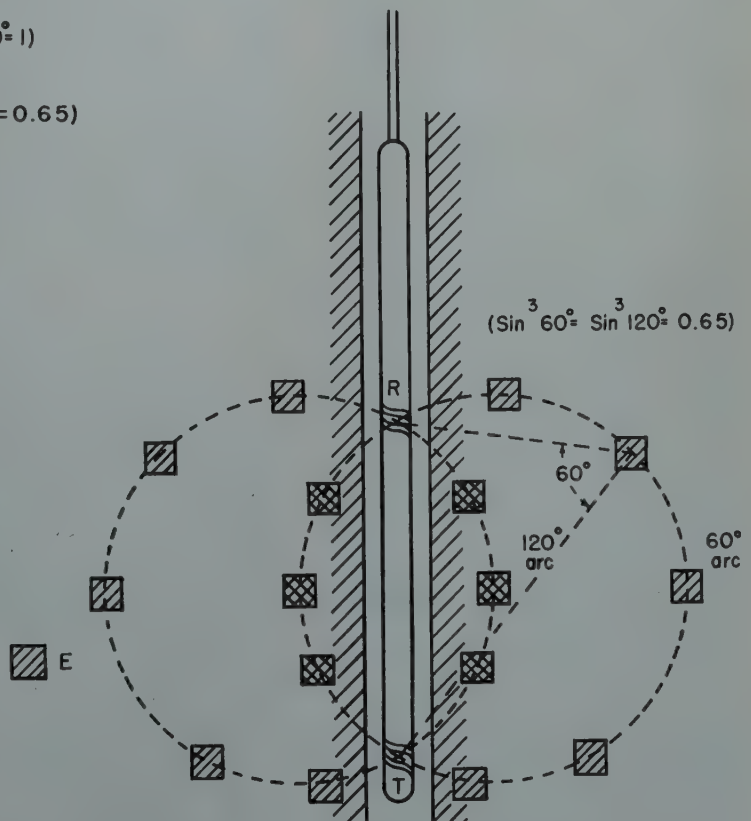


FIG. 4B — LOCUS OF UNIT CROSS SECTION LOOPS HAVING EQUAL GEOMETRICAL FACTOR.

THE GEOMETRY OF INDUCTION LOGGING—RESPECTIVE INFLUENCE OF THE DIFFERENT REGIONS OF THE GROUND SURROUNDING THE COIL SYSTEM

In the logging method using electrodes for the determination of the ground resistivity, the flow of current is of the radial type, and it is not possible to study separately the influence of the different regions of ground surrounding the electrode system. The reason is that the lines of current flow cross the boundaries between the different media, such as, for example, the boundary between the mud and a bed. If the resistivity of any given medium is changed, this affects the lines of current flow even in their path through the other media. This is why the mathematical computation of departure curves is rather complicated, and can only lead to a fair approximation as soon as the beds are neither very thick nor homogenous.

In the induction logging, the situation is entirely different. If the hole is vertical, as will be assumed to simplify the discussion, the lines of current flow are horizontal circumferences having their center on the axis of the hole. Since there is generally a symmetry of revolution of the ground around the axis of the drill hole, each line of current flow remains in the same medium all along its path, and never crosses a boundary between media of different conductivities. On the other hand, and provided that the frequency is not too high, the reaction of the different circular currents on each other can be neglected. In this condition, the action of the different regions of ground, which individually have a symmetry of revolution around the hole, can be considered separately, and the measured signal is simply the sum of the individual signals given by the different regions. The consequence is that the theoretical computation of charts or of typical logs, corresponding to any distribution of ground conductivities, is always possible, provided, of course, that there be a symmetry of revolution, as is practically the case, and particularly so when the dip of the formations is small.

In the discussion that follows, use will be made of charts representing the cross section of the ground intercepted by a vertical plane containing the axis of the hole. Each "region" of ground—which means here a volume of ground having a symmetry of revolution around the hole—will be represented on such charts by its cross section by the plane of the figure, and these sections will be identified by letters like A, B, etc. . . or otherwise. To simplify the wording, reference will be made, for instance, to the contribution of "section A" to the total signal; this will, of course, have to be construed as meaning the contribution of "region A", represented on the figure by "section A." This being stated, it becomes easy to discuss the contribution of a "section" of ground (meaning that of the corresponding volume or "region"). This contribution is a function of the area of the section and of a certain "geometrical factor" defined hereinafter, which factor depends on the position of the section with respect to the coil system.

All the mathematical computations, whose results are given in a later section, have been made with the assumption that the dimensions of the coils are small with respect to the diameter of any ground loop whose influence it is proposed to determine. This assumption, which simplifies substantially the mathematical work, is certainly reasonable and leads to quantitative values that can be considered as accurate for all practical purposes.

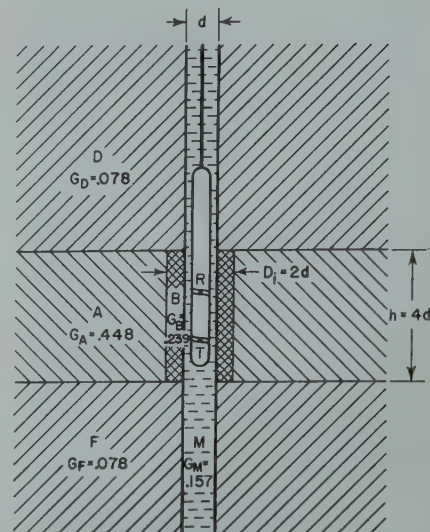


FIG. 5—EXAMPLE OF RELATIVE VALUES OF GEOMETRICAL FACTOR (TWO-COIL SONDE; SPACING = 1.25 HOLE DIAMETER).

The characteristics of the electronic circuit adopted as such that only the resistive component of the signal is measured, i.e., the component of the e.m.f. in the receiver which is in phase with the current in the transmitter. The theoretical discussion that follows is based on formulae which, theoretically, apply only to low frequencies, but which are still sufficiently accurate, for all practical purposes, at the frequency of 20 kilocycles presently used.

The Unit Ground Loop and Its Geometrical Factor

By definition, the expression unit ground loop, as used in this paper, will

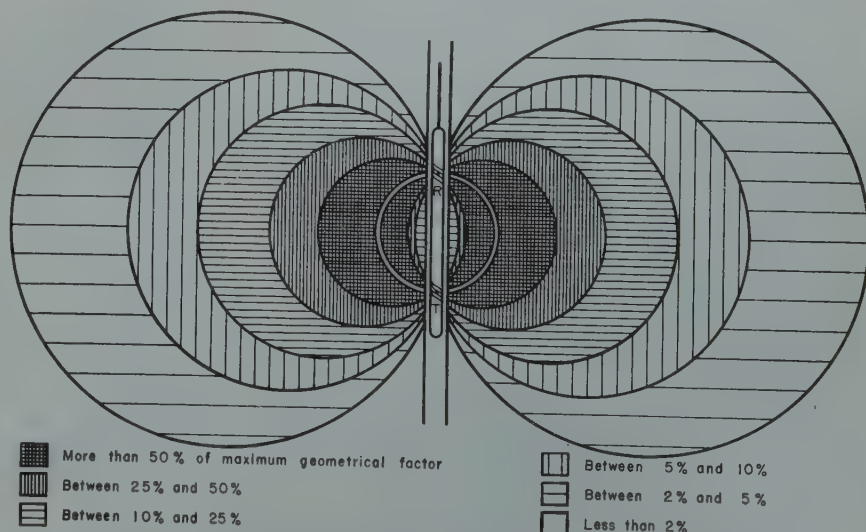


FIG. 6—CHART OF THE GEOMETRICAL FACTOR FOR THE DIFFERENT REGIONS OF GROUND AROUND THE COIL SYSTEM.

what proportion of the whole signal is contributed by that section, it is necessary to take into account the respective conductivities of the different sections, as is evident from relation (9) above. It can, in fact, very well happen that a region having only a small geometrical coefficient has a great influence on the measurement, simply because it has a proportionally large conductivity. This would, for instance, be the case for the beds D and F of Fig. 5 where their conductivity is much higher than that of bed A whose conductivity the system is supposed to measure.

Detailed Study of the Geometrical Factor

It is interesting at this point to consider in more detail the geometrical factors, starting with that of the unit loop. Instead of expressing factor g as a function of r and z , as in relation (3), this unit geometrical factor can also be related to an angle A (see Figs. 1A and 1B) through which the two coils T and R are seen from a point P of the unit loop. This relation is:

$$g = \frac{\sin^3 A}{2L^2} \quad \dots \quad (12)$$

which can be easily deduced from (3). It shows that all unit loops for which the angle A has the same sine have the same geometrical factor, and, therefore, contribute the same amount to the total signal, provided, of course, that they have the same conductivity. On a figure representing a cross section of the ground by a plane containing the axis of the hole, all the unit loops having the same g are, therefore, on a circumference which passes through the centers T and R of the two coils. Such a circumference, corresponding to loops for which the angle A is either 60° or 120° , with the sine equal to 0.866 in both cases, is represented on Fig. 4B. The g is maximum for unit loops such as B or C on Fig. 4A, for which the angle A is 90° . The cross sections of such horizontal loops by the plane of the figure lie on a vertical circumference having TR for diameter.

The chart of Fig. 6 illustrates a certain number of the circumferences corresponding, respectively, to a given value of g . The circumference (in

white) having TR for diameter corresponds to the maximum possible value for g which is used as reference. The other circumferences correspond to g 's which are, respectively, 50%, 25%, 10%, 5% and 2% of the maximum g . This chart gives a good idea of the depth of investigation of the induction logging system, or, more generally, of the relative extent of that investigation.

As indicated by relation (7), the geometrical factor G_A depends not only on the average unit geometrical factor g for that region, but also depends to a large extent on the area of its section. This is well illustrated by Fig. 7, which corresponds to Fig. 6. In Fig. 7, however, the space has been divided into

ten sections having the same geometrical factor. In the case of ground with the same conductivity throughout, each of these sections contributes 1/10 of the total signal.

In order to study the lateral investigation qualities of the induction logging system and the effect of formations adjacent to the bed under investigation, it is convenient to divided the space either into cylindrical shells or into thin horizontal beds. The features of these aspects will be discussed in the following paragraphs.

Geometrical Factor of a Unit Cylindrical Shell; Lateral Investigation Characteristic

In a bed of great thickness, which might be invaded laterally up to a certain radius by mud fluid, the conductivity does not vary along the vertical, but it varies along the radius. Such a medium can be considered as the combination of a large number of cylinders, coaxial with the hole, which are individually homogeneous, but whose conductivity may vary from one cylinder to another. To study that case, it is advantageous to divide the space into an infinite number of cylindrical shells, coaxial with the hole, having unit thickness, referred to hereafter as "unit cylinders", and to determine the geometrical factor of each of these cylindrical shells as a function of its radius. This geometrical factor for each cylindrical shell of radius r , designated by G_r , is related to g by the following equation:

$$G_r = \int_{-\infty}^{+\infty} g \, dz \quad \dots \quad (13)$$

The integration of (13) does not lead to a simple expression for G_r , but gives, however, the following relation which permits the computation of G_r by means of tabulated elliptic integrals:

$$G_r = \frac{1}{2L} \frac{u}{(u^2 + 1)^2} \left[\frac{(u^3 + 3)(\sqrt{u^2 + 1} - 1)}{(u^2 - 1)(\sqrt{u^2 + 1} + 1)} K(\sin a) - E(\sin a) \right] \quad \dots \quad (14)$$

where:

$$u = \frac{2r}{L} \quad \dots \quad (15a)$$

$$\sin a = 2\sqrt{u^2 + 1} \sqrt{u^2 + 1 - 1} \quad (15b)$$

Geometrical factor for a cylindrical shell of ground of unit thickness, of infinite length, and of radius r -

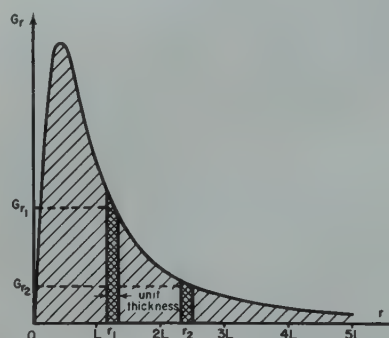


FIG. 8 - RADIAL INVESTIGATION CHARACTERISTIC FOR A TWO-COIL SYSTEM (L = SPACING = DISTANCE BETWEEN COILS).

Geometrical factor for a cylinder of ground of infinite length

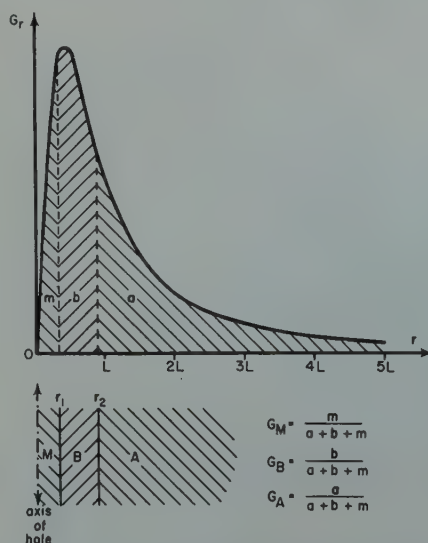


FIG. 9 - RADIAL INVESTIGATION CHARACTERISTIC (TWO-COIL SYSTEM SPACING "L").

while K and E are the elliptical functions defined by:

$$K(\sin a) = \int_0^{\frac{\pi}{2}} \frac{d\theta}{\sqrt{1 - \sin^2 a \sin^2 \theta}}$$

$$E(\sin a) = \int_0^{\frac{\pi}{2}} \frac{2}{\sqrt{1 - \sin^2 a \sin^2 \theta}} d\theta$$

for which the numerical values can be found in tables of functions.¹

The value of G_z , as a function of r , has been computed by the above relation (14), and it is represented by the curve of Fig. 8, which will be referred to as the "radial investigation characteristic." This curve shows the relative contribution of the different cylinders of ground in the case of a thick bed of uniform conductivity.

It is now easy to determine the relative values of the geometrical factor opposite a permeable bed. The geometrical factors for the regions indicated in Fig. 9 are, respectively, proportional to the corresponding areas m , b and a under the radial investigation characteristic. For reasons of normalization, the geometrical factor for the whole space is taken as a unity, so that G_m , G_b and G_a are really given by:

$$G_m = \frac{m}{m+b+a} \quad (17a)$$

$$G_b = \frac{b}{m+b+a} \quad (17b)$$

$$G_a = \frac{a}{m+b+a} \quad (17c)$$

Geometrical Factor of a Unit Horizontal Bed; Vertical Investigation Characteristic

When the induction logging system is located opposite a bed of finite thickness, the signal it measures is primarily responsive to the conductivity of that bed. In many cases, however, and in particular when the bed is rather thin and is surrounded by more conductive formations, the signal is quite appreciably influenced by these adjacent formations; in such instances, the apparent conductivity C_a , as measured, does not coincide with the true conductivity C_t of the bed under investigation.

To study that effect, it is convenient to disregard the effect of the mud column and the effect of mud filtrate penetration. The space can then be divided into an infinite number of horizontal beds of unit thickness, referred to hereafter as unit beds, individually characterized by their altitude with respect to the center of the coil system. The geometrical factor of such a unit bed, designated by G_z , is related to its altitude z by the following equation:

$$G_z = \int_0^\infty g \, dr \quad (18)$$

The integration of (18) gives for G_z the following relations:

$$G_z = \frac{1}{2L} \quad \text{when } -\frac{L}{2} < z < +\frac{L}{2} \quad (19a)$$

$$G_z = \frac{L}{8z^2} \quad \text{when } z < -\frac{L}{2} \text{ or } z > +\frac{L}{2} \quad (19b)$$

Relation (19a) applies to unit beds which are between the two coils, while relation (19b) applies to unit beds which are outside of the interval between the two coils.

The value of G_z , as a function of z , is represented by the dashed line of Fig. 10, which will be referred to as the "vertical investigation characteristic." This curve shows the relative contribution of the different layers of ground.

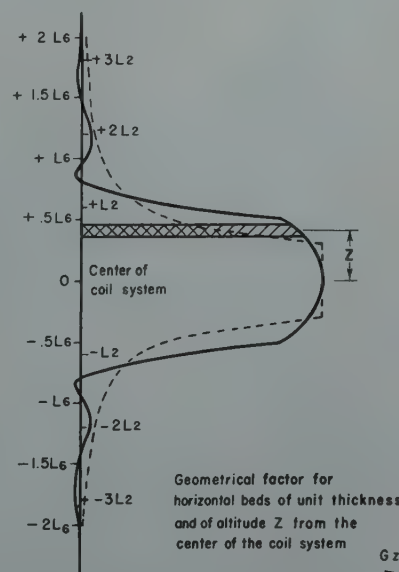


FIG. 10 — VERTICAL INVESTIGATION CHARACTERISTICS
 - - - - TWO-COIL (SPACING L_2)
 ——— FOCUSSING SONDE TYPE 6F
 (MAIN SPACING L_6)

It is interesting to consider the geometrical factor of beds of finite thickness whose boundaries have a definite altitude with respect to the center O of the coil system. As an example, Fig. 11 shows the division of the ground in three regions, A, D and F. The region A, which is opposite the coil system, corresponds to a bed of finite thickness whose conductivity is to be measured, and which is referred to as "the bed." Regions D and F correspond to very thick beds which constitute what is generally referred to as "the surrounding formations." The geometrical factors G_A , G_D and G_F of the three regions, for the position of a coil system centered at O on Fig. 11, are measured, respectively, by the corresponding areas a , d and f under the vertical investigation characteristic. Taking into account the normalization already mentioned, which makes the geometrical factor for the whole space equal to unity, the geometrical factors G_A , G_D and G_F of beds A, D and F are given by:

$$G_A = \frac{a}{a+d+f} \quad (20a)$$

$$G_D = \frac{d}{a+d+f} \quad (20b)$$

$$G_F = \frac{f}{a+d+f} \quad (20c)$$

As can be seen from the figure, the geometrical factors G_D and G_F are far from being negligible unless the bed A is very thick. This means that the surrounding formations D and F can have appreciable influence, especially when they are more conductive than the bed A under investigation. It is for that reason that special coil combinations, referred to hereafter as "focussing systems", have been developed in order to minimize to a very large extent the effect of the surrounding formations, by reducing the corresponding geometrical factors.

Focussing Systems of Coils

It has been found that it is possible to obtain systems which have much better vertical investigation characteristics than two-coil devices. This is done through a proper combination of additional coils using special arrangements of spacings and numbers of turns. Fig. 10 shows, in solid line, the vertical in-

vestigation characteristic for a focussing system of coils (reference type 6F). It also shows, for comparison, and in dashed line, the vertical investigation characteristic for a two-coil combination. The spacing indicated for the focussing system is that of its two main coils, and is referred to as the "main spacing." The spacing for the two-coil system has been taken smaller than the main spacing of the focussing sonde to obtain a vertical investigation characteristic which corresponds as closely as possible to that of the focussing system. This, however, gives a slightly smaller lateral depth of investigation to the two-coil sonde, as shown in Fig. 12, where the radial investigation characteristics of both systems are shown. In spite of this reduction of spacing for the two-coil system, Fig. 10 illustrates that this system cannot compete with the focussing system when it is desired to minimize the effect of the surrounding formations, as, for instance, when measuring conductivity of a bed of small thickness. Provided that the bed thickness be more than 1.5 times the main spacing, the geometrical factor of the surrounding formations, as measured by the area under the vertical investigation characteristic, is extremely small for the focussing system. The use of the focussing system, therefore, results in more direct determination of the conductivity of the formations. It also results in a sharper determination of the boundaries.

In designing the focussing system whose vertical and radial characteristics are respectively given in Figs. 10 and 12, precautions were taken to reduce the geometrical factor for small radii, as illustrated by Fig. 12. This reduces, of course, in the same proportion, the influence of the regions of space, like the mud column and the invaded zone, which correspond to these small radii. With that type of coil system, the focussing, therefore, is both vertical and lateral.

The investigation properties of the focussing system of coils is further illustrated by Fig. 13, which is a chart of the unit geometrical factor for that system.* A comparison of this chart

with that of Fig. 6 shows very clearly the advantages of the focussing system; namely, a sharper definition for the region of ground whose average conductivity is measured.

Geometrical Factor of a Given Region of Ground as a Function of the Position of the Coil System

The geometrical factor for a region of ground depends on its position with respect to the coil system. In practice, the region of ground is fixed, and it is the coil system that moves vertically along the hole. It is, therefore, normal to define the position of the coil system by the displacement of x of its center point with respect to a reference level. The geometrical factor G_A for a given region A of ground then becomes a function of x , which shall hereafter be written $G_A(x)$. Functions $G_A(x)$, $G_B(x)$, $G_D(x)$, etc. . . . can be tabulated for regions A , B , D , etc., of various shape

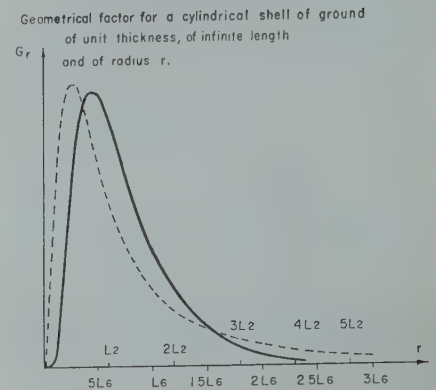


FIG. 12 — RADIAL INVESTIGATION CHARACTERISTICS
- - - - TWO-COIL (SPACING L_2)
———— FOCUSING SONDE TYPE 6F (MAIN SPACING L_6)

Geometrical factor for a horizontal bed at altitude Z from the center of the coil system

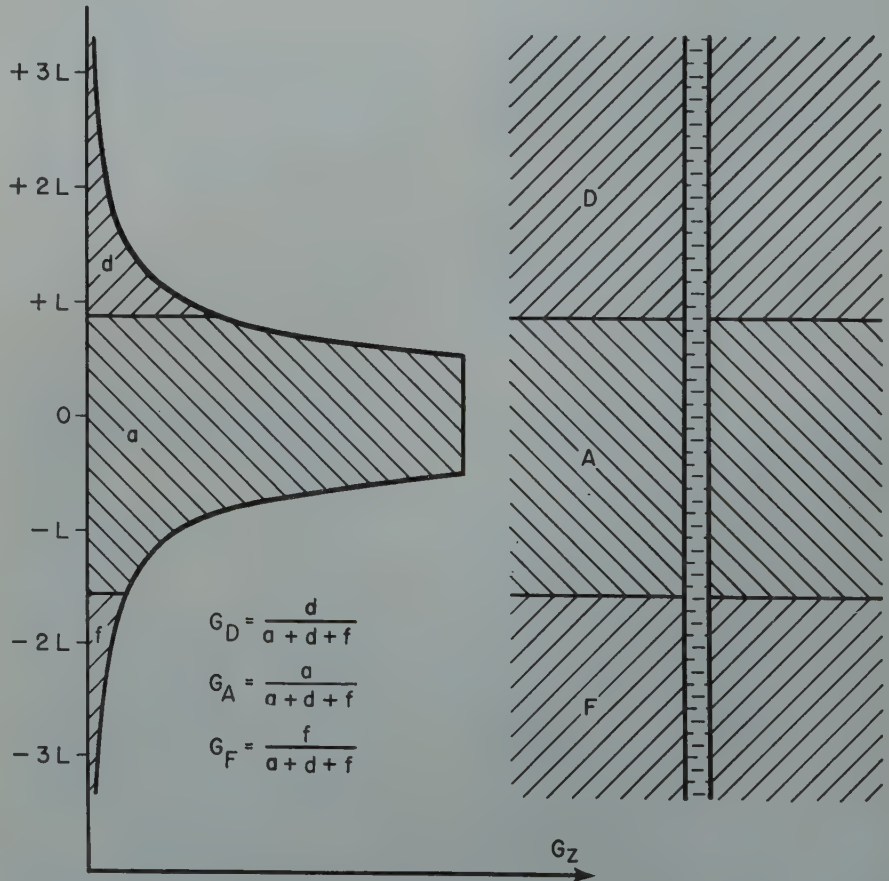


FIG. 11 — VERTICAL INVESTIGATION CHARACTERISTICS (TWO-COIL SYSTEM SPACING " L ").

* Fig. 13 corresponds to an earlier type of focussing system, similar to present type 6F, but in which the focussing had been exaggerated with the consequence that certain regions show slightly negative g 's. The corresponding chart for the present type 6F will probably be very similar, except that it will show less negative areas.

and dimension, and can then be used to compute typical logs or correction charts for various combinations of conductivities for the different media A, B, D . . .

THE MEASURED SIGNAL AND THE APPARENT CONDUCTIVITY

According to equation (9), the apparent conductivity for a given position of the coil system is given by:

$$C_a = C_A G_A + C_B G_B + \dots \quad (21)$$

When the coil system moves along the hole, the geometrical factors G_A , G_B , etc., vary with the displacement x of the coil system. In that case, the expression for C_a becomes:

$$C_a = C_A G_A(x) + C_B G_B(x) + \dots \quad (22)$$

Equation (22) shows that it is very easy to compute the "apparent conductivity logs" for any particular system of conductivities attributed to the media A, B, etc., once the functions $G_A(x)$, $G_B(x)$. . . have been determined. The computation of the G factors by integration of equation (7), represents a substantial amount of work, since it has to be done

for many shapes of ground types of coil system. It is, however, only a matter of time and, contrary to what occurs for analysis of electrical logs with electrodes, there is no theoretical difficulty which prevents the accurate computation of any particular case; the only requirement here is that there be symmetry of revolution. The consequence is that departure curves and correction charts can be computed for beds of finite thickness, whether invaded by the mud fluid or not, whatever the respective conductivities of the adjacent beds. Some examples of such departure curves or correction charts, corresponding to different coil systems or spacings, are given as examples in the next sections.

Computed Logs and Departure Curves

The principles and formulae discussed in this paper have been used to compute induction logs and departure curves, corresponding to different distributions of ground conductivities, some of which are given here as examples. In all cases, it has been assumed that the mud was highly resistive, as is normally the case with oil base mud.

The logs of Figs. 14, 16, and the departure curves of Fig. 16 were established to compare the respective qualities of the two-coil device and the focussing system for the determination of the true resistivity of beds of finite thickness. In order to show the influence of bed thickness in its extreme aspect, beds that are less conductive than the surrounding medium were considered as not being invaded by the mud filtrate; otherwise, the effect of the surrounding formations, which corresponds to an increase of the apparent conductivity in that case, would be partially compensated by the effect of invasion, which corresponds to a decrease of the apparent conductivity. Conversely, beds which are more conductive than the surrounding formations were considered as invaded, because, in that case, both the invasion and the surrounding formations will tend to decrease the apparent conductivity.

Following the practice introduced in connection with electrical logging with electrodes, the curves given here are calibrated in resistivity units. Logarithmic

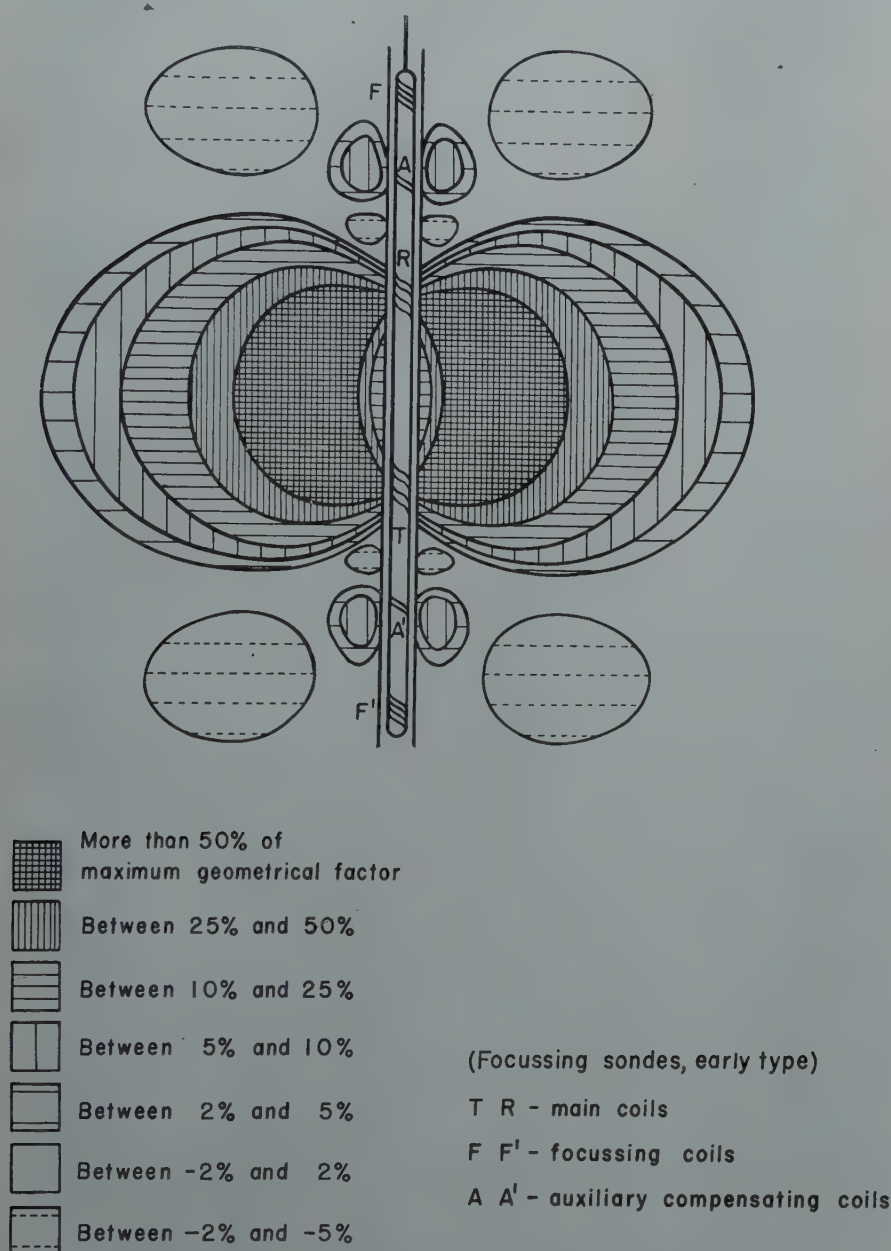


FIG. 13 — CHART OF THE GEOMETRICAL FACTOR FOR THE DIFFERENT REGIONS OF GROUND AROUND THE COIL SYSTEM.

mic scales are used for the resistivities on the logs and on the departure curves in order to show more clearly the percentage of departure of the apparent resistivities R_a with respect to the true resistivities R_t .

Both the computed logs of Figs. 14 and 15 and the departure curves of Fig. 16 verify that the two-coil system is much more sensitive to the influence of bed thickness, as expected, than the focussing device. Among the two coil systems, those having a spacing between one and two times the hole diameter seem to give the best over-all results, but the apparent resistivity differs appreciably from the true resistivity, even in beds whose thickness is sixteen times the hole diameter. This, however, is not too serious because corrections can be applied, as will be explained herein-after.

The focussing system has the definite advantage of giving a good approximation to the true resistivity directly on the log. For the ground conditions assumed for Figs. 14 and 15, a main spacing between two and three times the hole diameter seems to give the best over-all results. The superiority of the focussing system over the two-coil system is well illustrated by Fig. 15, in which the logs corresponding to the best average spacing for both systems are superimposed. With the focussing type of sonde, corrections for bed thickness are practically not needed except for rather thin beds, in which case they can be made by use of special charts.

The departure curves of Fig. 16 show in a more complete form the information given by Figs. 14 and 15. On this figure, the left hand side corresponds to the two-coil system, and the right hand side to the focussing system. The full line curves correspond to the case of no invasion, whereas the dashed line curves are for invasion. It is particularly interesting to remark that there is no spacing for which the two-coil system is not too sensitive to bed thickness and to the conductivity of the surrounding formations. On the contrary, a focussing system with a main spacing from two to three times the diameter of the hole gives an apparent resistivity which is always between 80% and 125% of the true resistivity, as long as the bed thickness is more than five times the

diameter of the hole and the surrounding formations have a conductivity not more than twenty times that of the bed. If the permeable beds are invaded by the mud fluid to a larger diameter D_i than that corresponding to the departure curves of Fig. 16, a larger spacing would be preferred, and the minimum

thickness of the beds for good quantitative determination would be raised accordingly.

Correction Charts for Beds of Finite Thickness

Fig. 17, given here as example, is a correction chart for beds of finite thick-

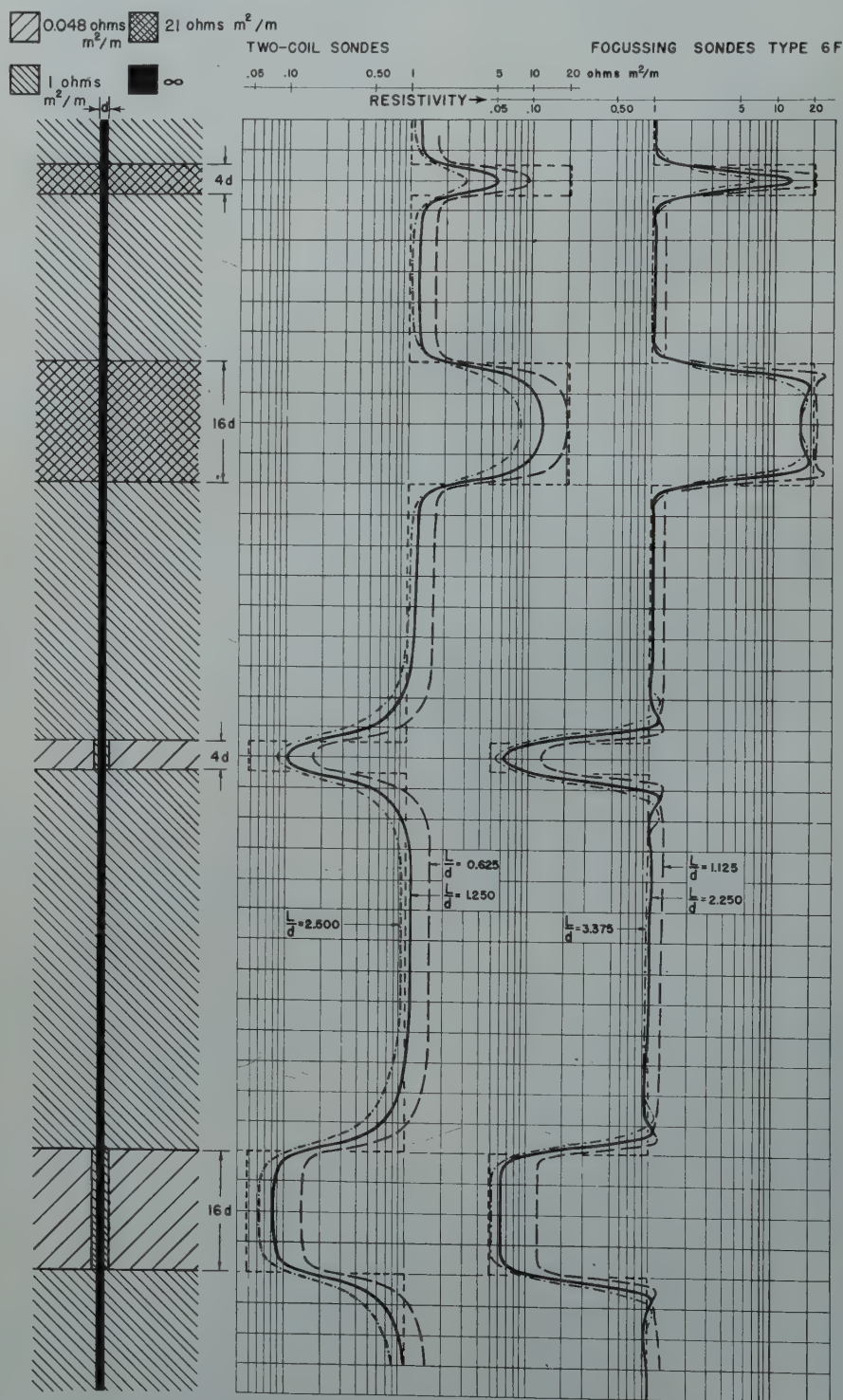


FIG. 14 — EXAMPLE OF COMPUTED INDUCTION LOGS FOR DIFFERENT
VALUES OF RATIO SPACING "L".

ness, and corresponds to a two-coil system whose spacing is 1.25 times the hole diameter. Theoretically, such a chart applies only to a homogeneous bed of finite thickness surrounded by two homogeneous beds, referred to as surrounding beds, which are supposed to be very thick. This, of course, is an ideal case. Such charts are useful, however, even in the case of formations

which are only approximately homogeneous, provided the surrounding beds are thick enough so that their average apparent resistivity can be determined from the log.

The chart has been calibrated in resistivity units, as done for the departure curves and the computed logs. It is, however, much easier to determine the necessary data from the induction log in

conductivity units, for reasons that will be obvious. This is a quite logical choice, since the field logs are recorded with a linear scale for the conductivities. In using the chart, the abscissae, which are expressed as the ratio of R_{sa}/R_a are then simply taken equal to C_a/C_{sa} , which has the same value.

Fig. 18 shows schematically an induction log for a bed of finite thickness represented with a linear scale for the conductivities. It shows how the different data necessary for the use of the correction chart are determined from that log.

C_a is the apparent conductivity opposite the center part of the bed;

$C_{sa} = \frac{C_{sa1} + C_{sa2}}{2}$ is the average apparent conductivity of the surrounding formations;

h_a is the apparent* thickness, which is the difference between the two depths at which the conductivities are, respectively,

$$\frac{C_a + C_{sa1}}{2} \quad \text{and} \quad \frac{C_a + C_{sa2}}{2}$$

The value of C_a/C_{sa} is entered in abscissae on the correction chart, and the ratio R_t/R_a , or correction factor, is read on the ordinate scale for the curve corresponding to the thickness h_a .

When the logs have a linear scale for the resistivities, the boundaries determining h_a are taken at the depths where the apparent resistivity is equal to

$$\frac{2}{\frac{1}{R_a} + \frac{1}{R_{sa1}}} \quad \text{or} \quad \frac{2}{\frac{1}{R_a} + \frac{1}{R_{sa2}}}$$

Obviously, such determination is less practical than the one made on logs recorded with the linear conductivity scale.

The particular chart of Fig. 17 combines, for a given hole diameter and for a given coil system, the correction due to the bed thickness and the correction due to the highly resistive mud column. Other means can be conceived to take care of these corrections. In particular,

* The apparent thickness h_a , as determined from the log, is practically equal to the true thickness for beds whose thickness is at least three times the main spacing of the coil system.

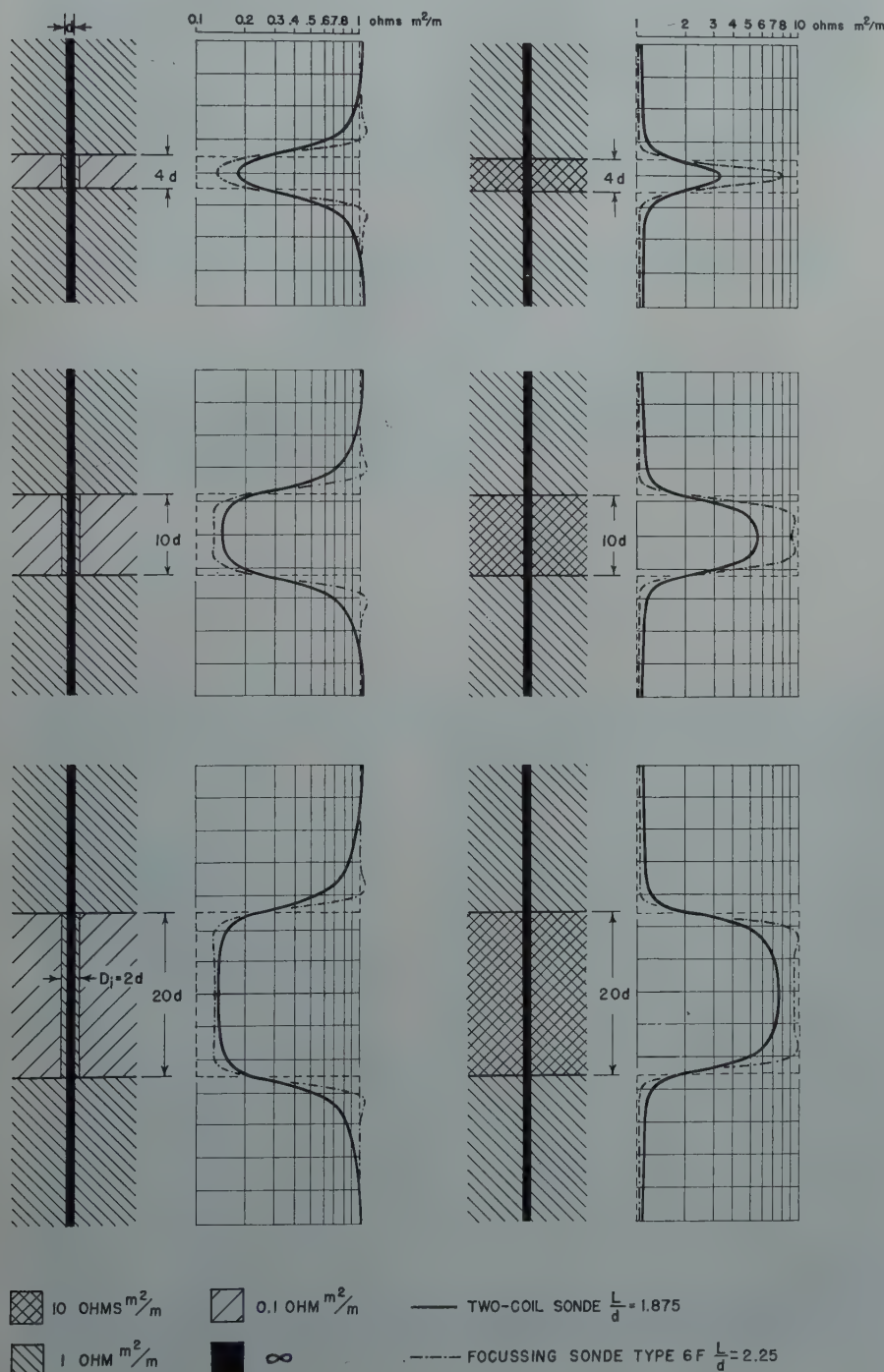


FIG. 15 — EXAMPLE OF COMPUTED INDUCTION LOGS SHOWING COMPARISON BETWEEN A TWO-COIL SONDE AND A FOCUSING SONDE TYPE 6 F.

the correction for the mud column can be done directly when recording the log, through proper adjustment of the scale, since the correction ratio is constant for a given hole diameter. Such adjustment steps will probably be developed commercially in the near future, and practical charts corresponding to the coil system actually used for the induction logging will be made available.

Correction Charts for Mud Filtrate Invasion

The value of R_t , as determined from the correction charts for beds of finite thickness, can further be corrected, if desired, for the effect of invasion, provided the diameter of invasion and the resistivity of the invaded zone can be estimated. Since the correction is generally not large, a fair estimation of these factors is sufficient in most cases.

Fig. 19 shows an example of a correction chart for mud fluid invasion corresponding to a two-coil system with a spacing of 1.25 times the diameter of the drill hole.

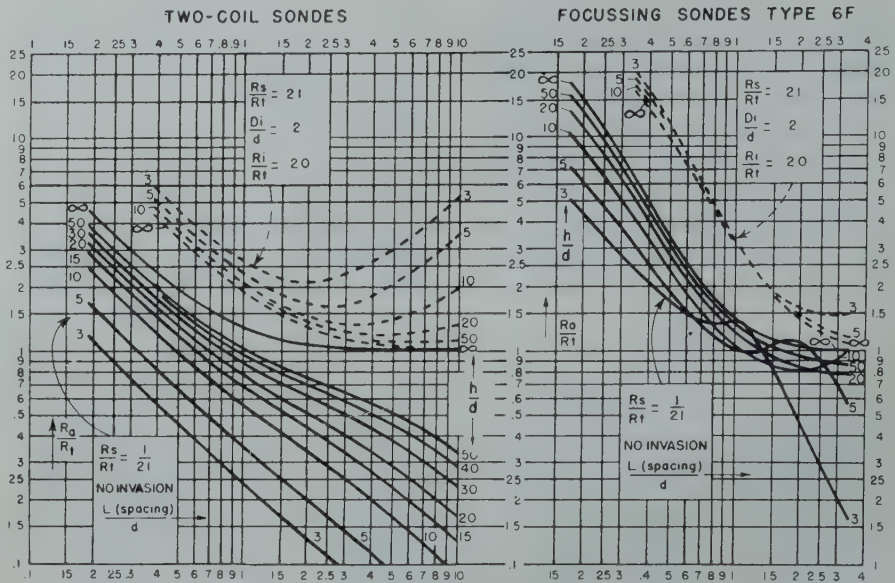


FIG. 16 — DEPARTURE CURVES FOR INDUCTION LOGGING IN OIL BASE MUD—BEDS OF FINITE THICKNESS.

- d = hole diameter
- h = bed thickness
- Di = invaded zone diameter
- L = spacing
- R_t = bed resistivity
- R_i = invaded zone resistivity
- R_a = apparent bed resistivity
- R_s = resistivity of surrounding formation

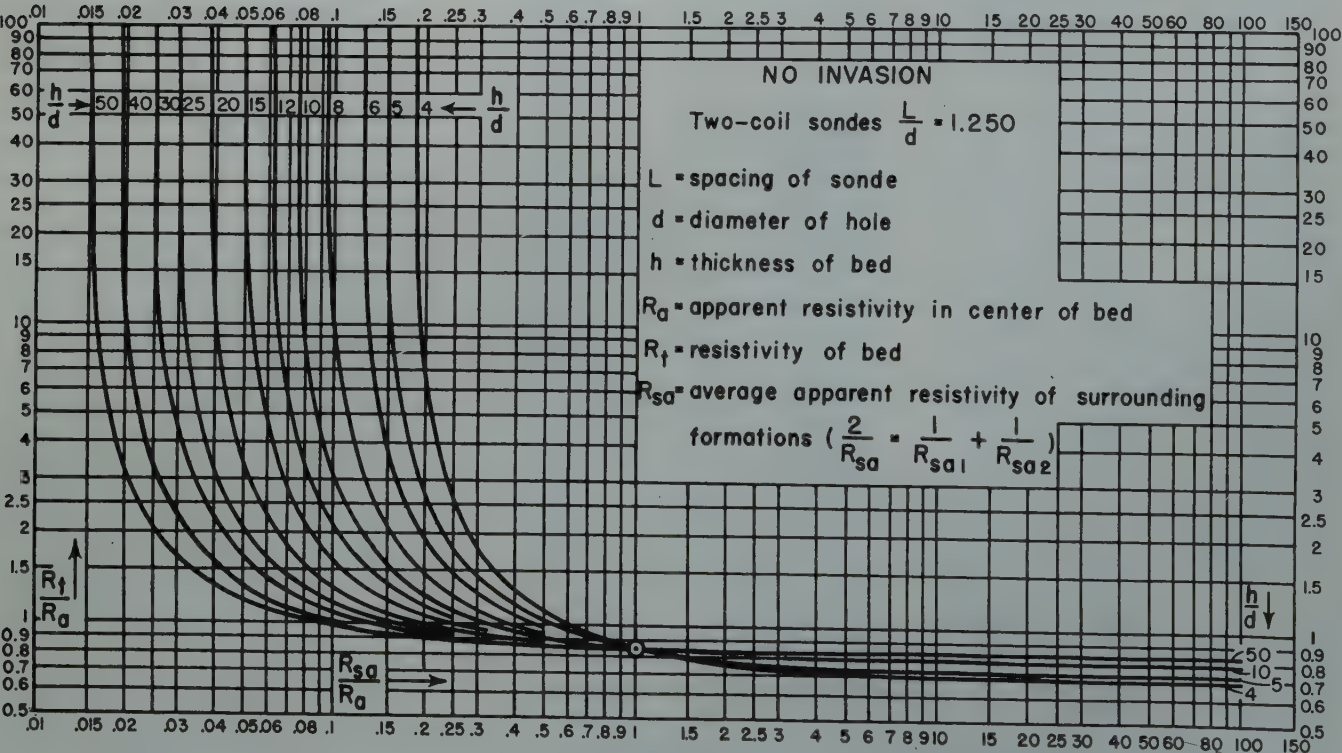


FIG. 17 — INDUCTION LOGGING IN OIL-BASE MUD, CORRECTION CHART FOR BEDS OF FINITE THICKNESS.

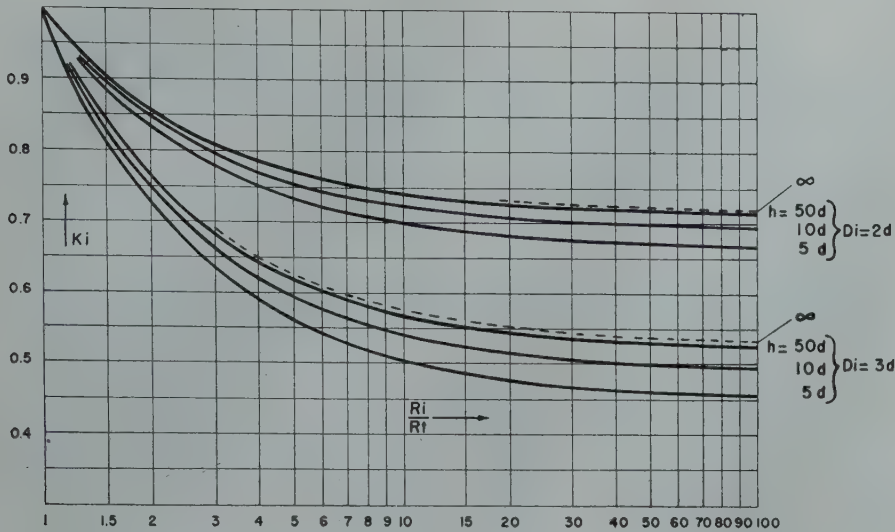


FIG. 19 — INDUCTION LOGGING IN OIL BASE MUD, BEDS OF FINITE THICKNESS. CORRECTION FACTOR FOR INVASION.

L
Two-coil sondes = 1.25
 D
 h = thickness of bed
 L = spacing of sonde

d = hole diameter
 D_i = diameter of invaded zone
 R_i = resistivity of invaded zone
 R_t = resistivity of formation (from chart for no invasion)
 K_i = correction factor
 R Corrected = $K_i \times R_t$

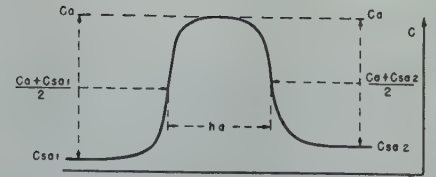


FIG. 18 — SCHEMATIC INDUCTION LOG SHOWING DETERMINATION OF APPARENT THICKNESS OF BED.

Numerical Examples of Quantitative Computations

Fig. 20 shows a computed log for a bed of finite thickness, corresponding to the same spacing as the examples of correction charts. This log is given to illustrate the method of correction. From the log, the following data is obtainable:

$C_a = 19.2$ mmhos/m or
 $R_a = 52$ ohm-m
 $C_{sa} = 1.9$ mmhos/m
 $h_a = 4.2$ d

The correction chart of Fig. 17 for the entry with the value 10 for C_a/C_{sa} and the value 4.2 d for h gives $R_t/R_a = 0.7$, or R_t (assuming no invasion) = $52 \times 0.7 = 36.4$ ohm-m. This value of R_t is to be corrected for the effect of invasion where the diameter D_i and the resistivity R_i of the invaded zone can be estimated. Assuming for R_i and D_i the values 10 R_t and 2 d, as indicated on Fig. 20, the chart of Fig. 19 gives $K_i = 0.69$. Therefore, R_t (corrected for invasion) = $36.4 \times 0.69 = 25.1$ ohm-m, which corresponds very nearly to the true resistivity of 25 ohm-m for the bed, as used for the computation of the log.

Fig. 21 gives another example of a log, corresponding to a resistive bed without invasion. In that case:

$C_a = 190$ mmhos/m
 $C_{sa} = 845$ mmhos/m
 $h_a = 4.2$ d
 $R_a = 5.3$ ohm-m
 $\frac{C_a}{C_{sa}} = 0.225$

and the correction chart of Fig. 17 gives $R_t/R_a = 3.4$; therefore, $R_t = 5.3 \times 3.4 = 18$ ohm-m, whereas the R_t of the bed was 20 ohm-m.

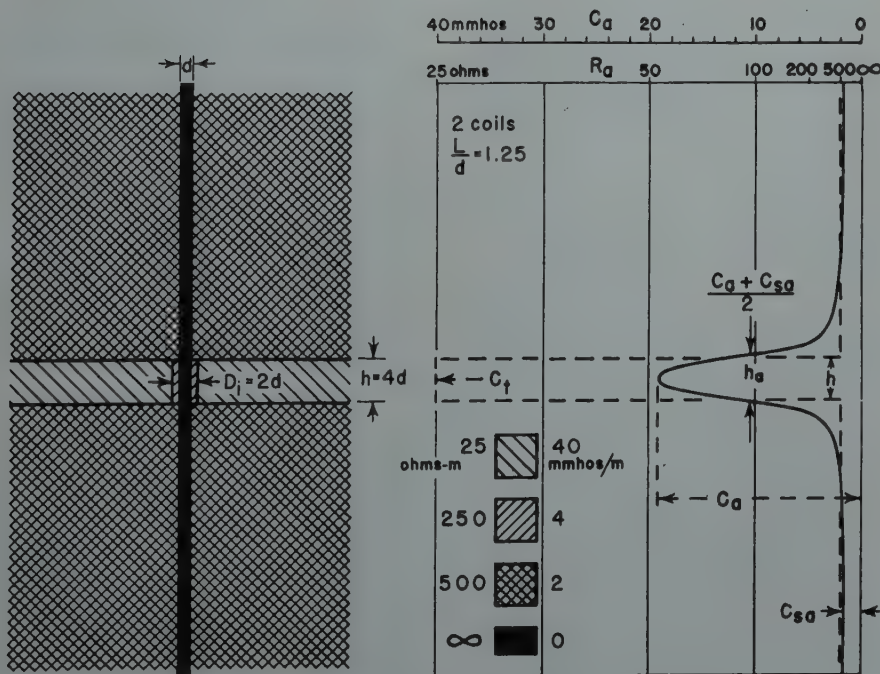


FIG. 20 — COMPUTED INDUCTION LOG SHOWING DETERMINATION OF APPARENT THICKNESS OF BED.

Remark on the Scale Calibration

The deflections recorded on field logs are proportional to the variations of the conductivity, and the scale is adjusted to a given number of mmhos/m, per division, by means of a test signal. In that respect, the calibration is, therefore, maintained accurate. In addition to the determination of the scale, it is necessary to position the zero on the logs. At present, this is accomplished by adjusting the apparatus when the sonde is located in the drill hole opposite a bed of very high resistivity, where the signal must be practically negligible. As the instrument is quite stable as long as it remains in the hole, the zero adjustment thus made is satisfactory for quantitative interpretation of strata of lower resistivity than that of the bed used for the adjustment. On the other hand, it would not be possible, with the present equipment, to obtain an accurate value of the conductivity of formations which are among the most resistive encountered in the open hole. Systems with a predetermined zero, sufficiently accurate for quantitative determination in all cases, are under development.

CONCLUSION

The conductivity, or the resistivity, of formations traversed by a drill hole can be determined by the induction logging method. This new technique is particularly useful at present for logging dry holes and holes filled with oil base mud, in which direct contact with the formations is difficult to establish.

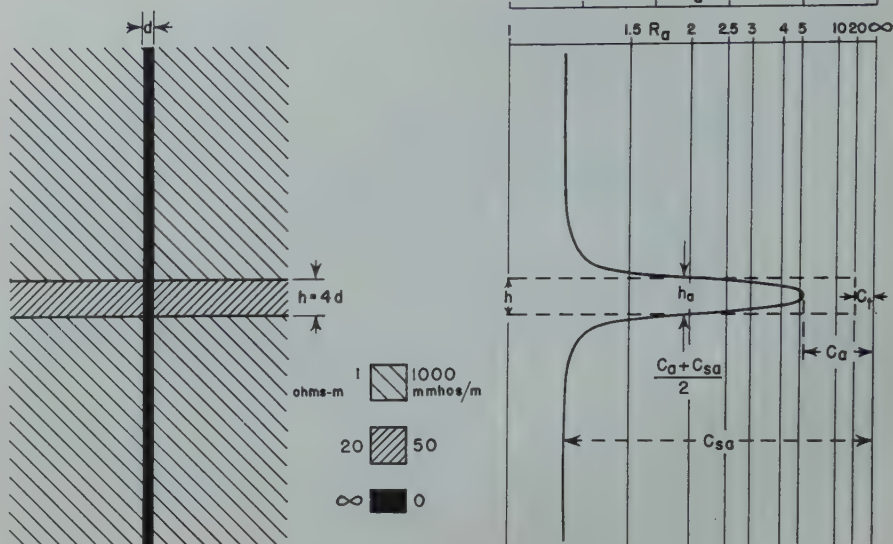


FIG. 21 — COMPUTED INDUCTION LOG FOR A NON-INVADED BED.

The method has great flexibility, and is quite promising. Coil systems can be designed to give a focussing effect in order to obtain directly on the log a more accurate value for the conductivity of beds of finite thickness.

Since the different regions of ground have generally a symmetry of revolution around the axis of the hole, and since, therefore, the induced currents have circular paths around that axis, the currents never cross the boundary from one region to the other. In these conditions, the contributions of the different regions to the measured signal can be considered independently. For that reason, it is relatively easy to compute typical logs and correction charts,

which should greatly improve the possibilities of quantitative interpretation.

ACKNOWLEDGMENTS

The author wishes to acknowledge the valuable assistance of F. Perrin, A. Blanchard and A. Poupon, who worked on the mathematical computations; he also wishes to acknowledge the contribution of O. H. Huston who had an important part in the design and construction of the apparatus.

REFERENCE

1. Jahnke and Emde, *Tables of Functions and Formulae and Curves*, (Dover Publications, New York). ★

PRODUCTION OF OIL UNDER UNITIZATION IN WERTZ DOME FIELD, WYOMING

E. A. SWEDENBORG, U. S. GEOLOGICAL SURVEY, CASPER, WYOMING

ABSTRACT

The unit agreement for the Wertz Dome field, Wyoming, was approved by the Acting Secretary of the United States Department of the Interior on November 4, 1937, effective on December 1, 1937. The stated objectives of the agreement are to conserve and put to beneficial use all oil and gas produced; to make possible a uniform withdrawal of oil and gas in order to maintain equalized reservoir pressures; to provide for an orderly determination of the structural features of the productive horizons; and to permit the injection of gas for pressure maintenance. The purpose of this paper is to show by a discussion of the problems involved and the engineering practices employed by the unit operator, how well the objectives of the unit agreement have been accomplished in the development and production of oil and gas from the field.

HISTORY AND DEVELOPMENT

The Wertz Dome oil and gas field is located 88 miles southwest of Casper and 38 miles north and westerly from Rawlins, Wyoming. It is served by a state secondary oiled road connecting with U. S. Highway No. 220 at Lamont, a distance of 3 miles from the field. It has been a producing field for 27 years,

first as an important producer of gas and more recently of oil.

The Producers and Refiners Corp. completed Well No. 1, NE $\frac{1}{4}$ SW $\frac{1}{4}$ sec. 7, T. 26 N., R. 89 W., the first productive well in the field, in September, 1921, in the Muddy sandstone of Upper Cretaceous age, at a depth of 3435 feet for an initial production of 42,000,000 cu. ft. of gas per day. In 1922 pipe lines were laid to Casper, Wyoming, for supplying fuel to the Standard of Indiana refinery, the adjoining town of Mills, and the Producers and Refiners Corp. pump station No. 6 in Mills; and to Parco (now Sinclair), Wyoming, for supplying that refinery with fuel. The gasoline content of the gas was extracted in an absorption plant located near the town of Mills. No compressors were used as the line pressure was sufficiently high to flow the gas through the absorbers. As high as 30,000,000 cu. ft. of gas per day were treated in the plant extracting 6000 gallons of gasoline. In September 1937, the pipe line was discontinued and the plant was dismantled at which time 61,000,000,000 cu. ft. of gas had been produced from the seven Muddy, Cloverly, and Sundance gas wells drilled in the field. Of this volume of gas 800,000,000 cu. ft. were produced from the Frontier formation, 34,200,000,000 cu. ft. from the Muddy sandstone, 24,000,000,000 cu. ft. from the Cloverly, locally called Dakota, and 2,000,000,000 cu. ft. from the Sundance formation. The pipe line was discontinued because of the near depletion of the gas reserves in Wertz and nearby fields, and because of the local

field requirements demanding the retention of the remaining gas reserves.

In December 1936, the Sinclair Wyoming Oil Co. completed Well No. 10, SE $\frac{1}{4}$ NW $\frac{1}{4}$ sec. 7, T. 26 N., R. 89 W., at a depth of 5886 feet, as the first Tensleep sand producer with an initial of 1700 barrels of oil per day. The well was originally drilled only 14 feet into the sand and in August 1939 was deepened to a depth of 6161 feet, 289 feet in the sand, and the daily production increased to 8350 barrels of oil. In February 1948 Well No. 22, SE $\frac{1}{4}$ SE $\frac{1}{4}$ sec. 1, T. 26 N., R. 90 W., was deepened from the Tensleep to the Basal Amsden sand and completed at a depth of 6635 feet for an initial of 600 barrels of oil per day in the Basal Amsden. In April 1948, Well No. 2, SW $\frac{1}{4}$ NE $\frac{1}{4}$ sec. 1, T. 26 N., R. 90 W., was deepened from the Tensleep to the Madison limestone and was completed at a depth of 7193 feet for an initial of 1145 barrels of oil per day in the Madison. Well No. 26, SE $\frac{1}{4}$ SE $\frac{1}{4}$ sec. 1, T. 26 N., R. 90 W., was deepened from the Tensleep to the Cambrian and in October 1948 it was completed in the Cambrian for an initial of 277 barrels of oil per day.

GEOLOGY AND PRODUCTIVE ACREAGE

The surface is Steele shale of Upper Cretaceous age, covered in part by gravel beds. The topography of the field is that of a rolling hill with a steep draw or gulch along the northern edge of the field. The Steele shale lies conformably on the lower formations as

Manuscript received at the Petroleum Branch Office January 20, 1949. Paper presented at AIME Annual Meeting in San Francisco, February 13-17, 1949.

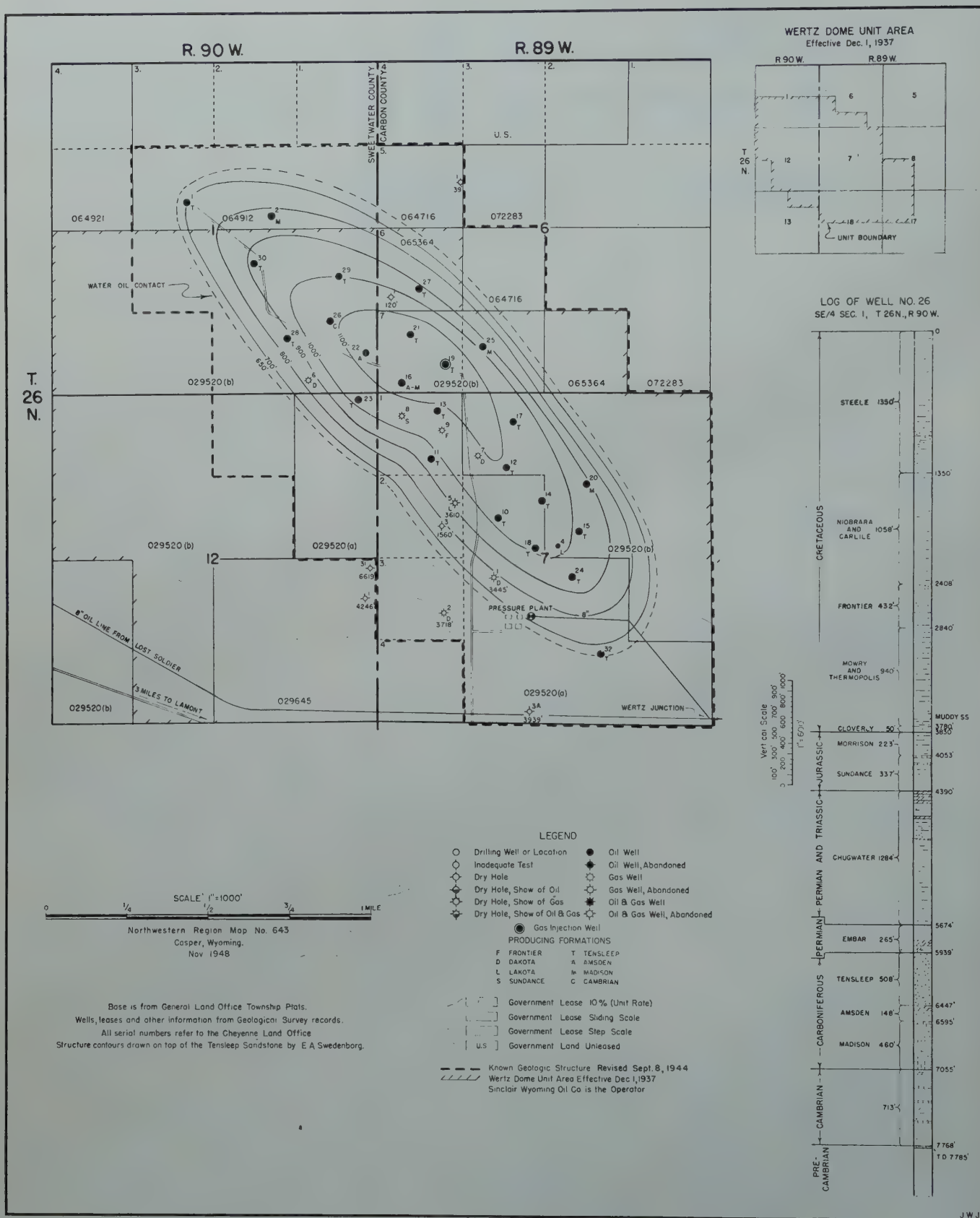


FIG. 3 — MAP OF WERTZ DOME, SWEETWATER AND CARBON COUNTIES, WYOMING.

TABLE I

Analysis of composite sample of gas produced with oil from Tensleep sandstone, Wertz Dome field, Wyoming:

	Per Cent by Volume
Oxygen	0
Nitrogen	4.09
Carbon dioxide	52.00
Hydrogen sulphide	1.11
Methane	26.80
Ethane	6.35
Propane	5.35
Iso Butane	0.79
Normal Butane	2.05
Iso Pentane	0.49
Normal Pentane	0.54
Hexane plus	0.43
Specific gravity by Pod:	1.241
Gross B.t.u. by Pod:	677

indicated on the log of Well No. 26, SE $\frac{1}{4}$ SE $\frac{1}{4}$ sec. 1, T. 26 N., R. 90 W., shown on the accompanying map. The structure is a sharply folded anticline, 3 miles long and 1 mile wide lying across the boundary between Carbon and Sweetwater counties, Wyoming in Township 26 N., Ranges 89 and 90 West.

There is no state or patented land within the productive area and all mineral rights are vested in the United States and operations are subject to the Federal oil and gas operating regulations. The Tensleep reservoir has a proven productive oil area of 650 acres. The Amsden, Madison, and Cambrian formations have not been sufficiently drilled to determine the limits of production but it is believed that they ex-

tend over acreages somewhat smaller than that of the Tensleep sandstone.

TENSLEEP SANDSTONE

The Tensleep sandstone thickness in four of the wells drilled through averages 450 feet, whereas in three of the wells wherein the sand was drilled through, it averages 540 feet. This fact along with similarity of crude oil, gas, and water found in the Tensleep, Amsden, Madison, and Cambrian formations indicates that at some time there may have been migration through faulting with respect to the above mentioned formations. See analyses of crudes from each formation. However there is no indication of faulting at the surface.

The Tensleep sandstone is found at depths ranging from 5800 feet on top of the structure to 6300 feet near the productive limits. The sand is hard and is composed of fine to medium grained sandstone streaked with dolomite. The fact that the sand is hard permits the cementing of casing on top of the sand leaving the well bore uncased through the sand section. No caving of sand has been experienced in any of the wells. The porosity of the sand varies from 3.3 to 18.9 per cent, averaging 14 per cent. The permeability ranges from 0 to 337 millidarcies with an average of 70 millidarcies. The connate water as determined by core analyses of cores taken from wells drilled, varies from a trace to 11 per cent, averaging 10 per cent for the oil saturated sand section.

DRILLING AND PRODUCTION

The drilling time of Tensleep sand wells has varied from three to five months depending on location of well on structure. The drilling of wells on the flanks of the structure required more time because weight on the drilling bit had to be reduced to keep the hole straight, and because of thickening of formations due to greater dip on flanks. The drilling was not done hurriedly since under the unit agreement there were no drilling requirements involving offset acreage which made possible an orderly determination of the structural features of the productive horizon. The market for the crude prior to 1941

TABLE II

Representative laboratory analysis of Tensleep oil, Wertz Dome field, Wyoming, by Casper laboratory of U. S. Geological Survey:

Per cent sulphur	1.33
API gravity	35.3
Pour point	Below 0°F.
Color	Greenish-brown

Distillation, Bureau of Mines, Hempel Method

Dry distillation; Barometer 635 mm.; First drop 26°C. (79°F.)

	Per cent cut	Sum per cent	Gravity of cut
Temperature			
Up to 122	2.8	2.8	89.6
122 to 167	3.3	6.1	82.2
167 to 212	4.0	10.1	71.5
212 to 257	5.0	15.1	62.6
257 to 302	4.9	20.0	55.7
302 to 347	6.2	26.2	51.1
347 to 392	5.6	31.8	46.0
392 to 437	5.2	37.0	43.4
437 to 482	6.1	43.1	39.6
482 to 527	7.0	50.1	36.2

Vacuum distillation at 40 mm.

Up to 392	2.4	52.5	32.3
392 to 437	6.6	59.1	30.6
437 to 482	6.0	65.1	27.9
482 to 527	5.2	70.3	25.6
527 to 572	5.9	76.2	23.0
Carbon residue of residuum:	9.5 per cent		
Carbon residue of crude:	2.6 per cent		

Approximate Summary

	Per cent	Gravity
Light gasoline	10.1	79.7
Total gasoline and naphtha	31.8	61.0
Kerosene distillate	5.2	43.4
Gas oil	20.9	35.4
Nonviscous lubricating distillate	10.8	
Medium lubricating distillate	6.3	
Viscous lubricating distillate	1.2	
Residuum	23.8	14.1
Distillation loss	0	

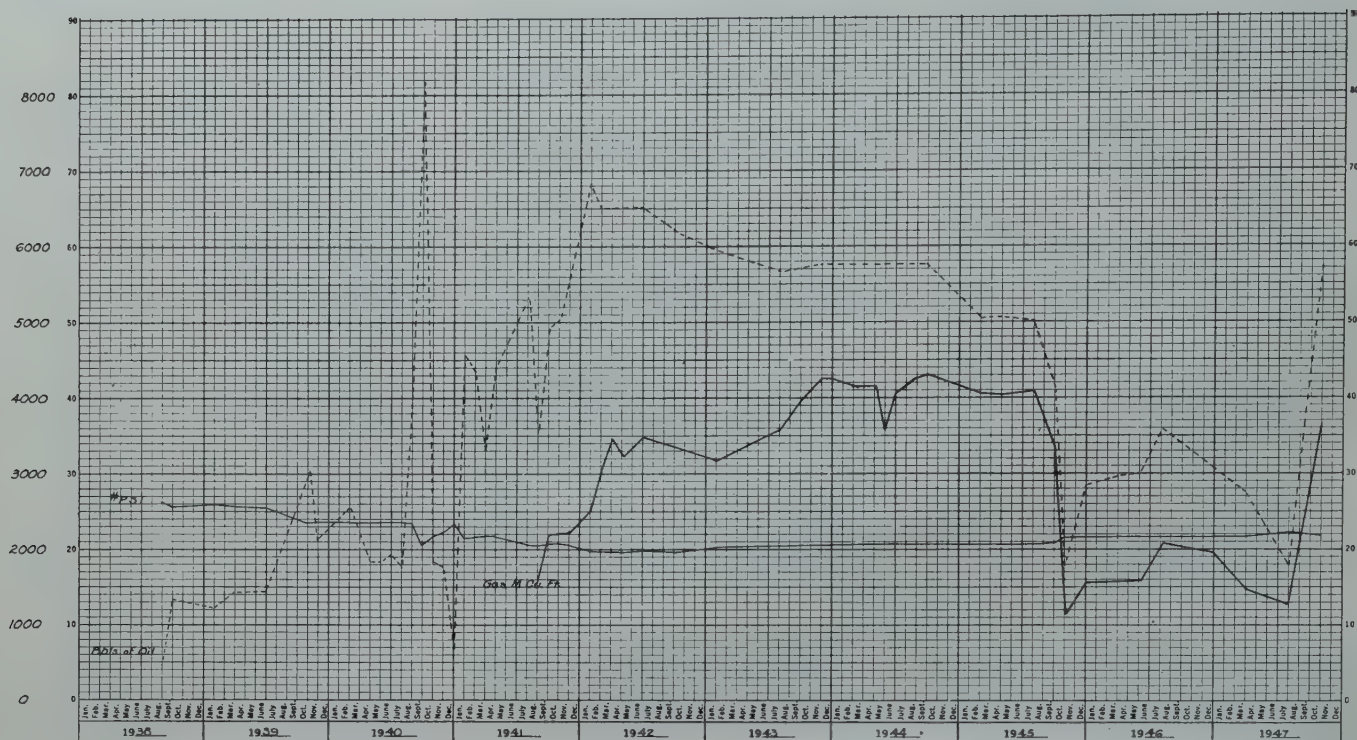


FIG. 1 — DAILY PRODUCTION, INJECTION AND B.H.P. IN THE WERTZ DOME TENSLEEP.

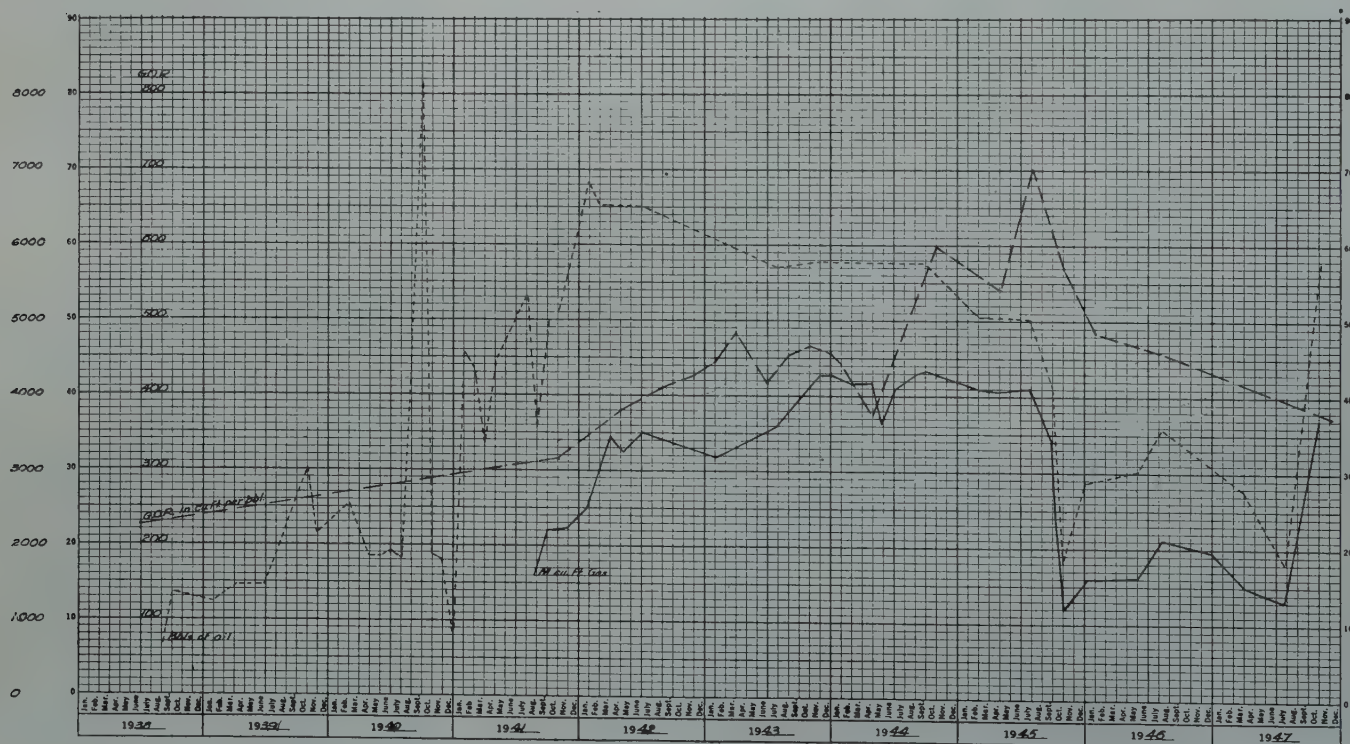


FIG. 2 — DAILY PRODUCTION, INJECTION AND G.O.R. IN THE WERTZ DOME TENSLEEP.

also restricted the development rate. One well was completed each year over the period of 1936 to 1940 inclusive. Ten wells were completed in 1941, five in 1942, and three in 1943. The continued demand for crude, prompted the testing of formations below the Tensleep sandstone in 1948 and upon finding oil in the Amsden, Madison and Cambrian formations, seven Tensleep wells were deepened. Six of the deepened wells were recompleted in the lower formations and one, an edge well, was plugged back and recompleted in the Tensleep after finding water in all formations below the Tensleep.

Twenty-five wells have been drilled

to the Tensleep; one was outside of the producing limits and one at the water oil contact. Twenty-four were producers ranging in productive capacities from 35 barrels of oil per day on the pump to 8350 barrels of oil flowing. Twenty wells were good flowing producers of oil whereas four wells along the northern flank were small producers and were pumped. The four pumping wells were the last drilled in the field and had small amounts of water with the oil, but did not flow because the bottom hole pressure of the reservoir had been reduced to or was approaching 2000 psi, which is the minimum pressure required for natural flow of oil for wells of their

depth considering the temperature and specific gravity of the crude produced.

It had become obvious by 1940, as the result of flowing production at various rates and observing drop in bottom hole pressures, that it would not be long before all the wells would be placed on artificial lift or, the producing rate drastically reduced to equal the rate of water encroachment in order to utilize hydrostatic pressure. The question of injecting the Tensleep gas produced with the oil was considered but in as much as the produced gas had a carbon dioxide content of 52 per cent and hydrogen sulphide content of 1.11 per cent, the problem of corrosion was a serious one in compressing the gas to pressures necessary for injection. (See analysis of gas.) The Sinclair Wyoming Oil Co., unit operator, decided on a method of dehydrating the gas to prevent corrosion rather than removal of the hydrogen sulphide and carbon dioxide. The decision has been proven sound as the corrosion of equipment in the compression of the dehydrated gas has not been serious over a period of 7½ years of operation. The dehydration method also avoided shrinkage of gas volume that would have resulted from the removal of corrosive components in the gas.

PRESSURE MAINTENANCE PLANT

Three Cooper-Bessemer 600 hp gas engine-compressor units boost the gas from an intake pressure of 30 pounds to a discharge pressure of 1825 pounds. The engines are of the six-cylinder, two cycle, angle type, with three compression cylinders each. The gas is boosted in three stages with the compressors operating in parallel through a common header system. In the first stage the pressure is boosted to 140 pounds, in the second to 485 pounds, and in the third and final stage to 1825 pounds. Check valves in the final stage discharge lines protect the plant should the final stage go out and permit the field pressures to back up in the gas return system.

Dehydration of the gas takes place between the first and second stages of compression, and is accomplished by

TABLE III

Representative laboratory analysis of Amsden oil, Wertz Dome field, Wyoming, by Casper laboratory of U. S. Geological Survey:

Per cent sulphur	0.36
API gravity	35.4
Pour point	Below 5°F.
Color	Greenish-brown

Distillation, Bureau of Mines, Hempel Method

Dry distillation; Barometer 636 mm.; First drop 29°C. (84°F.)

	Per cent cut	Sum per cent	Gravity of cut
Temperature Up to 122	2.8	2.8	89.6
122 to 167	3.4	6.2	81.9
167 to 212	4.2	10.4	70.9
212 to 257	5.0	15.4	62.6
257 to 302	5.4	20.8	55.2
302 to 347	6.1	26.9	50.6
347 to 392	4.8	31.7	46.7
392 to 437	5.4	37.1	43.2
437 to 482	6.0	43.1	39.6
482 to 527	7.4	50.5	35.8

Vacuum distillation at 40 mm.

Up to 392	2.3	52.8	32.5
392 to 437	6.2	59.0	31.0
437 to 482	5.7	64.7	28.2
482 to 527	5.9	70.6	25.4
527 to 572	5.8	76.4	23.2
Carbon residue of residuum:	9.6 per cent		
Carbon residue of crude:	2.57 per cent		

Approximate Summary

	Per cent	Gravity
Light gasoline	10.4	79.4
Total gasoline and naphtha	31.7	61.3
Kerosene distillate	5.4	43.2
Gas oil	20.6	35.4
Nonviscous lubricating distillate	10.9	30.6-25.0
Medium lubricating distillate	6.2	25.0-22.5
Viscous lubricating distillate	1.6	22.5-21.8
Residuum	23.4	14.1
Distillation loss	0.2	

passing the gas through a column containing one flourite and three activated alumina beds. There are two of these columns operating in alternate 24-hour periods, one being reactivated while the other is in use. The columns are reactivated by cycling preheated gas through them to take up the water vapor from the beds, and then cooling the gas and collecting the resulting condensate in a receiving tank for removal from the system. Gas in the system is dehydrated to a dew point of 14°F. below zero at the discharge pressure of 1825 pounds.

The plant is semi-automatic, and ordinarily only one man is needed on each shift. An electrically operated emergency shut down system has been provided. Switches have been placed at three convenient points in the plant and yard and pulling any one of these cuts off the fuel to the boiler, quenches the boiler fire boxes with steam, shorts the magnetos on the engine, shuts off the incoming gas and turns all production through the separators direct to storage instead of through the plant. Man power requirements for the operation of the plant are at a minimum. Because of severe cold weather during the winter months, all equipment is enclosed in steel buildings which are heated by exhaust steam from the turbines which drive the electric generators thereby maintaining a uniform temperature in the buildings.

Production of both oil and gas is delivered directly to the plant. The crude oil is passed through two banks of oil to oil heat exchangers and a steam heater to a flash tower for stabilization of the crude. The crude stream from the flash tower is cooled, first in the heat exchangers with the incoming cold crude and then in a final water to oil cooler from which it goes to storage. Approximately 70 per cent of the gas produced with the oil is taken off at the oil and gas separators. The remaining gas is vented from the flash tower in the stabilization of the crude and is delivered with the gas from the separators to the intake of the low stage compressors. This method of delivering the oil and gas direct to the plant from the wells for stabilization prevents any loss of oil vapors by evaporation. In reality

the gravity of the oil is increased in the stabilization process. The light gasoline fractions obtained in the compression of produced gas to injection pressures are added to the oil stream as it goes to the tanks for pipe line shipment.

PRODUCTION AND PRESSURE MAINTENANCE

Production schedules have been restricted at rates below 6000 barrels per day since 1942. During the years 1943, 1944 and 1945 the average daily rate was approximately 5500 barrels and during 1946 and 1947 the daily rate averaged 3000 barrels. In 1948 the rate

was again increased to approximately 5500 barrels per day.

Until gas injection into the Tensleep sandstone was started, a free gas cap was not present in the reservoir. The oil was under-saturated with gas. The original gas-oil ratio was 210 cu. ft. per barrel of oil. Since gas has been returned to the formation the gas-oil ratio has fluctuated depending on injection volumes, producing rates and shutting in of wells high on structure. See graph, Fig. 2. By progressive control in high-structure wells as their respective ratios increased, the average gas-oil ratio has been held within reasonable limits, thus

TABLE IV

Representative laboratory analysis of Madison oil, Wertz Dome field, Wyoming, by Casper laboratory of U. S. Geological Survey:

Per cent sulphur	1.28
API gravity	35.2
Pour point	Below 0°F.
Color	Greenish-brown

Distillation, Bureau of Mines, Hempel Method

Dry distillation; Barometer 635 mm.; First drop 27°C. (81°F.)

	Per cent cut	Sum per cent	Gravity of cut
Temperature			
Up to 122	2.7	2.7	88.9
122 to 167	3.3	6.0	81.9
167 to 212	4.0	10.0	70.9
212 to 257	5.2	15.2	62.6
257 to 302	4.6	19.8	55.7
302 to 347	6.2	26.0	50.0
347 to 392	4.9	30.9	46.9
392 to 437	5.3	36.2	43.4
437 to 482	5.8	42.0	39.8
482 to 527	7.3	49.3	36.0

Vacuum distillation at 40 mm.

Up to 392	1.9	51.2	32.3
392 to 437	6.6	57.8	30.8
437 to 482	6.5	64.3	28.0
482 to 527	5.7	70.0	25.6
527 to 572	6.6	76.6	22.8
Carbon residue of residuum:	10.1 per cent		
Carbon residue of crude:	2.7 per cent		

Approximate Summary

	Per cent	Gravity
Light gasoline	10.0	79.1
Total gasoline and naphtha	30.9	61.3
Kerosene distillate	5.3	43.4
Gas oil	20.5	35.4
Nonviscous lubricating distillate	11.4	29.8-25.0
Medium lubricating distillate	7.0	25.0-22.0
Viscous lubricating distillate	1.5	22.0-21.3
Residuum	23.3	13.3
Distillation loss	0.1	

TABLE V

Representative laboratory analysis of Cambrian oil, Wertz Dome field, Wyoming, by Sinclair Refinery, Sinclair, Wyoming:

			1600 cc Distillation:		
			Temperature		% Evaporated
			Sea Level	Sinclair	
			140	129	2.13
			160	148	3.44
			180	168	5.18
			200	187	6.94
			220	207	9.06
Gravity	36.1		240	227	11.00
Sulphur	1.39		260	246	12.9
			280	266	14.4
Over to 330	19.9	66.3	300	286	16.9
330 to 400	10.0	50.6	320	305	18.7
400 to 520	15.3	41.3	330	315	19.9
520 to Off	13.6	33.3	340	325	21.3
			360	344	24.6
<i>Tests on Bottoms:</i>			380	364	27.3
			400	383	29.9
Gravity	19.0		420	403	32.2
Visc. @ 210 S.U.	.70		440	423	34.7
Sulphur	2.33		460	442	37.3
			480	462	39.8
			500	482	42.3
			520	502	45.2
			540	521	47.5
			560	541	50.0
			580	560	53.0
			620	600	58.8

avoiding the necessity of handling excessive volumes of gas.

The volume of gas produced from the Tensleep formation is not sufficient to maintain desired formation pressure, consequently gas from the Cloverly and Sundance sand wells is used to make up any deficiency in volume needed to maintain volumetric balance in the reservoir.

Gas injection was started in July 1941 and has been continued since then. As of December 31, 1947, 7,043,000,000 cu. ft. of gas have been injected into the Tensleep sandstone. Of this, 4,668,800,000 cu. ft. were gas produced with the oil and reinjected and 2,374,800,000 cu. ft. make up gas produced from sands above the Tensleep sandstone. It is estimated that there are 5,442,800,000 cu. ft. of gas in the gas cap on top of the structure as of December 31, 1948. Although 7,043,600,000 cu. ft. have been injected, 1,600,800,000 cu. ft. of that volume is gas that has been recycled in the process of production and reinjection. Average pressure at this time is 2140 pounds, which is 190 pounds over the low of 1950 in 1942. See graph,

TABLE VII

Tensleep Sandstone Production by Wells and by Years

Well No.	Location	Completion Date	1937-38	1939	1940	1941	1942	1943	1944	1945	1946	1947	1948	Total Bbls. Oil
10(a)	NW sec 7	12-20-36	232238	295127	238098	202976	165500	189408	232854	179122	105577	133557	134062	2,018,519
11(a)	NW sec 7	11-21-37	126602	143343	194154	191452	175399	221399	210668	168342	103562	116709	193093	1,844,306
12-B	NW sec 7	4-4-38	101527	163826	209121	202061	175401	142088	134568	60738	28768	49697	89991	1,357,786
13-a	NW sec 7	7-24-39		158559	220808	192314	121486	46153	39074	26549	25206	21713	8937	860,799
14	NW sec 7	8-10-40			166419	202746	175408	163403	127598	88828	94833	108733	111995	1,239,963
15	SE sec 7	2-11-41				155120	175414	120818	99429	150833	94363	71598	75391	942,966
16	SW sec 6	1-15-41				164537	121500				5180	9937	1400	302,554
17	NW sec 7	5-8-41				117587	175440	121958	75116	43093	54607	56861	41580	686,222
18	NW sec 7	4-3-41				204489	175441	234953	23657	57194	4328	66264	164778	1,144,026
19	SW sec 6	5-13-41				31653								31,653
20	NE sec 7	7-24-41				64534				600	6653	7470	2095	81,352
21	SW sec 6	9-15-41				52858	144105	22034	257					219,254
22	SE sec 1	8-7-41				64411	175527	80672	26148	21117	14920	10150		392,945
23	NE sec 12	8-23-41				59905	175532	196807	162000	153687	122946	124710	211037	1,206,624
24	SE sec 7	4-17-42					118811	115922	140122	108188	104888	92284	160216	841,431
25	SW sec 6	1-25-42					674	17571	14150	23968	8780	12362	5016	82,521
26	SE sec 1	12-16-41				640	162144	108408	123380	95669	47383	32118	16932	586,674
27	SW sec 6	3-12-42					20669	68454	90100	81653	75019	63023	82500	481,418
28	SE sec 1	12-17-42					7114	155118	180703	136789	107526	125161	185999	898,410
29	SE sec 1	10-20-42					8211	18338	28564	21952	43339	28045	50512	198,961
30	SE sec 1	8-19-42					42724	58905	98774	84584	81158	91352	166369	623,866
32	SE sec 7	8-28-43								0			1522	1,531
1*	NW sec 1	4-4-43						3271	14631	16551	16236	13975	14327	78,991
2*	NE sec 1	11-15-46										2657		2,657
Total			460367	760755	1028600	1907263	2316500	2085363	2034715	1519466	1145272	1239376	1717752	16,215,429

*Outside unit area.

Fig. 1. Production prior to the starting of gas injection in July 1941 totaled approximately 3,400,000 barrels of oil. Original reservoir pressure was estimated at 2600 lbs. psi. By the time pressure maintenance was started the pressure had dropped to 2040 pounds, a drop of 560 pounds. As a result of pressure maintenance and restricting producing rates the reservoir pressure as of December 31, 1947, was 2134 pounds with a total oil production as of that date of 14,410,260 barrels. A total of 11,010,260 barrels of oil has been produced since July 1941 when gas injection was started up to December 31, 1947. During the period, the reservoir pressures increased approximately 100 lbs. psi whereas before the pressure maintenance program was started, only 3,400,000 barrels were produced, with a reservoir drop of 560 lbs. psi.

Two injection wells were used for a time but at present only one well is used. The original well is located on top of the structure, while the second well, now discontinued, is located about 250 feet down structure. The down structure injection of gas was somewhat of a departure from general practice in the early history of a pressure maintenance program. It was thought that by down structure injection, gas would have an opportunity to saturate the under-saturated oil with gas in its movement up structure, and in so doing reduce the viscosity of the oil and stimulate its movement to producing wells. However, it was found that eventually the gas injected in the down structure well channelled to adjoining wells and its use was discontinued. The volume of gas injected has been guided by the rate of oil withdrawal. It is calculated that 3000 barrels of water per day move up structure to replace oil withdrawn at a reservoir pressure differential of 460 lbs. psi. This calculation is based not only on graph, Fig. 1, but also on a volumetric balance of fluids produced as against fluids in place in the reservoir. The water head is equivalent to 2600 lbs. psi as indicated by reservoir pressure prior to oil withdrawal. Therefore, when oil is produced at a rate in excess of 3000 barrels per day, an equivalent volume replacement in the reservoir

TABLE VI
Representative analysis of Tensleep sandstone water, Wertz Dome field, Wyoming, by Casper laboratory of U. S. Geological Survey:

	Parts per million	Reacting value	Value in per cent
Sodium and Potassium (calculated as Sodium)	2456	106.82	40.35
Calcium (Cal)	433	21.61	8.16
Magnesium (Mg)	48	3.95	1.49
Sulphate (SO ₄)	3838	79.83	30.15
Chloride (Cl)	1302	36.72	13.87
Bicarbonate (HCO ₃)	965	15.83	5.98

Total solids in
parts per million

By evaporation	8400
After ignition	8260
Calculated	8552

Properties of reaction in per cent

Primary salinity	80.70%
Secondary salinity	7.34%
Primary alkalinity	0.00%
Secondary alkalinity	11.96%
Chloride salinity	31.51%
Sulphate salinity	68.49%

has to be made by gas injection in order to stabilize the reservoir pressure some where near 2140 lbs. psi. (See graph, Fig. 1). It has been stated previously in this paper that a minimum of 2000 lbs. psi reservoir pressure is required to maintain flow of the wells in the field. It is therefore important that the reservoir pressure be maintained at some pressure in excess of 2000 lbs. psi. It is estimated that 1200 cu. ft. of gas is required to replace one barrel of oil under reservoir conditions. This estimate is based on bottom hole samples and field tests made by the unit operator.

The success of the gas injection program in the Wertz Dome field is attributable to the maintenance of a volumetric balance between oil withdrawal, gas injection and edgewater encroachment at a reservoir pressure that will support the flowing of production and yet utilize some energy of the hydrostatic head. Maximum recovery will not only be realized as a result of the maintenance of such a program, but it will make possible a depletion of the oil in the reservoir at a much shorter period of time than would be ordinarily required, and at considerably less cost.

The unit operator is employing practices that are beneficial to the participants in the unit agreement. Everything is being done to promote economical and efficient development of the field,

and to insure efficient recovery of the unitized substances to the end that the maximum ultimate yield may be obtained without waste. The benefits of unitization with respect to operations in the Wertz Dome field may be summarized as follows:

1. Realization of maximum economical recovery of oil.
2. The gas produced with the oil has been conserved and utilized in spite of its character. Ordinarily it would have been largely wasted if not used in pressure maintenance of the reservoir.
3. Elimination of offset wells resulting in wells being advantageously located on structure.
4. Retention of the wells in a flowing status by maintaining a reservoir balance.
5. Provides a fair distribution of revenue from oil produced to the parties entitled to share in it.

ACKNOWLEDGMENT

The writer wishes to acknowledge the assistance and helpful suggestions of Supervisor J. R. Schwabrow and the engineers and draftsman in the Northwestern Regional Office, Oil and Gas Leasing Branch, Conservation Division, United States Geological Survey; and F. H. Rhees, Division Superintendent, and other personnel of the Sinclair Wyoming Oil Co. ★ ★ ★

RESERVOIR PERFORMANCE OF A HIGH RELIEF POOL

E. P. BURTCHAELL, MEMBER AIME, HONOLULU OIL CORP., SAN FRANCISCO, CALIF.

ABSTRACT

A method is presented for evaluating the effect of gravity drive upon the reservoir performance of a high relief pool. Conventional forms of reservoir analysis do not consider the alterations in the basic material balance data caused by gravity segregation of reservoir fluids. A procedure is outlined for structurally weighting physical and chemical data for use in the material balance equation. It is demonstrated how actual pool performance data can be utilized to evaluate the future reservoir performance of a gravity drive pool.

INTRODUCTION

Conventional reservoir engineering procedure is inadequate for the analysis of an oil pool which has considerable structural relief, steep dips, and good permeability development. In pools of this type, gravity drainage has an important part in the movement of oil to the wells and the effects of gravity on the overall pool performance should be included in any analysis of reservoir behavior. Many engineers have the opinion that the force of gravity in the movement of oil is not important until the later life of a pool.¹ Probably the basis for this belief is that gravitational effects may not be readily discernible until a pool is nearing depletion. This would be especially true for pools not having a high degree of structural relief and permeability development. Actually the effects of gravitational forces are at a maximum when the pool pressure is high, for during this period the hydrostatic head of the oil column is at a maximum and the viscosity of the oil is at a minimum.

Oil recoveries from pools having favorable gravity drive characteristics may equal or even exceed recoveries which might be expected from water displacement. Field evidence indicates that in some reservoirs gravity drive has resulted in recoveries greater than that which could have been expected from gas expansion or water drive.^{2,3} Unfortunately, the possible effects of gravity drive on pool performance have been underestimated and other reasons have been sought to explain the high recoveries obtained. There are unquestionably many reservoirs to which the principles of gravity drainage can be effectively applied.

It is the purpose of this paper to illustrate one method whereby gravity drive is included in the reservoir analysis

of an oil pool. A hypothetical pool, typical of many California reservoirs, is used as an example. As used in this paper, "gravity drive" is defined as the overall effect of gravitational influences on the recovery of petroleum from the reservoir; "gravitational segregation" as the gravity separation of oil and gas within the reservoir; and "gravity drainage" as the downward movement of oil as caused by the force of gravity.

SAND VOLUME DATA

Fig. 1 presents a structural contour map of the pool under study. Maximum closure is 1950 feet with dips on the south flank approaching 45°. The original gas-oil interface was set at -5200 feet. Average thickness of the producing sand was 200 feet.

For use in subsequent calculations in this paper, the pool was subdivided into 100-foot vertical increments and the sand-volume content of each increment was obtained. If the gross sand thickness is small, under 100 feet, the sand-volume content can be obtained by superimposing an isopachous map upon a structural contour map and planimetry the average thickness of each 100-foot increment. For sand thicknesses over 100 feet, one approach would be to construct a sufficient number of cross-sections of the pool from which the weighted sand-volume of each 100-foot increment could be obtained. Variations in the sand body with depth, as determined by core data, can also be included in the above process.

Table I presents a summary of sand-volume calculations, core data, and the original distribution of reservoir hydrocarbons in the pool. Fig. 2 illustrates the structural distribution of the sand-volume content. A total of 171,398 acre-feet is contained within the productive limits of the pool. Assuming an average porosity of 25% and an interstitial water content of 20%, the original hydrocarbon content was computed to be 227,075,000 barrels.

DEPTH-PRESSURE DATA

The determination of the initial vertical pressure arrangement in the pool is necessary for PVT and material balance calculations. Whenever sufficient data are available, a plot of pressure versus subsea depth of measurement should be made. From this plot a representative fluid pressure gradient can be established. Lacking sufficient initial pressure data, an initial pressure gradient may be estimated or calculated from available PVT data.

Manuscript received at Petroleum Branch Office September 3, 1948. Paper presented at Branch Fall Meeting in Los Angeles October 14, 1948.

¹ References are given at end of paper.

TABLE I
Summary of Sand Volume and Reservoir Oil Content

Interval	Acre-Feet	Cumulative Acre-Feet	Reservoir Oil	Cumulative Reservoir Oil
—5000 to —5100.....	13,615	13,615	Gas	Gas
—5100 to —5200.....	11,434	25,049	Gas	Gas
—5200 to —5300.....	7,478	32,527	11,602,865	11,602,865 bbls.
—5300 to —5400.....	6,635	39,162	10,294,866	21,897,731
—5400 to —5500.....	6,899	46,061	10,704,488	32,602,219
—5500 to —5600.....	6,991	53,052	10,847,236	43,449,455
—5600 to —5700.....	7,245	60,297	11,241,342	54,690,797
—5700 to —5800.....	7,245	67,542	11,241,342	65,932,139
—5800 to —5900.....	7,752	75,294	12,028,003	77,960,142
—5900 to —6000.....	7,752	83,046	12,028,003	89,988,145
—6000 to —6100.....	8,006	91,052	12,422,110	102,410,255
—6100 to —6200.....	8,260	99,312	12,816,216	115,226,471
—6100 to —6300.....	8,260	107,572	12,816,216	128,042,687
—6300 to —6400.....	8,767	116,339	13,602,877	141,645,564
—6400 to —6500.....	9,021	125,360	13,996,984	155,642,548
—6500 to —6600.....	9,528	134,888	14,783,645	170,426,193
—6600 to —6700.....	9,782	144,670	15,177,751	185,603,944
—6700 to —6800.....	10,289	154,959	15,964,412	201,568,356
—6800 to —6900.....	10,543	165,502	16,358,519	217,926,875
—6900 to —6950.....	5,896	171,398	9,148,234	227,075,109

Core Data
Porosity = 25%
Interstitial Water = 20%
Hydrocarbon Content = 1,551.6 Bbls. per Acre-Feet
Average Sand Thickness = 200 feet

TABLE III
Structural Weighting of PVT Data
Example for Datum Plane Pressure of 2660 p.s.i.a.

Interval	Reservoir Oil	Pressure	FVF	FVF x Res. O.	GORs	GORs x Res. O.
5200—5300.....	11,602,865	2,375	1.268	14,712	448	5,198
5300—5400.....	10,294,866	2,405	1.271	13,085	453	4,664
5400—5500.....	10,704,488	2,435	1.274	13,638	458	4,903
5500—5600.....	10,847,236	2,465	1.277	13,852	463	5,022
5600—5700.....	11,241,342	2,495	1.280	14,389	468	5,261
5700—5800.....	11,241,342	2,525	1.282	14,411	467	5,250
5800—5900.....	12,028,003	2,555	1.279	15,384	461	5,545
5900—6000.....	12,028,003	2,585	1.277	15,360	455	5,473
6000—6100.....	12,422,110	2,615	1.274	15,826	449	5,577
6100—6200.....	12,816,216	2,645	1.271	16,289	443	5,677
6200—6300.....	12,816,216	2,675	1.267	16,238	437	5,801
6300—6400.....	13,602,877	2,705	1.264	17,194	431	5,863
6400—6500.....	13,996,984	2,735	1.262	17,664	425	5,949
6500—6600.....	14,783,645	2,765	1.259	18,613	419	6,194
6600—6700.....	15,177,751	2,795	1.256	19,063	413	6,268
6700—6800.....	15,964,412	2,825	1.253	20,003	407	6,497
6800—6900.....	16,358,519	2,855	1.250	20,448	401	6,560
6900—6950.....	9,148,234	2,870	1.248	11,417	398	3,641
Total or Weighted.....	227,075,109	2,660	1.2665	287,586	437	99,143

Reservoir Oil = Subsurface barrels (Table I)
Pressure = Midpoint of interval, psia (Fig. 3)
FVF = Oil phase formation volume factor (Fig. 4)
GORs = Solution gas-oil ratio, cu. ft. per bbl. (Fig. 5)

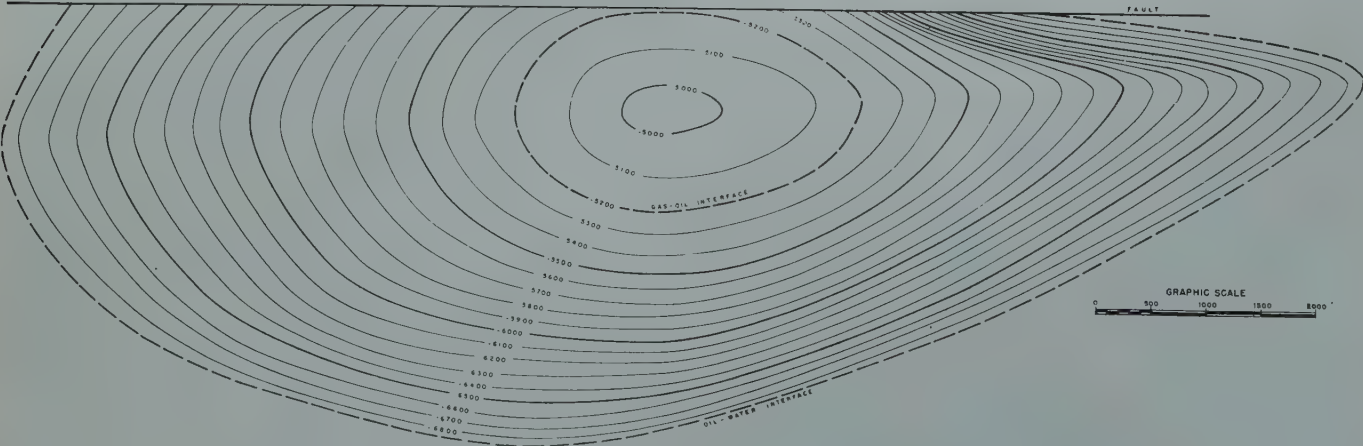


FIG. 1 — REPRESENTATIVE HIGH RELIEF OIL FIELD — CONTOURS ON TOP OF PAY.

The problem of establishing a standard pressure datum plane becomes exceedingly complex for high relief pools. Theoretically, the correct pool pressure at any given time is that pool pressure which represents the fluid mass within the producing reservoir. Initially this pressure would be the pressure at the volumetric mid-point of the reservoir. Oil and gas production from the pool, and the occurrence of gravity drainage in the pool causes a rearrangement of the structural distribution of the reservoir fluids. The continual downward migration of oil would necessitate a continual shifting of the pressure datum plane if a correct expression of pool pressure is to be maintained. Obviously the mechanics of determining the correct pressure datum position at succeeding time intervals would require the use of questionable assumptions as to fluid distribution in the reservoir. Secondly, most material

TABLE II

Calculated Composition of Well Effluent

	Mol Per Cent
Methane	43.3
Ethane	5.0
Propane	4.3
Iso-Butane	2.2
N-Butane	1.1
Iso-Pentane	1.2
N-Pentane	1.2
Hexanes, plus	41.7
	<hr/> 100.00

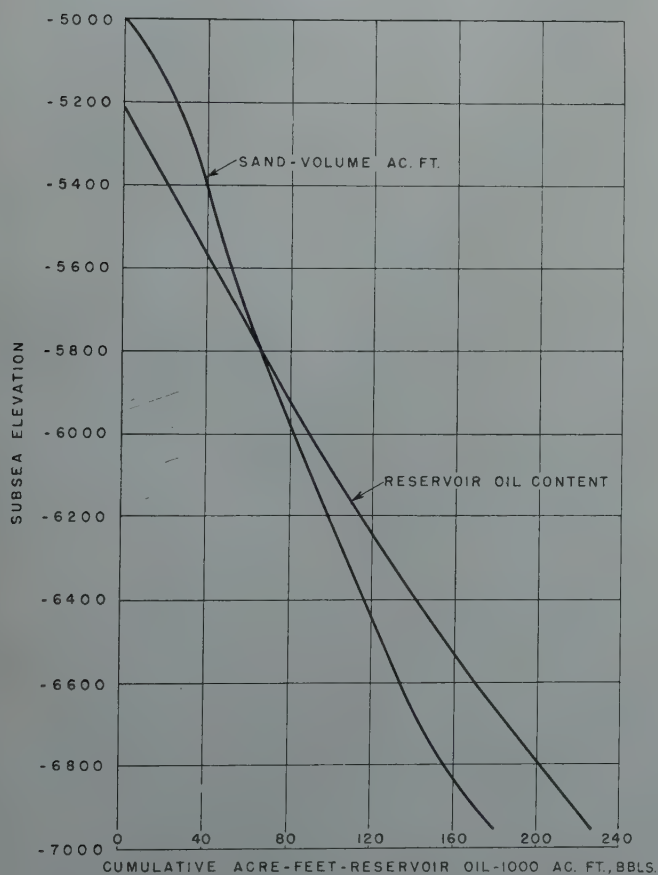


FIG. 2 — STRUCTURAL DISTRIBUTION OF SAND CONTENT.

balance data are dependent upon pressure and/or temperature. Changing the pressure datum position would require the continual alteration of basic PVT data which, from a practical standpoint, could nullify the value of the benefits to be gained.

The correction of well pressures to datum pressure in high relief pools requires an accurate determination of the fluid pressure gradient. In many cases it is necessary to correct pressures as much as 1,000 feet involving the addition or subtraction of 200 to 300 pounds to the bottom hole pressure. Through the application of conventional PVT calculations, it is possible to calculate the fluid density at any position on the structure and to predict the change in the density with pressure decline. However, before these refinements could be applied to pressure data, it would be necessary to know the reservoir fluid distribution surrounding each well. The difficulties to be overcome in determining fluid distribution nullify the value of the refinement. The use of a constant gradient correction factor is simple in application and accurately illustrates pressure differences between wells and surveys.

Therefore, it is believed that the most useable and reliable pressure data can be obtained by correcting bottom hole well pressures to a constant datum plane by the use of a constant fluid gradient correction factor. Weighted pool average pressures can be determined on an areal basis or a volumetric basis, as desired. Basic material balance and PVT

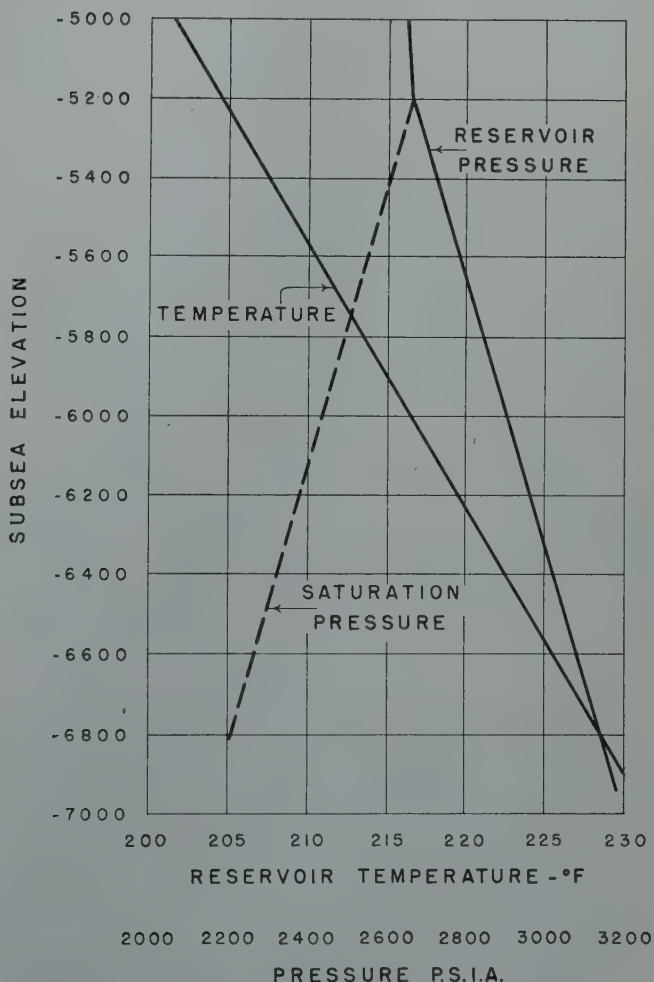


FIG. 3 — DISTRIBUTION OF PRESSURE AND TEMPERATURE.

data can be corrected to the same pressure base, allowing for rapid and straightforward performance calculations. Subsequent calculations in this paper will indicate how the small errors caused by the use of a constant pressure datum and pressure gradient are compensated.

PVT DATA

Pronounced pressure and temperature differences between the crest and flank of the reservoir due to high structural relief require a correction of all PVT data for structural location. If bottom-hole fluid samples are to be used, it is necessary to analyze the samples in the laboratory at two or more different

temperatures so that the proper temperature corrections can be made. To illustrate the magnitude of temperature and pressure variations, Fig. 3 is presented, in which it is seen that for the pool under study, temperatures ranged from 201°F. to 231°F. and pressures from 2600 to 3200 pounds.

For thin sand reservoirs of low relief it is commonly accepted that the determined bubble point pressure will be constant for all locations in the pool. Also if the pool contains an initial gas cap, it is automatically assumed to have been initially gas saturated. For thick sand and/or high relief pools, the above conditions usually are not found. In pools of this type, the bubble point pressure may follow one of three forms:

TABLE IV
Influence of Reservoir Pressure Upon Reservoir Gas Composition

	Mol Per Cent at				
	2800 psia	2500 psia	2000 psia	1500 psia	1000 psia
Methane.....	87.70	87.85	87.22	85.92	83.54
Ethane.....	5.07	5.24	5.55	6.21	7.15
Propane.....	2.57	2.63	2.79	3.10	3.93
Iso-Butane.....	1.07	1.08	1.15	1.27	1.49
N-Butane.....	0.43	0.44	0.46	0.50	0.60
Iso-Pentane.....	0.39	0.39	0.41	0.45	0.52
N-Pentane.....	0.33	0.33	0.34	0.38	0.44
Hexanes Plus.....	2.44	2.04	2.08	2.17	2.33
	100.00	100.00	100.00	100.00	100.00

Temperature=220° F.
Molecular Wt. Hexanes plus=120.

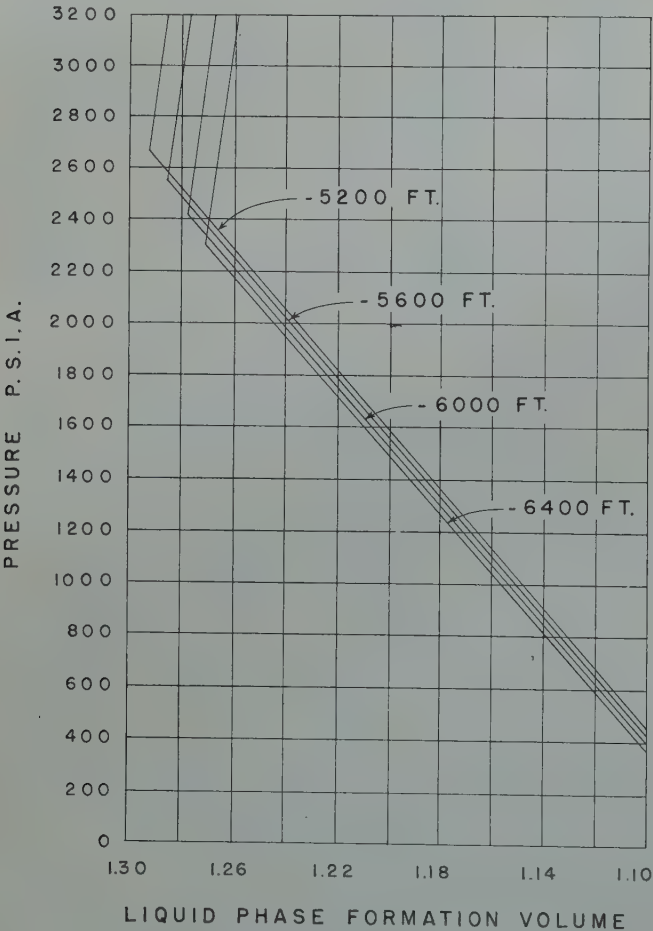


FIG. 4—OIL SHRINKAGE.

TABLE V
Summary of Relative Volume Factor of Oil and Original Solution Gas — u

Pressure	Weighted For Structure	Weighted For Field Performance
2960	1.0000	1.0000
2860	1.0018	1.0017
2760	1.0041	1.0041
2660	1.0068	1.0066
2460	1.0162	1.0159
2260	1.0338	1.0325
2060	1.0633	1.0568
1660	1.1787	1.1390
1400	1.2950	1.2270
1000	1.6270	1.4620
800	1.9470	1.6820
600	2.4100	1.9780

Pressure=p.s.i.a. at -6135 ft. datum.

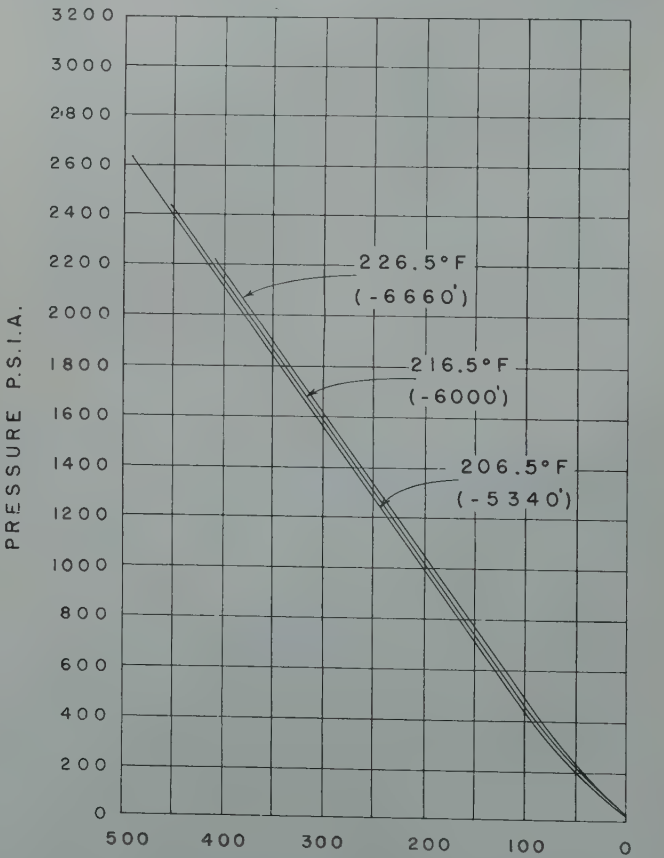


FIG. 5—SOLUBILITY DATA.

1. The bubble point pressure at any structural position is equal to initial pressure existing at that depth. Pools of this type can be classified as completely gas saturated.

2. The bubble point pressure is equal to the existing pressure at one point on the structure. Pools of this type can be classified as both gas saturated and undersaturated, as it is conceivable to have the bubble point pressure equal to the initial pressure existing at some point below the crest of the structure, in which case all elevations about this point would be gas saturated and all points below would be undersaturated.

3. The bubble point pressure would decrease with depth. Pools of this type can also be classified as either gas saturated or undersaturated, depending upon the structural location of the maximum saturation pressure.

Experience to date indicates that the majority of high relief pools are of Type 2 or exhibit a constant bubble point pressure regardless of depth.⁶ If free gas exists in the pool in the form of a gas cap, the oil at the gas-oil interface would be gas saturated but due to the degree of structural relief present, the oil below the interface would be undersaturated. This condition has been observed in several fields in California and may be explained by secondary movement of the structure after the oil was in place. This condition plus the existence of a tilted water table would indicate that complete reservoir equilibrium had not been attained at the time of discovery of the pool.

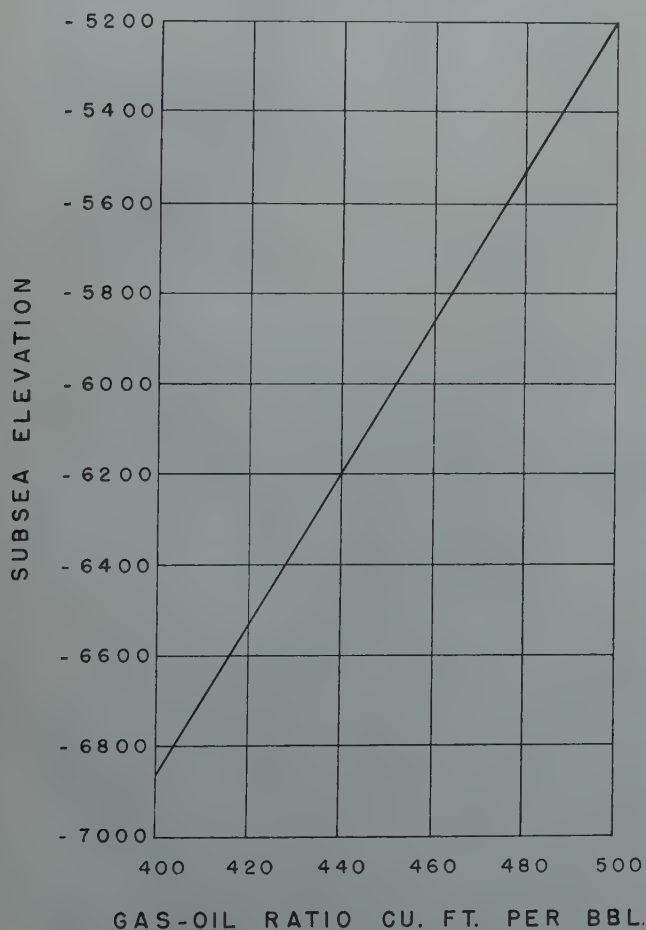


FIG. 6—GAS-OIL RATIO VS. DEPTH.

There are field data⁶ and analytical calculations⁷ indicating the existence of Type 3 pools in California. The presence of a decreasing bubble point pressure with depth is evidenced by a decrease in produced gas-oil ratio with depth. Usually oil gravities will be lower on the flank wells.

Conventional procedure can be followed for performance calculations on Type 1 and Type 2 pools, once the bubble point pressure has been established. Calculations on Type 3 pools are more involved because of the variations in saturation conditions. The pool example of this paper was assumed to be of Type 3 characteristics with a bubble point pressure distribution as illustrated by Fig. 3. As shown by Fig. 3, the bubble point pressure decreases from 2660 psia at the gas-oil contact of -5200 feet to 2160 psia at the water-oil contact of -6950 feet.

To determine the effect of structural relief upon the PVT data, a representative vertical distribution of oil and gas samples should be obtained. Lacking this type of information, initial well gas-oil ratios and oil gravities may be correlated by the Standing⁴ method to obtain bubble point pressures.

In Table II is presented the hydrocarbon analysis of the well stream effluent as calculated from a recombination of surface oil and gas samples. In Figs. 4 and 5 are presented oil shrinkage and solubility data for the pool under study. Fig. 6, gas-oil ratio versus depth, and Fig. 7, bubble point formation volume versus gas-oil ratio, are calculated from the data of Figs. 4 and 5. Fig. 8 presents oil and gas relative volume data as referred to bubble point oil, also plotted for various structural depths.

Before the above data can be readily applied in pool calculations it is necessary, for each item, to combine the variations due to structural depth into one composite curve which will represent the entire pool behavior. This procedure eliminates the cumbersome and intricate task of performing balance calculations on each vertical 100-foot block and will give results within the accuracy of the basic data. One method of calculating weighted PVT curves is illustrated in Table III in which the structural distribution of reservoir oil, as presented in Table I, is used as the basis of weighting the individual component curves.

Fig. 9 presents the resultant weighted pool shrinkage and solubility curves as calculated by the above procedure. Initial values calculated were 441 cu. ft. per barrel for solution gas-oil ratio and 1.2646 for reservoir oil formation volume factor—both values for the initial pressure of 2960 psia at the -6135 foot datum.

RESERVOIR GAS DATA

The method presented by Brown⁸ was used to calculate the gas compressibility factor with one addition, and that was to include in the computations the changes in composition of the reservoir gas due to pressure decline. Brown's method assumes the composition of the reservoir gas will remain constant with reduction in pressure. However, as the composition does change,⁷ as illustrated by Table IV, the effect of these changes should be included in the compressibility calculations.

Computations of the gas conversion or *v* factor were made in the conventional manner utilizing the above discussed gas compressibility factors. Due to the higher structural location and corresponding lower temperature of the gas cap, it was necessary to calculate a separate gas conversion factor for the cap gas. In Fig. 10 are presented *v* factor determinations for the oil zone gas and cap gas expressed in terms of pool datum pressure. Also on Fig. 10 are presented the results of the compressibility factor calculations. Utilizing the data of Fig. 10 and the sand volume content of the gas cap as presented in Table I, the original volume of the gas cap was calculated to be 35,000,000 Mcf. at standard conditions.

EFFECT OF GRAVITY ON POOL PERFORMANCE

It is pertinent at this time to discuss briefly the reasons why direct applications of conventional material balance equations cannot be applied to high relief pools. The material

balance approach assumes the entire pool will follow the behavior represented by a sample increment of fluid which remains in its original reservoir position and environment. The physical properties of this sample can be accurately determined by laboratory procedure. However, in the presence of steep dips, high relief, and good permeability development, gravity segregation alters the original reservoir environment of the sample increment.

Actual pool performance is the best indicator that gravity segregation is occurring in a high relief pool. A study of the gas-oil ratio history of individual wells in a pool will indicate whether or not segregation of oil and gas is occurring. The structurally lower wells will exhibit a decreasing gas-oil ratio trend with time, while the crestal wells will prematurely go to gas. Theoretical calculations performed on gas drive pools indicate a definite upward trend in gas-oil ratios should occur as the pool liquid saturation approaches 89%. Actual performance data on gas drive pools indicate that this "gas

TABLE VI
Summary of Material Balance Data

P	FVF	GOR _s	u	u-u ₀	v ₀	v _g	F
2800	1.267	440	1.2680	0.0034	0.001074	0.00117	37,900
2600	1.265	434	1.2755	0.0109	0.001156	0.00124	39,580
2400	1.260	421	1.2897	0.0251	0.001253	0.00137	39,900
2200	1.251	400	1.3125	0.0479	0.001370	0.00151	39,350
2000	1.238	371	1.3486	0.0840	0.001513	0.00171	39,000
1800	1.221	337	1.3949	0.1303	0.001692	0.00200	37,700
1600	1.204	302	1.4638	0.1992	0.001919	0.00233	36,200
1400	1.186	268	1.5517	0.2871	0.002215	0.00277	34,050
1200	1.169	232	1.6807	0.4161	0.002612	0.00331	31,650
1000	1.151	197	1.8488	0.5842	0.003169	0.00396	29,050
800	1.134	160	2.1018	0.8372	0.004017	0.00480	25,750
600	1.116	125	2.5014	1.2368	0.005436	0.00600	22,450
400	1.099	90	3.0856	1.8210	0.008282	0.00828	16,250
200	1.081	52	4.2048	2.9402	0.016856	0.01686	9,320
100	1.070	26	5.2860	4.0214	0.033986	0.03399	5,100

- P = Pressure at -6135 ft. p.s.i.a.
- FVF = Oil phase formation volume factor.
- GOR_s = Solution gas-oil ratio, cu. ft. per barrel.
- u = Reservoir volume of one barrel stock tank oil and original solution gas at reservoir pressure.
- v₀ = Reservoir volume of free gas in oil band, bbls./std. cu. ft.
- v_g = Reservoir volume of free gas in gas cap—bbls./std. cu. ft.
- F = Gas-oil ratio conversion factor—bbl/bbl reservoir conditions to cu. ft. per bbl. std. conditions.
- r₀ = Original solution gas-oil ratio=441 cu. ft. per barrel.
- v_g = Original v_g factor=0.00116.

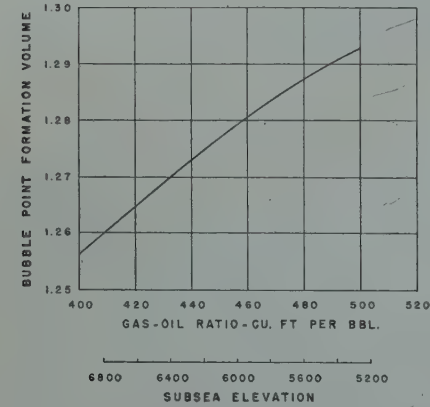


FIG. 7—BUBBLE POINT FORMATION VOLUME FACTOR VS. SOLUTION GAS OIL RATIO.

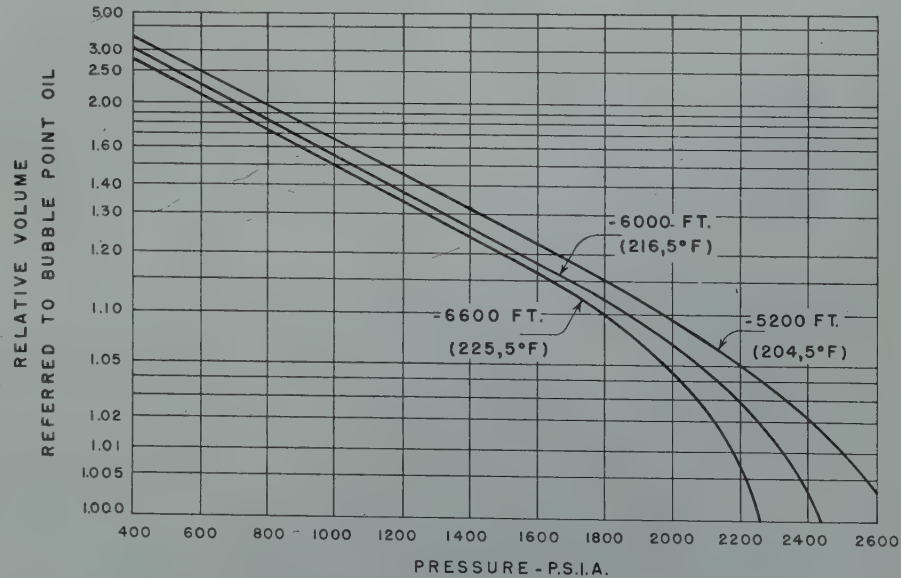


FIG. 8—UNWEIGHTED TWO PHASE RELATIVE VOLUME DATA.

equilibrium point" can be reached at liquid saturations as high as 96%.⁹ It has been the author's experience, based on the performance of gravity-drive pools in California, that where gravity segregation is occurring, gas-oil ratios will show no increase or a slight increase, even when the withdrawal data indicate the pool liquid saturation to be as low as 80%. It is conceivable that many wells, if the conditions are satisfactory, can produce to lower liquid saturations before the gas-oil ratios will increase. The attainment of continued low gas-oil ratios is an indication of the maintenance of a high liquid saturation readily explainable by gravity segregation.

It is necessary to evaluate the effect of gravity segregation on future pool performance before material balance calculations can be applied. If available, past pool performance should be used as it provides the most reliable index for future predictions. Using our type pool as an example, the following procedure illustrates one method of including the effects of gravity drive in the material balance equation.

First, the relative oil and gas volume referred to bubble point oil data, or u factor, were structurally weighted as previously illustrated in Table III. In Table V is presented a summary of the u factor as so weighted for structure. Fig. 11 presents the structurally weighted u curve as tabulated in Table V. At this point, no correction for gravity segregation has been made.

Second, material balance calculations were made for the weighted pressure averages of regularly scheduled pool pres-

sure surveys. The results of these calculations are graphically presented in Fig. 12 on which the calculated original oil content is plotted versus the cumulative oil production at the time of the pressure determination.

The calculation of a progressively lower initial oil content, as illustrated by Fig. 12, is evidence of gravity segregation. These calculations indicate, that for the volume of reservoir oil in place, too high an expansibility factor was used. By considering the original oil band volume as a constant unit, the passage of time will find a progressively increasing percentage of oil located farther and farther down structure, where, due to the higher pressures present, the oil and gas expansibility will be lower. In the absence of gravity segregation, the reservoir oil would be distributed over the entire oil band rather than concentrated in the lower structural areas. This would result in the computation of a higher weighted u factor than that computed if the oil were influenced by gravity. All other factors being comparable, the higher the u factor the lower the initial oil content, which effect has been observed in Fig. 12.

To correct the effect of gravity segregation, the material balance equation was recalculated by holding the initial oil content constant and solving for the u factor. The modified u factor so obtained was plotted on Fig. 11 and extrapolated to lower pressure points. It is reasoned that this approach combines into one factor the effects of gravity segregation on the basic material balance, and thus provides a means of forecasting the future performance of the pool. The important requirement for such a procedure to be valid is an accurate determination of the original oil content by the pore volume method.

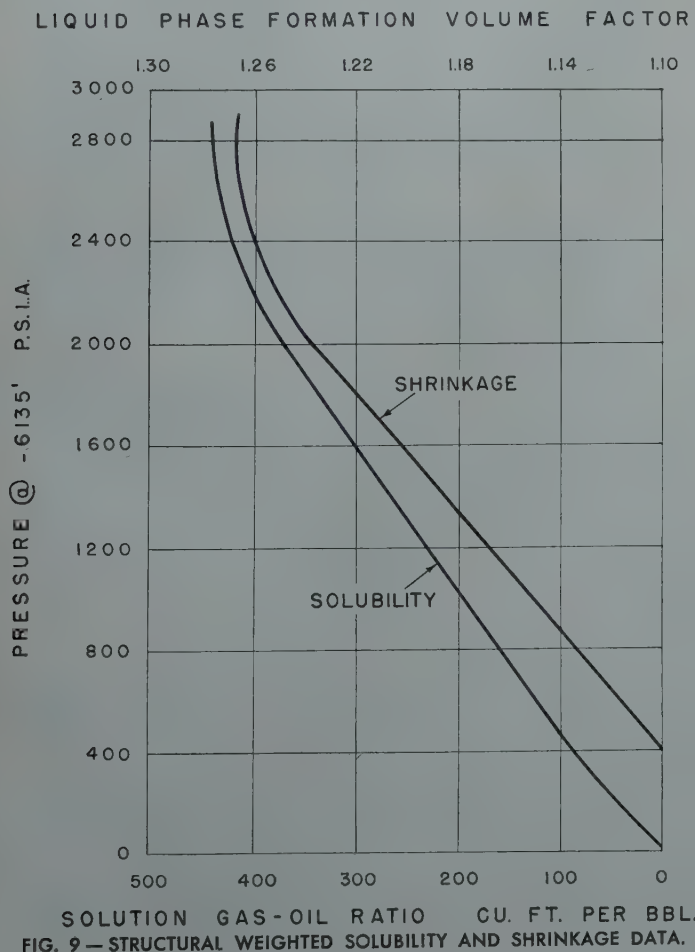


FIG. 9—STRUCTURAL WEIGHTED SOLUBILITY AND SHRINKAGE DATA.

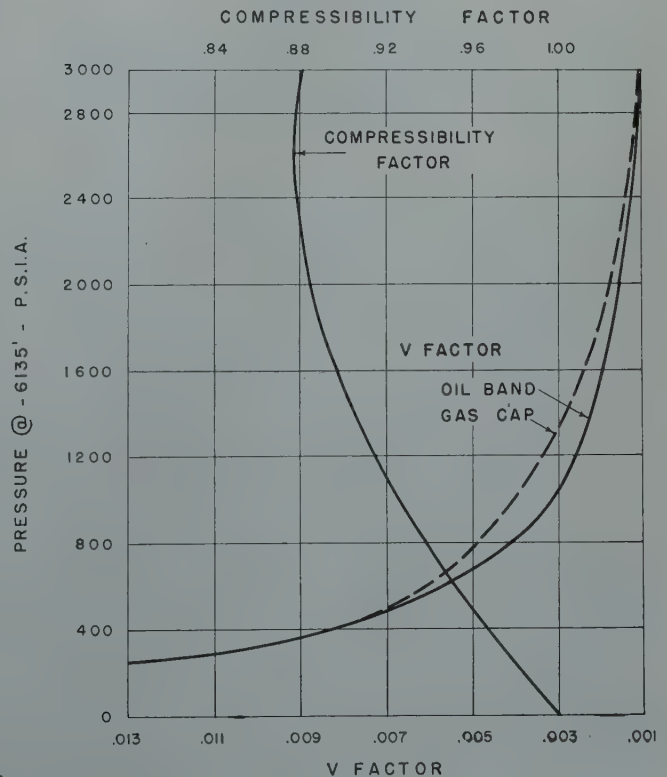


FIG. 10—GAS DATA.

PREDICTIONS OF FUTURE RESERVOIR BEHAVIOR

Predictions of future reservoir behavior depend upon a knowledge of the saturation changes in the pool. Recent studies performed on other pools⁹ have indicated that a determination of the change in the ratio of effective permeabilities of gas and oil (K_g/K_o) with changes in liquid saturation can be utilized to determine the type of reservoir drive existing and the influence of external agents upon this drive. As the produced gas-oil ratio is empirically related to the relative permeability ratio, which is related in turn to liquid and gas saturation, an analysis of gas-oil ratio performance will serve as a means of establishing the magnitude and distribution of existing saturations. The necessary requirements to apply such an analysis is a knowledge of relative permeability relationships for the pool.

As has been previously discussed, gravitational effects are responsible for the pool's average producing gas-oil ratio being considerably lower than that which would exist if the pool performance followed straight gas depletion drive. Past field performance on high relief pools indicates, that when controlled, produced gas-oil ratios will be low and will decrease rather than increase with pressure decline. For future predictions of gas-oil ratio performance, it is necessary to weight this effect of gravity segregation upon the composite pool behavior. Relative permeability relationships are controlled primarily by the liquid saturation in a reservoir and the physical nature of the rock comprising the reservoir. The laboratory procedure for the determination of relative permeability data from individual core samples satisfactorily analyzes the permeability-saturation behavior of a single core sample only. However, when such data are applied to an entire reservoir it is directly assumed that the behavior of the total reservoir is instantaneously equal to the behavior of the single core sample. In other words, it is assumed that the liquid saturation of the pool is distributed equally throughout the reservoir and maintains that distribution during the life of the pool, which assumption is incorrect if fluid migration occurs.

The existence of pressure differentials between wells, permeability variations, variations in well spacing in a pool, unequal distribution of withdrawals due to well productivities, competition, etc., and the formation of a secondary gas cap, are common conditions in most oil pools. Obviously the saturation distribution varies from well to well depending on the differences in the above variables between wells. The application of laboratory determined relative permeability data to an entire pool can easily result in an erroneous prediction of the future performance of the pool. Unfortunately the actual degree and magnitude of variation of many of the above variables cannot be correlated over an entire reservoir. The difficulty of determining the actual permeability distribution in a pool is an excellent illustration of this problem.

The use of actual pool performance data provides for a satisfactory solution of the problem. Primarily the resultant purpose of reservoir calculations is the determination of the entire pool performance. The use of weighted pool data combines into one item the differences of the variables between wells and between areas of the pool and expresses the data in terms of a single unit, namely, the pool. An analysis of past pool performance can give information as to the type and behavior drive present and the influence of external agents upon this drive.

Relative permeability relationships can be obtained from weighted pool data. The relative permeability ratios so obtained might be termed "apparent" K_g/K_o data as they would reflect the actual behavior of the pool rather than the empirical behavior as would be calculated from laboratory determined K_g/K_o data. Changes in the withdrawal policy of the pool, such as production of excessive free gas, effect of gravity segregation on the pool, and numerous other factors, would alter the "apparent K_g/K_o " curve. The effect of these changes on the future performance of the pool could then be evaluated.

The one controlling limitation to this approach is the assumption that the pool operating factors do not materially change over the period analyzed. For example, in an efficiently

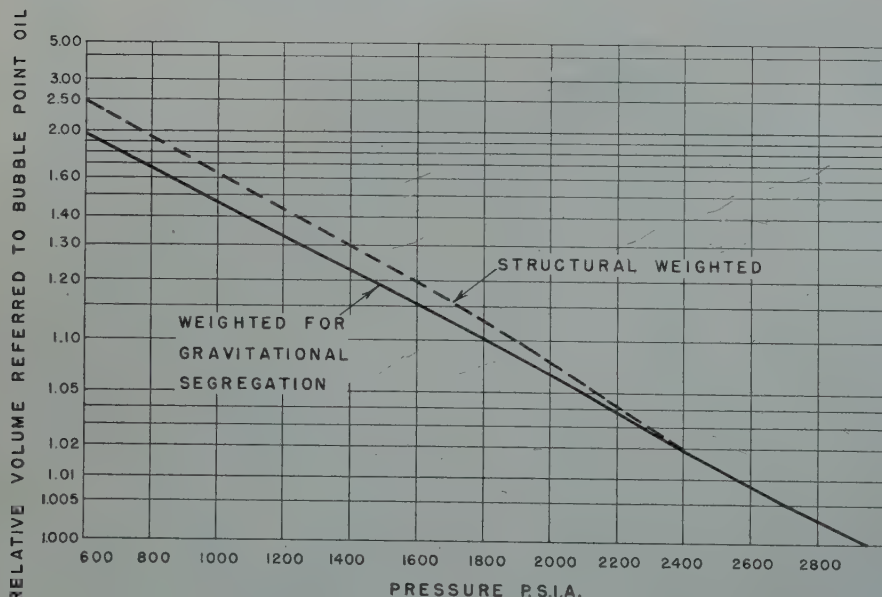


FIG. 11 — TWO PHASE RELATIVE VOLUME DATA.

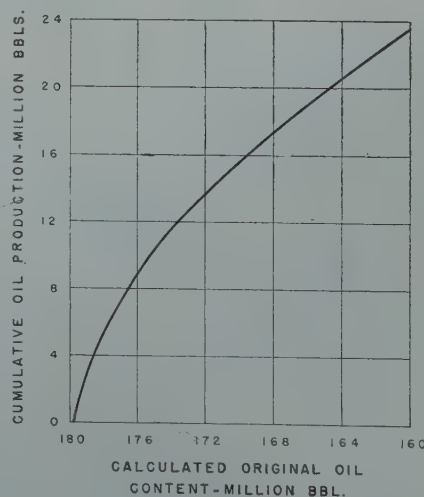


FIG. 12 — CALCULATED ORIGINAL OIL CONTENT VS. PRODUCTION.

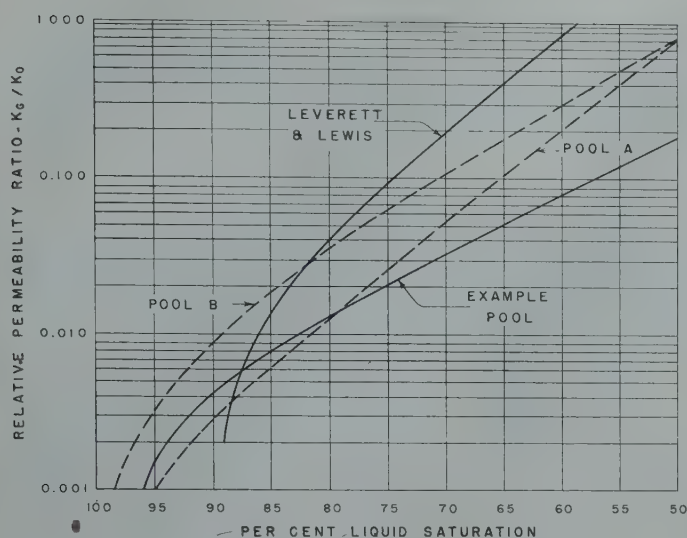


FIG. 13 — RELATIVE PERMEABILITY RELATIONSHIPS.

operated gravity drive pool, the policy of shutting in crestal wells when they go to gas must be assumed to continue in future operations. This limitation does not destroy the value of the method. Actually, the reservoir engineer can determine the future performance of a pool, if operated under past conditions, or he can determine the performance under various plans of operations by adjusting the "apparent K_g/K_o " curve to the conditions desired. This is possible as the "apparent K_g/K_o " ratio reflects instantaneous changes in pool performance caused by the influence of external agents.

In Fig. 13 are presented typical "apparent K_g/K_o " curves for several pools in California which are performing under various degrees of gravity drive. Also presented are empirical laboratory determined K_g/K_o data for unconsolidated sands.¹⁰ The effects of gravity drive on the fields performance are readily apparent in a distinct flattening of the K_g/K_o curve.

Table VI presents a complete summary of all material balance data used in predicting future field performance of the example pool. Future pressure-production and gas-oil ratio history was calculated on a trial and error material balance approach. Fig. 14 presents the calculated pressure-production and gas-oil ratio history of the pool under gravity drive performance. Also presented on Fig. 14 is the pool pressure-production and gas-oil ratio history representing performance under gas drive which would have been calculated if laboratory determined K_g/K_o data were used. It is readily apparent that by the use of the latter data future reservoir performance would have been erroneously predicted.

SUMMARY

The procedures outlined in this paper for evaluating the effects of gravity drive upon pool performance can be summarized as follows:

1. Basic material balance data should be structurally weighted to compensate for structural differences in pressure and temperature.

2. Relative permeability relationships as computed from actual field performance data should be used in preference to laboratory determined data.

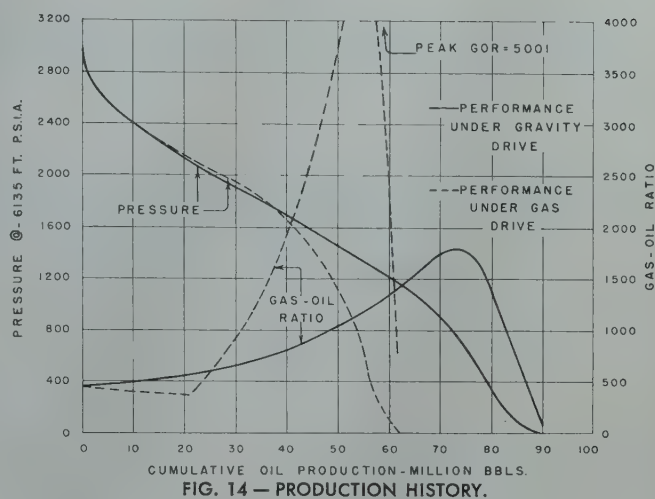


FIG. 14 — PRODUCTION HISTORY.

3. The oil and gas relative volume factor, or u factor, should be corrected for gravity segregation effects using actual field performance data as a guide.

The methods presented above are certainly not the complete solution to the problem of analyzing the reservoir behavior of a gravity-drive pool. Their use will provide refinement in procedure which will permit a more representative interpretation of reservoir performance.

ACKNOWLEDGMENTS

The author wishes to express his gratitude to F. M. Cole for his advice and guidance, and to the management of the Honolulu Oil Corp. for permission to publish this paper.

REFERENCES

1. "Gravitational Drainage of Liquids from Unconsolidated Wilcox Sand", Roscoe F. Stahl, W. A. Martin, and R. L. Huntington—*Trans. AIME*, 1943.
2. "Gravity Drainage in Oil Fields", James O. Lewis—*Trans. AIME*, 1942.
3. "Possibilities of Secondary Recovery for the Oklahoma City Wilcox Sand", Donald L. Katz—*Trans. AIME*, 1942.
4. "A General PVT Correlation for Mixtures of California Oils and Gases," M. B. Standing, A.P.I. Paper No. 801-23, May 1947.
5. Personal Communication, N. R. Williams, Core Laboratories, Inc., 1948.
6. Field Data on Sesnon Pool, A. C. Tutschulte, 1948.
7. "Gravitational Concentration Gradients in Static Columns of Hydrocarbon Fluids", B. H. Sage and W. N. Lacey—*Trans. AIME*, 1939.
8. "Deviations of Natural Gas from Ideal Gas Law", George Granger Brown—Pamphlet, Clark Bros., Inc., 1940.
9. The Importance of Injected Gas as a Driving Medium in Limestone Reservoirs as Indicated by Recent Gas Injection Experiments and Reservoir Performance History", L. E. Elkins, A.P.I. *Drill. and Prod. Prac.*, 1946.
10. "Steady Flow of Gas-Oil-Water Mixtures Through Unconsolidated Sands", M. C. Leverett and W. B. Lewis—*AIME Tech. Pub. No. 1206*, 1940.

★ ★ ★

PILOT GAS INJECTION — ITS CONDUCT AND CRITERIA FOR EVALUATION

LINCOLN F. ELKINS, MEMBER AIME, SOHIO PETROLEUM CO., OKLAHOMA CITY, OKLA.

JOHN T. COOKE, SOHIO PETROLEUM CO., OKLAHOMA CITY, OKLA.

INTRODUCTION

Injection of gas to increase oil recovery has been considered for almost all important discoveries during the past ten or fifteen years. However, the number of gas injection projects having sufficient history and data is too limited to permit valid generalities of effectiveness of gas injection. Management and engineers are faced with a difficult problem of selecting those reservoirs which are susceptible to profitable application of gas injection.

Injection of gas to maintain high pressure favors some factors affecting reservoir performance such as viscosity, surface tension, and formation volume factor of oil by keeping gas in solution and favors some operating features such as extending flowing life of wells and storing part of the produced gas for future use or sales. Injection of gas at low pressure involves lower compression ratio, or at least a single gas-gathering system, larger displacement volume in the reservoir per unit of gas handled, and permits effective utilization of the naturally existing energy and agent for oil displacement that is gas dissolved in oil. Each program is thus a compromise to meet optimum economic conditions while striving to attain maximum recovery of this important natural resource.

The statement has often been made that pressure maintenance would greatly

increase oil recovery by permitting abandonment of formation oil inflated with gas in solution rather than abandonment of the same liquid volume of tank oil, if the same terminal oil saturation could be attained. Simple calculations indicate increases in oil recovery

as high as one hundred per cent on this basis for high formation volume factor oil encountered in current deep drilling. Important in this statement is "if the same terminal oil saturation could be attained." Implicit in this statement are the requirement of physical

TABLE I—DATA PERTAINING TO GAS INJECTION PROJECTS

Field*	Viscosity of Oil Centipoises	Formation Pressure During Injection - Psia	Shrinkage of Formation Oil From Initial Conditions to Last Point Shown†
A†	.57 - .80	1750 - 800	11.5%
B	.5	2400 - 2100	9.0
C	1.4	300 - 50	10.0
D	1.5	400 - 40	12.0
E	.9 - 1.1	900 - 75	13.0
F	1.6	125 - 30	20.0
G	1.8	1200 - 1080	2.0
H	.52	1020 - 960	2.5
I	2.6 - 3.0	625 - 200	3.0

* Letters conform with curves shown in Fig. 1.

† Based on formation oil at initial conditions as 1.00.

† Pennsylvania sand field discussed in this paper.

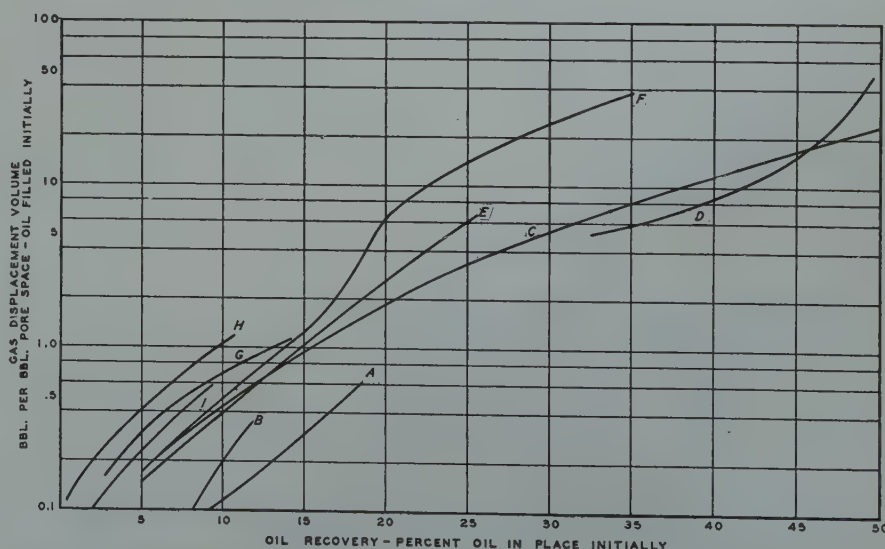


FIG. 1 — GAS INJECTION REQUIREMENTS FOR OIL RECOVERY — SANDSTONE RESERVOIRS.

Manuscript received at Petroleum Branch Office October 3, 1948. Paper presented at Branch Fall Meeting in Dallas, Texas, October 4-6, 1948.

¹ References are given at end of paper.

performance and of economics of operation of displacement of oil from heterogeneous rock. The problem is not that simple.

Except in those instances where rock, fluid properties and structural conditions combine to permit effective gravity drainage, oil must be displaced by gas or by water to be recovered. From numerous laboratory experiments the so-called relative permeability-saturation theory of oil displacement by gas has been developed. Natural production performance of many gas expansion reservoirs has shown good qualitative agreement with this theory. However, it has yet to be demonstrated that the primary production performance can be extrapolated quantitatively to accurately predict reservoir performance with gas injection.

Relation between gas displacement volumes and percentage oil recovery for nine gas injection projects in sand reservoirs is plotted in Fig. 1 and important properties of crude oil and formation pressures during injection are presented in Table I. Since oil displaced by injected gas cannot be segregated from the total oil produced, gas expansion in the reservoir has been added to volume of gas injected. Regional gravity segregation is believed to be negligible in all cases except "F", but even in this field gas injection has been dispersed in the down-structure area to drive the oil into producing wells.

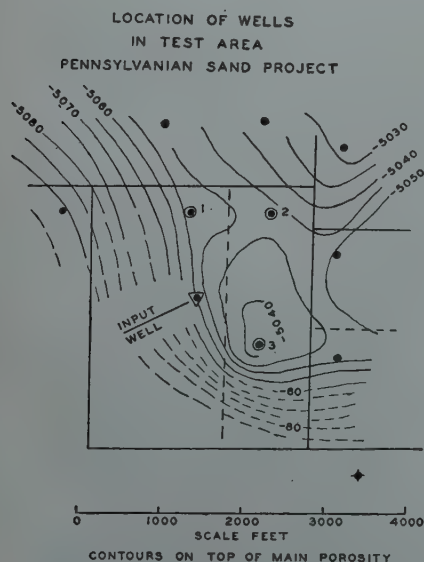


FIG. 2 — LOCATION OF WELLS IN TEST AREA,

With reservoir pressures ranging from 30 to 2200 psia for these projects, it is striking that total gas volume and oil viscosity appear to be the principal factors causing deviation from the mean and that pressure per se does not appear to be important. A nearly linear relation exists between viscosity and gas volume requirements except for Field "H", for the same oil recovery at least in the lower ranges. In the higher ranges variation in sand properties probably become more important although no definitive criteria are obvious. Injection of gas at high pressure requires considerably more gas handling to inject the same formation volume of gas than does injection at low pressure.

Even though these case histories of gas injection which include all the vicissitudes of field operation, well completion, gas channeling, etc., show good general agreement, it does not follow that circulation of a particular volume of gas measured under reservoir conditions will guarantee that indicated oil recovery will necessarily be attained. Since it has been demonstrated that oil is recovered primarily due to actual displacement by gas, it is necessary that the introduction of gas into the reservoir be controlled to insure that it will flow through the maximum possible part

of the oil-filled pore space. Herein lies an important distinction between the displacing ability of gas dissolved in oil in a reservoir and gas injected through wells. Expansion of gas released from solution in oil provides energy and a displacing agent in each pore in which oil exists, while injected gas of necessity, in following the line of least resistance, is capable of displacing oil from only a part of a reservoir before gas circulation ratio to oil recovery becomes economically prohibitive.

This part of the reservoir which can be effectively swept by injected gas—a function of permeability profile—can be partly determined for particular reservoirs by relatively short-term pilot gas injection tests. Case histories of pilot gas injection in one sand reservoir and two lime reservoirs are presented to show the procedures used, results obtained, and methods of interpretation.

Pilot gas injection tests also provide direct measure of well intake capacities which aid in designing compressor pressure requirements and in determining number of input wells required. The primary answer of economic importance, however, is reaction of the reservoir to injected gas.

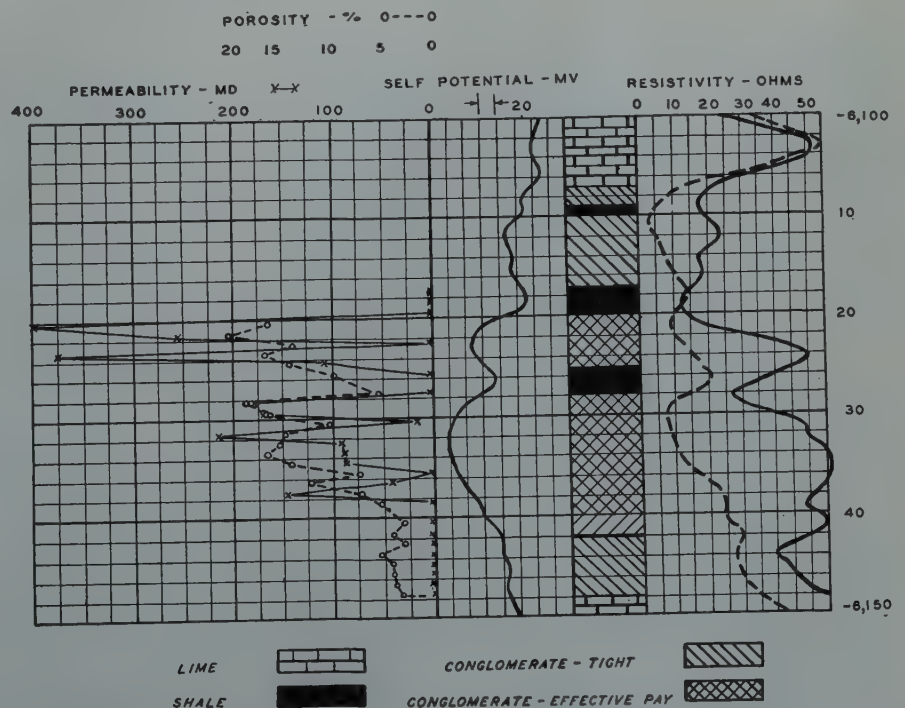


FIG. 3 — TYPICAL LOG, PENNSYLVANIAN SAND PROJECT.

LOWER PENNSYLVANIAN SAND RESERVOIR

A pilot injection experiment was conducted in the Second Conglomerate Reservoir, Lower Pennsylvanian sand, in a field in Texas. Location of input well and offset producing test wells are shown on the map in Fig. 2 on which contours on top of main porosity are super-imposed. Although this test area is a separate nose of the main structure, all wells involved are within fifteen feet of the same elevation, so gravity segregation effects should be minor. Typical characteristics of this reservoir are outlined on the composite log in Fig. 3. Unfortunately, no core analyses were available for any of the test wells, but general correspondence with the log shown is believed to exist.

Individual production facilities including separators, gas meters, and oil meters were installed for each of the test wells so that continuous daily measurement of the produced fluids would provide a complete and accurate record of detailed reservoir performance. Fig. 4 shows performance of well No. 1, the north offset to the input well throughout the test period. Gas-oil ratios rose distinctly within three months after gas injection started and increased to a

maximum of about 3500 cubic feet per barrel just before gas injection was curtailed. Gas-oil ratios then fell off rapidly, and within six months after gas injection was completely stopped they had declined to nearly the same value existing before gas injection started. The cross-hatched area on the curve represents difference between actual produced gas-oil ratio and that which probably would have existed without gas injection. Similar individual well performance of other wells more remote from the input well showed no significant variation in gas-oil ratio during this period.

Performance of well No. 2, the northeast diagonal offset to the input well is illustrated in Fig. 5. Gas-oil ratio performance similar to that of well No. 1 existed, though the peak gas-oil ratio was just slightly in excess of 2000 cubic feet per barrel. Here, too, the gas-oil ratio declined to its original value following cessation of gas injection.

Performance of well No. 3, the east offset to the input well, is illustrated in Fig. 6. Gas-oil ratios increased significantly about six months after gas injection started and also declined following cessation of gas injection. Gas-oil ratio without gas injection outlined on this curve is probably conservative with reference to excess gas production, since

ratios of other wells in the area remained low throughout most of 1945, but at least it indicates minimum channeling of injected gas.

Reservoir pressure when gas injection started was 2000 to 2050 psi—just 50 to 100 psi below the original saturation pressure of oil in the reservoir. Thus gas injection began before significant free gas saturation had developed in the reservoir—a condition considered essential by many engineers. Maximum gas channeling was experienced at well No. 1 which produced double allotment due to transfer of allowable production from the input well. More concentrated withdrawal may easily have directed injected gas toward this well to create this gas channel of higher capacity.

Gas injection was discontinued in September, 1945, and the input well remained shut in until January 22, 1946, when it was returned to production. Performance of this well is illustrated in Fig. 7. It should be noted that oil was obtained the first day of production and that within two months the gas-oil ratio and oil production had reached a status not greatly different than other wells in that area of the field, even though cumulative back-flow gas production from the input well was only 10 per cent of the volume of gas injected into the reservoir.

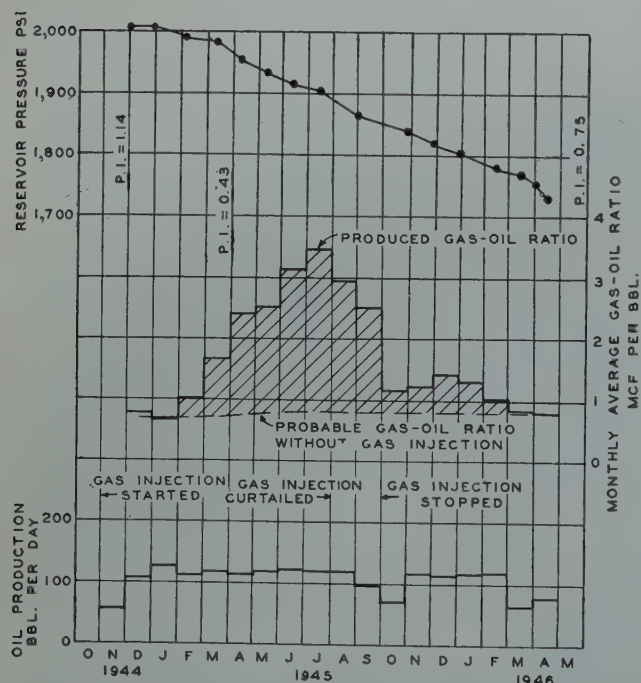


FIG. 4 — PERFORMANCE OF WELL NO. 1, PENNSYLVANIAN SAND PROJECT.

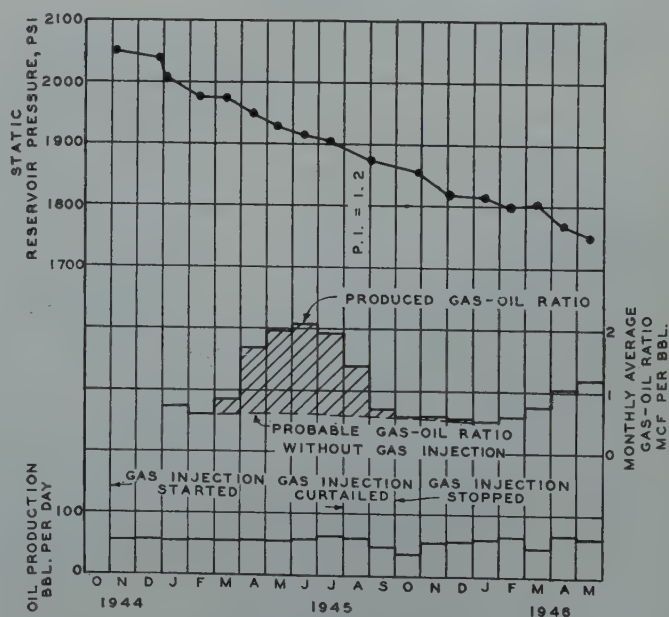


FIG. 5 — PERFORMANCE OF WELL NO. 2, PENNSYLVANIAN SAND PROJECT.

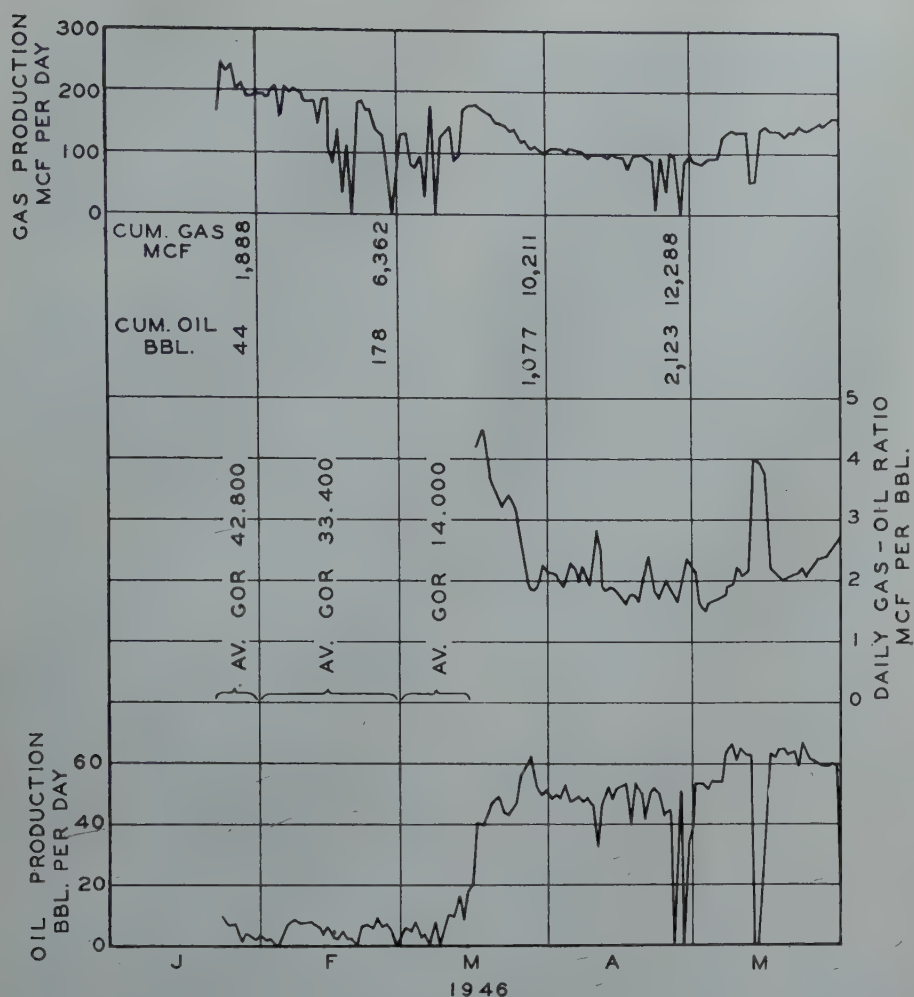


FIG. 7—PERFORMANCE OF INPUT WELL RETURNED TO PRODUCTION.

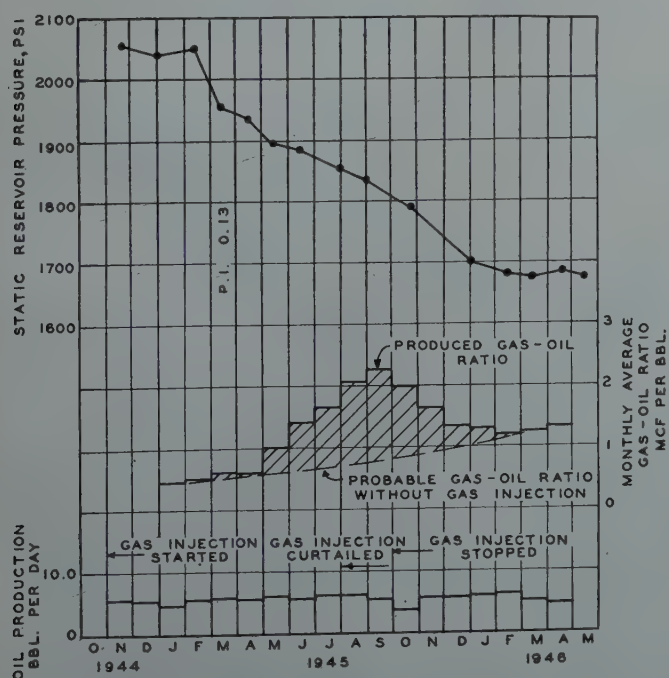


FIG. 6—PERFORMANCE OF WELL NO. 3, PENNSYLVANIAN SAND PROJECT.

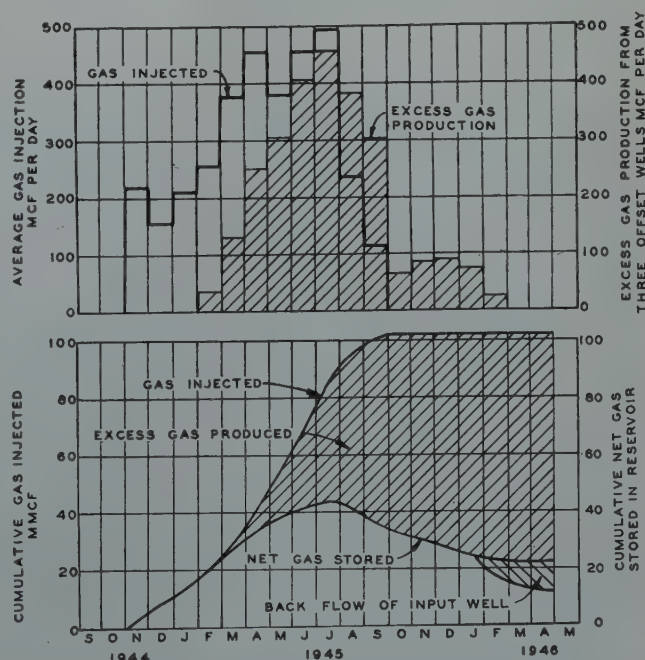


FIG. 8—GAS INJECTION RATE AND EXCESS GAS PRODUCTION IN 3 TEST WELLS, PENNSYLVANIAN SAND PROJECT.

Detail of gas injection rate and of excess gas production from these three test wells is outlined in Fig. 8. Within nine months of beginning gas injection, rate of excess gas production of three offset wells was nearly equal to the rate of gas injection. Gas injection was primarily gas circulation without significantly effecting further oil recovery.

Cumulative gas injection and cumulative excess gas production from these three offset wells are shown in the lower part of this chart. Of the 102 M³cf gas injected, maximum amount "stored" in the reservoir was about 44 M³cf occupying some 50,000 barrels in reservoir environment. Reservoir pore space in the area is about 26,000 barrels per acre or 4,200,000 barrels for the assumed 160-acre drainage area of the four wells involved. Thus these gas channels occupied only 1.2 per cent of the pore space involved when rate of excess gas production was essentially equal to rate of gas injection. Considering "stored" gas to be confined within linear bounds of the wells raises the fraction of pore space occupied to about four per cent, but it is unlikely that such condition existed entirely and at least all production did not come from these confines.

Reaction of oil productivity to injected gas is illustrated by PI history of well No. 1. Productivity index, which

was 1.14 barrels oil per day per psi prior to gas injection, declined to 0.43 before excess gas production reached its peak. It increased considerably to 0.75 after gas injection was stopped and gas-oil ratio had returned to normal. Both gas-oil ratio and oil productivity performance indicate these gas channels became at least partly resaturated with oil when gas injection was stopped. Much of this oil probably came from adjoining by-passed portions of the reservoir, but part might have come from outside the test area. If these conclusions are generally applied to this reservoir, they mean that no lasting effect was obtained from the gas injection. To maintain this "stored" gas volume at existing pressure would require circulation of about 450 Mcf per day till flow of oil from by-passed parts of the reservoir declined to uneconomic rate. At 2c per Mcf compression cost this would amount to \$3,300 per year plus the pro rata share of gas gathering and gas injection system expense to maintain 50,000 barrels of pore space (containing about 36,000 barrels of tank oil initially) swept free of oil. Not all of this oil could be considered increase in ultimate recovery since very little free gas existed at time of gas injection began and oil recovery by natural means would be expected to be highest in these most permeable channels. Such cost calculation is probably very inaccurate, but at least it shows magnitude involved.

Gas injection was continued in this field at the top of the main structure. Over-all pool performance—obtained by totaling individual well production of oil and gas measured by separate meters—is summarized in Fig. 9. Of importance is gas-oil ratio performance during March, April and May, 1946, covering a period when gas injection was stopped. Normal interpretation of this composite data is that gas-oil ratios were not sensitive to gas injection and thus that gas injection was successful—contrary to the inferences of pilot gas injection.

Analysis of detailed performance of individual wells, however, indicates interpretation of composite data to be erroneous. Fig. 10 shows performance of one 40-acre diagonal offset to the injection well. Immediate reaction to stopping gas injection on March 23,

1946 and resuming it on May 20, 1946 was noted. So striking, in fact, was this reaction that gas-oil ratios of this well alone indicated time almost to the day of stopping and starting the compressor. Decline in gas-oil ratio during this period for this and four other wells multiplied by their respective oil rates equals about 40 per cent of the gas injection rate just prior to the period—and none of these wells had attained a stabilized minimum gas-oil ratio. Thus much of the injected gas was being cycled to five producing wells. Small effect on pool average gas-oil ratio

was apparent because edge wells remote from the injection area had reached a stage of depletion where gas-oil ratios were increasing rapidly. Reduction in pool gas-oil ratio at beginning of 1947 was attained by shutting in high gas-oil ratio wells when the field was unitized.

Performance of this reservoir has illustrated the importance of detailed analysis performance of individual wells. It has indicated ease of making false conclusions even though over-all pool performance data are accurate.

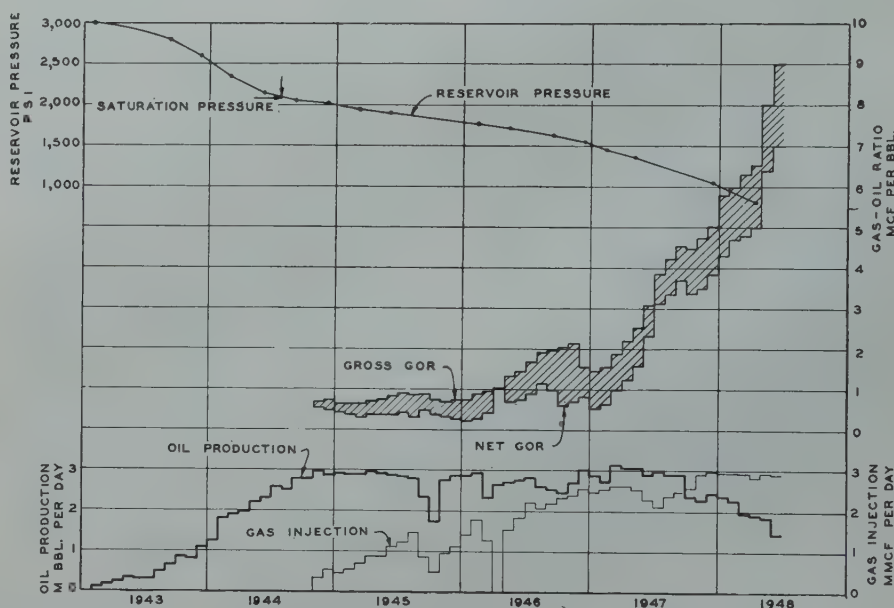


FIG. 9 — POOL PERFORMANCE, PENNSYLVANIAN SAND PROJECT.

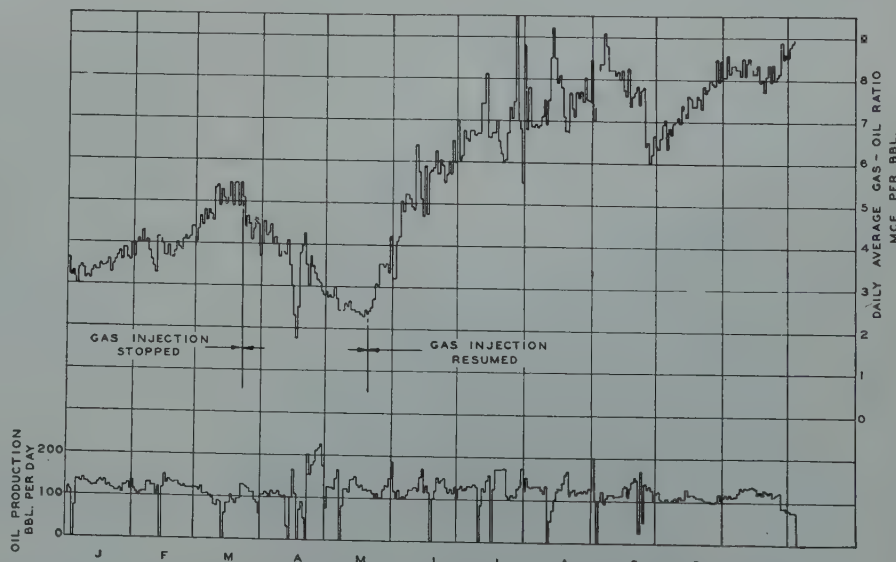


FIG. 10 — WELL PERFORMANCE OF 40-ACRE DIAGONAL OFFSET TO INPUT WELL, PENNSYLVANIAN SAND PROJECT.

SAN ANDRES LIMESTONE RESERVOIR

A series of pilot gas injection tests was conducted in a San Andres lime reservoir to determine intake capacities of wells and finally to determine effect of gas injection on gas-oil ratios of producing wells near the input well. Fig. 11 shows location of wells grouped by tank batteries for the final long-term injection test. All wells were set on fixed positive chokes of such size to permit production of allowable each month with a flowing schedule of six hours each day, and no chokes were changed during the pilot injection program. Total gas and oil production of wells in each tank battery were measured continuously for one month prior to gas injection, through the five-month injection period, and for at least one month following gas injection.

Fifty million cubic feet of gas were injected which at formation conditions represent about 88,000 barrels or less than 30 per cent of the volume of oil and gas produced from the test area during injection and less than 0.25 per cent of reservoir pore volume in the test area. The input well back-flowed about 12 per cent of the injected gas before any oil was produced; about 31

per cent when its gas-oil ratio declined to 4000 cubic feet per barrel, and about 45 per cent when it had declined to 2000 cubic feet per barrel.

Possible gas-oil ratios without gas injection are outlined for tank batteries 1, 3, 5, 6 and 7, based on reduced trends in gas-oil ratio when gas injection was stopped. These hatched areas indicate that as much as 16 per cent of the injected gas may have been produced. However, these indicated gas-oil ratios without gas injection should be considered just as reasonable possibilities since none of the changes in gas-oil ratio trend exceeded 200 cubic feet per barrel, and particularly since there is no assurance that wells in each tank battery contributed uniformly to oil production even though chokes were fixed.

The only valid conclusion that can be made regarding this test is that daily gas injection rate and total gas injection volume were too small to effect changes in reservoir performance that were significant enough to permit accurate interpretation.

GRAYBURG LIME GAS INJECTION EXPERIMENT

The paper *Importance of Injected Gas as a Driving Medium in Limestone Reservoirs*, by L. E. Elkins¹, reports an

experimental gas injection project in a West Texas Grayburg lime field. Map of test area is presented in Fig. 15, showing location of input and producing wells. First and second row offsets to the input well on 40-acre spacing were included in the test.

Performance of this group of wells is outlined on the chart in Fig. 16, showing average reservoir pressure, gas injection rate, oil production rate, average gas-oil ratio and reservoir fluid withdrawal. Eleven months of gas injection totaled 52 M³cf before significant rise in gas-oil ratio. This increase occurred simultaneously with a large increase in oil production rate and with a large increase in gas injection rate, so effects of gas injection cannot be segregated. Rate of gas production in excess of that calculated from a possible linear trend of gas-oil ratio from August, 1945 to January, 1945 is almost always in excess of gas injection rate. Much of this performance must have been due to oil production from permeable channels at a rate faster than oil flowed from the less permeable parts of the reservoir with then existing pressure differences. Approximate increase in gas-oil ratio during gas injection and approximate reduction in gas-oil ratio during six months after gas injection was stopped are shown for each well on the map in Fig. 15.

Formation volume of total 167 M³cf injected was about 300,000 barrels, or about 1.8 per cent of the estimated

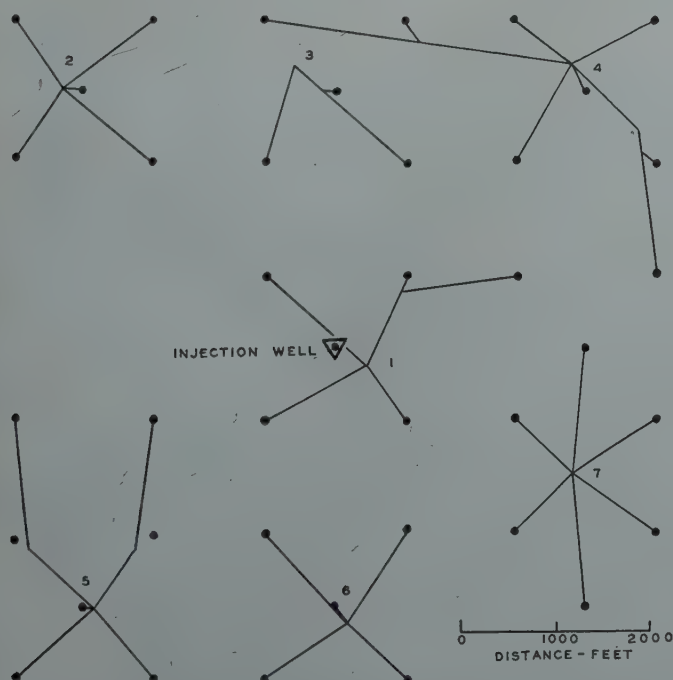


FIG. 11 — LOCATION OF TEST TANK BATTERIES, SAN ANDRES LIME PROJECT.

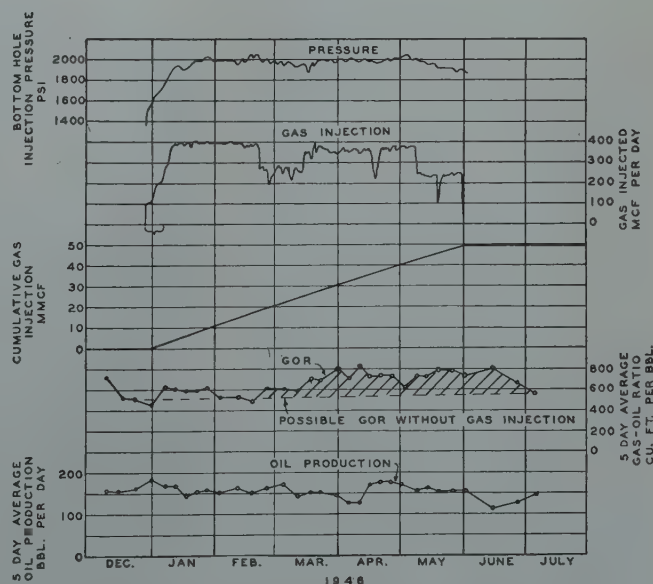


FIG. 12 — GAS INJECTION DATA AND PERFORMANCE OF BATTERY NO. 1, SAN ANDRES LIME PROJECT.

16,500,000 barrels pore space in the test area. Whatever injected gas contributed to observed gas-oil ratio performance thus occurred at a relatively low saturation of injected gas.

Reduction in gas-oil ratio from 3400 cubic feet per barrel in July, 1944 to 1700 cubic feet per barrel in January, 1945, during reduction in average oil saturation, was probably due to equalization of oil saturation between flow channels and more massive rock. Fluid flow from massive rock into permeable channels during this period was probably at a gas-oil ratio at least as low as 1700 cubic feet per barrel. If the reasonable assumption be made that a volume of gas and oil equal to production of about 1,000,000 barrels entered the permeable channels, this would include about 237,000 barrels of tank oil at a gas-oil ratio of 1700 cubic feet per barrel. Production of 172,000 barrels of tank oil in permeable channels, 0.4 per cent of total pore space, to reduce average produced gas-oil ratio from 3400 to 1700 cubic feet per barrel. Flow channels thus appear to be a relatively small fraction of the total pore space.

Rapid drop in pressure following increase in production rate in September, 1943 provides another approach to calculating effective fraction of reservoir voids in which action of injected gas may be presumed to be concentrated. Reservoir pressure and fluid withdrawal rates are plotted versus cumulative net fluid withdrawal in Fig. 17. During September and October, 1943, reservoir pressure dropped 150 psi with a net fluid withdrawal of 90,000 barrels. This amounts to only 600 barrels per psi while the calculated expansibility of reservoir fluids in the test area is of the order of 5700 barrels per psi. Apparent reservoir fluid expansibility was only ten per cent of the theoretical value assuming pressure equilibrium in all parts of the reservoir. At only 60 psi lower pressure in March, April and May, 1944, production of 2500 barrels per day was maintained with no drop in pressure which might represent rate of flow into the permeable channels. The 600-barrel production per psi includes some of this flow, but it is in any event the maximum indicated expansibility.

The fraction of total reservoir pore space indicated to comprise these channels is roughly ten per cent.

The only other plausible explanation of reservoir performance considered in these two analyses is lack of equalization of pressure and oil saturation be-

tween that portion of the reservoir near the wells and those portions more remote. Effects of drainage area and of fluid flow into permeable channels tend to offset each other in the pressure-production analysis, but to what degree cannot be determined.

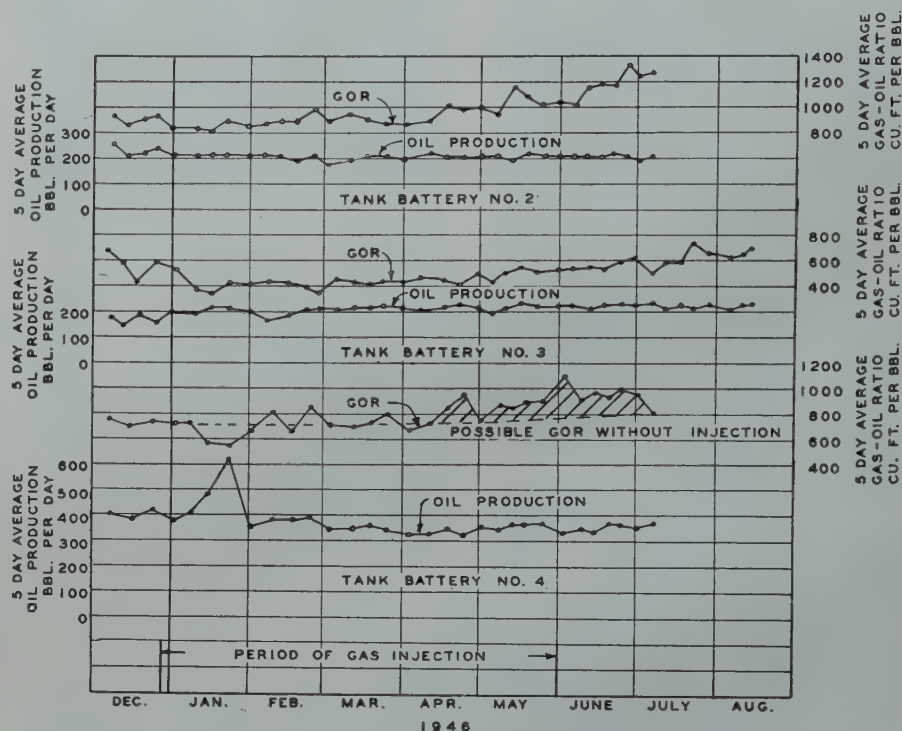


FIG. 13 — PERFORMANCE OF TANK BATTERIES NO. 2, 3 AND 4, SAN ANDRES DOLOMITE PROJECT.

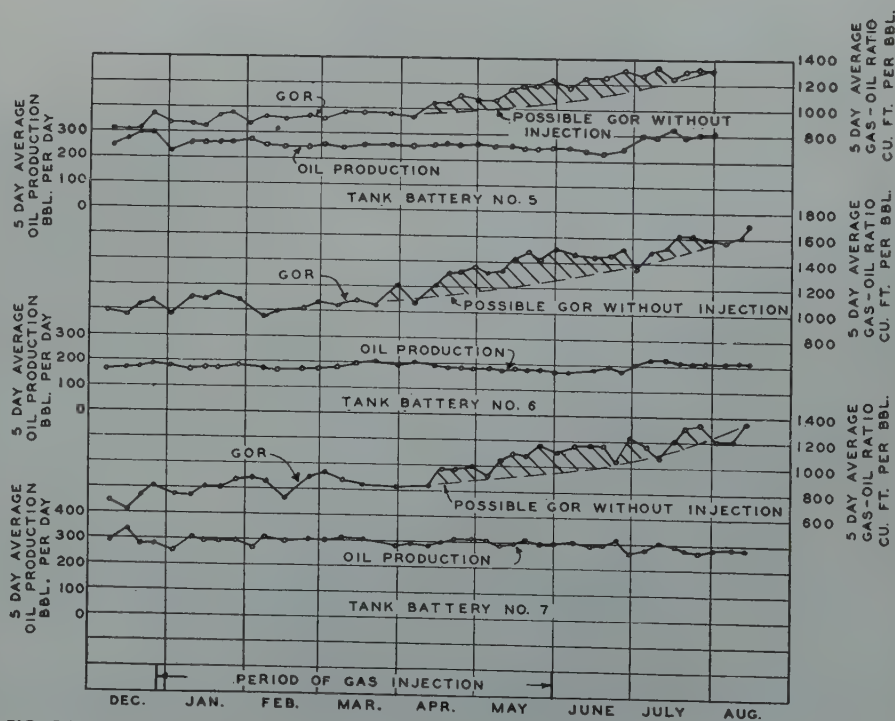


FIG. 14 — PERFORMANCE OF TANK BATTERIES NO. 5, 6 AND 7, SAN ANDRES LIME PROJECT.

Performance of eight gas injection projects in sand reservoirs has demonstrated that recovery of oil by injection of gas is primarily due to displacement. Thus the fraction of the reservoir through which injected gas will flow—

controlled by effective permeability profile—is of utmost importance. Three case histories of pilot gas injection have been presented showing results obtained and methods of interpretation. Continued gas injection in one field confirmed the implications of pilot gas injection.

So-called "conformance factors"³² or reservoir sweep efficiencies were found to be quite low—of the order of 10 to 20 per cent—in the two cases having gas injection at sufficient rate and volume to permit reliable interpretation. It appears that injection of sufficient gas to maintain formation pressure in these two instances would be inadvisable. Reduction of pressure to permit expansion of gas in those parts of the reservoir unaffected by injected gas would be necessary to effect recovery of oil therefrom.

From these pilot injection projects and others it appears to the authors that reliable conclusions depend upon:

(1) Injection of gas at sufficient rate and for a long enough period to cause significant changes in produced gas-oil ratio. Daily injection should at least replace volume of fluids produced by first-row offset wells.

(2) Adequate measurement of performance of individual wells to provide accurate data. Continuous measurement is desirable.

(3) Adequate test period before and after gas injection to determine normal trend in gas-oil ratio without gas injection.

(4) Conduction of pilot gas injection

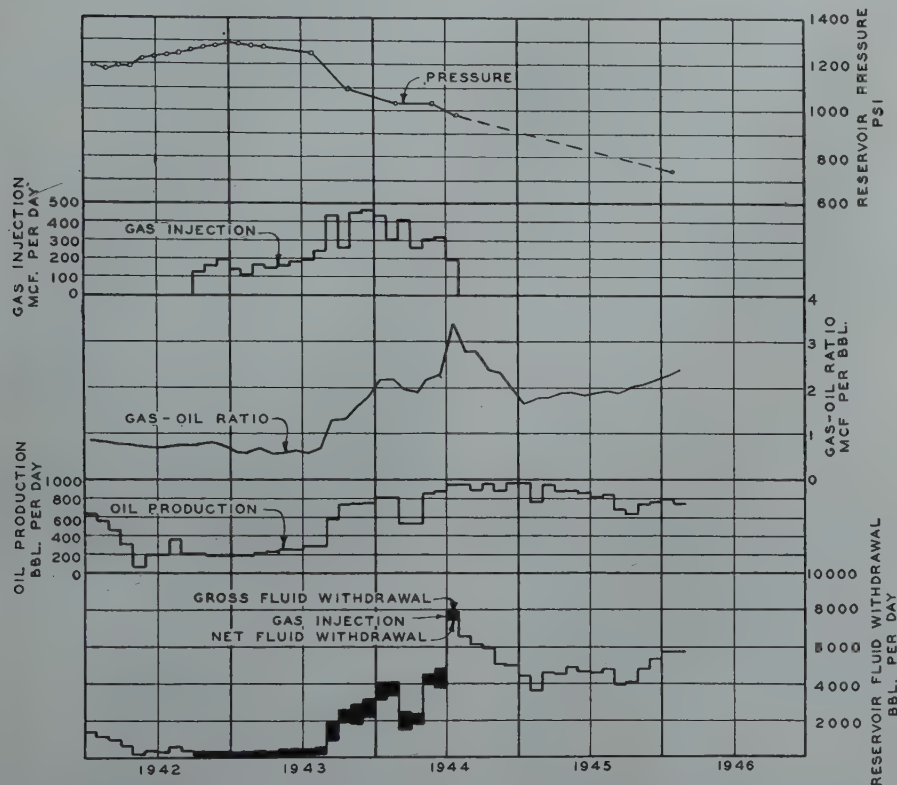


FIG. 16 — GRAYBURG LIME GAS INJECTION EXPERIMENT.

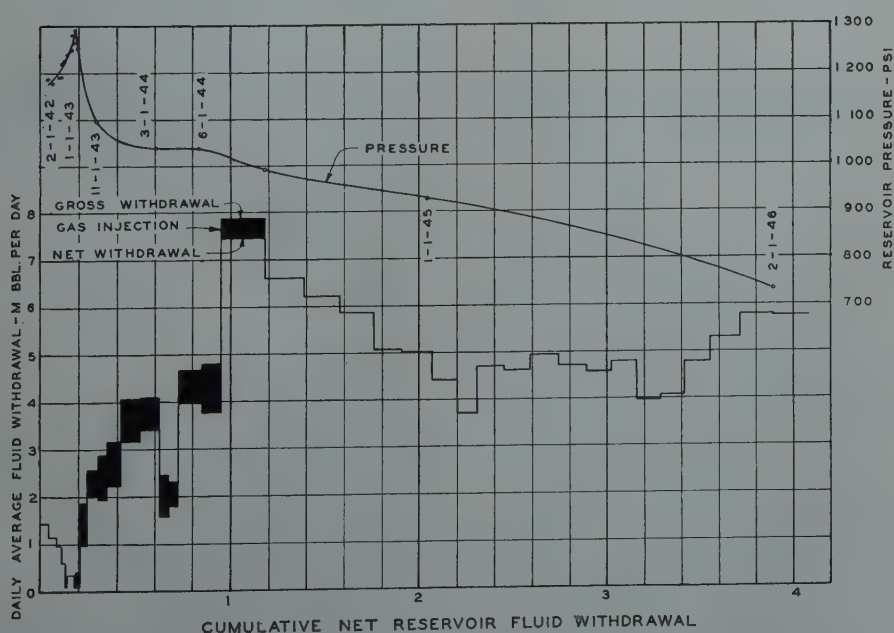


FIG. 17 — RESERVOIR PRESSURE AND FLUID WITHDRAWAL RATES VS. CUMULATIVE NET FLUID WITHDRAWAL, GRAYBURG LIME PROJECT.

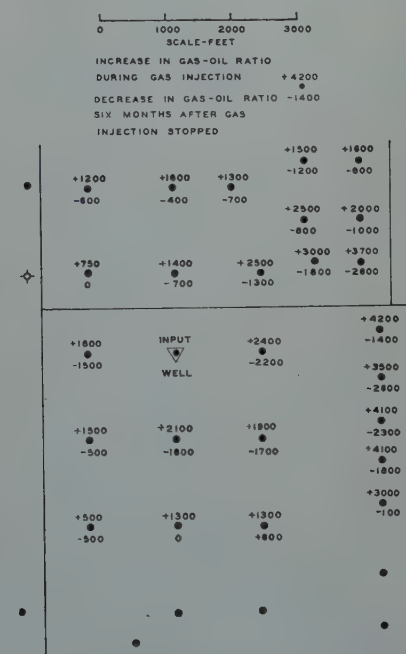


FIG. 15 — WEST TEXAS, GRAYBURG LIME GAS INJECTION EXPERIMENT.

early in pool life to reduce error involved in estimate of gas-oil ratio without gas injection.

ACKNOWLEDGMENT

The authors wish to express their thanks for these data to the companies which conducted these field tests and to Sohio Pet. Co. for permission to publish this paper.

REFERENCES

1. "Importance of Injected Gas as a Driving Medium in Limestone Reservoirs", Lloyd E. Elkins, *A.P.I. Drill. and Prod. Practice*, 1946, pp. 160-174.
2. "Evaluation of Pressure Maintenance by Internal Gas Injection in Volumetrically Controlled Reservoirs", E. Charles Patton, Jr., *AIME Trans.*, 1947, pp. 112-155.

DISCUSSION

By Ralph U. Fitting, Jr., *Fitting, Fitting & Jones, Midland, Texas.*

This paper is one for which there has been great need, as it presents additional evidence on a very important current problem. Are those limestone reservoirs which are characterized by two systems of porosity susceptible to the increase of oil recovery by gas injection? These two porosity systems are the intergranular type and the heterogeneous type; the latter being important because it tends to short-circuit fluid flow.

No one should approach this ques-

tion with the view that economics is the governing control as to feasibility; the physics of fluid flow in these porosity types is yet unsolved. Everyone should be fully aware that, as the authors state, the experience, history, and interpretation is too limited to permit valid generalities as to the effectiveness of gas injection in reservoirs of this type.

In Texas, oil operators are being confronted with the problem of the injection of gas into the oil reservoirs for the purpose of saving that gas from destruction. Yet it must be recognized that in some fields such a procedure actually results in the cycling of gas selectively through portions of the reservoir and when this occurs, no gas storage is feasible. Creation of such gas-filled layers in the reservoir allows excessive loss of solution gas, which otherwise would do effective work; such gas moves to the well bore in the zone of high gas saturation.

Furthermore, the cycling of dry gas through the reservoir may cause the reservoir oil to assume the very characteristics which pressure maintenance by gas injection is presumed to avoid. These characteristics are that the reservoir oil becomes more viscous rather than less viscous, this being due to the loss of the higher gaseous fractions in solution in that liquid into the dry gas in much the same manner as the reverse process occurs in the gasoline plant.

Certainly, the maintenance of pressure tends to nullify the pressure gradient causing vertical migration of oil

from the dense to the permeable rock. In those reservoirs where the oil volume contained in the dense rock is large as compared with that contained in the permeable rock, oil recovery could be materially affected adversely by gas introduction into the portions of the reservoir with high permeability. These adits, permitting communication of the recesses of the reservoir with the well, must be continued with high liquid saturation for as long as it is possible to do so.

Another of the problems which must be solved in this matter of gas injection is to determine at what time gas should be introduced into a limestone oil field, if ever; that is, before or after primary pressure has been depleted. This paper would evidence that total gas volume and oil viscosity, even in sandstone fields, appear to be the principal factors causing variations in the quantity of oil recovered in gas injection and that the remaining pressure of the reservoir at the time of gas injection does not appear to be important. The paper further indicates that there is no axiom that circulation through an oil reservoir of any particular volume of gas will guarantee additional oil recovery.

It is important that those people who dictate the policy practices in the oil industry understand the mounting evidence as to the experimental nature of gas injection projects in limestone reservoirs, particularly those in West Texas.

★ ★ ★

EXPERIMENTS ON THE CAPILLARY PROPERTIES OF POROUS SOLIDS

JOHN C. CALHOUN, JR., MEMBER AIME, DEPT. OF PETROLEUM ENGINEERING, UNIV. OF OKLA.
MAURICE LEWIS, JR., JUNIOR MEMBER AIME, and R. C. NEWMAN, STUDENT ASSOCIATE AIME

ABSTRACT

A report is made of experimental work performed on the capillary retention of water within porous solid systems, the displacement being accomplished with air and various organic liquids. A portion of the experiments were designed to measure the lowering of vapor pressure of water within a porous solid with subsequent conversion of such vapor pressure data to capillary pressure values. The form of the capillary pressure curve at high capillary pressures has been elucidated from this data. Certain theoretical approaches are presented to indicate the correlation between work done by previous investigators. The present work is correlated also with theory. Surface area values are calculated for the various core systems studied.

INTRODUCTION

Leverett¹ in 1941 presented a paper which gave the essential concepts of capillary behavior in porous solids. His presentation included both theoretical and experimental aspects of the problem. He defined the term "capillary pressure" and applied it to an ideal porous system. His work included the definition of a dimensionless quantity which was a function of fluid saturation and which could be correlated with porosity and permeability for clean, unconsolidated sands. His experimental work was performed by the drainage of water from packed columns of unconsolidated sands.

Subsequently, other authors have presented experimental techniques which permit the determination of capillary pressure data on small core samples. Data have been presented on porous systems other than unconsolidated sand and with the use of liquids

other than water. Notable among these are the works of Hassler, Brunner and Deahl,² Bruce and Welge,³ Amyx and Yuster,⁴ and Purcell.⁵ Others^{6,7} have indicated the applicability of such data to field problems without regard to the theoretical aspects of the capillary pressure saturation function. Within the recent published literature there have also been reported studies of the correlations between capillary pressure data and other fundamental properties of porous solids.^{8,9}

It was the intent of the present reported work to investigate the behavior noted by water and various other liquids within porous systems in an attempt to amplify existing correlations between capillary properties, surface properties, and other fundamental characteristics of porous systems. The experimental work described here was performed as two different investigations but due to its nature it is reported as separate phases of the same general topic.

CAPILLARY PRESSURE AND VAPOR PRESSURE LOWERING

It has long been recognized that the vapor pressure above the curved surface of a liquid is a function of the curvature of the liquid surface.¹⁰ The capillary pressure is also a function of the curvature of the liquid surface. Both capillary pressure values and vapor pressure lowering are, therefore, functions of the liquid saturation of a porous solid. A quantitative relationship between the vapor pressure lowering and the capillary pressure can be simply developed by considering a porous solid system containing water in equilibrium with its vapor.

The capillary pressure at any height within the system is defined as

$$P_c = P_v - P_l \quad (1)$$

where P_v is the pressure in the vapor phase and P_l is the pressure in the

liquid phase. Consider that both the water and its vapor are continuous phases within the system and that at any point the two phases are in equilibrium.

The gradients in the liquid and vapor columns within the porous system are:

$$dP_l = \rho_l g dh$$

$$dP_v = \rho_v g dh$$

By integrating these gradients from the point where $h = 0$ to the height h , values of P_l and P_v at the point h are found. Let the point where $h = 0$ be that where $P_c = 0$. At this point also P_v is equal to P_{v0} , the equilibrium vapor pressure of the liquid above a flat surface.

From the first of these integrations since ρ_l is independent of height:

$$P_l = \rho_l g h + P_{v0}$$

From the second, by substituting

$$\rho_v = \frac{P_v M}{RT}, \text{ where } M \text{ is the molecular}$$

weight:

$$\ln \frac{P_v}{P_{v0}} = \frac{M}{RT} g h$$

By combining the two last equations to eliminate h , one obtains:

$$P_l = \frac{RT}{M} \rho_l \ln \frac{P_v}{P_{v0}} - P_{v0}$$

Substituting values for P_v and P_l in equation (1) gives

$$P_c = \frac{\rho_v RT}{M} - \frac{RT}{M} \rho_l \ln \frac{P_v}{P_{v0}} - P_{v0}$$

$$\text{or } P_c = \frac{RT \rho_v}{M} \left[1 - \frac{\rho_l}{\rho_v} \ln \frac{P_v}{P_{v0}} \right] - P_{v0}$$

which is approximately

$$P_c = \frac{RT}{M} \rho_l \ln \frac{P_{v0}}{P_v} \quad (2)$$

This equation relates the vapor pressure above a curved surface with the capillary pressure across the curved surface in terms of measurable quantities. The equivalent of this equation is given by Freundlich.¹⁰

Manuscript received at office of the Branch January 24, 1949. Presented at AIME Annual Meeting, San Francisco, Calif., February 13-17, 1949.

¹References are given at end of paper.

There is much data in the literature on vapor pressures within porous solids at partial liquid saturations. Such data are often procured for adsorption measurements. To illustrate the conversion of data by equation (2), data on the adsorption of water vapor by silica gel were taken from the literature.¹¹ The data, given as pressure of adsorption versus saturation, were converted to values of P_c by equation (2). The vapor pressure curves and corresponding capillary pressure curves are shown in Fig. 1. The hysteresis loop is similar to that shown by Leverett¹ on his capillary pressure curves for unconsolidated sands.

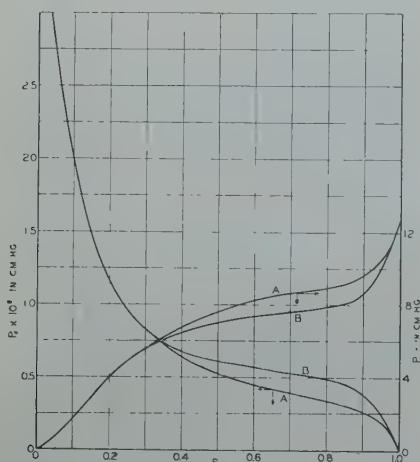


FIG. 1 — CONVERSION OF VAPOR PRESSURE DATA TO CAPILLARY PRESSURE DATA. VAPOR PRESSURE DATA FROM REFERENCE 11.

EXPERIMENTS ON VAPOR PRESSURE LOWERING

Equation (2) offered itself as a medium for evaluating capillary pressures at low saturation values and high values of the capillary pressure. With this in mind an apparatus was constructed to measure the difference in vapor pressure above a flat surface of water and that within a porous body at partial water saturation. The apparatus used is diagrammed in Fig. 2. Although it was not sufficiently sensitive to detect small changes in vapor pressure, it sufficed to give accuracy over the range of saturation. The porous media employed were composed of consolidated quartz. They were manufactured in the laboratory by consolidating sand grains with silica by deposition from colloidal suspension and by the hydrolysis of tetraethyl orthosilicate. The sand grains before consolidation were in the sieve

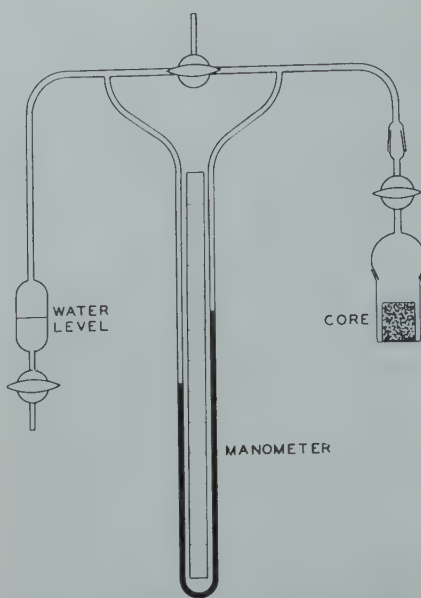


FIG. 2 — DIAGRAMATIC SKETCH OF APPARATUS FOR MEASURING VAPOR PRESSURE LOWERING.

range, 140-170.

Data were taken on four separate cores. They were first saturated fully with water and by the use of a conventional type capillary pressure cell

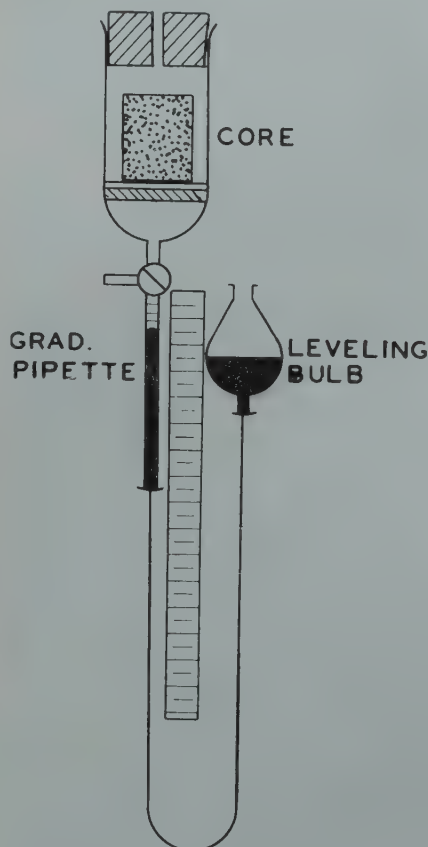


FIG. 3 — DIAGRAMATIC SKETCH OF APPARATUS FOR MEASURING CAPILLARY PRESSURES BY DISPLACEMENT.

(shown in Fig. 3) the capillary pressure curve for each core was determined in a routine fashion. The core was then placed in the vapor pressure apparatus, maintained at a constant temperature of 97°F., where further desaturation was accomplished by evacuating water vapor from the core side of the system. After sufficient evacuation had taken place, the system was closed and allowed to come to equilibrium, after which the manometer read directly the amount of vapor pressure lowering. Saturations were determined by removing and weighing that portion of the assembly which contained the core. It was necessary after each weighing to purge the apparatus of the air which entered when the assembly was unjoined for the weighing.

Both the routine capillary pressure data and the vapor pressure lowering data are given in Table 1. In Fig. 4 are plotted curves which show the data taken by the customary method of obtaining capillary pressures for the cores listed in Table 1 and for several other similar cores. The curves of Figs. 5, 6 and 8 show the capillary pressure data calculated from the vapor pressure data shown in Fig. 4. The logarithm scale is used to permit showing the high values and at the same time showing the lower plateau region. One experimental point on two of these curves was determined neither with the apparatus of Fig. 2 nor Fig. 3 but by means of an applied air pressure above

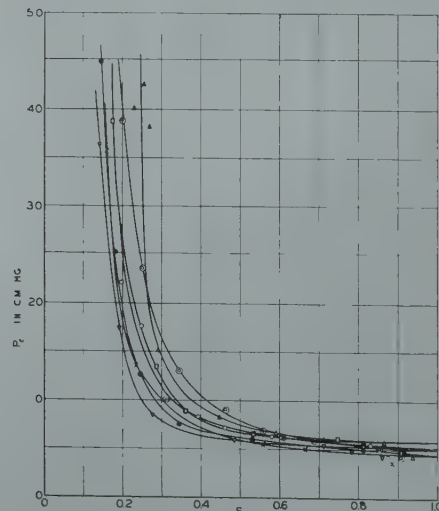


FIG. 4 — CAPILLARY PRESSURE CURVES WITH AIR DISPLACEMENT; ○ CORE NO. 2; ▽ CORE NO. 3; □ CORE NO. 5; ● CORE NO. 6; ▢ CORE NO. 8; △ CORE NO. 9; X CORE NO. 10.

TABLE 1
Capillary Pressure Data by Routine Displacement and by
Vapor Pressure Lowering

Core #2 K=2100 md. $\phi=0.322$			Core #3 K=855 md. $\phi=0.291$			Core #6 K=760 md. $\phi=0.279$			Core #8 K=3000 md. $\phi=0.321$		
S_w	P_{vo}/P_v	P_c Cm Hg	S_w	P_{vo}/P_v	P_c Cm Hg	S_w	P_{vo}/P_v	P_c Cm Hg	S_w	P_{vo}/P_v	P_c Cm Hg
0.830		5.43	0.712		5.38	0.811		5.05	0.856		5.19
0.603		6.19	0.486		5.93	0.530		6.02	0.691		5.89
0.578		6.34	0.276		8.48	0.343		7.51	0.558		6.86
0.459		7.05	0.192		17.46	0.246		12.60	0.464		8.99
0.394		8.26	0.142		36.4	0.181		25.3	0.346		13.0
0.361		8.85	0.0962	1.052	5,430	0.146		45.0	0.252		23.6
0.315		9.93	0.0744	3.289	127,000	0.103		305.0	0.201		38.8
0.248		17.6	0.0668	4.367	158,000	0.144	1.101	10,250	0.121		305.0
0.197		22.1	0.0560	6.369	198,000	0.079	3.344	129,000	0.0909	1.337	31,000
0.0667	1.304	28,350	0.0533	11.111	257,000	0.069	4.796	168,000	0.0798	1.782	61,900
0.0549	2.016	75,000	0.0407	20.833	325,000	0.058	7.692	217,000	0.0676	2.941	116,000
0.0527	2.066	77,500				0.0536	9.709	243,000	0.0570	3.922	147,000
0.0493	2.155	82,000				0.0479	19.157	316,000	0.0496	5.917	191,000
						0.0382	28.903	360,000	0.0487	9.346	239,000
						0.0325	37.313	387,000	0.0375	10.526	252,000
									0.0319	24.096	340,000

a diaphragm on which the core was placed. These are the data at approximately 300 cm. Hg. on cores No. 6 and No. 8.

Although no overlap of data between the vapor pressure method and the

routine displacement was procured, the data give, in each case, continuous curves from one hundred per cent saturation to zero saturation.

A significant point to this correlation is that there is, strictly speaking, no

absolute irreducible minimum of saturation. All of the curves turn into the zero saturation axis at a finite positive capillary pressure. Fig. 9 shows an expanded plot of the capillary pressures in the lower saturation region as calculated from the vapor pressure data. Within the range of average reservoir pressures, however, there is a saturation plateau, which from a practical view point is equivalent to an irreducible minimum. However, this plateau is reached at capillary pressures somewhat above those normally taken as the maximum in routine laboratory work. From Fig. 4, for example, on all cores it appears that the irreducible minimum saturation would be approximately that saturation shown at the highest capillary pressure, which is about 45 cm. Hg. As shown by Figs. 5 to 8, however, all of these cores at a capillary pressure of 45 cm. Hg. are several per cent away from the saturation plateau.

DISPLACEMENT WITH VARIOUS LIQUIDS

It is common to use the capillary displacement of water by air as a measure of the connate water content of a given reservoir material. Following Leverett's presentation of capillary pressure in the form

$$P_c = \delta \sqrt{\frac{\Phi}{K}} J(S_w) \quad (3)$$

it has been suggested that, with two different displacing fluids, the ratio of capillary pressures for a given value of water saturation would be the ratio of the δ values. Work with systems other than air-water have been reported by several authors. Hassler, et al³ did not find a constant ratio as expected. Purcell,⁵ whose work was done with mercury, gives good correlations between capillary pressure curves with water and with mercury using a ratio of $\delta \cos \theta$ values rather than a ratio of δ values. Bruce and Welge³ give a series of different irreducible water saturations using air and oil displacement.

In the present work several different pure liquids were used to displace distilled water from three of the laboratory prepared silica porous bodies. Liquids used were toluene, benzene, cyclohexane, tetradecane, and oleic acid. Air was used as a displacing medium as

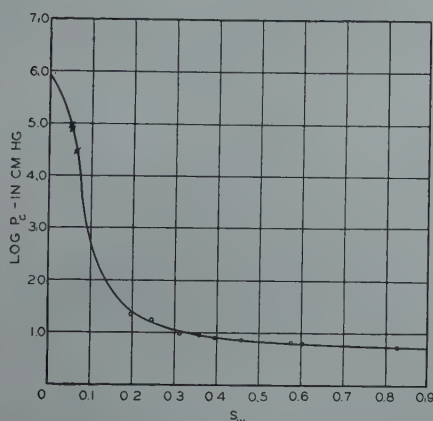


FIG. 5—CAPILLARY PRESSURE DATA CORE NO. 2. ○ DETERMINED BY DISPLACEMENT; ● DETERMINED BY VAPOR PRESSURE LOWERING.

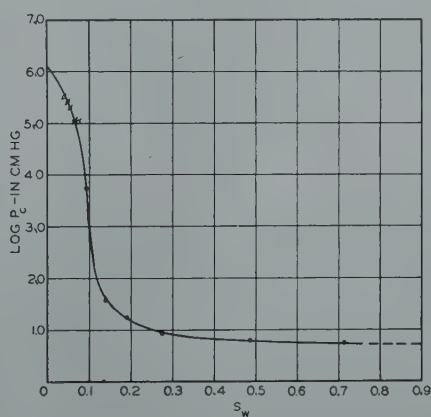


FIG. 6—CAPILLARY PRESSURE DATA CORE NO. 3. ○ DETERMINED BY DISPLACEMENT; ● DETERMINED BY VAPOR PRESSURE LOWERING.

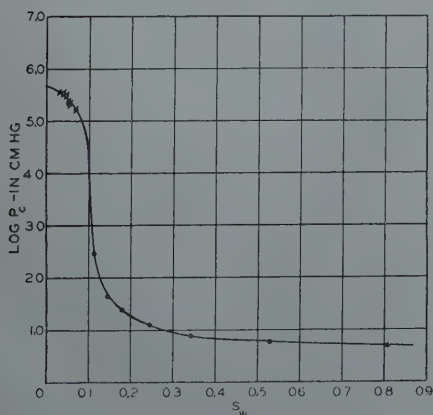


FIG. 7—CAPILLARY PRESSURE DATA CORE NO. 6. ○ DETERMINED BY DISPLACEMENT; ● DETERMINED BY VAPOR PRESSURE LOWERING.

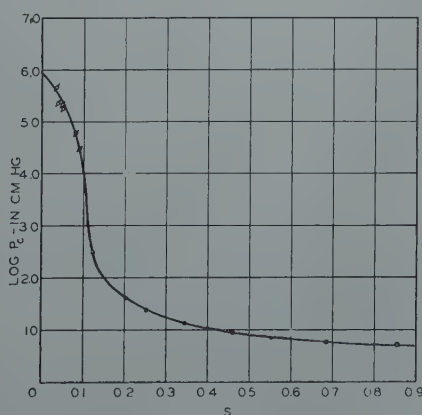


FIG. 8—CAPILLARY PRESSURE DATA CORE NO. 8. ○ DETERMINED BY DISPLACEMENT; ● DETERMINED BY VAPOR PRESSURE LOWERING.

TABLE 2
Capillary Pressure Data Obtained by Displacement with Various Fluids
Core 1—L K = 1.22 Darcys $\phi = .249$

Air		Tetradecane		Oleic Acid		Toluene		Benzene		Hexane	
P _c Cm Hg	S _w	P _c Cm Hg	S _w	P _c Cm Hg	S _w	P _c Cm Hg	S _w	P _c Cm Hg	S _w	P _c Cm Hg	S _w
1.6	98.01	0.5	98.80	0.2	99.08	1.7	88.1	0.8	99.19	1.43	98.89
2.7	96.46	1.4	93.38	0.3	96.63	2.1	76.0	1.3	96.60	1.74	90.11
3.4	91.22	2.1	84.4	0.7	91.73	2.4	57.7	1.4	91.68	2.14	77.20
4.2	79.0	2.4	71.7	0.9	82.9	2.7	44.7	1.5	88.9	2.54	68.80
5.1	68.3	2.7	56.3	1.0	64.5	3.0	33.3	1.6	83.7	3.40	47.30
6.2	41.6	3.4	36.1	1.3	45.8	4.1	30.0	1.7	80.6	5.65	45.20
8.6	24.7	4.7	23.3	1.6	32.4	5.8	28.8	1.9	72.2	14.4	39.50
15.4	22.9	8.1	21.4	2.0	26.0	9.8	28.0	2.0	70.4	14.7	40.20
23.9	20.3			7.7	19.9	15.8	22.3	2.1	67.3	15.2	41.00
						16.0	22.6	2.2	65.4	15.7	42.10
								2.7	62.0	16.3	43.00
								2.9	58.0	16.6	43.60
								3.4	55.0	16.5	43.30
								7.3	54.3	16.7	43.90
								23.9	53.7	16.6	43.90
										16.8	44.20

TABLE 3
Capillary Pressure Data Obtained by Displacement with Various Fluids
Core 2—L K = 1.83 Darcys $\phi = .251$

Air		Tetradecane		Oleic Acid		Cyclohexane		Toluene	
P _c Cm Hg	S _w	P _c Cm Hg	S _w	P _c Cm Hg	S _w	P _c Cm Hg	S _w	P _c Cm Hg	S _w
1.7	96.25	0.4	98.82	0.6	92.88	0.5	98.10	0.8	98.16
3.2	83.7	1.1	97.04	0.7	85.9	0.7	92.66	1.0	92.61
3.5	72.8	1.3	89.1	0.9	59.9	1.0	80.5	1.5	79.1
3.8	56.7	1.6	77.5	1.0	47.0	1.2	69.1	1.6	67.2
4.1	45.9	2.2	62.2	1.2	30.0	1.6	51.3	2.2	51.5
4.4	36.6	2.7	39.0	2.3	22.8	2.1	40.8	2.5	41.4
4.9	27.7	3.4	29.6	5.4	20.2	2.2	33.6	4.9	28.2
8.4	21.8	5.8	25.0	10.0	19.7	3.5	25.5	7.2	27.7
14.2	20.9	10.1	20.5			5.3	21.6	16.0	25.9
14.4	20.4	15.6	19.3			10.2	20.0	24.3	25.7
		20.6	18.0			16.9	19.0		
						16.7	18.5		

TABLE 4
Capillary Pressure Data Obtained by Displacement with Various Fluids
Core 3—L K = 1.11 Darcys $\phi = .258$

Air		Tetradecane		Oleic Acid		Hexane	
P _c Cm Hg	S _w	P _c Cm Hg	S _w	P _c Cm Hg	S _w	P _c Cm Hg	S _w
0.8	98.40	0.6	99.04	0.7	91.60	0.1	99.08
1.8	97.69	1.9	95.20	0.75	77.4	2.2	94.20
3.2	95.13	2.5	72.7	1.1	61.5	3.0	83.4
5.0	79.6	3.8	51.7	1.3	48.8	3.5	70.8
5.7	66.6	4.3	33.4	2.2	35.2	3.8	56.7
6.9	44.9	6.0	24.5	2.9	26.6	4.2	41.3
8.8	33.3	8.0	19.0	4.9	20.7	4.4	35.0
12.1	20.5	12.1	18.0	7.3	18.7	6.9	27.2
15.9	19.8	17.4	17.1			14.5	25.8
25.3	16.6					14.7	26.5
						15.2	27.5
						16.1	28.9
						17.0	30.8

well. Saturations were determined by the volumetric measurement of the amount of displaced saturant in an apparatus similar to that shown in Fig. 3. The results of these tests are given graphically in Figs. 10, 11 and 12. Tables 2, 3 and 4 list the data taken in chronological sequence. Not shown in these tables are several duplicate runs made with several of the displacing liquids.

The irreducible water saturations which were attained were approximately

equivalent on each core with the exceptions of benzene displacement on core 1-L, toluene displacement on cores 1-L and 2-L, and hexane displacement on cores 1-L and 3-L. There is some basis for believing that these apparently high values were due to faulty technique because there was on some of these particular tests an apparent regression of the desaturation process. It could also be true that the apparently high values of saturation found by displacement with these fluids is a manifestation of a

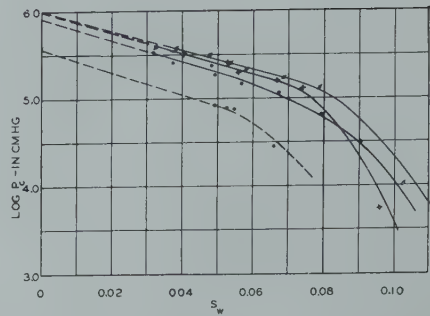


FIG. 9—EXPANDED PLOT SHOWING CAPILLARY PRESSURES AT EXTREMELY HIGH VALUES.

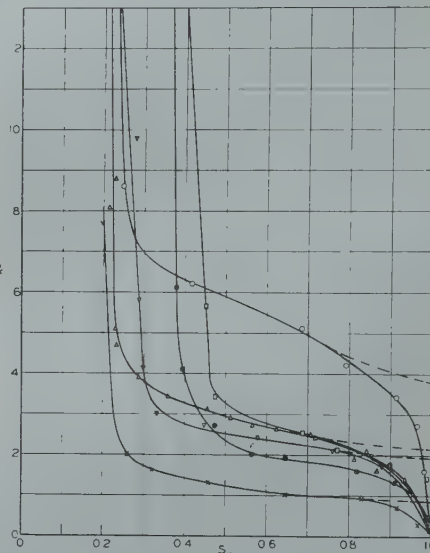


FIG. 10—CAPILLARY PRESSURE CURVES CORE NO. 1-L; DISPLACEMENT OF WATER WITH VARIOUS FLUIDS. ● AIR; △ TETRADECANE; x OLEIC ACID □ HEXANE; ▽ TOLUENE; ● BENZENE.

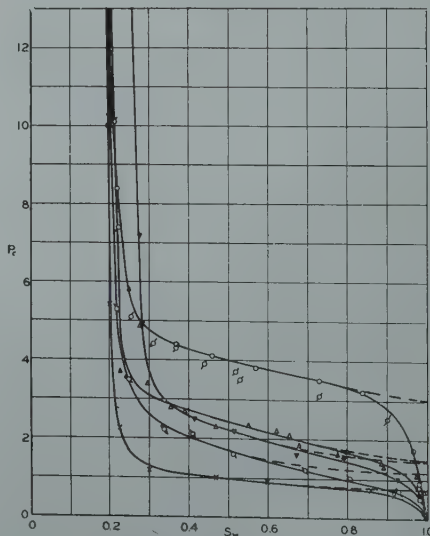


FIG. 11—CAPILLARY PRESSURE CURVES CORE NO. 2-L. DISPLACEMENT OF WATER WITH VARIOUS FLUIDS; ● AIR, FIRST RUN; ○ AIR, SECOND RUN; △ TETRADECANE; x OLEIC ACID; ◇ CYCLOHEXANE; ▽ TOLUENE.

true characteristic of these core systems.

Interfacial tensions between water and the various liquids were measured with the du Nouy tensiometer and values were also taken from the International Critical Tables. This data is given in Table 5. It is apparent from these measurements that impurities may have been present in some of the liquids which were employed.

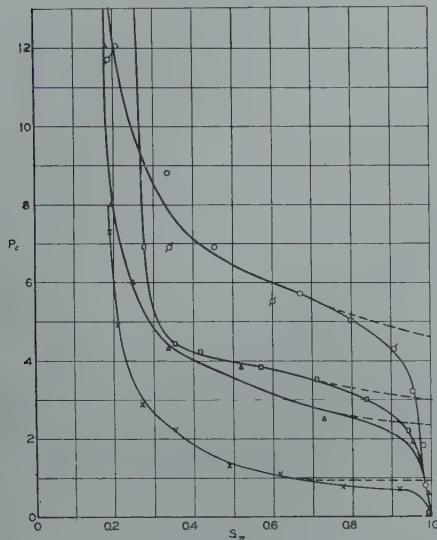


FIG. 12—CAPILLARY PRESSURE CURVES CORE NO. 3-L. DISPLACEMENT OF WATER WITH VARIOUS FLUIDS; ○ AIR; FIRST RUN; □ AIR, SECOND RUN; □ HEXANE; △ TETRADECANE; × OLEIC ACID.

For a given water saturation, values of capillary pressure with air displacing divided by the values for liquid displacing were always greater than unity. These ratios are shown in Figs. 13 and 14. The dotted lines on the graphs show the ratios of the interfacial tension for air against water to

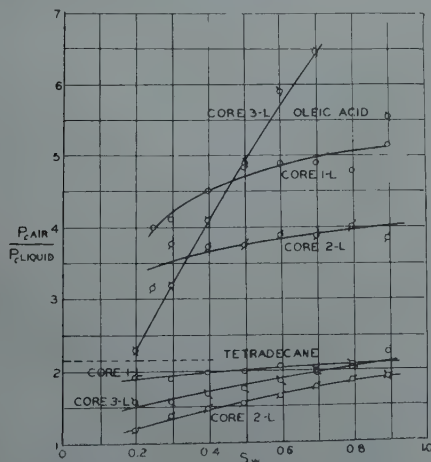


FIG. 13—RATIO OF EXPERIMENTAL CAPILLARY PRESSURES AND COMPARISON WITH INTERFACIAL TENSION RATIOS.

Consecutive Readings	Liquid System					
	δ Water-Air	δ Water-Tetradecane	δ Water-Toluene	δ Water-Benzene	δ Water-Oleic Acid	δ Water-Hexane
1.....	70.2	32.5	26.3	24.6	8.5	45.7
2.....	70.0	31.7	26.2	24.6	8.5	45.6
3.....		31.7	25.9	25.4	8.4	45.8
4.....		31.4	25.7	23.7	7.2	45.1
5.....		31.4	25.7	23.6	7.8	46.5
6.....						45.7
7.....						21.5
8.....						13.7
9.....						14.4
10.....						13.8
11.....						12.6
12.....						11.5
13.....						9.8
14.....						9.2
15.....						8.8
International Critical Tables.....			36.1 (25°C.)	35.00 (25°C.)	15.59 (20°C.)	51.1 (25°C.)
						9.4

that of the given liquid against water. In some instances, there is excellent agreement between the measured ratios and theoretical ratios, in particular, hexane on core No. 3-L, benzene on core No. 1-L and tetradecane on core No. 1-L. In the majority of instances, although the ratios at 100% saturation are near the expected theoretical values the ratios show a decrease as desaturation proceeds. There is no readily apparent explanation for this drop in ratio.

Theoretical Correlations:

In recent publications it has been suggested, and the suggestions have been supported to a certain degree by experimental data, that definite correlations can be obtained between various fundamental measurable quantities of porous bodies. Purcell⁵ has offered the

following equation to compute the permeability from capillary pressure data:

$$K = \frac{F \delta^2 \Phi \cos^2 \theta}{2} \int_0^{1.0} \frac{dS_w}{P_c^2} \quad (4)$$

Rose⁸ has developed certain relative permeability concepts on the basis of the Kozeny equation which he gives as:

$$K = \frac{\Phi}{A^2 t} \quad (5)$$

Rose furthermore states that from Leverett's $J(S_w)$ function the following is true:

$$\lim_{S_w \rightarrow 1.0} J(S_w) = \left(\frac{1}{t} \right)^{1/2} \quad (6)$$

The $J(S_w)$ function as given by Leverett is equation (3). To extend its applicability to all liquids it is now written as:

$$J(S_w) = \frac{P_c}{\delta \cos \theta} \sqrt{\frac{K}{\Phi}} \quad (7)$$

The value of the capillary pressure as the saturation approaches unity is the displacement pressure, P_d . At this limit, equation (7) is:

$$J(S_w)_{1.0} = \frac{P_d}{\delta \cos \theta} \sqrt{\frac{K}{\Phi}}$$

This can be rearranged to give an expression for the permeability. Thus:

$$K = \frac{[J(S_w)_{1.0}]^2 \Phi \delta^2 \cos^2 \theta}{P_d^2} \quad (8)$$

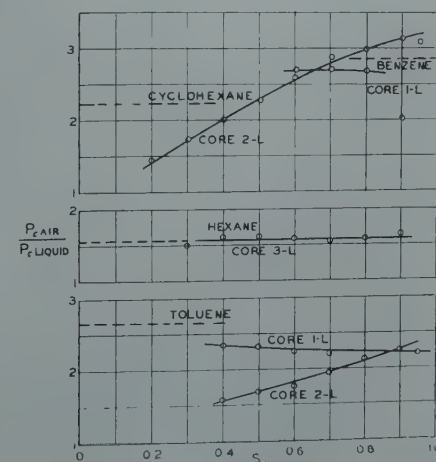


FIG. 14—RATIO OF EXPERIMENTAL CAPILLARY PRESSURES AND COMPARISON WITH INTERFACIAL TENSION RATIOS.

Comparing equations (8) and (5) and considering equation (6) the following equality is found:

$$A^2 = \frac{P_D^2}{\delta^2 \cos^2 \theta}$$

For a straight bore capillary this equality is known to be true. A is defined as the surface area per unit of pore space which, for a capillary of radius R and length L, would be:

$$A = \frac{2 \pi R L}{\pi R^2 L} = \frac{2}{R}$$

The displacement pressure is, in terms of R:

$$P_D = \frac{2 \delta \cos \theta}{R} = A \delta \cos \theta \quad (9)$$

which is the equation given above.

Comparing equation (8) with equation (4) gives the following equality:

$$\frac{F}{2} \int_0^{1.0} \frac{dS_w}{P_c^2} = \frac{[J(S_w)_{1.0}]^2}{P_D^2} \quad (10)$$

An examination of the data presented in this report leads to the conclusion that:

$$\frac{1}{P_D^2} = 2 \int_0^{1.0} \frac{dS_w}{P_c^2} \quad (11)$$

which then produces the equalities that follow:

$$F = 4[J(S_w)_{1.0}]^2 \quad (12)$$

or $F = \frac{4}{t}$
and also

$$\frac{1}{A^2} = 2\delta^2 \cos^2 \theta \int_0^{1.0} \frac{dS_w}{P_c^2} \quad (13)$$

Equation (11) is given as a result of observations made on the data given in Tables 1, 2, 3 and 4. There is no readily apparent theoretical basis for the relationship. In examining the data of Table 7 for air displacement only, the capillary pressure curves were converted to plots of the reciprocal of P_c^2 versus S_w similar to that of Figure 15. These were then planimetered to obtain the values of the integral and from the relationship of equation (11) values of P_D were calculated. Values of the integral and P_D values are listed in Table 6. Comparison is also given in Table 6 between the calculated values of P_D and those read from the curves of Fig. 4 by extrapolation to a saturation of 1.0.

TABLE 6

Core No.	Displacing Fluid	$\int_0^{1.0} \frac{dS_w}{P_c^2}$ Cm ⁻²	Calc. P_D Cm Hg	Observed P_D Cm Hg	A Cm ² /Cm ³	A (Carman Method) Cm ² /Cm ³
2.....	Air	.0186	5.18	5.20	960	840
3.....	Air	.0223	4.72	5.15	872	1120
5.....	Air	.0181	5.25	5.30	970	1125
6.....	Air	.0228	4.68	4.60	866	1115
8.....	Air	.0172	5.40	4.70	998	705
9.....	Air	.0158	5.62	5.80	1,040	920
10.....	Air	.0252	4.45	4.50	823	364

TABLE 7

Core No.	Displacing Fluid	$\int_0^{1.0} \frac{dS_w}{P_c^2}$ Cm ⁻²	Calc. P_D Cm Hg	Calc. $\delta \cos \theta$ dynes/cm	A Cm ² /Cm ³
1-L.....	Air.....	.0278	4.25		785
	Tetradecane.....	.109	2.14	36.2	
	Oleic Acid.....	.710	0.84	14.25	
	Toluene.....	.139	1.90	32.2	
2-L.....	Air.....	.056	2.99		554
	Tetradecane.....	.228	1.48	35.6	
	Oleic Acid.....	.890	0.75	18.0	
	Toluene.....	.234	1.46	35.1	
3-L.....	Cyclohexane.....	.362	1.18	28.3	854
	Air.....	.023	4.62		
	Tetradecane.....	.090	2.35	36.6	
	Oleic Acid.....	.560	0.945	14.7	
	Hexane.....	.056	2.99	46.5	

The data of Tables 2, 3 and 4 were also replotted to give curves similar to Fig. 15. Agreement with equation (11) was obtained for this data by noting the values of P_D which balanced the equation. The values are given in Figs. 10, 11 and 12. On these graphs the dashed lines are drawn to indicate the curve which satisfies equation (11). In Table

7 are listed the integral values and the calculated values of P_D . The values of $\delta \cos \theta$ in Table 7 were obtained from the calculated values of P_D by reference to the value of P_D for air displacing water, in which case the contact angle was assumed to be zero.

It is of interest to note that the values of $\delta \cos \theta$ are in good agreement with the previously tabulated value of δ . The fact that the agreement is close indicates that in every instance the contact angle was probably zero or approximately zero.

The internal surface area of the porous bodies was found by equation (9). Calculated values of P_D and $\delta \cos \theta$ were used rather than the experimental values for this determination. The surface area values so found are given in Tables 6 and 7.

It is possible also to determine the internal surface area from the vapor pressure data which was taken. The following equation is given without derivation as being applicable to the adsorption of a liquid within a porous material:¹²

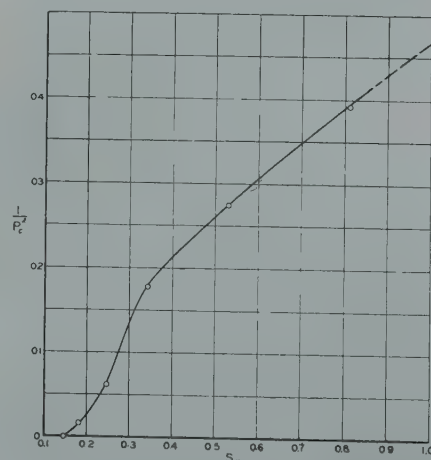


FIG. 15 — TYPICAL GRAPH FOR DETERMINATION OF

$$\int_0^{1.0} \frac{dS_w}{P_c^2}$$

$$\frac{P_v}{V(P_{vo} - P_v)} = \frac{1}{V_m C} + \frac{C-1}{V_m C} \frac{P_v}{P_{vo}} \quad (14)$$

where V_m = the volume of water adsorbed in a single layer on the entire porous surface.

V = the volume of water adsorbed at the pressure, P_v

P_{vo} = the vapor pressure of water above a flat surface

C = a constant.

Thus, by plotting the obtained vapor pressure data in the form of equation (14) the slope and intercept of the expected linear plot will suffice to calculate V_m . A knowledge of the space covered by a single water molecule suffices then to calculate the surface area covered. Figs. 16, 17 and 18 show the adsorption data for three cores as given in Table 1 plotted according to equation (14), using weights of water adsorbed in place of volumes. Assuming that one water molecule covers an area of 11.5×10^{-16} cm², the total surface is calculated in the three instances as 204, 228, and 172 square meters per cubic centimeter of void space. Values for the surface area as given in Table 6 for these cores are 872, 866, and 998 square centimeters per cubic centimeter of void space. The latter values are more in agreement with that which would be expected for uniformly packed spheres than are the former.

A third method of obtaining the internal surface area of these core specimens would be by use of the relationship:

$$A = \frac{-1}{\delta_{S-W} - \delta_{S-A}} \int_0^{1.0} P_c dS_w \quad (15)$$

Leverett¹ has given the free surface energy change per unit of pore volume between two different saturations of the same core as:

$$\Delta F = - \int_{S_{w1}}^{S_{w2}} P_c dS_w$$

By choosing the limits of saturation as zero and one hundred per cent the surface energy change is:

$$\Delta F = A\delta_{S-W} - A\delta_{S-A}$$

because the unit free surface energy when the core is dry is δ_{S-A} and the unit free surface energy when the core is fully saturated is δ_{S-W} . Combining the two expressions for ΔF gives equation

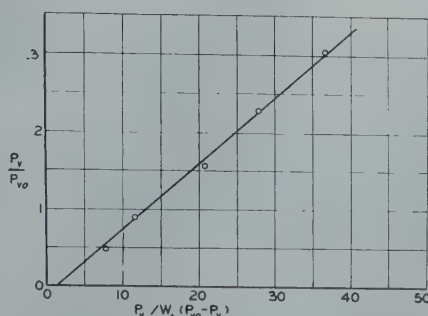


FIG. 16 — VAPOR PRESSURE DATA PLOTTED AS WATER ADSORPTION FOR DETERMINATION OF SURFACE AREA. CORE NO. 3.

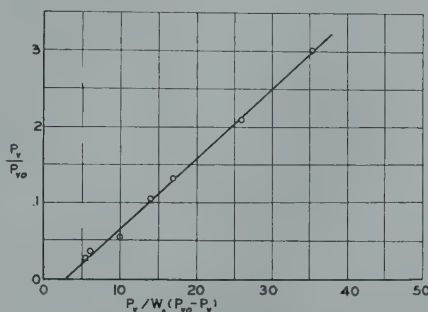


FIG. 17 — VAPOR PRESSURE DATA PLOTTED AS WATER ADSORPTION FOR DETERMINATION OF SURFACE AREA. CORE NO. 6.

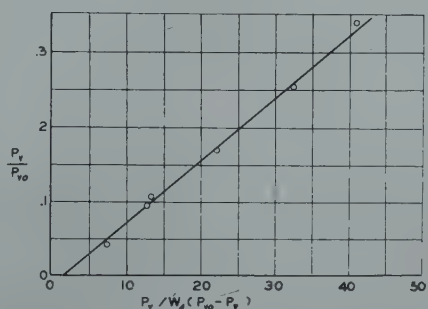


FIG. 18 — VAPOR PRESSURE DATA PLOTTED AS WATER ADSORPTION FOR DETERMINATION OF SURFACE AREA. CORE NO. 8.

(15). This equation cannot be used to solve for A because the interfacial tension values are not known. It could be used to obtain the difference in the interfacial tensions if A and the value of the integral were known. This has been done for cores Nos. 3, 6 and 8, for which the capillary pressure function is complete from zero to full saturation. A choice of the most logical A value was necessary for this calculations. Using the values obtained from the vapor pressure data yields values of $(\delta_{S-A} - \delta_{S-W})$ of 214, 204, and 206 dynes per centimeter. Using the lower values of A would have given negligible differences.

Bartell¹³ has defined the above difference in interfacial tensions as the adhesion tension and for the system

silica-water he gives the value of $(\delta_{S-A} - \delta_{S-W})$ to be 75.1 dynes per centimeter. It would appear from this that the A values as calculated by the adsorption method were too large.

Carman has evaluated the surface area of powders by a method based upon permeability and porosity measurement, a discussion of which method is given by Brunauer¹². Using this method and the experimentally determined porosity and permeability values specific surface areas were calculated. These are listed in Table 6. It will be noted that they do not agree numerically with A values calculated from P_D but the two are comparable in magnitude.

It is apparent that two different surface area values are being measured. So far as flow properties and total void space are concerned the roughness of the internal surfaces will not be apparent. With the measurement of wettability and adsorption phenomena the intricacies of the surface will be apparent. The adsorption measurement should give the higher values of A where there is roughness or etching of the internal surfaces. In the particular measurements reported here the porous bodies were prepared by consolidating sand grains by depositing silica from colloidal suspension and by the hydrolysis of tetraethylorthosilicate. This deposition is in the form of fine flaky particles, a condition which would enhance the amount of surface area which would be evident from a wettability or adsorption measurement.

SUMMARY AND CONCLUSIONS

The experiments reported here lead one to the conclusion that for the practical purpose of obtaining connate water values by capillary pressure curves, caution should be used in choice of a displacing liquid. The experiments demonstrate the desirability of determining such values at a maximum pressure which is a considerable distance above the capillary pressure plateau. From a strictly theoretical standpoint the experiments indicate that there is no "irreducible minimum" and that zero water saturation is reached at some finite value of capillary pressure.

The possible usefulness of vapor pressure measurements or adsorption

data to give characteristics of porous reservoir materials has been outlined. Good agreement was obtained between capillary pressure data by displacement and that calculated from the vapor pressure data.

Following the lead of previous authors, the capillary pressure data have been used to characterize the individual porous systems. It has been shown that the displacement pressure bears a defi-

nite relationship to $\int \frac{d S_w}{P_c^2}$.

Surface area values were calculated from the displacement pressures, from the adsorption data and from the Carman equation. It is apparent that difference quantities are being measured by the different methods.

ACKNOWLEDGMENTS

The experimental work which is reported in this paper was performed by Mr. Newman and Mr. Lewis while they were graduate students in Petroleum Engineering at the University of Oklahoma. Further details of their work is embodied in the theses which they submitted in partial fulfillment of requirements for the Master's degree. During this period Mr. Newman held the Phillips Petroleum Company Fellowship in Petroleum Engineering and Mr. Lewis held the Shell Oil Company Fellowship in Petroleum Engineering. The authors wish to express their deep appreciation for this support, without which their work would have been seriously curtailed.

NOMENCLATURE

P_c	= Capillary pressure
P_D	= Displacement pressure
P_v	= Vapor phase pressure at equilibrium
P_{v0}	= Equilibrium vapor pressure above a flat liquid surface
P_l	= Liquid phase pressure at equilibrium
ρ_v	= Vapor phase density
ρ_l	= Liquid phase density
h	= Height above a free water surface
M	= Molecular weight
R	= Gas constant
T	= Temperature of porous solid system
Φ	= Porosity as a fraction
K	= Permeability
S_w	= Water saturation, fractional
δ	= Interfacial tension
δ_{S-A}	= Interfacial tension, silica air
δ_{S-W}	= Interfacial tension, silica water
θ	= Contact angle
ΔF	= Free surface energy change per unit pore volume
A	= Internal surface area
F	= Lithology factor as defined by Purcell
t	= Tortuosity constant in Kozeny equation

REFERENCES

1. Leverett, M. C., "Capillary Behavior in Porous Solids," *Trans. AIME*, 142, (1941), 152-169.
2. Hassler, G. L., Brunner, E., and Deahl, T. J., "The Role of Capillarity in Oil Production," *Trans. AIME*, 155 and 160. Reprint (1944-1945), 153-172.
3. Bruce, W. A., and Welge, H. J., "Restored State Method for Determination of Oil in Place and Connate Water," *Oil and Gas Journal*, 156, No. 21 (July, 1947), 223-238.

4. Amyx, J. W., and Yuster, S. T., "Capillary Pressure in Secondary Recovery," *Producer's Monthly*, 11, No. 2 (December, 1946), 10-13.
5. Purcell, W. R., "Capillary Pressures—Their Measurement Using Mercury and the Calculation of Permeability Therefrom," *Int. Petr. Tech.* 1, No. 2, (February, 1948).
6. Thornton, O. F., and Marshall, D. L., "Estimating Interstitial Water by the Capillary Pressure Method," *Trans. AIME*, 170, (1947), 69-80.
7. McCullough, J. J., Albaugh, F. W., and Jones, P. H., "Determination of the Interstitial-Water Content of Oil and Gas Sand by Laboratory Tests of Core Samples," *API Drilling and Production Practice*, (1944), 180-188.
8. Rose, Walter, Theoretical Generalizations Leading to the Evaluation of Relative Permeability," presented at Petroleum Division, AIME, meeting at Dallas, Texas, October 4-5-6, 1948.
9. Popovich, M. J., "A Study of the Relationship Between Grain Size and Capillary Pressure Curves," *Producer's Monthly*, 11, No. 12 (October, 1947), 27-43.
10. Freundlich, H., *Colloidal and Capillary Chemistry*, E. P. Dutton and Co., New York, 1926.
11. Anderson, J. S., *Zeitschrift Physical Chemistry* 88, 191, 1914.
12. Brunauer, S., *The Adsorption of Gases and Vapors, Volume I, Physical Adsorption*, Princeton, 1945, p. 303.
13. Bartell, F. E., and Benner, F. C., *Adsorption at Solid-Liquid Interfaces*. Fundamental Research on Occurrence and Recovery of Petroleum, 1943, p. 94. ★ ★ ★

FACTORS INVOLVED IN REMOVAL OF SULPHATE FROM DRILLING MUDS BY BARIUM CARBONATE

W. E. BERGMAN, H. B. FISHER, AND P. G. CARPENTER, MEMBER AIME
PHILLIPS PETROLEUM CO., RESEARCH DEPARTMENT, BARTLESVILLE, OKLA.

ABSTRACT

The conditions under which barium carbonate can be used to remove sulfates from drilling muds are limited. The amount of sulfate remaining in solution in the system after treatment with barium carbonate is shown to be a function of the concentration of the carbonate and barium ions and the concentration of other electrolytes. Barium hydroxide may advantageously replace barium carbonate when the contamination is not entirely due to anhydrite (calcium in the system is then stoichiometrically less than sulfate) or when the carbonate concentration is high. The effect of substances such as quebracho, phosphates, and chromates, which form complexes or precipitates with barium, is discussed.

INTRODUCTION

As the complexity of the operations in drilling for oil has increased, more attention has of necessity been directed to the problems pertaining to the maintenance of good drilling mud properties. As a result, chemical treatment of muds has become an important factor in recent years. Some of these treatments have been designed to eliminate the deleterious effects of contaminants in aqueous mud systems by precipitation or other means. The most common of substances encountered during drilling include sodium chloride, cement, and calcium sulfate while various other contaminants, usually in small amounts, may be introduced from the water, clays, and other materials used in preparation of the mud. In certain cases, for example where continued salt-water flow is encountered or massive anhydrite is drilled, special muds may be used so that the physical properties of the mud will remain satisfactory for drilling. In other cases, it is desirable to remove the contaminants so that soluble electrolytes in the system are maintained at low values.

For sulfate contamination, the common practice in the field is to add barium carbonate to precipitate the sulfate as barium sulfate^{1,2}. Ordinarily such a procedure gives satisfactory results. There have been important instances, however, where addition of barium carbonate was not effective in removal of soluble sulfates from drilling muds, and it is to these cases that the present paper is directed.

While it is generally known that barium carbonate is not always effective in removing soluble sulfates from drilling muds, certain inconsistencies appear in the literature as to the limitations of its use, and little explanation for the limitations are given. Varnell and Kimbrell³ state that "the treatment (with barium carbonate for removal of sulfate) is simple and

consists in maintaining a pH of 9 with caustic soda and quebracho." They caution that concentrations of quebracho greater than 1 lb./bbl. may inhibit the reaction. In another publication⁴, a pH of 10.5 is considered "the maximum desirable," and the indication is that as much as 2.5 lb. quebracho per barrel may be present in the particular mud under discussion. Lancaster and Mitchell⁵ state that appreciable amounts of phosphates in the mud will inhibit the reaction with barium carbonate and that the phosphate treatment should be discontinued at least 24 hours before addition of the carbonate.

Experimental work was initiated to ascertain the factors involved in using barium carbonate for the removal of sulfate contamination in drilling muds. While the experimental data herein reported are limited, they focus attention on the pertinent factors which must be considered for successful treatment. These factors are discussed from a practical and a theoretical view, the latter being supported by equilibrium data found in the literature. Further, it will be appreciated that the factors involved in this specific study will be closely analogous to those in certain of the other chemical treatments which involve a precipitation of the soluble contaminant. A thorough comprehension of these factors should result in a more fruitful application of this type of chemical reaction to the treatment of drilling muds.

EXPERIMENTAL

A. Reagents

Two muds were used during this investigation. For one series of tests, bentonite suspensions were prepared by dilution of a stock suspension containing 8 per cent by weight of bentonite (Aquagel). For another series, a 6.4 per cent bentonitic mud weighted to 9.7 lb./gal. with barium sulfate (Magcobar) was used. Distilled water was used in all preparations.

The quebracho (72% tannin extract) was obtained from the Thompson-Hayward Co. of Tulsa and contained 11.4 per cent moisture (105 C.).

All other materials were reagent grade, and concentrations were corrected for water of crystallization, if any. All concentrations are expressed in pounds per barrel (42 gallons).

B. Technique

The systems—either mud or water—were contaminated with either sodium or calcium sulfate after treatment with the desired amounts of sodium hydroxide and quebracho. For treatments with barium carbonate an approximately 3-fold excess (5 lb./bbl.) was used over that computed to be required to precipitate all the sulfate as barium sulfate. Barium hydroxide was used in concentrations of 2 lb./bbl.—about

Manuscript received at office of Petroleum Branch August 16, 1949.
Paper presented at Branch Fall Meeting in Dallas October 4-6, 1948.
¹References are given at end of paper.

1.6 times that required to precipitate the sulfate. An error of about one per cent was involved in preparing these systems.

The treated suspensions were aged in sealed bottles at room temperature (about 25 C.) or at 95 C. for various periods of time. The suspensions were stirred intermittently during all prolonged aging periods and continuously for all 0.5 hour aging periods. At the end of the desired aging period, the muds were filtered on Baroid presses at 100 psi gage, while other systems were filtered twice without pressure through Whatman No. 42 paper (for fine-grained precipitates). For these latter experiments—no clay present—some very fine material would pass through the filter paper even after four filtrations through the same filter. Consequently, the filtrates were allowed to settle about one hour, and the supernatant liquid was taken for analysis.

The physical properties of the muds were determined in accordance with the procedure given in A.P.I. Code 29. The muds were stirred 30 minutes with a high speed mixer before conducting these tests.

The sulfate was determined by evaporating aliquots of the filtered solutions, acidified with HCl, to dryness and then extracting the residue with hydrochloric acid. The extract was then filtered and the soluble sulfate was precipitated with barium chloride. The precipitated barium sulfate was ignited and weighed. It should be mentioned that this procedure determines only that soluble sulfate which is present in excess of soluble barium and hence gives a *minimum value* for the soluble sulfate which is present in the system.

EXPERIMENTAL RESULTS AND DISCUSSION

One of the factors which was considered to be one of some importance in the effectiveness or at least the rate of precipitation of sulfate by barium carbonate, was that the barium carbonate might become coated with clay and not be solubilized at an appreciable rate. This effect, if real, would be of significance particularly in any system having a low water-loss value. By using concentrations of bentonite from 0 to 8 per

cent with calcium sulfate as contaminant in fixed amount (1 lb./bbl.) the water-loss values were varied between 6.5 and 44 ml./30 min. The results of the tests (Table I) show that water-loss value has no close relationship to the effectiveness of the barium carbonate. The barium carbonate treatment decreased the sulfate to about 154 ppm. within 0.5 hour as compared to values of 21 to 49 ppm. achieved with barium hydroxide. After aging the suspensions at 95 C. for 20 hours the sulfate was reduced to 50 ± 25 ppm. in all cases.

It will be noted that the control tests (No. 3, 6, and 8 of Table I) show increasing sulfate concentrations with increase in concentration of bentonite. This is explained by the fact that the concentration of added sulfate is based on volume of mud and not on volume of water. The values for sulfate agree within experimental error with those computed for the amount present per unit volume of water corrected for a small amount present as impurity in the clay.

The next tests (Table II) were intended to show possible limits both for the pH of the mud and the concentration of quebracho required to render the barium carbonate ineffective for the removal of sulfate. At the same time, a comparison was made between the effects when using barium hydroxide and the carbonate. The bentonitic mud was treated with various amounts of caustic and quebracho and contaminated with calcium sulfate (1 lb./bbl.). The sulfate in the filtrate from the muds was determined after the muds had aged 16 hours at 95 C. The physical properties (A.P.I. Code 29) were also determined for the aged muds.

The results of these tests (Table II) show that the barium carbonate reduced the sulfate to 245 ± 25 ppm. in the low pH systems (Parts A and B of Table II), but was essentially ineffective in the high pH systems (Parts B and C). The fact that the quebracho in amounts greater than 1 lb./bbl. was not completely solubilized before aging the mud at pH 8.3 precludes any definite conclusion regarding the effect of the quebracho. In the high pH, high quebracho systems, the ineffectiveness of the barium carbonate could be attributed to either the pH or the quebracho. The results definitely prove that an initial pH of 12.4 is sufficiently high to render the

TABLE I

Removal of Sulfate with Barium Carbonate and Barium Hydroxide from Bentonite Suspensions

Test No.	Bentonite, % by wt.	CaSO ₄ , lb/bbl	BaCO ₃ lb/bbl	Ba(OH) ₂ , lb/bbl	pH of Mud		Water-loss of Treated Suspension*, ml/30 min.	ppm SO ₄ ²⁻ in filtrate from	
					Mud Aged 0.5 hr. at 25° C.	Mud Aged 20 hr. at 95° C.		Mud Aged 0.5 hr. at 25° C.	Mud Aged 20 hr. at 95° C.
1.....	0	1.0	5.0	—	8.8	9.5	—	177	25
2.....	1.14	1.0	5.0	—	8.7	9.6	44	165	95
3.....	2.28	1.0	—	—	—	—	—	2,144	—
4.....	2.28	1.0	5.0	—	8.9	9.4	20	152	45
5.....	2.28	1.0	—	2.0	12.5	11.8	—	33	—
6.....	4.56	1.0	—	—	—	—	—	2,597	—
7.....	4.56	1.0	5.0	—	9.2	8.9	11	156	37
8.....	8.0	1.0	—	—	—	—	—	2,996	—
9.....	8.0	1.0	5.0	—	9.3	9.7	6.5	177	53
10.....	8.0	1.0	—	2.0	12.1	11.0	—	21	66
11.....	8.0	1.0	—	5.0	12.5	12.4	—	49	45

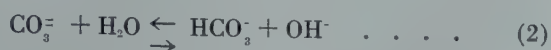
*These values were determined 0.5 hour after treating the suspension with BaCO₃ or Ba(OH)₂.
Values after aging the muds were not appreciably different.

barium carbonate ineffective in this system. Further, since the pH of the muds used for parts C and D decreased to 11.8 and 10.0, respectively, with the barium carbonate treatment, the indications are that a pH of 10.0 is sufficiently high so that the reaction proceeds very slowly.

It should be noted that the pH of the low pH systems treated with BaCO_3 increased upon aging. This may be explained by the liberation of carbonate from the reaction:



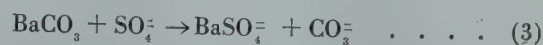
The carbonate then hydrolyzes in water:



In other words, the effect is analogous to the addition of a soluble carbonate which buffers the system.

The physical properties of the muds shown in Table II should be noted. Firstly, in the absence of any barium hydroxide or carbonate (tests 1, 2, 3, and 4) the viscosities and 10-minute gel strengths are increased by increasing the pH and the quebracho. Secondly, treatments with barium hydroxide did not adversely affect the properties of the muds and since it decreased the sulfate concentration more readily than the barium carbonate, the indications are that it could be used more advantageously than barium carbonate. This factor will be mentioned in another section.

In an attempt to determine more closely the effect of pH and of quebracho additional tests were conducted (Table III). For these tests, aqueous systems without clay were used. This simplified the experimental procedure as well as the interpretation of the results. For most of these tests sodium sulfate was used since it was realized that calcium sulfate would promote the reaction



by precipitation of the carbonate—at least in high pH systems—as calcium carbonate. When calcium sulfate is used one is assured that the amount of calcium which is present will be stoichiometrically equivalent to the carbonate liberated by the reaction given above.

Another major difference between the use of calcium and sodium sulfate in the presence of quebracho should be emphasized also. Addition of calcium sulfate to an alkaline quebracho solution precipitates some quebracho. The amount precipitated, on the basis of qualitative observations, is a function of pH (or NaOH), or ratio of sodium to calcium in the system. For example, quebracho is essentially insoluble in a saturated solution of calcium hydroxide (pH 12.6). The amount which will dissolve may be increased by addition of sodium hydroxide.

TABLE II

Removal of Sulfate with BaCO_3 and Ba(OH)_2 from a Bentonitic Mud Containing Caustic and Quebracho

Composition of Stock Mud Used:

Water.....	78.9%
Sodium hydroxide.....	0.226% (1.0 lb/bbl)
Quebracho.....	0.226% (1.0 lb/bbl)
Bentonite.....	6.4%
Barium Sulphate.....	13.3%

Test No.	Total Present in Mud, lb/bbl					Initial pH*	API Code 29 Physical Properties After Aging Mud 16 hr. at 95° C.					SO ₄ ⁼ in filtrate from Aged Mud, ppm
	NaOH	Quebracho	CaSO ₄	BaCO ₃	Ba(OH) ₂		Viscosity, cps	Init. gel, g.	10-min. gel, g.	Water-loss, ml/30 min.	pH of Mud	
A. Low pH—low quebracho												
1.....	1.0	1.0	1.0	—	—	8.5	16.5	0	2	11.3	8.4	2782
1a.....	1.0	1.0	1.0	5.0	—	8.5	75	0	2	7.0	8.9	267
1b.....	1.0	1.0	1.0	—	2.0	8.5	32	0	0	9.0	12.0	292
B. Low pH—high quebracho												
2.....	1.0	3.0†	1.0	—	—	8.3	20	0	12	10.0	8.3	3045
2a.....	1.0	3.0†	1.0	5.0	—	8.3	74	0	40	6.3	8.8	226
2b.....	1.0	3.0	1.0	—	2.0	8.3	59	0	20	6.3	9.8	251
C. High pH—low quebracho												
3.....	3.0	1.0	1.0	—	—	12.4	61	0	10	8.0	12.1	3053
3a.....	3.0	1.0	1.0	5.0	—	12.4	62	0	0	8.7	11.8	2609
3b.....	3.0	1.0	1.0	—	2.0	12.4	54	0	4	8.0	12.7	383
D. High pH—high quebracho												
4.....	3.0	3.0	1.0	—	—	11.9	70	0	20	6.0	10.4	2642
4a.....	3.0	3.0	1.0	5.0	—	11.9	60	0	7	6.7	10.0	2119
4b.....	3.0	3.0	1.0	—	2.0	11.9	71	0	2	7.2	12.2	383

*pH just prior to addition of BaCO_3 or Ba(OH)_2 .

†The quebracho did not disperse completely in this mud upon stirring for 0.5 hr. at 25° C.

The results (Table III) show that in the absence of added alkali or quebracho (test No. 1) the sulfate was decreased to only 646 ppm. The pH of the suspension increased due to liberation of carbonate (reactions 1 and 2). For test No. 2, where 0.03 lb. NaOH per barrel was present, the result is essentially the same as for test No. 1. Tests 3, 4, and 5 show the effect of increasing the quebracho concentration to 2.3 lb./bbl. when the initial pH of the system is about 8.2. Compared with tests 1 and 2, the major effect of the quebracho appears to be a decrease in the rate at which the sulfate is removed, since the rate is markedly accelerated by heating the suspension.

Tests 6 and 7 (initial pH of 9.8) and test 8 and 9 (initial pH of 11.1-11.2) do not reveal any major effect of the quebracho in the concentration range of 1.2 to 2.3 lb./bbl., except that the value obtained for test 8 after aging seven days is about 25 per cent lower than for test 9. For all these tests the sulfate concentration remains high, and the overall data reveal that barium carbonate will not effectively remove sulfate from these sodium sulfate contaminated systems if the pH is higher than about 9.8 and when the quebracho is 1.2 lb./bbl. or more. However, when barium hydroxide (test 14) is used in place of the carbonate the sulfate is decreased to 29 ppm. in the high pH-high quebracho system which could not be treated with barium carbonate (test 9). Although carbonate ion concentrations in these systems were not determined, the success of the barium hydroxide treatment may be attributed in part to the fact that the carbonate ion concentration was decreased by the reaction:



The excess barium hydroxide was then available to precipitate the sulfate. The effect of carbonate ion concentration will be discussed in a later section.

When calcium sulfate is used as the contaminant (tests 10-13), the sulfate is effectively removed by barium carbonate in the absence of quebracho, but when the quebracho is increased to 1.2 or 2.3 lb./bbl. as for tests 12 and 13, the sulfate is but slightly decreased.

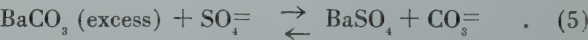
It was expected, at first, that these tests would show definite limits for both the pH of the system and the concentration of quebracho in order for the sulfate to be precipitated com-

pletely by barium carbonate. The tests show no sharply defined limits for either of these two factors and merely show that the barium carbonate treatment may not be effective. Treatments with barium hydroxide, however, were effective under conditions for which barium carbonate was not. This emphasized that removal of sulfate from such systems was not an impossibility. A study of the factors involved, as presented in Section IV of this report, showed that *no sharply defined limits could be expected*. Rather, a multi-component system is involved and the extent of the reaction (equilibrium) is controlled by the components and their concentration in the system at equilibrium. A knowledge of the effect of these variables can then be used to determine either the conditions under which barium carbonate may completely precipitate the sulfate or indicate treatments which are required to render the precipitation complete.

THEORETICAL DISCUSSION

The limited tests which have been presented show that treatment with barium carbonate is far from a simple panacea for the difficulties which may be encountered due to sulfate contamination in a drilling fluid. The tests have also served to show that certain factors, not readily apparent from the data, are involved which require an explanation.

Consider the reaction which is involved in the precipitation of sulfate by barium carbonate:



For this reaction the equilibrium constant is given by the equation

K₁ = ^aCO₃⁼ / ^aSO₄⁼ (6)

where ^aCO₃⁼ and ^aSO₄⁼ are the activities of the carbonate and sulfate ions in the solution at equilibrium. Using the values for the solubility product constants for barium sulfate and barium carbonate as reported by Latimer⁶.

^KBaSO₄ = (^aBa⁺⁺ ^aSO₄⁼) = 9.9 x 10⁻¹¹ . . (7)

and ^KBaCO₃ = (^aBa⁺⁺ ^aCO₃⁼) = 4.93 x 10⁻⁹ . . (8)

the value of K₁ in equation (6) may be evaluated

TABLE III
Removal of Sulfate from Aqueous Suspensions

Test No.	In Suspension lb/bbl						pH of Suspension			ppm of SO ₄			
	NaOH	Quebracho	Na ₂ SO ₄	CaSO ₄	BaCO ₃	Ba(OH) ₂	Before addn. of Ba	5 min. after addn.	24 hr. after addn.	Added	Found (1 day)	Found* (1 day)	Found 7 days
1.....	0	0	1.17	—	5.0	—	6.0	10.7	11.3	2250	646	582*	—
2.....	0.03	0	1.17	—	5.0	—	10.8	10.9	11.4	2250	640	578*	—
3.....	0.03	0.58	1.17	—	5.0	—	8.1	9.7	10.4	2250	944	922*	—
4.....	0.06	1.2	1.17	—	5.0	—	8.2	9.1	9.8	2250	1,067	695*	—
5.....	0.12	2.3	1.17	—	5.0	—	8.2	8.7	9.3	2250	1,066	702*	—
6.....	0.23	1.2	1.17	—	5.0	—	9.8	9.8	10.1	2250	1,511	—	—
7.....	0.47	2.3	1.17	—	5.0	—	11.2	11.2	11.1	2250	1,621	—	—
8.....	0.47	1.2	1.17	—	5.0	—	11.1	11.0	11.0	2250	1,906	—	1440
9.....	0.93	2.3	1.17	—	5.0	—	11.2	11.2	11.1	2250	1,910	—	1903
10.....	0	0	—	1.17	5.0	—	6.3	9.8	9.5	2350	8	—	—
11.....	0.03	0	—	1.17	5.0	—	11.2	11.2	11.0	2350	14	—	—
12.....	0.47	1.2	—	1.17	5.0	—	10.7	10.6	9.9	2350	1,891	—	1918
13.....	0.93	2.3	—	1.17	5.0	—	10.7	10.6	9.9	2350	2,237	—	2319
14.....	0.93	2.3	1.17	—	—	2.0	10.7	—	12.6	2250	29	—	—

*Just prior to filtration, the suspensions were heated to boiling and cooled to room temperature with continuous stirring for one hour.

$$K_1 = \frac{{}^a\text{CO}_3^=}{{}^a\text{SO}_4^=} = \frac{4.93 \times 10^{-9}}{9.9 \times 10^{-11}} = \text{about } 50 \quad (9)$$

It should be stated that other values in the literature for the solubility product constants for barium sulfate and carbonate vary by a factor of about 5 from those given by Latimer. This fact does not invalidate the discussion which follows; and it is believed that Latimer's data is the most consistent with other data in the literature, and will be used for the source of other solubility product data herein reported.

Since the activity of an ion is equal to its concentration, m , multiplied by its activity coefficient, γ , equation (9) may also be written as:

$$K_1 = \frac{(m\text{CO}_3^= \gamma \text{CO}_3^=)}{(m\text{SO}_4^= \gamma \text{SO}_4^=)} = \text{about } 50 \quad (10)$$

For any finite concentration the activity coefficients are generally less than unity and are functions of the average ionic strength, μ , of the solution. The ionic strength⁷ is defined by

$$\mu = \frac{Z^2 + m^+ + Z^2 - m^-}{2} = 1/2 \sum m_i Z_i^2 \quad (11)$$

TABLE IV

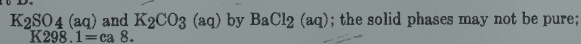
Equilibria in Aqueous Systems Containing Barium Sulfate and Barium Carbonate. Data from International Critical Tables, Vol. VII, p. 300

Part A.



In Solution, moles/1000 g of H ₂ O		Ionic Strength μ	Equil. Constant, K _m	In Solution, ppm of Water		
K ₂ SO ₄	K ₂ CO ₃			SO ₄	CO ₃	Cl-
t=25° C.						
0.00331	0.0690	0.217	20.9	318	4,140	—
.01218	.1873	.598	15.4	1,170	11,230	—
.0580(s)	.5243	1.747	9.03	5,570	31,400	—
t=100° C.						
.01533	.0571	0.217	3.73	1,470	3,430	—
.03639	.1131	.448	3.11	3,500	6,790	—
.2279(s)	.4144	1.927	1.82	21,850	24,860	—

Part B.



In Solution, moles/1000 g of H ₂ O			Ionic Strength, μ	Equil. Constant, Km	In Solution, ppm of Water		
K ₂ SO ₄	K ₂ CO ₃	KCl					
t=20° C.							
0.0005	.0072	.00068	.0238	14.5	48	432	241
.0009	.0068	.00068	.0238	7.6	86	408	241
.0028	.0164	.0017	.0593	5.9	269	984	602
.0032	.0160	.0017	.0593	5.0	307	960	602
.0147	.0619	.0068	.2366	4.2	1,410	3,710	2,410
.0159	.0607	.0068	.2366	3.8	1,530	3,640	2,410
.096	.287	.034	1.183	3.0	9,220	17,200	1,200
.104	.279	.034	1.183	2.7	10,000	16,940	1,200
t=96° C.							
.083	.300	.034	1.183	3.6	7,970	18,000	1,200
.089	.294	.034	1.183	3.3	8,540	17,600	1,200

*This question mark suggests that the carbonate would be hydrolyzed to HCO_3^- , that the original data did not indicate ratio of carbonate to bicarbonate in solution, and that the bicarbonate is reported as carbonate.

where Z_+ and Z_- are the charges of the positive and negative ions, respectively, in solution at concentrations m^+ and m_- . Thus, unless the activity coefficients of the sulfate and carbonate ions in a given solution are equal, the mol ratio (as determined by solubility) of the carbonate to sulfate ion for equation (9) need not be equal to 50. If the activity coefficient of the sulfate ion is lower than that of the carbonate ion at any given ionic strength, the mol ratio will be less than 50. That this is true was shown by inspection of values for the activity of potassium carbonate and of potassium sulfate at corresponding concentrations as reported by Latimer⁶. Calculation of the individual ion activities, ${}^a\text{CO}_3^=$ and ${}^a\text{SO}_4^=$, using values reported for K_2SO_4 , K_2CO_3 and KCl at corresponding ionic strengths, revealed that for values of ionic strengths greater than about 0.003, the activity of the carbonate was greater than that of the sulfate ion.

The above discussion can be summarized as follows. In any simple system saturated with barium sulfate and barium carbonate: (a) the mol ratio of carbonate to sulfate in solution will be less than the value of 50 indicated by the equilibrium constant for the system, (b) the concentration of sulfate ion will be increased by addition of soluble carbonates or by other electrolytes (NaOH , NaCl) not having the common ion Ba^{++} .

Supporting these conclusions are data reported in Table IV taken from the International Critical Tables. The last three columns of the table were computed from the data in order to report the concentrations in familiar terms.

In view of the previous discussion little need be said about these data. The equilibrium constant, K_m , reported in the table represents the mol ratio of carbonate to sulfate in the mixtures at equilibrium. It can be seen that this ratio decreases rapidly with increase in ionic strength of the solution. The data of part A of Table IV show that the ratio is highly dependent on temperature, so that at 100 C. the removal of sulfate from the potassium sulfate solution by barium carbonate is not as effective as at 25 C.

Part B of Table IV is quite analogous to that of Part A except that barium chloride was used so that the solution in equilibrium contains potassium chloride. This, in effect, increases the ionic strength of the solution and the equilibrium constant, K_m , given by the ratio of the moles of carbonate to moles of sulfate in solution is decreased. The data in Part B do not indicate high dependence on temperature.

The data of Table IV, and the theoretical treatment given, apply only to simple systems involving the equilibrium between barium carbonate and barium sulfate with sulfate and carbonate ions. In drilling mud systems the situation becomes far more complicated, but some of the factors may be partially evaluated by comparison with the effect in the simple system which was considered.

1. Effect of the concentration of carbonate: Obviously, the reaction



can be made to proceed to completion by removal of the carbonate. The procedure employed is to add calcium (as lime) to precipitate calcium carbonate. Complete removal of carbonate by calcium would be favored by a pH sufficiently high

(>10) so that bicarbonate is eliminated. However, in view of the fact that the solubility product for calcium carbonate



is but slightly less than that for barium carbonate

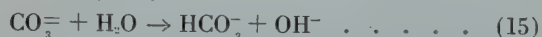


the effect of lime in the presence of excess barium carbonate is due not only to removal of carbonate but also to decomposition of barium carbonate according to the equation:

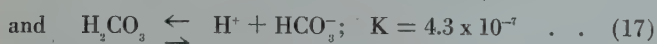
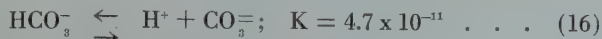


The effective concentration of the barium ion is thereby increased with a proportional decrease in the sulfate concentration. Obviously, application of barium hydroxide, rather than barium carbonate and lime, for the precipitation of sulfate, is a direct approach. The use of barium hydroxide is particularly indicated when the sulfate contamination is not primarily due to anhydrite (calcium sulfate) or when the carbonate concentration in the mud is high. Under these conditions the barium carbonate treatment can only be effective when lime or other soluble calcium or barium salt is added so that the carbonate ion concentration will be decreased.

2. Effect of pH: The effect of pH has been briefly mentioned. In the simple system— BaCO_3 , BaSO_4 , H_2O —it was assumed that only the carbonate ion was present. In reality, the carbonate ion hydrolyzes in water:

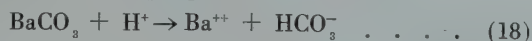


so that appreciable bicarbonate may be present unless the hydrolysis is repressed by addition of alkali. If acid is added to the system, the following equilibria become involved:



(In a given system, the pH will determine the ratio of carbonate to bicarbonate ion in solution.)

Therefore, a decrease in pH promotes the reaction



The barium ion concentration is increased, and the sulfate ion concentration would be decreased in accordance with the solubility product for barium sulfate as previously given.

In terms of drilling mud practice, two pH ranges may be considered. In high pH (>11) where bicarbonate ion is practically eliminated, the effective removal of sulfate by barium carbonate requires that the carbonate be removed.

In such high pH systems the removal of carbonate could be effectively accomplished by addition of a soluble calcium or barium compound. In connection with this, it should be emphasized that even if the sulfate contamination is from anhydrite, the amount of calcium in the system may be stoichiometrically less than that required to remove the carbonate. Alkaline muds would pick up carbonate from decomposition of organic matter in the system and from absorption of carbon dioxide from the atmosphere. There would also be some adsorption of calcium on the clay present.

In low pH systems, the carbonate may not be effectively decreased by calcium. Effective removal of sulfate would then depend upon increasing the concentration of barium ion. This could be accomplished by lowering the pH to dissolve barium carbonate or by addition of a soluble barium salt (e.g. BaCl_2).

3. Effect of inorganic ions which may or may not react with components of the system: The effect of ions which do not enter into the reaction was shown to result in an increase in the ionic strength with a resulting increase in the amount of sulfate which may remain in solution at equilibrium. The data of Table IV could be used to estimate the concentration of sulfate which would exist in the solution at equilibrium for values of ionic strength up to 1.9. The presence of such electrolytes puts a premium upon either the effective decrease in the carbonate ion concentration (by addition of calcium) or an increase in the concentration of barium (by decrease in pH to solubilize BaCO_3 or addition of a soluble barium compound).

In the presence of other constituents which may form precipitates with barium ion, the solubility product relationships for all the insoluble products must hold simultaneously. Consequently, any ion which forms with barium a compound having a low solubility product may be suspected as an interfering substance. For example, one such interfering ion might be chromate which is added to some drilling muds to inhibit corrosion:

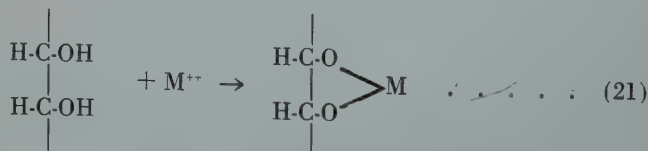


Others might include permanganate and metasilicate:



No solubility product data were found for barium metasilicate; but the solubility is believed to be low. Considerable silicate should be present particularly in high pH muds. In such systems the alkali would decompose the clay with the formation of soluble silicates. As indicated in the introduction, the phosphates also precipitate, or form complexes with barium ion.

4. The effect of quebracho and other organic matter: The fact that quebracho renders the barium carbonate treatment ineffective for removal of sulfate suggests that the barium ion forms a complex with or precipitates quebracho. It is well known that quebracho or other tannins may form precipitates with metal ions. However, even if a precipitate is not formed, organic material, particularly those containing hydroxyl groups, frequently form extremely stable complexes with polyvalent metal ions. A classic example of this phenomenon is the formation of complexes with tartrate or oxalate for which the reaction is formulated as



where M^{++} represents any divalent metallic ion. The complexes thus formed are frequently so stable that qualitative tests for the metal ion in such solutions may not reveal the presence of the metallic constituent until the organic matter is destroyed. Obviously to overcome the effect of such organic material a considerable excess of barium carbonate must be used or else the organic matter must be removed or its concentration decreased.

5. The effect of the clay: In drilling mud systems the effect of the clay will always be a factor. Firstly, clays, particularly those with a high base exchange capacity, will con-

tribute to the ionic strength of the system. This effect may be small except in high pH systems where sorption of hydroxyl ion is appreciable so that highly charged particles are formed.

Secondly, clays could undergo base exchange reactions. At pH values much below 9, the concentration of barium derived from solution of barium carbonate would certainly be sufficiently high so that an appreciable amount of barium would be exchanged for other cations sorbed on the clay. Further, in view of the very low activities which have been reported⁸ for monovalent cations in clay suspensions at pH values to about 11, it is quite probably that the concentration of barium ion derived from barium carbonate in most muds would be sufficiently high so that barium would be exchanged for other ions adsorbed on the clay.

It should be mentioned that in publications concerning drilling muds the statement is frequently made that chemicals having a low solubility in water are "inert" materials toward the clay. As shown by the data herein reported, even barium sulfate, which has an exceedingly low solubility in pure water, cannot be considered an inert material. For example, upon addition of barium sulfate to a mud containing carbonate considerable barium sulfate may be dissolved and affect the properties of the clay.

SUMMARY

The factors involved in the removal of sulfate from aqueous systems or drilling muds when using barium carbonate have been presented in considerable detail. The experimental data and the theoretical discussion have emphasized that the precipitation of sulfate by barium carbonate may not be as effective as generally presented in the literature and that the concentration of sulfate remaining in the system at equilibrium may be high. The amount of sulfate remaining in solution at equilibrium was shown to be primarily a function of the carbonate ion concentration, the barium ion concentration, and the ionic strength of the system. In addition, the presence of interfering substances—those which form difficultly soluble compounds or complexes with barium—may complicate the removal of sulfate by barium carbonate. A thorough comprehension of these factors should permit more fruitful application of the treatment.

Successful treatment of a drilling mud for removal of sulfate with barium carbonate requires at least that either the barium carbonate be appreciably solubilized (by having a low pH) or that the carbonate ion concentration be kept low. A decrease in the concentration of carbonate ion can be achieved by addition of a soluble calcium or barium salt (for example, calcium hydroxide or barium hydroxide). Complete precipitation of carbonate as the calcium or barium salt is favored by a high pH. For these reasons, the use of barium hydroxide is particularly indicated when the sulfate contamination is not primarily due to anhydrite or when the carbonate concentration in the mud is high.

REFERENCES

1. Hoeppe, R. W. U.S. Patent 2,393,165.
2. Gray, G. R. *Petroleum Engineer*. 18, 142 (1947).
3. D. D. Varnell and W. B. Kimbrell. Paper presented at Regional Meeting, AIME, Denver, Colo. Sept. 28-Oct. 2, 1947.

4. "Principles of Drilling Mud Control." Issued by Industrial Business Extension Training Bureau. Univ. of Texas (1946) p. 51-2.
5. E. H. Lancaster and M. E. Mitchell. Paper presented at Texas Section AIME Meeting at College Station, Texas, Dec. 4-5 (1947).
6. W. M. Latimer. "Oxidation Potentials." Prentice-Hall, Inc. N. Y. (1938).
7. G. N. Lewis and M. Randall. *Thermodynamics*. McGraw-Hill Book Co. New York (1923). p. 373.
8. C. E. Marshall and W. E. Bergman. *Jour. Phys. Chem.* 46, 52 (1942); *ibid.* 46, 325 (1942).

DISCUSSION

By O. W. Van Dyke, Magnet Cove Barium Corp.,
Houston, Texas

I would like to compliment Bergman, Fisher and Carpenter for the work that they have reported in this paper. We should also express appreciation to the Phillips Petroleum Co. for making this work possible.

This paper is of particular interest because it reports the results of research into a seemingly very simple chemical reaction that has been used in mud treating for quite a long time. It is work such as this that is bringing about refinements in drilling mud control that are necessary for today's deep holes. The authors have explained with experimental data the reason for some of the erratic behaviors we have all observed in using barium carbonate for removing sulphate from drilling mud. These data point out that pH, carbonate content, presence of quebracho or other complexing agents are only a few of the factors influencing the results that might be expected when using barium carbonate for the removal of sulphate. This work certainly points out that the reactions involving barium carbonate in drilling mud are complex and effected by numerous conditions.

It would have been of interest to have had some consideration given to the removal of calcium as well as the sulphate ion because such cations have a much greater effect upon mud than anions such as sulphate. We have done work which indicates that the sulphate ion is no more detrimental to drilling mud than the chloride ion. The fact that the sulphate ion usually enters the mud as calcium sulphate has perhaps prompted the misnomer of "sulphate contamination" for calcium sulphate where the major offender actually is the soluble calcium rather than the sulphate ion. In view of the fact that the most common application for barium carbonate has been treating out the detrimental effects of calcium sulphate, specific reference to this problem would have been timely in this paper.

DISCUSSION

By G. E. Saunders, Sohio Pet. Co., Cleveland, Ohio

This paper furnishes the industry with some very good theoretical data concerning sulfate removal in drilling muds.

One of the conclusions very worthwhile is that a high pH and high quebracho mud greatly reduces the effectiveness of the barium carbonate treatment. In this case, would the recommended testing procedure be to dilute the system with water in order to lower the pH and then carry on routine carbonate treatment?

It seems that some tests would have been advisable concerning the use of sodium carbonate, particularly when the sulfate content is due primarily to gypsum in low concentrations.

Barium hydroxide was shown to be much more effective in sulfate removal in some types of mud. The question arises as to cost and availability of the hydroxide instead of the carbonate. Barium carbonate is a native material, quite cheap and found in large quantities. It seems that using an excess (as is usually done in the field) of perhaps 15 to 20 pounds per barrel might be a more economical treatment.

The fact that high pH and high quebracho content in the mud inhibits the carbonate reaction should be very useful information. In some instances, such as at Carthage, Texas, anhydrite is found at known depths and the mud engineer can keep the pH and quebracho content at low values so that the carbonate will be effective when anhydrite is encountered.

Additional work in connection with sulfate removal where the treatment is done with polyphosphates instead of carbonates would be very useful to the industry.

Authors' reply to O. W. Van Dyke

The authors wish to point out that this paper has been purposely directed toward an emphasis on removal of sulfate ion. While sulfate may be no more detrimental than chloride or certain other inorganic anions, there are field problems in which even relatively small concentrations of sulfate arising

possibly from the mud make-up water, may contribute to the difficulty or complexity of maintaining specific mud properties, for example, low 10 minute gel strengths. The cations present are relatively unimportant in cases such as these.

The problems of muds heavily contaminated with anhydrite certainly poses the additional problem of handling the calcium ions in many of the methods of treating these muds. In the case of treatment with sodium carbonate or sodium hydroxide, the resultant high concentration of sulfate demands either a special mud to handle the sulfates or a method for their removal. This paper has made no attempt to answer all the ramifications of this system and the resultant effects on the mud properties.

Authors' reply to G. E. Saunders

In the case of the high-pH, high-quebracho systems, water dilution may be preferred particularly if no expenditure of weighting agent or other chemicals is required upon dilution. Treatment with sodium carbonate to precipitate the calcium might be recommended if the amount of anhydrite is small. Treatment with barium carbonate might be preferable if pilot tests indicate that the treatment is effective. It should be emphasized that where barium carbonate does not function the use of an excessive amount, as is sometimes done in the field, is unwarranted. The only alternative is to condition the system so that the barium carbonate will function or to use barium hydroxide.

★ ★ ★

BOTTOM HOLE FLOW SURVEYS FOR DETERMINATION OF FLUID AND GAS MOVEMENTS IN WELLS

C. R. DALE, DALE COMPANY, LOS ANGELES, CALIFORNIA

The need for instruments to measure the movement of fluids and gas in wells has been recognized by engineers for many years. Information regarding flow in the producing interval has a direct bearing on completion practices in new wells and also provides information on the production characteristics of the well. Many hours of engineering time are spent in planning and completing wells but knowledge as to whether or not the original planning has produced the desired results has not always been complete. Many questions such as the following often arise: Why is it that two wells are completed under supposedly identical conditions, yet one well is a good one and the other is a poor one? Are the sands that look the best on the electric log contributing to the production? These and many other conditions in the producing well need to be under-

stood in order to develop more efficient production practices and to improve on methods of completing new wells. It is the purpose of this paper to briefly describe one type of instrument, outline the methods of running the equipment and show the results of surveys made under various conditions. With an understanding of the use of this type of survey its importance can be evaluated in relation to the problems encountered by the operator.

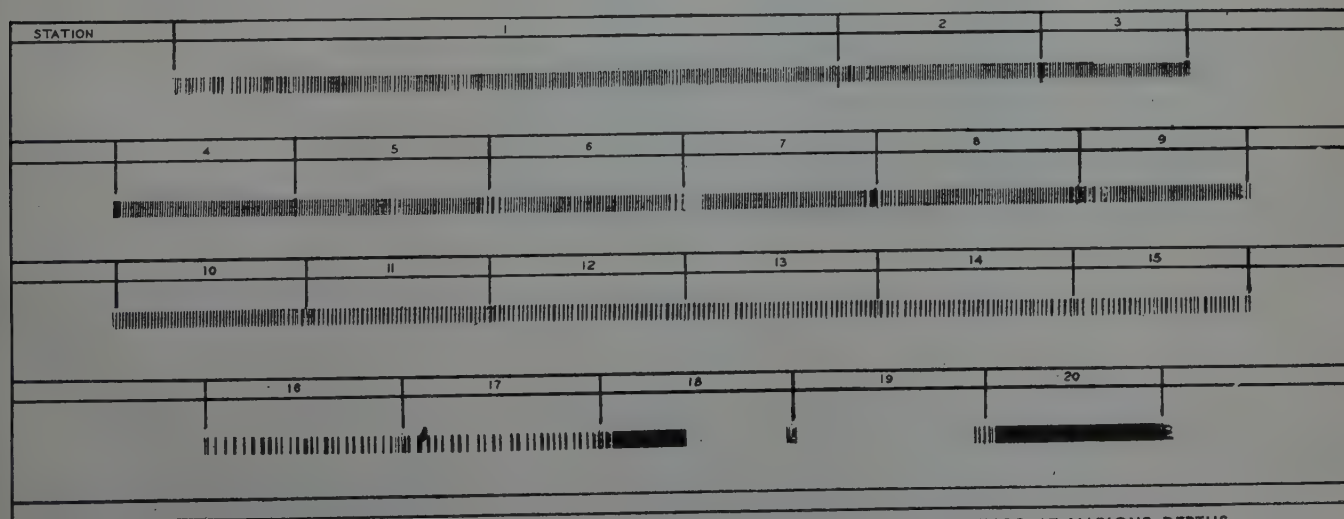
DESCRIPTION OF INSTRUMENT

The instrument is a velocity recorder employing a clock-controlled 16mm film for recording the rpm of an extremely sensitive rotor which is rotated by the flow of fluids or gas in a well. The helical-vaned rotor and shaft, weighing one-half of one ounce are an integral unit exposed to the well fluids and are the only moving parts not enclosed in the fluid-tight housing. No packing or fluid seal of these parts is necessary

and the shaft is mounted top and bottom on special jeweled bearings. Fig. A is the lower part of the instrument showing rotor and shaft with the protecting housing sleeve removed. The rpm of the rotor is recorded on the moving film by a combination electrical and optical system. The record is a series of dashes on the film, each dash and space representing twenty (20) revolutions of the rotor. (Film record of survey made in California well showing station recordings at various depths.) As the movement of the film is controlled by the clock the number of dashes and spaces in one minute of film travel represents the rpm of the rotor. The range of the instrument is from 0 to 2,500 rpm. The barrel or housing is 1-11/16 in. OD and seven feet long. Various types of expanding fluid traps are attached to the lower end of the instrument to direct the flow through the 1 in. orifice containing the rotor. The fluid trap for upward flow is shown in Figs. B and C. This assembly consists of eight arms with light spring

Manuscript received at office of Petroleum Branch September 1, 1948. Paper presented at Branch Fall Meeting in Los Angeles October 14-15, 1948.

¹References are given at the end of the paper.



FILM RECORD OF A SURVEY MADE IN A CALIFORNIA WELL SHOWING STATION RECORDINGS AT VARIOUS DEPTHS

steel leaves attached to each arm. The arms are free to move in but their outward movement is restricted so that when the trap is open the arms form a circle. Two sizes of these traps are used depending on the velocity to be measured,

one 3½ in. and the other 5 in. in diameter. For running in the well the assembly is held in a collapsed position by a restrictor shown in Fig. C. The restrictor is made of a light piece of aluminum tubing with four aluminum arms. In flowing wells the instrument is run in through the tubing into the liner. The instrument is pulled up and the extending arms of the restrictor catch in the perforations or between casing joints and it is pulled off and left in the well. For surveys in pumping wells the instrument is run through the annulus to below the pump with the same type of restrictor. The instrument is pulled up through the liner and the restrictor pulled off by the same procedure as used in flowing wells. For downward flow a fluid trap made of aluminum tubing and light leaf spring steel is used. This fluid trap is made in 3½ in. and 6 in. diameters and is held in position on the instrument sleeve just below the fluid ports by a friction fit as shown in Fig. D. The instrument is run in the well, the readings taken,

and the trap is pulled off and left in the well as illustrated in Fig. E.

METHODS OF OPERATION

In flowing wells the instrument is run through the tubing (2 in. or larger) under pressure on a measuring line and is lubricated into the well with the same procedure used in running a pressure bomb. For a survey in a flowing well it is necessary that the tubing be above the area to be surveyed.

Surveys in pumping wells are made by running the instrument in the annulus between the casing and tubing. The annular space must be large enough to allow free passage for the instrument but no further preparation of the well is required.

In pumping wells upward fluid movement is recorded if the pump is above the producing zone. However, if the tubing extends into the producing zone, downward flow to the pump can be recorded, and upward flow can be recorded below the bottom of the tubing. In making a survey for upward flow the instrument is stopped at various depths called stations. The first station is usually in the blank section above the perforations where the velocity of all fluids and gas moving past this point is recorded. The instrument is then lowered to the next station, a reading taken there, and so on to the lowest depth that can be reached. For downward flow the same procedure is used except that an inverted fluid trap is used.

INTERPRETATION OF SURVEYS

All precision measurements in wells require some interpretation to get the true picture, and flow surveys are no exception. In making interpretation of surveys made inside of perforated pipe it must be remembered that the fluid may not be entering the perforations directly opposite the formation that is contributing the production. In most wells surveyed to date however, the production seems to be coming through the perforations directly opposite the contributing sands. The results of surveys in a number of wells indicate the flow in machine cut perforated pipe is more steady than in gun perforated

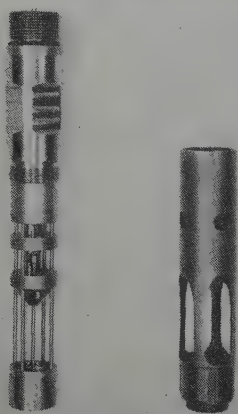


FIG. A — LOWER PART OF A VELOCITY RECORDER SHOWING ROTOR AND SHAFT WITH PROTECTIVE HOUSING SLEEVE REMOVED

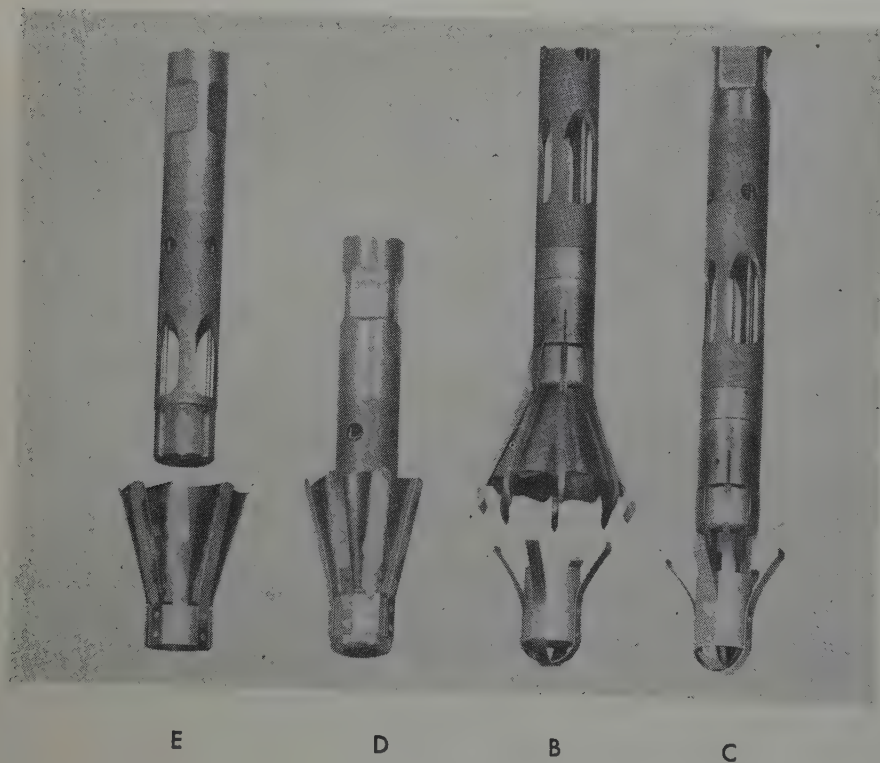


FIG. E — TRAP PULLED OFF AND LEFT IN THE WELL AFTER READINGS ARE TAKEN

FIG. D — FLUID TRAP HELD IN POSITION ON THE INSTRUMENT SLEEVE BY FRICTION FIT

FIG. B — FLUID TRAP FOR UPWARD FLOW

FIG. C — FLUID TRAP ASSEMBLY HELD IN COLLAPSED POSITION BY RESTRICTOR

pipe. In this case it is the writer's opinion that the recorded variations of rpm is due to the fewer perforations and the fluid jetting through them. In some wells the flow in the producing zone is intermittent or irregular and several runs may be required to catch a period of steady movement of fluid. Changes in viscosity and density of the fluid effect the rpm of the rotor. For example a steady flow of oil may move up the hole to a point of gas entry. From this point the rising fluid has less

density and viscosity, therefore less efficiency in turning the rotor. This results in a decrease in rpm at the point of gas entry. Temperature and pressure surveys are used in conjunction with the flow surveys and have aided a great deal in confirming interpretation. Although bottom hole flow surveys are a comparative new work and much experience is yet to be gained, only a few wells of the large number surveyed have presented a difficult problem of interpretation.

SATISFACTORY WELL FLOW CONDITIONS

The well shown in Fig. 1 was completed with oil base mud and a $5\frac{1}{2}$ in. liner was run into the $6\frac{1}{8}$ -in. hole after the well had been conditioned. Two-inch tubing was landed at 4,915 ft with a $1\frac{1}{2}$ in. tail to 5,635 ft. The tail pipe was retrieved for the flow survey and the well allowed to flow through the casing to obtain a steadied flow than could be maintained through the tubing. The well was producing 97 barrels per

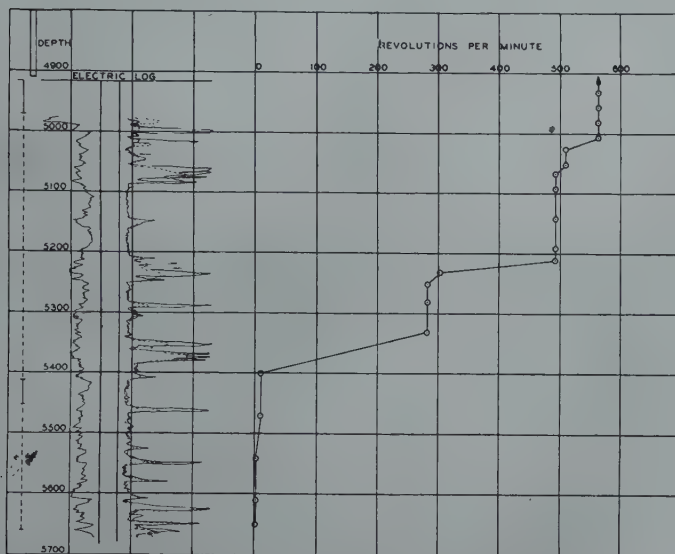


FIG. 1 — ELECTRIC LOG AND FLOW SURVEY SHOWING SATISFACTORY WELL CONDITIONS

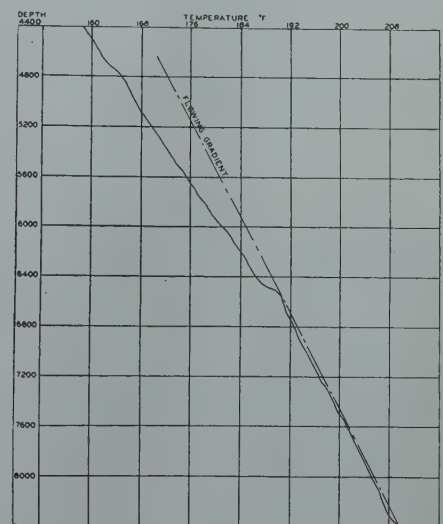


FIG. 2 — OIL AND GAS MIGRATION SHOWN BY TEMPERATURE SURVEY

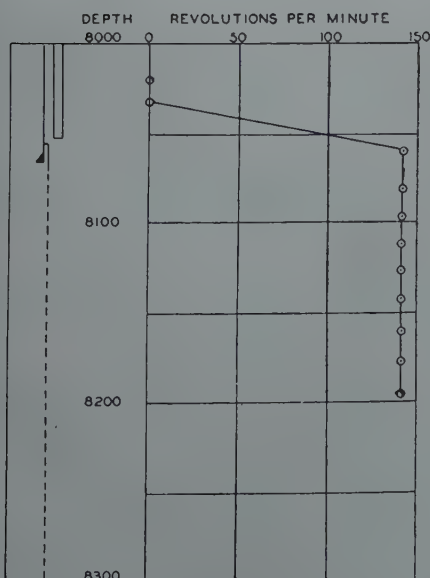


FIG. 3 — OIL AND GAS MIGRATION SHOWN BY FLOW SURVEY

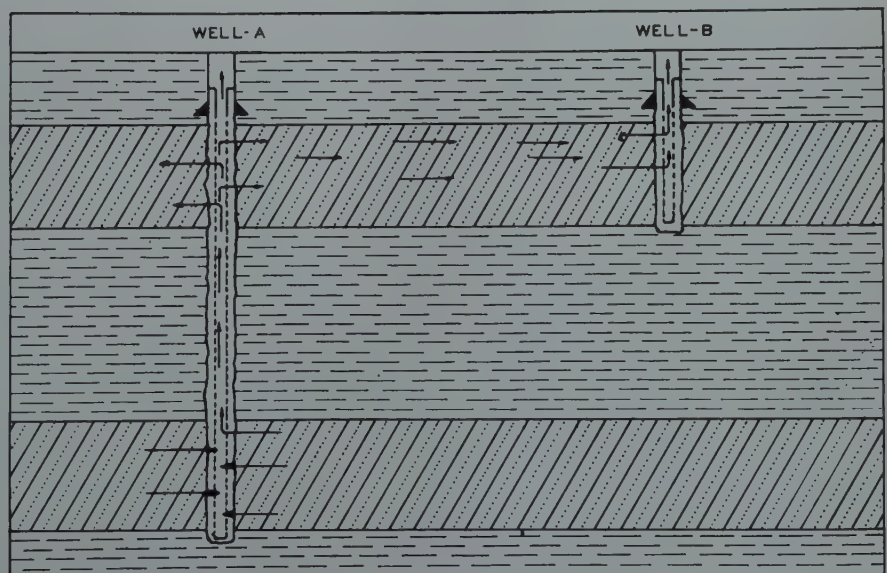


FIG. 4 — CONDITIONS FAVORABLE TO OIL AND GAS MIGRATION

day of 28 API gravity oil with 106 Mcf of gas. The electric log shows three oil sands of considerable width each separated from the other by approximately 100 ft of shale. The flow survey indicates all three sands are contributing production. Ten rpm recorded between 5,400 ft and 5,470 ft was probably caused by a small amount of gas flowing through fluid standing below 5,400 ft.

The lower 300 ft of formation that was not contributing production has productive sands that would probably produce if they were separated from the three upper sands. It is also possible that these sands may contribute production later on as pressures decline. One of the most important uses of this type of survey is to determine if sands that do not contribute production in the early life of the well will produce as the pressures subsequently become lower.

In several wells with long intervals it has been found that only a fraction of the formation in the upper part of the zone contributes any production. Attempts have been made to increase the productive area by producing the wells at a high rate, thereby reducing the pressure against the sands. In these wells there was no change in the producing areas.

With mud, water or dense fluids against the face of a sand for a long period of time it is possible that the sand will remain ineffective even after the pressures decline. For this reason knowledge of the areas contributing production in the early life of a well is quite important. To survey one well in a field and find conditions as satisfactory as they were in this well (Fig. 1) might lead an operator to feel that all his wells were in the same favorable conditions. This may not be true.

OIL AND GAS MIGRATION

Migration of fluids and gas from one sand to another or from the producing interval into formations that are supposed to be excluded from the well is a condition that is difficult to detect by normal operating procedure. Where the migration of oil takes place into dry or depleted sands it is possible that a substantial part will not be recovered. Casing failure may occur allowing large quantities of oil and gas to escape without causing any appreciable change

in surface operating pressures. Fig. 2, a temperature survey and Fig. 3, a flow survey, were made in a well where this condition existed.

A flow survey was first made with the well flowing and indicated upward migration. The well was shut in and the flow survey, Fig. 3, was run. This clearly showed upward movement from the producing interval to the bottom of the tubing. Readings taken in the tubing did not record any fluid movement. From the results of the survey it was quite evident that the fluid was flowing up through the annulus between the tubing and casing.

The temperature survey was then run (Fig. 2) in the tubing with the well

shut in. This survey disclosed a flowing temperature gradient to 6,500 ft and a change that approached the shut-in temperature gradient above this point. It also indicated that oil was flowing up through the annulus for 1,700 ft and migrating through a hole in the casing at 6,550 ft. Other wells in the area were producing from this same depth. Although it is probable that the oil escaping from this well will be recovered in the wells producing from the thief sand, if a dry sand or formation of high porosity existed opposite the hole in the casing the oil would have been permanently lost.

The extent to which migration is taking place from one sand to another

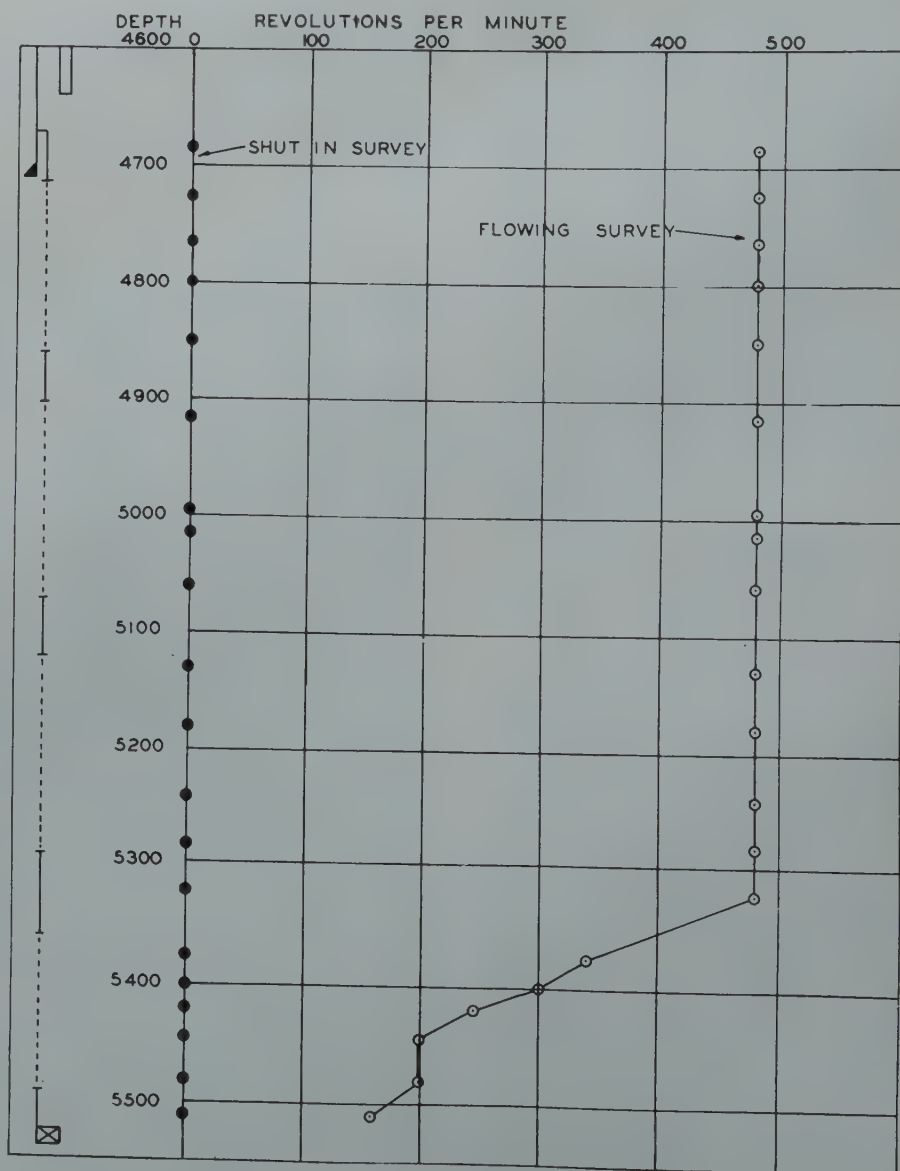


FIG. 5 — FLOW SURVEY SHOWING BRIDGE PLUG LEAKING

is partly the result of the way in which the various wells in the field are completed. Where zones of different pressures are included in a single well and separated by mechanical means the failure of the separating device may lead to migration of oil and gas from one zone to another. The manner in which wells are completed can set up conditions that are favorable to migration. This is illustrated in the sketch (Fig. 4) where Well A is completed in two zones while Well B is completed in the upper zone only. The lower zone of Well A may be contributing a substantial part of the production of Well B, and of other wells producing from only the upper zone.

The study of migration of fluids and gas in wells encompasses a wide field. Considerable experience over a period

of time will be required to explain fully the unusual conditions found in many wells.

BRIDGE PLUG LEAKING

In the well represented in Fig. 5, the operator knew that something was wrong because the pressures were abnormally high for the zones above 5,500 ft. Also the temperature at 5,500 ft was 226°F, while in an adjacent well at this depth the geothermal temperature was approximately 214°F. The flow survey revealed that the plug in the blank section below 5,500 ft was leaking. The plug had been placed to exclude production from lower zones. A survey was made with the well shut in to determine if fluid was moving into the lower pressure zones above the plug,

but no movement was indicated. Although production was coming from the perforated interval 5,360 ft to 5,495 ft when the well was producing it seemed quite possible that failure of the formations opposite the upper three sets of perforations to produce was due to high pressure from the lower zone. The pressures and temperatures recorded in this well were substantial evidence that the plug was leaking, and the flow survey, in addition to confirming this fact, also showed the failure of the three upper sets of perforations to contribute to the well production.

WELL COMPLETED WITH 3 IN. LINER IN 10 $\frac{5}{8}$ IN. HOLE

In the well shown in Fig. 6 a three-inch perforated liner was hung on 2 $\frac{1}{2}$

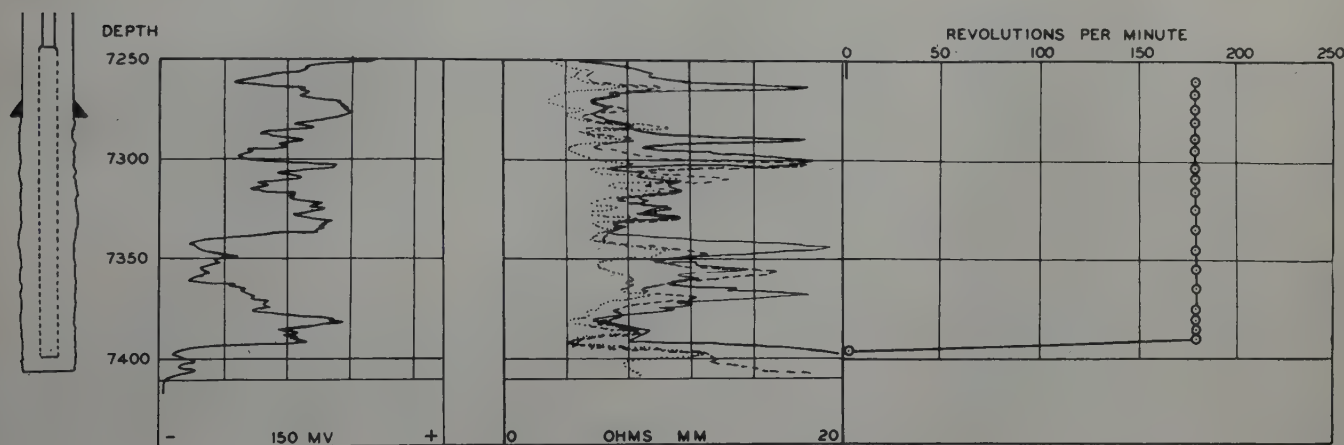


FIG. 6 — WELL PRODUCING FROM LOWER SANDS ONLY

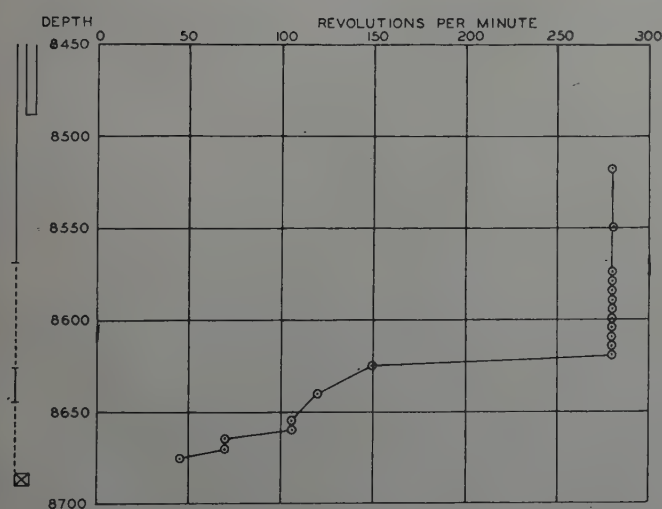


FIG. 7 — FLOW SURVEY SHOWING TWO POINTS OF WATER ENTRY

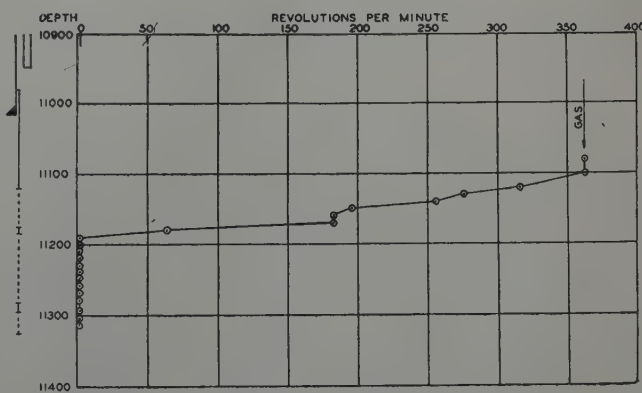


FIG. 8 — FLOW SURVEY OF A GAS INJECTION WELL

in. tubing in a 10 $\frac{5}{8}$ in. hole. The operator had originally planned to pull the liner after a test, but the results of the flow survey and the satisfactory performance of the well show that the liner should be left in place. The flow survey indicates that all the production is coming from the sand in the bottom fifteen feet of the well and operating data confirms this finding. A pressure traverse recorded a flowing gradient to the bottom of the well. Adjacent wells completed in only the lower sand affected this well when produced at a high rate indicating that it, too, was producing from the lower sand. It will be noted that here again sands shown on the electric log are not contributing to the production of the well.

FLOW SURVEY — LOCATE WATER SOURCE

The full extent to which flow surveys can be used in locating water sources in wells has not as yet been determined. Where a well is producing all water the method can be applied very successfully. In a well (Fig. 7) 110 barrels of water and 3 barrels of oil per day were being gas-lifted through the tubing. The flow survey indicated water entering at the blank section 8,627 ft to 8,645 ft, and at another point below 8,660 ft. The effective depth of the well was 8,676 ft. These results confirmed a water location survey that had previously located a major source of water at the top of the blank section and a minor source at the bottom of the well. At the lowest station only 45 rpm was recorded on the flow survey, representing a fluid velocity of less than one foot per minute.

GAS-INJECTION WELL

At the time of the survey of a gas-injection well, Fig. 8, four million feet of gas was being injected through the tubing with a surface injection pressure of approximately 400 lbs. The flow survey was made in two runs. On the first run readings were taken at every other station plotted in Fig. 8, and on the second survey at the stations between those of the first run. This procedure shows how closely two runs check when the conditions remain constant in the well. Temperature surveys indicated that there were only a few feet of fluid

in the well and that some gas was going out in the lower part of the second set of perforations. From the flow survey it is quite evident that most of the gas was going into the formation opposite the top of perforations and just below the blank at 11,190 ft. The gas indicated moving downward below this point on the temperature survey was such a small amount that it was impossible to record it on the flow survey.

LOCATING GAS ENTRY

The well represented in Fig. 9 was producing 3 barrels of oil and one million feet of gas at the time the flow and temperature surveys were made. Both surveys show the gas coming from the upper set of perforations. A pressure traverse was made which recorded a gas column to the blank section, 3,379 ft-3,412 ft and a fluid gradient below the blank. The blank section was cemented with plastic and tested for shut-off. A packer was then run in on tubing and set in the blank section. The upper set of perforations was then tested by flowing through the annulus between the tubing and casing. For several days the well produced considerable oil and

then went to gas, indicating that oil had migrated into the gas sand during the shut-in period.

It had been found that the use of continuously recorded temperature surveys is a good check and in many cases confirms information obtained on the flow survey.

CONCLUSION

In this brief paper it is not possible to set forth the applications and limitations of bottom hole flow surveys. The examples given illustrate a few applications and will serve to suggest many others.

The bottom hole flow survey supplies an important link in the chain of information necessary for complete understanding of the conditions existing in the producing wells. The data can be obtained with a minimum of equipment; no great amount of time is required for the field work; the average survey requires no special knowledge for interpretation. Used in conjunction with other precision measurements bottom hole flow surveys give the engineer a more complete picture of conditions existing in the well. ★ ★ ★

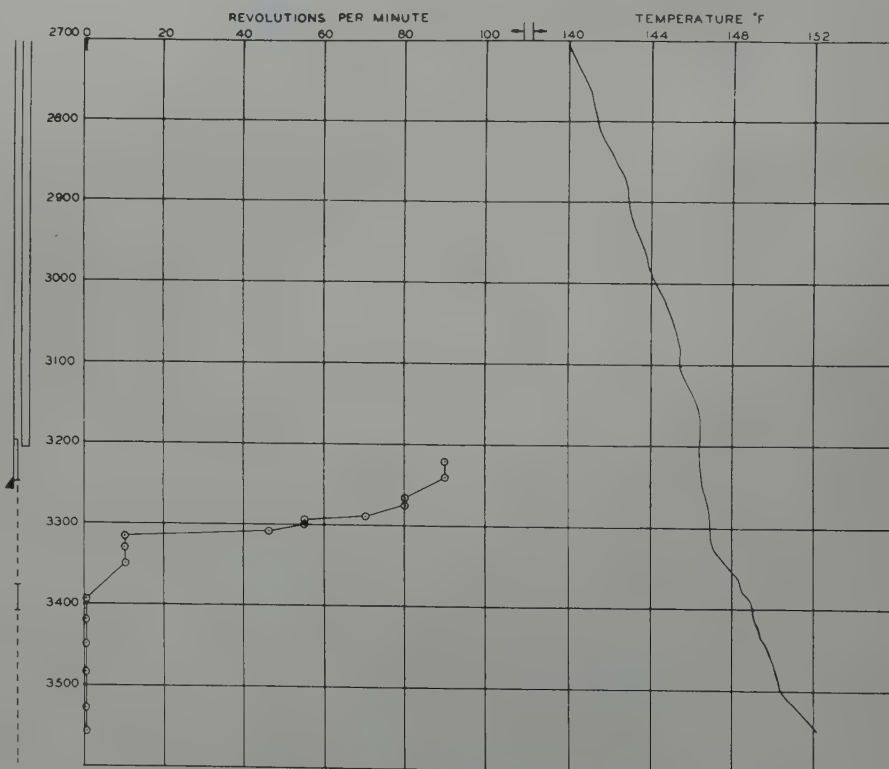


FIG. 9 — FLOW AND TEMPERATURE SURVEYS SHOWING GAS ENTRY

THE EFFECT OF WELL SPACING AND DRAWDOWN ON RECOVERY FROM INTERNAL GAS DRIVE RESERVOIRS*

RAYMOND G. LOPER, JUNIOR MEMBER AIME, AND JOHN C. CALHOUN, JR., MEMBER AIME
PETROLEUM ENGINEERING DEPARTMENT, UNIVERSITY OF OKLAHOMA, NORMAN, OKLAHOMA

ABSTRACT

Theoretical calculations for the decline of pressure and the variation of instantaneous producing gas-oil ratio with increased cumulative production have been made for reservoir systems under various producing drawdown values and for various spacings. These variables have been included by a modification of previously published techniques. This consists essentially of utilizing a radial system flowing gas and oil in a succession of steady state calculations. The results of the calculations do not show any variation in the predicted behavior of the internal gas drive reservoir when either the drawdown or the spacing are changed.

* A summary of material presented by Raymond G. Loper to the Graduate Faculty, Univ. of Oklahoma, in partial fulfillment of the master's degree.
Manuscript received at the Petroleum Branch office October 1, 1948. Paper presented at Branch Fall Meeting in Dallas, Texas, October 4-6, 1948.

INTRODUCTION

The prediction of performance on an internal gas drive reservoir has been presented by various authors.^{1,2,3} These predictions are in the form of a pressure decline and an instantaneous producing gas-oil ratio as a function of cumulative oil withdrawal. In making these predictions a basic assumption has been that the saturation of the reservoir is uniform throughout at any time, or that the pressure differential imposed on the reservoir system is zero. Because of these assumptions the validity of such predictions has been questioned. Their application to actual systems, where saturations are not uniform and where producing differentials exist, has been a hazardous procedure.

The authors cited^{1,2,3} have used different methods of approach to the

derivation of equations for making their predictions and for arriving at a solution of both equations, but basically the same relationships are utilized in each case. In all instances the instantaneous producing gas-oil ratio is calculated from the equation:

R = (k_g / k_o) * (μ_o / μ_g) * (β / v) + s (1)

In utilizing this equation an average reservoir pressure and an average reservoir saturation must be known, the former to define β, v, s, and μ_o/μ_g and the latter to define k_g/k_o. Predictions can be made, therefore, only for the conditions of a uniform reservoir saturation and a uniform reservoir pressure.

This restriction of requiring a uniform oil saturation can be resolved by applying two-phase steady state flow for the radial system to the reservoir's history. Radial steady state flow is defined when the ratio of phases flowing,

Nomenclature is listed at close of paper.
¹ References are given at end of paper.

TABLE Ia
TYPICAL CALCULATION OF PREDICTED QUANTITIES
Conditions: r_w = 0.25 ft.; r_e = 750 ft.; (P_e - P_w) = 1,000 psi; 39° API Oil
CALCULATION NO. 2 FOR TIME WHEN P_e = 2,300 psia
Assumed R_1 = 2,100

P_x	β	v	s	μ_o/μ_g	μ_o	k_g/k_o	S_o	k_o/k	k_o/k / μ_oβ	∫ ₁₃₀₀ ^{P_x} (k_o/k / μ_oβ) dp	ln r_x / r_w	r_x
						(a)					(b)	
2300	1.463	.00126	761	18.6	.356	.0620	.7032	.544	1.044	926.0	8.01	750
2200	1.452	.00134	737	19.6	.364	.0639	.7010	.537	1.016	823.0	7.11	308
2100	1.441	.00140	713	20.6	.373	.0654	.6995	.534	0.993	722.6	6.24	130
2000	1.431	.00148	689	21.6	.381	.0676	.6970	.528	0.968	624.6	5.40	55.5
1900	1.420	.00155	664	22.6	.390	.0694	.6950	.526	0.950	528.7	4.57	24.2
1800	1.408	.00165	640	23.7	.400	.0722	.6923	.523	0.929	435.2	3.76	10.8
1700	1.397	.00173	616	24.8	.407	.0741	.6905	.518	0.911	343.2	2.96	4.8
1600	1.386	.00185	592	26.0	.416	.0774	.6870	.510	0.885	253.4	2.19	2.2
1500	1.375	.00200	568	27.1	.425	.0822	.6825	.502	0.859	166.2	1.44	1.05
1400	1.364	.00217	544	28.3	.435	.0875	.6780	.492	0.829	81.8	0.71	
1300	1.353	.00235	520	29.4	.444	.0933	.6730	.484	0.806	0	0	

(a). Calculated from Equation (1)
(b). Calculated from Equation (3)

the pressures imposed, and the dimensions of the system are fixed. The system then possesses definite saturation and pressure distributions, both of which can be calculated.

The procedure to be outlined below, therefore, consists of fixing the gas-oil ratio, the pressure drawdown, and spacing (or drainage radius) for a radial system which is flowing oil and gas of known characteristics. The saturation distribution calculated for the system then permits the determination of stock tank oil removed from the system, and the pressure distribution calculated for the system permits the determination of the average pressure of the system. The gas oil ratio chosen, the stock tank oil produced, and the average pressure on the reservoir must then balance according to material balance concepts. If a balance is not obtained, trial changes of the fixed quantities are made and the calculation repeated until a balance is reached. By making a series of such calculations, the history of the reservoir can be determined, under whatever spacing and pressure drawdown values are assigned.

RADIAL, TWO-PHASE STEADY STATE FLOW

The development of Darcy's law as applied to a radial system for oil and gas mixtures under steady state flow has been given in the literature.⁴ Steady state implies not only constancy of pressure with time but also constancy of the relative amounts of gas and oil flowing at any place in the system. The most convenient place at which to fix the relative amounts of oil and gas is at the well radius, where they can correspond to an instantaneous producing gas-oil ratio.

For a radial system with an assigned value of instantaneous producing ratio, R, the flow of oil is given by:

$$Q_o = \frac{7.07 \text{ kh}}{\ln \frac{r_e}{r_w}} \int_{-P_w}^{P_e} \frac{k_o/k \text{ dp}}{\mu_o \beta} \quad (2)$$

Since this flow can be expressed across a fraction of the system from well radius r_w to any radius r_x , as well as across the whole system, the following is true:

TABLE Ib

Radii of Volume Increment in Feet	Fraction of Total Volume	Average Pressure for Increment	Volumetrically Weighted Pressure	Average S _o for Increment	Average β for Increment	Volumetrically Weighted S _o /β
308 —750	.8313	2250	1870	.7021	1.4575	.4004
130 —308	.1387	2150	298	.7003	1.4465	.0671
55.5—130	.0245	2050	50	.6982	1.4360	.0119
24.2—55.5	.0044	1950	9	.6960	1.4255	.0021
10.8—24.2	.0009	1850	2	.6937	1.4140	.0004
4.8—10.8	.0003	1750	1	.6914	1.4025	.0002
	1.0001		2230 = avg. pres.			.4821

Initial value of S_o = .80;
Equivalent initial stock tank oil = $\frac{.80}{.154} = .5195$;

$$\left(\frac{n_1}{N}\right)_{\text{avg}} = \frac{.5195 - .4821}{.5195} = .0720$$

From previous calculation the following values are known:
R₁₋₁ = 1180
u_o = 1.54
 $\frac{n_{1-1}}{N} = .0244$
s_o = 930
From P = 2230 the following values are found:
u₁ = 1.6984
v₁ = .00131

From calculation for previous step:
$$\sum_{i=1}^{i=i-1} \left(\frac{R_{1-1} + R_i}{2}\right) \left(\frac{n_i}{N} - \frac{n_{i-1}}{N}\right) = 25.74$$

Substituting the above known values in Equation (4) and solving for R₁:
$$\frac{219.16 - 1912 (.7020)}{.0720 - .0244} = 1713 = \text{calc. value of } R_1$$

Since 1,713 ≠ 2,100 Repeat Calculation by assuming R₁ = 2,045

TABLE IIa
Summary of All Calculations 39° API Oil

Curve Identification No. Fig. 7	Assumed Conditions	Predicted Quantities	Calculation No.						
			1	2	3	4	5	6	7
1	(P _e —P _w)=0 S _o Uniform	P..... R..... n/N.....	2772 1108 .0208	2275 1968 .0640	1775 3125 .1045	1275 4525 .1408	775 5300 .1733	450 4695 .1948	200 3840 .2278
4	r _e =300 ft. (P _e —P _w)=1000 psi	P _{avg} R..... (n/N) _{avg}	2716 1190 .0255	2223 2060 .0686	1726 3250 .1099	1230 4653 .1454	743 5316 .1767	448 4730 .1979	250 4050 .2240
2	r _e =750 ft. (P _e —P _w)=1000 psi	P _{avg} R..... (n/N) _{avg}	2728 1180 .0244	2230 2045 .0680	1730 3240 .1085	1232 4625 .1437	745 5375 .1778	449 4745 .1985	251 3625 .2256
3	r _e =1500 ft. (P _e —P _w)=1000 psi	P _{avg} R..... (n/N) _{avg}	2735 1150 .0240	2233 2047 .0681	1734 3225 .1088	1237 4560 .1488	745 5373 .1768	449 4738 .1975	250 3950 .2230
5	r _e =750 ft. (P _e —P _w)=200 psi	P _{avg} R..... (n/N) _{avg}	2278 1096 .0202	2278 1979 .0638	1778 3100 .1051	1278 4505 .1412	779 5297 .1736	479 4905 .1944	279 3960 .2187
6	r _e =750 ft. (P _e —P _w)=1000 psi Using Eq. (5)	P _{avg} R..... (n/N) _{avg}	2729 1190 .0262	2228 2055 .0682	1729 3230 .1080	1236 4640 .1437	746 5255 .1745	472 5050 .1970	279 3800 .2151

TABLE IIb
Summary of All Calculations 30° API Oil

Assumed Conditions	Predicted Quantities	1	2	3	4	5	6	7
(P _e —P _w)=0 S _o Uniform	P..... R..... n/N.....	2724 1365 .0237	2230 2960 .0543	1735 5315 .0903	1234 7390 .1015	746 8530 .1188	449 7085 .1265	250 4895 .1347
r _e =750 ft. (P _e —P _w)=1000 psi	P..... R..... (n/N) _{avg}	2724 1313 .0241	2231 3005 .0547	1735 5495 .0905	1234 7235 .1018	746 8760 .1190	449 7000 .1264	250 5150 .1348

$$\ln \frac{r_x}{r_w} = \frac{\int_{P_w}^{P_x} \frac{k_o/k}{\mu_o \beta} dp}{\int_{P_w}^{P_e} \frac{k_o/k}{\mu_o \beta} dp} \dots (3)$$

Equation (3) is used to obtain the values of pressure and radius which correspond throughout the system. The calculation of the integral quantities in equation (3) is made by use of equation (1) as given in the following paragraph.

For an assigned value of R , k_g/k_o can be calculated if the pressure is fixed. From k_g/k_o a value of k_o/k can be found. Therefore, the value of the quantity $\frac{k_o/k}{\mu_o \beta}$ can be calculated as a function of pressure. The variation is valid only for the R value assigned. By plotting $\frac{k_o/k}{\mu_o \beta}$ versus pressure the value

of the integral $\int_{P_w}^{P_e} \frac{k_o/k}{\mu_o \beta} dp$ is then

made definite as values of P_e and P_w are chosen. The first ten columns of Table Ia give a calculation of $\frac{k_o/k}{\mu_o \beta}$ between pressures of 1,300 psia and

2,300 psia for a gas-oil ratio of 2,100 cubic feet per barrel. The numerical

value of the integral $\int_{P_w}^{P_x} \frac{k_o/k}{\mu_o \beta} dp$

is determined from equation (3) when values of r_x , r_e , and r_w are chosen. Fixing the value of the integral fixes P_x , the pressure which corresponds to the radius r_x . It is a simpler calculation to work this process in reverse by choosing P_x . Then a value of r_x can be calculated from equation (3).

The saturation existing at this pressure and radius can be determined by referring to the value of k_o/k as determined from $\frac{k_o/k}{\mu_o \beta}$ versus pressure from which the integral values of Table Ia were determined. Fig. 1 is the plot of $\frac{k_o/k}{\mu_o \beta}$ versus pressure from Table Ia, and Fig. 2 is the variation of pressure versus radius and saturation versus radius calculated from the same information.

In summary, therefore, the steady state situation is completely defined by the quantities chosen for r_e , r_w , P_e , P_w , and R , from which the saturation and pressure distributions of Fig. 2 have been calculated. A similar calculation

can be made for any set of chosen quantities.

CALCULATION OF PRESSURE DECLINE

In utilizing the above steady state character to predict reservoir performance, systems with different drainage radii and different $(P_e - P_w)$ values were chosen. The equations for predicting performance are essentially those used by Turner.² Gas-oil ratio values were at first estimated and both pressure and saturation distributions within the producing system were calculated. If the chosen gas-oil ratio and the calculated pressure and saturation values did not check by material balance, a new gas-oil ratio was estimated and the process repeated.

The equation expressing a balance between pressure, stock tank production, and producing gas-oil ratio is:

$$\frac{(u_i - u_o) - \frac{n_i}{N} u_i + \frac{n_i}{N} s_o v_i}{v_i} = \sum_{i=1}^i \left(\frac{R_i + R_{i-1}}{2} \right) \left(\frac{n_i - n_{i-1}}{N} \right) \quad (4)$$

which equation is valid for the assumptions of no water encroachment, no gas

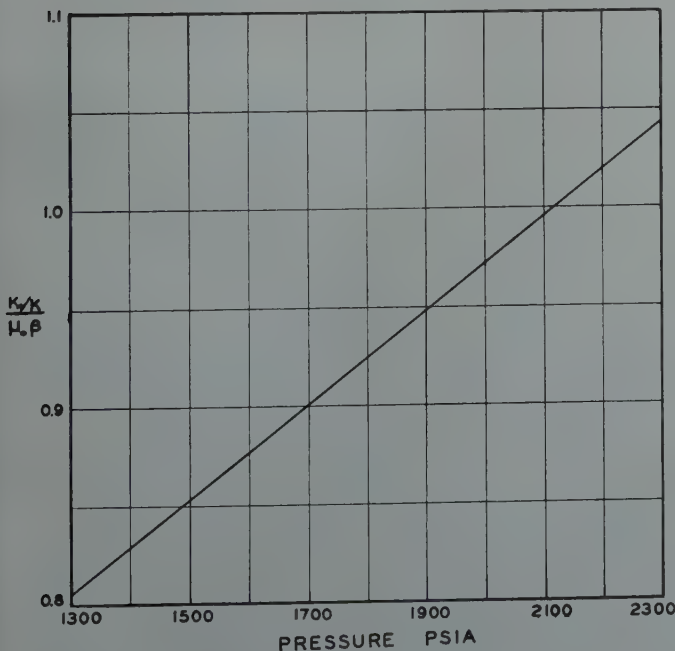


FIG. 1 — VARIATION OF $\frac{k_o/k}{\mu_o \beta}$ WITH PRESSURE

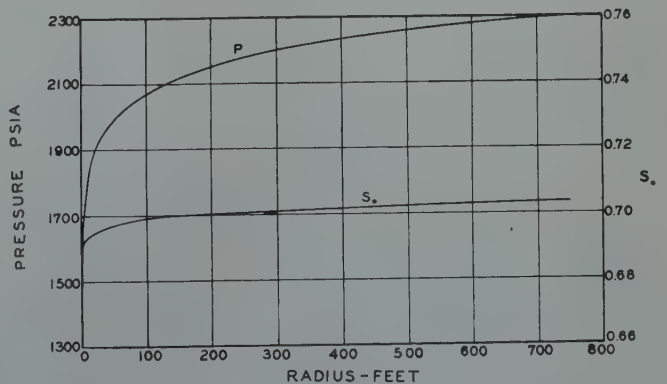


FIG. 2 — DISTRIBUTION OF PRESSURE AND OIL SATURATION WITHIN THE RADIAL FLOW SYSTEM

cap, and no gas reinjection. This equation is simply a statement of the equality of total produced gas obtained by two independent methods. The left-hand side gives total produced gas as found in the basic material balance equation. The right-hand side gives the total produced gas as found by the area under a plot of producing gas-oil ratio versus cumulative oil production.

To arrive at a set of values for $\frac{n_1}{N}$, P_i , and R_1 to balance in the above equation the procedure was as follows: (this procedure is tabulated in Table I)

(1) Values of r_e , r_w , and $(P_e - P_w)$ were chosen for the particular system.

(2) A value of R_1 was chosen and the variation of $\frac{k_o/k}{\mu_o\beta}$ with pressure values between P_e and P_w was calculated according to equation (1).

(3) Values of P_x between P_e and P_w were chosen and used to calculate r_x values according to equation (3).

(4) S_o values were calculated for each value of r_x by use of the pressure values found at r_x , the quantity $\frac{k_o/k}{\mu_o\beta}$ at that pressure, and the dependence of k_o/k on saturation.

These first four steps are essentially calculation of the steady state system as outlined above and tabulated in Table Ia.

(5) Each value of reservoir saturation S_o was converted to an equivalent stock tank oil value by dividing by the value of β for the pressure existing at that saturation point. An average value of stock tank oil remaining in the entire system was obtained by averaging these point values volumetrically over the system, and subtracting the average from the total original oil in place to give n_1/N . This is shown in Table Ib.

(6) An average pressure for the entire system was obtained by averaging the point values volumetrically over the entire system. This is shown in Table Ib.

(7) Values for R_1 , n_1/N , and for fluid characteristics as determined by

the average pressure were substituted in equation (4) to obtain a balance. If a balance was not obtained, a new value of R_1 was chosen and the steps from (2) to (7) were repeated.

As indicated by equation (4) the subscript i refers to any time point in the reservoir's history. The complete history was determined by a succession of such calculations, choosing in each case the time when the pressure at the drainage radius had fallen to some convenient value.

The above calculation was applied to three different well systems with $r_e = 300$ ft, $r_e = 750$ ft, and $r_e = 1,500$ ft (corresponding roughly to spacings of 10, 40, and 160 acres) and for values

TABLE III
Calculation Using Increment Reservoirs

CONDITIONS: $r_e = 750$ ft; $\sqrt{w} = .25$ ft; $(P_e - P_w) = 1000$ psi
Calculations for time when $P_e = 2300$ psia³
Assume $R_1 = 2040$

Radii of Increment	f_x	Average Pressure of Increment	Average S_o	u_{ix}	$\frac{n_{ix}}{N}$	$\frac{f_x(u_{ix} - u_o) + \frac{n_{ix}}{N}(v_{ix}S_o - u_{ix})}{N}$
315 — 850	.8236	(a) 2250	(a) .7055	1.6928	(b)(c) .05628	75.862
135 — 315	.1440	2150	.7034	1.7233	.00920	15.200
60 — 135	.0260	2050	.7015	1.7681	.00155	3.641
25 — 60	.0053	1950	.6988	1.8050	.00030	.853
11 — 25	.0009	1850	.6967	1.8460	.00005	.163
5 — 11	.0002	1750	.6943	1.9142		
2.5 — 5						
1 — 2.5						
0.5 — 1.0					$\frac{n_i}{N} = .06738$	
.25 — 0.5						95.719

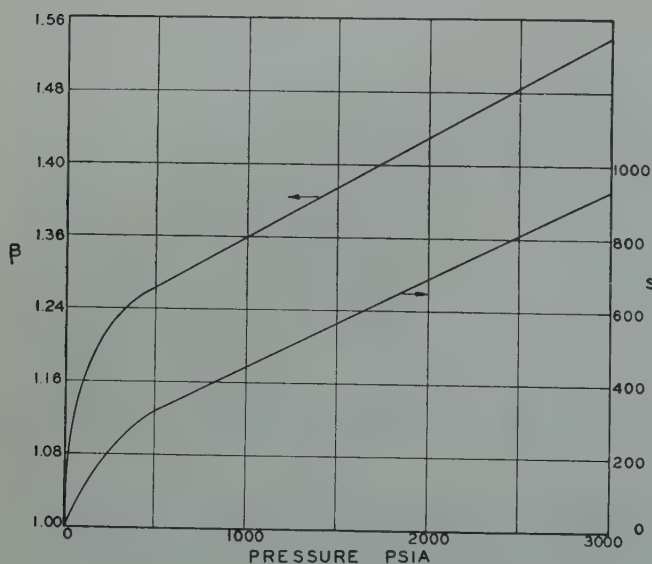


FIG. 3 — FORMATION VOLUME FACTOR AND GAS SOLUBILITY
CHARACTERISTICS OF 39° API RESERVOIR OIL

From previous calculation: $\frac{n_{i-1}}{N} = .02615$

$$R_{i-1} = 1,190$$

$$\sum_{i=1}^{i=i-1} \left(\frac{R_i + R_{i-1}}{2} \right) \left(\frac{n_i}{N} - \frac{n_{i-1}}{N} \right) = 27.72$$

$$27.72 + \frac{(2,040 + 1,190)}{2} (.06738 - .02615) = 94.31$$

Since $94.31 \neq 95.72$ Repeat Calculation using $R_1 = 2,055$

(a) Determined by procedure shown in Table Ia

$$(b) \frac{n_{ix}}{N} = \frac{\left(.5195 - \frac{S_o}{\beta} \right) f_x}{.5195}$$

$$(c) \frac{n_1}{N} = \sum_{x=1}^{x=10} \frac{n_{ix}}{N}$$

of $(P_e - P_w)$ equal to 200 pounds and 1,000 pounds. Fluid characteristics approximating a 39°API crude and a 30°API crude were used in two different sets of calculations. Calculation was also made of the reservoir predictions as ordinarily carried out for uniform

reservoir saturation and zero drawdown conditions to use as a basis for comparison.

Tabulation of a typical calculation is given in Table I, and results of all calculations are listed in Table II. In every case original reservoir pressure

was chosen as 3,000 psia and the connate water was chosen as 20 per cent. Variations of β and s with pressure (as used in all calculations with the exception of these marked 30° API) are given in Fig. 3. Dependence of the quantity v on pressure is given by Fig. 4. Variation of μ_o and μ_o/μ_g with pressure are shown in Fig. 5. The dependence of k_o/k with gas saturation is shown in Fig. 6, and the dependence of k_g/k_o with gas saturation in Fig. 7. Fig. 6 is taken from Leverett and Lewis⁶ (their Fig. 9) for 15-25 per cent connate water. Fig. 7 was computed using the k_o/k values of Fig. 6 and an assumed k_g/k curve such that gas flow would begin as soon as gas formed in the flow channels. Even though this k_g/k_o curve may not be identical with that measured by actual experiment the same curve was used for calculations assuming zero drawdown and finite drawdown. The results reported therefore, should reflect variation in the assumed variables rather than in the k_g/k_o curve.

Fig. 8 shows the predicted results graphically. It is noted that the calculated variation of pressure and instantaneous producing gas-oil ratio with withdrawals is equivalent, for all circumstances calculated, to that determined using the simple equilibrium conditions. This leads to the conclusion that the recovery to be derived from an internally gas driven reservoir is a function only of the fluid properties and flow properties. The economic rate at which these withdrawals occur has been ignored in this analysis. Should any variation of time and abandonment be necessitated by circumstances which give low rates of withdrawal the ultimate recovery would be variable. This approach has been treated by another author.⁵

CALCULATION AS A SERIES OF SEPARATE RESERVOIRS

In considering possible shortcomings to the analysis outlined, it was thought that the method of averaging stock tank saturation and pressure over the drainage system and using fluid characteristics at the average pressure for substitution in the material balance equation might give an erroneous picture. Therefore, the analysis was extended to consider the chosen radial system as a

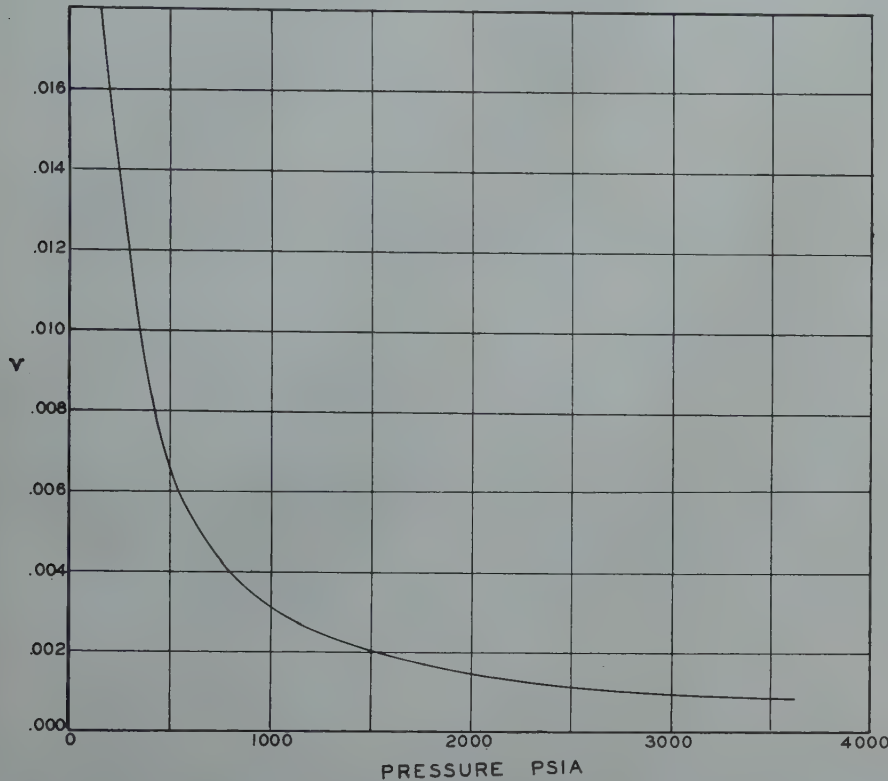


FIG. 4—GAS CONVERSION FACTOR-BARRELS RESERVOIR GAS SPACE PER STANDARD CUBIC FOOT

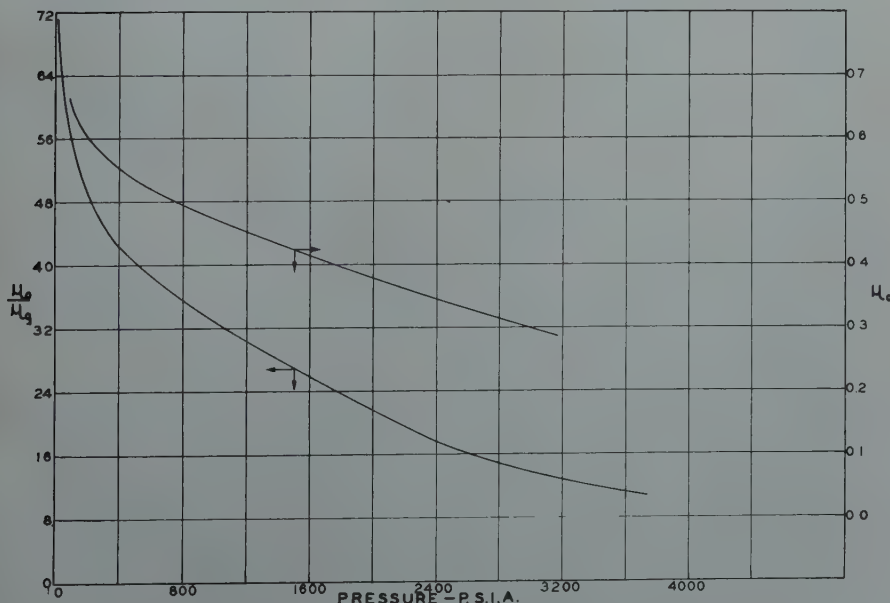


FIG. 5—VISCOSITY CHARACTERISTICS OF RESERVOIR OIL AND GAS

number of separate reservoirs each at its own pressure and saturation but with a common instantaneous producing gas-oil ratio. To do this, the system was first divided into a number of increments of assigned radii, the volumes of which were denoted as fractions of the total, $f_1, f_2, f_3, \dots, f_x$, x denoting any given volume increment. Ten volume increments were used. The material balance equation can be shown to apply in summation to the group of increment reservoirs to give the following:

$$\sum_{x=1}^{x=10} \frac{f_x (u_{1x} - u_o) + \frac{n_{1x}}{N} s_o v_{1x} - \frac{n_{1x}}{N} u_{1x}}{v_{1x}} = \sum_{i=1}^{i=i} \left(\frac{R_i - R_{i-1}}{2} \right) \left(\frac{n_i - n_{i-1}}{N} \right) \quad (5)$$

The assumption that the producing gas-oil ratio is the same at any time for each reservoir increment is in agreement with the use of the steady state flow at any time across the system. A tabulation of calculations in which this technique was used is given in Table III, the results are listed in Table II and are plotted in Fig. 8. This calculation gave a decline of reservoir pressure and variation of gas-oil ratio identical with that from the simpler approach, thereby indicating that an averaging of fluid characteristics was justifiable.

It might be noted that equation (5) can be used for any number of reservoirs producing simultaneously provided the producing gas-oil ratios of the separate reservoirs are equal and provided f_x represents the fraction of the total which each separate reservoir represents.

DECLINE OF PRODUCTIVITY INDICES

The data calculated in this analysis can also be used to indicate the relative decline in theoretical productivity indices. The rate of oil flow from the steady state system at any time is given by equation (2). The productivity index is equal to this rate of oil flow divided by the pressure differential of flow, or

$$P.I. = \frac{7.07 \text{ } kh}{(P_e - P_w) \ln \frac{r_e}{r_w}} \int_{P_w}^{P_e} \frac{k_o/k}{\mu_o \beta} dp \quad (6)$$

For unit permeability and thickness, the relative P.I. values between any two times will be given simply by the values of the integral divided by the respective values of $(P_e - P_w)$ and $\ln \frac{r_e}{r_w}$.

These ratios are plotted in Fig. 9. They show the effect of $(P_e - P_w)$ and drainage radius on the P.I. decline. Each decline curve is for a constant drawdown and spacing value. Curves 1, 2, and 3 are for a constant drawdown of 1,000 psi and for r_e values of 300 feet, 750 feet, and 1,500 feet respectively. Curves 2 and 4 are for drawdown values of 1,000 psi and 200 psi respectively at a constant drainage radius of 750 feet. Since the history of a reservoir has been shown by preceding calculations to be independent of drainage radius and

drawdown, the actual P.I. change in a reservoir due to change in operating drawdown or drainage radius could be found by interpolation on Fig. 9, after having established equilibrium values of reservoir pressure, gas-oil ratio, and cumulative withdrawal.

Calculation of the producing history of an internal gas drive reservoir with a definite drainage radius and pressure drawdown can be made by considering the reservoir to be a radial system flowing oil and gas under steady state. A succession of steady state calculations combined with the material balance concepts suffices to calculate withdrawals, gas-oil ratios, and pressure decline for the reservoir which possesses at any given time a pressure differential and a saturation differential from well radius to drainage radius. Although the method used involves several simplifying assumptions, the results are felt to be fairly representative of the internal gas drive reservoir.

It may be concluded from the calculations described that the history of an

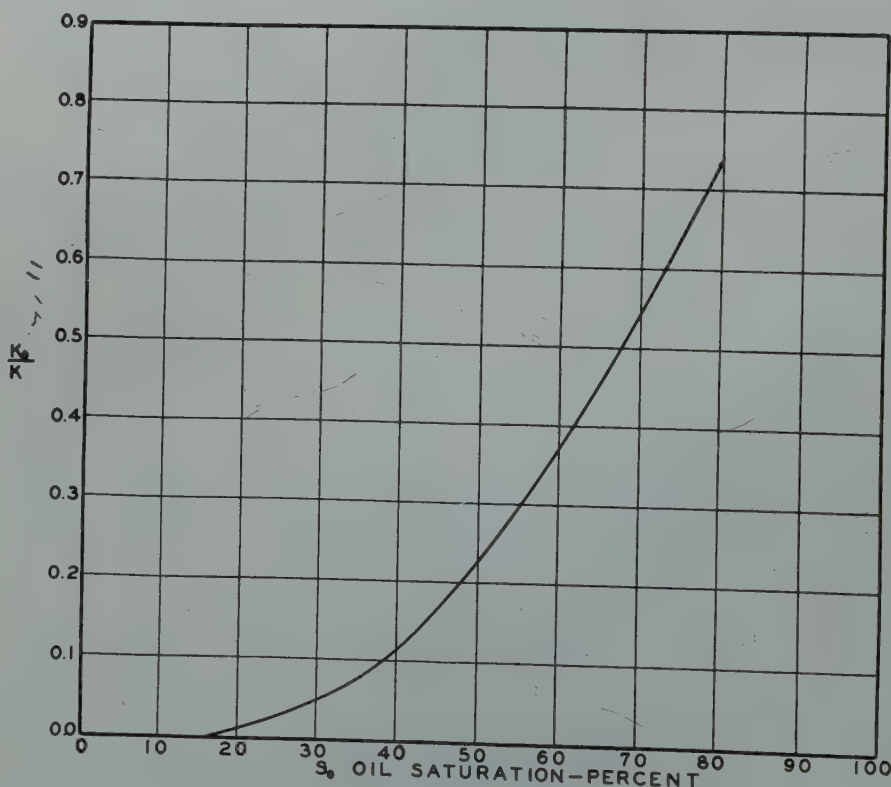


FIG. 6 — RELATIVE PERMEABILITY TO OIL

internal gas drive reservoir is independent of the spacing or pressure drawdown. In other words, from original pressure down to a given value of average reservoir pressure, one well will suffice to produce the same fraction of the total oil in place as will several wells. This conclusion does not consider possible economic limitations. From a standpoint of reservoir mechanics, the same result might have been anticipated from the generally accepted belief that the relative perme-

ability to reservoir fluids is dependent only upon the fluid saturations.

It should be reiterated that in order to make such calculations as are reported here simplifying assumptions are necessary. The primary assumption has been that the reservoir is at any time flowing oil and gas under steady state conditions. In addition it has been assumed that the reservoir is homogeneous, that water within the reservoir is uniformly distributed, that no water is produced, that gas and oil phases do

not segregate by density differential within the reservoir, that there is no vertical flow within the reservoir, and that capillary forces can be neglected. Nevertheless, most of these assumptions apply to any analytical approach to reservoir behavior that can presently be made. The results of the present calculations are offered as a simplified approach to a difficult problem, and the results should be interpreted in that light.

The application of the predicted history of an internal gas drive reservoir as commonly made to practical operations would appear to be justifiable because the zero drawdown calculations give a result identical to that under all other assumed conditions. Further, the prediction of productivity indices on a theoretical basis to take into account pressure drawdown would appear to be simplified.

The implications of the above analysis can be applied only to reservoirs where gas from solution is the sole producing mechanism.

NOMENCLATURE

β = formation volume factor, barrels of reservoir oil per barrel of stock tank oil

μ_o = reservoir oil viscosity, centipoises

μ_g = reservoir gas viscosity, centipoises

N = original stock tank oil in place in reservoir system, bbl

P_e = pressure at drainage radius, psia

P_w = pressure at well radius, psia

P_x = pressure at radius r_x , psia

P_i = reservoir pressure at time i , psia

Q_o = rate of stock tank oil production, bbl per day

R = producing gas-oil ratio, standard cubic feet per barrel of stock tank oil

R_i = producing gas-oil ratio at time i

R_{i-1} = producing gas-oil ratio at time $i-1$

S_o = fractional reservoir oil saturation

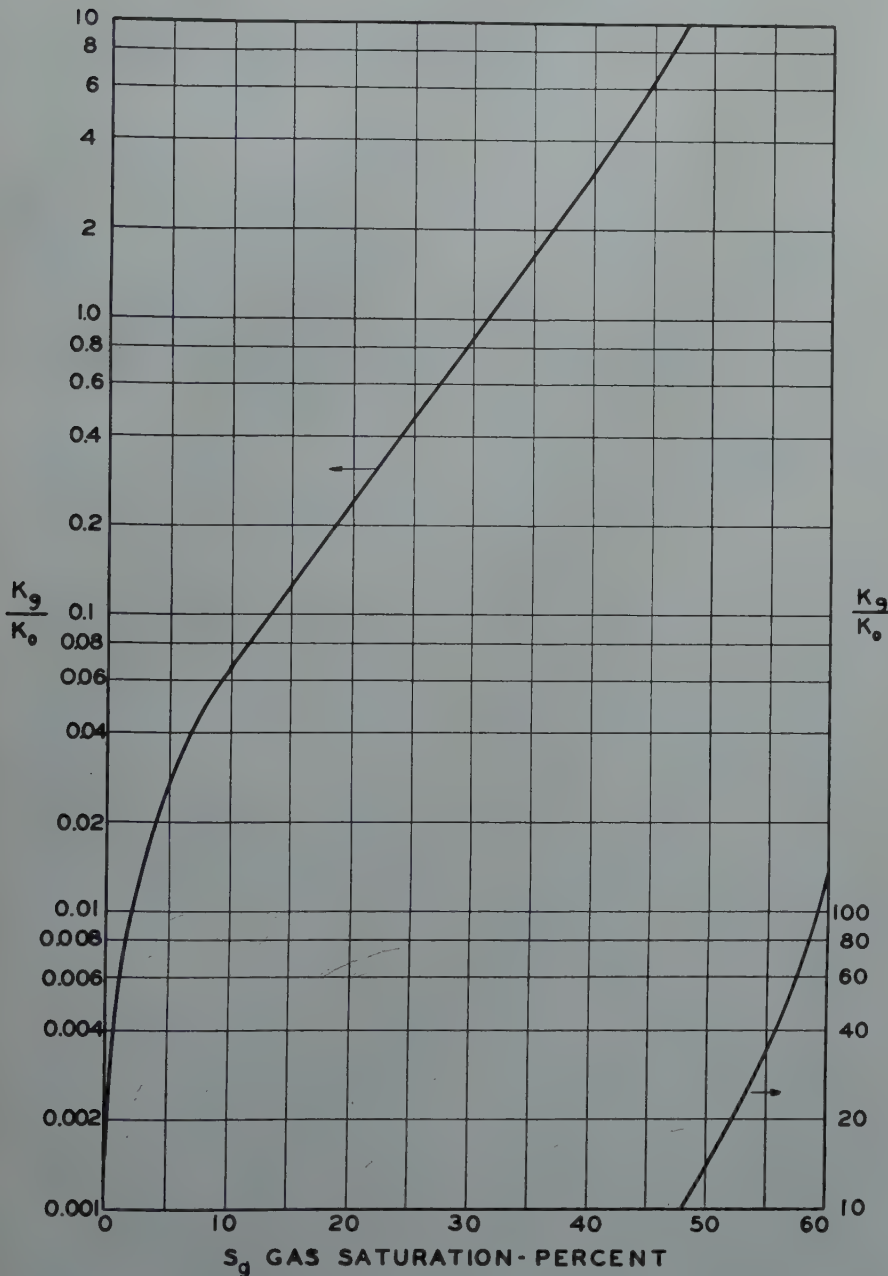


FIG. 7 — LOGARITHMIC RELATION BETWEEN RELATIVE PERMEABILITY RATIO AND RESERVOIR SATURATION

- S_g = fractional reservoir gas saturation
- f_x = fraction of the total reservoir volume represented by the producing increment x
- h = sand thickness, feet
- k = permeability, darcies
- k_g/k_o = relative permeability ratio, gas to oil
- k_o/k = relative permeability to oil
- \ln = natural logarithm
- n_i = stock tank oil produced up to time i , bbl
- n_{i-1} = stock tank oil produced up to time i , bbl
- n_{ix} = stock tank oil removed from producing increment x up to time $i-1$, bbl
- r_o = drainage radius, feet
- r_w = well radius, feet
- r_x = any radius between r_o and r_w
- s = gas in solution, SCF per stock tank bbl
- s_o = value of s at original reservoir pressure
- u = two-phase formation volume factor $= \beta + (s_o - s)v$
- u_o = two-phase formation volume factor at original reservoir pressure
- u_{ix} = two-phase formation volume factor at time i and increment x
- v = gas conversion factor, bbl reservoir gas space per SCF
- v_i = value of v at time i
- v_{ix} = value of v at time i and increment x

REFERENCES

1. Babson, E. C.: Prediction of Reservoir Behavior From Laboratory Data, *AIME, Trans.*, Vol. 155 (1944).
2. Turner, Jack: How Different Size Gas Caps and Pressure Maintenance Affect Amount of Recoverable Oil, *Oil Weekly*, 114, 2, June 12, 1944.
3. Muskat, M.: The Production Histories of Oil Producing Gas Drive Reservoirs, *Applied Physics*, Vol. 16, 3, March, 1945, 147-149.
4. Evinger and Muskat: Calculation of Theoretical Productivity Factor, *AIME Trans.* Vol. 146, (1942).

5. Moyer: Some Theoretical Aspects of Well Drainage and Economic Ultimate Recovery, *Petr Tech*, May, 1947.

6. Leverett and Lewis: Steady Flow of Gas-Oil-Water Mixtures through Unconsolidated Sands, *AIME Trans.*, Vol. 142 (1941). ★ ★ ★

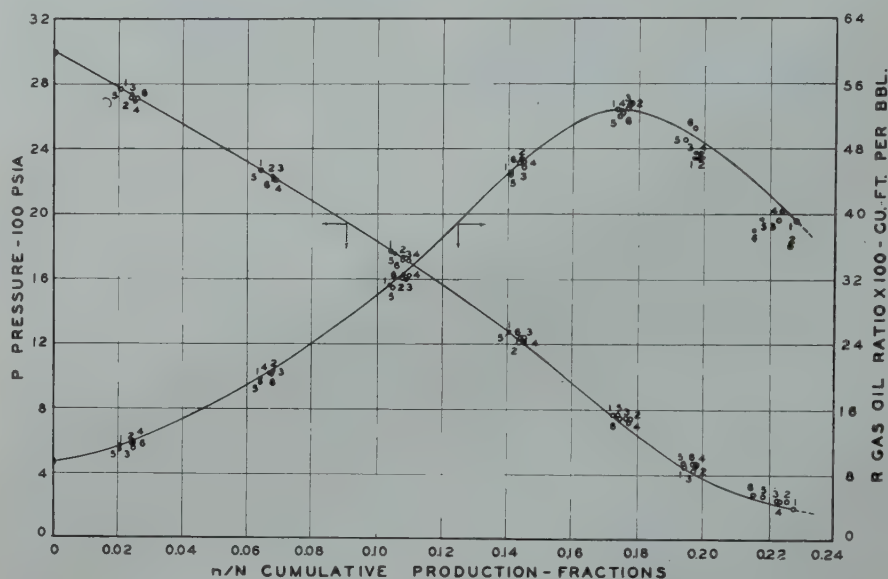


FIG. 8—PREDICTED RELATIONSHIP BETWEEN PRESSURE AND CUMULATIVE PRODUCTION AND BETWEEN PRODUCING GAS-OIL RATIO AND CUMULATIVE PRODUCTION. NUMBERS REFER TO CALCULATIONS AS SHOWN IN TABLE II

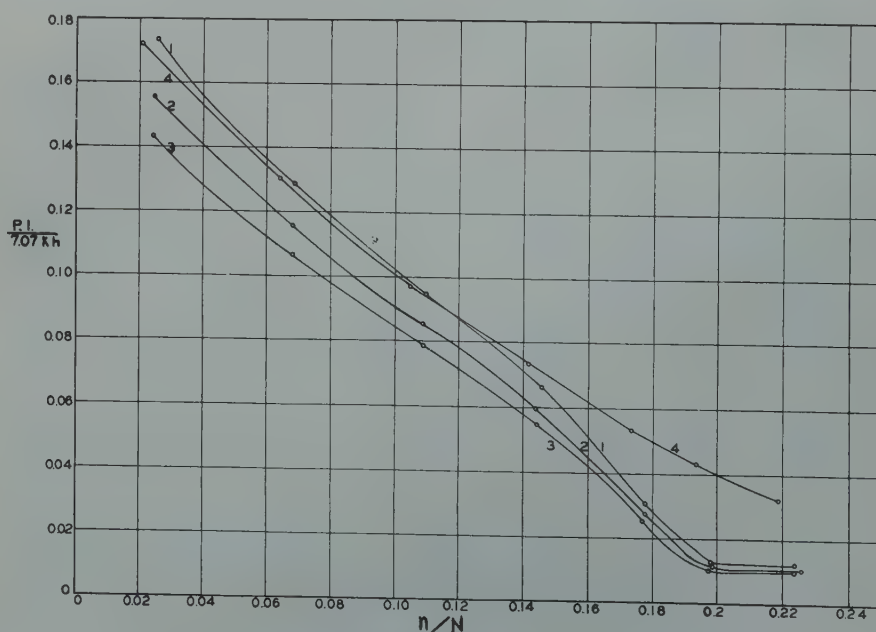


FIG. 9—DECLINE OF PRODUCTIVITY INDEX FOR VARIOUS WELL SYSTEMS

A NEW COMPRESSIBILITY CORRELATION FOR NATURAL GASES AND ITS APPLICATION TO ESTIMATES OF GAS-IN-PLACE

E. B. ELFRINK, C. R. SANDBERG, AND T. A. POLLARD, MEMBER AIME

MAGNOLIA PETROLEUM COMPANY, FIELD RESEARCH LABORATORIES, DALLAS, TEXAS

ABSTRACT

This paper presents an evaluation of compressibility factor data and a discussion of their application to the estimation of gas reserves.

A correlation is presented which provides compressibility factors for use in both two-phase and single-phase hydrocarbon systems. Accuracies comparable to those obtained previously for single-phase systems only can be expected. A simple means of predicting the presence or absence of a liquid phase in a condensate system of known composition is illustrated.

The correlation is based on 1,030 compressibility determinations from 21 hydrocarbon samples taken from eight oil fields. Of the data used, 75 per cent were from California, 15 per cent were from the Mid-Continent area, and 10 per cent were from South America. The average numerical deviation of the experimental data from this compressibility chart is 1.22 per cent.

Charts and tables are included and discussed which illustrate the errors involved through the misuse or nonuse of compressibility factors in estimates of gas-in-place.

INTRODUCTION

The compressibility factor is a coefficient which expresses the deviation of a gas of given composition from the Perfect Gas Laws. A factor such as this is necessary in any calculation involving volumes of gaseous mixtures, and finds extensive application in the estimation

of natural gas and condensate reserves. It is used in the decline curve, the volumetric, and the material balance methods of gas reserves estimation.

The behavior of gases at high pressures has been investigated extensively in recent years and considerable data have been assembled on the compressibility characteristics of a number of gases. Notable among the investigators of high pressure gas relationships are Kvalnes and Gaddy⁶, Kay⁵, Sage and Lacey⁸, and Brown¹, Standing¹⁴ and Katz⁴. Other contributors are Smith and Watson¹², Roland and Kaveler⁷, and Stevens and Vance¹⁵. The data on compressibility factors assembled by these investigators have been presented and correlated in numerous ways; particularly noteworthy is the method first presented by Kay⁵ which relates compressibility factor "Z" to pseudo-reduced temperature and pseudo-reduced pressure. Other investigators have used this empirical relationship successfully and numerous charts covering a large number of gases have been constructed on this basis.

It is the purpose of this paper to evaluate compressibility factor data and to illustrate the importance of their proper use in the estimation of gas-in-place for both gas and condensate reservoirs.

EVALUATION OF COMPRESSIBILITY FACTOR DATA

The compressibility chart presented by Standing, Katz, Brown and Holcomb⁴ in 1941 is probably the most recent and reliable chart for natural gases. The reliability of the Katz chart has been investigated by the writers for a fairly large number of gases (single-phase) in the pressure range from 500 to 10,000

psia and temperature range from 80 to 400°F. A summary of this comparison is presented in Table I. The numerical average deviation of the chart compressibility factors from the experimental compressibility factors is 1.05 per cent, and the algebraic deviation is -0.28 per cent.

The Katz correlation appears to be quite accurate for single-phase hydrocarbon systems. It was based on single-phase systems and does not necessarily provide a means of accurately predicting the behavior of two-phase systems which might be encountered in condensate work. Data published recently by Sage and Olds¹⁰ have enlarged the knowledge of phase behavior in condensate systems by covering extensively the compressibilities of systems in the two-phase as well as single-phase regions for a wide range of temperatures, pressures and gas-oil ratios. An evaluation of these data indicates that conditions can arise, especially in condensate systems having fairly low gas-oil ratios, in which two phases occur and the usual gaseous compressibility factors do not accurately apply.

The measured PVT data of Sage and Olds covering two-phase systems have been correlated with additional such data from the Mid-Continent² area and South America; these are presented in Fig. 1. This chart is the result of 1,030 compressibility* determinations from 21 hydrocarbon samples taken from eight oil and condensate fields. Of the data used, 74.75 per cent were from California, 15.45 per cent were from the Mid-Continent area, and 9.80 per cent were from South America. The chart construction is based on the original

Manuscript received at office of Petroleum Branch January 28, 1949. Paper presented at AIME Annual Meeting in San Francisco, February 13-17, 1949.

* References are given at end of paper.

* In this paper the term "compressibility" refers to the term "Z" in the equation $PV = ZNRT$, for either single- or two-phase systems.

two correlations. It has been found for a temperature of 150°F. this disagreement is 1.5 per cent at the dew point and for a temperature of 250°F. the disagreement is 0.5 per cent. The relationship between temperature and per cent disagreement is essentially linear between 150 and 250°F.

A sample calculation of gas-in-place for an actual condensate system, using Fig. 1, is presented in Table VI. Comparison of the result of this calculation with one using single-phase compressibility values shows that in the latter case a sizeable over-estimation of the gas-in-place would have resulted. Appropriate adjustments must, of course, be made in the final reserve estimates for effect of unrecoverable liquid phases left in the reservoir, for two-phase systems.

CONCLUSIONS

The present work demonstrates the feasibility of applying two-phase compressibility factors to two-phase systems for purposes of gas-in-place estimations, where representative composition data are available. Accuracies comparable to those obtained in single-phase systems using single-phase compressibility factors can be expected. A simple means of predicting the presence or absence of a liquid phase in a condensate reservoir is indicated, and the proper use of compressibility factors has been evaluated and illustrated.

ACKNOWLEDGMENTS

This paper originated as part of the work of the Subcommittee on Gas Reserves of the AIME Production Technology Committee; helpful comments of members of that committee are hereby acknowledged.

The authors wish to express their appreciation to the Magnolia Petroleum Company for permission to publish this paper, and to operating department personnel of Magnolia and its affiliates, Socony-Vacuum and General Petroleum,

for their helpful suggestions and comments. Appreciation is also extended to Dr. D. L. Katz for use of certain portions of his graphical correlation of pseudo-reduced properties vs. compressibility⁴.

TABLE VI

Example of Gas-in-Place Estimation Using Fig. 1 and the Katz Correlation
Given:

Reservoir Pressure, $P = 2,500$ psia
Reservoir Temp., $T = 150^\circ\text{F}$.
Porosity, $\phi = 0.30$
Interstitial Water Content, $S_w = 0.23$
 $r_P R$ (Total Product at Reservoir Cond.) = 3.89
 $r_T R$ (Total Product at Reservoir Cond.) = 1.25
 $r_P R$ (Produced Gas at Std. Cond.) = 0.02179
 $r_T R$ (Produced Gas at Std. Cond.) = 1.259
Produced Gas-Oil Ratio = 6,241 cu ft/bbl
Trap Gas/Day = 2,754,000 cu ft
Vent Gas/Day = 223,116 cu ft
Tank Oil/Day = 477 bbl
Specific Vol of Tank Oil = 0.021314 cu ft/lb
Molecular Wt of Tank Oil = 120.06

A. Using Fig. 1

$$Q = \frac{43,560 \times \phi \times (1 - S_w) \times 379.3 \times Z_1 \times P \times \text{E.R.}}{Z_2 RT}$$

$$Z_1 \text{ from Fig. 1} = 0.996$$

$$Z_2 \text{ from Fig. 1} = 0.720$$

$$\text{E.R.} = \frac{2,977,116}{2,977,116 + (477 \times 5.615 \times 379.3)} = 0.8823$$

$$(0.021314 \times 120.06)$$

$$\therefore Q = \frac{43,560 \times 0.30 \times 0.77 \times 379.3 \times 0.996 \times 2,500 \times 0.8823}{0.720 \times 10.73 \times 609.6}$$

$$= 1,781,300 \text{ cu ft gas/acre-ft}$$

B. Katz Chart

$$Z_2 \text{ from Katz Chart} = 0.623$$

$$\therefore Q = \frac{43,560 \times 0.30 \times 0.77 \times 379.3 \times 0.996 \times 2,500 \times 0.8823}{0.623 \times 10.73 \times 609.6}$$

$$= 2,057,475 \text{ cu ft gas/acre-ft}$$

$$\text{Per Cent Over-Estimation} = \frac{2,057,475 - 1,781,300}{1,781,300} \times 100 = 15.6$$

TABLE V

Comparison of Single-Phase and Two-Phase Compressibility Factors for Condensate Systems in Which Liquid Was Present at the State Point Chosen

Gas-Oil Ratio cu. ft./bbl.	Reservoir Pressure, psia	Reservoir Temperature, °F.	P_{TR}	P_{PR}	Single-Phase Compressibility Factor	Two-Phase Compressibility Factor	Per Cent Deviation	Phase
4000	2000	160	1.169	3.203	0.5200	0.6900	32.69	Two-Phase
6241	2500	150	1.250	3.890	0.6230	0.7200	15.56	
9260	3000	190	1.447	4.609	0.7600	0.8015	5.46	
24000	2600	130	1.330	3.950	0.6700	0.7150	6.72	
6241	4500	200	1.356	7.015	0.8990	0.8990	0.00	
								Two-Phase
								Two-Phase
								Two-Phase
								Single-Phase

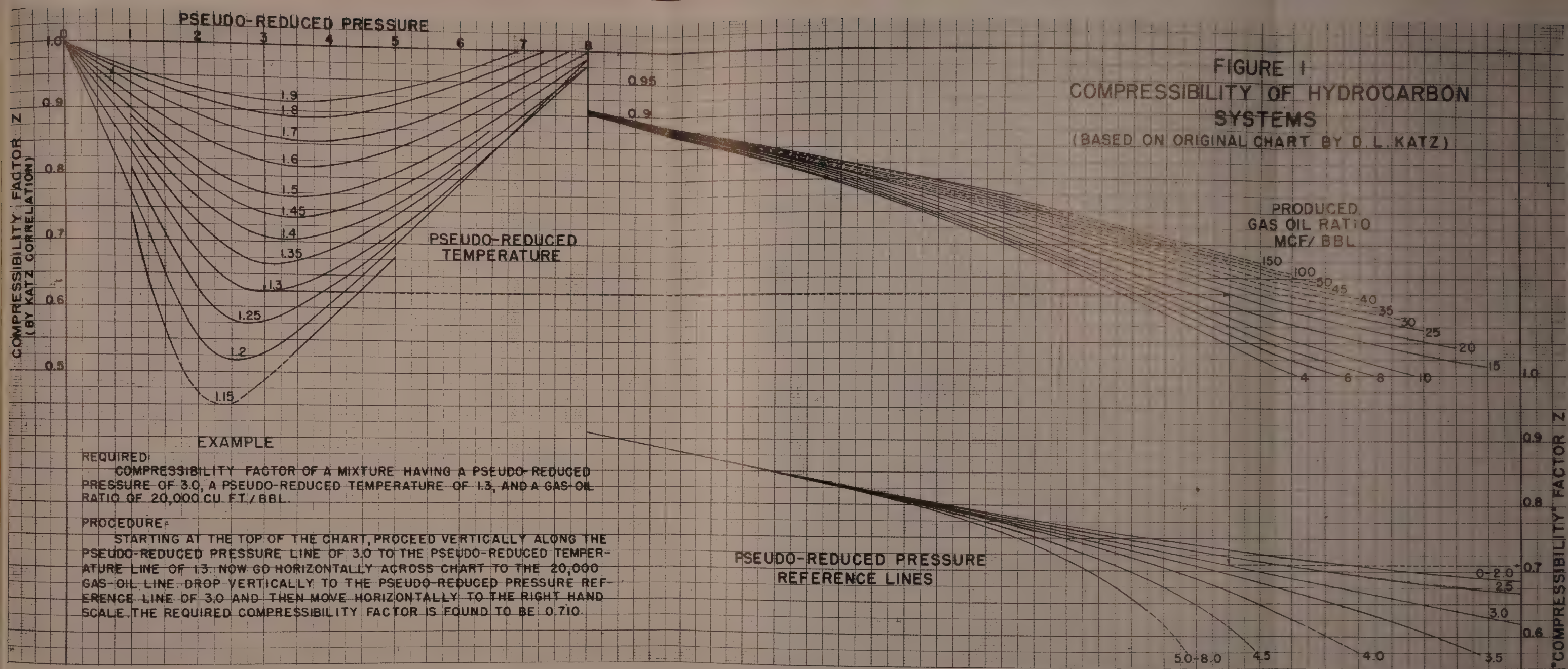


FIG. 1 — COMPRESSIBILITY OF HYDROCARBON SYSTEMS
(BASED ON ORIGINAL CHART BY D. L. KATZ)

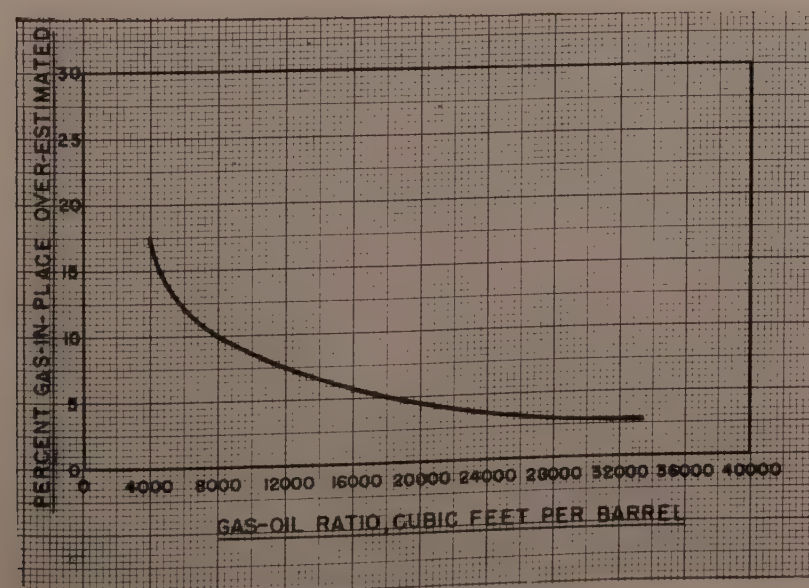


FIG. 2 — PER CENT ERROR RESULTING FROM OMISSION OF EQUIVALENT RATIO IN VOLUMETRIC EQUATION

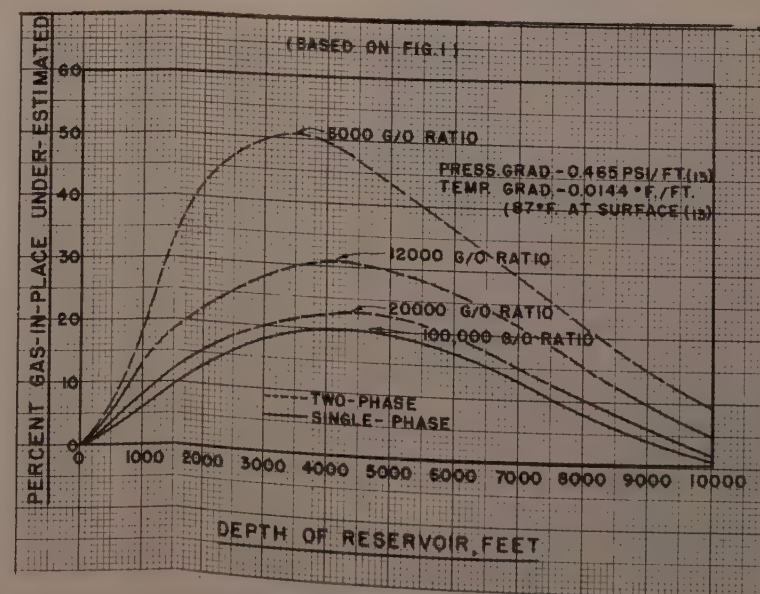


FIG. 3 — PER CENT ERROR RESULTING FROM OMISSION OF COMPRESSIBILITY FACTOR IN VOLUMETRIC EQUATION

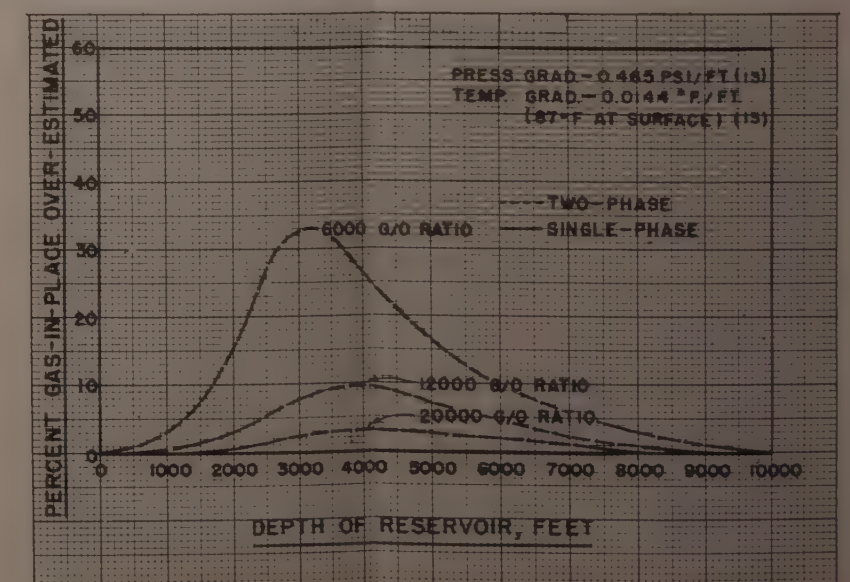


FIG. 4 — PER CENT ERROR RESULTING FROM USE OF SINGLE-PHASE COMPRESSIBILITY FACTORS IN THE TWO-PHASE REGION

NOMENCLATURE

$$\left[\frac{\text{cu ft gas}}{\text{cu ft gas} + \left(\frac{\text{bbl oil} \times 5.615 \times 379.3}{\text{sp vol of oil} \times \text{mol wt of oil}} \right)} \right] = \text{E.R. (equivalent ratio)}$$

P = reservoir pressure, psia

P_R = pseudo-reduced pressure

T_R = pseudo-reduced temperature

Q = cubic feet of gas-in-place per acre-foot at 60°F. and 14.7 psia

R = 10.73

S_w = interstitial water content of reservoir, expressed as a decimal fraction

T = reservoir temperature, °R (459.6 + °F)

Z_1 = compressibility factor of produced gas at 60°F. and 14.7 psia (can be determined from Fig. 1 by using left ordinate)

Z_2 = "compressibility" factor of entire system at reservoir conditions

ϕ = porosity, expressed as a decimal fraction

379.3 = volume in cubic feet occupied by one pound mol of gas at 60°F. and 14.7 psia

43,560 = number of cubic feet per acre-foot

REFERENCES

1. Brown, G. G.: The Compressibility of Gases, *Pet. Engr. 11*, No. 4, 21-4, 1940.
2. Eilerts, Kenneth, and Smith, R. Vincent: Specific Volumes and Phase-Boundary Properties of Separator-Gas and Liquid-Hydrocarbon Mixtures, Bureau of Mines, R.I. 3642, April, 1942.
3. Gruy, J. A., and Crichton, H. J.: A Critical Review of Methods Used in the Estimation of Natural Gas Reserves, *AIME Petr. Tech.*, July, 1948.
4. Katz, D. L.: High Pressure Gas Measurement, Proceedings of the Twenty-first Annual Convention, N.G.A.A., May, 1942.
5. Kay, W. B.: Density of Hydrocarbon Gases and Vapors at High Temperature and Pressure, *Ind. Eng. Chem.*, Vol. 28, p. 1014, 1936.
6. Kvalnes, H. M., and Gaddy, V. L.: The Compressibility Isotherms of Methane at Pressures to 1,000 Atmospheres and at Temperatures from -70 to 200°, *J. Am. Chem. Soc.*, 53, 394-9, 1931.
7. Roland, C. H., Smith, D. E., and Kaveler, H. H.: Equilibrium Constants for a Gas-Distillate System, *Oil and Gas Jnl.*, March 27, 1941.
8. Sage, B. H., and Lacey, W. N.: Series of publications in *Ind. Eng. Chem.* and *A.P.I.*, 1933 to date.
9. Sage, B. H., and Lacey, W. N.: Partial Volumetric Behavior of the Lighter Paraffin Hydrocarbons in the Gas Phase, A.P.I. Annual Meeting, Nov. 17, 1939.
10. Sage, B. H., and Olds, R. H.: Volumetric Behavior of Oil and Gas from Several San Joaquin Valley Fields, *AIME Petr. Tech.*, March, 1947.
11. Sage, B. H., and Reamer, H. H.: Volumetric Behavior of Oil and Gas from the Rio Bravo Field, *Trans. AIME*, Vol. 142, 1941.
12. Smith, R. L., and Watson, K. M.: Boiling Points and Critical Properties of Hydrocarbon Mixtures, *Ind. Eng. Chem.*, Vol. 29, p. 1408, 1937.
13. Spoor, H. C., Jr.: Estimation of Gas Reserves, Report of Composite Study Group Papers Texas Gulf Coast, Houston Geological Society, 1946.
14. Standing, M. B., and Katz, D. L.: Density of Natural Gases, *AIME Petr. Tech.*, July, 1941.
15. Stevens, A. B., and Vance, Harold: Experimental Determinations of the Compressibility Factors of Several Natural Gases and the Application of These Data to Simple Gas Computations, *Oil Weekly*, p. 21, June 8, 1942. ★ ★ ★

SOME EXAMPLES OF FLUID FLOW MECHANISM IN LIMESTONE RESERVOIRS

W. O. KELLER AND R. A. MORSE, JUNIOR MEMBERS AIME
STANOLIND OIL AND GAS COMPANY, TULSA, OKLAHOMA

ABSTRACT

The properties of limestone reservoir rocks such as the distribution and degree of continuity of the pore systems, and the relative volumes and permeabilities of the systems making up the complex cause large variations between performance of individual limestone reservoirs and their susceptibility to secondary recovery methods. The effects of these factors on the mechanism of fluid flow cannot be adequately evaluated with presently developed concepts, laboratory data, and geological information. The observance and interpretation of the performance of individual limestone reservoirs provides, at present, the most adequate approach for evaluating the integrated effects upon performance of the many, now immeasurable variations in the properties of limestone reservoirs.

INTRODUCTION

The development and application of techniques for increasing the efficiency of oil recovery from natural reservoirs is a problem of primary importance to the industry. During the past several years, a great deal of effort has been expended by the technical personnel of the industry toward the improvement of present known methods of oil recovery, and evaluating the factors which control the susceptibility of particular reservoir types to economic application of

secondary recovery methods. Providing adequate and accurate laboratory data on the properties of the reservoir rock and its contained fluids, together with good production statistics, are available, methods have been evolved for estimating with reasonable accuracy the performance of an oil reservoir under either continued natural depletion or conditions imposed by introducing additional displacing fluid into the reservoir from an extraneous source through the injection of gas and/or water.

The susceptibility of limestone reservoirs to secondary recovery by gas injection is very much dependent upon gas-oil relative permeability relationships for the reservoir in question. In a rock formation in which the porosity is of the intergranular type such as is found in sand stones and some non-fractured dolomites, a representative sample of the pore structure can be obtained in a small core plug. In this type of reservoir, it has been shown that relative permeability data obtained from laboratory experiments can be properly applied to evaluate the flow relationships actually observed during the depletion of a reservoir. In addition, a good idea of the fraction of the reservoir which will be swept by the injected gas may be obtained from the spacing pattern used and the permeability profile of cored wells. From these data, it has been demonstrated that reliable estimates of performance and recoveries under gas injection operations can be made for reservoirs in which the porosity is of the intergranular type.

Limestone reservoirs on the other hand often present much more complex problems. One reason that the performance of limestone reservoirs is so variable is that there may be, in reality, two or more pore systems, the integrated performance of which will depend upon the physical properties of each system and their inter-relationship. For instance, in a limestone reservoir, the main pore structure, as far as void spaces for storage of hydrocarbons is concerned, may be represented by the intergranular openings of the rock. Usually in limes and dolomites, the intergranular pore openings are very small and the matrix permeabilities extremely low. Often, as in the case of many dolomite and oolitic lime reservoirs, this is the only pore system, and performance is observed to be very similar to that of a sand stone of similar permeability. However, in the great majority of the limestone reservoirs, there is present, in addition to the intergranular pore system, a complementary system of openings caused by fracturing or solution.^{1,2} The openings in the latter system are usually many times more permeable than the intergranular pore system due to their much larger size, and may contribute almost all the fluid carrying capacity of the formation, even though their volume may be a very small part of the total pore space in the reservoir. Obviously, the performance of such a complex under either primary or secondary control will depend upon the distribution and degree of continuity of both systems, the relative volumes and permeabilities of the

Manuscript received at office of Petroleum Branch September 25, 1948. Paper presented at Branch Fall Meeting in Dallas October 4-6, 1948.

¹References are given at end of paper.

two systems; and in some instances, the rate of fluid withdrawals from the reservoir. For instance, if the volume of a *highly interconnected* secondary pore system is relatively small and of much higher permeability, compared to the intergranular system, the properties of the secondary pore system will exercise considerable control over performance. On the other hand, if the intermediate porosity is dispersed such that interconnection is largely through the matrix pore system, then the extent to which performance will be governed by properties of the secondary system will be minimized.

The infinite variety of possible combinations of continuity, relative volumes and permeabilities of intergranular and secondary pore spaces makes the study of performance of limestone reservoirs an enormously complex problem. Obviously, laboratory relative permeability relationships determined on matrix of the reservoir rock cannot be depended upon, at least under all conditions of production that might be encountered. Usually, due to the size and distribution of the openings in the secondary system of porosity, it is impossible to obtain a representative sample of the reservoir rock with a reasonably sized core. Hence, laboratory data cannot be relied upon completely, at least at the present stage of development, to provide relative permeability data which can be applied directly to limestone reservoir

performance problems. For this reason, it has been found desirable to calculate, from field performance data, the relative permeability relationships for a particular field and to extrapolate these data to evaluate future performance either under primary or gas injection operations. Even this method is open to the objection that the relationships obtained at one condition of production rate and rate of pressure decline may not be strictly applicable to another set of conditions. For this reason, with our present knowledge, it is impossible to set up as rigid a depletion program for such limestone reservoirs. The best approach that can be made at present is to use field performance data as an indication of the behavior to be expected under secondary recovery operations, and set up a program on the basis of such indications, followed by constant engineering surveillance of the project, making such changes as are dictated by performance of the field and experience on similar projects.

Obviously, such gas injection projects must be experimental and exploratory in nature, with the better engineering of future projects being based on close study of good data on similar projects in like reservoirs. Following are brief reviews of performance data from a number of limestone reservoirs. It is believed that the study of these and other limestone reservoirs will enable the development of increasingly better engineering analyses of second-

ary recovery possibilities by gas injection, as well as increase the general fund of knowledge on the complex problem of the displacement processes in limestone reservoirs.

FIELD "A"

Field "A" is a volumetrically controlled, relatively tight, dolomitic limestone reservoir.

Production is obtained from the San Andres formation, of Permian age, encountered at an average depth of approximately 4,750 feet. Seventy producing wells, located in the center of 40-acre units have been drilled to date within the presently developed area consisting of approximately 3,000 acres. Some development is still under way.

Although the oil accumulation is located on a structural high with approximately 100 feet of closure, the productive limits of the field are apparently controlled primarily by lack of porosity and permeability development rather than structural conditions. A definite water level has not been established, although there is some evidence that indicates that the water saturated porosity underlying the oil reservoir is not a level surface but tends to follow the structure.

The producing zone, consisting predominantly of gray crystalline dolomite, has a gross thickness of approximately 200 feet; however, based on core analysis from 14 wells in the field, the pay zone, consisting of erratically distributed streaks of permeable, porous rock, amounts to only ten to fifty per cent of the gross section. The vertical permeability distribution is illustrated by the core graphs shown in Fig. 1. As can be seen from the key map on Fig. 1, the four wells represented are all mutually direct or diagonal offsets, so that the variation shown exists at the four corners of a 40-acre area represented by the location of the wells. The permeability profile is highly irregular in any particular well, which might indicate poor sweeping of the formation by an injected medium, due to by-passing in the more highly permeable zones. It can be noted from Fig. 1 that the individual stringers of high and low permeability do not appear to be continuous between wells. This suggests the possibility that the producing for-

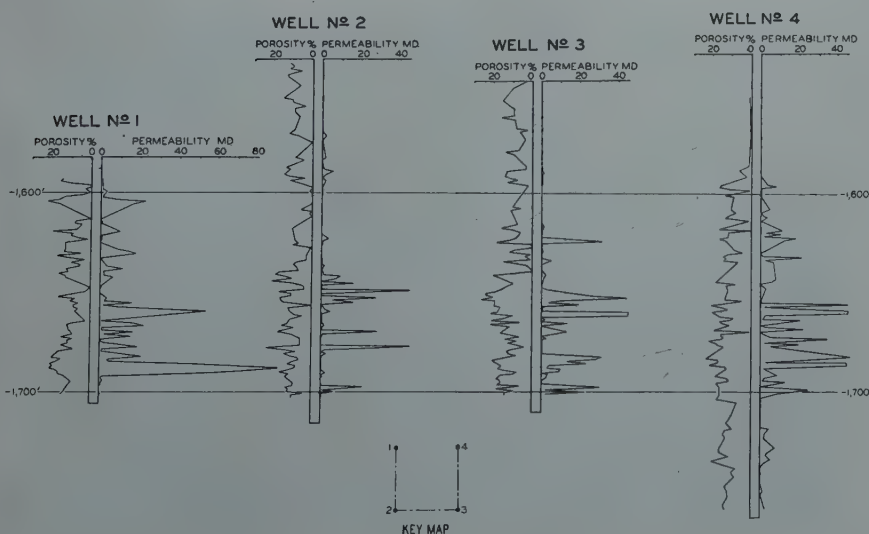


FIG. 1 — FIELD "A", CORE GRAPH CROSS SECTION

mation is made up of areally irregular zones of varying permeability and size, interfingering so that the effects of vertical variations in permeability, indicated in individual core analysis are greatly minimized to the extent that the flow of injected gas through the formation would be fairly evenly distributed throughout the productive zone. The probability that the areal distribution of the more permeable portions of the pay may be interfingering and erratic, as is the vertical distribution, has been borne out by the performance of the gas injection program initiated in April, 1946, as will be illustrated.

The wells are characterized by very low productivities, with initial productivity indices, after shooting, ranging from .05 to .5 barrels per day per pound pressure drop. The average productivity index is in the neighborhood of .2 barrels per day per psi. All the wells were completed as pumping wells, or were put on the pump very soon after completion. Completion practices in the field have consisted of setting casing at the top of the pay and shooting with solid nitroglycerin. A few wells have been acidized; however, acidization to stimulate productivity has been unsuccessful.

Based on several bottom hole sample analyses, the reservoir oil which was undersaturated at the initial reservoir pressure of 1,954 psig (-1,500 feet datum), has the following characteristics:

1. Bubble point pressure at reservoir temperature of 94°F. = 326 psia
2. Solubility (by differential vaporization) = 140 cu ft/bbl
3. Reservoir volume factor of bubble point oil = 1.091.
4. Viscosity at 326 psia and 94°F. = 2.25 cp
5. H₂S content of solution gas 1,776 grains/100 cu ft

As shown by Fig. 3, the average producing gas-oil ratio has been approximately equal to the solution ratio.

Because of the undersaturated nature of the reservoir oil, the expulsive force causing oil production during the period preceding gas injection was furnished entirely by the expansion of the liquid oil in the reservoir. It was apparent early in the development of the field that, due to the undersaturated

condition, a very rapid drop in reservoir pressure would occur down to the bubble point pressure, resulting in a rapid drop in the productivity of the wells, due primarily to the reduction in the available pressure differential. It was also apparent that, under natural depletion, the productivities of the wells would be further drastically reduced at such time as the reservoir pressure declined below the bubble point since, at this time, the presence of liberated solution gas would materially reduce the effective permeability to oil and, at the same time, there would be very little pressure differential to accomplish flow. This reservoir pressure and well productivity performance is depicted graphically by Figs. 2 and 3.

Based on these factors, it was estimated that a small percentage of the oil could be produced at economic rates by internal gas expansion. Engineering estimates indicated that the abandonment of the reservoir under natural depletion would have been necessary when the reservoir liquid-saturation was still in excess of 90 per cent, with approximately 20 per cent of the expected ultimate recovery being attributed to liquid expansion above the bubble point pressure. Although it was not possible to calculate precisely what the expected effect of this performance would be upon the oil production rate from the field since complete data on relative permeabilities were not available, an

approximation of the rates to be expected is shown by the extrapolated curve of expected oil rates on Fig. 2. Those estimated rates under primary production were calculated using a typical relative permeability to oil curve from laboratory data and an average initial P.I. of .2 bbls. per day per psi.

Although very little primary performance data, upon which to base studies of the anticipated performance under secondary recovery methods could be obtained prior to the time such methods were necessary, the high abandonment liquid saturation anticipated under primary operations made almost mandatory the early injection of gas or water. It was realized that such opera-

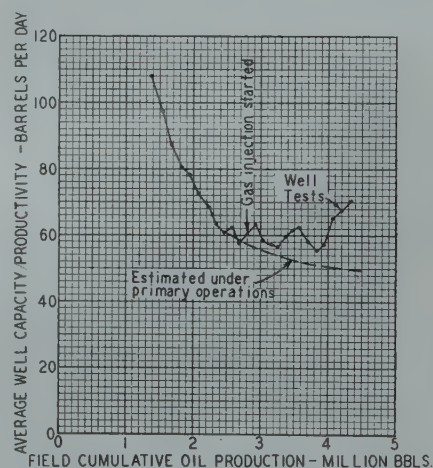


FIG. 2 — FIELD "A", AVERAGE WELL PRODUCTIVITY VS. CUMULATIVE PRODUCTION

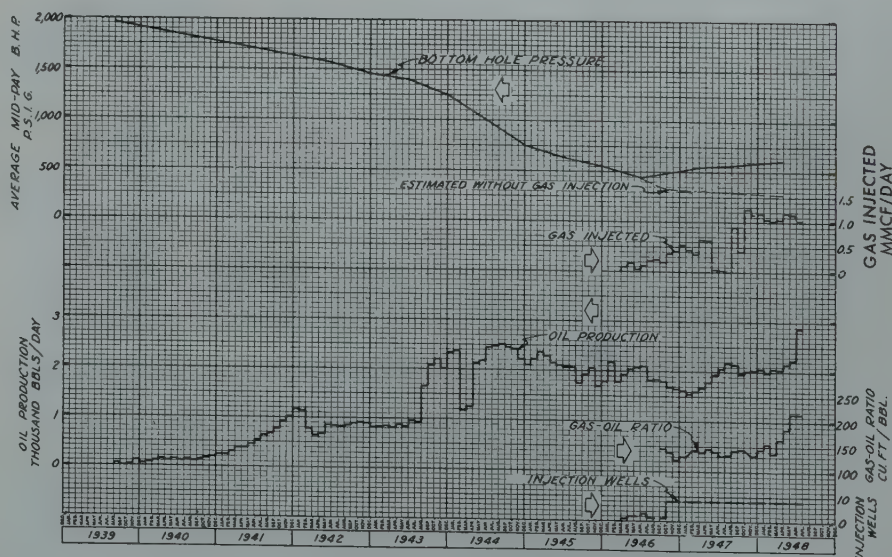


FIG. 3 — FIELD "A", RESERVOIR PERFORMANCE

tions would entail considerable risk. in view of the many unknown reservoir factors involved, probably the most important of which was the areal extent and continuity of the more permeable streaks, which would control the amount of by-passing of the injected medium to be expected. It was felt, however, that the possible gains to be derived from depletion of the reservoir by secondary methods more than outweighed the risk involved. Moreover, it was believed that the information derived from this project would be of considerable benefit in planning the depletion programs for similar limestone reservoirs encountered in West Texas. After study of all the available data, the decision was made to install an experimental gas injection program in the field to maintain the reservoir pressure at a level somewhat in excess of the bubble point of the reservoir oil, in order to

provide an adequate pressure differential to produce oil at economic rates, supplement the available displacing fluid, and improve the recovery efficiency by maintaining more favorable saturation conditions within the reservoir.

For the purpose of conducting the injectivity tests, and also to provide injection facilities until a permanent plant could be constructed, a portable compressor was moved into the field and gas injection started in April, 1946, as shown by the performance curves in Fig. 3. Injection tests were made on all the contemplated injection wells, and fairly continuous gas injection into one well was accomplished by the use of the portable compressor. The injection tests indicated that gas could be injected in sufficient volumes to maintain reservoir pressures by the use of an injection pressure of approximately

1,000 psi. Fluid level depression tests, made in conjunction with the injection tests, indicated that the gas was being forced fairly uniformly into the entire formation.

In September, 1947, the permanent compressor station was put into operation, along with the electrical generating station to furnish power to operate the pumping wells. Gas has been injected into seven injection wells almost continuously since that time. Gas is currently being injected into eight wells on a nine-spot pattern at rates adjusted to replace all withdrawals from the surrounding wells and, at the time time, eliminate large pressure differentials across the field.

Bottom hole pressure, oil production rate, gas injection rate, and gas-oil ratio performance of the field are illustrated on Fig. 3. The bottom hole pressure had declined to slightly less than

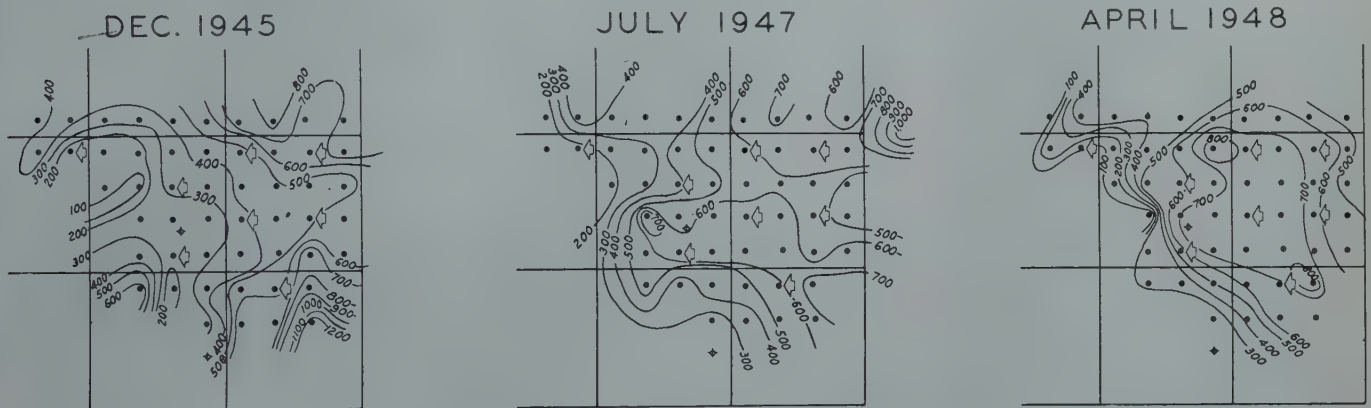


FIG. 4A—FIELD "A" RESERVOIR PRESSURE MAPS

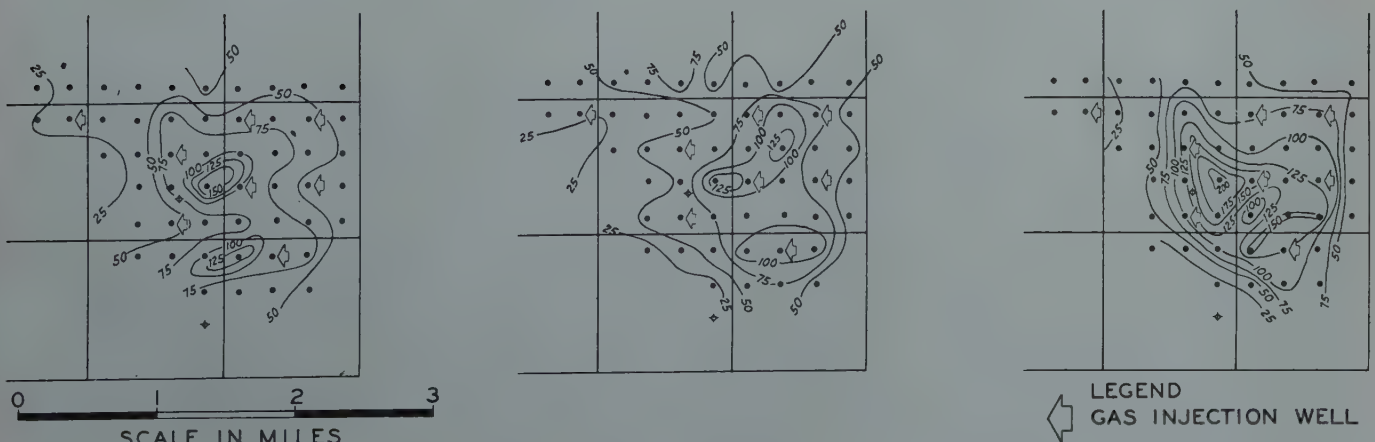


FIG. 4B—FIELD "A" WELL PRODUCTIVITY MAPS

400 pounds prior to gas injection, and since the start of gas injection operations, the pressure has been gradually increased and maintained at slightly in excess of 500 psig. The effect of the gas injection program upon the pressure performance of the field and upon the producing capacities of the wells is illustrated by Fig. 4 which shows the pressure distribution and the well productivity distribution in the gas injection area immediately preceding the start of the gas injection program, 16 months following the start of injection, and at the present time, after 2½ years of injection operations.

It will be noted, from Fig. 4, that productivity decline has been arrested and, in most of the area, substantial increases in productivities have been experienced. At the same time, individual well productivities are considerably more uniform than they were prior to gas injection. As a result of the improved performance characteristics, the producing rate for the field has been increased from 2,037 bbl/day before gas injection to approximately 3,000 bbl/day at present. It will be noted from Fig. 4 that, in general, the reservoir pressure has been increased, the pressure differentials throughout the field minimized, and that this change in pressure distribution has resulted in a corresponding change in distribution and magnitude of the producing ability of the wells. The effect of the program upon the producing capacity of the wells is further illustrated by the curve shown on Fig. 2, which shows the average well capacity based on production tests, both before and after the start of gas injection.

In connection with the gas injection program in the field, an attempt is being made to record the engineering information in enough detail to allow very close study of the results. Individual well productivity and gas-oil ratio tests are made at intervals of two months, and all gas produced is metered by individual tank batteries, each of which handle the production from three or four wells. Individual well gas-oil ratio tests taken bi-monthly since the start of gas injection operations show that no changes in the gas-oil ratios resulted from gas injection until March, 1948, at which time an increase in gas-oil ratio from approximately 150 cubic

feet to 400-800 cubic feet was noted on three wells offsetting the same injection well. With the exception of these three wells in the field, all of the wells are still producing at approximately the solution ratio. An analysis of this area, where the injection gas has apparently broken through to the producing wells indicates that the gas injection volumes are equivalent to an average gas saturation of approximately 4.1 per cent assuming that the gas is uniformly distributed throughout the vertical pay section, and 28.1 per cent assuming that the gas entered only the portion of the reservoir indicated by core analysis to have a permeability in excess of 5 millidarcys.

In planning this program, it was recognized that no appreciable benefits could be expected if the injected gas confined itself to the more permeable channels of flow within the reservoir and did not disseminate gas through the denser, less permeable portions of the reservoir which, based upon core analysis data, probably contained from 60 per cent to 70 per cent of the initial oil in place. There is considerable weight of opinion among engineers which contends that gas injection in a limestone reservoir such as Field "A" cannot be successful for the reason that the injected gas would selectively flow through only the more permeable channels and, therefore, could not be effective in displacing oil in the denser, less

permeable portions of the reservoir which contain the majority of the oil in place. In order to arrive at tentative conclusions in this respect, the gas saturation in the area surrounding each input well has been calculated, utilizing two extreme assumptions. It was first assumed that all the injected gas entered into only the zones having a permeability in excess of 5 millidarcys. The gas saturation was then calculated utilizing the other extreme assumption, that is, that the injected gas displaced oil uniformly throughout the entire permeable zone, irrespective of the magnitude of the permeability. The results of these calculations are shown by the following table:

Injection Well	Calculated Gas Saturation in 160-Acre Area		% of Net Pay With Permeability in Excess of 5 Md
	Net Pay Above .05 Md	Net Pay Above 5 Md	
1	4.1	28.1	14.6
2	3.0	8.1	36.6
3	4.8	22.0	21.9
4	4.5	11.3	40.1
5	2.4	9.3	26.1
6	1.9	6.2	31.1
7	2.8	7.6	36.3
Weighted Average	3.4	11.3	32.0

As can be seen from the above table, it is indicated that, if the injected gas had displaced oil only in the more permeable zones, gas saturations ranging from 6.2 to 28.1 per cent would exist in these zones. Either of these gas saturations are believed to be considerably in excess of the equilibrium gas saturation and, if this had occurred, gas

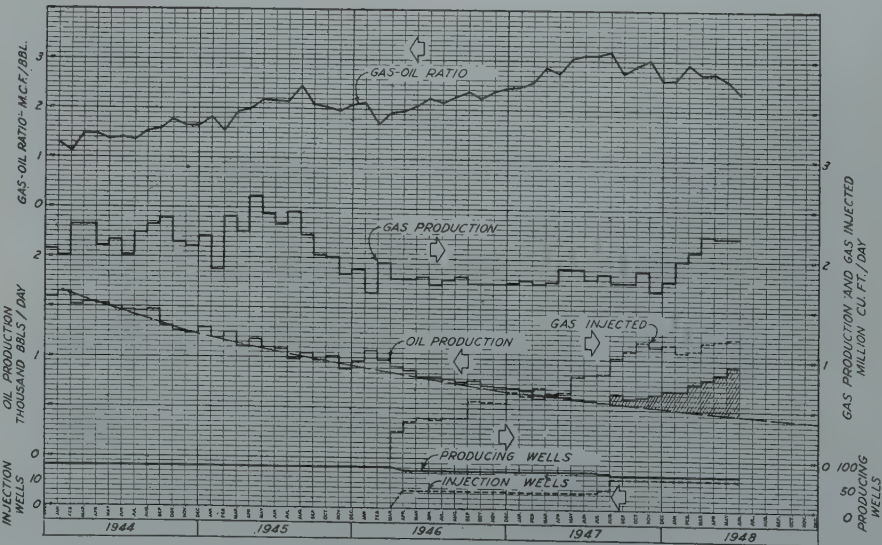


FIG. 5 — FIELD "B" TYPICAL GAS INJECTION PERFORMANCE

should have broken through to the offsetting producing wells, which would experience very rapid increases in gas-oil ratios. This has not been the case. On the assumption that all of the gas entered into the entire permeable pay section, the above table shows that a gas saturation of from 1.9 to 4.8 per cent would exist. These gas saturation values are of the order of magnitude of the equilibrium gas saturation to be expected, so it is anticipated that the producing wells will soon experience increasing gas-oil ratios. The time required before this occurs, and the subsequent increases in the gas-oil ratio of producing wells should provide a basis for an approximate quantitative estimate of the equilibrium gas saturation and some idea of the gas saturation distribution.

Although the project has not been in operation for sufficient length of time to arrive at definite conclusions as to the sweep efficiency of the injected gas and the ultimate benefits to be expected from the program, the following tentative conclusions are drawn: (1) The injected gas has not channeled to producing wells by selectively entering the more permeable portions of the reservoir to the exclusion of the less permeable portions. To the contrary, it appears that the more permeable sections of the reservoir are so interfingered, and the areal distribution of the permeable streaks sufficiently erratic to allow the injected gas to displace oil out of a large per cent of the reservoir rock. This tentative conclusion does not mean that channeling of injected gas will not occur. In a dispersed gas injection program, it necessarily follows that the injected gas must be produced sooner or later; otherwise, the displacement efficiency of the injected gas would be 100 per cent. Prior to the time gas break-through occurs in the producing wells, the displacement efficiency of the injected gas, in terms of pore volumes of oil displaced per pore volume of gas injected, is 100 per cent since all the gas injected has displaced oil. Once gas breaks through to the producing wells the producing gas-oil ratio can be expected to increase at a rate which will be governed by the nature and distribution of the permeable portions of the reservoir, the gas saturation gradients developed, and by

relative permeability relations. After break-through, the displacement efficiency of the injected gas will probably decrease very rapidly; however, it is expected that a large increase in recoverable oil can be obtained in this field prior to the time it becomes no longer economical to inject gas due to high producing gas-oil ratios. (2) The reservoir pressure has been maintained above the bubble point and pressure gradients throughout the gas injection area minimized, thus preventing the rapid decline in producing capacity of the wells which would undoubtedly have occurred if the reservoir pressure had been allowed to decline below the bubble point. (3) The rapid decline in producing capacity of the wells in the gas injection area observed prior to the gas injection program has not only been halted, but the producing capacity has been very materially improved.

FIELD "B"

Field "B" is a volumetrically controlled, North Texas, dolomitic limestone field, which has been operated under a fieldwide dispersed type gas injection program for the past $2\frac{1}{4}$ years.

Structurally the field is a broad, plunging anticlinal nose, cut by a steeply dipping anticlinal fold or fault roughly parallel to the main axis of the anticline. The productive limits of the field are defined by the oil-water and gas-oil contacts which are irregular surfaces and, also the variation in porosity and permeability development. In general, a concentration of non-porous zones exists above the oil pay and below the gas saturated porosity. This same general condition exists at the base of the oil saturation above the water-oil contact. Very restricted communication exists between the oil reservoir and the overlying gas zone in minor localized areas. The primary depletion performance has essentially been by internal or solution gas drive.

Unfortunately, lack of core data makes difficult a very satisfactory understanding of the characteristics of the reservoir rock as to the nature, magnitude, and distribution of the porosity and permeability development. The gross pay interval is composed of four major stratigraphic zones which are fairly persistent. The lithology of the

gross pay zone is very heterogeneous and varies over a wide range from cherty granular dolomite to white crystalline dolomite, and from oolitic limestone containing varying amounts of secondary cementing material to arkosic limestone intermingled with green shale. From microscopic examination of bit cuttings, it is observed that the character of the porosity ranges from fine grained crystalline type porosity to pore openings containing numerous vugular scattered pores. Although a quantitative estimate of the relative volumes of the reservoir represented by different types of porosity is not possible, it appears that the nature and magnitude of both the permeability and porosity represented vary over an extremely wide range.

The field was produced under primary control throughout its depletion history prior to gas injection, and had recovered approximately 85 to 90 per cent of the expected primary oil reserves at the time the gas injection program was initiated. The field had been producing at substantially capacity rates for several years prior to gas injection. At the time gas injection operations were started, the average well was producing at capacity of 13 barrels per day with a gas-oil ratio in the neighborhood of 1,350 cubic feet per barrel. This ratio is 8 to 10 times the solution ratio at the existing reservoir pressure of about 250 psi, thus indicating that, prior to gas injection, appreciable gas saturation and permeability to gas had been developed within the reservoir.

Typical performance data, based on several properties in the gas injection area, are illustrated by Fig. 5 for a $2\frac{1}{4}$ year period before and an equal period after commencement of gas injection. Two outstanding results of the gas injection program are obvious from Fig. 5: (1) The apparent gas-oil ratio trend observed during the period prior to gas injection has remained substantially unchanged during the life of the gas injection program to date. (2) Oil production capacities have been leveled out and increased to approximately the same magnitude as of the time gas injection operations were started.

It should be pointed out that some of the improvement in production rate is attributable to workovers (cleanouts

and acidizations) which were performed on some of the wells after gas injection was commenced. However, comparisons of well performance following workovers before and after the start of gas injection indicate that most of the sustained increases in production rate can be credited to the gas injection program.

Unfortunately, reservoir pressure data is inadequate to enable the interpretation of these results in terms of the magnitude of the oil and gas saturation and relative permeability values; however, it is obvious from the gas-oil ratio curve on Fig. 5 that the apparent permeability to gas has not been materially increased as a result of the gas injection program. Adopting the interpretation that there has been no change in the gas-oil ratio as a result of gas injection, the injected gas volume to date, which is approximately equivalent to 6.8 million barrels of reservoir space, must have displaced oil and accomplished a redistribution of oil saturation such that no increase in the apparent relative permeability ratio (K_g/K_o) resulted. The external gas drive displacement efficiency (reservoir volume of oil displaced per reservoir volume of gas injected) is thus indicated to be approximately equal to the displacement efficiency by internal gas drive during the injection period to date.

Adopting the other extreme interpretation of the effects of gas injection on the gas-oil ratio trend it might be interpreted that the gas-oil ratio curve during the injection period would have levelled out at approximately 2,000 cubic feet per barrel under primary operations. On this basis, it is calculated that the excess gas production represented by the increase in gas-oil ratios during the gas injection period is 52 per cent of the total injected gas volume. Even under this extreme interpretation, it is obvious that the injected gas must have displaced oil rather efficiently and adjusted the saturation distribution so that the displacement efficiency by external gas drive to date is approximately equal to one-half the displacement efficiency of solution gas drive.

Following is a tabulation of the pertinent production statistics from these leases for the 2½ year periods preceding and following start of gas injection:

	2½ Years Before	2½ Years After
Oil Production	1,020,000 bbl	625,000 bbl
Gas Production	1,780,000 Mcf	1,533,000 Mcf
Gas Injection	0	655,500 Mcf
Net Gas Production	1,780,000 Mcf	877,700 Mcf
Gross gas-oil ratio	1,745 cu ft/bbl	2,450 cu ft/bbl
Net gas-oil ratio	1,745 cu ft/bbl	1,405 cu ft/bbl

Since the ultimate oil recovery from a volumetric field is a function of the efficiency of utilization of the available gas volumes to displace oil, the relative recovery efficiency can be qualitatively evaluated by a comparison of net gas-oil ratios. As can be seen from the above table, the net gas-oil ratio during injection is 20 per cent less than the net gas-oil ratio prior to gas injection, and from 43 to 30 per cent less than the maximum and minimum gas-oil ratios that could have been predicted under primary operations during the gas injection period. The fact that the net gas-oil ratio has been materially improved certainly indicates that the increase in producing rate, above normal decline, shown by the shaded area on Fig. 5 represents, to some extent, an increase in ultimate recovery as well as an increase in recovery rate.

For the gas injection program to have been ineffectual in improving ultimate

oil recoveries, the increase in produced gas volumes attributable to gas injection should have approached the same magnitude as the injected volumes; however, the most pessimistic interpretation indicates that the increase in gas production due to gas injection to date has been approximately 50 per cent of the injected gas.

FIELD "C"

Field "C" is located in West Texas and produces from cavernous porosity of the El Capitan reef limestone of Permian Age at an average depth of 2,900 feet. The field was drilled on a spacing of approximately 10 acres per well. Wells in the field were characterized by very high initial productivities ranging up to 20,000 barrels per day. For the past 10 years, wells have been in the stripper status due to the high volumes of water produced with the oil.

Even at the very high rates of production experienced in the early life of the field, it is doubtful if the reservoir pressure was, at any time, reduced enough to cause significant volumes of solution gas to be liberated from the reservoir oil. The extremely active water drive has maintained the reservoir pressure to the extent that the present pres-

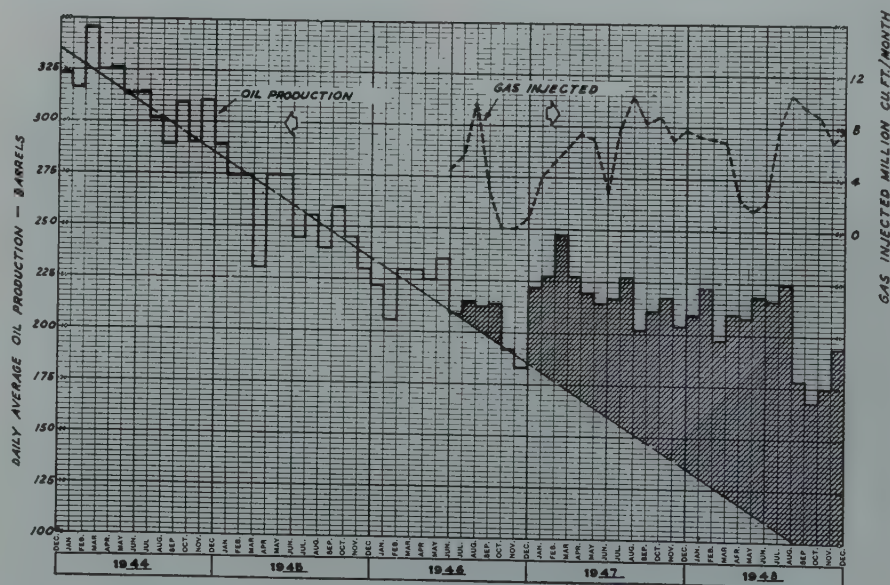


FIG. 6 — FIELD "C" GAS INJECTION AND DAILY OIL PRODUCTION RATE, EXPERIMENTAL GAS INJECTION PROJECT

tures in the latter stage of depletion are little, if any, lower than the original pressure. It is economically feasible to produce the wells at present water-oil ratios in excess of 100 only because of the high operating fluid levels.

Oil production, for the past 15 years, has declined at a fairly constant rate until, at present, most of the wells are producing at oil rates near the minimum possible for profitable operation. An idea of the oil decline rate may be gained from Fig. 6 showing the oil production rate of a number of wells in the area of a current gas injection project obtained from production data prior to the start of gas injection.

The peculiar behavior of several wells in the field suggested the possibility of recovery, by secondary means, of considerable quantities of oil which had been trapped in the reservoir by encroaching water. At intervals during

recent years normal, high water-oil ratio wells have been observed to suddenly start producing oil at greatly reduced ratios, sometimes producing several thousand barrels of oil before returning to their normal status. It was visualized, as shown in Fig. 7-a, that sizeable volumes of oil could have been trapped by the encroaching water in irregular upper surfaces of cavernous openings of the limestone. The only means whereby oil so entrapped could be produced is through being forced downward, by some lighter medium such as gas, into the fluid stream moving to the producing wells, as shown in Fig. 7-b. If pressure reduction during past production had been sufficient to cause the liberation of enough solution gas from the reservoir oil to fill these pockets, this oil would have been recovered by natural depletion methods. However, the pressure, as aforesaid, has been maintained by the encroaching water to the extent that it is probable that little, if any, solution gas liberation has occurred in the reservoir. If oil is trapped as visualized, then the only possibility for its recovery would be through the injection of gas to replace the oil.

In order to test the above discussed possibility, a small scale experimental gas injection project was planned for the field in which gas would be injected by the use of a portable compressor into one well, and the effects on oil production of offset wells observed. The well chosen for injection service was a temporarily abandoned well located centrally in a group of still active producing wells, and about 50 feet below the crest of the structure.

Gas injection was initiated in June, 1946, and has continued to date with operations being somewhat erratic, due to difficulty in maintaining sufficient gas supply, and mechanical trouble with the compressor. The average daily gas injection rate has been somewhat less than 200 Mcf per day. In Fig. 6, it can be observed that the oil production from the wells adjacent to the gas injection well is considerably above the expected decline under primary methods. The increased oil attributable to the injection program, indicated by the shaded area between the expected production curve, is 38,800 barrels. The volume of increased oil was obtained

by injection of a total of 135,323 Mcf of gas for an injected gas to increased oil production of 3.49 Mcf per barrel which, of course, is an economically attractive proposition for any reasonable cost of injecting gas.

FIELD "D"

This field is located in Central Kansas and produces from the Viola lime at an average depth of 3,850 feet. The productive area of the field is 520 acres, on which have been drilled 22 producing wells. The producing formation varies from a crystalline lime with cavernous solution porosity to a granular dolomite. Coring of several wells in the field has resulted in very poor recoveries, so it is impossible to establish definitely what fraction of the 40 feet of gross pay interval is porous and permeable. Laboratory analyses of the samples recovered from the cored section indicate an average permeability of less than 10 millidarcys. However, the productivities of the wells are several hundred to several thousand per cent higher than would be predicted from the core data, so it is obvious that communication in the reservoir is through a system of comparatively large secondary channels. From visual observation of drill cuttings and the cores recovered, it is indicated that this system is more probably made up of erosion channels than an extensive fracture system. Further indications of the presence of a system of relatively large interconnected secondary openings is shown by the excellent response to acid treatment.

Wells in the field were completed by setting pipe at the top of the producing zone, drilling in with cable tools, and acidizing with from 1,000 to 3,000 gallons of acid. Increases of productivities after acid treatment varied from a few per cent, on initially very good wells, up to 1,000 per cent of pre-acid productivities on initially small wells. Productivity indices after acid treatment range from 7.0 up to values immeasurably high. On some wells the decrease in the bottom hole pressure from static conditions is too small to be measured at reasonable rates of oil production. Productivities indicated from P.I. data in some cases are in excess of 20,000 barrels of oil per day.

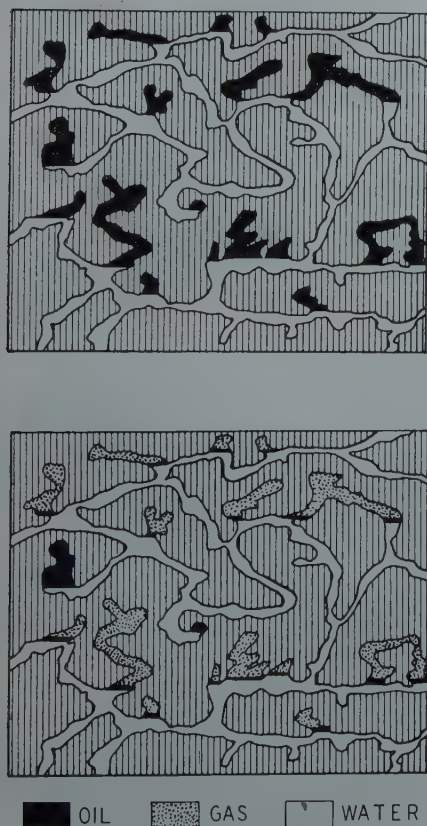


FIG. 7A (TOP) AND 7B (BOTTOM)—RESIDUAL OIL DISTRIBUTION WATER DRIVE CAVERNOUS LIME

The productive structure is an anticline, with the limits of production being defined on all sides by the water-oil contact. The oil filled closure between the crest of the structure and the original water-oil contact was approximately 70 feet. Despite the fact that most of the wells were completed close to the water-oil contact, little water coning was observed due to the slight pressure draw-down experienced under the limited withdrawal rates. The rise of the water-oil contact has been relatively uniform throughout the field. At present, as indicated by Fig. 8, the average water percentage of the producing wells is about 65 per cent. Properties of the original reservoir oil as shown by several bottom hole sample analyses are as follows:

Saturation Pressure at	
Reservoir Temperature.....	1,100 psia
Gas in Solution.....	350 cu ft/bbl
Relative Volume Compared	
to Residual Oil.....	1.214
Viscosity of Bubble	
Point Oil	1.05 cp
API Gravity of	
Residual Oil	41°

The original reservoir pressure at a datum of 1,950 subsea was 1,328 psig. During the depletion of the field, it has been possible to obtain excellent bottom hole pressure data since complete pressure build-up occurs in the producing wells within a very short time after they are shut in. Reservoir pressures obtained from quarterly surveys of several key wells distributed throughout the field indicate very slight pressure differences between different parts of the field. Usually the pressure differences between key wells in any survey are in the range of 10 to 30 p.s.i., which is another definite indication of the practically unlimited communication between all parts of the reservoir.

Fig. 8 is a graph of the pertinent production performance data on the field since the time of discovery in 1940. As shown by the figure, a rather sharp pressure decline was experienced in the early depletion of the field. During this period, up to the end of 1943, the field performance data indicated almost complete volumetric control. This was evidenced both by the sharp pressure de-

cline and the start of increase in gas-oil ratios occurring in late 1942 and 1943. However, when the reservoir withdrawal rate was curtailed toward the end of 1943 by reducing the oil production rate from approximately 1,400 barrels to 900 barrels per day, the tendency toward increasing gas-oil ratios was actually reversed and the rate of pressure decline was markedly decreased. At the lower rates of withdrawals experienced during the past 4½ years, the limited water drive has effectively altered the producing characteristics of the reservoir. The sensitivity of the relationship between rate of withdrawals and rate of reservoir pressure decline is shown by Fig. 9, which is a plot of bottom hole pressure and producing rate against cumulative reservoir withdrawals. It can be readily observed from this figure that the sharpest rate of pressure decline experienced during the life of the field was obtained during the period in which the reservoir pressure declined from the original pressure of 1,328 to approximately 1,100 psi. Replacement of reservoir withdrawals during this time was by liquid expansion alone. Below a pressure of 1,100 psi, gas coming out of solution from the reservoir oil supplemented liquid expansion to the extent that,

even though withdrawal rates were progressively increasing, the rate of reservoir pressure decline was arrested. It will also be noted from this figure that each time the rate of reservoir withdrawals was changed significantly, a corresponding change in rate of reservoir pressure decline was experienced, with the bottom hole pressure versus withdrawal relationships being practically linear over any period of constant withdrawal rate.

Although it is believed that the nature of the porosity in Field "D" is very similar to that visualized in Field "C", as pictured in Fig. 7, the combined gas expansion and the simultaneous encroachment of water will result in a recovery efficiency higher than is expected in Field "C", due to the fact that released solution gas will be stored in the irregular pockets of the reservoir, and displace the oil therefrom. It is estimated that between 50 and 70 per cent of the original oil in place will be produced under present depletion methods before this field is abandoned, and that the possibilities for future production by secondary recovery methods will be practically nil. As evidenced by gas-oil ratios increasing slightly above solution ratio, the maximum possible quantity of liberated solu-

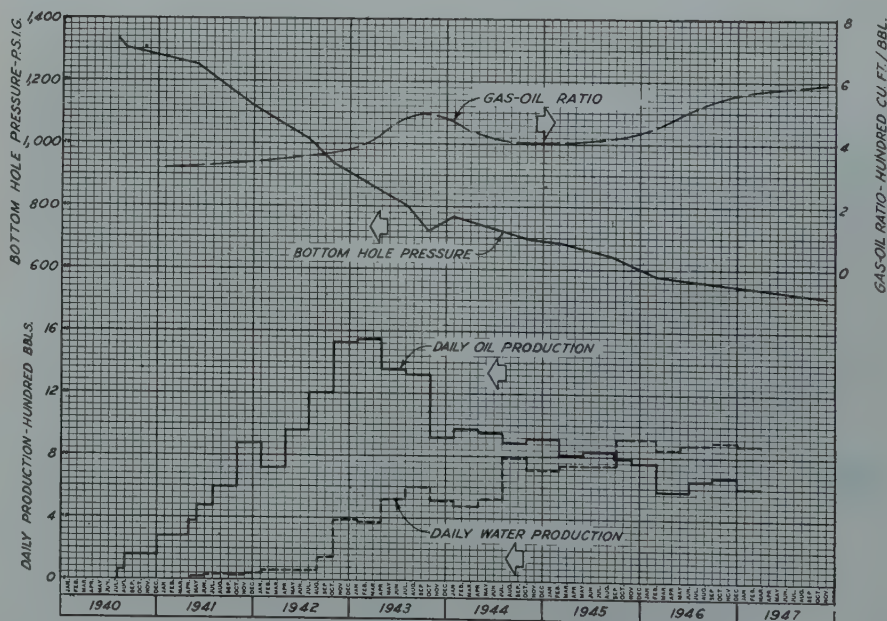


FIG. 8 — FIELD "D" RESERVOIR PERFORMANCE CURVES

tion gas has been stored in the reservoir. Gas-oil ratios have not become excessive, because gas saturation increases and the resulting gas permeability increases have been minimized by practically complete replacement of withdrawn fluids by encroaching water during the past few years. At the same time, pressure maintenance by the encroaching water has minimized losses due to shrinkage of the reservoir oil. This building up of the gas saturation in the reservoir to the maximum possible, without excessive free gas flow at the same time the water was encroaching, has eliminated the possibility of significant volumes of oil being trapped in irregular pockets by the water as shown in Fig. 7-a. In this reservoir, the type of depletion program being undertaken in Field "C" by gas injection has been effectively accomplished by natural means, solely through control of production rates.

Undoubtedly, the depletion program providing the maximum recoverable oil from a reservoir of this type, is fast pressure reduction early in the producing life of the reservoir before significant volumes of water have invaded the fully liquid saturated zones, followed by controlled pressure decline. The first phase of pressure reduction should continue as rapidly as possible to a pressure in the reservoir sufficiently below the bubble point of the oil to cause liberation of enough solution gas to establish the maximum gas saturation that can be maintained without excessive flow of free gas. After this condition has been attained, further pressure reduction should be at low enough rate such that the encroaching water will replace withdrawals to the extent that excessive gas-oil ratios and oil shrinkage will be avoided. If the pressure were allowed to decline rapidly after having reached the above discussed stage of gas saturation, and before encroaching water displaced, to the producing well bores, the oil which had been forced downward from irregular pockets, subsequent encroachment of water could recompress the gas trapped in these pockets and refill them partially with oil. The recovery of this oil then would depend on injecting high pressure gas to again displace this oil

downward, and would result in considerably lower efficiency than would be possible under simultaneous pressure reduction and water encroachment. Field "D" probably is one of few fields wherein reservoir conditions are such as to allow this almost perfect control over the natural producing mechanisms.

SUMMARY

There has been proposed, in the literature, a concept of the nature of limestone reservoirs and an interpretation which leads to the conclusion that limestone reservoirs in general are not susceptible to a dispersed type injection program and that such a program cannot materially increase the ultimate recovery of oil. In brief, this concept proposes that limestone reservoir rocks are made up of two types of porosity, intermediate and intergranular. It has been visualized that the intergranular rock, constituting a large portion of the reservoir void space, and having low permeability, is interconnected by fissures or by continuous, relatively thin zones of intermediate porosity having considerable greater permeability. It is then reasoned that this system of continuous highly permeable intermediate porosity acts as a system of short circuiting conduits which enable the production of oil from portions of

low permeability rock, remote from the well bore, that otherwise would produce into the wells at impractical rates.

Furthermore, this theory concludes that the presence of such interconnected passages may nullify the benefits of gas injection by unduly concentrating the flow of the injected gas; resulting in a program whereby the injected gas is cycled through a small portion of the reservoir, represented by the interconnected intermediate type porosity, without appreciably increasing the ultimate recovery of oil. It is quite possible that these conditions do exist in some limestone fields, and may be critical in determining the success of either a gas injection or water flood program; however, performance of many limestone fields indicate that the above proposition is possibly the exception rather than the rule for limestone reservoirs.

It must be recognized that the term "limestone reservoirs" denotes a class of reservoirs in which there are many different types having a wide range of characteristics. The four example fields discussed in this paper represent a few limestone reservoirs where an interpretation of performance definitely indicates that the concept stated above and its implications, in regard to the susceptibility of such reservoirs to secondary recovery efforts, does not apply.

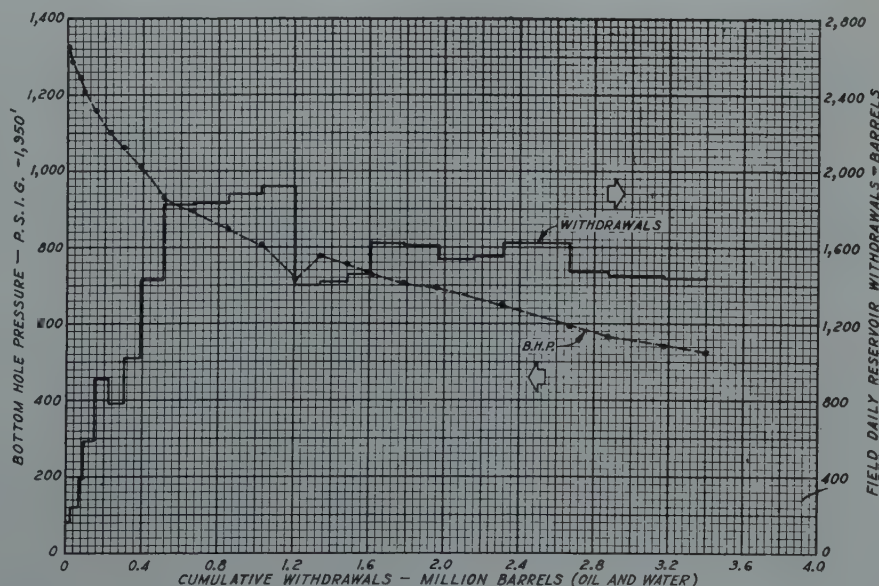


FIG. 9 — FIELD "D", RESERVOIR PERFORMANCE CURVES

Prospective secondary recovery programs in limestone fields in general should not be condemned on the basis of tentative conclusions as to the nature of limestone reservoir rocks, and an interpretation of these characteristics which leads to the conclusion that it is impossible to displace oil by means of an extraneous displacing medium except in a very small portion of the reservoir, represented by the intermediate type porosity.

It appears impossible to adequately evaluate the properties of the various type of porous media found in limestone reservoirs and their inter-relation from presently developed core data and

geological information. The problem of predicting, in advance, the susceptibility of a limestone reservoir to secondary recovery methods can only be solved, at present, by a comprehensive analysis of the performance history of that field. This must necessarily remain the case until more adequate methods are evolved to account for the effects upon performance of the many, now immeasurable, variations of limestone reservoir properties.

ACKNOWLEDGMENTS

The authors wish to acknowledge, with thanks, the cooperation of R. M.

Leibrock, Julian Huzarevich, and L. W. Barnhart in preparation of some of the material for this paper.

We also wish to thank the Stanolind Oil and Gas Company for permission to publish the paper.

REFERENCES

1. Littlefield, Max; Gray, L. L.; Godbold, A. C.: "A Reservoir Study of the West Edmond Hunton Pool, Oklahoma"—*Petr Tech*, No., 1947.
2. Bulnes, A. C.; Fitting R. U.: "An Introductory Discussion of the Reservoir Performances of Limestone Formations"—*Petr Devel and Tech*, 1945.

★ ★ ★

A CALCULATION OF THE EFFECT OF PRODUCTION RATE UPON ULTIMATE RECOVERY BY SOLUTION GAS DRIVE

CHARLES C. MILLER, E. R. BROWNSCOMBE, MEMBERS AIME, AND W. F. KIESCHNICK, JR.,
JR. MEMBER AIME, THE ATLANTIC REFINING CO., DALLAS

ABSTRACT

The possibility has been mentioned that large pressure gradients in a solution gas driven field caused by high production rates might lead to a reduction in the ultimate recovery obtainable compared to that which would be obtained by a very slow rate of production. In the present study the reservoir conditions accompanying a high rate of production and the corresponding ultimate recovery were compared with those obtained if the reservoir were produced at some marginal rate throughout its entire life. The method of calculation involved the application of fluid flow-material balance analysis to a series of successive steady state conditions in the reservoir. In the case studied very little difference in recovery was obtained at the abandonment pressure. An analysis of the basic factors involved indicates that the same results would hold for considerable variation in properties of reservoir fluids, permeability of the formation or well spacing. Even if the reservoir has a water drive it appears that no harm will be done by open flow production if the rate is cut back before any appreciable free gas is produced. However, any condition which leads to disproportionate withdrawal rates and which causes large pressure differences over large areas might result in substantial loss in ultimate recovery.

INTRODUCTION

When the pressure declines in a reservoir, gas is evolved from solution causing a shrinkage in the reservoir oil so that a stock tank barrel of oil with its residual dissolved gas occupies a smaller volume than originally. For a given reservoir oil saturation, therefore, stock tank oil content will be higher at the lower pressure. At the same time the evolved gas which remains in the reservoir reduces the reservoir oil

saturation, and this would be expected perhaps to cause a reduction in stock tank oil content. However, around the well the shrinkage occurs so rapidly that stock tank oil may actually accumulate in this region in spite of the simultaneous reduction in reservoir oil saturation. If this accumulation should continue, spreading into a larger zone, the loss might be appreciable and because larger pressure gradients accompany higher rates the accumulation might possibly be large if wells are produced at too high a rate. It is the purpose of this paper to determine the effect of rate of flow on ultimate recovery by solution gas drive.

The problem under consideration involves the unsteady state flow of oil in a closed radial system from which oil is produced by the evolution of gas as a finite drawdown is established and the reservoir pressure declines. A somewhat similar unsteady state production problem dealing, however, with a linear system has been considered by Muskat and Meres,¹ but these authors do not discuss the effects which rate may have on recovery. Other methods have been reported^{2,3,4} for estimating recovery as a function of pressure decline when producing at an infinitesimal rate, and Muskat and Taylor² have shown the effect of fluid and reservoir characteristics on recovery under these conditions. Assuming steady state to exist, Babson³ has given a procedure for computing the decline in well productivity as the field is depleted, and Moyer⁵ has combined these methods to estimate abandonment conditions and the resulting ultimate recovery. These latter approaches to the problem either do not consider the effect of rate or assume steady state can be established.

In detail this paper presents the behavior of the reservoir producing under unsteady state conditions and considers the effect of production rate during this unsteady state flow on the recovery attained. The analysis also shows that there will exist at abandonment a type of steady state, and on this basis a method has been developed for rapid calculation of abandonment conditions.

¹ References are given at end of paper.

Manuscript received at office of Petroleum Branch September 22, 1948.
Paper presented at Branch Fall Meeting in Dallas October 4-6, 1948.

RESERVOIR AND OPERATING CONDITIONS

The case chosen for this study considers the production of an undersaturated solution gas driven reservoir from a single well in a closed drainage area of 2000 feet radius and 30 feet thickness. For purposes of simplicity the permeability in this formation was assumed to be uniform throughout the entire region. The reservoir was taken to be at a pressure of 4900 psi initially but to contain an oil having a saturation pressure of 4460 psi.

Reservoir characteristics include a porosity of 16.9 per cent, a connate water saturation of 52 per cent, initial reservoir oil saturation of 48 per cent, and an initial effective oil permeability of 6 millidarcies. Fig. 1 presents the effective permeability of oil and the ratio of permeability to gas to permeability to oil, as a function of oil saturation.

The reservoir fluid selected has a formation volume factor of 2.70 reservoir barrels of oil per barrel of residue oil* and a gas solubility of 2720 standard cu ft of gas per residue barrel at saturation pressure. The viscosity of the reservoir oil at saturation pressure is 0.09 centipoise. The manner in which these factors change as pressure declines is shown in Figs. 2 and 3. Gas viscosities were taken from Katz and Bicher.⁹

The reservoir was produced at about 250 stock tank barrels per day until it reached open flow conditions. Thereafter, of course, the production rate fell steadily until abandonment conditions (10 bbl/day) were reached. Throughout the declining rate period the bottom hole flowing pressure was maintained at 1000 psi. This value was taken to be the minimum pressure under which natural flow would occur, and no attempt was made to consider the effect of artificial lifting.

METHODS OF ANALYSIS

Fluid Flow Material Balance Calculations

Since no rigorous analytical methods have been developed for the solution of the flow of fluid problems when both oil and gas are flowing through a reservoir, the methods used in the solution of this problem involve an approximation approach employing a succession of steady states. By this method the reservoir is subdivided into a number of annular rings surrounding a well, and it is assumed that steady state exists in each of these rings over a short time interval. This calculation considers a reservoir initially undersaturated at a uniform pressure and producing only the liquid phase. It then proceeds to deal with the reservoir in a transition state at some later time when pressure has fallen below saturation pressure and both oil and gas are flowing in the region near the well bore. A third phase of the calculation then deals with the reservoir completely below saturation pressure with both oil and gas flowing throughout the reservoir. Although the same general approach was used throughout the study it was necessary to modify the procedure somewhat when considering each of the three phases of the production history outlined above.

Expanding Liquid Production

At the start of the operation when the reservoir fluid was entirely in the liquid phase, a graphical method⁸ for the solution of unsteady flow problems was employed. After a short producing interval a steady state condition was found to be established in which each zone of the reservoir contributes to production in direct proportion to its size. A material balance - fluid flow analysis based on these conditions⁸ gives:

$$\frac{p - p_i}{2\pi a h k_o \left(1 - \frac{r_1^2}{r_e^2}\right)} = \frac{\mu_o q_1 F}{2\pi a h k_o \left(1 - \frac{r_1^2}{r_e^2}\right)} \left[\ln_e \frac{r}{r_1} - \frac{r^2 - r_1^2}{2r_e^2} \right] \quad (1)$$

† See Appendix.

Expressing the reservoir fluid content in terms of the compressibility and the average reservoir pressure decline as obtained by integrating the pressure distribution given by this equation, the total withdrawal up to the time saturation pressure reaches the well bore may be expressed as

$$\Delta Q_{we} = \frac{\pi r_e^2 h f (1 - C_w)}{5.61 F_1} \left[(p_i - p_w) \left(1 - \frac{r_w^2}{r_e^2}\right) - \left(\frac{\mu_o q_w}{2\pi a h k_o \left(1 - \frac{r_w^2}{r_e^2}\right)} \right) \left(\ln_e \frac{r_e}{r_w} - \frac{3}{4} + \frac{r_w^2}{r_e^2} - \frac{r_w^4}{4r_e^4} \right) \right] \quad (2)$$

The time interval to obtain this production is then determinable from the constant production rate assumed at the well bore. From the pressure distribution equation and the

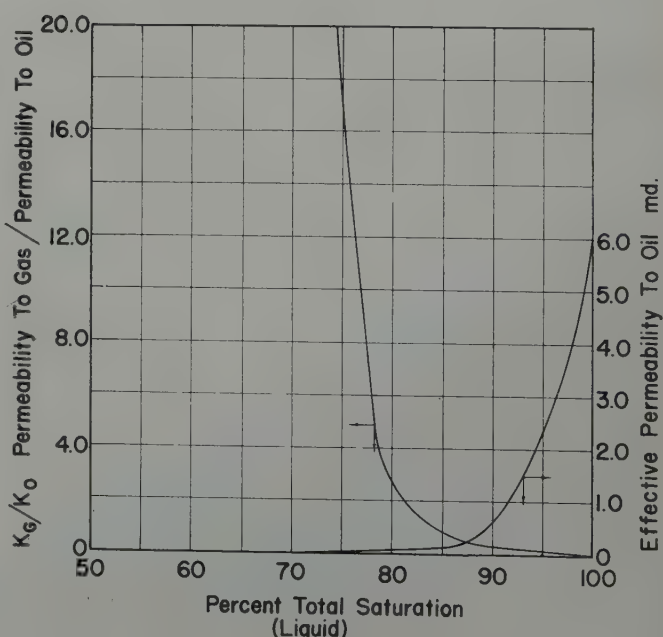


FIG 1 — RATIO OF PERMEABILITY TO GAS TO PERMEABILITY TO OIL AND EFFECTIVE PERMEABILITY TO OIL

* Refers to oil differently stabilized at reservoir temperature, see page 238.

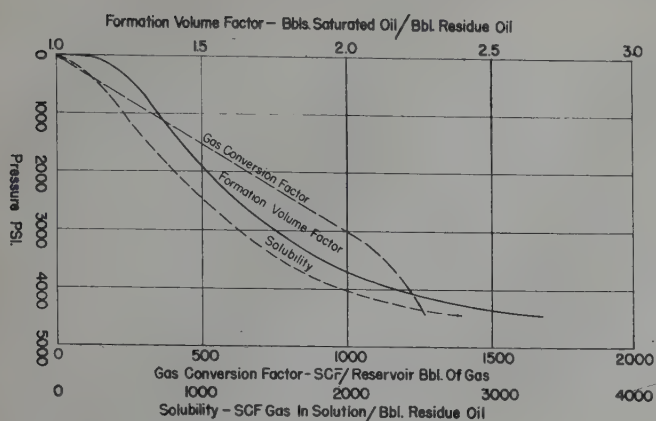


FIG. 2 — PRESSURE VOLUME DATA

compressibility of the fluid the distribution of residue oil may be determined, and all the conditions within the reservoir are completely defined.

Transition Phase

The uniform withdrawal rate and corresponding uniform pressure decline over the reservoir during the single phase production history is followed by a transition period as the pressure falls below saturation, first near the well bore and later out into the reservoir. While the outer portion of the reservoir, therefore, is still producing by an expanding liquid drive, the inner portion has entered the secondary or two-phase period of its production history.

Since the production rate at the well is to be held constant and a larger proportion of the total flow will be contributed from the region near the well bore where the reservoir fluids are more expansible, the flow rates in the expanding liquid region must necessarily decline. It was assumed, however, that this decline would be gradual and that steady state conditions could be assumed in this region. A modification of equation (2) has been derived in the Appendix to allow the computation of the withdrawals from the expanding liquid portion of the reservoir. Knowing these withdrawals the withdrawals from the remainder of the reservoir may be computed by the methods outlined below under two-phase production.

Two-Phase Production

In the region where both oil and gas are flowing it is necessary to consider changes in reservoir oil saturation and the resulting decline in relative permeability along with changes in pressure as the formation is depleted. The necessary equations for these steps are given and discussed in detail in the Appendix. Briefly, the method is one of trial and error. Assuming a pressure at the inner boundary of a zone, the oil saturation may be calculated by successive approximations employing Darcy's Law and a material balance on the residue oil. As a check that the assumed pressure is correct, the average gas-oil ratio at the inner boundary may be calculated from a gas balance and compared with the initial and final values determined on the basis of the pressure and saturation conditions at this point.

In order to apply the approximation formulas used in the two-phase case, it is necessary to have a relationship between

the saturation and the pressure at the boundary. Since the pressure gradient is zero at the boundary, an analysis by Muskat⁴ for the zero drawdown solution gas drive problem gives the desired relationship.

Stock Tank Recovery and Surface Gas-Oil Ratio Calculations

It is well known that different pressure volume relationships are obtained as a function of pressure decline by differentially lowering the pressure and removing gas as compared with flashing the reservoir fluid to the desired pressure. E. C. Patton⁷ has pointed out that these differences are significant when making an analysis of a reservoir. He suggests that the differential type of data should be used to represent these fluids in the reservoir while an equilibrium flash separation best represents the separation which occurs at the surface of the ground and should be used to correct the well stream materials to stock tank conditions. In the course of the present studies it was found necessary to consider one further factor in connection with the proper interpretation of the PV results. The particular reservoir under consideration is at an elevated pressure, and the reservoir fluid contains a large amount of intermediate components. Under these conditions it may be expected that the gas reaching the well will contain a large amount of condensable liquids, a portion of which will condense in the separator and be recovered as stock tank oil. To estimate the amount of such condensation the composition of the oil and gas produced was calculated and the two fluids were mixed in proportion to the gas-oil ratio. This mixture was assumed to be flashed through the separator to the stock tank in order to obtain the stock tank oil recovery. Because of the high pressure of separation in the reservoir no great degree of accuracy can be claimed for these results. However, the trends and the order of magnitude of recovery from the gas phase are significant. During the early stages of production history the results do not differ materially from those which would be obtained by assuming a flash separation of dissolved gas and oil. In the latter stages of the operation, however, when large volumes of gas are produced along with the oil as much stock tank oil is recovered from the gas phase as from the liquid phase.

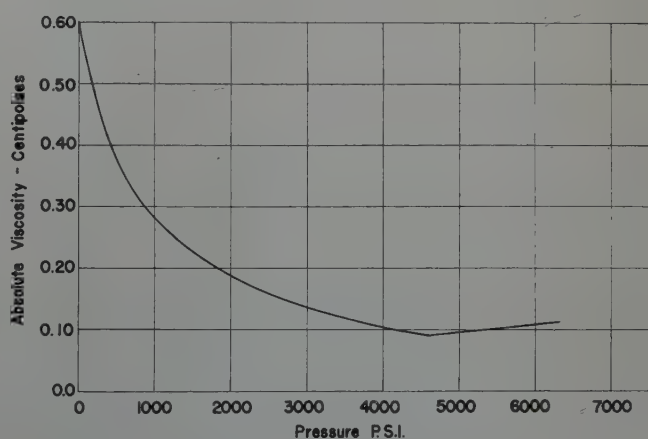


FIG. 3 — VISCOSITY OF OIL

DISCUSSION OF CHANGES OCCURRING
IN THE RESERVOIR

The results of these calculations which describe the transient history of the reservoir producing under open flow conditions are presented in Figs. 4-7 in which isochronic (same time) curves are shown for pressure and saturation distribution and the resulting gas-oil ratio and stock tank oil distribution. For comparison the conditions which would obtain if the reservoir were produced at an infinitesimally slow rate are also indicated. Since the present discussion deals with conditions existing within the reservoir, all quantities of oil are referred to "residue oil" rather than stock tank oil. "Residue oil" is defined as the oil remaining at atmospheric pressure after differential separation of the reservoir fluid at reservoir temperature.

The early, expanding liquid-drive phase of the production history is characterized by a short transient followed by a uniform decline of pressure and residue oil content over the reservoir. This uniform decline of pressure and residue oil content is attained during the first week and continues until the pressure begins to fall below saturation pressure. The large gradients of pressure and residue oil content are seen to be confined to the vicinity of the well bore. As pressure falls below the bubble point in the area near the well bore, considerable gas is evolved but does not leave the area because there is insufficient permeability to gas at this time, and the oil saturation then declines sharply near the well as gas displaces oil (Fig. 5). Other effects of this gas saturation increase are (1) a sharp drop in productivity index because of the sharply reduced permeability to oil and (2) a more rapid withdrawal from zones near the well (Fig. 8) because the oil and gas system now present is more expansible here than the oil in the rest of the reservoir. The effect of gas evolution prior to its leaving the area where evolved is further in evidence in the gas-oil ratio curves, where a decline near the well is noted in the early curves (Fig. 7).

As the pressure drop below the bubble point proceeds farther out into the reservoir, the region of gas accumulation and declining gas-oil ratios occurs farther from the well. Near the well the gas saturation continues to increase and free gas begins to flow. This behavior accounts for the minimum in several of the early gas-oil ratio curves (Fig. 7). When gas begins to flow, the liquid saturation declines more slowly, and in the vicinity of the well this decline is not sufficient to keep pace with the oil shrinkage accompanying the pressure decline in this region. Therefore, a portion of the oil withdrawn from more remote regions of the reservoir is accumulated here. This accumulation of residue oil (also of stock tank oil) is the principal effect of producing the reservoir wide open, and conclusions concerning the over-all and ultimate effect upon recovery of an open flow production operation depend upon the magnitude of this accumulation.

With further pressure decline and gas evolution, the accompanying reduced oil permeability results in larger gradients throughout the reservoir, and the oil accumulates in a larger portion of the reservoir (Fig. 6). This accumulation is shown by the increase in residue oil as the well is approached. The distribution of residue oil per barrel of pore space is plotted here as a function of area of drainage rather than radius of

drainage so that the area under any curve will represent the amount of residue oil in the reservoir at any given time. The area between any two constant-time curves then represents production during that time interval from the entire reservoir. Successive curves which converge or cross therefore indicate the accumulation effect. Successive parallel curves imply that the various zones in the reservoir are contributing proportionate shares of production and that there is no further accumulation.

When open flow conditions are reached, the pressure around the well falls more slowly because less oil is flowing and the total drawdown and the permeability gradient in this area decrease. The amount of accumulated oil reaches a maximum

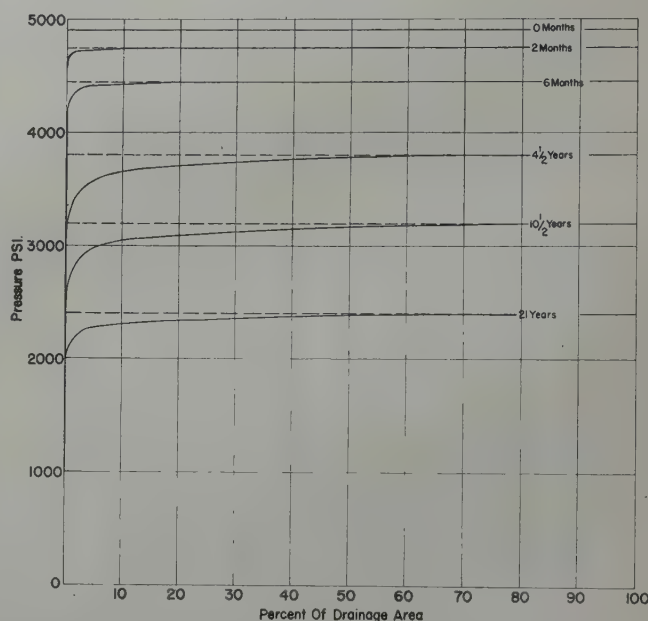


FIG. 4 — DISTRIBUTION OF PRESSURE WITHIN RESERVOIR
ONLY SIX CURVES INCLUDING ORIGINAL CONDITIONS AND ABANDONMENT OF CONDITIONS ARE SHOWN — CALCULATIONS EMBRACE
A TOTAL OF FOURTEEN CONSTANT — TIME CURVES

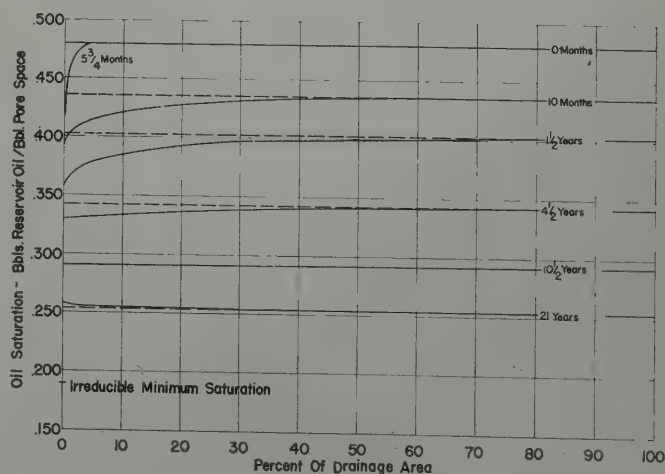


FIG. 5 — DISTRIBUTION OF RESERVOIR OIL SATURATION
ONLY SEVEN CURVES SHOWN INCLUDING ORIGINAL CONDITIONS
AND ABANDONMENT CONDITIONS — CALCULATIONS EMBRACE A
TOTAL OF FOURTEEN CONSTANT-TIME CURVES

value when the oil saturation is decreasing as rapidly as the liquid is shrinking.

The liquid and gas saturations in the reservoir are determined by the gas evolution and accompanying oil shrinkage as well as by the relative abilities of these fluids to escape, as

expressed by the ratio of effective permeability, $\frac{k_g}{k_o}$, when a sufficient gas saturation is developed gas can escape almost as fast as it is liberated from solution as shown by the rising gas-oil ratio in the reservoir, first only near the well and later throughout the reservoir. Large oil saturation gradients are set up in the reservoir during the early part of the production history because the large amount of gas evolved near the well bore accumulates at first. Later as the gas accumula-

tion moves back into the reservoir and gas begins to flow in sizable amounts near the well bore, the oil gradient begins to level out. Finally as gas flows freely throughout the reservoir and only very slight decreases in oil saturation allow very large increases in gas flow, the oil saturation gradient further flattens and approaches a condition of constant distribution at any subsequent time. In fact, the saturation gradient decreases to such an extent that at abandonment conditions (21-year curve, Fig. 5), the oil saturation is essentially constant over the entire reservoir.

Fig. 8, describing the rate of flow of residue oil within the reservoir, offers a concise review of the transient history just described by the other various figures. At first as the liquid expansion phase of production establishes a steady state of proportionate withdrawals from the various zones in the reservoir, the distribution of rate of residue oil flow is linear with area of drainage. Then as gas accumulation near the well causes greater production from this area, the flow rate increases as the well is approached. As accumulation of residue oil begins near the well, the rates decline. Finally as the steady state-proportionate withdrawal condition is again approached, the distribution of rate again becomes essentially linear. It is to be noted that throughout the production history the departure from linearity of the rate distribution curves because of gas and residue oil accumulation effects is essentially confined to the area near the well bore.

The decline of productivity index and reservoir boundary pressure (Fig. 9) and the change of gas-oil ratio and decline of stock tank oil production (Fig. 10) show the changes as a function of time that would be expected in light of the above discussion. Theoretically, the produced gas-oil ratio should decrease as gas accumulates near the well in the early history. This effect was too small to observe in the present calculations. One factor tending to minimize it is the production of free gas near the well as the pressure drops tending to offset the accumulation of gas farther out in the reservoir. Comparing the abandonment gas-oil ratio at the surface (SCF/Stock Tank bbl) with that at the well bore in the reservoir (SCF/Residue bbl), the surface ratio is found to be about half the reservoir ratio. In part, this is due to the difference between flash separation at atmospheric conditions and differential stabilization at reservoir conditions. However, the principal difference is due to the condensable materials in the reservoir gas which are partly recovered by the atmospheric stabilization.

EFFECT OF RATE UPON ULTIMATE RECOVERY

In order to determine whether any loss in ultimate recovery has resulted from the open flow production, the results of this study are compared with the recovery obtainable by producing the field at an infinitesimal rate (Fig. 11). This latter case was taken to give the maximum recovery since there are no pressure and saturation gradients in the field and therefore oil accumulation will not occur. Figs. 4 through 7 presented and discussed in the previous section contain the production history curve (in dashed lines) for the infinitesimal rate operation. It will be noted that the comparison between the open flow case and that of infinitesimal drawdown is made on the basis of the same reservoir pressure at the outer

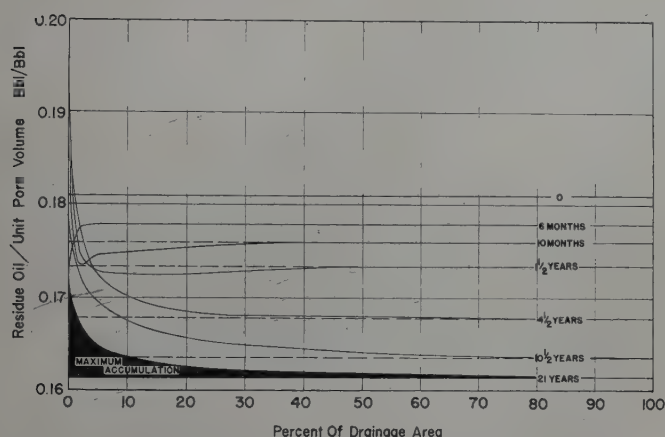


FIG. 6—DISTRIBUTION OF RESIDUE OIL WITHIN RESERVOIR ONLY SEVEN CURVES SHOWN INCLUDING ORIGINAL AND ABANDONMENT CONDITIONS
— OPEN FLOW CONDITIONS
- - - INFINITESIMAL DRAWDOWN CONDITIONS

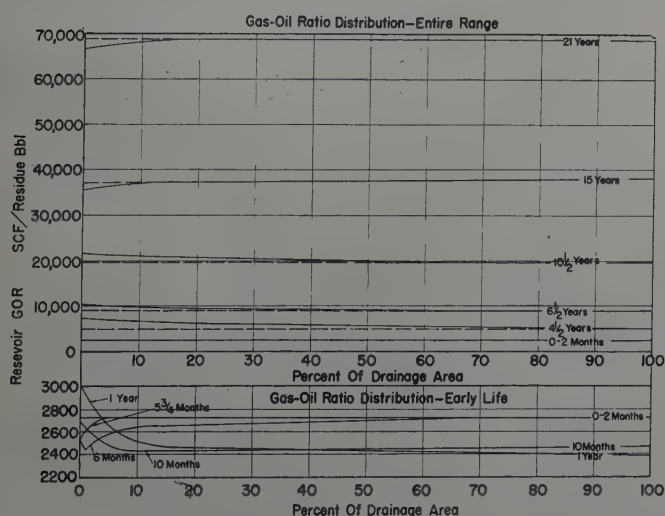


FIG. 7—DISTRIBUTION OF GAS-OIL RATIO WITHIN RESERVOIR RATIOS ARE RESERVOIR VALUES AND DO NOT INCLUDE CONSIDERATION OF CONDENSABLES DURING FLASH PRODUCTION TO STOCK TANK
— OPEN FLOW CONDITIONS
- - - INFINITESIMAL DRAWDOWN CONDITIONS

boundary. Although this basis of comparison might be regarded as somewhat arbitrary, it will suffice for the purpose and has the advantage of pointing out (Fig. 6) that the recovery of residue oil is less under open flow conditions although the pressure decline in the reservoir is everywhere greater. If the infinitesimal rate case is assumed to be at the average pressure of the open flow case instead of at the boundary pressure, more recovery than above will be obtained in the infinitesimal rate case and the loss due to open flow production will be greater. The difference between these two methods of comparison, however, is not appreciable, being less than 1 per cent of the recovered oil.

In Fig. 6, showing the distribution of residue oil in the reservoir, it is seen that at abandonment the amount of accumulated oil is appreciable, amounting to about 8 per cent of the produced oil. This loss accruing from the open flow operation is expressed on a residue oil basis and represents the loss in reservoir oil recovery. In this particular study, since the reservoir was at high pressure, the gas phase contained appreciable quantities of condensable vapors which were recovered in the stock tank. Further, the large drawdown in the open flow case gave appreciably lower pressures over large areas at abandonment than those obtaining in the infinitesimal case, so that at abandonment the open flow case had produced substantially more gas than the infinitesimal case. Taking the recovery of these materials into consideration the loss was reduced from 8 per cent to about 2 per cent.

It has already been pointed out that as abandonment conditions are approached the oil saturation becomes practically constant throughout the reservoir and the flow rate increases in proportion to the area traversed as the well is approached. Assuming these two conditions to hold it may be shown that a steady state exists similar to that which is set up during the expanding liquid phase of production. Equation (1) represents the pressure distribution if the permeability k_o is taken to be the effective oil permeability at the abandonment saturation. Since the saturation is constant the residue oil distribution can then be computed from the pressure distribution. A comparison at abandonment between the conditions of pressure and oil distribution at the end of the unsteady state production and conditions under the steady state assumptions indicates that a steady state has been attained.

The above analysis implies that the ultimate recovery will be determined primarily by the operating conditions at abandonment; the previous history of operation in this solution gas driven reservoir will have little effect. The same conclusion may be arrived at from a consideration of the time required to reach steady state conditions at abandonment.

As mentioned previously, approximately one week is required after production is started in the reservoir for a steady state condition to be set up such that oil is being withdrawn equally from all parts of the reservoir. A set of general solutions of the differential equation governing unsteady state compressible liquid flow is given by Muskat.¹ In each case the parameter containing time also contains the ratio: distance squared over diffusivity. Thus, in this type of problem the time required to reach an equivalent condition is proportional to this ratio:

$$t \text{ is in proportion to } \frac{\text{distance squared}}{\text{diffusivity}} = \frac{r^2 \mu c f}{k} \quad (3)$$

Since at abandonment the oil saturation is essentially uniform throughout the reservoir, and since the rate of flow of the gas is much higher than the rate of flow of the oil and the compressibility of the gas much higher than the compressibility of the oil, it may be anticipated that the rate of pressure decline in each part of the reservoir and therefore the time to reach a steady flow state under such conditions will be governed primarily by the gas phase factors. Although equation (3) is derived from a compressible liquid flow

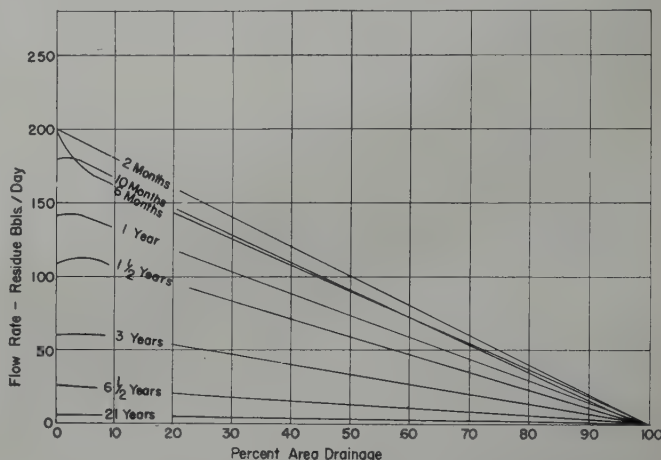


FIG. 8 — VARIATION OF OIL FLOW RATES WITHIN RESERVOIR

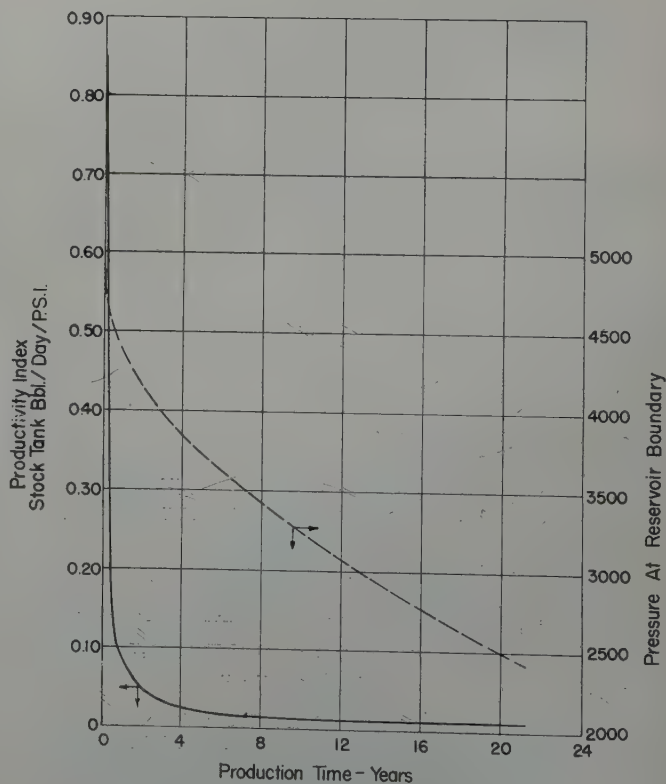


FIG. 9 — PRODUCTIVITY INDEX AND PRESSURE DECLINE

analysis, it may be used in the present case for gas flow since as may be seen from Fig. 4, the pressure variation over 90 per cent of the reservoir is less than 10 per cent of the drawdown, which gives a relatively constant compressibility for the gas permitting use of liquid flow equations over this portion of the reservoir. A comparison of the fluid factors initially and at abandonment gives:

	Initially (oil)	At Abandonment (gas)
μ viscosity	.088 cp	0.17 at 1750 psi
c compressibility	4.02×10^{-5} psi ⁻¹	2.9×10^{-4} at 2340 psi
f porosity filled	.081	.038
k permeability	5.6 md	.37
diffusivity	19.6×10^6 md x psi per cp	1.97×10^6

Since the distance factor is the same in both cases the time required to come to equilibrium is inversely proportional to the diffusivity; thus, since one week is required initially ten weeks would be required to level out any transient and establish a steady state flow condition in the reservoir when it is nearing depletion. This time is very short compared to the period of time required for the last stages of depletion. For this reason it may be expected that the ultimate recovery, which depends upon the final state of the reservoir, will be a function of operating conditions in the last stages of depletion and will be independent of operating conditions earlier in the life of the field. This is in line with the conclusion reached in the detailed analysis of the transient history of the field.

GENERAL APPLICABILITY OF CONCLUSIONS

The above considerations may be used to estimate the effect of rate upon recovery from solution gas driven reservoirs which have properties different from those assumed in the present example. The time required to reach a steady state flow under abandonment conditions may be used as a criterion of whether or not ultimate recovery will be affected by rate of flow since the attainment of a steady state will eliminate differences due to variations in previous operating conditions. The determination of how widely the conclusions developed from the present example apply requires the estimation of the range of values corresponding to abandonment conditions likely to occur in equation (3) for commercial fields. The present example represents a case of very wide spacing and low permeability. The gas viscosity will not vary greatly with type of gas or pressure. The porosity filled with gas will vary only over a rather limited range. The gas compressibility may vary considerably, however, being approximately inversely proportional to reservoir pressure. Also the well spacing, proportional to r^2 , may vary considerably. In general, these two important variables will tend to compensate each other since wider spacing usually follows deeper wells and higher pressures. In the present example the spacing was 288 acres per well and the abandonment pressure 2400 psi. As a widely different case, consider a shallow field with a 5-acre spacing. Assuming a permeability of 100 md, the minimum average reservoir pressure likely to be attained is estimated to be 50 psi (the abandonment reservoir pressure will be related to the assumed permeability and abandonment rate of flow). Since the spacing and compressibility factors approximately compensate, the greater permeability of the shallow field reduces the time to come to equilibrium in the shallow field at abandonment to one week. Thus, it seems likely that in general rate of production has no significant effect on ultimate recovery by a solution gas driven mechanism. If gravitational effects or other rate-sensitive factors are present, then these must be evaluated before applying the above generalization to any specific case.

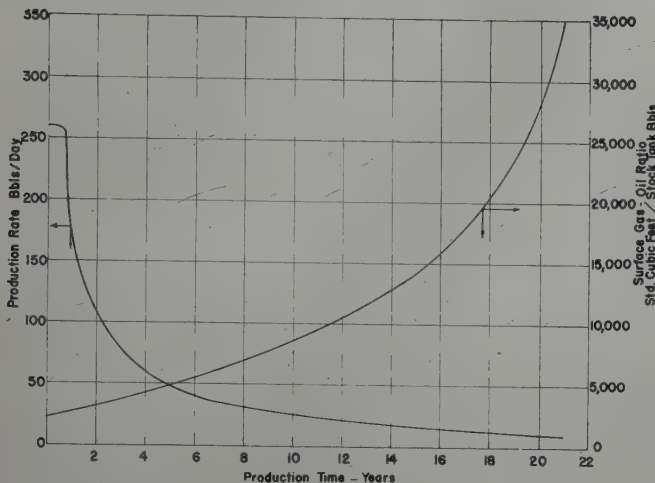


FIG. 10—STOCK TANK OIL PRODUCTION RATE DECLINE AND SURFACE GAS-OIL RATIO HISTORY

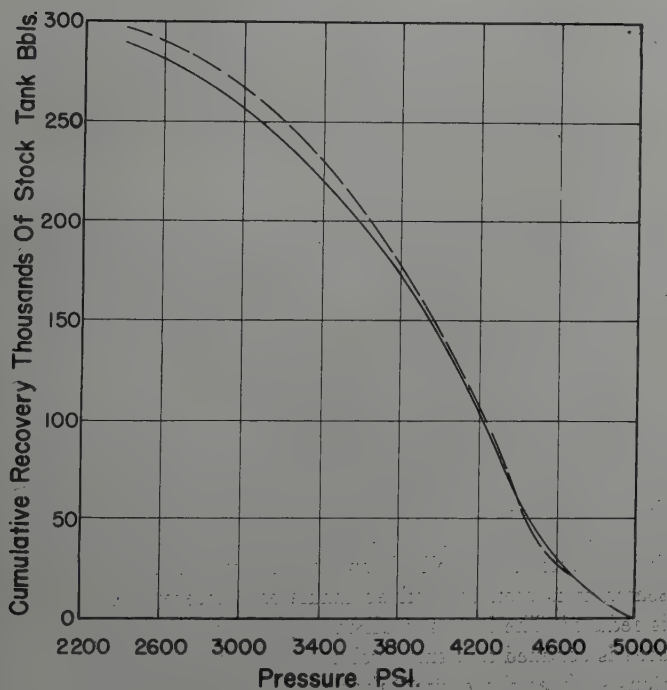


FIG. 11 — CUMULATIVE RECOVERY OF STOCK TANK OIL VS. RESERVOIR BOUNDARY PRESSURE
— OPEN FLOW CONDITIONS
--- INFINITESIMAL DRAWDOWN CONDITIONS

STEADY STATE ABANDONMENT CONDITIONS

A type steady state in which the various zones in the reservoir contribute in proportion to their volume is the type steady state to be referred to in the ensuing discussion. In the course of calculating the transient history of the reservoir studied in this discussion it is noted that successive curves of oil saturation, C_L , assume progressively flatter proportions until near abandonment when the distribution of C_L throughout the reservoir is essentially constant. This is readily acceptable upon noting that near abandonment the gas saturation has increased to such an extent that any gas produced essentially is merely bled off, assisting practically nil in producing oil by displacement. The rapid increase in gas permeability with very slight decrease in oil saturation near abandonment then tends to establish the flat distribution of C_L throughout the reservoir at abandonment. Also near abandonment, since saturation is essentially constant over the reservoir, the distribution of relative permeability to oil over the reservoir is quite uniform. This leads to a series of several pressure distributions near abandonment that decline quite uniformly; that is, successive pressure curves are essentially parallel over most of the reservoir. This combination of circumstances leads to successive C_L/F curves that are essentially parallel, which is a graphical expression of the fact that the various zones of the reservoir are producing residue oil in proportion to their respective volumes. This is expressed in another manner by the linearity of the curves of rate of residue oil flow within the reservoir as functions of area of drainage.

The condition described above can be taken advantage of in simplifying calculations of abandonment conditions by use of the single-phase, radial-flow adaptation of Darcy's Law to the type steady state described (equation 1). By making use of the constancy of C_L near abandonment conditions and using the effective permeability to oil characteristic of this constant saturation along a given curve, as well as using an average value of $\mu_o F$ which changes only slightly with pressure, an entire curve may be calculated with only a few points, and quickly, using:

$$p - p_i = \frac{(\mu_o F)_{ave} Q_1}{2\pi a h k_o \left(1 - \frac{r_1^2}{r_c^2}\right)} \left[\ln_c \frac{r}{r_1} - \frac{r^2 - r_1^2}{r_c^2} \right] \quad (4)$$

EFFECT OF WELL SPACING

The well whose transient history for open flow production has been calculated had a radius of drainage of 2,000 ft, corresponding to a well spacing of 288 acres. It may be noted from Figs. 4-7 that throughout the majority of this reservoir the pressure and saturation gradients are very low. Thus the ultimate recovery from this solution gas driven reservoir appears to be essentially independent of well spacing.

To confirm this an evaluation will be made of the recovery to be expected by 10-acre spacing. This will be based on the approximation of the steady state two-phase abandonment conditions described earlier. By assuming the same abandonment rate for the 10-acre reservoir as was taken in the transient history calculations, the distribution of pressure at abandonment for the 10-acre reservoir may be calculated when the

bottom hole flowing pressure is known (open flow conditions) and the boundary pressure can then be computed. The saturation at the boundary can be readily determined, and since it is justified to assume saturation in the reservoir to be constant, the complete distribution of oil in the 10-acre reservoir is described. Such calculations show that the 10-acre reservoir would be abandoned at a lower pressure and oil saturation than the 288-acre reservoir because much of the oil has to flow a shorter distance to a well. With the close spacing the productivity index corresponding to a given perimeter pressure would be improved by 20 per cent and the field depleted to the lower pressure of 2200 psi (2400 psi for 288-acre reservoir) giving about 1 per cent more recovery. Since this advantage is certainly minor in view of the large number of wells required, the question of well spacing essentially would reduce to an economic balance between added capital expenditure for drilling and saving in time of depletion.

WATER DRIVE AND PRESSURE MAINTENANCE

Following the conclusion that for any desired spacing a field produced solely by solution gas driven mechanism may be produced wide open without fear of decreasing ultimate recovery, questions naturally arise as to what harm, if any, will be done if a field is opened up and later found to be water driven or if a field is opened and it is later decided to institute a pressure maintenance program. The danger in such a situation would lie in the shrinkage that would accompany a decline in pressure and the subsequent loss of more stock tank oil in the form of residual oil trapped back of the water or gas front.

During the early life of such a water driven field that has been produced at open flow the evolved gas does not flow appreciably but rather remains in the individual pores until the gas saturation has built up sufficiently for the gas permeability to permit flow. Upon increasing the reservoir pressure, for example by water encroachment during a shut-in period, this dispersed gas would be redissolved in the oil and the net shrinkage would be negligible. It follows then that producing a water driven field initially at open flow causes no permanent loss in ultimate recovery if production at open flow is terminated before appreciable amounts of excess free gas are produced. However, the operation must be followed carefully and the absence of water drive established at an early date.

LARGE SCALE FIELD PRESSURE GRADIENTS

The previous discussion has dealt with production from a formation having a uniform horizontal distribution of permeability and produced from uniformly spaced wells. Large pressure gradients may develop across some fields, usually because of pronounced horizontal permeability variations, irregular well spacing, or disproportionate distribution of production among the wells. From the analysis of the results presented it is seen that oil accumulates wherever the pressure is reduced. The loss is small merely because the low pressure area is confined to a small volume of the reservoir. Any conditions such as those cited above which would result in a low pressure region of considerable areal extent, therefore, could cause a substantial loss in ultimate recovery in a solution gas driven field. The authors have made no detailed analysis of the loss possible under such circumstances.

CONCLUSIONS

The results discussed in this paper lead to the following conclusions:

1. In commercial solution gas driven fields a steady state condition will be approached during the long period of essentially constant rate near abandonment, the time required to reach steady state being short when compared with the time during which production occurs at a low, essentially constant marginal rate.

2. Since the particular steady state established in any solution gas driven field is determined solely by the production rate at abandonment and the reservoir and fluid characteristics, the ultimate recovery will not depend on the manner in which the field is produced during the earlier history. In other words this type field may be produced wide open with no fear of loss in ultimate recovery.

3. Since throughout the production history of such a reservoir the pressure and oil saturation gradients in the majority of the drainage area are very small, a single well will effectively drain a large area given sufficient time and a close well spacing will not materially improve ultimate recovery. The slight increase for a very close spacing compared to a wide spacing (10 acres to 288 acres) resulted from the lower average pressure at abandonment due to the smaller radius of drainage.

4. If a field were produced under open flow conditions initially and the presence of a water drive were later discovered, no serious harm would result provided the field is kept under close surveillance and the production of appreciable quantities of excess free gas is prevented.

5. The foregoing conclusions apply to solution gas driven fields of uniform permeability produced by uniformly spaced wells. The presence of large pressure differences existing over large areas such as might be caused by differences in permeability, irregular spacing, or disproportionate production of wells could cause a decrease in ultimate recovery.

APPENDIX

Single Phase Production Analysis

Brownscombe and Collins⁸ have developed a method for calculating pressure distribution by a material balance-fluid flow analysis. Their equation (10), by letting $\bar{q}_e = 0$ because there is no flow across the outer boundary, becomes:

$$\bar{\Delta p} = \frac{1}{\bar{r}_e^2 - 1} \left[\bar{r}_e^2 \ln_e \bar{r} - \frac{\bar{r}^2 - 1}{2} \right] \quad \dots \quad (5)$$

Changing from dimensionless variables, where $\bar{r} = r/r_w$ and $\bar{r}_e = r_e/r_w$,

$$\Delta p = \frac{1}{1 - \frac{r_w^2}{r_e^2}} \left[\ln_e \frac{r}{r_w} - \frac{r^2 - r_w^2}{2r_e^2} \right] \quad \dots \quad (6)$$

Instead of r_w , use r_1 as a reference radius across which rate is maintained constant at value q_1 until steady state is reached,

$$\bar{\Delta p} = \frac{1}{1 - \frac{r_1^2}{r_e^2}} \left[\ln_e \frac{r}{r_1} - \frac{r^2 - r_1^2}{2r_e^2} \right] \quad \dots \quad (7)$$

In converting from dimensionless $\bar{\Delta p}$ to Δp , rate q_1 (defined in reservoir bbl by Brownscombe and Collins⁸) is used at r_1 , and pressure p_1 at r_1 ,

$$\Delta p = \frac{2\pi h k_o}{\mu_o q_1 F} (p - p_1) \quad \dots \quad (8)$$

in which formation volume factor F was inserted along with q_1 to put it on a residue barrel basis. This is an approximation, but is well taken because of the relative constancy of F in this one-phase production. Inserting (8) into equation (7), and including the dimensional constant a to convert to units used in this paper,

$$p - p_1 = \frac{\mu_o q_1 F}{2\pi a h k_o} \left(\frac{1}{1 - \frac{r_1^2}{r_e^2}} \right) \left[\ln_e \frac{r}{r_1} - \frac{r^2 - r_1^2}{2r_e^2} \right] \quad \dots \quad (9)$$

which is equation (1) in the body of the paper.

Expressing the reservoir fluid content in terms of the compressibility and the average reservoir pressure decline as obtained by integrating the pressure distribution given by (9), the total withdrawal up to the time saturation pressure reaches the well may be expressed as:

$$\Delta Q_{wc} = \frac{\pi r_e^2 h f (1 - C_w)}{5.61 F_1} \left[(p_1 - p_w) \left(1 - \frac{r_w}{r_e} \right) - \left(\frac{\mu_o q_w}{2\pi a h k_o} \left(1 - \frac{r_w^2}{r_e^2} \right) \right) \left(\ln_e \frac{r_e}{r_w} - \frac{3}{4} + \frac{r_w^2}{r_e^2} - \frac{r_w^4}{4r_e^4} \right) \right] \quad (10)$$

Transition Phase Analysis

The pressure distribution after a uniform pressure decline over the reservoir has been established during the one-phase production history. This phase is followed by a transition period as the pressure falls below saturation pressure, first around the well bore and later out into the reservoir and is characterized by the outer portion producing by an expanding liquid drive, whereas the inner portion has entered the secondary or two-phase part of its history.

The production rate at the well is to be held constant at this stage of the production history. Since a larger proportion of the total flow will be contributed from the region near the well where the reservoir fluid system is more expandable, flow rates in the expanding liquid region must decline. Assuming this decline to be gradual, steady state conditions can nevertheless be assumed in this region over short time intervals.

Considering a zone from r_1 to r_2 entering into the transition region such that at time t_b saturation pressure occurred at r_1 and at time t_a , saturation pressure occurred at r_2 , the method

of Brownscombe and Collins³ may be modified to describe the pressure distribution with reference to saturation pressure if the flow rate at r_s is known:

$$p - p_s = \frac{\mu_o q_s F}{2\pi a h k_o \left(1 - \frac{r_s^2}{r_e^2}\right)} \left(\ln_e \frac{r}{r_s} - \frac{r^2 - r_s^2}{2r_e^2} \right) \quad (11)$$

The withdrawal, ΔQ_{2e} , from the expanding liquid region r_{s2} to r_e between time t_b and time t_a is:

$$\Delta Q_{2e} = \frac{hf}{5.61} \int_{\pi r_{s2}^2}^{\pi r_e^2} \left[\left(\frac{C_L}{F} \right)_{t_b} - \left(\frac{C_L}{F} \right)_{t_a} \right] d\pi r^2 \quad (12)$$

and since $F = F_e e^{(p_1 - p)}$ and $e^x = 1 + x$, when x is small,

$$\Delta Q_{2e} = \frac{hfcC_{L1}}{5.61F_1} \int_{\pi r_{s2}^2}^{\pi r_e^2} (P_{t_b} - P_{t_a}) d\pi r^2 \quad (13)$$

Evaluating equation (11) for the pressure at any point r at time t_b and t_a gives

$$P_{t_b} - P_{t_a} = \frac{\mu_o F}{2\pi a k_o h} \left[\frac{q_{s1}}{1 - \frac{r_{s1}^2}{r_e^2}} \left(\ln_e \frac{r}{r_{s1}} - \frac{r^2 - r_{s1}^2}{2r_e^2} \right) - \frac{q_{s2}}{1 - \frac{r_{s2}^2}{r_e^2}} \left(\ln_e \frac{r}{r_{s2}} - \frac{r^2 - r_{s2}^2}{2r_e^2} \right) \right] \quad (14)$$

Substitute (14) into (13) and integrating:

$$\Delta Q_{2e} = \left(\frac{hfcC_{L1}}{5.61F_1} \right) \left(\frac{\mu_o F_1}{2\pi a k_o h} \right) \left[\frac{q_{s1}}{1 - \frac{r_{s1}^2}{r_e^2}} \left(\pi r_e^2 \ln_e \frac{r_e}{r_{s1}} - \frac{\pi r_{s1}^2}{2} \right) - \frac{q_{s2}}{1 - \frac{r_{s2}^2}{r_e^2}} \left(\pi r_e^2 \ln_e \frac{r_e}{r_{s2}} - \frac{\pi r_{s2}^2}{2} \right) \right] \quad (15)$$

Let

$$A = \left(\frac{hfcC_{L1}}{5.61F_1} \right) \left(\frac{\mu_o F_1}{2\pi a k_o h} \right) \left(\frac{\pi r_e^2}{1 - \frac{r_{s1}^2}{r_e^2}} \right) \left(\ln_e \frac{r_e}{r_{s1}} - \frac{r_{s1}^2}{r_e^2} \right) \quad (16)$$

$$B = \left(\frac{hfcC_{L1}}{5.61F_1} \right) \left(\frac{\mu_o F_1}{2\pi a k_o h} \right) \left(\frac{\pi r_e^2}{1 - \frac{r_{s2}^2}{r_e^2}} \right) \left(\ln_e \frac{r_e}{r_{s2}} - \frac{3}{4} - \frac{r_{s2}^4}{4r_e^4} + \frac{r_{s2}^2}{r_e^2} \right) \quad (17)$$

$$(Note A = B \text{ when } r_{s1} = r_{s2}) \quad (18)$$

then $Aq_{s1} - Bq_{s2} = \Delta Q_{2e}$ (liquid). Since A and B are merely functions of the two radii, r_{s1} and r_{s2} , once the fluid and reservoir characteristics are defined, a knowledge of q_{s1} and q_{s2} will allow the withdrawal ΔQ_{2e} to be calculated (see Fig. 12-A). The value of q_{s1} is known from the curve previous in time. To establish the value of q_{s2} a trial and error approach is necessary. The value of q_{s2} must be estimated and then confirmed by obtaining a desired flow rate at the well at the time the saturation pressure occurs at r_2 .

Having calculated ΔQ_{2e} for $r = r_{s2}$, then

$$\frac{\Delta Q_{2e}}{q_{s2}} = t_a - t_b \quad (19)$$

since q_{s2} is the constant flow rate over the interval $t_b - t_a$ and the progress of saturation pressure out in the reservoir may be described thereby. It is to be noted that before establishing the progress of the saturation pressure out into the reservoir, it was necessary to define the production rates desired at the well.

Two-Phase Production Analysis

As in the earlier analysis, the reservoir is divided into a series of annular rings or zones surrounding the well for the two-phase production calculations. Over short time intervals and within each zone steady state conditions are assumed and an integrated form of Darcy's Law can be used. In the absence of a rigorous analytical approach to describe the unsteady state flow of two phases within the reservoir, this approximation by a series of successive steady state conditions has been combined with material balance calculations to describe the two-phase production. An additional consideration in the region below saturation pressure is the decline in oil saturation resulting in a decline in relative permeability to oil.

Using the afore-described general approach a method has been developed to calculate the distribution of pressure and the other variables between the well bore and the position at which saturation pressure occurs. Stepwise calculations describing the distribution of pressure and the other variables at a given time depend upon knowledge of such a distribution at some previous time. Dealing with two such constant time distributions of variables, material balance considerations may be applied by considering the change in the various variables over a time interval t_b to t_a and within a zone bounded by r_1 and r_2 . The shaded area in Fig. 12-B describes such a zone between t_b and t_a . It is to be noted that in a typical calculation, conditions at point 1_b, 2_b, and 2_a are known and conditions at 1_a are to be calculated. The calculation of conditions at point 1_a is begun by estimating the

pressure at that point. The oil saturation at l_a may be calculated by a relationship between pressure p and oil saturation C_L obtained by simultaneous solution of the equations relating p to q/k_o , permeability k_o to saturation C_L , and withdrawal of oil ΔQ_L or $\Delta t(q_1 - q_2)$ to saturation C_L . A modification of Darcy's Law allows the relationship between pressure p and the ratio of oil flow rate to permeability q/k_o to be evaluated from r_1 to r_2 at $t = t_a$:

$$\int_{r_1}^{r_2} \frac{q}{k_o} \frac{dr}{r} = 2\pi ah \int_{p_1}^{p_2} \frac{dp}{\mu_o F} \quad (20)$$

Assuming that over a short interval q/k_o is a linear function of $\log_{10} r$ and integrating:

$$\int_{p_1}^{p_2} \frac{dp}{\mu_o F} = \frac{2.303}{4\pi ah} \left(\frac{q_1}{k_{o1}} + \frac{q_2}{k_{o2}} \right) \log_{10} \frac{r_2}{r_1} \quad (21)$$

We have now an approximate implicit expression for Δp (or p_{1a} , given p_{2a}) in terms of $\left(\frac{q}{k_o} \right)_1$. Since $\left(\frac{q}{k_o} \right)_2$ and r_2/r_1 are known, the approximation of k_o as a function of C_L by a series of straight line segments has been assumed to relate these two quantities by means of the equation:

$$m = \frac{C'_L - C_L}{k'_o - k_o} \quad (22)$$

Where m is the slope of the straight-line segment in the region containing saturation $C_{L_{1a}}$ and C'_L and k'_o are the saturation and permeability respectively locating the upper limit of this straight-line segment. It now remains only to express the oil flow rate q in terms of the oil saturation in order to obtain a relationship between pressure and saturation. This is accomplished by material balance consideration in which the withdrawal of residue oil from the zone r_1 to r_2 during the time interval t_a to t_b is readily given by:

$$\Delta Q_{L_{12}} = (q_{1a} - q_{2a}) \Delta t = \frac{hf}{5.61} \int_{\pi r_1^2}^{\pi r_2^2} \left[\left(\frac{C_L}{F} \right)_b - \left(\frac{C_L}{F} \right)_a \right] d\pi r^2 \quad (23)$$

By assuming C_L/F to be a linear function of r , this assumption being well taken if sufficiently short distances are involved in defining zones, and the above integration performed analytically,

$$\Delta Q_{L_{12}} = \frac{\pi hf}{3 \times 5.61} (r_2 - r_1) \left[\left(\Delta \frac{C_L}{F} \right)_1 (2r_1 + r_2) + \left(\Delta \frac{C_L}{F} \right)_2 (r_1 + 2r_2) \right] \quad (24)$$

$$\text{where } \left(\Delta \frac{C_L}{F} \right)_1 = \left(\frac{C_L}{F} \right)_{1b} - \left(\frac{C_L}{F} \right)_{1a} \quad \text{and} \quad (25)$$

$$\left(\Delta \frac{C_L}{F} \right)_2 = \left(\frac{C_L}{F} \right)_{2b} - \left(\frac{C_L}{F} \right)_{2a} \quad (26)$$

and where $\left(\frac{C_L}{F} \right)_{1b}$ equals value at r_1 at time t_b and $\left(\frac{C_L}{F} \right)_{2b}$ equals value at r_2 at time t_b , and $\left(\frac{C_L}{F} \right)_{2a}$ equals value at r_2 at time t_a , known from previous calculations, and $\left(\frac{C_L}{F} \right)_{1a}$ equals value at r_1 at time t_a of present calculation.

The calculation of gas production over the interval, $\Delta Q_{G_{12}}$, may be carried out by a similar formula with the $\frac{C_L}{F}$ replaced by $\left(\rho C_G + S \frac{C_L}{F} \right)$ the sum of the free gas and the solution gas within a barrel of pore space.

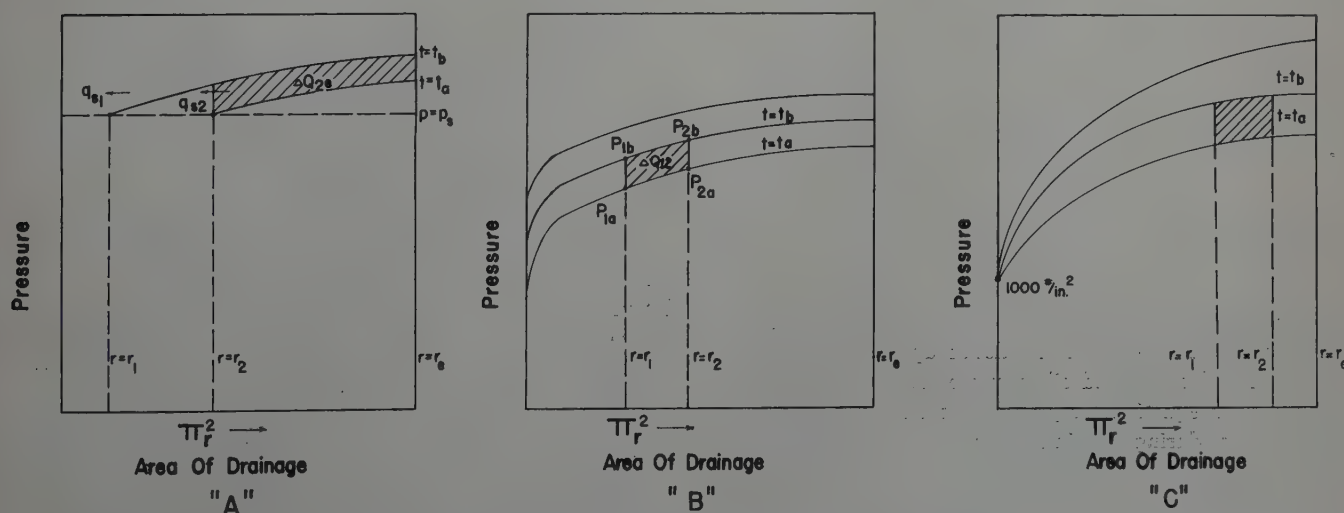


FIG. 12 — SCHEMATIC DRAWINGS OF ZONES USED IN CALCULATIONS

By simultaneous solution of equations (21), (22), and (24), the oil saturation $C_{L_{1a}}$ may now be expressed as a function of p_{1a} :

$$mC'_L - k'_o - \frac{q_2 + \frac{H}{G}}{\frac{q_2}{k_{o_{2a}}} - E\phi}$$

$$C_{L_{1a}} = \frac{2r_1 + r_2}{m - G \left(\frac{q_2}{k_{o_{2a}}} - E\phi \right) F_{1a}} \quad (27)$$

where

$$E = \frac{4\pi ah}{2.303 \log_{10} \frac{r_2}{r_1}}$$

$$G = \frac{3 \times 5.61 \times \Delta t}{\pi h f (r_2 - r_1)}$$

$$H = (2r_1 + r_2) \left(\frac{C_L}{F} \right)_{1b} - (r_1 + 2r_2) \left[\left(\frac{C_L}{F} \right)_{2b} - \left(\frac{C_L}{F} \right)_{2a} \right], \text{ and}$$

$$\phi = \int_{p_1}^{p_2} \frac{dp}{\mu_o F}$$

In evaluating the quantity ϕ in equation (27) it was found

$$\text{convenient to divide the curve of } \int_{p_1}^{p_2} \frac{dp}{\mu_o F} \text{ vs } p$$

into a number of straight-line segments and write linear equations for those segments.

Having estimated p_{1a} and calculated the oil saturation $C_{L_{1a}}$ associated with it, it now remains to confirm the assumed pressure. This is done by a consideration of the average gas-oil ratio over the interval. One method by which to calculate this average value assumes a linear variation of R with time, giving

$$R_F = \frac{1}{2} (R_a + R_b) \quad (28)$$

R_a , gas-oil ratio at $r = r_1$ and $t = t_a$, may be calculated by Darcy's Law,

$$R_a = \frac{\frac{k_G}{k_o}}{\frac{\mu_G}{\mu_o F}} + S_a \quad (29)$$

Another method by which the average gas-oil ratio may be calculated involves a material balance approach. Calculating the withdrawal of gas and oil from the zone by equation (24) and a similar equation for gas, the total flow of gas and oil past radius r_1 during the time interval Δt may be calculated by adding each respective withdrawal from the zone to the entry into the rear of the zone at r_2

$$\Delta Q_{L_{1a}} = \Delta Q_{L_{12}} + \Delta Q_{L_{2a}} \quad (30)$$

$$\text{and } \Delta Q_{G_{1a}} = \Delta Q_{G_{12}} + \Delta Q_{G_{2a}} \quad (31)$$

The average gas-oil ratio then is

$$R_M = \frac{\Delta Q_{G_{1a}}}{\Delta Q_{L_{1a}}} \quad (32)$$

The estimation of pressure which initiated the series of calculations may now be considered correct if $R_M = R_F$.

To review the calculation of the several variables at r_1 on time curve t_a , the procedure may be briefly summarized as follows. All data are known at the beginning of the interval, time t_b , and at radius r_2 , and calculations are to be made at the end of the interval, at time $t_a = t_b + \Delta t$ and at radius r_1 .

(1) A value of pressure p_{1a} at time t_a and distance r_1 is estimated.

(2) The corresponding value of oil saturation $C_{L_{1a}}$ is calculated by equation (27).

(3) The average value of the gas-oil ratio R_M over the time interval is calculated by material balance from equation (32).

(4) The value of the gas-oil ratio R_a at the end of the time interval is calculated by means of the permeability-viscosity relationship (see equation 29).

(5) Assuming that gas-oil ratio varies linearly with time over a short time interval, a second average value, R_F , is calculated from equation (28).

(6) The values of R calculated by (28) and (32) are compared to provide a check on the value of p estimated in (1).

As successive curves are calculated and saturation pressure reaches the boundary of the reservoir, curves later in time must originate below saturation pressure and at the rear boundary, viz. curve for $t = t_a$ and $t = t_b$ in Fig. 12-C. Coincidentally with saturation pressure reaching the rear boundary, the bottom hole pressure fell to 1000 psi, bottom hole flowing pressure for open flow production, and the pressure isochrones now originating at the rear boundary converge at the well bore at 1000 psi. This calls for a slight revision in technique of calculation. Whereas before, the rate that occurred at the well bore upon completion of a calculation of a curve served as a check on the original estimate of the rate at $t = t_a$ and $p = p_s$ where curve crossed saturation pressure, now the check consists of reaching a bottom hole flowing pressure of 1000 psi, and the curve's calculation is originated at the rear boundary by estimating the elapsed time Δt since the previous curve and making use of knowledge of transient history conditions at the rear boundary. This latter point is quite important. Isochrones originating at or above saturation pressure made use of knowledge of saturation conditions as one of the three known points bounding the calculation "zone" prior to calculation of the fourth point. However, with the initial zone at the rear boundary below $p = p_s$, a means must be employed to describe the history of a barrel of pore space at the rear boundary. This may be done by a series of gas solution drive calculations of the type that assumes infinitesimal drawdown.⁴

It is believed that this type of mechanism sufficiently well describes the rear boundary across which there is no flow of fluid. Since this type calculation excludes time as a variable, curves originating at the rear boundary may be begun at regu-

lar intervals. e.g. every 100 or 200 psi, and the elapsed time between curves, Δt , estimated and confirmed by the curve in question reaching a bottom hole pressure of 1000 psi, the open flow pressure.

It will be recalled that C_L/F is assumed to be a linear function of the radius r . This consideration more than any other determines the number of zones and frequency of points to be calculated on any given curve, for as the C_L/F curve assumes a greater curvature near the well bore, a greater frequency of points is demanded to establish the curve. By the means described heretofore, the curve is calculated into a point near the well bore, e.g. in the reservoir in this study, in $\pi r^2 = 0.1 \times 10^5 \text{ ft}^2$ (boundary = 125.7×10^5). In the short distance left through which the C_L/F values change rapidly, advantage is taken of the fact that little additional contribution of oil and gas is made from this zone and, essentially, the rate across the zone is constant so that the conventional type steady state condition describes this zone fairly well. This is called upon to calculate the bottom hole flowing pressure for the entire series of curves describing the transient history of the reservoir.

NOMENCLATURE

Symbols

- α Dimensional constant converting to system of units used in this analysis $\alpha = 0.001127$
- c Compressibility of saturated oil, $\frac{1}{\text{psi}}$
- C_L Oil saturation, fraction of pore space
- C_G Gas saturation, fraction of pore space
- C_w Water saturation, fraction of pore space
- f Fractional porosity of rock
- F Formation volume factor, oil, $\frac{\text{bbls reservoir oil}}{\text{bbl residue oil}}$
- h Thickness of reservoir, ft
- k Effective permeability to oil or gas, millidarcies
- μ Viscosity, centipoises
- p Pressure at radius r , lb per sq in.
- Δp Pressure difference over some distance indicated by subscripts
- q Flow rate of oil across radius r , residue bbl per day
- ΔQ_L Production of oil over a time interval $t_a - t_b$ and from a zone as indicated by subscripts, residue bbl
- ΔQ_G Production of gas over a time interval $t_a - t_b$ and from a zone as indicated by subscripts, standard cu ft
- r Radial distance to well bore center, ft
- ρ Gas conversion factor, SCF gas/bbl reservoir gas
- R Gas-oil ratio SCF gas/bbl residue oil
- S Solubility of gas in oil, SCF gas/bbl residue oil
- t Time since beginning production, days
- Δt Difference in time, days

Dimensionless Variables

$$\frac{\Delta p}{\mu q_w} = \frac{2\pi k h \Delta p}{\mu q_w} \quad (\text{here, } k \text{ and } \mu \text{ refer to oil and are equivalent to } k_o \text{ and } \mu_o \text{ used in this paper})$$

$$\frac{r}{r_e} = r_e/r_w$$

$$\frac{r}{r_e} = r/r_w$$

$$\frac{q_e}{q_w} = q_e/q_w$$

Abbreviations

- Bbl Barrels
- SCF Standard cu ft of gas (Atmospheric pressure and 60°F)
- STB Stock tank bbl of oil
- \ln_e Natural logarithm = 2.303 x common logarithm

Subscripts

- 1 Conditions at radius $r = r_1$
- 2 Conditions at radius $r = r_2$
- i Initial conditions
- e Conditions at $r = r_e$, boundary of reservoir
- w Conditions at $r = r_w$, well bore
- s Conditions at $p = p_s$, saturation pressure
- o Identifies as property of oil phase
- L Identifies as property of oil phase
- G Identifies as property of gas phase
- W Identifies as property of connate water
- a Conditions at time $t = t_a$
- b Conditions at time $t = t_b$
- M Refers to average gas-oil ratio calculated by material balance
- F Refers to average gas-oil ratio calculated by arithmetically averaging gas-oil ratios calculated by Darcy's Law.

ACKNOWLEDGMENT

The authors wish to acknowledge the valuable assistance rendered by F. A. Collins in the mathematical development in this study.

REFERENCES

1. M. Muskat and M. W. Meres: "The Flow of Heterogeneous Fluids Through Porous Media," *Physics* (September, 1936).
2. M. Muskat and M. O. Taylor: "Effect of Reservoir Fluid and Rock Characteristics on Production Histories of Gas-Drive Reservoirs," *Trans. AIME* (1946) 165.
3. E. C. Babson: "Predictions of Reservoir Behavior From Laboratory Data," *Trans. AIME* (1944) 155.
4. M. Muskat: "Production Histories of Oil Producing Gas-Drive Reservoirs," *Journal of Applied Physics*, Vol. 16, No. 3 (March, 1945).
5. Vaughn Moyer: "Some Theoretical Aspects of Well Drainage and Economic Ultimate Recovery," *Petroleum Technology* (May, 1947).
6. T. C. Patton: "Graphical Methods for Temperature Distribution with Unsteady Heat Flow," *Industrial and Engineering Chemistry* (November, 1944) 36, 990.
7. E. C. Patton, Jr.: "Evaluation of Pressure Maintenance by Internal Gas Injection in Volumetrically Controlled Reservoirs," *Petroleum Technology* (November, 1946).
8. E. R. Brownscombe and F. A. Collins: "Steady States in Single Phase Reservoirs," Presented February 16, 1949 at meeting of AIME in San Francisco, California. In press *AIME Petroleum Technology*.
9. Leo B. Bicher, Jr., and Donald L. Katz: "Viscosity of Natural Gases," *Trans. AIME* (1944) 155. ★ ★ ★

CORRECTION OF GAS VOLUMES FOR COMPRESSIBILITY AND TEMPERATURE

ALBERT D. BROKAW, BROKAW, DIXON & McKEE, NEW YORK, N. Y.

The accompanying charts are presented to extend and improve a chart published under the title "A Chart to Provide Approximate Correction for Temperature and Deviation from Boyle's Law."¹ The applicability of this earlier chart was limited by the fact that it was based on the work of Burke and Keyes² and Kvalnes and Gaddy³ whose experiments were conducted with pure methane, the adjustments suggested for natural gases of higher specific gravity were unsatisfactory except within limited ranges of temperatures and pressures, and precise interpolation was difficult.

The extensive work of G. G. Brown, D. L. Katz and their associates on the heavier natural gases has provided better bases for the needed corrections, and the present charts, which are based largely on their work, are intended to simplify the computations involved.

The design of the charts has been changed by plotting temperatures as a function of pressure and correction factor, on a semilogarithmic or "ratio" grid, which gives fairly even spacing of the graphs and simplifies interpolation. Charts have been prepared for natural gas with specific gravities of .60, .65, .70, .75 and .80.

The standard computation for use in estimating the quantity of gas in a reservoir may be expressed as follows:

$$Q = \frac{PA \times 520 \times VR}{ZT}$$

where: Q is the volume of gas at 60°F and one atmosphere pressure

PA is the absolute formation pressure in atmospheres

¹ Original manuscript received at the Petroleum Branch Office June 23, 1947. Revised manuscript received July 8, 1949.

² References given at end of paper.

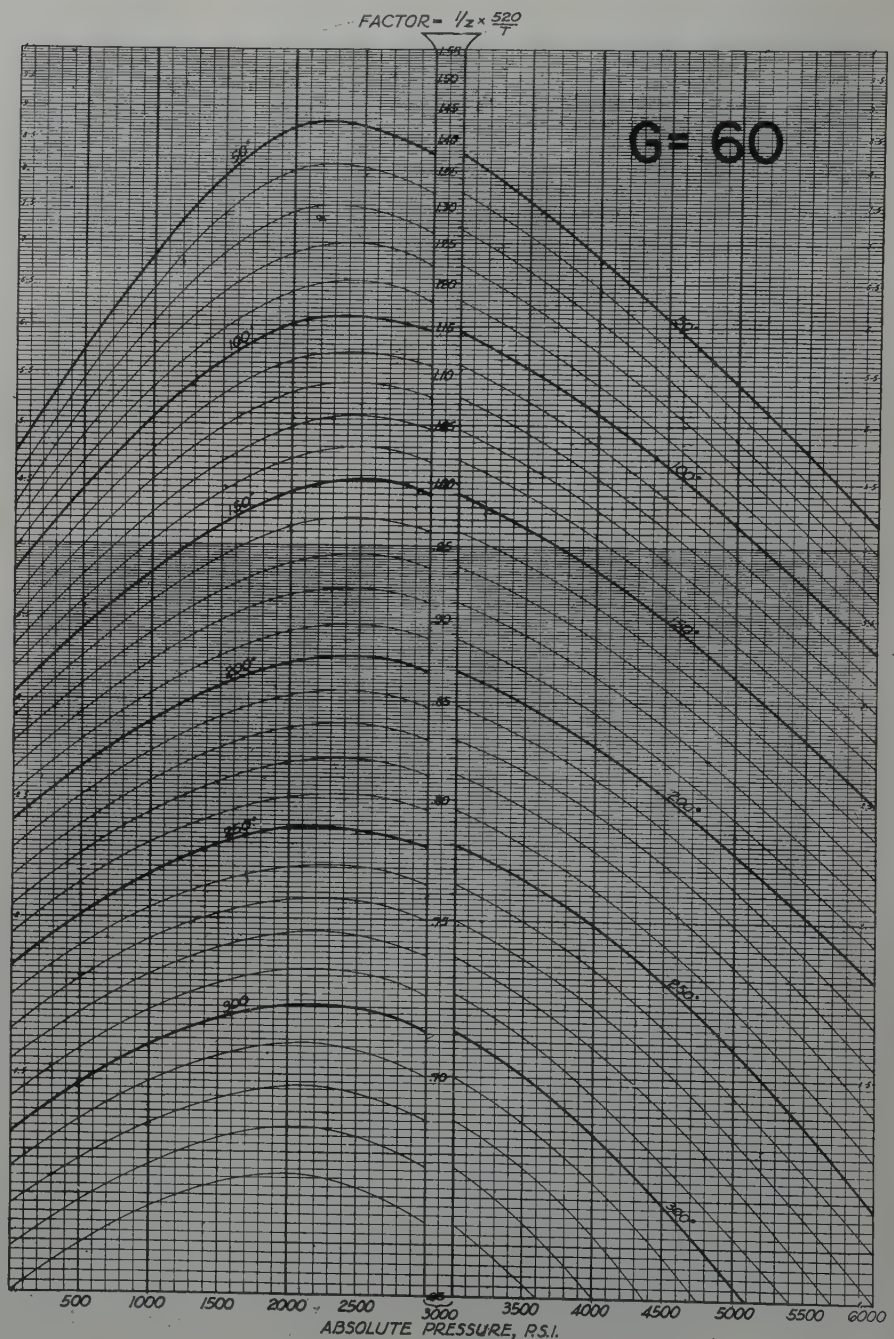


FIG. 1 — MULTIPLIERS FOR CORRECTING GAS-VOLUME CALCULATING (PV) FOR
TEMPERATURE AND DEVIATION FROM BOYLE'S LAW (G=.60)

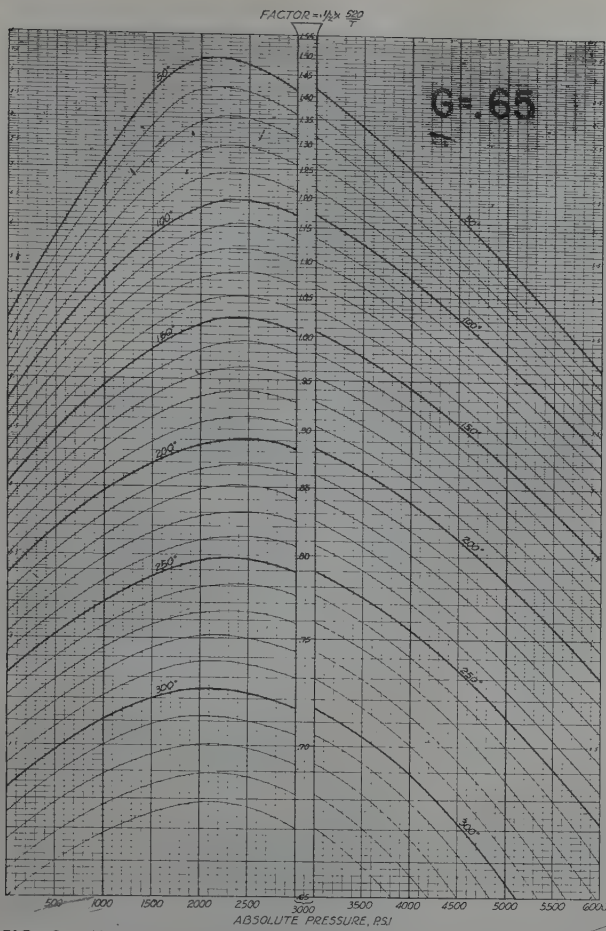


FIG. 2 — MULTIPLIERS FOR CORRECTING GAS-VOLUME CALCULATIONS (PV) FOR TEMPERATURE AND DEVIATION FROM BOYLE'S LAW (G = .65)

FACTOR = $\frac{1}{2} \times \frac{520}{T}$

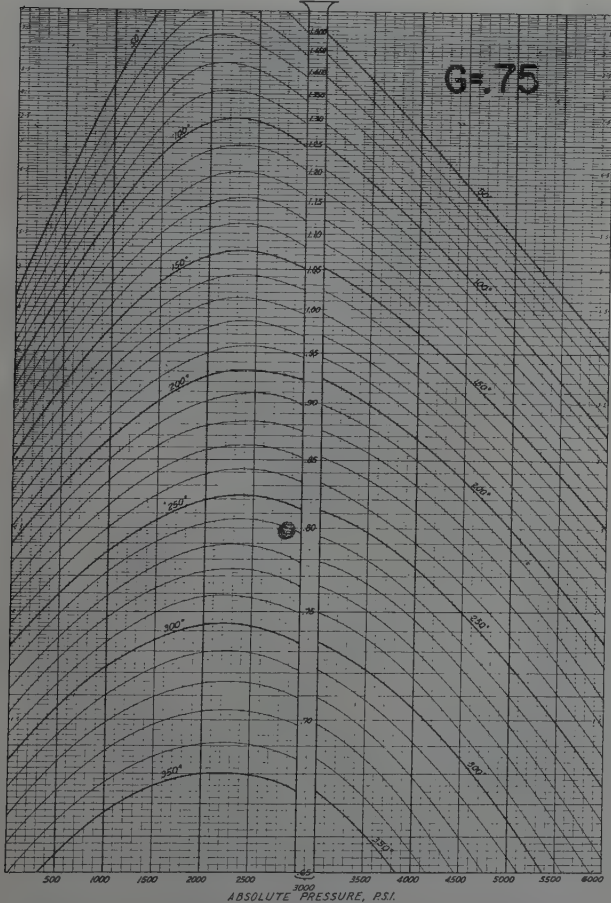


FIG. 4 — MULTIPLIERS FOR CORRECTING GAS-VOLUME CALCULATIONS (PV) FOR TEMPERATURE AND DEVIATION FROM BOYLE'S LAW (G = .75)

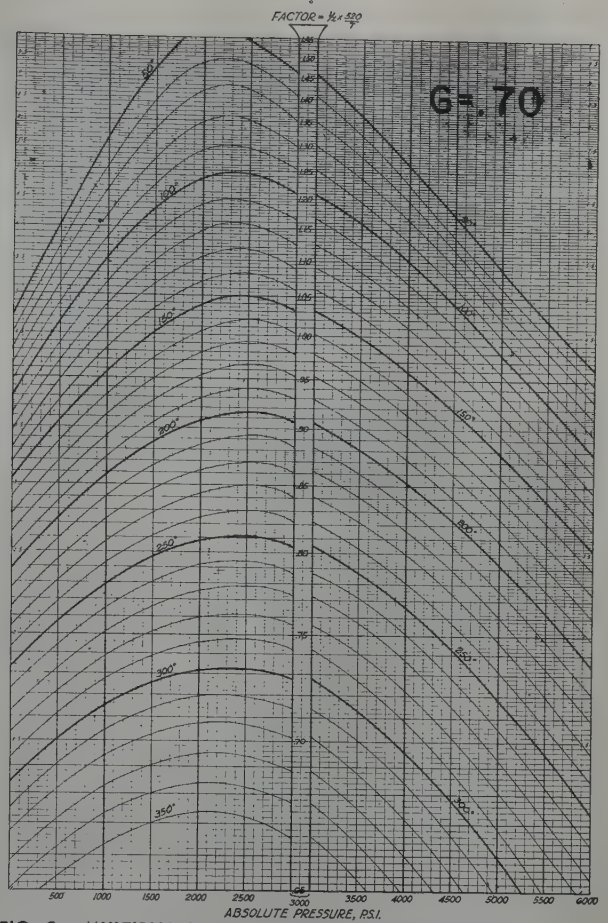


FIG. 3 — MULTIPLIERS FOR CORRECTING GAS-VOLUME CALCULATIONS (PV) FOR TEMPERATURE AND DEVIATION FROM BOYLE'S LAW (G = .70)

FACTOR = $\frac{1}{2} \times \frac{520}{T}$

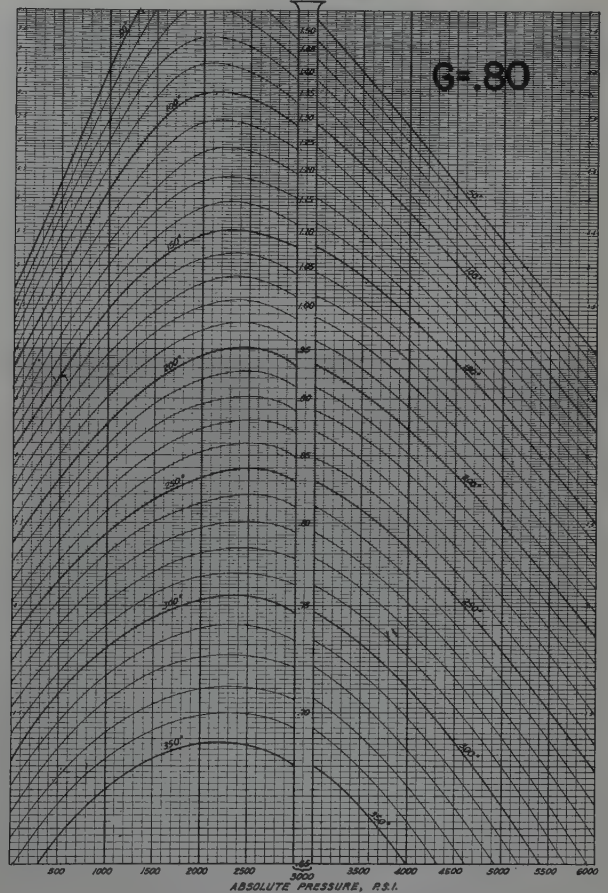


FIG. 5 — MULTIPLIERS FOR CORRECTING GAS-VOLUME CALCULATIONS (PV) FOR TEMPERATURE AND DEVIATION FROM BOYLE'S LAW (G = .80)

VR is the net effective reservoir volume

T is the absolute temperature (Rankine)

Z is the compressibility factor

The correction Factor F, given by the charts is $F = \frac{520}{ZT}$ and the equation above becomes:

$$Q = PA \times VR \times F$$

The charts are probably self explanatory but their use may be illustrated as follows:

Assume: Specific Gravity of gas .65

Absolute Formation Pressure 2100 psia

Temperature 165°F

Starting at 2100 psia on the axis of abscissas on the chart for $G = .65$ proceed upward to a point halfway between the 170° and 160° temperature lines, thence horizontally to the Factor column in the middle of the chart, where we may read, $F = .973$. The probable error is very small compared to the errors attendant upon estimation of net effective reservoir volume. In order to illustrate the saving in time we may carry out the computation without use of the chart:

Read from Chart⁴

Pseudo Critical Temperature for $G = .65$ 371°R

Pseudo Critical Pressure 671 psia

Calculate:

Pseudo Reduced Temperature

$$\frac{460 + 165}{371} = 1.68$$

Pseudo Reduced Pressure

$$\frac{2100}{671} = 3.13$$

Interpolate for Compressibility Factor Z on Chart⁵ = .852

Compute Factor:

$$\frac{520}{.852 \times (460 + 165)} = .977$$

In view of the generalized relationship between pseudo critical pressures and temperatures and the specific gravity of natural gases, and the known deviation of values for individual gases from the plotted graphs there seems to be little basis for choice between the values obtained by the two methods.

For gases differing in specific gravity from the bases of the charts not more than .01, results sufficiently accurate for use in reserve estimates may be obtained by using the prepared charts without correction. For intermediate specific gravities interpolation between the values of two charts may be desired.

For gases much above .70 in specific gravity it is probably desirable to carry

out the routine computation because of the fairly wide divergence of pseudo critical temperature and pressure from the graphs cited.

All of the necessary graphs may be found in an excellent chapter on estimation of gas reserves prepared by H. C. Spoor, Jr.⁶ and published by the Houston Geological Society.

It may not be out of place to inject a note of caution against basing estimates of gas reserves for gas condensate wells on the composition or specific gravity of separator gas, as this will result in an over-estimate of recoverable gas. While the compressibility of reservoir gas in such fields is greater than that of the separator gas, the excess compressibility is not sufficient to offset the shrinkage due to condensation.

REFERENCES

1. Brokaw: AIME Tech. Pub. No. 1375 (1941).
2. Burke and Keyes: *Jnl. Amer. Chem. Soc.* (1927) 49, 1409.
3. Kvalnes and Gaddy: *Jnl. Amer. Chem. Soc.* (1931) 53, 349.
4. Rzasa and Katz: AIME Tech. Pub. No. 1814.
5. Standing and Katz: *Trans. AIME* 146, 144.
6. Houston Geological Society: Report of Composite Study Group Papers, Texas Gulf Coast 1946, 41FF.

★ ★ ★

THE PERFORMANCE OF THE TEN SECTION OIL FIELD

W. TEMPELAAR LIETZ, SHELL OIL COMPANY, INC., LOS ANGELES, CALIFORNIA

INTRODUCTION

The Ten Section oil field is located in the San Joaquin Valley in Kern County, California, about 12 miles southwest of Bakersfield in Township 30 South, Ranges 25 and 26 East. The accumulation is in a low relief anticlinal dome and has a productive area of approximately 2,200 acres. Discovered in 1936 as a result of seismic work, it was the first field on the floor of the Valley to obtain production. It had a small primary gas cap, and since its inception has been produced by depletion with controlled withdrawal from the gas cap to minimize blowthrough.

STRUCTURE AND STRATIGRAPHY

The Ten Section structure is an elongated anticlinal dome with flank dips of only about 7 degrees. A map of the field, now fully developed, and a composite log are shown in Figs. 1 and 2. Contours shown on the map are on the top of the first zone, or Marker XA as indicated on the composite log.

As shown, the field has a productive closure of only some 350 feet, and there apparently is no faulting in the reservoir.

The productive measures in Ten Section are of Upper Miocene age and are known as the Stevens sand. They contain thin, irregular shale or siltstone streaks which vary considerably in stratigraphic position and thickness and apparently are rather discontinuous. As a result, individual sands and shales cannot be correlated over any appreciable area, which makes it difficult to subdivide the sand body into separate

zones which are distinct throughout the field. However, there are two fairly persistent siltstone bodies that at the time of development were considered to divide the productive measures into three general zones.

The first, or uppermost zone is productive over the entire field and has an average thickness of 180 feet, of which some 65 per cent is sand. It had a primary gas cap in the crestal area with an areal extent of 930 acres. The second zone has a productive area somewhat smaller than the first zone, but it did not have any original gas cap. It has an average thickness of about 360 feet, of which 55 per cent is sand. The third zone has a very limited areal extent and a maximum productive thickness of 100 feet, of which 80 per cent is sand. Recently, a deeper oil accumulation, termed the "53" sand, was discovered, but it is not discussed in this analysis. In the first and second zones the water table was at 7,980 feet subsea, while in the third zone it was at 8,080 feet subsea.

RESERVOIR CHARACTERISTICS

Sand Characteristics

The Stevens sand in Ten Section is hard and well consolidated, and numerous wells were cored for core analysis. Core data on four representative wells are shown, plotted beside the electric logs in Figs. 3 to 6. The average porosity is 20 per cent, with porosities ranging from 15 to 30 per cent. It is estimated, from cores taken with oil base muds, that the interstitial water content is about 40 per cent. The average weighted permeability is approximately 140, with measured permeabilities ranging from 10 to 3,000 md. As might be expected with practically no correlation of individual sand

Manuscript at office of Petroleum Branch October 14, 1948. Paper presented at Branch Fall Meeting in Los Angeles October 14, 1948.

layers over an appreciable area, there are no definite stratigraphic layers of high or low permeability.

Physical Properties of Oil

The oil produced from this reservoir originally had a gravity of 36° API and was produced with an initial gas-oil ratio of 780 cu ft/bbl. PVT analyses have been carried out on several oil and gas samples, and data on the most representative well, 58-20, are represented in Figs. 7 and 8. It appears in these analyses that the bubble point pressure of the reservoir crude was 2,920 psia. The bubble point pressures in the PVT analyses of other samples were all of the same order of magnitude. This is rather surprising, since the oil had been in contact with the gas cap in which the pressure before development was some 3,525 psi. The viscosity of the oil at subsurface temperature of 211°F and a pressure of 3,525 psia was 0.4 cp.

RESERVOIR VOLUMES

Initially, the Stevens sand in Ten Section contained 340,000,000 barrels of reservoir oil, consisting of 240,000,000 barrels of tank oil combined with 190,000,000 Mcf of gas in solution. The gas cap originally had a reservoir pore space of 60,000,000 barrels occupied by gas, which amounted to 72,000,000 Mcf at standard conditions.

HISTORY

The first well, 1-29, was completed June 2, 1936, to produce from the first zone. The initial production was 745 barrels of 60° API gravity oil and 12,450 Mcf of gas. No bottom hole pressure was determined at the time of the completion; however, from pressure data obtained after the well was recompleted on April 20, 1937, an original gas cap pressure of 3,525 psia was indicated. In that period, a total of 222,000

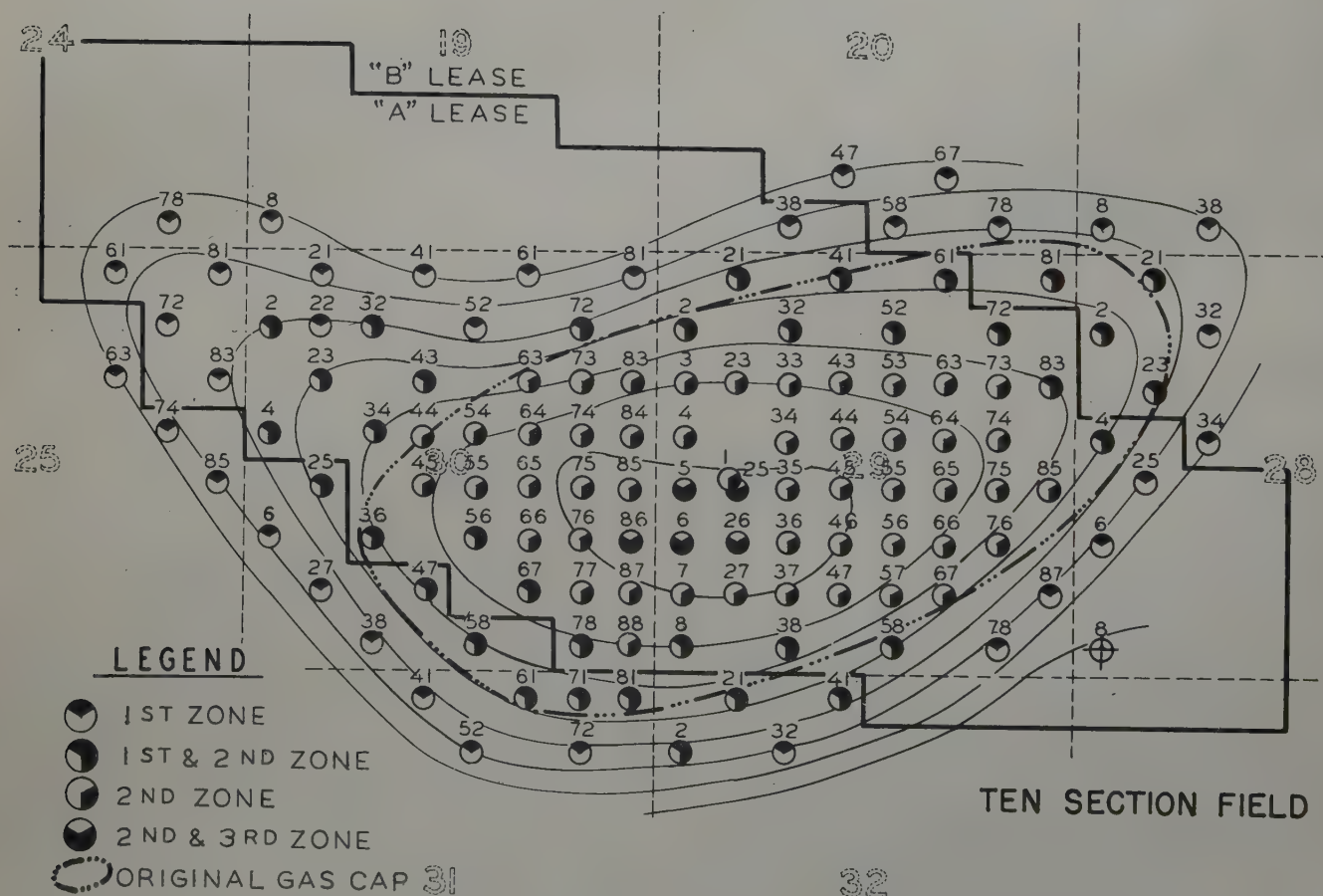


FIG. 1 — MAP OF TEN SECTION FIELD SHOWING CONTOURS ON ELECTRIC LOG MARKER XA

barrels of 60° gravity oil and 4,000,000 Mcf of gas was produced.

The second well, 6-29*, was completed in October, 1936, in what was later found to be the third zone, and had a reservoir

* The first number indicates the position of the well in the section on a 10-acre grid; the second number indicates the section.

pressure of 3,660 psia at the midpoint of the perforations. The third well, 34-29, completed in February, 1937, produced from the second zone and had an initial reservoir pressure of 3,500 psia at the midpoint of the perforations.

The next wells were drilled in 20-acre locations selected to establish the limits of the oil accumulation. After completion of the 20-acre development, it appeared that the first zone had an original gas cap as outlined in Fig. 1. Since the field was developed rapidly, the information on well performance at the time the 20-acre development was completed was limited, and no definite conclusions could be drawn about the productive character of the reservoir. However, the edge wells had not shown any signs of increasing cuts, and it was assumed tentatively that Ten Section was not producing under water drive conditions.

As mentioned before, the lack of correlation between streaks of siltstone left some uncertainty regarding the continuity of the separation between the zones. Also, because of the drilling costs of these comparatively deep wells, separate development of the three zones was not justified. As a result, wells were completed to produce four combinations of zones: (a) First-zone wells, located in a belt near the periphery of the oil accumulation; (b) Combination first and second-zone wells, located in the next belt upstructure and sufficiently down-structure from the gas cap to prevent an early blowthrough; (c) Second-zone wells located in the reservoir underlying the first-zone gas cap; and (d) Second and third-zone wells in the crestal area.

RESERVOIR PERFORMANCE

The 20-acre development was completed in March, 1941, and a critical review was made of the performance of the reservoir. At that time about 12,000,000 barrels of oil had been produced from the reservoir, and the average pressure had dropped to 3,080 psig. There were no indications of water drive, since none of the edge wells had shown an increase in water production, although the pressure in the edge wells had declined to about 3,080 psig. If any water-drive effect existed in these sands, it should have shown up in the edge wells. Moreover, a material balance calculation at that time indicated that practically no water had entered the oil reservoir.

In addition to a material balance calculation, an analysis was made of the possible effect of changed rates upon the apparent productive character of the reservoir.

It is a well known fact that the production characteristics of an oil reservoir often can be modified by changing the rate of withdrawal from the reservoir. Since (as a rule) recoveries obtained under water-drive conditions usually are higher than those under depletion conditions, an analysis was made for the Ten Section field.

In exceptional cases, the waterbearing portion of a reservoir may have an outside source of water supply, for instance, an outcrop. If no faults or other obstructions are present between this outcrop and the oil reservoir and if there is an ample supply of water, conditions are favorable for water-drive production. In other cases, the water supply will be a function

TEN SECTION FIELD

SCALE 1" = 200'

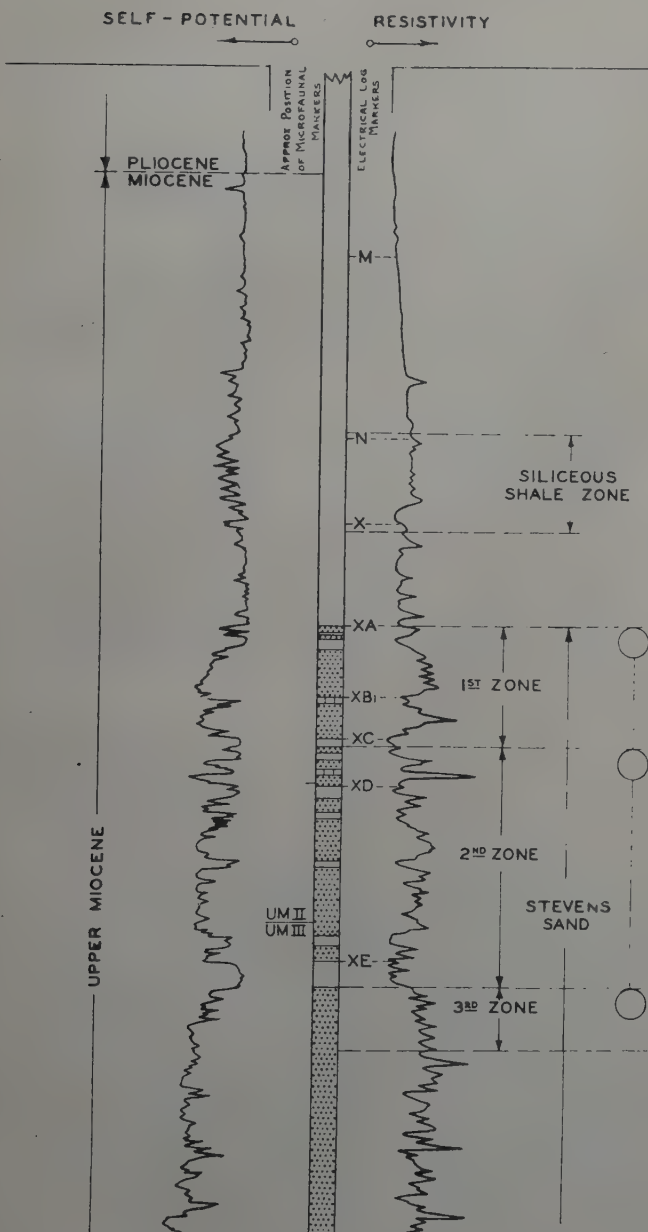


FIG. 2 — COMPOSITE LOG OF TEN SECTION FIELD.

of the extent of the water reservoir and water inflow into the oil reservoir will be a result of liquid expansion caused by the drop in pressure in the waterbearing portion of the reservoir. As a result thereof, the weight of the overburden will cause additional compression of the reservoir rock. This additional compression will reduce the pore volume of the water bearing part of the reservoir and cause water to move from there into the oil bearing portion of the reservoir. Although this compression may be relatively small, the large volume of the water bearing portion of the reservoir may cause an appreciable additional inflow of water into the oil reservoir.

If the rate of withdrawal from the oil wells is high, the pressure in the oil reservoir will be low and it will take time for this pressure drop to affect fully the waterbearing portion of the reservoir. Continued high rates of withdrawal will finally develop into the release of dissolved gas and further delay in the pressure adjustment. By adjusting the rate of oil withdrawal, this delay will be kept within a reasonable time and should result in improved recoveries.

The effect of reduced rates can be calculated if the following factors are known: the sizes of the water and oil-bearing portions of the reservoir, the permeabilities to oil and water, the viscosities of the two liquids, and the original and present pressures in the oil reservoir.

Although the size of the waterbearing reservoir can sometimes be estimated from the regional subsurface maps of the area, there is still no assurance that there are no barriers. The size of the water reservoir contiguous with the oil reservoir can be found from material balance calculations and compressible flow equations.

Such calculations, as indicated above, were carried out for the Ten Section reservoir, and it was found that the contiguous water reservoir is of about the same size as the oil reservoir. It is self-evident that the expansion of the water in such a small reservoir is not sufficient to replace the producible oil. It can therefore be concluded that it is impossible to produce the Ten Section field under water-drive conditions by changing the rate of production.

The major driving force in this reservoir, therefore, was gas, partly in solution and partly present as free gas in the gas cap in the first zone. In the first horizon there were three possible ways of producing:

- (a) Produce the wells under expansion of the gas cap, using the energy of the high pressure free gas as the main driving agent to move oil towards the wells.
- (b) Follow the procedure under (a) but keep the pressure of the gas cap constant by injection of gas.
- (c) Produce each well as an individual unit, draining its allocated area under depletion conditions. When adopting this system, production rates of individual wells have to be adjusted at intervals to ensure equal pressure declines in the individual drainage areas, thereby preventing movement of fluid between drainage areas.

Early in 1941, gas-oil ratios in several wells open in the first zone had increased considerably, while only a portion of the expected ultimate recoveries from those wells had been produced, as shown in the following table:

Well	Gas-Oil Ratio		Cumulative Oil
	Cu Ft/Bbl		
	Original	3-1-41	3-1-41
32-29	700	1000	218,000
52-29	800	1100	32,500
72-29	700	2300	234,500
23-28	800	2400	121,000
58-29	800	2500	205,500
8-29	800	3200	135,500

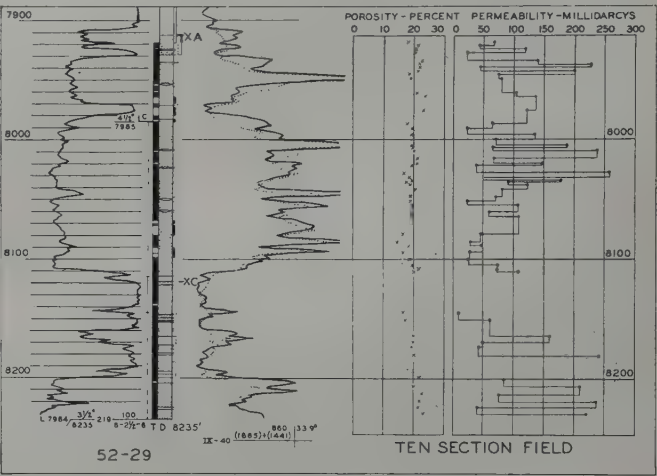


FIG. 3 — CORE DATA AND ELECTRIC LOG ON WELL 52-29

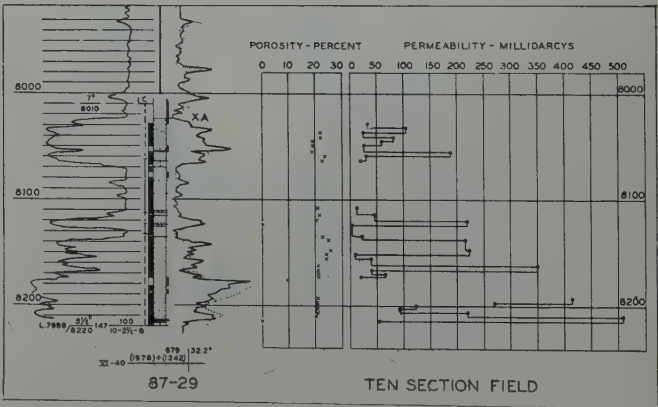


FIG. 4 — CORE DATA AND ELECTRIC LOG ON WELL 87-29

At this time the pressure in the reservoir had declined to 3,080 psig, which was about 175 psi above the bubble point pressure, indicating that the high gas-oil ratios were caused by blowthrough from the gas cap, probably in streaks of high permeability. Subsequent temperature surveys strongly indicated this interpretation to be correct.

Under production by gas cap expansion (a) or pressure maintenance (b), it would be necessary to close in or repair the wells with excessive gas-oil ratios and produce the oil from the next downstructure line of wells. As a great number of wells were combination first and second-zone wells, each

well shut in would mean the loss of a drainage point in the second zone. Because of the irregular character of the shale bodies, repair would for all practical purposes mean shutting off the entire first zone. Following this procedure consistently would mean that after a short time only the wells completed solely in the first zone would be available to drain that zone. There are only two rows of first-zone wells on the south flank, three rows on the north flank, and a regular 20-acre development in the northwest end of the field. When the gas cap blew through in those single zone wells, repairs would be impossible because:

(1) Temperature runs have shown that gas often enters through more than one interval.

(2) Even in wells in which only one point of entry is observed, the irregularities in the shale bodies will permit vertical migration and a rapid blowthrough in other portions of the sand body. Further repairs are then practically impossible, and it would thereafter be necessary to close in the wells in order to prevent wastage of the gas in the gas cap. In the case of pressure maintenance, an ever-increasing size of the compressor plant would be necessary if the first-zone wells were kept on production.

Summarizing, it appeared that as a result of reservoir characteristics, production by gas drive or pressure maintenance in the first horizon in Ten Section was not feasible; and after due consideration of all the factors involved, it was decided to produce the wells in the first zone under depletion conditions.

In order to reduce the expansion of the size of the gas cap to a minimum, the rates of withdrawal of the blowthrough wells were set for pressure equilibrium throughout the first zone. It was realized that at no time should the pressure in the gas cap be lower than that in the oil belt in order to prevent encroachment of oil into the dry sand with subsequent loss of recovery. The pressure in the gas cap, therefore, was held some 70 psi above the average in the oil belt.

In the second zone, no original gas cap was present, and the production problems in that horizon were different from those in the first zone. Consideration was given to producing this zone by depletion or as a pressure maintenance project by injecting gas into the horizon, attempting to keep the pressure close to the original pressure. Electric logs in the Ten Section wells showed the same irregularities in the second zone as observed in the first zone, and it was feared that blowthrough as observed in the first zone might be repeated if gas was injected.

The third zone has only a limited extent, and production from this sand body is obtained through five wells which are also producing from the second zone.

INTERSPACING

In many cases, it has been observed that in a depletion reservoir, recovery efficiencies can be improved substantially

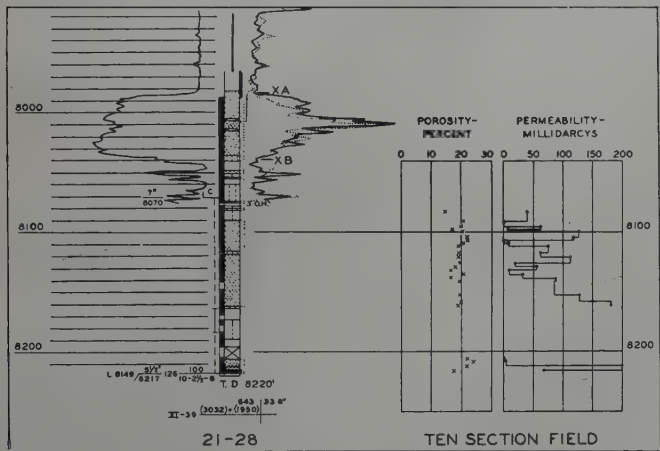


FIG. 5 -- CORE DATA AND ELECTRIC LOG ON WELL 21-28

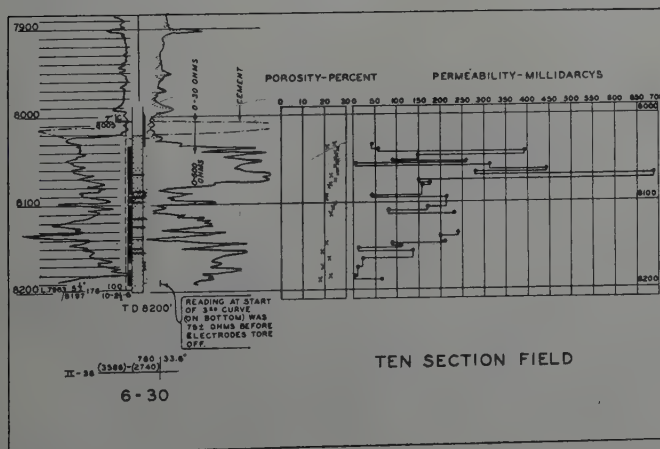


FIG. 6 -- CORE DATA AND ELECTRIC LOG ON WELL 6-30

by reducing the spacing. There are no strict rules by which the extent of these improvements can be predicted; but the many irregularities observed in the Stevens sand made such an interspacing project attractive, and for that reason 10-acre wells were drilled in the central portion of the second horizon as shown in Fig. 1.

In order to obtain full benefit from the closer spacing, rates of withdrawal from the individual wells were balanced to maintain pressure equilibrium throughout the field.

The interspaced development of Ten Section was halted in August, 1942, because of Government regulations and in the next years the field was produced on the basis of the principles laid down above. Fig. 9 is a graphical representation of the reservoir performance. It will be noted that the rate of withdrawal was increased considerably during the period August, 1942, to March, 1943, owing to war requirements. In that period the gas-oil ratio increased from 1,900 to 2,500 for a cumulative production of about 4,000,000 barrels. A continuation of such a high rate might have had a detrimental effect upon the ultimate recovery from the reservoir, and in the next month the rate was reduced to 18,000 bbl/day. In the next two years further reductions brought the rate down to 12,000 bbl/day, but gas-oil ratios kept increasing, although in the period July 1, 1944, to January 1, 1945, it was fairly constant at 4,000 cu ft/bbl. The gas-oil ratio reached a maximum of 4,800 cu ft/bbl in September, 1945. Thereafter, the rate was reduced to 9,000 bbl/day, after which the gas-oil ratio started a downward trend which has continued to the present time. In January, 1949, the oil rate was 6,000 bbl/day with a gas-oil ratio of 3,700 cu ft/bbl.

COMPARISON WITH CANAL FIELD

At the time of the completion of the 20-acre development, a pressure maintenance project had been started in the Canal field, a field situated close to Ten Section and producing from the Stevens sand. In order to obtain a basis for comparison, it was decided to observe the performance of the Canal field under pressure maintenance and produce the second zone in Ten Section as a depletion or internal gas-drive reservoir. If the experience in Canal indicated that pressure maintenance would lead to increased recoveries, gas injection in the second zone could still be applied at an early date.

In the April, 1946, Spring Meeting of the API, Pacific Coast District, R. P. Mangold presented a paper entitled *Canal Field Gas Injection Project*, in which he discussed the performance of that field under pressure maintenance. It was clearly demonstrated that (1) after 2½ years of gas injection in two crestal wells, serious blowthrough occurred in wells within a distance of 2,000 ft and that this blowthrough was concentrated in a small portion of the zone open in the wells; these portions were located at different depths in different wells but mostly at the top of the zone; (2) wells more than 2,000 ft distant from the injection wells experienced very little blowthrough and were pumping at nominal rates; (3) in the wells

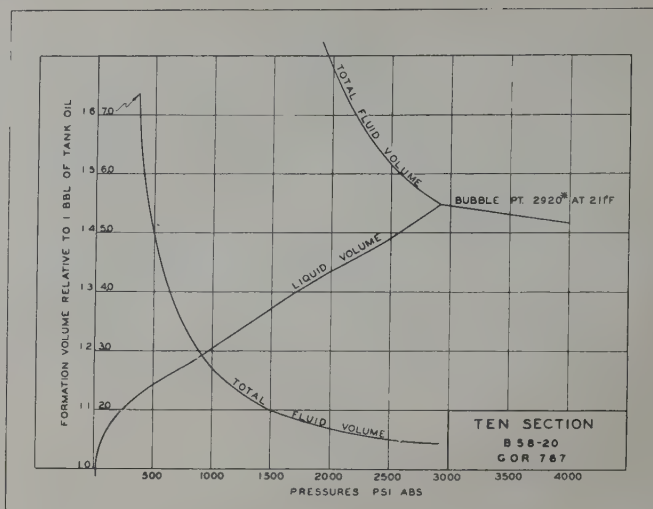


FIG. 7 — PVT ANALYSIS OF REPRESENTATIVE WELL 58-20 SHOWING BUBBLE POINT PRESSURE

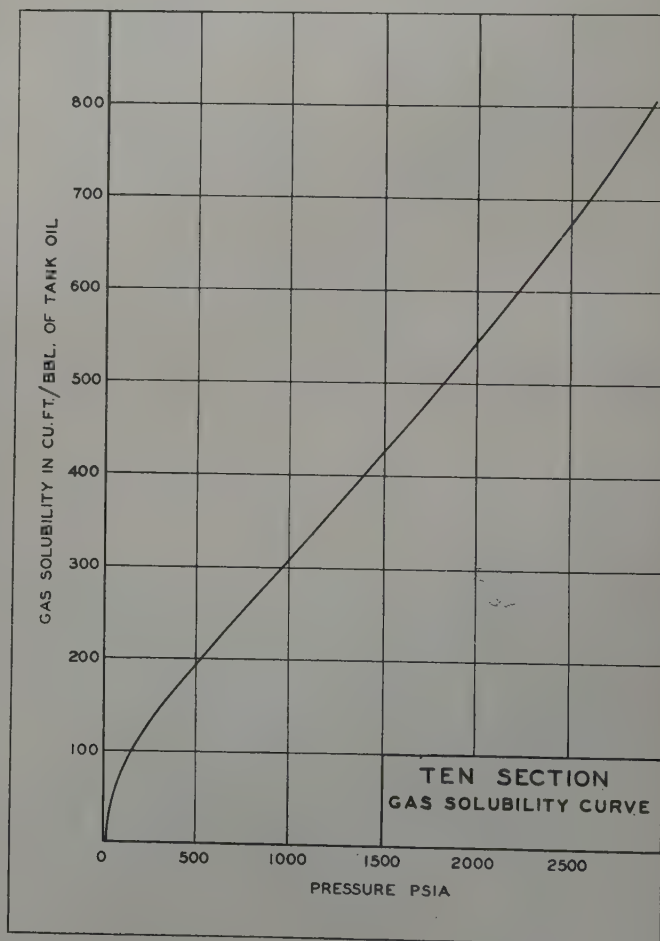


FIG. 8 — PVT ANALYSIS OF REPRESENTATIVE WELL 58-20 SHOWING GAS SOLUBILITY CURVE

in which blowthrough had been observed, pressure readings after 24 hours shut-in built up to about equal values throughout the central area of the field; and (4) after 2½ years of gas injection into two crestal wells, one injection well was closed in and the full quantity was injected in one well, while the other was closed in; the wells surrounding the latter showed a rapid pressure decline of the order of 400 psi in 6 months' time, in which period comparatively little oil was withdrawn from that area. Although it was still too early to draw definite conclusions, Mangold felt that very little, if any movement of oil to downstructure wells could be observed.

Subsequent to Mangold's report, a well was recompleted by pulling the shop-perforated liner and cementing a blank liner in the productive interval. This liner was gun-perforated in four sections and each section was tested separately. These tests showed that gas was entering mainly through the upper 15 ft of the sand which confirmed the results of a temperature survey run before the repair. In the other three sections very

little production was obtained, and there were no signs of any blowthrough. Apparently in the lower three-quarters of the zone there was no direct connection with the injection well, in which for several years the pressure had been maintained at least 500 psi above the operating pressure in the repaired well.

At the present time, pressures in the wells surrounding the closed-in injection well have declined to values which could reasonably have been expected if no pressure maintenance had been applied; and the effect of the gas injection, if any, would seem to be small.

Because of the close similarity of the productive measures in Ten Section and Canal, serious blowthrough probably would have been experienced in Ten Section if the field had been produced under pressure maintenance.

Recent Ten Section material balance calculations for the field and also for individual wells and drainage areas showed the following:

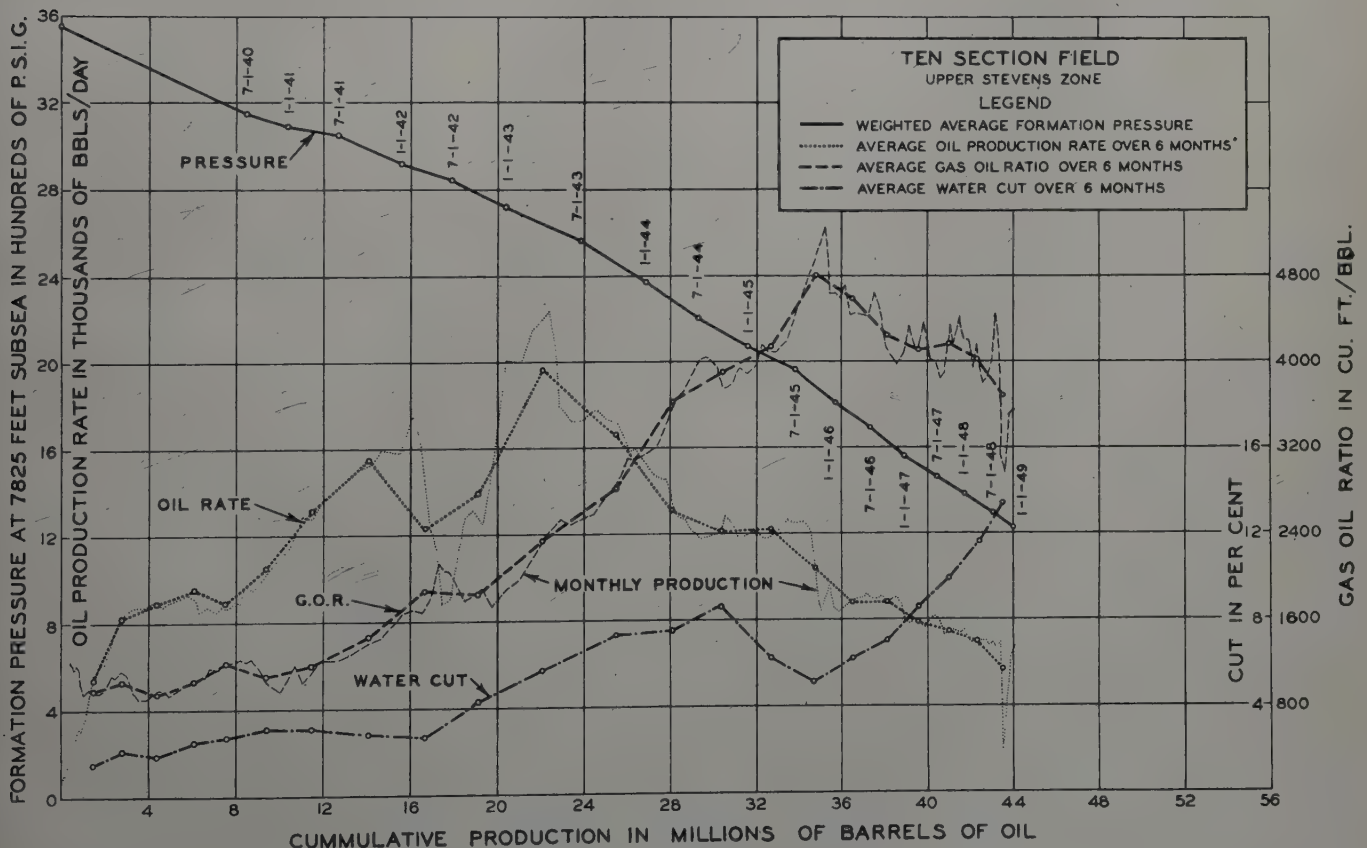


FIG. 9 — RESERVOIR PERFORMANCE FROM JULY, 1940, TO JANUARY, 1949

(a) As of 1-1-48 the net inflow of water into the oil reservoir is zero for all practical purposes.

(b) A considerable migration of gas from the gas cap.

(c) An appreciable inflow of gas into the oil-bearing portion of the first zone and into the second zone.

Gas-oil ratios in several of the second-zone wells have increased appreciably; and the distribution of high and medium gas-oil ratio wells in this zone is not directly related to their structural positions, thereby indicating that gas cap gas is entering into the second zone through discontinuities in the separating shale.

CONCLUSIONS

This study of the Ten Section field has lead to the following conclusions.

(1) The Ten Section field has been produced primarily as a depletion-type reservoir. Calculations have shown that the amount of water available in the contiguous reservoir is too small to permit producing this field as a natural water-drive reservoir.

(2) Consideration has been given repeatedly to pressure maintenance by gas injection. Because of the flat structure and the large variations in permeability, it appears that this would not be feasible. This conclusion is further supported by the performance of the Canal field, in which gas has been injected since 1941.

(3) Production by expansion of the gas cap was also rejected because early blowthrough had been experienced in wells near the gas cap; and if this had been allowed to expand further downstructure, control of the gas cap pressure would have required either repair or shut-in of the combination zone wells.

These conclusions should not be construed to condemn gas injection in Ten Section in the future as a possible means of secondary recovery.

ACKNOWLEDGMENT

The author wishes to thank the management of the Shell Oil Co., Inc. for permission to publish the data used in this paper.

★ ★ ★

THE RELATION BETWEEN ELECTRICAL RESISTIVITY AND BRINE SATURATION IN RESERVOIR ROCKS

HENRY F. DUNLAP, HARRELL L. BILHARTZ, MEMBERS AIME, ELLIS SHULER, AND
C. R. BAILEY, MEMBER AIME, THE ATLANTIC REFINING CO., DALLAS, TEXAS

ABSTRACT

Data are presented which indicate that the saturation exponent, n , in the equation, $R_s = R_{100}S^{-n}$, relating core resistivity, R_s , to the resistivity at 100 per cent saturation, R_{100} , and to the saturation, S , may vary appreciably from the value of two which is usually assumed for this exponent when interpreting well logs. Values ranging from one to two and one-half have been found on core samples investigated to date. Attempts to correlate this saturation exponent with porosity or permeability of the core have not been successful. The saturation exponent is apparently not a function of the interfacial tension between the brine and the displacing fluid. Some evidence is given indicating that the resistance of the core is not a unique function of the saturation but depends upon the manner in which this saturation was achieved. Equipment and technique are discussed for measurement of resistivities in core plugs in which water saturation can be varied.

INTRODUCTION

A number of investigations¹⁻⁴ of the resistivity-saturation relationship for unconsolidated sands and consolidated core samples have been reported in the literature. According to most of these, $R_s = R_{100}S^{-2}$, where R_s = the resistivity of a formation at saturation S , and R_{100} = the resistivity of the formation at 100 per cent water saturation. Much of this work was done on unconsolidated sands desaturated by gas or oil. Henderson and Yuster⁵ worked exclusively

with dynamic systems, flowing oil or gas through consolidated cores. There is some doubt as to how well this reproduces static reservoir conditions. Jakosky and Hopper³ considered also the case of consolidated core plugs, but the oil-water distribution in the emulsions which they used to saturate their cores is almost certainly different from that occurring in reservoirs. Recently Guyod⁷ quotes the results of some Russian work which indicates that n may vary from 1.7 to 4.3. No experimental details of this work are available.

In connection with electric log interpretation it is important to know the value of the saturation exponent. For example, if in a given reservoir it is found that the resistivity is three times the resistivity observed when the reservoir is 100 per cent saturated with water, this fact would be interpreted as indicating a water saturation of 33 per cent if the saturation exponent were 1 and a water saturation of 64 per cent if the saturation exponent were 2.5.

EXPERIMENTAL METHOD

In the work to be described it was assumed that reservoir conditions are most nearly obtained when core plugs are desaturated by the capillary pressure technique referred to in numerous places in the literature, as for example, in Bruce and Welge's paper.⁸ In this technique the core, saturated 100 per cent with brine, is placed in contact with a ceramic disc permeable to brine but not to the displacing medium for the displacement pressures used. Pressure is then applied to the displacing medium and brine forced out of the core through the ceramic disc. Fig. 1 shows the core plug in place in the cell

in which resistivity and saturation measurements are made. Fig. 2 shows the schematic electrical diagram used to make resistivity measurements on the core plug. A four-electrode type circuit is used, employing a Hewlett-Packard model 400A, AC vacuum tube voltmeter. The 60-cycle AC current through the core is adjusted to 1 milliamperere and measured by noting the voltage drop across the calibrated 100-ohm resistor. The voltages appearing at probes 1, 2, 3, and 4 are then successively measured. Voltage drops across the top, center, and bottom portions of the core are obtained by subtracting the voltages appearing at successive probes. This technique avoids any polarization or other high contact resistance phenomena which may develop at the current input electrodes. Resistances which may develop between the core and the probes, and which are small compared to the 1-megohm input impedance of the vacuum tube voltmeter will obviously not affect the measurements appreciably. Any very appreciable resistances which may develop at any of the probe wires are detected and allowed for by inserting a 1-megohm resistor in series with the voltage measuring probe. If the probe resistance is actually zero, the new voltage measured after insertion of the 1-megohm resistor will be approximately one-half of that previously measured, since the input impedance of the vacuum tube voltmeter is itself 1 megohm. If any appreciable probe resistance has developed, the new voltage is found to be appreciably greater than one-half of the previously measured voltage. Such probe resistances have been found to develop only occasionally and usually can be traced to poor connections between the core

¹ References given at end of paper.

Manuscript at office of Petroleum Branch, August 3, 1949. Paper presented at Branch Fall Meeting in San Antonio October 5-7, 1949.

and the probe, or to conditions prevailing at low core saturations where poor contact is established between the probe and the capillary water remaining in the core. These resistances develop often enough, however, to make the taking of this precaution very desirable.

Some additional specific precautions which should be observed in making measurements of this type are discussed below. In most of the work reported here nitrogen was used as a displacing medium, although a few runs were made using naphtha, kerosene, or crude oil samples. When gas is the displacing medium, it is extremely important to reduce to a minimum any fluctuations in temperature in the neighborhood of the displacement cell, since any appreciable temperature cycle will cause water to evaporate from the core and condense, usually upon the sides of the cell. Such evaporation and condensation phenomena lead to loss of water from the core due to means other than capillary displacement and hence to erroneous results. In the equipment used these temperature cycles were held to plus or minus 1°F.

It is also important to allow enough time to elapse after pressure is applied on the core to permit equilibrium conditions to be achieved. Some cores studied have not reached resistance equilibrium after periods as long as one month. Usually intervals of one or two weeks are required to reach equilibrium, even for cores of high perme-

ability. The time required for equilibrium to be reached after the core is saturated and placed on the ceramic disc, but before pressure is applied, has also been found to be very long, often running from one to two days. Fig. 3 shows the way in which resistance varied as a function of time when desaturating pressure was applied to a typical core.

The question of a suitable contact material between the core and the ceramic disc and between the core and the top current electrode has not been solved to our complete satisfaction. The most suitable material tried to date has been moistened diatomaceous earth, which has performed considerably better from an electrical standpoint than has Kleenex, which has a tendency to dry out and pull away from the upper current contact. Diatomaceous earth, however, has disadvantages such as a tendency to clog the core and to reduce the accuracy of weight measurements.

Experience has taught that volumetric measurements, especially those obtained when gas is used as the displacing medium, are not so reliable as gravimetric or distillation estimates of core saturation. When a liquid rather than a gas is used as the desaturating fluid, volumetric measurements are considerably more reliable. It is felt that the most accurate technique, however, is to distill the desaturated core to obtain final saturation values, since the densities of the desaturating liquid and the water are usually so nearly the same that gravimetric methods fail if high precision is desired.

Care should be taken in cleaning the core or formation sample before beginning the saturation and resistivity measurements. The original salt as well as initial hydrocarbons should be removed from the core before it is saturated with brine and placed in the displacement cell.

An example of procedures used for making the measurements on consolidated cores is given below. Core plugs 2.0 cm in diameter by 2.0 cm long are usually used, although longer cores have been run. The core is cleaned by flowing acetone (to dissolve the hydrocarbons) followed by distilled water (to dissolve the salt) through the core for several hours. Fifty to 100 pore volumes of each are used. Four No. 22 B and S gauge wires are then twisted tightly about the core at equal intervals. Platinum, copper, and chromel wires have been used with about equal effectiveness. The core is then dried by baking at 220°F in an evacuated oven overnight, after which it is weighed. The core is saturated by placing in a chamber, which is then evacuated, and allowing de-aerated sodium chloride brine containing 5000 ppm chloride ions (to give a convenient conductivity) to enter slowly from below. (If bentonite is present or suspected in the core, it would be desirable to saturate with formation water.) When the core is covered by the brine, atmospheric pressure is admitted and the system allowed to stand for several hours. Tests made upon cores saturated in this manner using a Boyle's law type saturation

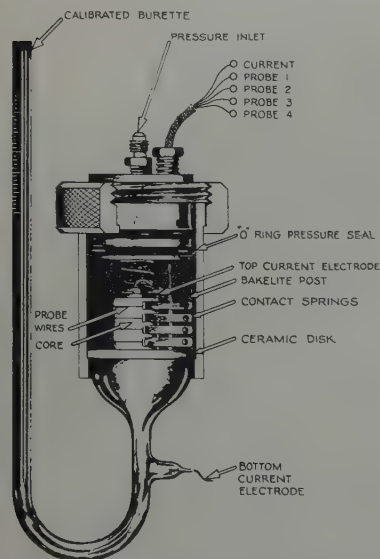


FIG. 1 — EXPERIMENTAL SET-UP SHOWING CORE IN PLACE IN CELL.

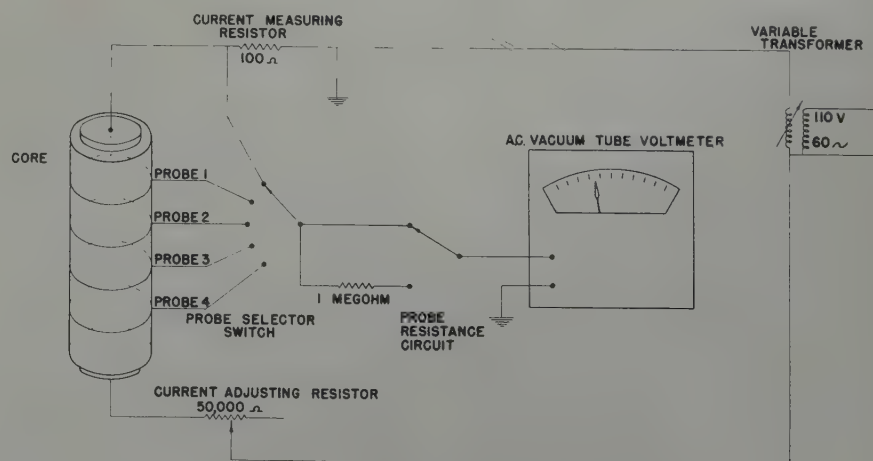


FIG. 2 — CIRCUIT DIAGRAM FOR RESISTIVITY MEASUREMENTS (THE PROBE RESISTANCE SWITCH IS NORMALLY IN THE POSITION SHOWN, THE ONE MEGOHM RESISTOR BEING INCLUDED ONLY WHEN CHECKING FOR PROBE RESISTANCE).

tester have indicated that this technique yields saturations ranging from 98 to 100 per cent. The saturated core is then weighed, placed on a porous disc saturated with the same brine and any excess water allowed to drain for about 24 hours. A negative or desaturating head of one-half inch of water (referred to the base of the core) is usually used. It is necessary to use this small negative head in order to insure that no excess water remains on the ceramic disc or on the sides of the core. The capillaries in most cores are small enough so that no interstitial water is removed by the procedure. A core thus equilibrated is then placed in the cell shown in Fig. 1. The cell is mounted in a constant temperature box maintained at 100°F plus or minus 1°F. Further equilibrium amounting to about 12 hours at the half inch negative head of water is allowed after assembling into the cell, until resistance measurements show no further change with time. Pressure is then applied to the desaturating fluid, usually nitrogen. In some

cases the final desaturating pressure is applied immediately; in others, the pressure is increased stepwise. Resistance changes as a function of time for a given applied pressure are measured, and equilibrium conditions at a given pressure estimated from the constancy of this resistance value over an interval of several days. In many cases practical time limitations prevented equilibrium from being achieved. Simultaneous volumetric measurement of brine displaced is also made in order to estimate roughly the degree of saturation of the core. After resistance equilibrium is reached at the highest pressure used, the core is removed from the cell, and a final accurate saturation value obtained by weighing, distilling, or both. Since available evidence indicates that the saturation exponent, n , does not vary with saturation, determination of resistivity at two saturations determines the exponent.

Techniques for unconsolidated formation samples follow the above procedure as closely as the material permits. Un-

consolidated samples containing bentonite are cleaned by flushing with acetone followed by formation water or a laboratory sample made up to match a formation water analysis. After the effluent water has the same resistivity as the incoming water, the sample saturated with the formation water is poured into the cell in which measurements are to be taken and allowed to equilibrate overnight with zero desaturating pressure (referred to the top of the sample. See Fig. 4). Using this technique there is no visual or other evidence to indicate stratification of the unconsolidated material occurring in the lucite cell. Desaturating pressure is then applied as before, and resistance and volumetric measurements are made. In this case gravimetric or distillation values of final saturation are not so important since considerably larger volumes of both sand sample and brine are involved and small volumetric errors do not affect the results so markedly. In some of the work reported here these final saturation checks were nevertheless made.

RESULTS

In order to obtain the value of the saturation exponent, n , from measured values of the resistance and saturation, the resistance was plotted against the per cent saturation on log-log paper for each section of the core, and the saturation exponent obtained by measuring the slope of this line. Plotted saturation values, of course, represent

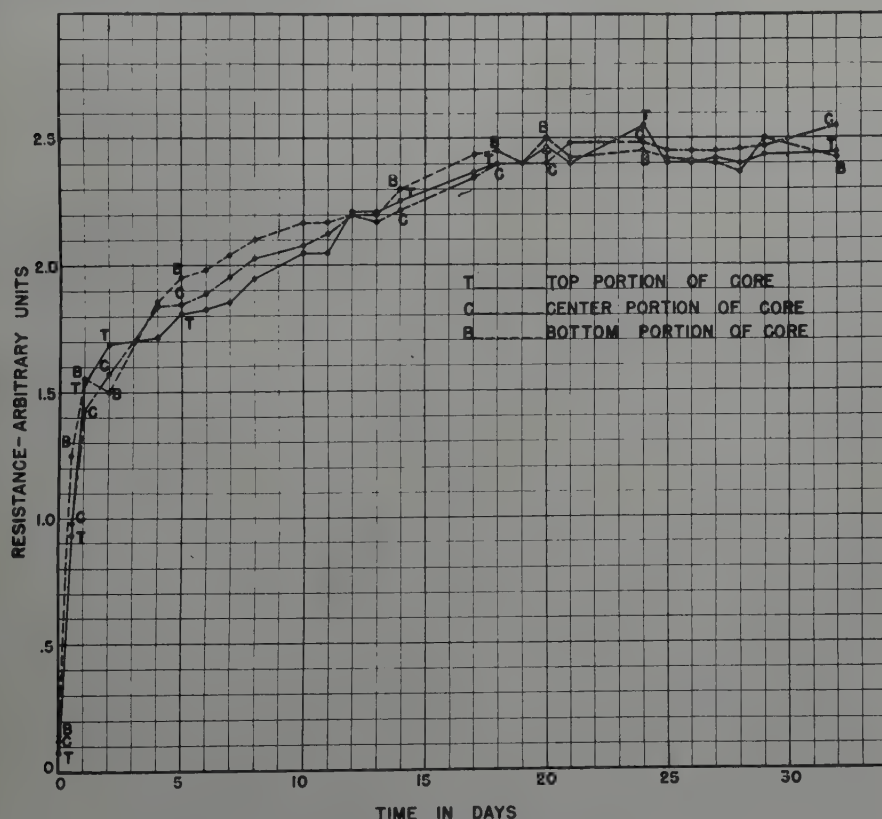


FIG. 3 — RESISTANCE AS A FUNCTION OF TIME FOR A CONSTANT DESATURATING PRESSURE OF 12 PSI.

CORE
POROSITY
AIR PERMEABILITY
DISPLACING MEDIUM

— COTTON VALLEY SANDSTONE
— 18.6%
— 924 MD
— N_2

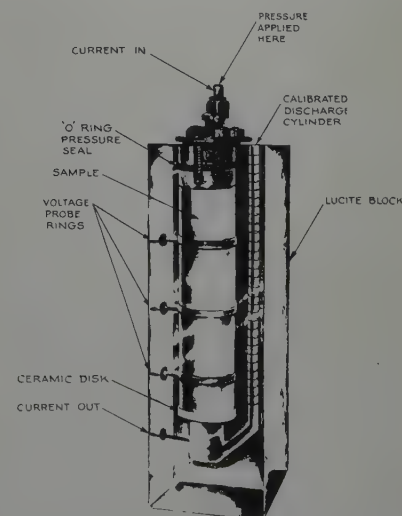


FIG. 4 — CELL FOR MAKING RESISTIVITY VS. SATURATION MEASUREMENTS ON UNCONSOLIDATED SAMPLES.

the average value for the entire core. The technique of measuring the resistance across several sections of the core permits estimates to be made of the degree of saturation at these sections, assuming that the core is homogeneous. Constancy of the saturation exponent for the various sections of the core was interpreted as indicating uniform saturation conditions throughout. It was considered necessary that this condition be fulfilled in order to obtain reliable values for n . In many cases cores which had reached apparent equilibrium at high desaturating pressures exhibited widely varying values for the saturation exponent in different parts of the core. The reason for this behavior is not completely clear, but there is some evidence to indicate that it may be due to (1) variation in properties of the core from point to point, (2) a small saturation gradient which appears to exist in some cases, with the most highly desaturated part of the core appearing closest to the disc. Whatever the cause these data were considered unreliable and have not been included in the results reported here.

Typical plots of resistance versus saturation are shown in Figs. 5, 6, and 7. Constant displacement pressures were applied during these runs and only the final points were brought to resistance equilibrium with time. Other runs on unconsolidated sands and consolidated sandstones indicate that the saturation exponents determined from points equilibrated at different saturations were the same. Hence subsequent exponents were determined using only the initial and final equilibrium points as shown in Fig. 7. Fig. 5 is typical of what we have considered to be reliable data obtained for clean, unconsolidated sands. The initial curvature in the plot of resistance versus saturation is believed to be associated with the rapid flow of brine through the core which occurs at this time. When pressure is applied slowly, these early deviations from linearity are much smaller or absent. Fig. 6 indicates a typical run with a bentonitic, unconsolidated sample. The data shown on this figure are not considered reliable, since the saturation exponent varies markedly and in a systematic manner from one part of the sample to another. The apparent trapping off of water in the upper section of the sample as illustrated in this run has been

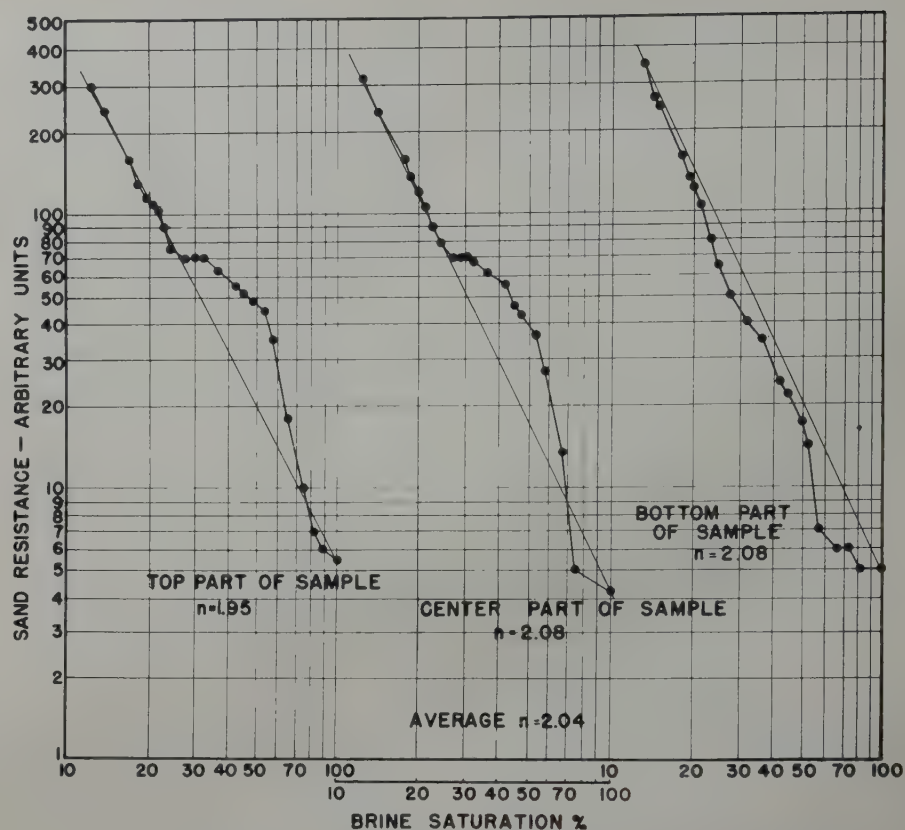


FIG. 5—RESISTANCE AS A FUNCTION OF BRINE SATURATION FOR A CLEAN UNCONSOLIDATED SAND.

POROSITY = 37%
DISPLACING MEDIUM = N_2
CONSTANT DISPLACEMENT PRESSURE = 2 PSI

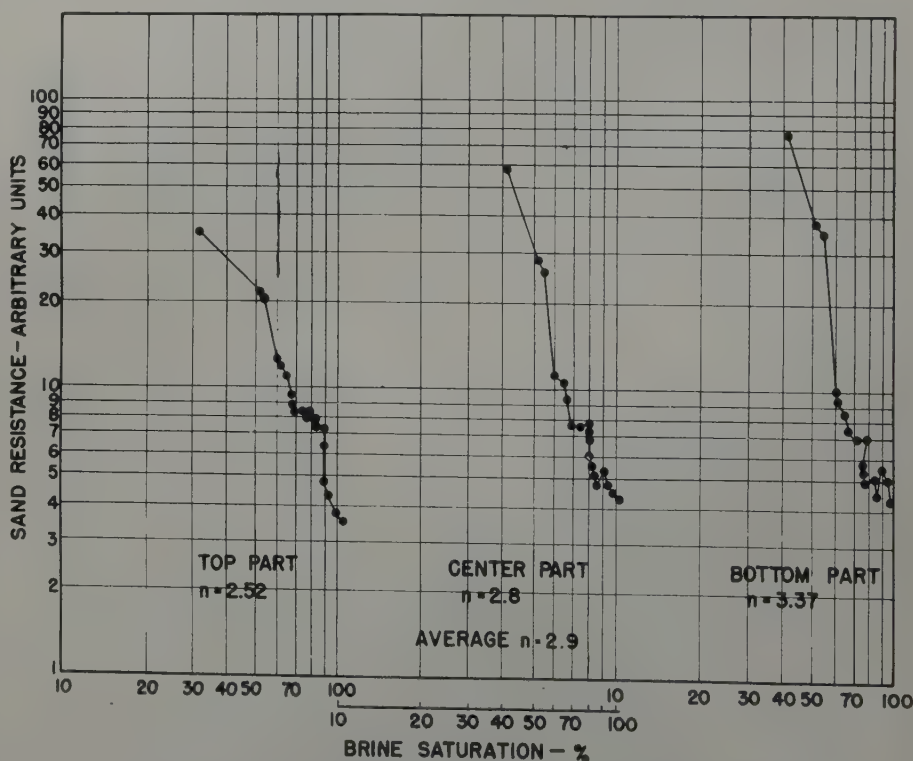


FIG. 6—RESISTANCE AS A FUNCTION OF BRINE SATURATION FOR AN UNCONSOLIDATED SAMPLE CONTAINING 1/2% BENTONITE BY DRY WEIGHT.
DISPLACING MEDIUM = N_2
CONSTANT DISPLACEMENT PRESSURE = 3.6 PSI

TABLE I
Reproducibility of Results Obtained from Consolidated Samples
(Brine Displaced by N₂)

Core No.	Porosity %	Air Permeability (md)	Core Description	Run No.	Saturation Exponent, n.				
					Top Part of Core	Center Part of Core	Bottom Part of Core	Average of Top, Center and Bottom	% Deviation of Average n.
1	18.5	266	Cotton Valley Sandstone	1	1.86	1.75	1.49	1.70	14%
1	18.5	266	Sandstone	2	1.39	1.69	1.70	1.59	
1	18.5	266	Sandstone	3	1.96	1.66	1.88	1.83	
2	19.9	416	Sandstone	1	1.53	1.45	1.43	1.47	
2	19.9	416	Sandstone	2	1.48	1.43	1.43	1.45	1%
3	20.2	736	Sandstone	1	2.24	2.02	1.84	2.03	10%
3	20.2	736	Sandstone	2	1.90	1.90	1.73	1.84	
4	22.5	770	Sandstone	1	1.87	1.67	1.55	1.70	9%
4	22.5	770	Sandstone	2	1.85	1.82	1.57	1.75	
4	22.5	770	Sandstone	3	1.85	1.90	1.82	1.86	
5	23.0	1450	Strawn Sandstone	1	1.15	1.21	1.15	1.17	1%
5	23.0	1450	Sandstone	2	1.11	1.08	1.34	1.18	
6	23.4	2190	Cotton Valley Sandstone	1	1.90	2.01	2.16	2.02	16%
6	23.4	2190	Sandstone	2	1.68	1.68	1.72	1.69	
6	23.4	2190	Sandstone	3	1.98	2.06	1.97	2.00	
6	23.4	2190	Sandstone	4	1.98	1.98	1.97	1.98	
7	18.6	924	Sandstone	1	2.05	1.94	1.82	1.94	12%
7	18.6	924	Sandstone	2	1.88	1.68	1.61	1.72	

observed frequently, particularly when the sample contains bentonite. Fig. 7 shows what is considered to be reliable data on a consolidated core of Cotton Valley sandstone. Resistivity measurements of three portions of the core were repeated on four runs which show good reproducibility.

The reproducibility of what we have considered average reliable data is shown in Table I, which gives the re-

sults of repeat runs on several cores of varying permeability. If the saturation exponents found for the top, center, and bottom sections of each core are averaged for each run, the data indicate differences in the average saturation exponent found on successive runs as great as 16 per cent.

The results obtained for unconsolidated samples, shown in Table II, have not been so consistent, fluctuations in

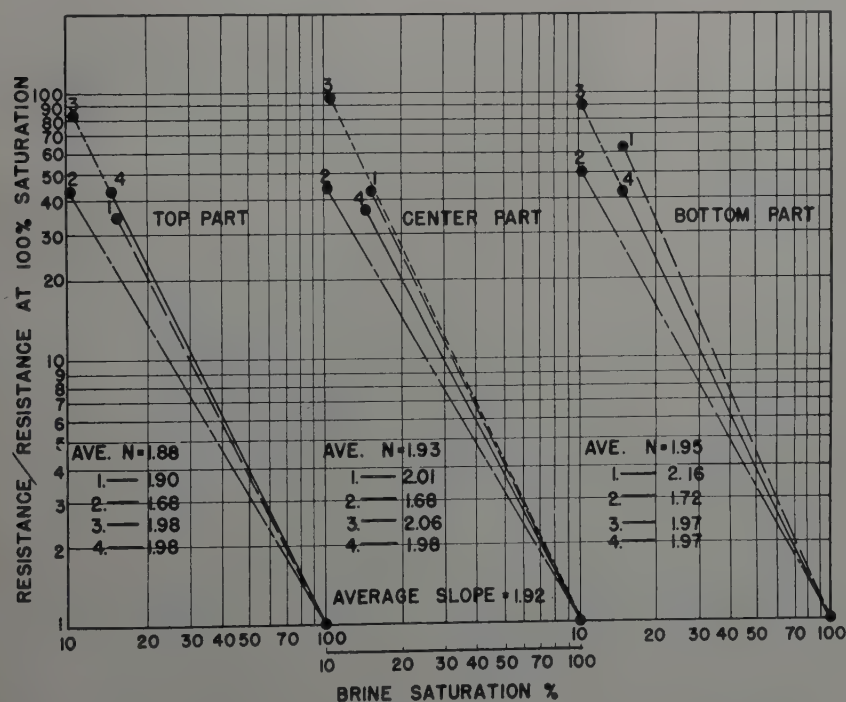


FIG. 7—SEVERAL DETERMINATIONS OF RESISTANCE AS A FUNCTION OF BRINE SATURATION FOR A COTTON VALLEY SANDSTONE.

CONSTANT DISPLACEMENT PRESSURE = 12 PSI
DISPLACING MEDIUM = N₂
POROSITY = 23.4%
AIR PERMEABILITY = 2190 MD

the value of n as determined by repeat runs reaching values as high as 37 per cent. It is believed that this difficulty is at least partly associated with variations in packing the sample for the various runs.

The range of observed values of n for both consolidated and unconsolidated samples has been from about one to two and one-half with some questionable data which indicate that n may take on values as high as three. For consolidated cores, n is usually less than two. To date it has not been possible in general to correlate the saturation exponent with permeability or porosity of the core. Fortunately, the saturation exponent does not appear to change as the interfacial tension between the brine and the desaturating medium varies. This is in agreement with theory, since for a static system variation in interfacial tension would be expected to vary the pressure at which a given saturation is reached, but not the geometrical arrangement of the water at that saturation. Table III gives some data on repeat runs on a core and an unconsolidated sample using nitrogen (interfacial tension 74 dynes/cm) and various liquid desaturants (interfacial tensions 30 to 35 dynes/cm). The variation in the saturation exponent with interfacial tension is not thought to be significant. This is very fortunate as it means that laboratory data obtained using a convenient desaturant, such as nitrogen or naphtha, may be used to represent reservoir conditions as far as interfacial tension is concerned.

The over-all question of how best to reproduce reservoir conditions in the laboratory as far as resistivity-saturation relationships are concerned is an important one, particularly since this work as well as that of other investigators appears to indicate that the resistance-saturation relationship is not a unique one, but that the resistance at a given saturation depends on how that saturation was attained. This appears to be so even after what appear to be equilibrium conditions are reached, and saturation changes appear to have ceased. For example, the saturation exponent obtained from the capillary pressure technique is quite different from that obtained when a given saturation is arrived at as a result of dynamic flood-

ing experiments. Furthermore, the saturation exponents are different depending upon the order in which various materials are flowed through the core. For example, when careful resistivity measurements were made on a long Strawn sandstone outcrop having a porosity of 20 per cent, permeability of about 800 md, and which had been saturated with brine and flooded with naphtha, a saturation exponent of 1.19 was observed. An end point saturation was obtained from a material balance of the fluids flowing into and out of the core. When this core was then flooded with brine, a saturation exponent of 1.68 was observed. In each case an attempt to reach equilibrium was made, although it is not certain that this was achieved. Saturation exponent values observed using the capillary pressure technique when displacing brine are closer to the former than the latter. The difference between the static and dynamic results is probably due to viscous effects entering in the dynamic case.

The question of how to achieve a given saturation in order best to represent reservoir conditions is a very per-

tinent one and one which has not yet been answered. A completely satisfying answer, indeed, probably cannot be arrived at until a satisfactory solution to the problem of the accumulation and migration of hydrocarbons has been achieved. At the present time it appears that the capillary pressure technique offers the best hope of arriving at a fair representation of reservoir conditions, but as stated before, this is by no means certain. At least, the capillary pressure technique simulates reservoir conditions to the extent that it is a static system.

In order best to utilize data of this type in the interpretation of electric well logs it is important that a large statistical accumulation of the saturation exponents be available, measured on many types of formation and in many parts of the country. This is important particularly when attempts are made to interpret the logs of wildcat wells, which frequently are not cored. It was one of the aims of this paper to stimulate interest in the field so that other companies might perhaps undertake similar work, the results of which might be published.

In conclusion, acknowledgment should be made to the late Emil Kaye for early contributions to some of the techniques, to E. R. Brownscombe for many discussions and suggestions, and to John Cave for considerable experimental work in various stages of the investigation.

REFERENCES

1. G. E. Archie: *Trans. AIME*, Vol. 146, pp. 54-62, 1942.
2. G. E. Archie: *Bulletin AAPG*, Vol. 31, No. 2, p. 350, February, 1947.
3. J. J. Jakosky and R. H. Hopper: *Geophysics*, Vol. 2, No. 1, January, 1937.
4. R. D. Wyckoff and H. G. Botset: *Physics*, Vol. 7, No. 9, September, 1936.
5. M. C. Leverett: *Trans. AIME*, Vol. 132, 1939.
6. M. Martin, G. H. Murray, W. J. Gillingham: *Geophysics*, Vol. 3, No. 3, July, 1938.
7. H. Guyod: *World Oil*, August, 1948, p. 120.
8. J. H. Henderson and S. T. Yuster: *Producers Monthly*, Vol. 12, No. 3, January, 1948.
9. W. A. Bruce and H. J. Welge: *Oil and Gas Journal*, July, 1947, p. 223.

TABLE II
Reproducibility of Results Obtained from
Unconsolidated Samples
(Brine Displaced by N₂)

Sample Description	Run No.	Saturation Exponent, n				
		Top Part of Sample	Center Part of Sample	Bottom Part of Sample	Average of Top, Center, Bottom	Maximum % Deviation of Average n.
Graded Ottawa Silica Mortar Testing Sand..	1	1.95	2.08	2.08	2.04	37%
Graded Ottawa Silica Mortar Testing Sand..	2	2.05	*	2.12	2.04	
Graded Ottawa Silica Mortar Testing Sand..	3	2.49	2.59	2.51	2.53	
Graded Ottawa Silica Mortar Testing Sand..	4	1.81	*	1.69	1.75	
Same + 1/2% by dry weight of Aquagel.....	1	1.97	2.5	2.79	2.45	17%
Same + 1/2% by dry weight of Aquagel.....	2	2.52	2.80	3.37	2.90	

*These runs were made in the cell shown in Figure 3. Other runs shown in this table were made in a cell of slightly different design which permitted resistivity measurements to be made on three rather than two intervals in the sample.

TABLE III
Effect of Interfacial Tension on Saturation Exponent

Desaturating Fluid	Interfacial Tension (dynes-cm)	Core Description	n
Naphtha*	35	Smackover Lime 186 md, 12.9% Porosity	1.72
N ₂ *	74	Smackover Lime 186 md, 12.9% Porosity	1.76
Crude Oil	about 30	Unconsolidated Cockfield Sample, 48% Porosity	2.12
N ₂	74	Unconsolidated Cockfield Sample, 48% Porosity	2.30
Naphtha	35	Unconsolidated Sand, 37% Porosity	2.11
N ₂	74	Unconsolidated Sand, 37% Porosity	2.04
N ₂	74	Unconsolidated Sand, 37% Porosity	2.17

*Equilibrated for four hours before pressure was applied. All other runs reported in this work were equilibrated for one to two days before pressure was applied.

MULTIPLE CONDENSED PHASES IN THE METHANE-DECANE-TETRALIN-BITUMEN SYSTEM

J. S. BILLHEIMER, AEROJET ENGINEERING CORP., AZUSA, CALIFORNIA, C. G. YUNDT, 1030
PROSPECT BLVD., PASADENA, CALIFORNIA, B. H. SAGE, Member AIME, and W. N. LACEY,
CALIFORNIA INSTITUTE OF TECHNOLOGY, PASADENA, CALIFORNIA

ABSTRACT

As a part of a general investigation of the separation of bitumen from hydrocarbon mixtures a study was made of a restricted quaternary system composed of methane, decane, tetralin, and bitumen. The work was limited to a pressure of 8000 psi, a temperature of 220°F, and to a fixed relative proportion of decane, tetralin, and bitumen. The measurements permitted the determination of the distribution of these components in each of the fluid phases. It was not possible to distinguish a second liquid phase in the course of these measurements. Gas-liquid equilibrium "constants" of each of the components were found to vary markedly with the composition of the system while temperature and pressure remained fixed.

INTRODUCTION

The separation of bitumen from naturally occurring hydrocarbon mixtures has been of importance for a number of years in the production of petroleum, especially in the California area. The deposition of this material from crude oils was noted in earlier studies^{1,2,3,4} of the solubility of natural gas in crude oil. Studies of the separation of bitumen from crude oils from the Greeley and Santa Fe Springs fields were carried out.^{5,6} The behavior of these systems appeared complex and studies of two restricted ternary systems involving mixtures of n-pentane, tetralin, and bitumen,⁷ and of decane, tetralin, and bitumen,⁸ confirmed this belief. Reviews of the literature pertaining to the separation of bitumen from naturally occurring and refined hydrocarbons are available.^{7,8}

The important effect of methane in the separation of bitu-

men from naturally occurring hydrocarbon mixtures was apparent from the earlier studies^{2,3,4} and for that reason it appeared desirable to investigate a restricted quaternary system involving mixtures of methane, decane, tetralin, and bitumen; data concerning the behavior of mixtures of decane, tetralin, and bitumen having already been obtained.⁸ This study was restricted to a pressure of 8000 psi,^a a temperature of 220°F, and fixed relative proportions of bitumen, decane, and tetralin. This composite constituent, hereinafter designated as the less volatile constituent, was made up of 0.0455 weight fraction bitumen, 0.0909 weight fraction decane, and 0.8636 weight fraction tetralin.

The experimental method involved bringing together mixtures of methane and the less volatile constituent in varying proportions in a constant volume container at the pressure and temperature indicated above. The composition of each of the phases was determined and from this the extent of the separation of bitumen was established.

MATERIALS

The bitumen used in this investigation was obtained from the same stocks employed in earlier studies.^{7,8} The crude material from the North Coles Levee field was stored in the laboratory in a closed drum for a period of five years. Several samples from this stock were subjected to refining operations which were described earlier,⁷ and every effort was made to follow the same procedure in all cases. It was necessary to prepare supplies of bitumen for this investigation at two rather widely different times. These materials have been identified as samples 1 and 2. The composition of the crude bitumen after it was washed with n-pentane at room temperature

¹ References are given at end of paper.
Manuscript received at office of Petroleum Branch August 3, 1949.

^a All pressures cited are absolute.

is recorded in Table 1, together with the ultimate analysis of the two samples of refined bitumen. Some difference exists between the two refined samples of bitumen despite the fact that they were prepared by the same procedures.

The tetralin was obtained from a commercial source and was fractionated in a Hempel column⁹. After purification, the index of refraction was found to be 1.5380 for the D-lines of sodium at a temperature of 78°F. This may be compared with a published value of 1.53919 at 77°F.¹⁰ The specific weight was 59.56 lb. per cu. ft. at 100°F.

The decane was obtained commercially and was purified by fractionation in a glass column with 30 plates at a reflux ratio of approximately 10 to 1. The purified material had an index of refraction of 1.4087 at 81°F as compared to the published value of 1.40986 for n-decane at 77°F.¹¹ Its specific weight was found to be 44.69 lb per cu ft at 100°F and atmospheric pressure.

PROCEDURES

The methods used in carrying out this study have already been described.⁷ In principle, they involve the transfer of known quantities of the less volatile constituent and of methane into a weighing bomb.^{5,11} The quantity of each of the constituents was determined from the corresponding change in weight of the bomb. The pressure was brought to a value of 8000 psi by introducing methane after the weighing bomb containing the less volatile constituent had been brought to a temperature of 220°F. The temperature was controlled by placing the bomb in an agitated air bath, the temperature of which was within 0.2° of 220°F. Equilibrium was obtained by oscillating the weighing bomb for a period of 2 hours. Methane was added as needed to keep the pressure at 8000 psi during the approach to equilibrium. The bomb was then placed in a centrifuge and upon rotation any separated bitumen was deposited as a firm coating on the walls of the container. The phases were then separated by withdrawing fluid from the top of the bomb through a valve while introducing mercury through the lower valve in order to maintain isobaric conditions. The composition of each of the displaced phases was determined by volumetric measurement of the separated methane and from information concerning the specific weight of the methane-free liquid collected and the quantity of bitumen present in this latter material. The quantity of bitumen was determined by pentane precipitation in accordance with procedures described earlier.⁷ No effort was made to determine the quantities of methane, decane, and tetralin actually associated with the solid bitumen phase. However, from qualitative observation it appeared that the amounts of these components in the separated bitumen phase were very small.

EXPERIMENTAL RESULTS

To aid in the determination of the composition of decane-tetralin-bitumen mixtures the specific weights of mixtures of tetralin and decane and of mixtures of tetralin and bitumen were determined. From these measurements values of the partial specific volume of the bitumen in tetralin were established. It was assumed that the partial volume of the bitumen in the decane-tetralin mixtures would be substantially the same as in tetralin since the variation in the partial volume of the bitumen over a relatively wide range of weight fractions of

TABLE 1 — *Composition of Bitumen Samples*

Sample	Carbon	Hydrogen	Nitrogen	Sulfur	Ash	Mercury	Carbon-Hydrogen Ratio
Crude Bitumen, Pentane Washed	0.8625 ^a	0.0842	0.0109	0.0118	0.0133		10.24
Refined Bitumen Sample 1	0.8417	0.0716	0.0080	0.0122	0.0097		11.76
Refined Bitumen Sample 2	0.8494	0.0752	0.0061	0.0227	0.0136	0.0041	11.30

^a—Compositions are expressed as weight fractions.

TABLE 2 — *Specific Weight of Decane-Tetralin Mixtures at 100°F and Atmospheric Pressure*

Weight Fraction Tetralin	Specific Weight Lb./Cu. Ft.
0.0000	44.69
0.2492	47.74
0.4985	51.17
0.7485	55.11
1.0000	59.56

TABLE 3 — *Partial Specific Volume of Bitumen in Mixtures of Bitumen and Tetralin at 77°F. and Atmospheric Pressure*

Weight Fraction Bitumen	Partial Specific Volume Cu. Ft./Lb.
0.0000	0.013664
0.0500	0.013725
0.1000	0.013835
0.1500	0.013946
0.2000	0.014036

TABLE 4—Comparison of Analyses of Decane-Tetralin-Bitumen Mixtures

Method	Decane	Tetralin	Bitumen
Gravimetric Preparation	0.8637 ^a	0.0904	0.0458
Specific Weight Analysis ^b	0.8600	0.094	0.046

^a—Composition expressed as weight fraction.^b—Compositions were determined from specific weight of mixtures.

TABLE 5—Comparison of Gravimetric and Refractive Index Methods of Determining Composition of the Liquid Phase

Component	Analysis	
	Gravimetric	Refractive Index
Methane ^b	0.131 ^a	0.132
Decane	0.067	0.064
Tetralin	0.781	0.785
Bitumen	0.022	0.018
Methane ^c	0.130	0.135
Decane	0.073	0.076
Tetralin	0.784	0.777
Bitumen	0.013	0.013

^a—Composition expressed as weight fraction.^b—Composition of system corresponds to 0.442 weight fraction methane. See Table 6.^c—Composition of system corresponds to 0.283 weight fraction methane. See Table 6.

bitumen was only 2.7 per cent. Table 2 presents the specific weight of mixtures of decane and tetralin of varying composition at 100°F. and atmospheric pressure. The partial specific volume of bitumen used in the estimation of the composition of the methane-free liquids is recorded in Table 3. The weight fraction of bitumen in these methane-free liquids was determined in this case with an uncertainty of approximately 0.5 per cent of the quantity present. The uncertainty in the weight fraction of decane and tetralin was approximately 0.003. Table 4 compares the analysis of a mixture of tetralin, decane, and bitumen as determined from the data submitted in Tables 2 and 3 with values calculated from the gravimetric preparation of the sample. In addition the refractive index of the bitumen-free decane-tetralin mixtures recovered from the gas phase was determined and a satisfactory agreement between the specific weight and refractive index techniques was obtained as is shown in Table 5, which presents results for two different states.

The work reported in this discussion involves eight measurements with bitumen sample 1 and ten measurements with bitumen sample 2, the weight fraction of the bitumen separated being determined for the eighteen cases. The weight fractions of the system represented by the liquid, gas, and solid phases were established at two states for bitumen sample 1 and for the ten states investigated with bitumen sample 2. The compositions of the coexisting phases were determined for only two states in the case of bitumen sample 1 and for the ten states involving sample 2. The latter sample was investigated in much greater detail because of a need for such measurements found during the studies with bitumen sample 1. The less complete data for bitumen sample 1 are included since the results are directly applicable to the over-all study. In a number of instances where direct analyses were not available the composition of the liquid phase was ascertained by difference between the over-all composition of the system and the weight and compositions of the gas and bitumen phases. The fact that under the conditions investigated a second liquid phase was not observed made this possible.

Table 6 presents the detailed results of all of the measurements made. The two parts of the table relate respectively to bitumen samples 1 and 2. Values are given of the weight fraction of the components in each of the phases and in the system as a whole. The weight fraction of the total bitumen which separated out as a solid is presented.

Fig. 1 shows the influence of methane in the liquid phase upon the weight fraction of bitumen sample 2 in the liquid phase of the restricted methane-decane-tetralin-bitumen system at 8000 psi and 220°F. These results indicate a relatively rapid reduction in the weight fraction of dissolved bitumen with an increase in the weight fraction of methane in the liquid phase.

Fig. 2 shows the weight fractions of the system contributed by the gas, liquid, and solid bitumen phases as related to the weight fraction of methane in the system as a whole. The bubble-point and dew-point compositions have been indicated. The dew point in this instance is the state at which the liquid phase disappears on increasing the weight fraction of methane, even though solid phase is present. The weight fraction of the solid bitumen phase is shown on the very much enlarged scale indicated on the right-hand side of the figure. The

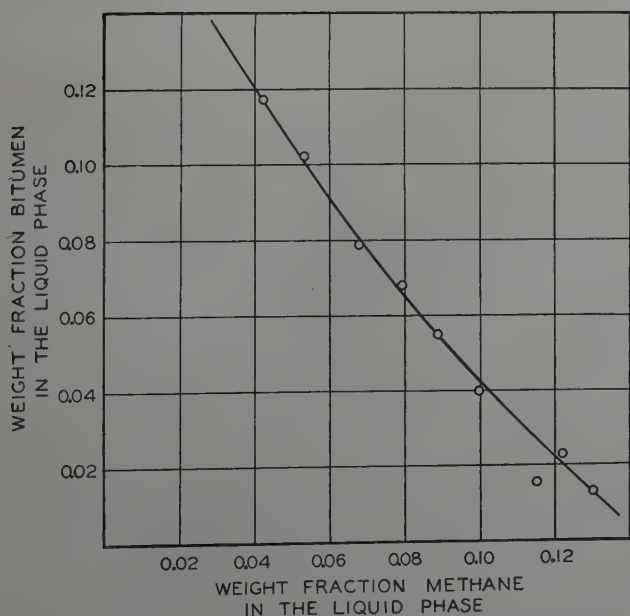


FIG. 1—INFLUENCE OF DISSOLVED METHANE ON THE SOLUBILITY OF BITUMEN IN THE LIQUID PHASE AT 8000 PSI AND 220°F.

maximum quantity of bitumen separated was less than 0.025 weight fraction of the system. The data for the two bitumen samples agree well in regard to the weight fraction of liquid and gas phases. The experimental points indicated in Fig. 2 include all the data that were available. The complex behavior of the solid phase was shown by both bitumen samples. However, a marked difference in this behavior was found at weight fractions of methane below 0.45. The weight fraction methane in the system as a whole has been used as the independent variable in this and subsequent figures because the investigation was limited to constant temperature and pressure and to a restricted system involving fixed relative proportions of decane, tetralin and bitumen, the only variation being in the weight fraction of methane. The weight fraction of the total bitumen present which separated as a solid phase is shown in Fig. 3 as a function of the weight fraction of methane in the system as a whole. Again the marked difference in behavior at low weight fractions of methane is indicated for the two samples of bitumen. At present, the cause for this difference can be ascribed only to the difference in the composition of the bitumen as indicated in Table 1.

Throughout this work it was assumed that a negligible quantity of bitumen was present in the gas phase. This was substantiated by the relatively light color of the tetralin and decane obtained from the gas phase upon its withdrawal from the weighing bomb. In accordance with this assumption the

weight fraction of the bitumen separated is indicated in Fig. 3 as unity at the dew point.

The composition of the liquid phase is shown in Fig. 4. The weight fraction of methane in the liquid phase increased rapidly to bubble point which was at approximately 0.1 weight fraction methane in the system and continued to increase gradually until there was approximately 0.3 weight fraction methane in the system as a whole. At higher weight fractions of methane in the system its weight fraction in the liquid phase gradually decreased until at dew point the small amount of liquid remaining contained little more than 0.04 weight fraction methane.

The weight fraction of decane in the liquid phase decreased gradually and that of tetralin remained substantially constant as the weight fraction of methane in the system increased. The decreasing solubility of methane in the liquid phase might be expected from the decreasing ratio of decane to tetralin in the phase. The minimum in the weight fraction of bitumen occurring at a weight fraction methane in the system as a whole of approximately 0.3 corresponds to the maximum values of bitumen separated as indicated in Fig. 2 and 3. The logarithmic ordinate scales used in both Fig. 2 and 4 serve to magnify the changes relating to bitumen as compared to those for the other components. Because methane in the liquid phase is effective as a precipitant for bitumen, the maxi-

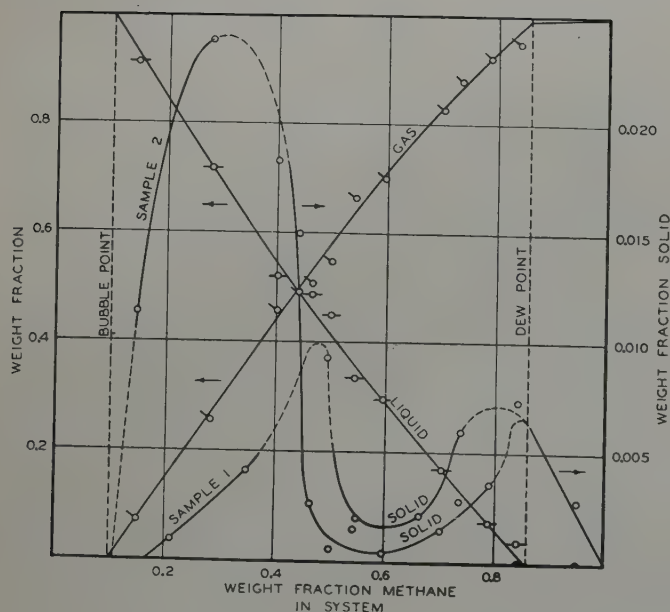


FIG. 2 — DISTRIBUTION OF THE PHASES AT 8000 PSI AND 220°F.

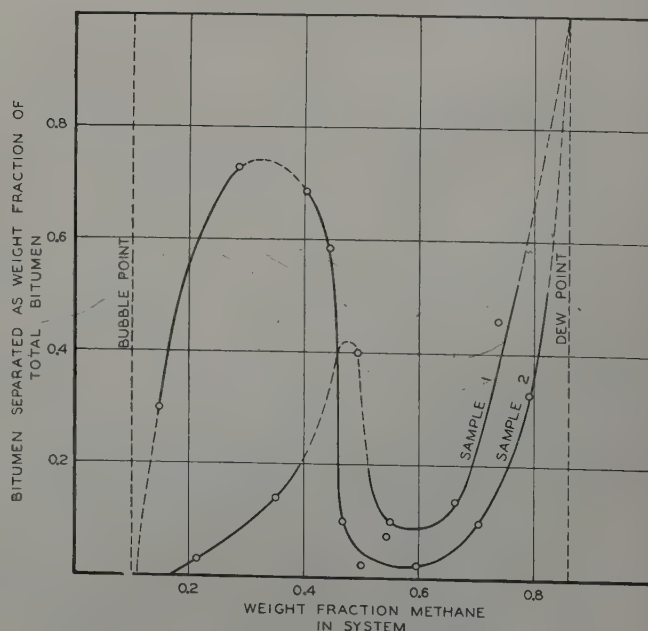


FIG. 3 — BITUMEN SEPARATED AS A SOLID PHASE AT 8000 PSI AND 220°F EXPRESSED AS WEIGHT FRACTION OF TOTAL BITUMEN.

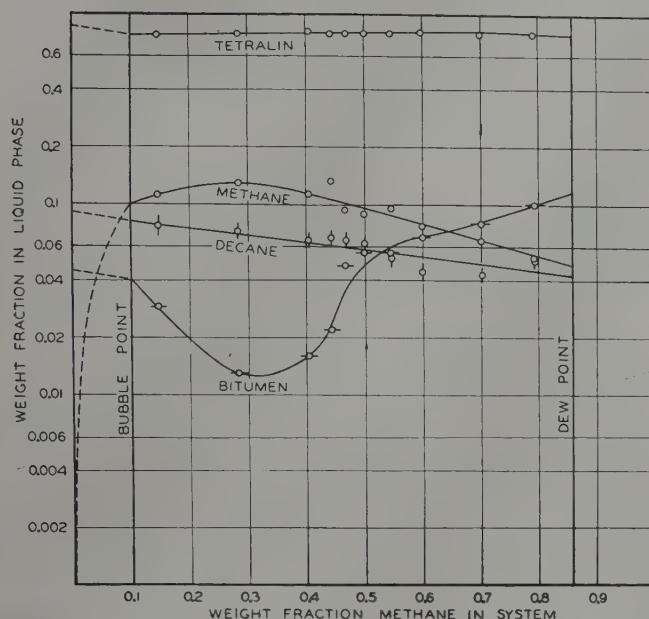


FIG. 4—COMPOSITION OF THE LIQUID PHASE AT 8000 PSI AND 220°F.

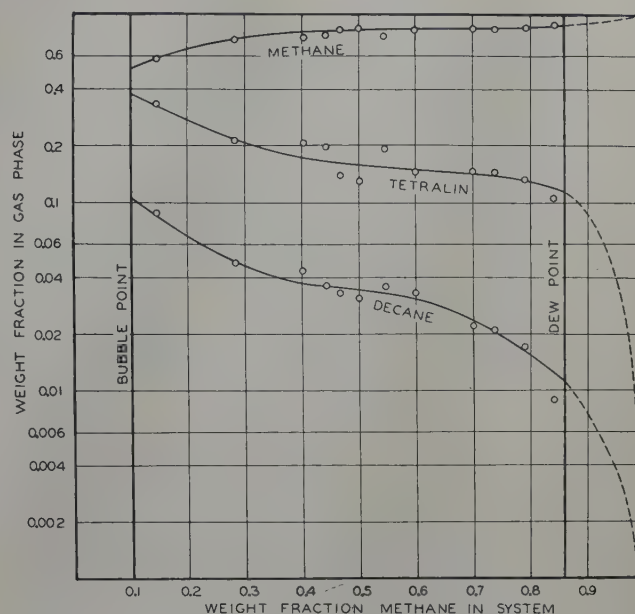


FIG. 5 — COMPOSITION OF THE GAS PHASE AT 8000 PSI AND 220°F.

mum in its weight fraction could well account for the minimum in the bitumen weight fraction.

The weight fraction of methane in the gas phase, as shown in Fig. 5, increased gradually with the weight fraction of methane in the system as a whole, the change being more rapid at the lower weight fractions of methane. Conversely the weight fractions of tetralin and decane both decreased. Data for both bitumen samples were included in Fig. 4 and 5 and no marked divergence appeared. At states richer in methane than dew point, the weight fractions in the gas phase

have been indicated as linear functions of the increasing weight fraction of methane in the system.

Table 7 presents values of the gas-liquid equilibrium constants for methane, decane, and tetralin as calculated from the phase compositions corresponding to the curves of Fig. 4 and 5. For this purpose a value of 1500 was taken as the molecular weight of the bitumen. This was an average of values obtained from the freezing point lowerings of benzene, carbon tetrachloride, and tetralin as solvents for the bitumen. Relatively large uncertainties were encountered in these measurements.

TABLE 6 — Characteristics of the Restricted Methane-Decane-Tetralin-Bitumen System at 8000 PSI and 220°F

Weight Fraction Methane in System	Weight Fraction Bitumen Separated	Weight Fraction of Phase in System			Compositions of Phases ^a						
		Solid	Liquid	Gas	Gas Phase			Liquid Phase			
					Methane	Decane	Tetralin	Methane	Decane	Tetralin	Bitumen
0.211 ^a	0.027	0.0010									
0.350	0.140	0.0042									
0.493	0.399	0.0093									
0.550	0.099	0.0020									
0.663	0.137	0.0021									
0.737	0.459	0.0060	0.113	0.881	0.835	0.021	0.144	0.013	0.049	0.876	0.062
0.842	1.000	0.0078	0.041	0.951	0.885	0.009	0.106				
0.949	1.000	0.0028									
0.147 ^b	0.209	0.0114	0.914	0.074	0.581	0.088	0.331	0.113	0.077	0.780	0.029
0.283	0.727	0.0239	0.720	0.256	0.737	0.048	0.215	0.130	0.073	0.784	0.013
0.403	0.685	0.0183	0.522	0.459	0.750	0.043	0.207	0.113	0.065	0.806	0.016
0.442	0.585	0.0150	0.493	0.492	0.766	0.036	0.198	0.131	0.067	0.781	0.022
0.466	0.101	0.0026	0.489	0.508	0.827	0.033	0.140	0.094	0.065	0.794	0.048
0.500	0.021	0.0005	0.451	0.549	0.839	0.031	0.130	0.088	0.063	0.793	0.056
0.544	0.073	0.0015	0.336	0.663	0.771	0.036	0.193	0.096	0.052	0.796	0.056
0.598	0.022	0.0005	0.299	0.700	0.821	0.033	0.145	0.078	0.044	0.811	0.068
0.703	0.097	0.0014	0.171	0.828	0.835	0.024	0.141	0.068	0.043	0.809	0.082
0.791	0.329	0.0036	0.073	0.924	0.852	0.017	0.132	0.053	0.051	0.796	1.000

^a—Prepared from Bitumen Sample 1.

^b—Prepared from Bitumen Sample 2.

^c—All phase compositions are expressed as weight fractions.

TABLE 7—*Equilibrium Constants for Methane, Decane, and Tetralin in Restricted Quaternary System at 8000 PSI and 220°F.*

Weight Fraction Methane in System	Methane	Decane	Tetralin
0.10	1.83	0.452	0.175
0.20	1.74	0.294	0.114
0.30	1.73	0.204	0.0798
0.40	1.84	0.158	0.0590
0.50	2.03	0.142	0.0480
0.60	2.29	0.130	0.0399
0.70	2.55	0.0963	0.0349
0.80	2.88	0.0617	0.0290
0.85	2.98	0.0484	0.0256

Values varying between 1100 and 1800 were found with different samples of the bitumen and different solvents. In each case the measurements were carried out at several weight fractions of bitumen and the results were extrapolated to infinite dilution. Fortunately, variations in the molecular weight of the bitumen do not markedly influence the values of the equilibrium constants reported in Table 7. Fig. 6 shows the value of the equilibrium constants for methane, decane, and tetralin in relation to the weight fraction of methane in the system. The data contained in Fig. 6 and Table 7 afford an indication of the influence of the composition of the system upon equilibrium constants for three of the components at the chosen pressure and temperature. The rather marked decrease in the equilibrium "constants" of decane and tetralin with increase in the weight fraction of methane apparently results from progressively larger deviations from ideal solution behavior in the liquid phase as dew point is approached.

The experimental results presented indicate the complexity of behavior that may be expected in hydrocarbon systems involving components of relatively high molecular weight. However, the limited data obtained leave much to be desired in the way of completeness, relating only to the characteristics of a restricted quaternary system at a single temperature and pressure.

ACKNOWLEDGMENT

This paper is a contribution from American Petroleum Institute Research Project 37 located at the California Institute of Technology. The assistance of N. D. Zimmerman, H. H. Reamer, and J. D. Yanak in connection with the experimental program is acknowledged.

REFERENCES

1. Morris: Amer. Petr. Inst. Drill. and Prod. Prac. (1937) 220.
2. Lacey, Sage and Kircher: *Ind. and Eng. Chem.* (1934) 26, 652.
3. Olds, Sage and Lacey: AIME *Tech. Pub.* 1588 (1943).
4. Olds and Sage: AIME *Tech. Pub.* 2153 (1947) (*Petr. Tech.*, 1947).

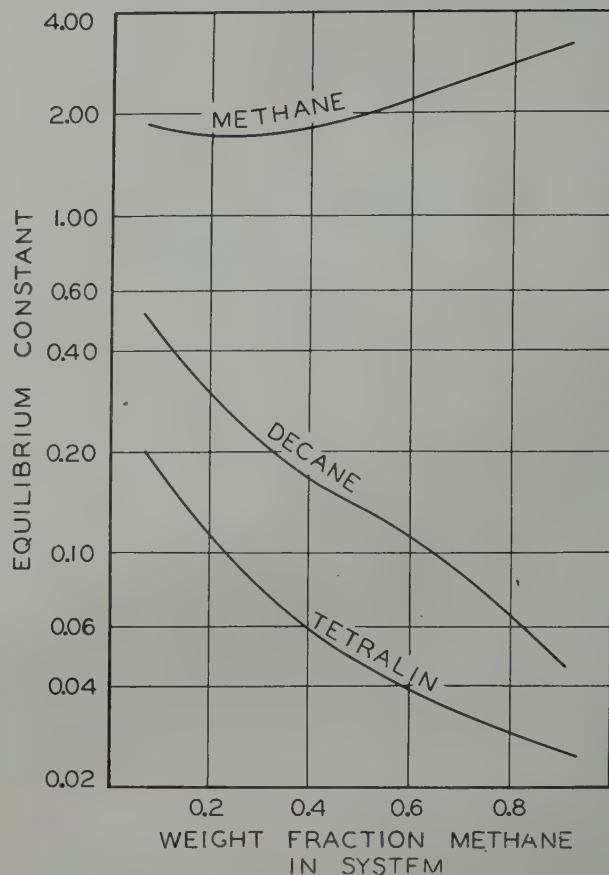


FIG. 6—EQUILIBRIUM CONSTANTS FOR METHANE, DECANE, AND TETRALIN IN THE RESTRICTED QUATERNARY SYSTEM AT 8000 PSI AND 220°F.

5. Botkin, Reamer, Sage and Lacey: *Fundamental Res. on Occurrence and Recovery of Pet.* Amer. Petr. Inst. (1943) 62.
6. Botkin, Reamer, Sage and Lacey: *Fundamental Res. on Occurrence and Recovery of Pet.* Amer. Petr. Inst. (1945) 42.
7. Billheimer, Sage and Lacey: "Multiple Condensed Phases in the n-Pentane-Tetralin-Bitumen System" (1949) (submitted to Amer. Petr. Inst.).
8. Billheimer, Reamer and Sage: "Multiple Condensed Phases in the Decane-Tetralin-Bitumen System" (1949) (submitted to Amer. Petr. Inst.).
9. Hempel: *Zeit. f. Anal. Chem.* (1881) 20, 502.
10. Mair and Streiff: *Bur. Stand. Jnl. Res.* (1941) 27, 343.
11. Shepard, Henne and Midgley: *Jnl. Amer. Chem. Soc.* (1931) 53, 1948.
12. Sage and Lacey: *Trans. AIME* (1940) 136, 136. ★ ★ ★

FUNDAMENTAL FORCES INVOLVED IN THE USE OF OIL WELL PACKERS

Reprinted from JOURNAL of PETROLEUM TECHNOLOGY

JACK C. WEBBER, THE ATLANTIC REFINING CO., DALLAS

INTRODUCTION

The successful use of oil well packers requires, in part, an understanding of the pressures which exist at the packer in various applications and an understanding of the characteristics of the various types of packers. It is with these pressures, the resultant forces, and the characteristics of packers, that this paper is primarily concerned.

An oil well packer may be defined as a mechanical device for blocking the passage of fluids in an annular space. In the more usual case, the annular space is that between the tubing or drill pipe in a well and the casing, and packers which block such an annular space are broadly referred to as casing packers. In the other case, the annular space is that between the tubing or drill pipe and the walls of an open hole, and packers for blocking this space are generally called formation packers. While the hydraulics involved are essentially the same for casing and formation packers, a greater variety of conditions are encountered in the use of casing packers and only casing packers will be discussed.

After a packer has been set and a pressure seal effected between tubing and casing, the packer is comparable to a piston in a cylinder. Pressures acting upon a piston result in forces which will move the piston unless some means is provided to prevent such movement. In the same manner, pressures acting upon a packer will move the packer unless there is present a sufficiently great restraining force.

PACKER CLASSIFICATIONS

Packers may be classified according to the pressure conditions under which they are capable of blocking the annular space between tubing and casing. Fig. 1 shows schematically two types of packers in common use. These packers are capable of blocking the annular space against the passage of fluids under a differential pressure of significant magnitude only when the pressure in the annular space above the packing element is greater than the pressure below. It may be seen that in Fig. 1-a, slips with teeth which bite into the casing and prevent downward movement are provided. In Fig. 1-b, an

anchor prevents downward movement. In each case, there is only the tubing to prevent upward movement when differential pressures act to move the packers upwardly. Packers which hold only a significant differential pressure acting downwardly have been in use since the early days of the oil industry and will hereafter be referred to as conventional type packers.

In many packer applications operating conditions will result in differential pressures across the packer which will at times act to move the packer upwardly, and at other times, act to move the packer downwardly. For these applications, designs are available which will block the annular space and resist movement in either direction. Fig. 2-a shows schematically a packer of this type which is designed to be run into a well and set, and removed when desired by merely pulling the tubing. It will be noted that two sets of slips are provided—one set above the packing element to prevent upward movement, and another set below the packing element to prevent downward movement. This packer is built around a mandrel which is essentially a part of the tubing, and which is free to move longitudinally within certain limits through the set packer. Fig. 2-b shows schematically a permanent type packer which is capable of holding pressures from either direction. Here again, two sets of slips are provided to prevent movement of the packer. This packer is designed to become virtually a part of the casing when set and it is made of drillable material so that it may be drilled out when its removal is desired. The seal nipple shown effects a pressure seal between the tubing and the packer. This seal nipple is a part of the tubing, and the nipple and tubing may be withdrawn from the well without disturbing the packer. It should be noted that these figures are not representative of all available packers which are designed to hold pressures from both above and below. Packers which resist movement in either direction will hereafter be referred to as universal type packers.

There is a third type of packer in general use and this type is designed to block the passage of fluids when the pressure below the packing element is greater than that above. This type is provided with slips which prevent upward movement of the packer and is somewhat similar to a conventional type packer run upside-down. Packers designed to hold pressure only from below are made in a variety of designs and are usually owned and operated by service companies.

Manuscript received at office of Petroleum Branch November 22, 1948. Paper presented at Joint Meeting of the Texas Sections in Austin, Texas, December 16-17, 1948.

There are, then, three types of packers to be considered—conventional packers designed to hold a differential pressure acting downwardly; universal packers designed to hold pressure from above or below; and special packers designed to hold only an upwardly acting differential pressure.

FACTORS AFFECTING PACKERS

Fig. 3 shows schematically the essential elements which must be considered in evaluating the pressures and forces which occur in the use of conventional and universal type packers. In the case of conventional packers, Support 2 should be regarded as fixed against downward movement. In the case of universal packers, Support 1 should be regarded as fixed against upward movement, and Support 2 again regarded as fixed against downward movement. In each case, the mandrel is permitted at least a limited upward movement without disturbing the packer setting.

Factors which must be considered include the tubing load required to compress the packing element, the changes in tubing load as well conditions change, pressures above and below the packer, the unbalanced valve area on packers having circulating valves, and the unbalanced area inside the packing element and outside the tubing on valveless packers.

It is convenient in nearly all cases to evaluate the pressures and forces on the tubing separately from the pressures and forces on the packer, and this will be done in all cases considered in this discussion. With few exceptions, the mandrel which passes through conventional and universal type packers has an inside diameter substantially equal to the inside diameter of the tubing upon which the packer is run, and an outside diameter equal to or greater than that of the tubing. Since any pressure which acts to move the packer upwardly will also act to move the mandrel upwardly, the outside diameter of a full opening mandrel in a conventional packer is not a factor, and it may be considered as having an outside diameter equal to that of the tubing.

Pressure Force on Packer

Pressures from above or below conventional packers may be regarded as acting over an annular area from the outside of the tubing to the inside of the casing tending to move the packer up or down. Annular areas for tubing-casing combinations in common use are tabulated in Table I.

The pressure force on a conventional packer may be expressed as

$$F_p = p(\pi/4) [(casing ID)^2 - (nominal tubing OD)^2] \quad (1)$$

$$= p A_p$$

where

F_p = pressure force on the packer, lbs.

p = pressure acting to move packer, psi.

A_p = annular area—tubing OD to casing ID, sq. in.

Unbalanced Valve Area

Most of the packers in common use have circulating valves which may be opened without disturbing the packer setting. Some of these valves are pressure balanced and some are not. The unbalanced valve area now considered is that area which tends to keep the valve closed under a differential pressure

from above. Referring to Fig. 3, it will be seen that a differential pressure acting downwardly acts over an annular area from the outside diameter of the valve to the outside diameter of the tubing tending to keep the valve closed. Some packers in common use have sufficiently great valve areas to prevent opening of the valve and pulling of the packer under conditions where a high differential pressure acting downwardly exists. Instances have occurred where several hours were spent unsuccessfully in attempting to unseat and pull a packer under these conditions. It is sometimes necessary to at least partially fill the tubing or otherwise reduce the differential pressure across the packer before it can be pulled.

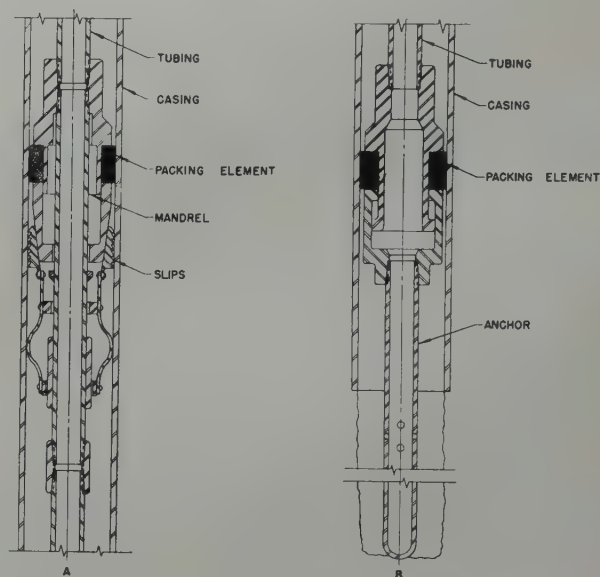


FIG. 1 — CONVENTIONAL TYPE PACKERS

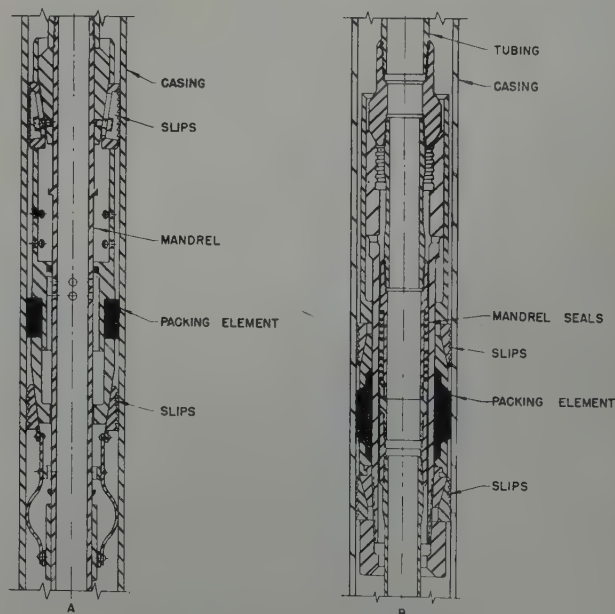


FIG. 2 — UNIVERSAL TYPE PACKERS

Mandrel in Universal Type Packers

The mandrel in universal packers is usually sealed inside the packer and is sometimes larger than the nominal outside diameter of the tubing. Since the tubing is to be considered separately, it is convenient to regard the annular area of the mandrel from the outside diameter of the tubing to the

TABLE I

Annular Area Exclusive of Tubing Over Which Pressure Acts to Move Full Opening Conventional Packers Upwardly or Downwardly

API Casing Size	API Tubing Size	Annular Area - Sq. In.
5½ in. - 15.5 lb	2 in.	16.1
5½ in. - 17 lb	2 in.	15.6
5½ in. - 20 lb	2 in.	14.8
5½ in. - 23 lb	2 in.	14.0
7 in. - 23 lb	2½ in.	25.3
7 in. - 26 lb	2½ in.	24.4
7 in. - 29 lb	2½ in.	23.5
7 in. - 32 lb	2½ in.	22.7

Annular Area = Area of nominal ID of casing - area of OD of tubing

Cross Sectional Area of Tubing Entering into Buoyancy Calculations

2 in. API tubing, 2⅜ in. OD, 1.995 in. ID - 1.31 sq in.

2½ in. API tubing, 2⅞ in. OD, 2.441 in. ID - 1.81 sq in.

maximum diameter of the packer sealed by the mandrel as a separate and distinct area. Pressure acting over this area will act to move the mandrel up or down.

FACTORS AFFECTING TUBING LOAD ON PACKER

Friction of Tubing Against Casing

Tubing in longitudinal compression is supported horizontally by the casing, and when tubing is subjected to excessive compression loading the distortion usually results in "corkscrewed" tubing. This indicates that tubing in compression is probably in a gentle spiral bearing against the casing. Since tubing load must almost always be applied to compress the packing element, a portion of the length of the tubing must be supported horizontally by the casing. This condition results in friction of an indeterminate amount which resists movement of the tubing. The amount of this friction varies with the straightness of the hole and other factors and very little experimental data are available on the subject. In one instance, 16,000 lb. was slacked-off at the surface before shear pins designed to shear at 8,000 lb. were sheared. In this case the packer containing the shear pins was run on 2½ in. upset tubing and set at 10,270 ft in 7-in. OD casing. This is considered unusual, but there is always a definite possibility, because of friction of the tubing against the casing, or the resistance of a tubing coupling to movement past a casing joint, that all the weight slacked off at the surface will not reach the packer.

Buoyancy

When any pipe is lowered into fluid in a well, the fluid exerts a buoyant force which supports a portion of the weight of the pipe. The extent of this buoyant force may be determined with negligible error in the case of tubing by neglecting the couplings and obtaining the product of the pressure within the fluid column at the lower end of the tubing string and the cross sectional area of the walls of the tubing. Unless there is a considerable amount of tubing beneath the packer, buoyancy calculations may be further simplified without significant error by disregarding the tubing beneath the packer and assuming that the tubing only extends to setting depth. Thus, the pressure value to use in determining the effect of buoyancy may usually be taken as the fluid pressure existing in the annular space below the packer. The buoyant force tending to raise the tubing may be expressed as

$$F_b = p(\pi/4) [(\text{nominal tubing OD})^2 - (\text{nominal tubing ID})^2] \\ = p A_t \quad (2)$$

where

p = pressure below packer, psi.

F_b = buoyant force on tubing, lbs.

A_t = annular area—tubing ID to tubing OD, sq. in.

It must be clearly understood, however, that no buoyant force can be exerted on the pipe unless the fluid has an opportunity to act over the annular area of the pipe. Fluid about a pipe suspended vertically has no vertical component and can exert no buoyant force. (There is a very small buoyant force on the couplings and upsets but it is strictly negligible.) Reference to Fig. 3 will show that there can be no buoyant force on the tubing with fluid in the annulus above the packer when there is no fluid or pressure within the tubing. There

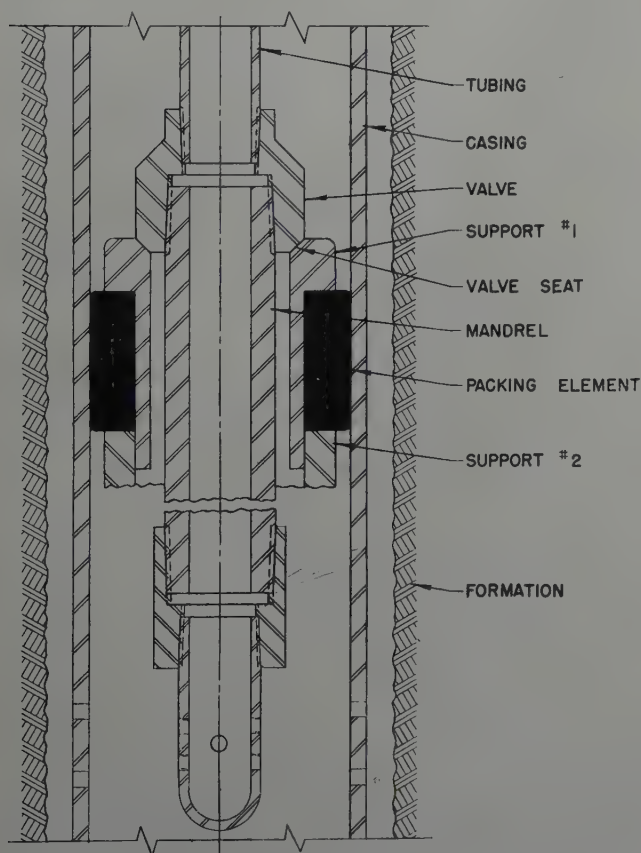


FIG. 3—ELEMENTS TO BE CONSIDERED IN EVALUATING THE PRESSURES AND FORCES WHICH OCCUR IN THE USE OF CONVENTIONAL AND UNIVERSAL TYPE PACKERS

is no opportunity for the fluid to act over the annular area of the tubing.

The effect of buoyancy complicates the determination of forces at a packer. In the case of a string of tubing freely suspended in a hole filled with fluid, where the fluid has access to and fills the interior of the tubing, the lower portion of the tubing is in longitudinal buoyant compression. This results simply from the pressure at the lower end of the tubing acting over the annular area of the tubing to exert an upward (buoyant) force on the tubing at that point. If this buoyant force is reduced or removed, a corresponding tubing force is transferred to and must be supported by the packer. Thus, the force which the tubing exerts on a packer will vary with the pressure below the packer.

The weight of the tubing initially buoyed by fluid may be considered a separate and distinct force. It acts downwardly, and at the time a packer is set it is exactly counteracted by the buoyant force on the tubing.

Pressure Change

John P. DeHetre¹ has developed equations for determining the change in casing load at the well head for changing pressures and temperatures about the casing. These equations are also applicable to the change in tubing load on a packer when pressures and temperatures about the tubing change, provided that the tubing does not move at the surface or at the packer. DeHetre's equation for the effect of pressure change is

$$P = 0.0434W\Delta pD/t \quad (3)$$

where

P = change in load, lbs

W = nominal pipe weight, lb per ft

Δp = average net pressure change on free pipe, psi

D = pipe OD, in.

t = pipe wall thickness, in.

The effect of pressure change about the tubing is frequently significant in the use of packers. It is easily possible to build up sufficient pressure in the tubing when using universal type packers to lift all tubing weight from the packer, and this pressure, which also acts to increase the buoyant force on the tubing, may be great enough to lift the mandrel entirely out of the packer with resultant passage of fluid to the space above the packer. This pressure effect also makes more difficult the holding of a differential pressure below a conventional packer without damaging the tubing when the initial required tubing load is placed on the packer. It results in changing tubing loads on the packer in all cases where the pressures about the tubing are changed from the conditions existing when the packer was set.

Fig. 4 is a graphical solution of Equation (3). Tubing friction, and the effect of spiraling of the tubing inside the casing are neglected. Internal pressure increase results in decreased tubing load on the packer.

Temperature Change

DeHetre's equation for the effect of temperature change is

$$P = 58.2W\Delta T \quad (4)$$

¹ "Casing Landing Practice", by John P. DeHetre, API Drilling and Production Practice, 1946.

where

P = change in load, lb

W = nominal pipe weight, lb per ft

ΔT = average temperature change of free pipe, °F

The effect of temperature change of the tubing is also frequently significant in the use of packers. The difficulty here lies in determining the average temperature changes that may occur. However, the direction of the expected temperature change will usually be known and it will usually be possible to make an estimate of the degree of change. An allowance can then be made in the amount of tubing weight set on the packer to care for the expected temperature change.

Fig. 5 is a graphical solution of Equation (4). Tubing friction, and the effect of spiraling of the tubing inside the casing are neglected. Temperature increase results in increased tubing load on the packer.

DETERMINING NET TUBING LOAD ON PACKER

Analyzing a packer application is simplified by considering the tubing separately. In nearly all cases the mandrel on which a packer is built is simply a continuation of the tubing, and anything larger than the nominal size of the tubing on which the packer is run may be considered a part of the packer.

In practically all conventional and universal packer installations at least some tubing weight on the packer is essential or desired. For this reason it is convenient to regard downward tubing forces, and any change which tends to increase the downward forces, as positive. Negative forces will then include all upward forces, and all changes which act to decrease the tubing load on the packer. These forces and changes of force are then combined to determine the net tubing load on the packer. In the examples given later, the positive and negative tubing forces are tabulated separately for clarity.

NET FORCE ON PACKER

It is characteristic of practically all conventional packers that tubing weight must be applied to expand the packing element into sealing contact with the casing. It is further characteristic of these packers that the packing element strives to return to its unset shape and will do so if sufficient tubing weight is removed. For this reason such packers must always* have sufficient tubing load applied to them if a seal is to be maintained. The amount of tubing load required, or what might be called the minimum setting load, varies with the make and size of packer.

If a conventional packer is to remain in place, the downward forces must at least equal the upward force. If the seal is to be maintained, the downward forces must exceed the upward forces by the minimum setting load, and the downward forces must include a tubing load at least equal to the minimum setting load.

* There is an exception. Where the differential pressure acting downwardly is great, little or no tubing load is necessary to maintain packing element compression. This may be understood by reference to Fig. 3. It will be noted that there is an annular area existing between the inside diameter of the packing element and the outside diameter of the tubing. In most of the available conventional packers, this area is in the neighborhood of one-third of the annular area between the tubing and casing. A differential pressure from above acts over this area to aid in maintaining packing element compression. Also, after varying periods and usage, many packing elements assume a permanent set and exert much less tendency to return to their unset shapes. These characteristics, if considered, should be regarded as safety factors.

The major downward force on a packer is usually the pressure force resulting from pressure above acting downwardly over the annular area of Equation (1). The net tubing load is the only other downward force on a packer.

Since the tubing load is to be determined separately, the only upward force on a packer is the pressure force resulting from pressure below the packer acting over the annular area of Equation (1).

An upward force not considered is that exerted on the slips, or on an anchor. Where the downward forces exceed the upward, the excess is carried by slips or an anchor.

EXAMPLES

Some examples of packer applications will emphasize many salient features which must be considered in the use of packers. Assume the following conditions:

Conventional type packer with circulating valve
API Casing — 7 in., 29 lb, N-80, at setting depth, 6.14 in. ID
API Tubing — 27/8 in. OD x 2.441 in. ID, 6.5 lb/ft, EUE, Grade J-55
Setting Depth — 10,000 ft
Mud in Well — 9.6 lb/gal; pressure gradient—0.5 psi/ft

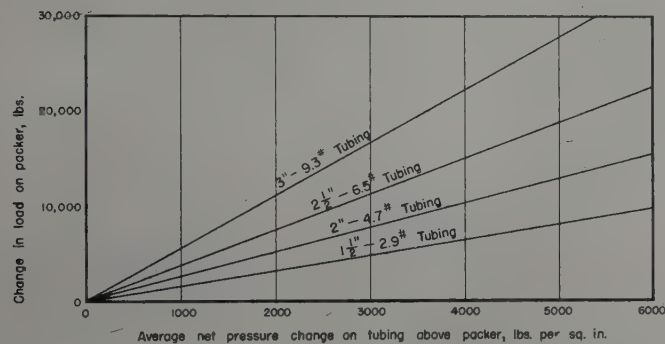


FIG. 4 — EFFECT OF PRESSURE CHANGE ON TUBING LOAD ON PACKER

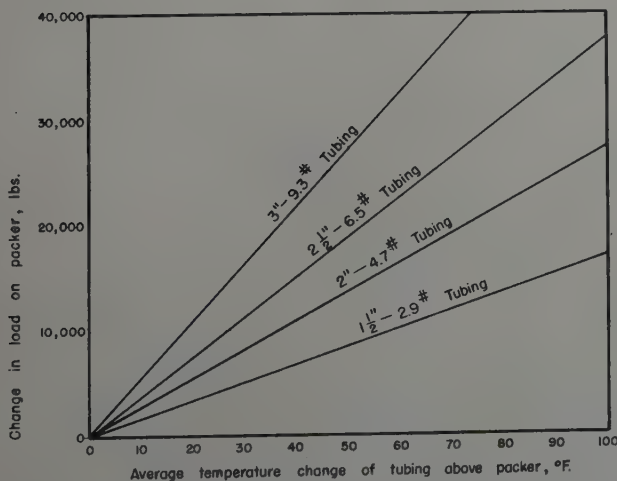


FIG. 5 — EFFECT OF TEMPERATURE CHANGE ON TUBING LOAD ON PACKER

Minimum tubing weight to compress packing element—10,000 lb

Unbalanced valve area — 10.8 sq in.

Annular Area, Tubing to Casing: $A_p = 23.5$ sq in., from Table I

Annular Area of Tubing: $A_t = 1.81$ sq in., from Table I

When the packer has been run to 10,000 ft, there is all about the packer a pressure of 5,000 psi. The buoyant force on the tubing is

$$\begin{aligned} F &= pA_t \\ &= (5,000)(1.81) \\ &= 9,050 \text{ lb} \end{aligned}$$

When the packer is set with a tubing load of 10,000 lb, the net tubing load on the packer may be determined in the following manner:

Positive Tubing Forces

1. Tubing setting load	10,000 lb
2. Weight of tubing initially buoyed by fluid	9,050

Total Positive Forces	19,050 lb
-----------------------	-----------

Negative Tubing Forces

1. Buoyant force on tubing	9,050 lb
----------------------------	----------

Net Tubing Load on Packer

$$\begin{aligned} &(\text{Positive Forces} - \text{Negative Forces}) \\ &= 19,050 - 9,050 \\ &= 10,000 \text{ lb} \end{aligned}$$

The forces on the packer may be tabulated in the following manner:

Downward Forces on Packer

1. Pressure force on packer: $pA_p = (5000)(23.5) = 117,500$ lb	
2. Net tubing load on packer, from above	10,000

Total Downward Forces	127,500 lb
-----------------------	------------

Upward Force on Packer

$$pA_p = (5000)(23.5) = 117,500 \text{ lb}$$

It is seen that the downward forces exceed the upward forces by 10,000 lb, and that the downward forces include a tubing load of 10,000 lb. Since this is the amount of excess downward force, and tubing force, to maintain compression of the packing element, conditions are satisfactory at this point for this type of packer.

Effect of Swabbing

Next assume that the casing has been perforated a few feet below the packer setting and that when the tubing is swabbed to bring the well in, the well will not flow. The tubing is consequently swabbed to bottom. Pressure conditions and forces are now considerably different. It will be noted that there is no longer a column of fluid in the tubing to exert an upward force on the packer and tubing and hence the upward forces are now zero. Prior to swabbing, the column of fluid outside the tubing was balanced by a column of fluid inside the tubing, but with the removal of fluid from the tubing, the annular space above the packer exerts a pressure tending to collapse the tubing. This decrease in internal tubing pressure results in an additional downward force on the packer. The average internal pressure decrease is $5,000/2$ or

2,500 psi. The wall thickness of the tubing is $(2.875 - 2.441)/2$ or 0.217 in. The additional downward force is

$$\begin{aligned} P &= 0.0434 W_p D/t \\ &= (0.0434) (6.5) (2,500) (2.875) / (0.217) \\ &= 9,350 \text{ lb} \end{aligned}$$

The net tubing load on the packer may be determined in the following manner:

Positive Tubing Forces

1. Tubing setting load	10,000 lb
2. Weight of tubing initially buoyed by fluid	9,050
3. Increase due to pressure change	9,350
Total Positive Forces	28,400 lb

Negative Tubing Forces

None

Net Tubing Load on Packer

28,400 lb

The forces on the packer may be tabulated in the following manner:

Downward Forces on Packer

1. Pressure force on packer: $pA_p = (5000) (23.5) = 117,500$ lb	
2. Net tubing load on packer, from above	28,400
	145,900 lb

Upward Force on Packer

None

This is a considerable downward force. The example chosen is not an unusual one. Swabbing a well to bottom with the tubing set on a packer and with mud in the annulus above the packer is a common occurrence, and in many cases the depth is deeper and the mud heavier so that larger downward forces exist.

The 10,000 lb tubing weight slacked off at the surface in setting the packer represents only 6.8 per cent of the total downward force on the packer. It is thus evident that the weight with which a packer is set is a relatively insignificant portion of the load carried by a packer when a well is swabbed down. Had it been decided to set the packer with say 20,000 lb to make certain that the packing element was adequately expanded, irrespective of frictional or other forces, the additional weight would have been less than 7 per cent of the total load on the packer. Since the setting load is such a small percentage of the total load to which packers are often subjected, there are few valid arguments favoring the setting of packers with the minimum possible setting weight. It is the effect of high setting weights upon the tubing and the disadvantages of tubing in compression that must be considered, and not the effect upon the packer.

Fig. 1-a shows an anchor type packer which depends upon an anchor pipe to prevent downward movement of the packer. This example shows that where an anchor is used to support a packer, it may be subjected to a large longitudinal compression load and it must therefore have sufficient column strength to prevent failure.

It should be noted that when a conventional packer is swabbed down on, it is fulfilling a purpose for which it is

particularly suited; i.e., holding downwardly acting forces and pressures. If a failure occurs, it is usually due to the inadequacy of the packer and not to the application.

Effect of Unbalanced Valve Area

To pull the packer of this example loose and remove it from the well without first pumping fluid into the tubing, it is necessary to exert a sufficient pull on the tubing to support the entire weight of the tubing, and to open the circulating valve against the pressure above the packer. The tubing weighs 65,000 lbs., and the force required to open the valve is $(10.8) \times (5,000)$ or 54,000 lb, for a total required pull at the surface of 119,000 lb. The tubing in such a well as this example would usually be grade J-55 which has a minimum yield strength listed at 99,660 lb. In this case, as in many similar ones, it would be advisable to fill the tubing at least partially before attempting to unseat the packer.

Conventional packers without circulating valves sometimes offer a similar problem which requires at least partially filling the tubing before the packer can be unseated.

Effect of Gas Wells

Again using the data of the example, assume now that the formation just below the packer contains gas at a static pressure of 4,500 psi and that the shut in surface pressure is 3,500 psi. The average external pressure on the tubing is still 2,500 psi. The average internal pressure is now $(3,500 + 4,500)/2$ or 4,000 psi. The decrease in the force exerted by the tubing on the packer because of this average internal pressure increase of 1,500 psi is 5,700 lb from Fig. 4.

The net tubing load on the packer in this application is determined as follows:

Positive Tubing Forces

1. Tubing setting load	10,000 lb
2. Weight of tubing initially buoyed by fluid	9,050
Total Positive Forces	19,050

Negative Tubing Forces

1. Buoyant force on tubing, $(4,500) (1.81) =$	8,150 lb
2. Decrease due to pressure change	5,700
Total Negative Forces	13,850 lb

Net Tubing Load on Packer

$$19,050 - 13,850 = 5,200 \text{ lb}$$

The forces on the packer may be tabulated in the following manner:

Downward Forces on Packer

1. Pressure force on packer: $(5000) (23.5) =$	117,500 lb
2. Net tubing load on packer	5,200
	122,700 lb

Upward Force on Packer

$$pA_p = (4500) (23.5) = 105,700 \text{ lb}$$

Net Downward Force on Packer

$$122,700 - 105,700 = 17,000 \text{ lb}$$

In this case, the total downward forces exceed the upward forces by a comfortable margin. However, the net tubing load

on the packing element, which is the primary force maintaining packing element compression, is only 5,200 lb. It would be advisable in an installation such as this to increase the tubing setting load by some 5,000 lb to insure maintenance of packing element compression.

If the packer in the above example had been set a considerable distance above the producing formation, the pressure of the mud acting downwardly would be decreased significantly while the pressure of the gas acting upwardly would be decreased only slightly. This could result in insufficient downward force to maintain packing element compression or to prevent upward movement, and it is likely that such a packer installation would fail.

It sometimes happens that a liner of considerable length is set in a well and the well completed on a packer which is set in the casing above the liner. The pressure conditions which will exist in such an installation of a conventional packer should be carefully investigated to see if the downward forces will exceed the upward forces by a sufficient amount to maintain the compression of the packing element.

Bottom hole chokes and regulators are sometimes run inside the tubing. Such devices will usually result in an average pressure inside the tubing which is less than that when the packer was set, and thus tend to place a greater tubing load on the packer. However, the chokes offer a piston effect due to the differential pressure across the choke and this tends to lift the tubing. The cooling effect of the expanding gas above the chokes may result in a significant average temperature drop within the tubing and the effect of this may be to raise the tubing from the packer. Unless proper care is exercised in this type of installation, the downward forces may not be sufficient to maintain compression of the packing element and prevent upward movement of the packer, and the packer may fail in its purpose.

Effect of Upwardly Acting Differential Pressure on Conventional Packers

Assume that it is desired to hold a differential pressure of 1,000 psi underneath the conventional packer of the example in an operation such as acidizing the formation below. Assume further that the acid used has a pressure gradient of 0.5 psi per foot and that pumping the acid down the tubing will lower the temperature of the tubing an average of 30°F. The only means available for holding a differential pressure below a conventional packer is tubing weight, and the amount of tubing weight which is required when friction is neglected will be determined. The pressure within the acid at the packer is 5,000 psi due to the fluid column, plus 1,000 psi pump pressure applied at the surface for a total pressure at the packer of 6,000 psi.

The upward pressure force on the packer will be:

$$pA_p = (6000) (23.5) = 141,000 \text{ lb}$$

The downward pressure force on the packer will remain at 117,500 lb. Since the total downward forces must exceed the upward pressure force by 10,000 lb, the net tubing load on the packer when acidizing must be

$$(141,000 + 10,000) - 117,500 = 33,500 \text{ lb}$$

The tubing setting load applied prior to acidizing will decrease when pressure is applied to the tubing. The decrease in load for 1,000 psi average increase in internal pressure is 3,700 lb from Fig. 4.

The tubing setting load will also be decreased when the tubing is cooled by the acid pumped down. This decrease in load for a 30°F temperature decrease is 11,300 lb from Fig. 5.

The tubing setting load required may be determined in the following manner:

Positive Tubing Forces

1. Tubing setting load	X
2. Weight of tubing initially buoyed by fluid	9,050
Total Positive Forces	(X + 9,050) lb

Negative Tubing Forces

1. Buoyant force on tubing, (6000) (1.81)	= 10,900 lb
2. Decrease due to pressure change	3,700
3. Decrease due to temperature change	11,300
Total Negative Forces	25,900

The net tubing load on the packer as determined above is 33,500 lb

Then

Net tubing load on packer = (Positive tubing forces) - (Negative Tubing Forces)

$$33,500 = (X + 9,050) - 25,900$$

$$X = 50,350$$

In practice, some assistance is received from friction, so it probably would not be necessary to slack off as much as 50,000 lb tubing weight onto the packer to maintain 1,000 psi differential pressure under the packer. Further, when pressure must be applied to the tubing as in this example, it is almost always possible to apply pressure to the casing also, so that there would actually be little or no differential pressure across the packer. This example explains the difficulties experienced with conventional packer leakage when substantially equivalent fluid columns are in the tubing and casing and pressure is applied only to the tubing.

In many dually completed wells, changing pressure differentials across the packer result in large upward and downward forces. If a conventional packer is used to isolate the two producing zones, there may not be sufficient tubing weight available to maintain the packer setting against upwardly acting differential pressure, and this will result in intercommunication between the two zones.

Upwardly Acting Differential Pressure on Universal Type Packers

Universal type packers are suitable for holding pressure differentials acting upwardly, but care must be taken to place sufficient tubing weight on the packer, or otherwise arrange the installation, so that the mandrel will not be moved upwardly out of the packer when pressure and temperature changes occur. If pressure and temperature changes of considerable magnitude are expected, it is advisable to analyze the resultant effect upon the tubing. Attention must be paid the particular design to be used, as in some designs the mandrel diameter and sealing arrangement permit pressure from above and below to exert forces tending to move the mandrel which are independent of and in addition to the various forces affecting tubing load. Difficulties have been experienced in using universal type packers simply because changed well conditions

caused an upward movement of the mandrel with resultant leakage about the mandrel.

Effect of Squeeze Cementing Pressures

Destructive pressures sometimes occur when using packers, as in squeeze cementing. In this application, the pressures below the packer are often very high. There is a column of cement slurry which usually has a pressure gradient of about 0.84 psi/ft, plus high pressures applied to the tubing. This pressure is sometimes transmitted upwardly outside the casing and acts to collapse the casing above the packer. The casing in the above example has a published minimum collapse pressure of 6,370 psi. If it is assumed that the tubing is completely filled with cement slurry and that a squeeze pressure of 5,000 psi is applied, the pressure below the packer is $(0.84)(10,000)$ psi plus 5,000 psi, or 13,400 psi. The pressure above the packer is $(0.5)(10,000)$, or 5,000 psi. If channels exist which permit the application of the pressure below the packer to the outside of the casing above the packer, there is a net differential pressure of 8,400 psi tending to collapse the casing. Since there is danger of casing collapse when the minimum collapse

pressure is exceeded, there is a good possibility that the casing in this example would have collapsed above the packer. Collapsing the casing above a packer is ordinarily very expensive to remedy, and is usually avoided in a case such as this by applying sufficient internal pressure to the casing to counteract the collapsing pressure.

CONCLUSIONS

The type of packer required for a given installation may be determined from an analysis of the conditions to be met. The amount of tubing load necessary to maintain the installation when expected pressure and temperature changes occur may be determined by analysis. When the proper type of packer is set with the proper tubing load for the application, chances for a successful installation are enhanced.

ACKNOWLEDGMENT

The author is indebted to The Atlantic Ref. Co. for permission to release this paper and wishes to express his appreciation for the aid received from various members of the engineering staff of the company.

★ ★ ★

MULTIPLE CONDENSED PHASES IN THE DECANE-TETRALIN-BITUMEN SYSTEM

J. S. BILLHEIMER, AEROJET ENGINEERING CORPORATION, AZUSA, CALIFORNIA, H. H. REAMER,
AND B. H. SAGE, MEMBER AIME, CALIFORNIA INSTITUTE OF TECHNOLOGY, PASADENA, CALIF.

ABSTRACT

The influence of pressure, temperature, and relative quantity of decane on the separation of plastic or solid phases rich in bitumen from the decane-tetralin-bitumen system has been investigated in a restricted range of composition. Measurements were made at atmospheric pressure and at 8000 psi^a for temperatures of 70, 160, and 220°F. Behavior similar to that of the n-pentane-tetralin-bitumen system was found except that the influence of pressure upon the separation of bitumen was radically different in the decane-tetralin-bitumen system than that found in any of the earlier studies.

INTRODUCTION

The separation of solid asphaltic or bituminous material from hydrocarbon liquids has been noted in petroleum operations and studied in the laboratory. Publications relating to the separation of bitumen from naturally occurring hydrocarbon mixtures were reviewed in a recent publication.¹ Early investigations^{2,3} of these mixtures showed a relatively complex behavior, with the quantity of separated bitumen increasing with increased weight fraction of the lighter hydrocarbons until a state was reached at which the separation of a second liquid phase (liquid II) began. Further increase in the weight fraction of the lighter component caused a decrease in the amount of solid bitumen. However, the total quantity of bitumen in liquid II and in the separated solid phase continued to increase in a regular fashion. This type of behavior was also found in the n-pentane-tetralin-bitumen system.¹

Because of this similarity in behavior of the simpler system and more complex naturally occurring hydrocarbon mixtures, it became desirable to extend the study to aliphatic hydrocarbons of higher molecular weight. As a part of this study an investigation of the decane-tetralin-bitumen system was carried out at 70, 160, and 220°F. The details of the techniques employed in the preparation of a purified bitumen from the natural product have already been described.¹ An adequate quantity was prepared from a crude bitumen obtained from the San Joaquin Valley by leaching, solution, and precipitation processes. The purified material was similar in all measured respects to that employed in the earlier investigation of the n-pentane-tetralin-bitumen system.

The tetralin used, after purification by fractional distillation, had a specific weight at 77°F of 59.906 lb per cu ft and an index of refraction relative to D-lines of sodium at 77°F of 1.5401. No significant difference in these properties was shown by several samples prepared. The decane was obtained from the Eastman Kodak Company and was purified by repeated fractionation in a 30-plate glass column at reduced pressure. The fractionated material when dried over metallic sodium had a specific weight at 100°F of 44.686 lb per cu ft and an index of refraction relative to the D-lines of sodium at 78.9°F of 1.4091.

PROCEDURES

The measurements reported in this investigation were made by use of

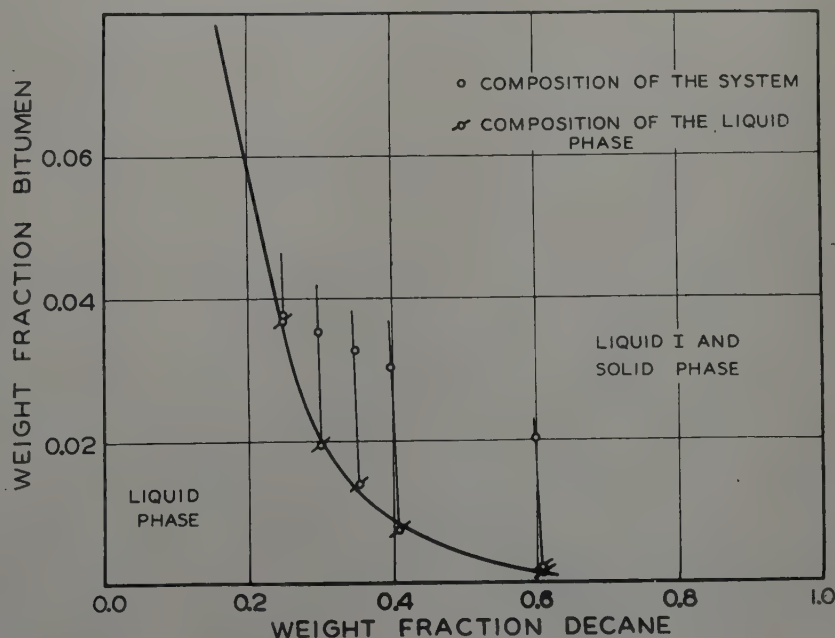


FIG. 1 — COMPOSITION OF LIQUID PHASE IN EQUILIBRIUM WITH BITUMEN
AT 160°F AND 15 PSI.

Manuscript received at office of Petroleum Branch August 1, 1949.

¹ References are given at end of paper.

^a All pressures cited are absolute.

weighing bomb techniques⁴ with either glass or steel bombs depending upon whether the pressure was atmospheric or 8000 psi. The general procedure used in these bitumen investigations^{1,2} consisted of adding known quantities of each of the components to the weighing bomb and bringing the mixture to equilibrium at a prescribed pressure and temperature. The contents of the weighing bomb were then displaced under equilibrium conditions by mercury and the compositions of the phases determined. For measurements with the steel weighing bomb, the solid bitumen was separated from the liquid phases by rotating the bomb about its major axis for a period of about 30 minutes at a speed which would produce at its inner surface an acceleration of approximately 1500 times that of gravity. For measurements with the glass equipment, the solid phase was separated without difficulty from the liquid by centrifuging in a conventional laboratory centrifuge and decanting.

Some difficulty was experienced in obtaining equilibrium between the separated bitumen and the corresponding liquid phase, especially at decane concentrations near that corresponding to the phase boundary. Under these conditions at least 60 hours were required for an approach within 0.5 per cent of the complete equilibrium separation. This difficulty was greater with this system than with the n-pentane-tetralin-bitumen system.

EXPERIMENTAL RESULTS

Fig. 1 shows the compositions of the several mixtures investigated at atmospheric pressure (approximately 15 psi) and a temperature of 160°F. The corresponding compositions of the liquid phase have also been indicated. The system has been treated as if it were ternary even though the bitumen contains a range of components of undetermined but high molecular weight. Parts of the combining lines are shown also. Because the weight fraction of bitumen in solution is small throughout the system the scale of plotting this quantity was enlarged markedly. The phases present in each of the composition fields have been indicated and the estimated location of the phase boundary shown. The upper end of the boundary line was located from separate investigations of the solubility of

bitumen in tetralin.¹ A pair of points indicating coincidence of the composition of the liquid phase and of the system as a whole has been indicated at approximately 0.1 weight fraction decane. Corresponding results obtained at 220°F are presented in Fig. 2. The weight fraction of bitumen miscible with tetralin increases with an increase in temperature, and this trend also persists in mixtures containing at least 0.2 weight fraction decane. All of the measurements included in these figures were carried out upon systems containing a

weight ratio of bitumen to tetralin of 0.0526, and were at a pressure of approximately 15 psi. Attempts were made to carry out similar measurements at 70°F but difficulty was experienced in obtaining equilibrium.

The quantitative results obtained in the course of the investigation, at 15 psi, graphically portrayed in Fig. 1 and 2, are recorded in Table I. These data include for each case the composition of the system as a whole, the separated bitumen as a weight fraction of the total bitumen, and the composition of

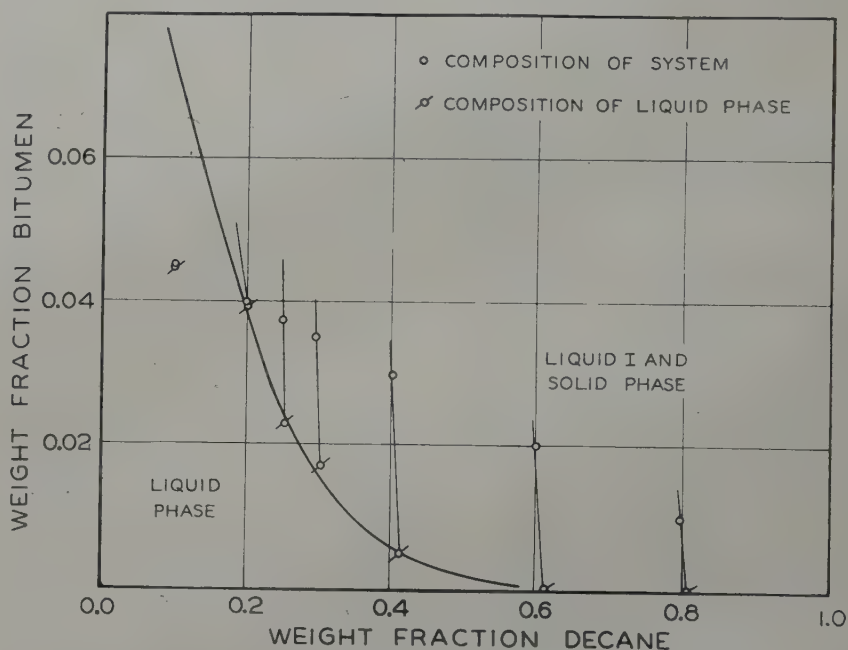


FIG. 2 — COMPOSITION OF LIQUID PHASE IN EQUILIBRIUM WITH BITUMEN AT 220°F AND 15 PSI.

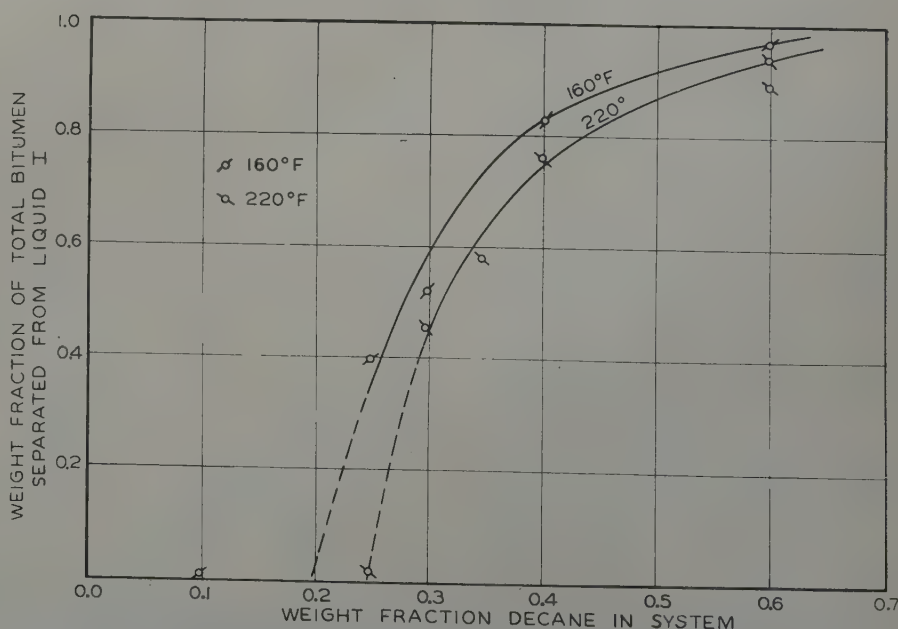


FIG. 3 — SEPARATION OF BITUMEN AS A SOLID PHASE FROM DECANE-TETRALIN-BITUMEN SYSTEM AT 15 PSI AND A WEIGHT RATIO OF BITUMEN TO TETRALIN OF 0.0526.

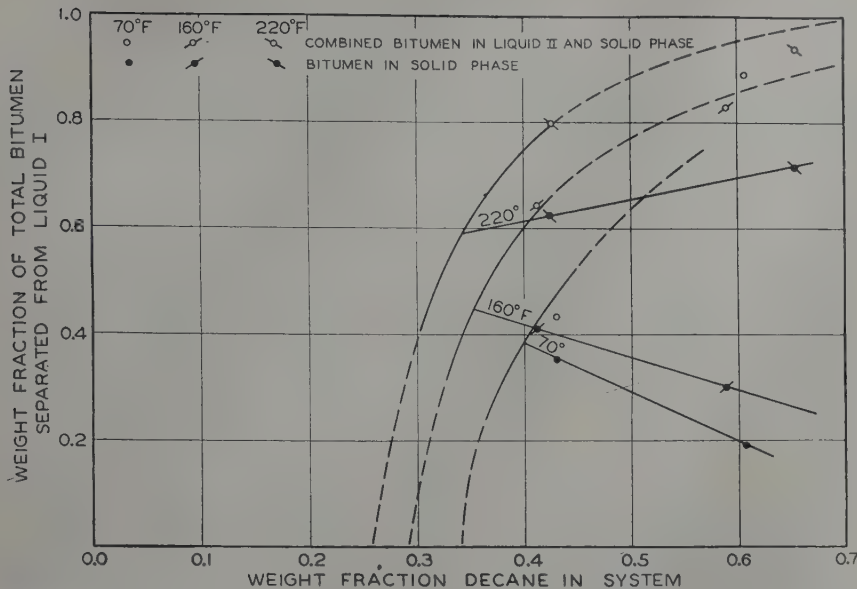


FIG. 4—SEPARATION OF BITUMEN FROM THE DECANE-TETRALIN-BITUMEN SYSTEM AT 8000 PSI AND A WEIGHT RATIO OF BITUMEN TO TETRALIN OF 0.0526.

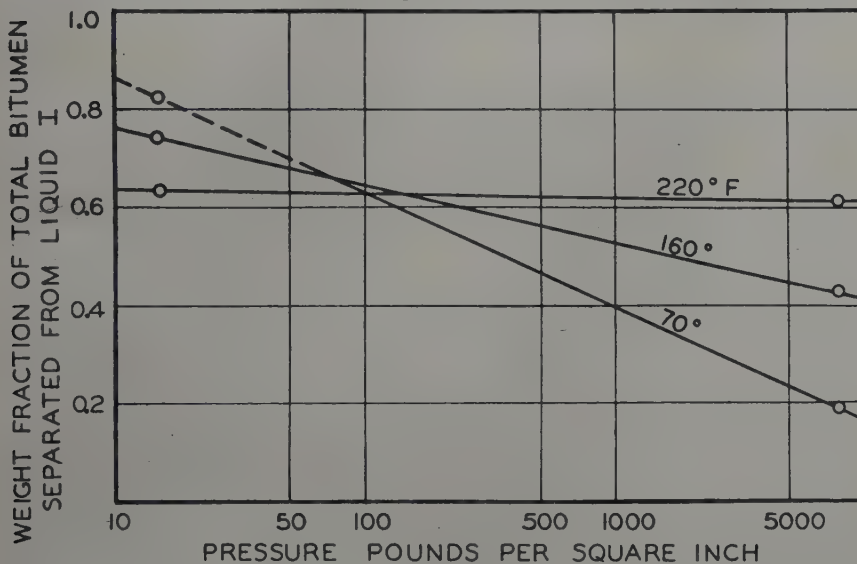


FIG. 5—INFLUENCE OF PRESSURE UPON SEPARATION OF BITUMEN FROM LIQUID I IN A RESTRICTED DECANE-TETRALIN-BITUMEN SYSTEM CONTAINING 0.350 WEIGHT FRACTION DECANE AND 0.0325 WEIGHT FRACTION BITUMEN.

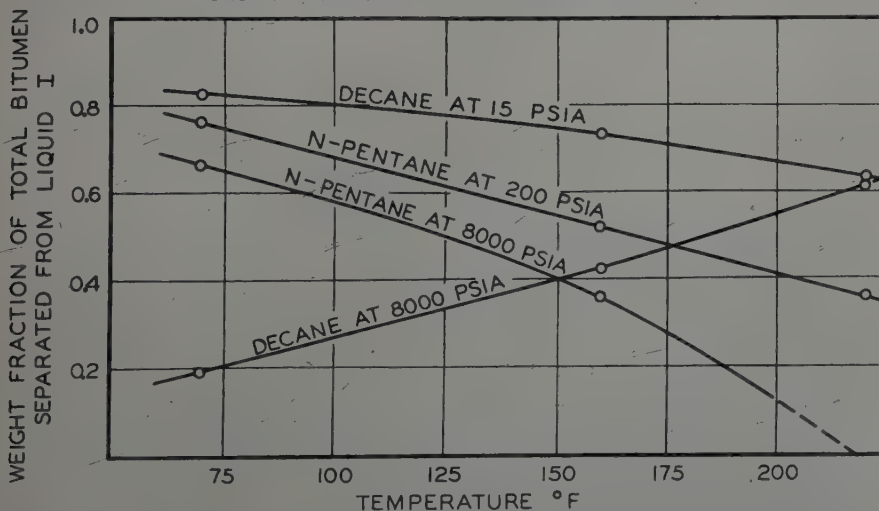


FIG. 6—COMPARATIVE INFLUENCE OF TEMPERATURE UPON SEPARATION OF BITUMEN FROM LIQUID I IN THE N-PENTANE-TETRALIN-BITUMEN AND DECANE-TETRALIN-BITUMEN SYSTEMS CONTAINING 0.0350 WEIGHT FRACTION PARAFFIN AND 0.0325 WEIGHT FRACTION BITUMEN.

the liquid phase. The solid phase separating from the liquid upon addition of decane was mainly bitumen but contained very small amounts of tetralin and decane. The influence of the weight fraction of decane in the system upon the separation of bitumen as solid phase at 15 psi is presented in Fig. 3. At this pressure an increase in the weight fraction of decane resulted in a corresponding increase in the relative quantity of the bitumen separated and there was no observed tendency for the separation of a second liquid phase, thus differing from behavior at high pressure.

At a pressure of 8000 psi the relative quantity of solid phase increased with increasing weight fraction of decane until a second liquid phase (liquid II) appeared. Further increase in the weight fraction of decane in the system caused a decrease in the amount of solid at 70° and 160°F. However, the combined quantity of bitumen in liquid II and in the solid phase continued to increase with rising weight fraction of decane in the system. The latter behavior is shown in Fig. 4 for the three temperatures investigated. The data obtained at 8000 psi are recorded in Table II. The accuracy and extent of the results presented in Fig. 4 and recorded in Table II leave much to be desired. However, much effort was required for the accumulation of such data and quantitative approach to equilibrium is difficult to obtain. It is believed that the trends indicated in Fig. 4 are significant and at least semi-quantitatively descriptive of fact. The composition of the bitumen separated as a solid phase from the decane-tetralin-bitumen system is recorded in Table

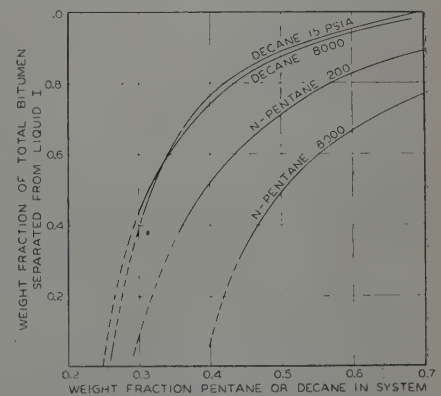


FIG. 7—COMPARISON OF SEPARATION OF BITUMEN FROM LIQUID I IN THE N-PENTANE-TETRALIN-BITUMEN AND THE DECANE-TETRALIN-BITUMEN SYSTEMS AT 220°F.

III. Data obtained at 15 psi and 70°F have been included although difficulty was experienced in obtaining equilibrium at this temperature and pressure.

An appropriate representation of the influence of pressure upon the separation of bitumen from liquid I in the restricted decane-tetralin-bitumen system is presented in Fig. 5. These data indicate a much more complex influence of pressure at the several temperatures than was found in the case of the n-pentane-tetralin-bitumen system.¹ The experimental background upon which Fig. 5 was based is limited to pressure measurements at 15 psi and 8000 psi. It would be desirable to obtain information at intermediate pressures but the experimental effort required was such as to limit the number of measurements made. Fig. 5 indicates only a small effect of pressure change upon the separation of bitumen at a temperature of 220°F but larger effects at lower temperatures.

For comparison, Fig. 6 shows the influence of temperature upon the separation of bitumen from liquid I in the n-pentane-tetralin-bitumen¹ and the decane-tetralin-bitumen systems. These data indicate the same trends for both restricted ternary systems at low pressures but a radical difference appears in their behavior at a pressure of 8000 psi. As indicated in this figure and also in Fig. 7, decane causes greater separation of bitumen from liquid I than does pentane at 220°F.

ACKNOWLEDGMENT

This paper is a contribution from American Petroleum Institute Research Project 37 located at the California Institute of Technology. Neal Zimmerman contributed substantially to the experimental program.

REFERENCES

1. Billheimer, Sage and Lacey: Multiple Condensed Phases in the n-Pentane-Tetralin-Bitumen System, *Journal of Petroleum Technology*, November, 1949.
2. Katz and Singleterry: *Trans. AIME* (1939) 132, 103.
3. Botkin, Reamer, Sage and Lacey: Amer. Petr. Inst., Fundamental Res. on Occurrence and Recovery of Petr. (1943).
4. Sage and Lacey: *Trans. AIME* (1940) 136, 136. ★ ★ ★

TABLE I—Separation of Bitumen as Solid Phase From the Restricted Decane-Tetralin-Bitumen System at 15 PSI

Composition of System Weight Fraction			Separated Bitumen as Weight Fraction of Total Bitumen	Composition of the Liquid Phase Weight Fraction		
Decane	Tetralin	Bitumen		Decane	Tetralin	Bitumen
160° F.						
0.099	0.856	0.0450*	0.009	0.099	0.855	0.0459*
0.199	0.761	0.0400	0.002	0.199	0.761	0.0399
0.249	0.713	0.0376	0.397	0.253	0.724	0.0231
0.298	0.667	0.0351	0.521	0.304	0.679	0.0171
0.403	0.567	0.0298	0.837	0.413	0.582	0.0050
0.600	0.380	0.0200	0.973	0.611	0.388	0.0005
0.800	0.190	0.0100	0.996	0.808	0.192	0.0000
220° F.						
0.248	0.714	0.0376	0.019	0.248	0.715	0.0369
0.297	0.668	0.0351	0.456	0.301	0.679	0.0194
0.347	0.620	0.0326	0.582	0.354	0.632	0.0139
0.398	0.572	0.0301	0.761	0.407	0.586	0.0074
0.598	0.382	0.0201	0.942	0.609	0.390	0.0012
0.599	0.381	0.0201	0.892	0.610	0.388	0.0022

*Composition of system falls in single phase region.

TABLE II—Separation of Bitumen From the Restricted Decane-Tetralin-Bitumen System at 8000 PSI

Composition of System Weight Fraction			Distribution of the Bitumen Weight Fraction of Total Bitumen		
Decane	Tetralin	Bitumen	Solid	Liquid I	Liquid II
70° F.					
0.430	0.542	0.0285	0.354	0.568	0.078
0.607	0.373	0.0196	0.191	0.109	0.700
160° F.					
0.412	0.559	0.0294	0.0409	0.358	0.333
0.589	0.390	0.0206	0.0301	0.170	0.529
220° F.					
0.425	0.546	0.0287	0.622	0.202	0.176
0.654	0.329	0.0173	0.716	0.063	0.221

TABLE III—Composition of Bitumen Separated as a Solid Phase From the Decane-Tetralin-Bitumen System

Pressure, PSI	Composition of System Weight Fraction			Weight Fraction of Constituents				Weight Ratio of Carbon to Hydrogen
	Decane	Tetralin	Bitumen	Carbon	Hydrogen	Nitrogen	Ash	
70° F.								
15	0.40	0.570	0.030	0.8157	0.0737	0.0119	0.0057	11.10
15	0.60	0.380	0.020	0.8143	0.0754	0.0105		10.80
15	0.40*	0.570	0.030	0.8137	0.0758	0.0081		10.75
220° F.								
15	0.40	0.570	0.030	0.8477	0.0755		0.0002 0.0002	11.20
8,000	0.40	0.570	0.030	0.7442	0.0718			10.38

*Additional solid phase separated from the liquid phase after seven days.

MULTIPLE CONDENSED PHASES IN THE N-PENTANE-TETRALIN-BITUMEN SYSTEM

J. S. BILLHEIMER, AEROJET ENGINEERING CORP., AZUSA, CALIFORNIA, B. H. SAGE, MEMBER AIME, AND W. N. LACEY, CALIFORNIA INSTITUTE OF TECHNOLOGY, PASADENA, CALIFORNIA

ABSTRACT

A restricted ternary system made up of n-pentane, tetralin, and a purified bitumen was investigated at 70, 160, and 220°F. Most of the experimental observations were at atmospheric pressure or at 200 psi.^a However, some experimental measurements were carried out at a pressure of approximately 8000 psi.

It was found that the purified bitumen was precipitated from its solution or dispersion in tetralin by the addition of n-pentane and that the separation occurred at lower weight fractions of n-pentane at the lower temperatures. The bitumen-tetralin solutions show some colloidal characteristics at temperatures below 160°F when near compositions at which the bitumen separates as a solid phase. At states remote from the phase boundaries and at temperatures above 160°F these characteristics become less evident. Under these latter circumstances the mixtures tend to follow the behavior of true solutions, particularly in regard to the approach to heterogeneous equilibrium. An increase in pressure appears to increase the solubility of bitumen in tetralin-n-pentane solutions. This effect is more pronounced at temperatures above 160°F than at lower temperatures.

INTRODUCTION

Asphaltic phases of plastic or solid nature have appeared in numerous instances during the recovery of petroleum from underground reservoirs. Such depositions occurring underground appear to have caused adverse

production histories for particular wells or zones. Because of this field experience, it is desirable to understand the factors which influence the formation or separation of the asphaltic phases from petroleum. The problem is unusually complex because the number of true components involved is very large and the details of the phase behavior encountered are difficult to ascertain experimentally.

The literature relating to asphalts, asphaltines, and bitumen is voluminous and widespread.¹ Only those references which are directly pertinent to the work at hand are cited. The separation of an asphaltic phase, hereinafter called bitumen, from naturally occurring hydrocarbon mixtures has been the subject of several investigations.^{2,3,4,5,6} It has been found that as many as four phases⁴ may be produced from a crude oil by the solution of a natural gas and propane at a pressure of 1500 psi and a temperature of 70°F. The separation of bitumen from such naturally occurring mixtures results in at least one liquid phase which is substantially free of high molecular weight components.³ The influence of the solution of lighter hydrocarbons on the separation of bitumen from a Santa Fe Springs crude oil has been investigated.⁵ The results indicate that in the case of the methane-crude oil system, the quantity of plastic or solid phase separated reaches a maximum between 0.14 and 0.19 weight fraction methane and then decreases until negligible at higher weight fractions of methane. Similiar behavior was encountered in the case of mixtures of ethane and crude oil. The decrease in the quantity of the solid phase with an increase in the weight fraction of the lighter component appears to result

from the formation of an additional liquid phase⁵ in which the bitumen is relatively soluble. The formation of this additional phase probably occurs at a weight fraction of methane close to that at which the quantity of separated solid reaches a maximum. A comparison of the deposition of bitumen in the field with the separation of asphalts from lubrication oil has been made⁷ and apparently the phenomena are similar. The phase behavior of bitumen also appears to be comparable to that of coal tar.^{8,9} The chemical and physical characteristics of asphalts and bitumen have been the subject of extended investigations which have been reviewed in some detail by Katz.¹⁰ The conclusion was reached that the dispersion of bitumen in a number of organic liquids was not entirely colloidal since it was impossible to isolate individual dispersed particles even with the electron microscope. However, the evidence appeared to indicate that at states close to phase boundaries the extent of the dispersion of the phases influenced the equilibrium to a greater extent than is encountered in many simpler systems.

From earlier study of field samples^{5,6} it became apparent that the phase behavior of bitumen-hydrocarbon systems was unusually complex. It was difficult to characterize in detail the phase behavior involved in naturally occurring hydrocarbon systems, even after a relatively extended investigation. For this reason, the study of a somewhat simpler system which still behaved in a similar manner became desirable. Three major constituents were necessary as follows: a bituminous solid, a liquid constituent which was a reasonably good solvent, and a constituent in which bitumen was largely insoluble. A sam-

Manuscript received at office of Petroleum Branch August 1, 1949.

¹ References are at the end of the paper.

^a All pressures reported are expressed in pounds per square inch absolute.

ple of bitumen from the field was purified to give the solid constituent. Tetralin was chosen as one component because of its effectiveness as a solvent, or possibly a dispersing agent, for the solid bitumen. Because the low molecular weight paraffin hydrocarbons are poor solvents for bitumen, n-pentane was employed as the third component. The data reported for the ternary system was restricted to the behavior of mixtures of only one ratio of bitumen to tetralin. A general study of the ternary system would involve many times the effort represented by the investigation reported here.

The present work upon the restricted n-pentane-tetralin-bitumen system includes studies at temperatures of 70, 160, and 220°F and covers nearly the entire range of compositions possible with one fixed ratio of bitumen to tetralin. The measurements were made with a bitumen-tetralin mixture containing 0.05 weight fraction bitumen. From a consideration of the relatively small values of the partial volumes of all the components and their nearness to equality it was not expected that pressure would exert such a major effect upon the equilibrium as was found. The investigations were limited to measurements at atmospheric pressure and at 200 psi, with a few measurements at 8000 psi.

MATERIALS

The bitumen used in this investigation was obtained from a production well of a field located on the west side of the San Joaquin Valley in California. It was obtained from the surface separator and was contaminated with crude oil and sand. This crude bitumen was leached repeatedly with n-pentane at a temperature of 220°F. The leaching was repeated until the liquid obtained by filtration contained less than 0.001 weight fraction of nonvolatile material. The initial filtrate from the leaching contained considerable quantities of a waxlike hydrocarbon material which was nearly white. A large part of this wax was separated from the n-pentane solution by cooling to the ice point. Upon evaporation of the residual solution after separation of the wax, a red-colored resinlike material was obtained.

The residual bitumen after leaching with n-pentane was dissolved in sufficient tetralin to produce a solution con-

taining not over 0.05 weight fraction bitumen. The resulting solution, after decanting from undissolved solids, was centrifuged at approximately 1000 times the acceleration of gravity for a period of one hour. Usually a negligible amount of precipitate was obtained in this operation. No segregation of the bitumen into discreet particles was ap-

parent, indicating that the bitumen can be dissolved at least partially in tetralin. The bitumen was recovered from the tetralin solution by dilution with sufficient n-pentane to give a mixture containing at least 0.90 weight fraction pentane. The mixture was agitated for two hours at 70°F and centrifuged for 30 minutes. The solid phase was washed

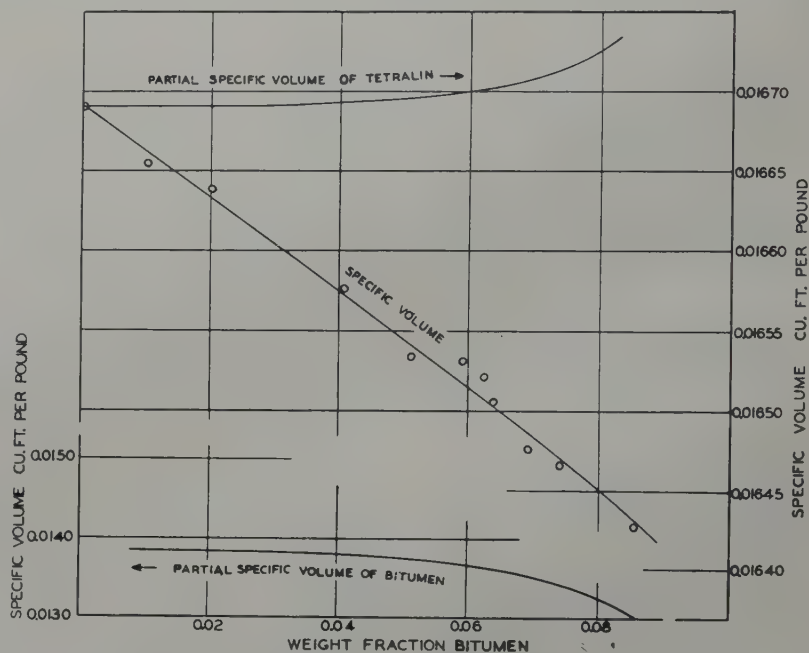


FIG. 1 — PARTIAL SPECIFIC VOLUMES IN BITUMEN-TETRALIN MIXTURES AT 77°F.

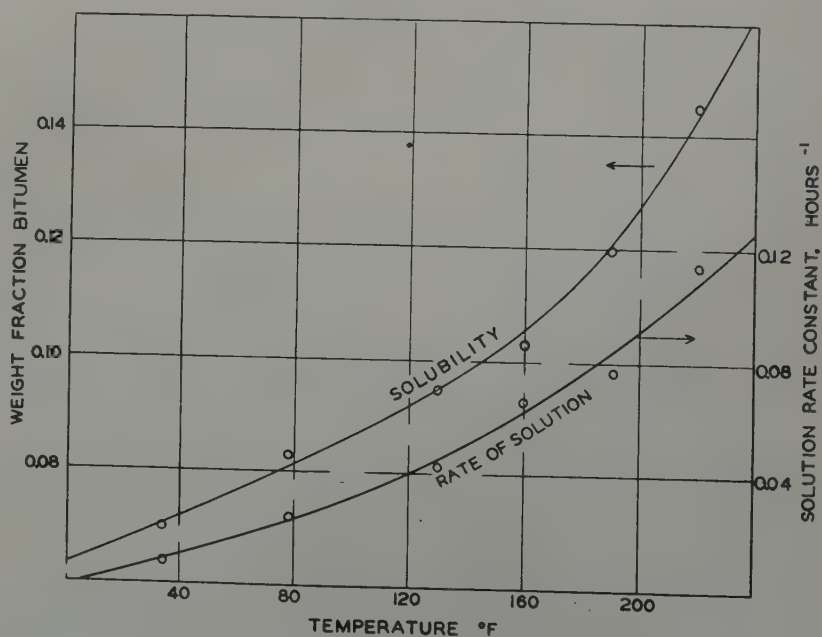


FIG. 2 — THE SOLUTION OF BITUMEN IN TETRALIN AT ATMOSPHERIC PRESSURE.

three times with n-pentane and dried for an extended period at a temperature of 100°F and a pressure of less than 0.1 inch of mercury. It was assumed that all of the n-pentane was removed when the weight of the bitumen changed less than 0.02 per cent per day.

Ultimate analyses of the purified bitumen, the resinous material, and the waxlike byproduct are given in Table I. The carbon-hydrogen ratio decreases progressively from the bitumen to the wax. Attempts to measure the average molecular weight of the bitumen from the lowering of the freezing point of benzene or tetralin were not particularly successful.

The tetralin used in these investigations was obtained from E. I. du Pont de Nemours and Company. The material was fractionated in a thirty-plate glass column at a pressure of approximately 1 psi. The initial and final 10 per cent portions were discarded. The purified tetralin showed an index of refraction relative to the D-line of sodium of 1.5401 at 77°F (25°C). Its specific volume at 77°F was 0.016699 cu ft per lb.

The n-pentane was obtained from the Phillips Petroleum Company with an analysis which indicated that it contained less than 1 mol per cent of material other than n-pentane, which was mainly iso-pentane. The n-pentane was

used without further treatment for all operations associated with the purification of bitumen. However, supplies of n-pentane were fractionated at reduced pressure in a glass ring-packed column for use in the majority of the measurements involved in the study of the restricted ternary system. The primary objective of the limited purification of n-pentane was to remove the dissolved non condensable gases such as nitrogen. The pertinent physical characteristics of the n-pentane were obtained from data available in the literature.^{11,12}

EQUIPMENT AND PROCEDURE

The equipment utilized in this experimental investigation may be divided into two categories. The first, which was described earlier,^{5,13} was used for the investigation of the behavior at elevated pressures. No important changes in either procedure or equipment were made, except that several jigs and fixtures were installed to permit more effective handling of the weighing bomb in the several stages of the separation and displacement processes. In addition, provision was made to avoid the removal of the weighing bomb from the agitated air bath in order to accomplish the displacement operations.

The procedures involved the introduction into the weighing bomb of the desired quantities of each of the components of the restricted ternary system. In each series of measurements with a fixed ratio of bitumen to tetralin an accurately prepared stock solution of these components was used. The quantities introduced were determined gravimetrically by measurement of the change in weight of the equilibrium vessel. After the weighing bomb and contents reached the chosen temperature in a thermostat bath, the pressure was brought to the desired value by introduction of mercury. The pressure was measured with an uncertainty of less than 0.3 per cent, by use of a pressure balance. The system was then agitated by rotating the vessel around its minor axis slowly for a period of at least 6 hours. It was then placed in a centrifuge maintained at the equilibrium temperature and rotated about its major axis for 30 minutes at approximately 10,000 revolutions per minute. This served to deposit the solid phase

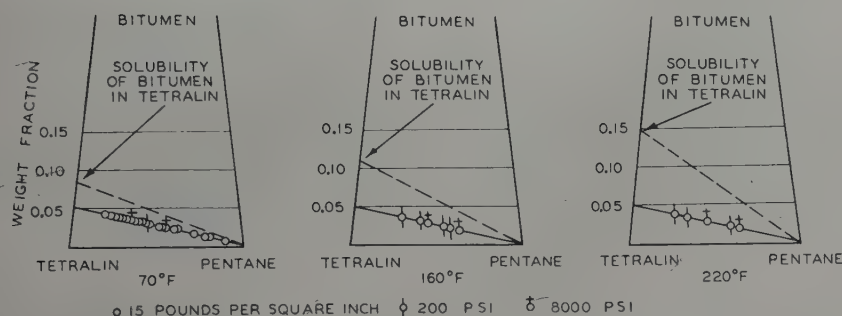


FIG. 3 — STATES INVESTIGATED IN RESTRICTED N-PENTANE-TETRALIN-BITUMEN SYSTEM. BITUMEN SCALE IS GREATLY ENLARGED.

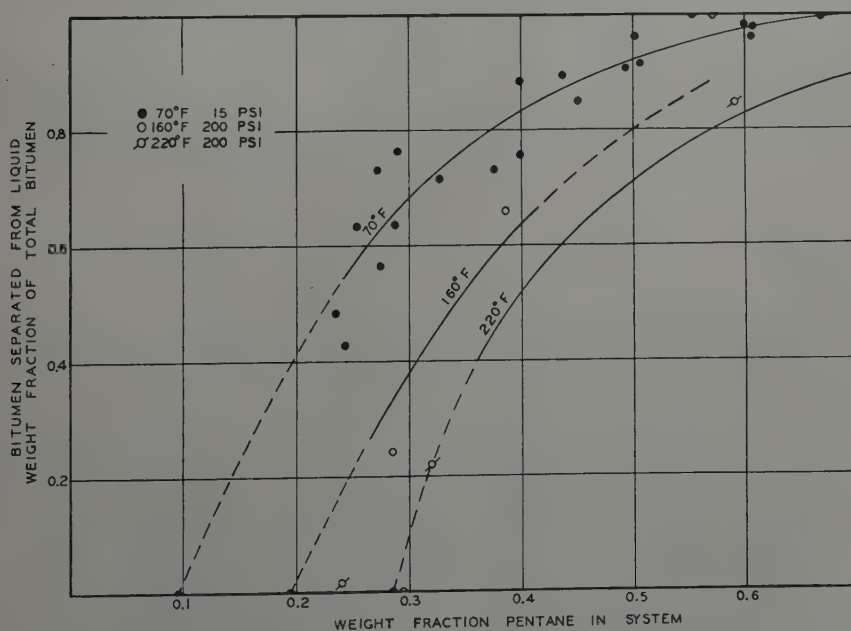


FIG. 4 — BITUMEN SEPARATED AT LOW PRESSURES EXPRESSED AS WEIGHT FRACTION OF TOTAL BITUMEN IN THE RESTRICTED N-PENTANE-TETRALIN-BITUMEN SYSTEM.

tightly upon the interior surface of the weighing bomb and permitted the segregation and displacement of the liquid phases from the vessel at the same elevated pressure at which equilibrium was attained. The separated bitumen was then removed from the walls by solution in tetralin at 190°F.

Glass equipment was used for the work at atmospheric pressure. Known quantities of the samples were introduced into a centrifuge tube by appropriate gravimetric techniques. Equilibrium was obtained by oscillating the sample in the centrifuge tube in a temperature-controlled air bath. After the system had been permitted to stand in a quiescent state for an extended period in the air bath at the temperature of the original equilibrium, it was removed from the bath and centrifuged. Although some change in temperature occurred in the course of this latter operation it produced little effect upon the equilibrium because the area of contact between the separated solid and the liquid phase decreased rapidly upon centrifuging. Duplicate measurements with carefully controlled temperature failed to show appreciable disagreement with the simpler technique. The measurements in the glass equipment were carried out at pressures below 20 psi.

It was necessary to utilize defined and closely controlled analytical techniques in determining the quantity of bitumen present in the several phases under investigation. If this was not done variations in the apparent quantity of bitumen present resulted. After consideration of a number of possibilities, the n-pentane precipitation techniques outlined in the literature¹ were employed.

In order to establish a weight balance of the components, the quantity of bitumen remaining in the liquid phase of the equilibrium mixture was determined by precipitation with n-pentane. The effectiveness of this analytical technique² to be satisfactory. As a matter of interest the solubility of the solid bitumen in pentane was determined at atmospheric pressure. The results were obtained by evaporation of the pentane extract after prolonged agitation at the cited temperature. It is probable that the material dissolved in this manner

was partially impurities remaining from the solid stock. It was concluded that the solubility of bitumen was less than 0.0008 weight fraction at 70°F and less than 0.0015 weight fraction at 220°F.

N-pentane and tetralin are completely miscible in the liquid phase at temperatures of 70, 160, and 220°F and at pressures slightly above the bubble point.

EXPERIMENTAL RESULTS

Tetralin-Bitumen System

As an initial part of the investigation a study was made of the behavior of the binary tetralin-bitumen system. The specific volume of mixtures of tetralin and bitumen in the liquid phase at 77°F is recorded in Table II as a function of the weight fraction bitumen. The uncertainties of the actual measurements of specific volume were probably less than 0.05 per cent. They were carried out in glass pycnometers which were temperature conditioned in an agitated air bath. The temperature of this bath relative to the international platinum scale was known within 0.1°F. The partial specific volumes of tetralin

and bitumen were evaluated graphically by the method of Roozeboom.¹⁴ The results reported in Table II are presented graphically in Fig. 1 as a function of the weight fraction bitumen in the mixture. The deviations of these data from a smooth curve are somewhat greater than the uncertainty of the specific weight measurements. This may result in part from variations in the nature of the solution or dispersion of bitumen in tetralin. However, for most engineering purposes it appears possible to assume that the partial volumes of both the tetralin and bitumen remain substantially constant throughout the range of compositions up to 0.06 weight fraction bitumen. The deviations from constancy increased as the concentration of bitumen approached the saturation value at this temperature.

As is shown by the data in Fig. 2, if tetralin were brought to equilibrium with solid bitumen at a temperature of 70°F, approximately 0.08 weight fraction bitumen could be dissolved or possibly dispersed in the tetralin. At 220°F this value increased nearly to 0.15 weight fraction. Upon cooling an equi-

TABLE I—Ultimate Analyses of the Constituents Obtained From Crude Bitumen

Constituent	Weight Fraction of Constituent					Wt. Ratio of Carbon to Hydrogen
	Carbon	Hydrogen	Nitrogen	Sulfur	Ash	
Wax*	0.8481	0.1283	0.0090			6.61
Resin†	0.8373	0.0097	0.0185	0.0120	0.0120	8.40
Bitumen‡	0.8208	0.0742	0.0119	0.0160	0.0043	11.07

*Wax is defined as the constituent insoluble in pentane at the ice point.

†Resin is defined as the constituent obtained from evaporation of the pentane extracts.

‡Bitumen is defined as the constituent insoluble in pentane at 220°F.

TABLE II—Partial Specific Volume of Components in Tetralin-Bitumen Mixtures at 77°F

Weight Fraction Bitumen	V (cu.ft./lb)	\bar{V}_T (cu.ft./lb)	\bar{V}_B (cu.ft./lb)
0.0000	0.016692	0.016691	
0.0102	0.016655	0.016691	
0.0200	0.016639	0.016691	0.01385
0.0406	0.016577	0.016691	0.01380
0.0511	0.016534	0.016692	0.01379
0.0593	0.016531	0.016695	0.01372
0.0624	0.016521	0.016699	0.01365
0.0637	0.016505	0.016701	0.01360
0.0692	0.016476	0.016702	0.01356
0.0741	0.016466	0.016707	0.01354
0.0855	0.016427	0.016715	0.01340
		0.016755	0.01292

*Experimental uncertainty somewhat greater at these high weight fractions of bitumen.

librium mixture from 220 to 70°F, a relatively stiff gel was obtained. After breaking up the gel mechanically and centrifuging for an extended period the separated bitumen could be recovered. The quantity remaining in the solution agreed well with the equilibrium value for 70°F.

Because of the possible instability at 70°F of mixtures prepared with more than 0.008 weight fraction bitumen, no stock solutions of bitumen and tetralin containing more than 0.05 weight fraction bitumen were used in this investigation. The solutions used appeared to be relatively stable and could be centrifuged repeatedly without loss of solid bitumen. Furthermore, such solutions did not show appreciable deposition of the bitumen on the surfaces of the glass container in which they were stored, although difficulties of this sort were experienced with mixtures having higher bitumen content.

Limited experimental work was conducted upon the rate of solution of bitumen in tetralin at a number of temperatures. It was found that, for the conditions of agitation employed and

the original condition of the purified solid bitumen, a period of approximately 100 hours was required to approach within 2 per cent of the equilibrium concentration at temperatures as high as 130°F. At a temperature of 220°F the same percentage of the equilibrium composition could be reached in approximately 60 hours. The measurements as reported in Fig. 2 were not of great accuracy but serve to show that an extended contact period was required in order to obtain the equilibrium data. Most of the solubility values discussed later were obtained by extrapolation of the measurements of the rate of solution of bitumen in tetralin to apparent equilibrium.

An unsuccessful attempt was made to supplement this information by determining the temperature at which bitumen would separate upon cooling a solution which had been nearly saturated with bitumen at a somewhat higher temperature. A gel formed which, at this state close to the phase boundary, was not separated by centrifuging at 1000 times the acceleration of gravity for 30 minutes.

In the course of the investigation of the tetralin-bitumen system the variation in the composition of the bitumen which dissolved from an excess quantity of the solid phase was established roughly. Table III shows the average ultimate analysis of the bitumen. Corresponding analyses of the bitumen dissolved by tetralin at 34°F and at 220°F from an excess of the solid phase are given. The composition of the residue remaining after dissolving approximately half of the bitumen at 220°F is also recorded. The precision of ultimate microanalysis is probably insufficient to justify detailed consideration of the data. Although some differences in composition appear, nevertheless the analyses indicate that only small variations in the characteristics of this material are to be expected in the course of phase changes. The variation in composition reported in Table III is markedly less than that found among the three constituents obtained from the crude bitumen as indicated in Table I.

The analytical precipitation techniques were tested for use with the tetralin-bitumen system. Table IV compares the composition of tetralin-bitumen solutions as determined from the weight of bitumen added and from duplicate measurements of the precipitate obtained upon dilution with n-pentane at a temperature of approximately 70°F to yield a filtrate containing approximately 0.91 weight fraction n-pentane. The greatest divergence between the analytical values is less than 4 per cent and the average deviation from the prepared composition is 1.8 per cent.

Pentane-Tetralin-Bitumen System

A series of measurements was made utilizing a stock mixture of bitumen and tetralin containing 0.05 weight fraction bitumen, (0.0526 weight ratio of bitumen to tetralin), to establish the phase behavior of a restricted system made up of n-pentane, tetralin and bitumen. The relation of the mixtures investigated to the ternary system as a whole is indicated in Fig. 3.

Fig. 4 shows the extent of separation of solid bitumen from the restricted n-pentane-tetralin-bitumen system at atmospheric pressure (approximately 15 psi) and 70°F. The bitumen separated is expressed as weight fraction of the

TABLE III—Composition of Bitumen

	Weight Fraction				Wt. Ratio of Carbon to Hydrogen
	Carbon	Hydrogen	Nitrogen	Ash	
Bitumen before extraction with tetralin.....	0.8254	0.0789	0.0070	0.0003	10.48
Bitumen dissolved at 34° F.....	0.8144	0.0789	0.0058	0.0002	10.32
Bitumen dissolved at 220° F.....	0.8250	0.0753	0.0050	0.0001	10.96
Undissolved Bitumen (in residue from extraction by tetralin at 220° F.).....	0.8482	0.0772	0.0094		11.00

TABLE IV—Comparison of Determinations of Composition of Tetralin-Bitumen Solutions

Weight Fraction Bitumen			
As Prepared	By Pentane Precipitation		Average
0.0513*	0.0524†	0.0519†	0.0522
0.0500	0.0508	0.0508	0.0508
0.0499	0.0511	0.0505	0.0508
0.0499	0.0516	0.0520	0.0518

*Established from gravimetric measurements made in course of preparing solutions.

†Duplicate determinations by normal pentane precipitation procedures.

total bitumen present in the system. The components are entirely miscible up to a composition corresponding to about 0.10 weight fraction n-pentane in the system. Above this fraction of n-pentane, increasing amounts of solid bitumen separate. At compositions corresponding to 0.7 weight fraction n-pentane substantially all of the bitumen separates as solid phase. The experimental data indicated in Fig. 4 for 70°F are recorded in Table V. When less than 0.25 weight fraction n-pentane was present especial difficulty was experienced in obtaining reproducible values.

Table VI presents data indicating the influence of time upon the separation of bitumen at 70°F and 15 psi. If compositions of less than 0.21 weight fraction are considered, the bitumen separating in a period of two hours is only one-fourth of the quantity obtained after standing for seven days. Efforts to perform direct experiments at weight fractions less than 0.20 n-pentane were not successful and it was necessary to employ indirect methods. The trend of the indirectly obtained data at 70°F has been indicated by a dashed curve in Fig. 4. This curve was established by determining the composition of liquid phase in equilibrium with solid bitumen at 70°F and 15 psi with varying weight fractions of n-pentane, as shown in Fig. 5. These data were combined with the corresponding solubility value for the tetralin-bitumen system as a limit. From such information the dashed curve of Fig. 5 was established and the point on it corresponding to a weight ratio of 0.0526 for bitumen to tetralin (the restriction applied to the ternary system) indicated a weight fraction of n-pentane of 0.1, which was taken as the abscissa at the lower end of the 70°F curve in Fig. 4. Similar data for 160 and 220°F at a pressure of 200 psi are presented in Fig. 4 and Table VII.

Information concerning the behavior of the ternary system at 70, 160 and 220°F for a pressure of 8000 psi is presented graphically in Fig. 6. The experimental data are recorded in Table VIII. These data resemble those in Fig. 4 obtained for lower pressures, except that a somewhat higher weight fraction of n-pentane was required to effect the same relative separation of solid bitumen. Less difficulty was ex-

perienced in determining the amount of bitumen separated at the higher pressures even at a temperature of 70°F. The curves shown in Fig. 6 are at best only approximations of the behavior of the system.

Substantial quantities of a relatively dense second liquid phase were obtained at temperatures of 70 and 160°F. This phase will be designated as liquid II.

Apparently the decrease in the quantity of bitumen separated as a solid with an increase in the weight fraction of pentane, as indicated in Fig. 6, results from redissolving the separated bitumen in this second liquid phase. The total quantity of bitumen in the original liquid phase (liquid I) continues to decrease as the weight fraction of pentane is increased. An indi-

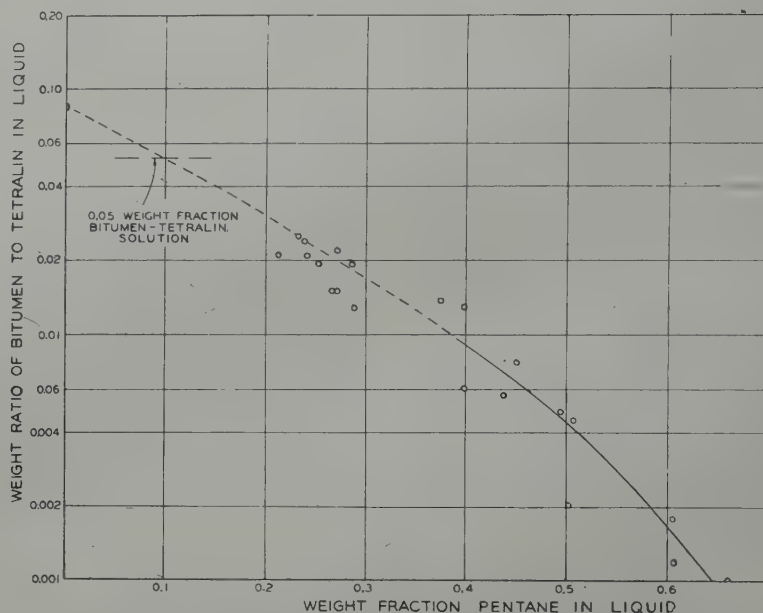


FIG. 5 — COMPOSITION OF LIQUID PHASE IN RESTRICTED N-PENTANE-TETRALIN-BITUMEN SYSTEM IN EQUILIBRIUM WITH SOLID BITUMEN AT 70°F. AND 15 PSI.

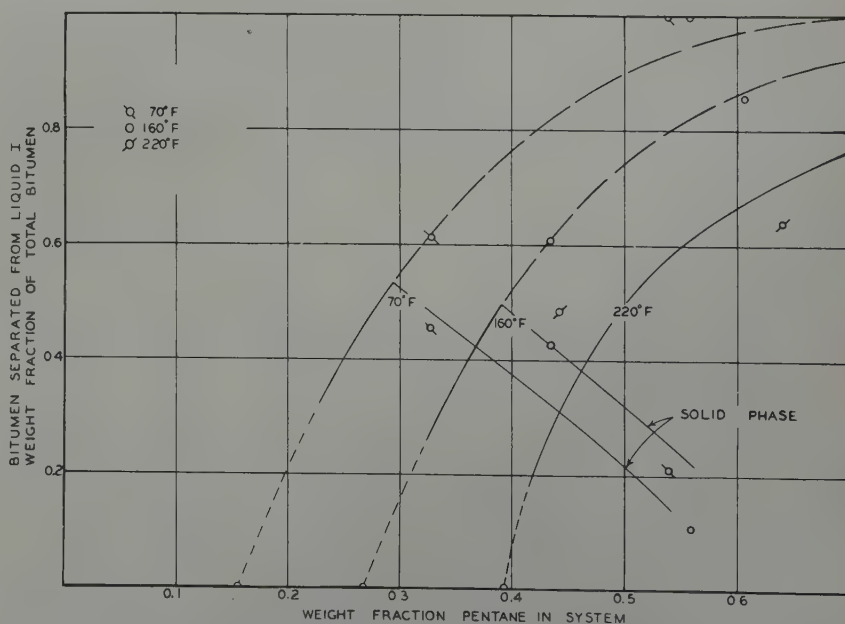


FIG. 6 — BITUMEN SEPARATED FROM LIQUID I OF THE RESTRICTED N-PENTANE-TETRALIN-BITUMEN SYSTEM AT 8000 PSI.

TABLE V — *The Separation of Bitumen in the n-Pentane-Tetralin-Bitumen System at 70° and 15 psi*

Weight Fraction Pentane in System*	Separated Bitumen as Fraction of Total Bitumen	Composition of the Liquid Phase Weight Fraction		
		Pentane	Tetralin	Bitumen
0.208	0.483†	0.210†	0.766†	0.0240†
0.213	0.484	0.218	0.767	0.0153
0.233	0.527	0.237	0.744	0.0188
0.239	0.547	0.244	0.739	0.0170
0.242	0.597	0.248	0.736	0.0155
0.253	0.632	0.259	0.727	0.0139
0.271	0.730	0.277	0.713	0.0103
0.273	0.599	0.277	0.703	0.0197
0.286	0.634	0.292	0.695	0.0133
0.289	0.760	0.297	0.694	0.0089
0.375	0.727	0.384	0.6074	0.0086
0.399	0.883	0.407	0.5855	0.0075
0.399	0.753	0.408	0.5840	0.0076
0.437	0.891	0.448	0.5489	0.0031
0.450	0.849	0.462	0.5340	0.0042
0.494	0.906	0.507	0.4906	0.0024
0.501	0.960	0.513	0.4860	0.0010
0.506	0.911	0.516	0.4820	0.0021
0.600	0.981	0.610	0.3896	0.0004
0.605	0.965	0.616	0.3830	0.0007
0.606	0.978	0.620	0.3790	0.0004
0.668	1.000	0.679	0.3210	0.0000
0.709	1.000	0.719	0.2810	0.0000
0.801	1.000	0.809	0.1910	0.0000
0.803	1.000	0.811	0.1890	0.0000
0.890	1.000	0.895	0.1050	0.0000

*Data limited to systems containing a weight ratio of bitumen to tetralin of 0.0526.

†Separation accomplished in a period of 7 days at 70° F. under quiescent conditions.

‡Weight fraction of the component in the liquid phase in equilibrium with the plastic or solid phase.

TABLE VI — *Influence of Time Upon Separation of Bitumen at Low n-Pentane Weight Fractions at 70° and 15 psi*

Weight Fraction n-Pentane	Bitumen Separated in 2 Hours	Additional Bitumen Separated in one Week	Total Bitumen Separated	Pct. of the Separated Bitumen Obtained in 2 Hours
0.271	0.730	0.000	0.730	100
0.253	0.632	0.000	0.632	100
0.242	0.427	0.170	0.597	71.5
0.239	0.335	0.212	0.547	61.2
0.213	0.198	0.286	0.484	35.2
0.208	0.168	0.315	0.483	23.6

TABLE VII — *Separation of Bitumen From a Restricted n-Pentane-Tetralin-Bitumen System at 200 psi*

Weight Fraction Pentane in System	Separated Bitumen as Weight Fraction of Total Bitumen	Composition of the Liquid Phase, Weight Fraction		
		Pentane	Tetralin	Bitumen
160° F., 200 PSI				
0.285	0.242	0.267*	0.706*	0.0267*
0.386	0.659	0.393	0.596	0.0111†
0.553	1.000			
220° F., 200 PSI				
0.240	0.017	0.241	0.722	0.0373
0.320	0.220	0.322	0.651	0.0267
0.591	0.843	0.600	0.396	0.0034

*Weight fraction of the component in the liquid phase in equilibrium with the solid phase.

†Because of the formation of liquid II at this state, the composition of liquid I was not determined.

cation of the quantity of bitumen in liquid II may be obtained from Fig. 6 as the difference between the weight fraction of total bitumen separated and that appearing as a solid. This information is fragmentary since difficulty was experienced in sampling this viscous liquid.

Fig. 7 indicates approximately the influence of pressure on the separation of bitumen from liquid I in the restricted n-pentane-tetralin-bitumen system which was investigated. An increase in the solubility of bitumen in liquid I accompanies an increase in pressure since the quantity of total bitumen separated from it decreases with increase in pressure. The effect of pressure is greater at higher temperatures.

In Table IX is presented the information available concerning the weight fraction of carbon, hydrogen, nitrogen, and ash in the solid bitumen separated from the n-pentane-tetralin-bitumen system at 70, 160, and 220°F. This information indicates a small decrease in the carbon-hydrogen ratio in cases in which the separation of bitumen was accomplished at high pressures. This shows that, as might be expected, the system cannot be considered strictly as a ternary system.

The data submitted in Tables V, VII, VIII, IX, and presented in Fig. 4, 5, and 6 are based upon the assumption that the separation of the solid bitumen from the liquid phase is completed by centrifuging the weighing bomb. This procedure involves rotation of the weighing bomb for a period of 30 minutes at such a speed as to yield an acceleration of approximately 1500 times that of gravity. In some instances small quantities of bitumen amounting to as much as 0.03 weight fraction of the total present were separated by more extended periods of high acceleration. However, with the exception of states at low temperatures and at low concentrations of pentane the prolonged treatment was not believed to be justified.

The results obtained indicate a fairly reproducible separation of the solid bitumen from the n-pentane-tetralin-bitumen system. The liquids, gases, and solids appearing in this system behave essentially as homogeneous phases except at states in the vicinity of the phase boundaries where difficulty in obtaining reproducible separation of the

bitumen was experienced. It appears that in this region surface energy is relatively important and the precipitated bitumen tends to remain in the liquid phases as a dispersed colloid.

The results obtained in this study of the n-pentane-tetralin-bitumen system leave much to be desired in the way of completeness and reproducibility. However, the marked similarity in the behavior of this restricted ternary system to that encountered in the mixtures of natural gas and crude oils gives some hope that the general characteristics of the complex naturally occurring hydrocarbon mixtures may be studied by investigation of simpler systems such as that discussed here. The problem is inherently complex and the present investigation has only added a small part of the information that will be required to permit a complete understanding of the separation of plastic or solid phases of relatively high molecular weight from naturally occurring hydrocarbon systems.

ACKNOWLEDGMENT

This paper is a contribution from American Petroleum Institute Research Project 37, located at the California Institute of Technology. The sample of crude bitumen was supplied by The Texas Company. The assistance of J. D. Yanak, C. E. Erickson, and N. D. Zimmerman in connection with the experimental work is gratefully acknowledged.

REFERENCES

1. Abraham: *Asphalts and Allied Substances*, 5th Ed., D. Van Nostrand Co., 1945.
2. von Pilat: *Oil and Gas Jnl.* (1936) 35 (10), 54.
3. Katz and Singleterry: *Trans. AIME* (1939) 132, 103.
4. Katz, Vink and David: *Trans. AIME* (1940) 136, 106.
5. Botkin, Reamer, Sage and Lacey: *Fundamental Res. on Occurrence and Recovery of Petr. Amer. Petr. Inst.* (1943).
6. Botkin, Reamer, Sage and Lacey: *Fundamental Res. on Occurrence and Recovery of Petr. Amer. Petr. Inst.* (1945).
7. Graff and Forrest: *Ind. and Eng. Chem.* (1940) 32, 294.
8. Kuhn: *Ind. and Eng. Chem. Anal. Ed.* (1940) 12, 86.

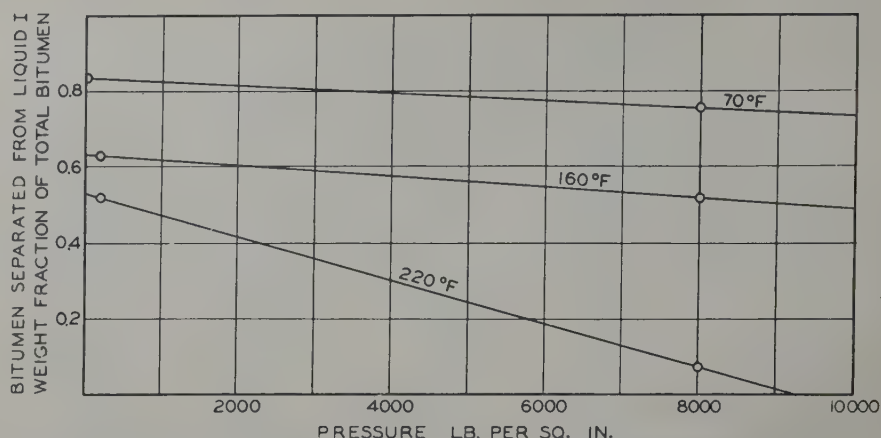


FIG. 7 — INFLUENCE OF PRESSURE ON THE SEPARATION OF BITUMEN FROM LIQUID I OF A N-PENTANE-TETRALIN-BITUMEN MIXTURE CONTAINING 0.40 WEIGHT FRACTION N-PENTANE AND 0.543 WEIGHT FRACTION TETRALIN.

TABLE VIII — The Separation of Bitumen From a Restricted n-Pentane-Tetralin-Bitumen System at 8000 psi

Temperature Deg. F.	Weight Fraction Pentane in System	Distribution of the Bitumen		
		Solid Phase	Liquid I	Liquid II
70	0.328	0.458*	0.389*	0.153*
70	0.535	0.645	0.355	0.000
70	0.539	0.210	0.000†	0.790
160	0.434	0.429	0.394	0.177
160	0.558	0.111	0.000†	0.889
160	0.606	0.416‡	0.139	0.445
160	0.655	0.655	0.130	
220	0.442	0.487	0.513	0.000
220	0.640	0.640	0.360	0.000

*Bitumen in the phase expressed as weight fraction of the total bitumen in the system.

†No bitumen was present in liquid I at these states.

‡Separation of bitumen as the solid phase and liquid II not made with certainty and bitumen separated as solid phase for this state has been omitted from Figure 6.

*The distribution of bitumen between the solid phase and liquid II was not determined at this state.

TABLE IX — Composition of the Bitumen Separated From the n-Pentane-Tetralin-Bitumen System

Temp. Deg. F.	Pressure, Psi	Weight Fraction n-Pentane in System	Phase from which Bitumen Obtained	Weight Fraction of Constituents				Weight Ratio of Carbon to Hydrogen
				Carbon	Hydrogen	Nitrogen	Ash	
Low Pressures								
70	15	0.90	solid	0.8281	0.0731	0.0065	0.0002	11.32
220	200	0.60	solid	0.8411	0.0746		0.0002	11.28
High Pressures								
70	8000	0.40	solid	0.7552	0.0678	0.0085		11.15
160	8000	0.60	solid	0.7735	0.0735	0.0071	0.0001	10.50
160	8000	0.60	liquid II	0.7605	0.0686	0.0055	0.0001	11.10
220	8000	0.60	solid	0.7754	0.0730		0.0002	10.63
220	8000	0.60	liquid II	0.7842	0.0788		0.0005	9.95

9. Hoiberg: *Petr. Ref.* (1947) 26 (1), 77.
10. Katz and Beu: *Ind. and Eng. Chem.* (1945) 37, 195.
11. Sage, Lacey and Schaafsma: *Ind. and Eng. Chem.* (1935) 27, 48.
12. Sage and Lacey: *Ind. and Eng. Chem.* (1942) 34, 730.
13. Sage and Lacey: *Trans. AIME* (1940) 136, 136.
14. Roozeboom: *Heterogenen Gleichgewichte*, 228-289, Braunschweig, 1904.

★ ★ ★

AN ELECTRICAL COMPUTER FOR SOLVING PHASE EQUILIBRIUM PROBLEMS

M. MUSKAT, MEMBER AIME, AND J. M. McDOWELL, GULF RESEARCH & DEVELOPMENT CO.,
PITTSBURGH, PENNSYLVANIA

INTRODUCTION

In both production and refining operations of the oil industry many processes are controlled by the gas-liquid phase relationships of the hydrocarbon mixtures of interest. The quantitative behavior of fractionating or distillation columns and stills depends on the changes in the equilibrium distributions of the hydrocarbon components between the gas and liquid phases as the pressure or temperature conditions may vary along the length of the column or as the gross operating parameters and compositions are varied. In oil producing operations the nature and amount of gas phase developed within an underground reservoir as it is being depleted and its pressure declines also involve the basic equilibrium gas-liquid phase interactions. The influence of surface conditions of temperature and pressure and various separation procedures on the nature and amount of stock tank oil and natural gas recovered from a given well stream is likewise determined by the same basic phase equilibrium characteristics of the hydrocarbon systems. Such equilibrium separation of the gas and liquid phases in a well stream is of importance both in establishing optimum separator conditions for obtaining maximum stock tank oil yields and in the general problem of crude stabilization.

The phenomena involved in these problems and their quantitative aspects can, of course, be established in each individual instance by appropriate laboratory experimentation. It has been found, however, that by associating with the individual hydrocarbon components functional characteristics de-

scribing their individual gas-liquid phase equilibrium behavior, the phase properties of the composite mixtures can be predicted by mathematical computation. These characteristics have been termed "equilibrium constants", or "equilibrium ratios",* and are defined by the general equation:

$$K_j = \frac{y_j}{x_j} \dots \dots \dots (1)$$

where K_j is the equilibrium ratio for the j th component, y_j is the mol fraction of that component in the gas phase, and x_j is the corresponding mol fraction in the coexisting liquid phase.

Considering the K_j as representing available and measurable properties of the individual components of a mixture, and as defined by Eq. (1), it is readily shown that in a coexisting gas-liquid system the mol fraction concentrations of the individual components in the gas phase, y_j , and those in the liquid phase, x_j , are given by the expressions:

*The latter term has been introduced to get away from the implication that the ratios y_j/x_j are really constant, as was apparently hoped when these ratios were originally proposed for phase equilibrium analysis.

$$y_j = \frac{n_j K_j}{1 + n_g (K_j - 1)} ;$$
$$x_j = \frac{n_j}{1 + n_g (K_j - 1)} \dots (2)$$

where the n_j are the corresponding mol fraction concentrations in the composite system, and n_g is the mol fraction of the whole which is in the gas phase. The basic unknown in Eq. (2) is n_g , which gives the gross separation between the gas and liquid phases. This may be determined in principle by imposing the requirement that the sums of the mol fractions in both the gas and liquid phases are unity, i.e. by the equations:

$$\sum \frac{n_j K_j}{1 + n_g (K_j - 1)} = 1$$
$$\sum \frac{n_j}{1 + n_g (K_j - 1)} = 1 \dots (3)$$

The solution of the equivalent Eqs. (3) lying between 0 and 1, when inserted into Eqs. (2), provides a complete description of the compositions of the coexisting gas and liquid phases. While the Eqs. (3) are essentially equivalent to polynomial equations, such transformations are of little value when dealing with multicomponent sys-

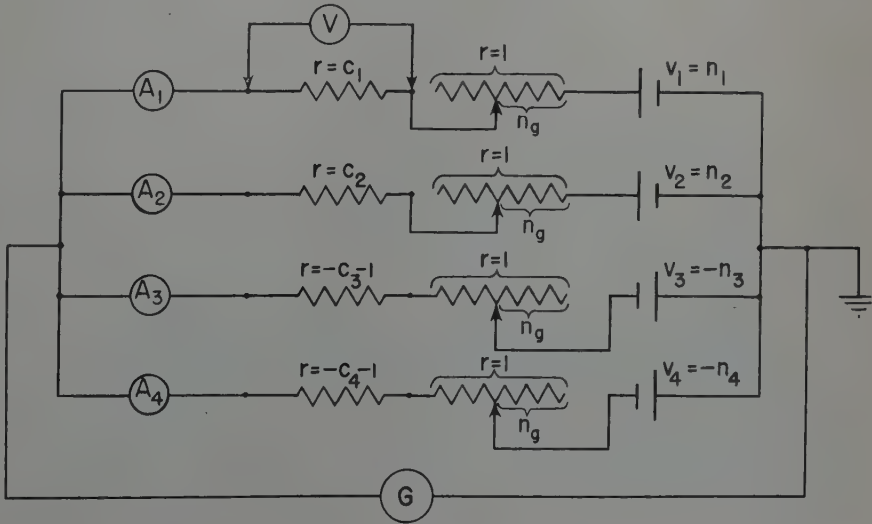


FIG. 1 — SIMPLIFIED SCHEMATIC DIAGRAM OF THE PHASE EQUILIBRIUM COMPUTER.

Manuscript received at office of Petroleum Branch August 3, 1949. Paper presented at San Antonio meeting of the Petroleum Branch, October 5-7, 1949.

tems. It has therefore been common practice to resort to direct numerical trial and error methods of solution, often supplemented by graphical interpolation. Such procedures are especially laborious when 7 or more components are involved and when a single problem requires multiple sequences of phase determinations, as in tray-to-tray or stage separation studies. An apparatus has therefore been developed for the purpose of solving Eqs. (3) by a special electrical circuit analog. This will be described in the following sections.

DEVELOPMENT OF THE ANALOGOUS CIRCUIT FOR THE ELECTRICAL COMPUTER

Electrical analogs of both algebraic and differential equations have been used for many years to facilitate their numerical solution. That which has been developed for the solution of Eqs. (3) is unique in that it is comprised of linear circuit elements, although the

basic unknown appears in an essentially non-linear manner.

The electrical circuit analog of Eqs. (3) can be formally expressed in a variety of ways, such as:

$$\begin{aligned} \sum I_j R_j &= 1; \\ \sum \frac{E_j}{I_j} &= 1; \\ \sum \frac{E_j}{R_j} &= 1 \dots \dots \dots (4) \end{aligned}$$

where I_j , R_j , E_j denote appropriate current, resistance or potential drop analogs of the individual terms in Eqs. (3). It is the last which has been taken as the basis for the computer to be described here. The direct equivalent of the last of Eqs. (4) would comprise a set of parallel variable resistances in which voltages proportional to the n_j are imposed on the individual elements and their resistances are made proportional to $1 + n_g (K_j - 1)$. By varying the n_g so that the measured resultant current is unity, or an appropriate scale factor, the correct value of n_g or the

solution to the equations will be obtained.

A transformation of Eqs. (3) to the form:

$$\sum \frac{c_j n_j}{n_g + c_j} = 1; \quad c_j = \frac{1}{K_j - 1} \dots (5)$$

leads to simplified circuit adjustments, since the variable resistors in the various circuit elements would be the common term n_g , which could be ganged together to insure identical values and variations. However, a still simpler equivalent of Eqs. (3) and (5), and the one which has been chosen for designing the Computer,* is:

$$\sum \frac{n_j}{c_j + n_g} = 0 \dots \dots (6)$$

In Eq. (6) the voltages applied to the separate component analogs are given directly by the total composition

*It may be noted here that Eq. (6) is itself of interest as providing a means for substantially reducing the time required for direct numerical solution of the equilibrium equations, as generally used in the form of Eqs. (3), provided the K_j are converted into the corresponding c_j by preliminary calculations.

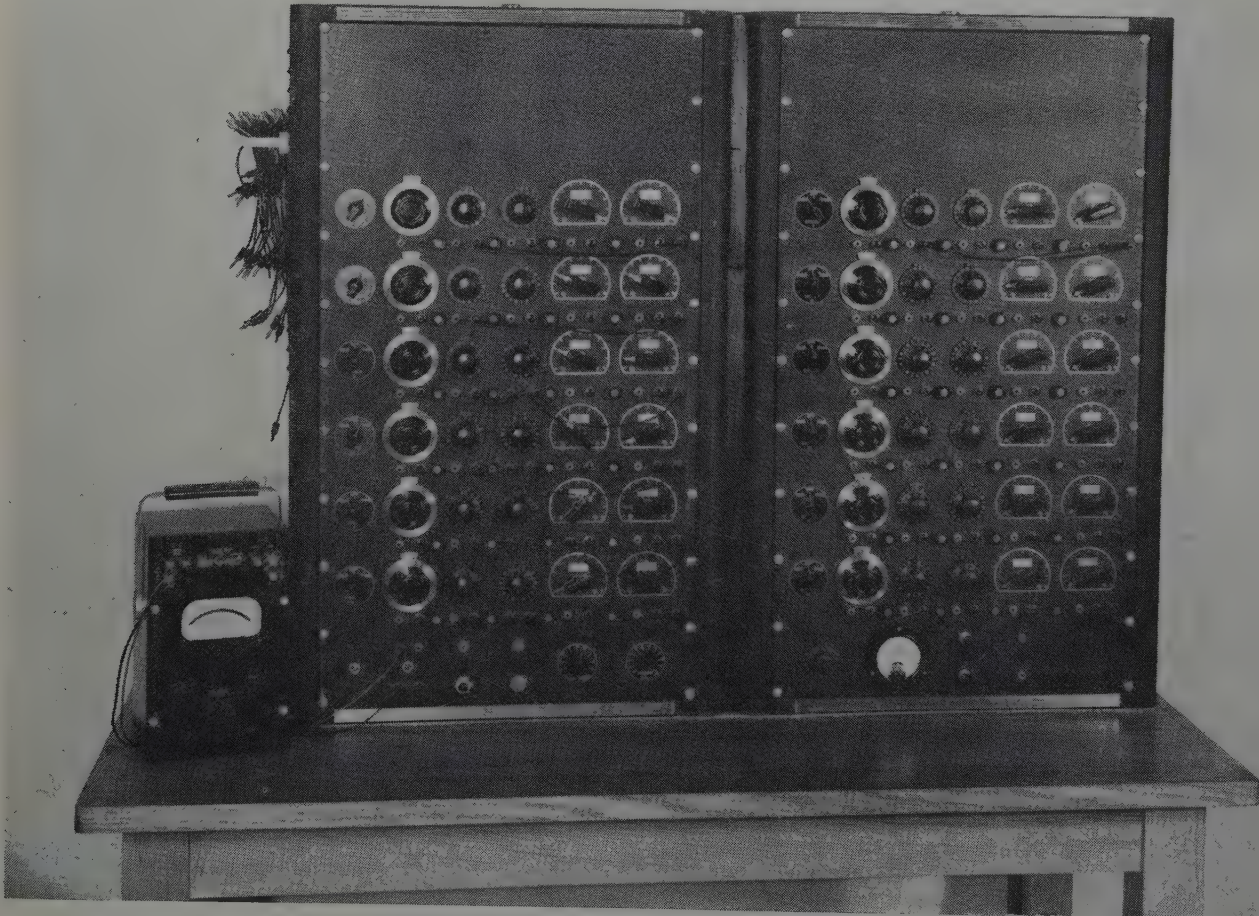


FIG. 2 — PHOTOGRAPH OF THE 12 COMPONENT PHASE EQUILIBRIUM COMPUTER.

mol fractions n_j . The physical characteristics of the individual components enter only as the fixed resistance elements c_j . And the basic unknown n_g can again be simulated by a set of ganged identical variable resistors. Moreover, Eq. (6) permits the use of a null method—zero resultant current—for locating the desired solution n_g .

As is obvious from the form of Eq. (6), and as is to be expected physically, in any equilibrium mixture comprised of coexisting gas and liquid phases it is necessary that for some of the components $K_j > 1$ while for others $K_j < 1$. In terms of the c_j this means that for some of the components $c_j > 0$, while for the others $c_j < 0$. This fact requires that the actual composite circuit be constructed of 2 basic groups,

in one of which the c_j are positive, and in the other the c_j are negative, as shown diagrammatically in Fig. 1. Here only two circuit branches are shown to represent components of the mixture for which $c_j > 0$ and two circuit branches for $c_j < 0$, but it is obvious that any number of components in a mixture could be handled simply by adding more parallel branches to the circuit.

In Fig. 1 the current in the first group of branches in which c_j is positive ($K_j > 1$) is obviously:

$$\frac{V_j}{c_j + n_g} = \frac{n_j}{c_j + n_g} \dots (7)$$

The current in the second group of branches in which c_j is negative ($K_j < 1$) can be written:

$$\frac{V_j}{-c_j - 1 + (1 - n_g)} = \frac{-n_j}{-c_j - n_g} = \frac{n_j}{c_j + n_g} \quad (8)$$

Since $-n_j$ is a negative quantity in Eq. (8), it is simply represented as a negative voltage. And since the c_j are negative for the branches represented by Eq. (8), the sums of the resistances in the various branches are $|c_j| - n_g$. Therefore Eq. (8) gives the values of negative currents. The expression for the summation of the currents in the branches of Fig. 1 thus reduces to Eq. (6) when the current through the galvanometer, G , is zero.

In addition to using such a circuit to solve for n_g it can be used either to determine the x_j for $K_j > 1$ by measuring the voltages across the resistors c_j in the first group of branches, or to determine the y_j for $K_j < 1$ by measuring the absolute values of the voltages across the resistors $-c_j - 1$ in the second

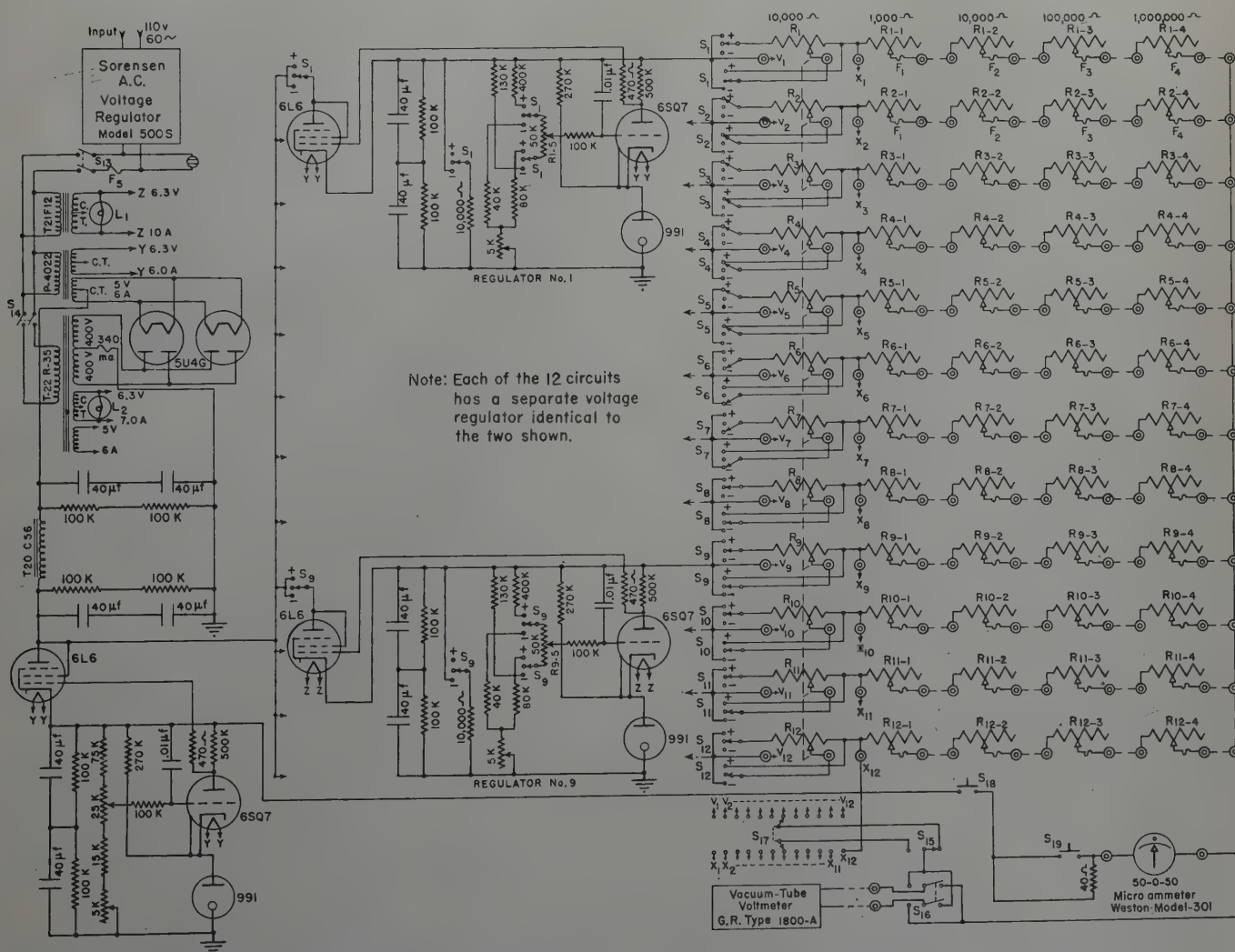


FIG. 3 — CIRCUIT DIAGRAM OF THE PHASE EQUILIBRIUM COMPUTER.

group of branches. The remaining values of x_j and y_j can be calculated from Eq. (1) or Eqs. (2). However, Eqs. (2) will usually give more accurate results than Eq. (1), and for this reason Eqs. (2) have been used in all examples presented in this study.

DESCRIPTION OF THE ELECTRICAL COMPUTER

The Computer to be described here is a twelve component instrument. A photograph of this Computer is reproduced in Fig. 2. The controls for each circuit representing a single component are arranged in horizontal lines across each cabinet. Starting on the left side the first controls are switches for turning the voltage on in each circuit and simultaneously determining whether it is a positive or negative voltage. The second control from the left in each series adjusts the value of this voltage to represent the quantity n_j . The other

four controls for each component adjust the value of four resistors which can be put in series by means of patch cords, and the total resistance will represent c_j (or $-c_j-1$) if $K < 1$.

The vacuum-tube-voltmeter used for measuring all voltages can be seen at the lower left of Fig. 2. There are a number of switches at the bottom of the left-hand cabinet which permit this voltmeter to be connected to any of the voltage points corresponding to the n_j or the x_j or y_j .

The value of n_g is read directly, when the circuits are balanced, from the dial shown in Fig. 2 at the lower left of the right-hand cabinet. This dial adjusts simultaneously the value of the n_g resistors in all of the component branches. The condition of balance is indicated on the microammeter just to the right of this dial.

The main power supply and a separate electronic voltage regulator for each voltage source is contained in the cabinets. A Sorensen voltage regulator is also used to regulate the 60 cycle line voltage. The detailed circuit diagram of these units is given in Fig. 3.

The overall accuracy of the Computer will depend primarily on the precision of the resistor elements and the control of the voltages. To provide for the former extremely accurate precision resistor units were selected to represent c_j and n_g . To obtain stable voltages the high degree of regulation previously mentioned was provided. It has been found that in general the computer will give results accurate to within 0.5 per cent to 1 per cent depending somewhat upon the problem.

The time necessary for the solution of each flash vaporization will, of course, depend upon the number of

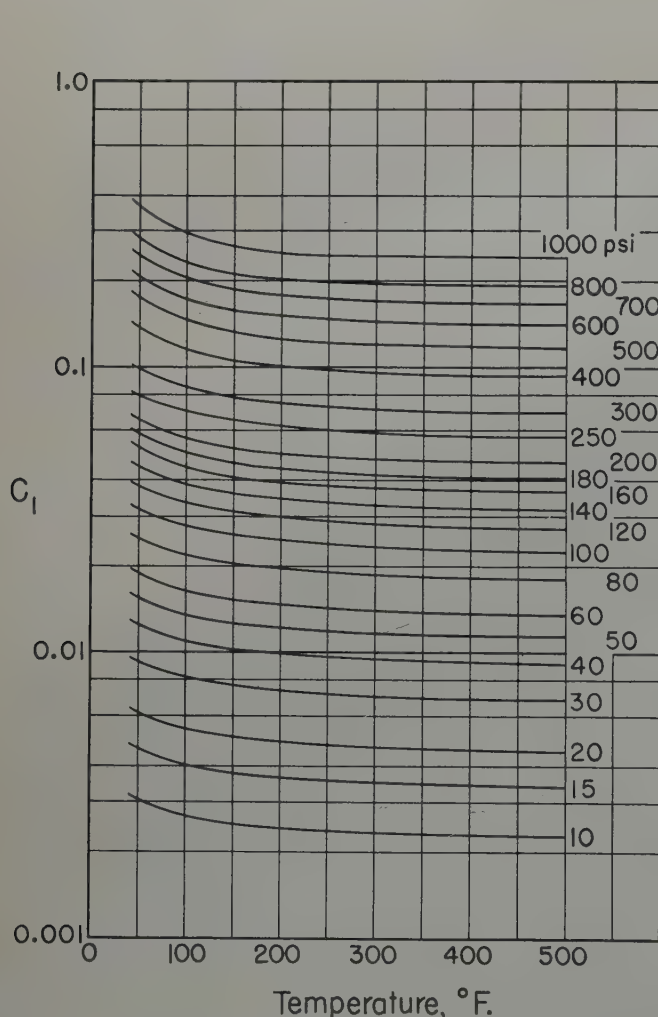


FIG. 4—ISOBARIC CHART OF THE EQUILIBRIUM RATIO FUNCTION FOR METHANE, c_1 , VS. THE TEMPERATURE.

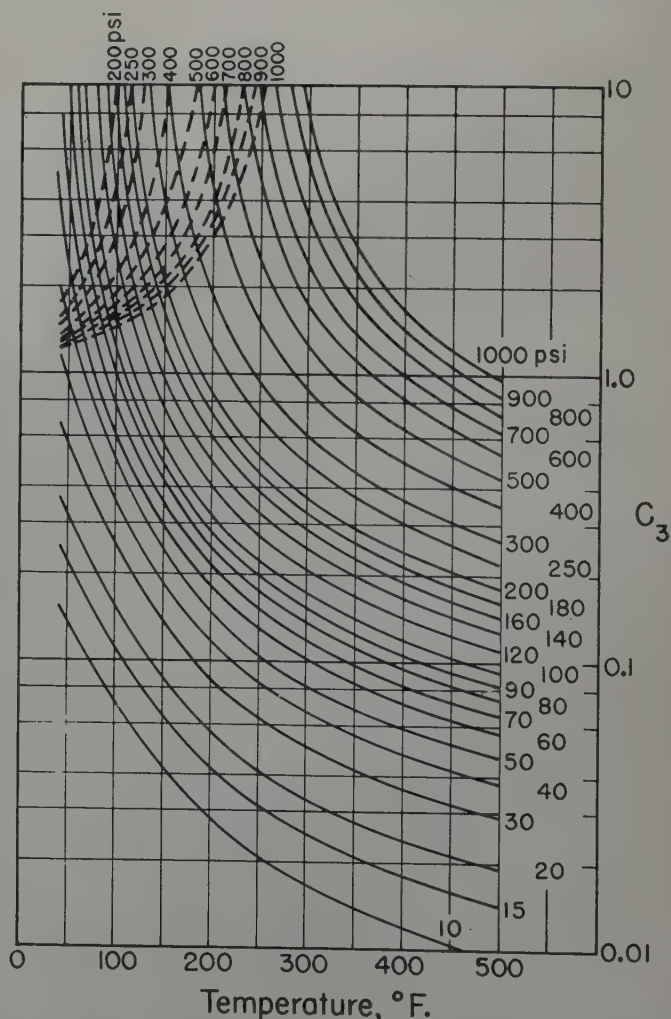


FIG. 5—ISOBARIC CHART OF THE EQUILIBRIUM RATIO FUNCTION FOR PROPANE, c_3 , VS. THE TEMPERATURE. DASHED SEGMENTS GIVE ABSOLUTE VALUES WHERE $c_3 < 0$.

components used, since most of the time is spent in setting the values of the resistors and voltages. It is usually necessary to reset the voltage dials two or three times as the voltages will vary slightly as the n_g dial is adjusted to the position of circuit balance. However, an experienced operator can make a complete solution on the Computer in from ten to twenty minutes, as the number of components ranges from 6 to 12, half of which time is generally consumed in adjusting the n_i voltage settings.

SAMPLE PROBLEMS AND USES OF THE ELECTRICAL COMPUTER

Tests of the general operational performance of the Computer readily demonstrated that it functioned in accordance with the planned circuit design, and as a true analog of the transformed phase equilibrium equations. To eval-

uate its practical value, however, it was necessary to check on the overall accuracy of the instrument, the ease of operation, and the time saving it would afford over direct numerical solution of the equilibrium equation. Accordingly, systematic comparative calculations have been made, numerically and with the Computer, both on purely theoretical problems and some of direct interest in oil production. Several of these will be discussed in the following sections.

As a preliminary to making actual calculations on the Computer it is convenient to convert the equilibrium ratios K_i to the equivalent c_i . These may be prepared in graphical form to take the place of the charts usually used for the K_i . To show the nature of such c_i charts those for methane, propane, n-pentane and n-heptane, as calculated from the corresponding K_i charts published by the NGAA, are reproduced

in Figs. 4-7. In the case of Fig. 4 for methane the c_i are all positive, since the corresponding K_i exceed 1, and give smooth continuous curves. For propane, n-pentane, and n-heptane, however, the c_i curves each have two segments, joining where the K_i equal 1. At these junction points the c_i theoretically become infinite, and they change sign on passing the singularities, although for simplicity only the absolute values are plotted in Figs. 5-7. The overlapping of the curves on Figs. 5-7 thus do not imply any ambiguity in the c_i values, and experience has shown that these charts can be used with the Computer quite as conveniently as the K_i charts in the conventional numerical calculations.

Theoretical Problem

A theoretical problem was chosen which involved the determination of the phase equilibrium in a mixture of me-

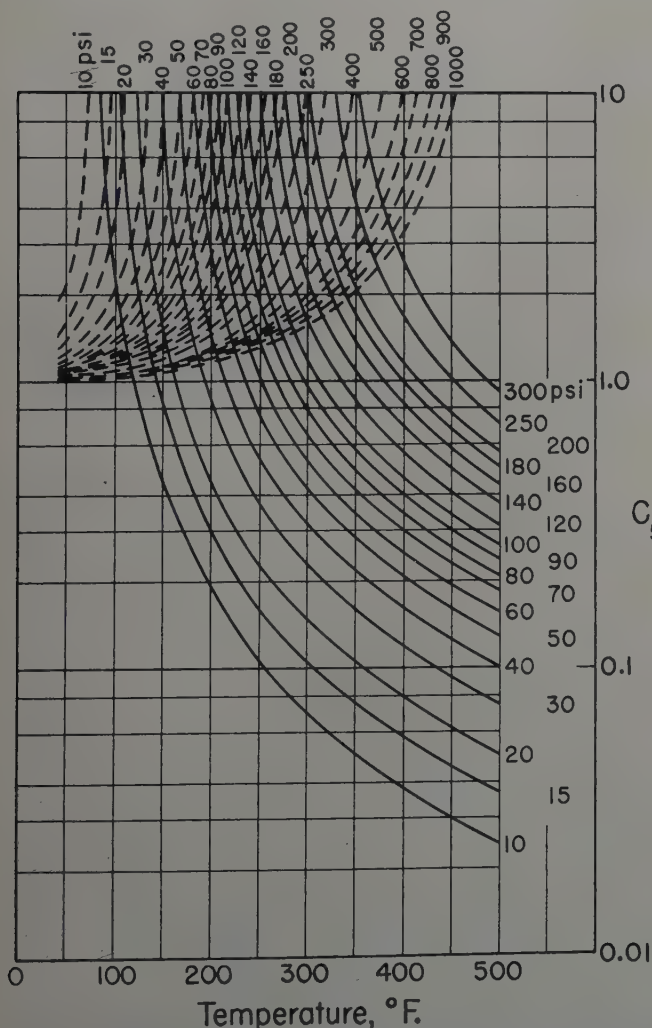


FIG. 6 — ISOBARIC CHART OF THE EQUILIBRIUM RATIO FUNCTION FOR N-PENTANE, c_5 , VS. THE TEMPERATURE. DASHED SEGMENTS GIVE ABSOLUTE VALUES WHERE $c_5 < 0$.

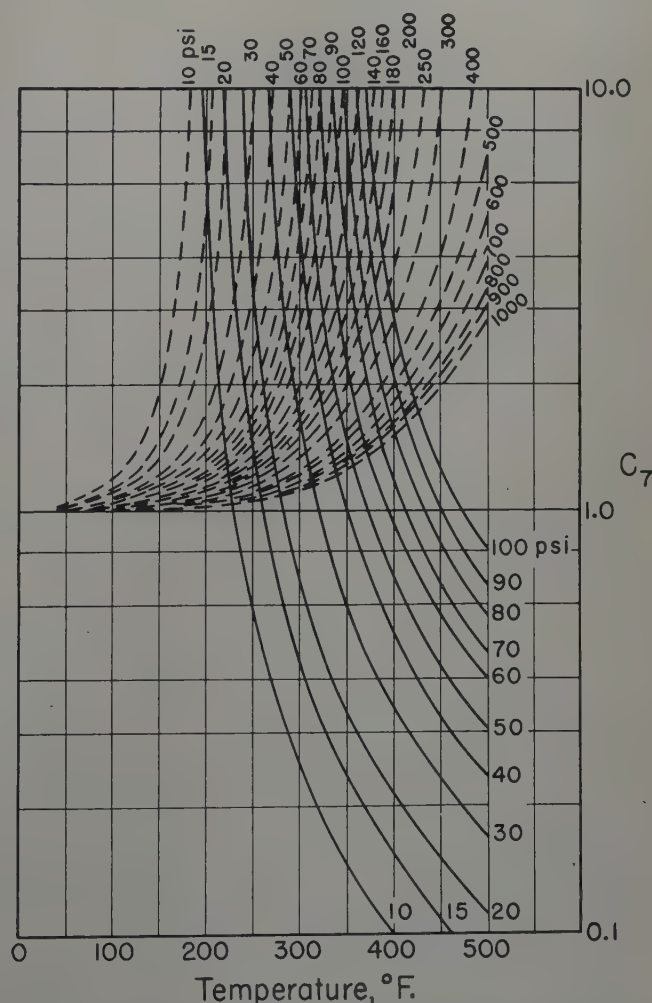


FIG. 7 — ISOBARIC CHART OF THE EQUILIBRIUM RATIO FUNCTION FOR N-HEPTANE, c_7 , VS. THE TEMPERATURE. DASHED SEGMENTS GIVE ABSOLUTE VALUES WHERE $c_7 < 0$.

thane, ethane, pentanes, and heptanes at a temperature of 245°F, and a pressure of 500 psia. The relative amounts of methane and heptanes present in the mixture were changed keeping a constant percentage, 10 per cent, of both ethane and pentanes. The value of n_g and the x_j 's were calculated numerically using Eqs. (2) and (3), and the results were compared with those obtained by using the Computer. These results and comparisons are presented in Table I. The errors in n_g and Σx_j are tabulated for each case. The largest error in n_g is 0.0015. Although this error amounts to 3.2 per cent of the value of n_g in one case, the resulting error in Σx_j for this case is only 0.0004 or 0.04 per cent. The largest error in Σx_j is 0.6 per cent. It thus appears that an error of ± 0.002 may result in the value of n_g . However, with care, better accuracy can be obtained, especially if the resistor settings are made by the use of a resistance measuring bridge to obtain more accurate values.

A Sample Problem for Determining Optimum Separator Pressures

As an example of an application of the Computer to a study of crude oil separation in field operations, Computer calculations were made on the effect of separator conditions on the gas-oil ratio, stock tank gravity and yield for the oil produced from the Witcher pool in Oklahoma. Equivalent complete numerical calculations had been previously made on this problem,* thus providing a basis for comparison of the two methods. For purposes of brevity only a typical set of results will be shown here.

Fig. 8 gives a series of curves for the case of single stage separation only, and thus shows the comparison of the results of Wilkins with the Computer calculations in graphical form. The differences between the smooth curves and the plotted points indicating the laboratory results are quite small, except for two points on the per cent increase in oil recovery curve. While the latter discrepancies seem quite large because of the scales used, the differences in absolute yields are only 0.13 per cent and 0.24 per cent. The Computer results would indicate that a maximum

TABLE I—Accuracy of the Electrical Computer as Indicated By an Equilibrium Problem Involving a Mixture of Four Hydrocarbons

% Methane	% Heptanes	n_g Calculated	n_g from Computer	Error in n_g	Σx_j using n_g	Error in Σx_j
10	70	0.0465	0.0450	0.0015	0.9996	-0.0004
20	60	0.1902	0.1900	0.0002	1.0000	0.0000
30	50	0.3270	0.3255	0.0015	0.9987	-0.0013
35	45	0.3942	0.3935	0.0007	0.9991	-0.0009
40	40	0.4613	0.4600	0.0013	0.9983	-0.0017
45	35	0.5285	0.5270	0.0015	0.9978	-0.0022
50	30	0.5959	0.5960	0.0001	1.0002	+0.0002
55	25	0.6638	0.6626	0.0012	0.9977	-0.0023
60	20	0.7325	0.7320	0.0005	0.9989	-0.0011
65	15	0.8026	0.8032	0.0006	1.0020	+0.0020
70	10	0.8747	0.8750	0.0003	1.0013	+0.0013
75	5	0.9501	0.9508	0.0007	1.0060	+0.0060

Note: For this theoretical problem a four component mixture was used having 10% Ethane, 10% Pentanes, in addition to hydrocarbons above.

Temperature was 245°F., pressure 500 psia, $K_1 = 9.7$, $K_2 = 2.7$, $K_5 = 0.38$, and $K_7 = 0.03$.

TABLE II—Indication of Accuracy of Two Sample Calculations of Two Successive Flash Vaporizations Using the Electrical Computer

Component	n_j	Pres.=300 psia., Temp.=95° F.			Pres.=14 psia., Temp.=65° F.		
		$x_j = n_j$	$\bar{x}_j = \bar{n}_j$	Error in x_j	x_j	\bar{x}_j	Error in x_j
C ₁	0.4548	0.0633	0.0629	+0.0004	0.0009	0.0010	-0.0001
C ₂	0.0987	0.0625	0.0617	+0.0008	0.0068	0.0068	0.0000
C ₃	0.0699	0.0864	0.0864	0.0000	0.0310	0.0304	+0.0006
C ₄	0.0475	0.0812	0.0814	-0.0002	0.0575	0.0575	0.0000
C ₅	0.0289	0.0580	0.0582	-0.0002	0.0599	0.0601	-0.0002
C ₆₊	0.3002	0.6476	0.6494	-0.0018	0.8452	0.0842	+0.0010
	1.0000	0.9990	1.0000	-0.0010	1.0013	1.0000	+0.0013

$n_g = 0.545$, $\bar{n}_g = 0.5464$
Error = 0.0014

$n_{g'} = 0.263$, $\bar{n}_{g'} = 0.2596$
Error = 0.0034

Component	n_j	Pres.=150 psia., Temp.=75° F.			Pres.=14 psia., Temp.=65° F.		
		$x_j = n_j$	$\bar{x}_j = \bar{n}_j$	Error in x_j	x_j	\bar{x}_j	Error in x_j
C ₁	0.4548	0.0318	0.0320	-0.0002	0.0008	0.0008	0.0000
C ₂	0.0987	0.0415	0.0419	-0.0004	0.0069	0.0069	0.0000
C ₃	0.0699	0.0729	0.0729	0.0000	0.0342	0.0338	+0.0004
C ₄	0.0475	0.0796	0.0795	+0.0001	0.0640	0.0631	+0.0009
C ₅	0.0289	0.0619	0.0618	+0.0001	0.0631	0.0630	+0.0001
C ₆₊	0.3002	0.7135	0.7119	+0.0016	0.8344	0.8324	+0.0020
	1.0000	1.0012	1.0000	+0.0012	1.0034	1.0000	+0.0034

$n_g = 0.589$, $\bar{n}_g = 0.5880$
Error = 0.001

$n_{g'} = 0.163$, $\bar{n}_{g'} = 0.1628$
Error = 0.0002

Note: \bar{x}_j and \bar{n}_g represent accurate calculated results. The primed symbols, such as $x_{j'}$ or $\bar{x}_{j'}$, represent values of the quantities for the second flash vaporization in each of the two examples.

TABLE III—Comparison of Electrical Computer Results with Calculated Results of Buckley for a Flash Vaporization at 130°F and 0 PSIG

Component	Weight in %	Molecular Weight	Mol Fraction n_j	Equi. Ratio $K=y/x$	x_j Buckley	x_j Elec. Comp.	y_j Buckley	y_j Elec. Comp.
Methane.....	7.45	16.03	0.4380	256.0	0.0031	0.0032	0.7925	0.7924
Ethane.....	1.22	30.05	0.0382	28.0	0.0024	0.0024	0.0673	0.0674
Propane.....	1.06	44.06	0.0227	13.0	0.0030	0.0029	0.0387	0.0388
Iso-butane.....	0.91	58.08	0.0148	6.7	0.0036	0.0037	0.0239	0.0240
N-butane.....	0.73	58.08	0.0119	4.9	0.0038	0.0038	0.0185	0.0185
Iso-pentane.....	0.50	72.09	0.0065	2.1	0.0041	0.0042	0.0085	0.0085
N-pentane.....	0.79	72.09	0.0104	1.66	0.0076	0.0078	0.0126	0.0127
Hexanes.....	2.11	86.17	0.0231	0.83	0.0290	0.0290	0.0183	0.0178
Heptanes.....	3.27	100	0.0307	0.245	0.0525	0.0526	0.0129	0.0132
Octanes.....	3.21	114	0.0265	0.087	0.0533	0.0533	0.0047	0.0046
Nonanes.....	4.21	128	0.0309	0.032	0.0661	0.0662	0.0021	0.0020
Heavier.....	74.54	203	0.3463	0.000	0.7715	0.7713		
	100.00		1.0000		1.0000	1.0004	1.0000	0.9999

Buckley's $n_g = 0.551$; Elec. Comp. $n_g = 0.551$

* This study has been made by R. B. Wilkins, and is being published in the Oil and Gas Journal. The authors are indebted to him and the management of the Gulf Oil Corporation at Tulsa for making this work available to them.

value (or minimum) of each curve would be reached at a separator pressure of about 150 psia instead of 110 psia. However, the difference in oil recovery, oil gravity or gas-oil ratio would be almost negligible at these two pressures, and the use of the optimum conditions indicated by the Computer would lead to results which would not be significantly less satisfactory from a practical standpoint. The agreement between the calculated and Computer results on the whole were within 0.5 per cent.

In addition to the above discussed comparison of the gross results, a com-

parison between the Computer and accurate numerical calculations of the complete compositions for several flash vaporizations was made. The results are given in Table II for, (1) a flash vaporization at 300 psia and 95°F, and the resulting liquid flashed again at atmospheric pressure and 65°F, and (2) a flash vaporization at 150 psia and 75°F and the resulting liquid flashed at atmospheric pressure and 65°F. It will be noted that the error in the Computer values for Σx_i ranges up to 0.0034. However, this represents an accumulated error of two successive computations, since no attempt was made to

correct the mol fractions of each component in the liquid phase after the first flash vaporization so that their sums would equal one. It can be seen that the errors in the values of x_i vary somewhat as the magnitude of the x_i 's. The error in n_g ranges up to 0.0034, but this also represents an accumulated error. These results should serve to indicate the accuracy of the various quantities involved in using the Phase Equilibrium Computer.

Sample Problems Showing Variation of n_g with the Composition

In Fig. 9 are shown the variations in the mol fractions in the gas phase, n_g , with the composition of various hydrocarbon mixtures. The basic data for the solid and dot-dash curves were obtained from Table II, the methane and hexane + components being varied so that their total would remain the same. The data for the dashed curve were obtained from Table I. In all cases the curves are nearly straight lines, and the corresponding curves for each problem are nearly parallel. The position of the curves will of course depend on the other components in the mixture and the pressure and temperature. However, all the graphs have slight curvatures, which tend to increase in some cases as the percentage of methane (or the heavier component) approaches either zero or its maximum value.

This type of calculation serves to show the sensitivity of the phase equilibrium separation to the exact composition of the mixture, and the effect of errors in the latter on the quantitative features of the phase separation. By using the Computer, studies of this kind can be made perhaps a hundred times as fast as by direct numerical solution of the equilibrium equations.

The Sensitivity of the Phase Equilibrium Separation to the Accuracy of the Equilibrium Ratios

An especially interesting and valuable application of the Computer is the investigation of the effect of the sensitivity of the phase calculations to the accuracy of the equilibrium data. While such a study would require laborious repeat calculations, if done numerically, it is solved with extreme simplicity on the Computer by merely observing the change in the null setting of the n_g

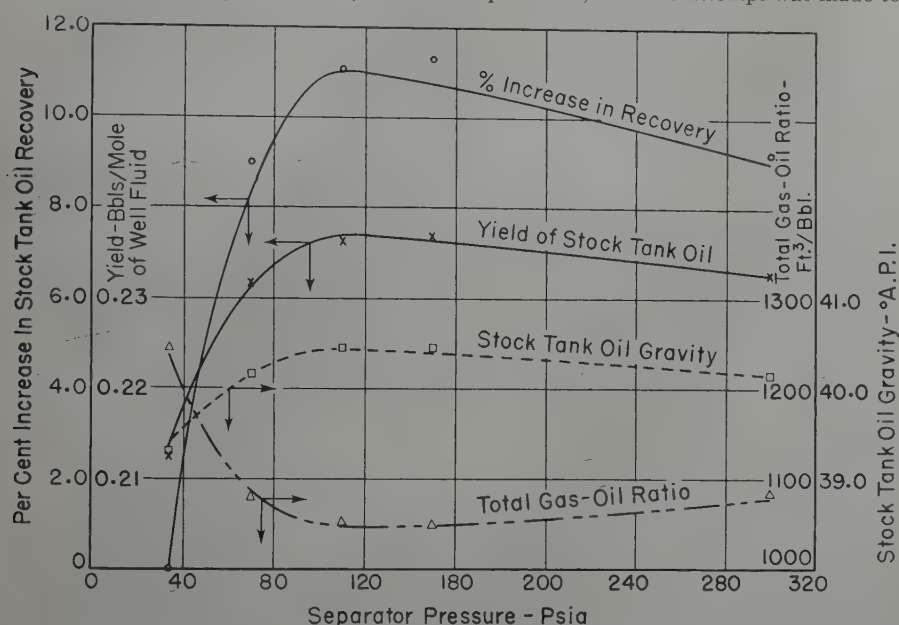


FIG. 8—COMPARISON OF CALCULATED (CURVES) AND PHASE EQUILIBRIUM COMPUTER RESULTS (POINTS) FOR SINGLE STAGE SEPARATION AS A FUNCTION OF THE SEPARATOR PRESSURE.

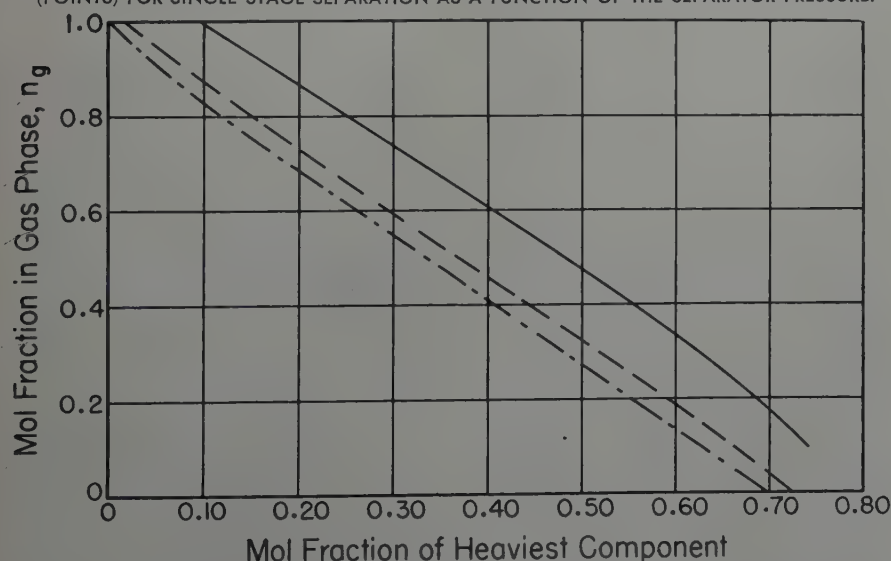


FIG. 9—THE VARIATION OF THE MOL FRACTION OF HYDROCARBON MIXTURES IN THE GAS PHASE WITH THE CONCENTRATION OF THE HEAVIEST COMPONENT, WHILE KEEPING THE SUM OF THE LATTER AND OF METHANE FIXED.

—: 6 COMPONENT MIXTURE AT 14 PSIA, 65°F, WITH $n_1 + n_{6+} = 0.744$;
 ---: 6 COMPONENT MIXTURE AT 300 PSIA, 95°F, WITH $n_1 + n_{6+} = 0.755$;
 - · - ·: 4 COMPONENT MIXTURE AT 500 PSIA, 245°F, WITH $n_1 + n_7 = 0.80$.

dial as the corresponding c_i dial is changed. Figs. 10 and 11 show typical results of such an application. While the curves of these figures show rather systematic variations of the values of n_g with changes in the values of the K_i , they are to be considered only as illustrative of a type of application of the Computer. The absolute magnitudes given in these figures and the relative values for the different components are undoubtedly rather complex functions of the values of the individual components and the compositions of the component mixtures. It is undoubtedly for this reason that the characteristics of the curves for Fig. 10, which roughly simulates a reservoir crude oil-natural gas mixture, is radically different from those of Fig. 11, which refers to a low pressure gas depleted crude oil. In any case, however, it does appear from these preliminary and illustrative results that the absolute value of n_g is not very sensitive to the accuracy with which the equilibrium ratios are determined. This, in itself, is of considerable practical interest.

Problem Checking the Use of All Twelve Components

A final problem was solved to check the operation of the Computer when all twelve components are used. This problem is the same as one treated numerically by Buckley.¹ Table III gives the necessary data and the results of the flash vaporizations at 130°F. and 0 psi gauge. The agreement here is extremely close. To check if this agreement was entirely accidental, the problem was solved twice, but the results were almost identical. The x_i 's were measured with the voltmeter through n-pentane, and calculated for the hexanes and heavier components using Eq. (2). The y_i 's were calculated using Eq. (2) for methane through n-pentane, and measured with the voltmeter for the hexanes and heavier components.

CONCLUSIONS

The Phase Equilibrium Computer described in this paper should be of value in the solution of problems involving the phase equilibrium between gas and liquid in any hydrocarbon mixture, especially if such determinations must be made a large number of times. Depending on the number of components, each flash vaporization can be calculated in 10 to 20 minutes

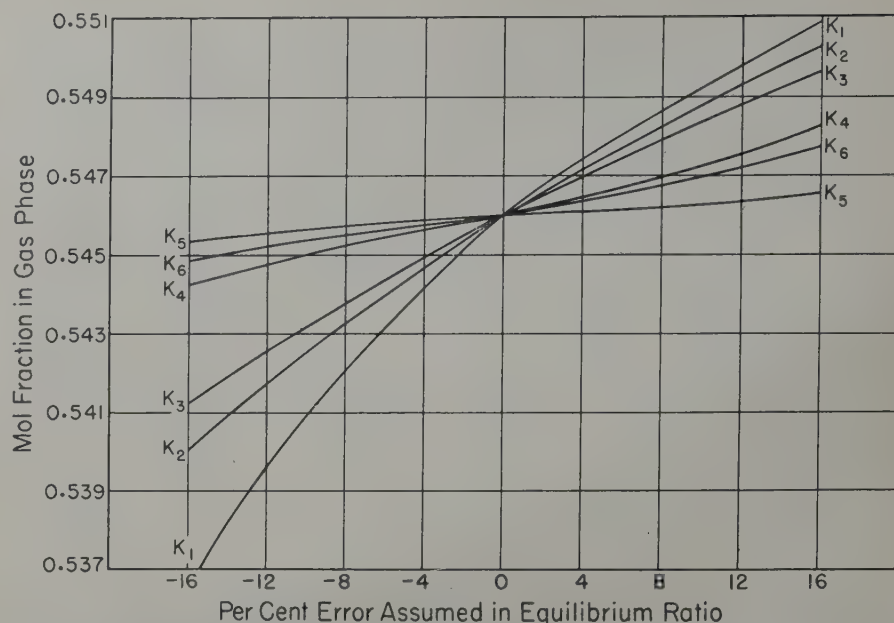


FIG. 10 — THE EFFECT OF ERRORS IN THE EQUILIBRIUM RATIO ON THE COMPUTED VALUES OF THE MOL FRACTION IN THE GAS PHASE OF A HYDROCARBON MIXTURE WITH A COMPOSITION: $n_1, n_2, n_3, n_4, n_5, n_6 = 0.4548, 0.0987, 0.0699, 0.0475, 0.0289, 0.3002$. INDIVIDUAL CURVES REFER TO INDIVIDUAL K VALUES IN WHICH ERRORS WERE INTRODUCED. ASSUMED CORRECT K VALUES ARE: $K_1, K_2, K_3, K_4, K_5, K_6 = 12.4, 2.1, 0.65, 0.238, 0.079, 0.0157$.

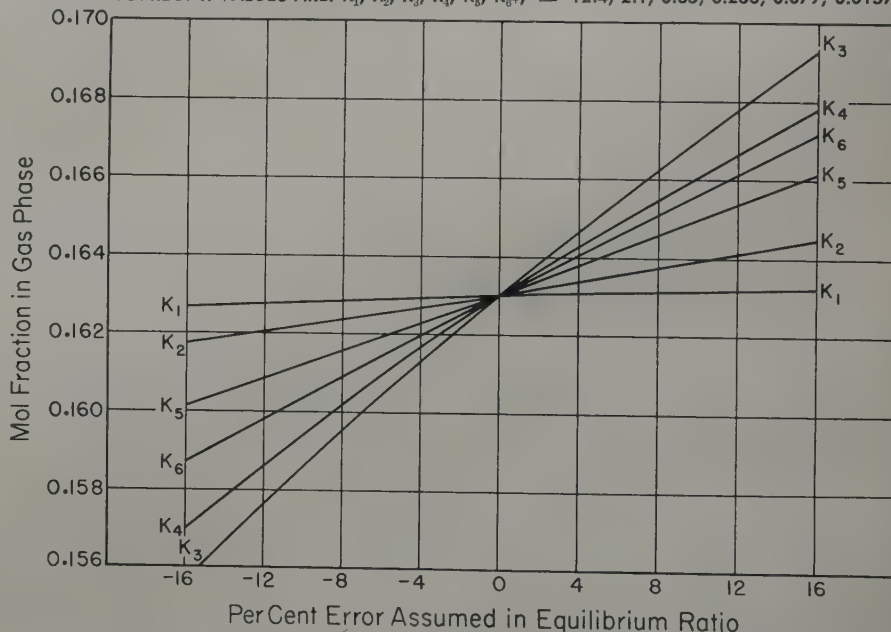


FIG. 11 — THE EFFECT OF ERRORS IN THE EQUILIBRIUM RATIO ON THE COMPUTED VALUES OF THE MOL FRACTION IN THE GAS PHASE OF A HYDROCARBON MIXTURE WITH A COMPOSITION: $n_1, n_2, n_3, n_4, n_5, n_6 = 0.0320, 0.0419, 0.0729, 0.0795, 0.0618, 0.7119$. INDIVIDUAL CURVES REFER TO INDIVIDUAL K VALUES IN WHICH ERRORS WERE INTRODUCED. ASSUMED CORRECT K VALUES ARE: $K_1, K_2, K_3, K_4, K_5, K_6 = 250, 32.0, 8.1, 2.6, 0.88, 0.111$.

using the Computer. These time requirements can be substantially reduced by providing more stable voltage supplies to eliminate the readjustment in initial voltage settings required as the result of interactions between the parallel circuits representing the individual components in the first model of the Computer. The error in the final results will be no greater than 0.5% for most problems, and may be reduced if the

resistors representing the c_i are set according to their calibrated values.

The authors are indebted to Miss M. O. Taylor for calculating the c_i charts given in this paper, and to P. D. Foote, executive vice president of Gulf Research and Development Company, for permission to publish it.

REFERENCES

1. S. E. Buckley, *Trans. AIME*, 127, 178 (1938).

★ ★ ★

WAVE FORCES COMPUTED FOR A TYPICAL OFFSHORE DRILLING SITE

PAUL L. HORRER, SCRIPPS INSTITUTION OF OCEANOGRAPHY, LA JOLLA, CALIFORNIA

ABSTRACT

Costly damage by severe wave attack to many engineering structures has illustrated the need for a consideration of the nature of wave action in plans for offshore drilling operations. Using wave data it is possible to answer questions pertaining to engineering problems such as platform elevation, structure orientation, and expected wave forces. For locations where wave records are not available a technique can be used to obtain information about wave characteristics from past meteorological data and near shore submarine topography. Forces exerted on structures by waves may be divided into four parts. A completed study is given in which frequencies of various wave heights and maximum frictional drag forces are computed for a typical offshore drilling site.

INTRODUCTION

Waves of tremendous proportions accompanying hurricane winds crash against breakwaters and other offshore structures causing untold damages. Wave forces exerted on structures at these times are enormous, as shown by past records of incidents where massive portions of breakwaters have been broken off and moved by waves. On other similar occasions, whole structures have been unloosed and smashed or floated away. These incidents, which seem almost incredible, serve to illustrate the great amount of energy contained in large waves, and to show that this energy results in powerful forces destructive to offshore installations which are not designed sufficiently strong to withstand wave attack.

In the past the expected frequencies of waves having various characteristics have rarely been considered in the design of structure affected by wave action. As a result, many structures have failed to accomplish the purpose for

which they were designed or have collapsed under wave attack. Others have been constructed to withstand greater wave energy than is ever encountered, with resulting waste of material and construction time.

In this study an analysis is made of the frequencies of waves having different characteristics which affect the plans for offshore drilling installations. After such an analysis the erection of these structures can proceed with less risk involved and with more efficiency and economy.

ENGINEERING ASPECTS

In the offshore drilling program wave forces play an extremely important part in design and construction of drilling rigs in shallow water. The design of a platform or other structure from which drilling equipment is operated is critical, because any damage to the platform may endanger personnel and result in complete loss of equipment. Since a platform built too close to the water would be battered by breakers, and one built unnecessarily high would involve undue expense, it is necessary to know the most desirable elevation at which the platform should be erected. This is only one of many questions about structural planning which can be answered using existing technique for determining wave characteristics.

The purpose of efficient design for the portions of many types of offshore structures which are acted upon by wave forces is the same as that of all designs which deal with frictional forces of a fluid on a solid. For these structures the problem is comparable to that encountered by undersea craft moving through water, except that in the case of a fixed structure the force is produced by the water moving past the model. For offshore structures which are extremely rigid the frictional forces may be nearly negligible compared with the impact or shock forces imparted by breaking waves. In all cases the better design is that which offers

the least resistance to the opposing forces.

From a consideration of wave forces, each drilling structure varies in efficiency depending upon the type and amount of superstructure in contact with the waves. For example, round piling and bracing offer less resistance to wave forces than do I-shaped ones. All network superstructure such as cross bracing should be kept to a minimum and at as low an elevation as possible, so that it will not experience the pressure exerted at the tops of breaking waves. Models of proposed structures can be tested in wave tanks and in the field to ascertain the efficiency of specific designs.

Past experience in beach and shoreline engineering has shown that, although changes in the topography of the bottom very near shore do not seem to be occurring, the natural forces involved may be in a delicate balance such that a static state exists. Interruptions of any of these natural forces by erecting offshore structures are likely to cause undesirable effects. Changes in beach profile result partly from sediment being brought into suspension by the orbital motion of waves and partly from the transport of sediment by longshore currents. With the erection of an offshore structure and consequent change in the combined effects of these two forces, unfavorable deposition upon, or erosion of, the bottom at the site may occur. Therefore, combination wave and current studies are essential for the solution of problems involved in the design of most marine structures.

TECHNIQUE FOR OBTAINING WAVE INFORMATION

In determining the probable effect of wave action on an offshore drilling structure, it is first necessary to know the usual frequencies of certain wave types for the given location. A technique^{1,8,9,11,12} has been developed which provides a means for obtaining information about wave characteristics in the

Manuscript received at office of the Petroleum Branch August 12, 1949. Presented at Branch Fall Meeting, San Antonio, Texas, October 5-7, 1949.

¹References are given at end of paper.

past using meteorological data and the known submarine topography of the region. The procedure for obtaining this information at a given location involves three steps: the first utilizes past weather maps, which are readily available, for the computation of wave characteristics in deep water; the second determines the modification of these characteristics as the waves travel into shallow water towards shore; the third, using the shallow water wave characteristics, provides the expected frequencies of forces and moments on engineering structures at the proposed location.

METEOROLOGICAL CONSIDERATIONS

Waves are produced in an area where moderate to strong winds are blowing over the ocean and exerting frictional drag on the water surface. The higher waves result from strong winds when there are relatively large areas over which the winds are blowing. After formation, waves move out of the generating area and proceed with gradually diminishing heights through areas of calm or variable winds until, after traveling hundreds of miles, their heights may become insignificant. It is therefore necessary in computations of waves to consider storms occurring in all parts of the sea or ocean in which the drilling site is located. As an example⁶ of wave propagation over great distances, the nature of the surf and character of the beach in some parts of Southern California in summer are largely determined by waves which have traveled from the southern hemisphere.

At any given instant, ocean waves are usually not uniform but have a variety of heights and periods. The procedures for determining the characteristics of waves in deep water which progress toward a given location immediately offshore have been devised so as to give the average height and period of the highest one-third of all waves present. An analysis¹³ of Pacific Coast wave records indicates that the average height of the highest 10 per cent of the waves is equal to 1.29 times the height of the highest one-third. The maximum highest wave measured each day has a height which is equal to 1.87 times the average height of the highest one-third. The computations made in this study are completed for both the highest 10

per cent and the maximum highest waves which are expected.

EFFECT OF IRREGULAR BOTTOM NEAR SHORE

As waves enter shallow water they are transformed under the influence of bottom topography. Refraction occurs when the wave crest advances over an uneven bottom. The portions of the wave which are in deeper water have a greater velocity than those in shallow water. This causes a bending of the crest. Under such circumstances the wave energy is concentrated in some shore areas and reduced in others. Consequently, wave height may be either

increased or decreased as waves travel into shallow water towards the breaker zone.

The drawing⁹ of refraction diagrams is a portion of the technique essential to the accurate computation of wave forces in shallow water. In Fig. 1 is shown a sample refraction diagram⁹ illustrating convergence and divergence of wave energy due to refraction over irregular bottom. The magnitude of the refraction factors, to which the wave heights are directly proportional, is indicated by the length of the bars shown in Fig. 1. The wave heights, as determined by these refraction factors, vary from 20 per cent to 350 per cent of the heights the same waves would have if no refraction occurred.

Refraction diagrams are useful in determining the best location for a drilling site. The importance of selecting a location where convergence does not occur cannot be over emphasized.

NATURE OF WAVE FORCES

In shallow water the maximum wave height at any depth is that of a wave whose characteristics are such that it breaks at that depth. Although the total energy of a wave is slightly reduced as it comes into water shallow enough to alter its form, a greater portion of its total energy then lies above still water level and moves forward with the wave form. Consequently a breaker produces a much greater stress on structures than would a wave of equal height in deep water. The frequency of breakers of different kinds at a given location depends upon the

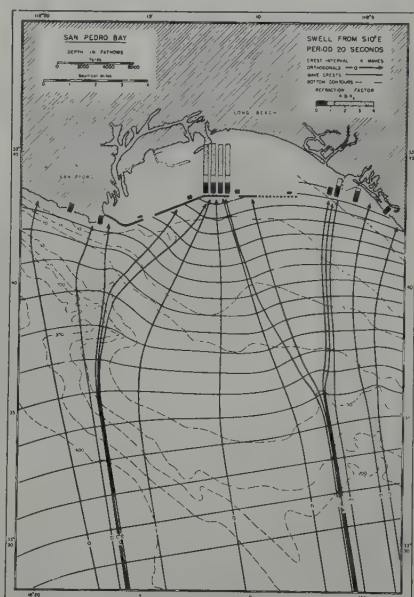


FIG. 1—A SAMPLE REFRACTION DIAGRAM ILLUSTRATING CONVERGENCE AND DIVERGENCE OF WAVE ENERGY DUE TO REFRACTION OVER IRREGULAR BOTTOM.

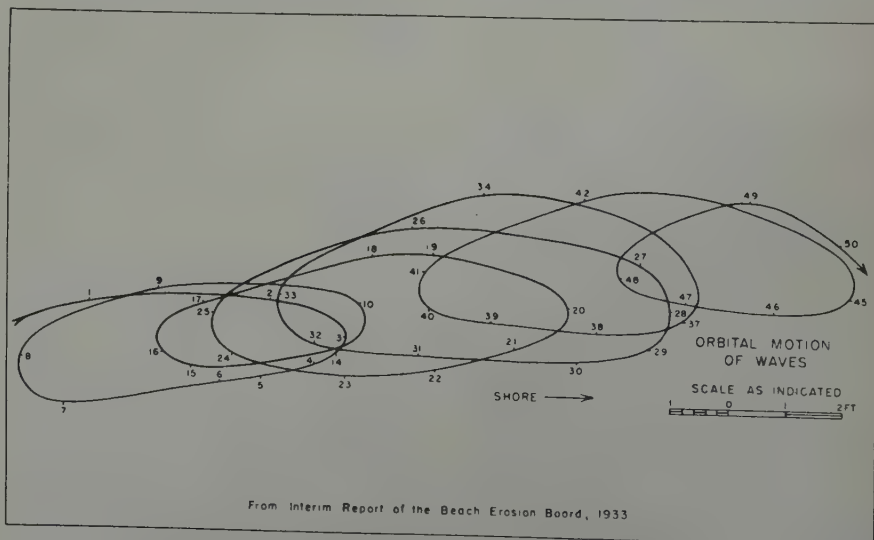


FIG. 2—ORBITAL MOTION OF WAVES 5 FT TO 7 FT BELOW SURFACE OF WATER. TIME INTERVAL TWO SECONDS FOR EACH CONSECUTIVE NUMBER.

frequency of waves of different heights in deep water offshore, refraction characteristics over shallow bottom near the location, and the depth of water at the location.

For all but very short period waves a linear relationship exists between the height of breakers and the depth of water in which breaking waves occur. The depth at a drilling site may vary due to regular astronomical tides and also due to storm tides which result from piling up water along the coast by wave transport and transport due to wind stress on the sea surface. For this reason at a given location there are a number of different breaker heights possible, of which the greatest may occur only in connection with intense storms. Rather large depth changes at a given location are especially characteristic in the case of hurricanes, and special consideration must be given to the associated problems in the Gulf of Mexico where hurricane waves are not infrequent.

The forces exerted by waves on struc-

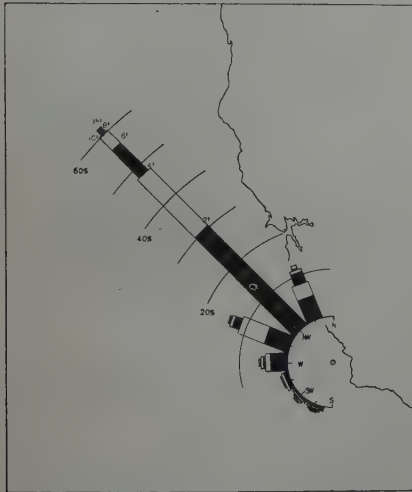


FIG. 3 — WAVE HEIGHT AND DIRECTION IN DEEP WATER.

tures in or near the breaker zone are due to (1) acceleration, (2) friction, (3) impact, and (4) hydrostatic head.

It has been shown^{6,7} that the acceleration force and frictional drag force are related to the particle or orbital motion of the waves. The nature of the particle movement in waves has been studied³ using motion pictures of a float in a wave, and a picture is shown in Fig. 2. The dynamic pressures exerted by the tops of breaking waves represent the greatest frictional drag to which structures may be subjected by wave action because at the very crests of breaking waves the orbital velocity is at a maximum. The acceleration force is a maximum prior to the arrival of the crest.

The magnitude of each of the four types of force may vary depending upon the design characteristics of a given structure as well as the wave characteristics. For example, an analysis⁵ of breakwater damage indicated that a breakwater erected on a random rubble foundation may be less subject to damage by wave impact or shock force than a breakwater built upon a more rigid cut stone foundation. Wave tank studies² show that impact forces of extremely short duration due to waves breaking on certain structures may be at least one order of magnitude greater than forces due to friction and acceleration. The pressure due to hydrostatic head is of importance only in the case of structures such as breakwaters where a water level difference is maintained by waves.

STUDY FOR TYPICAL DRILLING SITE

For illustrative purposes an application of the entire wave computation

technique has been made for a location off the coast of California at 35°N latitude in 20 feet depth, mean low water. Fig. 3 shows statistics on wave height and direction in deep water calculated¹⁰ for the three years 1936 to 1938. In deep water it can be seen that the greater percentage of higher waves is from the northwest. These statistics shown in Fig. 3 provide the basis upon which the wave forces at the site are computed.

In order to examine the effects of the bottom on waves approaching the sample drilling site, 17 refraction diagrams were drawn for waves of different directions and periods. Fig. 4 summarizes the refraction effects at the drilling site for all of the 17 individual diagrams. It shows what portions of deep water wave height remain after refraction for waves of different periods and deep water directions. Since no portion shown is greater than unity, it can be seen that little or no convergence is present at this location. A region of approximately no change in wave height due to refraction exists for directions in the westerly quadrant. As the directions change, either toward the north or toward the south, the waves are seen to diverge in traveling over the shallow depths adjacent to the coast. Using the frequencies of waves greater than a given height at the site, after the shallow water corrections have been applied, it is possible to compute a weighted average of the refraction factors. This can be done for the site and nearby areas to determine whether waves at the site will be larger or smaller on the average than waves in areas adjacent to the site.

Fig. 5 summarizes the directions of wave crest advance at the site for waves

TABLE I
Height and Period Frequencies (in days) at Site for Highest 10 Per Cent of Waves (Total Time 3 Years)
H (Feet)

T(seconds)	Less Than 2 ft.	2-4	4-6	6-8	8-10	10-12½	12½-15	15-17½	17½-19½ (Breakers)	Total
2-4	73.6	41.7	.3	.4						116.0
4-6	168.4	110.0	10.7	9.0	2.4	.3				300.8
6-8	83.1	59.4	25.4	15.1	7.2	2.4				192.6
8-10	50.1	47.9	5.8	5.4	3.6	2.7	.4	.5	.1	116.5
10-12	41.8	40.3	10.9	1.0	3.4	.1	.2		.6	98.3
12-14	43.4	54.5	.3	10.6		2.3	1.4	.8	.4	113.7
14-16	46.8	35.5	20.6	5.6		.2			.1	109.0
16-18	35.2	32.3	17.9	2.2	.1				.9	87.6
18-20	18.8	12.4	5.8	1.4	.3				.1	39.4
Greater than 20	3.4	2.5	.2	.2						6.7
Total	564.6	436.5	97.9	50.9	17.0	8.0	2.2	1.3	2.2	1,180.6

approaching the site and having any given period and direction in deep water. Wave refraction changes not only the wave height, but changes the direction of wave advance, and the change is such that the wave crests tend to become parallel to the bottom contours as the waves approach shore, thereby decreasing the variability in direction of wave approach at the shore. Fig. 5 shows that the waves at the site have a direction varying from 240° to 300° and that this variation in wave direction is greater for the shorter period waves which are less influenced by the bottom topography than waves of longer period. For the longer period waves the direction varies from about 255° to 290°. The weighted average direction at the site for waves higher than a given value can be determined. This direction can be used in determining the orientation of engineering structures which will offer the least resistance or maximum breakwater action, depending on the purpose for which the engineering structures to be employed.

In Fig. 6 is shown the maximum breaker heights associated with a 25-foot depth (mean high water at site) and the corresponding deep water wave heights for different period waves. Because 25-foot depth provides, on the average, the worst possible breaker conditions at the site unless a storm tide is produced, this depth was used for calculating the wave and breaker heights at the site. In most cases the duration of periods having fairly large waves was greater than the time between high and low tide. Fig. 6 does not include refraction effects. It is noted that change in wave height due to shallowing of the water alone varies considerably with period.

Using the refraction effects shown in Fig. 4 and applying other shallow water corrections, the height and period frequencies in days at the site for the highest 10 per cent of the waves and for the maximum highest waves were calculated and are tabulated in Tables 1 and 2. Data of this type may be used for calculating dimensions of waves to be used in model experiments. After refraction, a rather large proportion of the deep water waves had heights which were less than two feet. Consequently, the number of days in

which actual breakers at the site occurred was considerably less than would be expected. Out of the 1180.6 computed days only on 81.6 days were 10 per cent of the waves greater than 6 feet at the site. If only the maximum highest wave is considered, then on 176.4 days were the waves greater than 6 feet. On only 2.2 days were 10 per cent of the waves breaking at the site. On 6.8 days the very highest waves were breaking at the site. These breakers, however, occur with a number of different storms such that there is 100

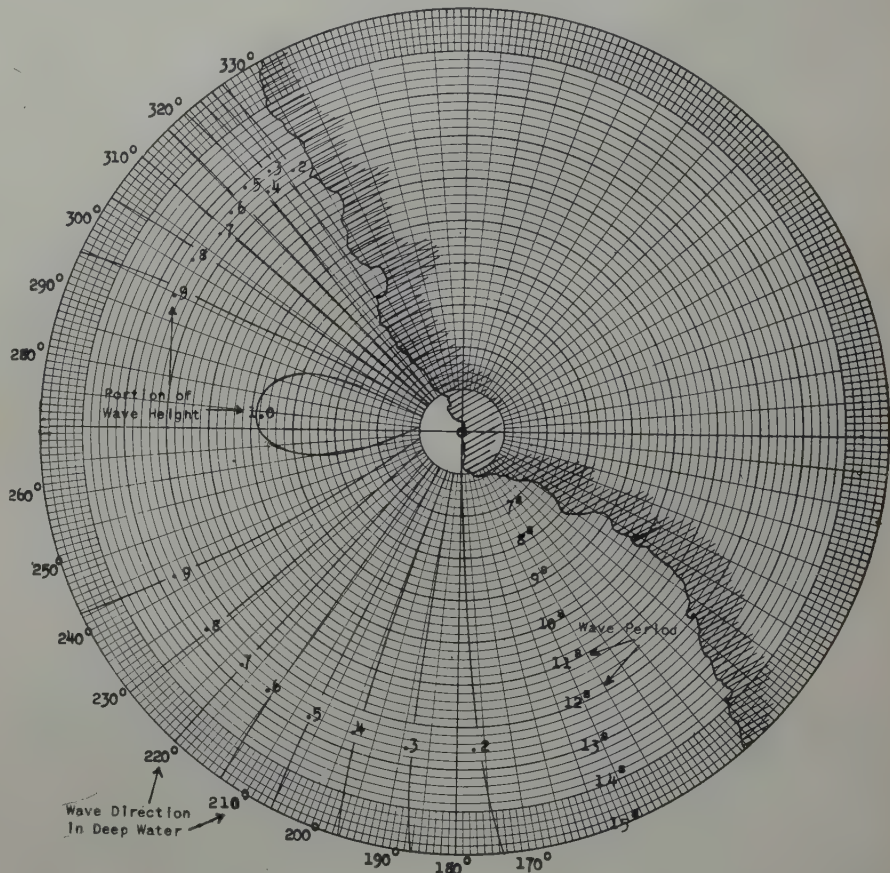


FIG. 4 — PORTION OF DEEP WATER WAVE HEIGHT REMAINING AFTER REFRACTION FOR WAVES OF DIFFERENT PERIODS AND DEEP WATER DIRECTION.

TABLE II

Height and Period Frequencies (in days) at site for Maximum Highest Waves (Total Time 3 Years)
H (Feet)

T(seconds)	Less Than 2 ft.	2—4	4—6	6—8	8—10	10—12½	12½—15	15—17½	17½—19½ (Breakers)	Total
2—4	73.2	35.2	7.8	1.1	.4					116.7
4—6	161.4	60.0	51.5	9.7	7.1	2.3	2.4	.3		294.7
6—8	61.7	43.1	38.5	24.5	3.9	11.4	8.0	1.6		192.7
8—10	49.8	31.0	17.2	5.3	5.2	7.5	3.1	2.3		122.8
10—12	42.8	19.1	21.2	2.8	8.1	3.4			1.4	98.3
12—14	43.0	32.9	22.1	.3	3.1	7.5	2.3		.9	113.8
14—16	27.3	19.5	35.5	20.6	.7	3.8	.2		.3	107.9
16—18	22.8	12.5	32.2	17.7	.9	1.5				87.6
18—20	11.6	7.7	17.7		.4	1.0				39.4
Greater than 20	1.5	1.9	2.5	.2					1.0	6.7
Total	495.1	262.9	246.2	81.2	29.8	38.4	16.0	4.2	6.8	1,180.6

per cent probability that in any given year breakers whose height is 19.5 feet will be formed at the site. If a storm tide of 5 feet had occurred at the times when the largest waves were present, 23.4 foot breakers could also have been formed at the site.

In Fig. 7 is shown the cumulative per cent frequency of various wave heights greater than 6 feet for both the 10 per cent highest and the maximum highest waves. Because a larger number of the maximum highest waves are associated with the larger wave heights, this curve is more steep for the values

of greater height than is the curve for the highest 10 per cent. In computing the wave forces in piling, it has been assumed that it would be desirable to know the forces exerted for various stands of the tide, and also when a storm tide occurred. Therefore, four representative cases have been studied. These cases are tabulated in Table III. Cases 2 and 3 occur frequently as the tide is largely semi-diurnal in character, and Case 2 gives the lowest breakers which could be formed at the site. The maximum horizontal velocities were computed using the solitary wave theory.⁸

Methods for computing forces due to impact and acceleration are not available. However, maximum horizontal dynamic pressures due to frictional drag on circular pile at various elevations above the bottom for these four cases are shown graphically in Fig. 8. For circular pile a drag coefficient of .33 was used in the computations. On a flat plate perpendicular to flow a value of 1.9 should be used such that all pressures in Fig. 8 would be 5.8 times as large for square or I-shaped pile. The total frictional forces on a pile may be obtained by integrating the area to the left of the curves in Fig. 8. The turning moment can be calculated by using the difference between the forces near the top of the curve and that near the bottom. The small pressures of Case 1 are typical of non-breaking waves.

Although forces of acceleration and impact are not shown in Fig. 8 the curves are useful for relative comparison of the effect of wave action from waves having different dimensions.

CONCLUSIONS

Wave forces play an extremely important part in the design and erection of offshore drilling structures. An adequate technique exists for the determination of expected frequencies of waves having different characteristics from past weather data and the known submarine topography of the region, but methods for computing wave forces are not yet complete. The entire procedure has been illustrated by an example in which wave height frequencies and the frictional forces on circular pile are given. Although the techniques used herein have been described elsewhere, an application of all these techniques to one location has not previously been made generally available.

ACKNOWLEDGMENT

I wish to express my thanks to Paula M. Horrer for assistance in computations and in preparing Figs. 3-8.

REFERENCES

1. Arthur, R. S., 1947, "Revised Wave Forecasting Graphs and Procedures," Scripps Institute of Oceanography Wave Report No. 73, 14 pp., 10 plates.
2. Bagnold, R. A., 1939, "Interim Report on Wave-Pressure Research," *Journal Institution of Civil Engineers*, London, v. 12, pp. 202-226.

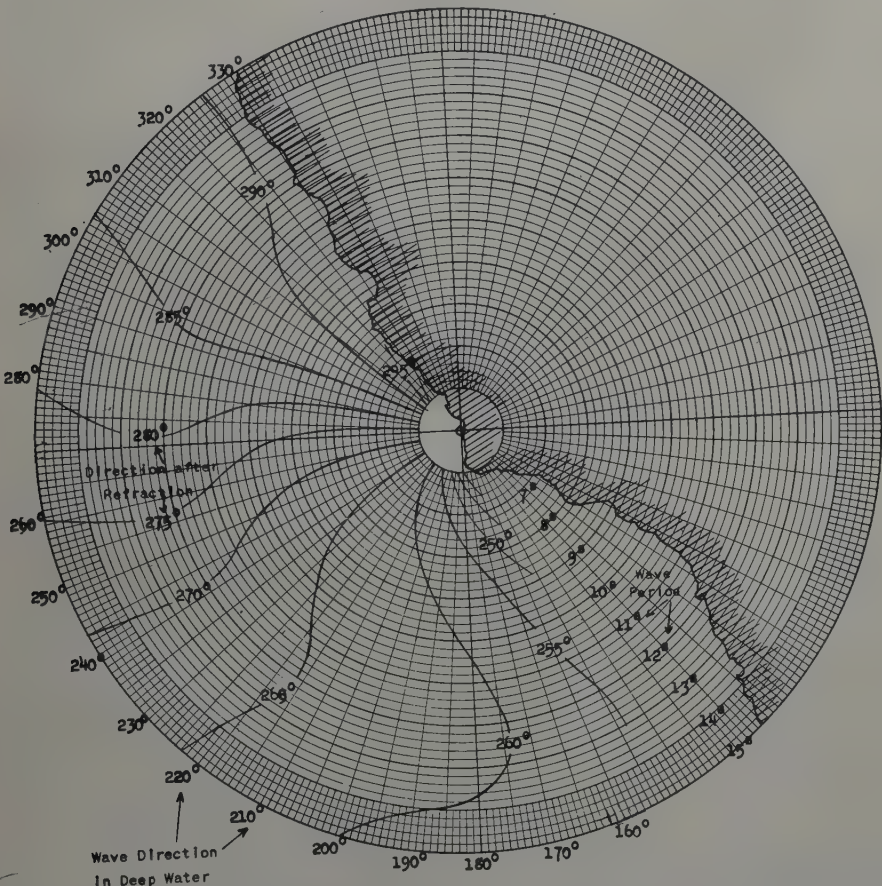


FIG. 5—WAVE DIRECTION AFTER REFRACTION FOR DEEP WATER WAVES OF DIFFERENT PERIODS AND DIRECTIONS.

TABLE III

Representative Cases for Which Maximum Horizontal Dynamic Pressures Due to Frictional Drag Have Been Calculated

	Case 1	Case 2*	Case 3*	Case 4*
Sea (water) Level.....	mean high water	mean low water	mean high water	mean high water and 5' storm tide
Still water depth (feet).....	25	20	25	30
Wave height (feet).....	10.0	15.6	19.5	23.4
Height to crest above bottom (feet).....	32.2	31.7	39.6	47.5
Wave velocity (feet per sec.).....	29.7	32.5	37.9	41.5
Max. Horizontal orbital velocity (feet per sec.).....	10.6	32.5	37.9	41.5
Max. horizontal dynamic pressure due to frictional drag on circular pile (pounds per sq.ft.).....	37	344	473	567

*Breakers

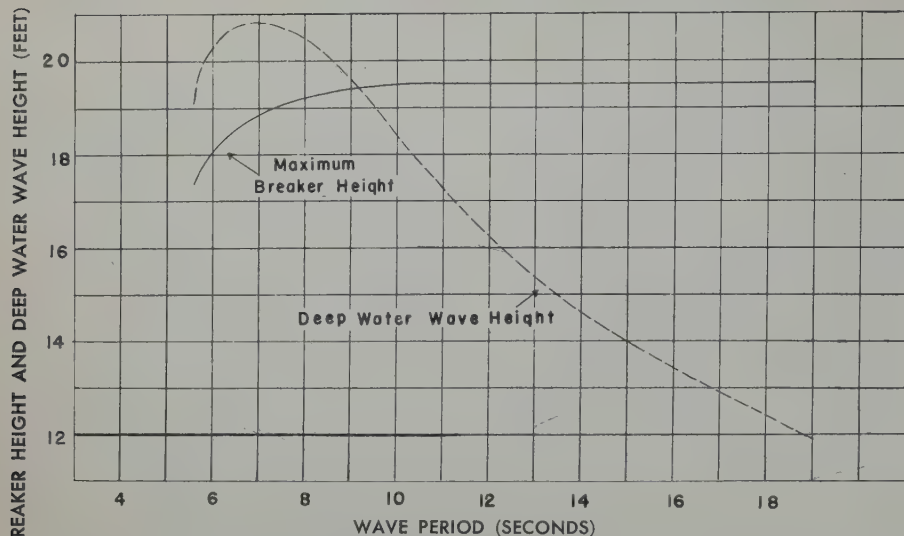


FIG. 6 — MAXIMUM BREAKER HEIGHTS AT 25-FOOT DEPTH AND CORRESPONDING DEEP WATER WAVE HEIGHTS FOR DIFFERENT PERIOD WAVES.

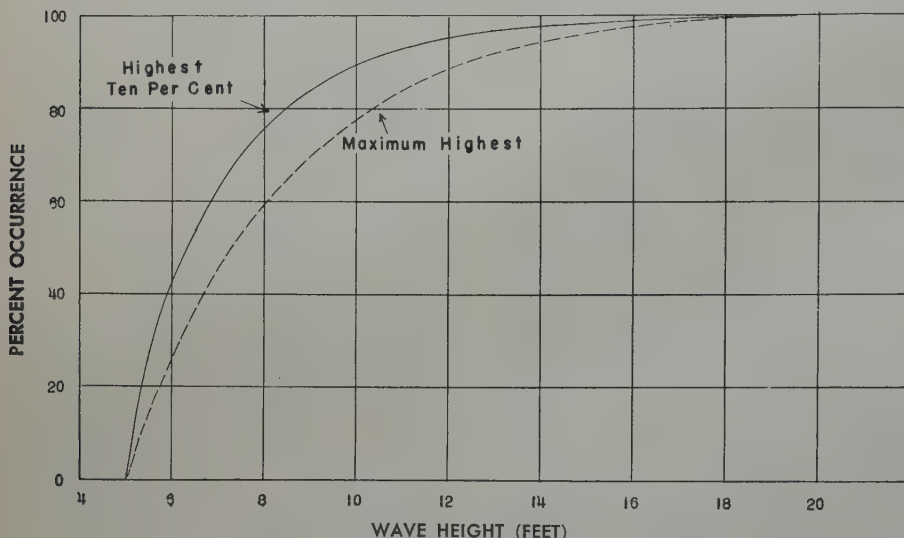


FIG. 7 — CUMULATIVE PERCENTAGE FREQUENCY OF WAVE HEIGHTS FOR HIGHEST TEN PER CENT AND FOR MAXIMUM HIGHEST WAVES WHICH ARE 6 FOOT OR HIGHER AT 25-FT. DEPTH.

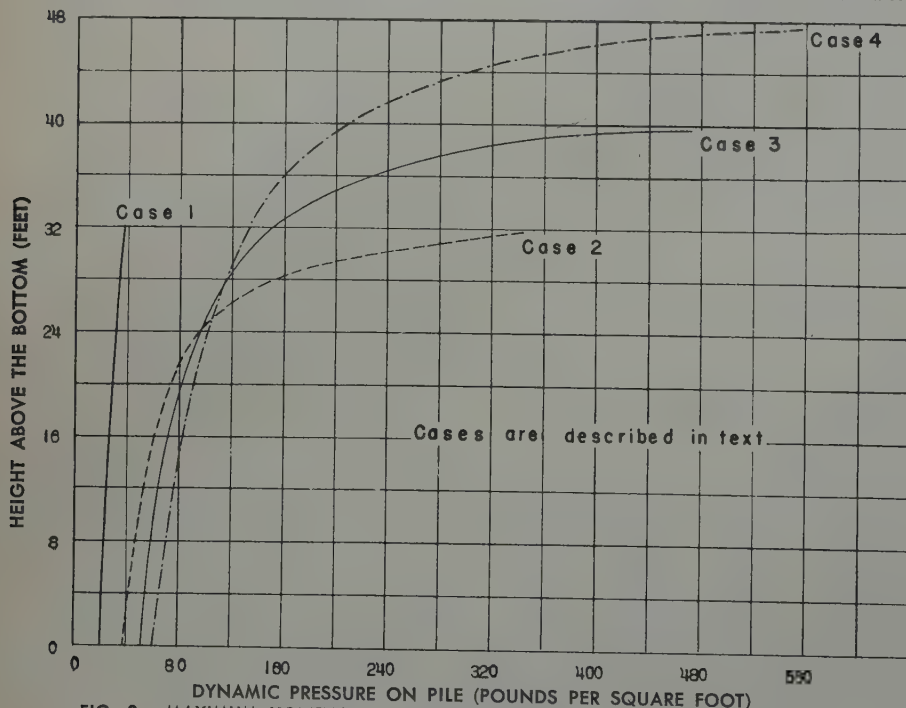


FIG. 8 — MAXIMUM HORIZONTAL DYNAMIC PRESSURES DUE TO FRICTIONAL DRAG EXERTED BY WAVES ON CIRCULAR PILE.

3. Beach Erosion Board, 1933, Interim Report of the Beach Erosion Board, Office of the Chief of Engineers, U. S. Army.
4. Bigelow, H. B., and W. T. Edmondson, 1948, "Wind Waves at Sea, Breakers and Surf," U. S. Hydrographic Office, H. O. Pub. No. 602, 176 pp.
5. Horrer, P. L., 1948, "Southern Hemisphere Swell and Waves from a Tropical Storm at Long Beach, California," Wave Project Report No. 76, Scripps Institution of Oceanography of the Univ. of California, 12 pp.
6. Morison, J. R., O'Brien, M. P., Johnson, J. W., and Schaaf, "The Force Exerted by Surface Waves on Piles", to be published in *Jnl. Petr. Tech.*, AIME.
7. Munk, W. H., 1948, "Wave Action on Structures," Technical Publication No. 2322, *Petr. Tech.*, AIME, 18 pp.
8. Munk, W. H., 1949, "The Solitary Wave Theory and its Application to Surf Problems," *Annals of the New York Academy of Sciences* 51 (3), pp. 376-424.
9. Munk, W. H., and Traylor, M. E., 1947, *Refraction of Ocean Waves. "A Process Linking Underwater Topography to Beach Erosion,"* *Journal Geology* 55 (1), pp. 1-26.
10. Saur, T., Anderson, R. E., Burt, W. V., and Thompson, W., 1947, "A Statistical Study of Wave Conditions at Five Open Sea Localities Along the California Coast," Wave Project Report No. 68, Scripps Institution of Oceanography of the Univ. of California, 34 pp.
11. Sverdrup, H. U., and Munk, W. H., 1947, "Wind, Sea and Swell: Theory of Relations for Forecasting," U. S. Hydrographic Office, Technical Report No. 1, H. O. Pub. No. 6 pl., 44 pp.
12. U. S. Navy Hydrographic Office, 1945, "Breakers and Surf: Principles in Forecasting," H. O. Pub. 234, 55 pp., 4 plates.
13. Wiegel, R. L., 1949, "An Analysis of Data from Wave Recorders on the Pacific Coast of the United States," Technical Report HE-116-246, Fluid Mechanics Laboratory of the Univ. of California, Berkeley, California, 5 pp. ★ ★ ★

THE APPLICATION OF THE LAPLACE TRANSFORMATION TO FLOW PROBLEMS IN RESERVOIRS

A. F. VAN EVERDINGEN, SHELL OIL CO., HOUSTON, AND W. HURST, PETROLEUM
CONSULTANT, HOUSTON, MEMBERS AIME

ABSTRACT

For several years the authors have felt the need for a source from which reservoir engineers could obtain fundamental theory and data on the flow of fluids through permeable media in the unsteady state. The data on the unsteady state flow are composed of solutions of the equation

$$\frac{\partial^2 P}{\partial r^2} + \frac{1}{r} \frac{\partial P}{\partial r} = \frac{\partial P}{\partial t}$$

Two sets of solutions of this equation are developed, namely, for "the constant terminal pressure case" and "the constant terminal rate case." In the constant terminal pressure case the pressure at the terminal boundary is lowered by unity at zero time, kept constant thereafter, and the cumulative amount of fluid flowing across the boundary is computed, as a function of the time. In the constant terminal rate case a unit rate of production is made to flow across the terminal boundary (from time zero onward) and the ensuing pressure drop is computed as a function of the time. Considerable effort has been made to compile complete tables from which curves can be constructed for the constant terminal pressure and constant terminal rate cases, both for finite and infinite reservoirs. These curves can be employed to reproduce the effect of any pressure or rate history encountered in practice.

Most of the information is obtained by the help of the Laplace transformations, which proved to be extremely helpful for analyzing the problems encountered in fluid flow. The application of this method simplifies the more tedious mathematical analyses employed in the past. With the help of Laplace transformations some original developments were obtained (and presented) which could not have been easily foreseen by the earlier methods.

INTRODUCTION

This paper represents a compilation of the work done over the past few years on the flow of fluid in porous media. It concerns itself primarily with the transient conditions prevailing in oil reservoirs during the time they are produced. The study is limited to conditions where the flow of fluid obeys the

diffusivity equation. Multiple-phase fluid flow has not been considered.

A previous publication by Hurst¹ shows that when the pressure history of a reservoir is known, this information can be used to calculate the water influx, an essential term in the material balance equation. An example is offered in the literature by Old² in the study of the Jones Sand, Schuler Field, Arkansas. The present paper contains extensive tabulated data (from which work curves can be constructed), which data are derived by a more rigorous treatment of the subject matter than available in an earlier publication.¹ The application of this information will enable those concerned with the analysis of the behavior of a reservoir to obtain quantitatively correct expressions for the amount of water that has flowed into the reservoirs, thereby satisfying all the terms that appear in the material balance equation. This work is likewise applicable to the flow of fluid to a well whenever the flow conditions are such that the diffusivity equation is obeyed.

DIFFUSIVITY EQUATION

The most commonly encountered flow system is radial flow toward the well bore or field. The volume of fluid which flows per unit of time through each unit area of sand is expressed by Darcy's equation as

$$v = \frac{K}{\mu} \frac{\partial P}{\partial r}$$

where K is the permeability, μ the viscosity and $\partial P / \partial r$ the pressure gradient at the radial distance r . A material balance on a concentric element AB , expresses the net fluid traversing the surfaces A and B , which must equal the fluid lost from within the element. Thus, if the density of the fluid is expressed by ρ , then the weight of fluid per unit time and per unit sand thickness, flowing past Surface A , the surface nearest the well bore, is given as

$$2\pi r \rho \frac{K}{\mu} \frac{\partial P}{\partial r} = \frac{2\pi K}{\mu} \left(\rho r \frac{\partial P}{\partial r} \right)$$

The weight of fluid flowing past Surface B , an infinitesimal distance δr , removed from Surface A , is expressed as

$$\frac{2\pi K}{\mu} \left[\rho r \frac{\partial P}{\partial r} + \frac{\partial \left(\rho r \frac{\partial P}{\partial r} \right)}{\partial r} \delta r \right]$$

Manuscript received at office of Petroleum Branch January 12, 1949.
Paper presented at the AIME Annual Meeting in San Francisco, February 18-17, 1949.

¹ References are given at end of paper.

The difference between these two terms, namely,

$$-\frac{2\pi K}{\mu} \frac{\partial \left(\rho r \frac{\partial P}{\partial r} \right)}{\partial r} \delta r,$$

is equal to the weight of fluid lost by the element AB, or

$$-2\pi f r \frac{\partial \rho}{\partial T} \delta r$$

where f is the porosity of the formation.

This relation gives the equation of continuity for the radial system, namely,

$$\frac{K}{\mu} \frac{\partial \left(\rho r \frac{\partial P}{\partial r} \right)}{\partial r} = f r \frac{\partial \rho}{\partial T} \quad \dots \quad (II-1)$$

From the physical characteristics of fluids, it is known that density is a function of pressure and that the density of a fluid decreases with decreasing pressure due to the fact that the fluid expands. This trend expressed in exponential form is

$$\rho = \rho_o e^{-c(P_o - P)} \quad \dots \quad (II-2)$$

where P is less than P_o , and c the compressibility of the fluid. If we substitute Eq. II-2 in Eq. II-1, the diffusivity equation can be expressed using density as a function of radius and time, or

$$\left(\frac{\partial^2 \rho}{\partial r^2} + \frac{1}{r} \frac{\partial \rho}{\partial r} \right) \frac{K}{f\mu c} = \frac{\partial \rho}{\partial T} \quad \dots \quad (II-3)$$

For liquids which are only slightly compressible, Eq. II-2 simplifies to $\rho \cong \rho_o [1 - c(P_o - P)]$ which further modifies Eq. II-3 to give

$$\left(\frac{\partial^2 P}{\partial r^2} + \frac{1}{r} \frac{\partial P}{\partial r} \right) \frac{K}{f\mu c} = \frac{\partial P}{\partial T} \quad \dots \quad (II-4)$$

radius of the well or field, R_b , is referred to as a unit radius, then the relation simplifies to

$$\frac{\partial^2 P}{\partial r^2} + \frac{1}{r} \frac{\partial P}{\partial r} = \frac{\partial P}{\partial t} \quad \dots \quad (II-4)$$

where $t = KT/f\mu c R_b^2$ and r now expresses the distance as a multiple of R_b , the unit radius. The units appearing in this paper are always used in connection with Darcy's equation, so that the permeability K must be expressed in darcys, the time T in seconds, the porosity f as a fraction, the viscosity μ in centipoises, the compressibility c as volume per volume per atmosphere, and the radius R_b in centimeters.

LAPLACE TRANSFORMATION

In all publications, the treatment of the diffusivity equation has been essentially the orthodox application of the Fourier-Bessel series. This paper presents a new approach to the solution of problems encountered in the study of flowing fluids, namely, the Laplace transformation, since it was recognized that Laplace transformations offer a useful tool for solving difficult problems in less time than by the use of Fourier-Bessel series. Also, original developments have been obtained which are not easily foreseen by the orthodox methods.

If $P_{(t)}$ is a pressure at a point in the sand and a function of time, then its Laplace transformation is expressed by the infinite integral

$$\bar{P}_{(p)} = \int_0^\infty e^{-pt} P_{(t)} dt \quad \dots \quad (III-1)$$

where the constant p in this relationship is referred to as the operator. If we treat the diffusivity equation by the process

implied by Eq. III-1, the partial differential can be transformed to a total differential equation. This is performed by multiplying each term in Eq. II-4 by e^{-pt} and integrating with respect to time between zero and infinity, as follows:

$$\int_0^\infty e^{-pt} \left(\frac{\partial^2 P}{\partial r^2} + \frac{1}{r} \frac{\partial P}{\partial r} \right) dt = \int_0^\infty e^{-pt} \frac{\partial P}{\partial t} dt \quad (III-2)$$

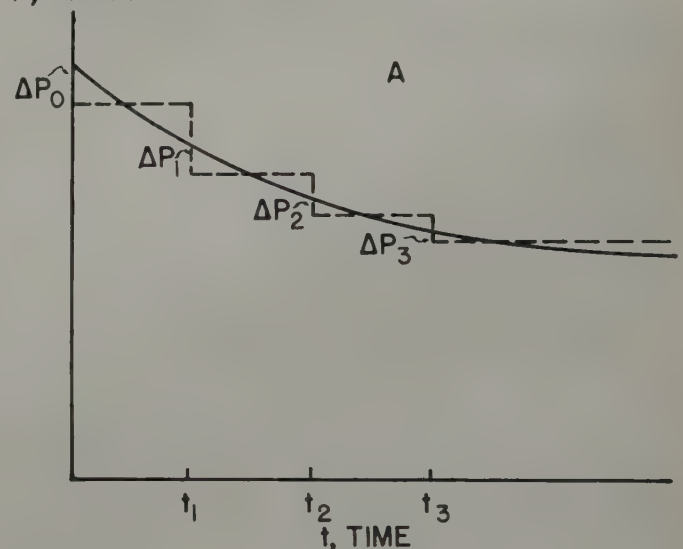
Since P is a function of radius and time, the integration with respect to time will automatically remove the time function and leave P a function of radius only. This reduces the left side to a total differential with respect to r , namely,

$$\int_0^\infty e^{-pt} \frac{\partial^2 P}{\partial r^2} dt = \frac{\partial^2 \int_0^\infty e^{-pt} P dt}{\partial r^2} = \frac{d^2 \bar{P}_{(p)}}{dr^2} \quad \text{etc.}$$

and Eq. III-2 becomes

$$\frac{d^2 \bar{P}_{(p)}}{dr^2} + \frac{1}{r} \frac{d \bar{P}_{(p)}}{dr} = \int_0^\infty e^{-pt} \frac{dP}{dt} dt$$

P, PRESSURE



q(t), RATE

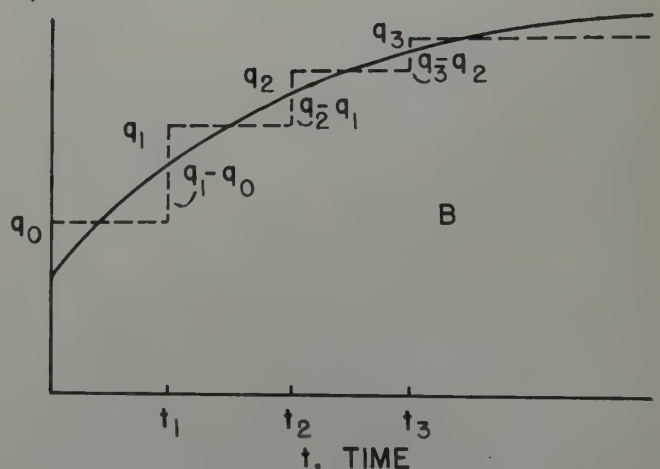


FIG. 1A — SEQUENCE CONSTANT TERMINAL PRESSURES.
1B — SEQUENCE CONSTANT TERMINAL RATES.

Furthermore, if we consider that $P_{(t)}$ is a cumulative pressure drop, and that initially the pressure in the reservoir is everywhere constant so that the cumulative pressure drop $P_{(t=0)}=0$, the integration of the right hand side of the equation becomes

$$\int_0^{\infty} e^{-pt} \frac{dP}{dt} dt = e^{-pt} P_{(t)} \Big|_0^{\infty} + p \int_0^{\infty} e^{-pt} P_{(t)} dt$$

$$= p \int_0^{\infty} e^{-pt} P_{(t)} dt$$

As this term is also a Laplace transform, Eq. III-2 can be written as a total differential equation, or

$$\frac{d^2 \bar{P}_{(p)}}{dr^2} + \frac{1}{r} \frac{d\bar{P}_{(p)}}{dr} = p \bar{P}_{(p)} \quad \dots \quad (\text{III-3})$$

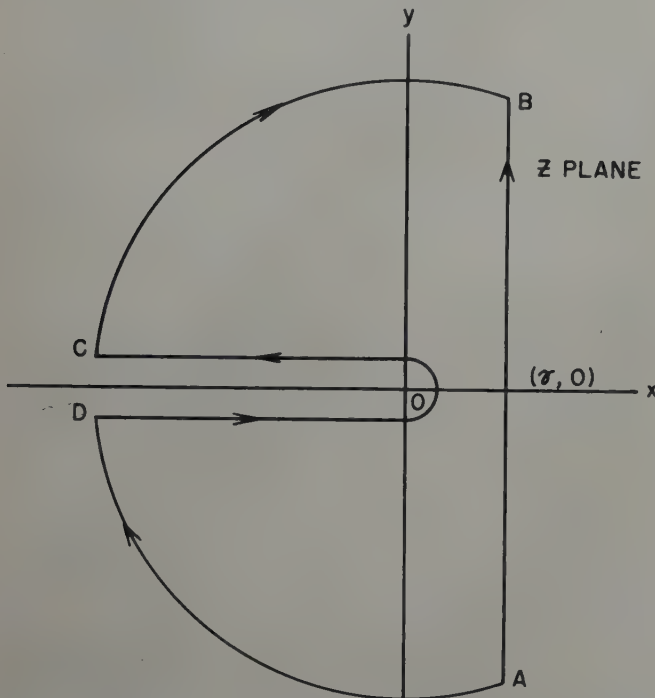


FIG. 2 — CONTOUR INTEGRATION IN ESTABLISHING THE CONSTANT TERMINAL RATE CASE FOR INFINITE EXTENT.

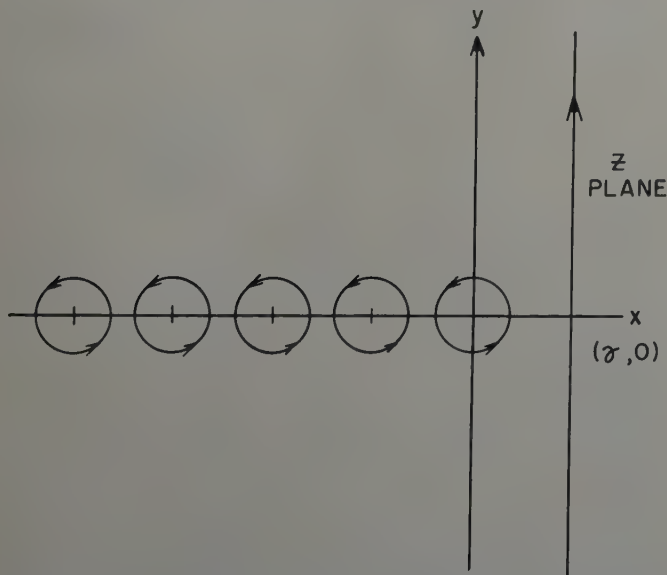


FIG. 3 — CONTOUR INTEGRATION IN ESTABLISHING THE CONSTANT TERMINAL RATE CASE FOR LIMITED RESERVOIR.

The next step in the development is to reproduce the boundary condition at the well bore or field radius, $r=1$, as a Laplace transformation and introduce this in the general solution for Eq. III-3 to give an explicit relation

$$\bar{P}_{(p)} = f_{(p,r)}$$

By inverting the term on the right by the Mellin's inversion formula, or other methods, we obtain the solution for the cumulative pressure drop as an explicit function of radius and time.

ENGINEERING CONCEPTS

Before applying the Laplace transformation to develop the necessary work-curves, there are some fundamental engineering concepts to be considered that will allow the interpretation of these curves. Two cases are of paramount importance in making reservoir studies, namely, the constant terminal pressure case and the constant terminal rate case. If we know the explicit solution for the first case, we can reproduce any variable pressure history at the terminal boundary to determine the cumulative influx of fluid. Likewise, if the rate of fluid influx varies, the constant terminal rate case can be used to calculate the total pressure drop. The constant terminal pressure and the constant terminal rate case are not independent of one another, as knowing the operational form of one, the other can be determined, as will be shown later.

Constant Terminal Pressure Case

The constant terminal pressure case is defined as follows: At time zero the pressure at all points in the formation is constant and equal to unity, and when the well or reservoir is opened, the pressure at the well or reservoir boundary, $r=1$, immediately drops to zero and remains zero for the duration of the production history.

If we treat the constant terminal pressure case symbolically, the solution of the problem at any radius and time is given by $P = P_{(r,t)}$. The rate of fluid influx per unit sand thickness under these conditions is given by Darcy's equation

$$q_{(x)} = \frac{2\pi K}{\mu} \left(r \frac{\partial P}{\partial r} \right)_{r=1} \quad \dots \quad (\text{IV-1})$$

If we wish to determine the cumulative influx of fluid in absolute time T , and having expressed time in the diffusivity equation as $t = KT/\mu c R_b^2$, then

$$Q_{(x)} = \int_0^T q_{(x)} dT = \frac{2\pi K}{\mu} \times \frac{f\mu c R_b^2}{K} \int_0^t \left(\frac{\partial P}{\partial r} \right)_{r=1} dt$$

$$= 2\pi f c R_b^2 Q_{(t)} \quad \dots \quad (\text{IV-2})$$

where

$$Q_{(t)} = \int_0^t \left(\frac{\partial P}{\partial r} \right)_{r=1} dt \quad \dots \quad (\text{IV-3})$$

In brief, knowing the general solution implied by Eq. IV-3, which expresses the integration in dimensionless time, t , of the pressure gradient at radius unity for a pressure drop of one atmosphere, the cumulative influx into the well bore or into the oil-bearing portion of the field can be determined by Eq. IV-2. Furthermore, for any pressure drop, ΔP , Eq. IV-2 expresses the cumulative influx as

$$Q_{(T)} = 2\pi f c R_b^2 \Delta P Q_{(t)} \quad \dots \quad (\text{IV-4})$$

per unit sand thickness.*

* The set of symbols now introduced and the symbols reported in Hurst's¹ earlier paper on water-drive are related as follows:

$$G(\alpha^2 \theta/R^2) = Q_{(t)} \quad \text{and} \quad \bar{G}(\alpha^2 \theta/R^2) = \int_0^t Q_{(t)} dt \quad \text{where} \quad \alpha^2 \theta/R^2 = t$$

When an oil reservoir and the adjoining water-bearing formations are contained between two parallel and sealing faulting planes, the flow of fluid is essentially parallel to these planes and is "linear." The constant terminal pressure case can also be applied to this case. The basic equation for linear flow is given by

$$\frac{\partial^2 P}{\partial x^2} = \frac{\partial P}{\partial t} \quad \dots \quad (IV-5)$$

where now $t = KT/\mu c$ and x is the absolute distance measured from the plane of influx extending out into the water-bearing sand. If we assume the same boundary conditions as in radial flow, with $P = P(x, t)$ as the solution, then by Darcy's law, the rate of fluid influx across the original water-oil contact per unit of cross-sectional area is expressed by

$$q_{(T)} = \frac{K}{\mu} \left(\frac{\partial P}{\partial x} \right)_{x=0} \quad \dots \quad (IV-6)$$

The total fluid influx is given by

$$Q_{(T)} = \int_0^T q_{(T)} dT = \frac{K}{\mu} \cdot \frac{f\mu c}{K} \int_0^t \left(\frac{\partial P}{\partial x} \right)_{x=0} dt = f c Q_{(t)} \quad \dots \quad (IV-7)$$

where $Q_{(t)}$ is the generalized solution for linear flow and is equal to

$$Q_{(t)} = \int_0^t \left(\frac{\partial P}{\partial x} \right)_{x=0} dt \quad \dots \quad (IV-8)$$

Therefore, for any over-all pressure drop ΔP , Eq. IV-7 gives

$$Q_{(T)} = fc\Delta P Q_{(t)} \quad \dots \quad (IV-9)$$

per unit of cross-sectional area.

Constant Terminal Rate Case

In the constant terminal rate case it is likewise assumed that initially the pressure everywhere in the formation is constant but that from the time zero onward the fluid is withdrawn from the well bore or reservoir boundary at a unit rate. The pressure drop is given by $P = P_{(r, t)}$, and at the boundary of the field, where $r = 1$, $(\partial P / \partial r)_{r=1} = -1$. The minus sign is introduced because the gradient for the pressure drop relative to the radius of the well or reservoir is negative. If the cumulative pressure drop is expressed as ΔP , then

$$\Delta P = q_{(t)} P_{(r, t)} \quad \dots \quad (IV-10)$$

where $q_{(t)}$ is a constant relating the cumulative pressure drop with the pressure change for a unit rate of production. By applying Darcy's equation for the rate of fluid flowing into the well or reservoir per unit sand thickness

$$q_{(T)} = \frac{-2\pi K}{\mu} \left(\frac{\partial \Delta P}{\partial r} \right)_{r=1} = \frac{-2\pi K}{\mu} q_{(t)} \left(\frac{\partial P_{(r, t)}}{\partial r} \right)_{r=1}$$

which simplifies to $q_{(t)} = \frac{q_{(T)}\mu}{2\pi K}$. Therefore, for any constant

rate of production the cumulative pressure drop at the field radius is given by

$$\Delta P = \frac{q_{(T)}\mu}{2\pi K} P_{(t)} \quad \dots \quad (IV-11)$$

Similarly, for the constant rate of production in linear flow, the cumulative pressure drop is expressed by

$$\Delta P = \frac{q_{(T)}\mu}{K} P_{(t)} \quad \dots \quad (IV-12)$$

where $q_{(T)}$ is the rate of water encroachment per unit area of cross-section, and $P_{(t)}$ is the cumulative pressure drop at the sand face per unit rate of production.

Superposition Theorem

With these fundamental relationships available, it remains to be shown how the constant pressure case can be interpreted for variable terminal pressures, or in the constant rate case, for variable rates. The linearity of the diffusivity equation allows the application of the superposition theorem as a sequence of constant terminal pressures or constant rates in such a fashion that it reproduces the pressure or production history at the boundary, $r = 1$. This is essentially Duhamel's principle, for which reference can be made to transient electric circuit theory in texts by Karman and Biot,⁵ and Bush.⁶ It has been applied to the flow of fluids by Muskat,⁴ Schilthuis and Hurst,⁷ in employing the variable rate case in calculating the pressure drop in the East Texas Field.¹

The physical significance can best be realized by an application. Fig. 1-A shows the pressure decline in the well bore or a field that has been flowing and for which we wish to obtain the amount of fluid produced. As shown, the pressure history is reproduced as a series of pressure plateaus which represent a sequence of constant terminal pressures. Therefore, by the application of Eq. IV-4, the cumulative fluid produced in time t by the pressure drop ΔP_0 , operative since zero time, is expressed by $Q_{(T)} = 2\pi fcR_b^2 \Delta P_0 Q_{(t)}$. If we next consider

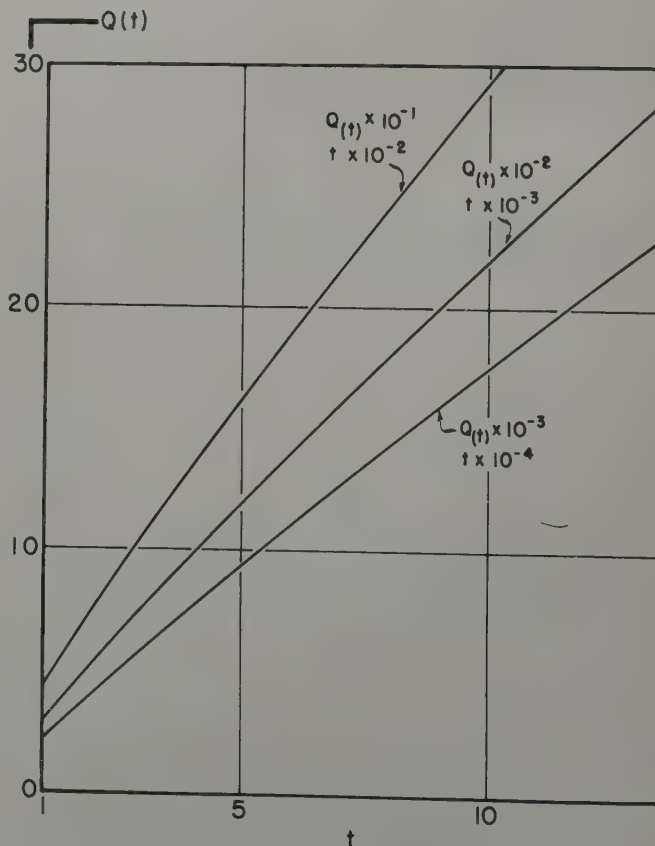


FIG. 4 — RADIAL FLOW, CONSTANT TERMINAL PRESSURE CASE, INFINITE RESERVOIR, CUMULATIVE PRODUCTION VS. TIME.

the pressure drop ΔP_1 , which occurs in time t_1 , and treat this as a separate entity, but take cognizance of its time of inception t_1 , then the cumulative fluid produced by this increment of pressure drop is $Q_{(t)} = 2\pi f c R_b^2 \Delta P_1 Q_{(t-t_1)}$. By superimposing all these effects of pressure changes, the total influx in time t is expressed as

$$Q_{(t)} = 2\pi f c R_b^2 [\Delta P_0 Q_{(t)} + \Delta P_1 Q_{(t-t_1)} + \Delta P_2 Q_{(t-t_2)} + \Delta P_3 Q_{(t-t_3)} + \dots] \quad (IV-13)$$

when $t > t_3$. To reproduce the smooth curve relationship of Fig. 1-A, these pressure plateaus can be taken as infinitesimally small, which give the summation of Eq. IV-13 by the integral

$$Q_{(t)} = 2\pi f c R_b^2 \int_0^t \frac{\partial \Delta P}{\partial t'} Q_{(t-t')} dt' \quad (IV-14)$$

By considering variable rates of fluid production, such as shown in Fig. 1-B, and reproducing these rates as a series of constant rate plateaus, then by Eq. IV-11 the pressure drop in the well bore in time t , for the initial rate q_0 is $\Delta P_0 = q_0 P_{(t)}$. At time t_1 , the comparable increment for constant rate is expressed as $q_1 - q_0$, and the effect of this increment rate on the corresponding increment of pressure drop is $\Delta P_1 = (q_1 - q_0) P_{(t-t_1)}$. Again by superimposing all of these effects, the determination for the cumulative pressure drop is expressed by

$$\Delta P = q_{(0)} P_{(t)} + [q_1(t_1) - q_{(0)}] P_{(t-t_1)} + [q_{(t_2)} - q_{(t_1)}] P_{(t-t_2)} + [q_{(t_3)} - q_{(t_2)}] P_{(t-t_3)} + \dots \quad (IV-15)$$

If the increments are infinitesimal, or the smooth curve relationship applies, Eq. IV-15 becomes

$$\Delta P = q_{(0)} P_{(t)} + \int_0^t \frac{dq_{(t')}}{dt'} P_{(t-t')} dt' \quad (IV-16)$$

If $q_{(0)} = 0$, Eq. IV-16 can also be expressed as

$$\Delta P = \int_0^t q_{(t')} P'_{(t-t')} dt' \quad (IV-17)$$

where $P'_{(t)}$ is the derivative of $P_{(t)}$ with respect to t .

Since Eqs. IV-13 and IV-15 are of such simple algebraic forms, they are most practical to use with production history in making reservoir studies. In applying the pressure or rate plateaus as shown in Fig. 1, it must be realized that the time interval for each plateau should be taken as small as possible, so as to reproduce within engineering accuracy the trend of the curves. Naturally, if an exact interpretation is desired, Eqs. IV-14 and IV-16 apply.

FUNDAMENTAL CONSIDERATIONS

In applying the Laplace transformation, there are certain fundamental operations that must be clarified. It has been stated that if $P_{(t)}$ is a pressure drop, the transformation for $P_{(t)}$ is given by Eq. III-1, as

$$\bar{P}_{(p)} = \int_0^\infty e^{-pt} P_{(t)} dt$$

To visualize more concretely the meaning of this equation, if the unit pressure drop at the boundary in the constant terminal pressure case is employed in Eq. III-1, its transform is given by

$$\bar{P}_{(p)} = \int_0^\infty e^{-pt} 1 dt = \left. \frac{-e^{-pt}}{p} \right|_0^\infty = \frac{1}{p} \quad (V-1)$$

The Laplace transformations of many transcendental functions have been developed and are available in tables, the most complete of which is the tract by Campbell and Foster.⁸ It is therefore often possible after solving a total differential such as Eq. III-3 to refer to a set of tables and transforms and determine the inverse of $\bar{P}_{(p)}$ or $P_{(t)}$. It is frequently necessary to simplify $\bar{P}_{(p)}$ before an inversion can be made. However, Mellin's inversion formula is always applicable, which requires analytical treatment whenever used.

There are two possible simplifications for $\bar{P}_{(p)}$ when time is small or time is large. This is evident from Eq. III-3, where p can be interpreted by the operational calculus as the operator d/dt . Therefore, if we consider this symbolic relation, then if t is large, p must be small, or inversely, if t is small, p will be large. To understand this, if $\bar{P}_{(p)}$ is expressed by an involved Bessel relationship, the substitution for p as a small or large value will simplify $\bar{P}_{(p)}$ to give $P_{(t)}$ for the corresponding times.

Mellin's inversion formula is given on page 71 of Carslaw and Jaeger.⁹

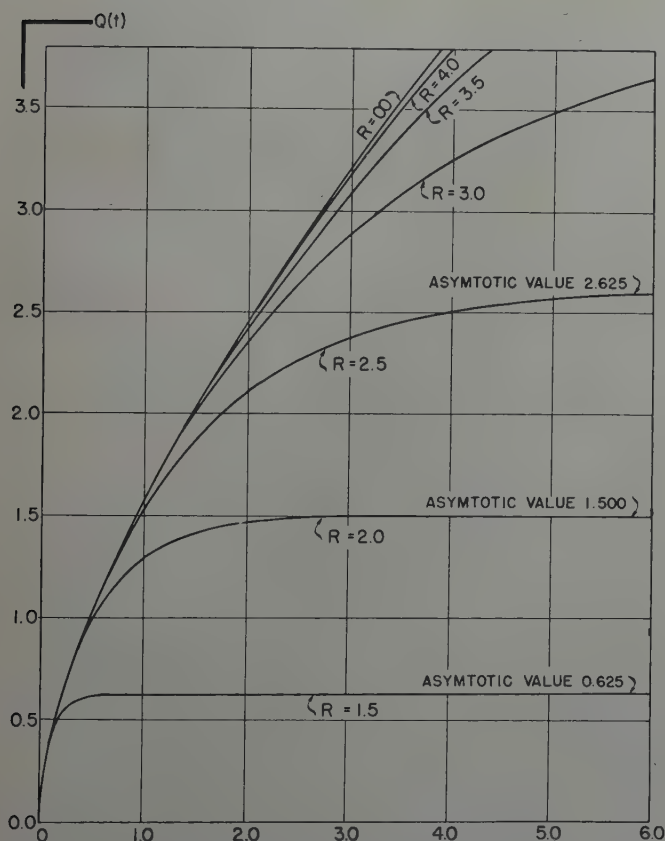


FIG. 5—RADIAL FLOW, CONSTANT TERMINAL PRESSURE CASE, CUMULATIVE PRODUCTION VS. TIME FOR LIMITED RESERVOIRS.

$$P(t) = \frac{1}{2\pi i} \int_{\gamma-i\infty}^{\gamma+i\infty} e^{\lambda t} \bar{P}(\lambda) d\lambda$$

where $\bar{P}(\lambda)$ is the transform $\bar{P}(p)$. Where this report is concerned with pressure drops, the above can be written as

$$P(t_1) - P(t_2) = \frac{1}{2\pi i} \int_{\gamma-i\infty}^{\gamma+i\infty} (e^{\lambda t_1} - e^{\lambda t_2}) \bar{P}(\lambda) d\lambda. \quad (V-2)$$

The integration is in the complex plane $\lambda = x + iy$, along a line parallel to the y -axis, extending from minus to positive infinity, and a distance γ removed from the origin, so that all poles are to the left of this line, Fig. 2. The reader who has a comprehensive understanding of contour integrals will recognize that this integral is equal to the integration around a semi-circle of infinite radius extending to the left of the line $x = \gamma$, and includes integration along the "cuts," which joins the poles to the semi-circle. Since the integration along the semi-circle in the second and third quadrant is zero for radius infinity and $t > 0$, this leaves the integration along the "cuts" and the poles, where the latter, as expressed in Eq. V-2, are the residuals.

Certain fundamental relationships in the Laplace transformations are found useful:¹⁰

Theorem A—If $\bar{P}(p)$ is the transform of $P(t)$, then

$$\int_0^\infty e^{-pt} \frac{dP(t)}{dt} dt = e^{-pt} P(t) \Big|_0^\infty + p \int_0^\infty e^{-pt} P(t) dt$$

$$= p \bar{P}(p) - P(t=0)$$

or the transform of $\frac{dP(t)}{dt} = p \bar{P}(p) - P(t=0)$, provided $e^{-pt} P(t)$

approaches zero as time approaches infinity.

Theorem B—The transform of $\int_0^\infty P(t') dt'$ is expressed by

$$\int_0^\infty e^{-pt} \int_0^t P(t') dt' dt = \frac{-e^{-pt}}{p} \int_0^t P(t') dt' \Big|_0^\infty + \frac{1}{p} \int_0^\infty e^{-pt} P(t) dt$$

$$= \frac{\bar{P}(p)}{p}$$

or the transform of the integration $P(t')$ with respect to t' from zero to t is $\bar{P}(p)/p$, if $e^{-pt} \int_0^t P(t') dt'$ is zero for time infinity.

Theorem C—The transform for $e^{\pm ct} P(t)$ is equal to

$$\int_0^\infty e^{-pt} e^{\pm ct} P(t) dt = \int_0^\infty e^{-(p \mp c)t} P(t) dt = \bar{P}(p \mp c)$$

if $p - c$ is positive.

Theorem D—If $\bar{P}_1(p)$ is the transform of $P_1(t)$, and $\bar{P}_2(p)$ is the transform of $P_2(t)$, then the product of these two transforms is the transform of the integral

$$\int_0^t P_1(t') P_2(t-t') dt'$$

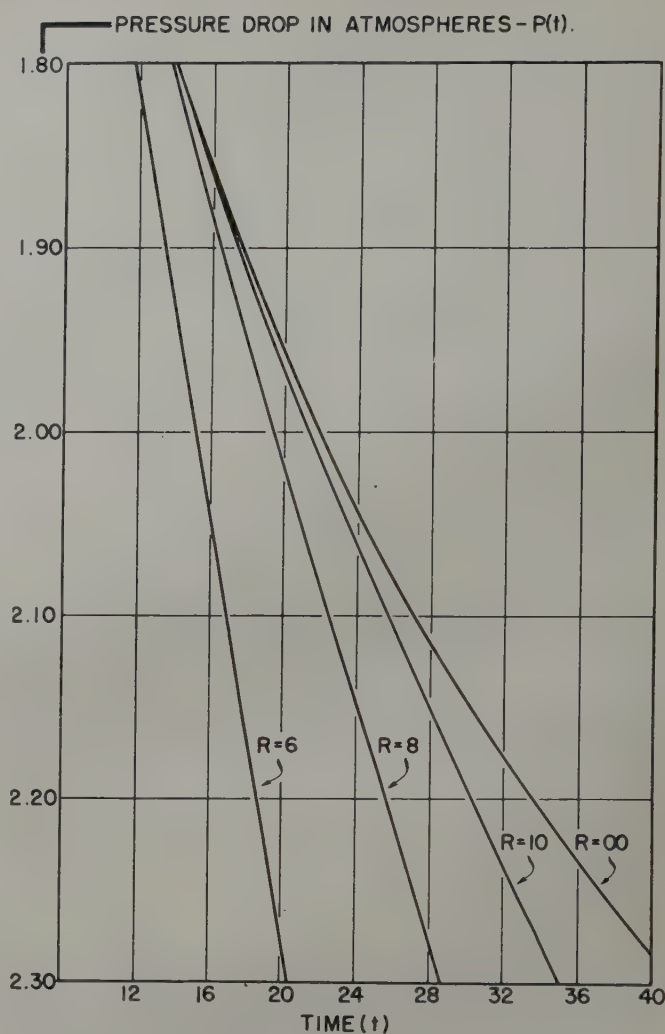


FIG. 6—RADIAL FLOW, CONSTANT TERMINAL RATE CASE, PRESSURE DROP VS. TIME, $P(t)$ VS. t

This integral is comparable to the integrals developed by the superimposition theorem, and of appreciable use in this paper.

CONSTANT TERMINAL PRESSURE AND CONSTANT TERMINAL RATE CASES, INFINITE MEDIUM

The analytics for the constant terminal pressure and rate cases have been developed for limited reservoirs^{3,4} when the exterior boundary is considered closed or the production rate through this boundary is fixed. In determining the volume of water encroached into the oil-bearing portion of reservoirs, few cases have been encountered which indicated that the sands in which the oil occurs are of limited extent. For the most part, the data show that the influx behaves as if the water-bearing parts of the formations are of infinite extent, because within the productive life of oil reservoirs, the rate of water encroachment does not reflect the influence of an exterior boundary. In other words, whether or not the water sand is of limited extent, the rate of water encroachment is such as if supplied by an infinite medium.

Computing the water influx for an infinite reservoir with the help of Fourier-Bessel expansions, an exterior boundary can be assumed so far removed from the field radius that the production for a considerable time will reflect the infinite case. Unfortunately, the poor convergence of these expansions invalidates this approach. An alternative method consists of using increasing values for exterior radius, evaluating the water influx for each radius separately, and then drawing the envelope of these curves, which gives the infinite case, Fig. 5. In such a procedure, each of the branch curves reflects a water reservoir of limited extent. Inasmuch as the drawing of an envelope does not give a high degree of accuracy, the solutions for the constant terminal pressure and constant terminal rate cases for an infinite medium are presented here, with values for $Q_{(t)}$ and $P_{(t)}$ calculated directly.

The constant terminal pressure case was first developed by Nicholson¹¹ by the application of Green's function to an instantaneous circular source in an infinite medium. Goldstein¹² presented this solution by the operational method, and Smith¹³ employed Carslaw's contour method in its development. Carslaw and Jaeger^{14,21} later gave the explicit treatment of the constant terminal pressure case by the application of the Laplace transformation. The derivation of the constant terminal rate case is not given in the literature, and its development is presented here.

The Constant Rate Case

As already discussed, the boundary conditions for the constant rate case in an infinite medium are that (1) the pressure drop $P_{(r,t)}$ is zero initially at every point in the formation, and (2) at the radius of the field ($r=1$) we have

$$\left(\frac{\partial P}{\partial r} \right)_{r=1} = -1 \text{ at all times.}$$

A reference to a text on Bessel functions, such as Karman and Biot,⁵ pp. 61-63, shows that the general solution for Eq. III-3 is given by

$$\bar{P}_{(r,p)} = A I_0(r\sqrt{p}) + B K_0(r\sqrt{p}) \quad (\text{VI-1})$$

where $I_0(r\sqrt{p})$ and $K_0(r\sqrt{p})$ are modified Bessel functions of the first and second kind, respectively, and of zero order. A and B are two constants which satisfy a second order differential equation. Since $\bar{P}_{(r,p)}$ is the transform of the pressure drop at a point in the formation, and because at a point not yet affected by production the absolute pressure equals the initial pressure, it is required that $\bar{P}_{(r,p)}$ should approach zero as r becomes large. As shown in Karman and Biot,⁵ $I_0(r\sqrt{p})$ becomes increasingly large and $K_0(r\sqrt{p})$ approaches zero as the argument ($r\sqrt{p}$) increases. Therefore, to obey the initial condition, the constant A must equal zero and (VI-1) becomes

$$\bar{P}_{(r,p)} = B K_0(r\sqrt{p}) \quad (\text{VI-2})$$

To fulfill the second boundary condition for unit rate of production, namely $(\partial P / \partial r)_{r=1} = -1$, the transform for unity gives

$$\left(\frac{\partial \bar{P}}{\partial r} \right)_{r=1} = -\frac{1}{p} \quad (\text{VI-3})$$

by Eq. V-1. The differentiation of the modified Bessel function of the second kind, Watson's Bessel Functions,¹⁶ W.B.F., p. 79, gives $K_0'(z) = -K_1(z)$. Therefore, differentiation Eq.

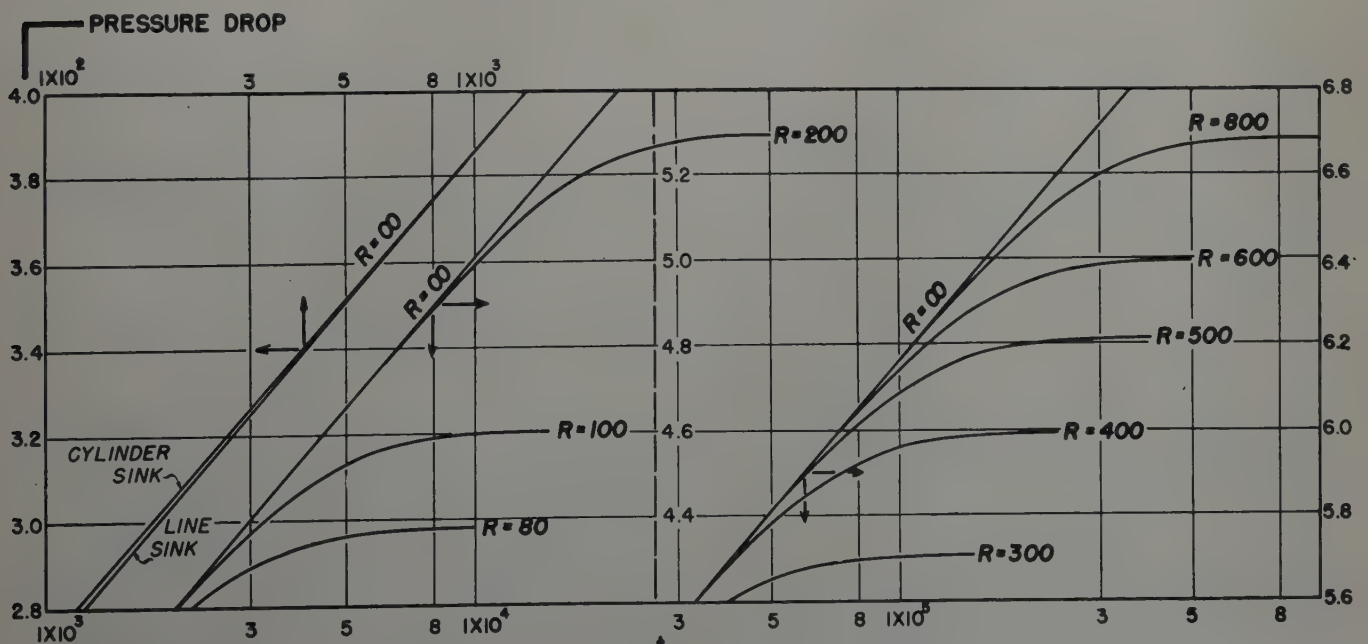


FIG. 7 — RADIAL FLOW, CONSTANT TERMINAL RATE CASE, CUMULATIVE PRESSURE DROP VS. TIME $P(t)$ VS. t

VI-2, with respect to r at $r = 1$, gives

$$\left(\frac{\partial \bar{P}}{\partial r} \right)_{r=1} = -B \sqrt{p} K_1(\sqrt{p})$$

and since

$$\left(\frac{\partial \bar{P}}{\partial r} \right)_{r=1} = -\frac{1}{p}$$

the constant $B = 1/p^{3/2} K_1(\sqrt{p})$. Therefore, the transform for the pressure drop for the constant rate case in an infinite medium is given by

$$\bar{P}_{(r,p)} = \frac{K_0(r\sqrt{p})}{p^{3/2} K_1(\sqrt{p})} \quad \text{VI-4}$$

To determine the inverse of Eq. VI-4 in order to establish the pressure drop at radius unity, we can resort to the simplification that for small times the operator p is large. Since

$$K_n(z) = \sqrt{\frac{\pi}{2z}} e^{-z} \quad \text{VI-5}$$

for z large, W.B.F., p. 202, then

$$\bar{P}_{(1,p)} = \frac{1}{p^{3/2}} \quad \text{VI-6}$$

The inversion for this transform is given in Campbell and Foster, Eq. 516, as

$$P_{(t)} = \frac{2}{\sqrt{\pi}} t^{1/2} \quad \text{VI-7}$$

In brief, Eq. VI-7 states that when $t = K T / f \mu c R_b^2$ is small, which can be caused by the boundary radius for the field, R_b , being large, the pressure drop for the unit rate of production approximates the condition for linear flow.

To justify this conclusion, the treatment of the linear flow equation, Eq. IV-5, by the Laplace transformation gives

$$\frac{d^2 \bar{P}_{(p)}}{dx^2} = p \bar{P}_{(p)} \quad \text{VI-8}$$

for which the general solution is the expression

$$\bar{P}_{(x,p)} = A e^{-x\sqrt{p}} + B e^{+x\sqrt{p}} \quad \text{VI-9}$$

By repeating the reasoning already employed in this development, the transform for the pressure drop at $x = 0$ gives

$$\bar{P}(0\sqrt{p}) = 1/p^{3/2}$$

which is identical with (VI-6) with p the operator of $t = KT/f\mu c$.

The second simplification for the transform (VI-4) is to consider p small, which is equivalent to considering time, t , large. The expansions for $K_0(z)$ and $K_1(z)$ are given in Carslaw and Jaeger,¹⁹ p. 248.

$$K_0(z) = -I_0(z) \left\{ \log \frac{z}{2} + \gamma \right\} + \left(\frac{z}{2} \right)^2 + \frac{\left(1 + \frac{1}{2} \right) \left(\frac{z}{2} \right)^4}{(2!)^2} + \frac{\left(1 + \frac{1}{2} + \frac{1}{3} \right) \left(\frac{z}{2} \right)^6}{(3!)^2} + \quad \text{VI-10}$$

$$K_1(z) = -(-1)^{n+1} I_n(z) \left\{ \log \frac{z}{2} + \gamma \right\} + \frac{1}{2} (-1)^n \sum_{r=0}^{\infty} \frac{\left(\frac{z}{2} \right)^{n+2r}}{r! (n+r)!} \left[\sum_{m=1}^{n+r} m^{-1} + \sum_{m=1}^r m^{-1} \right] + \frac{1}{2} \sum_{r=0}^{n-1} (-1)^r \left(\frac{z}{2} \right)^{-n+2r} \frac{(n-r-1)!}{r!} \quad \text{VI-11}$$

where γ is Euler's constant 0.57722, and the logarithmic term consists of natural logarithms. When z is small

$$K_0(z) \cong - \left[\log \frac{z}{2} + \gamma \right] \quad \text{VI-12}$$

$$K_1(z) \cong 1/z \quad \text{VI-13}$$

Therefore, Eq. VI-4 becomes

$$\bar{P}_{(1,p)} = \frac{-\log p}{2p} + \frac{(\log 2 - \gamma)}{p} \quad \text{VI-14}$$

The inversion for the first term on the right is given by Campbell and Foster, Eq. 892, and the inverse of the second term by

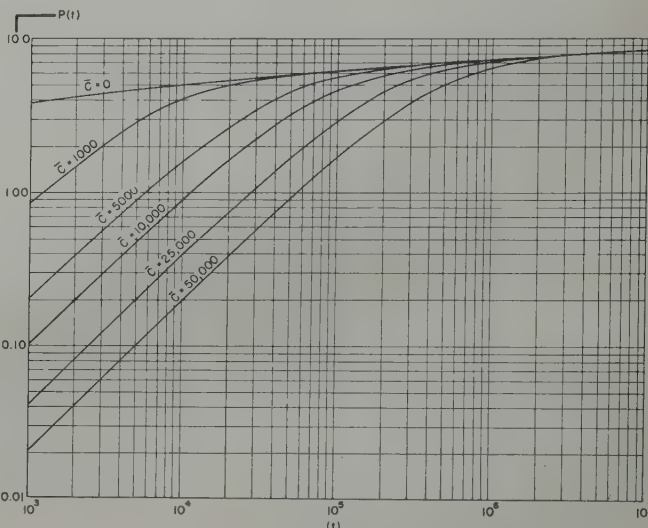


FIG. 8—CONSTANT RATE OF PRODUCTION IN THE STOCK TANK, ADJUSTING FOR THE UNLOADING OF FLUID IN THE ANNULUS, $P(t)$ VERSUS t WHERE $c = c/2\pi f c R_b^2$, AND c IS THE VOLUME OF FLUID UNLOADED FROM THE ANNULUS, CORRECTED TO RESERVOIR CONDITIONS, PER ATMOSPHERE BOTTOM-HOLE PRESSURE DROP, PER UNIT SAND THICKNESS.

Eq. V-1. Therefore, the pressure drop at the boundary of the field when t is large is given by

$$P_{(t)} = \frac{1}{2} [\log 4t - \gamma] = \frac{1}{2} [\log t + 0.80907] \quad \text{VI-15}$$

The solution given by Eq. VI-15 is the solution of the continuous point source problem for large time t . The relationship has been applied to the flow of fluids by Bruce,¹⁹ Elkins,²⁰ and others, and is particularly applicable for study of interference between flowing wells.

The point source solution originally developed by Lord Kelvin and discussed in Carslaw¹⁸ can be expressed as

$$P_{(r,t)} = \frac{1}{2} \int_{-\infty}^{\infty} \frac{e^{-n}}{n} dn = \frac{1}{2} \left\{ -\text{Ei} \left(-\frac{1}{4t} \right) \right\} \quad \text{VI-16}$$

often referred to as the logarithmic integral or the Ei-function. Its values are given in Tables of Sine, Cosine, and Exponential Integrals, Volumes I and II, Federal Works Agency, W.P.A., City of New York. For large values of the time, t ,

Eq. VI-16 reduces to $P_{(r,t)} = \frac{1}{2} [\log 4t - \gamma]$ which is Eq. VI-15, and this relation is accurate for values of $t > 100$.

By this development it is evident that the point source solution does not apply at a boundary for the determination of the pressure drop when t is small. However, when the radius, R_b , is small, such as a well radius, even small values of the absolute time, T will give large values of the dimensionless time t , and the point source solution is applicable. On the other hand, in considering the pressure drop at the periphery of a field (in which case R_b can have a large numerical value) the value of t can be easily less than 100 even for large values of absolute time, T . Therefore, for intermediate times, the rigorous solution of the constant rate case must be used, which we will now proceed to obtain.

To develop the explicit solution for the constant terminal rate case, it is necessary to invert the Laplace transform, Eq. VI-4, by the Mellin's inversion formula. The path of integration for this transform is described by the "cut" along the negative real axis, Fig. 2, which gives a single valued function on each side of the "cut." That is to say that Path AB required by Eq. V-2 is equal to the Path AD and CB, both of which are described by a semi-circle of radius infinity. Since its integration is zero in the second and third quadrant, this leaves the integration along Paths DO and OC equal to AB. The integration on the upper portion of the "cut" can be obtained by making $\lambda = u^2 e^{+i\pi}$, which yields

$$\frac{1}{2\pi i} \int_{-\infty}^{\infty} \frac{(e^{\lambda t_1} - e^{\lambda t_2}) K_0(\sqrt{\lambda} r)}{\lambda^{3/2} K_1(\sqrt{\lambda})} d\lambda = \frac{1}{\pi i} \int_{-\infty}^{\infty} \frac{(e^{-u^2 t_1} - e^{-u^2 t_2}) K_0(u e^{i\pi/2} r)}{u^2 e^{i\pi/2} K_1(u e^{i\pi/2})} du \quad \text{---(VI-17)}$$

Carslaw and Jaeger⁹ (page 249) shows that modified Bessel functions of the first and second kind of arguments $z e^{\pm i\pi/2}$ can be expressed by the regular Bessel functions as complex values, as follows:

$$I_0(z e^{\pm i\pi/2}) = J_0(z) \\ K_0(z e^{\pm i\pi/2}) = \mp \frac{\pi i}{2} \{ J_0(z) \mp i Y_0(z) \}$$

$$I_1(z e^{\pm i\pi/2}) = \pm i J_1(z) \quad \text{---(VI-18)}$$

and

$$K_1(z e^{\pm i\pi/2}) = -\frac{\pi}{2} [J_1(z) \mp i Y_1(z)]$$

The substitution of the corresponding values for $K_0(u e^{i\pi/2} r)$ and $K_1(u e^{i\pi/2})$ from Eq. VI-18 in Eq. VI-17 gives the integration along the upper portion of the negative real "cut" as

$$\frac{1}{\pi i} \int_{-\infty}^{\infty} \frac{(e^{-u^2 t_1} - e^{-u^2 t_2}) [Y_1(u) J_0(ur) - J_1(u) Y_0(ur)] du}{u^2 [J_1^2(u) + Y_1^2(u)]} \quad \text{---(VI-19)}$$

where the imaginary term has been dropped.

Likewise, the integration along the under portion of the negative real "cut" is expressed by $\lambda = u^2 e^{-i\pi}$ and

$$\frac{1}{2\pi} \int_{-\infty}^{\infty} \frac{(e^{\lambda t_1} - e^{\lambda t_2}) K_0(\sqrt{\lambda} r) d\lambda}{\lambda^{3/2} K_1(\sqrt{\lambda})} = -\frac{1}{\pi} \int_{-\infty}^{\infty} \frac{(e^{-u^2 t_1} - e^{-u^2 t_2}) K_0(u e^{-i\pi/2} r) du}{u^2 e^{-i\pi/2} K_1(u e^{-i\pi/2})}$$

Using Eq. VI-18, yields the relationship

$$\frac{1}{\pi} \int_{-\infty}^{\infty} \frac{(e^{-u^2 t_1} - e^{-u^2 t_2}) [Y_1(u) J_0(ur) - J_1(u) Y_0(ur)] du}{u^2 [J_1^2(u) + Y_1^2(u)]} \quad \text{---(VI-20)}$$

The integration along Paths DO and OC is the sum of the relations VI-19 and VI-20, or

$$P(r, t_1) - P(r, t_2) = \frac{2}{\pi} \int_{-\infty}^{\infty} \frac{(e^{-u^2 t_1} - e^{-u^2 t_2}) [Y_1(u) J_0(ur) - J_1(u) Y_0(ur)] du}{u^2 [J_1^2(u) + Y_1^2(u)]}$$

Initially, that is at time zero, the cumulative pressure drop at any point in the formation is zero, $P(r, t=0) = 0$. Hence, the pressure drop since zero time equals:

$$P(r, t) = \frac{2}{\pi} \int_{-\infty}^{\infty} \frac{(1 - e^{-u^2 t}) [J_1(u) Y_0(ur) - Y_1(u) J_0(ur)] du}{u^2 [J_1^2(u) + Y_1^2(u)]} \quad \text{---(VI-21)}$$

which is the explicit solution of the constant terminal rate case for an infinite medium.

To determine the cumulative pressure drop for a unit rate of production at the well bore or field radius, (where $r = 1$) then Eq. VI-21 changes to

$$P(1, t) = \frac{2}{\pi} \int_{-\infty}^{\infty} \frac{(1 - e^{-u^2 t}) [J_1(u) Y_0(u) - Y_1(u) J_0(u)] du}{u^2 [J_1^2(u) + Y_1^2(u)]} \quad \text{---(VI-22)}$$

By the recurrence formula given in W.B.F., p. 77

$$J_1(u) Y_0(u) - J_0(u) Y_1(u) = \frac{2}{\pi u} \quad \text{---(VI-23)}$$

Equation VI-22 simplifies to

$$P(1, t) = \frac{4}{\pi^2} \int_{-\infty}^{\infty} \frac{(1 - e^{-u^2 t}) du}{u^3 [J_1^2(u) + Y_1^2(u)]} \quad \text{---(VI-24)}$$

Constant Terminal Pressure Case

As already shown, the transform of the pressure drop in an infinite medium is $\bar{P}_{(r,p)} = B K_0(\sqrt{p} r)$. In the constant terminal pressure case it is assumed that at all times the pressure drop at $r = 1$ will be unity, which is expressed as a transform by Eq. V-1

$$\bar{P}_{(1,p)} = 1/p$$

By solving for the constant B at $r = 1$ in the above formula, we find $B = 1/p K_0(\sqrt{p})$, so that the transform for the pressure at any point in the reservoir is expressed by

$$\bar{P}_{(r,p)} = \frac{K_0(\sqrt{p} r)}{p K_0(\sqrt{p})} \quad \text{---(VI-25)}$$

The comparable solution of VI-25 for a cumulative pressure drop can be developed as before by considering the paths of Fig. 2, with a pole at the origin, to give the solution

$$P(r, t_1) - P(r, t_2) = \frac{2}{\pi} \int_0^\infty \frac{(e^{-u^2 t_1} - e^{-u^2 t_2}) [J_0(u) Y_0(ur) - Y_0(u) J_0(ur)] du}{u^2 [J_0^2(u) + Y_0^2(u)]} \quad (VI-26)$$

If we are interested in the cumulative fluid influx at the field radius, $r = 1$, then the relationship Eq. IV-3 applies, or

$$Q(t) = \int_0^t \left(\frac{\partial P}{\partial r} \right)_{r=1} dt \quad (IV-3)$$

The determination of the transform of the gradient of the pressure drop at the field's edge follows from Eq. VI-25,

$$\left(\frac{\partial \bar{P}_{(r,p)}}{\partial r} \right)_{r=1} = - \frac{K_1(\sqrt{p})}{p^{1/2} K_0(\sqrt{p})}$$

since $K_0'(z) = -K_1(z)$. Since the pressure drop $P(r, t)$ corresponds to the difference between the initial and actual pressure, the transform of the gradient of the actual pressure at $r = 1$ is given by

$$\left(\frac{\partial \bar{P}}{\partial r} \right)_{r=1} = \left(\frac{-\partial \bar{P}_{(r,p)}}{\partial r} \right)_{r=1}$$

or

$$\left(\frac{\partial \bar{P}}{\partial r} \right)_{r=1} = \frac{K_1(\sqrt{p})}{p^{1/2} K_0(\sqrt{p})}$$

which corresponds to the integrand of Eq. IV-3. Further, from

the definition given by Theorem B, namely, that if $\bar{P}(p)$ is the transform of $P(t)$, then the transform of $\int_0^t P(t') dt'$ is given by $\bar{P}(p)/p$ and the Laplace transform for $Q(t)$ is expressed by

$$\bar{Q}(p) = \frac{K_1(\sqrt{p})}{p^{3/2} K_0(\sqrt{p})} \quad (VI-27)$$

The application of the Mellin's inversion formula to Eq. VI-27 follows the paths shown in Fig. 2, giving

$$Q(t) = \frac{4}{\pi^2} \int_0^\infty \frac{(1 - e^{-u^2 t}) du}{u^3 [J_0^2(u) + Y_0^2(u)]} \quad (VI-28)$$

With respect to the transform $\bar{Q}(p)$, there is the simplification that for time small, p is large, or Eq. VI-27 reduces to

$$\bar{Q}(p) = 1/p^{3/2} \quad (VI-29)$$

and the inversion is as before

$$Q(t) = \frac{2}{\sqrt{\pi}} t^{1/2} \quad (VI-30)$$

which is identical to the linear flow case. For all other values of the time, Eq. VI-28 must be solved numerically.

Relation Between $\bar{Q}(p)$ and $\bar{P}(p)$

It is evident from the work that has already gone before, that the Laplace transformation and the superimposition theorem offer a basis for interchanging the constant terminal pressure to the constant terminal rate case, and vice versa. In any reservoir study the essential interest is the analyses of the flow either at the well bore or the field boundary. The purpose of this work is to determine the relationship between $Q(t)$, the constant terminal pressure case, and $P(t)$, the constant terminal rate case, which explicitly refer to the boundary $r = 1$. Therefore, if we conceive of the influx of fluid into a

TABLE I—Radial Flow, Constant Terminal Pressure and Constant Terminal Rate Cases for Infinite Reservoirs

t	Q(t)	P(t)	t	Q(t)
1.0(10) ⁻²	0.112	0.112	1.5(10) ³	4.136(10) ³
5.0 "	0.278	0.229	2.0 "	5.315 "
1.0(10) ⁻¹	0.404	0.315	2.5 "	6.466 "
1.5 "	0.520	0.376	3.0 "	7.590 "
2.0 "	0.606	0.424	4.0 "	9.757 "
2.5 "	0.689	0.469	5.0 "	11.88 "
3.0 "	0.758	0.503	6.0 "	13.95 "
4.0 "	0.898	0.564	7.0 "	15.99 "
5.0 "	1.020	0.616	8.0 "	18.00 "
6.0 "	1.140	0.659	9.0 "	19.99 "
7.0 "	1.251	0.702	1.0(10) ⁴	21.96 "
8.0 "	1.359	0.735	1.5 "	3.146(10) ³
9.0 "	1.469	0.772	2.0 "	4.079 "
1.0 "	1.570	0.802	2.5 "	4.994 "
1.5 "	2.032	0.927	3.0 "	5.891 "
2.0 "	2.442	1.020	4.0 "	7.634 "
2.5 "	2.838	1.101	5.0 "	9.342 "
3.0 "	3.209	1.169	6.0 "	11.03 "
4.0 "	3.897	1.275	7.0 "	12.69 "
5.0 "	4.541	1.362	8.0 "	14.33 "
6.0 "	5.148	1.438	9.0 "	15.95 "
7.0 "	5.749	1.500	1.0(10) ⁵	17.56 "
8.0 "	6.314	1.556	1.5 "	2.538(10) ⁴
9.0 "	6.861	1.604	2.0 "	3.308 "
1.0(10) ¹	7.417	1.651	2.5 "	4.066 "
1.5 "	9.965	1.829	3.0 "	4.817 "
2.0 "	1.229(10) ¹	1.960	4.0 "	6.267 "
2.5 "	1.455 "	2.067	5.0 "	7.699 "
3.0 "	1.681 "	2.147	6.0 "	9.113 "
4.0 "	2.088 "	2.282	7.0 "	10.51 "
5.0 "	2.482 "	2.388	8.0 "	11.89 "
6.0 "	2.860 "	2.476	9.0 "	13.26 "
7.0 "	3.228 "	2.550	1.0(10) ⁶	14.62 "
8.0 "	3.599 "	2.615	1.5 "	2.126(10) ⁵
9.0 "	3.942 "	2.672	2.0 "	2.781 "
1.0(10) ²	4.301 "	2.723	2.5 "	3.427 "
1.5 "	5.980 "	2.921	3.0 "	4.064 "
2.0 "	7.586 "	3.064	4.0 "	5.313 "
2.5 "	9.120 "	3.173	5.0 "	6.544 "
3.0 "	10.58 "	3.263	6.0 "	7.761 "
4.0 "	13.48 "	3.408	7.0 "	8.965 "
5.0 "	16.24 "	3.516	8.0 "	10.16 "
6.0 "	18.97 "	3.608	9.0 "	11.34 "
7.0 "	21.60 "	3.684	1.0(10) ⁷	12.52 "
8.0 "	24.23 "	3.750		
9.0 "	26.77 "	3.809		
1.0(10) ³	29.31 "	3.860		

TABLE I—Continued

t	Q(t)	t	Q(t)
1.5(10) ⁷	1.828(10) ⁵	1.5(10) ¹¹	1.17(10) ¹⁰
2.0 "	2.398 "	2.0 "	1.55 "
2.5 "	2.961 "	2.5 "	1.92 "
3.0 "	3.517 "	3.0 "	2.29 "
4.0 "	4.610 "	4.0 "	3.02 "
5.0 "	5.689 "	5.0 "	3.75 "
6.0 "	6.758 "	6.0 "	4.47 "
7.0 "	7.816 "	7.0 "	5.19 "
8.0 "	8.866 "	8.0 "	5.89 "
9.0 "	9.911 "	9.0 "	6.58 "
1.0(10) ⁸	10.95 "	1.0(10) ¹²	7.28 "
1.5 "	1.604(10) ⁷	1.5 "	1.08(10) ¹¹
2.0 "	2.108 "	2.0 "	1.42 "
2.5 "	2.607 "		
3.0 "	3.100 "		
4.0 "	4.071 "		
5.0 "	5.032 "		
6.0 "	5.984 "		
7.0 "	6.928 "		
8.0 "	7.865 "		
9.0 "	8.797 "		
1.0(10) ⁹	9.725 "		
1.5 "	1.429(10) ⁸		
2.0 "	1.880 "		
2.5 "	2.328 "		
3.0 "	2.771 "		
4.0 "	3.645 "		
5.0 "	4.510 "		
6.0 "	5.368 "		
7.0 "	6.220 "		
8.0 "	7.066 "		
9.0 "	7.909 "		
1.0(10) ¹⁰	8.747 "		
1.5 "	1.288(10) ⁹		
2.0 "	1.697 "		
2.5 "	2.103 "		
3.0 "	2.505 "		
4.0 "	3.299 "		
5.0 "	4.087 "		
6.0 "	4.868 "		
7.0 "	5.643 "		
8.0 "	6.414 "		
9.0 "	7.183 "		
1.0(10) ¹¹	7.948 "		

TABLE II—Constant Terminal Pressure Case
Radial Flow, Limited Reservoirs

R = 1.5 $\alpha_1 = 2.8899$ $\alpha_2 = 9.3452$		R = 2.0 $\alpha_1 = 1.8606$ $\alpha_2 = 4.6458$		R = 2.5 $\alpha_1 = 0.8663$ $\alpha_2 = 3.0875$		R = 3.0 $\alpha_1 = 0.6256$ $\alpha_2 = 2.3041$	
t	Q _(t)	t	Q _(t)	t	Q _(t)	t	Q _(t)
5.0(10) ⁻²	0.276	5.0(10) ⁻²	0.278	1.0(10) ⁻¹	0.408	3.0(10) ⁻¹	0.755
6.0 "	0.304	7.5 "	0.345	1.5 "	0.509	4.0 "	0.895
7.0 "	0.330	1.0(10) ⁻¹	0.404	2.0 "	0.599	5.0 "	1.023
8.0 "	0.354	1.25 "	0.458	2.5 "	0.681	6.0 "	1.143
9.0 "	0.375	1.50 "	0.507	3.0 "	0.758	7.0 "	1.256
1.0(10) ⁻¹	0.395	1.75 "	0.553	3.5 "	0.829	8.0 "	1.363
1.1 "	0.414	2.00 "	0.597	4.0 "	0.897	9.0 "	1.465
1.2 "	0.431	2.25 "	0.638	4.5 "	0.962	1.00	1.563
1.3 "	0.446	2.50 "	0.678	5.0 "	1.024	1.25	1.791
1.4 "	0.461	2.75 "	0.715	5.5 "	1.083	1.50	1.997
1.5 "	0.474	3.00 "	0.751	6.0 "	1.140	1.75	2.181
1.6 "	0.486	3.25 "	0.785	6.5 "	1.195	2.00	2.353
1.7 "	0.497	3.50 "	0.817	7.0 "	1.248	2.25	2.507
1.8 "	0.507	3.75 "	0.848	7.5 "	1.299	2.50	2.646
1.9 "	0.517	4.00 "	0.877	8.0 "	1.348	2.75	2.772
2.0 "	0.525	4.25 "	0.905	8.5 "	1.395	3.00	2.888
2.1 "	0.533	4.50 "	0.932	9.0 "	1.440	3.25	2.990
2.2 "	0.541	4.75 "	0.958	9.5 "	1.484	3.50	3.084
2.3 "	0.548	5.00 "	0.983	1.0	1.526	3.75	3.170
2.4 "	0.554	5.50 "	1.028	1.1	1.605	4.00	3.247
2.5 "	0.559	6.00 "	1.070	1.2	1.679	4.25	3.317
2.6 "	0.565	6.50 "	1.108	1.3	1.747	4.50	3.381
2.8 "	0.574	7.00 "	1.143	1.4	1.811	4.75	3.439
3.0 "	0.582	7.50 "	1.174	1.5	1.870	5.00	3.491
3.2 "	0.588	8.00 "	1.203	1.6	1.924	5.50	3.581
3.4 "	0.594	9.00 "	1.253	1.7	1.975	6.00	3.656
3.6 "	0.599	1.00	1.295	1.8	2.022	6.50	3.717
3.8 "	0.603	1.1	1.330	2.0	2.106	7.00	3.767
4.0 "	0.606	1.2	1.358	2.2	2.178	7.50	3.809
4.5 "	0.613	1.3	1.382	2.4	2.241	8.00	3.843
5.0 "	0.617	1.4	1.402	2.6	2.294	9.00	3.893
6.0 "	0.621	1.6	1.432	2.8	2.340	10.00	3.928
7.0 "	0.623	1.7	1.444	3.0	2.380	11.00	3.951
8.0 "	0.624	1.8	1.453	3.4	2.444	12.00	3.967
		2.0	1.468	3.6	2.491	14.00	3.985
		2.5	1.487	4.2	2.525	16.00	3.993
		3.0	1.495	4.6	2.551	18.00	3.997
		4.0	1.499	5.0	2.570	20.00	3.999
		5.0	1.500	6.0	2.599	22.00	3.999
				7.0	2.613	24.00	4.000
				8.0	2.619		
				9.0	2.622		
				10.0	2.624		

TABLE II—Continued

R = 3.5 $\alpha_1 = 0.4851$ $\alpha_2 = 1.8374$		R = 4.0 $\alpha_1 = 0.3935$ $\alpha_2 = 1.5267$		R = 4.5 $\alpha_1 = 0.3296$ $\alpha_2 = 1.3051$		R = 5.0 $\alpha_1 = 0.2823$ $\alpha_2 = 1.1392$		R = 6.0 $\alpha_1 = 0.2182$ $\alpha_2 = 0.9025$	
t	Q _(t)	t	Q _(t)	t	Q _(t)	t	Q _(t)	t	Q _(t)
1.00	1.571	2.00	2.442	2.5	2.835	3.0	3.195	6.0	5.148
1.20	1.761	2.20	2.598	3.0	3.196	3.5	3.542	6.5	5.440
1.40	1.940	2.40	2.748	3.5	3.537	4.0	3.875	7.0	5.724
1.60	2.111	2.60	2.893	4.0	3.859	4.5	4.193	7.5	6.002
1.80	2.273	2.80	3.034	4.5	4.165	5.0	4.499	8.0	6.273
2.00	2.427	3.00	3.170	5.0	4.454	5.5	4.792	8.5	6.537
2.20	2.574	3.25	3.334	5.5	4.727	6.0	5.074	9.0	6.795
2.40	2.715	3.50	3.493	6.0	4.986	6.5	5.345	9.5	7.047
2.60	2.849	3.75	3.645	6.5	5.231	7.0	5.605	10.0	7.293
2.80	2.976	4.00	3.792	7.0	5.464	7.5	5.854	10.5	7.533
3.00	3.098	4.25	3.932	7.5	5.684	8.0	6.094	11	7.767
3.25	3.242	4.50	4.068	8.0	5.892	8.5	6.325	12	8.220
3.50	3.379	4.75	4.198	8.5	6.089	9.0	6.547	13	8.651
3.75	3.507	5.00	4.323	9.0	6.276	9.5	6.760	14	9.063
4.00	3.628	5.50	4.560	9.5	6.453	10	6.965	15	9.456
4.25	3.742	6.00	4.779	10	6.621	11	7.350	16	9.829
4.50	3.850	6.50	4.982	11	6.930	12	7.706	17	10.19
4.75	3.951	7.00	5.169	12	7.208	13	8.035	18	10.53
5.00	4.047	7.50	5.343	13	7.457	14	8.339	19	10.85
5.50	4.222	8.00	5.504	14	7.680	15	8.620	20	11.16
6.00	4.378	8.50	5.653	15	7.880	16	8.879	22	11.74
6.50	4.516	9.00	5.790	16	8.060	18	9.338	24	12.26
7.00	4.639	9.50	5.917	18	8.365	20	9.731	25	12.50
7.50	4.749	10	6.035	20	8.611	22	10.07	31	13.74
8.00	4.846	11	6.246	22	8.809	24	10.35	35	14.40
8.50	4.932	12	6.425	24	9.068	26	10.59	39	14.93
9.00	5.009	13	6.580	26	9.097	28	10.80	51	16.05
9.50	5.078	14	6.712	28	9.200	30	10.98	60	16.56
10.00	5.138	15	6.825	30	9.283	34	11.26	70	16.91
11	5.241	16	6.922	34	9.404	38	11.46	80	17.14
12	5.321	17	7.004	38	9.481	42	11.61	90	17.27
13	5.385	18	7.076	42	9.532	46	11.71	100	17.36
14	5.435	20	7.189	46	9.565	50	11.79	110	17.41
15	5.476	22	7.272	50	9.586	60	11.91	120	17.45
16	5.506	24	7.332	60	9.612	70	11.96	130	17.46
17	5.531	26	7.377	70	9.621	80	11.98	140	17.48
18	5.551	30	7.434	80	9.623	90	11.99	150	17.49
20	5.579	34	7.464	90	9.624	100	12.00	160	17.49
25	5.611	38	7.481	100	9.625	120	12.0	180	17.50
30	5.621	42	7.490					200	17.50
35	5.624	46	7.494					220	17.50
40	5.625	50	7.497						

well or field as a constant rate problem, then the actual cumulative fluid produced as a function of the cumulative pressure drop is expressed by the superposition relationship in Eq. IV-14 as

$$Q_{(T)} = 2\pi f c R_b^2 \int_0^T \frac{d\Delta P}{dt'} Q_{(T-t')} dt' \quad \text{IV-14}$$

when ΔP is the cumulative pressure drop at the well bore affected by producing the well at constant rate which is established by

$$\Delta P = \frac{q_{(T)} \mu P_{(T)}}{2\pi K} \quad \text{IV-11}$$

The substitution of Eq. IV-11 in IV-14 gives

$$Q_{(T)} = \frac{q_{(T)} \mu c R_b^2}{K} \int_0^T \frac{d P_{(t')}}{dt'} Q_{(T-t')} dt'$$

Since the rate is constant, $Q_{(T)} = q_{(T)} \times T$, and as $t = KT / \mu c R_b^2$ this relation becomes

$$t = \int_0^T \frac{d P_{(t')}}{dt'} Q_{(T-t')} dt' \quad \text{VI-31}$$

To express Eq. VI-31 in transformation form, the transform for t is $1/p^2$, Campbell and Foster, Eq. 408.1. The transform

for $P_{(t)}$ at $r = 1$ is $\bar{P}_{(p)}$, and it follows from Theorem A that

the transform of $\frac{dP_{(t)}}{dt}$ is $p\bar{P}_{(p)}$ as the cumulative pressure

drop $P_{(t)}$ for constant rate is zero at time zero. Finally from Theorem D, the transform for the integration of the form Eq. VI-31 is equal to the product of the transforms for each of the two terms in the integrand, or

TABLE II—Continued

R = 7.0 $\alpha_1 = 0.1767$ $\alpha_2 = 0.7534$		R = 8.0 $\alpha_1 = 0.1476$ $\alpha_2 = 0.6438$		R = 9.0 $\alpha_1 = 0.1264$ $\alpha_2 = 0.5740$		R = 10.0 $\alpha_1 = 0.1104$ $\alpha_2 = 0.4979$	
t	Q _(t)	t	Q _(t)	t	Q _(t)	t	Q _(t)
9.00	6.861	9	6.861	10	7.417	15	9.965
9.50	7.127	10	7.398	15	9.945	20	12.32
10	7.389	11	7.920	20	12.26	22	13.22
11	7.902	12	8.431	22	13.13	24	14.09
12	8.397	13	8.930	24	13.98	26	14.95
13	8.876	14	9.418	26	14.79	28	15.78
14	9.341	15	9.895	28	15.59	30	16.59
15	9.791	16	10.361	30	16.35	32	17.38
16	10.23	17	10.82	32	17.10	34	18.16
17	10.65	18	11.26	34	17.82	36	18.91
18	11.05	19	11.70	36	18.52	38	19.65
19	11.46	20	12.13	38	19.19	40	20.37
20	11.85	22	12.95	40	19.85	42	21.07
22	12.58	24	13.74	42	20.48	44	21.76
24	13.27	26	14.50	44	21.09	46	22.42
26	13.92	28	15.23	46	21.69	48	23.07
28	14.53	30	15.92	48	22.26	50	23.71
30	15.11	34	17.22	50	22.82	52	24.33
35	16.39	38	18.41	52	23.36	54	24.94
40	17.49	40	18.97	54	23.89	56	25.53
45	18.43	45	20.26	56	24.39	58	26.11
50	19.24	50	21.42	58	24.88	60	26.67
60	20.51	55	22.46	60	25.36	65	28.02
70	21.45	60	23.40	65	26.48	70	29.29
80	22.13	70	24.98	70	27.52	75	30.49
90	22.63	80	26.26	75	28.48	80	31.61
100	23.00	90	27.28	80	29.36	85	32.67
120	23.47	100	28.11	85	30.18	90	33.66
140	23.71	120	29.31	90	30.93	95	34.60
160	23.85	140	30.08	95	31.63	100	35.48
180	23.92	160	30.58	100	32.27	120	38.51
200	23.96	180	30.91	120	34.39	140	40.89
500	24.00	200	31.12	140	35.92	160	42.75
		240	31.34	160	37.04	180	44.21
		280	31.43	180	37.85	200	45.36
		320	31.47	200	38.44	240	46.95
		360	31.49	240	39.17	280	47.94
		400	31.50	280	39.56	320	48.54
		500	31.50	320	39.77	360	48.91
				360	39.88	400	49.14
				400	39.94	440	49.28
				440	39.97	480	49.36
				480	39.98		

$$\frac{1}{p^2} = p \overline{P}_{(p)} \overline{Q}_{(p)} \dots \dots \dots \text{(VI-32)}$$

Evidence of this identity can be confirmed by substituting Eqs. VI-4 and VI-27 in Eq. VI-32. In brief, Eq. VI-32 is the relationship between constant terminal pressure and constant terminal rate cases. If the Laplace transformation for one is known, the transform for the other is established. This interchange can only take place in the transformations and the final solution must be by inversion.

Computation of $P_{(t)}$ and $Q_{(t)}$

To plot $P_{(t)}$ and $Q_{(t)}$ as work-curves, it is necessary to determine numerically the value for the integrals shown in Eqs. VI-24 and VI-28. In treating the infinite integrals for $P_{(t)}$ and $Q_{(t)}$, the only difficult part is in establishing the integrals for small values of u . For larger values of u the integrands converge fairly rapidly, and Simpson's rule for numerical integration has proved sufficiently accurate.

To determine the integration for $Q_{(t)}$ in the region of the origin, Eq. VI-28 can be expressed as

$$Q_{\delta(t)} = \frac{4}{\pi^2} \int_0^{\delta} \frac{(1 - e^{-u^2 t})}{u^2 [J_0^2(u) + Y_0^2(u)]} du \dots \dots \text{(VI-33)}$$

where the value for δ is taken such that $1 - e^{-u^2 t} \cong u^2 t$, which is true for $u^2 t$ equal to or less than 0.02, or $\delta = \sqrt{0.02/t}$ and the simplification for Eq. VI-33 becomes

$$Q_{\delta(t)} = \frac{4t}{\pi^2} \int_0^{\delta} \frac{du}{u [J_0^2(u) + Y_0^2(u)]}$$

For u less than 0.02, $J_0(u) = 1$, and

$$Y_0(u) \cong \frac{2}{\pi} \left\{ \log \frac{u}{2} + \gamma \right\} = \frac{2}{\pi} \left\{ \log u - 0.11593 \right\}$$

As the logarithmic term is most predominant in the denominator for small values of u , this equation simplifies to

$$Q_{\delta(t)} = t \int_0^{\delta} \frac{du}{u [\log u - 0.11593]^2} = \frac{t}{[0.11593 - \log \delta]} \dots \text{(VI-34)}$$

The integration for $P_{(t)}$ close to the origin is expressed by

$$P_{\delta(t)} = \frac{4}{\pi^2} \int_0^{\delta} \frac{(1 - e^{-u^2 t})}{u^2 [J_1^2(u) + Y_1^2(u)]} du \dots \text{(VI-35)}$$

For u equal to or less than 0.02, $J_1(u) = 0$, and $Y_1(u) = 2/\pi u$ so that Eq. VI-35 reduces to

$$P_{\delta(t)} = \int_0^{\delta} \frac{(1 - e^{-u^2 t})}{u} du \dots \dots \text{(VI-36)}$$

If we let $n = u^2 t$

$$P_{\delta(t)} = \frac{1}{2} \int_0^{\delta^2 t} \frac{(1 - e^{-n})}{n} dn \dots \dots \text{(VI-37)}$$

Further,

$$\int_0^{\delta^2 t} \frac{(1 - e^{-n})}{n} dn = \int_0^1 \frac{(1 - e^{-n})}{n} dn - \int_{\delta^2 t}^1 \frac{(1 - e^{-n})}{n} dn \dots \text{(VI-38)}$$

Since Euler's constant γ is equal to

$$\gamma = \int_1^{\infty} \frac{(1 - e^{-n})}{n} dn = \int_0^{\infty} \frac{e^{-n}}{n} dn$$

Substitution of this relation in Eq. VI-38 gives

$$\int_0^{\delta^2 t} \frac{(1 - e^{-n})}{n} dn = \gamma + \int_{\delta^2 t}^{\infty} \frac{e^{-n}}{n} dn - \int_{\delta^2 t}^1 \frac{1}{n} dn$$

and since the second term on the right is the Ei-function already discussed in the earlier part of this work, Eq. VI-37 reduces to

$$P_{\delta(t)} = \frac{1}{2} [\gamma - \text{Ei}(-\delta^2 t) + \log \delta^2 t] \dots \text{(VI-39)}$$

TABLE III — Constant Terminal Rate Case Radial Flow — Limited Reservoirs

$R_1 = 1.5$ $\beta_1 = 6.3225$ $\beta_2 = 11.924$		$R = 2.0$ $\beta_1 = 8.1965$ $\beta_2 = 6.3118$		$R = 2.5$ $\beta_1 = 2.1564$ $\beta_2 = 4.2230$		$R = 3.0$ $\beta_1 = 1.6358$ $\beta_2 = 3.1787$		$R = 3.5$ $\beta_1 = 1.3218$ $\beta_2 = 2.5526$		$R = 4$ $\beta_1 = 1.1120$ $\beta_2 = 2.1342$		$R = 4.5$ $\beta_1 = 0.9609$ $\beta_2 = 1.8356$	
t	$P_{(t)}$	t	$P_{(t)}$	t	$P_{(t)}$	t	$P_{(t)}$	t	$P_{(t)}$	t	$P_{(t)}$	t	$P_{(t)}$
6.0(10) ⁻²	0.251	2.2(10) ⁻¹	0.443	4.0(10) ⁻¹	0.565	5.2(10)	0.627	1.0	0.802	1.5	0.927	2.0	1.023
8.0 "	0.288	2.4 "	0.459	4.2 "	0.576	5.4 "	0.636	1.1	0.830	1.6	0.948	2.1	1.040
1.0(10) ⁻¹	0.322	2.6 "	0.476	4.4 "	0.587	5.6 "	0.645	1.2	0.857	1.7	0.968	2.2	1.056
1.2 "	0.355	2.8 "	0.492	4.6 "	0.598	6.0 "	0.662	1.3	0.882	1.8	0.988	2.3	1.072
1.4 "	0.387	3.0 "	0.507	4.8 "	0.608	6.5 "	0.683	1.4	0.906	1.9	1.007	2.4	1.087
1.6 "	0.420	3.2 "	0.522	5.0 "	0.618	7.0 "	0.703	1.5	0.929	2.0	1.025	2.5	1.102
1.8 "	0.452	3.4 "	0.536	5.2 "	0.628	7.5 "	0.721	1.6	0.951	2.2	1.059	2.6	1.116
2.0 "	0.484	3.6 "	0.551	5.4 "	0.638	8.0 "	0.740	1.7	0.973	2.4	1.092	2.7	1.130
2.2 "	0.516	3.8 "	0.565	5.6 "	0.647	8.5 "	0.758	1.8	0.994	2.6	1.123	2.8	1.144
2.4 "	0.548	4.0 "	0.579	5.8 "	0.657	9.0 "	0.776	1.9	1.014	2.8	1.154	2.9	1.158
2.6 "	0.580	4.2 "	0.593	6.0 "	0.666	9.5 "	0.791	2.0	1.034	3.0	1.184	3.0	1.171
2.8 "	0.612	4.4 "	0.607	6.5 "	0.688	1.0	0.806	2.25	1.083	3.5	1.255	3.2	1.197
3.0 "	0.644	4.6 "	0.621	7.0 "	0.710	1.2	0.865	2.50	1.130	4.0	1.324	4.0	1.222
3.5 "	0.724	4.8 "	0.634	7.5 "	0.731	1.4	0.920	2.75	1.176	4.5	1.392	3.6	1.246
4.0 "	0.804	5.0 "	0.648	8.0 "	0.752	1.6	0.973	3.0	1.221	5.0	1.460	4.0	1.269
4.5 "	0.884	6.0 "	0.715	8.5 "	0.772	2.0	1.076	4.0	1.401	5.5	1.527	4.5	1.292
5.0 "	0.964	7.0 "	0.782	9.0 "	0.792	3.0	1.328	5.0	1.579	6.0	1.594	5.0	1.349
5.5 "	1.044	8.0 "	0.849	9.5 "	0.812	4.0	1.578	6.0	1.757	6.5	1.660	5.5	1.403
6.0 "	1.124	9.0 "	0.915	1.0	0.832	5.0	1.828			7.0	1.727	6.0	1.457
		1.0	0.982	2.0	1.215					8.0	1.861	6.5	1.510
		2.0	1.649	3.0	1.596					9.0	1.994	7.0	1.615
		3.0	2.316	4.0	1.977					10.0	2.127	8.0	1.719
		5.0	3.649	5.0	2.358							9.0	1.823
												10.0	1.927
												11.0	2.031
												12.0	2.135
												13.0	2.239
												14.0	2.343
												15.0	2.447

The values for the integrands for Eqs. VI-24 and VI-28 have been calculated from Bessel Tables for or greater than 0.02 as given in W.B.F., pp. 666-697. The calculations have been somewhat simplified by using the square of the modulus of

$|H_0^{(1)}(u)| = |J_0(u) + i Y_0(u)|$ and $|H_1^{(1)}(u)| = |J_1(u) + i Y_1(u)|$ which are the Bessel functions of the third kind or the Hankel functions.

Table I shows the calculated values for $Q_{(t)}$ and $P_{(t)}$ to three significant figures, starting at $t = 0.01$, the point where linear flow and radial flow start deviating. $P_{(t)}$ is calculated only to $t = 1,000$ since beyond this range the point source solution of Eq. VI-15 applies. The values for $Q_{(t)}$ are given up to $t = 10^{12}$.

The reader may reproduce these data as he sees fit; Fig. 4 is an illustrative plot for $Q_{(t)}$, and Fig. 7 is a semi-logarithmic relationship for $P_{(t)}$.

LIMITED RESERVOIRS

As already mentioned, the solutions for limited reservoirs of radial symmetry have been developed by the Fourier-Bessel type of expansion.^{3,4,21} Their introduction here is not only to show how the solutions may be arrived at by the Laplace transformation, but also to furnish data for $P_{(t)}$ and $Q_{(t)}$ curves when such cases are encountered in practice.

No Fluid Flow Across Exterior Boundary

The first example considered is the constant terminal pressure case for radial flow of limited extent. The boundary conditions are such that at the well bore or field's edge, $r = 1$, the cumulative pressure drop is unity, and at some distance removed from this boundary at a point in the reservoir $r = R$,

there exists a restriction such that no fluid can flow past this barrier so that at that point $\left(\frac{\partial P}{\partial r}\right)_{r=R} = 0$.

The general solution of Eq. VI-1 still applies, but to fulfill the boundary conditions it is necessary to re-determine values for constants A and B. The transformation of the boundary condition at $r = 1$ is expressed as

$$\frac{1}{p} = A I_0(\sqrt{p}) + B K_0(\sqrt{p}) \quad \text{. . . (VII-1)}$$

and at $r = R$ the condition is

$$0 = A I_1(\sqrt{p}R) - B K_1(\sqrt{p}R) \quad \text{. . . (VII-2)}$$

since it is shown in W.B.F., p. 79, that $K_0'(z) = -K_1(z)$, and $I_0'(z) = I_1(z)$. The solutions for A and B from these two simultaneous algebraic expressions are

$$A = K_1(\sqrt{p}R) / p [K_1(\sqrt{p}R) I_0(\sqrt{p}) + K_0(\sqrt{p}) I_1(\sqrt{p}R)]$$

and

$$B = I_1(\sqrt{p}R) / p [K_1(\sqrt{p}R) I_0(\sqrt{p}) + K_0(\sqrt{p}) I_1(\sqrt{p}R)]$$

By substituting these constants in Eq. VI-1, the general solution for the transform of the pressure drop is expressed by

$$\bar{P}_{(r,p)} = \frac{[K_1(\sqrt{p}R) I_0(\sqrt{p}r) + I_1(\sqrt{p}R) K_0(\sqrt{p}r)]}{p [K_1(\sqrt{p}R) I_0(\sqrt{p}) + I_1(\sqrt{p}R) K_0(\sqrt{p})]} \quad \text{(VII-3)}$$

To find $Q(t)$ the cumulative fluid produced for unit pressure drop, then the transform for the pressure gradient at $r = 1$ is obtained as follows:

$$-\left(\frac{\partial \bar{P}}{\partial r}\right)_{r=1} = \frac{[I_1(\sqrt{p}R) K_1(\sqrt{p}) - K_1(\sqrt{p}R) I_1(\sqrt{p})]}{p^{1/2} [K_1(\sqrt{p}R) I_0(\sqrt{p}) + I_1(\sqrt{p}R) K_0(\sqrt{p})]}$$

where the negative sign is introduced in order to make $Q(t)$

TABLE III—Continued

R = 5 $\beta_1 = 0.8472$ $\beta_2 = 1.6112$		R = 6.0 $\beta_1 = 0.6864$ $\beta_2 = 1.2963$		R = 7.0 $\beta_1 = 0.5782$ $\beta_2 = 1.0860$		R = 8.0 $\beta_1 = 0.4999$ $\beta_2 = 0.9352$		R = 9.0 $\beta_1 = 0.4406$ $\beta_2 = 0.8216$		R = 10 $\beta_1 = 0.3940$ $\beta_2 = 0.7333$	
t	$P_{(t)}$	t	$P_{(t)}$	t	$P_{(t)}$	t	$P_{(t)}$	t	$P_{(t)}$	t	$P_{(t)}$
3.0	1.167	4.0	1.275	6.0	1.436	8.0	1.556	10.0	1.651	12.0	1.732
3.1	1.180	4.5	1.322	6.5	1.470	8.5	1.582	10.5	1.673	12.5	1.750
3.2	1.192	5.0	1.364	7.0	1.501	9.0	1.607	11.0	1.693	13.0	1.768
3.3	1.204	5.5	1.404	7.5	1.531	9.5	1.631	11.5	1.713	13.5	1.784
3.4	1.215	6.0	1.441	8.0	1.559	10.0	1.653	12.0	1.732	14.0	1.801
3.5	1.227	6.5	1.477	8.5	1.586	10.5	1.675	12.5	1.750	14.5	1.817
3.6	1.238	7.0	1.511	9.0	1.613	11.0	1.697	13.0	1.768	15.0	1.832
3.7	1.249	7.5	1.544	9.5	1.638	11.5	1.717	13.5	1.786	15.5	1.847
3.8	1.259	8.0	1.576	10.0	1.663	12.0	1.737	14.0	1.803	16.0	1.862
3.9	1.270	8.5	1.607	11.0	1.711	12.5	1.757	14.5	1.819	17.0	1.890
4.0	1.281	9.0	1.638	12.0	1.757	13.0	1.776	15.0	1.835	18.0	1.917
4.2	1.301	9.5	1.668	13.0	1.801	13.5	1.795	15.5	1.851	19.0	1.943
4.4	1.321	10.0	1.698	14.0	1.845	14.0	1.813	16.0	1.867	20.0	1.968
4.6	1.340	11.0	1.757	15.0	1.888	14.5	1.831	17.0	1.897	22.0	2.017
4.8	1.360	12.0	1.815	16.0	1.931	15.0	1.849	18.0	1.926	24.0	2.063
5.0	1.378	13.0	1.873	17.0	1.974	17.0	1.919	19.0	1.955	26.0	2.108
5.5	1.424	14.0	1.931	18.0	2.016	19.0	1.986	20.0	1.983	28.0	2.151
6.0	1.469	16.0	1.988	19.0	2.058	21.0	2.051	22.0	2.037	30.0	2.194
6.5	1.513	16.0	2.045	20.0	2.100	23.0	2.116	24.0	2.090	32.0	2.236
7.0	1.556	17.0	2.103	22.0	2.184	25.0	2.180	26.0	2.142	34.0	2.278
7.5	1.598	18.0	2.160	24.0	2.267	30.0	2.340	28.0	2.193	36.0	2.319
8.0	1.641	19.0	2.217	26.0	2.351	35.0	2.499	30.0	2.244	38.0	2.360
9.0	1.725	20.0	2.274	28.0	2.434	40.0	2.658	34.0	2.345	40.0	2.401
10.0	1.808	25.0	2.560	30.0	2.517	45.0	2.817	38.0	2.446	50.0	2.604
11.0	1.892	30.0	2.846					40.0	2.496	60.0	2.806
12.0	1.975							45.0	2.621	70.0	3.008
13.0	2.059							50.0	2.746		
14.0	2.142										
15.0	2.225										

positive. Theorem B shows that the integration with respect to time introduces an additional operator p in the denominator to give

$$\bar{Q}_{(p)} = \frac{[I_1(\sqrt{p} R) K_1(\sqrt{p})] - K_1(\sqrt{p} R) I_1(\sqrt{p})}{p^{3/2}[K_1(\sqrt{p} R) I_0(\sqrt{p}) + I_1(\sqrt{p} R) K_0(\sqrt{p})]}$$

(VII-4)

In order to apply Mellin's inversion formula, the first consideration is the roots of the denominator of this equation

which indicate the poles. Since the modified Bessel functions for positive real arguments are either increasing or decreasing, the bracketed term in the denominator does not indicate any poles for positive real values for p . At the origin of the plane of Fig. 2 a pole exists and this pole we shall have to investigate first. Thus, the substitution of small and real values for z (Eqs. VI-12 and VI-13) in Eq. VII-4, gives

$$\bar{Q}_{(p)} = \frac{(R^2 - 1)}{2p}$$

$p \rightarrow 0$

TABLE IV — Constant Terminal Rate Case Radial Flow
Pressure at Exterior Radius Constant

R = 1.5 λ ₁ = 3.4029 λ ₂ = 9.5207		R = 2.0 λ ₁ = 1.7940 λ ₂ = 4.8021		R = 2.5 λ ₁ = 1.2426 λ ₂ = 3.2265		R = 3.0 λ ₁ = 0.9596 λ ₂ = 2.4372		R = 3.5 λ ₁ = 0.7852 λ ₂ = 1.9624	
t	P _(t)	t	P _(t)	t	P _(t)	t	P _(t)	t	P _(t)
5.0(10) ⁻²	0.230	2.0(10) ⁻¹	0.424	3.0(10) ⁻¹	0.502	5.0(10) ⁻¹	0.617	5.0(10) ⁻¹	0.620
5.5 "	0.240	2.2 "	0.441	3.5 "	0.535	5.5 "	0.640	6.0 "	0.665
6.0 "	0.249	2.4 "	0.457	4.0 "	0.564	6.0 "	0.662	7.0 "	0.705
7.0 "	0.266	2.6 "	0.472	4.5 "	0.591	7.0 "	0.702	8.0 "	0.741
8.0 "	0.282	2.8 "	0.485	5.0 "	0.616	8.0 "	0.738	9.0 "	0.774
9.0 "	0.292	3.0 "	0.498	5.5 "	0.638	9.0 "	0.770	1.0 "	0.804
1.0(10) ⁻¹	0.307	3.5 "	0.527	6.0 "	0.659	1.0 "	0.799	1.2 "	0.858
1.2 "	0.328	4.0 "	0.552	7.0 "	0.696	1.2 "	0.850	1.4 "	0.904
1.4 "	0.344	4.5 "	0.573	8.0 "	0.728	1.4 "	0.892	1.6 "	0.945
1.6 "	0.356	5.0 "	0.591	9.0 "	0.755	1.6 "	0.927	1.8 "	0.981
1.8 "	0.367	5.5 "	0.606	1.0 "	0.778	1.8 "	0.955	2.0 "	1.013
2.0 "	0.375	6.0 "	0.619	1.2 "	0.815	2.0 "	0.980	2.2 "	1.041
2.2 "	0.381	6.5 "	0.630	1.4 "	0.842	2.2 "	1.000	2.4 "	1.065
2.4 "	0.386	7.0 "	0.639	1.6 "	0.861	2.4 "	1.016	2.6 "	1.087
2.6 "	0.390	7.5 "	0.647	1.8 "	0.876	2.6 "	1.030	2.8 "	1.106
2.8 "	0.393	8.0 "	0.654	2.0 "	0.887	2.8 "	1.042	3.0 "	1.123
3.0 "	0.396	8.5 "	0.660	2.2 "	0.895	3.0 "	1.051	3.5 "	1.158
3.5 "	0.400	9.0 "	0.665	2.4 "	0.900	3.5 "	1.069	4.0 "	1.183
4.0 "	0.402	9.5 "	0.669	2.6 "	0.905	4.0 "	1.080	5.0 "	1.215
4.5 "	0.404	1.0 "	0.673	2.8 "	0.908	4.5 "	1.087	6.0 "	1.282
5.0 "	0.405	1.2 "	0.682	3.0 "	0.910	5.0 "	1.091	7.0 "	1.242
6.0 "	0.405	1.4 "	0.688	3.5 "	0.913	5.5 "	1.094	8.0 "	1.247
7.0 "	0.405	1.6 "	0.690	4.0 "	0.915	6.0 "	1.096	9.0 "	1.250
8.0 "	0.405	1.8 "	0.692	4.5 "	0.916	6.5 "	1.097	10.0 "	1.251
		2.0 "	0.692	5.0 "	0.916	7.0 "	1.097	12.0 "	1.252
		2.5 "	0.693	5.5 "	0.916	8.0 "	1.098	14.0 "	1.253
		3.0 "	0.693	6.0 "	0.916	10.0 "	1.099	16.0 "	1.253

TABLE IV — Continued

R = 4.0 λ ₁ = 0.6670 λ ₂ = 1.6450		R = 6.0 λ ₁ = 0.4205 λ ₂ = 1.0059		R = 8.0 λ ₁ = 0.3090 λ ₂ = 0.7286		R = 10 λ ₁ = 0.2448 λ ₂ = 0.5726		R = 15 λ ₁ = 0.1616 λ ₂ = 0.3745	
t	P _(t)	t	P _(t)	t	P _(t)	t	P _(t)	t	P _(t)
1.0	0.802	4.0	1.275	7.0	1.499	10.0	1.651	20.0	1.960
1.2	0.857	4.5	1.320	7.5	1.527	12.0	1.730	22.0	2.003
1.4	0.905	5.0	1.361	8.0	1.554	14.0	1.798	24.0	2.043
1.6	0.947	5.5	1.398	8.5	1.580	16.0	1.856	26.0	2.080
1.8	0.986	6.0	1.432	9.0	1.604	18.0	1.907	28.0	2.114
2.0	1.020	6.5	1.462	9.5	1.627	20.0	1.952	30.0	2.146
2.2	1.052	7.0	1.490	10.0	1.648	25.0	2.043	35.0	2.218
2.4	1.080	7.5	1.516	12.0	1.724	30.0	2.111	40.0	2.279
2.6	1.106	8.0	1.539	14.0	1.786	35.0	2.160	45.0	2.332
2.8	1.130	8.5	1.561	16.0	1.837	40.0	2.197	50.0	2.379
3.0	1.152	9.0	1.580	18.0	1.879	45.0	2.224	60.0	2.455
3.4	1.190	10.0	1.615	20.0	1.914	50.0	2.245	70.0	2.513
3.8	1.222	12.0	1.667	22.0	1.943	55.0	2.260	80.0	2.558
4.5	1.266	14.0	1.704	24.0	1.967	60.0	2.271	90.0	2.592
5.0	1.290	16.0	1.730	26.0	1.986	65.0	2.279	10.0(10) ¹	2.619
5.5	1.309	18.0	1.749	28.0	2.002	70.0	2.285	12.0 "	2.655
6.0	1.325	20.0	1.762	30.0	2.016	75.0	2.290	14.0 "	2.677
7.0	1.347	22.0	1.771	35.0	2.040	80.0	2.293	16.0 "	2.689
8.0	1.361	24.0	1.777	40.0	2.055	90.0	2.297	18.0 "	2.697
9.0	1.370	26.0	1.781	45.0	2.064	10.0(10) ¹	2.300	20.0 "	2.701
10.0	1.376	28.0	1.784	50.0	2.070	11.0 "	2.301	22.0 "	2.704
12.0	1.382	30.0	1.787	60.0	2.076	12.0 "	2.302	24.0 "	2.706
14.0	1.385	35.0	1.789	70.0	2.078	13.0 "	2.302	26.0 "	2.707
16.0	1.386	40.0	1.791	80.0	2.079	14.0 "	2.302	28.0 "	2.707
18.0	1.386	50.0	1.792			16.0 "	2.303	30.0 "	2.708

and by the application of Mellin's inversion formula applied at the origin, then

$$\frac{1}{2\pi i} \oint_{\lambda=0} e^{\lambda t} \frac{1}{2} \frac{(R^2-1)}{\lambda} d\lambda = \frac{R^2-1}{2} \quad \text{(VII-5)}$$

An investigation of the integration along the negative real "cut" both for the upper and lower portions, Fig. 2, reveals that Eq. VII-4 is an even function for which the integration along the paths is zero. However, poles are indicated along the negative real axis and these residuals together with Eq. VII-5 make up the solution for the constant terminal pressure case for the limited radial system. The residuals are estab-

lished by the Mellin's inversion formula by letting $\lambda = u^2 e^{i\pi}$; then by Eqs. VI-18

$$\frac{1}{2\pi i} \oint_{\lambda_1, \lambda_2, \text{ etc.}} e^{\lambda t} \bar{Q}(\lambda) d\lambda = -\frac{1}{\pi i} \oint e^{-u^2 t} \frac{[J_1(uR) Y_1(u) - Y_1(uR) J_1(u)] du}{u^2 [J_1(uR) Y_0(u) - Y_1(uR) J_0(u)]} \quad \text{(VII-6)}$$

$a_1, a_2, \text{ etc.}$

where a_1, a_2 , and a_n are the roots of

$$[J_1(a_n R) Y_0(a_n) - Y_1(a_n R) J_0(a_n)] = 0 \quad \text{(VII-7)}$$

and the poles are represented on the negative real axis by $\lambda_n = -a_n^2$, Fig. 3. The residuals of Eq. VII-6 are the series expansion

TABLE IV — Continued

R = 20 $\lambda_1 = 0.1208$ $\lambda_2 = 0.2788$		R = 25 $\lambda_1 = 0.09648$ $\lambda_2 = 0.2223$		R = 30 $\lambda_1 = 0.08032$ $\lambda_2 = 0.1849$		R = 40 $\lambda_1 = 0.06019$ $\lambda_2 = 0.1384$		R = 50 $\lambda_1 = 0.04813$ $\lambda_2 = 0.1106$	
t	P(t)	t	P(t)	t	P(t)	t	P(t)	t	P(t)
30.0	2.148	50.0	2.389	70.0	2.551	12.0(10) ¹	2.813	20.0(10) ¹	3.064
35.0	2.219	55.0	2.434	80.0	2.615	14.0 "	2.888	22.0 "	3.111
40.0	2.282	60.0	2.476	90.0	2.672	16.0 "	2.953	24.0 "	3.154
45.0	2.338	65.0	2.514	10.0(10) ¹	2.723	18.0 "	3.011	26.0 "	3.193
50.0	2.388	70.0	2.550	12.0 "	2.812	20.0 "	3.063	28.0 "	3.229
60.0	2.475	75.0	2.583	14.0 "	2.886	22.0 "	3.109	30.0 "	3.263
70.0	2.547	80.0	2.614	16.0 "	2.950	24.0 "	3.152	35.0 "	3.339
80.0	2.609	85.0	2.643	16.5 "	2.965	26.0 "	3.191	40.0 "	3.405
90.0	2.658	90.0	2.671	17.0 "	2.979	28.0 "	3.226	45.0 "	3.461
10.0(10) ¹	2.707	95.0	2.697	17.5 "	2.992	30.0 "	3.259	50.0 "	3.512
10.5 "	2.728	10.0(10) ¹	2.721	18.0 "	3.006	35.0 "	3.331	55.0 "	3.556
11.0 "	2.747	12.0 "	2.807	20.0 "	3.054	40.0 "	3.391	60.0 "	3.595
11.5 "	2.764	14.0 "	2.878	25.0 "	3.150	45.0 "	3.440	65.0 "	3.630
12.0 "	2.781	16.0 "	2.936	30.0 "	3.219	50.0 "	3.482	70.0 "	3.661
12.5 "	2.796	18.0 "	2.984	35.0 "	3.269	55.0 "	3.516	75.0 "	3.688
13.0 "	2.810	20.0 "	3.024	40.0 "	3.306	60.0 "	3.546	80.0 "	3.713
13.5 "	2.823	22.0 "	3.057	45.0 "	3.332	65.0 "	3.568	85.0 "	3.735
14.0 "	2.835	24.0 "	3.085	50.0 "	3.351	70.0 "	3.588	90.0 "	3.754
14.5 "	2.846	26.0 "	3.107	60.0 "	3.375	80.0 "	3.619	95.0 "	3.771
15.0 "	2.857	28.0 "	3.126	70.0 "	3.387	90.0 "	3.640	10.0(10) ²	3.787
16.0 "	2.876	30.0 "	3.142	80.0 "	3.394	10.0(10) ²	3.655	12.0 "	3.833
18.0 "	2.906	35.0 "	3.171	90.0 "	3.397	12.0 "	3.672	14.0 "	3.862
20.0 "	2.929	40.0 "	3.189	10.0(10) ²	3.399	14.0 "	3.681	16.0 "	3.881
24.0 "	2.958	45.0 "	3.200	12.0 "	3.401	16.0 "	3.685	18.0 "	3.892
28.0 "	2.975	50.0 "	3.207	14.0 "	3.401	18.0 "	3.687	20.0 "	3.900
30.0 "	2.980	60.0 "	3.214			20.0 "	3.688	22.0 "	3.904
40.0 "	2.992	70.0 "	3.217			25.0 "	3.689	24.0 "	3.907
50.0 "	2.995	80.0 "	3.218					26.0 "	3.909
		90.0 "	3.219					28.0 "	3.910

TABLE IV — Continued

R = 60		R = 70		R = 80		R = 90		R = 100	
t	P(t)	t	P(t)	t	P(t)	t	P(t)	t	P(t)
3.0(10) ²	3.257	5.0(10) ²	3.512	6.0(10) ²	3.603	8.0(10) ²	3.747	1.0(10) ³	3.859
4.0 "	3.401	6.0 "	3.603	7.0 "	3.680	9.0 "	3.803	1.2 "	3.949
5.0 "	3.512	7.0 "	3.680	8.0 "	3.747	1.0(10) ³	3.858	1.4 "	4.026
6.0 "	3.602	8.0 "	3.746	9.0 "	3.805	1.2 "	3.949	1.6 "	4.092
7.0 "	3.676	9.0 "	3.803	10.0 "	3.857	1.3 "	3.988	1.8 "	4.150
8.0 "	3.739	10.0 "	3.854	12.0 "	3.946	1.4 "	4.025	2.0 "	4.200
9.0 "	3.792	12.0 "	3.937	14.0 "	4.019	1.5 "	4.058	2.5 "	4.303
10.0 "	3.832	14.0 "	4.003	15.0 "	4.051	1.6 "	4.144	3.0 "	4.379
12.0 "	3.908	16.0 "	4.054	16.0 "	4.080	1.8 "	4.192	3.5 "	4.434
14.0 "	3.959	18.0 "	4.095	18.0 "	4.130	2.0 "	4.285	4.0 "	4.478
16.0 "	3.996	20.0 "	4.127	20.0 "	4.171	2.5 "	4.349	4.5 "	4.510
18.0 "	4.023	25.0 "	4.181	25.0 "	4.248	3.0 "	4.394	5.0 "	4.534
20.0 "	4.043	30.0 "	4.211	30.0 "	4.297	3.5 "	4.426	5.5 "	4.552
25.0 "	4.071	35.0 "	4.228	35.0 "	4.328	4.0 "	4.448	6.0 "	4.565
30.0 "	4.084	40.0 "	4.237	40.0 "	4.347	4.5 "	4.464	6.5 "	4.579
35.0 "	4.090	45.0 "	4.242	45.0 "	4.360	5.0 "	4.482	7.0 "	4.583
40.0 "	4.092	50.0 "	4.245	50.0 "	4.368	5.5 "	4.491	7.5 "	4.588
45.0 "	4.093	55.0 "	4.247	60.0 "	4.376	6.0 "	4.496	8.0 "	4.593
50.0 "	4.094	60.0 "	4.247	70.0 "	4.380	7.0 "	4.498	9.0 "	4.598
55.0 "	4.094	65.0 "	4.248	80.0 "	4.381	8.0 "	4.499	10.0 "	4.601
		70.0 "	4.248	90.0 "	4.382	9.0 "	4.499	12.5 "	4.604
		75.0 "	4.248	10.0(10) ³	4.382	11.0 "	4.500	15.0 "	4.605
		80.0 "	4.248	11.0 "	4.382	14.0 "	4.500		

$$-2 \sum_{\substack{\infty \\ a_1, a_2 \\ \text{etc.}}} \frac{e^{-a_n^2 t} [J_1(a_n R) \cdot Y_1(a_n) - Y_1(a_n R) J_1(a_n)]}{a_n^2 \lim_{u \rightarrow a_n} \frac{d}{du} [J_1(u R) Y_0(u) - Y_1(u R) J_0(u)]}$$

(VII-8)

since

$$J_1'(z) = J_0(z) - J_1(z)/z \quad \dots \quad \text{(VII-9)}$$

and

$$J_0'(z) = -J_1(z)$$

which are recurrence formulae for both first and second kind of Bessel functions, W.B.F., p. 45 and p. 66, then by the identities of Eqs. VII-7 and VI-23, the relation VII-8 reduces to

$$-2 \sum_{\substack{\infty \\ a_1, a_2 \\ \text{etc.}}} \frac{e^{-a_n^2 t} J_1^2(a_n R)}{a_n^2 [J_0^2(a_n) - J_1^2(a_n R)]}$$

Therefore, the solution for $Q(t)$ is expressed by

$$Q(t) = \frac{R^2 - 1}{2} - 2 \sum_{\substack{\infty \\ a_1, a_2 \\ \text{etc.}}} \frac{e^{-a_n^2 t} J_1^2(a_n R)}{a_n^2 [J_0^2(a_n) - J_1^2(a_n R)]}$$

(VII-10)

This is essentially the solution developed in an earlier work,* but Eq. VII-10 is more rapidly convergent than the solution previously reported.

The values of $Q(t)$ for the constant terminal pressure case for a limited reservoir have been calculated from Eq. VII-10 for $R = 1.5$ to 10 and are tabulated in Table 2. A reproduction of a portion of these data is given in Fig. 5. As Eq. VII-10 is rapidly convergent for t greater than a given value, only two

TABLE IV — Continued

R = 200		R = 300		R = 400		R = 500		R = 600	
t	P(t)	t	P(t)	t	P(t)	t	P(t)	t	P(t)
1.5(10) ³	4.061	6.0(10) ³	4.754	1.5(10) ⁴	5.212	2.0(10) ⁴	5.356	4.0(10) ⁴	5.703
2.0 "	4.205	8.0 "	4.898	2.0 "	5.356	2.5 "	5.468	4.5 "	5.762
2.5 "	4.317	10.0 "	5.010	3.0 "	5.556	3.0 "	5.559	5.0 "	5.814
3.0 "	4.408	12.0 "	5.101	4.0 "	5.689	3.5 "	5.636	6.0 "	5.904
3.5 "	4.485	14.0 "	5.177	5.0 "	5.781	4.0 "	5.702	7.0 "	5.979
4.0 "	4.552	16.0 "	5.242	6.0 "	5.845	4.5 "	5.759	8.0 "	6.041
5.0 "	4.663	18.0 "	5.299	7.0 "	5.889	5.0 "	5.810	9.0 "	6.094
6.0 "	4.754	20.0 "	5.348	8.0 "	5.920	6.0 "	5.894	10.0 "	6.139
7.0 "	4.829	24.0 "	5.429	9.0 "	5.942	7.0 "	5.960	12.0 "	6.210
8.0 "	4.894	28.0 "	5.491	10.0 "	5.957	8.0 "	6.013	14.0 "	6.262
9.0 "	4.949	30.0 "	5.517	11.0 "	5.967	9.0 "	6.055	16.0 "	6.299
10.0 "	4.996	40.0 "	5.606	12.0 "	5.975	10.0 "	6.088	18.0 "	6.326
12.0 "	5.072	50.0 "	5.652	12.5 "	5.977	12.0 "	6.135	20.0 "	6.345
14.0 "	5.129	60.0 "	5.676	13.0 "	5.980	14.0 "	6.164	25.0 "	6.374
16.0 "	5.171	70.0 "	5.690	14.0 "	5.983	16.0 "	6.183	30.0 "	6.387
18.0 "	5.203	80.0 "	5.696	16.0 "	5.988	18.0 "	6.195	35.0 "	6.392
20.0 "	5.227	90.0 "	5.700	18.0 "	5.990	20.0 "	6.202	40.0 "	6.395
25.0 "	5.264	10.0(10) ⁴	5.702	20.0 "	5.991	25.0 "	6.211	50.0 "	6.397
30.0 "	5.282	12.0 "	5.703	24.0 "	5.991	30.0 "	6.213	60.0 "	6.397
35.0 "	5.290	14.0 "	5.704	26.0 "	5.991	35.0 "	6.214		
40.0 "	5.294	15.0 "	5.704			40.0 "	6.214		

TABLE IV — Continued

R = 700		R = 800		R = 900		R = 1000		R = 1200	
t	P(t)	t	P(t)	t	P(t)	t	P(t)	t	P(t)
5.0(10) ⁴	5.814	7.0(10) ⁴	5.983	8.0(10) ⁴	6.049	1.0(10) ⁵	6.161	2.0(10) ⁵	6.507
6.0 "	5.905	8.0 "	6.049	9.0 "	6.108	1.2 "	6.252	3.0 "	6.704
7.0 "	5.982	9.0 "	6.108	10.0 "	6.161	1.4 "	6.329	4.0 "	6.833
8.0 "	6.048	10.0 "	6.160	12.0 "	6.251	1.6 "	6.395	5.0 "	6.918
9.0 "	6.105	12.0 "	6.249	14.0 "	6.327	1.8 "	6.452	6.0 "	6.975
10.0 "	6.156	14.0 "	6.322	16.0 "	6.392	2.0 "	6.503	7.0 "	7.013
12.0 "	6.239	16.0 "	6.382	18.0 "	6.447	2.5 "	6.605	8.0 "	7.038
14.0 "	6.305	18.0 "	6.432	20.0 "	6.494	3.0 "	6.681	9.0 "	7.056
16.0 "	6.357	20.0 "	6.474	25.0 "	6.587	3.5 "	6.738	10.0 "	7.067
18.0 "	6.398	25.0 "	6.551	30.0 "	6.652	4.0 "	6.781	12.0 "	7.080
20.0 "	6.430	30.0 "	6.599	40.0 "	6.729	4.5 "	6.813	14.0 "	7.085
25.0 "	6.484	35.0 "	6.630	45.0 "	6.751	5.0 "	6.837	16.0 "	7.088
30.0 "	6.514	40.0 "	6.650	50.0 "	6.766	5.5 "	6.854	18.0 "	7.089
35.0 "	6.530	45.0 "	6.663	55.0 "	6.777	6.0 "	6.868	19.0 "	7.089
40.0 "	6.540	50.0 "	6.671	60.0 "	6.785	7.0 "	6.885	20.0 "	7.090
45.0 "	6.545	55.0 "	6.676	70.0 "	6.794	8.0 "	6.895	21.0 "	7.090
50.0 "	6.548	60.0 "	6.679	80.0 "	6.798	9.0 "	6.901	22.0 "	7.090
60.0 "	6.550	70.0 "	6.682	90.0 "	6.800	10.0 "	6.904	23.0 "	7.090
70.0 "	6.551	80.0 "	6.684	10.0(10) ⁵	6.801	12.0 "	6.907	24.0 "	7.090
80.0 "	6.551	100.0 "	6.684			14.0 "	6.907		
						16.0 "	6.908		

terms of the expansion are necessary to give the accuracy needed in the calculations.

Likewise from the foregoing work it can be easily shown that the transform of the pressure drop at any point in the formation in a limited reservoir for the constant terminal rate case, is expressed by

$$\bar{P}_{(r,p)} = \frac{[K_1(\sqrt{p} R) I_0(\sqrt{p} r) + I_1(\sqrt{p} R) K_0(\sqrt{p} r)]}{p^{3/2} [I_1(\sqrt{p} R) K_1(\sqrt{p} r) - K_1(\sqrt{p} R) I_1(\sqrt{p} r)]} \quad (\text{VII-11})$$

An examination of the denominator of Eq. VII-11 indicates that there are no roots for positive values of p . However, a double pole exists at $p = 0$. This can be determined by expanding $K_0(z)$ and $K_1(z)$ to second degree expansions for small values of z and third degree expansions for $I_0(z)$ and $I_1(z)$, and substituting in Eq. VII-11. It is found for small values of p , Eq. VII-11 reduces to

$$\bar{P}_{(r,p)} = \frac{1}{p} \left\{ \frac{R^2}{(R^2-1)} \log \frac{R}{r} - \frac{(R^2-r^2)}{2(R^2-1)} + \frac{R^2 \log R}{(R^2-1)^2} - \frac{(R^2+1)}{4(R^2-1)} \right\} + \frac{1}{p^2} \frac{2}{(R^2-1)} \quad (\text{VII-12})$$

This equation now indicates both a single and double pole at the origin, and it can be shown from tables or by applying Cauchy's theorem to the Mellin's formula that the inversion of Eq. VII-12 is

$$P_{(r,t)} = \frac{2}{(R^2-1)} \left[\frac{r^2}{4} + t \right] - \frac{R^2}{(R^2-1)} \log r - \frac{[3R^4-4R^2 \log R-2R^2-1]}{4(R^2-1)^2} \quad (\text{VII-13})$$

which holds when the time, t , is large

As in the preceding case, there are poles along the negative real axis, Fig. 3, and the residuals are determined as before by letting $\lambda = u^2 e^{i\pi}$, and Eqs. VI-18 give

TABLE IV—Continued

R = 1400		R = 1600		R = 1800		R = 2000		R = 2200	
t	P _(t)	t	P _(t)	t	P _(t)	t	P _(t)	t	P _(t)
2.0(10) ⁵	6.507	2.5(10) ⁵	6.619	3.0(10) ⁵	6.710	4.0(10) ⁵	6.854	5.0(10) ⁵	6.966
2.5 "	6.619	3.0 "	6.710	4.0 "	6.854	5.0 "	6.966	5.5 "	7.013
3.0 "	6.709	3.5 "	6.787	5.0 "	6.965	6.0 "	7.056	6.0 "	7.057
3.5 "	6.785	4.0 "	6.853	6.0 "	7.054	7.0 "	7.132	6.5 "	7.097
4.0 "	6.849	5.0 "	6.962	7.0 "	7.120	8.0 "	7.196	7.0 "	7.133
5.0 "	6.950	6.0 "	7.046	8.0 "	7.188	9.0 "	7.251	7.5 "	7.167
6.0 "	7.026	7.0 "	7.114	9.0 "	7.238	10.0 "	7.298	8.0 "	7.199
7.0 "	7.082	8.0 "	7.167	10.0 "	7.280	12.0 "	7.374	8.5 "	7.229
8.0 "	7.123	9.0 "	7.210	15.0 "	7.407	14.0 "	7.431	9.0 "	7.256
9.0 "	7.154	10.0 "	7.244	20.0 "	7.459	16.0 "	7.474	10.0 "	7.307
10.0 "	7.177	15.0 "	7.334	30.0 "	7.489	18.0 "	7.506	12.0 "	7.390
15.0 "	7.229	20.0 "	7.364	40.0 "	7.495	20.0 "	7.530	16.0 "	7.507
20.0 "	7.241	25.0 "	7.373	50.0 "	7.495	25.0 "	7.566	20.0 "	7.579
25.0 "	7.243	30.0 "	7.376	51.0 "	7.495	30.0 "	7.584	25.0 "	7.631
30.0 "	7.244	35.0 "	7.377	52.0 "	7.495	35.0 "	7.593	30.0 "	7.661
31.0 "	7.244	40.0 "	7.378	53.0 "	7.495	40.0 "	7.597	35.0 "	7.677
32.0 "	7.244	42.0 "	7.378	54.0 "	7.495	50.0 "	7.600	40.0 "	7.686
33.0 "	7.244	44.0 "	7.378	56.0 "	7.495	60.0 "	7.601	50.0 "	7.693
						64.0 "	7.601	60.0 "	7.695
								70.0 "	7.696
								80.0 "	7.696

TABLE IV—Continued

R = 2400		R = 2600		R = 2800		R = 3000	
t	P _(t)	t	P _(t)	t	P _(t)	t	P _(t)
6.0(10) ⁵	7.057	7.0(10) ⁵	7.134	8.0(10) ⁵	7.201	1.0(10) ⁶	7.312
7.0 "	7.134	8.0 "	7.201	9.0 "	7.260	1.2 "	7.403
8.0 "	7.200	9.0 "	7.259	10.0 "	7.312	1.4 "	7.480
9.0 "	7.259	10.0 "	7.312	12.0 "	7.403	1.6 "	7.545
10.0 "	7.310	12.0 "	7.401	16.0 "	7.542	1.8 "	7.602
12.0 "	7.398	14.0 "	7.475	20.0 "	7.644	2.0 "	7.651
16.0 "	7.526	16.0 "	7.536	24.0 "	7.719	2.4 "	7.732
20.0 "	7.611	18.0 "	7.588	28.0 "	7.775	2.8 "	7.794
24.0 "	7.668	20.0 "	7.631	30.0 "	7.797	3.0 "	7.820
28.0 "	7.706	24.0 "	7.699	35.0 "	7.840	3.5 "	7.871
30.0 "	7.720	28.0 "	7.746	40.0 "	7.870	4.0 "	7.908
35.0 "	7.745	30.0 "	7.765	50.0 "	7.905	4.5 "	7.935
40.0 "	7.760	35.0 "	7.799	60.0 "	7.922	5.0 "	7.955
50.0 "	7.775	40.0 "	7.821	70.0 "	7.930	6.0 "	7.979
60.0 "	7.780	50.0 "	7.845	80.0 "	7.934	7.0 "	7.992
70.0 "	7.782	60.0 "	7.856	90.0 "	7.936	8.0 "	7.999
80.0 "	7.783	70.0 "	7.860	10.0(10) ⁶	7.937	9.0 "	8.002
90.0 "	7.783	80.0 "	7.862	12.0 "	7.937	10.0 "	8.004
95.0 "	7.783	90.0 "	7.863	13.0 "	7.937	12.0 "	8.006
		10.0(10) ⁶	7.863			15.0 "	8.006

$$\frac{1}{2\pi i} \oint_{\lambda_1, \lambda_2, \text{etc.}} e^{\lambda t} \bar{P}_{(r, \lambda)} d\lambda$$

$$= \frac{1}{\pi i} \oint_{\beta_1, \beta_2, \text{etc.}} e^{-\beta^2 t} \frac{[J_1(uR) Y_0(ur) - Y_1(uR) J_0(ur)]}{u^2 [J_1(uR) Y_1(u) - J_1(u) Y_1(uR)]} du \quad (\text{VII-14})$$

where $\beta_1, \beta_2, \text{etc.}$, are roots of

$$[J_1(\beta_n R) Y_1(\beta_n) - Y_1(\beta_n) J_1(\beta_n R)] = 0 \quad (\text{VII-15})$$

with $\lambda_n = -\beta_n^2$. The residuals at the poles in Eq. VII-14 give the series

$$2 \sum_{\beta_1, \beta_2, \text{etc.}} \frac{e^{-\beta_n^2 t} [J_1(\beta_n R) Y_0(\beta_n R) - Y_1(\beta_n R) J_0(\beta_n R)]}{\beta_n^2 \lim_{u \rightarrow \beta_n} \frac{d}{du} [J_1(uR) Y_1(u) - J_1(u) Y_1(uR)]} \quad (\text{VII-16})$$

By the recurrence formulae Eqs. VII-9, the identity VII-15, and Eq. VI-23, this series simplifies to

$$\pi \sum_{\beta_1, \beta_2, \text{etc.}} \frac{e^{-\beta_n^2 t} J_1(\beta_n R) [J_1(\beta_n) Y_0(\beta_n R) - Y_1(\beta_n) J_0(\beta_n R)]}{\beta_n [J_1^2(\beta_n R) - J_1^2(\beta_n)]} \quad (\text{VII-17})$$

Therefore, the sum of all residuals, Eqs. VII-13 and VII-17 is the solution for the cumulative pressure drop at any point in the formation for the constant terminal rate case in a limited reservoir, or

$$P_{(r,t)} = \frac{2}{(R^2-1)} \left(\frac{r^2}{4} + t \right) - \frac{R^2}{(R^2-1)} \log r - \frac{(3R^4-4R^4 \log R-2R^2-1)}{4(R^2-1)^2}$$

$$+ \pi \sum_{\beta_1, \beta_2} \frac{e^{-\beta_n^2 t} J_1(\beta_n R) [J_1(\beta_n) Y_0(\beta_n R) - Y_1(\beta_n) J_0(\beta_n R)]}{\beta_n [J_1^2(\beta_n R) - J_1^2(\beta_n)]} \quad (\text{VII-18})$$

which is essentially the solution given by Muskat,⁴ now developed by the Laplace Transformation. Finally, for the cumulative pressure drop for a unit rate of production at the well bore, $r = 1$, this relation simplifies to

$$P_{(t)} = \frac{2}{(R^2-1)} \left(\frac{1}{4} + t \right) - \frac{(3R^4-4R^4 \log R-2R^2-1)}{4(R^2-1)^2}$$

$$+ 2 \sum_{\beta_1, \beta_2} \frac{e^{-\beta_n^2 t} J_1^2(\beta_n R)}{\beta_n^2 [J_2^2(\beta_n R) - J_1^2(\beta_n)]} \quad (\text{VII-19})$$

The calculations for the constant terminal rate case for a reservoir of limited radial extent have been determined from Eq. VII-19. The summary data for $R = 1.5$ to 10 are given in Table 3. An illustrative graph is shown in Fig. 6. The effect of the limited reservoir is quite pronounced as it is shown that producing the reservoir at a unit rate increases the pressure drop at the well bore much faster than if the reservoir were infinite, as the constant withdrawal of fluid is reflected very soon in the productive life by the constant rate of drop in pressure with time.

Pressure Fixed at Exterior Boundary

As a variation on the condition that $\left(\frac{dP}{dr} = 0 \right)_{r=R}$ we may assume that the pressure at $r = R$ is constant. In effect, this assumption helps to explain approximately the pressure history of flowing a well at a constant rate when, upon opening, the bottom hole pressure drops very rapidly and then levels out to become constant with time. The case has been developed by Hurst³ using a cylinder source and by Muskat⁴ using a point source solution.

When developing the solution by means of the Laplace transformation, it is assumed that the exterior boundary $r = R$, $\bar{P}(R, p) = 0$, which fixes the pressure at the exterior boundary as constant. Since the above-quoted references contain complete details, the final solutions are only quoted here for completeness' sake.

Cylindrical source:

$$P_{(t)} = \log R - 2 \sum_{n=1}^{\infty} \frac{e^{-\lambda_n^2 t} J_0^2(\lambda_n R)}{\lambda_n^2 [J_1^2(\lambda_n) - J_0^2(\lambda_n R)]} \quad (\text{VII-20})$$

where λ_n is the root established from

$$J_1(\lambda_n) Y_0(\lambda_n R) - Y_1(\lambda_n) J_0(\lambda_n R) = 0 \quad (\text{VII-21})$$

Point source:

$$P_{(t)} = \log R - \frac{2}{R^2} \sum_{n=1}^{\infty} \frac{e^{-\mu_n^2 t} J_0(\mu_n)}{\mu_n^2 J_1^2(\mu_n R)} \quad (\text{VII-22})$$

where the root μ_n is determined from $J_0(\mu_n R) = 0$, W.B.F., p. 748. Table 4 is the summary of the calculated $P(t)$ employing Eq. VII-20 for $R = 1.5$ to 50 , the cylinder source solution, which applies for small as well as large times. The data given for $R = 60$ to $3,000$ are calculated from the point source solution Eq. VII-22. Plots of these data are given in Fig. 7.

SPECIAL PROBLEMS

The work that has gone before shows the facility of the Laplace transformation in deriving analytical solutions. Not yet shown is the versatility of the Laplace transformation in arriving at solutions which are not easily foreseen by the orthodox methods. One such solution derived here has shown to be of value in the analysis of flow tests.

When making flow tests on a well, it is often noticed that the production rates, as measured by the fluid accumulating in the stock tanks, are practically constant. Since it is desired to obtain the relation between flowing bottom hole pressure and the rate of production from the formation, it is necessary to correct the rate of production as measured in the flow tanks for the amount of oil obtained from the annulus between casing and tubing. To arrive at the solution for this problem, we use the basic equation for the constant terminal rate case given by Eq. IV-11, where $q_{(T)}$ is the constant rate of fluid produced at the stock tank corrected to reservoir conditions, but $P_{(t)}$ is a pseudo pressure drop which is adjusted mathematically for the unloading of the fluid from the annulus to give the pressure drop occurring in the formation.

It is assumed that the unloading of the annulus is directly reflected by the change in bottom hole pressure as exerted by a hydrostatic head of oil column in the casing. Therefore, the rate of unloading of the annulus $q_{A(T)}$, expressed in cc. per second corrected to reservoir conditions, is equal to

$$q_{A(T)} = C \frac{\Delta P}{dT} \quad (\text{VIII-1})$$

where C is the volume of fluid unloaded from the annulus per atmosphere bottom hole pressure drop per unit sand thickness. The rate of fluid produced from the formation is then given by $q_{(T)} - q_{A(T)}$. As the bottom hole pressure is continuously changing, the problem becomes one of a variable rate. The substitution of the form of Eq. IV-11 in the superposition theorem, Eq. IV-16, gives

$$\Delta P = \frac{\mu}{2\pi K} \int_0^t [q_{(t')} - q_{A(t')}] P'_{(t-t')} dt'$$

and from Eq. VIII-1

$$\Delta P = \frac{\mu}{2\pi K} \int_0^t \left[q_{(t')} - C \frac{d\Delta P}{dt'} \right] P'_{(t-t')} dt' \quad \text{(VIII-2)}$$

Since $T = f\mu c R_b^2 t/K$, and the unit rate of production at the surface corrected to reservoir conditions is $\bar{q}_{(t)} = \frac{q_{(t)}\mu}{2\pi K}$, Eq. VIII-2 becomes

$$\Delta P = \int_0^t \left[q_{(t')} - \bar{C} \frac{d\Delta P}{dt'} \right] P'_{(t-t')} dt' \quad \text{(VIII-3)}$$

where $\bar{C} = C/2\pi f c R_b^2$.

Eq. VIII-3 presents a unique situation and we are confronted with determination of ΔP , the actual pressure drop, appearing both in the integrand and to the left side of the equation. The Laplace transformation offers a means of solving for ΔP which, by orthodox methods, would be difficult to accomplish.

It will be recognized that Theorem D, from Chapter V, is applicable. Therefore, if Eq. VIII-3 can be changed to a Laplace transformation, ΔP can be solved explicitly. If we express the transform of the constant rate $q_{(t)}$ as q/p , the transform of $P'_{(t)}$ as $\bar{p} \bar{P}_{(p)}$ and the transform of ΔP as $\bar{\Delta P}$, so that the transform for $d\Delta P/dt$ is $p \bar{\Delta P}$, then it follows that

$$\bar{\Delta P} = \left[\frac{q}{p} - \bar{C} p \bar{\Delta P} \right] \bar{p} \bar{P}_{(p)} \quad \text{(VIII-4)}$$

and on solution gives

$$\bar{\Delta P} = \frac{q \bar{P}_{(p)}}{[1 + \bar{C} p^2 \bar{P}_{(p)}]} \quad \text{(VIII-5)}$$

Since $q = q_{(T)}\mu/2\pi K$, then the term $\frac{\bar{P}_{(p)}}{[1 + \bar{C} p^2 \bar{P}_{(p)}]}$ in Eq.

VIII-5 can be interpreted as the transform of the pseudo pressure drop for the unit rate of production at the stock tank.

No mention has been made as to what value can be substituted for $\bar{P}_{(p)}$. If we wish to apply the cylinder source, Eq. VI-4 applies, namely,

$$\bar{P}_{(p)} = \frac{K_o(\sqrt{p})}{p^{3/2} K_1(\sqrt{p})} \quad \text{(VIII-6)}$$

However, from the previous discussion it has been shown that for wells, t is usually large since the well radius is small, and the point source solution of Lord Kelvin's applies, namely,

$$P_{(t)} = \frac{1}{2} \frac{1}{t^{1/4}} \int_0^\infty \frac{e^{-u}}{u} du \quad \text{(VI-16)}$$

the Ei-function. Therefore, to apply this expression in Eq. VIII-5, it is necessary to obtain the Laplace transform of the point source solution of Eq. VI-16. By an interchange of variables, this equation becomes

$$P_{(t)} = \frac{1}{2} \int_0^t \frac{e^{-1/4t}}{t} dt \quad \text{(VIII-7)}$$

and it will be recognized from Campbell and Foster, Eq. 920.1,

that the integrand is the transform for $K_o(\sqrt{p})$. Further, the integration with respect to time follows from Theorem B, Chapter V, so that the transform of Eq. VIII-7 is the relation

$$\bar{P}_{(p)} = \frac{K_o(\sqrt{p})}{p} \quad \text{(VIII-8)}$$

The same result can be gleaned from Eq. VIII-6 since for t large, p is small and $K_1(\sqrt{p}) = 1/\sqrt{p}$. Substitution of this approximation in Eq. VIII-6 yields Eq. VIII-8. Therefore, introducing the expression for $\bar{P}_{(p)}$ in Eq. VIII-5 gives

$$\bar{\Delta P} = \frac{q K_o(\sqrt{p})}{p [1 + \bar{C} p K_o(\sqrt{p})]} \quad \text{(VIII-9)}$$

for which it is necessary only to find the inverse of

$$\frac{K_o(\sqrt{p})}{p [1 + \bar{C} p K_o(\sqrt{p})]} \quad \text{(VIII-10)}$$

to obtain values for $P_{(t)}$, the cumulative pressure drop for unit rate of production in the stock tank which automatically takes cognizance of the unloading of the annulus.

The inverse of the form of VIII-10 by the Mellin's inversion formula can be determined by the path described in Fig. 2. The analytical determination is identical with the constant terminal rate case given in Section VI. Therefore, the cumulative pressure drop in the well bore, for a unit rate of production at the surface, corrected for the unloading of the fluid in the casing, is the relation

$$P_{(t)} = \int_0^\infty \frac{(1 - e^{-ut}) J_0(u) du}{u [(1 + u^2 \bar{C} \frac{\pi}{2} Y_0(u))^2 + (u^2 \bar{C} \frac{\pi}{2} J_0(u))^2]} \quad \text{(VIII-11)}$$

Fig. 8 presents a plot of the computed values for $P_{(t)}$ corresponding to \bar{C} from 1,000 to 75,000. It can be observed that the greater the unloading from the casing, the smaller the actual pressure drop is in a formation due to the reduced rate of fluid produced from the sand. For large times, however, all curves become identified with the point source solution which is the envelope of these curves. After a sufficient length of time, the change in bottom hole pressure is so slow that the rate of production from the formation is essentially that produced by the well, and the point source solution applies.

ACKNOWLEDGMENTS

The authors wish to thank the Management of the Shell Oil Co., for permission to prepare and present this paper for publication. It is hoped that this information, once available to the industry, will further the analysis and understanding of the behavior of oil reservoirs.

The authors acknowledge the help of H. Rainbow of the Shell Oil Co., whose suggestions on analytic development were most helpful, and of Miss L. Patterson, who contributed the greatest amount of these calculations with untiring effort.

REFERENCES

1. "Water Influx into a Reservoir and Its Application to the Equation of Volumetric Balance," William Hurst, *Trans., AIME*, 1943.

2. "Analysis of Reservoir Performance," R. E. Old, *Trans.*, AIME, 1943.
3. "Unsteady Flow of Fluids in Oil Reservoirs," William Hurst, *Physics*, January, 1934.
4. "The Flow of Compressible Fluids Through Porous Media and Some Problems in Heat Conduction," M. Muskat, *Physics*, March, 1934.
5. *Mathematical Methods in Engineering*, Karman and Biot, p. 403, McGraw-Hill, 1940.
6. *Operational Circuit Analysis*, Vannevar Bush, Chapter V, John Wiley and Sons, 1929.
7. "Variations in Reservoir Pressure in the East Texas Field," R. J. Schilthuis and W. Hurst, *Trans.*, AIME, 1935.
8. "Fourier Integrals for Practical Applications," G. A. Campbell and R. M. Foster, American Telephone and Telegraph Company.
9. *Operational Methods in Applied Mathematics*, H. S. Carslaw and J. C. Jaeger, Oxford Univ. Press, 1941. (Chapter IV).
10. *Ibidum*. p. 5 to 7.
11. "A Problem in the Theory of Heat Conduction," J. W. Nichol森, p. 226, *Proc. Royl. Soc.*, 1921.
12. "Some Two-Dimensional Diffusion Problems with Circular Symmetry," S. Goldstein, p. 51, *Proc. London Math. Soc.* (2), Vol. XXXIV, 1932.
13. "Heat Flow in an Infinite Solid Bounded Internally by a Cylinder," L. P. Smith, p. 441, *J. App. Physics*, 8, 1937.
14. "Some Two-Dimensional Problems in Conduction of Heat with Circular Symmetry," H. S. Carslaw and J. C. Jaeger, p. 361, *Proc. London Math. Soc.* (2), Vol. XVI.
15. "Heat Flow in the Region Bounded Internally by a Circular Cylinder," J. C. Jaeger, p. 223, *Proc. Royal Soc.*, Edinb. A, 61, 1942.
16. *A Treatise on the Theory of Bessel Functions*, G. W. Watson, Cambridge Univ. Press, 1944.
17. *Modern Analysis*, E. T. Whittaker and G. W. Watson, Cambridge Univ. Press, 1944.
18. *The Conduction of Heat*, H. S. Carslaw, pp. 149-153, MacMillan and Company, 1921.
19. "Pressure Prediction for Oil Reservoirs," W. A. Bruce, *Trans.*, AIME, 1943.
20. "Reservoir Performance and Well Spacing," Lincoln F. Elkins, *Oil and Gas Journal*, Nov. 16, 1946, API, 1946.
21. *Conduction of Heat in Solids*, H. S. Carslaw and J. C. Jaeger, Oxford at the Clarendon Press, 1947.

Note: This book came to our notice only after the text of this paper was prepared and for that reason references to its contents are incomplete. The careful reader will observe that, for instance, equation VI-21 in this paper is similar to equation (16), p. 283 when k and a are given unit values; also that "Limited Reservoirs" contains equations quite similar to those appearing in Section 126, "The Hollow Cylinder," of Carslaw and Jaeger's book. ★ ★ ★

DISCUSSION

Comments on "The Relation Between Electrical Resistivity and Brine Saturation in Reservoir Rocks," by H. F. Dunlap, H. L. Bilhartz, Ellis Shuler, and C. R. Bailey. Published in the October, 1949 issue of the JOURNAL OF PETROLEUM TECHNOLOGY.

By G. E. Archie, Shell Oil Co., Houston, Texas

I wish to compliment the authors on their experimental work of measuring the resistivities of cores. Measurements of this nature are difficult, particularly on small core samples.

The conclusion that the saturation exponent, n , used when interpreting electrical logs, varies appreciably from 2.0 does not follow from the data. It is true that individual samples indicated an n value considerably different, for instance, the Strawn sandstone given in Table I where $n = 1.18$. Rocks are heterogeneous, however, and more than one sample must be measured. One sample is of little value in predicting any property of the formation as a whole; therefore, only data where several pieces of the formation have been analyzed can be considered conclusive to be used to predict a value for n . Of the data presented in this paper, the measurements made on the Cotton Valley sandstone seem to meet this requirement, see Table I, where six samples were measured. The average value of n equals 1.8. This value cannot be said to vary appreciably from 2.0. (It is true that n varied from 1.5 to 2.0, but experimental error variations on the same sample were 1.7 to 2.0, see sample No. 6, Table I.) In view of the experimental error involved and the limited number of analyses run, the more logical conclusion would be that the data on the Cotton Valley sandstone give weight to the assumption that n may be expected to be of the order of 2.0 for sandstones.

This later data, together with the data given on a chart presented with my comments on the paper, "Estimation of Interstitial Water from the Electrical Log," by Milton Williams, also presented at the San Antonio meeting, indicates that the average value of n for consolidated sandstone "in situ" may be closer to 1.9 than 2.0 which has formerly been used.

★ ★ ★

Author's Reply to G. E. Archie—

The average of all of our own measurements on saturation exponents for various consolidated sandstone and limestone cores is about 1.75, and, as Archie properly points out, the scatter in the determinations on cores taken from a single formation is considerable. However, we have never measured a saturation exponent for a consolidated core which was significantly greater than two, and the great majority are somewhat less, the lowest value measured being that of 1.17 for the Strawn sandstone sample reported in the paper. For unconsolidated material, the values have usually been two or above. Exactly what the most nearly correct average value to use of consolidated sandstones would be is difficult to estimate in view of the limited data available, but we would estimate a value of 1.7 to 1.8 rather than 1.9 to 2.0. However, more data might well change this average value. For formations of particular interest, it is believed desirable to determine an average exponent from measurements on a number of core samples rather than to use any assumed universal average value. The fact that variation could occur, rather than the use of any particular average number for the exponent, was the thesis of the paper.

★ ★ ★

DISCUSSION

Comments on "The Relation Between Electrical Resistivity and Brine Saturation in Reservoir Rocks" by H. F. Dunlap, H. L. Bilhartz, Ellis Shuler and C. R. Bailey. Published in the October, 1949 issue of *Journal of Petroleum Technology*.

By M. R. J. Wyllie and Walter D. Rose, Gulf Research and Development Company, Pittsburgh, Pennsylvania

This paper and the results it gives concerning the numerical value of the exponent n in the resistivity index-saturation relationship, $I = S_w^{-n}$, is a most valuable and timely contribution to the rather sparse literature on a subject vital to electric log interpretation. Inasmuch as the results obtained provide some opportunity for checking certain theoretical conclusions we reached in a recent paper,¹ it is of particular interest to us.

The results obtained by the authors clearly show that the exponent n is not a constant with a value of about 2.0 as is generally assumed, but varies from core to core and may thus be considered some function of rock texture. On the basis of our theoretical development, we forecast that the exponent n would vary with rock texture (as measured in terms of irreducible wetting phase saturation, S_{wi}) and with saturation of the wetting phase itself. It is the latter prediction which is denied by Dunlap et al when they explicitly state that the available evidence indicates that the saturation exponent, n , does not vary with saturation. While we would like to believe this to be true (since an exponent n which was always independent of saturation, if albeit dependent upon rock texture, would introduce one welcome simplification in a complex problem) we do not believe that this is the only interpretation of all the results extant, including those of Dunlap et al. The results of Wyckoff and Botset,³ Leverett⁴ and other workers on essentially unconsolidated sands do indeed show a relatively constant exponent n , but those of Morse, Terwilliger and Yuster⁵ and those of the Russian workers quoted by Guyod⁶ show a marked dependence of n on saturation in certain instances. The variation of the exponent n with saturation shown in Fig. 5 of the paper of Dunlap et al is apparently attributed by these workers to non-equilibrium conditions. Elsewhere, however, it is stated that when, at high desaturating pressures and apparent equilibrium, widely varying values of the saturation exponent were found in different parts of the core, the results were considered unreliable and not reported.

We have shown¹ that an analytical expression for the exponent n can be found of the form:

$$n = \frac{\ln S_w^2 T/T_e}{\ln S_w^2},$$

Where,

S_w = the wetting phase saturation as a fraction of the pore volume,

T = the tortuosity of the porous medium at 100 per cent wetting phase saturation, and is defined as the square of the ratio of mean actual pore length to bed length,

T_e = the effective tortuosity, similarly defined, for the saturation, S_w .

From the above expression if n is to be a constant independent of saturation, it follows that $T/T_e = S_w^{x-2}$, where x is a constant having the value $2n$. The ratio T/T_e is itself a measure of fluid distribution and may be expected to vary somewhat with the manner in which a particular saturation has been obtained. Thus, the fact that the exponent n for a Strawn sandstone sample was found by Dunlap et al to vary when the mode of saturation was changed from flooding to capillary pressure desaturation is quite explicable in terms of a variation in the T/T_e ratio at a particular saturation. That the ratio T/T_e for any particular mode of saturating or desaturating a porous medium should be uniquely related to the degree of saturation by an expression of the form $T/T_e = S_w^{x-2}$ appears to us to be possible in certain cases, but we see no reason to believe that this relationship is universally true of all porous media. In particular we would expect to find pore size distribution as a big factor in determining T/T_e , since the tendency for the wetting phase to be displaced first from the larger pores by an entering non-wetting phase must necessarily affect T/T_e in a manner which is not always expressible in terms of S_w^{x-2} with x a constant.

We would thus like to ask Dunlap and his co-workers whether upon further consideration they are convinced that there is never a genuine variation of the exponent n with saturation. In addition, we would be interested to learn whether any of the results discarded because of their apparent unreliability showed apparent values of n between 3 and 4.5, i.e., in a range covering certain observations made by Williams and by the Russian workers quoted by Guyod and considered possible by us on theoretical grounds. In general, however, it would appear that to a first approximation and in the absence of more specific knowledge a value for n of about 2.0-2.5 is still the best average value to assume for log interpretation. In the light of the results reported by Williams we would particularly query the conclusion that n is generally less than 2 for consolidated media.

REFERENCES

1. "Some Theoretical Considerations Related to the Quantitative Evaluation of the Physical Characteristics of Reservoir Rock from Electrical Log Data." M. R. J. Wyllie and Walter D. Rose. (Submitted for publication in the *Jour. of Petr. Tech.*)
2. "Estimation of Interstitial Water from the Electric Log." M. Williams. AIME, San Antonio, Oct. 7, 1949.
3. "The Flow of Gas-Liquid Mixtures through Unconsolidated Sands." R. D. Wyckoff and H. G. Botset. *Physics*, 7, (9), 325, (1936).
4. "Flow of Oil-Water Mixtures through Unconsolidated Sands." M. C. Leverett. *Trans. AIME*, 132, 149, (1939).
5. "Relative Permeability Measurements on Small Core Samples." R. A. Morse, P. L. Terwilliger and S. T. Yuster. *Oil and Gas Jour.*, 46, (16), 109, (1947).
6. "Electrical Logging Developments in the U.S.S.R.": Part 6. H. Guyod, *World Oil*, 128 (4), 110, (1948). ★ ★ ★

Author's Reply to M. R. J. Wyllie and Walter D. Rose

In reply to the specific questions posed by Wyllie and Rose, we would like to make the following comments:

First, we are of course not convinced on the basis of our rather limited experimental evidence that there is *never* a genuine variation of the saturation exponent, n , with saturation. Our own data on several consolidated sandstone cores do not show any evidence of this variation, even in the region close to irreducible water, where the theory of Wyllie and Rose would indicate that n should approach a value of minus infinity. (See Fig. 4 in Wyllie and Rose's forthcoming paper, which the authors have kindly furnished us.) This figure is of interest, also, in that it indicates that for cores having irreducible waters of less than 30%, n is approximately constant with saturation until the water saturation reaches a value not greatly different from irreducible water. Most of the material which we worked with had irreducible waters of less than 30%. This variation close to the irreducible water sat-

uration, which is postulated by Wyllie and Rose, could not be expected to be detected by our experiments.

In answer to the second question, some of the results which we discarded indicated saturation exponents as high as six. However, as was stated in our paper, the criterion used for the reliability of the data was not the value of the saturation exponent, but the constancy of this value as obtained on different sections of the same core. If large and systematic variations in n were obtained for various sections of the core from top to bottom, this was taken to mean that the average brine saturation obtained for the entire core was not the same as the saturation in the individual sections. If this is so, a plot of resistance vs. an incorrect saturation would of course be meaningless.

Regarding the average value of the saturation exponent for consolidated and unconsolidated media, we can only reiterate that in our limited experience we have never observed a saturation exponent which was significantly greater than two for consolidated material, whereas for unconsolidated material the values have nearly always been two or above. ★ ★ ★

Technical Notes

A Note on the Application of the Capillary Pressure Method for the Determination of Oil Recovery

By Walter Rose

Gulf Research and Development Co.
Pittsburgh, Pa.

Experimentation which measures differences in pressure across the interfaces of immiscible fluids in the interstitial spaces of porous media may be termed "capillary pressure experimentation". In the literature of petroleum technology since 1941 there have appeared twelve papers popularizing capillary pressure concepts and developing applications of these concepts for the solution of problems of practical reservoir engineering importance, such as the determination of connate water, fluid distribution in transition zones, reservoir rock textural properties, and oil recovery from petroleum reservoirs.^a Although a review of the literature would be justified at this time in order to reconcile the conflicting viewpoints which are contained in the cited papers, the object of this note will be of more limited scope. It is believed that the recent paper of Muskat⁸ calls sufficient attention to many of the uncertainties which arise upon examination of the published literature, such that until satisfactory counter-proposals can be made it will serve our purpose only to mention some other like uncertainties. This will emphasize further the need confronting petroleum technologists to reconsider and reformulate the application possibilities of capillary pressure experimentation. In particular, I sug-

gest that we examine the thesis that capillary pressure experimentation as above defined can lead to measurements reflecting the recovery of oil from petroleum reservoirs, as was proposed first^b by Amyx and Yuster⁶ and was first reduced to practice by the experimentation of Welge⁹. In fact, I shall deal exclusively with the Welge papers since it is the principle one on this subject which has appeared to date. I shall attempt to show that the possibility of describing oil recovery features in terms of capillary pressure phenomena has not been established entirely.

The Welge paper was a pioneering effort to evaluate this recovery application possibility. P. P. Reichertz' comments on the Welge paper state that non-wetting phase discontinuities are developed occasionally in the Welge experiment, and restate Muskat's argument⁸ that discontinuous fluid elements (partially saturating the interstices of porous media which are elsewhere saturated with some other immiscible phase or phases) are not subject to the requirements of hydrostatic equilibrium. It is the purpose of my comment to show that it is unnecessary to make Reichertz' postulation regarding non-wetting phase discontinuities (however valid) when it is desired to criticize Welge's theoretical treatment of his problem. It can be shown that Welge's method of measuring values for "capillary pressure" is invalid in many instances of application, such that his reported curves of capillary pressure versus fluid saturation often have no physical meaning, even throughout the interval of fluid saturation where it might be otherwise suspected that no phase discontinuities occur.

By considering established principles of capillary pressure experimentation it can be shown that the pressure difference experimentally observed between wetting and non-wetting fluid phases which are contained in external reservoirs will reflect on the capillary pressure difference at the interfaces of contact between these phases only when the following conditions are satisfied:

(a) There shall be a balance between the opposing forces of gravity and capillarity, as obtains under conditions of hydrostatic equilibrium when the positions of the interfaces of contact become fixed in pore spaces of certain geometry

(b) The wetting and non-wetting fluids within the interstitial spaces shall everywhere be continuous with the external wetting phase reservoir and the external non-wetting phase reservoir, respectively.

It will become apparent immediately that in any instance when a greater pressure is recorded in the external wetting phase reservoir than in the external non-wetting phase reservoir, one may establish either that static equilibrium has not been attained or that discontinuities in one or more of the fluids have been developed. This is because the pressure otherwise is *always* greatest in the non-wetting phase at each static interstitial interface of contact with the wetting phase, such that the externally measured pressure in the non-wetting phase likewise must be greatest if the above conditions are to be satisfied.

^a The basic papers of Leverett¹ and Hassler, Brunner and Deahl² initially treated the major theoretical considerations; and these were followed by a series of papers^{3,4,5,6,7} developing the technique for the determination of connate water and fluid distribution in transition zones, the theory of the latter having been discussed in detail by Muskat⁸. The papers pertaining to the evaluation of rock texture character by the capillary pressure method are those of Purcell⁹ and Rose and Bruce¹⁰, and those pertaining to the determination of oil recovery are those of Welge¹¹ and Yuster and Stahl¹². In addition, there are to be found in these twelve cited papers numerous references to the soil science and related literature where other consideration has been given to capillary pressure phenomena.

^b As a matter of interest a suggestion of this application possibility can be found in the paper of Hassler, Brunner and Deahl (loc. cit.).

To illustrate the difficulty one faces in the application of Welge's method to determine oil recovery, an example can be cited. Let us consider a porous body of known wettability character. The surfaces of the interstitial spaces of the porous body may be described either as completely hydrophilic with respect to the saturating fluids; as completely lyophilic; or as of intermediate character where certain portions will be hydrophilic, and others lyophilic, and still others perhaps best described as neutral. Since an equivalent argument can be developed to apply to any of these assumed conditions of wettability character, we may choose to consider only the case of the hydrophilic porous body. The initial part of the Welge experiment concerns itself with the establishment of a definite distribution of connate water and oil within the interstitial spaces, and this is accomplished according to well-known capillary pressure methods which for the present discussion will be accepted as valid.^c

Another part of the Welge experiment concerns itself with the production of oil by water drive and the establishment of a static distribution of connate-plus-drive-water and oil which is described by identifying an externally measured pressure difference between immiscible fluid phases with macroscopic values of fluid saturation. The difficulty in this treatment arises from the fact that whereas the externally measured pressures indicates the pressure as greater in the wetting phase, water, than in the non-wetting phase, oil, we know the reverse condition is the one which actually obtains for this chosen case. That is, we measure the greater pressure in the wetting phase although in hydrophilic porous media the greater pressure must necessarily be in the non-wetting phase if static equilibrium is to obtain.

In attempting to reconcile these theoretical considerations with Welge's results one is faced with the additional problem of explaining how intermediate saturations of displaced non-wetting phase apparently are established under conditions of greater pressure in the displacing wetting phase.

Let us consider a capillary tube con-

taining oil and water. All of the oil will be displaced therefrom (vis. if the water is continuous to some external reservoir source and if there is an escape path for the oil) simply by an imbibition process and certainly if a driving pressure is imposed on the water. If there are cul de sac extensions to the capillary tube, a real non-recoverable oil saturation can be developed, measuring however a discontinuous oil phase. Thus, there are apparently no possibilities for intermediate saturations of oil to occur under conditions of static equilibrium, as indicated by Welge's graphical results, unless the pressure in the non-wetting phase remains greater than that in the wetting phase. Therefore the explanation must be that Welge measured his intermediate saturations of oil, not under conditions of static equilibrium as he believed, but under conditions of dynamic displacement when the flow of oil had become too small for him to observe. Such oil saturation data can have but little significance, especially since these data are associated with pseudo capillary pressure values which have little physical meaning. Although the writer is aware that this explanation implies that any capillary pressure experimentation may be in error due to lack of equilibrium attainment, there appears to be no other satisfactory explanation, unless we postulate a *variable* wettability which changes with time according to the dynamics of the system. However, although such a postulation perhaps might explain some of the observed results, at the same time it would introduce other complexities which would make solution of the problem extremely difficult either by theory or by experiment. This is because of the hysteretic uncertainties associated with transient contact angle and related effects. And in any event, the postulation of a variable wettability has not been made by the cited investigators of oil recovery phenomena to explain their results.

Figure 1 has been prepared to indicate in a generalized manner the description of the capillary displacement of oil by water in hydrophilic porous media (Curve A). This curve is seen everywhere to lie under the drainage curve describing the initial fluid distribution (Curve B) characterizing the virgin reservoir, according to well-es-

tablished concepts of drainage-imbibition hysteresis. However, in contrast to the experimental results reported in the literature no negative values of capillary pressure are encountered. In fact, a definite minimum value of capillary pressure greater than zero is shown identified with the minimum non-wetting phase saturation where non-wetting phase continuity still exists according to the requirements set forth by Muskat⁸ in his recent analysis.^d It must be

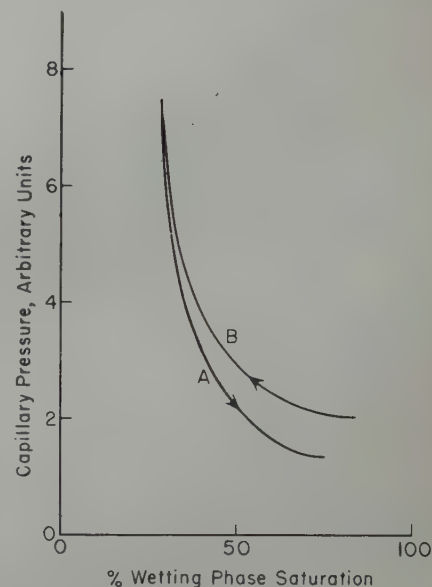


FIG. 1—Capillary Displacement of Oil by Water in Hydrophilic Porous Media.

emphasized at this point, however, that the curves given in Figure 1 apply only to conditions of static equilibrium, and therefore reflect on fluid distributions in petroleum reservoirs only to the extent that static equilibrium conditions obtain in the reservoirs.

To conclude, it may be noted that the above comments per se do not disprove the usefulness of the Welge type experimentation to predict oil recovery. Indeed, if it can be established in a particular instance that the reservoir recovery features are adequately simulated in the laboratory experiment, the values of non-recoverable oil so obtained can be accepted with little or no consideration being given to the significance and interpretation of the various values of pressure recorded during the experiment. In any event we are assured that capillary pressure type experimentation

^c Actually, the validity of this portion, as well as subsequent portions, of the experiment can be questioned according to the arguments of Muskat⁸, although such is not necessary for our immediate purpose.

^d The original data of Leverett are suggestive of finite minimum capillary pressures associated with imbibition processes, although Hassler *et al* show a zero value and Welge shows a negative value (loc. cit.).

will be required ultimately for detailed oil recovery studies, at least to the extent that oil recovery is controlled by capillary pressure phenomena. On the other hand, the writer is inclined to question the Welge speculation that: "... it may not be necessary to run a laboratory experiment exactly as the field will be exploited in order to predict its behavior . . ." For whereas this statement may apply fortuitously in some instances,* the implications are such that core analysis investigators can ill afford to be guided by such a concept in the organization of fluid behavior laboratory experimentation. Indeed this is the substance of the argument, not only as it has been directed against the work of Welge, but also as it can be directed against other reported capillary pressure experimentation: the laboratory experiment *must* simulate adequately the reservoir mechanism under study if the laboratory measurements are to reflect correctly on reservoir

phenomena. And although we may be forced sometimes for reasons of expediency or ignorance to improperly simulate the reservoir prototype by the laboratory model, we should not express our results except in terms of the assumptions, approximations, and experimental error which may affect the results.

The writer acknowledges the permission of Paul D. Foote, executive vice president of the Gulf Research and Development Company, to submit this note for publication.

* Actually, this quoted statement is ambiguous in that it can be made to apply in any and every instance according to how loosely we define the term "exactly".

REFERENCES

1. Leverett, *Trans. AIME*, 142, 152-169 (1941).
2. Hassler, Brunner and Deahl, *Trans. AIME*, 155, 154-174 (1944).

3. McCullough, Albaugh and Jones, *A.P.I. Drill. & Prod. Pract.*, 180 (1944).
4. Hassler and Brunner, *Trans. AIME*, 160, 114-123 (1945).
5. Thornton and Marshall, *Petroleum Technology*, Tech. Pub. 2126, (Jan. 1947).
6. Amyx and Yuster, *Prod. Monthly*, 9, Number 2, Page 10, (December, 1946).
7. Bruce and Welge, *API Drill. & Prod. Pract.*, 166 (1947).
8. Muskat, *Petroleum Tech.*, Tech. Pub. No. 2405, (July, 1948).
9. Purcell, *J. Petr. Tech.*, 1, in press (1949).
10. Rose and Bruce, *J. Petr. Tech.*, 1, in press (1949).
11. Welge, *Petroleum Technology*, Tech. Pub. No. 2433, (Sept., 1948).
12. Yuster and Stahl, *Prod. Monthly*, 13, Number 2, page 24, (December, 1948).

A NOTE ON WELL CEMENTING AT LOW TEMPERATURES

by

ROSCOE C. CLARK, JR.

Stanolind Oil and Gas Co., Tulsa, Okla.

In October 1945, R. F. Farris, in an AIME paper entitled *Method For Determining Minimum Waiting On Cement Time*, presented a method for calculating the minimum WOC* time required in oil well cementing operations. Briefly, this method consisted of shutting in a well, after the cement had been placed, and noting the time required for the wellhead pressure to reach a maximum. This time was then multiplied by a factor of 1.5 to determine when the cement had reached sufficient strength to support the weight of the casing.

As a result of this work, a number of areas have reduced their WOC time requirements with the subsequent saving of considerable rig time.

*WOC, abbreviation for "waiting on cement", indicates the time from when the cement is mixed to the time when sufficient strength has been obtained to allow the drilling of the plug.

The tests conducted by Farris were, for the most part, conducted under cementing temperatures in excess of 70°F. This was done because in the overwhelming majority of cases, cementing temperatures are in excess of 70°F (only in the northern part of the country, primarily in the Rocky Mountain area, in cementing surface casing are temperatures below 70°F. encountered, and such temperatures occur only during the winter months). The Stanolind Research Laboratory since that time has performed a number of tests both in the laboratory and in the field to evaluate this WOC factor when cementing temperatures are lower than 70°F. The results of these tests indicated the need for greater WOC time in areas affected by abnormally low cementing temperatures. These tests indicated that a WOC factor of 2 (Time

from start to mix cement to maximum wellhead pressure $\times 2 =$ Time to drill plug) will allow sufficient time for the cement to develop adequate strength.

A field test under abnormally low cementing temperatures (surface temperature 35°F., mud discharge temperature <70°F. and cementing depth 500 ft.) in the Rangely Field, Colorado, using the WOC factor of 2, indicated the time to drill the plug as 45 hours. Well conditions preventing getting back into the well until a 48-hour WOC time had elapsed. At this time, the plug drilled firm to hard indicating that the cement had reached its final set.

It is contemplated that during next winter additional field tests will be performed to further check the results of the laboratory and field tests conducted to date. ★ ★ ★

A NOTE ON THE VALUATION OF RELATIVE PERMEABILITY

By OWEN F. THORNTON
The Texas Co., Houston, Texas

Recently equations have been presented by Rose and Bruce¹ and by Rose², showing how the relative permeability of a reservoir rock may be determined from the capillary character of the rock. In particular, equations were developed to show the relationship between capillary pressure and the effective permeability to the wetting phase in a poly-phase flow system. The equations are as follows (nomenclature the same as in the Rose and Bruce paper):

$$K = f \left(\frac{1}{k} \right) \left(\frac{r}{P_r} \right)^2 \dots (1)$$

$$K_w = f S_w \left(\frac{1}{k} \right) \left(\frac{r}{P_c} \right)^2 \dots (2)$$

$$\frac{1}{k} = \frac{1}{2} \left(\frac{L}{L_a} \right)^2 \dots (3)$$

Rose and Bruce assume that the average length of path (L_a), which the wetting fluid follows in flowing through a porous media is independent of the saturation to the wetting phase, so that $\frac{1}{k}$ is a constant dependent only on the rock, and the permeability to the wetting phase is a function of the saturation and of the capillary pressure:

$$K_w = \frac{K_r}{K} = S_w \left(\frac{P_r}{P_c} \right)^2 \dots (4)$$

In measuring the flow of electric current through partially saturated core samples, it has been observed that the electrical resistance usually is not a simple linear function of saturation. This fact indicates that the average length of path in the flow of electric current is not independent of saturation, but rather that the tortuosity of the path depends upon the average saturation to the conducting fluid as well as upon the characteristics of the rock.

Itself. Inasmuch as the flow of fluid and the flow of electric current in many respects are analogous, it may be indicated further that the length of path for fluid also may not be independent of saturation. The following relationship can be derived to express the resistance to flow of electric current through a core sample partially saturated with conductive wetting phase, the non-wetting phase being non-conductive:

$$\frac{R_o}{R_s} = \frac{1}{S_w} \frac{L_a^1}{L_s^1} \dots (5)$$

where L_a^1 is the average length of path followed by the current in flowing through a length L of partially saturated core, where L_s^1 is the length of current path when the core is fully saturated, and where R_s and R_o are the specific resistivities of the partially saturated and saturated core sample, respectively.

It will be noted that R_o , the specific resistivity of the core sample when $S_w = 1.0$, is equal to the "formation resistivity factor"³ multiplied by the specific resistivity of the saturating fluid.

If it be assumed that the average lengths of path for fluid flow and for the flow of electric current are the same, then equation (5) may be combined with equations (1), (2) and (3) to give the following relationship:

$$K_w = \frac{K_r}{K} = S_w \left(\frac{L_a^1}{L_s^1} \right)^2 \left(\frac{P_r}{P_c} \right)^2 = \frac{1}{S_w} \left(\frac{R_o}{R_s} \right)^2 \left(\frac{P_r}{P_c} \right)^2$$

The above equation suggests including a correction for tortuosity when calculating the relative permeability of a reservoir rock to a wetting phase. The correction factor may be obtained from the resistivity-saturation relationship. For instance, the following calculations are obtained for the unconsolidated sands described by Leverett^{4,5}:

lutions are obtained for the unconsolidated sands described by Leverett^{4,5}:

S_w	R_o/R_s^4	P_r/P_c^1	K_w (Calc.)	K_w (Obs.) ⁴
0.30	0.08	0.88	0.02	0.0
0.40	0.16	0.94	0.06	0.04
0.50	0.27	0.97	0.14	0.11
0.60	0.40	0.98	0.26	0.21
0.70	0.53	0.98	0.39	0.35
0.80	0.68	0.99	0.57	0.54
0.90	0.84	0.99	0.77	0.76
1.00	1.00	1.00	1.00	1.00

It will be noted that the agreement between the calculated points and the observed data is rather good. Further investigation of the above method for obtaining relative permeabilities may be merited.

For many sands within specified ranges of saturations the following relationship has been found to hold approximately³:

$$\frac{R_o}{R_s} = S_w^n \dots (7)$$

The exponent n in the above equation has been found to equal two for many sands so that equation (6) reduces to the following:

$$K_w = S_w^{n^2} \left(\frac{P_r}{P_c} \right)^2 = S_w^2 \left(\frac{P_r}{P_c} \right)^2$$

The writer acknowledges the permission of The Texas Co. to submit this note for publication.

1. Walter Rose and W. A. Bruce—*Jnl. of Pet. Tech.*, Vol. 1, No. 5, p. 127 (1949).
2. Walter Rose—*Jnl. of Petr. Tech.*, Vol. 1, No. 5, p. 111 (1949).
3. G. E. Archie—*Trans. AIME*, 146, 54 (1942).
4. M. C. Leverett—*Trans. AIME*, 142, 152 (1941).
5. M. C. Leverett—*Trans. AIME*, 132, 149 (1939). ★ ★ ★

A NOTE ON THE THEORETICAL DESCRIPTION OF WETTING LIQUID RELATIVE PERMEABILITY DATA

By

WALTER ROSE AND M. R. J. WYLLIE

Gulf Research & Development Company, Pittsburgh, Pa.

In a recent technical note, Owen Thornton¹ suggests that wetting liquid relative permeability may be derived from the relationship:

$$k_{rw} = \left(\frac{P_d}{P_c} \right)^2 \cdot \frac{1}{I^2 S_w} \quad \dots (1)$$

where P_d/P_c is the ratio of displacement pressure to capillary pressure at the wetting liquid saturation S_w , and I is the resistivity index at this saturation. Thornton shows that this expression gives values for relative permeability in good agreement with those experimentally determined by Leverett. We have recently developed another expression for k_{rw} , which seems preferable to Equation 1 since it requires fewer experimental data for its verification. This equation may be derived in the following manner. Making use of the analogy between mass transfer of fluid in a porous medium and electrical conductivity through the fluid in the same medium, we can postulate a hydraulic formation resistivity factor analogous to an electrical formation resistivity factor. From Poiseuille's Law the resistivity to flow in a tube of radius R is of the form $8\mu/R^2$, where μ is the viscosity of the fluid. Similarly, the resistivity to flow in a porous medium of the same dimensions as the tube is given by D'Arcy's Law as μ/k , where k is the permeability of the medium. The hydraulic formation resistivity factor, F_r , is thus the quotient of these two resistivities, or:

$$F_r = \frac{R^2}{8k}$$

But permeability is defined by the Kozeny equation as:

$$k = \frac{\phi \bar{r}^2}{8} \left(\frac{L}{L_a} \right)^2 \quad (\text{cgs units})$$

where: \bar{r} is the average pore radius of the porous medium, L_a is the average tortuous length of the average pore, ϕ is the porosity, and L is the bed length.

This gives F_r as a function of the (L_a/L) tortuosity ratio and porosity, or in explicit form:

$$F_r = \frac{NT}{\phi^2}$$

where: $T = (L_a/L)^2$, and N is the number of pores of radius, \bar{r} , which will be found in any cross sectional area, πR^2 . That is, $N = \phi R^2/\bar{r}^2$. It will be clear from the foregoing considerations that the hydraulic formation factor should be dependent on the value of R which in every case must be arbitrarily selected.

By analogy, the hydraulic formation factor, F_{ef} , characterizing the porous medium at $S_w < 1$, will be given by:

$$F_{ef} = \frac{R^2}{8k_e} = \frac{NT_e}{\phi^2 S_w^2}$$

where k_e is the effective wetting liquid permeability obtaining at $S_w < 1$, and T_e is the square of the (L_{as}/L) ratio defined by Thornton. Therefore, the hydraulic resistivity index, I_r , is:

$$I_r = \frac{F_{ef}}{F_r} = \frac{k}{k_e} = \frac{1}{k_{rw}} = \left(\frac{T_e}{T} \right) \left(\frac{1}{S_w^2} \right)$$

However, Thornton gives I as:

$$I = \left(\frac{T_e}{T} \right)^{1/2} \frac{1}{S_w}$$

and it follows that:

$$k_{rw} = \frac{1}{I^2} \quad \dots (2)$$

Equation 2, when checked against the data of Wyckoff and Botset² and some of the Morse et al data³, gives comparisons as shown at the bottom of this page.

Computations based on Leverett's data, quoted by Thornton, gives computed k_{rw} values somewhat lower than the experimental values. Moreover, other instances can be cited where we find that neither Equation 1 nor Equation 2 is checked by experimental data. The work of Botset⁴ on the Nichols

Buff sandstone and Morse et al on oil wetted Bradford sandstone are such instances.

A reason for these discrepancies may lie in the fact that if both Equations 1 and 2 are presumed always to give accurate values for k_{rw} , it follows that $P_c = P_d/S_w^{1/2}$. Such an expression, it is well known, is too simple to describe accurately the capillary pressure behavior of all porous media. However, it is believed that a particular advantage resides on the use of Equation 2, since it is not dependent for its utility on a knowledge of the capillary pressures obtaining in dynamic flow systems. No practical technique for measuring the capillary pressures characterizing the fluid distributions in dynamic flow systems has yet been proposed.

Acknowledgment is given to Dr. Paul D. Foote, executive vice-president of the Gulf Research and Development Company, for permission to publish this note.

1. Owen F. Thornton, "A Note on the Valuation of Relative Permeability," *J. Pet. Tech.*, 1:7, Section 1, July, 1949.
2. R. D. Wyckoff and H. G. Botset, "The Flow of Gas-Liquid Mixtures through Porous Media," *Physics*, 7:325-345, 1936.
3. R. A. Morse, P. L. Terwilliger, and S. T. Yuster, "Relative Permeability Measurements of Small Core Samples," *Oil and Gas J.*, 46:109-125, Aug. 23, 1947.
4. H. G. Botset, "Flow of Gas-Liquid Mixtures Through Consolidated Sand," *Trans. AIME*, 136:91, 1940.

★ ★ ★

S_w	1.0	0.90	0.80	0.70	0.60	0.50	0.40	0.30
k_{rw} (a)	1.0	0.66	0.42	0.25	0.14	0.07	0.03	0.01
(b)	1.0	0.70	0.45	0.29	0.16	0.09	0.04	0.02
(c)	1.0	0.72	0.47	0.30	0.16	0.08	0.05	0.01
(d)	1.0	0.74	0.51	0.32	0.20	0.11	0.03	0.02

(a) and (b) refer to the Wyckoff and Botset computed and experimental values, respectively.

(c) and (d) refer to the Morse et al computed and experimental values, respectively.

(Plus reference to Articles and Editorials published in *Journal of Petroleum Technology* in 1949)

A

- ALCORN, I. W.: Editorial, Jan. JPT
Application of the Capillary Pressure Method for the Determination of Oil Recovery, by Walter Rose (Tech. Note), 326
Application of the LaPlace Transformation to Flow Problems in Reservoirs, by A. F. van Everdingen and W. Hurst, 305
ARCHIE, G. E.: *Discussion of the Relation Between Electrical Resistivity and Brine Saturation in Reservoir Rocks*, 324

B

- BABSON, E. C.: *Discussion of Estimation of Reserves and Water Drive from Pressure and Production History*, 97
BAILEY, C. R., DUNLAP, HENRY F., BILHARTZ, HARRELL L., and SHULER, ELLIS: *The Relation Between Electrical Resistivity and Brine Saturation in Reservoir Rocks*, 259
Banausia — or the Greeks Had a Word for It, by Reese H. Taylor, Mar. JPT
BEACH, WALTER G.: *Travelling Block Deflector in Drilling Operations* (Tech. Note), Nov. JPT
Behavior of Binary, Ternary, and Multi-component Systems at States Similar to Those Encountered in Condensate Fields, by B. H. Sage and W. N. Lacey, 143
BERGMAN, W. E., FISHER, H. B. and CARPENTER, P. G.: *Factors Involved in Removal of Sulphate from Drilling Muds by Barium Carbonate*, 197
BESSE, C. P. and OSBORNE, G. W.: *Gulf of Mexico Floating Drilling Tender*, 87
BILHARTZ, HARRELL L., SHULER, ELLIS, BAILEY, C. R., and DUNLAP, HENRY F.: *The Relation Between Electrical Resistivity and Brine Saturation in Reservoir Rocks*, 259
BILLHEIMER, J. S., REAMER, H. H. and SAGE, B. H.: *Multiple Condensed Phases in the Decane-Tetralin-Bitumen System*, 279
BILLHEIMER, J. S., SAGE, B. H. and LACEY, W. N.: *Multiple Condensed Phases in the N-Pentane-Tetralin-Bitumen System*, 283
BILLHEIMER, J. S., YUNDT, C. G., SAGE, B. H. and LACEY, W. N.: *Multiple Condensed Phases in the Methane-Decane-Tetralin-Bitumen System*, 265
BINCKLEY, C. W., BURGESS, F. R., and HAYMAKER, E. R.: *Method of Establishing a Stabilized Back-Pressure Curve for Gas Wells Producing from Reservoirs of Extremely Low Permeability*, 71
Bottom Hole Flow Surveys for Determination of Fluid and Gas Movements in Wells, by C. R. Dale, 205
BOYD, JAMES: *Technology and Low Grade Mineral Deposits* (Editorial) Nov. JPT
BRANTLY, J. E.: *Suggested National Oil Policy* (Editorial), Sept. JPT
BRESTON, JOSEPH and HUGHES, RICHARD V.: *Relation Between Pressure and Recovery in Long Core Water Floods*, 100
BROKAW, ALBERT D.: *Correction of Gas Volumes for Compressibility and Temperatures*, 248
BROWNSCOMBE, E. R., and COLLINS, FRANCIS: *Estimation of Reserves and Water Drive from Pressure and Production History*, 92

- BROWNSCOMBE, E. R., KIESCHNICK, W. F., JR., and MILLER, CHARLES C.: *A Calculation of the Effect of Production Rate Upon Ultimate Recovery by Solution Gas Drive*, 235
BRUCE, W. A. and ROSE, WALTER: *Evaluation of Capillary Character in Petroleum Reservoir Rock*, 127
BRYANT, F. S.: *Some Aspects of Unitization—California Oil and Gas Fields*, Feb. JPT
BULNES, A. C.: *Discussion of Theoretical Generalizations Leading to the Evaluation of Relative Permeability*, 125
BURTCHAELL, E. P.: *Reservoir Performance of a High Relief Pool*, 171
BURGESS, F. R., HAYMAKER, E. R., and BINCKLEY, C. W.: *Method of Establishing a Stabilized Back-Pressure Curve for Gas Wells Producing from Reservoirs of Extremely Low Permeability*, 71

C

- Calculation of the Effect of Production Rate upon Ultimate Recovery by Solution Gas Drive, by Charles C. Miller, E. R. Brownscombe, and W. F. Kieschnick, Jr., 235
CALHOUN, JOHN C., JR., LEWIS, MAURICE, JR., and NEWMAN, R. C.: *Experiments on the Capillary Properties of Porous Solids*, 189
CALHOUN, JOHN C., JR., and LOPER, RAMOND G.: *The Effect of Well Spacing and Drawdown on Recovery from Internal Gas Drive Reservoirs*, 211
Capillary pressures and capillarity: Calculation of permeability from, 39
Evaluation of character, 127
Experiments on retention of water, 189
Measurement by mercury, 39
Capillary Pressures — Their Measurement Using Mercury and the Calculation of Permeability Therefrom, by W. R. Purcell, 39
CARPENTER, P. G., BERGMAN, W. E. and FISHER, H. B.: *Factors Involved in Removal of Sulphate from Drilling Muds by Barium Carbonate*, 197
CARTER, D. V.: *Function of Petroleum Engineering Departments and Their Relationship to Management*, Sept. JPT
CLARK, J. B.: *A Hydraulic Process for Increasing the Productivity of Wells*, 1
CLARK, ROSCOE C., JR.: *Well Cementing at Low Temperatures* (Tech. Note) 327
COLLINS, FRANCIS and BROWNSCOMBE, E. R.: *Estimation of Reserves and Water Drive from Pressure and Production History*, 92
Conservation of oil and gas in Pickton field, 55
COOKE, JOHN T. and ELKINS, LINCOLN F.: *Pilot Gas Injection—Its Conduct and Criteria for Evaluation*, 180
Coring core recording, 33
Core Recorder, by Clark Millison, 33
Correction of Gas Volumes for Compressibility and Temperatures, by Albert D. Brokaw, 248

D

- DALE, C. R.: *Bottom Hole Flow Surveys for Determination of Fluid and Gas Movements in Wells*, 205
Developments in the Petroleum Field in Canada and Their Impact on the Economy of Canada, by H. H. Hewetson, Mar. JPT

Directional Drilling—Trespass to Technique (Editorial), by Howard C. Pyle, Oct. JPT

DOLL, H. G.: *Introduction to Induction Logging and Application to Logging of Wells Drilled with Oil Base Mud*, 148

Drilling

- equipment, for offshore operation, 87
equipment, semi-automatic, 27
muds, removal of sulphate from, 197
tenders, 87
DUNLAP, HENRY F., BILHARTZ, HARRELL L., SHULER, ELLIS, and BAILEY, C. R.: *The Relation Between Electrical Resistivity and Brine Saturation in Reservoir Rocks*, 259

E

- Effects of Transient Conditions in Gas Reservoirs, by D. T. MacRoberts, 36
Effect of Well Spacing and Drawdown on Recovery from Internal Gas Drive Reservoirs, by Raymond G. Loper and John C. Calhoun, Jr., 211
Electrical Computer for Solving Phase Equilibrium Problems, by M. Muskat and J. M. McDowell, 291
Electric logging effect of brine saturation, 259
electrochemical component, 17
induction logging, 148
resistivity relationships, 14
S. P. curves, analysis, 17
ELFRINK, E. B., SANDBERG, C. R. and POLLARD, T. A.: *New Compressibility Correlation for Natural Gases and Application to Estimates of Gas-In-Place*, 219
ELKINS, LINCOLN F. and COOKE, JOHN T.: *Pilot Gas Injection—Its Conduct and Criteria for Evaluation*, 180
ELKINS, L. E.: Editorial, Feb. JPT
ELKINS, L. E.: *A Preface to the Dues Referendum* (Editorial), Apr. JPT
ELKINS, L. E.: Editorial, Mar. JPT
ELKINS, L. E.: *Vote Yes on Dues Increase* (Editorial), May JPT
Engineering Profession and the Socialization of Industry, by L. E. Young, Nov. JPT
Estimation of Reserves and Water Drive from Pressure and Production History, by E. R. Brownscombe and Francis Collins, 92
Evaluation of Capillary Character in Petroleum Reservoir Rock, by Walter Rose and W. A. Bruce, 127
Experiments on the Capillary Properties of Porous Solids, by John C. Calhoun, Jr., Maurice Lewis, Jr., and R. C. Newman, 189
Factors Involved in Removal of Sulphate from Drilling Muds by Barium Carbonate, by W. E. Bergman, H. B. Fisher and P. G. Carpenter, 197

F

- FISHER, H. B., CARPENTER, P. G., and BERGMAN, W. E.: *Factors Involved in Removal of Sulphate from Drilling Muds by Barium Carbonate*, 197
FITTING, RALPH U., JR.: *Discussion of Pilot Gas Injection—Its Conduct and Criteria for Results*, 188
FITZGERALD, P. E.: *Discussion of a Hydraulic Process for Increasing the Productivity of Wells*, 7
Formation fracture, 1
Fundamental Forces Involved in the Use of Oil Well Packers, by Jack D. Webber, 271
Function of Petroleum Engineering Departments and Their Relationship to Management, by D. V. Carter, Sept. JPT

- back-pressure testing of wells, 71
compressibility correlation for, 219
conservation in Pickton field, 55
correction of volumes for compressibility and temperature, 248
determination of movement in wells, 205
hydrates, 66, 83
injection, 180
reservoirs, effects of transient conditions in, 37
solution gas drive, 235
- Gas Hydrates of Carbon Dioxide—Methane Mixture, by Carl H. Unruh and Donald L. Katz, 83
- GLENN, A. H. and GRAHAM, J. E.: *Outline of Weather and Wave Forecasting Techniques*, 49
- GRAHAM, J. E. and GLENN, A. H.: *Outline of Weather and Wave Forecasting Techniques*, 49
- Gravity drainage, 171
- Gulf of Mexico Floating Drilling Tender, by C. P. Besse and G. W. Osborne, 87
- GUYOD, HERBERT: *Discussion of a Quantitative Analysis of the Electrochemical Component of the S. P. Curve*, 25
- GUSTAFSON, J. D.: *Recent Canadian Oil Developments*, Dec. JPT

H

- HAWKINS, WALLACE: *Oil and Gas Conservation*, 1949, Jun. JPT
- HAYMAKER, E. R., BINCKLEY, C. W., and BURGESS, F. R.: *Method of Establishing a Stabilized Back-Pressure Curve for Gas Wells Producing from Reservoirs of Extremely Low Permeability*, 71
- HEWETSON, H. H.: *Developments in the Petroleum Field in Canada and Their Impact on the Economy of Canada*, Mar. JPT
- HORRER, PAUL L.: *Wave Forces Computed for a Typical Offshore Drilling Site*, 299
- HUGHES, RICHARD V. and BRESTON, JOSEPH N.: *Relation Between Pressure and Recovery in Long Core Water Floods*, 100
- HURST, W. and VAN EVERDINGEN, A. F.: *The Application of the Laplace Transformation to Flow Problems in Reservoirs*, 305
- Hydrates
carbon dioxide-methane mixtures, 83
methane, 66
- Hydraulic Process for Increasing the Productivity of Wells, by J. B. Clark, 1
- Hydrocarbon Mixtures
computer for equilibrium problems, 291
phase behavior, 143, 265, 279, 283

I

- Induction logging, 148
- Introduction to Induction Logging and Application to Logging of Wells Drilled with Oil Base Mud, by H. G. Doll, 148

K

- KATZ, DONALD L. and KOBAYASHI, RIKI: *Methane Hydrate at High Pressure*, 66
- KATZ, DONALD L. and UNRAH, CARL H.: *Gas Hydrates of Carbon Dioxide—Methane Mixture*, 83
- KAVELER, H. H.: *More Banausia* (Editorial), Dec. JPT
- KELLER, W. O. and MORSE, R. A.: *Some Examples of Fluid Flow Mechanism in Limestone Reservoirs*, 224

- KIESCHNICK, W. F., JR., MILLER, CHARLES C., and BROWNSCOMBE, E. R.: *A Calculation of the Effect of Production Rate Upon Ultimate Recovery by Solution Gas Drive*, 235
- KOBAYASHI, RIKI and KATZ, DONALD L.: *Methane Hydrate at High Pressure*, 66

L

- LACEY, W. N. BILLHEIMER, J. S., and SAGE, B. H.: *Multiple Condensed Phases in the N-Pentane-Tetralin-Bitumen System*, 283
- LACEY, W. N., BILLHEIMER, J. S., YUNDT, C. G., and SAGE, B. H.: *Multiple Condensed Phases in the Methane-Decane-Tetralin-Bitumen System*, 265
- LACEY, W. N. and SAGE, B. H.: *Behavior of Binary, Ternary, and Multicomponent Systems at States Similar to Those Encountered in Condensate Fields*, 143
- LEWIS, MAURICE, JR., NEWMAN, R. C., and CALHOUN, JOHN C., JR.: *Experiments on the Capillary Properties of Porous Solids*, 189
- Liquid Fuels from Coal and Oil Shales, by George Roberts, Jr. and Paul R. Schultz, Sept. JPT
- LIVERMORE, GEORGE P.: *Place of the Engineer in the Drilling Industry*, Apr. JPT
- LOPER, RAYMOND G. and CALHOUN, JOHN C., JR.: *The Effect of Well Spacing and Drawdown on Recovery from Internal Gas Drive Reservoirs*, 211

M

- MACROBERTS, D. T.: *Effects of Transient Conditions in Gas Reservoirs*, 36
- MCDOWELL, J. M. and MUSKAT, M.: *An Electrical Computer for Solving Phase Equilibrium Problems*, 291
- Mercury injection
to determine capillary pressures, 39
- Meteorology
application to offshore operation, 49
- Method of Embedding Large Cores in Plastic for Fluid Flow Studies, by Penn. State Coll. Pet. and Nat. Gas Div., Aug. JPT
- Middle Eastern Oil and Its Importance to the World, by John R. Suman, Jan. JPT
- MILLER, CHARLES C., BROWNSCOMBE, E. R., and KIESCHNICK, W. F., JR.: *A Calculation of the Effect of Production Rate upon Ultimate Recovery by Solution Gas Drive*, 235
- MILLISON, CLARK: *The Core Recorder*, 33
- MOORE, CARL A.: *Preparation of Lantern Slide Copy*, Sept. JPT
- More Banausia (Editorial), by H. H. Kaveler, Dec. JPT
- MORSE, R. A. and KELLER, W. O.: *Some Examples of Fluid Flow Mechanism in Limestone Reservoirs*, 224
- MUSKAT, MORRIS: *Discussion of Estimation of Reserves and Water Drive from Pressure and Production History*, 98
- MUSKAT, MORRIS: *Production Research—Present and Future*, Jul. JPT
- MUSKAT, M. and MCDOWELL, J. M.: *Electrical Computer for Solving Phase Equilibrium Problems*, 291
- Method of Establishing a Stabilized Back-Pressure Curve for Gas Wells Producing from Reservoirs of Extremely Low Permeability, by E. R. Haymaker, C. W. Binckley, and F. R. Burgess, 71
- Multiple Condensed Phases in the Decane-Tetralin-Bitumen System, by J. S. Billheimer, H. H. Reamer and B. H. Sage, 279
- Multiple Condensed Phases in the Methane-Decane-Tetralin-Bitumen System, by J. S. Billheimer, C. G. Yundt, B. H. Sage and W. N. Lacey, 265

- Multiple Condensed Phases in the N-Pentane-Tetralin-Bitumen System, by J. S. Billheimer, B. H. Sage and W. N. Lacey, 283
- Methane Hydrate at High Pressure, by Riki Kobayashi and Donald L. Katz, 66

N

- New Compressibility Correlation for Natural Gases and Application to Estimates of Gas-in-Place, by E. B. Elfrink, C. R. Sandberg, and T. A. Pollard, 219
- NEWMAN, R. C., CALHOUN, JOHN C., JR., and LEWIS, MAURICE, JR.: *Experiments on the Capillary Properties of Porous Solids*, 189
- Oceanography
application to offshore operation, 49, 299
- Oil and Gas Conservation, 1949, by Wallace Hawkins, June JPT
- Oil base mud
use with induction logging, 148
- OSBORNE, G. W. and BESSE, C. P.: *Gulf of Mexico Floating Drilling Tender*, 87
- Outline of Weather and Wave Forecasting Techniques, by A. H. Glenn and J. E. Graham, 49

O

P

- Packers
fundamentals involved in use, 271
requirements for formation fracture, 3
- PARSONS, C. P.: *Discussion of a Hydraulic Process for Increasing the Productivity of Wells*, 7
- PATNODE, H. W.: *Relationship of Drilling Mud Resistivity to Mud Filtrate Resistivity*, 14
- Penn State Coll. Pet. and Nat. Gas Div., *Method of Embedding Large Cores in Plastic for Fluid Flow Studies*, Aug. JPT
- Performance of the Ten Section Oil Field, by W. Tempelaar Lietz, 251
- Permeability
calculation from capillary pressures, 39
distribution, use of in water flood calculations, 9
relative, evaluation of, 111
- Permeability Distribution in Water Flood Calculations, by W. E. Stiles, 9
- Pickton field, Texas, 55
- Pilot Gas Injection—Its Conduct and Criteria for Evaluation, by Lincoln F. Elkins and John T. Cooke, 180
- Place of the Engineer in the Drilling Industry, by George P. Livermore, Apr. JPT
- POLLARD, T. A., ELFRINK, E. B., and SANDBERG, C. R.: *A New Compressibility Correlation for Natural Gases and Application to Estimates of Gas-in-Place*, 219
- Preface to the Dues Referendum (Editorial), by L. E. Elkins, Apr. JPT
- Preparation of Colored Lantern Slides, by G. Zuloaga, Sept. JPT
- Preparation of Lantern Slide Copy, by Carl A. Moore, Sept. JPT
- Pressure
relation to recovery in water floods, 100
use of pressure history in reserve estimation, 92
- Private Financing of Oil Producing Properties, by C. L. Rice, Jr., Jan. JPT
- Production of Oil Under Unitization in Wertz Dome Field, Wyoming, by E. A. Swendenborg, 163
- Production Research—Present and Future, by Morris Muskat, July JPT

- PURCELL, W. R.: *Capillary Pressures—Their Measurement Using Mercury and the Calculation of Permeability Therefrom*, 39
- PYLE, HOWARD C.: *Directional Drilling—Trespass to Technique* (Editorial), Oct. JPT
- Q
- Quantitative Analysis of the Electrochemical Component of the S. P. Curve, by M. R. J. Wyllie, 17
- R
- REAMER, H. H., SAGE, B. H., and BILLHEIMER, J. S.: *Multiple Condensed Phases in the Decane-Tetralin-Bitumen System*, 279
- Recent Canadian Oil Developments, by J. D. Gustafson, Dec. JPT
- REISTLE, CARL E., JR.: *Reservoir Engineering and Conservation* (Editorial), Jun. JPT
- Relation between Electrical Resistivity and Brine Saturation in Reservoir Rocks, by Henry F. Dunlap, Harrell L. Bilhartz, Ellis Shuler and C. R. Bailey, 259
- Relation between Pressure and Recovery in Long Core Water Floods, by Joseph N. Breston and Richard V. Hughes, 100
- Relationship of Drilling Mud Resistivity to Mud Filtrate Resistivity, by H. W. Patnode, 14
- Reserves
- estimation of, 92
 - gas, estimation, compressibility, correlation, 219
- Reservoir Engineering and Conservation (Editorial), by Carl E. Reistle, Jr., June JPT
- Reservoir performance
- gravity drive type, 171
 - limestone reservoirs, examples, 224
 - Pickton field, 55
 - Ten Section field, 251
 - Wertz Dome field, 163
- Reservoir Performance of a High Relief Pool, by E. P. Burtchael, 171
- Resistivities
- of drilling mud, 14
 - relation to brine saturation, 259
 - of mud filtrates, 14
- RICE, C. L., JR.: *Private Financing of Oil Producing Properties*, Jan. JPT
- ROBERTS, GEORGE, JR. and SCHULTZ, PAUL R.: *Liquid Fuels from Coal and Oil Shales*, Sept. JPT
- ROSE, WALTER: *Application of the Capillary Pressure Method for the Determination of Oil Recovery* (Tech. Note), 325
- ROSE, WALTER: *Discussion of Capillary Pressures, Their Measurement Using Mercury and the Calculation of Permeability Therefrom*, 46
- ROSE, WALTER: *Theoretical Generalizations Leading to the Evaluation of Relative Permeability*, 111
- ROSE, WALTER and BRUCE, W. A.: *Evaluation of Capillary Character in Petroleum Reservoir Rock*, 127
- ROSE, WALTER D., and WYLLIE, M. R. J.: *Discussion of The Relation Between Electrical Resistivity and Brine Saturation in Reservoir Rocks*, 324A
- ROSE, WALTER and WYLLIE, M. R. J.: *Theoretical Description of Wetting Liquid Relative Permeability* (Tech. Note), 329
- RYDER, HARRY M.: *Discussion of Relation Between Pressure and Recovery in Long Core Water Floods*, 109
- S
- SAGE, B. H., BILLHEIMER, J. S. and REAMER, H. H.: *Multiple Condensed Phases in the Decane-Tetralin-Bitumen System*, 279
- SAGE, B. H. and LACEY, W. N.: *Behavior of Binary, Ternary, and Multicomponent Systems at States Similar to those Encountered in Condensate Fields*, 143
- SAGE, B. H., LACEY, W. N., and BILLHEIMER, J. S.: *Multiple Condensed Phases in the N-Pentane-Tetralin-Bitumen System*, 283
- SAGE, B. H., LACEY, W. N., BILLHEIMER, J. S., and YUNDT, C. G.: *Multiple Condensed Phases in the Methane-Decane-Tetralin-Bitumen System*, 265
- SANDBERG, C. R., POLLARD, T. A., and ELFRINK, E. B.: *A New Compressibility Correlation for Natural Gases and Application to Estimates of Gas-In-Place*, 219
- SAUNDERS, G. E.: *Discussion of Factors Involved in Removal of Drilling Muds by Barium Carbonate*, 203
- SCHULTZ, PAUL R. and ROBERTS, GEORGE, JR.: *Liquid Fuels from Coal and Oil Shales*, Sept. JPT
- SELLS, H. R.: *Discussion of Method of Establishing a Stabilized Back-Pressure Curve for Gas Wells Producing from Reservoirs of Extremely Low Permeability*, 82
- Semi-Automatic Power Operated Drilling Equipment, by M. E. True and B. L. Stone, 27
- SHULER, ELLIS, BAILEY, C. R., DUNLAP, HENRY F., and BILHARTZ, HARRELL L.: *The Relation Between Electrical Resistivity and Brine Saturation in Reservoir Rocks*, 259
- SIMPSON, R. E., SMITH, J. W., YUST, C. S. and WELSH, J. R.: *A Study of Oil and Gas Conservation in the Pickton Field*, 55
- SMITH, J. W., YUST, C. S., WELSH, J. R. and SIMPSON, R. E.: *A Study of Oil and Gas Conservation in the Pickton Field*, 55
- SOLLIDAY, A. L.: *When Do We Need a Synthetic Fuel Industry?* Oct. JPT
- Some Aspects of Our Future Mineral Supplies, by W. E. Wrather, Feb. JPT
- Some Aspects of Unitization—California Oil and Gas Fields, by F. S. Bryant, Feb. JPT
- Some Examples of Fluid Flow Mechanisms in Limestone Reservoirs, by W. O. Keller and R. A. Morse, 224
- STILES, W. E.: *Use of Permeability Distribution in Water Flood Calculations*, 9
- STONE, B. L. and TRUE, M. E.: *Semi-Automatic Power Operated Drilling Equipment*, 27
- Study of Oil and Gas Conservation in the Pickton Field, by J. R. Welsh, R. E. Simpson, J. W. Smith and C. S. Yust, 55
- Suggested National Oil Policy (Editorial), by J. E. Brantly, Sept. JPT
- SUMAN, JOHN R.: *Middle Eastern Oil and its Importance to the World*, Jan. JPT
- SUTER, HANS H.: *We the Banasians* (Editorial), July JPT
- SWEDENBORG, E. A.: *Production of Oil Under Unitization in Wertz Dome Field, Wyoming*, 163
- T
- TAYLOR, REESE H.: *Banasia — or the Greeks Had a Word for It*, Mar. JPT
- Technology and Low Grade Mineral Deposits (Editorial), by James Boyd, Nov. JPT
- TEMPELAAR, LIETZ W.: *The Performance of the Ten Section Oil Field*, 251
- Theoretical Description of Wetting Liquid Relative Permeability (Tech. Note), by Walter Rose and M. R. J. Wyllie, Sept. JPT
- Theoretical Generalizations Leading to the Evaluation of Relative Permeability, by Walter Rose, 111
- THORNTON, OWEN: *Valuation of Relative Permeability* (Tech. Note), 328
- Travelling Block Deflector in Drilling Operations (Tech. Note), by Walter G. Beach, Nov. JPT
- TRUE, M. E. and STONE, B. L.: *Semi-Automatic Power Operated Drilling Equipment*, 27
- U
- UNRUH, CARL H. and KATZ, DONALD L.: *Gas Hydrates of Carbon Dioxide—Methane Mixture*, 83
- Valuation of Relative Permeability (Tech. Note), by Owen Thornton, 329
- V
- VAN DYKE, O. W.: *Discussion of Factors Involved in Removal of Sulphate From Drilling Muds*, 203
- VAN EVERDINGEN, A. F. and HURST, W.: *The Application of the Laplace Transformation to Flow Problems in Reservoirs*, 305
- Vote Yes on Dues Increase (Editorial), by L. E. Elkins, May JPT
- W
- Water Drive
- estimation of, 92
- Water flooding
- calculations, 9
 - study by long cores, 100
- WATSON, C. P.: *California Post-War Production and Demand*, Feb. JPT
- Wave Forces Computed for a Typical Off-shore Drilling Site, by Paul L. Horner, 299
- We the Banasians (Editorial), by Hans H. Suter, July JPT
- Weather forecasting, 49
- WEBBER, JACK C.: *Fundamental Forces Involved in the Use of Oil Well Packers*, 271
- Well Cementing at Low Temperatures (Tech. Note), by Roscoe C. Clark, Jr., 328
- Well spacing, 211
- WELSH, J. R., SIMPSON, R. E., SMITH, J. W. and YUST, C. S.: *A Study of Oil and Gas Conservation in the Pickton Field*, 55
- Wertz Dome field, Wyoming, 163
- When Do We Need a Synthetic Fuel Industry?, by A. L. Solliday, Oct. JPT
- WILLIAMS, MILTON: *Discussion of a Quantitative Analysis of the Electrochemical Component of the S. P. Curve*, 24
- WRATHER, W. E.: *Some Aspects of Our Future Mineral Supplies*, Feb. JPT
- WYLLIE, M. R. J. and ROSE, WALTER D.: *Discussion of The Relation Between Electrical Resistivity and Brine Saturation in Reservoir Rocks*, 325
- WYLLIE, M. R. J.: *A Quantitative Analysis of the Electrochemical Component of the S. P. Curve*, 17
- WYLLIE, M. R. J. and ROSE, WALTER: *Theoretical Description of Wetting Liquid Relative Permeability* (Tech. Note), Sept. JPT
- Y
- YOUNG, L. E.: *Engineering Profession and the Socialization of Industry*, Nov. JPT
- YUNDT, C. G., SAGE, B. H., LACEY, W. N., and BILLHEIMER, J. S.: *Multiple Condensed Phases in the Methane-Decane-Tetralin-Bitumen System*, 265
- YUST, C. S., WELSH, J. R., SIMPSON, R. E., and SMITH, J. W.: *A Study of Oil and Gas Conservation in the Pickton Field*, 55
- Z
- ZULOAGA, G.: *Preparation of Colored Lantern Slides*, Sept. JPT ★ ★ ★

